Synthesis of Biologically Active Glycosylphosphatidylinositol Derivatives Bearing Unsaturated Lipids

Inaugural-Dissertation
to obtain the academic degree
Doctor rerum naturalium (Dr. rer. nat.)

Submitted to the Department of Biology, Chemistry, Pharmacy
of the Freie Universität Berlin

by

PAULA ANDREA GUERRERO MUÑOZ

2022

This work was performed between March 2019 and July 2022 under the supervision of Prof. Dr. Daniel Varón Silva in the Department of Biomolecular Systems at the Max-Planck-Institute of Colloids and Interfaces, Potsdam-Germany, the Institute of Chemistry and Biochemistry at the Free University Berlin, and the Institute for Chemistry and Bioanalytics at the University of Applied Sciences and Arts Northwestern Switzerland, Muttenz-Switzerland.

1st Reviewer: Prof. Dr. Daniel Varón Silva

2nd Reviewer: Prof. Dr. Christoph A. Schalley

Date of defense: 21/11/2022

Declaration of Independence

Herewith I certify that I have prepared and written my thesis independently and that I have not used any sources and aids other than those indicated by me. I also declare that I have not submitted the dissertation in this or any other form to any other institution as a dissertation

_____ _____

(Date, Place) (Signature)

Outline

Summary

Several eukaryotic proteins are attached to the cell membrane using glycosylphosphatidylinositol (GPI) anchors, a family of complex glycolipids. GPIs are post-translationally added to the *C*-terminus of proteins and contain a conserved pseudopentasaccharide glycan core structure, a phosphoethanolamine (PEtN) unit, and a phospholipid. Deficiencies in the GPI-anchored proteins (GPI-APs) biosynthesis lead to a series of rare and complicated disorders associated with inherited GPI deficiencies (IGDs) in humans. Currently, there is no treatment for patients suffering from IGDs, and there is a lack of understanding of the biological events derived from the GPI deficiency.

Deciphering the GPIs biological functions and the application of these molecules as tools in chemical biology require homogeneous samples. GPIs are naturally found as heterogeneous mixtures that are difficult to separate for getting single compounds in pure form. Several strategies have been reported to obtain pure GPIs by chemical synthesis; nevertheless, incorporating unsaturated fatty acids remains challenging. GPIs and GPI fragments containing unsaturated lipids are not only predominant intermediates during the GPI biosynthesis but are also highly present on the cell surface of protozoan parasites and exhibit prominent proinflammatory activity. Thus, developing a reliable strategy to access these complex glycolipids is of great interest.

This work aimed to develop a general and convergent synthesis of GPIs bearing unsaturated lipids. In previous work, our group established a strategy using 2-naphthylmethyl (Nap) ether as permanent protection for incorporating unsaturated lipids in a GPI derivative synthesis. In this work, the process was expanded and optimized to get biologically active and structurally diverse GPIs and GPI fragments containing unsaturated fatty acid chains.

In the first part of this work, nine GPI fragments resembling the products of the initial steps of the GPI biosynthesis (Figure 1) were designed and synthesized to determine the activity of synthetic GPI-glycolipids in restoring the GPI-APs biosynthesis in GPI-AP deficient cells (chapter 2).

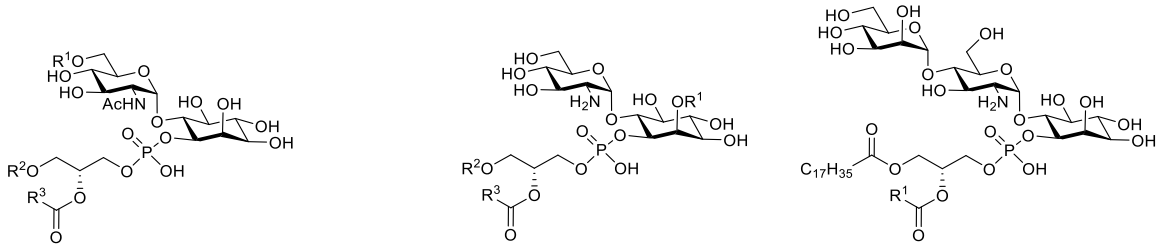

1a R^1= H, R^2= $COC_{17}H_{35}$, R^3= $(CH_2)_7CH{=}CH(CH_2)_7CH_3$
1b R^1= H, R^2= $COC_{17}H_{35}$, R^3= $C_{17}H_{35}$
1c R^1= H, R^2= $C_{18}H_{37}$, R^3= $(CH_2)_7CH{=}CH(CH_2)_7CH_3$
1d R^1= $(CH_2)_3N_3$, R^2= $COC_{17}H_{35}$, R^3= $(CH_2)_7CH{=}CH(CH_2)_7CH_3$

2a R^1= H, R^2= $COC_{17}H_{35}$, R^3= $(CH_2)_7CH{=}CH(CH_2)_7CH_3$
2b R^1= $COC_{15}H_{31}$, R^2= $COC_{17}H_{35}$, R^3= $(CH_2)_7CH{=}CH(CH_2)_7CH_3$
2c R^1= H, R^2= $COC_{17}H_{35}$, R^3= $C_{17}H_{35}$
2d R^1= H, R^2= $C_{18}H_{37}$, R^3= $(CH_2)_7CH{=}CH(CH_2)_7CH_3$

3 R^1= $(CH_2)_7CH{=}CH(CH_2)_7CH_3$

Figure 1. Designed GPI fragments (**1** to **3**) to rescue the expression of GPI-APs.

Glycolipids **1**, **2**, and **3** were synthesized by assembling first the glycan part using Nap-protected inositol, glucosamine, and mannose building blocks. The lipids were installed at the late synthesis stage before the global deprotection. Removal of the Nap ethers was optimized and successfully performed under oxidative conditions with DDQ. Pure compounds were purified by size exclusion chromatography and trituration in methanol. The glycolipids were biologically evaluated at Osaka University to determine the activity of the synthetic fragments to rescue the GPI-APs production in GPI-AP deficient HEK cells having knockout genes involved in the first four steps of GPI biosynthesis.

The biological assays demonstrated that the synthetic fragments **1a**, **2a**, **2b,** and **3** rescue the GPI biosynthesis in HEK cells having PIGA or PIGL knockout genes *in vitro*. The glycolipids showed concentration-dependent recovery of GPI biosynthesis and were highly active on the steps at the ER's cytoplasmic face. However, the synthetic compounds could not restore the biosynthesis process in cells having knock-out genes affecting the steps on the luminal side of the ER. The activity absence was attributed to the lack of compounds transport across the ER membrane.

A set of biological studies using glycolipids **1b**, **1c, 1d, 2c,** and **2d** are in progress to determine the transport mechanisms for incorporating GPI fragments in the knockout cells and to evaluate the lipid influence on the fragments' incorporation into the GPI biosynthesis. Compounds **1b** and **2c** were synthesized without unsaturated lipids to disclose the role of unsaturation in the activity; fragments **1c** and **2d** were designed to evaluate the effect of alkyl and acyl chains on compound activity. Additionally, the azide-labeled fragment **1d** was synthesized to analyze the transport of the compounds inside the cells.

Altogether, this work showed the application of a synthetic strategy to obtain active GPI fragments and their suitability as tools for future development of glycan-based treatments of IGDs involving mutations in the PIGA and PIGL genes. Additional studies are required to expand the structure-activity relationship understanding, tune the activity of the glycolipids, and establish methods for efficient GPI fragments delivery into the ER Lumen to cover mutations in genes affecting further steps of the GPI-AP biosynthesis.

In the second part of this work, the synthetic strategy was expanded for the total synthesis of a GPI of *Plasmodium falciparum*—the parasite that causes Malaria—having unsaturated lipids (chapter 3). The strategy was based on using Nap ether protecting groups, the global deprotection developed for the synthesis of GPI fragments **1** to **3**, and a previous strategy to access GPIs with saturated lipids. The assembly of the GPI glycan core relied on a set of fully orthogonally protected building blocks **4** to **7** that enabled the regioselective introduction of phosphodiesters at the late synthesis stage (Scheme 1). Mannose building blocks **4**, **5** and **9** were equipped with an allyl protecting group on the anomeric position that was converted into a trichloroacetimidate to perform the glycosylation reactions. The stereoselectivity of glycosylations was controlled by the

reaction conditions and neighboring group participation of the levulinoyl and acetyl esters, delivering the desired α configuration.

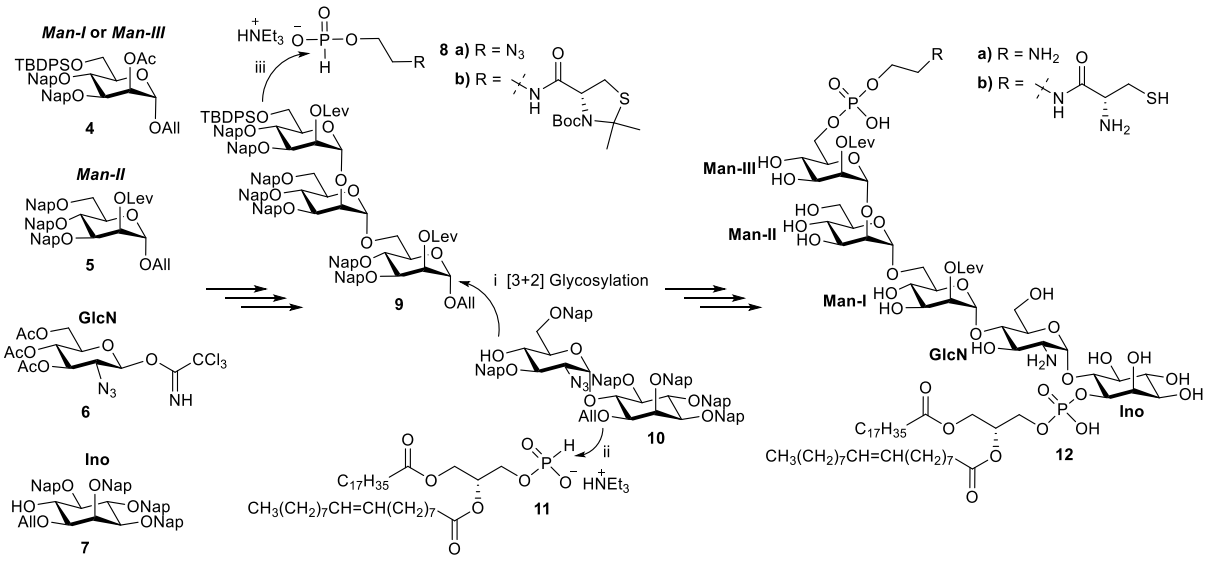

Scheme 1. Total synthesis of a *P. falciparum* GPI bearing unsaturated lipids. The roman numbers represent the order of the reactions.

The assembly of the glycan core via a [3+2] glycosylation was followed by the introduction of the phospholipid using H-phosphonate **11** and a two-step phosphorylation with H-phosphonate **8a** to introduce the PEtN unit. A three-step protocol was performed for global deprotection to furnish the desired *P. falciparum* GPI **12a** bearing unsaturated lipids. Additionally, the GPI **12b** was synthesized using H-phosphonate **8b** to incorporate a protected cysteine attached to phosphoethanolamine in the second phosphorylation. The cysteine in GPI **12b** allows the coupling with a protein through native chemical ligation to obtain a GPI-AP.

In the third part of this work, the strategy was applied to synthesize a GPI of the parasite *Trypanosoma cruzi*, the causing agent of Chagas disease (chapter 4). The synthesis required a modified strategy to incorporate two GPI-glycan modifications: an additional mannose attached to the Man-III unit and an aminoethylphosphonate (AEP) unit attached to glucosamine (Scheme 2). The process required an additional mannose unit into the glycan that was incorporated using [4+2] glycosylation strategy instead of [3+2]. The lipidated pseudohexasaccharide **18** was synthesized using the same route used for synthesizing the *P. falciparum* GPI and involved a phosphorylation using the H-phosphonate **16**. An extra level of orthogonality was achieved by including a PMB protecting group at the O-6 position of glucosamine at an early stage of the route. This differentiated position in the pseudodisaccharide **15** was selectively deprotected to incorporate the AEP component, a characteristic modification of *T. cruzi* GPIs. The attachment of the AEP moiety was more challenging than expected. Attempts to optimize this reaction with a small model molecule presented unexpected results for the NMR and Mass spectra, so additional studies are still

required to achieve the desired transformation and complete the synthesis. Further steps include the phosphorylation using the H-phosphonate **8a** to obtain the final protected *T. cruzi* GPI, which can be transformed into the final target **19** using the three-step deprotection protocol established to get GPI **12**.

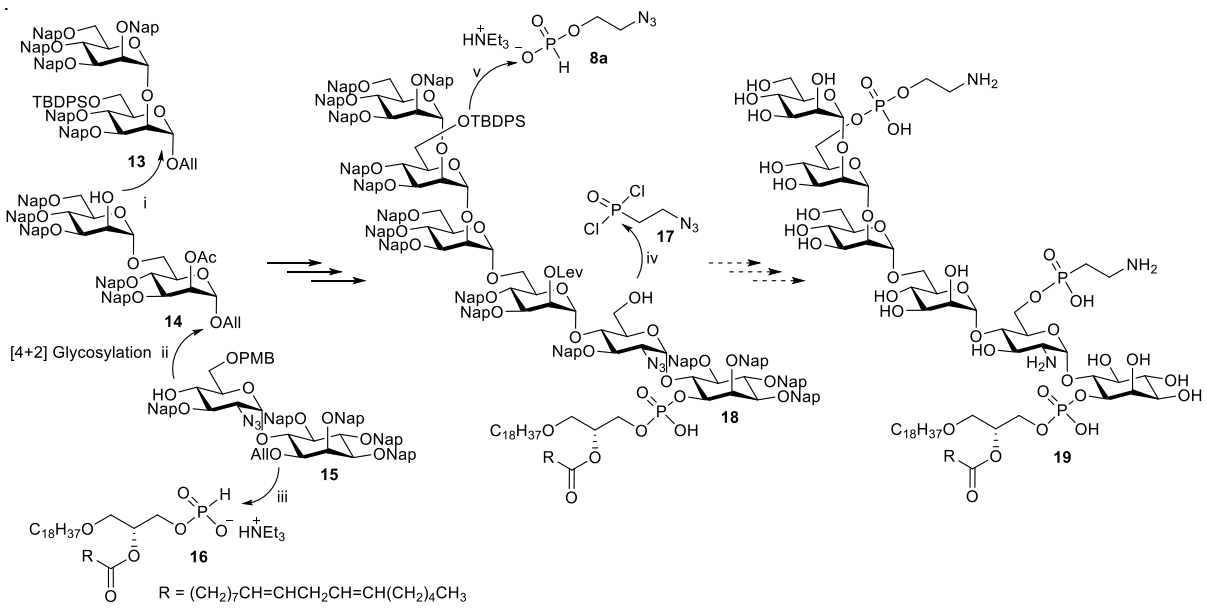

Scheme 2. Synthesis of *T. cruzi* GPI bearing unsaturated lipids. The roman numbers represent the order of the reactions.

This work established a general approach for synthesizing diverse GPIs and GPI fragments bearing unsaturated lipids. The developed strategy allows not only to produce homogeneous native GPI structures but also provides the flexibility to accommodate further modifications to give unnatural analogs. Access to these complex glycolipids will enable extensive investigation into their biological roles and expand their potential applications in biomedical research.

Zusammenfassung

Viele eukaryotische Proteine sind mittels einer Stoffklasse komplexer Glykolipide, den Glykosylphosphatidylinositol(GPI)-Ankern, an die Zellmembran gebunden. Alle GPIs bestehen aus einer Pseudopentasaccharid-Glykan-Kernstruktur, einer Phosphoethanolamin(PEtN)-Einheit und einem Phospholipid. Die GPIs werden posttranslational an den *C*-Terminus von Proteinen angeknüpft. Mängel in der Biosynthese von GPI-verankerten Proteinen (GPI-APs) führen zu einer Reihe seltener und komplizierter Erkrankungen, die mit vererbten GPI-Mangelzuständen (IGD, für das englische Acronym „inherited GPI deficiencies“) beim Menschen verbunden sind. Derzeit gibt es keine Behandlungsmöglichkeiten von Patienten, die an IGDs leiden. Zusätzlich sind die biologischen Prozesse, die aus einem GPI-Mangel resultieren, nicht ausreichend erforscht und verstanden.

Für die Entschlüsselung der biologischen Funktionen von GPIs und deren Verwendung als Werkzeuge in der chemischen Biologie werden homogenen Proben benötigt. GPIs können in der Natur aber lediglich als heterogene Mischungen gefunden werden. Es ist äußerst schwierig die einzelnen GPIs voneinander zu trennen, was es herausfordernd macht einzelne Verbindungen in reiner Form zu erhalten. Einige Strategien zur chemischen Synthese von reinen, homogenen GPIs wurden bereits veröffentlicht, jedoch stellt die Synthese von GPIs mit ungesättigten Fettsäuren nach wie vor eine große Herausforderung dar. GPIs und GPI-Fragmente mit ungesättigten Lipiden sind nicht nur wichtige Intermediate während der GPI-Biosynthese, sie kommen auch zahlreich auf der Zelloberfläche von Protozoen-Parasiten vor und zeigen eine herausragende proinflammatorische Eigenschaft. Daher ist die Entwicklung einer zuverlässigen Synthesestrategie, die Zugang zu diesen komplexen Glykolipiden schafft, von großer Bedeutung.

Das Ziel dieser Arbeit bestand darin eine allgemeine und konvergente Synthesestrategie von GPIs mit ungesättigten Lipiden zu entwickeln. In vergangenen Arbeiten hat unsere Gruppe eine Strategie entwickelt, bei der 2-Naphthylmethyl(Nap)-Ether als permanente Schutzgruppen zur Einführung ungesättigter Lipide in die Synthese von GPI-Derivaten verwendet wurden. Im Rahmen dieser Arbeit wurde der Prozess erweitert und optimiert, um biologisch aktive und strukturell vielseitige GPIs und GPI-Fragmente mit ungesättigten Fettsäureketten zugänglich zu machen.

Im ersten Teil dieser Arbeit wurden neun GPI-Fragmente, welche den Produkten der ersten Schritte der GPI-Biosynthese ähneln, entworfen und synthetisiert (Figur 1). Mit diesen Fragmenten sollte die Aktivität synthetischer GPI-Glykolipide bei der Wiederherstellung der GPI-APs-Biosynthese in GPI-AP-defizienten Zellen bestimmt werden (Kapitel 2).

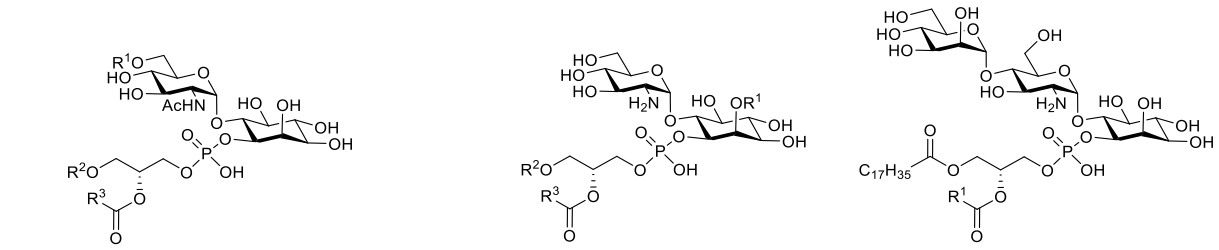

1a R^1= H, R^2= $COC_{17}H_{35}$, R^3= $(CH_2)_7CH{=}CH(CH_2)_7CH_3$
1b R^1= H, R^2= $COC_{17}H_{35}$, R^3= $C_{17}H_{35}$
1c R^1= H, R^2= $C_{18}H_{37}$, R^3= $(CH_2)_7CH{=}CH(CH_2)_7CH_3$
1d R^1= $(CH_2)_3N_3$, R^2= $COC_{17}H_{35}$, R^3= $(CH_2)_7CH{=}CH(CH_2)_7CH_3$

2a R^1= H, R^2= $COC_{17}H_{35}$, R^3= $(CH_2)_7CH{=}CH(CH_2)_7CH_3$
2b R^1= $COC_{15}H_{31}$, R^2= $COC_{17}H_{35}$, R^3= $(CH_2)_7CH{=}CH(CH_2)_7CH_3$
2c R^1= H, R^2= $COC_{17}H_{35}$, R^3= $C_{17}H_{35}$
2d R^1= H, R^2= $C_{18}H_{37}$, R^3= $(CH_2)_7CH{=}CH(CH_2)_7CH_3$

3 R^1= $(CH_2)_7CH{=}CH(CH_2)_7CH_3$

Figur 1. Entworfene GPI-Fragmente (**1** bis **3**), um die Expression von GPI-APs zu retten.

Die Glykolipide **1**, **2** und **3** wurden beginnend mit dem Aufbau der Glykan-Kernstruktur durch Verwendung von Nap-geschützten Inositol-, Glucosamin- und Mannose-Bausteinen erreicht. Die Lipide wurden gegen Ende der Synthesesequenz vor der vollständigen Entschützung der Glykolipide eingeführt. Die Abspaltung der Nap-Ether wurde optimiert und erfolgreich unter oxidativen Bedingungen mittels DDQ bewerkstelligt. Die reinen Verbindungen wurden durch Größenausschlusschromatographie und Trituration in Methanol erhalten. Die Glykolipide wurden an der Universität Osaka biologisch bewertet, bezogen auf deren Aktivität zur Rettung der GPI-AP-Produktion in GPI-AP-defizienten HEK-Zellen mit Knockout-Genen, die an den ersten vier Schritten der GPI-Biosynthese beteiligt sind.

Die biologischen Assays zeigten, dass die synthetischen Fragmente **1a**, **2a**, **2b** und **3** die GPI-Biosynthese in vitro in HEK-Zellen mit PIGA- oder PIGL-Knockout-Genen retten. Die Glykolipide zeigten eine konzentrationsabhängige Wiederherstellung der GPI-Biosynthese und waren hochaktiv in den Stufen an der zytoplasmatischen Seite des ER. Die synthetischen Verbindungen konnten jedoch nicht den Biosyntheseprozess in Zellen mit Knock-out-Genen wiederherstellen, die die Schritte auf der luminalen Seite des ER beeinflussen. Das Fehlen der Aktivität wurde auf den mangelnden Transport der Moleküle durch die ER-Membran zurückgeführt.

Eine Reihe biologischer Studien mit den Glykolipiden **1b**, **1c**, **1d**, **2c** und **2d** sind im Gange, um die Transportmechanismen für die Aufnahme von GPI-Fragmenten in die Knockout-Zellen zu bestimmen und den Einfluss der Lipide auf den Einbau der Fragmente in die GPI-Biosynthese zu bewerten. Die Verbindungen **1b** und **2c** wurden ohne ungesättigte Lipide synthetisiert, um die Rolle der Ungesättigtheit bezogen auf die Aktivität der Moleküle herauszufinden. Die Fragmente **1c** und **2d** wurden entwickelt, um die Wirkung von Alkyl- und Acylketten auf die Aktivität der Moleküle zu testen. Zusätzlich wurde das Azid-markierte Fragment **1d** synthetisiert, um den Transport der Verbindungen innerhalb der Zellen verfolgen zu können.

Zusammenfasend zeigte diese Arbeit die Anwendung einer synthetischen Strategie, um biologisch aktive GPI-Fragmente herzustellen, und deren Eignung als Hilfsmittel für zukünftige Entwicklungen glykanbasierter Behandlungen von IGDs mit Mutationen in den PIGA- und PIGL-Genen. Zusätzliche Studien sind erforderlich, um das Verständnis der Struktur-Aktivitäts-Beziehung zu verbessern, die Aktivität der Glykolipide einstellen zu können, und Methoden für die effiziente Aufnahme von GPI-Fragmenten in das ER-Lumen zu

etablieren, um Mutationen in Genen abdecken zu können, die weitere Schritte der GPI-AP-Biosynthese beeinflussen.

Im zweiten Teil dieser Arbeit wurde die Synthesestrategie für die Totalsynthese eines GPI von *Plasmodium falciparum* – dem Parasiten, der Malaria verursacht – mit ungesättigten Lipiden erweitert (Kapitel 3). Die Strategie basiert auf der Verwendung von Nap-Ether-Schutzgruppen, der globalen Entschützung, die für die Synthese der GPI-Fragmente **1**-**3** entwickelt wurde, und einer früheren Strategie, welche Zugang zu GPIs mit gesättigten Lipiden liefert. Für den Aufbau des GPI-Glykan-Kerns wurde eine Kombination aus den vollständig orthogonal geschützten Bausteine **4** bis **7** verwendet, welche die regioselektive Einführung von Phosphodiestern im späten Verlauf der Synthese ermöglichten (Schema 1). Die Mannose-Bausteine **4**, **5** und **9** wurden mit einer Allyl-Schutzgruppe am anomeren Zentrum versehen, die mittels Entschützung und anschließender Funktionalisierung in eine Trichloracetimidat-Gruppe umgewandelt wurde, um die Glykosylierungsreaktionen durchführen zu können. Die Stereoselektivität der Glykosylierungen wurde durch geeignete Reaktionsbedingungen und den Nachbargruppen-Effekt der Lävulinsäure- und Acetylester gesteuert. Dadurch wurde die gewünschte α-Konfiguration erzielt.

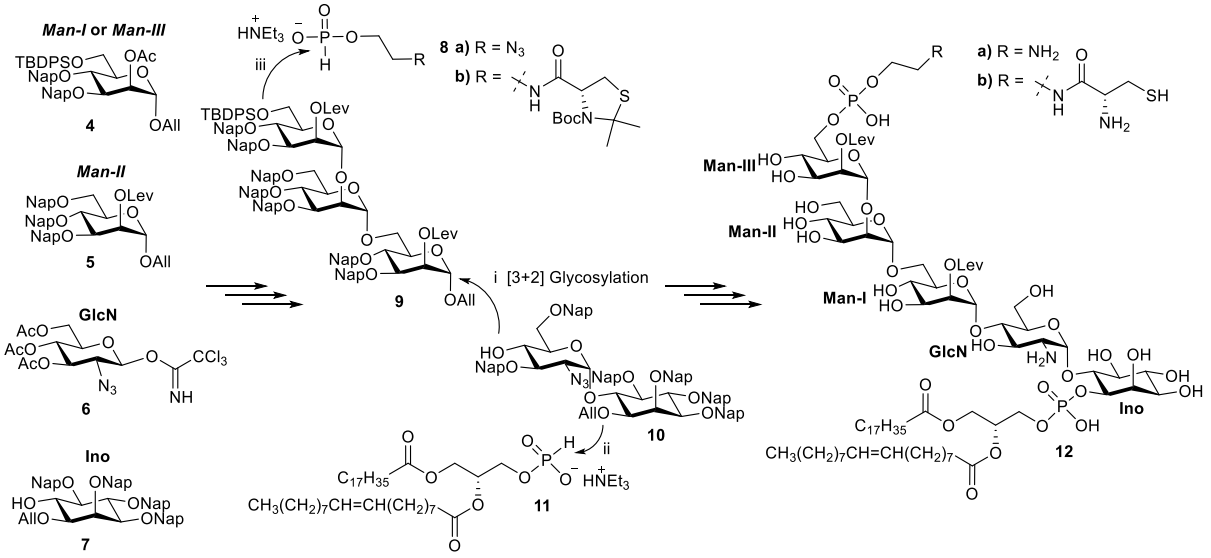

Schema 1. Totalsynthese eines GPI aus *P. falciparum* mit ungesättigten Lipiden. Die römischen Zahlen geben die Reihenfolge der Reaktionen wieder.

Nach dem Aufbau des Glykan-Kerns mittels [3+2]-Glykosylierung folgte die Anknüpfung des Phospholipids durch H-Phosphonat **11** und eine zweistufige Phosphorylierung mit H-Phosphonats **8a** zur Einführung der PEtN-Einheit. Um das gewünschte GPI **12a** aus *P. falciparum* mit ungesättigten Lipiden bereitzustellen, wurde eine dreistufige Synthesesequenz zur globalen Entschützung verwendet. Zusätzlich wurde das GPI **12b** unter Verwendung von H-Phosphonat **8b** synthetisiert, um bei der zweiten Phosphorylierung ein an das Phosphoethanolamin gebundenes, geschütztes Cystein in das Molekül einbauen zu können. Das Cystein in GPI **12b** ermöglicht die Kupplung mit einem Protein durch native chemische Ligation, wodurch ein GPI-AP erhalten werden kann.

Im dritten Teil dieser Arbeit wurde diese Strategie auf die Synthese eines GPI des Parasiten *Trypanosoma cruzi* – dem Erreger der Chagas-Krankheit – übertragen (Kapitel 4). Die Synthese benötigte eine angepasste Strategie, um zwei GPI-Glykan-Modifikationen einzubauen: Einen zusätzlichen Mannose-

Baustein, der an die Man-III-Einheit gebunden ist, und eine Aminoethylphosphonat(AEP)-Einheit, die an das Glucosamin gebunden ist (Schema 2). Das lipid-modifizierte Pseudohexasaccharid **18** wurde nach der Synthesestrategie des *P. falciparum* GPI hergestellt. Die [3+2]-Glykosylierungsstrategie wurde in diesem Fall zu einer [4+2]-Glykosylierungsstrategie geändert, um eine zusätzliche Mannose-Einheit in das Glykan einzubauen. Die Phospholipid-Einheit wurde durch Verwendung des H-Phosphonats **16** eingeführt. Durch das Anknüpfen einer PMB-Schutzgruppe an die O-6-Position des Glucosamins am Anfang der Synthese-route wurde eine zusätzliche Orthogonalitätsstufe gewonnen. Diese Position wurde im Pseudodisaccharid **15** selektiv entschützt, um die AEP-Komponente, eine charakteristische Modifikation von *T. cruzi*-GPIs, anzubringen. Die Anknüpfung der AEP-Einheit erwies sich jedoch schwieriger als erwartet. Diese Reaktion wurde an einem kleinen Modellmolekül getestet bzw. optimiert, wobei die Transformation nicht eindeutige NMR- und Massenspektren lieferte. Deshalb werden hier noch weitere Studien benötigt, um die gewünschte Modifikation erreichen und die Synthese abschließen zu können. Diese Schritte umfassen die Phosphorylierung unter Verwendung des H-Phosphonats **8a**, um das finale, geschützte *T. cruzi*-GPI zu erhalten. Dieses kann gemäß dem dreistufigen Entschützungsprotokoll, das sich bei der Synthese von GPI **12** bewährt hat, zum Zielmolekül **19** umgesetzt werden.

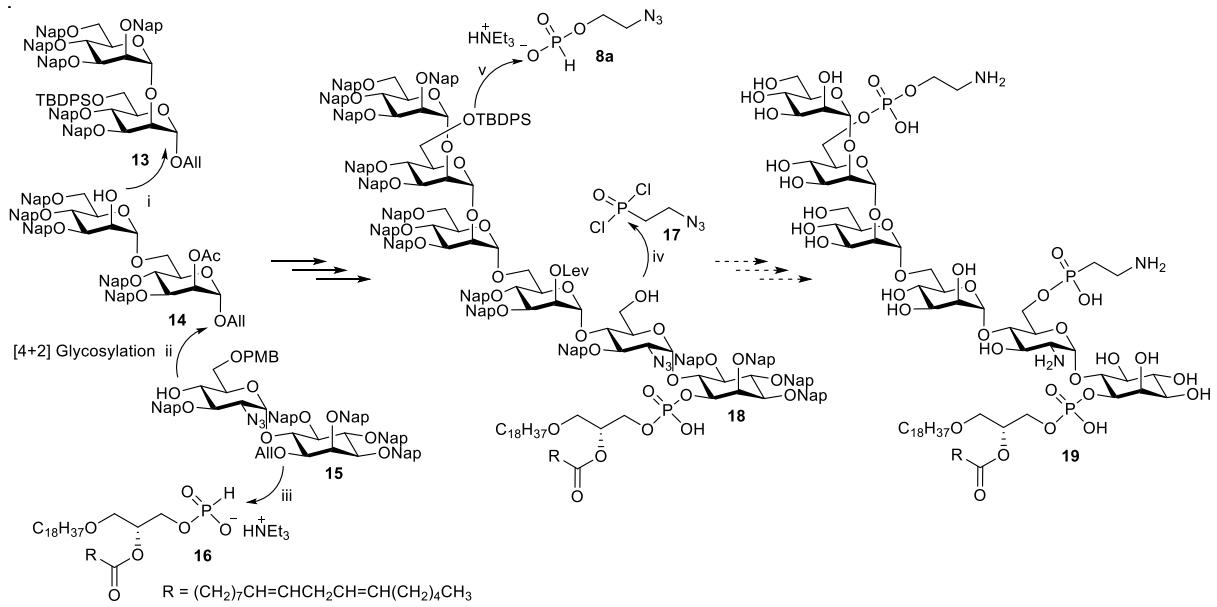

Schema 2. Synthese von *T. cruzi* GPI mit ungesättigten Lipiden. Die römischen Zahlen geben die Reihenfolge der Reaktionen wieder.

Diese Arbeit etablierte einen allgemeinen Ansatz zur Synthese verschiedener GPIs und GPI-Fragmente mit ungesättigten Lipiden. Die entwickelte Strategie ermöglicht nicht nur die Herstellung homogener nativer GPI-Strukturen, sondern bietet auch die Flexibilität weitere Modifikationen vorzunehmen, um unnatürliche Analoga herzustellen. Der Zugang zu diesen komplexen Glykolipiden ermöglicht es ihre biologische Funktion genauer zu untersuchen und ihre potenziellen Anwendungen in der biomedizinischen Forschung zu überprüfen.

List of Abbreviations

$(Bu_3Sn)_2O$	Bis(tributyltin) oxide
$[IrCOD(PPh_2Me)_2]PF_6$	(1,5-Cyclooctadiene)bis(methyldiphenylphosphine)iridium(I) Hexafluorophosphate
AAG	1-alkyl-2-acyl-*sn*-glycerophosphate
Ac	Acetyl
Ac_2O	Acetic anhydride
ACN	Acetonitrile
AcOH	Acetic acid
AEP	Aminoethylphoshonate
AllBr	Allyl bromide
$BF_3{\cdot}Et_2O$	Boron trifluoride diethyl etherate
Bn	Benzyl
Boc	*tert*-Butoxycarbonyl
Bu_2SnO	Dibutyltinoxide
Bz	Benzoyl
CAN	Ceric ammonium nitrate
Cbz	Benzyl chloroformate
CD	Circular dichroism
CER	Ceramide
$CHCl_3$	Chloroform
COSY	Correlated spectroscopy
CSA	Camphor sulfonic acid
$Cu(OTf)_2$	Copper(II) trifluoromethanesulfonate/Copper(II) triflate
DAG	1,2-Diacyl-*sn*-glycerophosphate
DBU	1,8-diazabicycloundec-7-ene
DCC	*N,N'*-Dicyclohexylcarbodiimide
DCM	Dichloromethane
DDQ	2,3-Dichloro-5,6-dicyano-1,4-benzoquinone
DIC	*N,N'*-Diisopropylcarbodiimide
DIPEA	*N,N*-Diisopropylethyl amine
DMAP	4-Dimethylaminopyridine
DMES	Dimethyl ethyl silane
DMF	Dimethylformamide
DMSO	Dimethyl sulfoxide
Dol-P-Man	Dolicholphosphatemannose
ER	Endoplasmic reticulum
Et_2O	Diethyl ether
Et_3N	Triethylamine
EtOH	Ethanol
FLAER	Fluorescent-labeled inactive toxin aerolysin
Gal	Galactose
GalNAc	N-acetylglactosamine
GIPLs	Glycoinositol phospholipids
GlcN-acylPI	Glucosamine-acylphosphatidylinositol
GlcN-PI	Glucosamine-phosphatidylinositol
GlcNAc	N-acetylglucosamine
GlcNAc-PI	N-acetylglucosamine-phosphatidylinositol
GPI-APs	Glycosylphosphatidylinositol anchored proteins
GPI	Glycosylphosphatidylinositol
GSL	Glycosphingolipid
HCl	Hydrochloric acid
HF·Py	Pyridine hydrofluoride
HSQC	Heteronuclear single quantum coherence spectroscopy
IFN- γ	Interferon-γ

IGDs	Inherited GPI deficiencies
IL	Interleukin
Ino	Inositol
KLH	Keyhole limpet hemocyanin
KO	knockout
Lev	Levulinoyl
LevOH	Levulinic acid
LPGs	Lipophosphoglycans
MALDI	Matrix-assisted laser desorption/ionization
Man	Mannose
Man-GlcN-PI	Mannosyl-glucosamine-phosphatidylinositol
MeOH	Methanol
$MeP(O)Cl_2$	Methylphosphonyl dichloride
MFI	Mean Fluorescence Intensity
MS	Mass spectrometry
N_3 GlcNAc-PI	Azido-labelled glucosamine-phosphatidylinositol
$NaBH(OAc)_3$	Sodium triacetoxyborohydride
NaOAc	Sodium acetate
NaOMe	Sodium methoxide
Nap	2-Naphthylmethyl
NCL	Native chemical ligation
NMR	Nuclear magnetic resonance
O.N.	Overnight
OVA	Ovalbumin
Pal	Palmitoyl
PEtN	Phosphoethanolamine
Pf-GPI	*Plasmodium falciparum* glycosylphosphatidylinositol
PGAP	Post glycosylphosphatidylinositol attachment to protein
PhSH	Thiophenol
PI	Phosphatidylinositol
PIG	Phosphatidylinositol Glycan
PI-PLC	Phosphoinositol-specific phospholipase C
PivCl	Pivaloyl chloride
PMB	4-Methoxybenzyl
PNH	Paroxysmal Nocturnal Hemoglobinuria
PPTS	Pyridinium *p*-toluenesulfonate
PrP^C	Cellular prion protein
PrP^{Sc}	Scrapie isoform of the prion protein
p-TsOH	*p*-Toluenesulfonic acid
Py	Pyridine
QTOF	Quadrupole time-of-flight
r.t.	Room temperature
SEM	Trimethylsilylethoxymethyl
SO_3-Py	Sulfur trioxide pyridine complex
TBAB	Tetrabutylammonium bromide
TBAF	Tetrabutylammonium fluoride
TBAI	Tetrabutylammonium iodide
TBDPS	*tert*-Butyldiphenylsilyl
TBS	*tert*-Butyldimethylsilyl
TES	Triethylsilyl
Tf_2O	Trifluoromethanesulfonic anhydride/Triflic anhydride
TFA	Trifluoroacetic acid
THF	Tetrahydrofuran
TIPS	Triisopropylsilane
TLC	Thin Layer Chromatography
TMS	Trimethylsilyl

TMSOTf	Trimethylsilyltrifluoromethanesulfonate
TNF-α	Tumor necrosis factor-alpha
TOF	Time-of-flight
TrtCl	Trityl chloride
TSSA	Trypomastigote Small Surface Antigen
VSG	Variant Surface Glycoproteins

1 Introduction

1.1 Occurrence and structural diversity of GPIs

Eukaryotes possess many essential proteins on the cell surface that participate in vital processes, such as regulation of innate immunity, cell-to-cell communication, and molecular transport. The association of proteins with cellular membranes occurs in diverse forms. Peripheral proteins loosely adhere to the membranes, and integral proteins insert into the lipid bilayer to have a tighter attachment. Among the integral proteins, transmembrane proteins establish contact with the hydrophobic part within the membrane using hydrophobic peptide fragments and cross the lipid bilayer once or multiple times. In contrast, post-translationally modified proteins use additional moieties, such as lipids, to insert into the membrane. The modification can be *via* a palmitoylation, myristoylation, or prenylation of cysteine and serine residues or glypiation, a covalent attachment of a complex glycosylphosphatidylinositol (GPI) anchor to the C-terminus of a protein forming GPI-Anchored proteins (GPI-APs).[1,2] GPI-APS are functionally diverse and include protease inhibitors, receptors, adhesive proteins, and immune system regulators.[2]

Since the discovery of the GPI anchors in the late 1970s, the research efforts of several groups led to the elucidation of the GPI structure in 1988.[3–5] These complex glycolipids consist of a glycan core, a phosphoethanolamine (PEtN) linker connecting the *C*-terminus of a protein to the glycan, and a phospholipid tail that anchors the GPI-AP to the cell membrane (Figure 1-1). The glycan core contains a *myo*-inositol, glucosamine, and three mannoses (Man-I, Man-II, and Man-III, as depicted in figure 1-1); the phospholipid moiety is heterogenous and can be a diacylglycerol, alkyl acylglycerol or ceramide with chains of different saturation degree and length ranging from 14 to 28 carbons. The GPI core is conserved and ubiquitous across eukaryotes, but the glycan can be further modified with carbohydrates, phosphates, and acyl chains depending on the specific species and cell type (Table 1-1).[6] Besides anchoring proteins to the cell surface, GPIs can be present as free GPIs on the cell surface of protozoa and mammalians. In addition, part of the GPI glycan structure is present in extracellular glycoconjugates such as glycoinositol phospholipids (GIPL) and lipophosphoglycans (LPGs), which are considered a sub-class of GPIs.[6–8]

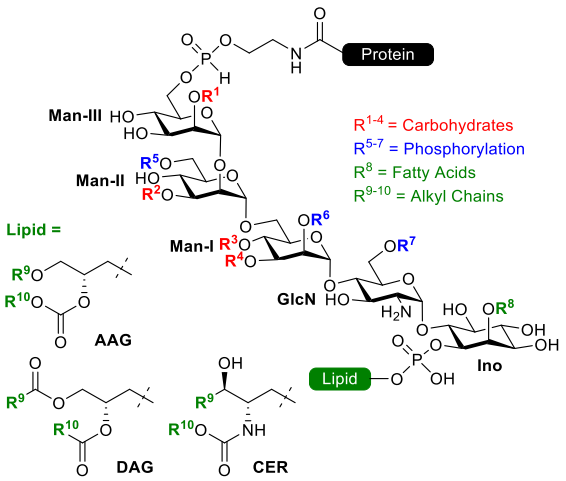

Figure 1-1. The conserved core structure of GPI with possible modifications. AAG = 1-alkyl-2-acyl-*sn*-glycerophosphate, DAG = 1,2-diacyl-*sn*-glycerophosphate, CER = Ceramide, Man = mannose, Ino = inositol, GlcN = glucosamine.

The most common carbohydrate modification in GPIs incorporates an additional mannose at the nonreducing end of the glycan core. Different oligosaccharide branches at the O-4 and O-3 positions of Man-III result in the most structural diversity of GPIs (Table 1-1). A β-galactose residue can also be present at the O-3 position of Man-II, and a fatty acid chain—usually in mammals—can be attached to the O-2 position of inositol. Additional phosphoethanolamines have been detected at the O-6 position of Man-II and the O-2 position of Man-I; the latter is a conserved modification in mammalian GPIs.[6,9] These additional phosphoethanolamines have not been found in protozoan or yeast GPIs, suggesting that this modification might be specific for metazoan eukaryotes.[3,10] Interestingly, a (2-aminoethyl)phosphonate unit at the O-6 position of glucosamine is a parasite-specific modification only found in GPIs of *Trypanosoma cruzi*.[11] Regarding the lipid moiety, alkyl acylglycerol, and diacylglycerol with two saturated fatty acids are the major components for mammalian GPIs, with a small portion containing one unsaturation in the *sn*2-linked chain.[12] In contrast, ceramide is the most common lipid in the GPI anchors of yeast and *Dictyostelium discoideum*. Some parasites such as *Trypanosoma cruzi* and *Plasmodium falciparum* present a significant concentration of GPIs bearing unsaturated lipids on their cell surface.[3,11,13]

Table 1-1. Selected examples of the GPI structural diversity.[6]

Origin	R^1	R^2	R^3	R^4	R^5	R^6	R^7	R^8	Lipid
***T. brucei* VSG 121**	H	Galβ	H	$Gal_{2\text{-}4}α$	H	H	H	H	DAG
***T. congolense* VSG**	H	H	Gal-Glc-NAcβ	H	H	H	H	H	DAG
***T. cruzi* NETNES**	Manα	H	H	H	H	H	AEP	H	AAG
A. fumigatus	Man1-2α	H	H	H	H	H	H	H	CER
P. falciparum	±Manα	H	H	H	H	H	H	Acyl	DAG
T. gondii	H	H	±Glc-Gal-NAcβ	H	H	H	H	H	DAG
Mouse muscle NCAM	±Manα	H	±GalNAcβ	H	H	PEtN	H	H	n.d.
Human erythrocyte AChe	H	H	H	H	± PEtN	PEtN	H	Pal.	AAG
Human CD52	±Manα	H	H	H	H	PEtN	H	±Pal.	DAG
Human erythrocyte CD59	H	H	±GalNAcβ	H	PEtN	PEtN	H	Pal.	AAG

Captions ($R^{1\text{-}8}$ and Lipid correspond those presented in figure 1-1). Man = mannose, Gal = galactose, GalNac = N-acetyl galactosamine, PEtN = phosphoethanolamine, AEP = aminoethylphoshonate, Pal. = palmitoyl, DAG = diacylglycerol, AAG = alkyl acylglycerol, CER = ceramide, n.d. = not determined.

1.2 Biological function of GPIs

Despite the complexity and high occurrence of GPIs in nature, as protein anchors or free glycolipids, the only well-established biological function of GPIs is the anchoring of proteins to the cell surface. GPIs and GPI-anchored proteins have also been associated with signal transduction events, cell-cell communication, protein trafficking, immune system regulation during infections, the pathophysiology of parasites, among others.[10] Unique properties of the GPI-APs are linked to the GPI glycolipid. The hydrophobic lipid tail of the GPI allows the protein to interact with membrane microdomains known as lipid rafts, which are enriched with glycosphingolipids, phospholipids, cholesterol, and lipidated proteins.[10,14] Due to the tight packing of its components, lipid rafts are believed to be less fluid than the rest of the membrane, having unique physicochemical properties that allow them to serve as platforms for several processes, such as vesicular trafficking and signal transduction events.[10] For instance, the GPI-AP CD14, which is involved in the innate immune response of mononuclear phagocytes, has been associated with lipid rafts. The lipid raft might provide the dynamic microenvironment needed for the CD14-dependent clustering of some receptors involved in inflammation and atherogenesis.[15]

The ability of GPIs to associate the protein with lipid rafts also facilitates the participation of the protein in signal transduction events. Even if the GPI anchor doesn't span the cell membrane, its physical interaction with transmembrane proteins involved in intracellular signaling might allow the GPI-mediated activation signal to be transmitted across the membrane to the cell's interior.[16] Signal transduction proteins that are thought to interact with GPI-APs include protein tyrosine kinases, integrins, and heterotrimeric GTP-binding proteins.[10]

Contrary to transmembrane proteins, the insertion of GPI-APs to the cell membrane using their phospholipid moiety doesn't extend through the whole lipid bilayer. This results in a relatively transient association that allows GPI-APs to be transferred from one membrane to another.[17,18] Protein transfer between cells might aid the regulation of their surface expression without depending on their gene expression in a given cell.[17] More than 40 years ago, before the elucidation of the GPI structure, the human GPI-AP DAF was already inserted onto sheep erythrocytes.[19] Since then, many GPI-APs have been translocated into natural and artificial membranes.[17,20–24] Interestingly, exogenous GPI-AP inserted into different cells retain their original function. The ability of GPI-APs to undergo intermembrane transfer has been observed in both *in vitro* and *in vivo* studies. The exact mechanism of the process is unknown but relies on the presence of the full-length GPI anchor.[17] The intercellular transferability of GPI-APs has been used to regulate host immune responses.[25] For example, the immunogenicity of tumor cells was increased after the insertion of GPI-modified versions of the B7-1 and B7-2 proteins, which induce co-stimulatory signals responsible for cytotoxic T cell activation. Mice immunized with the EG7 tumor cell line expressing the GPI-anchored proteins showed protection in challenge experiments with live wild-type tumor cells.[26,27] These experiments unravel the potential of exogenously added GPI-Anchored proteins to act as therapeutic agents.

GPI anchors may influence the protein conformation and provide the protein with hydrophobicity that enhances interaction with cellular membranes. Circular dichroism (DC) spectra and antibody binding experiments demonstrated that the conformation of the human GPI-AP Thy-1 changed after delipidation with phospholipases C or D.[28] Moreover, other studies suggest a role of protein-GPI interactions in modulating the functions of the GPI-APs. The catalytic activity and immunoreactivity of GPI-APs are altered after treatment with phospholipases or if the GPI-AP didn't undergo correct fatty acid remodeling during their biosynthesis.[29–31]

GPI anchors are also associated with prion diseases, which are fatal progressive neurodegenerative disorders affecting animals and humans. These diseases can propagate from host to host and are caused by an infectious protein known as a prion.[32] The prion protein (PrP^C) is a GPI-AP on the neuronal surface. A misfolding of the PrP^C produces its pathogenic isoform known as PrP

scrapie (PrP^{Sc}), which can transmit the misfolded shape onto normal variants of the same protein and leads to brain damage and the characteristic symptoms of the prion disease.[33] Numerous studies indicate that the prion protein glypiation promotes the formation and intercellular transfer of protein aggregates, which increases the transmission and pathogenetic potential of prion diseases compared to other protein misfolding diseases; however, these results are a subject of controversy.[25,33,34]

Many protozoan parasites express more GPI-APs on their cell surface than higher eukaryotes.[35] Besides anchoring proteins, parasitic GPIs are important for virulence and are directly involved in the host's immune regulation during infections.[36] For example, the GPIs from the malarial parasite *P. falciparum*, the Chaga's disease parasite *T. cruzi,* and the sleeping sickness' parasite *T. brucei* act as pro-inflammatory agents during eukaryotic parasitism.[11,13,37] Moreover, some parasitic GPIs are packed densely to form a glycocalyx, a layer that allows the parasite to evade the host immune system and interact with its external environment.[38]

GPI-APs can be released from the cell membrane by phospholipases; thus, it has been suggested that cells use the GPI anchor as a site of degradation to regulate GPI-APs by selectively secreting them at a given time.[39] Other remarkable potential functions that have been attributed to the GPI anchors include the assistance of cellular communication by providing the proteins with greater mobility on the cell surface and the sorting of proteins to the apical and basolateral domains of polarized epithelial cells by acting as apical targeting signals; nonetheless, these affirmations have been questioned.[40–42]

1.3 Biosynthesis of GPI-Anchors

Glypiation is one of the most complex post-translational modifications of proteins that presents a high structural diversity among different species and tissues. GPIs are assembled in the endoplasmic reticulum (ER) by a membrane-bound sequential addition of monosaccharides, phosphoethanolamine, and acyl chain to phosphatidyl inositol (Figure 1-2). The process starts on the cytoplasmic side of the ER and finishes on the luminal side after the flipping of one of the early intermediates through the membrane.

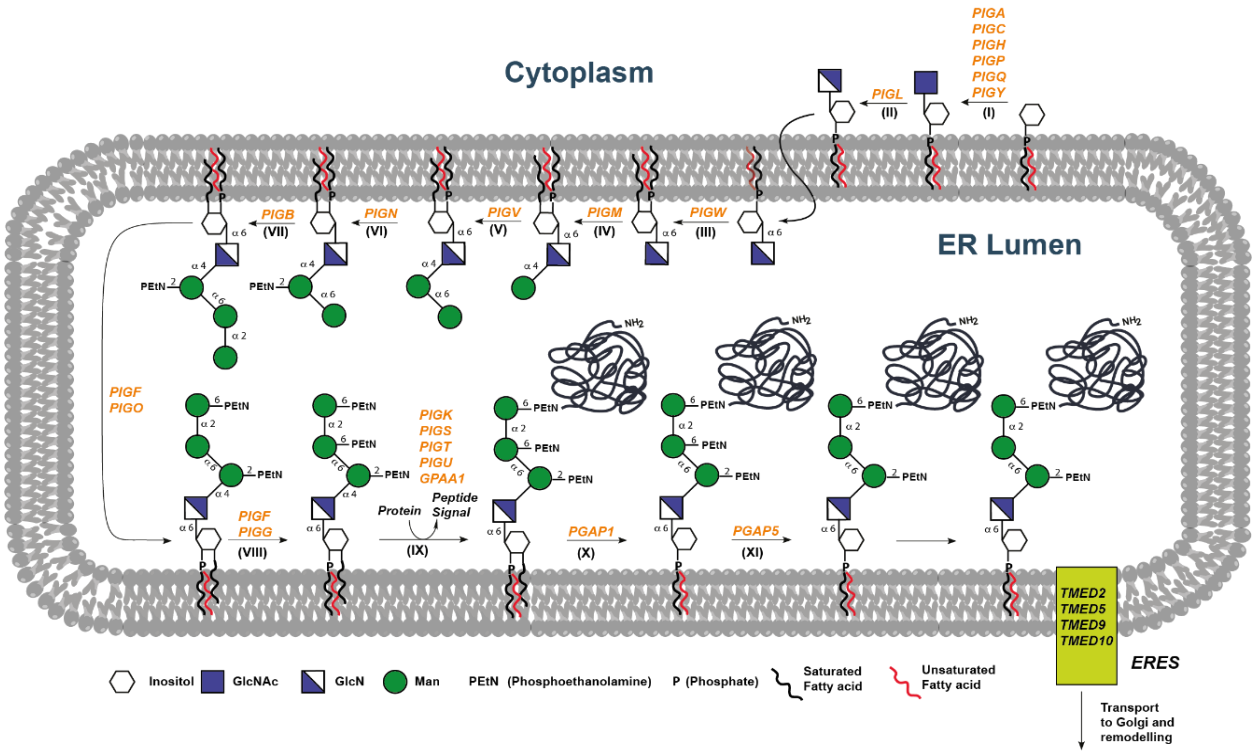

Figure 1-2. Schematic representation of GPI-AP biosynthesis. (Figure by Daniel Varón Silva).

The GPI-AP biosynthesis can be divided into three parts: synthesis of the GPI anchor, attachment to the protein, and further remodeling of the glycan and lipid moieties. In mammalian cells, the GPI synthesis starts on the cytoplasmic side of the ER with the transfer of glucosamine (GlcNAc) to phosphatidyl inositol (PI) to generate the pseudodisaccharide GlcNAc-PI. This step is mediated by a multi-subunit GPI-GlcNAc transferase comprising six proteins (PIGA, PIGC, PIGH, PIGP, PIGQ, and PIGY). In this complex, PIGA provides catalytic activity, and the roles of the other subunits are unclear. In the second step, the GlcNAc-PI is deacetylated by the mammalian PIGL enzyme to form GlcN-PI, which is then translocated across the ER membrane into the luminal side by an unknown mechanism. Next, an acyl chain—usually palmitic acid—is transferred from Acyl-CoA to the O-2 position of the inositol unit of GlcN-PI furnishing GlcN-AcylPI. This intermediate should also undergo lipid remodeling in this step. The precursor GlcN-PI has the same lipid composition as the endogenous PI, which is predominantly stearoyl(*sn*1)-arachidonoyl(*sn*2), while in the resulting GlcN-AcylPI the lipid composition is replaced by an alkyl(*sn*1)-acyl(*sn*2), which is predominant in most mammalian GPIs.[6,12,43–46]

In the following two biosynthesis steps, the GPI glycan is elongated with two mannoses by the action of the PIGM and PIGV enzymes, generating the Man-Man-GlcN-(acyl)PI structure. A PEtN side branch is next added to the O-2 position of Man-I of this intermediate, and the third mannose unit is incorporated by the PIGB enzyme. All three mannoses are transferred from dolicholphosphatemannose (Dol-P-Man) as a substrate donor. Finally, two additional PEtN units

are added to the O-6 position of Man-III and Man-II, giving the GPI anchor ready for attachment to a protein.[6,12,43–46]

Proteins that will be GPI-anchored contain an *N*-terminal signal peptide for translocation across the ER membrane and a *C*-terminal signal peptide for GPI attachment. Once the protein is on the luminal side of the ER, the *N*-terminal signal peptide is removed, and a GPI-transamidase complex including five proteins (PIG-K, PIG-S, PIG-T, PIG-U, and GPAA1) recognizes and cleaves the signal peptide and transfers the GPI precursor in a simultaneous process.[6,12,43–46]

Upon generation of the GPI-AP, the acyl chain attached to the inositol unit is often removed through the action of the deacylase PGAP1, and the side chain PEtN from Man-II is cleaved by PGAP5. Finally, the GPI-AP is transported to the Golgi *via* secretory vesicles, where it undergoes remodeling of the glycan and lipid moieties.[6,46] The high structural diversity of the GPI anchors results from these additional enzymatic modifications in the Golgi. Little is known about GPI remodeling, but it depends on the glycosylation machinery of the cell and the protein attached to the anchor.[8]

In mammals, GPI-AP biosynthesis requires several proteins and enzymes, which are named after the genes encoding them. Currently, 27 genes coding for enzymes responsible for most transformations in the GPI biosynthesis have been identified. [45,47] From these, 22 genes are called Phosphatidyl Inositol Glycan (PIG) genes and are involved in the assembly and protein attachment of GPIs. The other five genes are known as Post GPI Attachment to Protein (PGAP) and are responsible for the lipid and glycan remodeling of GPI-APs.[12,45] GPI-APs are involved in many pathways and developmental events; therefore, defects in the genes compromising their biosynthesis result in a variety of genetic disorders that affected individuals manifest in a wide spectrum of features.[48] These genetic disorders will be discussed in detail in Chapter 2.

It is important to remark that the biosynthetic pathway of GPI-AP in mammals exhibits several distinct features compared to biosynthesis in parasites. For example, acylation of the inositol unit takes place in *T. brucei* after incorporating the first mannose into the glycan chain, and only the PEtN for protein attachment is attached to the structure.[6] The structural differences between the intermediates of the GPI biosynthesis in mammals and parasites have been considered for developing antiparasitic treatments.[6]

1.4 Chemical Synthesis of GPI-Anchors

The structural complexity of GPIs suggests a higher functional capacity beyond acting as membrane anchors for proteins. However, there is relatively limited knowledge about the biological functions of GPIs that results from the limited access to a pure and homogeneous material. The isolation of GPIs from natural sources is challenging because of their heterogeneity and amphiphilic character. Thus, the biological information obtained from isolated heterogenic GPI samples has been contradictory or controversial in a few cases. There is a high interest in getting pure homogeneous GPIs using chemical synthesis to overcome the challenging isolation and accurately elucidate and exploit the biological functions of these complex structures.
Several groups have developed clever strategies for synthesizing structurally diverse GPIs and GPI derivatives. These strategies rely on the design of orthogonally protected building blocks and the selection of suitable reaction conditions and activation methods to achieve the desired regio- and stereoselectivity required for the assembly of the glycan core and the introduction of the phosphate moieties.[49–59] The challenging incorporation of carbohydrate, lipid, and phosphate chemistry is aggravated by the critical selection of permanent protecting groups which determine the global deprotection conditions. The global deprotection of these complex glycolipids is problematic not only because the conditions have to be compatible with the different functionalities present in the molecule but also because of the poor solubility profiles and amphiphilic character of the native GPIs.[9]

In most of the reported synthetic routes to GPIs, the glycan core is assembled first and the phosphorylations are performed at a late stage, avoiding the phosphate removal and having more flexibility during the construction of the glycan.[6,8,9,60] Generally, the strategies to obtain GPI structures can be divided into two categories: linear and convergent. In a linear strategy, the glycan core is built from individual monosaccharides stepwise, but the yield quickly drops after each reaction step (Figure 1-3a). In a convergent strategy, bigger fragments of the GPI are assembled separately and coupled in later stages of the synthesis to build the GPI core structure (Figure 1-3b). Most published routes are linear due to the more complex protection strategies required for convergent approaches. However, convergent synthetic strategies are preferable not only to improve efficiency by reducing the number of transformations on advanced intermediates but also to provide high flexibility to introduce additional functionalities to the final structure.[9,59]

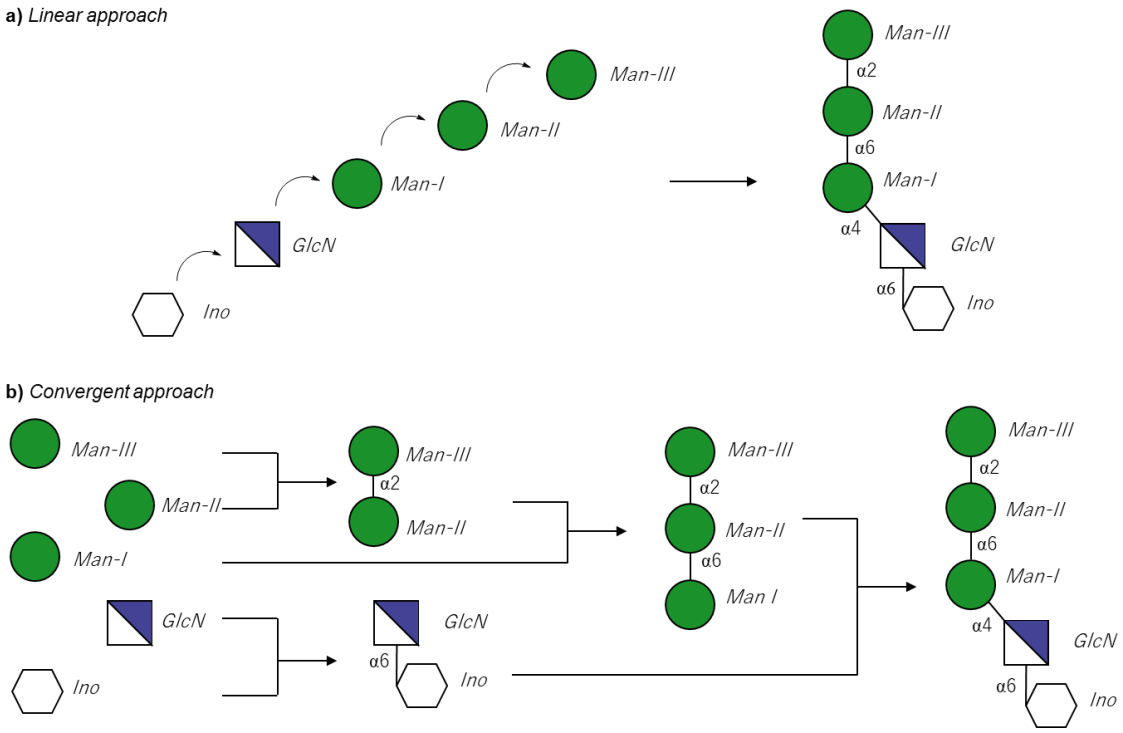

Figure 1-3. Schematic representation for the synthesis of a GPI glycan core: a) A linear strategy; b) A convergent strategy

1.4.1 Linear Synthesis of GPIs

The first linear synthesis of a GPI glycan was reported by the konradson group in 2002 (Scheme 1-1).[61] In this work, the inositol unit of the pseudodisaccharide **1-4** was prepared using the 1,2-L-camphanyliden acetal of racemic *myo*-inositol **1-7**. The camphor acetal served as a chiral auxiliary and moderated the individual reactivity of the remaining hydroxyl groups, making possible the regioselective introduction of protecting groups into the inositol.[62] The glycan core of the GPI **1-5** was assembled after a linear five-step glycosylation sequence of the pseudodisaccharide **1-4** with the three different ethyl thiomannoside donors **1-1** to **1-3**, which were obtained from the common building block **1-6**. After removal of the orthogonal temporary protecting groups of the trimanno-side component in **1-5**, phosphates were incorporated into the O-2 position of Man-I and Man-III, and into the O-6 position of Man-II and Man-III. Next, removal of the camphor acetal afforded a 1,2-inositol diol, which was converted to a 1,2-cyclic phosphate. Finally, one-step deprotection using sodium in liquid ammonia afforded the target tetraphosphorylated GPI core structure **1-8**.

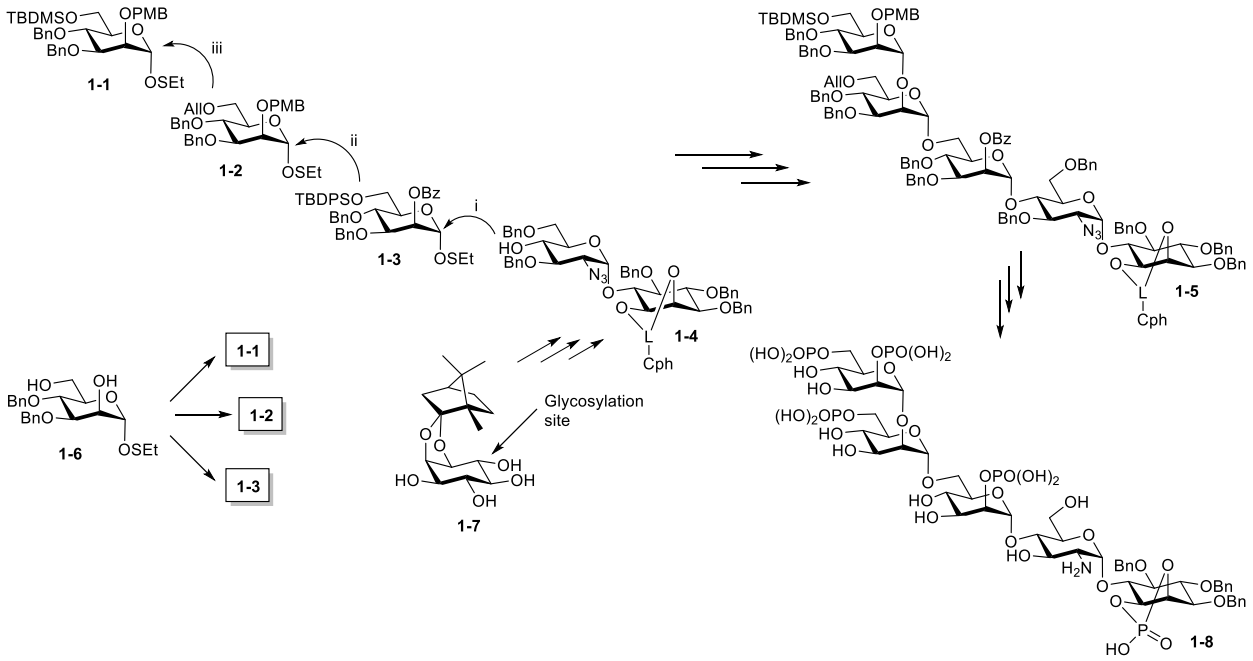

Scheme 1-1. konradson-Oscarson linear synthesis of a polyphosphorylated GPI anchor core structure.[61] The roman numbers represent the order of the glycosidic bond formation to build the glycan core **1-5**.

After this work, many other linear strategies were reported. Among them, the route for the total synthesis of a fully lipidated GPI anchor of *P. falciparum* presented by Fraser-Raid in 2004 constituted a hallmark for GPI chemical synthesis.[56,63] In their work, they developed a new methodology for the preparation of the optically pure and differentially protected *myo*-inositol building block, involving oxidation of α-D-methylglucoside, a Ferrier type II rearrangement to convert the heterocycle to a carbocycle, and a stereoselective reduction of the resulting ketone (Scheme 1-2a). This strategy was later modified by the Seeberger group (Scheme 1-2b), and it is now a standard alternative for preparing the inositol unit during the synthesis of GPI structures.[64]

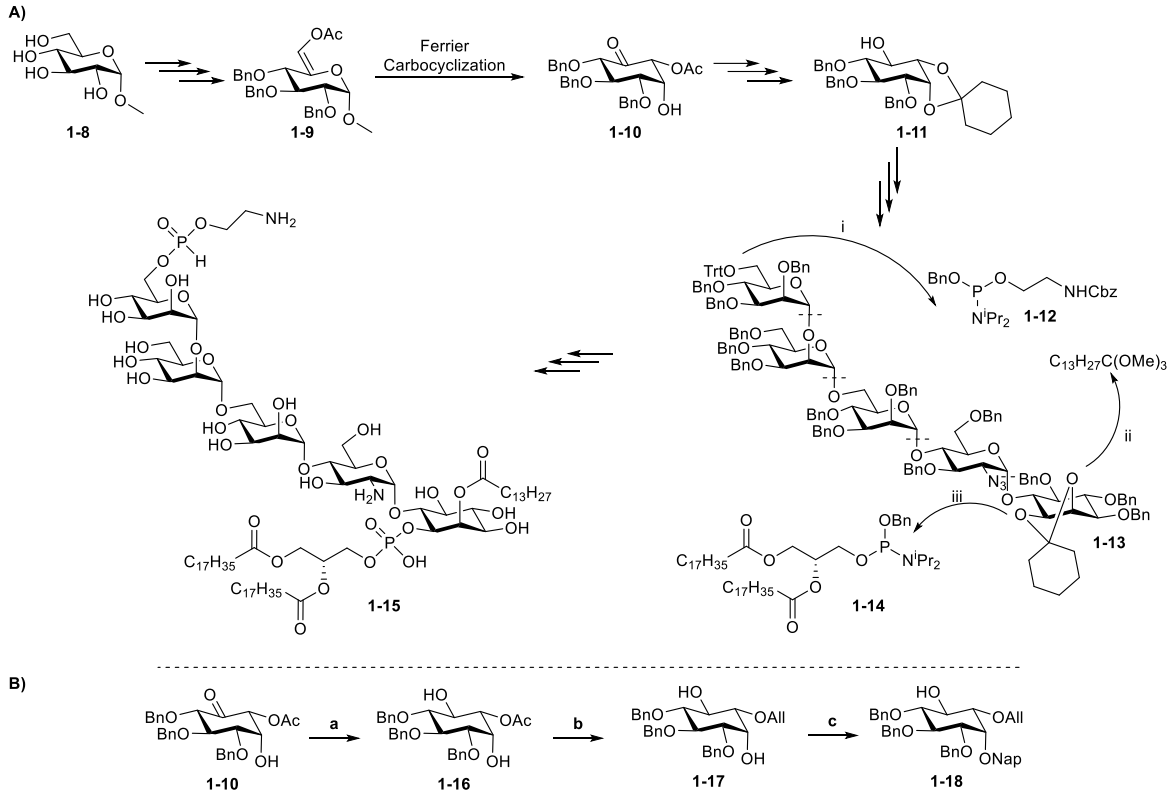

Scheme 1-2. A) Fraser-Reid linear synthesis of a *P. falciparum* GPI anchor using a new *de novo* synthesis of an optically pure *myo*-inositol derivative.[56,63] The roman numbers represent the order of the reactions. B) Modification of the *de novo* synthesis of the *myo*-inositol building block by the Seeberger group.[64] *Reagents and conditions*: a) $NaBH(OAc)_3$, AcOH, ACN, 79%; b) i. CH_2=CHOEt, PPTS, DCM; ii. NaOMe, MeOH; iii. AllBr, NaH, TBAB, DMF; iv. 2 M aq HCl, THF, 50 °C; c) NapBr, NaH, TBAB, DMF, -20 °C to r.t., 65% (2 steps).

The assembly of the pseudopentasaccharide core **1-13** was completed using n-pentenyl-ortho-ester glycosyl donors and ytterbium (III) triflate and NIS as promotors to obtain the desired α-selectivity**.** The phosphoethanolamine unit was attached using phosphoramidite **1-12** (Scheme 1-2a). The selective introduction of the additional lipid (myristoyl) moiety at the axial O-2 position at the inositol unit was followed by the late-stage phosphorylation with the phosphoramidite **1-14**. In the end, global deprotection by hydrogenolysis (first in an organic solvent followed by the addition of water) gave the desired *P. falciparum* GPI anchor **1-15** in 87% yield.

A combined linear-convergent synthesis of the phosphorylated pseudohexasaccharide of a GPI anchor of *P. falciparum* **1-28** was reported by the Seeberger group.[65] A hallmark of this strategy was the implementation of automated solid-phase synthesis for the linear preparation of tetra-mannoside **1-24**. The automated synthesis was carried out on an automated oligosaccharide synthesizer using octenediol functionalized Merrifield resin **1-23** and trichloroacetimidate mannosyl donors. Each chain elongation cycle was followed by the acetyl group removal with NaOMe. After

cleavage of the octendiol linker with Grubbs' catalyst, the n-pentenyl tetramannoside **1-23** was obtained and converted to the corresponding glycosyl trichloracetimidate donor**.** The challenging α-linkage between glucosamine and inositol impedes a fully automated approach. Therefore, the pseudodisaccharide **1-25** was prepared in solution. The glycan core **1-27** was obtained by coupling the tetramannoside trichloracetimidate donor and the pseudodisaccharide acceptor through a [4+2] glycosylation strategy. The 1,2-diol in the myo-inositol moiety was deprotected and cyclophosphorylated with $MeP(O)Cl_2$, followed by O-demethylation with aqueous HCl. After O-desilylation of Man-III, the phosphoethanolamine unit was introduced *via* 1H-tetrazole-catalyzed coupling with the phosphoramidite **1-26**, oxidation with *tert*-butyl hydroperoxide and removal of the cyanoethyl ether with DBU. Global deprotection was achieved by Birch reduction, furnishing the phosphorylated *P. falciparum* GPI anchor **1-28**.

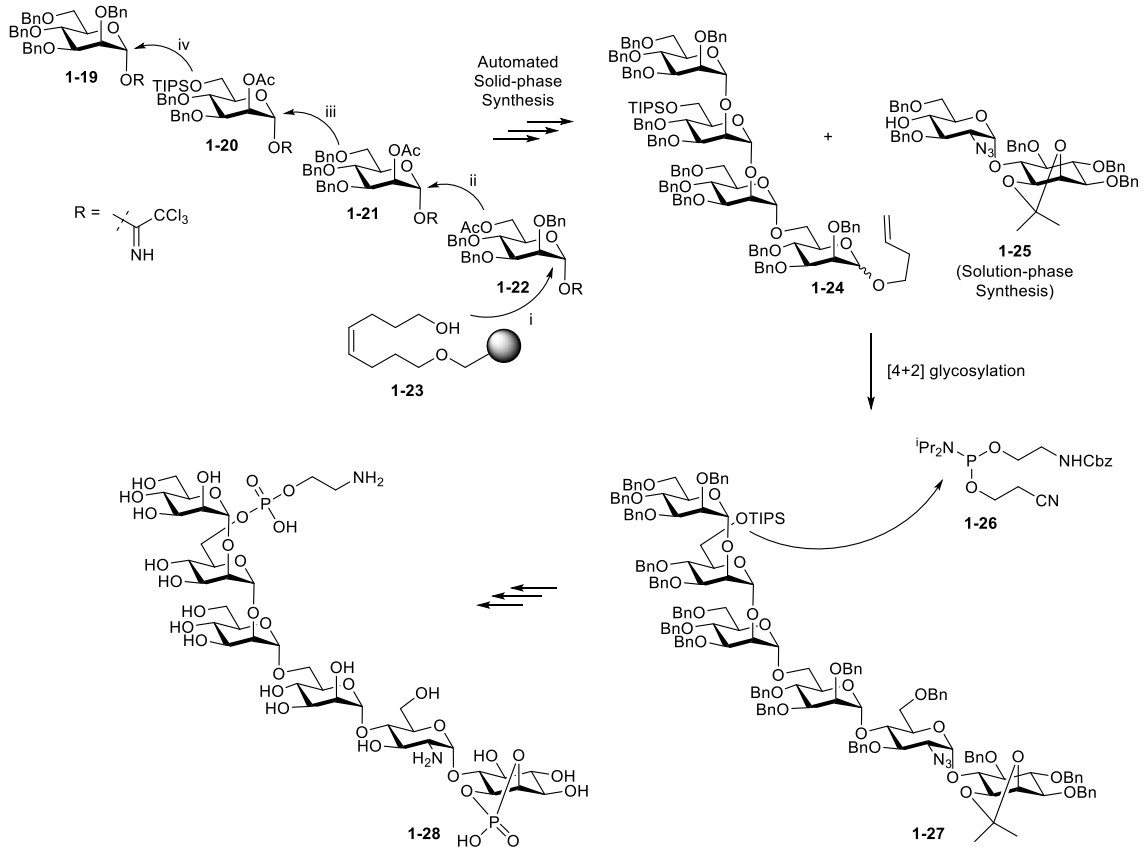

Scheme 1-3. Seeberger's group combined linear-convergent synthesis of a phosphorylated *P. falciparum* GPI glycan incorporating automated solid-phase oligosaccharide synthesis.[65] The roman numbers represent the order of the glycosidic bond formation to build the tetramannoside **1-24**.

Reichardt and Martin-Lomas also used manual solid phase synthesis to assemble the glycan core of a GPI anchor using trichloroacetimidate donors.[66] For this purpose, the O-2 position of the inositol unit of the pseudodisaccharide component was attached to the solid support, and it was

further elongated by the stepwise glycosylation reactions with orthogonally protected mannosyl trichloroacetimidates.

1.4.2 Convergent Synthesis of GPIs

A convergent strategy was used for the first total synthesis of a GPI anchor, reported by Murakata and Ogawa in the early 1990s.[49,67,68] In this work, the glycan core of a *T. brucei* GPI anchor was built first, and the incorporation of the phosphate residues was performed in a later stage to enable the synthesis of analogs with variations in the lipid composition (Scheme 1-4). The synthesis started with the preparation of an optically active inositol derivative **1-33** from the racemic diol **1-37**. The inositol was coupled to the disaccharide **1-32** to obtain a pseudotrisaccharide, which was elongated using the digalactosyl fluoride **1-29**. Further reactions with the mannosyl chloride **1-31** and mannosyl fluoride **1-30** furnished the key pseudoheptasaccharide **1-35**, equipped with two orthogonal protecting groups (Ac and PMB). A sequential introduction of the phospholipid and phosphoethanolamine units used the H-phosphonates **1-36** and **1-34**, respectively. Finally, the removal of the benzyl ethers used as permanent protecting groups and reduction of the azide was achieved by hydrogenolysis, furnishing the desired native GPI of *T. Brucei*.

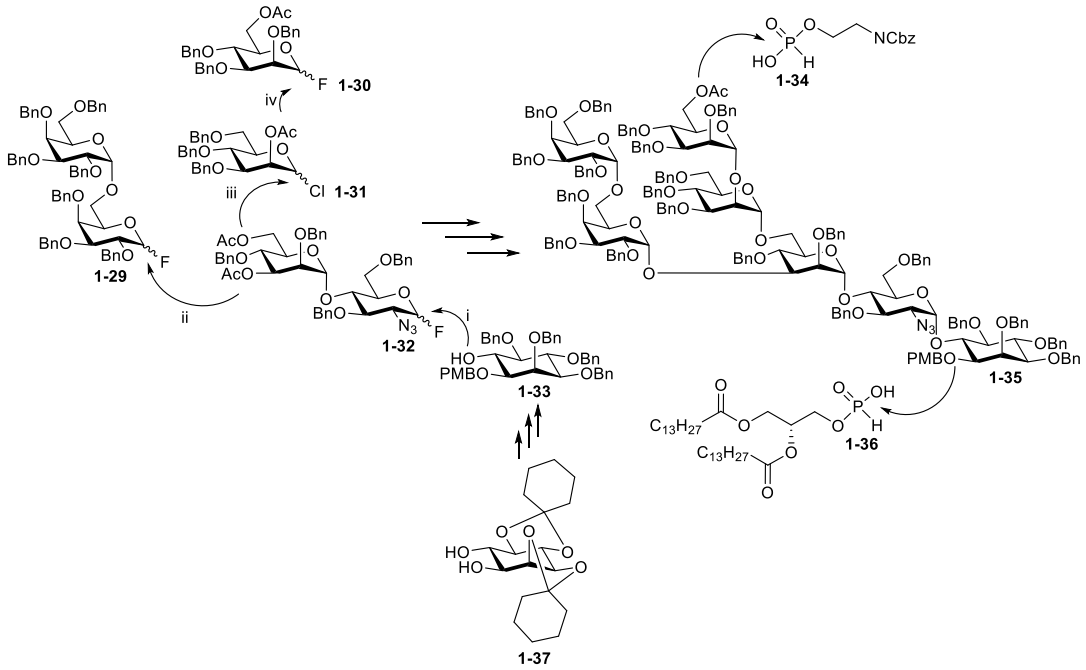

Scheme 1-4. Ogawa's synthesis of the *T. brucei* GPI anchor.[49,67,68] The roman numbers represent the order of the glycosidic bond formation to build the glycan core **1-35**.

In the next decades, Ogawa's synthetic convergent strategy was adapted and modified by many authors for the target-oriented synthesis of different GPI anchors.[9,50,54,69] However, there was still

a lack of a general route that could enable the efficient preparation of a wide range of structurally varied GPI anchors. To address this, our group published the first general and convergent synthesis of diverse GPIs in 2013 (Scheme 1-5), which relied on a set of interchangeable orthogonally protected building blocks **1-40** to **1-42** that enabled the efficient assemble of the glycan core **1-39** after a [X+2] glycosylation strategy, where X represents the length of the oligosaccharide chain that is coupled to the pseudodisaccharide **1-43**.[58] In this case, *de novo* synthesis of the inositol unit started from α-D-methylglucoside following the methodology developed by Fraser-Raid and modified by the Seeberger group. As in most synthetic routes, phosphorylations were done at the late stage of the synthesis, and benzyl ethers were employed as permanent protecting groups, which were removed under reductive conditions.[6,58]

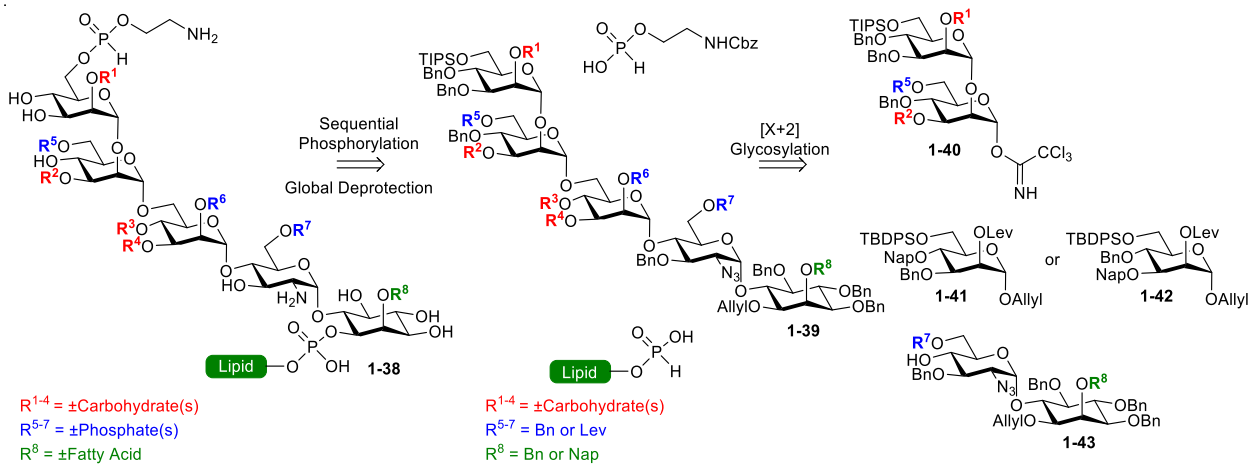

Scheme 1-5. Retrosynthetic analysis for the general and convergent GPI synthesis developed by the Varon Silva group.[58]

The disconnections during the design of this synthetic route and the protection pattern of the building blocks were selected based on the naturally occurring substitution patterns of the preserved GPIs pseudopentasaccharide core. The selected protecting groups would also assist the stereoselectivity control during the glycosylation through neighboring group participation. Four levels of orthogonality were achieved by incorporating allyl ethers, levulinoyl esters, silyl ethers, and naphthylmethyl ethers as protecting groups. The orthogonality provided the flexibility to accommodate other moieties to the structure such as additional oligosaccharide branches, phosphates, and fatty acids. The reaction conditions were readily transferable to other syntheses and allowed the preparation of structurally different GPIs (GPI of *T. gondii*, the low molecular weight antigen of *T. gondii*, the GPI anchor of *T. congolense* VSG and the GPI of *T. brucei* VSG 117), thereby achieving maximum structural diversity from a minimum number of common building blocks.

1.4.3 Synthesis of GPIs bearing unsaturated lipids

The general and convergent strategy developed by our group represented a great advance for preparing natural and unnatural GPI structures. However, the need for reductive conditions to remove the benzyl ethers commonly used as permanent protecting groups precludes its application for synthesizing GPIs bearing unsaturated lipids or other reductive-sensitive groups such as azides and alkynes. GPIs containing unsaturated lipids are present on the cell surface of human cells and some parasites. Parasites such as *Trypanosoma cruzi*, the causing agent of Chagas' disease, and *Plasmodium falciparum* which causes Malaria present a significant concentration of GPIs bearing unsaturated lipids on their cell surface.[3,11,13] Particularly, the GPIs of *T. cruzi* exhibit proinflammatory activities comparable to bacterial lipopolysaccharides, making them one of the most potent proinflammatory agents known (for more details, see chapter 4).[70] The immunoreactivity of these GPIs has been associated with lipid unsaturations; nevertheless, to accurately determine the structure-activity relationship of these structures, pure structurally well-defined samples are required.

To obtain GPIs with unsaturated lipids, in 2006 Nikolaev's group proposed a convergent strategy using base-labile (benzoic esters) and acid-labile (acetals and N-Boc) groups for O,N permanent protection for the synthesis of two GPI anchors of *T. cruzi* (Scheme 1-6).[71] As in previous strategies, various silyl ethers were employed as orthogonal protecting groups at the phosphorylation sites. The pseudohexasaccharide core **1-48** of the GPIs was assembled via a [4+2] glycosylation between the tetramannosyl trichloroacetimidate donor **1-43** (built in a linear approach) and the pseudodisaccharide acceptor **1-44**. The (2-aminoethyl)phosphonate unit at the O-6 position of glucosamine, a *T. cruzi*-specific modification,[11] was introduced using the 2-azidoethylphosphonodichloridate **1-47** with 1H-tetrazole activation. The azido groups were reduced and re-protected as *tert*-butyl carbamates. The phosphoethanolamine incorporation required the N-Boc protected H-phosphonate **1-46** and two different triethylammonium 2-acyl-1-alkyl-*sn*-glycero-3-H-phosphonates **1-45a** and **1-45b** were used for the attachment of the phospholipid, one containing an oleic chain at the *sn*-2 position and the other with a linoleic chain instead.

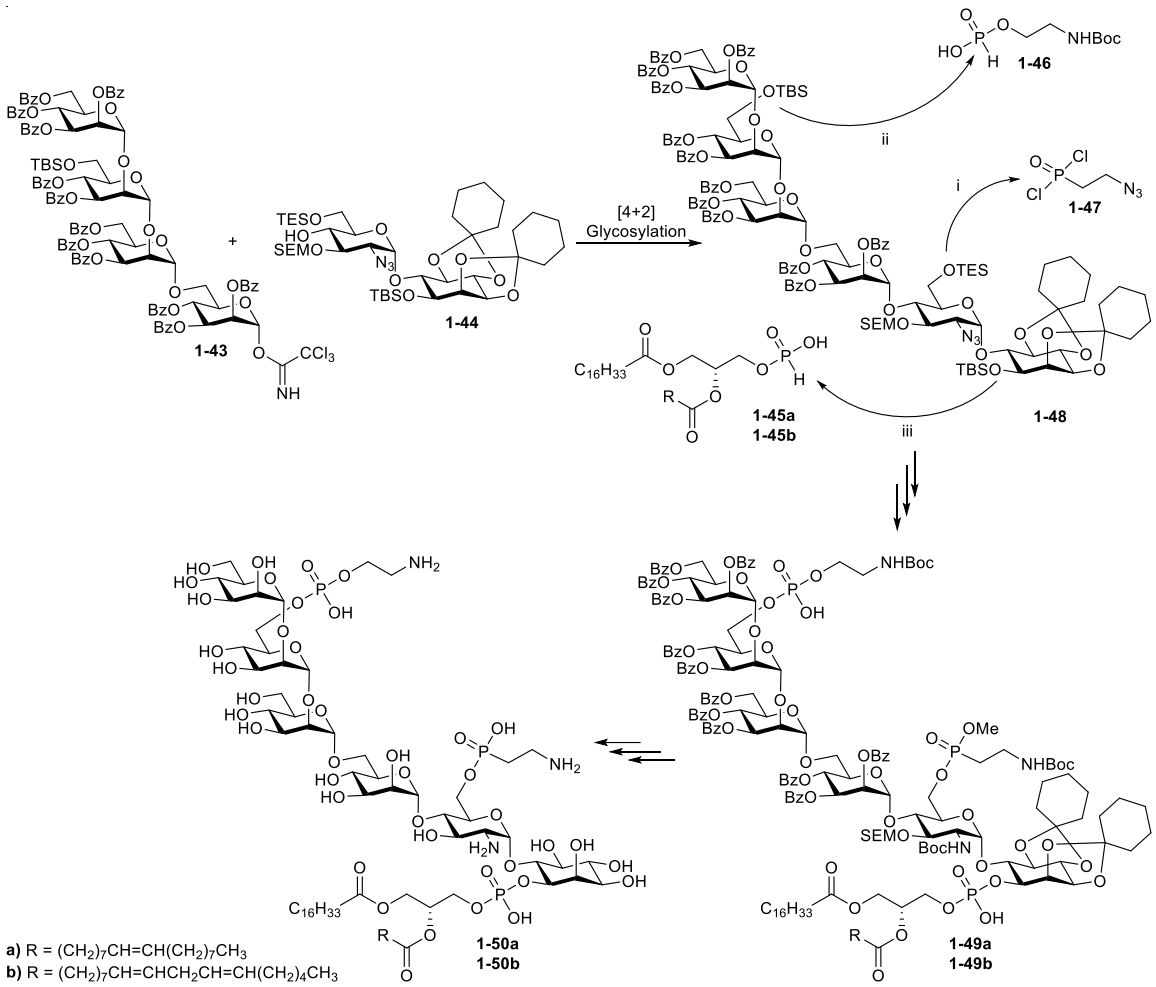

Scheme 1-6. Synthesis of a *T. cruzi* GPI anchor bearing unsaturated lipids reported by Nikolaev's group.[71] The roman numbers represent the order of the reactions.

Final deprotection of the two GPIs **1-49a** and **1-49b** involved three steps: demethylation at the aminoethylphosphonate moiety with PhSH/Et_3N; removal of the benzoyl protecting groups by treatment with 0.05 M NaOMe in methanol, and cleavage of O-acetal and N-Boc protecting groups with aqueous 90% TFA. These reactions delivered the two desired *T. cruzi* GPI anchors bearing unsaturated lipids **1-50a** and **1-50b** in ~35% yield (Scheme 1-6). Nikolaev's pioneer work constituted the first synthesis of this type of GPI. Nonetheless, it was still a target-oriented synthesis, and it could not be used for the syntheses of structurally diverse GPIs with unsaturated lipids. In addition, using benzoic esters as permanent protecting groups shows low compatibility with esters and/or peptides/glycopeptides in the target molecule, which are sensitive to deprotection under basic conditions. The cleavage of the benzoic esters during Nikolaev's synthesis delivers the products in low yield (~40%), probably due to saponification of the ester-linked lipid chains.

In a similar effort to replace benzyl permanent protection with a strategy that allows the incorporation of reductive-sensitive groups, Guo and Swarts synthesized in 2010 a GPI anchor employing the acid-labile PMB ethers as a permanent protecting group (Scheme 1-7).[72] Contrary to most

protocols, the phospholipid moiety was introduced in an early stage of the synthesis: the phosphoramidite **1-52** was coupled to the pseudodisaccharide **1-53**, and the resulting phospholipidated pseudodisaccharide was reacted with the trimannosyl trichloroacetimidate donor **1-51** through a [3+2] glycosylation in 64% yield. The phosphoethanolamine unit was installed using the phosphoramidite **1-54** and the global deprotection of the phospholipidated GPI **1-56** was performed over three steps. First, the azide was reduced using zinc and acetic acid. Second, the Fmoc and cyanoethoxy groups were removed with DBU. Third, a final hydrolysis of PMB ethers using 10% TFA delivered the GPI **1-57** containing unsaturated lipids in 81% yield. Guo and Swarts used the same protection strategy to synthesize GPI anchors with saturated lipids having reductive-sensitive groups at the O-2 position of Man-I such as an alkyl azide and alkynes.[73]

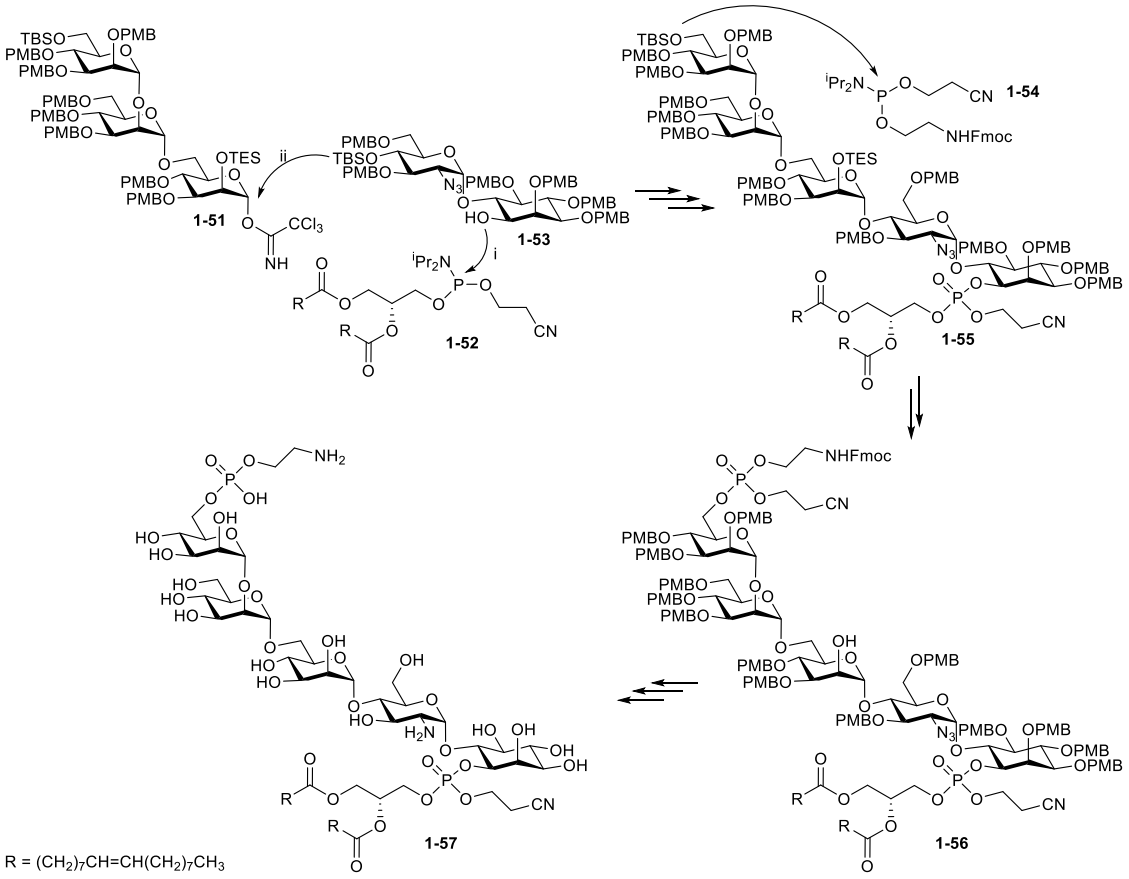

Scheme 1-7. Synthesis of a GPI bearing unsaturated lipids by Guo and Swarts.[72] The roman numbers represent the order of the reactions.

Guo's approach represented a significant improvement over Nikolaev's work regarding the efficiency of the global deprotection; nevertheless, the strategy was still not ideal for synthesizing GPIs of high complexity due to the low stability of PMB ethers under acidic conditions, which are commonly employed for glycosylation reactions. The reported glycosylation reactions in Guo's synthesis resulted in modest to low yields, likely due to the cleavage of the PMB ethers under the

reaction conditions. Syntheses of complex GPI structures with oligosaccharide branches would inevitably involve several glycosylation reactions.

The previous syntheses do not represent a general strategy to access GPIs bearing unsaturated lipids due to incompatibilities of the chosen permanent protecting groups with fatty acid esters (or other base-sensitive moieties) or with acidic conditions during glycosylation reactions. Therefore, our group proposed the usage of 2-naphthylmethyl (Nap) ethers as permanent protecting groups, which present significant advantages over benzoyl esters and PMB ethers. The Nap group is not only orthogonal to acyl esters, silyl ethers, and even PMB ethers, but it is also stable during glycosylation reactions and can be removed under acidic or oxidative conditions.

In 2016, our group reported a strategy using 2-naphthylmethyl ether as a permanent protecting group to synthesize the pseudodisaccharide from *T. cruzi* bearing an unsaturated phospholipid (Scheme 1-8).[74] The strategy was based on the reported general and convergent synthesis of GPIs presented in scheme 1-5. The glucosamine and inositol building blocks were obtained by exchanging the benzyl ethers for Nap ethers in all established protocols. The phospholipid moiety containing a linoleic chain at the *sn*-2 position was incorporated into the pseudodisaccharide using phosphoramidite **1-58**. Once the PMB ether was selectively removed under acidic conditions, the 2-azidoethylphosphonodichloridate **1-47** was used to introduce the *T. cruzi* characteristic (2-aminoethyl)phosphonate unit at the O-6 position of glucosamine. Finally, a three-step protocol was followed to remove the protecting groups: removal of the cyanoethoxy group of the phospholipid using DBU, azide reduction using zinc in acetic acid, and final cleavage of Nap ethers using TFA in toluene. The final *T. cruzi* fragment **1-61** bearing unsaturated lipids was obtained in 72% yield.

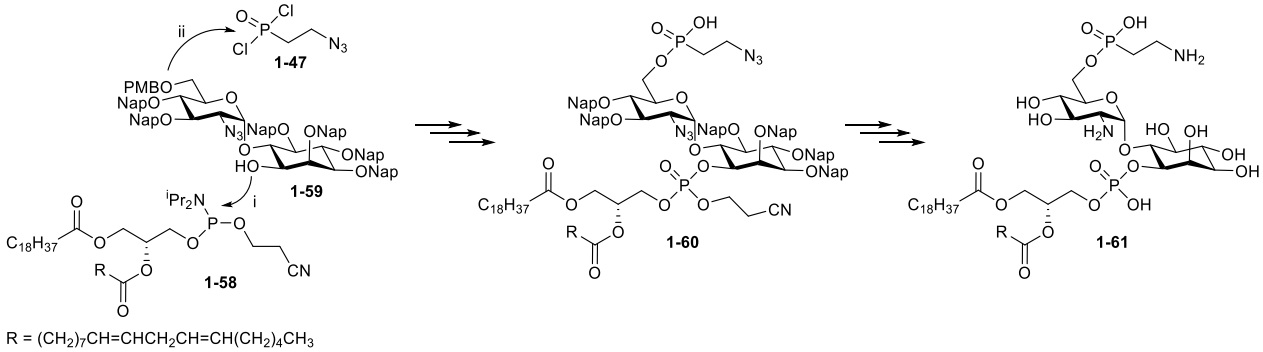

Scheme 1-8. Synthesis of a *T. cruzi* GPI fragment bearing unsaturated lipids using 2-naphthylmethyl ether protecting groups.[74] The roman numbers represent the order of the reactions.

Boons and coworkers used this Nap protection strategy in 2017 to synthesize a derivative of a *Leishmania donovani* lipophosphoglycan (LPG) that can be functionalized by a Cu-catalyzed azide−alkyne cycloaddition (Scheme 1-9).[75] The targeted LPG derivative didn't have unsaturated

lipids nor acyl chains, but it contained an alkyne tag at the top of the glycan core that made Nap protection indispensable for the synthesis. The global deprotection was achieved under oxidative conditions using DDQ to remove the Nap protection, followed by basic conditions to cleave the levulinoyl esters delivering the target LPG **1-64** in 65% yield.

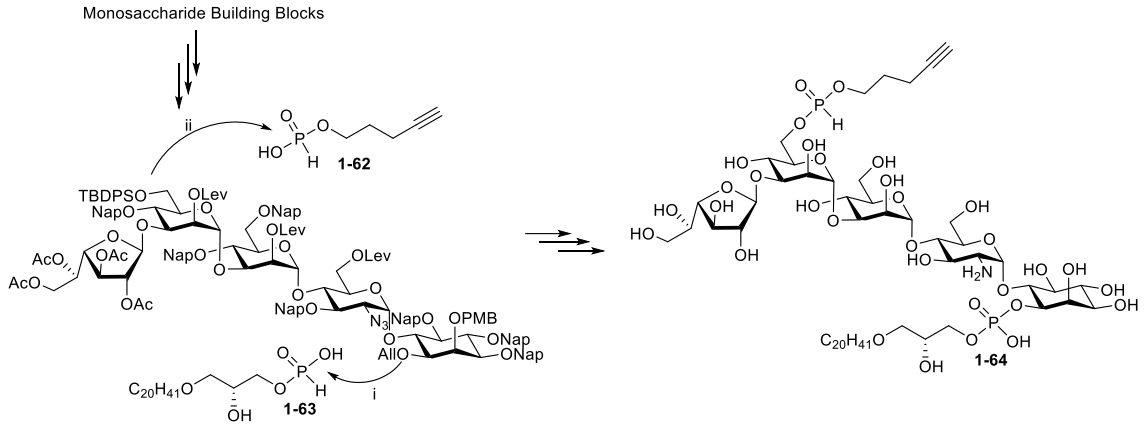

Scheme 1-9. Synthesis of a *Leishmania donovani* lipophosphoglycan derivative bearing unsaturated lipids by Boons and coworkers.[75] The roman numbers represent the order of the reactions.

The synthesis of a GPI fragment having unsaturated lipids performed in our group and Boons' synthesis of an LPG derivative having a reductive-sensitive group shows that naphthylmethyl ethers have enormous potential as permanent protecting groups in GPI synthesis. However, further studies are still required to probe their applicability to obtain complete and diverse GPI structures bearing unsaturated lipids.

To decipher the structure-activity relationship of GPIs bearing unsaturated lipids and to evaluate the potential application of these glycolipids in the prevention, diagnosis, and/or treatments of parasitic infections, it is necessary to establish synthetic reliable strategies to get well-defined GPI structures. Several synthetic methods to access GPIs have been developed during the last decades. However, most routes involve protecting groups strategies requiring a final hydrogenolysis step that restricted the application for getting GPIs containing saturated lipids. Some strategies have been explored for the synthesis of GPIs or GPI fragments bearing unsaturated lipids; these strategies are either target-oriented or have not been applied for GPIs total synthesis. Therefore, there is still a lack of a general route that enables the efficient preparation of a wide range of structurally diverse GPI anchors containing reductive-sensitive moieties.

1.5 Aim of the thesis

The presence of unsaturated alkyl chains has been associated with the high immunoreactivity obtained with isolated GPIs glycolipids from parasites. Particularly, the GPIs of *T. cruzi* and *P.*

falciparum expressed in significant amounts on the cell surface may be responsible for the strong immunoreactivity during the Chagas disease and Malaria infection.

This thesis aims to develop a general and convergent strategy for synthesizing GPIs and GPI fragments bearing unsaturated lipids. For this purpose, different protecting group combinations and a reported strategy using 2-naphthylmethyl ethers as permanent protecting group will be expanded and optimized for GPI synthesis. The strategy should be flexible to accommodate additional modifications such as acylation of the O-2 position of myo-inositol, elongation of the glycan core with additional monosaccharide units, and incorporation of specific modifications such as the *T. cruzi* characteristic (2-aminoethyl)phosphonate at the O-6 position of glucosamine. A combination of protecting groups including acyl esters, allyl ethers, Nap ethers, PMB ether and silyl ethers will be evaluated. Different lipid compositions including diacyl and 1-alkyl-2-acyl-*sn*-glycerophosphates with one or two unsaturations will be incorporated, and suitable removal conditions for all protecting groups in the presence of unsaturated lipids or other reductive-sensitive moieties such as the azido group will be established.

The strategy will be applied to synthesize biologically relevant GPI structures containing various lipids compositions with unsaturated fatty acid chains. The project will initiate synthesizing GPI fragments containing unsaturated lipids to evaluate their activities as substrates in GPI biosynthesis in mammals. These studies should provide tools for the development of treatments for patients having genetic disorders affecting this biosynthesis pathway and give insights into mechanistic aspects of GPI biosynthesis.

The established methods will be expanded for the total synthesis of pure homogeneous parasitic GPIs bearing unsaturated lipid chains. The synthesis of two GPIs will serve as a model: the GPI anchor of *P. falciparum* and a GPI anchor of *T. cruzi*. These GPIs have been synthesized by other strategies and represent a good reference structure to test new strategies. In addition, the total syntheses are motivated to enable extensive investigation into the biological roles of these and other GPI structures during parasitic infections, which can lead to the development of prophylactics, diagnosis methods, and/or treatments for the affected populations.

2 Rescue of GPI-Anchored Protein Biosynthesis Using Synthetic GPI-fragments

2.1 Inherited GPI Deficiencies

The GPI-AP biosynthesis starts from phosphatidylinositol, is encoded by around 27 genes, and requires several proteins and enzymes (Figure 1-2).[12,47] Most genes (22) belong to the so-called Phosphatidyl Inositol Glycan (PIG) genes involved in the GPI assembling and GPI protein attachment. The other five genes are known as Post GPI Attachment to Protein (PGAP) and are responsible for the lipid and glycan remodeling of GPI-APs.[12] Defects on 21 GPI biosynthesis genes compromise the biosynthesis process and can lead to two different results.[45] On one side, a defective gene can cause total loss of GPI-APs and lead to embryonic death.[76] On the other side, the defect can result in GPI-APs expression reduction on the cell surface and lead to inherited GPI deficiencies (IGDs) manifesting as intellectual disability, organ malformations, developmental delay, seizures, among others.[44,48,77,78]

Depending on the role of the affected gene in the GPI biosynthesis and if the mutation occurred in the coding or noncoding region of the gene, patients with IGD present different pathologies.[78] The severity of the symptoms is also influenced by other factors, such as the type of mutation at the nucleotide level and the nature of the amino acid changes.[78] Some symptoms are common across patients with different PIG or PGAP mutated genes. Patients with PIGA and PIGL variants—involved in the first two steps of the GPI biosynthesis—mostly present intellectual deficiency, developmental delay, epileptic encephalopathies, brain anomalies, elevated alkaline phosphatase levels, cardiac anomalies, dental problems, visual impairments, deafness, among others.[48] In the case of PIGL mutations, many patients present colobomas, an ophthalmological anomaly that patients with mutations in other PIG genes don't have.[78] Mutations in PIGL have also been identified in patients with CHIME syndrome, which is the acronym for a multisystem disorder characterized by colobomas, heart defects, ichthyosiform dermatosis, mental retardation, and ear anomalies.[79]

For the third step of the GPI biosynthesis, PIGW encodes the enzyme involved in the inositol acylation, which is critical for the attachment of the phosphoethanolamine linker to the third mannose.[44,80] Besides the common phenotypes in other IGD patients, mutations in this gene do not present many additional features.[48] On the contrary, patients with PIGV variants typically show nail anomalies.[48,78] As for the later stage of GPI biosynthesis, PIGV, PIGO, PGAP2, PGAP3, PIGW, and PIGY variants have been reported to cause Mabry syndrome, an autosomal recessive

disorder characterized by intellectual disability, distinctive facial features and abnormal alkaline phosphatase levels in the blood.[44,77]

The IGD cases described above are caused by germline mutation of the PIG or PGAP genes. Nonetheless, GPI biosynthesis deficiencies can also result from the somatic mutation of a PIG gene. For example, somatic PIGA mutation leads to paroxysmal nocturnal hemoglobinuria (PHN), an acquired hematopoietic stem cell disorder characterized by thrombosis, bone marrow failure, and complement-mediated red blood cell destruction due to deficiency of two GPI-APs that are complement inhibitors, the complement-accelerating factor (CD55) and glycoprotein CD59.[44,81–83] Clinical diagnosis of PHN is confirmed by determination of GPI-APs deficiency with peripheral blood flow cytometry with at least two different blood cell lineages.[81] Treatments for PNH patients include immunosuppression to protect the bone marrow; bone marrow transplantation which is the only curative option for PNH; and a humanized monoclonal antibody (eculizumab) to inhibit terminal complement activation, which is the only approved medication for PNH.[81,84–87]

Many other pathologies have been associated with mutations in genes encoding several proteins involved in GPI biosynthesis. The amount is expected to increase with the growing development of sequencing technologies.[12,78] However, treatment and diagnosis development for GPI biosynthesis deficiencies have been mainly focused on PNH patients. This is primarily due to the lack of a reliable, sensitive biomarker to detect GPI biosynthesis deficiencies. Specific symptoms suggest an inherited GPI deficiency, such as seizures with aplastic/hypoplastic nails or increased alkaline phosphatase levels.[48] Most commonly, diagnosis can be achieved by detecting GPI-APs deficiencies with flow cytometry without sequencing using antibodies; however, in certain mutations, the overall amount of GPI-APs is still within the expected values.[44] Other alternatives include genetic analysis, sequencing, and computer-assisted phenotype comparison[88]. Moreover, since IGDs manifest in a broad spectrum of clinical phenotypes, developing treatments is also challenging. Only symptomatic treatments, such as oral or intravenous use of vitamin B6, are available to control seizures in some IGD patients.[44,89] But, no cure or therapy addresses the primary cause of these rare but life-threatening disorders, and new strategies are urgently needed.

2.2 Hypothesis

To address the urgent need for treatments for IGDs, we hypothesized that GPI biosynthesis deficiencies originated from defective genes and mutations should be treatable with a synthetic version of the intermediate that is not produced in the deficient cell. The synthetic GPI-fragment could enter the biosynthesis process and restore the GPI-AP expression on the cell surface (Figure

2-1). If the process is successful, synthetic GPI fragments could be used to develop glycan-based treatments for patients suffering from IGDs. Thus, we started the evaluation and applicability of synthetic GPI fragments, synthesizing and evaluating these compounds to rescue the GPI-APs expression in cells with knock-out genes affecting the initial four steps of GPI biosynthesis.

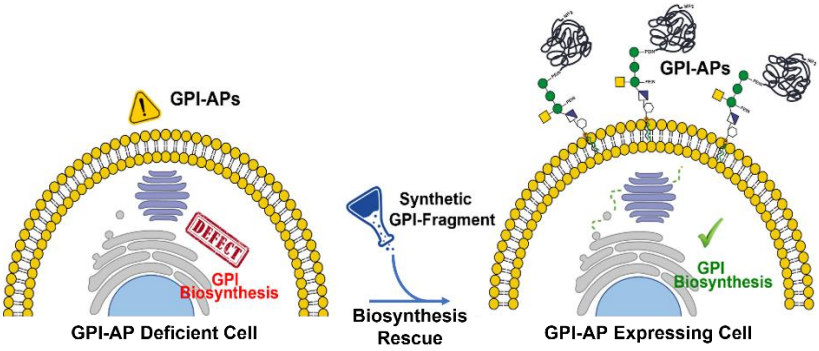

Figure 2-1. Graphical representation of the hypothesis. Synthetic GPI fragments restore GPI-APs expression on the cell surface.

2.3 Glycolipid design

To evaluate the *in vitro* activity of synthetic GPI fragments to rescue the GPI-APs biosynthesis, we designed a series of glycolipids that resemble the products and substrates of the enzymes involved in the four initial steps of GPI biosynthesis in eukaryotes (Figure 2-2). The pseudodisaccharide **2-1** (GlcNAc-PI) was designed to resemble the product of the first biosynthesis step: the transfer of GlcNAc to PI. GPI-fragment **2-2** (GlcN-PI) was designed to replace the product of GlcNAc-PI deacetylation. The triacylated glycolipid **2-3** (GlcN-acylPI) should resemble the first GPI precursor obtained in the ER lumen. This compound contains in addition to a DAG a palmitate (C16:0) at the C-2 position of *myo*-inositol. Finally, the pseudotrisaccharide **2-4** (Man-GlcN-PI) was devised to replace the product generated after transferring the first mannose to the growing glycan core.

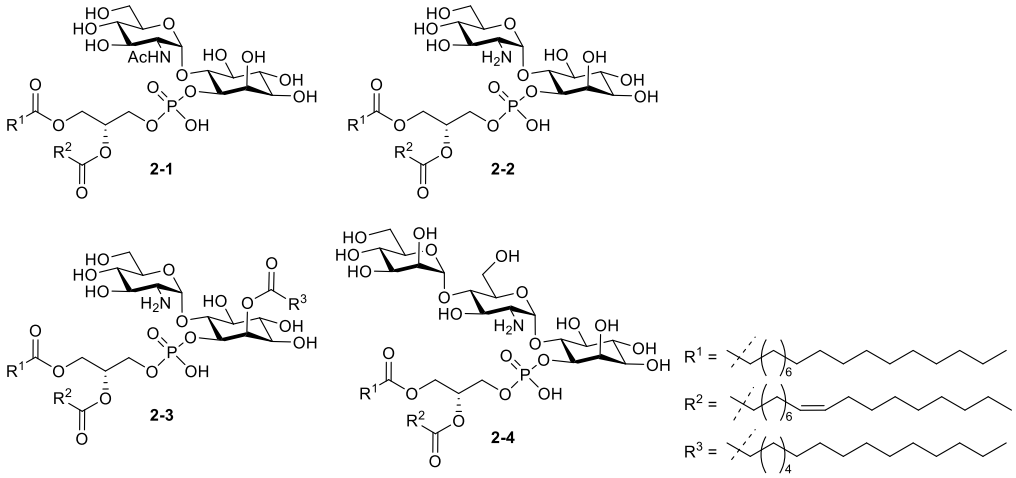

Figure 2-2 Designed fragments to rescue GPI biosynthesis.

A phospholipid containing 1-stearoyl(C18:0)-2-oleoyl(C18:1)-*sn*-glycerophosphate was selected for the lipid part of the glycolipids **2-1** to **2-4**. This moiety was designed with an unsaturated chain at the *sn*-2 position to mimic the lipid of the endogenous phosphatidylinositol (PI) that contains predominantly 1-stearoyl-2-arachidonoyl(C20:4)-*sn*-glycerolipid.[45,90]

2.4 Retrosynthetic analysis

The strategy for synthesizing GPI fragments bearing unsaturated lipids requires a glycan assembly using the mannose **2-12**, glucosamine **2-11,** and *myo*-inositol building blocks **2-9** and **2-10** (Scheme 2-1). These building blocks will contain a 2-naphthylmethyl (Nap) ether as a permanent protecting group. Nap ethers are stable under glycosylation conditions and orthogonal to acyl esters, allyl ethers, and PMB ether required during the synthesis. A neighboring participating group or the proper solvent and temperature selection will control the stereoselectivity of glycosylations. Phosphorylation will be performed at a late synthesis stage to preserve the phosphate and the unsaturation in the lipid chain. Finally, Nap ethers should be readily removed under acidic conditions without compromising the unsaturation in the lipid part to give the desired glycolipids.[74]

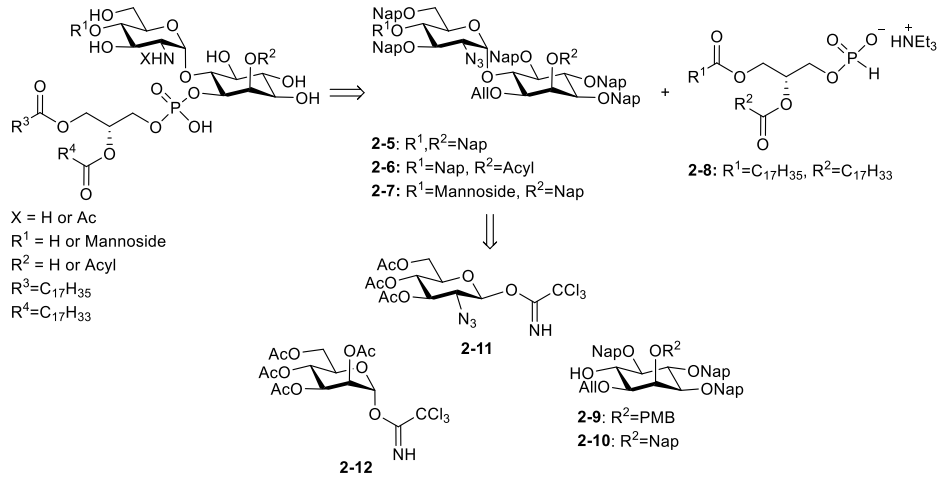

Scheme 2-1. Retrosynthetic analysis of GPI fragments **2-1** to **2-4**. Nap = 2-Naphthylmethyl, PMB = para-methoxybenzyl.

2.5 Results and discussion

2.5.1 Synthesis of GPI-fragments

2.5.1.1 Synthesis of Building Blocks

Two different inositol building blocks are required for the assembly of the desired glycolipids: inositol **2-9** having a PMB group at the 2-O position to enable the latter introduction of the third lipid and get glycolipid **2-3**, and inositol **2-10** having a Nap group at the 2-O position for the synthesis of the target glycolipids without inositol modification. The synthesis of both *myo*-inositol acceptors **2-9** and **2-10** started from methyl α-D-glucopyranoside **2-13** using a protocol established by our group (Scheme 2-2).[74] The primary alcohol of glucose was initially protected with a trityl group and followed by protection with 2-naphthylmethyl ether of the remaining hydroxyl groups. After removal of the trityl group, the resulting alcohol **2-15** was oxidized with SO_3-pyridine complex to the corresponding aldehyde, which was immediately converted into an enol and acetylated. The obtained enol ester **2-16** was rearranged into cyclohexanone **2-17** *via* Ferrier type II carbocyclization in moderate yield (60%). The ketone in **2-17** was reduced in high stereoselectivity with $NaBH(OAc)_3$, and the acetyl group was removed using NaOMe to give the triol **2-19**. The allyl ether was regioselectively installed *via* tin-acetal to provide the diol **2-20**. Selective etherification of the 2-O position using para-methoxybenzyl (PMB) chloride and NaH afforded the optically pure D-myo-inositol **2-9** in 85% yield while performing the same reaction using 2-naphthylmethyl bromide gave the D-myo-inositol **2-10** in 66% yield.

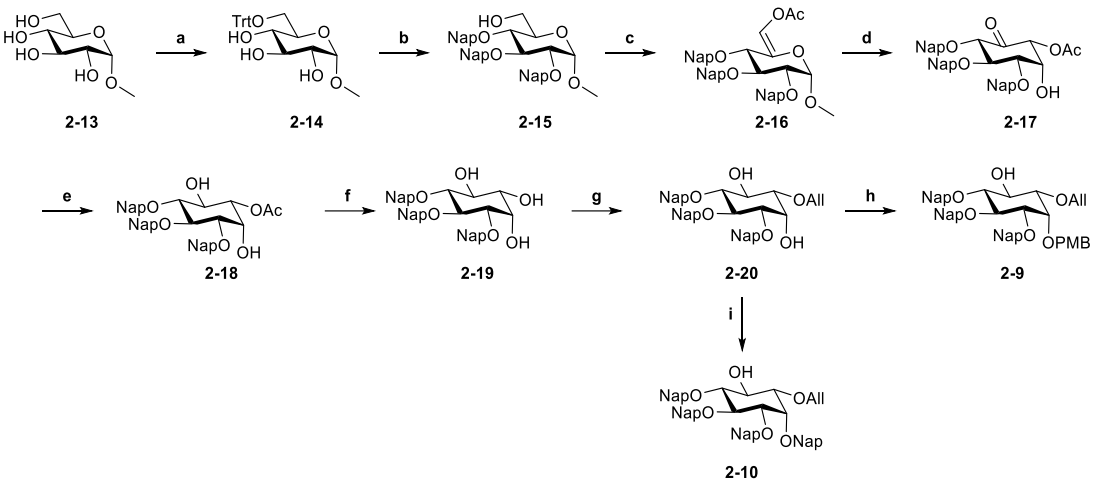

Scheme 2-2. Synthesis of *myo*-inositols **2-9** and **2-10**. *Reagents and conditions*: a) TrtCl, Et_3N, DMF, r.t., 12 h, 92%; b) i. NapBr, NaH, DMF, r.t., 76 h; *ii. p*-TsOH, DCM/MeOH, rt, 19 h, 71%; c) i. SO_3-Py, DIPEA, DMSO, DCM, 0 °C, 1 h; *ii.* Ac_2O, K_2CO_3, ACN, 85 °C, 2 h, 81% (two steps); d) i. $Hg(CF_3COO)_2$, acetone, rt, 1 h; *ii.* H_2O, NaOAc, NaCl, 0 °C to rt, O.N., 60%; e) $NaBH(OAc)_3$, ACN, AcOH, r.t., 25 h, 78%; f) NaOMe, DCM/MeOH, r.t., 1 h, 97%; g) i. $(Bu_3Sn)_2O$, toluene, reflux, 4 h; *ii.* AllBr, TBAI, 65 °C, 14 h, 68%; h) PMBCl, NaH, DMF, 0 °C, 3 h, 85%; i) NapBr, NaH, DMF, 0 °C, 2 h, 66%.

The synthesis of glucosamine donor **2-11** (Scheme 2-3) was initiated with a two-step protocol involving the diazotransfer reaction between D-glucosamine hydrochloride **2-21** and *in situ* generated triflic azide and followed peracetylation to the glucosamine azide **2-22** in good yield. Anomeric deacetylation with hydrazine acetate and subsequent treatment of the hemiacetal with trichloroacetonitrile and catalytic amount of DBU delivered the trichloroacetimidate donor **2-23** in 79% yield over two steps and 4:6 α/β ratio (Scheme 2-3). Anomers were separated during product purification by flash silica gel column chromatography.

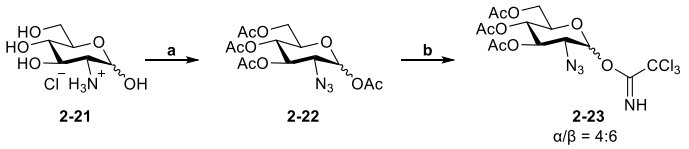

Scheme 2-3. Synthesis of glucosamine donor. *Reagents and conditions*: a) i. Tf_2O, NaN_3, $CuSO_4{\cdot}5H_2O$, Et_3N, H_2O/ACN, 0 °C, 24 h; *ii.* DMAP, Ac_2O/Pyridine, 0 °C, O.N., 95% (two steps); b) i. hydrazine acetate, THF, r.t. O.N., 92%; *ii.* DBU, CCl_3CN, 0 °C, 1 h, 86%. DMAP = 4-Dimethylaminopyridine.

The mannose building block **2-12** required for synthesizing glycolipid **2-4** was synthesized in two steps from peracetylated mannose **2-24**. The anomeric acetyl group was removed with hydrazine

acetate, and the formed hemiacetal was treated with trichloroacetonitrile and catalytic DBU to afford the trichloroacetimidate donor **2-12** in 68% yield (Scheme 2-4).

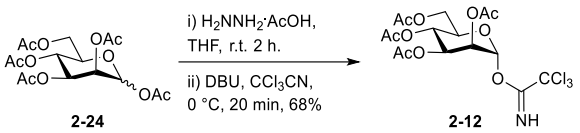

Scheme 2-4. Synthesis of the mannose donor **2-12**.

The retrosynthetic analysis identified the H-phosphonate **2-8** as a common building block for all designed glycolipids (Scheme 2-1). The synthesis of this building block started from commercially available (S)-(+)-1,2-Isopropylideneglycerol **2-25** (Scheme 2-5). The alcohol was protected as *p*-methoxybenzyl ether, and the acetal was opened under aqueous acidic conditions to afford the diol **2-27**. The free primary alcohol was selectively acylated with stearic acid under Steglich esterification conditions using equimolar amounts of the acid. Then, the remaining secondary alcohol was acylated with oleic acid under similar conditions to give the fully protected diacyl glycerol **2-29** in 75% yield over the two steps. Finally, the PMB group was removed under oxidative conditions with DDQ, and the resulting alcohol was phosphitylated using phosphorous acid with pivaloyl chloride activation to afford the desired H-phosphonate **2-8**.

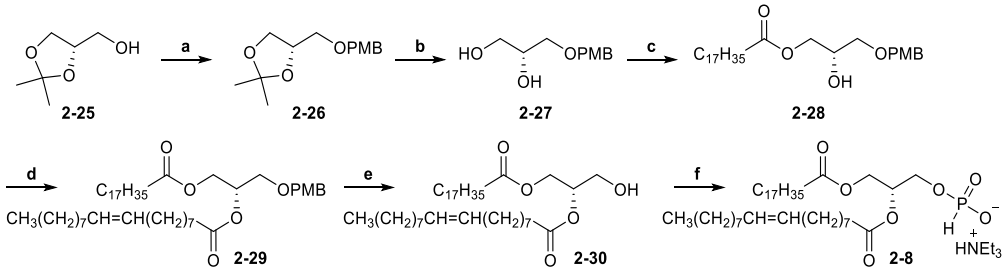

Scheme 2-5. Synthesis of H-phosphonate **2-8**. *Reagents and conditions*: a) PMBCl, NaH, DMF, r.t., 30 min; b) AcOH/H_2O, 70 °C, 1 h, 92% (two steps); c) Stearic acid, DCC, DMAP, DCM, r.t., O.N., 82%; d) Oleic acid, DIC, DMAP, DCM, r.t., O.N., 92%; e) DDQ, DCM/H_2O, r.t., O.N., 78%; f) H_3PO_3, PivCl, pyridine, r.t., O.N., 53%. DCC = *N,N′*-Dicyclohexylcarbodiimide, DIC = *N*,*N′*-Diisopropylcarbodiimide, PivCl = pivaloyl chloride.

2.5.1.2 Synthesis of GPI-fragments 2-1 and 2-2

The pseudodisaccharide **2-33** was required to synthesize glycolipids **2-1** and **2-2** (scheme 2-6). The assembly of this glycan started with the glycosylation of inositol acceptor **2-10** with the β-configurated glucosamine imidate donor **2-11** using TMSOTf activation to yield the pseudodisaccharide **2-31** in an 11:1 α/β ratio (Scheme 2-6). The α/β-product mixture of **2-31** was deacetylated using NaOMe and the anomers were separated by silica gel column chromatography to afford

the α-configurated triol **2-32**. Protection of **2-32** using NapBr and NaH delivered the fully protected pseudodisaccharide **2-5**, which was deallylated with palladium chloride in methanol to obtain the alcohol **2-33** ready for phospholipid installation. The phospholipid moiety was introduced by a two-step protocol involving phosphitylation with the H-phosphonate **2-8** using pivaloyl chloride activation and the following oxidation with iodine/water to deliver the phospholipidated protected pseudodisaccharide **2-34**. An initial attempt to remove the 2-naphthylmethyl ethers was performed according to the reported procedure using treatment of the fully protected product with TFA in toluene.[74] This reaction resulted in partial removal of the protecting groups or in starting material decomposition after a long reaction time. Similar results were observed at different temperatures and replacing toluene with anisole.

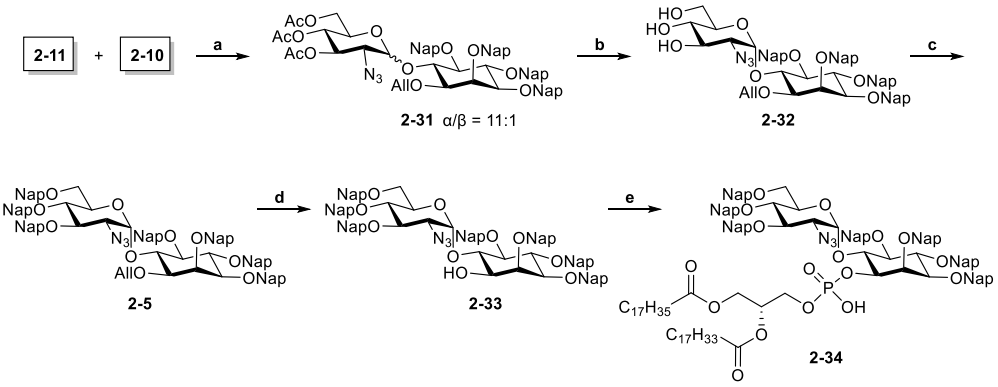

Scheme 2-6. Synthesis of pseudodisaccharide **2-34**. *Reagents and conditions*: a) TMSOTf, Et_2O/DCM, r.t., 2 h, b) NaOMe, MeOH, 40 °C, 3 h, 94% (two steps); c) NapBr, TBAI, NaH, DMF, r.t., O.N. 92%; d) $PdCl_2$, DCM/MeOH, r.t., 3 h, 85%; e) **2-8**, *i.* PivCl, pyridine, r.t., 1.5 h; *ii.* I_2, H_2O, r.t. 1 h, 98%.

To optimize the conditions for Nap protecting groups removal without using the precious compound **2**-**34**, the dimannoside **2-35** having an oleic acid chain was synthesized as a model compound (Scheme 2-7). Starting with the removal of TBDPS from **4-11** with TBAF the desired product was obtained by subsequent acylation of the free alcohol with oleic acid. Treatment of **2-35** with TFA in toluene or anisole as a solvent at different temperatures also resulted in partial removal of Nap ethers. Thus, other conditions, such as oxidative conditions, were considered for this process. A removal of benzyl ether was reported using biphasic oxidative conditions without affecting reduction-sensible groups.[91] These conditions were tested to remove the Nap groups by treating **2-35** with aqueous solutions of $NaBrO_3$ and $Na_2S_2O_4$ in ethyl acetate considering the similar reactivity of benzyl and Nap ether. However, partial removal of the protecting group was again observed. Better results were obtained treating **2-35** with DDQ in DCM/MeOH, which resulted in the complete removal of Nap protecting groups delivering **2**-**36**.

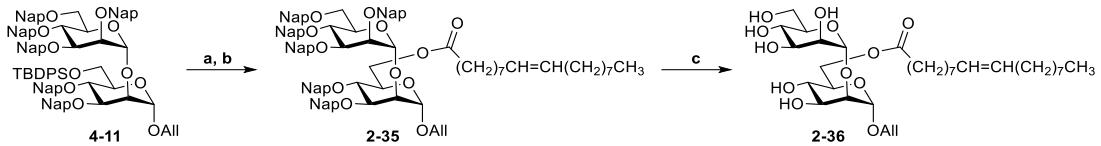

Scheme 2-7. Deprotection of model dimannoside **2-35**. *Reagents and conditions*: a) TBAF, THF, r.t., O.N., 97%; b) Oleic acid, DIC, DMAP, r.t., 4 h, 85%; c) DDQ, MeOH/DCM, r.t., 4 h. TBAF = tetra-N-butylammonium fluoride.

Similarly, all Nap groups of glycolipid **2-34** were also removed under oxidative conditions using DDQ in DCM/MeOH giving the O-deprotected pseudodisaccharide azide. Due to the amphiphilic character and low solubility in most solvents of this deprotected glycolipid, purification by normal phase silica gel column chromatography or RP-HPLC was not suitable. Initial attempts to remove excess DDQ and its colored by-products by manual LH-20 size exclusion chromatography using THF or MeOH/$CHCl_3$/H_2O 3:3:1 using short columns (50 cm x 1.5 cm) were unsuccessful. Therefore, a 1.5 m x 5 cm column packed with LH-20 resin was coupled to an HPLC system and the *O*-deprotected glycolipid was eluted using MeOH/$CHCl_3$ 9:1. The proportion of chloroform had to be kept low due to its incompatibility with the tubing of the system. Although the solubility of the glycolipid in the eluent was not ideal, most of the colored impurities were readily removed obtaining the molecule spread within several fractions with a remaining yellow impurity.

Following treatment with zinc dust in acetic acid to reduce the azide did not deliver the desired product **2-2** and caused the decomposition of the glycolipid. Inverting the order of the two steps did not improve the outcome of the process. Thus, an azide reduction using Staudinger reaction was evaluated. The Nap groups of **2-34** were removed under oxidative conditions using DDQ, and the azide was reduced with trimethylphosphine in THF, providing the expected GPI fragment **2-2**. The trimethyl phosphine oxide produced during the Staudinger reduction was removed by manual LH-20 size exclusion chromatography eluting with MeOH/$CHCl_3$/H_2O 3:3:1; however, the yellow impurity remained in the product. During the screening for a suitable solvent for NMR characterization, it was found that the glycolipid abundantly precipitated as a white solid in methanol. Therefore, the product was triturated in this solvent obtaining the desired GPI fragment **2-2** in pure form in 47% yield over two steps (Scheme 2-8).

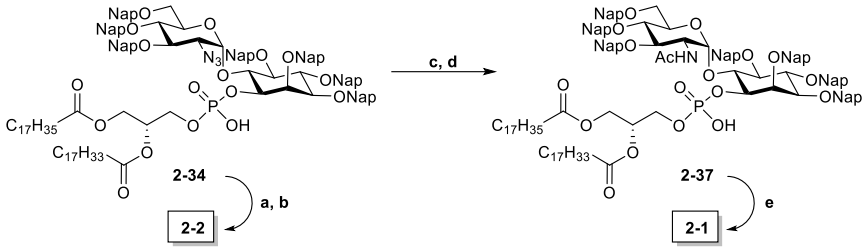

Scheme 2-8. Synthesis of GPI-fragments **2-1** and **2-2**. *Reagents and conditions*: a) DDQ, MeOH/DCM, r.t., 5 h; b) $P(CH_3)_3$, THF, r.t., 2 h, 47% (two steps); c) $P(CH_3)_3$, THF, r.t., 1 h; d) Ac_2O, pyridine, r.t., 1 h; e) DDQ, MeOH/DCM, r.t., 3 h, 62% (three steps).

For the preparation of the second GPI-fragment **2-1**, the azide in **2-34** was reduced under Staudinger conditions with trimethylphosphine in THF and the obtained amine was acetylated using acetic anhydride and pyridine to give the fully protected pseudodisaccharide **2-37**. Removal of the Nap ethers by treatment with DDQ in MeOH/DCM followed by purification with LH-20 size exclusion chromatography and trituration with methanol provided the glycolipid **2-1** in good yield (62%, over three steps).

2.5.1.3 Synthesis of GPI-fragment 2-3

The synthesis of trilipidated structure **2-3** required the modified pseudodisaccharide **2-40** having an orthogonal PMB group at the 2-O position of inositol for the late-stage acylation with the third lipid chain (Scheme 2-9). The process initiated with the glycosylation of inositol **2-9** with glycosyl donor **2-11** with TMSOTf activation to obtain pseudodisaccharide **2-38** in a 7:1 α/β ratio. The following deacetylation with sodium methoxide in methanol and etherification with 2-naphthylmethyl bromide delivered the protected pseudodisaccharide **2-40** in 61% yield over the three steps. The PMB group on inositol was selectively removed under acidic conditions, and the resulting alcohol was acylated with palmitic acid under Steglich esterification conditions to give **2-6**. The allyl group was removed using palladium chloride, and the phospholipid was installed using the H-phosphonate **2-8** under similar conditions as described for **2-34**. Finally, the 2-naphthylmethyl groups were removed with DDQ, and Staudinger reduction was performed to deliver trilipidated fragment **2-3** in 48% yield.

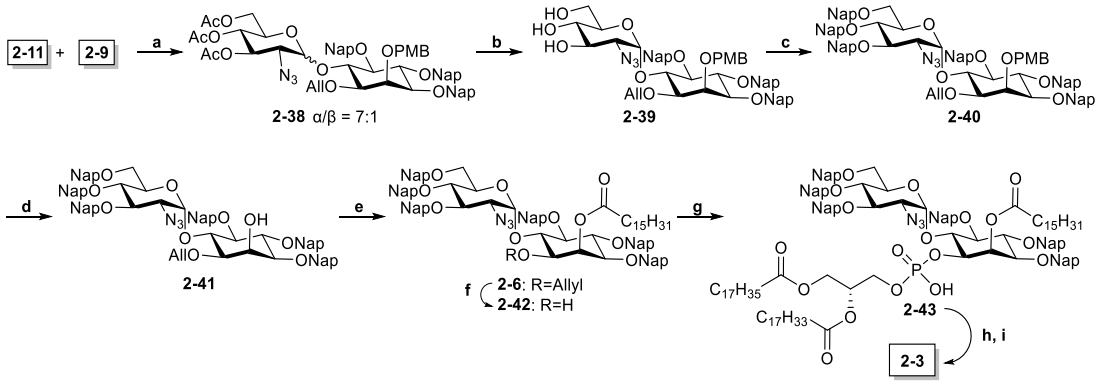

Scheme 2-9. Synthesis of GPI-fragment **2-3**. *Reagents and conditions*: a) TMSOTf, Et_2O/DCM, 0 °C, 2 h, 7:1 (α/β); b) NaOMe, MeOH, 40 °C, 1 h, 77% (two steps); c) NapBr, NaH, DMF, r.t., 79%; d) TFA, DCM, 0 °C, 40 min, 97%; e) Palmitic acid, DIC, DMAP, DCM, r.t., 15 h, 86%; f) $PdCl_2$, DCM/MeOH, r.t., 2.5 h, 85%; g) *i.* **2-8**, PivCl, pyridine, r.t., 1.5 h; *ii*. I_2, H_2O, r.t., 1.5 h, 82%; h) DDQ, MeOH/DCM, r.t., 5 h; i) $P(CH_3)_3$, THF, r.t., 2 h, 48% (two steps). TFA = trifluoroacetic acid.

2.5.1.4 Synthesis of GPI-fragment 2-4

The synthesis of pseudotrisaccharide fragment **2-4** required the preparation of pseudodisaccharide **2-46** having the 4-O position of glucosamine free for glycan core elongation with the mannose donor **2-12** (Scheme 2-10). The route started with treating triol **2-32** with freshly prepared 2-(dimethoxymethyl)naphthalene under acidic conditions to give the 4,6-cyclic acetal **2-44**. The remaining free hydroxyl group was protected as a 2-naphthylmethyl ether to obtain the fully protected pseudodisaccharide **2-45**. Selective opening of the cyclic acetal using dimethyl ethyl silane (DMES) and a catalytic amount of $Cu(OTf)_2$ afforded pseudodisaccharide glycosyl acceptor **2-46** in 74% yield and good regioselectivity. Following glycosylation of the resulting alcohol with the mannose donor **2-12** under TMSOTf activation delivered the elongated glycan in 84% yield. The resulting pseudotrisaccharide was deacetylated and re-protected under Williamson conditions with 2-naphthylmethyl bromide to give the fully protected pseudotrisaccharide **2-7**. Following deallylation of inositol with palladium chloride furnished alcohol **2-47**, and phospholipidation using the H-phosphonate **2-8** and oxidation with iodine and water delivered the phosphorylated pseudotrisaccharide **2-48**. Finally, a two-step global deprotection involving the removal of the Nap groups with DDQ and the reduction of the azide with trimethylphosphine delivered the GPI fragment **2-4** in good yield.

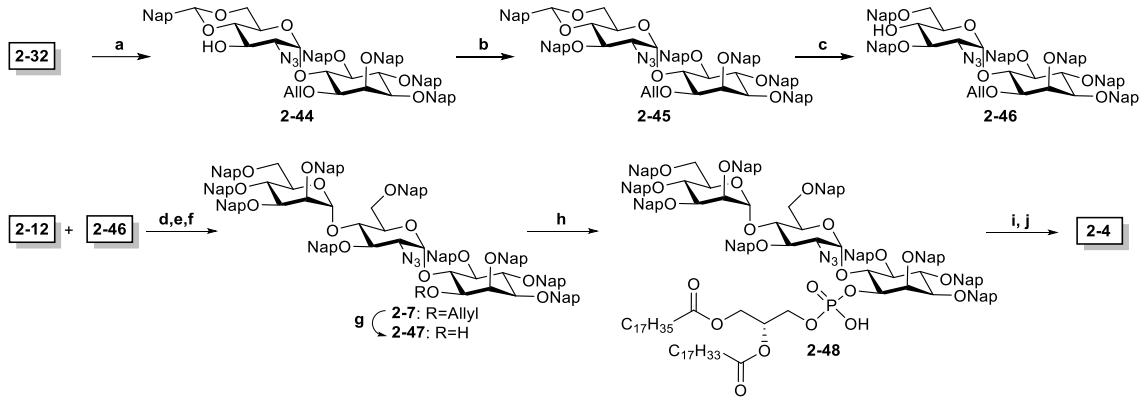

Scheme 2-10. Synthesis of the GPI-fragment **2-4**. *Reagents and conditions*: a) CSA, 2-(dimethoxymethyl)naphthalene, ACN, r.t., 3 h, 91%; b) TBAI, NapBr, NaH, DMF, r.t., 2 h, 98%; c) DMES, $Cu(OTf)_2$, ACN/DCM, 0 °C, 30 min, 74%; d) TMSOTf, Et_2O/DCM, 0 °C, 45 min, 84%; e) NaOMe, MeOH, r.t., 2 h; f) NapBr, NaH, DMF, r.t., 48 h, 75% (two steps); g) $PdCl_2$, DCM/MeOH, r.t., 5.5 h, 83%; h) *i.* **2-8**, PivCl, pyridine, r.t., 1.5 h; *ii.* I_2, H_2O, r.t., 1.5 h, 93%; i) DDQ, MeOH/DCM, r.t., 6 h; j) $P(CH_3)_3$, THF, r.t., 2 h, 56% (two steps). CSA = Camphorsulfonic acid.

2.5.2 Recovery of GPI-APs Biosynthesis in HEK293 Cells

To evaluate the activity of the synthetic GPI fragments in rescuing the GPI-APs biosynthesis, the highly pure glycolipids were sent to Osaka University for biological assays in the group of Dr. Prof. Taroh Kinoshita. Knock-out HEK293 cells lacking a specific gene involved in one of the first four steps of the GPI biosynthesis were treated *in vitro* with the synthetic structure corresponding to the product of the affected step. The GPI-APs biosynthesis rescue was analyzed by determining the cell expression of the GPI-anchored CD59 and DAF proteins by flow cytometry. The cells were labeled using either specific anti-CD59 or anti-DAF monoclonal antibodies or using fluorescent-labeled inactive toxin aerolysin (FLAER), which is a protein that binds to the GPI glycan and can be used to detect total GPI-APs.[81]

Evaluation of the compounds started with the *in vitro* studies using compound **2-1** to restore GPI-APs expression in cells having a defective gene that compromises the first step of the GPI biosynthesis. For this purpose, HEK293 cells having a knockout for the PIGA gene (PIGA-KO) were treated in a serum-free DMEM/F-12 culture medium with concentrations of compound **2-1** between 0.02 µM and 2 µM (GlcNAc-PI). The restored cell expression of total GPI-APs, CD59, and DAF was analyzed after 24 hours. To our delight, compound **2-1** was efficiently incorporated into the treated cells, reached the ER membrane, and was accepted as the substrate for PIGL in the next step, restoring the GPI-APs biosynthesis in the PIGA-KO cells in a concentration-dependent manner (Figure 2-3a).

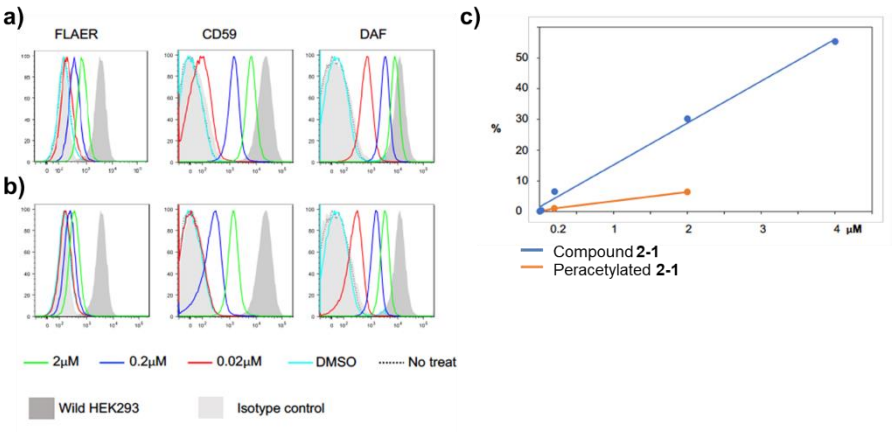

Figure 2-3. Determination of GPI-APs by flow cytometry after treatment PIGA-KO HEK293 cells with compounds **2-1** (GlcNAc-PI) and peracetylated **2-1** (peracetylated GlcNAc-PI). a) Production of total GPI-APs (detected with FLAER), CD59 and DAF after treatment with compound **2-1**; b) Production of total GPI-APs (detected with FLAER), CD59 and DAF after treatment with peracetylated **2-1**; c) Percent of CD59 expression rescue with various concentrations of **2-1** and peracetylated **2-1**. Histograms in (a and b): *y*-axis shows cell counts; the *x*-axis shows fluorescence intensity.

Acetylation is a common modification used for improving cell internalization of carbohydrates.[92] To evaluate the effect of this modification in the cell internalization of compound **2-1** (GlcNAc-PI), compound **2-1** was peracetylated (peracetylated GlcNAc-PI, prepared by a former colleague) and used to treat PIGA-KO HEK293 cells (Figure 2-3b). Cells treated with peracetylated **2-1** also showed a rescue of the GPI-APs biosynthesis in a dose-dependent manner; however, this compound showed lower activity than GlcNAc-PI **2-1** (Figure 2-3c). It is not clear if the peracetylation improved the compound's ability to cross the cell membrane and how much the removal of the acetyl groups by intracellular esterases affected the compound incorporation into biosynthesis. Thus, a combination of these two processes might have decreased the rescue efficiency of peracetylated **2-1**. Further studies are in progress by the Kinoshita group to determine the mechanistic steps involved in the compound **2-1** activity. Based on its activity, compound **2-1** is an ideal candidate for future *in vivo* studies and a reference structure to compare the activity of the other designed glycolipids to rescue GPIs biosynthesis.

An efficient incorporation of compound **2-1** and the GPI biosynthesis rescue was corroborated determining that the detected cell surface proteins were indeed GPI-APs. The levels of CD59 and DAF proteins was analyzed after treating the cells with phosphoinositol-specific phospholipase C (PI-PLC), an enzyme that cleaves at the phosphoinositol and release proteins from the membrane that are connected via a GPI (Figure 2-4a). The expression of CD59 and DAF was sensitive to

treatment with the PIPLC with nearly complete removal of CD59 and partial removal of DAF from the membrane, which confirmed that they were expressed as GPI-APs (Figure 2-4b).

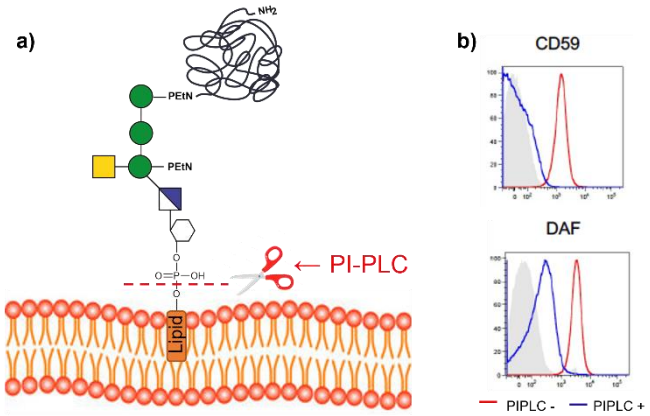

Figure 2-4. a) Graphic representation of GPI-AP cleavage by phosphoinositol-specific phospholipase C (PI-PLC). b) FACS analysis of the PI-PLC effect on cells treated with compound **2-1.** The *y*-axis shows cell counts; the *x*-axis shows fluorescence intensity.

The activity of GPI-fragment **2-2** (GlcN-PI) to rescue GPI-APs biosynthesis in PIGA-KO HEK293 cells was analyzed and compared to fragment **2-1** (GlcNAcPI). PIGA-KO HEK293 cells were treated with concentrations between 0.25 µM and 50 µM of glycolipids **2-1** and **2-2** (Figures 2-5a and b). Compound **2-2** also restored the expression of GPI-APs on the surface of the treated cells, although it was less efficient than **2-1** (Figure 2-5d). Pulse-chase analysis using compounds **2-1** and **2-2** in PIGA-KO cells was performed to compare their efficiencies further. The cells were incubated for 1 h with 10 µM of the corresponding compound at 4 °C; the cells were washed and then cultured at 37 °C for various periods to chase restoration of CD59. Compounds **2-1** and **2-2** showed different levels of CD59 production, but they showed similar kinetics of CD59 expression in which CD59 appeared after 1.5 hours and settled after 5-6 hours of culture (Figure 2-5e). It is not clear which factors reduced the activity of compound **2-2** compared to **2-1**, so further studies are necessary to evaluate the effects of the zwitterionic character of **2-2** and the introduction of modifications to improve the incorporation of this glycolipid into the GPI biosynthesis.

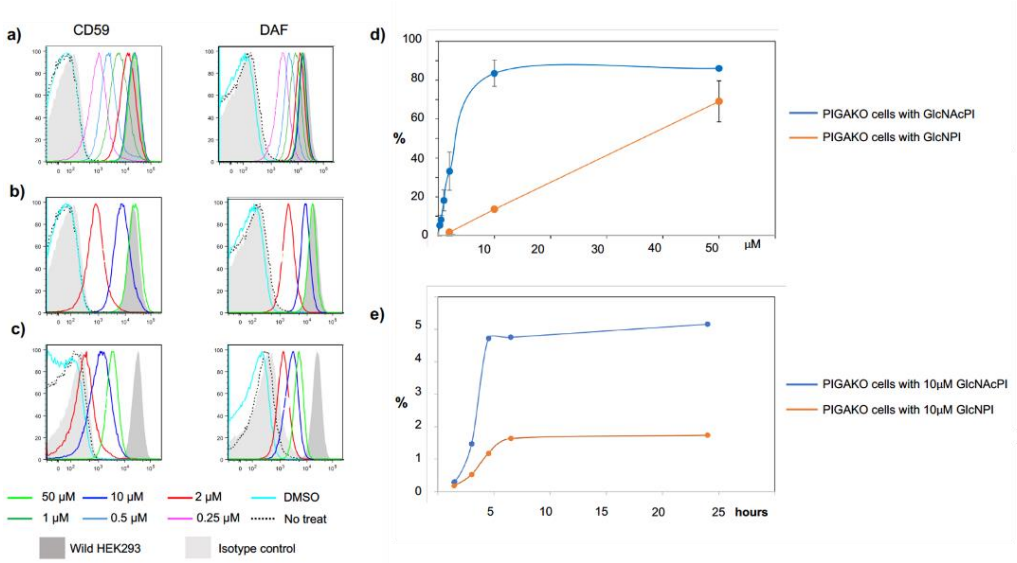

Figure 2-5. Determination of GPI-APs by flow cytometry after treatment of PIGA-KO HEK293 cells with compound **2-2** (GlcN-PI) and compound **2-1** (GlcNAcPI)**.** a) Restoration of CD59 and DAF expression on PIGA-KO cells after 24 h incubation with compound **2-1**; b) Restoration of CD59 and DAF expression on PIGA-KO cells after 24 h incubation with compound **2-2**; c) Restoration of CD59 and DAF expression on PIGL-KO cells after 24 h incubation with compound **2-2**; d) Percent CD59 restoration of wild-type cells at various concentrations of compounds **2-1** and **2-2** calculated from the fluorescence intensity in histograms (a and b); e) Percent restorations of CD59 expression were plotted at various time points. Histograms in (a−b): *y*-axis shows cell counts; the *x*-axis shows fluorescence intensity. The values plotted in charts (c) and (e) result from duplicate experiments.

The GPI-APs biosynthesis rescue was next evaluated on HEK293 cells having a knockout for the PIGL gene (PIGL-KO), which compromises the second step of the biosynthesis. PIGL-KO HEK293 were treated with glycolipid **2-2** (GlcN-PI), and the GPI-APs expression was analyzed. Synthetic GPI-fragment **2-2** also restored GPI-APs biosynthesis in PIGL-KO cells in a concentration-dependent manner. However, it showed lower activity in PIGL-KO than in PIGA-KO cells (Figure 2-5c). The lower rescue activity in PIGL-KO cells was attributed to an accumulation of the endogenous intermediate after the first step, which may inhibit the incorporation of synthetic intermediate **2-2** that should be flipped into the luminal side of the ER to continue the biosynthesis process. Little is known about the mechanisms involved in the GPI-intermediates flip from the cytoplasmic side to the luminal side of the ER membrane;[93] thus, further studies are still required to understand the differentiated activity of compound **2-2** in PIGA-KO and PIGL-KO cells.

The activity of glycolipids **2-3** and **2-4** was next evaluated to rescue the third and fourth steps of the GPI biosynthesis. Glycolipid **2-3** (GlcN-acylPI) was tested to restore GPI-APs expression in PIGW-KO cells, when the first step into the ER lumen is affected. In this step, PIGW catalyzes

the acylation of the 2-O position of inositol with a fatty acid. Surprisingly, the trilipidated compound **2-3** was not able to restore the expression of GPI-APs in PIGW-KO cells (Figure 2-6a bottom), suggesting that **2-3** is not an appropriate substrate for PIGW, or the compound cannot reach the luminal side of the ER, where the affected step takes place. Following this, we decided to determine whether the next step of GPI biosynthesis, also taking place in the ER lumen (mannosylation of the pseudodisaccharide by PIGM), could be restored by the incorporation of the synthetic GPI-fragment **2-4**. Unfortunately, treatment of PIGM-KO HEK293 cells with pseudotrisaccharide **2-4** did not rescue the surface expression of GPI-APs, suggesting that this synthetic GPI-Fragment was also unable to enter the ER lumen (Figure 2-6b bottom).

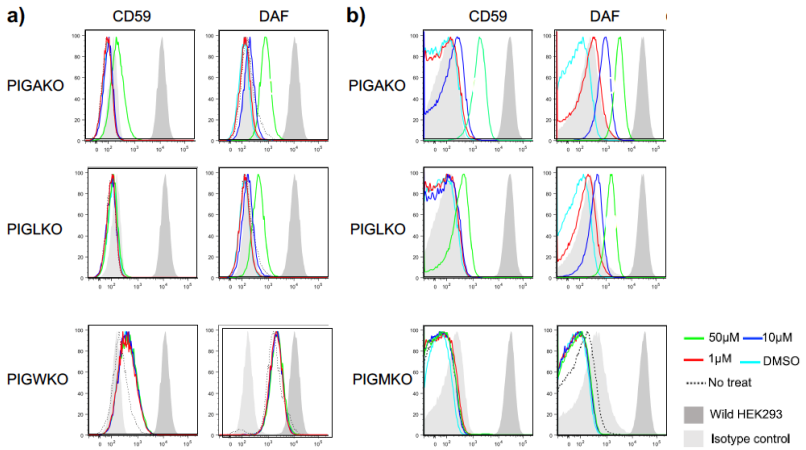

Figure 2-6. Determination of GPI-APs by flow cytometry after treatment of PIGA-, PIGL-, PIGW, and PIGM-KO cells with GPI-fragments **2-3** (GlcN-acylPI) and **2-4** (Man-GlcN-PI)**.** a) CD59 and DAF expression on PIGA-, PIGL- and PIGWKO cells after 24 h incubation with compound **2-3** b) CD59 and DAF expression on PIGA-, PIGL- and PIGMKO cells after 24 h incubation with compound **2-4**. Histograms in (a−b): *y*-axis shows cell counts; the *x*-axis shows fluorescence intensity.

To determine if compounds **2-3** and **2-4** entered the cells, the activity of these compounds in PIGA-KO and PIGL-KO cells was also evaluated. These fragments very weakly restored GPI-APs on both PIGA-KO cells and PIGL-KO cells (Figure 2-6a and 2-6b) with an activity 1/100 to 1/20 times lower than from compounds **2-1** and **2-2**. This corroborates that the fragments are entering the cell. But like peracetylated compound **2-1**, the reduced rescue activity of compounds **2-3** and **2-4** indicates the need for intracellular modifications of **2-3** and **2-4** before they can enter biosynthesis. These processes include the removal of inositol acylation from compound **2-3** by esterases or of the mannose unit from compound **2-4** to produce small amounts of compound **2-2** (GlcN-PI). Thus, only the small quantities of fragment **2-2** formed into the cells by degradation from **2-3** or **2-4** rescued the biosynthesis, explaining the low activity observed.

The difference in activity between the synthetic GPI fragments **2-1**/**2-2** and **2-3**/**2-4** correlated with the localization of the affected steps of the GPI biosynthesis. The rescue was efficient for the steps on the cytoplasmic side of the ER membrane but failed for the processes in the ER lumen. This suggests a lack of insertion into the ER membrane or the absence of the required transport or flip into the lumen of the ER for fragments **2-3** and **2-4**.

Additional approaches to support the incorporation of fragments **2-3** and **2-4** were evaluated, and rescue experiments with glycolipids **2-1**, **2-3**, and **2-4** were performed using either streptolysin O from Hemolytic streptococcus or formulation in liposomes to increase cell membrane permeability. Unfortunately, only glycolipid **2-1** presented activity under these conditions, which corroborates that crossing the ER membrane might be the limiting factor for the incorporation of glycolipids **2-3** and **2-4** into the GPI biosynthesis.

2.5.3 Additional Glycolipid design

Two structural modifications were envisioned to gain a better understanding of the structure-activity relationship of the glycolipids **2-1** (GlcNAcPI) and **2-2** (GlcNPI) and to evaluate the impact on their activity. Glycolipids **2-49** and **2-50** were designed to have 1,2-distearoyl-*sn*-glycerophosphate as a lipid moiety (Figure 2-7). Previous reports assigned that the unsaturation in the phospholipid tail of some parasitic GPIs might be responsible for their immunoreactivity.[70,71] The absence of unsaturation in the lipid part could provide insights into the role of the double bond in the activity of the compounds and the relevance of the lipid moiety in GPI biosynthesis. In addition, unpublished lipidomic analysis by our collaborators at Osaka University showed GPI substrates having a 1-alkyl-2-acyl-*sn*-glycerophosphate (AAG) with either 18:0e/22:6 or 16.0e/22.6 chains are preferentially used from the second step of the biosynthesis in HEK293 cells. It is important to determine if the AAG variants of **2-1** and **2-2** have higher incorporation and activity to rescue GPI-APs biosynthesis. Thus, glycolipids **2-51** and **2-52** were designed to have a 1-octadecanoyl-2-oleoyl-*sn*-glycerophosphate to resemble the substrates preferred by PIGL and PIGW (Figure 2-7).

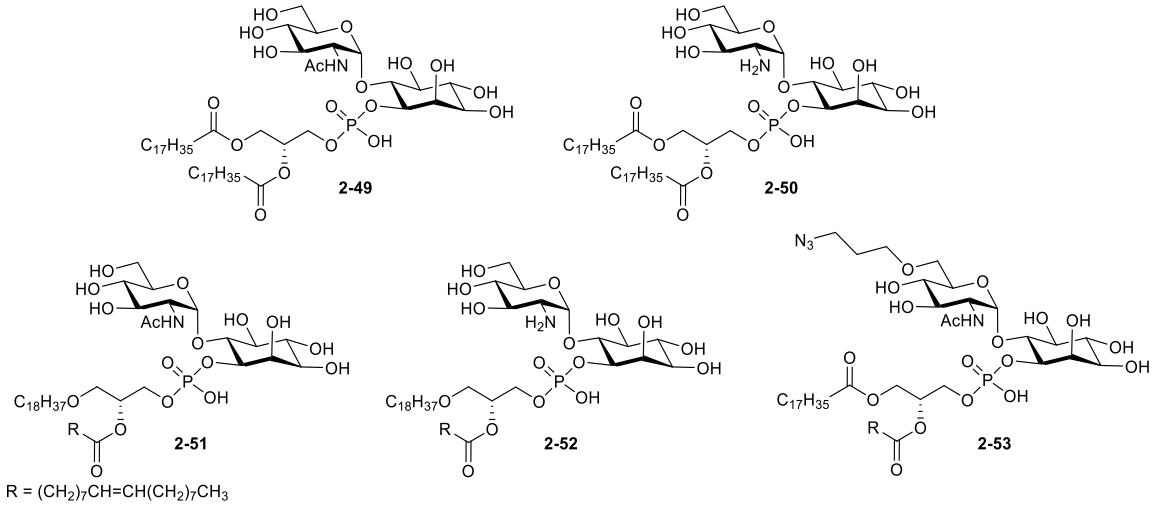

Figure 2.7 Additional designed GPI fragments to rescue GPI biosynthesis.

Additionally, fragment **2-53** bearing an azido propyl group in the 6-O position of glucosamine was designed to study the mechanisms and pathways involved in the incorporation of synthetic fragments into the GPI biosynthesis (Figure 2-7). The 6-O position of glucosamine was selected for the modification because it is easy to modify following the used synthetic route and it should not disturb the GPI biosynthesis since the glycan core elongation occurs through the 4-O position of glucosamine. The presence of the azido group in **2-53** would allow tracking of the compound, from the cell surface to the ER, in the various knockout cells using cycloaddition reactions to stain the treated cells. These studies could also give insights about the process hindering the transport of compounds **2-3** and **2-4** into the luminal side of the ER, and provide information about which structural modifications or transport mechanisms can be implemented for synthetic GPI fragments to increase their activity and transport in cells.

2.5.4 Synthesis of GPI-fragments 2-49 to 2-53

The retrosynthetic analysis presented in scheme 2-1 was also applied for the synthesis of GPI fragments **2-49** to **2-53**. However, two new H-phosphonates were required. Preparation of glycolipids **2-49** and **2-50** requires the saturated H-phosphonate **2-55** (Scheme 2-11). Glycolipids **2-51** and **2-52** require the H-phosphonate **2-59** with an alkyl acyl glycerol instead of the diacylglycerol used for all other GPI fragments (Scheme 2-11). H-phosphonate **2-55** was synthesized in 81% yield by phosphitylation of commercially available (S)-(+)-1,2-distearoyl-*sn*-glycerol **2-54** using phosphorous acid and pivaloyl chloride activation. The preparation of H-phosphonate **2-59** involved three steps. First, a selective alkylation of the diol **2-27** *via* tin-acetal, and acylation of the remaining alcohol with oleic acid under Steglich esterification conditions to furnish **2-57** in 80% yield over two steps. Next, the PMB group was removed under oxidative conditions with DDQ,

and the resulting alcohol was phosphitylated using phosphorous acid with pivaloyl chloride activation to afford H-phosphonate **2-59** (Scheme 2-11).

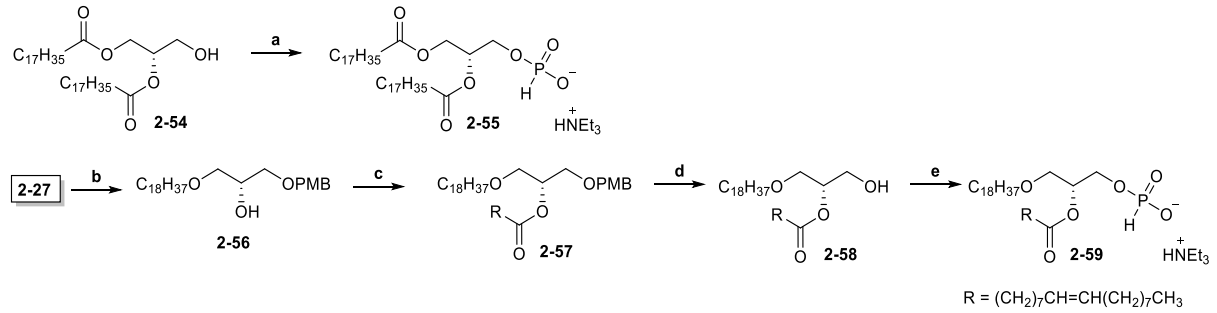

Scheme 2-11. Synthesis of H-phosphonates **2-55** and **2-59**. *Reagents and conditions*: a) H_3PO_3, PivCl, pyridine, r.t., O.N., 81%; b) *i.* $(Bu_2Sn)O$, toluene, reflux, 2.5 h; *ii.* $C_{18}H_{37}Br$, CsF, r.t., 20 h, 90%; c) Oleic acid, DIC, DMAP, DCM, r.t., 3 h, 89%; d) DDQ, DCM/H_2O, r.t., 1 h, 78%; e) H_3PO_3, PivCl, pyridine, r.t., 1 h, 40%.

The synthesis of glycolipids **2-49** and **2-50** began with the two-step phospholipidation of the pseudodisaccharide **2-33** using the H-phosphonate **2-55** to deliver the fully protected glycolipid **2-60** (Scheme 2-12). Then, the Nap groups were removed with DDQ, and the azide was reduced to give GPI fragment **2-50** in 40% yield. For the preparation of the glycolipid **2-49**, the azide in **2-60** was reduced and the resulting amine was acetylated in a two-step protocol to yield the fully protected pseudodisaccharide **2-61**. Next, removal of the Nap ethers by treatment with DDQ provided the glycolipid **2-49** in 53% yield over three steps.

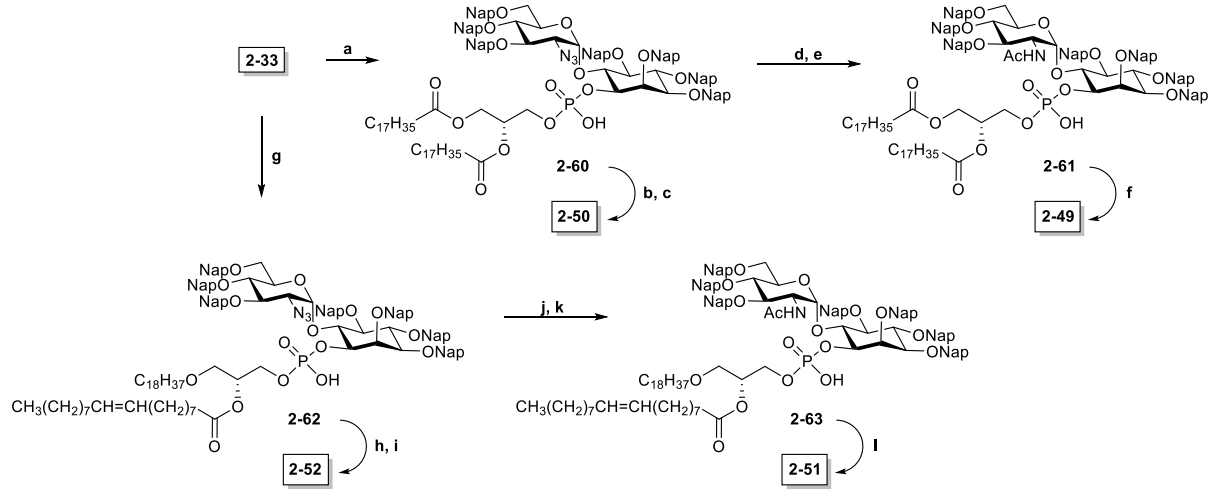

Scheme 2-12. Synthesis of GPI-fragments **2-50** to **2-52**. *Reagents and conditions*: a) *i.* **2-55**, PivCl, pyridine, r.t., 1 h; *ii.* I_2, H_2O, r.t., 1 h, 75%; b) DDQ, MeOH/DCM, r.t., 5.5 h; c) $P(CH_3)_3$, THF, r.t., 3 h, 40% (two steps); d) $P(CH_3)_3$, THF, r.t., 1 h; e) Ac_2O, pyridine, r.t., 1 h; f) DDQ, MeOH/DCM, r.t., 8 h, 53% (three steps) g) *i.* **2-59**, PivCl, pyridine, r.t., 1 h; *ii.* I_2, H_2O, r.t., 1 h, 82%; h) DDQ, MeOH/DCM, r.t., 5 h; i) $P(CH_3)_3$, THF, r.t., 30 min, 69% (two steps); j) $P(CH_3)_3$, THF, r.t., 1 h; k) Ac_2O, pyridine, r.t., 35 min; l) DDQ, MeOH/DCM, r.t., 5 h, 71% (three steps).

To prepare glycolipids **2-51** and **2-52**, pseudodisaccharide **2-33** was phospholipidated using the H-phosphonate **2-59** and oxidated with iodine and water to give the fully protected glycolipid **2-62** (Scheme 2-12). Contrary to the previous glycolipids, purification of the *O*-deprotected glycolipid after removal of the Nap protecting groups with DDQ was performed by manual LH-20 size exclusion chromatography using a 1.2 m x 2 cm column eluting with MeOH/$CHCl_3$/H_2O 3:3:1. This system improved the solubility of the product, which eluted without significant diffusion through the column. After Staudinger reduction of the azide, an additional purification step involving size exclusion chromatography to remove trimethyl phosphine oxide followed by trituration with methanol to remove the remaining yellow impurities delivered GPI fragment **2-52** in good yield (69%**,** two steps). Finally, a three-step protocol including reduction of the azide, amine acetylation, and removal of the Nap groups afforded the glycolipid **2-51** from **2-62** in 71% yield. The improved yield compared to the previous glycolipids is attributed to the change in the eluting system for the removal of excess DDQ and its by-products, which avoided product lost during the column due to a higher solubility of the deprotected glycolipid in the solvent mixture

The synthesis of the azido-alkylated fragment **2-53** started from triol **2-32** and required the introduction of an orthogonal protecting group at the 6-O position of glucosamine for azidopropyl chain installation in a later stage (Scheme 2-13). Initially, a trityl ether was selected as the orthogonal protecting group for the 6-O position of glucosamine; however, the steric hindrance of trytil difficulted the introduction of 2-naphthylmethyl ether groups in the 3-O and 4-O positions. Therefore, protection of the primary alcohol of **2-32** was done using the TBDMS group by treatment of **2-32** with TBDMS chloride and imidazole. Following 2-naphthylmethylation of the remaining hydroxy groups under Williamson conditions delivered the fully protected pseudodisaccharide **2-65**. Reduction of the azide with trimethylphospine in THF and subsequent acetylation of the free amine to yield **2-66** was done at an early stage of the route—prior to the introduction of the azidopropyl moiety—since it would not be possible to selectively reduce one of two azides in the structure. The primary alcohol in **2-66** was deprotected using TBAF and alkylated with freshly prepared 2-azidopropyl trifluoromethanesulfonate and NaH as base to afford the fully protected pseudodisaccharide **2-68** in 82% yield over two steps. The allyl group was removed using palladium chloride in methanol, and the resulting alcohol was phospholipidated using the H-phosphonate **2-8** to furnish the glycolipid **2-70**. Finally, removal of the 2-naphthylmethyl protecting groups under oxidative conditions delivered GPI-fragment **2-53** in a good yield of 73% over two steps.

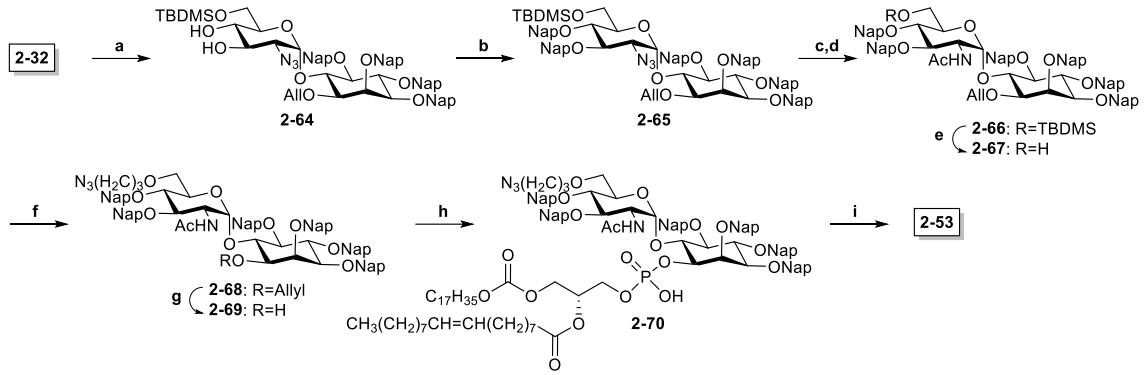

Scheme 2-13. Synthesis of GPI-fragments **2-53**. *Reagents and conditions*: a) TBDMSCl, imidazole, THF, r.t., 6 h, 94%; b) NapBr, TBAI, NaH, DMF, 50 °C, O.N., 70%; c) $P(CH_3)_3$, THF, r.t., 1.5 h; d) Ac_2O, pyridine, r.t., 1.5 h, 55% (two steps); e) TBAF, THF, r.t., 4 h, 86%; f) $TfO(CH_2)_3N_3$, NaH, THF, r.t., 2.5 h, 96%; g) $PdCl_2$, DCM/MeOH, r.t., 7 h, 77%; h) *i.* **2-8**, PivCl, pyridine, r.t., 2 h; *ii.* I_2, H_2O, r.t., 50 min; i) DDQ, MeOH/DCM, r.t., 5 h, 73% (two steps). TBDMS = *tert*-Butyldimethylsilyl chloride.

2.5.5 Preliminary Results: Recovery of GPI-APs Biosynthesis with fragments 2-49 to 2-53

The activity of compounds **2-49** and **2-50** to rescue GPI-APs biosynthesis in PIGA-KO HEK293 was evaluated. Both GPI fragments were able to rescue GPI-APs expression on the cell surface in a concentration-dependent manner (figure 2-8 a and b). Like fragments **2-1** and **2-2**, fragment **2-49** with acetylated glucosamine presented higher activity than compound **2-50** having a free amine. However, the difference in activity was higher than the observed between **2-1** and **2-2**. This result was unexpected considering that GlcNAc-PI is desacetylated to GlcN-PI in the ER during the first biosynthesis step. It was expected that a negative effect should result in GlcN-PI with saturated lipids having a similar activity to GlcNAc-PI with saturated lipids. Since this was not the case, it is conceivable that the zwitterionic character of **2-50** has a major effect in its incorporation into the GPI biosynthesis compared to **2-2**, but further studies are required to determine the factors reducing the activity of GPI-fragment **2-50** compared to **2-49**.

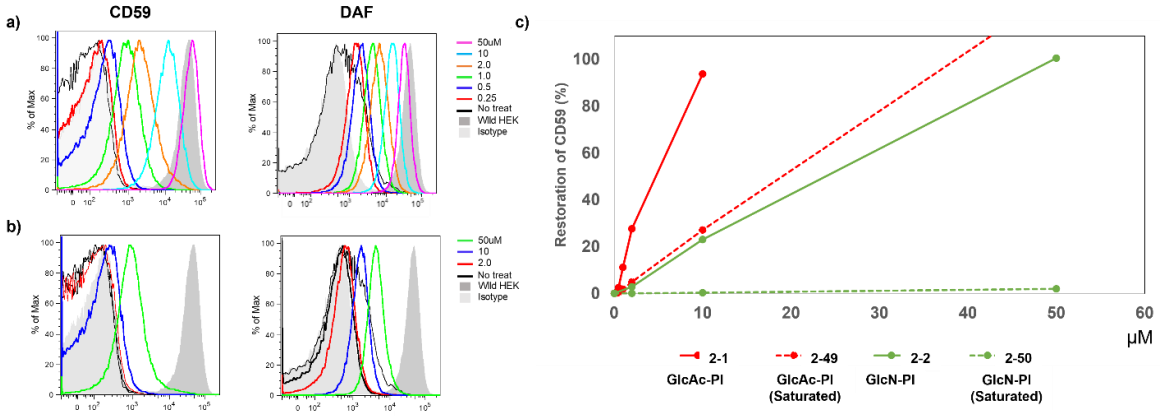

Figure 2-8. Determination of GPI-APs expression by flow cytometry after treatment of PIGA-KO HEK293 cells with GPI-fragments **2-49** (GlcNAc-PI, saturated) and **2-50** (GlcN-PI, saturated)**.** a) CD59 and DAF expression on PIGA-KO cells after 24 h incubation with compound **2-49** b) CD59 and DAF expression on PIGA-KO cells after 24 h incubation with compound **2-50**. C). Percent CD59 restoration of wild-type cells at various concentrations of compounds **2-1**, **2-2**, **2-49** and **2-50** calculated from the fluorescence intensity Histograms in (a and b) and Histograms in Figure 2-5 (a and b). Histograms in (a and b): *y*-axis shows cell counts; the *x*-axis shows fluorescence intensity.

GPI-fragments **2-49** and **2-50** bearing saturated lipids were less active in the rescue of GPI biosynthesis than fragments **2-1** and **2-2** having unsaturation in the lipid part, confirming that the presence of the double bond has an important effect on the incorporation of the synthetic glycolipids in the GPI biosynthesis. However, further studies are still necessary to determine the factors inducing activity reduction. Two potential factors could be a less effective transport of these compounds to the ER surface, or the need of lipid remodeling in GPI fragments with saturated lipids before they enter the biosynthesis.

The biosynthesis of GPI-APs was also rescued with compound **2-53** (N_3 GlcNAc-PI). However, this compound also showed lower activity compared to its unmodified analogue **2-1** (GlcNAc-PI) (figure 2-9). Although the biosynthesis generally does not involve the O-6 position of glucosamine, it is possible that the azido propyl modification affected the process by steric hindrance reducing the compound acceptance by the enzyme processing this intermediate. Current studies are focused on determining whether the observed activity is from **2-53** or derived from its intracellular conversion into **2-1**, which will lack the azide for a click reaction with alkynes fluorophore. Despite the lower activity, compound **2-53** is still a useful compound to evaluate the GPI fragments transport to the ER surface. These experiments have been in process during the preparation of this document and will be published in due time.

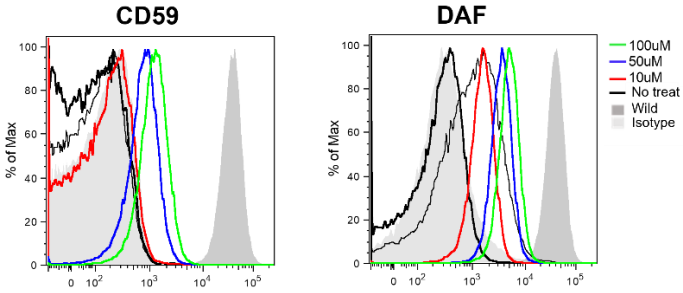

Figure 2-9. Determination of GPI-APs by flow cytometry of PIGA-KO HEK293 cells after overnight incubation with compound **2-53** (N_3 GlcNAc-PI). Histograms: *y*-axis shows cell counts; the *x*-axis shows fluorescence intensity.

2.5.6 Additional Application of the Synthetic GPI-Fragments

Besides the successful application for GPI biosynthesis deficiencies rescue, the synthetic GPI fragments **2-1** and **2-2** have been employed by our collaborators at the University of Osaka to elucidate other steps of GPI biosynthesis. Several enzymes involved in the transfer of monosaccharides and other substrates for the GPI glycan elongation have been identified and characterized.[12,45] However, the genetic bases for the translocation of GlcN-PI from the cytoplasmic to the luminal side of the ER have been unknown for the past decades, mainly because a mutant cell line defective in this step has never been obtained.[12] After treatment of PIGA-knockout cells with the synthetic fragment **2-1**, a genome-wide CRISPR knockout screen of genes required for rescuing the GPI-APs expression was performed, and the ER-resident multipass membrane protein CLPTM1L was identified as a GlcN-PI scramblase required for efficient GPI biosynthesis.[93] A CLPTM1L knockout from PIGA-KO cells reduced the GPI-APs biosynthesis rescue efficiency of GPI-fragments **2-1** and **2-2** (Figure 2-10). Since the efficiency was not completely lost, it is still possible that another protein acts redundantly with CLPTM1L to flip GlcN-PI into the luminal side of the ER.[93] This functional redundancy explains previous failures in identifying the enzyme responsible for this step, and these findings constitute important progress in the understanding of GPI biosynthesis and lipid scrambling. The results of these studies were recently published and are out of the scope of this thesis, so they will now be further discussed in detail.[93]

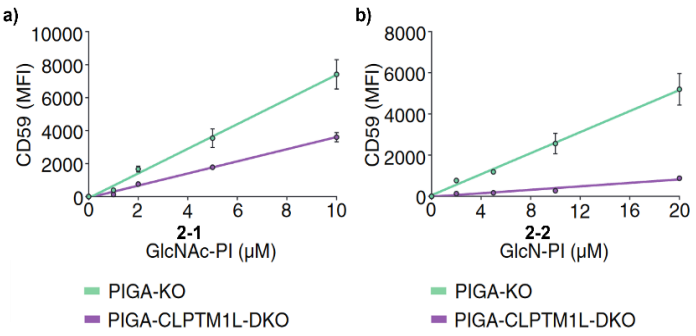

Figure 2-10. Restoration of CD59 expression in PIGA-KO and CLPTM1L-PIGA-DKO cells after treatment with GPI-fragments **2-1** (GlcNAc-PI) and **2-2** (GlcN-PI). a) Restoration of CD59 expression in PIGA-KO and CLPTM1L-PIGA-DKO cells in the presence of various concentrations of compound **2-1**; b) Restoration of CD59 expression in PIGA-KO and CLPTM1L-PIGA-DKO cells in the presence of various concentrations of compound **2-2**. MFI = mean fluorescence intensity; DKO = double knockout.

2.6 Conclusion and Outlook

A library of nine glycolipids resembling the initial intermediates of the GPI biosynthesis in eukaryotes was designed and synthesized. The assembly required a set of orthogonally protected building blocks that provided flexibility to accommodate further moieties and structural modifications to the targeted fragments such as an additional monosaccharide, acyl chain or an azido group. The 2-naphthylmethyl ethers used as permanent protecting groups proved to be orthogonal to the acyl esters, allyl ethers, silyl ether, and PMB ether required during the glycan assembly and other manipulations that were employed during the synthesis process. Oxidative conditions for removal of the permanent protecting groups with DDQ were optimized to preserve the unsaturation in the lipid part, affording the desired GPI-fragments in good to moderate yields. In addition, the Staudinger reaction was found to be the best alternative for azide reduction in the presence of unsaturated phospholipids. Outstanding purity of the final compounds for biological investigation was achieved by developing a purification protocol involving size exclusion chromatography and trituration with methanol. The column length and solvent selection were crucial for the efficient removal of excess of DDQ and its by-products and recovery of the desired deprotected glycolipid. The conditions for the assembly, global deprotection and purification of the glycolipids were transferable within all different GPI-fragments, proving the versatility of the developed methods.

The GPI fragments showed biological activity to rescue GPI biosynthesis deficiencies caused by mutations affecting the enzymes involved in the first two steps of the biosynthesis. PIGA-, PIGL-, PIGW-, and PIGM-KO HEK293 cells were treated with micromolar concentrations of the synthetic

GPI-fragments. Rescue of two GPI-APs (CD59 and DMF) expression was observed only in cells having knock out genes affecting the biosynthesis steps on the cytoplasmic side of the ER. GPI-fragments **2-1** and **2-2** were efficiently incorporated into the treated cells and restored the GPI-APs expression, suggesting them as suitable targets for the development of glycan-based treatments for IGD pathologies. Further structure-activity relationship studies are still required to decipher the mechanisms involved in the compounds activity and provide data before proceeding with *in vivo* evaluations of these compounds. Preliminary results with compounds **2-49** and **2-50** revealed that the absence of unsaturation in the lipid may negatively affect the incorporation of the glycolipids into the GPI biosynthesis. Thus, two additional compounds (**2-51** and **2-52**) were synthesized to evaluate further the lipid composition effect in the activity. In addition, an azide-labeled fragment **2-53** was synthesized to perform tracking and mechanistic studies on the GPI-APs expression rescue. Although fragment **2-53** showed lower efficiency than **2-1**, cells cultured with this compound can be stained using click chemistry to follow its incorporation to the GPI biosynthesis.

The fragments **2-3** and **2-4** were unable to reach the luminal side of the ER and enter the GPI biosynthesis. New carrier systems such as nanoparticles and nanodrops should be evaluated for the transport of **2-3**, **2-4** and bigger GPI-fragments glycolipids to the ER. In addition, using compounds **2-49** to **2-53** we expect to find information about structural modifications and support transport mechanism studies or evaluate delivery systems that will take them into the ER.

3 Total synthesis of a GPI of *Plasmodium falciparum*

3.1 Introduction

3.1.1 Plasmodium falciparum and Malaria

Malaria is a serious and fatal infectious disease in humans caused by five species of single-celled eukaryotic *Plasmodium* parasites. The disease is endemic in tropical regions and is transmitted by the bite of around 40 species of the *Anopheles* mosquito.[94–96] The severity and consequences of malaria symptoms depend on the *Plasmodium* species causing the infections and on host factors such as level of immunity and general health status. Malaria is a chronic disease tending to relapse or gets worse over months or years, and it can be classified as asymptomatic, uncomplicated, or severe. The initial symptoms usually include mild fever, muscle ache, shaking chills, anorexia, and nausea, and can progress to febrile attacks—also known as malarial paroxysms—occurring at either 48- or 72-hour intervals. The attacks include a cold stage with shivering and the sensation of cold, a hot stage with fever, muscle ache, and nausea, and a sweating stage accompanied by exhaustion. Severe malaria occurs when the infection is complicated by organ failures or abnormalities in the patient's blood or metabolism; It is often deadly and manifests as severe anemia, pulmonary complications, hypoglycemia, or cerebral malaria.[97] The latter is the most severe neurological complication of the infection and results in abnormal behavior, seizures, coma, or other neurologic abnormalities. Cerebral malaria is responsible for most malaria-related deaths globally, causing 15–20% mortality and the development of long-term neurological deficits for survivors.[97,98]

According to the World Health Organization, nearly half of the world's population was threatened by malaria in 2020, representing a significant public health problem in resource-limited areas in Africa, Asia, and Central and South America.[99,100] Malaria has caused hundreds of thousands of deaths worldwide and represents an exceptionally high risk for children, pregnant women, and immunosuppressed people.[94–96] *Plasmodium falciparum* and *Plasmodium vivax* are the most common parasite species responsible for malaria transmission to humans.[94] *Plasmodium falciparum* is the most dangerous species as it is responsible for cerebral malaria and is associated with complications in pregnancy.[94] Infection with *P. falciparum* causes most malaria-associated morbidity and mortality in sub-Saharan Africa and, in general, most malaria-related deaths.[94]

The life cycle of *Plasmodium* parasites is almost the same for all five species. It can be divided into three stages: infection of a human with sporozoites, asexual and sexual reproduction. A human infection starts when an infected female anopheline bites a person for a blood meal and

injects—along with anti-coagulating saliva—the *Plasmodium* parasites in the stage of sporozoites (Figure 3-1). Once in the human bloodstream, the asexual cycle stage begins and can be divided into the pre-erythrocytic phase and the erythrocytic phase. In the pre-erythrocytic phase, the sporozoites migrate within 30 to 60 minutes from the bloodstream to the liver and infect the hepatocytes, where they start mitotic (asexual) replication. This process takes up to two weeks and doesn't cause malaria symptoms. After this period, the liver cells rupture, releasing thousands of *Plasmodium* parasites in the stage of merozoites, which break out of the liver and reenter the bloodstream to start the erythrocytic phase. They invade red blood cells, grow, and reproduce asexually, destroying the blood cell and subsequentially inducing malaria symptoms.

During the replication in the red blood cells, instead of producing new merozoites, some of the merozoites develop into gametocytes, marking the start of the sexual stage of the life cycle. The gametocytes concentrate in the human skin capillaries and are taken up by a mosquito vector during a bite for a blood meal. In the mosquito's gut, the *Plasmodium* male and female gametocytes mate and undergo meiosis. After migration through the midgut wall, oocysts are formed, in which thousands of *Plasmodium* parasites in the stage of sporozoites develop, beak free, and migrate to the salivary glands of the mosquito, where they wait to be injected into the next human host and restart the cycle.[94–96,101]

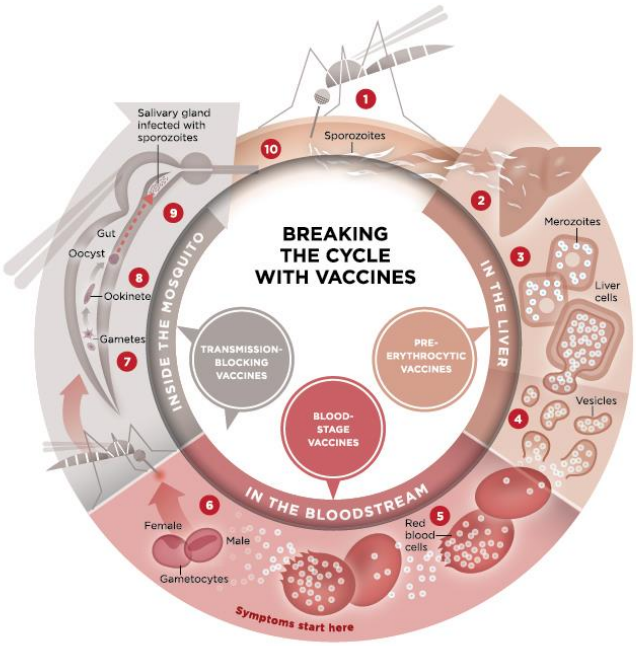

Figure 3-1. The life cycle of the malaria parasites.[102]

Different control approaches have been implemented to address the propagation of the *Plasmodium* parasites, including insecticide spraying, destruction of *Anopheles* mosquitos breeding grounds, and insecticide-treated beds.[94] These efforts have reduced the number of infections in some areas; however, malaria remains one of the most severe infectious diseases, with

approximately 241 million cases in 2020, increasing from 227 million in 2019 and 95% of the cases coming from Africa.[99]

Malaria can be suspected based on the patient's symptoms, travel history, or place of residence, and it is confirmed by laboratory blood tests to detect the parasites.[95] Currently, artemisinin-based combination therapies (ACT) are widely applied due to their high efficiency in treating uncomplicated malaria. Still, the emergence of artemisinin-resistant *Plasmodium falciparum* strains is limiting their use.[95,96,103] Due to the spread of drug-resistant parasites and insecticide-resistant *Anopheles* mosquitos, efforts to eradicate the *Plasmodium* seem impossible. Therefore, developing a highly efficient malaria vaccine is critical for malaria control activities.

Many malaria vaccines are designed to provide immunity against proteins expressed by the parasites. However, the development of these vaccines is particularly challenging due to the genetic complexity of the parasite, which presents thousands of antigens to the human immune system. In addition, the parasite changes through the different life stages in humans, exhibiting antigenic variations at each stage of its life cycle (Figure 3-1). Finding the right target for vaccine development represents a major challenge. Many different malaria vaccines have been developed, and many more are in clinical trials.[104–108] The most advanced and studied candidate is the RTS,S/AS01 vaccine that incorporates a recombinant protein with parts of the *P. falciparum* circumsporozoite protein. However, this vaccine has an efficacy of just 40% and doesn't provide long-term protection.[94]

3.1.2 GPIs of Plasmodium falciparum

Throughout its life cycle, *P. falciparum* produces several free GPIs and GPI-APs essential for its development and survival; GPI-anchoring constitutes around 95% of the carbohydrate modification in *P. falciparum* proteins.[109,110] *P. falciparum* GPIs (*Pf*-GPIs) that are either released into the patient's blood or anchored on the parasite membranes function as a prominent pro-inflammatory endotoxin in malaria and induce the inflammatory cytokines TNF-a and IL-1 that might be responsible for malarial pathology.[111–113] It has also been hypothesized that malarial GPIs contribute to hypoglycemia by mimicking the action of insulin.[114] In light of these findings, *Pf*-GPIs have been considered potential targets for developing an antitoxin malaria vaccine. Indeed, malaria-exposed individuals from malaria-endemic regions with a certain level of naturally acquired immunity to malaria pathogenesis possess a high level of anti-GPI antibodies in their blood, which increase with age and during malaria seasons.[112,115–118]

The structure of the GPIs anchoring proteins to the cell membrane and the free GPIs are highly conserved within the *Plasmodium* species. The *Pf*-GPIs incorporate two main modifications to the pseudopentasacchride core preserved in eucaryotes: an acyl chain at the O-2 position of the

inositol unit and an additional unsubstituted-mannose at the non-reducing end of the glycan core. At the same time, the free GPIs probably lack this Man-IV elongation (Figure 3-2).[13,119] The constitutive identity of the lipid moieties of *Pf*-GPIs is diverse, with chains of different lengths and degrees of unsaturation. In the case of the acylation at the O-2 position of the inositol, it incorporates a palmitoyl chain predominantly and, less often, a myristoyl chain. The phospholipid moiety is a diacylglycerol with a saturated chain at the *sn*-1 and an unsaturated chain at the *sn*-2 position. The chain length at the *sn*-1 position is diverse, but it is mainly a C18:0 chain. In contrast, the size of the *sn*-2 chain remains constant but with a varying number of unsaturations, being C18:1 the most common.[13]

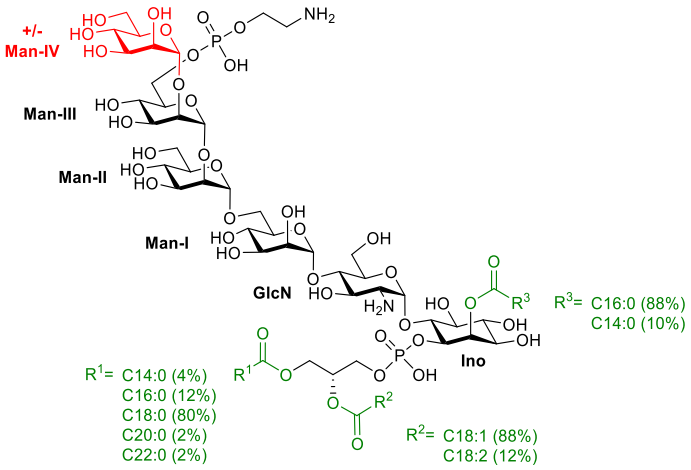

Figure 3-2. Structure and lipid composition of *P. falciparum* GPIs: *P. falciparum* GPIs anchors possess the additional Man-IV unity, while free *P. falciparum* GPIs lack this unit; the heterogenicity of the lipid chains is presented as percentages.

Several studies have used isolated *Pf*-GPIs to evaluate the anti-GPI immune response to protect against malaria. However, the results have been contradictory, probably due to the isolated material's heterogenicity and difference in purity. More reliable results have been obtained using pure and homogeneous synthetic GPIs, [13,64,65,118,120,121] which are helpful for vaccination and can prevent malarial pathology in animal models.[64] For developing such a vaccine, a *Pf*- GPI derivative was chemically synthesized, conjugated to a carrier protein such as maleimide-activated ovalbumin (OVA) or keyhole limpet hemocyanin (KLH), and used to immunize preclinical rodent models. The material was immunogenic and provided substantial protection against malarial pathogenesis and fatalities in mice. Vaccinated mice had a rate of around 70%, while just 0-9% of non-vaccinated mice survived after the infection. Recently, our group conjugated six different synthetic *Pf*-GPI fragments to a carrier protein and evaluated their immunogenicity and efficacy as antimalarial vaccines in mice.[120] This study provided insights into the role of structural modifications of *Pf*-GPIs in their activity. The orientation of the glycan, the number of mannoses in the structure, and the phosphoethanolamine and inositol moieties presence were identified as crucial factors in

the immunogenicity of malarial GPIs; however, the role of the lipid moiety in their activity was not covered.

To understand the structure-activity relationship of the *Pf*-GPIs during parasitic infection, this work aimed to contribute to the field synthesizing the *P. falciparum* GPI derivative **3-1,** having the most common lipid composition, *sn*-1 (C18:0) and *sn*-2 (c18:1), in the phospholipid moiety (Figure 3-3). This derivative should allow a biological activity comparison with the previous results obtained with GPI glycans to provide insights into the lipid moiety's role in *Pf*-GPIs activity. The synthesis of **3-1** requires a general and convergent route to access GPI-bearing unsaturated lipids. Thus, initial efforts focused on synthesizing structures without the acyl chain at the 2-O position of inositol to simplify the strategy design.

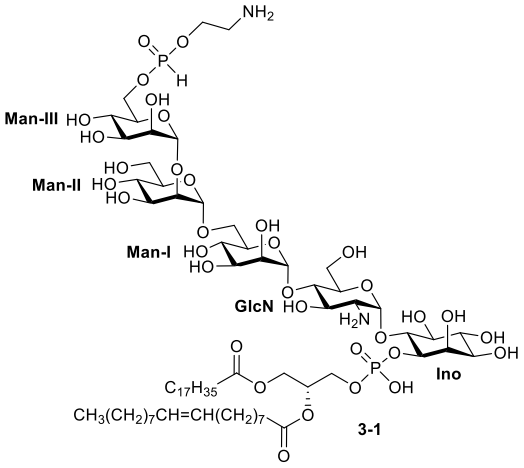

Figure 3-3. Target GPI structure from *P. falciparum* parasites.

3.2 Retrosynthetic analysis

The strategy for the total synthesis of a *Pf*-GPI is based on a general and convergent synthesis of GPIs published by our group in 2013,[58] and a strategy to obtain GPI derivatives with double bonds in the lipid structure.[47,74] Considering that the target GPI bears an unsaturated lipid, the route was adapted to incorporate the protection strategy and optimizations employed in synthesizing the GPI fragments presented in chapter 2. To preserve the unsaturation during the glycan modifications and global deprotection of the molecule, hydroxyl groups protection included a TBDPS silyl ether and an allyl ether for masking the positions requiring late-stage phosphorylation, and the 2-Naphtylmethyl ether (Nap) as permanent protecting group (Scheme 3-1).

The synthesis of GPI **3-1** bearing unsaturated lipids will require the assembly of the pseudodisaccharide **2-46** by glycosylation of *myo*-inositol **2-10** with glucosamine **2-11**, and the synthesis of the trisaccharide **3-4** from the mannose building blocks **3-5** and **3-6** (Scheme 3-1). A [3+2]

glycosylation reaction between the trimannoside **3-4** and the pseudodisaccharide **2-46** will deliver the glycan core **3-2.** Sequential removal of the orthogonal protecting groups and phosphorylations of **3-2** with H-phosphates **2-8** and **3-3** and a final global deprotection will deliver the target GPI structure **3-1**.

Mannose building blocks **3-4** to **3-6** will be equipped with an allyl protecting group on the anomeric position; these allyl glycosides will be converted into a trichloroacetimidate to perform the corresponding glycosylation reactions. The stereoselectivity of glycosylations will be controlled by neighboring group participation of the acetyl groups and the reaction conditions. Phosphorylations will be performed at a late synthesis stage using H-phosphonates. To preserve the unsaturation in the lipid chain, final deprotection will involve treatment with DDQ to remove the Nap groups and azide reduction with trimethylphosphine in THF (Scheme 3-1).

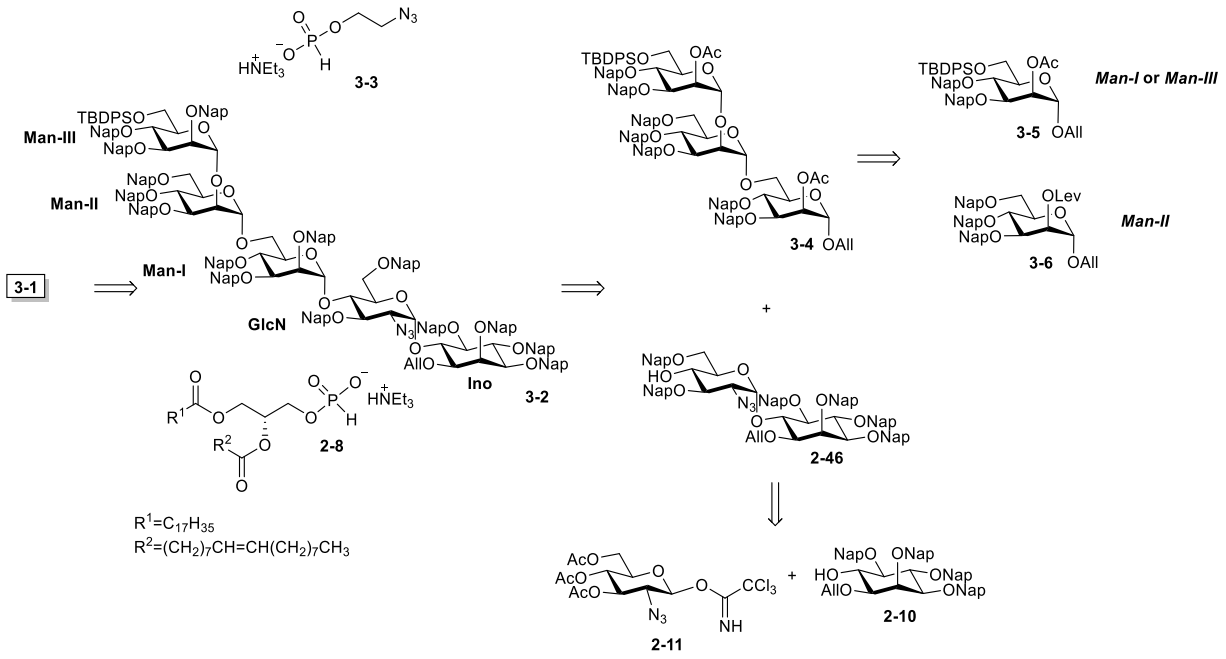

Scheme 3-1. Retrosynthetic analysis of *P. falciparum* GPI **3-1**. Nap = 2-Naphthylmethyl, TBDPS = *tert*-Butyldiphenylsilyl.

3.3 Results and discussion

3.3.1 Synthesis of glycan core (First strategy)

The general retrosynthetic analysis presented in scheme 3-1 identified the allyl trimannoside **3-4** and the pseudodisaccharide **2-46** as the key intermediates to obtain the glycan core of GPI **3-1** by a [3+2] glycosylation strategy. The pseudodisaccharide **2-46** was synthesized to assemble the GPI-fragment **2-4** (see Scheme 2-10, chapter 2 for details). Two mannose building blocks are

required to prepare the trimannose **3-4**: mannose **3-5** as a precursor for preparing Man-I or Man-III units and mannose **3-6** for the Man-II unit.

The synthesis started with the preparation of mannose building blocks for Man-III and Man-I, which are accessible from the common intermediate **3-7** available in our laboratory as a by-product of previous syntheses (Scheme 3-2).[58] Protection of the primary alcohol of **3-7** with TBDPS delivered the diol **3-8** that was selectively 2-naphthyl methylated at the O-3 position *via* tin-acetal. The remaining hydroxy group was acetylated using acetic anhydride and pyridine with catalytic amounts of DMAP to yield the fully protected mannose **3-5**. A selective removal of the TBDPS group in **3-5** with TBAF afforded the mannose alcohol **3-10** in 90% yield, which is the final building block to install the Man-I. Removal of the anomeric allyl group in **3-5** using $PdCl_2$ in methanol, followed by conversion of the hemiacetal into a trichloroacetimidate using trichloroacetonitril and DBU as a base furnished the Man-III building block **3-12** in 56% yield over two steps.

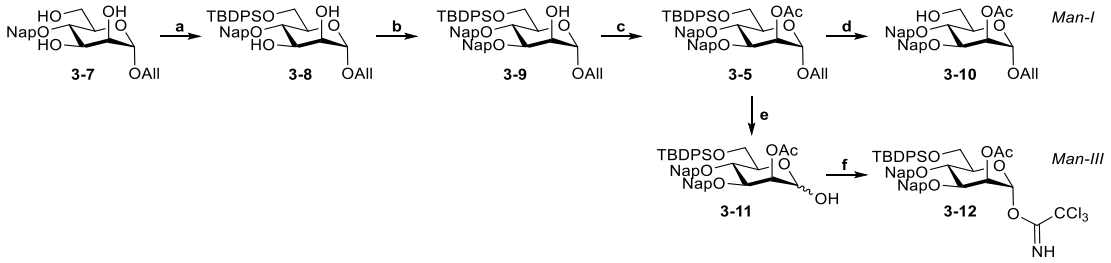

Scheme 3-2. Synthesis of mannose building blocks **3-12** (Man-III) and **3-10** (Man-I). *Reagents and conditions:* a) Imidazole, DMAP, TBDPSCl, DCM, r.t., 1 h, 80%; b) *i.* Bu_2SnO, toluene, reflux, 3 h; *ii.* TBAI, NapBr, DMF, 60 °C, 3 h, 83%; c) DMAP, Ac_2O, pyridine, DCM, r.t., 1.5 h, 82%; d) TBAF, THF, r.t., 1 h, 90%; e) $PdCl_2$, DCM/MeOH, r.t., 3 h, 67%; f) DBU, CCl_3CN, DCM, 0 °C, 40 min; 83%. DMAP= 4-Dimethylaminopyridine, TBAI = Tetra-n-butylammonium iodide, TBAF = Tetra-n-butylammonium fluoride.

The Man-II building block was synthesized starting from allyl mannoside **3-13** available in our laboratory (Scheme 3-3).[58] The TBDPS group in **3-13** was removed with TBAF, and the resulting diol was protected using 2-naphthylmethyl bromide and NaH to give the fully protected mannose **3-15**. Following acetal opening under acidic conditions to get diol **3-16** and a tin-acetal mediated selective naphthylmethylation at O-3 position delivered the alcohol in **3-17**. The remaining alcohol was quantitatively acylated with levulinic acid under Steglich conditions, and the allyl group was removed using $PdCl_2$ to afford the hemiacetal **3-18** in 61% yield over two steps. Finally, the hemiacetal **3-18** was treated with trichloroacetonitrile and catalytic DBU to afford the trichloroacetimidate **3-19** in 81% yield.

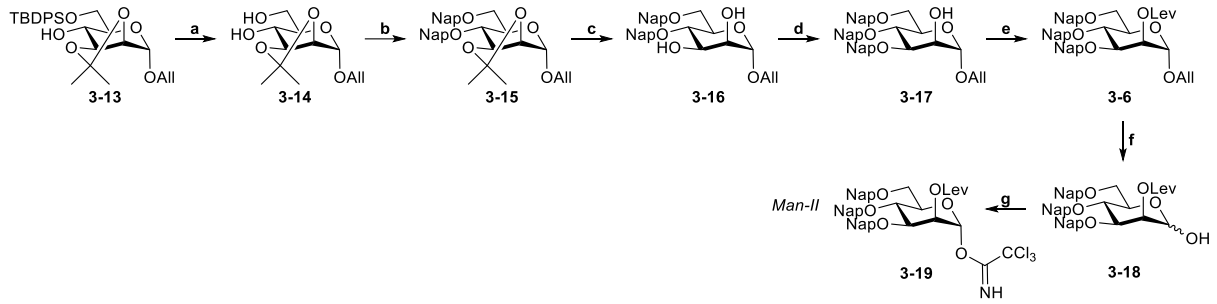

Scheme 3-3. Synthesis of mannose building block donor **3-19** (Man-II). *Reagents and conditions:* a) TBAF, THF, r.t., 1 h, 85%; b) NaH, NapBr, DMF, r.t., O.N.; c) CSA, DCM/MeOH, r.t., 7 h, 71% (two steps); d) *i.* Bu_2SnO, toluene, reflux, 3 h; *ii.* TBAI, NapBr, DMF, 60 °C, 3 h, 80%; e) LevOH, DMAP, DIC, DCM, r.t., O.N., 100%; f) $PdCl_2$, DCM/MeOH, r.t., 3 h, 61%; g) DBU, CCl_3CN, DCM, 0 °C, 40 min; 81%. LevOH = Levulinic acid, DIC = *N,N'*-Diisopropylcarbodiimide.

The assembly of the allyl trimannoside **3-4** was initiated with the glycosylation of the glycosyl acceptor **3-10** with the mannose donor **3-19** (Man-II) under TMSOTf activation to get the disaccharide **3-20**. Then, the dimannose **3-20** was treated with hydrazine acetate to remove the Lev group to deliver the alcohol **3-21** in 84% yield over two steps (Scheme 3-4). Glycosylation of the dimannoside acceptor **3-21** with the mannosyl imidate **3-12** (Man-III) gave the allyl trimannoside **3-4** in 90% yield as the pure α-anomer through neighboring group participation of the acetyl group. A trimannose byproduct without TBDPS protecting group was recovered in an 8% yield. The anomeric allyl group in **3-4** was removed with $PdCl_2$ in methanol, and the resulting hemiacetal was converted into the trichloroacetimidate to obtain the final trimannoside donor **3-23** in 73% yield after two steps.

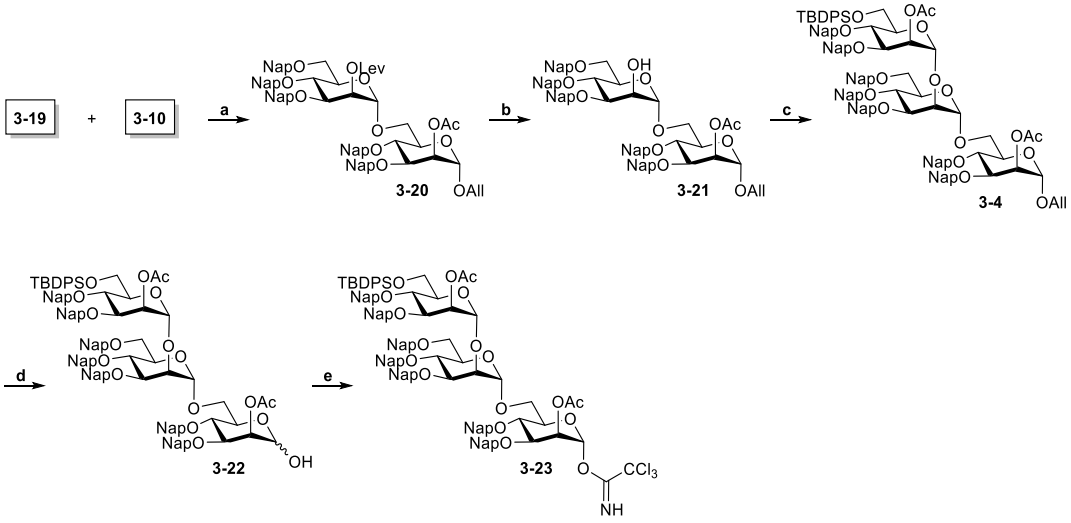

Scheme 3-4. Synthesis of trimannoside donor **3-23** (Man-II). *Reagents and conditions:* a) TMSOTf, DCM, 0 °C, 1 h, 87%; b) Hydrazine acetate, DCM, r.t., 4.5 h, 97%; c) **3-12**, TMSOTf, DCM, -10 °C, 1 h; d) $PdCl_2$, DCM/MeOH, r.t., 4 h, 88%; e) DBU, CCl_3CN, DCM, 0 °C, 45 min; 83%. TMSOTf = Trimethylsilyl trifluoromethanesulfonate, DBU = 1,8-Diazabicyclo[5.4.0]undec-7-ene.

Following the synthetic plan, the next step was the glycan core assembly using a [3+2] glycosylation strategy with trimannoside donor **3-23** and the pseudodisaccharide **2-46**. The reaction was completed using TMSOTf activation and neighboring group participation of the acetyl group in **3-23** to obtain the pseudopentasaccharide **3-24** as pure α-anomer (Scheme 3-5). Before removal of the allyl group from inositol to install the phospholipid, the acetyl groups in the O-2 position of Man-I and Man-III must be exchanged to Nap protecting groups to avoid deacetylation under basic conditions and subsequent saponification of the lipid chain. Therefore, the acetyl groups in pseudopentasaccharide **3-24** were removed with NaOMe to obtaing the diol **3-25** in 94% yield over two steps. Next, the diol **3-25** was treated with NaH and NapBr in DMF to prepare the fully protected pseudopentasaccharide **3-2**. However, the reaction did not proceed.

Different conditions were evaluated for the installation of the 2-naphthyl ether. However, similar results were observed using TBAI addition to improve the reactivity of NapBr and using the ether 15-Crown-5 to increase the basicity of NaH. A solvent exchange from DMF to THF didn't change the result and increasing the reaction temperature to 50 °C resulted in the decomposition of the starting material. Further attempts to protect the alcohols included a reaction under acidic conditions using freshly prepared 2-Naphthylmethyl trichloroacetimidate and TMSOTf activation, which also caused the decomposition of the starting material. As an alternative to Nap protection for the free hydroxy groups, **3-25** was treated with NaH, TBAI and PMBCl to introduce *p*-methoxybenzyl ethers as protecting groups. This reaction proceeded only when the pH was increased; however, under these conditions, the TBDPS was removed and replaced by PMB to provide the trimethoxybenzylated derivative of **3-25**.

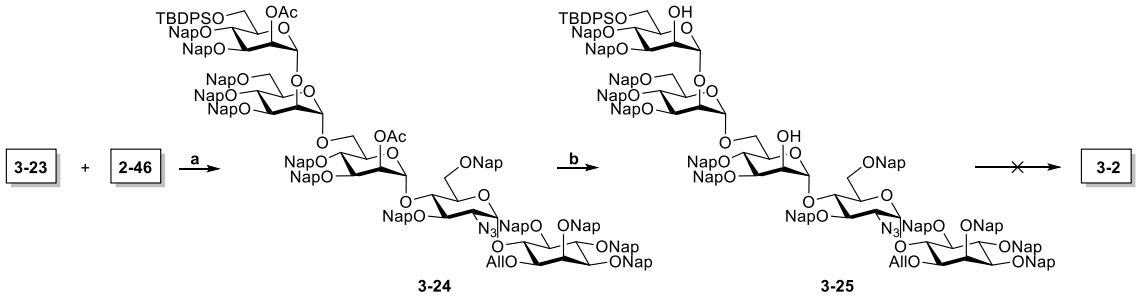

Scheme 3-5. Synthesis of the pseudopentasaccharide **3-2** using acetyl groups. *Reagents and conditions:* a) TMSOTf, DCM/Et_2O, -10 °C, 1 h; b) NaOMe, DCM/MeOH, 50 °C, O.N., 94% (two steps).

Attempting to install the Nap ether protection in the O-2 position of Man-III in an early stage of the synthesis, the trimannose **3-30** was synthesized with the aim of protecting its free hydroxy group with Nap ether (Scheme 3-6). The synthesis started with acylation of alcohol **3-9** with levulinic acid under Steglich conditions and the conversion of the fully protected mannose **3-26** into the

mannosylimidate donor **3-28** in 52% yield after two steps. The [1+2] glycosylation of donor **3-28** and acceptor **3-21** delivered the allyl trimanoside **3-29** in quantitative yield. To exchange the first ester at this stage, selective removal of the levulinoyl ester with hydrazine acetate furnished alcohol **3-30** in 66% yield. Next, the resulting alcohol **3-30** was treated with NaH and NapBr in DMF. Unfortunately, the basic conditions of the etherification caused partial migration of the acetyl group, yielding an inseparable mixture of **3-31** to **3-34** by silica gel column chromatography.

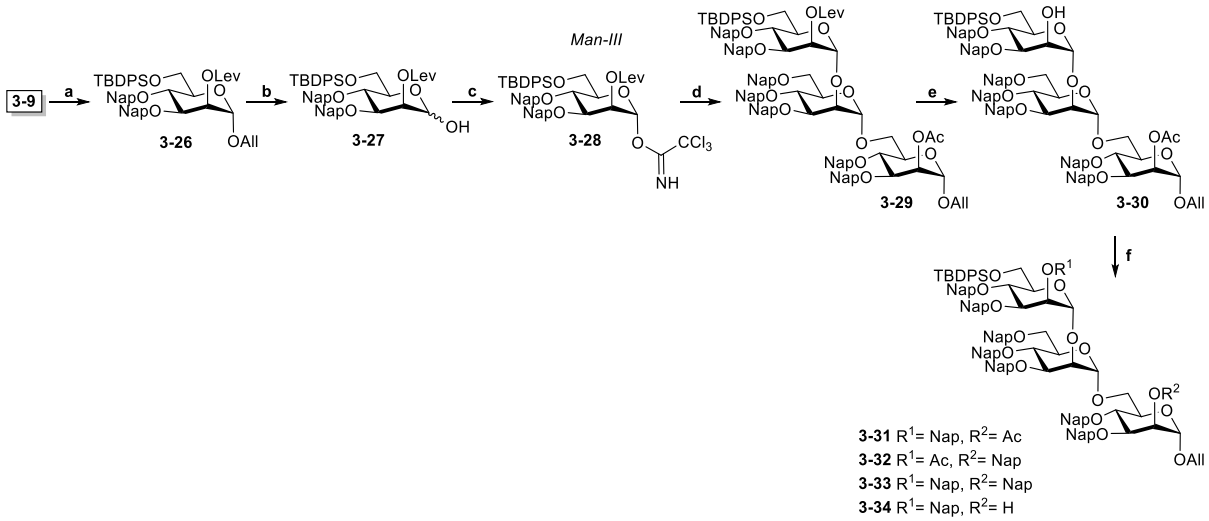

Scheme 3-6. Synthesis of the alternative trimannoside **3-31**. *Reagents and conditions:* a) LevOH, DMAP, DIC, DCM, r.t., O.N., 99%; b) $PdCl_2$, DCM/MeOH, r.t., 3.5 h, 60%; c) DBU, CCl_3CN, DCM, 0 °C, 1 h; 87%; d) **3-21**, TMSOTf, Et_2O, 0 °C, 1.5 h, 100%; e) Hydrazine acetate, DCM, r.t., O.N., 66%; f) NaH, NapBr, DMF, r.t., 1.5 h.

Since a replacement of acetyl groups by naphthyl methyl ethers is not possible in an earlier stage of the synthesis or removal once the phospholipid has been installed, it was decided to modify the protection strategy for the O-2 position of Man-I and Man-III. Levulinoyl esters were considered as a suitable alternative to acetyls; they are neighboring participating groups during glycosylation reactions and are selectively removed in the presence of the lipids using hydrazine acetate.

3.3.2 Synthesis of glycan core (Second strategy)

An acylation with levulinic acid of the free hydroxyl groups in pseudopentasaccharide **3-25** represented an alternative to the unsuccessful installation of Nap ether. However, most of the synthesized intermediate **3-25** was expended attempting protection with 2-Naphthyl methyl ether groups in these positions. Instead of preparing more **3-25** following the route in scheme 3-1, the strategy was modified by replacing the acetyls for levulinoyl groups in the 2-O positions of Man-I and Man-III in an early stage of the route. This change will reduce the number of reaction steps to get the

pseudopentasaccharide and the loss of complex intermediates in the latter stages of the synthesis.

The new assembly of the pseuopentasaccharide started with the treatment of trimannosides **3-4** or **3-29** with NaOMe in DCM/MeOH to get the diol **3-35**, which was acylated with LevOH using Steglich esterification conditions to provide the fully protected trimannose **3-36** in 93% yield (Scheme 3-7). A removal of the allyl group from **3-36** with palladium and further installation of the trichloroacetimidate delivered the trisaccharide donor **3-38** in 69% yield after two steps.

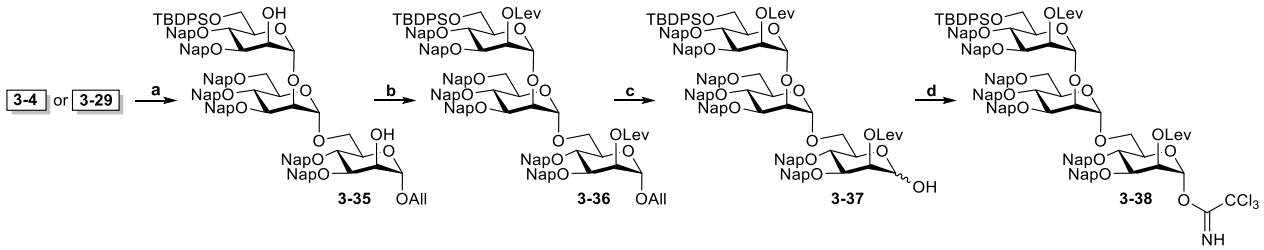

Scheme 3-7. Synthesis of the trimannoside donor **3-33**. *Reagents and conditions:* a) NaOMe, DCM/MeOH, r.t., 48 h, 87% b) LevOH, DMAP, DIC, DCM, r.t., 60 h., 93%; c) $PdCl_2$, DCM/MeOH, r.t., 6 h, 74%; d) DBU, CCl_3CN, DCM, 0 °C, 50 min; 82%.

The [3+2] glycosylation reaction between the modified trimannoside donor **3-38** and the pseudodisaccharide **2-46** using TMSOTf activation delivered the fully protected pseudopentasaccharide **3-39** in 96% yield (Scheme 3-8). In contrast, treatment of diol **3-25** with levulinic acid under Steglich conditions provided the pseudopentasaccharide **3-39** in a lower yield (69%), showing the advantage of introducing the levulonoyl esters in an earlier stage of the synthesis. The alcohol **3-40** ready for phosphorylation was obtained removing the allyl group in the inositol of **3-39** with $PdCl_2$ in 82% yield or with a freshly activated iridium complex using a two-step process, isomerization and hydrolysis, in 94% yield.

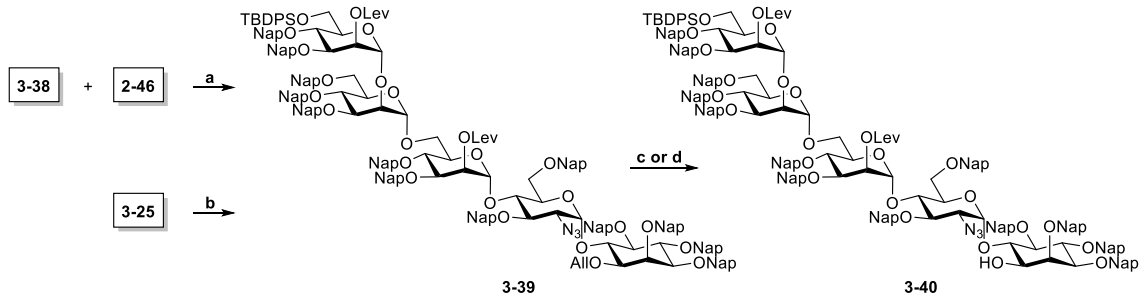

Scheme 3-8. Synthesis of the pseudopentasaccharide **3-40**. *Reagents and conditions:* a) TMSOTf, DCM/Et_2O, -10 °C, 1 h, 96%; b) LevOH, DMAP, DIC, DCM, r.t., O.N., 69%; c) $PdCl_2$, DCM/MeOH, r.t., 5 h, 82%; d) *i.* $[IrCOD(PPh_2Me)_2]PF_6$ freshly activated with H_2, THF, r.t., 3h; *ii.* $HgCl_2$, HgO, acetone/H_2O, 2 h, r.t., 94%.

3.3.3 Synthesis of *P. falciparum* GPI

A two-step protocol was followed to introduce the phospholipid moiety to the glycan core **3-40**. Starting with the phosphitylation with the H-phosphonate **2-8** using pivaloyl chloride activation, phosphorous oxidation of the diester with iodine/water provided the phospholipidated pseudopentasaccharide **3-41** in 92% yield (Scheme 3-9). Initially, scandium(III) triflate in DCM/ACN was used to selectively remove the TBDPS group at 50 °C; however, just partial removal was observed. Complete removal of this protecting group was achieved using HF·Py complex in THF at room temperature to furnish alcohol **3-42** ready for introducing the second phosphate of the *P. falciparum* GPI.

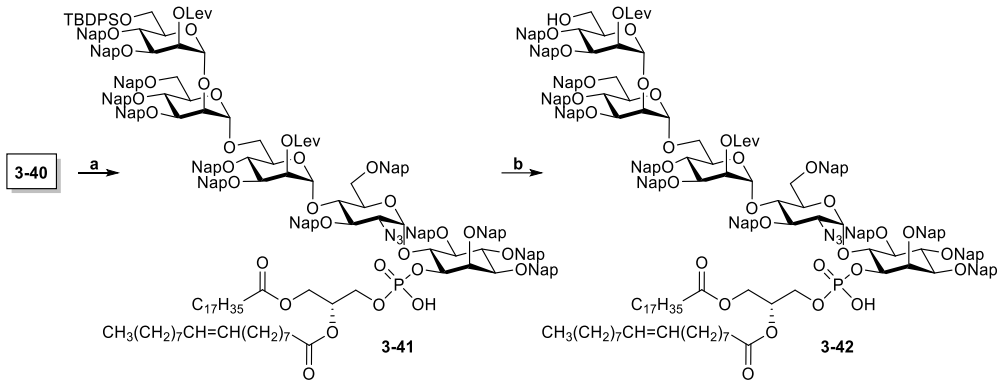

Scheme 3-9. Synthesis of the phospholipidated pseudopentasaccharide **3-40**. *Reagents and conditions:* a) **2-8**, *i.* PivCl, pyridine, r.t., 1 h; *ii.* I_2, H_2O, r.t., 1 h, 92%; b) HF·Py complex, THF, r.t., 24 h, 90%.

As presented in the retrosynthetic analysis (Scheme 3-1), the H-phosphonate **3-3** is required to introduce the phosphoethanolamine unit. The synthesis of this building block started with a monotosylation from ethylene glycol to obtain alcohol **3-44** in 93% yield (Scheme 3-10). Nucleophilic substitution of the tosyl group with the sodium azide delivered azido ethanol **3-45**, which was phosphitylated using phosphorous acid and pivaloyl chloride activation to afford the desired H-phosphonate **3-3** in 80% yield.

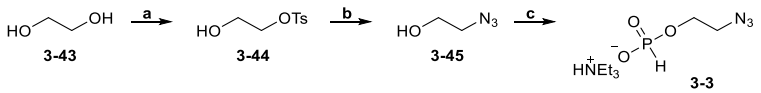

Scheme 3-10. Synthesis of H-phosphonate **3-3**. *Reagents and conditions:* a) p-toluenesulfonyl chloride, Et_3N, r.t., 1 h, 93%; b) NaN_3, H_2O/acetone, 65 °C, O.N., 79%; c) H_3PO_3, PivCl, pyridine, r.t., O.N., 80%.

The fully protected *P. falciparum* GPI **3-46** was obtained in 98% yield by phosphitylation of alcohol **3-42** with the H-phosphonate **3-3** using pivaloyl chloride activation and following oxidation with iodine/water. Next, all protecting groups were removed to complete the synthesis of *Pf*-GPI. The global deprotection started removing the Lev protecting groups by treatment of **3-46** with hydrazine acetate in THF using a pyridine/AcOH buffer to avoid lipid removal through the pH increase. Under these conditions, only one Lev protecting group was removed, probably due to steric hindrance caused by the Nap ethers. Therefore, the order of the deprotection strategy was inverted. First, the Nap protecting groups were removed under oxidative conditions using DDQ in DCM/MeOH to obtain GPI **3-47**. Then, levulinoyl esters were removed by treatment with hydrazine acetate in THF and pyridine/AcOH buffer. Finally, azides reduction using Staudinger conditions delivered the GPI of *P. falciparum* **3-1** in excellent yield (89%, three steps).

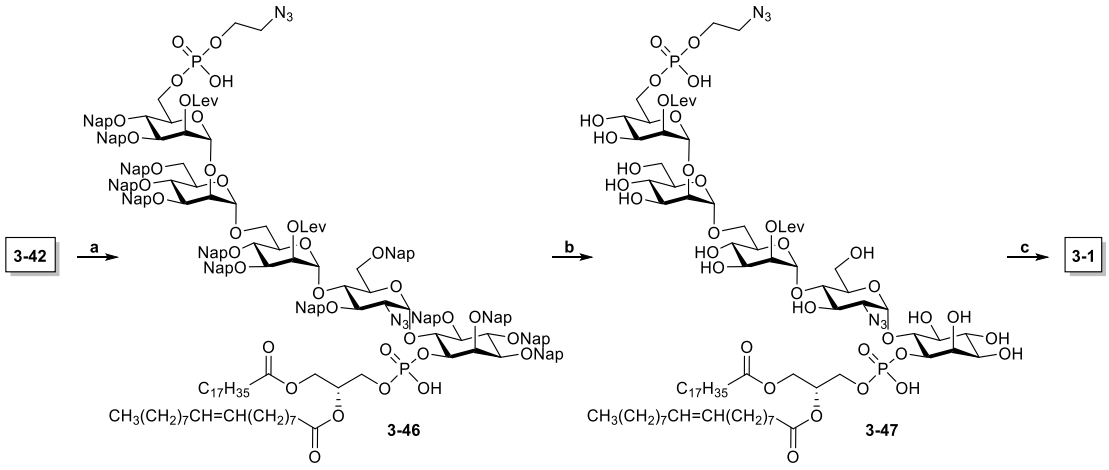

Scheme 3-11. Synthesis of *P. falciparum* GPI **3-1**. *Reagents and conditions:* a) **3-3**, *i.* PivCl, pyridine, r.t., 3 h; *ii.* I_2, H_2O, r.t., O.N., 98%; b) DDQ, MeOH/DCM, r.t., O.N.; c) *i.* Hydrazine acetate, Pyridine/AcOH, THF, O.N.; ii. $P(CH_3)_3$, THF, r.t., 30 min, 89% (three steps).

The synthesized *P. falciparum* GPI derivative **3-1** bearing unsaturated lipids was obtained with excellent purity, evidenced by NMR spectroscopy. This homogeneous material has strong potential for *in vitro* and *in vivo* assays to evaluate the GPIs role and activity in immunogenicity and protection efficacy against malaria infections and determine lipid composition effects in the GPI's activity.

To obtain a natural GPI of *P. falciparum* having an additional lipid chain in the O-2 position of inositol, further studies will include the pseudodisaccharide **2-39** having a PMB at the O-2 position of inositol, which was employed in the synthesis of the trilipidated GPI fragment **2-3** (Scheme 2-9, chapter 2). The PMB group gives an additional level of orthogonality to the route and will allow introduction of the palmitate typically found in *P. falciparum* GPIs.

Understanding the influence of GPIs on protein function and immunoreactivity during parasitic infection will provide additional tools for drugs and therapy development against malaria. In addition to direct evaluation of GPI **3-1**, this glycolipid can be coupled to *P. falciparum* proteins, such as the merozoite surface protein 1 (C-terminal 19-kDa region [PfMSP-1_{19}]), for further investigation. MSP1 is the most abundant protein on the surface of the erythrocyte-invading *Plasmodium* merozoite and it anchors to the parasite surface by a GPI. The structure and immunoreactivity of MSP1 during infection have been extensively studied, and it is considered a promising vaccine candidate for malaria.[122–128]

3.3.4 Synthesis of a *P. falciparum* GPI with cysteine modification

Different GPI-APs have been prepared *via* Native Chemical Ligation (Scheme 3-12a). In this strategy, the phosphoethanolamine of the GPI anchor requires a cysteine unit for the reaction with a protein thioester (Scheme 3-12b).[129,130] The cysteine thiol acts as a nucleophile to attack the C-terminal peptide or protein thioester to give a transthioestereification reaction in an aqueous buffer at pH 7 and room temperature. After the transthioesterification, the new thioester undergoes a rapid and spontaneous rearrangement by an intramolecular *S- to N*-acyl shift to form a native peptide bond at the ligation site.[131]

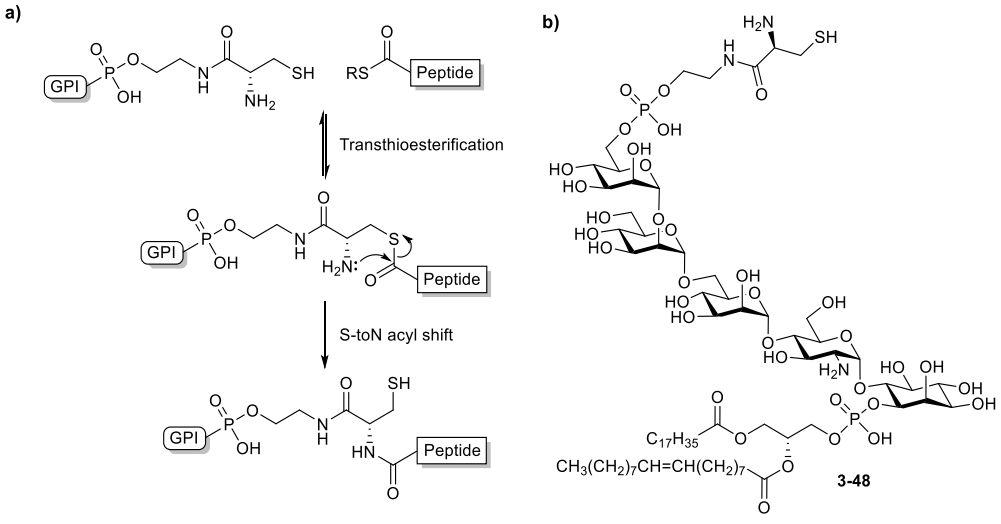

Scheme 3-12. a) Native Chemical Ligation between a GPI bearing a cysteine at the phosphoethanolamine and an unprotected peptide or protein; b) *Structure of a P. falciparum* GPI modified with a cysteine.

The phospholipidated pseudopentasaccharide **3-40** was phosphorylated using H-phosphonate **3-49**, already available in our laboratory, to synthesize a *Pf*-GPI having the cysteine modification (Scheme 3-13). Phosphorylation was carried out using a two-step protocol involving

phosphitylation with **3-49** and oxidation with I_2/water to give the protected *P. falciparum* GPI **3-50**. For deprotection of the glycolipid, the Nap protecting groups were removed under oxidative conditions; the levulinoyl esters were cleaved using buffered (pyridine/AcOH) hydrazine acetate in THF; and the azides were reduced with trimethyl phosphine in THF, furnishing the *P. falciparum* GPI **3-51** with a protected cysteine in 48% yield after four steps. Next, the deprotection of the cysteine in **3-51** was accomplished using TFA in toluene to remove Boc protection from the α-amino group of the cysteine. When the complete conversion was observed by MALDI-TOF, solvents were removed, and treatment with MeOH/Water to open the N,S-isopropylidene acetal was performed. The NMR spectra of the obtained product clearly showed a deprotected GPI structure bearing an unsaturated lipid. However, the complexity of the spectra doesn't allow it to corroborate with high accuracy if the cysteine was completely deprotected. Unexpectedly, mass spectrometry analysis by ESI-QTOF-MS showed an MS value 13 units higher than the expected molecular weight of the target molecule. It is unclear the reason for the mass difference; therefore, the opening of the *N,S*-acetal was completed using water instead of MeOH/Water to avoid any possible nucleophilic effect from methanol. Nonetheless, the same result was also obtained under these conditions.

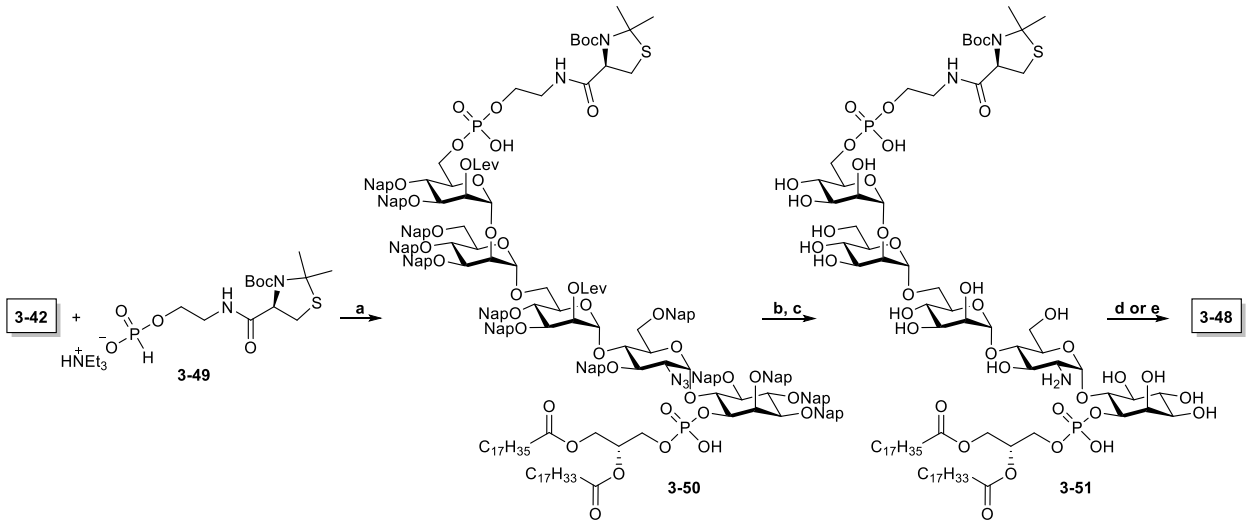

Scheme 3-13. Synthesis of the *P. falciparum* GPI **3-48** with cysteine modification. a) *i.* PivCl, pyridine, r.t., 2 h; *ii.* I_2, H_2O, r.t., O.N.; b) DDQ, MeOH/DCM, r.t., O.N.; c) *i.* Hydrazine acetate, Pyridine/AcOH, THF, O.N.; ii. $P(CH_3)_3$, THF, r.t., 30 min 48% (four steps); d) *i.* TFA, toluene, r.t., 1 h; ii. MeOH/Water, 40 °C, 5 min x 3 times; e) *i.* TFA, toluene, r.t., 1 h; *ii.* Aq. $AgNO_3$, MeOH/$CHCl_3$/MeOH 3:3:1, r.t., 1 h; *iii.* Mercaptoethanol, r.t., 1 h. TFA = Trifluoroacetic acid.

Previous reports described N-Boc-N,S-acetal-cysteine deprotection using an acid treatment to remove the Boc group and following reactions with an aqueous solution of sodium nitrate to open the N,S-acetal.[132] The resulting silver mercaptide can be treated with mercaptoethanol to obtain the desired aminothiol. These conditions where used with the GPI **3-51**; but again, the same unexpected mass was observed.

To understand, what caused the unexpected mass difference, a model molecule with less molecular complexity than **3-51** was synthesized. Mannose **3-52**—already available in our laboratory—was phosphitylated with **3-49** and oxidized with I_2/H_2O to deliver the model mannoside **3-53** (Scheme 3-14). A deprotection of cysteine with TFA in toluene and following treatment with water/MeOH to open the N,S-acetal delivered the allyl mannoside **3-54** in excellent yield. NMR and ESI-MS product analysis correlated with the expected cysteine derivative **3-54**. Similar results were obtained by reacting **3-53** TFA in toluene and acetal opening with aqueous sodium nitrate, mannose **3-54** was also obtained in good yield. The results with this model compound suggest that the unexpected mass difference observed in **3-48** could be a product formed during the MS ionization or by an unknown structural modification—probably in one of the phosphates—during the deprotection. To confirm if the structure of GPI **3-48** was altered and if the cysteine is in fact completely deprotected, NCL of GPI **3-48** with the MSP-1_{19} protein of *P. falciparum* will be evaluated to determine the reactivity of the structure in this reaction. If the coupling is successful, the obtained *P. falciparum* GPI-AP will be used for *in vitro* and *in vivo* assays.

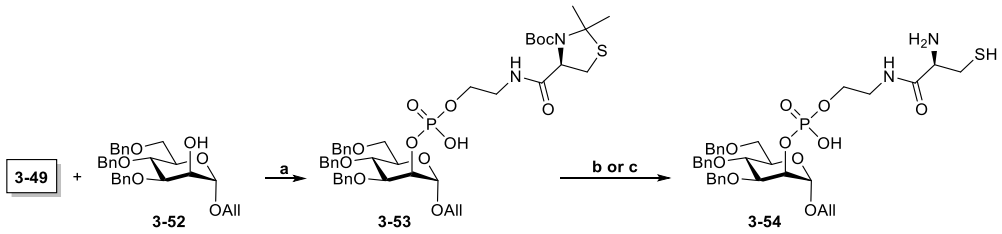

Scheme 3-14. Synthesis of a model mannoside **3-54** with cysteine modification. *Reagents and conditions:* a) *i.* PivCl, pyridine, r.t., 1.5 h; *ii.* I_2, H_2O, r.t., 2 h, 84%; b) *i.* TFA, toluene, r.t., 1 h; ii. MeOH/Water, 40 °C, 5 min x 3 times, 92% c) *i.* TFA, toluene, r.t., 1 h; *ii.* Aq. $AgNO_3$, MeOH/$CHCl_3$/MeOH 3:3:1, r.t., 1 h; *iii.* Mercaptoethanol, r.t., 1 h, 78%.

3.4 Conclusion and Outlook

A new strategy for the total synthesis of GPIs bearing unsaturated lipids was designed and successfully executed in preparing a *P. falciparum* GPI glycolipid. The convergent synthesis relied on a set of orthogonally protected building blocks that allowed the efficient assembly of the glycan core using 2-naphthylmethyl ethers as permanent hydroxyl protecting groups. The initial strategy involved acetyl esters as neighbor participating groups to control the selectivity of the glycosylation reactions. However, replacement of these groups for 2-naphthylmethyl ethers at the synthesis late stage was more challenging than expected and resulted in compound decomposition or protecting group migration of the structures. Therefore, a different strategy employing 2-naphthylmethyl ethers and levulinoyl esters as permanent protecting groups for the hydroxyls was envisioned

and executed. After the late-stage introduction of the phospholipid and phosphoethanolamine moieties, a three-step deprotection protocol involving oxidative removal of the Nap ethers, selective cleavage of the levulinoyl esters and Staudinger reduction of the azides was followed. The global deprotection was compatible with the presence of the unsaturated lipid chains and delivered the targeted *P. falciparum* GPI in high yield and with outstanding purity.

This strategy represents a potential and general method for the synthesis of GPIs having unsaturated lipids or other functionalities that are not accessible by employing traditional protection strategies such as benzyl or benzoyl groups. The developed strategy would not only allow the production of homogeneous native GPI structures but would also provide the flexibility to accommodate further moieties to give unnatural GPI analogs. Having access to GPI structures will facilitate extensive investigations to decipher the biological relevance of these glycolipids and to perform structure-activity relationship studies. The chemically synthesized *P. falciparum* GPI **3-1** will be used to evaluate the immune response toward this glycolipid and glycoconjugates having this GPI structure.

The established route also allowed the synthesis of a *P. falciparum* GPI bearing a cysteine attached to the phosphoethanolamine unit, which is an essential building block for getting a native *P. falciparum* protein through native chemical ligation. The three-step global deprotection protocol to get the GPI structure was successful; however, complete deprotection of the cysteine was uncertain. Although the NMR spectra suggest that the target GPI was obtained, an unexpected difference of 13 units was observed in the mass spectra. The reasons for this result could not be identified. A model molecule with less molecular complexity than the GPI showed efficient and expected products in the cysteine deprotection. Thus, further studies, such as native chemical ligation of the obtained GPI structure **3-48** with the MSP-1_{19} protein of *P. falciparum,* are required to corroborate the structure identity and activity of the chemically synthesized GPI anchor. In addition, the attachment of GPI **3-48** to proteins may provide data about the influence of the GPI anchor on the protein activity and in the interaction of GPI-anchored MSP1 with the immune system.

4 Total synthesis of a GPI anchor of *Trypanosoma cruzi*

4.1 Introduction

4.1.1 *Trypanosoma cruzi* and Chagas disease

Chagas disease, also known as American trypanosomiasis, is a neglected tropical infectious disease in humans caused by the protozoan parasite *Trypanosoma cruzi*, which can be transmitted through the feces of insects in the subfamily *Triatominae*, known as "kissing bugs" since they tend to bite people's face.[133] The fecal contaminative infection occurs when the insect vector defecates on the skin lesion generated after a bite for a blood meal. However, the parasite can also be transmitted congenitally (mother-to-baby), through blood transfusion, organ transplantation, or ingesting raw food contaminated with feces from infected triatomine bugs.[134] The symptoms change over the course of the infection and, when untreated, the infection is lifelong and can be fatal. The severity of the symptoms depends on the *T. cruzi* strain and on host factors such as age and health status. The Chagas disease develops in two phases: the acute phase, when there is a high concentration of parasites in the bloodstream, and the chronic phase, when the parasites are hidden in the heart and digestive system. Both phases can be symptom-free or life-threatening. The initial acute phase occurs right after the infection and lasts either for a few weeks or around two months after the infection. The symptoms, if present, are mild and include inflammation on the bite site (called a chagoma), fever, fatigue, headache, diarrhea, vomiting, and lack of appetite. These symptoms tend to be confused with many other illnesses, which hinders an early diagnosis and treatment with antiparasitic medication. After the acute phase, most people get into the chronic phase of the disease, which rarely presents symptoms and can last the whole life span of the patient. Around 10% of Chagasic patients experience gastrointestinal, neurological, or mixed complications. Moreover, due to the destruction of the heart muscle and its nervous system during the parasitic infection, around 30% of the infected people develop cardiac problems such as enlarged heart, heart failure, altered heart rate or rhythm, and cardiac arrest.[133–137]

Chagas disease is a major public health problem in Latin America, especially in low-resource areas where houses are usually built with precarious materials such as mud, adobe, straw, and palm thatch, which are ideal habitats for the vector. Nonetheless, due to the emigration of infected people, the number of detected cases is increasing worldwide. The infection affects around 6 to 7 million people worldwide and causes more than 12,000 deaths per year, being a special risk for immunosuppressed people. Vector control measures, such as improvement of housing and insecticide spraying to eliminate the insect vectors, have decreased the spread of Chagas disease;

however, the incidence remains high, reaching around 30,000 new cases per year, and 65 to 100 million people are at risk of acquiring the disease.[138,139]

The disease can be diagnosed through blood tests during its acute phase to detect the parasites, while the chronic phase can be suspected based on the patient's symptoms, travel history, or place of residence, and it is confirmed by testing for parasite-specific antibodies, requiring several tests to have a fairly accurate result. The foregoing added to the silent nature of the disease has resulted in most undetected cases.[134,136] Also, there is no drug or vaccine to prevent the infection. Chagas disease is treated with prescription drugs either to ameliorate the symptoms or to kill the parasites. The two available antiparasitic treatments include the two nitro-heterocyclic drugs benznidazole and nifurtimox. Both medicines can be effective against the disease if given soon after the infection; nevertheless, their use is limited due to their high cost, long treatment periods, serious side effects, and low antiparasitic activity in Chagasic patients with chronic infections.[134,140,141] Therefore, new prophylactic detection and treatment strategies against Chagas disease are direly needed.

When *T. cruzi* parasites, in the form of metacyclic trypomastigotes, enter the human host through the lesion left by the insect vector, they invade various cells at the bite site. There, the parasites develop into intracellular amastigotes and multiply through binary fission (Figure 4-1). Once they mature into trypomastigotes, they break out of the infected cells and enter the bloodstream. Trypomastigotes cannot reproduce in the bloodstream, so they infect cells of different tissues, transforming again into intracellular amastigotes to multiply and continue the infective cycle, which causes direct and indirect tissue damage and results in the pathologic features of Chagas disease. The bloodstream trypomastigotes in the human host can also be taken up by an insect vector during the bite for a blood meal. The ingested trypomastigotes transform into epimastigotes and multiply in the insect's midgut. After migration to the hindgut, the epimastigotes develop into highly infective trypomastigotes known as metacyclic trypomastigotes. When the infected insect feeds from a human, it ingests a significant amount of blood which forces the elimination of the bulk of accumulated excreta. Subsequently, the insect vector deposits its feces containing the parasite in the form of metacyclic trypomastigotes at the wound site, allowing the parasite to enter another human host to restart its life cycle.[137,142,143]

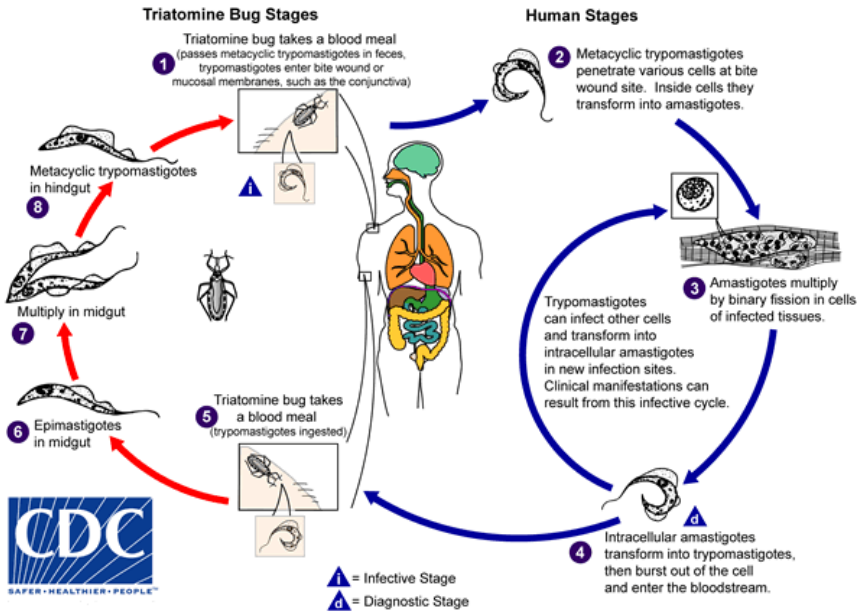

Figure 4-1. Life cycle of *T. cruzi* parasites.[139]

4.1.2 GPI anchors of Trypanosoma cruzi

T. cruzi exists in 4 different forms during its life cycle (metacyclic trypomastigote, amastigote, bloodstream trypomastigote, and epimastigote); each with stage-specific adaptative mechanisms that make complex the prevention, detection, and treatment methods development against it. Throughout its life cycle, *T. cruzi* produces common and stage-specific GPI-anchored cell-surface macromolecules such as highly glycosylated mucins and phosphoglycans.[71] The cell surface of *T. cruzi* contains a high concentration of these GPI-anchored molecules. It is believed that the release of GPI-Anchored mucins by the bloodstream trypomastigote triggers the parasite-elicited inflammation that causes cardiac complications and other pathologies associated with the Chagas disease.[11,144] In fact, highly purified GPI fractions of trypomastigote mucins present unusual proinflammatory activity comparable to bacterial lipopolysaccharide, making these GPIs one of the most potent microbial proinflammatory agents known.[70] More specifically, when presented to macrophages, isolated GPIs induced potent interleukin (IL)-12 expression that initiates interferon-γ (IFN- γ) production, which is a crucial cytokine mediating resistance during the acute infection with *T. cruzi*; nitric oxide (NO) which is essential for host resistance during the early stages of the parasitic infection; and the tumor necrosis factor (TNF)-α, a cytokine that has also been shown to have an essential role in controlling the disease.[11,70,145,146]

The structure of the highly bioactive GPIs of *T. cruzi* trypomastigote presents three characteristic features: a glycan branch of galactoses, a (2-aminoethyl)phosphonate unit at the O-6 position of glucosamine, which is a parasite-specific modification only found in *T. cruzi*, and the presence of

unsaturated fatty acids in the phospholipid moiety (Figure 4-2). The intense activity of these GPIs was associated with two of these modifications, the oligo-galactoses branch and, especially, the unsaturation in the lipid tail.[11,70]

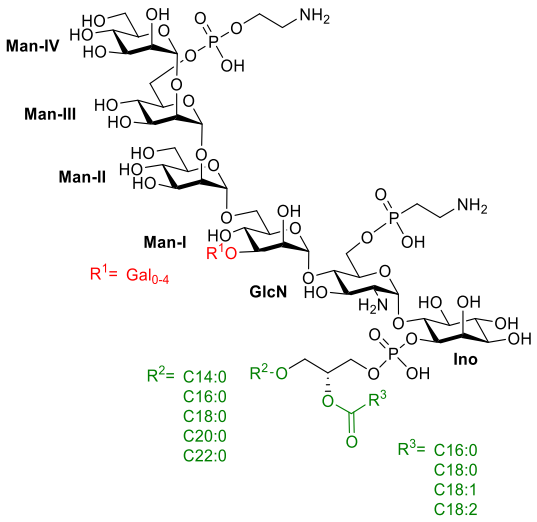

Figure 4-2. Structural diversity of *T. cruzi* GPIs with glycerophospholipids. Galactose residues are also attached to other mannoses in the glycan core.

Due to the small amount and heterogenic nature of isolated GPI structures from *T. cruzi,*[70] understanding of the stimulation of the innate immune system by these molecules is still sparse. Studies using chemically synthesized GPI and GPI fragments of *T. cruzi* might aid the further elucidation of the structural requirements and the molecular interactions involved during macrophage activation by these complex structures. This information could provide insights into the mechanisms to avoid excessive inflammatory responses during parasitic infection and develop new prevention and treatment methods for the Chagas disease. Therefore, this project aimed to perform the total synthesis of a GPI of *T. cruzi* (Figure 4-3) using the established synthetic strategy to access GPI structures bearing unsaturated lipids.

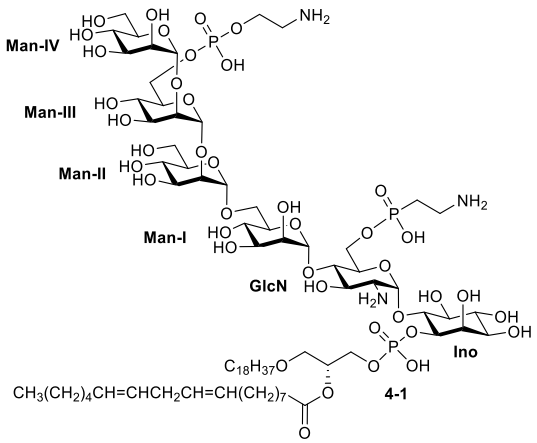

Figure 4-3. Target GPI of *T. cruzi.*

4.2 Retrosynthetic analysis

Following the general and convergent synthesis for GPIs bearing unsaturated lipids, the strategy for the total synthesis of a GPI of *T. cruzi* followed the methods used to synthesize the *P. falciparum* GPI presented in chapter 3. In this synthesis, the strategy must be adapted to include two modifications to the GPI pseudopentasaccharide core: an additional mannose (Man IV) at the non-reducing end of the glycan core and a (2-aminoethyl)phosphonate (AEP) unit at the O-6 position of glucosamine (Figure 4-3).

The assembly of the GPI **4-1** bearing unsaturated lipids will require the construction of the pseudodisaccharide **4-6** by the glycosylation between inositol **2-10** and glucosamine **2-11** (Scheme 4-1). Pseudodisaccharide **4-6** was devised with a PMB group at the O-6 position of glucosamine to provide the additional level of orthogonality required to introduce the AEP at a late stage of the route. To include the additional Man IV into the final structure, the synthesis of the allyl tetramannoside **4-5** was designed via a [2+2] glycosylation between the dimannose donor **4-7** and the dimannose acceptor **3-21**. A [4+2] glycosylation reaction of the tetramannoside donor **4-5** with the pseudodisaccharide acceptor **4-6** will provide the pseudohexasaccharide **4-3**. Then, the allyl protecting group will be removed to install the phospholipid using the H-phosphonate **4-4.** Removing the PMB protecting group and reacting with the phosphonodichloridate **4-2** will deliver the (2-aminoethyl)phosphonate modified core. A following TBDPS cleavage and installation of the phosphoethanolamine unit in the free alcohol will complete the assembly of the GPI. The final treatment of the protected compound under oxidative conditions to remove the 2-naphthylmethyl ethers permanent protecting groups and the reduction of remaining azides will deliver the desired glycolipid.

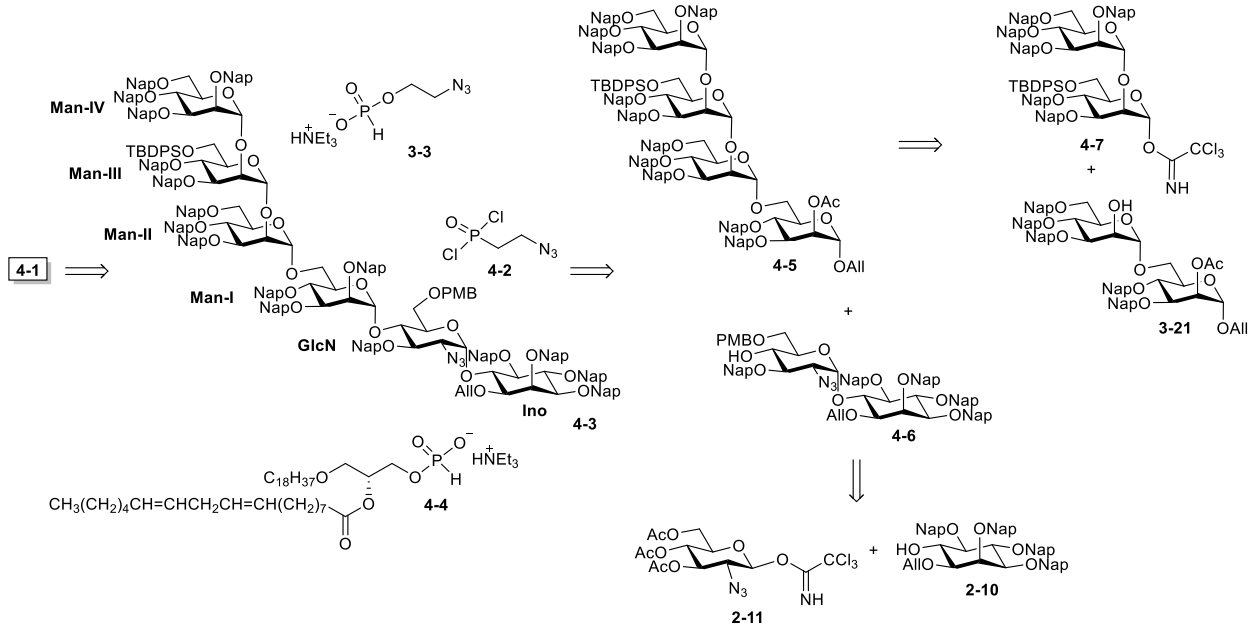

Scheme 4-1. Retrosynthetic analysis of *T. cruzi* GPI **4-1**. Nap = 2-Naphthylmethyl, TBDPS = *tert*-Butyldiphenylsilyl, PMB = *p*-Methoxybenzyl.

4.3 Results and discussion

4.3.1 Synthesis of building blocks

The triol **2-32** (Scheme 2-6, chapter 2) was used as starting material to synthesize the pseudodisaccharide acceptor **4-6** (Scheme 4-2). First, a *p*-methoxybenzylidene acetal between the O-6 and O-4 positions of glucosamine was formed using *p*-anisaldehyde dimethyl acetal. Then, the remaining hydroxyl group was protected as naphthylmethyl ether using Williamson conditions to give the fully protected pseudodisaccharide **4-9** in 77% yield over two steps. The acetal was selectively opened with sodium cyanoborohydride to furnish the desired pseudodisaccharide **4-6**, having the 4-O position of glucosamine free for glycan core elongation with tetramannoside donor **4-5**, and a PMB group at the 6-O position for the (2-aminoethyl)phosphonate unit incorporation at the late stage of the synthesis.

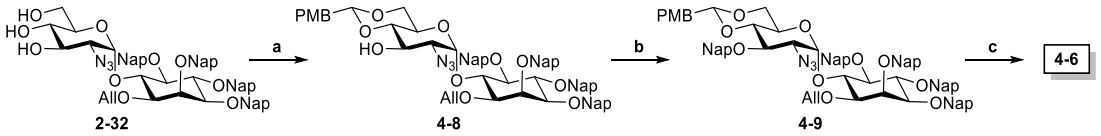

Scheme 4-2. Synthesis of the pseudodisaccharide **4-6**. *Reagents and conditions:* a) *p*-anisaldehyde dimethyl acetal, CSA, ACN, r.t., 40 min 88%; b) TBAI, NaH, NapBr, 0 °C, 1.5 h, 88%; c) $NaBH_3CN$, TFA, THF/DCM, r.t., 40 min, 6 h, 89%.

As depicted in the retrosynthetic analysis, tetramannose synthesis requires two building blocks. The dimannose **3-21** (ManI-ManII), which was previously obtained for the synthesis of a *P. falciparum* GPI (Scheme 3-4, chapter 3), and the ManIII-ManIV disaccharide **4-7** that can be obtained from the dimannose **4-10** that was already available in our laboratory (Scheme 4-3). The free hydroxy group of the allyl dimannoside **4-10** was protected in 88% yield as naphthylmethyl ether using NaH and NapBr in DMF. Following deallylation with $PdCl_2$ and hemiacetal treatment with trichloroacetonitrile and DBU delivered the dimannose donor **4-7**. The glycosylation between mannosyl donor **4-7** and acceptor **3-21** under TMSOTf activation provided the allyl tetramannoside **4-5**, which was deallylated at the reducing end with $PdCl_2$ in MeOH/DCM to furnish the hemiacetal **4-13** in 98% yield over two steps. Finally, carboximidation of the hemiacetal **4-13** with thrichloroacetonitrile and DBU afforded the desired tetramannose donor **4-14** in 77% yield.

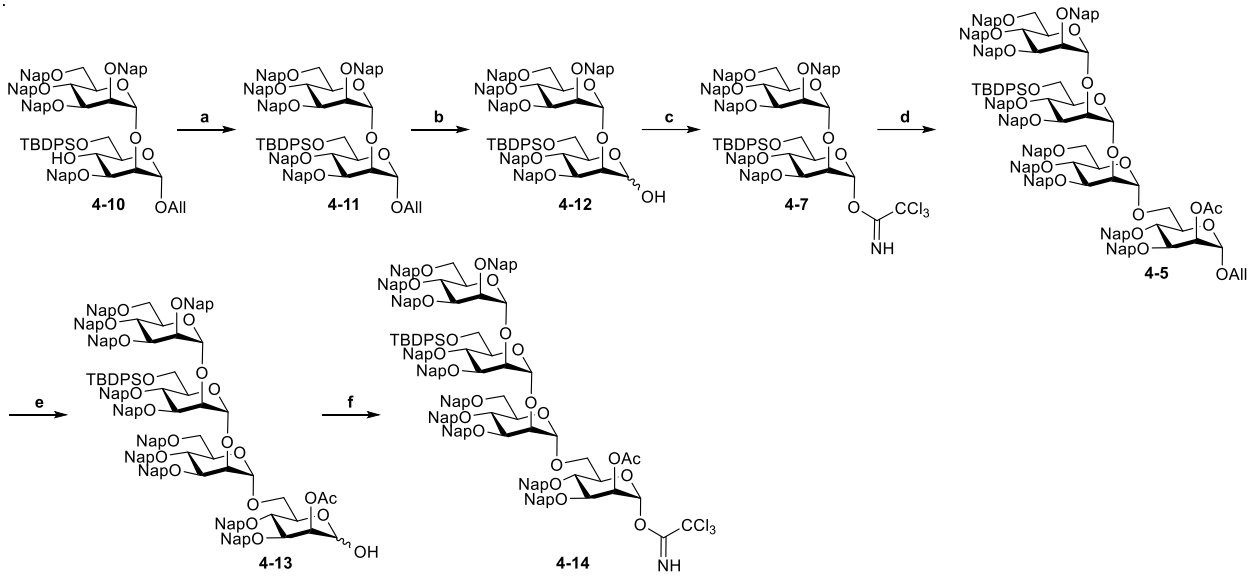

Scheme 4-3. Synthesis of the tetramannose donor **4-14**. *Reagents and conditions:* a) TBAI, NaH, NapBr, DMF, 50 °C, O.N., 88%; b) $PdCl_2$, DCM/MeOH, r.t., 7 h, 80%; c) DBU, CCl_3CN, DCM, 0 °C, 1.5 h; 83%; d) **3-21**, TMSOTf, Et_2O, -10 °C, 1 h; e) $PdCl_2$, DCM/MeOH, r.t., 3.5 h, 98% (two steps); f) DBU, CCl_3CN, DCM, 0 °C, 1 h; 77%.

The synthetic route continued with the preparation of the phospholipid moiety starting from alcohol **2-56**, an intermediate of the synthesis of H-phosphonate **2-59** (Scheme 2-11, chapter 2). The free alcohol of **2-56** was acylated with linoleic acid under *Steglich* esterification conditions in 92% yield, and the PMB group was removed under acidic conditions to give the alcohol **4-16** in 63% yield (Scheme 4-4). Finally, phosphitylation of **4-16** using phosphorous acid under pivaloyl chloride activation afforded H-phosphonate **4-4**.

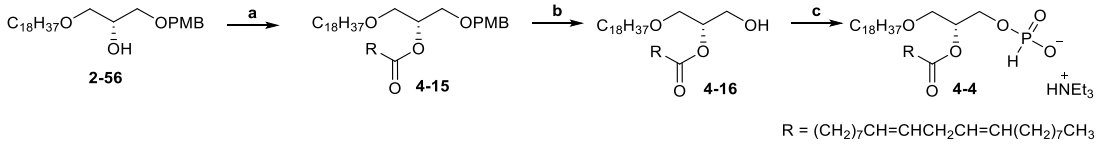

Scheme 4-4. Synthesis of H-phosphonates **4-4**. *Reagents and conditions*: a) Linoleic acid, DIC, DMAP, DCM, r.t., 1.5 h, 92%; d) TFA, DCM, -20 °C, 20 min, 63%; c) H_3PO_3, PivCl, pyridine, r.t., 1.5 h, 41%.

4.3.2 Synthesis of glycan core (First strategy)

Following the synthesis plan, the pseudodisaccharide acceptor **4-6** was glycosylated with the tetramannoside donor **4-14** using TMSOTf as the activator. The neighboring group participation of the acetyl group in **4-14** directed the reaction to obtain the pseudohexasaccharide **4-17** as its α-anomer (Scheme 4-5). Before removing the allyl group in **4-17** to install the phospholipid moiety,

the acetyl group in the O-2 position of Man-I must be exchanged with a Nap protecting group to avoid undesired removal of the fatty acid esters during the deacetylation. The pseudohexasaccharide **4-17** was treated with NaOMe to remove the acetyl group, giving the alcohol **4-18** in 57% yield over two steps. The low yield resulted from the loss of PMB protection under the harsh basic conditions required to remove the acetyl group. Next, alcohol **4-18** was treated with NaH, NapBr and 15-crown-5 in THF at 40 °C to prepare the fully protected pseudohexasaccharide **4-3**. However, as with the *P. falciparum* GPI, the reaction was more challenging than expected, probably due to steric hindrance. After a prolonged reaction time and successive additions of reagents, complete conversion was not achieved, and the small portion of the isolated product was highly contaminated. From the experience with the *P. falciparum* GPI synthesis, the protection strategy of the O-2 position of Man-I was changed instead of screening for additional reaction conditions. Thus, the acetyl protection was replaced with a levulinoyl ester in an early stage of the route.

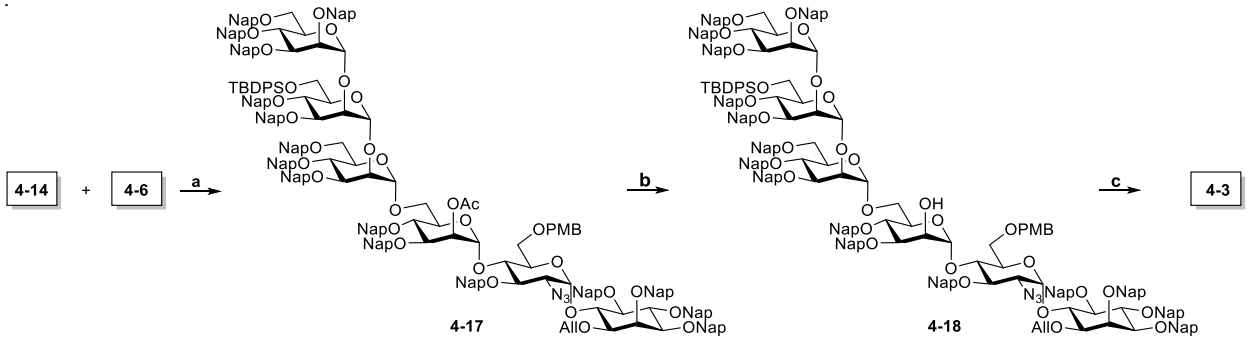

Scheme 4-5. Synthesis of the pseudohexasaccharide **4-3**. *Reagents and conditions:* a) TMSOTf, DCM/Et_2O, -10 °C, 1 h; b) NaOMe, DCM/MeOH, 50 °C, O.N., 57% (two steps); c) NaH, 15-crown-5, NapBr, THF, 40 °C, 24 h, <30%.

4.3.3 Synthesis of glycan core (Second strategy)

To exchange the protecting group at the O-2 position of Man-I at the earliest possible step of the synthesis, the allyl tetramannoside **4-5** was deacetylated with NaOMe in DCM/ MeOH, and the free alcohol was acylated with levulinic acid using Steglich esterification conditions, affording the tetramannose **4-20** in 85% yield over two steps (Scheme 4-6). Next, the allyl group was removed with $PdCl_2$, and the resulting tetramannose **4-21** was treated with trichloroacetonitrile and DBU to deliver the new trichloroacetimidate donor **4-22** in 77% yield over two steps.

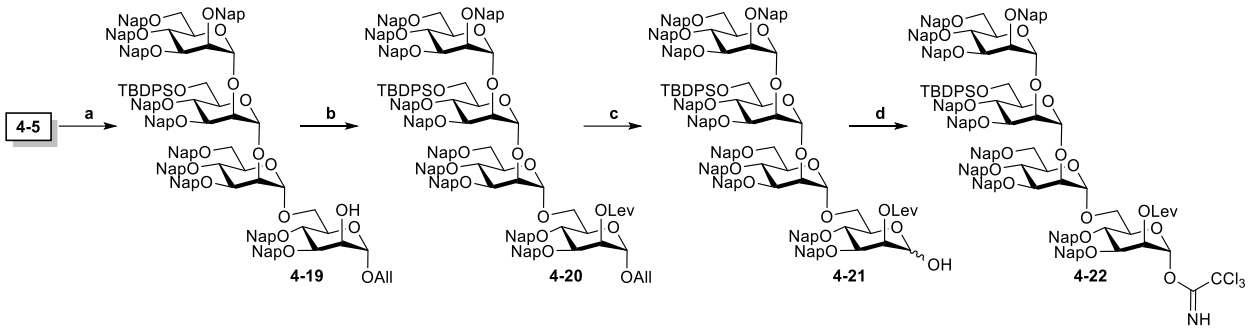

Scheme 4-6. Synthesis of the tetramannose donor **4-22**. *Reagents and conditions:* a) NaOMe, DCM/MeOH, 40 °C, 30 min, 100% b) LevOH, DMAP, DIC, DCM, r.t., O.N., 85%; c) $PdCl_2$, DCM/MeOH, r.t., 5 h, 85%; d) DBU, CCl_3CN, DCM, 0 °C, 1 h; 91%.

The [4+2] glycosylation of pseudodisaccharide acceptor **4-6** with tetramannose donor **4-22** afforded the pseudohexasaccharide **4-23** in quantitative yield as pure α-anomer thanks to the neighboring group participation of the levulinoyl ester (Scheme 4-7). The allyl protection at the myo-inositol was removed using a two-step protocol with an isomerization using a freshly activated iridium catalyst in THF, followed by hydrolysis with mercury salts in acetone/water, affording the glycan core **4-24** ready for the introduction of the phospholipid.

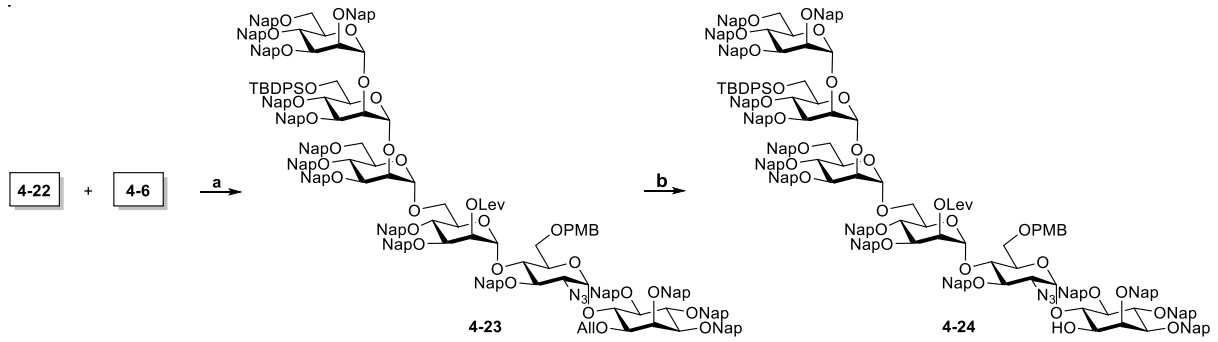

Scheme 4-7. Synthesis of the pseudohexasaccharide **4-24**. *Reagents and conditions:* a) TMSOTf, DCM/Et_2O, -10 °C, 1 h, 100%; b) *i.* $[IrCOD(PPh_2Me)_2]PF_6$ freshly activated with H_2, THF, r.t., 3 h; *ii.* $HgCl_2$, HgO, acetone/H_2O, 2 h, r.t., 85%

4.3.4 Synthesis of *T. cruzi* GPI

The alcohol **4-24** was reacted with the H-phosphonate **4-4** under pivaloyl chloride activation to get an H-phosphonate diester, which was oxidized with I_2/water to furnish the phospholipidated pseudohexasaccharide **4-25** in 82% yield. Next, the PMB group was selectively removed under acidic conditions to deliver the alcohol **4-26** in 96% yield, ready to incorporate the (2-aminoethyl)phosphonate unit (Scheme 4-8).

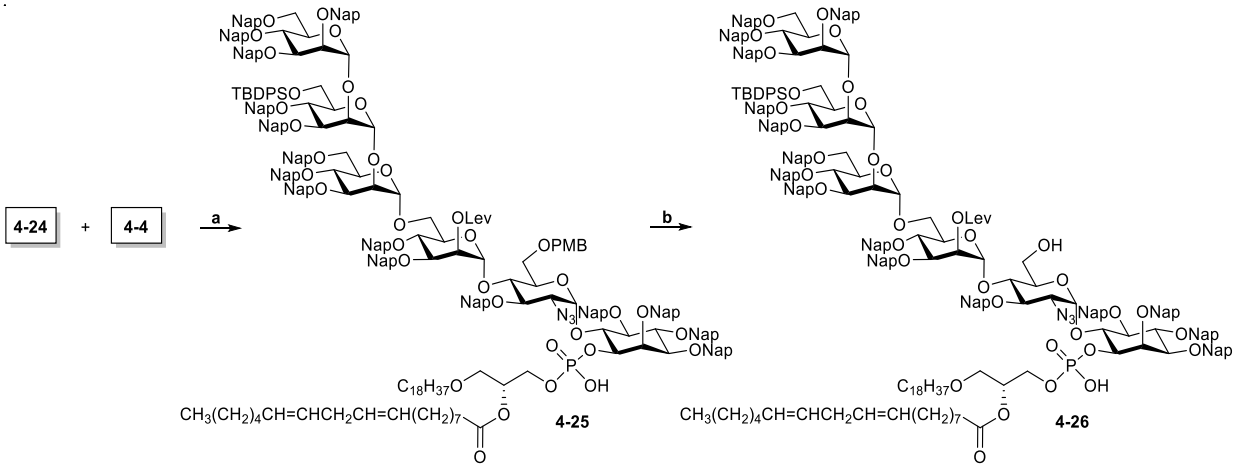

Scheme 4-8. Synthesis of the phospholipidated pseudohexasaccharide **4-26**. *Reagents and conditions:* a) *i.* PivCl, pyridine, r.t., 2 h; *ii.* I_2, H_2O, r.t., 1.5 h, 82%; b) TFA, DCM, -20 °C, 15 min, 96%.

Following the original synthetic plan, the phosphonodichloridate **4-2** was required to introduce the (2-aminoethyl)phosphonate moiety. The synthesis of this intermediated started from the commercially available diethyl (2-bromoethyl)phosphonate **4-27** (Scheme 4-9). First, the nucleophilic substitution of the bromide with sodium azide gave diethyl (2-azidoethyl)phosphonate **4-28** in 54% yield. Next, reaction with bromotrimethylsilane delivered the silylated intermediate **4-29**, which was treated with oxalyl chloride to afford the phosphonodichloridate **4-2**. Alcohol **4-26** was reacted with the crude phosphonodichloridate **4-2** in toluene; using 1H-tetrazole and DIPEA activation at 0 °C, followed by the hydrolysis of the remaining chloride by addition of water aiming to furnish the diphosphorylated GPI **4-30**. However, after purification by silica gel column chromatography and LH-20 size exclusion, a mixture of unidentified compounds was obtained, and the expected mass was not found with QTOF-MS. The complex mixture was treated with HF·Py in THF to remove the TBDPS protection. In this case, the expected mass for GPI **4-31** was observed by QTOF-MS, likely due to improvement of the ionization of the molecule after deprotection of the hydroxyl group. However, it was still highly contaminated with uncharacterizable by-products.

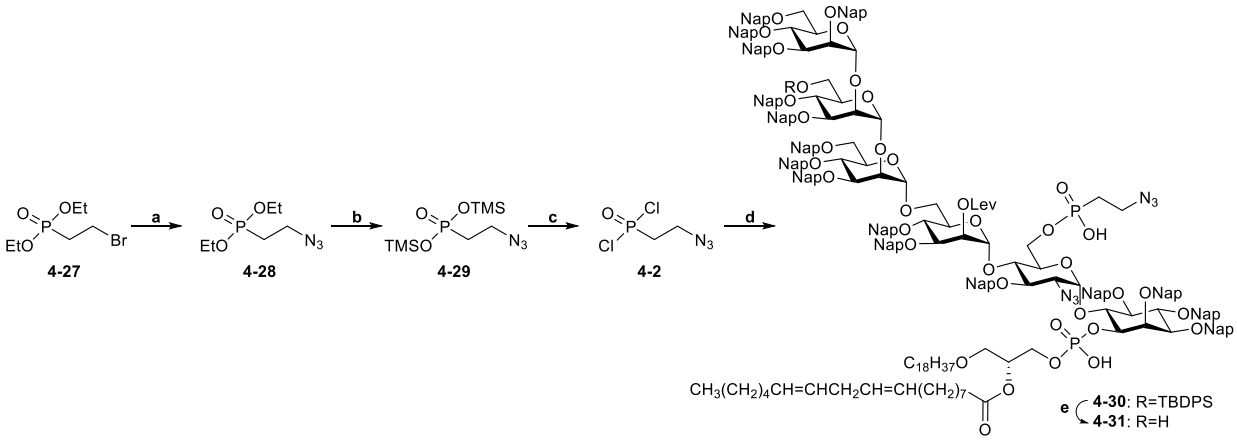

Scheme 4-9. Synthesis of the diphosphorylated pseudohexasaccharide **4-30**. *Reagents and conditions:* a) NaN_3, DMF, 65 °C, O.N., 54%; b) TMSBr, DCM, r.t., O.N.; c) Oxalylchloride, DMF cat.,

DCM, r.t., 1.5 h.; d) *i.* **4-26**, 1H-tetrazole, DIPEA, toluene, 0 °C, 2 h; *ii.* Water, r.t., 1 h; e) HF·Py complex, THF, r.t., 24 h.

To understand and optimize the outcome for the introduction of the AEP unit, the mannose **3-52** was reacted with the crude phosphonodichloridate **4-2** under the same conditions employed for alcohol **4-30** (Scheme 4-10). Two compounds were obtained after the reaction. The detected mass in positive mode for the minor product of the reaction corresponded to the starting material; nonetheless, some signals of the ^{1}H NMR spectrum were split compared to the original signals of the pure starting material. In addition, the ^{31}P NMR spectrum evidenced contamination with several phosphorous-containing compounds. The major product of the reaction presented a signal at 26 ppm in the ^{31}P NMR spectrum, which is in concordance with the signal reported for the AEP unit.[74] It also presented a significant shift towards the low field in the ^{1}H NMR spectrum for the proton of the C-2 position, indicating substitution at that position. However, the protons of the alkyl chain of the AEP unit were not observed. In addition, even if the expected mass of at 622 u.m.a. for **4-32** was observed in negative mode, the corresponding mass was not found in positive mode, instead two unexpected signals at 541 and 552 u.m.a. were observed.

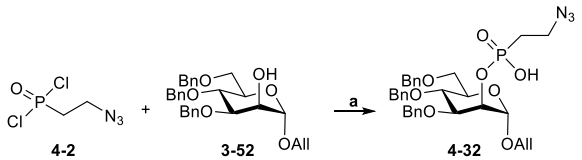

Scheme 4-10. Introcuction of the AEP unit to the model mannose **3-52**. *Reagents and conditions:* a) 1H-tetrazole, DIPEA, toluene or DCM, 0 °C, 2 h; *ii.* Water, r.t., 1 h; e) HF·Py complex, THF, r.t., 24 h.

To overcome solubility problems during the reaction of phosphonodichloridate **4-2** and alcohol **3-52**, the reaction was performed in DCM instead of toluene. Under these conditions, only the major product from previous attempts and the same unexpected results in the NMR and MS characterization were observed. The reasons behind these results are still unclear and further optimization and reaction conditions must be tested to introduce the AEP unit. Unfortunately, these studies were not possible within the available time for the experimental part of this thesis.

4.4 Conclusions and Outlook

The GPI glycan core of the *T. cruzi* GPI was synthesized containing orthogonal protecting groups for a selective installation of two specific modifications, a lipid with unsaturated fatty acid chains and the AEP unit. The glycan assembly showed significant problems during the last Nap protecting group installation at the Man-I unit. It required a change of the protection strategy and installing

levulinoyl ester at that position at an early stage of the synthesis. The unsaturated phospholipid installation was successful with the corresponding H-phosphonate **4-4**, while the attachment of the AEP moiety was more challenging than expected. Attempts to optimize this reaction with a small model molecule resulted in unexpected NMR and Mass spectra results; therefore, further studies are still required to achieve the desired transformation. Despite these results, the developed strategy showed high flexibility and allowed the synthesis of diverse protected GPI structures bearing unsaturated lipids.

The developed strategy can easily incorporate an additional mannose unit in the glycan structure by performing an [4+2] instead of [3+2] glycosylation reaction. In addition, this assembly protocol allowed the incorporation of additional orthogonality by including a PMB protecting group at the O-6 position of glucosamine. This differentiated position may allow a selective (2-aminoethyl)phosphonate incorporation in the GPI **4-30**. Further, TBDPS removal and installation of the phosphoethanolamine unit using the protocols used in the *P. falciparum* GPI will complete the synthesis of the target GPI. Finally, the three-step global deprotection protocol may provide the target *T. cruzi* GPI **4-1**.

We aimed the GPI **4-1** synthesis to perform structure-activity relationship and biological activity determinations of the GPI in the Chagas disease and to test the potential application of these molecules in diagnostic and Chagas disease prevention. Therefore, a successful synthesis of GPI **4-1** will not only prove the general applicability of the strategy to obtain GPIs bearing unsaturated lipids, but it will also provide the homogenous *T. cruzi* GPI samples for biological assays. Like the GPI of *P. falciparum*, future work will incorporate a cysteine modification at the phosphoethanolamine unit to couple GPI **4-1** with a *T. cruzi* glycoprotein —e.g., the Trypomastigote Small Surface Antigen (TSSA)— via native chemical ligation. This GPI-AP of *T. cruzi* should also provide information about the influence of the GPI anchor on the protein activity and its use as a diagnostic tool for Chagas disease.

The biological activity of the GPI anchor of *T. cruzi* is also associated with a glycan branch of galactoses. Further studies should consider incorporating this modification and the synthesis of *T. cruzi* GPIs containing different branched structures at the 3-O position of Man-I. Access to various *T. cruzi* GPI derivatives will allow the evaluation of the biological function of the different modifications of these structures.

5 Experimental Part

5.1 General Methods

All purchased chemicals were of reagent grade and all anhydrous solvents were of high-purity grade and used as received from commercial suppliers. The glassware was dried under vacuum with a flameless heat gun, and all reactions were carried out under an argon atmosphere. Reaction progress was monitored by thin layer chromatography (TLC) performed on aluminum plates coated with silica gel F254 with a 0.25 mm thickness. Visualization was performed with UV light and staining with developing agents, followed by heating. The staining solutions were 3-methoxyphenol-sulfuric ethanol solution containing sulfuric acid, cerium sulfate-ammonium molybdate (CAM), acidic ninhydrin-acetone solution and basic potassium permanganate solution. Flash column chromatography was performed using Sigma Aldrich silica gel high purity grade 60 Å (230–400 mesh). Yields refer to spectroscopically homogeneous materials, unless otherwise stated.

^{1}H, ^{13}C and ^{31}P-NMR as well as 2D-spectra (COSY, HSQC and HMBC) were recorded on a Bruker 400 (400 MHz) or a Bruker Ascend 400 (400 MHz) spectrometers; the chemical shifts are expressed in parts per million (pmm) referenced to solvent signals. Data for ^{1}H RMN are reported as follows: δ, chemical shift; multiplicity (recorded as br, broad; app, apparent; s, singlet; d, doublet; t, triplet; q, quadruplet; and m, multiplet), coupling constants (J in Hertz, Hz) and integration. Data for ^{13}C NMR and ^{31}P NMR are reported as the chemical shifts, expressed in parts per million. High resolution mass spectrometry (HRMS) was performed on a Waters Xevo G2-XS Q-TOF spectrometer with an Acquity H-class UPLC. Mass spectra (MS) were recorded on a 1260 Infinity II LC System with an Agilent LC/MSD iQ Mass Selective Detector (G6160AA). Ionization was done by Electrospray (ESI). Mass spectrum data are reported as m/z. Infrared spectra (IR) were obtained on a Perkin Elmer Spectrum 100 FTIR spectrophotometer with PIKE MIRacle ATR cell and are reported in terms of frequency of absorption (v, cm^{-1}). Optical rotation was determined on a Schmidt & Haensch UniPol L 1000 polarimeter and is reported as follows: $[\alpha]_{20}^{D}$: (c, solvent), where c = concentration is expressed in g/100 mL.

5.2 Methods for chapter 2

5.2.1 Synthesis of building blocks

Methyl 6-*O*-trityl-α-D-glucopyranoside (2-14)

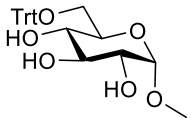

To a solution of Methyl-α,D-glucopiranose **2-13** (5.08 g, 26.2 mmol) in DMF (40 mL), trityl chloride (10.9 g, 39.2 mmol) and triethylamine (18.2 mL, 131 mmol) were added. The reaction mixture was stirred at room temperature for 12 h and volatiles were removed under reduced pressure. The remaining was dissolved with ethyl acetate, and the solution was extracted with water. The layers were separated, and the aqueous phase was extracted with ethyl acetate. Organic phases were combined, washed with brine, dried over Na_2SO_4, filtered, and concentrated under vacuum. The crude residue was purified by flash silica gel column chromatography to afford **2-14** in 92% yield (10.5 g, 24.05 mmol) as a white solid; R_f = 0.38 (hexane/EtOAc, 2:8).

^{1}H NMR (400 MHz, CD_3OD) δ (ppm) 7.42 – 7.51 (m, 6H, Ar), 7.18 – 7.32 (m, 9H, Ar), 4.75 (d, $J_{1,2}$ = 3.8 Hz, 1H, Glc-1), 3.76 (ddd, $J_{4,5}$ = 10.1 Hz, $J_{5,6b}$ = 6.7 Hz, $J_{5,6a}$ = 1.9 Hz, 1H, Glc-5), 3.60 (dd, $J_{2,3}$ = 9.7 Hz, $J_{3,4}$ = 8.8 Hz, 1H, Glc-3), 3.52 (s, 3H, C$\underline{H}_3$-O), 3.43 (dd, $J_{2,3}$ = 9.7 Hz, $J_{2,1}$ = 3.8 Hz, 1H, Glc-2), 3.40 (dd, $J_{6a,6b}$ = 9.8 Hz, $J_{5,6a}$ = 1.9 Hz, 1H, Glc-6a), 3.26 (dd, $J_{4,5}$ = 10.1 Hz, $J_{3,4}$ = 8.8 Hz, 1H, Glc-4), 3.22 (dd, $J_{6a,6b}$ = 9.8 Hz, $J_{5,6b}$ = 6.7 Hz, 1H, Glc-6b).

^{13}C NMR (101 MHz, CD_3OD) δ (ppm) 144.2 (C_q Ar), 128.6, 127.3, 126.6 (C Ar), 100.0 (Glc-1), 75.3 (Glc-3), 73.5 (Glc-2), 72.3 (Glc-5), 72.2 (Glc-4), 64.8 (Glc-6), 54.0 ($\underline{C}H_3$-O).

ESI-MS: 459.1 $[M+Na]^+$, 895.2 $[M+M+Na]^+$.

Methyl 2,3,4-tri-*O*-(2-naphthyl)methyl-α-D-glucopyranoside (2-15)

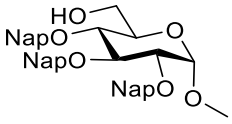

NaH (2.31 g, 96.2 mmol, 60% in mineral oil) was added to a solution of **2-14** (10.5 g, 24.0 mmol) in DMF (235 mL) at 0 °C. After 1 hour, 2-(Bromomethyl)naphthalene (18.6 g, 84.2 mmol) was added, and the reaction mixture was stirred at room temperature for 76 h. The reaction was quenched with aq. NH_4Cl, and volatiles were removed under reduced pressure. The remaining was dissolved with ethyl acetate, and the solution was extracted with water. The layers were separated, and the aqueous phase was extracted with ethyl acetate. Organic layers were combined, washed with brine, dried with Na_2SO_4, filtered, and evaporated. The crude compound (532 mg) was dissolved in a 1:1 DCM/MeOH mixture (9.6 mL), and *p*-Toluenesulfonic acid (22.5 mg,

0.130 mmol was added. The reaction mixture was stirred at room temperature for 24 h, neutralized using triethylamine and concentrated *in vacuo*. The resulting residue was purified by flash silica gel column chromatography using a gradient of hexane/EtOAc (1:5) to (4:6) give product **2-15** in 71% (10.5 g, 17.04 mmol) yield over two steps as a white solid; R_f = 0.23 (hexane/EtOAc, 5:1).

^{1}H NMR (400 MHz, $CDCl_3$) δ (ppm) 7.67 – 7.86 (m, 12H, Ar), 7.42 – 7.55 (m, 8H, Ar), 7.39 (dd, *J* = 8.4 Hz, 1.7 Hz, 1H, Ar), 5.21 & 5.05 (ABq, *J* = 11.2 Hz, 2H, C$\underline{H}_2$ Nap), 5.07 & 4.84 (ABq, *J* = 11.3 Hz, 2H, C$\underline{H}_2$ Nap), 4.99 & 4.88 (ABq, *J* = 12.2 Hz, 2H, C$\underline{H}_2$ Nap), 4.62 (d, $J_{1,2}$ = 3.5 Hz, 1H, Glc-1), 4.14 (app t, *J* = 9.22 Hz, 1H, Glc-3), 3.68 – 3.86 (m, 3H, Glc-5, Glc-6), 3.58 – 3.66 (m, 2H, Glc-2, Glc-4), 3.41 (s, 3H, C$\underline{H}_3$-O).

^{13}C NMR (101 MHz, $CDCl_3$) δ (ppm) 136.4, 135.7, 135.6, 133.4, 133.3, 133.3, 133.2, 133.1 (C_q Ar), 128.5, 128.4, 128.2, 128.1, 128.1, 127.8, 127.8, 127.2, 126.7, 126.6, 126.3, 126.2, 126.1, 126.6, 126.1, 126.1, 126.0, 125.9 (C Ar), 98.3 (Glc-1), 82.1 (Glc-3), 80.0 (Glc-2), 77.6 (Glc-4), 75.9 (C$\underline{H}_2$ Nap), 75.3 (C$\underline{H}_2$ Nap), 73.7 (C$\underline{H}_2$ Nap), 70.8 (Glc-5), 62.0 (Glc-6), 55.4 (C$\underline{H}_3$-O).

ESI-MS: 637.2 $[M+Na]^+$.

(*Z*)-Methyl 6-*O*-acetyl-2,3,4-tri-*O*-(2-naphthyl)methyl-α-D-*gluco*-hex-5-enopyranoside (2-16)

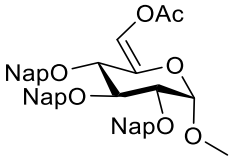

Sulfur trioxide-pyridine complex (8.89 g, 14.5 mmol) was added to a solution of **2-15** (8.89 g, 14.0 mmol) in anhydrous DCM (144 mL). The solution was cooled to 0 °C, and DIPEA (17 mL, 97.8 mmol) was added. After 10 min, DMSO (13.9 mL, 196 mmol) was added, and the reaction mixture was stirred at the same temperature for 1h. The reaction was quenched with aq. $NaHCO_3$, diluted with ethyl acetate and extracted with aq. $NaHCO_3$. The aqueous phase was extracted with EtOAc, and organic layers were combined, washed with brine, dried over Na_2SO_4, filtered and concentrated. The crude compound was dissolved in anhydrous ACN (140 mL), and acetic anhydride (7.9 mL, 83.8 mmol) was added, followed by potassium carbonate (7.72 g, 56.0 mmol). The mixture was brought to reflux (85 °C) for 3 h and allowed to cool to room temperature. The reaction was quenched with aq. $NaHCO_3$, diluted with ethyl acetate, and extracted with aq. $NaHCO_3$. The aqueous phase was extracted with EtOAc. Organic phases were combined, washed with brine, dried over Na_2SO_4, filtered and concentratedand concentrated *in vacuo*. The crude was purified by flash silica gel chromatography to afford **2-16** in 81% yield (7.66 g, 11.7 mmol) as a white solid; R_f = 0.36 (hexane/EtOAc, 3:1).

^{1}H NMR (400 MHz, $CDCl_3$) δ (ppm) 7.67 – 7.86 (m, 12H, Ar), 7.42 – 7.53 (m, 9H, Ar), 7.28 (d, $J_{6,4}$ = 1.4 Hz, 1H, Glc-6), 5.12 (d, *J* = 11.2 Hz, 1H, C$\underline{H}_2$ Nap), 4.99 – 5.08 (m, 2H, C$\underline{H}_2$ Nap), 4.95 (d, *J* = 2.6 Hz, 2H, C$\underline{H}_2$ Nap), 4.87 (d, *J* = 12.3 Hz, 1H, C$\underline{H}_2$ Nap), 4.75 (d, $J_{1,2}$ = 3.4 Hz, 1H, Glc-

1), 4.08 – 4.11 (m, 2H, Glc-3, Glc-4), 3.69 – 3.73 (m, 1H, Glc-2), 3.51 (s, 3H, C<u>H</u>$_3$-O), 2.17 (s, 3H, C<u>H</u>$_3$ Ac).

^{13}C NMR (101 MHz, CDCl$_3$) δ (ppm) 167.5 (C=O), 136.1 (Glc-5), 135.4, 135.2, 135.0, 133.4, 133.32, 133.27, 133.2, 133.14, 133.07 (C$_q$ Ar), 128.5, 128.4, 128.2, 128.13, 128.09, 128.0, 127.81, 127.78, 127.2, 126.9, 126.7, 126.4, 126.24, 126.19, 126.08, 126.06, 126.0, 125.95 (C Ar), 123.3 (Glc-6), 99.9 (Glc-1), 81.4 (Glc-3), 79.2(Glc-2), 77.8 (Glc-4), 75.9 (C<u>H</u>$_2$ Nap), 74.6 (C<u>H</u>$_2$ Nap), 74.0 (C<u>H</u>$_2$ Nap), 56.5 (C<u>H</u>$_3$-O), 20.8 (C<u>H</u>$_3$ Ac).
ESI-MS: 677.2 [M+Na]$^+$.

(1*R*,2*R*,3*S*,4*R*,5*S*)-3,4,5-tri-*O*-(2-naphthyl)methyloxy-2-hydroxy-6-oxocyclohexyl acetate (2-17)

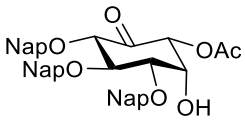

To a solution of **2-16** (100 mg, 0.153 mmol) in acetone (1.2 mL), mercury trifluoroacetate (78.1 mg, 0.183 mmol) was added, and the mixture was stirred for 1h. It was cooled to 0 °C, and water (0.2 mL) was added followed by aq. NaOAc (3 M, 0.15 mL) and brine (0.3 mL). The reaction was stirred at room temperature overnight, quenched with aq. $NaHCO_3$, diluted with ethyl acetate, and extracted with aq. $NaHCO_3$. The aqueous phase was extracted with EtOAc, and organic layers were combined, washed with brine, dried over Na_2SO_4, filtered and concentrated under reduced pressure. The desired product was crystalized from DCM/Et_2O to give **2-17** in 60% yield (59 mg, 0.0921 mmol) as a white solid; R_f = 0.29 (hexane/EtOAc, 3:2).
^{1}H NMR (400 MHz, CDCl$_3$) δ (ppm) 7.66 – 7.84 (m, 12H, Ar), 7.38 – 7.52 (m, 9H, Ar), 5.18 (d, $J_{1,2}$ = 2.7, 1H, H-1), 5.14 & 5.02 (ABq, J = 11.0 Hz, 2H, C<u>H</u>$_2$ Nap), 5.13 & 4.70 (ABq, J = 11.7 Hz, 2H, C<u>H</u>$_2$ Nap), 4.96 & 4.92 (ABq, J = 11.9 Hz, 2H, C<u>H</u>$_2$ Nap), 4.37 (app t, J = 2.9 Hz, 1H, H-2), 4.15 – 4.26 (m, 2H, H-4, H-5), 3.94 (dd, $J_{3,4}$ = 8.5 Hz, $J_{3,2}$ = 2.5 Hz, 1H, H-3), 2.61 (s, 1H, O<u>H</u>), 2.25 (s, 3H, C<u>H</u>$_3$-O).
^{13}C NMR (101 MHz, CDCl$_3$) δ (ppm) 198.1 (C-6), 170.0 (C=O Ac), 135.9, 134.8, 134.7, 133.4, 133.3, 133.2, 133.2, 133.1 (C$_q$ Ar), 128.7, 128.4, 128.2, 128.2, 128.1, 128.1, 127.8, 127.8, 127.8, 127.3, 127.2, 126.8, 126.7, 126.4, 126.2, 126.1, 126.0, 125.9 (C Ar), 83.4 (C-5), 81.9 (C-4), 78.8 (C-3), 76.3 (C<u>H</u>$_2$ Nap), 75.1 (C-1), 73.7 (C<u>H</u>$_2$ Nap), 73.6 (C<u>H</u>$_2$ Nap), 69.6 (C-2), 20.7 (C<u>H</u>$_3$-O).
ESI-MS: 663.2 [M+Na]$^+$.

1-Acetyl-3,4,5-tri-*O*-(2-naphthyl)methyl-D-*myo*-inositol (2-18)

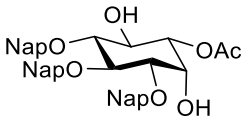

A solution $NaBH(OAc)_3$ (860 mg, 4.06 mmol) in ACN/AcOH (1:1, 13 mL) was added to a suspension of compound **2-17** (260 mg, 0.406 mmol) in ACN (13 mL) at 0 °C. The reaction mixture was allowed to warm to room temperature, and it was stirred for 24 h. The reaction was quenched with aq. $NaHCO_3$, diluted with ethyl acetate and extracted with aq. $NaHCO_3$. The aqueous phase was extracted with EtOAc. Organic layers were combined, washed with brine, dried over Na_2SO_4, filtered and concentrated *in vacuo*. The crude was purified by flash silica gel chromatography to afford **2-18** in 78% yield (204 mg, 0.317 mmol) as a white solid; R_f = 0.20 (hexane/EtOAc, 1:1).

^{1}H NMR (400 MHz, $CDCl_3$) δ (ppm) 7.61 – 7.86 (m, 12H, Ar), 7.46 (m, 9H, Ar), 5.12 & 5.04 (ABq, *J* = 11.1 Hz, 2H, C$\underline{H}_2$ Nap), 5.12 & 4.96 (ABq, *J* = 11.5 Hz, 2H, C$\underline{H}_2$ Nap), 4.90 & 7.85 (ABq, *J* = 11.6 Hz, 2H, C$\underline{H}_2$ Nap), 4.79 (dd, $J_{1,6}$ = 10.3 Hz, $J_{1,2}$ = 2.7 Hz, 1H, Ino-1), 4.38 (app t, *J* = 2.9 Hz, 1H, Ino-2), 4.19 (td, $J_{6,1\ \&\ 6,5}$ = 9.8 Hz, $J_{6,OH}$ = 3.0 Hz, 1H, Ino-6), 4.06 (t, *J* = 9.5 Hz, 1H, Ino-4), 3.68 (dd, $J_{3,4}$ = 9.5 Hz, $J_{3,2}$ = 2.7 Hz, 1H, Ino-3), 3.49 (t, *J* = 9.4 Hz, 1H, Ino-5), 2.51 (s, 1H, O$\underline{H}$-2), 2.32 (d, $J_{OH,6}$ = 3.1 Hz, 1H, O$\underline{H}$-6), 2.18 (s, 3H, C$\underline{H}_3$-O).

^{13}C NMR (101 MHz, $CDCl_3$) δ (ppm) 170.9 (C=O Ac), 136.1, 135.9, 134.9, 133.4, 133.4, 133.3, 133.2, 133.1, 133.1 (C_q Ar), 128.6, 128.6, 128.3, 129.0, 127.8, 127.8, 127.8, 127.0, 126.8, 126.6, 126.4, 126.3, 126.2, 126.12, 126.07, 126.01, 125.92, 125.90 (C Ar), 83.0 (Ino-5), 81.1 (Ino-4), 80.2 (Ino-3), 76.1 (C$\underline{H}_2$ Nap), 75.9 (C$\underline{H}_2$ Nap), 73.2 (Ino-1), 73.0 (C$\underline{H}_2$ Nap), 70.6 (Ino-6), 67.9 (Ino-2), 21.3 (C$\underline{H}_3$-O).

ESI-MS: 665.2 $[M+Na]^+$.

3,4,5-tri-*O*-(2-naphthyl)methyl-D-*myo*-inositol (2-19)

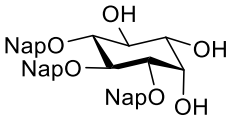

NaOMe (17.6 mg, 0.326 mmol) was added to a solution of **2-18** (1.05 g, 1.63 mmol) in 28 mL of MeOH/DCM (1:1), and the mixture was stirred at room temperature for 1 h. The reaction was neutralized with Amberlite IR 120 H^+ resin, filtered, and concentrated *in vacuo*. The resulting residue was purified by flash silica gel column chromatography to give the triol **2-19** in 97% yield (0.946 g, 1.57 mmol) as a white solid; R_f = 0.24 (DCM/EtOAc, 1:19).

^{1}H NMR (400 MHz, $CDCl_3$) δ (ppm) 7.71 – 7.80 (m, 7H, Ar), 7.64 – 7.68 (m, 4H, Ar), 7.35 – 7.50 (m, 10H, Ar), 5.07 & 4.96 (ABq, *J* = 11.0 Hz, 2H, C$\underline{H}_2$ Nap), 5.05 & 5.01 (ABq, *J* = 11.3 Hz, 2H, C$\underline{H}_2$ Nap), 4.94 & 4.82 (ABq, *J* = 11.9 Hz, 2H, C$\underline{H}_2$ Nap), 4.22 (t, *J* = 2.8 Hz, 1H, Ino-2), 4.03 (t, *J* = 9.5 Hz, 1H, Ino-4), 3.90 (t, *J* = 9.5 Hz, 1H, Ino-6), 3.55 (dd, $J_{3,4}$ = 9.7 Hz, $J_{3,2}$ = 2.7 Hz, 1H, Ino-3), 3.41 (t, *J* = 9.3 Hz, 1H, Ino-5), 3.36 (dd, $J_{1,6}$ = 9.8 Hz, $J_{1,2}$ = 2.8 Hz, 1H, Ino-1).

^{13}C NMR (101 MHz, $CDCl_3$) δ (ppm) 135.9, 135.8, 135.2, 133.0, 132.9, 132.7, 132.61, 132.59 (C_q Ar), 127.8, 127.6, 127.51, 127.49, 127.24, 127.21, 126.3, 126.11, 126.07, 125.70, 125.67, 125.65, 125.58, 125.56, 125.55, 125.4 (C Ar), 83.0 (Ino-5), 80.9 (Ino-4), 79.7 (Ino-3), 75.4 ($\underline{C}H_2$ Nap), 75.2 ($\underline{C}H_2$ Nap), 72.7 (Ino-6), 71.9 ($\underline{C}H_2$ Nap), 71.6 (Ino-1), 69.0 (Ino-2).
ESI-MS: 623.2 $[M+Na]^+$.

1-*O*-Allyl-3,4,5-tri-*O*-(2-naphthyl)methyl-D-*myo*-inositol (2-20)

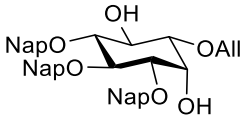

A mixture of compound **2-19** (153 mg, 0.255 mmol), 4 Å molecular sieves (400 mg), and bis(tributyltin)oxide (0.18 mL, 0.33 mmol) in toluene (5 mL) was refluxed using a Dean-Stark trap. After 5 h, TBAI (94 mg, 0.255 mmol) was added followed by allyl bromide (0.11 mL, 1.28 mmol). The reaction mixture was stirred at 65 °C overnight, solvent was evaporated *in vacuo*, and the product was purified by flash silica gel column chromatography to obtain **2-20** in 68% yield (112 mg, 0.175 mmol) as a white solid; R_f = 0.39 (hexane/EtOAc, 6:4).
^{1}H NMR (400 MHz, $CDCl_3$) δ (ppm) 7.72 – 7.84 (m, 12H, Ar), 7.43 – 7.52 (m, 9H, Ar), 5.89 – 6.99 (m, 1H, -C$\underline{H}$= Allyl), 5.27 (dd, *J* = 17.2 Hz, 1.6 Hz, 1H, =C$\underline{H}_{2a}$ Allyl), 5.18 (dd, *J* = 10.4 Hz, 1.6 Hz, 1H, =C$\underline{H}_{2b}$ Allyl), 5.14 & 5.04 (ABq, *J* = 11.1 Hz, 2H, C$\underline{H}_2$ Nap), 5.11 & 5.06 (ABq, *J* = 11.2 Hz, 2H, C$\underline{H}_2$ Nap), 4.96 & 4.92 (ABq, *J* = 12.0 Hz, 2H, C$\underline{H}_2$ Nap), 4.31 (app t, *J* = 2.8 Hz, 1H, Ino-2), 4.21 (ddt, *J* = 12.7, 5.8, 1.4 Hz, 1H, -C$\underline{H}_{2a}$- Allyl), 4.15 – 4.08 (m, 3H, Ino-4, Ino-6, -C$\underline{H}_{2b}$- Allyl), 3.55 (dd, $J_{3,4}$ = 9.6 Hz, $J_{3,2}$ = 2.7 Hz, 1H, Ino-3), 3.47 (t, *J* = 9.4 Hz, 1H, Ino-5), 3.20 (dd, $J_{1,6}$ = 9.6 Hz, $J_{1,2}$ = 2.7 Hz, 1H, Ino-1), 2.59 (s, 1H, O$\underline{H}$-6), 2.56 (s, 1H, O$\underline{H}$-2).
^{13}C NMR (101 MHz, $CDCl_3$) δ (ppm) 136.3, 136.2, 135.4 (C_q Ar), 134.5 (-$\underline{C}$H= Allyl), 133.42, 133.39, 133.3, 133.14, 133.06, 133.03 (C_q Ar), 128.5, 128.4, 128.2, 128.1, 128.0, 127.8, 127.8, 127.8, 126.8, 126.7, 126.6, 126.3, 126.2, 126.2, 126.13, 126.08, 126.05, 126.0, 125.93, 125.90 (C Ar), 118.0 (=$\underline{C}H_2$ Allyl), 82.8 (Ino-5), 81.1 (Ino-4), 80.0 (Ino-3), 79.0 (Ino-1), 76.0 ($\underline{C}H_2$ Nap), 75.6 ($\underline{C}H_2$ Nap), 72.9 ($\underline{C}H_2$ Nap), 72.4 (Ino-6), 71.4 (-$\underline{C}H_2$- Allyl), 67.1 (Ino-2).
ESI-MS: 663.2 $[M+Na]^+$.

1-*O*-Allyl-2-*O*-(*p*-methoxybenzyl)-3,4,5-tri-*O*-(2-naphthyl)methyl-D-*myo*-inositol (2-9)

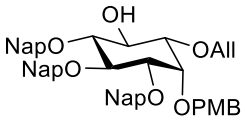

NaH (3.7 mg, 0.0917 mmol, 60% in mineral oil) was added to a solution of **2-20** (23.5 mg, 0.0367 mmol) in DMF (0.5 mL) at 0 °C. After 40 min, PMBCl (6.5 µL, 0.0477 mmol) was added, and it was stirred at the same temperature for 3 h. The reaction was quenched with water, and volatiles were removed under reduced pressure. The remaining was dissolved with DCM, and the solution

was extracted with water. The layers were separated, and the aqueous phase was extracted with DCM. Organic layers were mixed, washed with brine, dried with Na_2SO_4, filtered, and concentrated. The crude was purified by flash silica gel chromatography to afford **2-9** in 85% yield (23.7 mg, 0.0312 mmol) as a white solid; R_f = 0.33 (hexane/EtOAc, 7:3).

^{1}H NMR (400 MHz, $CDCl_3$) δ (ppm) 7.731 – 7.92 (m, 12H, Ar), 7.62 – 7.72 (m, 1H, Ar), 7.46 – 7.60 (m, 9H, Ar), 7.42 (d, *J* = 8.3 Hz, 2H, Ar), 6.87 – 6.95 (m, 2H, Ar), 5.89 – 6.01 (m, 1H, -C<u>H</u>= Allyl), 5.27 – 5.37 (m, 1H, =C<u>H</u>$_{2a}$ Allyl), 5.08 – 5.27 (m, 5H, =C<u>H</u>$_{2b}$ Allyl, C<u>H</u>$_2$ Nap), 4.81 – 4.96 (m, 4H, C<u>H</u>$_2$ Nap, C<u>H</u>$_2$ PMB), 4.21 – 4.35 (m, 2H, Ino-6, Ino-4), 4.15 – 4.19 (m, 1H, Ino-2), 4.08 (qd, *J* = 12.7, 5.5 Hz, 2H, -C<u>H</u>$_2$- Allyl), 3.82 (s, 3H, -OC<u>H</u>$_3$ PMB), 3.50 – 3.62 (m, 2H, Ino-5, Ino-3), 3.19 (dd, *J* = 9.8, 2.3 Hz, 1H, Ino-1).

^{13}C NMR (101 MHz, $CDCl_3$) δ (ppm) 159.1, 136.49, 136.48, 136.0 (C_q Ar), 134.6 (-<u>C</u>H= Allyl), 133.4, 133.3, 133.01, 132.99, 132.0 (C_q Ar), 129.6, 128.23, 128.20, 128.1, 128.03, 127.98, 127.8, 127.74, 127.71, 126.6, 126.5, 126.32, 126.26, 126.2, 126.05, 126.02, 126.00, 125.96, 125.79, 125.78 (C Ar), 117.4 (=<u>C</u>H$_2$ Allyl), 113.7 (C Ar), 83.4 (Ino-5), 81.6 (Ino-4), 81.1 (Ino-3), 80.0 (Ino-1), 75.9 (<u>C</u>H$_2$ Nap), 75.4 (<u>C</u>H$_2$ Nap), 73.8 (<u>C</u>H$_2$), 73.0 (Ino-6), 72.93 (<u>C</u>H$_2$), 72.89 (Ino-2), 71.2 (-<u>C</u>H$_2$- Allyl), 55.3 (O<u>C</u>H$_3$ PMB).

ESI-MS: 783.4 $[M+Na]^+$.

1-*O*-Allyl-2,3,4,5-tetra-*O*-(2-naphthyl)methyl-D-*myo*-inositol (2-10)

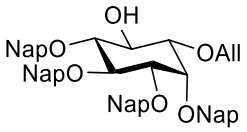

NaH (102 mg, 2.54 mmol, 60% in mineral oil) was added to a solution of **2-20** (651 mg, 1.02 mmol) in DMF (9.3 mL) at 0 °C. After 40 min, a solution of NapBr (270 mg, 1.22 mmol) in DMF (0.2 mL) was added, and it was stirred at the same temperature for 2 h. The reaction was quenched with water, and volatiles were removed under reduced pressure. The remaining was dissolved with ethyl acetate, and the solution was extracted with water. The layers were separated, and the aqueous phase was extracted with ethyl acetate. Organic layers were mixed, washed with brine, dried with Na_2SO_4, filtered, and concentrated. The crude was purified by flash silica gel chromatography to afford **2-10** in 66% yield (523 mg, 0.670 mmol) as a white solid; R_f = 0.34 (hexane/EtOAc, 3:1).

^{1}H NMR (400 MHz, $CDCl_3$) δ (ppm) 7.71 – 7.85 (m, 13H, Ar), 7.58 – 7.67 (m, 3H, Ar), 7.41 – 7.51 (m, 12H, Ar), 5.84 – 5.94 (m, 1H, -C<u>H</u>= Allyl), 5.23 (dd, *J* = 17.2 Hz, 1.8 Hz, 1H, =C<u>H</u>$_{2a}$ Allyl), 5.14 – 5.18 (m, 2H, =C<u>H</u>$_{2b}$ Allyl, C<u>H</u>$_2$ Nap), 5.05 – 5.10 (m, 5H, C<u>H</u>$_2$ Nap), 4.88 & 4.82 (ABq, *J* = 11.9 Hz, 2H, C<u>H</u>$_2$ Nap), 4.25 (m, 2H, Ino-4, Ino-6), 4.15 (app t, *J* = 2.4 Hz, 1H, Ino-2), 4.10 – 3.95 (m, 2H, -C<u>H</u>$_2$- Allyl), 3.49 – 3.53 (m, 2H, Ino-3, Ino-5), 3.16 (dd, $J_{1,6}$ = 9.9 Hz, $J_{1,2}$ = 2.3 Hz, 1H, Ino-1), 2.58 (s, 1H, O<u>H</u>).

^{13}C NMR (101 MHz, $CDCl_3$) δ (ppm) 136.44, 136.37, 136.0 (C_q Ar), 134.5 (-CH= Allyl), 133.44, 133.35, 133.3, 133.07, 133.06, 133.03 (C_q Ar), 128.32, 128.29, 128.16, 128.09, 128.0, 127.82, 127.79, 127.76, 126.7, 126.6, 126.4, 126.31, 126.30, 126.28, 126.09, 126.07, 126.0, 125.88, 125.86 (C Ar), 117.6 (=CH_2 Allyl), 83.5 (Ino-5), 81.6 (Ino-4), 81.2 (Ino-3), 80.0 (Ino-1), 76.0 (CH_2 Nap), 75.5 (CH_2 Nap), 74.1 (CH_2 Nap), 73.3 (Ino-2), 73.2 (CH_2 Nap), 73.0 (Ino-6), 71.4 (-CH_2-Allyl).

ESI-MS: 803.2 $[M+Na]^+$.

2-Azido-1,3,4,6-tetra-*O*-acetyl-2-deoxy-α,β-D-glucopyranose (2-22)

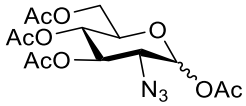

Triflic anhydride (0.46 mL, 2.78 mmol) was added dropwise to a suspension of NaN_3 (218 mg, 3.36 mmol) in ACN (4 mL) at 0 °C. After 2.5 h, this solution was added dropwise to a mixture of glucosamine hydrochloride **2-21** (500 mg, 2.32 mmol), copper sulfate pentahydrate (5.7 mg, 0.0231 mmol), and Et_3N (0.65 mL, 4.64 mmol) in water (2.5 mL) at the same temperature. After 24 h, solvents were removed under reduced pressure. The resulting oil was dissolved in 5 mL of anhydrous pyridine, and DMAP (28 mg, 0.232 mmol) was added followed by 5 mL of Ac_2O at 0 °C. The mixture was stirred overnight and concentrated by evaporation *in vacuo*. It was dissolved in EtOAc, washed with 1 M aq. HCl followed by saturated aqueous bicarbonate. Aqueous phases were combined and extracted once with EtOAc. Organic layers were mixed, washed with brine, dried over Na_2SO_4, filtered and concentrated. The crude was purified by flash silica gel column chromatography to give a 42:58 α:β mixture of compound **2-22** in 95 % yield over to steps (822 mg, 0.862 mmol) as a colorless oil; R_f = 0.35 (hexane/EtOAc, 7:3).

^{1}H NMR (400 MHz, $CDCl_3$) δ (ppm) 5.55 (d, $J_{1,2}$ = 8.6 Hz, 1H, Glc-1 β-anomer), 5.00 – 5.14 (m, 2H, Glc-3, Glc-4), 4.28 (m, 1H, Glc-6a), 4.08 (m, 1H, Glc-6b), 3.78 – 3.82 (m, 1H, Glc-5), 3.61 – 3.70 (m, 1H, Glc-2), 2.03 – 2.19 (m, 12H, CH_3 Ac).

^{13}C NMR (101 MHz, $CDCl_3$) δ (ppm) 170.7 (C=O Ac), 169.8 (C=O Ac), 169.7 (C=O Ac), 168.7 (C=O Ac), 92.7 (Glc-1 β-anomer), 72.8 (Glc-5), 72.7 (Glc-3), 67.8 (Glc-4), 62.6 (Glc-2), 61.4 (Glc-6), 21.03 (CH_3 Ac), 20.82 (CH_3 Ac), 20.78 (CH_3 Ac), 20.7 (CH_3 Ac).

ESI-MS: 396.0 $[M+Na]^+$.

2-Azido-3,4,6-tri-*O*-acetyl-2-deoxy-β-D-glucopyranosyl trichloroacetimidate (2-23)

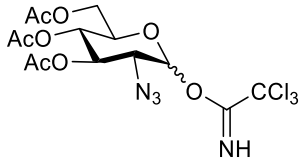

A mixture of compound **2-22** (2.92 g, 7.84 mmol) and hydrazine acetate (1.08 g, 11.8 mmol) in anhydrous THF (98 mL) was stirred overnight. It was concentrated, dissolved in DCM and washed twice with water. Aqueous phase was extracted twice with DCM. Organic layers were combined, washed with brine, dried over Na_2SO_4, filtered and concentrated. The resulting crude was purified by flash silica gel column chromatography eluting with Hexane/EtOAc (11:9, R_f =0.43) to afford the corresponding hemiacetal in 92% yield as a 64:36 α:β mixture (2.39 g, 7.21 mmol). To a solution of the hemiacetal (265 mg, 0.800 mmol) in anhydrous DCM (2.8 mL) at 0 °C, trichloroacetonitrile (0.8 mL, 8.00 mmol) was added followed by DBU (2.4 µL, 0.0160 mmol). After 1h, the solution was slightly concentrated under reduced pressure and immediately purified by silica gel column chromatography to give the imidate **2-23** in 86% yield (327 mg, 0.688 mmol) and 4:6 α/β ratio as a white solid; R_f = 0.40 (hexane/EtOAc, 2:1). The β anomer was isolated after silica gel column chromatography.

^{1}H NMR (400 MHz, $CDCl_3$) δ (ppm) 8.80 (s, 1H, NH), 5.69 (d, $J_{1,2}$ = 8.4 Hz, 1H, Glc-1), 5.11 – 5.04 (m, 2H, Glc-3, Glc-4), 4.29 (dd, $J_{6a,6b}$ = 12.5 Hz, $J_{6a,5}$ = 4.4 Hz, 1H, Glc-6a), 4.08 (dd, $J_{6b,6a}$ = 12.5 Hz, $J_{6b,5}$ 2.3 Hz, 1H, Glc-6b), 3.86 – 3.74 (m, 2H, Glc-2, Glc-5), 2.07 (s, 3H, CH_3 Ac), 2.04 (s, 3H, CH_3 Ac), 2.00 (s, 3H, CH_3 Ac).

^{13}C NMR (101 MHz, $CDCl_3$) δ (ppm) 170.5 (C=O Ac), 169.8 (C=O Ac), 169.5 (C=O Ac), 160.6 (C=NH), 96.4 (Glc-1), 90 (CCl_3), 72.7 (Glc-5), 72.6 (Glc-3), 67.8 (Glc-4), 63.2 (Glc-2), 61.4 (Glc-6), 20.8 (CH_3 Ac), 20.7 (CH_3 Ac), 20.6 (CH_3 Ac).

ESI-MS: 499.0 $[M+Na]^+$.

2,3,4,6-Tetra-*O*-acetyl-α-D-mannopyranosyl trichloroimidate (2-12)

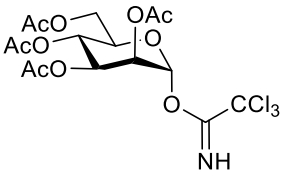

To a solution of peracetylated mannose **2-24** (600 mg, 1.54 mmol) in anhydrous DMF (5 mL), hydrazine acetate (156 mg, 1.69 mmol) was added at room temperature. After 2 h, the reaction mixture was diluted with DCM (30 mL) and washed with cold aq. sat. $NaHCO_3$ (4 x 30 mL). Organic layers were combined, washed with brine, dried over Na_2SO_4, filtered and concentrated. The resulting crude hemiacetal was dissolved in anhydrous DCM (12 mL), and trichloroacetonitrile (1.54 mL, 15.4 mmol) was added followed by DBU (57 µL, 0.384 mmol) at 0 °C. After 30 min, the solution was slightly concentrated under reduced pressure and immediately purified by silica

gel column chromatography to give the imidate **2-12** in 68% yield (512 mg, 1.04 mmol) as a white solid; R_f = 0.45 (hexane/EtOAc, 6:4).

^{1}H NMR (400 MHz, $CDCl_3$) δ (ppm) 8.78 (s, 1H, NH), 6.27 (d, $J_{1,2}$ = 2.0 Hz, 1H, Man-1), 5.46 (s, 1H, Man-2), 5.35 – 5.43 (m, 2H, Man-3, Man-4), 4.27 (dd, *J* = 12.0, 4.7 Hz, 1H, Man-6a), 4.12 – 4.21 (m, 2H, Man-5, Man-6b), 2.19 (s, 3H, CH_3 Ac), 2.08 (s, 3H, CH_3 Ac), 2.06 (s, 3H, CH_3 Ac), 2.00 (s, 3H, CH_3 Ac).

^{13}C NMR (101 MHz, $CDCl_3$) δ (ppm) 170.7 (C=O Ac), 169.9 (C=O Ac), 169.9 (C=O Ac), 169.8 (C=O Ac), 159.8 (C=NH), 94.6 (Man-1), 90.6 (CCl_3), 71.3 (Man-3), 68.9, 67.9, 65.4, 62.1 (Man-6), 20.9 (CH_3 Ac), 20.84 (CH_3 Ac), 20.82 (CH_3 Ac), 20.76 (CH_3 Ac).

ESI-MS: 513.9 $[M+Na]^+$.

3-(*p*-methoxybenzyl)-*sn*-glycerol (2-27)

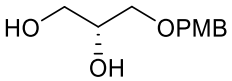

NaH (647 mg, 16.2 mmol, 60% in mineral oil) was added to a solution of (S)-(+)-1,2-Isopropylideneglycerol **2-25** (1.07 g, 8.10 mmol) in anhydrous DMF (40 mL) at 0 °C. After 30 min, 4-methoxybenzyl chloride (1.65 mL, 12.2) was added, and the solution was stirred at room temperature for 1 h before it was quenched with water at 0 °C. It was extracted with ethyl acetate (x4). Organic layers were combined, washed with brine, dried with Na_2SO_4, filtered, and evaporated. The resulting oil was dissolved in acetic acid (35 mL) and water (8.7 mL), and it was stirred at 70 °C for 1 hours. Solvents were removed *in vacuo* at 50°C, and the crude was purified by flash silica gel column chromatography to afford the desired diol **2-27** in 92% yield (1.59 g, 7.49 mmol) as a greasy white solid; R_f = 0.14 (hexane/EtOAc, 1:2).

^{1}H NMR (400 MHz, $CDCl_3$) δ (ppm) 7.23 – 7.27 (m, 2H, Ar of PMB), 6.85 – 6.91 (m, 2H, Ar of PMB), 4.48 (s, 2H, CH_2 PMB), 3.84 – 3.94 (m, 1H, CH sn-2), 3.81 (s, 3H, CH_3 PMB), 3.58 – 3.75 (m, 2H, CH_2 sn-1), 3.48 – 3.58 (m, 2H, CH_2 sn-3), 2.79 – 2.91 (m, 1H, OH-sn2), 2.34 – 2.48 (m, 1H, OH-sn1).

^{13}C NMR (101 MHz, $CDCl_3$) δ (ppm) 159.5 (C_q Ar of PMB), 129.8 (C_q Ar of PMB), 129.6 (CH Ar of PMB), 114.0 (CH Ar of PMB), 73.4 (CH_2 PMB), 71.7 (CH_2 sn-3), 70.7 (CH sn-2), 64.2 (CH_2 sn-1), 55.4 (CH_3 PMB).

ESI-MS: 235.1 $[M+Na]^+$.

3-(*p*-methoxybenzyl)-1-stearoyl-*sn*-glycerol (2-28)

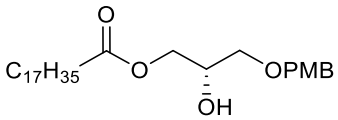

DMAP (84.7 mg, 0.693 mmol) and DCC (2.86 g, 13.9 mmol) were added to a solution of 3-(p-methoxybenzyl)-sn-glycerol **2-27** (1.23 g, 5.78 mmol) and stearic acid (1.64 g, 5.78 mmol) at 0 °C.

The mixture was stirred at this temperature for 1 h, then warmed up to room temperature and stirred overnight. Solids were removed by filtration through a pad of Celite, and the solution was concentrated under reduced pressure. The crude was purified by flash silica gel column chromatography to give product **2-28** (2.28 g, 4.77 mmol) in 82% yield as a white greasy solid; R_f = 0.52 (hexane/EtOAc, 7:3).

^{1}H NMR (400 MHz, $CDCl_3$) δ (ppm) 7.24 – 7.30 (m, 2H, Ar of PMB), 6.88 – 6.93 (m, 2H, Ar of PMB), 4.51 (s, 2H, C$\underline{H}_2$ PMB), 4.09 – 4.24 (m, 2H, C$\underline{H}_2$ sn-1), 3.98 – 4.09 (m, 1H, C$\underline{H}$ sn-2), 3.83 (s, 3H, C$\underline{H}_3$ PMB), 3.43 – 3.59 (m, 2H, C$\underline{H}_2$ sn-3), 2.53 (d, *J* = 4.8 Hz, 1H, O$\underline{H}$-sn2), 2.34 (t, *J* = 7.6 Hz, 2H, O-COC$\underline{H}_2$-CH_2 lipid), 1.65 – 1.57 (m, 2H, O-$COCH_2$-C$\underline{H}_2$ lipid), 1.27 (s, 28H, C$\underline{H}_2$ lipid), 0.90 (t, *J* = 6.7 Hz, 3H, C$\underline{H}_3$ lipid).

^{13}C NMR (101 MHz, $CDCl_3$) δ (ppm) 174.0 (C=O), 159.4 (C_q Ar of PMB), 129.7 (C_q Ar of PMB), 129.5 (C$\underline{H}$ Ar of PMB), 113.9 (C$\underline{H}$ Ar of PMB), 73.2 (C$\underline{H}_2$ PMB), 70.6 (C$\underline{H}_2$ sn-3), 68.9 (C$\underline{H}$ sn-2), 65.4 (C$\underline{H}_2$ sn-1), 55.3 (C$\underline{H}_3$ PMB), 34.2 (O-CO$\underline{C}H_2$-CH_2 lipid), 32.0 (C$\underline{H}_2$ lipid), 29.73 (C$\underline{H}_2$ lipid), 29.71 (C$\underline{H}_2$ lipid), 29.69 (C$\underline{H}_2$ lipid), 29.6 (C$\underline{H}_2$ lipid), 29.5 (C$\underline{H}_2$ lipid), 29.4 (C$\underline{H}_2$ lipid), 29.3 (C$\underline{H}_2$ lipid), 29.2 (C$\underline{H}_2$ lipid), 24.9 (O-$COCH_2$-C$\underline{H}_2$ lipid), 22.7 (C$\underline{H}_2$ lipid), 14.2 (C$\underline{H}_3$ lipid).

ESI-MS: 501.3 $[M+Na]^+$, 979.6 $[M+M+Na]^+$.

3-(p-methoxybenzyl)-2-oleoyl-1-stearoyl-*sn*-glycerol (2-29)

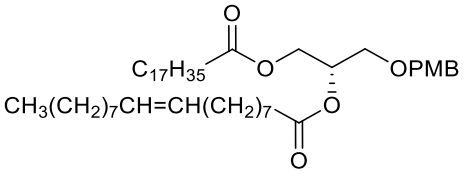

DMAP (63.6 mg, 5.20 mmol) and DIC (0.81 mL, 5.20 mmol) were added to a solution of 3-(p-methoxybenzyl)-1-stearoyl-*sn*-glycerol **2-28** (2.26 g, 4.73 mmol) and oleic acid (1.47 g, 5.20 mmol) in anhydrous DCM (20 mL). After 1.5 h, the reaction was quenched with water, and the layers were separated. The aqueous phase was extracted with DCM. Organic layers were washed with citric acid (1 M) followed by brine, dried over Na_2SO_4, filtered, and concentrated. Crude was purified by flash silica gel column chromatography to afford **2-29** (3.23 g, 4.34 mmol) in 92% yield as a white greasy solid; R_f = 0.66 (hexane/EtOAc, 4:1).

^{1}H NMR (400 MHz, $CDCl_3$) δ (ppm) 7.23 (d, *J* = 8.5 Hz, 2H, Ar of PMB), 6.87 (d, *J* = 8.5 Hz, 2H, Ar of PMB), 5.28 – 5.40 (m, 2H, -C$\underline{H}$=C$\underline{H}$- Oleoyl), 5.18 – 5.27 (m, 1H, C$\underline{H}$ sn-2), 4.40 – 4.52 (m, 2H, C$\underline{H}_2$ PMB), 4.32 (dd, *J* = 11.9, 3.8 Hz, 1H, C$\underline{H}_{2a}$ sn-1), 4.17 (dd, *J* = 11.9, 6.5 Hz, 1H, C$\underline{H}_{2b}$ sn-1), 3.80 (s, 3H, C$\underline{H}_3$ PMB), 3.55 (d, *J* = 5.2 Hz, 2H, C$\underline{H}_2$ sn-3), 2.22 – 2.36 (m, 4H, 2 x O-COC$\underline{H}_2$-CH_2 lipid), 1.93 – 2.05 (m, 4H, -C$\underline{H}_2$-CH=CH-C$\underline{H}_2$- Oleoyl), 1.51 – 1.68 (m, 4H, 2 x O-$COCH_2$-C$\underline{H}_2$ lipid), 1.20 – 1.37 (m, 48H, C$\underline{H}_2$ lipid), 0.88 (t, *J* = 6.7 Hz, 6H, 2 x C$\underline{H}_3$ lipid).

^{13}C NMR (101 MHz, $CDCl_3$) δ (ppm) 173.6 (C=O), 173.3 (C=O), 159.4 (C_q Ar of PMB), 130.1 (C_q Ar of PMB), 129.8 (-C$\underline{H}$=C$\underline{H}$- Oleoyl), 129.4 (C$\underline{H}$ Ar of PMB), 113.9 (C$\underline{H}$ Ar of PMB), 73.1 (C$\underline{H}_2$ PMB), 70.1 (C$\underline{H}$ sn-2), 68.0 (C$\underline{H}_2$ sn-3), 62.8 (C$\underline{H}_2$ sn-1), 55.4 (C$\underline{H}_3$ PMB), 34.4 (O-CO$\underline{C}H_2$-CH_2

lipid), 34.2 (O-CO<u>C</u>H$_2$-CH$_2$ lipid), 32.1, 32.05, 29.90, 29.85, 29.82, 29.81, 29.78, 29.7, 29.6, 29.51, 29.47, 29.44, 29.35, 29.3, 29.23, 29.20 (<u>C</u>H$_2$ lipid), 27.4 (-CH$_2$-CH=CH-<u>C</u>H$_2$- Oleoyl), 27.3 (-<u>C</u>H$_2$-CH=CH-CH$_2$- Oleoyl), 25.1 (O-COCH$_2$-<u>C</u>H$_2$ lipid), 25.0 (O-COCH$_2$-<u>C</u>H$_2$ lipid), 22.8 (<u>C</u>H$_2$ lipid), 14.2 (2 x <u>C</u>H$_3$ lipid).

ESI-MS: 765.5 [M+Na]$^+$.

2-Oleoyl-1-stearoyl-*sn*-glycerol (2-30)

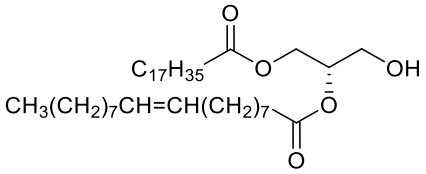

DDQ (183 mg, 0.808 mmol) and water (0.3 mL) were added to a solution of 3-(p-methoxybenzyl)-2-oleoyl-1-stearoyl-*sn*-glycerol **2-29** (300 mg, 0.404 mmol) in DCM (3 mL). The reaction mixture was stirred overnight before it was diluted with saturated aq. NaHCO$_3$ and extracted with DCM. Organic layers were washed with brine, dried with Na$_2$SO$_4$, filtered, and evaporated. The crude was purified by flash silica gel column chromatography to afford alcohol **2-30** (196 mg, 0.315 mmol) in 78% yield as a colorless oil; R_f = 0.34 (hexane/EtOAc, 4:1).

^{1}H NMR (400 MHz, CDCl$_3$) δ (ppm) 5.29 – 5.38 (m, 2H, -C<u>H</u>=C<u>H</u>- Oleoyl), 5.05 – 5.12 (m, 1H, C<u>H</u> sn-2), 4.33 (dd, *J* = 12.0, 4.2 Hz, 1H, C<u>H</u>$_{2a}$ sn-1), 4.21 (dd, *J* = 12.0, 5.9 Hz, 1H, C<u>H</u>$_{2b}$ sn-1), 3.71 (d, *J* = 5.0 Hz, 2H, C<u>H</u>$_2$ sn-3), 2.32 (q, *J* = 8.1 Hz, 4H, 2 x O-COC<u>H</u>$_2$-CH$_2$ lipid), 1.93 – 2.11 (m, 4H, -C<u>H</u>$_2$-CH=CH-C<u>H</u>$_2$- Oleoy), 1.53 – 1.59 (m, 4H, 2 x O-COCH$_2$-C<u>H</u>$_2$ lipid), 1.16 – 1.41 (m, 48H, C<u>H</u>$_2$ lipid), 0.87 (t, *J* = 6.7 Hz, 6H, 2 x C<u>H</u>$_3$ lipid).

^{13}C NMR (101 MHz, CDCl$_3$) δ (ppm) 173.9 (C=O), 173.5 (C=O), 130.0 (-<u>C</u>H=CH- Oleoyl), 129.7 (-CH=<u>C</u>H- Oleoyl), 72.1 (<u>C</u>H sn-2), 62.0 (<u>C</u>H$_2$ sn-1), 61.5 (<u>C</u>H$_2$ sn-3), 34.3 (O-CO<u>C</u>H$_2$-CH$_2$ lipid), 34.1 (O-CO<u>C</u>H$_2$-CH$_2$ lipid), 32.0, 31.9, 29.8, 29.74, 29.70, 29.66, 29.64, 29.56, 29.51, 29.49, 29.41, 29.36, 29.31, 29.29, 29.22, 29.15, 29.12, 29.09 (<u>C</u>H$_2$ lipid), 27.25 (-CH$_2$-CH=CH-<u>C</u>H$_2$-Oleoyl), 27.19 (-<u>C</u>H$_2$-CH=CH-CH$_2$- Oleoyl), 24.95 (O-COCH$_2$-<u>C</u>H$_2$ lipid), 24.91 (O-COCH$_2$-<u>C</u>H$_2$ lipid), 22.7 (<u>C</u>H$_2$ lipid), 14.2 (2 x <u>C</u>H$_3$ lipid).

ESI-MS: 645.5 [M+Na]$^+$.

Triethylammonium 2-oleoyl-1-stearoyl-*sn*-glycero-3-H-phosphonate (2-8)

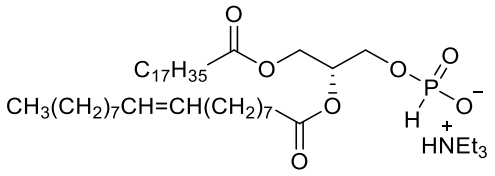

Phosphonic acid (587 mg, 7.16 mmol) and 2-Oleoyl-1-stearoyl-*sn*-glycerol **2-30** (1.49 g, 2.39 mmol) were subjected to azeotropic drying with anhydrous pyridine (3 x 5 mL of pyridine; last removal of pyridine was carried out for 1 h). The solid residue was dissolved in anhydrous pyridine

(60 mL). Pivaloyl chloride (0.88 mL, 7.16 mmol) was added, and the mixture was stirred for 2 h. Volatiles were removed under reduced pressure and the crude product was purified by column using silica gel deactivated with triethylamine (elution with MeOH/DCM 1:90 and gradually increasing the polarity to 1:10) to afford the H-phosphonate **2-8** in 53% yield (1.11 g, 1.27 mmol, 90% purity; excess triethylammonium salt) as a white solid; R_f = 0.28 (MeOH/DCM, 1:10).

^{1}H NMR (400 MHz, $CDCl_3$) δ (ppm) 11.97 (s, 1H, H-NEt_3), 7.50 (s, 0.5H, H-P), 5.86 (s, 0.5H, H-P), 5.25 – 5.37 (m, 2H, -CH=CH- Oleoyl), 5.19 (b s, 1H, CH sn-2), 4.40 – 4.29 (m, 1H, CH_{2a} sn-1), 4.19 – 4.07 (m, 1H, CH_{2b} sn-1), 4.00 (s, 2H, CH_2 sn-3), 3.17 – 3.01 (m, 6H, CH_2 Et_3N), 2.27 (q, *J* = 8.2 Hz, 4H, 2 x O-COCH_2-CH_2 lipid), 2.02 – 1.93 (m, 4H, -CH_2-CH=CH-CH_2- Oleoyl), 1.62 – 1.47 (m, 4H, 2 x O-$COCH_2$-CH_2 lipid), 1.38 (t, *J* = 7.3 Hz, 9H, CH_3 Et_3N), 1.33 – 1.17 (m, 48H, CH_2 lipid), 0.85 (t, *J* = 6.7 Hz, 6H, 2 x CH_3 lipid).

^{13}C NMR (101 MHz, $CDCl_3$) δ (ppm) 173.4 (C=O), 173.1 (C=O), 130.0 (-CH=CH- Oleoyl), 129.7 (-CH=CH- Oleoyl), 70.1 (CH sn-2), 62.5 (CH_2 sn-1), 62.3 (CH_2 sn-3), 45.8 (CH_2 Et_3N), 34.2 (O-COCH_2-CH_2 lipid), 34.1 (O-COCH_2-CH_2 lipid), 32.0, 31.9, 29.79, 29.77, 29.75, 29.7, 29.6, 29.40, 29.35 (CH_2 lipid), 27.2 (-CH_2-CH=CH-CH_2- Oleoyl), 24.89 (O-$COCH_2$-CH_2 lipid), 24.88 (O-$COCH_2$-CH_2 lipid), 22.7 (CH_2 lipid), 14.2 (2 x CH_3 lipid), 8.6 (CH_3 Et_3N).

^{31}P NMR (162 MHz, $CDCl_3$) δ (ppm) 3.59.

ESI-MS: 685.5 $[M-H]^-$.

Triethylammonium 1,2-distearoyl-*sn*-glycero-3-H-phosphonate (2-55)

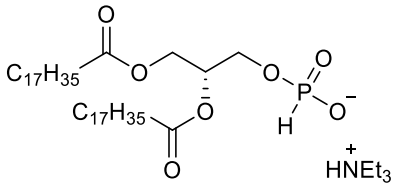

A mixture of 1,2-distearoyl-*sn*-glycerol **2-54** (200 mg, 0.320 mmol) and phosphonic acid (78.7 mg, 0.960 mmol) was co-evaporated with anhydrous pyridine (3 x 6 mL of pyridine; last removal of pyridine was carried out for 2 h). The solid residue was dissolved in anhydrous pyridine (8.5 mL). Pivaloyl chloride (43 µL, 0.352 mmol) was added, and the mixture was stirred overnight. Volatiles were removed under reduced pressure and the crude product was purified on a column of silica gel deactivated with triethylamine (eluting with MeOH/DCM 1:90 and gradually increasing the polarity to 1:10) to afford the H-phosphonate **2-55** in 81% yield (258 mg, 0.258 mmol, 79% purity, excess triethylammonium salt) as a white solid; R_f = 0.06 (MeOH/DCM, 1:10).

^{1}H NMR (400 MHz, $CDCl_3$) δ (ppm) 12.08 (s, 1H, H-NEt_3), 7.60 (s, 0.5H, H-P), 6.00 (s, 0.5H, H-P), 5.16 – 5.25 (m, 1H, CH sn-2), 4.35 (dd, *J* = 12.0, 3.6 Hz, 1H, CH_{2a} sn-1), 4.16 (dd, *J* = 12.0, 6.4 Hz, 1H, CH_{2b} sn-1), 3.95 – 4.05 (m, *J* = 6.9 Hz, 2H, CH_2 sn-3), 3.09 (br app s, 6H, CH_2 Et_3N), 2.28 (q, *J* = 7.5 Hz, 4H, 2 x O-COCH_2-CH_2 lipid), 1.58 (br s, 4H, 2 x O-$COCH_2$-CH_2 lipid), 1.39 (t, *J* = 7.2 Hz, 9H, CH_3 Et_3N), 1.23 (s, 56H, 2 x CH_2 lipid chain), 0.86 (t, *J* = 6.7 Hz, 6H, CH_3 lipid).

^{13}C NMR (101 MHz, $CDCl_3$) δ (ppm) 173.6 (C=O), 173.2 (C=O), 70.3 (CH sn-2), 62.5 (CH_2 sn-1), 62.4 (CH_2 sn-3), 45.8 (CH_2 Et_3N), 34.4 (O-COCH_2-CH_2 lipid), 34.2 (O-COCH_2-CH_2 lipid), 32.0, 29.85, 29.79, 29.7, 29.50, 29.47, 29.29, 29.26, 27.3 (CH_2 lipid), 25.00 (O-$COCH_2$-CH_2 lipid), 24.98 (O-$COCH_2$-CH_2 lipid), 22.8 (CH_2 lipid), 14.3 (2 x CH_3 lipid), 8.7 (CH_3 Et_3N).

^{31}P NMR (162 MHz, $CDCl_3$) δ (ppm) 4.49.

ESI-MS: 687.5 $[M-H]^-$.

3-(*p*-methoxybenzyl)-1-octadecanoyl-*sn*-glycerol (2-56)

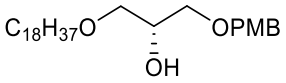

A mixture of diol **2-27** (441 mg, 2.08 mmol), and dibutyltin oxide (569 mg, 2.29 mmol) in toluene (21 mL) was refluxed at 118 °C for 2.5 h before it was concentrated at 50 °C by rotatory evaporation. The residue was dissolved in DMF (7 mL) and cooled to 0 °C. Cesium fluoride (802 mg, 5.28 mmol) was added followed by 1-bromooctadecane (763 mg, 2.29 mmol), and the reaction mixture was stirred at room temperature for 20 h. It was diluted with DCM, washed with water and brine, dried with Na_2SO_4, filtered, and concentrated. The crude compound was purified by silica gel column chromatography to give the alcohol **2-56** in 90% yield (865 mg, 1.86 mmol) as a white greasy solid; R_f = 0.76 (hexane/EtOAc, 1:2).

^{1}H NMR (400 MHz, $CDCl_3$) δ (ppm) 7.21 – 7.30 (m, 2H, Ar of PMB), 6.84 – 6.91 (m, 2H, Ar of PMB), 4.49 (s, 2H, CH_2 PMB), 3.92 – 4.01 (m, 1H, CH sn-2), 3.80 (s, 3H, CH_3 PMB), 3.40 – 3.56 (m, 6H, CH_2 sn-1, CH_2 sn-3, O-CH_2-CH_2 Octadecanoyl), 2.67 (d, J = 4.1 Hz, 1H, OH-sn2), 1.52 – 1.51 (m, 2H, O-CH_2-CH_2 Octadecanoyl), 1.21 – 1.37 (m, 32H, CH_2 Octadecanoyl), 0.89 (t, J = 6.7 Hz, 3H, CH_3 Octadecanoyl).

^{13}C NMR (101 MHz, $CDCl_3$) δ (ppm) 159.4 (C_q Ar of PMB), 130.2 (C_q Ar of PMB), 129.5 (CH Ar of PMB), 114.0 (CH Ar of PMB), 73.2 (CH_2 PMB), 71.9 (O-CH_2-CH_2 Octadecanoyl), 71.8 (CH_2 sn-1), 71.2 (CH_2 sn-3), 69.7 (CH sn-2), 55.4 (CH_3 PMB), 32.1, 29.84, 29.81, 29.77, 29.75, 29.6, 29.5, 26.2, 22.8 (CH_2 Octadecanoyl), 14.3 (CH_3 Octadecanoyl).

HRMS: $[M+Na]^+$ cald 487.3763; found 487.3750.

3-(p-methoxybenzyl)-2-oleoyl-1-octadecanoyl-*sn*-glycerol (2-57)

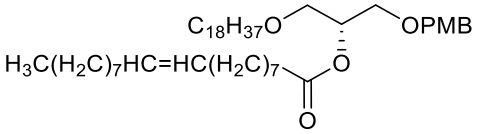

DMAP (54 mg, 0.442 mmol) and DIC (69.2 µL, 0.442 mmol) were added to a solution of 3-(p-methoxybenzyl)-1-octadecanoyl-*sn*-glycerol **2-56** (187 mg, 0.401 mmol) and oleic acid (139 µL, 0.442 mmol) in anhydrous DCM (1.7 mL). After 3 h, the reaction was quenched with water, and the layers were separated. The aqueous phase was extracted with DCM. Organic layers were

dried over Na_2SO_4, filtered, and concentrated. Crude was purified by flash silica gel column chromatography to afford **2-57** (268 mg, 0.356 mmol) in 89% yield as a colorless oil; R_f = 0.66 (hexane/EtOAc, 7:3).

^{1}H NMR (400 MHz, $CDCl_3$) δ (ppm) 7.21 – 7.25 (m, 2H, Ar of PMB), 6.84 – 6.89 (m, 2H, Ar of PMB), 5.30 – 5.40 (m, 2H, -C<u>H</u>=C<u>H</u>- Oleoyl), 5.16 (p, J = 5.1 Hz, 1H, C<u>H</u> sn-2), 4.40 – 4.52 (m, 2H, C<u>H</u>$_2$ PMB), 3.80 (s, 3H, C<u>H</u>$_3$ PMB), 3.51 – 3.61 (m, 4H, C<u>H</u>$_2$ sn-1, C<u>H</u>$_2$ sn-3), 3.36 – 3.46 (m, 2H, O-C<u>H</u>$_2$-CH$_2$ Octadecanoyl), 2.28 – 2.36 (m, 2H, O-COC<u>H</u>$_2$-CH$_2$ Oleoyl), 1.94 – 2.09 (m, 4H, -C<u>H</u>$_2$-CH=CH-C<u>H</u>$_2$- Oleoyl), 1.58 – 1.67 (m, 2H, O-COCH$_2$-C<u>H</u>$_2$ Oleoyl), 1.49 – 1.56 (m, 2H, O-CH$_2$-C<u>H</u>$_2$ Octadecanoyl), 1.21 – 1.37 (m, 55H, C<u>H</u>$_2$ lipid), 0.85 – 0.91 (m, 7H, 2 x C<u>H</u>$_3$ lipid).

^{13}C NMR (101 MHz, $CDCl_3$) δ (ppm) 173.5 (C=O Oleoyl), 159.4 (C_q Ar of PMB), 130.1 (C_q Ar of PMB), 129.9 (-<u>C</u>H=<u>C</u>H- Oleoyl), 129.4 (<u>C</u>H Ar of PMB), 113.9 (<u>C</u>H Ar of PMB), 73.0 (<u>C</u>H$_2$ PMB), 71.8 (O-<u>C</u>H$_2$-CH$_2$ Octadecanoyl), 71.4 (<u>C</u>H sn-2), 69.4 (<u>C</u>H$_2$ sn-1), 68.6 (<u>C</u>H$_2$ sn-3), 55.4 (<u>C</u>H$_3$ PMB), 34.6 (O-CO<u>C</u>H$_2$-CH$_2$ Oleoyl), 32.1, 32.1, 29.93, 29.86, 29.81, 29.80, 29.75, 29.7, 29.6, 29.52, 29.48, 29.4, 29.3, 29.2 (<u>C</u>H$_2$ lipid), 27.4 (-<u>C</u>H$_2$-CH=CH-CH$_2$- Oleoyl), 27.3 (-CH$_2$-CH=CH-<u>C</u>H$_2$- Oleoyl), 26.2 (<u>C</u>H$_2$ lipid), 25.2 (O-COCH$_2$-<u>C</u>H$_2$ Oleoyl), 22.8 (<u>C</u>H$_2$ lipid), 14.3 (2 x <u>C</u>H$_3$ lipid).

HRMS: $[M+Na]^+$ 751.6216 cald; found 751.6187.

2-Oleoyl-1-octadecanoyl-*sn*-glycerol (2-58)

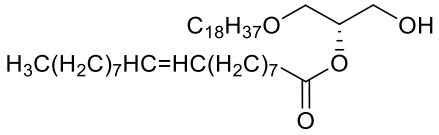

DDQ (45.2 mg, 0.199 mmol) was added to a solution of 3-(p-methoxybenzyl)-2-oleoyl-1-octadecanoyl-*sn*-glycerol **2-57** (100 mg, 0.133 mmol) in DCM:Water 95:5 (1 mL). The reaction mixture was stirred 1 h before it was diluted with saturated aq. $NaHCO_3$ and extracted with EtOAc. Organic layers were washed with brine, dried with Na_2SO_4, filtered, and evaporated. The crude was purified by flash silica gel column chromatography to afford alcohol **2-58** (64.7 mg, 0.104 mmol) in 78% yield as a yellow oil; R_f = 0.35 (hexane/EtOAc, 4:1).

^{1}H NMR (400 MHz, $CDCl_3$) δ (ppm) 5.27 – 5.40 (m, 2H, -C<u>H</u>=C<u>H</u>- Oleoyl), 4.99 (p, J = 4.8 Hz, 1H, C<u>H</u> sn-2), 3.74 – 3.86 (m, 2H, C<u>H</u>$_2$ sn-3), 3.56 – 3.67 (m, 2H, C<u>H</u>$_2$ sn-1), 3.39 – 3.48 (m, 2H, O-C<u>H</u>$_2$-CH$_2$ Octadecanoyl), 2.31 – 2.38 (m, 2H, O-COC<u>H</u>$_2$-CH$_2$ Oleoyl), 1.95 – 2.06 (m, 4H, -C<u>H</u>$_2$-CH=CH-C<u>H</u>$_2$- Oleoyl), 1.60 – 1.67 (m, 2H, O-COCH$_2$-C<u>H</u>$_2$ Oleoyl), 1.51 – 1.57 (m, 2H, O-CH$_2$-C<u>H</u>$_2$ Octadecanoyl), 1.22 – 1.37 (m, 62H, C<u>H</u>$_2$ lipid), 0.84 – 0.90 (m, 7H, 2 x C<u>H</u>$_3$ lipid).

^{13}C NMR (101 MHz, $CDCl_3$) δ (ppm) 173.8 (C=O Oleoyl), 130.1 (-<u>C</u>H=CH- Oleoyl), 129.8 (-CH=<u>C</u>H- Oleoyl), 73.0 (<u>C</u>H sn-2), 72.0 (O-<u>C</u>H$_2$-CH$_2$ Octadecanoyl), 70.1 (<u>C</u>H$_2$ sn-1), 63.0 (<u>C</u>H$_2$ sn-3), 34.5 (O-CO<u>C</u>H$_2$-CH$_2$ Oleoyl), 32.1, 32.0, 29.9, 29.84, 29.81, 29.76, 29.74, 29.71, 29.69, 29.66, 29.60, 29.59, 29.5, 29.4, 29.3, 29.24, 29.21 (<u>C</u>H$_2$ lipid), 27.4 (-<u>C</u>H$_2$-CH=CH-CH$_2$- Oleoyl),

27.3 (-CH_2-CH=CH-$\underline{C}H_2$- Oleoyl), 26.21 ($\underline{C}H_2$ lipid), 26.18 ($\underline{C}H_2$ lipid), 25.1 (O-$COCH_2$-$\underline{C}H_2$ Oleoyl), 22.8 ($\underline{C}H_2$ lipid), 14.2 (2 x $\underline{C}H_3$ lipid).

HRMS: $[M+Na]^+$ 631.5641 cald; found 631.5626.

Triethylammonium 2-oleoyl-1-octadecanoyl-*sn*-glycero-3-H-phosphonate (2-59)

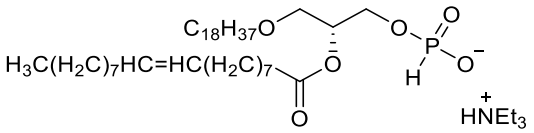

A mixture of 2-oleoyl-1-octadecanoyl-*sn*-glycerol **2-58** (105 mg, 0.173 mmol) and phosphonic acid (35.4 mg, 0.432 mmol) was co-evaporated with anhydrous pyridine (3 x 1 mL of pyridine; last removal of pyridine was carried out for 1 h). The solid residue was dissolved in anhydrous pyridine (4.3 mL). Pivaloyl chloride (52.9 µL, 0.432 mmol) was added, and the mixture was stirred 1 h. Volatiles were removed under reduced pressure and the crude product was purified on a column of silica gel deactivated with triethylamine (eluting with MeOH/DCM 1:90 and gradually increasing the polarity to 2:10) to afford the H-phosphonate **2-59** in 40% yield (61.1 mg, 0.0694 mmol, 88% purity, excess triethylammonium salt) as a slightly yellow oil; R_f = 0.22 (MeOH/DCM, 2:10).

^{1}H NMR (400 MHz, $CDCl_3$) δ (ppm) 12.08 (s, 1H, $\underline{H}$-NEt_3), 7.55 (s, 0.5H, $\underline{H}$-P), 5.95 (s, 0.5H, $\underline{H}$-P), 5.28 – 5.39 (m, 2H, -C$\underline{H}$=C$\underline{H}$- Oleoyl), 5.09 – 5.18 (m, 1H, C$\underline{H}$ sn-2), 3.90 – 4.14 (m, 2H, C$\underline{H}_2$ sn-3), 3.51 – 3.62 (m, 2H, C$\underline{H}_2$ sn-1), 3.34 – 3.47 (m, 2H, O-C$\underline{H}_2$-CH_2 Octadecanoyl), 3.04 – 3.18 (m, 6H, C$\underline{H}_2$ Et_3N), 2.31 (t, J = 7.6 Hz, 2H, O-COC$\underline{H}_2$-CH_2 Oleoyl), 1.95 – 2.07 (m, 4H, -C$\underline{H}_2$-CH=CH-C$\underline{H}_2$- Oleoyl), 1.57 – 1.65 (m, 2H, O-$COCH_2$-C$\underline{H}_2$ Oleoyl), 1.48 – 1.57 (m, 2H, O-CH_2-C$\underline{H}_2$ Octadecanoyl), 1.40 (t, J = 7.1 Hz, 9H, C$\underline{H}_3$ Et_3N), 1.21 – 1.36 (m, 56H, C$\underline{H}_2$ lipid), 0.88 (t, J = 6.8 Hz, 6H, 2 x C$\underline{H}_3$ lipid).

^{13}C NMR (101 MHz, $CDCl_3$) δ (ppm) 173.2 (C=O Oleoyl), 129.9 (-C$\underline{H}$=CH- Oleoyl), 129.7 (-CH=C$\underline{H}$- Oleoyl), 71.6 (C$\underline{H}$ sn-2, O-C$\underline{H}_2$-CH_2 Octadecanoyl), 69.1 (C$\underline{H}_2$ sn-1), 62.6 (C$\underline{H}_2$ sn-3), 45.8 (C$\underline{H}_2$ Et_3N), 34.4 (O-COC$\underline{H}_2$-CH_2 Oleoyl), 31.93, 31.90, 29.8, 29.74, 29.72, 29.67, 29.5, 29.5, 29.4, 29.3, 29.3, 29.23, 29.19, 29.14 (C$\underline{H}_2$ lipid), 27.2 (-C$\underline{H}_2$-CH=CH-C$\underline{H}_2$- Oleoyl), 26.1 (C$\underline{H}_2$ lipid), 25.0 (O-$COCH_2$-C$\underline{H}_2$ Oleoyl), 22.7 (C$\underline{H}_2$ lipid), 22.6 (C$\underline{H}_2$ lipid), 14.1 (2 x C$\underline{H}_3$ lipid), 8.6 (C$\underline{H}_3$ Et_3N).

^{31}P NMR (162 MHz, $CDCl_3$) δ (ppm) 3.82.

HRMS: $[M+Na]^+$ 671.5380 cald; found 671.5401.

5.2.2 Synthesis of GPI fragments 2-1 and 2-2

2-Azido-2-deoxy-α-D-glucopyranosyl-(1→6)-1-*O*-allyl-2,3,4,5-tetra-*O*-(2-naphthyl)methyl-D-*myo*-inositol (2-32)

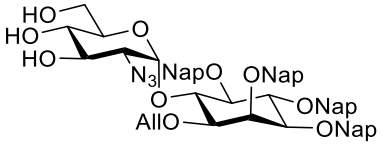

A solution of glycosyl acceptor **2-10** (49.1 mg, 0.0629 mmol) and glycosyl donor **2-11** (44.9 mg, 0.0943 mmol) in a 6:1 Et_2O/DCM anhydrous mixture (1 mL) was stirred at room temperature for 10 min. The mixture was cooled to 0 °C, and TMSOTf (3.4 µL, 0.0189 mmol) was added. After stirring for 2h at room temperature, the reaction was quenched with aq. $NaHCO_3$, diluted with ethyl acetate and extracted with aq. $NaHCO_3$. The aqueous phase was extracted with EtOAc. Organic layers were combined, washed with brine, dried over Na_2SO_4, filtered, and concentrated under reduced pressure. The obtained residue was purified by flash silica gel column chromatography to afford the pseudodisaccharide **2-31** (white solid) as a 11:1 α:β mixture that could not be separated; R_f = 0.28 (hexane/EtOAc, 3:1).

^{1}H NMR (400 MHz, $CDCl_3$) δ (ppm) 7.70 – 7.88 (m, 16H, Ar), 7.53 – 7.41 (m, 12H, Ar), 5.89–5.98 (m, 1H, -C<u>H</u>= Allyl), 5.87 (d, *J* = 3.7 Hz, 1H, Glc-1), 5.42 (dd, $J_{3,2}$ = 10.7 Hz, $J_{3,4}$ = 9.3 Hz, 1H, Glc-3), 5.34 (d, *J* = 12.3 Hz, 1H, C<u>H</u>$_2$ Nap), 5.14 – 5.26 (m, 3H, =C<u>H</u>$_2$ Allyl, C<u>H</u>$_2$ Nap), 5.05 – 5.10 (m, 3H, C<u>H</u>$_2$ Nap), 5.01 (d, *J* = 2.4 Hz, 1H, C<u>H</u>$_2$ Nap), 4.79 – 4.91 (m, 3H, C<u>H</u>$_2$ Nap Glc-4), 4.36 – 4.43 (m, 2H, Glc-5, Ino-6), 4.32 (t, *J* = 9.5 Hz, 1H, Ino-4), 4.16 (app t, *J* = 2.8 Hz, 1H, Ino-2), 4.04 (app dd, *J* = 13.3, 4.7 Hz, 1H, -C<u>H</u>$_{2a}$- Allyl), 3.96 (app dd, *J* = 12.1, 5.6 Hz, 1H, -C<u>H</u>$_{2b}$-Allyl), 3.79 (dd, *J* = 12.6, 2.3 Hz, 1H, Glc-6a), 3.53 – 3.59 (m, 3H, Glc-6b, Ino-1, C<u>H</u>-Ino), 3.46 (dd, *J* = 9.8, 2.1 Hz, 1H, C<u>H</u>-Ino), 3.21 (dd, *J* = 10.7 Hz, 3.7 Hz, 1H, Glc-2), 2.06 (s, 3H, C<u>H</u>$_3$ Ac), 1.90 (s, 3H, C<u>H</u>$_3$ Ac), 1.37 (s, 3H, C<u>H</u>$_3$ Ac). **^{13}C NMR (101 MHz, $CDCl_3$) δ (ppm)** 170.6 (C=O Ac), 170.2 (C=O Ac), 169.7 (C=O Ac), 136.2, 136.1, 135.9, 135.7 (C_q Ar), 134.1 (-<u>C</u>H= Allyl), 133.32, 133.28, 133.26, 133.12, 133.07, 133.04, 132.96, 132.8 (C_q Ar), 128.4, 128.2, 128.2, 128.14, 128.07, 128.03, 127.99, 127.9, 127.82, 127.80, 127.77, 127.7, 126.9, 126.8, 126.6, 126.5, 126.4, 126.32, 126.28, 126.24, 126.18, 126.12, 126.09, 126.01, 125.98, 125.88, 125.86, 125.8 (C Ar), 117.6 (=<u>C</u>H$_2$ Allyl), 97.3 (Glc-1), 82.0 (Ino-4), 81.8 (Ino), 81.5 (Ino), 80.8 (Ino), 76.0 (<u>C</u>H$_2$ Nap), 75.4 (<u>C</u>H$_2$ Nap), 74.9 (Ino-6), 74.4 (<u>C</u>H$_2$ Nap), 73.2 (<u>C</u>H$_2$ Nap), 72.9 (Ino-2), 71.1 (-<u>C</u>H$_2$- Allyl), 70.4 (Glc-3), 67.9 (Glc-4), 67.0 (Glc-5), 61.3 (Glc-6), 61.0 (Glc-2), 20.9 (<u>C</u>H$_3$ Ac), 20.7 (<u>C</u>H$_3$ Ac), 20.0 (<u>C</u>H$_3$ Ac).

ESI-MS: 1117.3 $[M+Na]^+$.

A solution of the α:β mixture **2-31** (0.0629 mmol) and NaOMe (10 mg, 0.189 mmol) in anhydrous MeOH (2 mL) was stirred at 40 °C for 3 h. The reaction was neutralized with Amberlite IR 120 H^+

resin, filtered, and concentrated *in vacuo*. The resulting residue was purified by flash silica gel column chromatography to give the desired product **2-32** in 94 % yield over two steps (57.5 mg, 0.0594 mmol) as a white solid. In this case, the α and β anomers were separated during the column; R_f α-anomer= 0.31, R_f β-anomer= 0.2 (hexane/EtOAc, 3:7).

IR (ATR) v(cm^{-1}) 3395 (O-H), 3047, 3019, 2925, 2872, 2106 (N=N=N), 1599, 1506, 1467, 1362, 1344, 1265, 1215, 1168, 1125, 1083, 1047, 1019, 957, 930, 890, 854, 814, 751, 665.

^{1}H NMR (400 MHz, $CDCl_3$) δ (ppm) 7.70 – 7.86 (m, 14H, Ar), 7.34 – 7.54 (m, 14H, Ar), 5.88 – 6.00 (m, 1H, -C<u>H</u>= Allyl), 5.69 (d, *J* = 3.7 Hz, 1H, Glc-1), 5.18 – 5.29 (m, 3H, C<u>H</u>$_2$ Nap, =C<u>H</u>$_{2a}$ Allyl), 5.15 (dd, *J* = 10.4 Hz, 1.5 Hz, 1H, =C<u>H</u>$_{2b}$ Allyl), 5.01 – 5.09 (m, 3H, C<u>H</u>$_2$ Nap), 4.76 – 4.88 (m, 3H, C<u>H</u>$_2$ Nap), 4.28 – 4.34 (m, 2H, Ino-4, Ino-6), 4.14 (app t, *J* = 2.3 Hz, 1H, Ino-2), 3.99 – 4.05 (m, 2H, -C<u>H</u>$_2$- Allyl), 3.94 – 3.99 (m, 1H, Glc-3), 3.87 – 3.92 (m, 1H, Glc-5), 3.50 – 3.54 (m, 2H, C<u>H</u>-Ino, C<u>H</u>-Ino), 3.38 – 3.43 (m, 2H, Glc-4, C<u>H</u>-Ino), 3.31 (m, 1H, Glc-6a), 3.15 (m, 1H, Glc-6b), 3.06 (dd, *J* = 10.4, 3.7 Hz, 1H, Glc-2), 2.92 (br s, 1H, O<u>H</u>-3'), 2.52 (br s, 1H, O<u>H</u>-4'), 1.36 (br s, 1H, O<u>H</u>-6').

^{13}C NMR (101 MHz, $CDCl_3$) δ (ppm) 136.3, 136.1, 136.0, 135.7 (C_q Ar), 134.3 (-<u>C</u>H= Allyl), 133.34, 133.29, 133.26, 133.1, 133.07, 133.0, 132.8 (C_q Ar), 128.3, 128.19, 128.17, 128.1, 128.04, 128.01, 128.0, 127.85, 127.82, 127.7, 126.8, 126.7, 126.45, 126.40, 126.3, 126.17, 126.15, 126.11, 126.09, 126.06, 126.02, 125.99, 125.9, 125.8, 125.5 (C Ar), 117.0 (=<u>C</u>H$_2$ Allyl), 97.7 (Glc-1), 82.1 (Ino-4), 81.9 (Ino), 81.6 (Ino), 81.0 (Ino), 76.0 (<u>C</u>H$_2$ Nap), 75.7 (<u>C</u>H$_2$ Nap), 75.4 (Ino-6), 74.2 (<u>C</u>H$_2$ Nap), 73.1 (<u>C</u>H$_2$ Nap), 72.8 (Ino-2), 71.6 (Glc-3), 71.5 (Glc-4), 71.2 (-<u>C</u>H$_2$- Allyl), 70.1 (Glc-5), 62.9 (Glc-2), 61.8 (Glc-6).

ESI-MS: 991.2 $[M+Na]^+$.

HRMS: $[M+Na]^+$ cald 990.3942; found 990.3983.

2-Azido-2-deoxy-3,4,6-tri-*O*-(2-naphthyl)methyl-α-D-glucopyranosyl-(1→6)-1-*O*-allyl-2,3,4,5-tetra-*O*-(2-naphthyl)methyl-D-*myo*-inositol (2-5)

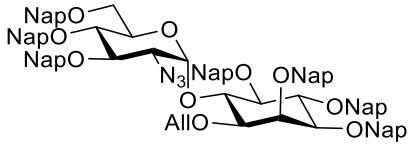

NaH (16.9 mg, 0.424 mmol, 60% in mineral oil) was added to a solution of isolated α-anomer **2-32** (68.5 g, 0.0708 mmol) and TBAI (118 mg, 0.318 mmol) in DMF (1.8 mL) at 0 °C. After 20 min, 2-(Bromomethyl)naphthalene (70.4 mg, 0.318 mmol) was added, and the reaction mixture was stirred at room temperature overnight. The reaction was quenched with water, and volatiles were removed under reduced pressure. The remaining was dissolved with ethyl acetate, and the solution was extracted with water. The layers were separated, and the aqueous phase was extracted with ethyl acetate. The organic layers were combined, washed with brine, dried with Na_2SO_4, filtered, and evaporated. The resulting residue was purified by flash silica gel column

chromatography to afford **2-5** in 92% (90.4 mg, 0.0651 mmol) yield as a white solid; R_f = 0.37 (hexane/EtOAc, 8:2).

$[\alpha]_D^{20}$**:** 43.5 (c = 1, $CHCl_3$).

IR (ATR) ν(cm^{-1}) 3056, 2866, 2106 (N=N=N), 1603, 1510, 1461, 1365, 1347, 1272, 1216, 1172, 1125, 1055, 953, 894, 856, 816, 753, 667.

^{1}H NMR (400 MHz, $CDCl_3$) δ (ppm) 7.65 – 7.89 (m, 23H, Ar), 7.61 (t, *J* = 7.5 Hz, 4H, Ar), 7.33 – 7.53 (m, 26H, Ar), 7.17 – 7.25 (m, 2H, Ar), 7.15 (s, 1H, Ar), 6.83 (dd, *J* = 8.5, 1.6 Hz, 1H, Ar), 5.93 – 6.04 (m, 1H, -C<u>H</u>= Allyl), 5.88 (d, *J* = 3.7 Hz, 1H, Glc-1), 5.29 (dd, *J* = 17.2, 1.6 Hz, 1H, =C<u>H</u>$_{2a}$ Allyl), 5.16 – 5.25 (m, 3H, =C<u>H</u>$_{2b}$ Allyl, C<u>H</u>$_2$ Nap), 4.98 – 5.14 (m, 6H, C<u>H</u>$_2$ Nap), 4.93 (d, *J* = 11.6 Hz, 1H, C<u>H</u>$_2$ Nap), 4.78 – 4.90 (m, 2H, C<u>H</u>$_2$ Nap), 4.76 (d, *J* = 11.2 Hz, 1H, C<u>H</u>$_2$ Nap), 4.63 (d, *J* = 12.3 Hz, 1H, C<u>H</u>$_2$ Nap), 4.44 (t, *J* = 9.6 Hz, 1H, Ino-6), 4.27 – 4.40 (m, 2H, Ino-4, C<u>H</u>$_2$ Nap), 4.15 – 4.23 (m, 2H, Ino-2, Glc-5), 4.04 – 4.11 (m, 3H, -C<u>H</u>$_2$- Allyl, Glc-3), 3.77 – 3.86 (m, 1H, Glc-4), 3.53 – 3.62 (m, 2H, Ino-3, Ino-5), 3.41 – 3.50 (m, 2H, Ino-1, Glc-2), 3.34 (dd, *J* = 11.0, 2.0 Hz, 1H, Glc-6a), 3.14 (dd, *J* = 10.9, 2.2 Hz, 1H, Glc-6b).

^{13}C NMR (101 MHz, $CDCl_3$) δ (ppm) 136.4, 136.2, 136.0, 135.81, 135.79, 135.7, 135.3 (C_q Ar), 134.4 (-<u>C</u>H= Allyl), 133.4, 133.33, 133.30, 133.27, 133.2, 133.12, 133.08, 133.06, 132.98, 132.95, 132.8, 132.7 (C_q Ar), 128.4, 128.32, 128.27, 128.2, 128.13, 128.09, 128.05, 128.03, 128.01, 127.9, 127.85, 127.82, 127.74, 127.72, 127.67, 127.0, 126.8, 126.7, 126.7, 126.5, 126.44, 126.39, 126.29, 126.26, 126.2, 126.12, 126.09, 126.03, 125.96, 125.94, 125.92, 125.91, 125.9, 125.81, 125.78, 125.7, 125.6, 125.5 (C Ar), 117.1 (=<u>C</u>H$_2$ Allyl), 97.9 (Glc-1), 82.2 (Ino-1), 82.1 (Ino-4), 81.6 (Ino-5), 80.8 (Ino-3), 80.4 (Glc-3), 78.2 (Glc-4), 76.0 (<u>C</u>H$_2$ Nap), 75.6 (Ino-6), 75.5 (<u>C</u>H$_2$ Nap), 75.4 (<u>C</u>H$_2$ Nap), 74.8 (<u>C</u>H$_2$ Nap), 74.2 (<u>C</u>H$_2$ Nap), 73.5 (<u>C</u>H$_2$ Nap), 73.0 (<u>C</u>H$_2$ Nap), 72.9 (Ino-2), 71.1 (-<u>C</u>H$_2$- Allyl), 70.2 (Glc-5), 67.7 (Glc-6), 63.6 (Glc-2).

HRMS: $[M+Na]^+$ cald 1410.5820; found 1410.5811.

ESI-MS: 1410.3 $[M+Na]^+$, 1286.3 $[M+K]^+$.

2-Azido-2-deoxy-3,4,6-tri-*O*-(2-naphthyl)methyl-α-D-glucopyranosyl-(1→6)-2,3,4,5-tetra-*O*-(2-naphthyl)methyl-D-*myo*-inositol (2-33)

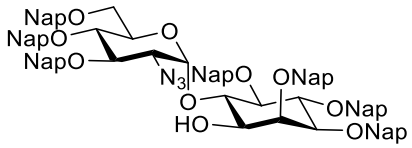

To a solution of the allylated pseudodisaccharide **2-6** (43.4 mg, 0.0312 mmol) in a 1:1 DCM/MeOH anhydrous mixture (1 mL), $PdCl_2$ (2.8 mg, 0.0156 mmol) was added at room temperature. After 3 h, the mixture was filtered through a pad of Celite, and the volatiles were evaporated *in vacuo*. The resulting oil was purified by flash silica gel column chromatography to obtain **2-33** in 85% yield (35.8 mg, 0.0265 mmol) as a white solid; R_f = 0.39 (hexane/EtOAc, 7:3).

$[\alpha]_D^{20}$**:** 35.8 (c = 1, $CHCl_3$).

IR (ATR) ν(cm^{-1}) 3458 (O-H), 3056, 3019, 2925, 2864, 2108 (N=N=N), 1603, 1510, 1462, 1366, 1344, 1272, 1248, 1216, 1171, 1124, 1044, 953, 893, 855, 815, 750, 667.

^{1}H NMR (400 MHz, $CDCl_3$) δ (ppm) 7.63 – 7.89 (m, 23H, Ar), 7.35 – 7.69 (m, 26H, Ar), 7.21 (s, 1H, Ar), 7.14 (d, *J* = 8.4 Hz, 1H, Ar), 6.91 (d, *J* = 8.4 Hz, 1H, Ar), 5.56 (d, *J* = 3.6 Hz, 1H, Glc-1), 5.15 – 5.29 (m, 3H, C$\underline{H}_2$ Nap), 4.97 – 5.12 (m, 4H, C$\underline{H}_2$ Nap), 4.84 – 4.92 (m, 3H, C$\underline{H}_2$ Nap), 4.78 & 4.38 (ABq, *J* = 11.5 Hz, 2H, C$\underline{H}_2$ Nap), 4.50 & 3.97 (ABq, *J* = 12.2 Hz, 2H, C$\underline{H}_2$ Nap), 4.32 (t, *J* = 9.6 Hz, 1H, Ino-4), 4.06 – 4.21 (m, 3H, Ino-1, Glc-3, Ino-6), 4.03 (d, *J* = 10.2 Hz, 1H, Glc-5), 3.82 (t, *J* = 9.5 Hz, 1H, Glc-4), 3.72 (d, *J* = 9.4 Hz, 1H, Ino-2), 3.61 – 3.69 (m, 2H, Glc-2, Ino-3), 3.54 (t, *J* = 9.3 Hz, 1H, Ino-5), 3.20 (d, *J* = 10.8 Hz, 1H, Glc-6a), 3.05 (d, *J* = 10.8 Hz, 1H, Glc-6b).

^{13}C NMR (101 MHz, $CDCl_3$) δ (ppm) 136.2, 136.1, 136.0, 135.6, 135.5, 135.4, 135.1, 133.36, 133.35, 133.3, 133.2, 133.12, 133.09, 133.0, 132.9, 132.8 (C_q Ar), 128.4, 128.3, 128.2, 128.14, 128.12, 128.09, 128.06, 128.04, 128.01, 127.98, 127.9, 127.83, 127.77, 127.73, 127.71, 127.68, 127.0, 126.82, 126.81, 126.6, 126.30, 126.26, 126.23, 126.21, 126.15, 126.12, 126.08, 126.05, 126.01, 125.93, 125.90, 125.88, 125.80, 125.75, 125.7, 125.5 (C Ar), 98.8 (Glc-1), 82.1 (Ino-4), 81.3 (Ino-5), 81.02 (Ino-1), 80.97 (Glc-3), 80.9 (Ino-3), 78.1 (Glc-4), 76.8 (Ino-6), 76.0 (C$\underline{H}_2$ Nap), 75.6 (C$\underline{H}_2$ Nap), 75.2 (C$\underline{H}_2$ Nap), 75.0 (C$\underline{H}_2$ Nap), 74.9 (C$\underline{H}_2$ Nap), 73.8 (Ino-2), 73.4 (C$\underline{H}_2$ Nap), 73.1 (C$\underline{H}_2$ Nap), 71.0 (Glc-5), 67.4 (Glc-6), 64.3 (Glc-2).

HRMS: $[M+Na]^+$ cald 1370.5507; found 1370.5432.

ESI-MS: 1371.3 $[M+Na]^+$.

2-Azido-2-deoxy-3,4,6-tri-*O*-(2-naphthyl)methyl-α-D-glucopyranosyl-(1→6)-2,3,4,5-tetra-*O*-(2-naphthyl)methyl-1-*O*-(2-oleoyl-1-stearoyl-*sn*-glycero-3-phosphonate)-D-*myo*-inositol (2-34)

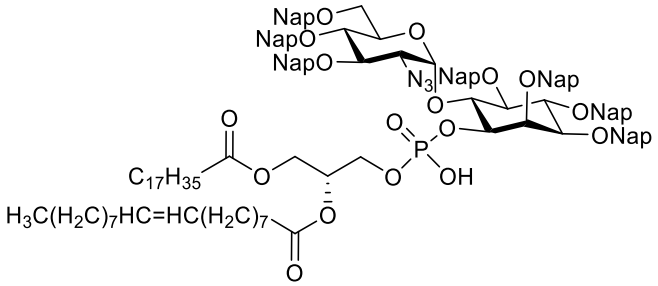

Alcohol **2-33** (79.7 mg, 0.0591 mmol) and H-phosphonate **2-8** (88% purity, 85.7 mg, 0.0946 mmol) were co-evaporated with anhydrous pyridine (3 x 3 mL) and placed under high vacuum for 1 h. The residue was dissolved in anhydrous pyridine (4.5 mL) and PivCl (18.8 µL, 0.154 mmol) was added. The reaction mixture was stirred for 1.5 h at room temperature before water (254 µL) and iodine (45 mg, 0.177 mmol) were added. The reaction mixture was stirred for additional 50 min, and solid $Na_2S_2O_3$ was added until the color of the reaction changed from orange to yellow. Volatiles were removed under reduced pressure. The remaining was triturated with DCM to remove

$Na_2S_2O_3$, and concentrated. Purification was performed by flash silica gel column chromatography (eluting with MeOH/DCM 1:90 and gradually increasing the polarity to 1:10). The obtained compound was dissolved in chloroform, and Amberlite IR 120 (Na^+) form resin was added. After stirring for 5 min, the solution was filtered and concentrated to afford the lipidated pseudodisaccharide **2-34** in 98% yield (0.119 mg, 0.0581 mmol) as a white solid; R_f = 0.54 (MeOH/DCM, 1:10).

$[\alpha]_D^{20}$**:** 37.7 (c = 1, $CHCl_3$).

IR (ATR) v(cm^{-1}) 3057, 2926, 2855, 2110 (N=N=N), 1742 (C=O), 1604, 1510, 1466, 1366, 1246, 1125, 1047, 893, 855, 816, 752.

^{1}H NMR (400 MHz, $CDCl_3$) δ (ppm) 7.90 (s, 1H, Ar), 7.50 – 7.84 (m, 22H, Ar), 7.27 – 7.47 (m, 22H, Ar), 7.09 – 7.20 (m, 3H, Ar), 6.79 (d, *J* = 8.5 Hz, 1H, Ar), 5.69 (s, 1H, Glc-1), 5.09 – 5.42 (m, 8H, -C<u>H</u>=C<u>H</u>- Oleoyl, C<u>H</u> sn-2, C<u>H$_2$</u> Nap), 4.98 – 5.08 (m, 2H, C<u>H$_2$</u> Nap), 4.77 – 4.96 (m, 4H, C<u>H$_2$</u> Nap), 4.64 – 4.75 (m, 2H, C<u>H$_2$</u> Nap, Ino-2), 4.44 – 4.62 (m, 3H, C<u>H$_2$</u> Nap, Ino-1, Ino-6), 4.05 – 4.37 (m, 9H, C<u>H$_2$</u> Nap, C<u>H$_2$</u> sn-1, C<u>H$_2$</u> sn-3, Glc-3, Ino-4, Glc-5), 3.69 – 3.83 (m, 2H, Ino-3, Glc-4), 3.57 (t, *J* = 8.7 Hz, 1H, Ino-5), 3.45 – 3.52 (m, 1H, Glc-2), 3.32 (d, *J* = 10.7 Hz, 1H, Glc-6a), 3.13 (d, *J* = 10.8 Hz, 1H, Glc-6b), 2.89 – 2.99 (m, 1H, Et_3N residue), 2.23 (q, *J* = 8.4 Hz, 4H, 2 x O-COC<u>H$_2$</u>-CH$_2$- lipid), 1.91 – 2.05 (m, 4H, -C<u>H$_2$</u>-CH=CH-C<u>H$_2$</u>- Oleoyl), 1.52 (b s, 4H, 2 x O-COCH$_2$-C<u>H$_2$</u>- lipid), 1.09 – 1.39 (m, 57H, C<u>H$_2$</u> lipid), 0.84 – 0.93 (m, 7H, 2 x C<u>H$_3$</u> lipid).

^{13}C NMR (101 MHz, $CDCl_3$) δ (ppm) 173.4 (<u>C</u>=O), 173.1 (<u>C</u>=O), 136.5, 136.1, 135.8, 135.7, 135.5, 135.2, 133.4, 133.33, 133.29, 133.23, 133.15, 133.10, 133.07, 133.01, 132.97, 132.9, 132.85, 132.75 (C_q Ar), 130.0 (-<u>C</u>H=CH- Oleoyl), 129.8 (-CH=<u>C</u>H- Oleoyl), 128.3, 128.21, 128.17, 128.14, 128.10, 128.05, 128.02, 128.00, 127.94, 127.91, 127.86, 127.79, 127.76, 127.73, 127.71, 127.6, 126.9, 126.7, 126.6, 126.5, 126.4, 126.3, 126.2, 126.4, 126.11, 126.09, 126.04, 126.01, 125.96, 125.92, 125.88, 125.85, 125.78, 125.7, 125.5 (C Ar), 97.7 (Glc-1), 81.9 (Ino-4), 81.0 (Ino-5), 80.7 (Ino-3), 80.16 (Glc-3), 79.6 (Ino-1), 78.2 (Glc-4), 76.7 (Ino-2), 76.0 (<u>C</u>H$_2$ Nap), 75.7 (<u>C</u>H$_2$ Nap), 75.6 (<u>C</u>H$_2$ Nap), 75.3 (<u>C</u>H$_2$ Nap), 74.8 (Ino-6), 73.4 (<u>C</u>H$_2$ Nap), 72.8 (<u>C</u>H$_2$ Nap), 70.5 (Glc-5), 69.74 (C<u>H</u> sn-2), 69.76 (<u>C</u>H$_2$ Nap), 67.69 (Glc-6), 65.3 (<u>C</u>H$_2$ sn-3), 63.5 (Glc-2), 62.0 (<u>C</u>H$_2$ sn-1), 34.2 (O-CO<u>C</u>H$_2$-CH$_2$ lipid), 34.1 (O-CO<u>C</u>H$_2$-CH$_2$ lipid), 32.1, 32.0, 29.90, 29.87, 29.8, 29.71, 29.67, 29.51, 29.48, 29.46, 29.41, 29.38, 29.32, 29.28, 29.2 (<u>C</u>H$_2$ lipid), 27.34 (-<u>C</u>H$_2$-CH=CH-CH$_2$- Oleoyl), 27.33 (-CH$_2$-CH=CH-<u>C</u>H$_2$- Oleoyl), 25.0 (O-COCH$_2$-<u>C</u>H$_2$- lipid), 24.9 (O-COCH$_2$-<u>C</u>H$_2$- lipid), 22.84 (<u>C</u>H$_2$ lipid), 22.82 (<u>C</u>H$_2$ lipid), 14.29 (2 x <u>C</u>H$_3$ lipid).

^{31}P NMR (162 MHz, $CDCl_3$) δ (ppm) -1.02.

HRMS: $[M-H]^-$ cald 2031.0625; found 2031.0488.

2-Acetamido-2-deoxy-α-D-glucopyranosyl-(1→6)-1-*O*-(2-oleoyl-1-stearoyl-s*n*-glycero-3-phosphonate)-D-*myo*-inositol (2-1)

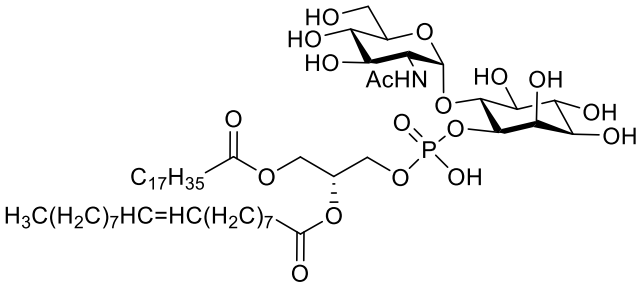

The glycolipid **2-34** (45 mg, 0.0219 mmol) was mixed with 0.83 mL of a 1M solution of $P(CH_3)_3$ in THF. Water (170 µL) was added, and the reaction was stirred at room temperature for 1.5 h. Volatiles were removed under reduced pressure and the residue was dissolved in a 2:1 pyridine/acetic anhydride mixture. The reaction was stirred for additional 2 h before it was concentrated *in vacuo*. Purification was performed by flash silica gel column chromatography (eluting with MeOH/DCM 1:90 and gradually increasing the polarity to 1:25). The obtained *N*-acetylated compound **2-37** (43.6 mg, 0.0213 mmol) was dissolved in a 3:1 DCM/MeOH mixture (1 mL), and DDQ (50.7 mg, 0.223 mmol) was added. The reaction mixture was stirred at room temperature for 3 h, and volatiles were removed under vacuum. The residue was purified by LH-20 size exclusion chromatography eluting with MeOH/$CHCl_3$ 9:1 followed by trituration with MeOH to afford the final GPI-fragment **2-1** in 62% yield (14.5 mg, 0.0136 mmol) as a slightly yellow solid. For the NMR sample, the compound was dissolved in a 3:3:1 $CD_3OD/CDCl_3/D_2O$ mixture.

^{1}H NMR (400 MHz, CD_3OD) δ (ppm) 5.00 – 5.09 (m, 2H, -C<u>H</u>=C<u>H</u>- Oleoyl), 4.91 – 5.00 (m, 1H, C<u>H</u> sn-2), 4.69 (d, *J*= 3.4 Hz, 1H, Glc-1), 4.09 – 4.16 (m, 1H, C<u>H</u>$_{2a}$ sn-1), 3.82 – 3.92 (m, 3H, C<u>H</u>$_{2b}$ sn-1), 3.71 – 3.79 (m, 2H, C<u>H</u>$_2$ sn-3), 3.64 – 3.70 (m, 2H, Glc-2), 3.53 – 3.59 (m, 1H, Glc-6a), 3.32 – 3.51 (m, 4H, Glc-6b), 3.12 – 3.19 (m, 1H), 3.04 – 3.12 (m, 2H), 1.98 – 2.09 (m, 4H, 2 x O-COC<u>H</u>$_2$-CH$_2$- lipid), 1.79 (s, 3H, C<u>H</u>$_3$ Ac), 1.69 – 1.75 (m, 4H, -C<u>H</u>$_2$-CH=CH-C<u>H</u>$_2$- Oleoyl), 1.26 – 1.34 (m, 4H, 2 x O-COCH$_2$-C<u>H</u>$_2$- lipid), 0.92 – 1.07 (m, 58H, C<u>H</u>$_2$ lipid), 0.58 (t, *J* = 6.7 Hz, 8H, 2 x C<u>H</u>$_3$ lipid).

^{13}C NMR (101 MHz, CD_3OD) δ (ppm) 174.0 (<u>C</u>=O), 173.7 (<u>C</u>=O), 129.6 (-<u>C</u>H=CH- Oleoyl), 129.3 (-<u>C</u>H=CH- Oleoyl), 99.0 (Glc-1), 81.4, 73.7, 72.8, 71.9, 71.2, 70.6, 70.2 (<u>C</u>H sn-2), 63.4 (<u>C</u>H$_2$ sn-3),62.6 (<u>C</u>H$_2$ sn-1), 60.8 (Glc-6), 53.6 (Glc-2), 33.8 (O-CO<u>C</u>H$_2$-CH$_2$- lipid), 33.7 (O-CO<u>C</u>H$_2$-CH$_2$- lipid), 31.5, 29.4, 29.33, 29.27, 29.22, 29.15, 29.1, 28.93, 28.90, 28.87, 28.83, 28.77, 28.7, 26.78 (-<u>C</u>H$_2$-CH=CH-CH$_2$- Oleoyl), 26.77 (-CH$_2$-CH=CH-<u>C</u>H$_2$- Oleoyl), 24.6 (O-COCH$_2$-<u>C</u>H$_2$- lipid), 24.5 (O-COCH$_2$-<u>C</u>H$_2$- lipid), 22.2 (<u>C</u>H$_3$ Ac), 21.9 (<u>C</u>H$_2$ lipid), 13.5 (2 x <u>C</u>H$_3$ lipid).

^{31}P NMR (162 MHz, CD_3OD) δ (ppm) -0.56.

HRMS: $[M-H]^-$ cald 1066.6443; found 1066.6547.

2-Amino-2-deoxy-α-D-glucopyranosyl-(1→6)-1-*O*-(2-oleoyl-1-stearoyl-*sn*-glycero-3-phosphonate)-D-*myo*-inositol (2-2)

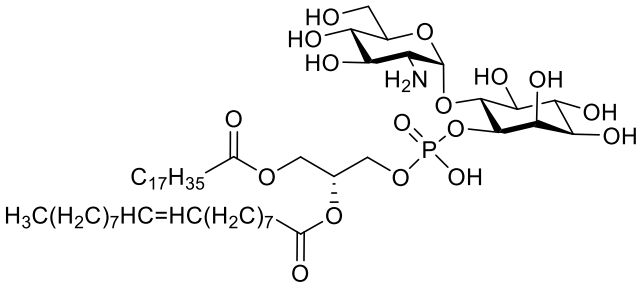

DDQ (79.0 mg, 0.348 mmol) was added to a solution of the protected glycolipid **2-34** (68.1 mg, 0.0331 mmol) in a 3:1 DCM/MeOH mixture (1.6 mL). The reaction mixture was stirred at room temperature for 5 h before volatiles were removed under reduced pressure. The residue was purified by LH-20 size exclusion chromatography eluting with MeOH/$CHCl_3$ 9:1. To the obtained deprotected glycolipid (26.1 mg, 0.0243 mmol), 0.49 mL of a 1M solution of $P(CH_3)_3$ in THF were added followed by water (89 µL). After 2h, the reaction was concentrated under vacuum, and purification was performed by LH-20 size exclusion chromatography eluting with MeOH/$CHCl_3$/H_2O 3:3:1 followed by trituration with MeOH to give the final GPI-fragment **2-2** in 47% yield (16.1 mg, 0.0157 mmol) as a slightly yellow solid. For the NMR sample, the compound was dissolved in a 3:3:1 CD_3OD/$CDCl_3$/D_2O mixture

^{1}H NMR (400 MHz, CD_3OD) δ (ppm) 5.24 (d, *J*= 4.0 Hz, 1H, Glc-1), 5.00 – 5.10 (m, 2H, -C<u>H</u>=C<u>H</u>- Oleoyl), 4.93 – 5.01 (m, 1H, C<u>H</u> sn-2), 4.09 – 4.16 (m, 1H, C<u>H</u>$_{2a}$ sn-1), 3.83 – 3.94 (m, 2H, C<u>H</u>$_{2b}$ sn-1), 3.61 – 3.83 (m, 5H, C<u>H</u>$_2$ sn-3, Glc-5), 3.49 – 3.59 (m, 2H, Glc-3, Glc-6a), 3.43 (dd, *J*= 12.5, 4.8 Hz, 1H, Glc-6b), 3.37 (t, *J* = 9.7 Hz, 1H), 3.10 – 3.19 (m, 2H, Glc-4), 3.03 – 3.05 (m, 1H),2.90 (dd, *J*= 10.5, 4.2 Hz, 1H, Glc-2), 1.96 – 2.12 (m, 4H, 2 x O-COC<u>H</u>$_2$-CH$_2$- lipid), 1.65 – 1.79 (m, 4H, -C<u>H</u>$_2$-CH=CH-C<u>H</u>$_2$- Oleoyl), 1.25 – 1.37 (m, 4H, 2 x O-COCH$_2$-C<u>H</u>$_2$- lipid), 0.99 (d, *J* = 16.1 Hz, 53H, C<u>H</u>$_2$ lipid), 0.59 (app t, *J* = 6.6 Hz, 6H, 2 x C<u>H</u>$_3$ lipid).

^{13}C NMR (101 MHz, CD_3OD) δ (ppm) 174.0 (<u>C</u>=O), 173.7 (<u>C</u>=O), 129.6 (-<u>C</u>H=CH- Oleoyl), 129.3 (-CH=<u>C</u>H- Oleoyl), 94.7 (Glc-1), 76.3, 72.7, 72.2, 71.9, 71.5 (Glc-5), 70.6, 70.04 (<u>C</u>H sn-2), 69.95, 69.8 (Glc-3), 69.4 (Glc-4), 63.3 (<u>C</u>H$_2$ sn-3), 62.5 (<u>C</u>H$_2$ sn-1), 60.2 (Glc-6), 53.8 (Glc-2), 33.8 (O-CO<u>C</u>H$_2$-CH$_2$- lipid), 33.7 (O-CO<u>C</u>H$_2$-CH$_2$- lipid), 31.5, 31.5, 29.40, 29.35, 29.31, 29.26, 29.2, 29.1, 29.0, 28.93, 28.90, 28.85, 28.80, 28.7 (<u>C</u>H$_2$ lipid), 26.81 (-<u>C</u>H$_2$-CH=CH-CH$_2$- Oleoyl), 26.80 (-CH$_2$-CH=CH-<u>C</u>H$_2$- Oleoyl), 24.6 (O-COCH$_2$-<u>C</u>H$_2$- lipid), 24.5 (O-COCH$_2$-<u>C</u>H$_2$- lipid), 22.3 (<u>C</u>H$_2$ lipid), 13.5 (2 x <u>C</u>H$_3$ lipid).

^{31}P NMR (162 MHz, CD_3OD) δ (ppm) -0.01.

HRMS: $[M-H]^-$ cald 1024.6338; found 1024.6212.

5.2.3 Synthesis of GPI fragment 2-3

2-Azido-2-deoxy-3,4,6-tri-*O*-(2-naphthyl)methyl-α-D-glucopyranosyl-(1→6)-1-*O*-allyl-3,4,5-tri-*O*-(2-naphthyl)methyl-2-*O*-(p-methoxybenzyl)-D-*myo*-inositol (2-40)

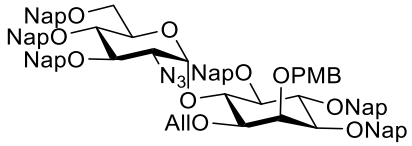

A solution of glycosyl acceptor **2-9** (30.8 mg, 0.0405 mmol) and glycosyl donor **2-11** (40 mg, 0.0606 mmol) in a 6:1 Et_2O/DCM anhydrous mixture (1 mL) was stirred at room temperature for 10 min. The mixture was cooled to 0 °C, and TMSOTf (2.1 µL, 0.0115 mmol) was added. After stirring for 2 h at room temperature, the reaction was quenched with Et_3N and concentrated under reduced pressure. The obtained residue was purified by flash silica gel column chromatography to afford the corresponding pseudodisaccharide **2-38** as a 7:1 α/β mixture that could not be separated; R_f = 0.34 (hexane/EtOAc, 7:3). The product was dissolved in an 11:1 MeOH/DCM anhydrous mixture and 61 µL (0.121 mmol) of a 5 M NaOMe solution in MeOH was added. The reaction was stirred at 40 °C for 1 h before it was neutralized with Amberlite IR 120 (H^+) resin, filtered, and concentrated *in vacuo*. The resulting residue was purified by flash silica gel column chromatography to give the desired triol **2-39** in 77% yield (29.6 mg, 0.0312 mmol) as a white solid. The α and β anomers were separated during the column; R_f α-anomer= 0.40, R_f β-anomer= 0.27 (hexane/EtOAc, 3:7).

NaH (20.3 mg, 0.509 mmol, 60% in mineral oil) was added to a solution of the isolated α-anomer **2-39** (80.4 g, 0.0848 mmol) and TBAI (141 mg, 0.382 mmol) in DMF (1.2 mL) at 0 °C. After 20 min, 2-(Bromomethyl)naphthalene (84.4 mg, 0.382 mmol) was added, and the reaction mixture was stirred at room temperature for 2 days. The reaction was quenched with water, and volatiles were removed under reduced pressure. The remaining was dissolved with ethyl acetate, and the solution was extracted with water. The layers were separated, and the aqueous phase was extracted with ethyl acetate. Organic layers were combined, washed with brine, dried with Na_2SO_4, filtered, and evaporated. The resulting residue was purified by flash silica gel column chromatography to give **2-40** in 76% (88.2 mg, 0.0644 mmol) yield as a white solid; R_f = 0.34 (hexane/EtOAc, 8:2).

$[\alpha]_D^{20}$: 41.4 (c = 1, $CHCl_3$).

IR (ATR) v(cm^{-1}) 3056, 2865, 2106 (N=N=N), 1603, 1511, 1462, 1365, 1248, 1172, 1125, 1037, 854, 893, 856, 817, 753.

^{1}H NMR (400 MHz, $CDCl_3$) δ (ppm) 7.66 – 7.88 (m, 14H, Ar), 7.57 – 7.66 (m, 4H, Ar), 7.31 – 7.51 (m, 22H, Ar), 7.13 – 7.24 (m, 3H, Ar), 6.86 – 6.92 (m, 2H, Ar PMB), 6.83 (dd, *J* = 8.4, 1.7 Hz, 1H, Ar), 5.92 – 6.05 (m, 1H, -C<u>H</u>= Allyl), 5.84 (d, *J*= 3.7 Hz, 1H, Glc-1), 5.30 (dd, *J* = 17.2, 1.8 Hz, 1H, =C<u>H</u>$_{2a}$ Allyl), 5.14 – 5.24 (m, 3H, =C<u>H</u>$_{2b}$ Allyl, C<u>H</u>$_2$ Nap), 5.08 (ABq, *J* = 11.0 Hz, 2H, C<u>H</u>$_2$ Nap), 4.99 (d, *J* = 10.9 Hz, 1H, C<u>H</u>$_2$ Nap), 4.92 (d, *J* = 11.6 Hz, 1H, C<u>H</u>$_2$ Nap), 4.79 – 4.89 (m, 4H, C<u>H</u>$_2$

PMB, C$\underline{H}_2$ Nap), 4.76 & 4.32 (ABq, *J* = 11.2 Hz, 2H, C$\underline{H}_2$ Nap), 4.63 & 4.20 (ABq, *J* = 12.2 Hz, 2H, C$\underline{H}_2$ Nap), 4.39 (t, *J* = 9.6 Hz, 1H, Ino-6), 4.27 – 4.35 (m, 1H, Ino-4), 4.15 – 4.22 (m, 1H, Glc-5), 4.12 – 4.15 (m, 1H, Ino-2), 4.03 – 4.11 (m, 3H, -C$\underline{H}_2$- Allyl, Glc-3), 3.81 (s, 3H, OC$\underline{H}_3$ PMB, Glc-4), 3.50 – 3.60 (m, 2H, Ino-3, Ino-5), 3.38 – 3.47 (m, 2H, Ino-1, Glc-2), 3.33 (dd, *J* = 11.0, 2.0 Hz, 1H, Glc-6a), 3.13 (dd, *J* = 11.0, 2.3 Hz, 1H, Glc-6b).

^{13}C NMR (101 MHz, $CDCl_3$) δ (ppm) 159.3, 136.2, 136.1, 135.89, 135.86, 135.7, 135.3 (C_q Ar), 134.5 (-C$\underline{H}$= Allyl), 133.40, 133.38, 133.35, 133.3, 133.21, 133.15, 133.11, 133.08, 133.01, 132.97, 132.87, 132.77, 131.0 (C_q Ar), 129.7, 128.31, 128.26, 128.13, 128.10, 128.07, 128.03, 128.01, 127.93, 127.90, 127.85, 127.83, 127.80, 127.75, 127.73, 127.68, 127.0, 126.8, 126.7, 126.4, 126.31, 126.26, 126.2, 126.13, 126.09, 126.03, 125.95, 125.93, 125.91, 125.87, 125.80, 125.77, 125.7, 125.6, 125.5 (C Ar), 117.0 (=C$\underline{H}_2$ Allyl), 113.8 (C Ar, PMB), 97.9 (Glc-1), 82.2 (Ino-1), 82.1 (Ino-4), 81.6 (Ino-5), 80.9 (Ino-3), 80.4 (Glc-3), 78.2 (Glc-4), 76.0 (C$\underline{H}_2$ Nap), 75.6 (Ino-6), 75.5 (C$\underline{H}_2$ Nap), 75.4 (C$\underline{H}_2$ Nap), 74.8 (C$\underline{H}_2$ Nap), 73.9 (C$\underline{H}_2$ PMB), 73.5 (C$\underline{H}_2$ Nap), 72.9 (C$\underline{H}_2$ Nap), 72.6 (Ino-2), 71.0 (-C$\underline{H}_2$- Allyl), 70.3 (Glc-5), 67.8 (Glc-6), 63.6 (Glc-2), 55.4 (OC$\underline{H}_3$ PMB).

HRMS: $[M+Na]^+$ cald 1390.5769; found 1390.6027; $[M+NH_4]^+$ cald 1385.6215; found 1385.6481.

2-Azido-2-deoxy-3,4,6-tri-*O*-(2-naphthyl)methyl-α-D-glucopyranosyl-(1→6)-1-*O*-allyl-3,4,5-tri-*O*-(2-naphthyl)methyl-D-*myo*-inositol (2-41)

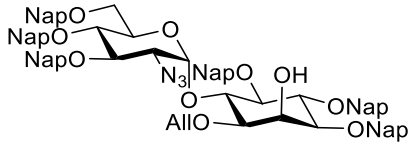

TFA (0.15 mL, 1.42 mmol) was added to a solution of pseudodisaccharide **2-40** (88.3 mg, 0.0645 mmol) in anhydrous DCM (1 mL) at 0 °C, and it was stirred for 40 min. The reaction was quenched with Et_3N and concentrated under reduced pressure. The crude product was purified by flash silica gel column chromatography to obtain **2-41** in 97% (78.4 mg, 0.0628 mmol) yield as a white solid; R_f = 0.15 (hexane/EtOAc, 7:3).

$[\alpha]_D^{20}$: 10.4 (c = 1, $CHCl_3$).

IR (ATR) ν(cm^{-1}) 3449 (O-H), 3055, 2927, 2106 (N=N=N), 1711, 1604, 1510, 1463, 1366, 1347, 1247, 1172, 1125, 1060, 953, 894, 856, 816, 752.

^{1}H NMR (400 MHz, $CDCl_3$) δ (ppm) 7.63 – 7.87 (m, 24H, Ar), 7.30 – 7.57 (m, 34H, Ar), 7.16 – 7.21 (m, 2H, Ar), 6.90 (d, *J* = 8.2 Hz, 1H, Ar), 6.85 (d, *J* = 8.4 Hz, 1H, Ar), 5.92 – 6.05 (m, 1H, -C$\underline{H}$= Allyl), 5.76 (d, *J*= 3.8 Hz, 1H, Glc-1), 5.28 (d, *J* = 17.2 Hz, 1H, =C$\underline{H}_{2a}$ Allyl), 5.11 – 5.22 (m, 4H, =C$\underline{H}_{2b}$ Allyl, C$\underline{H}_2$ Nap), 4.85 – 5.08 (m, 9H, C$\underline{H}_2$ Nap), 4.76 & 4.36 (ABq, *J* = 11.2 Hz, 2H, C$\underline{H}_2$ Nap), 4.59 – 4.65 (m, 2H, C$\underline{H}_2$ Nap), 4.10 – 4.33 (m, 10H, C$\underline{H}_2$ Nap, Ino-2, Ino-4, Glc-5, Ino-6, -C$\underline{H}_2$- Allyl), 4.06 (t, *J* = 9.6 Hz, 1H, Glc-3), 3.76 – 3.80 (m, 1H, Glc-4), 3.45 – 3.59 (m, 1H, Ino-1, Ino-3, Ino-5), 3.41 (dd, *J* = 10.4, 3.7 Hz, 1H, Glc-2), 3.35 (d, *J* = 10.9 Hz, 1H, Glc-6a), 3.20 (d, *J* = 10.7 Hz, 1H, Glc-6b).

^{13}C NMR (101 MHz, $CDCl_3$) δ (ppm) 136.1, 135.83, 135.80, 135.6, 135.39, 135.36 (C_q Ar), 134.2 (-CH= Allyl), 133.38, 133.36, 133.33, 133.27, 133.22, 133.19, 133.16, 133.1, 133.03, 132.99, 132.9, 132.8 (C_q Ar), 128.8, 128.5, 128.3, 128.18, 128.15, 128.1, 128.0, 128.0, 127.94, 127.90, 127.83, 127.75, 127.71, 127.68, 126.9, 126.8, 126.6, 126.4, 126.24, 126.20, 126.15, 126.1, 126.05, 125.94, 125.91, 125.86, 125.8, 125.7, 125.7 (C Ar), 118.0 (=CH_2 Allyl), 97.7 (Glc-1), 81.6 (Ino-4), 81.3 (Ino-1), 81.2 (Ino-5), 80.2 (Glc-3), 79.6 (Ino-3), 78.3 (Glc-4), 77.5 (CH_2 Nap), 77.4 (CH_2 Nap), 77.2 (CH_2 Nap), 76.8 (CH_2 Nap), 76.1 (CH_2 Nap), 75.8 (CH_2 Nap), 75.0 (Ino-6), 74.8, 73.5, 73.0, 71.2 (-CH_2- Allyl), 70.41 (Glc-5), 67.8 (Glc-6), 66.7 (Ino-2), 63.5 (Glc-2).
HRMS: $[M+Na]^+$ cald 1270.5194; found 1270.2440; $[M+K]^+$ cald 1286.4933; found 1286.2083.

2-Azido-2-deoxy-3,4,6-tri-*O*-(2-naphthyl)methyl-α-D-glucopyranosyl-(1→6)-1-*O*-allyl-3,4,5-tri-*O*-(2-naphthyl)methyl-2-*O*-(palmitoyl)-D-*myo*-inositol (2-6)

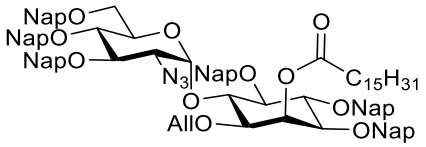

DMAP (3.6 mg, 0.0294 mmol) and DIC (4.6 µL, 0.0294 mmol) were added to a solution of alcohol **2-41** (22.9 mg, 0.0184 mmol) and palmitic acid (7.5 mg, 0.0294 mmol) in anhydrous DCM (1 mL). After 15 h, the reaction was quenched with water, and the layers were separated. The aqueous phase was extracted with DCM. Organic layers were washed with citric acid (1 M) followed by brine, dried over Na_2SO_4, filtered, and concentrated. Crude was purified by flash silica gel column chromatography to afford **2-6** (23.6 g, 0.0159 mmol) in 86% yield as a white solid; R_f = 0.44 (hexane/EtOAc, 8:2).
$[\alpha]_D^{20}$**:** 47.50 (c = 1, $CHCl_3$).
IR (ATR) ν(cm^{-1}) 3047, 2926, 2855, 2106 (N=N=N), 1740 (C=O), 1603, 1510, 1467, 1366, 1247, 1126, 1088, 953, 855, 816, 753.
^{1}H NMR (400 MHz, $CDCl_3$) δ (ppm) 7.77 – 7.85 (m, 8H, Ar), 7.70 – 7.75 (m, 6H, Ar), 7.57 – 7.69 (m, 5H, Ar), 7.38 – 7.52 (m, 21H, Ar), 7.33 (d, *J* = 8.2 Hz, 1H, Ar), 7.16 – 7.25 (m, 3H, Ar), 6.92 (dd, *J* = 8.4, 1.6 Hz, 1H, Ar), 5.94 – 6.07 (m, 2H, -CH= Allyl, Ino-2), 5.81 (d, *J*= 3.7 Hz, 1H, Glc-1), 5.32 (dd, *J* = 17.2, 1.8 Hz, 1H, =CH_{2a} Allyl), 5.23 (d, *J* = 10.8 Hz, 2H, =CH_{2b} Allyl, CH_2 Nap), 5.19 (d, *J* = 11.0 Hz, 1H, CH_2 Nap), 5.12 (ABq, *J* = 11.0 Hz, 2H, CH_2 Nap), 4.91 – 5.04 (m, 2H, CH_2 Nap), 4.99 & 4.76 (ABq, *J* = 11.3 Hz, 2H, CH_2 Nap) 4.83 & 4.38 (ABq, *J* = 11.2 Hz, 2H, CH_2 Nap), 4.65 & 4.22 (d, *J* = 12.2 Hz, 2H, CH_2 Nap), 4.28 (dd, *J* = 12.0, 5.6 Hz, 1H, -CH_2- Allyl), 4.16 – 4.25 (m, 2H, Glc-5, Ino-6), 4.05 – 4.15 (m, 3H, -CH_2- Allyl, Glc-3, Ino-4), 3.84 (t, *J* = 9.5 Hz, 1H, Glc-4), 3.68 (dd, *J* = 9.8, 2.8 Hz, 1H, Ino-3), 3.57 – 3.66 (m, 2H, Ino-1, Ino-5), 3.43 (dd, *J*= 10.4, 3.7 Hz, 1H, Glc-2), 3.33 (dd, *J* = 10.9, 2.1 Hz, 1H, Glc-6a), 3.22 (dd, *J* = 11.0, 2.4 Hz, 1H, Glc-6b), 2.50 (t, *J* = 7.3 Hz, 2H, O-COCH_2-CH_2- palmitoyl), 1.68 – 1.78 (m, 2H, O-$COCH_2$-CH_2- palmitoyl),

1.37 – 1.45 (m, 2H, C<u>H</u>$_2$ palmitoyl), 1.23 – 1.33 (m, 26H, C<u>H</u>$_2$ palmitoyl), 0.92 (t, *J* = 6.8 Hz, 3H, C<u>H</u>$_3$ palmitoyl).

^{13}C NMR (101 MHz, CDCl$_3$) δ (ppm) 173.4 (C=O), 136.0, 135.8, 135.7, 135.6, 135.2, 135.1 (C$_q$ Ar), 134.2 (-<u>C</u>H= Allyl), 133.37, 133.35, 133.3, 133.25, 133.18, 133.15, 133.1, 133.01, 132.99, 132.9, 132.8 (C$_q$ Ar), 128.33, 128.29, 128.18, 128.16, 128.1, 128.03, 128.00, 127.9, 127.78, 127.75, 127.72, 127.68, 127.6, 127.2, 127.0, 126.8, 126.6, 126.4, 126.3, 126.2, 126.13, 126.10, 126.05, 126.03, 125.98, 125.96, 125.9, 125.83, 125.78, 125.75 (C Ar), 117.7 (=<u>C</u>H$_2$ Allyl), 98.0 (Glc-1), 81.8 (Ino-4), 81.0 (Ino-1), 80.3 (Glc-3), 79.2 (Ino-5), 78.4 (Ino-3), 78.2 (Glc-4), 76.1 (<u>C</u>H$_2$ Nap), 76.0 (<u>C</u>H$_2$ Nap), 75.8 (Ino-6), 75.4 (<u>C</u>H$_2$ Nap), 74.9 (<u>C</u>H$_2$ Nap), 73.5 (<u>C</u>H$_2$ Nap), 72.3 (<u>C</u>H$_2$ Nap), 70.9 (-<u>C</u>H$_2$- Allyl), 70.4 (Glc-5), 67.6 (Glc-6), 65.6 (Ino-2), 63.5 (Glc-2), 34.5 (O-CO<u>C</u>H$_2$-CH$_2$- palmitoyl), 32.0, 29.85, 29.80, 29.7, 29.6, 29.5, 29.2 (<u>C</u>H$_2$ palmitoyl), 25.4 (O-COCH$_2$-<u>C</u>H$_2$-palmitoyl), 22.8 (<u>C</u>H$_2$ palmitoyl), 14.2 (<u>C</u>H$_3$ palmitoyl).

HRMS: [M+Na]$^+$ cald 1508.749032; found 1508.7793.

2-Azido-2-deoxy-3,4,6-tri-*O*-(2-naphthyl)methyl-α-D-glucopyranosyl-(1→6)-3,4,5-tri-*O*-(2-naphthyl)methyl-2-*O*-(palmitoyl)-D-*myo*-inositol (2-42)

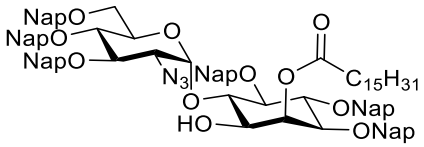

To a solution of pseudodisaccharide **2-6** (23.6 mg, 0.0159 mmol) in a 1:1 DCM/MeOH anhydrous mixture (0.5 mL), PdCl$_2$ (2.6 mg, 0.0147 mmol) was added at room temperature. After 2.5 h, the mixture was filtered through a pad of Celite, and the volatiles were evaporated under reduced pressure. The resulting oil was purified by flash silica gel column chromatography afford compound **2-42** in 72% yield (0.0166 mg, 0.0114 mmol) as a white solid; R$_f$ = 0.30 (hexane/EtOAc, 7:3).

$[\alpha]_D^{20}$: 34.8 (c = 1, CHCl$_3$).

IR (ATR) ν(cm^{-1}) 3460 (H-O), 3056, 2926, 2855, 2109 (N=N=N), 1738 (C=O), 1603, 1510, 1467, 1367, 1250, 1125, 1054, 953, 894, 855, 817, 754.

^{1}H NMR (400 MHz, CDCl$_3$) δ (ppm) 7.85 – 7.63 (m, 19H, Ar), 7.60 – 7.55 (m, 4H, Ar), 7.40 – 7.50 (m, 15H, Ar), 7.34 – 7.39 (m, 2H, Ar), 7.28 (s, 1H, Ar), 7.22 (s, 1H, Ar), 7.10 (dd, *J* = 8.4, 1.7 Hz, 1H, Ar), 6.95 (dd, *J* = 8.4, 1.7 Hz, 1H, Ar), 5.88 (app t, *J* = 2.8 Hz, 1H, Ino-2), 5.36 (d, *J*= 3.6 Hz, 1H, Glc-1), 5.30 & 4.85 (ABq, *J* = 11.4 Hz, 2H, C<u>H</u>$_2$ Nap), 5.16 & 4.95 (ABq, *J* = 10.8 Hz, 2H, C<u>H</u>$_2$ Nap), 5.09 (ABq, *J* = 11.0 Hz, 2H, C<u>H</u>$_2$ Nap), 4.98 & 4.72 (ABq, *J* = 11.3 Hz, 2H, C<u>H</u>$_2$ Nap), 4.78 & 4.37 (ABq, *J* = 11.0 Hz, 2H, C<u>H</u>$_2$ Nap), 4.45 & 3.89 (ABq, *J* = 12.2 Hz, 2H, C<u>H</u>$_2$ Nap), 4.07 (td, *J* = 9.5, 3.0 Hz, 2H, Glc-3, Ino-4), 3.93 – 4.01 (m, 3H, Glc-5, Ino-6), 3.82 (t, *J* = 9.5 Hz, 2H, Ino-1, Glc-4), 3.67 – 3.72 (m, 2H, Glc-2, Ino-3), 3.53 (t, *J* = 9.4 Hz, 1H, Ino-5), 3.14 (dd, *J* = 11.0, 2.2 Hz, 1H, Glc-6a), 2.90 (dd, *J* = 11.1, 2.1 Hz, 1H, Glc-6b), 2.51 (t, *J* = 7.4 Hz, 2H, O-COC<u>H</u>$_2$-CH$_2$-

palmitoyl), 1.69 – 1.78 (m, 2H, O-COCH$_2$-CH$_2$- palmitoyl), 1.35 – 1.45 (m, 2H, CH$_2$ palmitoyl), 1.19 – 1.32 (m, 26H, CH$_2$ palmitoyl), 0.90 (t, *J* = 6.7 Hz, 3H, CH$_3$ palmitoyl).

^{13}C NMR (101 MHz, CDCl$_3$) δ (ppm) 173.6 (C=O), 136.1, 135.9, 135.4, 135.3, 135.1, 135.0, 133.39, 133.35, 133.3, 133.2, 133.1, 133.03, 132.99, 132.9 (C$_q$ Ar), 128.3, 128.22, 128.15, 128.1, 128.04, 128.02, 127.98, 127.9, 127.8, 127.73, 127.70, 127.3, 127.0, 126.8, 126.5, 126.3, 126.21, 126.18, 126.12, 126.07, 125.97, 125.95, 125.9, 125.6, 125.5 (C Ar), 99.6 (Glc-1), 82.2 (Ino-4, Ino-6), 81.2 (Glc-3), 80.8 (Ino-5), 78.5 (Ino-3), 78.1 (Glc-4), 76.1 (CH$_2$ Nap), 75.7 (CH$_2$ Nap), 75.5 (CH$_2$ Nap), 74.9 (CH$_2$ Nap), 73.4 (CH$_2$ Nap), 72.2 (CH$_2$ Nap), 71.43 (Ino-1), 71.40 (Glc-5), 68.9 (Ino-2), 67.2 (Glc-6), 64.6 (Glc-2), 34.7 (O-COCH$_2$-CH$_2$- palmitoyl), 32.1, 29.85, 29.80, 29.8, 29.7, 29.6, 29.5, 29.2 (CH$_2$ palmitoyl), 25.5 (O-COCH$_2$-CH$_2$- palmitoyl), 22.8 (CH$_2$ palmitoyl), 14.3 (CH$_3$ palmitoyl).

HRMS: [M+Na]$^+$ cald 1468.7177; found 1469.7498.

2-Azido-2-deoxy-3,4,6-tri-*O*-(2-naphthyl)methyl-α-D-glucopyranosyl-(1→6)-3,4,5-tri-*O*-(2-naphthyl)methyl-1-*O*-(2-oleoyl-1-stearoyl-*sn*-glycero-3-phosphonate)-2-*O*-(palmitoyl)-D-*myo*-inositol (2-43)

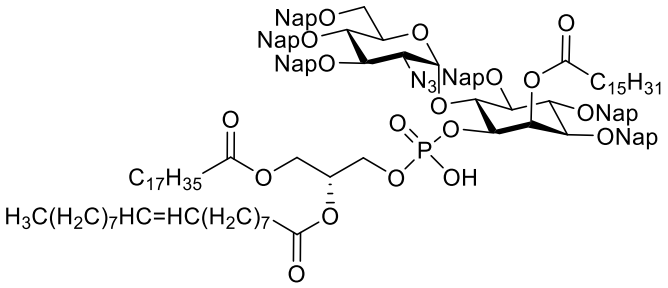

Alcohol **2-42** (70.4 mg, 0.0487 mmol) and H-phosphonate **2-8** (87% purity, 70.5 mg, 0.0778 mmol) were co-evaporated with anhydrous pyridine (3 x 2 mL) and placed under high vacuum for 1 h. The residue was dissolved in anhydrous pyridine (2.4 mL) and PivCl (15.5 µL, 0.126 mmol) was added. The reaction mixture was stirred for 1.5 h at room temperature before water (217 µL) and iodine (37.0 mg, 0.146 mmol) were added. The reaction mixture was stirred for additional 1.5 h, and solid $Na_2S_2O_3$ was added until the color of the reaction changed from orange to yellow. Volatiles were removed under reduced pressure. The remaining was triturated with DCM to remove $Na_2S_2O_3$. Purification was performed by flash silica gel column chromatography. The obtained compound was dissolved in chloroform, and Amberlite IR 120 (Na^+) form resin was added; after stirring for 8 min, the solution was filtered and concentrated. The compound was further purified by LH-20 size exclusion chromatography eluting with MeOH/$CHCl_3$ 1:2 to afford the protected glycolipid **2-43** in 82% yield (86.5 mg, 0.0402 mmol) as a white solid; R_f = 0.50 (MeOH/DCM, 1:10).

^{1}H NMR (400 MHz, CDCl$_3$) δ (ppm) 7.57 – 7.77 (m, 18H, Ar), 7.29 – 7.50 (m, 23H, Ar), 7.13 – 7.22 (m, 3H, Ar), 6.84 (dd, *J* = 8.4, 1.6 Hz, 1H, Ar), 6.03 (s, 1H, Ino-2), 5.50 (s, 1H, Glc-1), 5.29 –

5.39 (m, 3H, -CH=CH- Oleoyl, CH sn-2), 5.20 (d, *J* = 11.1 Hz, 1H, CH_2 Nap), 5.10 (d, *J* = 10.9 Hz, 1H, CH_2 Nap), 5.04 (s, 2H, CH_2 Nap), 4.94 & 4.66 (ABq, *J* = 11.0 Hz, 2H, CH_2 Nap), 4.87 – 4.97 (m, 2H, CH_2 Nap), 4.73 & 4.30 (d, *J* = 11.3 Hz, 2H, CH_2 Nap), 4.58 & 4.16 (ABq, *J* = 12.0 Hz, 2H, CH_2 Nap), 4.56 (s, 1H, Ino-1), 4.39 (dd, *J* = 11.9, 3.9 Hz, 1H, CH_{2a} sn-1), 4.15 – 4.34 (m, 5H, CH_{2b} sn-1, CH_2 sn-3, Glc-5, Ino-6), 4.08 (t, *J* = 9.6 Hz 1H, Glc-3), 3.99 (t, *J* = 9.5 Hz, 1H, Ino-4), 3.75 – 3.83 (m, 2H, Ino-3, Glc-4), 3.52 – 3.63 (m, 2H, Glc-2, Ino-5), 3.32 (d, *J* = 10.9 Hz, 1H, Glc-6a), 3.15 (d, *J* = 11.1 Hz, 1H, Glc-6b), 2.46 (t, *J* = 7.4 Hz, 2H, O-COCH_2-CH_2- palmitoyl), 2.26 – 2.39 (m, 5H, 2 x O-COCH_2-CH_2- lipid), 1.94 – 2.02 (m, 4H, -CH_2-CH=CH-CH_2- Oleoyl), 1.54 – 1.69 (m, 6H, 3 x O-COCH_2-CH_2-), 1.24 (d, *J* = 11.9 Hz, 97H, CH_2 lipid), 0.83 – 0.91 (m, 14H, 3 x CH_3 lipid).

^{13}C NMR (101 MHz, $CDCl_3$) δ (ppm) 173.4 (2 x C=O), 173.1 (C=O), 135.8, 135.6, 135.5, 135.3, 135.2, 135.0, 133.34, 133.31, 133.25, 133.18, 133.14, 133.10, 133.02, 133.00, 132.90, 132.87 (C_q Ar), 130.1 (-CH=CH- Oleoyl), 129.9 (-CH=CH- Oleoyl), 128.3, 128.24, 128.20, 128.16, 128.12, 128.08, 128.03, 128.00, 127.96, 127.9, 127.8, 127.72, 127.70, 127.4, 126.9, 126.8, 126.6, 126.5, 126.3, 126.18, 126.15, 126.1, 126.05, 126.02, 125.99, 125.9, 125.8, 125.7 (C Ar), 97.7 (Glc-1), 81.8 (Ino-4), 80.4 (Ino-5), 80.2 (Glc-3), 78.3 (Ino-3), 78.2 (Glc-4), 77.2 (Ino-1), 76.0 (2 x CH_2 Nap), 75.4 (Ino-6), 74.9 (CH_2 Nap), 73.5 (2 x CH_2 Nap), 72.5 (CH_2 Nap), 70.9 (Glc-5), 69.5 (CH sn-2), 68.5 (Ino-2), 67.6 (Glc-6), 65.8 (CH_2 sn-3), 63.6 (Glc-2), 61.9 (CH_2 sn-1), 34.6 (O-COCH_2-CH_2- palmitoyl), 34.3 (O-COCH_2-CH_2- lipid), 34.2 (O-COCH_2-CH_2- lipid), 32.1, 32.0, 29.9, 29.9, 29.82, 29.77, 29.70, 29.68, 29.6, 29.52, 29.50, 29.46, 29.44, 29.40, 29.35, 29.33, 29.27, 29.2 (CH_2 lipid), 27.4 (-CH_2-CH=CH-CH_2- Oleoyl), 25.5 (O-COCH$_2$-CH_2- palmitoyl), 25.0 (2 x O-COCH$_2$-CH_2- lipid), 22.84, 22.83 (CH_2 lipid), 14.3 (3 x CH_3 lipid).

^{31}P NMR (162 MHz, $CDCl_3$) δ (ppm) -0.82.

HRMS: $[M-H]^-$ cald 2129.2295; found 2129.2083.

2-Amino-2-deoxy-α-D-glucopyranosyl-(1→6)-1-*O*-(2-oleoyl-1-stearoyl-*sn*-glycero-3-phosphonate)- 2-*O*-(palmitoyl)-D-*myo*-inositol (2-3)

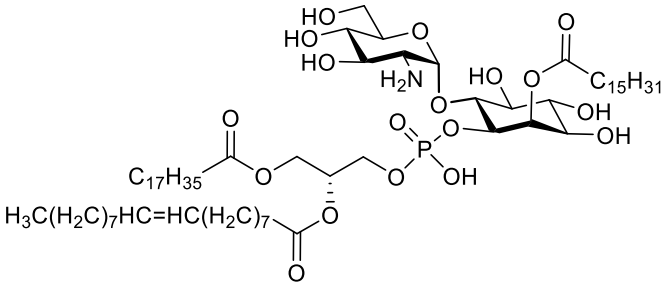

DDQ (60.7 mg, 0.267 mmol) was added to a solution of the protected glycolipid **2-43** (64 mg, 0.0297 mmol) in a 3:1 DCM/MeOH mixture (1.5 mL). The reaction mixture was stirred at room temperature for 5 h before volatiles were removed under reduced pressure. The residue was purified by LH-20 size exclusion chromatography eluting with MeOH/$CHCl_3$ 9:1. To the obtained deprotected glycolipid (29 mg, 0.0225 mmol), 0.45 mL of a 1 M solution of $P(CH_3)_3$ in THF were

added followed by water (82 µL). After 2h, the reaction was concentrated under vacuum, and the crude was purified by LH-20 size exclusion chromatography eluting with MeOH/$CHCl_3$/H_2O 3:3:1 followed by trituration with MeOH to give the final GPI-fragment **2-3** in 48% yield (18.2 mg, 0.0144 mmol) as a slightly yellow solid. For the NMR sample, the compound was dissolved in a 3:3:1 CD_3OD/$CDCl_3$/D_2O mixture.

^{1}H NMR (400 MHz, CD_3OD) δ (ppm) 5.13 – 5.25 (m, 2H, Glc-1, Ino-2), 4.96 – 5.06 (m, 2H, C<u>H</u>=C<u>H</u>- Oleoyl), 4.84 – 4.94 (m, 1H, C<u>H</u> sn-2), 3.96 – 4.11 (m, 2H, C<u>H</u>$_{2a}$ sn-1, Ino-1), 3.75 – 3.88 (m, 2H, C<u>H</u>$_{2b}$ sn-1, Glc-5), 3.45 – 3.68 (m, 5H, C<u>H</u>$_2$ sn-3, Glc-3, Glc-6a, Ino-6), 3.37 – 3.45 (m, 1H, Glc-6b), 3.20 – 3.35 (m, 2H, Ino-3), 2.99 – 3.15 (m, 2H, Glc-4), 2.78 – 2.88 (m, 1H, Glc-2), 2.04 – 2.12 (m, 2H, O-COC<u>H</u>$_2$-CH$_2$- palmitoyl), 1.94 – 2.03 (m, 4H, 2 x O-COC<u>H</u>$_2$-CH$_2$- lipid), 1.62 – 1.74 (m, 4H, -C<u>H</u>$_2$-CH=CH-C<u>H</u>$_2$- Oleoyl), 1.21 – 1.33 (m, 7H, 3 x O-COCH$_2$-C<u>H</u>$_2$-), 0.84 – 1.04 (m, 82H, C<u>H</u>$_2$ lipid), 0.54 (t, *J* = 6.6 Hz, 10H, 3 x C<u>H</u>$_3$ lipid).

^{13}C NMR (101 MHz, CD_3OD) δ (ppm) 173.7 (<u>C</u>=O), 173.4 (2 x <u>C</u>=O), 129.6 (-<u>C</u>H=CH- Oleoyl), 129.3 (-<u>C</u>H=CH- Oleoyl), 94.8 (Glc-1), 76.7 (Ino-6), 74.3 (Ino-1), 72.68 (Ino-2), 72.67, 72.6, 71.9 (Glc-5), 69.9 (<u>C</u>H sn-2, Glc-3), 69.4 (Glc-4), 69.1, 63.6 (<u>C</u>H$_2$ sn-3), 62.4 (<u>C</u>H$_2$ sn-1), 60.4 (Glc-6), 53.7 (Glc-2), 33.8 (O-CO<u>C</u>H$_2$-CH$_2$- palmitoyl), 33.7 (2 x O-CO<u>C</u>H$_2$-CH$_2$- lipid), 31.6, 29.41, 29.37, 29.32, 29.26, 29.1, 29.00, 28.97, 28.94, 28.91, 28.86 (<u>C</u>H$_2$ lipid), 26.8 (-<u>C</u>H$_2$-CH=CH-<u>C</u>H$_2$- Oleoyl), 24.6 (O-COCH$_2$-<u>C</u>H$_2$- palmitoyl), 24.5 (2 x O-COCH$_2$-<u>C</u>H$_2$- lipid), 22.3 (<u>C</u>H$_2$ lipid), 13.6 (3 x <u>C</u>H$_3$ lipid).

^{31}P NMR (162 MHz, CD_3OD) δ (ppm) -1.52.

HRMS: [M-H]$^-$ cald 1262.8634; found 1262.8473.

5.2.4 Synthesis of GPI fragment 2-4

2-(Dimethoxymethyl)naphthalene

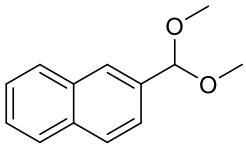

A mixture of 2-naphtaldehyde (250 mg, 1.60 mmol), trimethyl orthoformate (2.63 mL, 24.0 mmol), and *p*-Toluenesulfonic acid (61 mg, 0.320 mmol) in anhydrous MeOH (2 mL) was stirred at 85 °C for 4h. The reaction was cooled to room temperature and quenched with $NaHCO_3$. MeOH was removed under reduced pressure, and the remaining aqueous phase was extracted with DCM. Organic layers were combined, washed with brine, dried over Na_2SO_4, filtered and concentrated. The yellow residue was purified by flash silica gel column chromatography to give the desired dimethyl acetal in 95% yield (308 mg, 1.52 mmol) as a colorless oil; R_f = 0.35 (hexane/EtOAc, 30:2).

^{1}H NMR (400 MHz, $CDCl_3$) δ (ppm) 7.94 (d, *J* = 1.5 Hz, 1H, H-Ar), 7.82 – 7.89 (m, 3H, H-Ar), 7.56 (dd, *J* = 8.5, 1.7 Hz, 1H, H-Ar), 7.47 – 7.52 (m, 2H, H-Ar), 5.56 (s, 1H, C<u>H</u> Acetal), 3.38 (s, 6H, C<u>H</u>$_3$-O).

^{13}C NMR (101 MHz, $CDCl_3$) δ (ppm) 135.6, 133.5, 133.1 (C_q Ar), 128.4, 128.2, 127.8, 126.4, 126.25, 126.18, 124.5 (C Ar), 103.3 (<u>C</u>H-Acetal), 52.9 (<u>C</u>H$_3$-O).

ESI-MS: 241.1 $[M+K]^+$.

2-Azido-2-deoxy-4,6-*O*-((2-naphthyl)methylidene)-α-D-glucopyranosyl-(1→6)-1-*O*-allyl-2,3,4,5-tetra-*O*-(2-naphthyl)methyl-D-*myo*-inositol (2-44)

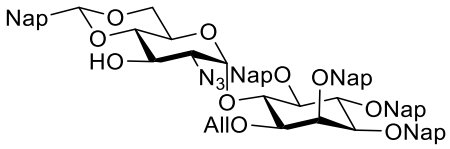

CSA (13.5 mg, 0.0580) was added to a mixture of the isolated α-anomer **2-32** (225 mg, 0.232 mmol) and 2-(dimethoxymethyl)naphthalene (80% purity, 176 mg, 0.696 mmol) in anhydrous ACN (6.4 mL). After stirring for 3 h, the reaction was quenched with aq. $NaHCO_3$, diluted with ethyl acetate and washed with aq. $NaHCO_3$. The aqueous phase was extracted with EtOAc. Organic layers were combined, washed with brine, dried over Na_2SO_4, filtered, and concentrated under reduced pressure. The crude was purified by silica gel column chromatography to afford **2-44** in 91% yield (233 mg, 0.211 mmol) as a white solid; R_f = 0.46 (hexane/EtOAc, 7:3).

$[\alpha]_D^{20}$: 51.48 (c = 1, $CHCl_3$).

IR (ATR) v(cm^{-1}) 3500 (O-H), 3057, 2867, 2109 (N=N=N), 1603, 1510, 1366, 1271, 1127, 1088, 856, 818, 745.

^{1}H NMR (400 MHz, $CDCl_3$) δ (ppm) 7.76 – 7.91 (m, 11H, Ar), 7.59 – 7.71 (m, 9H, Ar), 7.43 – 7.54 (m, 12H, Ar), 7.27 – 7.34 (m, 2H, Ar), 7.03 (dd, *J* = 8.5, 1.7 Hz, 1H, Ar), 5.95 – 6.05 (m, 1H, -C<u>H</u>= Allyl), 5.86 (d, *J* = 3.8 Hz, 1H, Glc-1), 5.53 (s, 1H, C<u>H</u> Naphtylidene acetal), 5.28 (dd, *J* = 17.2, *J* = 1.7 Hz, 1H, =C<u>H</u>$_{2a}$ Allyl), 5.16 – 5.24 (m, 4H, C<u>H</u>$_2$ Nap, =C<u>H</u>$_{2b}$ Allyl), 5.12 & 5.09 (ABq, *J* = 12.3 Hz, 2H, C<u>H</u>$_2$ Nap), 4.98 (d, *J* = 10.8 Hz, 1H, C<u>H</u>$_2$ Nap), 4.90 & 4.84 (ABq, *J* = 11.9 Hz, 2H, C<u>H</u>$_2$ Nap), 4.46 (t, *J* = 9.6 Hz, 1H, Ino-6), 4.30 – 4.39 (m, 2H, Ino-4, Glc-5), 4.22 – 4.30 (m, 2H, Glc-3, Glc-6a), 4.18 (app t, *J* = 2.3 Hz, 1H, Ino-2), 4.01 – 4.12 (m, 2H, -C<u>H</u>$_2$- Allyl), 3.60 – 3.67 (m, 2H, Glc-6b, Ino-5), 3.57 (dd, *J* = 9.8, 2.3 Hz, 1H, Ino-3), 3.46 – 3.53 (m, 2H, Ino-1, Glc-4), 3.26 (dd, *J*= 10.1, 3.8 Hz, 1H, Glc-2), 2.70 (br s, 1H, HO-Glc-3).

^{13}C NMR (101 MHz, $CDCl_3$) δ (ppm) 136.3, 136.1, 136.0, 135.8 (C_q Ar), 134.3 (-<u>C</u>H= Allyl), 133.7, 133.5, 133.33, 133.31, 133.29, 133.12, 133.07, 132.94, 132.92, 132.8 (C_q Ar), 128.4, 128.3, 128.19, 128.17, 128.14, 128.1, 128.03, 128.01, 127.84, 127.82, 127.71, 127.70, 127.7, 126.73, 126.71, 126.5, 126.43, 126.39, 126.3, 126.18, 126.16, 126.10, 126.08, 126.0, 125.93, 125.88, 125.86, 125.84, 125.80, 125.6, 125.3, 123.8 (C Ar). 117.5 (=<u>C</u>H$_2$ Allyl), 102.0 (<u>C</u>H Naphtylidene acetal), 98.2 (Glc-1), 82.1 (Ino-1), 82.06 (Ino-4), 82.02 (Glc-4), 81.6 (Ino-5), 80.8 (Ino-3), 76.0

(CH₂ Nap), 75.6 (CH₂ Nap), 75.4 (Ino-6), 74.3 (CH₂ Nap), 73.2 (CH₂ Nap), 73.0 (Ino-2), 71.1 (-CH₂- Allyl), 68.9 (Glc-6), 68.8 (Glc-3), 63.3 (Glc-2), 62.4 (Glc-5).

HRMS: $[M+Na]^+$ cald 1128.4411; found 1128.4623. $[M+K]^+$ cald 1144.4150; found 1144.4374.

ESI-MS: 1129.3 $[M+Na]^+$.

2-Azido-2-deoxy-3-*O*-(2-naphthyl)methyl-4,6-*O*-((2-naphthyl)methylidene)-α-D-glucopyranosyl-(1→6)-1-*O*-allyl-2,3,4,5-tetra-*O*-(2-naphthyl)methyl-D-*myo*-inositol (2-45)

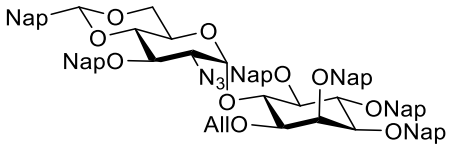

To a mixture of alcohol **2-44** (207 mg, 0.187 mmol) and TBAI (104 mg, 0.281 mmol) in DMF (2.6 mL), NaH (15.0 mg, 0.0374 mmol, 60% in mineral oil) was added at 0 °C. After 40 min, NapBr (62 mg, 0.281 mmol) was added and the mixture was stirred for additional 2h. The reaction was quenched with water, and volatiles were removed under reduced pressure. The remaining was dissolved with ethyl acetate, and the solution was extracted with water. The layers were separated, and the aqueous phase was extracted with ethyl acetate. Organic layers were washed with brine, dried with Na_2SO_4, filtered, and evaporated. The crude was purified by flash silica gel column chromatography to afford the fully protected pseudodisaccharide **2-45** in 98% yield (229.8 mg, 0.184 mmol) as a white solid; R_f = 0.28 (hexane/EtOAc, 5:1).

$[\alpha]_D^{20}$**:** 40.91 (c = 1, $CHCl_3$).

IR (ATR) v(cm^{-1}) 3057, 2863, 2107 (N=N=N), 1603, 1510, 1465, 1366, 1272, 1172, 1125, 1089, 1036, 893, 856, 817, 750.

^{1}H NMR (400 MHz, $CDCl_3$) δ (ppm) 7.75 – 7.91 (m, 15H, Ar), 7.60 – 7.75 (m, 9H, Ar), 7.41 – 7.60 (m, 18H, Ar), 5.93 – 6.07 (m, 1H, -CH= Allyl), 5.85 (d, *J* = 3.8 Hz, 1H, Glc-1), 5.65 (s, 1H, CH Naphtylidene acetal), 5.28 (dd, *J* = 17.2, 1.6 Hz, 1H, =CH$_{2a}$ Allyl), 5.16 – 5.25 (m, 2H, =CH$_{2b}$ Allyl, CH$_2$ Nap), 5.07 – 5.15 (m, 5H, CH$_2$ Nap), 4.95 – 5.01 (m, 2H, CH$_2$ Nap), 4.89 & 4.83 (ABq, *J* = 11.9 Hz, 2H, CH$_2$ Nap), 4.30 – 4.48 (m, 3H, Ino-4, Ino-6, Glc-5), 4.28 (dd, *J* = 10.2, 4.8 Hz, 1H, Glc-6a), 4.17 (s, 1H, Ino-2), 4.10 – 4.15 (m, 1H, Glc-3), 4.07 (app t, *J* = 6.5 Hz, 2H, -CH$_2$- Allyl), 3.77 (t, *J* = 9.4 Hz, 1H, Glc-4), 3.70 (t, *J* = 10.2 Hz, 1H, Glc-6b), 3.62 (t, *J* = 9.3 Hz, 1H, Ino-5), 3.56 (d, *J* = 7.8 Hz, 1H, Ino-3), 3.47 (d, *J* = 9.6 Hz, 1H, Ino-1), 3.43 (dd, *J* = 10.0, 3.8 Hz, 1H, Glc-2).

^{13}C NMR (101 MHz, $CDCl_3$) δ (ppm) 136.3, 136.2, 135.9, 135.8, 135.5, 134.9 (C_q Ar), 134.4 (-CH= Allyl), 133.6, 133.4, 133.3, 133.3, 133.11, 133.07, 133.0, 132.91, 132.90 (C_q Ar), 128.5, 128.33, 128.27, 128.19, 128.18, 128.15, 128.1, 128.0, 127.9, 127.84, 127.81, 127.76, 127.73, 127.69, 127.6, 127.1, 126.7, 126.6, 126.5, 126.4, 126.3, 126.23, 126.15, 126.10, 126.07, 126.05, 125.96, 125.95, 125.9, 125.8, 125.8, 125.7, 125.6, 125.6, 124.0 (C Ar), 117.4 (=CH$_2$ Allyl), 101.5 (CH Naphtylidene acetal), 98.2 (Glc-1), 83.1 (Glc-4), 82.1 (Ino-4), 82.0 (Ino-1), 81.4 (Ino-5), 80.9

(Ino-3), 75.91 (CH$_2$ Nap), 75.90 (Glc-3), 75.6 (CH$_2$ Nap), 75.4 (Ino-6), 74.9 (CH$_2$ Nap), 74.3 (CH$_2$ Nap), 73.2 (CH$_2$ Nap), 73.0 (Ino-2), 71.2 (-CH$_2$- Allyl), 69.0 (Glc-6), 63.3 (Glc-2), 62.7 (Glc-5).
HRMS: [M+Na]$^+$ cald 1268.5037; found 1268.5302.
ESI-MS: 1269.3 [M+Na]$^+$.

2-Azido-2-deoxy-3,6-di-*O*-(2-naphthyl)methyl-α-D-glucopyranosyl-(1→6)-1-*O*-allyl-2,3,4,5-tetra-*O*-(2-naphthyl)methyl-D-*myo*-inositol (2-46)

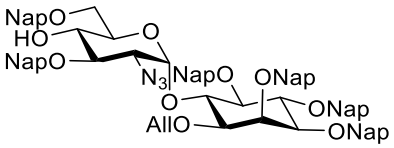

To a solution of the fully protected pseudodisaccharide **2-45** (45.2 mg, 0.0363 mmol) in a 4:1 ACN/DCM anhydrous mixture (1.2 mL), Me$_2$EtSiH (47.8 µL, 0.363 mmol) and Cu(OTf)$_2$ (3 mg, 8.29 µmol) were added at 0 °C. After 30 min, the reaction was quenched with aq. NaHCO$_3$, diluted with ethyl acetate and extracted with aq. NaHCO$_3$. The aqueous phase was extracted with EtOAc. Organic layers were combined, washed with brine, dried over Na$_2$SO$_4$, filtered, and concentrated by rotatory evaporation. The resulting colorless oil was purified by silica gel column chromatography to give the desired pseudodisaccharide **2-46** in 75% yield (33.8 mg, 0.0271 mmol) as a white solid; R_f = 0.56 (hexane/EtOAc, 7:3). The corresponding diol was also obtained as a result of complete acetal opening with 23% yield (9.3 mg, 0.00839 mmol); R_f = 0.17 (hexane/EtOAc, 7:3).
$[\alpha]_D^{20}$**:** 4.59 (c = 1, CHCl$_3$).
IR (ATR) ν(cm^{-1}) 3472 (O-H), 3055, 2926, 2108 (N=N=N), 1603, 1510, 1460, 1365, 1272, 1216, 1171.6, 1125, 1054, 953, 894, 856, 817, 751, 667.
^{1}H NMR (400 MHz, CDCl$_3$) δ (ppm) 7.77 – 7.91 (m, 16H, Ar), 7.58 – 7.72 (m, 10H, Ar), 7.45 – 7.51 (m, 10H, Ar), 7.31 – 7.40 (m, 5H, Ar), 7.17 (dd, *J* = 8.4, 1.7 Hz, 1H, Ar), 5.93 – 6.04 (m, 1H, -CH= Allyl), 5.82 (d, *J* = 3.7 Hz, 1H, Glc-1), 5.28 (dd, *J* = 17.2, 1.7 Hz, 1H, =CH$_{2a}$ Allyl), 5.16 – 5.26 (m, 3H, =CH$_{2b}$ Allyl, CH$_2$ Nap), 4.98 – 5.14 (m, 5H, CH$_2$ Nap), 4.91 (d, *J* = 11.5 Hz, 1H, CH$_2$ Nap), 4.87 & 4.82 (ABq, *J* = 11.9 Hz, 2H, CH$_2$ Nap), 4.31 – 4.45 (m, 3H, Ino-4, Ino-6, CH$_2$ Nap), 4.15 – 4.20 (m, 2H, Ino-2, CH$_2$ Nap), 4.10 – 4.15 (m, 1H, Glc-5), 4.02 – 4.10 (m, 2H, -CH$_2$- Allyl), 3.93 (dd, *J* = 10.3, 8.7 Hz, 1H, Glc-3), 3.78 (td, *J* = 9.3, 3.3 Hz, 1H, Glc-4), 3.54 – 3.63 (m, 2H, Ino-3, Ino-5), 3.47 (dd, *J* = 9.7, 2.1 Hz, 1H, Ino-1), 3.30 – 3.39 (m, 2H, Glc-2, Glc-6a), 3.19 (dd, *J* = 10.4, 3.5 Hz, 1H, Glc-6b), 2.19 (d, *J* = 3.3 Hz, 1H, HO-Glc-4).
^{13}C NMR (101 MHz, CDCl$_3$) δ (ppm) 136.4, 136.2, 136.0, 135.79, 135.78, 135.3 (C$_q$ Ar), 134.4 (-CH= Allyl), 133.4, 133.33, 133.29, 133.21, 133.17, 133.11, 133.06, 132.97, 132.95, 132.8 (C$_q$ Ar), 128.5, 128.3, 128.2, 128.13, 128.09, 128.06, 128.0, 127.9, 127.82, 127.79, 127.75, 128.0, 127.7, 127.0, 126.72, 126.66, 126.5, 126.4, 126.3, 126.21, 126.19, 126.14, 126.12, 126.09, 126.07, 126.06, 126.02, 125.97, 125.93, 125.88, 125.82, 125.77, 125.6, 125.5 (C Ar), 117.2 (=CH$_2$ Allyl),

97.8 (Glc-1), 82.12 (Ino-4), 82.09 (Ino-1), 81.7 (Ino-5), 80.9 (Ino-3), 79.5 (Glc-3), 76.0 (CH$_2$ Nap), 75.6 (CH$_2$ Nap), 75.3 (Ino-6), 75.0 (CH$_2$ Nap), 74.2 (CH$_2$ Nap), 73.4 (CH$_2$ Nap), 73.0 (CH$_2$ Nap), 72.9 (Ino-2), 72.4 (Glc-4), 71.2 (-CH$_2$- Allyl), 69.44 (Glc-5), 69.37 (Glc-6), 63.0 (Glc-2).
HRMS: $[M+Na]^+$ cald 1270.5194; found 1270.5620. $[M+K]^+$ cald 1286.4933; found 1286.5371.
ESI-MS: 1271.3 $[M+Na]^+$, 1286.3 $[M+K]^+$.

2,3,4,6-Tetra-*O*-(2-naphthyl)methyl-α-D-mannopyranosyl-(1→4)-2-azido-2-deoxy-3,6-di-*O*-(2-naphthyl)methyl-α-D-glucopyranosyl-(1→6)-1-*O*-allyl-2,3,4,5-tetra-*O*-(2-naphthyl)methyl-D-*myo*-inositol (2-7)

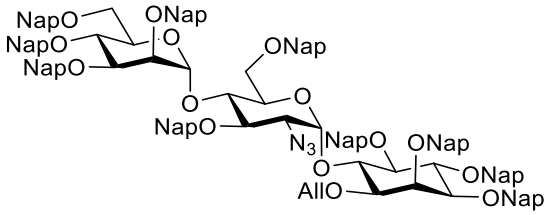

A solution of pseudodisaccharide acceptor **2-46** (100 mg, 0.0801 mmol) and the trimannose glycosyl donor **2-12** (59.1 mg, 0.120 mmol) in a 6:1 Et$_2$O/DCM anhydrous mixture (2 mL) was stirred at room temperature for 10 min. The mixture was cooled to 0 °C, and TMSOTf (4.3 µL, 24 µmol) was added. After stirring for 45 min, the reaction was quenched with Et$_3$N, and volatiles were removed under reduced pressure. The resulting crude was purified by flash silica gel column chromatography to give exclusively the α-anomer of the corresponding pseudotrisaccharide in 84% yield (0.106 mg, 0.0671 mmol) as a white solid; R_f = 0.54 (hexane/EtOAc, 1:1). This compound was mixed with NaOMe (17.3 mg, 0.320 mmol) and 5 mL of a 4:1 MeOH/DCM anhydrous mixture. The reaction was stirred at room temperature for 2 h before it was neutralized with Amberlite IR 120 (H^+) resin, filtered and concentrated. The obtained triol was dissolved in anhydrous DMF (2 mL), and NaH (33.4 mg, 0.835 mmol, 60% in mineral oil) was added at 0 °C. After 40 min, NapBr (146 mg, 0.660 mmol) was added, and the mixture was stirred for two days before it was quenched with water. Volatiles were removed under reduced pressure. The remaining was dissolved with ethyl acetate, and the solution was extracted with water. The layers were separated, and the aqueous phase was extracted with ethyl acetate. Organic layers were washed with brine, dried with Na_2SO_4, filtered, and evaporated. The resulting oil was purified by flash silica gel column chromatography to obtain **2-7** in 75% (98.7 mg, 0.0501 mmol) yield over two steps as a white solid; R_f = 0.31 (hexane/EtOAc, 1:3).
$[\alpha]_D^{20}$**:** 11.50 (c = 1, $CHCl_3$).
IR (ATR) ν(cm^{-1}) 3021, 3056, 2926, 2106 (N=N=N), 1699, 1635, 1603, 1510, 1462, 1366, 1346, 1266, 1216, 1125, 1096, 1053, 953, 894, 856, 816, 752, 668.
^{1}H NMR (400 MHz, $CDCl_3$) δ (ppm) 7.13 – 7.80 (m, 86H, Ar), 7.02 – 7.13 (m, 5H, Ar), 6.84 – 6.92 (m, 2H, Ar), 5.82 – 5.91 (m, 1H, -CH= Allyl), 5.80 (d, *J* = 3.6 Hz, 1H, Glc-1), 5.13 – 5.22 (m, 2H, =CH$_{2a}$ Allyl, Man-1), 5.08 (d, *J* = 10.5 Hz, 1H, =CH$_{2b}$ Allyl), 4.94 – 5.05 (m, 5H, CH$_2$ Nap), 4.91

(d, *J* = 10.8 Hz, 1H, C<u>H</u>$_2$ Nap), 4.69 – 4.82 (m, 4H, C<u>H</u>$_2$ Nap), 4.49 – 4.61 (m, 3H, C<u>H</u>$_2$ Nap), 4.31 – 4.46 (m, 3H, Ino-6, C<u>H</u>$_2$ Nap), 4.14 – 4.25 (m, 3H, Ino-4, C<u>H</u>$_2$ Nap), 4.05 – 4.15 (m, 4H, Ino-2, Man-4, Glc-5, C<u>H</u>$_2$ Nap), 3.88 – 4.00 (m, 3H, -C<u>H</u>$_2$- Allyl, C<u>H</u>$_2$ Nap), 3.81 – 3.88 (m, 2H, Glc-3, Glc-4), 3.73 (dd, *J* = 9.4, 2.7 Hz, 1H, Man-3), 3.60 (app t, *J* = 2.5 Hz, 1H, Man-2), 3.42 – 3.50 (m, 3H, Ino-3, Ino-5, Glc-6a), 3.31 – 3.41 (m, 2H, Ino-1, Man-6a), 3.16 – 3.26 (m, 3H, Glc-2, Glc-6b, Man-5), 3.01 (d, *J* = 10.8 Hz, 1H, Man-6b).

^{13}C NMR (101 MHz, CDCl$_3$) δ (ppm) 136.5, 136.3, 136.1, 136.11, 136.06, 136.03, 135.97, 135.8, 135.6 (C$_q$ Ar), 134.3 (-<u>C</u>H= Allyl), 133.38, 133.35, 133.32, 133.30, 133.28, 133.2, 133.13, 133.08, 133.06, 133.0, 132.9, 132.73, 132.69 (C$_q$ Ar), 128.6, 128.4, 128.21, 128.16, 128.12, 128.10, 128.07, 128.04, 128.01, 127.97, 127.9, 127.84, 127.79, 127.76, 127.74, 127.72, 127.67, 127.63, 127.60, 127.0, 126.8, 126.73, 126.71, 126.5, 126.43, 126.40, 126.36, 126.32, 126.29, 126.2, 126.1, 126.11, 126.07, 126.03, 125.99, 125.95, 125.91, 125.85, 125.81, 125.73, 125.68, 125.49, 125.46, 125.43, 125.40, 125.33, 125.29, 124.9, 124.7 (C Ar), 117.2 (=<u>C</u>H$_2$ Allyl), 101.2 (Man-1), 97.8 (Glc-1), 82.2 (Ino-4), 82.1 (Ino-1), 81.8 (Ino-5), 80.8 (Ino-3), 80.2 (Glc-3), 79.5 (Man-3), 78.2 (Glc-4), 76.8 (Man-2), 76.0 (<u>C</u>H$_2$ Nap), 75.5 (Ino-6), 75.4 (<u>C</u>H$_2$ Nap), 75.3 (<u>C</u>H$_2$ Nap), 74.6 (Man-4), 74.2 (<u>C</u>H$_2$ Nap), 74.0 (<u>C</u>H$_2$ Nap), 73.5 (<u>C</u>H$_2$ Nap), 73.4 (<u>C</u>H$_2$ Nap), 73.2 (Man-5), 73.0 (<u>C</u>H$_2$ Nap), 72.6 (Ino-2), 72.30 (<u>C</u>H$_2$ Nap), 72.26 (<u>C</u>H$_2$ Nap), 71.0 (-<u>C</u>H$_2$- Allyl), 70.0 (Glc-5), 69.0 (Glc-6), 68.6 (Man-6), 63.3 (Glc-2).

HRMS: [M+Na]$^+$ cald 1992.8226; found 1992.819.

ESI-MS: 1992.6 [M+Na]$^+$.

2,3,4,6-Tetra-*O*-(2-naphthyl)methyl-α-D-mannopyranosyl-(1→4)-2-azido-2-deoxy-3,6-di-*O*-(2-naphthyl)methyl-α-D-glucopyranosyl-(1→6)-2,3,4,5-tetra-*O*-(2-naphthyl)methyl-D-*myo*-inositol (2-47)

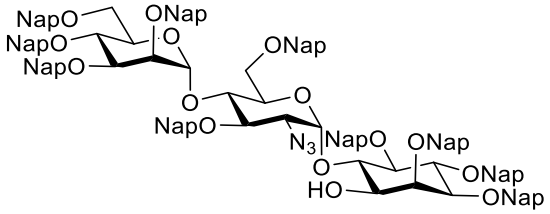

The fully protected pseudotrisaccharide **2-7** (94 mg, 0.0477 mmol) was dissolved in a 47:53 MeOH/DCM anhydrous mixture, and PdCl$_2$ (4.7 mg, 0.0265 mmol) was added at room temperature. After 5.5 h, the mixture was filtered through a pad of Celite, and the volatiles were evaporated under reduced pressure. The resulting oil was purified by flash silica gel column chromatography to obtain **2-47** in 83% yield (76.7 mg, 0.0397 mmol) as a white solid; R$_f$ = 0.60 (hexane/EtOAc, 13:7).

$[\alpha]_D^{20}$: 18.22 (c = 1, CHCl$_3$).

IR (ATR) ν(cm^{-1}) 3471 (O-H), 3056, 2926, 2108 (N=N=N), 1699, 1603, 1510, 1462, 1367, 1344, 1272, 1171, 1125, 1097, 1049, 954, 893, 856, 816, 752.

^{1}H NMR (400 MHz, $CDCl_3$) δ (ppm) 7.75 – 7.85 (m, 13H, Ar), 7.61 – 7.70 (m, 16H, Ar), 7.53 – 7.58 (m, 10H, Ar), 7.45 – 7.51 (m, 11H, Ar), 7.38 – 7.44 (m, 12H, Ar), 7.28 – 7.36 (m, 12H, Ar), 7.17 – 7.26 (m, 3H, Ar), 7.16 (s, 1H, Ar), 7.10 (t, *J* = 7.5 Hz, 1H, Ar), 6.98 (dd, *J* = 8.5, 1.7 Hz, 1H, Ar), 5.60 (d, *J* = 3.5 Hz, 1H, Glc-1), 5.33 (d, *J* = 2.1 Hz, 1H, Man-1), 5.20 (d, *J* = 11.8 Hz, 1H, C$\underline{H}_2$ Nap), 5.12 (app t, *J* = 11.1 Hz, 2H, C$\underline{H}_2$ Nap), 4.96 – 5.04 (m, 3H, C$\underline{H}_2$ Nap), 4.86 – 4.95 (m, 4H, C$\underline{H}_2$ Nap), 4.52 – 4.72 (m, 4H, C$\underline{H}_2$ Nap), 4.19 – 4.31 (m, 5H, C$\underline{H}_2$ Nap, Ino-4), 4.05 – 4.19 (m, 6H, C$\underline{H}_2$ Nap, Ino-2, Man-4, Glc-5, Ino-6), 3.87 – 3.97 (m, 3H, Glc-3, Man-3, Glc-4), 3.67 – 3.76 (m, 2H, Ino-1, Man-2), 3.63 (dd, *J* = 9.9, 2.3 Hz, 1H, Ino-3), 3.47 – 3.58 (m, 4H, Glc-2, Ino-5, Man-5, Man-6a), 3.40 (br s, 2H, Glc-6), 3.22 – 3.31 (m, 1H, Man-6b), 3.17 (d, *J* = 6.8 Hz, 1H, HO-Ino-1).

^{13}C NMR (101 MHz, $CDCl_3$) δ (ppm) 136.3, 136.11, 136.07, 136.0, 135.9, 135.6, 135.33, 133.34, 133.30, 133.27, 133.24, 133.17, 133.1, 133.04, 132.99, 132.95, 132.92, 132.81, 132.77 (C_q Ar), 128.5, 128.45, 128.37, 128.2, 128.14, 128.10, 128.08, 128.05, 128.02, 127.99, 127.96, 127.88, 127.86, 127.80, 127.77, 127.7, 127.6, 127.1, 126.9, 126.7, 126.6, 126.5, 126.43, 126.37, 126.35, 126.3, 126.24, 126.16, 126.11, 126.06, 126.03, 126.01, 125.96, 125.9, 125.8, 125.5, 125.4, 125.3, 125.1, 124.7 (C Ar), 100.9 (Man-1), 98.2 (Glc-1), 81.9 (Ino-4), 81.6 (Ino-5), 80.9 (Ino-3), 80.8 (Man-3), 80.3 (Glc-3), 77.8 (Glc-4), 77.4 (C-Ino), 77.1 (C-Ino), 76.7 (Man-2), 76.0 (C$\underline{H}_2$ Nap), 75.4 (C$\underline{H}_2$ Nap), 75.3 (C$\underline{H}_2$ Nap), 75.1 (C$\underline{H}_2$ Nap), 74.7 (Man-4), 74.4 (C$\underline{H}_2$ Nap), 73.6 (Ino-1), 73.5 (C$\underline{H}_2$ Nap), 73.3 (C$\underline{H}_2$ Nap), 73.2 (C$\underline{H}_2$ Nap, Man-5), 72.4 (C$\underline{H}_2$ Nap x2), 70.8 (Glc-5), 68.9 (Man-6), 68.8 (Glc-6), 64.2 (Glc-2).

HRMS: $[M+Na]^+$ cald 1952.7913; found 1952.7926.

ESI-MS: 1952.6 $[M+Na]^+$.

2,3,4,6-Tetra-*O*-(2-naphthyl)methyl-α-D-mannopyranosyl-(1→4)-2-azido-2-deoxy-3,6-di-*O*-(2-naphthyl)methyl-α-D-glucopyranosyl-(1→6)-2,3,4,5-tetra-*O*-(2-naphthyl)methyl-1-*O*-(2-oleoyl-1-stearoyl-*sn*-glycero-3-phosphonate)-D-*myo*-inositol (2-48)

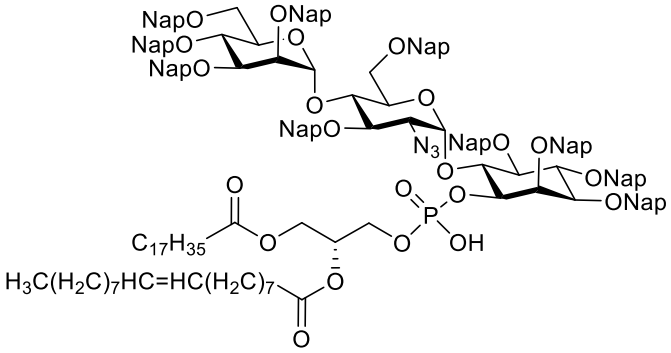

Alcohol **2-47** (39.1 mg, 0.0202 mmol) and H-phosphonate **2-8** (71% purity, 35 mg, 0.0315 mmol) were co-evaporated with anhydrous pyridine (3 x 2 mL) and placed under high vacuum for 1.5 h. The residue was dissolved in anhydrous pyridine (2 mL) and PivCl (6.4 µL, 0.0525 mmol) was added. The reaction mixture was stirred for 1.5 h at room temperature before water (90 µL) and

iodine (15.2 mg, 0.0600 mmol) were added. The reaction mixture was stirred for 2 h, and solid $Na_2S_2O_3$ was added until the orange color of the reaction disappeared. Volatiles were removed under reduced pressure. The remaining was triturated with DCM to remove $Na_2S_2O_3$. Purification was performed by flash silica gel column chromatography (eluting with MeOH/DCM 1:90 and gradually increasing the polarity to 1:10) to afford the lipidated pseudotrisaccharide **2-48** in 82% yield (43.9 mg, 0.0162 mmol) as a white solid; R_f = 0.68 (MeOH/DCM, 1:10).

$[\alpha]_D^{20}$**:** 30.1 (c = 1, $CHCl_3$).

IR (ATR) v(cm^{-1}) 2626, 2855, 2110 (N=N=N), 1740 (C=O), 1603, 1510, 1466, 1366, 1259, 1125, 1050, 892, 856, 815, 753, 668.

^{1}H NMR (400 MHz, $CDCl_3$) δ (ppm) 7.51 – 7.86 (m, 36H, Ar), 7.27 – 7.48 (m, 29H, Ar), 7.08 – 7.21 (m, 4H, Ar), 6.95 (d, *J* = 8.0 Hz, 1H, Ar), 5.78 (d, *J*= 3.6 Hz, 1H, Glc-1), 5.23 – 5.37 (m, 4H, -C<u>H</u>=C<u>H</u>- Oleoyl, C<u>H</u> sn-2, Man-1), 4.89 – 5.20 (m, 9H, C<u>H</u>$_2$ Nap), 4.72 – 4.88 (m, 3H, C<u>H</u>$_2$ Nap, H-Ino), 4.50 – 4.66 (m, 6H, C<u>H</u>$_2$ Nap), 4.39 – 4.47 (m, 3H), 4.09 – 4.36 (m, 10H, C<u>H</u>$_2$ sn-1, C<u>H</u>$_2$ sn-3, Ino-4), 3.89 – 4.06 (m, 3H, Glc-3, Glc-4), 3.71 – 3.83 (m, 2H, 2 x H-Ino), 3.55 – 3.68 (m, 3H, Man-2, Glc-6), 3.30 – 3.46 (m, 3H, Man-5, Glc-2, Man-6a), 3.17 (d, *J* = 10.6 Hz, 1H, Man-6b), 2.98 (d, *J* = 11.9 Hz, 1H, Et_3N residue), 2.21 (q, *J* = 7.3 Hz, 4H, 2 x O-COC<u>H</u>$_2$-CH$_2$- lipid), 1.91 – 2.03 (m, 4H, -C<u>H</u>$_2$-CH=CH-C<u>H</u>$_2$- Oleoyl), 1.45 – 1.56 (m, 4H, 2 x O-COCH$_2$-C<u>H</u>$_2$- lipid), 1.14 – 1.34 (m, 63H, C<u>H</u>$_2$ lipid), 0.85 – 0.92 (m, 6H, 2 x C<u>H</u>$_3$ lipid).

^{13}C NMR (101 MHz, $CDCl_3$) δ (ppm) 173.6 (<u>C</u>=O), 173.2 (<u>C</u>=O), 137.5, 136.4, 136.2, 136.14, 136.08, 136.01, 135.7, 133.38, 133.36, 133.3, 133.2, 133.13, 133.07, 133.0, 132.9, 132.8, 132.7 (C_q Ar), 130.1 (-<u>C</u>H=CH- Oleoyl), 129.9 (-CH=<u>C</u>H- Oleoyl), 128.8, 128.2, 128.11, 128.08, 128.04, 128.01, 127.97, 127.9, 127.8, 127.73, 127.69, 127.64, 127.59, 127.1, 126.8, 126.5, 126.4, 126.3, 126.2, 126.1, 126.05, 126.03, 125.99, 125.9, 125.8, 125.73, 125.68, 125.4, 125.35, 125.31, 125.2, 125.0 (C Ar), 101.4 (Man-1), 96.7 (Glc-1), 82.3 (Ino-4), 82.0, 80.9, 80.0 (Glc-3), 78.6 (Glc-4), 77.4, 77.0 (Man-2), 76.2, 76.0, 75.7, 75.4, 75.2, 75.0, 74.7, 74.2, 73.8, 73.5, 73.2 (Man-5), 72.5, 72.3, 70.8, 70.7, 69.9 (<u>C</u>H sn-2), 69.5, 69.1 (Glc-6, Man-6), 63.8 (Glc-2), 62.9 (<u>C</u>H$_2$ sn-1), 34.4, 34.2, 32.1, 32.0, 29.90, 29.86, 29.8, 29.7, 29.5, 29.5, 29.4, 29.29, 29.27, 29.22, 28.18, 27.4, 27.3, 26.6, 25.0, 22.8, 14.3.

^{31}P NMR (162 MHz, $CDCl_3$) δ (ppm) -0.80.

HRMS: $[M-H]^-$ cald 2613.3031; found 2613.4924.

α-D-Mannopyranosyl-(1→4)-2-amino-2-deoxy-α-D-glucopyranosyl-(1→6)-1-*O*-(2-oleoyl-1-stearoyl-s*n*-glycero-3-phosphonate)-D-*myo*-inositol (2-4)

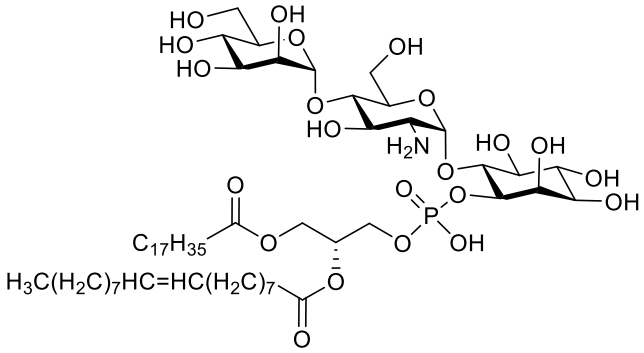

DDQ (70 mg, 0.308 mmol) was added to a solution of the protected glycolipid **2-48** (54.6 mg, 0.0207 mmol) in a 3:1 DCM/MeOH mixture (4 mL). The reaction mixture was stirred at room temperature for 6 h before volatiles were removed under reduced pressure. The residue was purified by LH-20 size exclusion chromatography eluting with MeOH/$CHCl_3$ 9:1. To the obtained deprotected glycolipid, 0.79 mL of a 1M solution of $P(CH_3)_3$ in THF were added followed by water (160 µL). After 2h, the reaction was concentrated under vacuum, and the crude was purified by LH-20 size exclusion chromatography eluting with THF followed by trituration with MeOH to give the final GPI-fragment **2-4** in 56% yield (13.8 mg, 0.0116 mmol) as a slightly yellow solid. For the NMR sample, the compound was dissolved in a 3:3:1 $CD_3OD/CDCl_3/D_2O$ mixture.

^{1}H NMR (400 MHz, CD_3OD) δ (ppm) 5.22 (d, *J*= 3.9 Hz, 1H, Glc-1), 5.02 – 5.10 (m, 2H, -C<u>H</u>=C<u>H</u>- Oleoyl), 4.90 – 5.01 (m, 2H, Man-1, C<u>H</u> sn-2), 4.09 – 4.16 (m, 1H, C<u>H</u>$_{2a}$ sn-1), 3.82 – 3.95 (m, 3H, C<u>H</u>$_{2b}$ sn-1), 3.67 – 3.79 (m, 4H, C<u>H</u>$_2$ sn-3, Glc-3), 3.63 (t, *J* = 9.4 Hz, 1H), 3.46 – 3.58 (m, 3H), 3.28 – 3.45 (m, 7H), 3.15 (dd, *J* = 10.0, 2.7 Hz, 1H), 2.98 – 3.06 (m, 1H), 2.93 (dd, *J* = 10.6, 3.9 Hz, 1H, Glc-2), 1.98 – 2.09 (m, 4H, 2 x O-COC<u>H</u>$_2$-CH$_2$- lipid), 1.69 – 1.76 (m, 4H, -C<u>H</u>$_2$-CH=CH-C<u>H</u>$_2$- Oleoyl), 1.24 – 1.35 (m, 4H, 2 x O-COCH$_2$-C<u>H</u>$_2$- lipid), 0.91 – 1.07 (m, 53H, C<u>H</u>$_2$ lipid), 0.59 (t, *J* = 6.7 Hz, 6H, 2 x C<u>H</u>$_3$ lipid).

^{13}C NMR (101 MHz, CD_3OD) δ (ppm) 174.0 (<u>C</u>=O), 173.7 (<u>C</u>=O), 129.6 (-<u>C</u>H=CH- Oleoyl), 129.3 (-CH=<u>C</u>H- Oleoyl), 101.0 (Man-1), 95.0 (Glc-1), 76.3, 73.6, 73.0, 72.3, 71.4, 70.2 (<u>C</u>H sn-2, Glc-3), 66.5, 63.4 (<u>C</u>H$_2$ sn-3), 62.5 (<u>C</u>H$_2$ sn-1), 60.9, 53.9 (Glc-2), 33.8 (O-CO<u>C</u>H$_2$-CH$_2$- lipid), 33.7 (O-CO<u>C</u>H$_2$-CH$_2$- lipid), 31.5, 29.3, 29.23, 29.17, 29.1, 28.94, 28.91, 28.88, 28.7 (<u>C</u>H$_2$ lipid), 26.8 (-<u>C</u>H$_2$-CH=CH-<u>C</u>H$_2$- Oleoyl), 24.6 (O-COCH$_2$-<u>C</u>H$_2$- lipid), 24.5 (O-COCH$_2$-<u>C</u>H$_2$- lipid), 22.2 (<u>C</u>H$_2$ lipid), 13.5 (2 x <u>C</u>H$_3$ lipid).

^{31}P NMR (162 MHz, CD_3OD) δ (ppm) 0.0023.

HRMS: $[M-H]^-$ cald 1186.6866; found 1186.6705.

5.2.5 Synthesis of GPI fragments 2-49 and 2-50

2-Azido-2-deoxy-3,4,6-tri-*O*-(2-naphthyl)methyl-α-D-glucopyranosyl-(1→6)-2,3,4,5-tetra-*O*-(2-naphthyl)methyl-1-*O*-(1,2-distearoyl-*sn*-glycero-3-phosphonate)-D-*myo*-inositol (2-60)

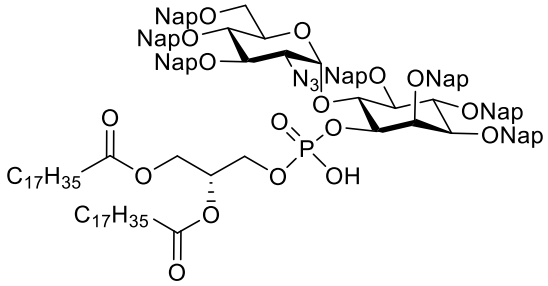

Alcohol **2-33** (90 mg, 0.0667 mmol) and H-phosphonate **2-55** (88% purity, 105 mg, 0.107 mmol) were co-evaporated with anhydrous pyridine (3 x 2.5 mL) and placed under high vacuum for 45 min. The solid mixture was dissolved in anhydrous pyridine (5.1 mL) and PivCl (21.2 µL, 0.173 mmol) was added. The reaction was stirred for 1 h at room temperature before water (154 µL) and iodine (50.8 mg, 0.200 mmol) were added. The reaction mixture was stirred for additional 60 min, and solid $Na_2S_2O_3$ was added until the color of the reaction changed from dark orange to light yellow. Volatiles were removed under reduced pressure. The remaining was triturated with DCM to leave behind solid $Na_2S_2O_3$, and concentrated. Purification was performed by flash silica gel column chromatography (eluting with MeOH/DCM 1:90 and gradually increasing the polarity to 1:10) to afford the lipidated pseudodisaccharide **2-60** in 75% yield with excess of triethyl ammonium salt (95% Purity, 113 mg, 0.0503 mmol) as a slightly yellow foam; R_f = 0.51 (MeOH/DCM, 1:10).

^{1}H NMR (400 MHz, $CDCl_3$) δ (ppm) 7.93 (s, 1H, Ar), 7.69 – 7.83 (m, 12H, Ar), 7.53 – 7.67 (m, 11H, Ar), 7.32 – 7.51 (m, 22H, Ar), 7.21 (d, *J* = 4.8 Hz, 1H, Ar), 7.07 – 7.12 (m, 1H, Ar), 6.85 (dd, *J* = 8.5, 1.7 Hz, 1H, Ar), 6.00 (d, *J* = 3.7 Hz, 1H, Glc-1), 5.27 – 5.33 (m, 1H, C$\underline{H}$ sn-2), 5.17 – 5.26 (m, 2H, C$\underline{H_2}$ Nap), 5.06 – 5.15 (m, 2H, C$\underline{H_2}$ Nap), 4.96 – 5.05 (m, 3H, C$\underline{H_2}$ Nap), 4.92 (dd, *J* = 10.5, 7.4 Hz, 3H, C$\underline{H_2}$ Nap, Ino), 4.84 (d, *J* = 11.8 Hz, 1H, C$\underline{H_2}$ Nap), 4.78 (d, *J* = 11.0 Hz, 1H, C$\underline{H_2}$ Nap), 4.68 (d, *J* = 12.2 Hz, 1H, C$\underline{H_2}$ Nap), 4.54 (t, *J* = 9.5 Hz, 1H, Ino), 4.39 – 4.48 (m, 3H, C$\underline{H_2}$ Nap, Ino, C$\underline{H_{2a}}$ sn-1), 4.30 – 4.37 (m, 2H, C$\underline{H_2}$ Nap, Glc-5), 4.26 (t, *J* = 9.5 Hz, 1H, Ino), 4.08 – 4.22 (m, 4H, C$\underline{H_{2b}}$ sn-1, C$\underline{H_2}$ sn-3, Glc-3), 3.82 (t, *J* = 9.5 Hz, 1H, Glc-4), 3.73 (dd, *J* = 9.8, 2.3 Hz, 1H, Ino), 3.63 (t, *J* = 9.3 Hz, 1H, Ino), 3.46 – 3.58 (m, 2H, Glc-6), 3.31 (dd, *J* = 10.3, 3.7 Hz, 1H, Glc-2), 3.03 (q, *J* = 7.3 Hz, 14H, C$\underline{H_2}$ Et_3NH), 2.19 – 2.28 (m, 4H, 2 x O-COC$\underline{H_2}$-CH_2- lipid), 1.49 – 1.60 (m, 4H, 2 x O-$COCH_2$-C$\underline{H_2}$- lipid), 1.32 (t, *J* = 7.3 Hz, 25H, C$\underline{H_3}$ Et_3NH), 1.14 – 1.30 (m, 77H, C$\underline{H_2}$ lipid), 0.88 (t, *J* = 6.7 Hz, 8H, 2 x C$\underline{H_3}$ lipid).

^{13}C NMR (101 MHz, $CDCl_3$) δ (ppm) 173.6 (C$\underline{}$=O), 173.3 (C$\underline{}$=O), 137.4, 136.4, 136.1, 135.9, 135.8, 135.7, 135.43, 133.39, 133.37, 133.3, 133.24, 133.19, 133.1, 133.05, 132.97, 132.92, 132.89, 132.87, 132.7 (C_q Ar), 128.2, 128.13, 128.11, 128.07, 128.02, 127.99, 127.95, 127.89,

127.85, 127.7, 127.63, 127.55, 126.8, 126.4, 126.2, 126.1, 126.05, 126.02, 125.99, 125.9, 125.83, 125.77, 125.7, 125.6, 125.6, 120.1 (C Ar), 96.9 (Glc-1), 82.01 (Ino), 81.99 (Ino), 81.0 (Ino), 79.9 (Glc-3), 78.4 (Glc-4), 78.1 (Ino), 77.3 (Ino), 76.1 ($\underline{C}H_2$ Nap), 75.8 ($\underline{C}H_2$ Nap), 75.2 ($\underline{C}H_2$ Nap), 74.9 ($\underline{C}H_2$ Nap), 74.1 (Ino), 73.4 ($\underline{C}H_2$ Nap), 72.5 ($\underline{C}H_2$ Nap), 70.6 ($\underline{C}H$ sn-2), 70.2 (Glc-5), 68.2 (Glc-6), 63.9 ($\underline{C}H_2$ sn-3), 63.4 (Glc-2), 62.8 ($\underline{C}H_2$ sn-1), 46.1 ($\underline{C}H_2$ Et_3NH), 38.6, 34.4 (O-CO$\underline{C}H_2$-CH_2- lipid), 34.2 (O-CO$\underline{C}H_2$-CH_2- lipid), 32.0, 29.82, 29.77, 29.7, 29.6, 29.5, 29.4, 29.2, 27.3 (-CH_2- lipid), 25.0 (O-COCH$_2$-$\underline{C}H_2$- lipid), 24.9 (O-COCH$_2$-$\underline{C}H_2$- lipid), 22.8 (-CH_2- lipid), 14.2 ($\underline{C}H_3$ lipid), 8.6 ($\underline{C}H_3$ Et_3NH).

^{31}P NMR (162 MHz, CDCl3) δ (ppm) -2.07.

HRMS: [M-H]$^-$cald 2033.0781; found 2033.0824.

2-Acetamido-2-deoxy-α-D-glucopyranosyl-(1→6)-1-*O*-(1,2-distearoyl-*sn*-glycero-3-phosphonate)-D-*myo*-inositol (2-49)

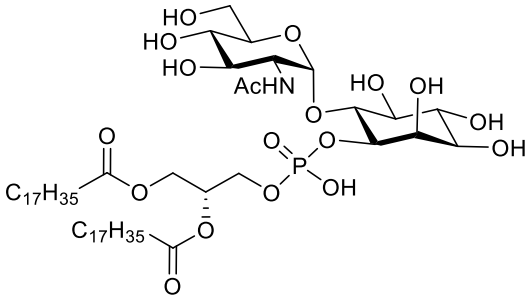

A solution of the glycolipid **2-60** (59.9 mg, 0.0266 mmol) in anhydrous THF (0.48 mL) was mixed with 0.53 mL of a 1 M solution of $P(CH_3)_3$ in THF. Water (200 µL) was added, and the reaction was stirred at room temperature for 1 h. Volatiles were removed under reduced pressure and the residue was dissolved in a 2:1 pyridine/acetic anhydride mixture (2.25 mL). The reaction was stirred for an additional hour before it was concentrated *in vacuo*. Purification was performed by flash silica gel column chromatography (eluting with MeOH/DCM 1:90 and gradually increasing the polarity to 1:10). The obtained *N*-acetylated compound **2-61** (48.3 mg, 0.0235 mmol) was dissolved in a 3:1 DCM/MeOH mixture (1.1 mL), and DDQ (56.1 mg, 0.247 mmol) was added. The reaction mixture was stirred at room temperature for 8 h, and volatiles were removed under vacuum. The residue was purified by LH-20 size exclusion chromatography eluting with MeOH/$CHCl_3$ 9:1 followed by trituration with MeOH to afford the final GPI-fragment **2-49** in 53% yield (15.2 mg, 0.0142 mmol) as a white solid. For the NMR sample, the compound was dissolved in a 3:3:1 CD_3OD/$CDCl_3$/D_2O mixture.

^{1}H NMR (400 MHz, CD_3OD) δ (ppm) 4.89 – 4.97 (m, 1H, C$\underline{H}$ sn-2), 4.62 (app s, 1H, Glc-1), 4.10 (dd, *J* = 12.2, 2.6 Hz, 1H, C$\underline{H}_{2a}$ sn-1), 3.76 – 3.90 (m, 3H, C$\underline{H}_{2b}$ sn-1, Ino, Ino), 3.60 – 3.76 (m, 4H, C$\underline{H}_2$ sn-3, Glc-5, Glc-2), 3.54 (dd, *J* = 12.0, 2.3 Hz, 1H, Glc-6a), 3.42 – 3.50 (m, 1H, Glc-3), 3.29 – 3.41 (m, 3H, Glc-6b, Ino, Ino), 3.13 (dd, *J* = 10.4, 1.8 Hz, 1H, Ino), 3.05 (t, *J* = 9.2 Hz, 2H,

Ino, Glc-4), 1.93 – 2.06 (m, 4H, 2 x O-COC$\underline{H}_2$-CH_2- lipid), 1.76 (s, 3H, C$\underline{H}_3$ Ac), 1.20 – 1.32 (m, 4H, 2 x O-$COCH_2$-C$\underline{H}_2$- lipid), 0.93 (s, 72H, C$\underline{H}_2$ lipid), 0.51 – 0.58 (m, 9H, 2 x C$\underline{H}_3$ lipid).

HSQC (400 MHz, CD_3OD) δ (ppm) 99.6 (Glc-1), 82.6 (Ino), 74.8 (Ino), 74.2 (Ino), 73.2 (Glc-5), 72.1 (Ino), 71.6 (Ino), 70.9 (Glc-3, Ino), 70.6 (Glc-4), 70.5 (C$\underline{H}$ sn-2), 63.4 (C$\underline{H}_2$ sn-3), 62.9, (C$\underline{H}_2$ sn-1), 61.3 (Glc-6), 54.0 (Glc-2), 34.2 (O-CO$\underline{C}H_2$-CH_2- lipid), 34.1 (O-CO$\underline{C}H_2$-CH_2- lipid), 31.8, 29.6, 29.5, 29.2 (-CH_2- lipid), 24.9 (O-$COCH_2$-$\underline{C}H_2$- lipid), 24.8 (O-$COCH_2$-$\underline{C}H_2$- lipid), 22.6 (-CH_2- lipid), 13.8 (-CH_3 lipid).

^{31}P NMR (162 MHz, CD_3OD) δ (ppm) -0.42.

HRMS: $[M-H]^-$ cald 1068.6600; found 1068.6608.

2-Amino-2-deoxy-α-D-glucopyranosyl-(1→6)-1-*O*-(1,2-distearoyl-*sn*-glycero-3-phospho-nate)-D-*myo*-inositol (2-50)

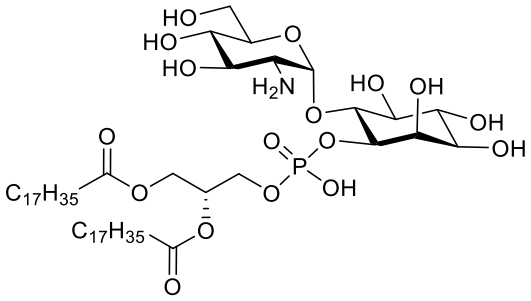

DDQ (67.6 mg, 0.298 mmol) was added to a solution of the protected glycolipid **2-60** (60.6 mg, 0.0284 mmol) in a 3:1 DCM/MeOH mixture (1.35 mL). The reaction mixture was stirred at room temperature for 5.5 h before volatiles were removed under reduced pressure. The residue was purified by LH-20 size exclusion chromatography eluting with MeOH/$CHCl_3$ 9:1. The obtained deprotected glycolipid (24.3 mg, 0.023 mmol) was dissolved in anhydrous THF (0.4 mL), and 0.46 mL of a 1 M solution of $P(CH_3)_3$ in THF were added followed by water (83.5 µL). After 3 h, the reaction was concentrated under vacuum, and purification was performed by LH-20 size exclusion chromatography eluting with MeOH/$CHCl_3$/H_2O 3:3:1 followed by trituration with MeOH to give the final GPI-fragment **2-50** in 40% yield (11.6 mg, 0.0113 mmol) as a white solid. For the NMR sample, the compound was dissolved in a 3:3:1 CD_3OD/$CDCl_3$/D_2O mixture.

^{1}H NMR (400 MHz, CD_3OD) δ (ppm) 5.24 (d, *J* = 3.9 Hz, 1H, Glc-1), 4.93 – 5.04 (m, 1H, C$\underline{H}$ sn-2), 4.06 – 4.17 (m, 1H, C$\underline{H}_{2a}$ sn-1), 3.84 – 3.95 (m, 2H, C$\underline{H}_{2b}$ sn-1, Ino), 3.70 – 3.82 (m, 3H, C$\underline{H}_2$ sn-3, Glc-5, Ino), 3.66 (t, *J* = 9.5 Hz, 1H, Ino), 3.50 – 3.60 (m, 2H, Glc-3, Glc-6a), 3.34 – 3.48 (m, 2H, Glc-6b, Ino), 3.11 – 3.20 (m, 2H, Glc-4, Ino), 3.05 – 3.08 (m, 1H, Ino), 2.91 (dd, *J* = 10.5, 3.9 Hz, 1H, Glc-2), 2.00 – 2.10 (m, 4H, 2 x O-COC$\underline{H}_2$-CH_2- lipid), 1.27 – 1.37 (m, 4H, 2 x O-$COCH_2$-C$\underline{H}_2$- lipid), 0.92 – 1.08 (m, 69H, C$\underline{H}_2$ lipid), 0.60 (t, *J* = 6.7 Hz, 8H, 2 x C$\underline{H}_3$ lipid).

^{13}C NMR (101 MHz, CD_3OD) δ (ppm) 174.0 (C$\underline{}$=O), 173.8 (C$\underline{}$=O), 95.1 (Glc-1), 77.0 (Ino), 76.2 (Ino),72.7 (Ino), 72.2 (Ino), 71.5 (Glc-5, Ino), 70.6 (Ino), 70.1 (C$\underline{H}$ sn-2), 69.9 (Glc-3), 69.4 (Glc-4), 63.4 (C$\underline{H}_2$ sn-3), 62.5 (C$\underline{H}_2$ sn-1), 60.3 (Glc-6), 60.1, 53.8 (Glc-2), 33.9 (O-CO$\underline{C}H_2$-CH_2- lipid),

33.8 (O-CO<u>C</u>H$_2$-CH$_2$- lipid), 31.6, 29.4, 29.32, 29.27, 29.2, 29.1, 29.0, 28.82, 28.77 (-CH$_2$- lipid), 24.6 (O-COCH$_2$-<u>C</u>H$_2$- lipid), 24.5 (O-COCH$_2$-<u>C</u>H$_2$- lipid), 22.3 (-<u>C</u>H$_2$- lipid), 13.5 (-<u>C</u>H$_3$ lipid).

^{31}P NMR (162 MHz, CD$_3$OD) δ (ppm) -0.75.

HRMS: [M-H]$^-$ cald 1026.6494; found 1026.6499.

5.2.6 Synthesis of GPI fragments 2-51 and 2-52

2-Azido-2-deoxy-3,4,6-tri-*O*-(2-naphthyl)methyl-α-D-glucopyranosyl-(1→6)-2,3,4,5-tetra-*O*-(2-naphthyl)methyl-1-*O*-(1-octadecanoyl-2-oleoyl-*sn*-glycero-3-phosphonate)-D-*myo*-inositol (2-62)

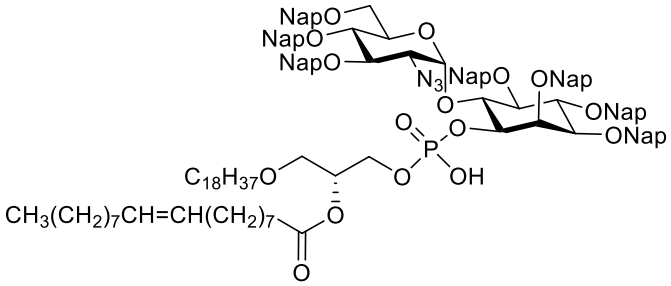

Alcohol **2-33** (62 mg, 0.0460 mmol) and H-phosphonate **2-59** (88% purity, 64.7 mg, 0.0736 mmol) were co-evaporated with anhydrous pyridine (3 x 1 mL) and placed under high vacuum for 45 min. The solid mixture was dissolved in anhydrous pyridine (3.5 mL) and PivCl (14.6 µL, 0.119 mmol) was added. The reaction was stirred for 1 h at room temperature before water (106 µL) and iodine (35 mg, 0.138 mmol) were added. The reaction mixture was stirred for additional 60 min, and solid $Na_2S_2O_3$ was added until the color of the reaction changed from dark orange to light yellow. Volatiles were removed under reduced pressure. The remaining was triturated with DCM to leave behind solid $Na_2S_2O_3$, and concentrated. Purification was performed by flash silica gel column chromatography (eluting with MeOH/DCM 1:90 and gradually increasing the polarity to 1:20) to afford the lipidated pseudodisaccharide **2-62** in 82% yield (77.2 mg, 0.0378 mmol) as a white foam; R_f = 0.25 (MeOH/DCM, 1:20).

^{1}H NMR (400 MHz, CDCl$_3$) δ (ppm) 7.03 – 7.88 (m, 122H, Ar), 5.67 – 5.87 (m, 1H, Glc-1), 4.41 – 5.39 (m, 41H), 4.04 – 4.37 (m, 14H), 3.08 – 3.89 (m, 21H), 2.11 – 2.37 (m, 2H), 1.73 – 2.07 (m, 6H), 1.03 – 1.33 (m, 118H), 0.83 – 0.93 (m, 14H).

^{13}C NMR (101 MHz, CDCl$_3$) δ (ppm) complemented with HSQC 135.7, 133.4, 132.98, 132.96, 132.93, 132.89, 132.87, 132.86, 132.85, 132.82, 132.80, 132.79, 132.78, 132.76, 132.73, 132.70, 132.67, 132.66, 130.4, 130.3, 130.25, 130.20, 130.16, 130.12, 130.07, 130.05, 129.97, 129.94, 129.90, 128.0, 127.74, 127.71, 126.5, 126.3, 125.95, 125.9, 125.2, 125.0, 124.65, 124.57, 97.6 (Glc-1), 34.45, 32.08, 32.05, 29.92, 29.89, 29.82, 29.69, 29.52, 29.47, 27.4, 26.1, 22.8, 22.8, 14.3.

^{31}P NMR (162 MHz, CDCl3) δ (ppm) -1.78.

HRMS: [M-H]$^-$cald 2017.0832; found 2017.0901.

2-Acetamido-2-deoxy-α-D-glucopyranosyl-(1→6)-1-*O*-(1-octadecanoyl-2-oleoyl-*sn*-glycero-3-phosphonate)-D-*myo*-inositol (2-51)

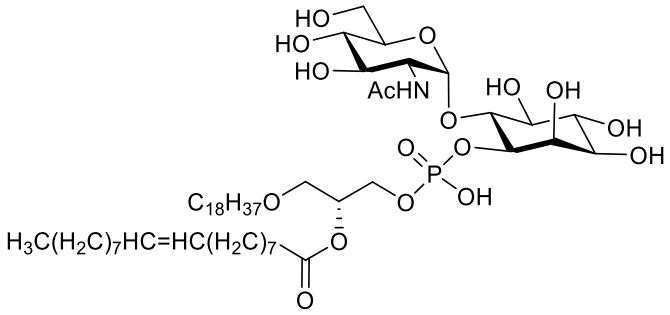

A solution of the glycolipid **2-62** (31.7 mg, 0.0155 mmol) in anhydrous THF (0.27 mL) was mixed with 0.31 mL of a 1 M solution of $P(CH_3)_3$ in THF. Water (120 µL) was added, and the reaction was stirred at room temperature for 1 h. Volatiles were removed under reduced pressure and the residue was dissolved in a 2:1 pyridine/acetic anhydride mixture (1.5 mL). The reaction was stirred for 35 min before it was concentrated *in vacuo*. Purification was performed by flash silica gel column chromatography (eluting with MeOH/DCM 1:90 and gradually increasing the polarity to 1:10). The obtained *N*-acetylated compound **2-63** was dissolved in a 3:1 DCM/MeOH mixture (0.88 mL), and DDQ (42.2 mg, 0.186 mmol) was added. The reaction mixture was stirred at room temperature for 5 h, and volatiles were removed under vacuum. The residue was purified by LH-20 size exclusion chromatography eluting with MeOH/$CHCl_3$/H_2O 3:3:1 followed by trituration with MeOH to afford the final GPI-fragment **2-51** in 71% yield (11.6 mg, 0.0110 mmol) as a white solid. For the NMR sample, the compound was dissolved in a 3:3:1 CD_3OD/$CDCl_3$/D_2O mixture.

^{1}H NMR (400 MHz, CD_3OD) δ (ppm) 4.99 – 5.10 (m, 2H, -C<u>H</u>=C<u>H</u>- Oleoyl), 4.88 (s, 1H, C<u>H</u> sn-2), 4.68 (s, 1H, Glc-1), 3.78 – 3.93 (m, 2H, Ino), 3.61 – 4.77 (m, 4H, Glc-2, Glc-5, C<u>H$_2$</u> sn-3), 3.57 (d, *J* = 12.0 Hz, 1H, Glc-6a), 3.26 – 3.53 (m, 7H, Glc-6b, C<u>H$_2$</u> sn-1), 3.05 – 3.26 (m, 6H, O-C<u>H$_2$</u>-CH$_2$ Octadecanoyl), 2.00 – 2.11 (m, 2H, O-COC<u>H$_2$</u>-CH$_2$ Oleoyl), 1.79 (s, 3H, C<u>H$_3$</u> Ac), 1.68 – 1.77 (m, 4H, -C<u>H$_2$</u>-CH=CH-C<u>H$_2$</u>- Oleoyl), 1.27 – 1.38 (m, 2H, O-COCH$_2$-C<u>H$_2$</u> Oleoyl), 1.21 – 1.27 (m, 2H, O-COCH$_2$-C<u>H$_2$</u> Oleoyl), 0.93 – 1.07 (m, 68H, C<u>H$_2$</u> lipid), 0.59 (t, *J* = 6.6 Hz, 8H, 2 x C<u>H$_3$</u> lipid).

HSQC (400 MHz, CD_3OD) δ (ppm) 174.1 (<u>C</u>=O), 129.6 (-<u>C</u>H=CH- Oleoyl), 129.3 (-CH=<u>C</u>H-Oleoyl), 99.1 (Glc-1), 81.7, 74.8, 73.7, 72.9 (Glc-5), 71.9, 71.6 (<u>C</u>H sn-2), 71.4 (O-<u>C</u>H$_2$-CH$_2$ Octadecanoyl), 71.2, 70.6, 70.2, 68.9 (<u>C</u>H$_2$ sn-1), 63.5 (<u>C</u>H$_2$ sn-3), 60.8 (Glc-6), 53.6 (Glc-2), 34.0 (O-CO<u>C</u>H$_2$-CH$_2$ Oleoyl), 31.54, 31.52, 29.41, 29.36, 29.3, 29.25, 29.19, 29.16, 29.1, 29.0, 28.93, 28.91, 28.86, 28.8, 28.7 (<u>C</u>H$_2$ lipid), 26.83 (-<u>C</u>H$_2$-CH=CH-CH$_2$- Oleoyl), 26.81 (-CH$_2$-CH=CH-<u>C</u>H$_2$-Oleoyl), 25.6 (<u>C</u>H$_2$ lipid), 24.6 (O-COCH$_2$-<u>C</u>H$_2$ Oleoyl), 22.7 (<u>C</u>H$_2$ lipid), 13.5 (2 x <u>C</u>H$_3$ lipid).

^{31}P NMR (162 MHz, CD_3OD) δ (ppm) -0.56.

HRMS: $[M-H]^-$ cald 1052.6650; found 1052.7013.

2-Amino-2-deoxy-α-D-glucopyranosyl-(1→6)-1-*O*-(1-octadecanoyl-2-oleoyl-s*n*-glycero-3-phosphonate)-D-*myo*-inositol (2-52)

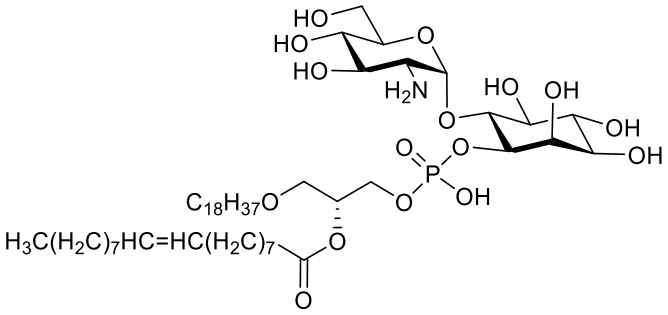

DDQ (43.8 mg, 0.193 mmol) was added to a solution of the protected glycolipid **2-62** (37.1 mg, 0.0184 mmol) in a 3:1 DCM/MeOH mixture (1 mL). The reaction mixture was stirred at room temperature for 5 h before volatiles were removed under reduced pressure. The residue was purified by LH-20 size exclusion chromatography eluting with MeOH/$CHCl_3$/H_2O 3:3:1. The obtained deprotected glycolipid was dissolved in anhydrous THF (0.32 mL), and 0.37 mL of a 1 M solution of $P(CH_3)_3$ in THF were added followed by water (146 µL). After 30 min, the reaction was concentrated under vacuum, and purification was performed by LH-20 size exclusion chromatography eluting with MeOH/$CHCl_3$/H_2O 3:3:1 followed by trituration with MeOH to give the final GPI-fragment **2-52** in 69% yield (12.8 mg, 0.0126 mmol) as a white solid. For the NMR sample, the compound was dissolved in a 3:3:1 CD_3OD/$CDCl_3$/D_2O mixture.

^{1}H NMR (400 MHz, CD_3OD) δ (ppm) 5.23 (d, *J* = 3.9 Hz, 1H, Glc-1), 4.99 – 5.10 (m, 2H, -C<u>H</u>=C<u>H</u>- Oleoyl), 4.83 – 4.92 (m, 1H, C<u>H</u> sn-2), 3.81 – 3.91 (m, 1H, Ino), 3.74 – 3.83 (m, 1H, Glc-5), 3.60 – 3.74 (m, 3H, C<u>H$_2$</u> sn-3, Ino), 3.49 – 3.59 (m, 2H, Glc-3, Glc-6a), 3.42 (dd, *J* = 12.4, 4.8 Hz, 1H, Glc-6b), 3.28 – 3.41 (m, 3H, C<u>H$_2$</u> sn-1, Ino), 3.10 – 3.23 (m, 3H, Glc-4, Ino, O-C<u>H$_2$</u>-CH$_2$ Octadecanoyl), 3.01 – 3.04 (m, 1H, Ino), 2.89 (dd, *J* = 10.6, 3.9 Hz, 1H, Glc-2), 2.02 – 2.11 (m, 2H, O-COC<u>H$_2$</u>-CH$_2$ Oleoyl), 1.67 – 1.77 (m, 4H, -C<u>H$_2$</u>-CH=CH-C<u>H$_2$</u>- Oleoyl), 1.29 – 1.36 (m, 2H, O-COCH$_2$-C<u>H$_2$</u> Oleoyl), 1.20 – 1.28 (m, 2H, O-CH$_2$-C<u>H$_2$</u> Octadecanoyl), 0.90 – 1.08 (m, 66H, C<u>H$_2$</u> lipid), 0.55 – 0.61 (m, 7H, 2 x C<u>H$_3$</u> lipid).

^{13}C NMR (101 MHz, CD_3OD) δ (ppm) 174.0 (<u>C</u>=O), 129.6 (-<u>C</u>H=CH- Oleoyl), 129.3 (-CH=<u>C</u>H- Oleoyl), 95.0 (Glc-1), 72.7, 72.2, 72.0, 71.5 (Glc-5, O-<u>C</u>H$_2$-CH$_2$ Octadecanoyl), 71.4 (<u>C</u>H sn-2), 70.6 (Glc-4), 69.8 (Glc-3), 69.4, 68.8 (<u>C</u>H$_2$ sn-1), 63.7 (<u>C</u>H$_2$ sn-3), 60.3 (Glc-6), 53.8 (Glc-2), 34.0 (O-CO<u>C</u>H$_2$-CH$_2$ Oleoyl), 31.52, 31.50, 29.4, 29.34, 29.31, 29.28, 29.23, 29.15, 29.1, 28.94, 28.91, 28.88, 28.82, 28.71 (<u>C</u>H$_2$ lipid), 26.80 (-<u>C</u>H$_2$-CH=CH-CH$_2$- Oleoyl), 26.78 (-CH$_2$-CH=CH-<u>C</u>H$_2$- Oleoyl), 25.62 (<u>C</u>H$_2$ lipid), 24.61 (O-COCH$_2$-<u>C</u>H$_2$ Oleoyl), 22.25 (<u>C</u>H$_2$ lipid), 13.49 (2 x <u>C</u>H$_3$ lipid).

^{31}P NMR (162 MHz, CD_3OD) δ (ppm) -0.07.

HRMS: $[M-H]^-$ cald 1010.6545; found 1010.6527.

5.2.7 Synthesis of GPI fragment 2-53

2-Azido-2-deoxy-6-*O*-*tert*-butyldimethylsilyl-α-D-glucopyranosyl-(1→6)-1-*O*-allyl-2,3,4,5-tetra-*O*-(2-naphthyl)methyl-D-*myo*-inositol (2-64)

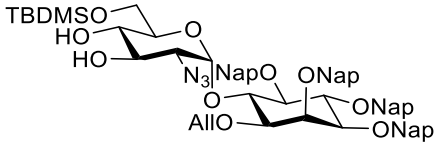

tert-Butyldimethylsilyl chloride (0.276 mL, 1 M solution in THF) was added to a solution of the isolated α-anomer **2-32** (71.4 mg, 0.0737 mmol) and imidazole (15.1 mg, 0.221 mmol) in anhydrous THF (0.28 mL). The reaction mixture was stirred at room temperature for 6 h before it was diluted with ethyl acetate, washed with water and brine, dried with Na_2SO_4, filtered, and concentrated. The resulting residue was purified by flash silica gel column chromatography to afford **2-64** in 94% (75.2 mg, 0.0695 mmol) yield as a white solid; R_f = 0.38 (heptane/EtOAc, 4:6).

IR (ATR) ν(cm^{-1}) 3352 (O-H), 2927, 2857, 2108 (N=N=N), 1510, 1459, 1332, 1343, 1254, 1217, 1168, 1124, 1086, 1032, 963, 853, 834, 816, 755.

^{1}H NMR (400 MHz, $CDCl_3$) δ (ppm) 7.70 – 7.88 (m, 15H, Ar), 7.57 – 7.69 (m, 5H), 7.31 – 7.55 (m, 15H, Ar), 5.88 – 6.02 (m, 1H, -C<u>H</u>= Allyl), 5.75 (d, J = 3.6 Hz, 1H, Glc-1), 5.18 – 5.29 (m, 1H, =C<u>H</u>$_{2a}$ Allyl), 5.22 & 4.92 (ABq, *J* = 11.7 Hz, 2H, C<u>H</u>$_2$ Nap), 5.12 – 5.20 (m, 1H, =C<u>H</u>$_{2b}$ Allyl), 5.18 & 4.02 (ABq, *J* = 10.2 Hz, 2H, C<u>H</u>$_2$ Nap), 5.07 (d, J = 3.6 Hz, 2H, C<u>H</u>$_2$ Nap), 4.76 – 4.88 (m, 2H, C<u>H</u>$_2$ Nap), 4.27 – 4.39 (m, 2H, Ino-6, Ino-4), 4.12 – 4.16 (m, 1H, Ino-2), 3.99 – 4.06 (m, 3H, -C<u>H</u>$_2$- Allyl, Glc-3), 3.92 – 3.99 (m, 1H, Glc-5), 3.47 – 3.58 (m, 3H, Ino-5, Ino-3, Glc-4), 3.37 – 3.45 (m, 2H, Ino-1, Glc-6a), 3.24 (dd, J = 10.8, 3.8 Hz, 1H, Glc-6b), 3.10 (dd, J = 10.5, 3.7 Hz, 1H, Glc-2), 0.70 (s, 9H, C<u>H</u>$_3$ tBu), -0.16 (s, 3H, C<u>H</u>$_3$), -0.25 (s, 3H, C<u>H</u>$_3$).

^{13}C NMR (101 MHz, CDCl3) δ (ppm) 136.4, 136.22, 136.16, 135.8 (C_q Ar), 134.4 (-<u>C</u>H= Allyl), 133.45, 133.38, 133.34, 133.2, 133.1, 133.0, 132.9 (C_q Ar), 128.3, 128.2, 128.13, 128.08, 128.05, 128.04, 127.84, 127.79, 127.70, 126.74, 126.70, 126.5, 126.4, 126.3, 126.20, 126.17, 126.14, 126.10, 126.07, 126.04, 126.02, 125.98, 125.95, 125.9, 125.8, 125.5 (C Ar), 117.4 (=<u>C</u>H$_2$ Allyl), 97.6 (Glc-1), 82.1 (Ino-1, Ino-4), 81.9 (Ino-5), 81.0 (Ino-3), 76.0 (<u>C</u>H$_2$ Nap), 75.7 (<u>C</u>H$_2$ Nap), 75.1 (<u>C</u>H$_2$ Nap), 74.3(<u>C</u>H$_2$ Nap), 73.1 (Ino-2), 72.6 (Glc-4), 71.6 (Glc-3), 71.2 (-<u>C</u>H$_2$- Allyl), 69.9 (Glc-5), 63.3 (Glc-6), 62.9 (Glc-2), 25.9 (<u>C</u>H$_3$ tBu), -5.67 (<u>C</u>H$_3$ x 2).

HRMS: $[M+Na]^+$ cald 1104.4806; found 1104.4801; $[M+H]^+$ cald 1082.4987; found 1082.514.

2-Azido-2-deoxy-3,4-di-*O*-(2-naphthyl)methyl-6-*O*-*tert*-butyldimethylsilyl-α-D-glucopyranosyl-(1→6)-1-*O*-allyl-2,3,4,5-tetra-*O*-(2-naphthyl)methyl-D-*myo*-inositol (2-65)

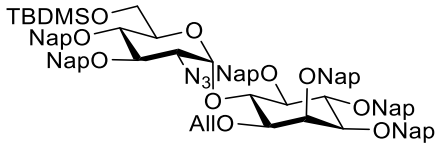

NaH (9.85 mg, 0.246 mmol, 60% in mineral oil) was added to a solution of **2-64** (66.6 mg, 0.0616 mmol) and TBAI (68.2 mg, 0.185 mmol) in DMF (0.5 mL) at 0 °C. After 20 min, 2-(Bromomethyl)naphthalene (40.8 mg, 0.185 mmol) was added, and the reaction mixture was stirred at 50 °C overnight. The reaction was cooled to room temperature, quenched with MeOH, and volatiles were removed under reduced pressure. The remaining was mixed with ethyl acetate/H_2O, and it was extracted with ethyl acetate. Organic layers were combined, washed with brine, dried with Na_2SO_4, filtered, and evaporated. Crude was purified by flash silica gel column chromatography to give **2-65** in 70% (58.6 mg, 0.0430 mmol) yield as a white solid; R_f = 0.57 (heptane/EtOAc, 7:3).

^{1}H NMR (400 MHz, $CDCl_3$) δ (ppm) 7.75 – 7.93 (m, 26H, Ar), 7.65 – 7.74 (m, 10H, Ar), 7.38 – 7.59 (m, 30H, Ar), 5.97 – 6.11 (m, 1H, -C<u>H</u>= Allyl), 5.78 (d, J = 3.7 Hz, 1H, Glc-1), 5.19 – 5.37 (m, 5H, =C<u>H</u>$_2$ Allyl, C<u>H</u>$_2$ Nap), 5.06 – 5.18 (m, 5H, C<u>H</u>$_2$ Nap), 4.95 – 5.09 (m, 2H), C<u>H</u>$_2$ Nap, 4.83 – 4.96 (m, 4H, C<u>H</u>$_2$ Nap), 4.72 (d, J = 11.3 Hz, 1H, C<u>H</u>$_2$ Nap), 4.47 – 4.34 (m, 2H, Ino-6, Ino-4), 4.21 (s, 1H, Ino-2), 4.07 – 4.21 (m, 4H, -C<u>H</u>$_2$- Allyl, Glc-3, Glc-5), 3.81 (t, J = 9.4 Hz, 1H, Glc-4), 3.54 – 3.66 (m, 2H, Ino-5, Ino-3), 3.42 – 3.53 (m, 2H, Ino-1, Glc-6a), 3.36 (dd, J = 10.3, 3.8 Hz, 1H, Glc-2), 3.23 (dd, J = 11.8, 2.6 Hz, 1H, Glc-6b), 0.83 (s, 9H, C<u>H</u>$_3$ tBu), -0.05 (s, 3H, C<u>H</u>$_3$), -0.15 (s, 3H, C<u>H</u>$_3$).

^{13}C NMR (101 MHz, CDCl3) δ (ppm) 136.45, 136.39, 136.25, 136.15, 135.9, 135.8, 135.7 (C_q Ar), 134.6 (-<u>C</u>H= Allyl), 133.5, 133.44, 133.42, 133.38, 133.37, 133.2, 133.1, 133.04, 133.01, 133.00, 132.8 (C_q Ar), 128.4, 128.33, 128.29, 128.25, 128.20, 128.18, 128.12, 128.09, 128.07, 128.05, 128.02, 127.98, 127.9, 127.84, 127.83, 127.80, 127.75, 127.69, 127.67, 127.0, 126.9, 126.8, 126.73, 126.70, 126.6, 126.54, 126.51, 126.47, 126.44, 126.40, 126.35, 126.3, 126.24, 126.22, 126.18, 126.13, 126.10, 126.07, 126.03, 126.00, 125.98, 125.96, 125.94, 125.90, 125.88, 125.81, 125.76, 125.7, 125.6 (C Ar), 117.3 (=<u>C</u>H$_2$ Allyl), 98.0 (Glc-1), 82.2 (Ino-1, Ino-4), 81.8 (Ino-5), 81.0 (Ino-3), 80.4 (Glc-3), 78.2 (Glc-4), 76.0 (Ino-6), 75.6 (<u>C</u>H$_2$ Nap), 75.51 (<u>C</u>H$_2$ Nap), 75.49 (<u>C</u>H$_2$ Nap), 74.8 (<u>C</u>H$_2$ Nap), 74.3 (<u>C</u>H$_2$ Nap), 73.2 (Ino-2), 73.1 (<u>C</u>H$_2$ Nap), 71.4 (Glc-5), 71.3 (-<u>C</u>H$_2$- Allyl), 63.9 (Glc-2), 61.5 (Glc-6), 26.0 (<u>C</u>H$_3$ tBu), -5.1(<u>C</u>H$_3$), -5.5 (<u>C</u>H$_3$).

HRMS: $[M+Na]^+$ cald 1384.6058; found 1384.6079; $[M+NH_4]^+$ cald 1379.6504; found 1379.6514.

2-Acetamido-2-deoxy-3,4-di-*O*-(2-naphthyl)methyl-6-*O*-*tert*-butyldimethylsilyl-α-D-gluco-pyranosyl-(1→6)-1-*O*-allyl-2,3,4,5-tetra-*O*-(2-naphthyl)methyl-D-*myo*-inositol (2-66)

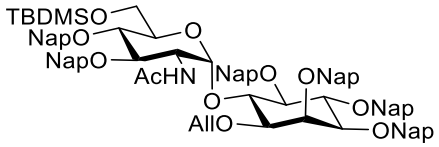

The pseudodisaccharide **2-65** (69.9 mg, 0.0513 mmol) was mixed with 1 mL of a 1M solution of $P(CH_3)_3$ in THF. Water (400 µL) was added, and the reaction was stirred at room temperature for 1.5 h. Volatiles were removed under reduced pressure, and the residue was dissolved in a 5:1 pyridine/acetic anhydride mixture (1.2 mL). The reaction was stirred for additional 1.5 h before it was concentrated in vacuo. Purification was performed by flash silica gel column chromatography to obtain the desired compound **2-66** in 55 % yield (38.8 mg, 0.0281 mmol); R_f = 0.10 (heptane/EtOAc, 7:3).

^{1}H NMR (400 MHz, $CDCl_3$) δ (ppm) 7.66 – 7.87 (m, 25H, Ar), 7.60 – 7.64 (m, 2H, Ar), 7.36 – 7.55 (m, 21H, Ar), 6.83 (d, J = 9.9 Hz, 1H, N-H), 5.59 – 5.74 (m, 1H, -CH= Allyl), 5.40 (d, J = 3.4 Hz, 1H, Glc-1), 5.16 (dd, J = 10.7, 4.8 Hz, 2H, CH_2 Nap), 5.09 – 5.11 (m, 1H, =CH_{2a} Allyl), 4.95 – 5.08 (m, 7H, =CH_{2b} Allyl, CH_2 Nap), 4.82 – 4.93 (m, 4H, CH_2 Nap), 4.41 (td, J = 10.1, 3.5 Hz, 1H, Glc-2), 4.19 – 4.27 (m, 2H, Ino-6, Ino-4), 4.11 (s, 1H, Ino-2), 4.01 – 4.08 (m, 1H, Glc-5), 3.91 (t, J = 9.4 Hz, 1H, Glc-4), 3.70 – 3.88 (m, 5H, -CH_2- Allyl, Glc-3, Glc-6), 3.45 – 3.53 (m, 2H, Ino-5, Ino-3), 3.25 (dd, J = 10.0, 2.3 Hz, 1H, Ino-1), 1.86 (s, 3H, CH_3 Ac), 0.80 (s, 9H, CH_3 tBu), -0.17 (s, 3H, CH_3), -0.19 (s, 3H, CH_3).

^{13}C NMR (101 MHz, CDCl3) δ (ppm) 170.1 (C=O Ac), 136.5, 136.3, 136.21, 136.18, 136.0, 135.7 (C_q Ar), 133.5 (-CH= Allyl), 133.44, 133.38, 133.35, 133.2, 133.12, 133.09, 133.06, 133.0 (C_q Ar), 128.4, 128.25, 128.21, 128.16, 128.14, 128.12, 128.09, 128.07, 128.03, 128.00, 127.9, 127.83, 127.78, 127.77, 127.69, 126.70, 126.6, 126.5, 126.44, 126.41, 126.35, 126.3, 126.23, 126.19, 126.14, 126.09, 126.06, 125.97, 125.91, 125.88, 125.8, 125.7 (C Ar), 119.0 (=CH_2 Allyl), 100.4 (Glc-1), 83.4 (Ino-5), 82.2 (Ino-4), 81.4 (Glc-3), 80.8 (Ino-3), 80.1 (Ino-1), 78.9 (Ino-6), 78.3 (Glc-4), 76.0 (CH_2 Nap), 75.7 (CH_2 Nap), 75.1 (CH_2 Nap), 75.0 (CH_2 Nap), 74.4 (CH_2 Nap), 73.29 (Glc-5), 73.26 (CH_2 Nap), 73.0 (Ino-2), 71.3 (-CH_2- Allyl), 62.2 (Glc-6), 53.8 (Glc-2), 26.0 (CH_3 tBu), 23.6 (CH_3 Ac), -5.3 (CH_3), -5.6 (CH_3).

HRMS: $[M+H]^+$ cald 1378.6440; found 1378.6449.

2-Acetamido-2-deoxy-3,4-di-*O*-(2-naphthyl)methyl-α-D-glucopyranosyl-(1→6)-1-*O*-allyl-2,3,4,5-tetra-*O*-(2-naphthyl)methyl-D-*myo*-inositol (2-67)

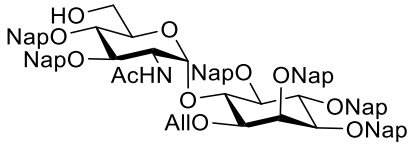

TBAF (0.25 mL, 1M in THF) was added to a solution of the silylated pseudodisaccharide **2-66** (32.8 mg, 0.0238 mmol) in THF (0.34 mL), and it was stirred at room temperature for 4 h. The reaction was quenched with water and extracted with ethyl acetate. Organic layers were washed with brine, dried over Na_2SO_4, filtered and concentrated. Purification was done by flash silica gel column chromatography to afford the alcohol **2-67** in 86% yield (25.9 mg, 0.0205 mmol) as a white solid; R_f = 0.37 (heptane/EtOAc, 4:6).

^{1}H NMR (400 MHz, $CDCl_3$) δ (ppm) 7.65 – 7.86 (m, 25H, Ar), 7.37 – 7.51 (m, 18H, Ar), 7.33 (dd, *J* = 8.4, 1.7 Hz, 1H, Ar), 6.75 (d, *J* = 9.9 Hz, 1H, N-H), 5.59 – 5.73 (m, 1H, -CH= Allyl), 5.35 (d, *J* = 3.5 Hz, 1H, Glc-1), 5.04 – 5.19 (m, 5H, =CH_{2a} Allyl, CH_2 Nap), 4.96 – 5.03 (m, 6H, =CH_{2b} Allyl, CH_2 Nap), 4.82 – 4.94 (m, 4H, CH_2 Nap), 4.78 (d, *J* = 11.1 Hz, 1H, CH_2 Nap), 4.37 (td, *J* = 9.9, 3.4 Hz, 1H, Glc-2), 4.15 – 4.28 (m, 2H, Ino-6, Ino-4), 4.11 (s, 1H, Ino-2), 4.04 (dt, *J* = 9.6, 3.2 Hz, 1H, Glc-5), 3.80 – 3.87 (m, 2H, -CH_{2a}- Allyl, Glc-3), 3.66 – 3.80 (m, 4H, -CH_{2b}- Allyl, Glc-4, Glc-6a), 3.58 (dd, *J* = 12.0, 3.7 Hz, 1H, Glc-6b), 3.41 – 3.51 (m, 2H, Ino-5, Ino-3), 3.25 (dd, *J* = 10.0, 2.3 Hz, 1H, Ino-1), 1.86 (s, 3H, CH_3 Ac).

^{13}C NMR (101 MHz, CDCl3) δ (ppm) 170.1 (C=O Ac), 136.3, 136.2, 136.0, 135.9, 135.7, 135.6 (C_q Ar), 133.43 (-CH= Allyl), 133.40, 133.35, 133.2, 133.14, 133.12, 133.10, 133.04, 132.95 (C_q Ar), 128.4, 128.3, 128.24, 128.19, 128.09, 128.07, 128.05, 128.01, 127.9, 127.84, 127.78, 127.75, 126.9, 126.8, 126.7, 126.6, 126.5, 126.4, 126.3, 126.25, 126.20, 126.14, 126.11, 126.07, 126.06, 126.03, 125.98, 125.95, 125.91, 125.88, 125.8, 125.3 (C Ar), 119.1 (=CH_2 Allyl), 100.3 (Glc-1), 83.3 (Ino-5), 82.0 (Ino-4), 80.8 (Glc-3, Ino-3), 80.0 (Ino-1), 79.0 (Ino-6), 78.4 (Glc-4), 76.0 (CH_2 Nap), 75.7 (CH_2 Nap), 75.3 (CH_2 Nap), 74.9 (CH_2 Nap), 74.5 (CH_2 Nap), 73.4 (CH_2 Nap), 73.0 (Ino-2), 72.5 (Glc-5), 71.3 (-CH_2- Allyl), 61.9 (Glc-6), 53.6 (Glc-2), 23.5 (CH_3 Ac).

HRMS: $[M+H]^+$ cald 1264.5575; found 1264.5585; $[M+Na]^+$ cald 1286.5394; found 1286.5404.

3-Azidopropan-1-ol

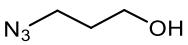

Sodium azide (1.55 g, 23.90 mmol) was added to a solution of 3 -Chloropropan-1-ol (1 mL, 11.95 mmol) in anhydrous DMF (16.3 mL) and it was stirred at 65 °C overnight. It was cooled to room temperature, filtered, and concentrated. The obtained residue was purified by flash silica gel column chromatography to afford 3-Azidopropan-1-ol in 79% yield (0.955 g, 9.44 mmol) as a colorless liquid.

^{1}H NMR (400 MHz, $CDCl_3$) δ (ppm) 3.74 (t, *J* = 6.0 Hz, 2H, HO-C<u>H</u>$_2$-), 3.44 (t, *J* = 6.6 Hz, 2H, -C<u>H</u>$_2$-N_3), 1.83 (p, *J* = 6.2 Hz, 2H, HO-CH_2-C<u>H</u>$_2$-CH_2-N_3), 1.74 (s, 1H, O-<u>H</u>).
^{13}C NMR (101 MHz, CDCl3) δ (ppm) 60.0 (HO-<u>C</u>H_2-), 48.61 (-<u>C</u>H_2-N_3), 31.55 (HO-CH_2-<u>C</u>H_2-CH_2-N_3).

2-Acetamido-2-deoxy-6-*O*-(3-Azidopropyl)-3,4-di-*O*-(2-naphthyl)methyl-α-D-glucopyranosyl-(1→6)-1-*O*-allyl-2,3,4,5-tetra-*O*-(2-naphthyl)methyl-D-*myo*-inositol (2-68)

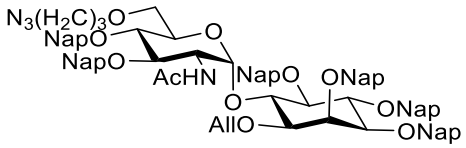

A mixture of 3-Azidopropan-1-ol (8.2 µL, 0.089 mmol), 2,6-dimethylpyridine (6.8 µL, 0.0588 mmol), and triflic anhydride (9.9 µL, 0.0588 mmol) in anhydrous DCM (0.14 mL) was stirred at -78 °C for 1 h. The reaction was quenched with H_2O and extracted with DCM (3x3 mL). The organic layers were dried over Na_2SO_4, filtered, and concentrated to give a pink oil. The alcohol **2-67** (23.7 mg, 0.0187 mmol) was dissolved in anhydrous THF (0.4 mL), and NaH (3 mg, 0.075 mmol, 60% in mineral oil) was added at 0 °C. A solution of the crude 2-azidopropyl trifluoromethanesulfonate in anhydrous THF (0.2 mL) was added to the reaction mixture, and it was stirred at room temperature for 2.5 h. The reaction was quenched with brine and extracted with ethyl acetate. Organic layers were washed with brine, dried over Na_2SO_4, filtered and concentrated. Crude was purified by flash silica gel column chromatography to afford **2-68** in 96% yield (24.2 mg, 0.0180 mmol) as a white solid; R_f = 0.38 (heptane/EtOAc, 6:4).
^{1}H NMR (400 MHz, $CDCl_3$) δ (ppm) δ 7.64 – 7.87 (m, 23H, Ar), 7.34 – 7.55 (m, 19H, Ar), 6.72 – 6.79 (m, 1H, N-<u>H</u>), 5.57 – 5.72 (m, 1H, -C<u>H</u>= Allyl), 5.36 (t, *J* = 3.6 Hz, 1H, Glc-1), 4.93 – 5.22 (m, 10H, =C<u>H</u>$_2$ Allyl, C<u>H</u>$_2$ Nap), 4.72 – 4.96 (m, 4H, C<u>H</u>$_2$ Nap), 4.36 – 4.48 (m, 1H, Glc-2), 4.22 (dt, *J* = 12.1, 9.6 Hz, 2H, Ino-6, Ino-4), 4.04 – 4.14 (m, 2H, Ino-2, Glc-5), 3.67 – 3.90 (m, 4H, -C<u>H</u>$_2$- Allyl, Glc-3, Glc-4), 3.18 – 3.62 (m, 10H, Ino-5, Ino-3, Ino-1, Glc-6, N_3-C<u>H</u>$_{2a}$-CH_2-C<u>H</u>$_{2a}$-), 2.99 – 3.12 (m, 2H, N_3-C<u>H</u>$_{2b}$-CH_2-C<u>H</u>$_{2b}$-), 1.85 (d, *J* = 3.3 Hz, 3H, C<u>H</u>$_3$ Ac), 1.45 – 1.59 (m, 2H, N_3-CH_2-C<u>H</u>$_2$-CH_2-).
^{13}C NMR (101 MHz, CDCl3) δ (ppm) 170.0 (C=O Ac), 136.4, 136.3, 136.25, 136.21, 136.19, 135.98, 135.97, 135.95, 135.7 (C_q Ar), 133.45 (-<u>C</u>H= Allyl), 133.39, 133.36, 133.35, 133.2, 133.12, 133.08, 133.04, 133.01, 132.98 (C_q Ar), 128.4, 128.22, 128.19, 128.17, 128.11, 128.06, 128.01, 127.99, 127.9, 127.84, 127.77, 127.71, 127.69, 126.8, 126.70, 126.68, 126.65, 126.62, 126.5, 126.45, 126.36, 126.30, 126.28, 126.23, 126.19, 126.17, 126.14, 126.08, 126.05, 126.02, 125.99, 125.94, 125.90, 125.88, 125.85, 125.80, 125.7 (C Ar), 119.0 (=<u>C</u>H_2 Allyl), 100.4 (Glc-1), 83.3 (Ino-5), 82.1 (Ino-4), 81.2 (Glc-3), 80.8 (Ino-3), 80.1 (Ino-1), 79.1 (Ino-6), 78.4 (Glc-4), 76.0 (<u>C</u>H_2 Nap), 75.7 (<u>C</u>H_2 Nap), 75.1 (<u>C</u>H_2 Nap), 74.9 (<u>C</u>H_2 Nap), 74.5 (<u>C</u>H_2 Nap), 73.3 (<u>C</u>H_2 Nap),

73.0 (Ino-2), 72.3 (Glc-5), 71.3 (-<u>C</u>H$_2$- Allyl), 70.8, 69.6 (Glc-6), 68.2 (N$_3$-CH$_2$-CH$_2$-<u>C</u>H$_2$-), 67.2, 53.6 (Glc-2), 48.6, 48.3 (N$_3$-<u>C</u>H$_2$-CH$_2$-CH$_2$-), 29.1 (N$_3$-CH$_2$-<u>C</u>H$_2$-CH$_2$), 23.5 (<u>C</u>H$_3$ Ac).
HRMS: [M+H]$^+$ cald 1347.6058; found 1347.6078; [M+Na]$^+$ cald 1369.5878; found 1369.5899.

2-Acetamido-2-deoxy-6-*O*-(3-Azidopropyl)-3,4-di-*O*-(2-naphthyl)methyl-α-D-glucopyranosyl-(1→6)-2,3,4,5-tetra-*O*-(2-naphthyl)methyl-D-*myo*-inositol (2-69)

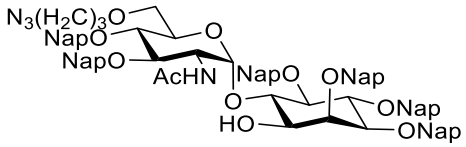

To a solution of the allylated pseudodisaccharide **2-68** (24.2 mg, 0.0180 mmol) in a 1:1 DCM/MeOH anhydrous mixture (0.8 mL), PdCl$_2$ (5.3 mg, 0.0299 mmol) was added at room temperature. After 7 h, the mixture was filtered through a pad of Celite, and the volatiles were evaporated *in vacuo*. The resulting brown oil was purified by flash silica gel column chromatography to obtain the alcohol **2-69** in 77% yield (18 mg, 0.0138 mmol) as a white solid; R_f = 0.24 (heptane/EtOAc, 6:4).
^{1}H NMR (400 MHz, CDCl$_3$) δ (ppm) 7.61 – 7.88 (m, 25H, Ar), 7.35 – 7.52 (m, 18H, Ar), 6.11 – 6.18 (m, 1H, N-<u>H</u>), 5.31 (dd, *J* = 7.4, 3.5 Hz, 1H, Glc-1), 5.25 (d, *J* = 11.7 Hz, 1H, C<u>H</u>$_2$ Nap), 5.17 (dd, *J* = 11.0, 2.2 Hz, 1H, C<u>H</u>$_2$ Nap), 5.09 (dd, *J* = 10.9, 8.0 Hz, 1H, C<u>H</u>$_2$ Nap), 4.83 – 5.04 (m, 8H, C<u>H</u>$_2$ Nap), 4.81 (d, *J* = 11.8 Hz, 1H, C<u>H</u>$_2$ Nap), 4.69 (dd, *J* = 11.3, 7.4 Hz, 1H, C<u>H</u>$_2$ Nap), 4.18 – 4.32 (m, 2H, Glc-2, Ino-4), 3.93 – 4.10 (m, 3H, Ino-6, Ino-2), 3.71 – 3.87 (m, 2H, Glc-3, Glc-4), 3.57 (dd, *J* = 9.7, 2.2 Hz, 1H, Ino-3), 3.40 – 3.51 (m, 2H, Ino-5, Ino-1), 2.96 – 3.38 (m, 9H), 2.43 – 2.53 (m, 1H, O-<u>H</u>), 1.69 (s, 3H, C<u>H</u>$_3$ Ac), 1.49 – 1.59 (m, 2H).
^{13}C NMR (101 MHz, CDCl3) δ (ppm) 170.3 (C=O Ac), 136.1, 136.0, 135.60, 135.56, 135.5, 133.41, 133.37, 133.34, 133.32, 133.24, 133.18, 133.1, 133.03, 132.97 (C$_q$ Ar), 128.78, 128.5, 128.2, 128.2, 128.10, 128.08, 128.06, 128.03, 128.01, 127.92, 127.88, 127.79, 127.77, 127.7, 127.3, 126.8, 126.73, 126.69, 126.66, 126.63, 126.61, 126.49, 126.47, 126.43, 126.39, 126.3, 126.25, 126.21, 126.15, 126.11, 126.08, 126.03, 125.96, 125.90, 125.88, 125.7 (C Ar), 99.0 (Glc-1), 81.5 (Ino-4), 81.4 (Ino-5), 81.0 (Ino-3), 80.5 (Glc-3), 80.4 (Ino-6), 78.1 (Glc-4), 77.4, 76.0 (<u>C</u>H$_2$ Nap), 75.2 (<u>C</u>H$_2$ Nap), 75.0 (<u>C</u>H$_2$ Nap), 74.8 (<u>C</u>H$_2$ Nap), 74.7 (<u>C</u>H$_2$ Nap), 73.6 (<u>C</u>H$_2$ Nap), 72.6 (Ino-1), 71.7 (Ino-2), 70.8, 68.0, 67.3, 53.2 (Glc-2), 48.6, 48.3, 29.8, 29.0, 26.4, 23.4 (<u>C</u>H$_3$ Ac).
HRMS: [M+H]$^+$cald 1307.5745; found 1307.5762; [M+Na]$^+$ cald 1329.5565; found 1329.5569.

2-Acetamido-2-deoxy-6-*O*-(3-Azidopropyl)-α-D-glucopyranosyl-(1→6)- 1-*O*-(2-oleoyl-1-stearoyl-sn-glycero-3-phosphonate)-D-*myo*-inositol (2-53)

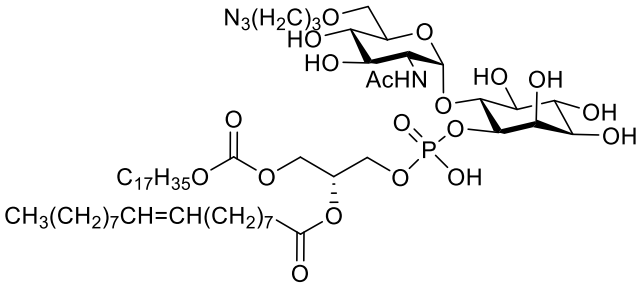

Alcohol **2-69** (15.9 mg, 0.0122 mmol) and H-phosphonate **2-8** (88% purity, 17.6 mg, 0.0195 mmol) were co-evaporated with anhydrous pyridine (3 x 1 mL) and placed under high vacuum for 1 h. The solid mixture was dissolved in anhydrous pyridine (0.9 mL) and PivCl (3.9 µL, 0.0316 mmol) was added. The reaction was stirred for 2 h at room temperature before water (54.4 µL) and iodine (9.26 mg, 0.0365 mmol) were added. The reaction mixture was stirred for additional 50 min, and solid $Na_2S_2O_3$ was added until the color of the reaction changed from dark orange to light yellow. Volatiles were removed under reduced pressure. The remaining was triturated with DCM to leave behind solid $Na_2S_2O_3$, and concentrated. Purification was performed by flash silica gel column chromatography (eluting with MeOH/DCM 1:90 and gradually increasing the polarity to 1:10). The obtained compound was dissolved in chloroform, and Amberlite IR 120 (Na^+) form resin was added. After stirring for 5 min, the solution was filtered and concentrated to afford the lipidated pseudodisaccharide **2-70** as a white solid; R_f = 0.46 (MeOH/DCM, 1:10). **HRMS:** $[M-H]^-$ cald 1990.0683; found 1990.0663.

The lipidated pseudodisaccharide **2-70** was dissolved in a 3:1 DCM/MeOH mixture (0.48 mL), and DDQ (19.8 mg, 0.0871 mmol) was added. The reaction mixture was stirred at room temperature for 5 h, and volatiles were removed under vacuum. The residue was purified by LH-20 size exclusion chromatography eluting with MeOH/$CHCl_3$ 9:1 followed by trituration with MeOH to afford the final GPI-fragment **2-53** in 73% yield (10.3 mg, 0.00894 mmol) as a slightly yellow residue. For the NMR sample, the compound was dissolved in a 3:3:1 $CD_3OD/CDCl_3/D_2O$ mixture.

^{1}H NMR (400 MHz, CD_3OD) δ (ppm) 5.31 – 5.36 (m, 2H, -C<u>H</u>=C<u>H</u>- Oleoyl), 5.21 – 5.29 (m, 1H, C<u>H</u> sn-2), 4.89 (d, *J* = 3.5 Hz, 1H, Glc-1), 4.40 – 4.47 (m, 1H, C<u>H_{2a}</u> sn-1), 4.09 – 4.22 (m, 3H, C<u>H_{2b}</u> sn-1), 3.96 – 4.07 (m, 4H, Glc-2, C<u>H_2</u> sn-3), 3.73 – 3.80 (m, 2H), 3.34 – 3.71 (m, 17H, N_3-C<u>H_2</u>-CH_2-C<u>H_2</u>-), 3.09 – 3.16 (m, 2H), 2.28 – 2.37 (m, 4H, 2 x O-COC<u>H_2</u>-CH_2- lipid), 2.08 (s, 3H, C<u>H_3</u> Ac), 1.97 – 2.04 (m, 5H, -C<u>H_2</u>-CH=CH-C<u>H_2</u>- Oleoyl), 1.80 – 1.90 (m, 3H, N_3-CH_2-C<u>H_2</u>-CH_2-), 1.55 – 1.67 (m, 7H, 2 x O-COCH_2-C<u>H_2</u>- lipid), 1.21 – 1.38 (m, 68H C<u>H_2</u> lipid), 0.84 – 0.90 (m, 8H, 2 x C<u>H_3</u> lipid).

^{13}C NMR (101 MHz, CD_3OD) δ (ppm) 175.1 (<u>C</u>=O), 174.8 (<u>C</u>=O), 130.7 (-<u>C</u>H=CH- Oleoyl), 130.4 (-CH=<u>C</u>H- Oleoyl), 100.6 (Glc-1), 75.2, 72.8, 71.9 (Glc-3), 71.5 (<u>C</u>H sn-2), 71.0, 69.0 (N_3-CH_2-CH_2-<u>CH_2</u>-), 64.2 (<u>CH_2</u> sn-3), 63.7 (<u>CH_2</u> sn-1), 54.7 (Glc-2), 48.9 (N_3-<u>CH_2</u>-CH_2-CH_2-), 47.3, 34.9

(O-CO$\underline{C}H_2$-CH_2- lipid), 34.8 (O-CO$\underline{C}H_2$-CH_2- lipid), 32.6, 30.4, 30.2, 30.0, 29.5 (N_3-CH_2-$\underline{C}H_2$-CH_2-), 27.9 (-$\underline{C}H_2$-CH=CH-$\underline{C}H_2$- Oleoyl), 26.7, 25.6 (O-COCH_2-$\underline{C}H_2$- lipid), 23.4, 23.0 ($\underline{C}H_3$ Ac), 14.6 ($\underline{C}H_3$ lipid).

^{31}P NMR (400 MHz, CD_3OD) δ (ppm) -0.50.

HRMS: $[M-H]^-$cald 1149.6927; found 1149.6936.

5.3 Methods for chapter 3

Allyl 6-*O*-*tert*-butyldiphenylsilyl-4-*O*-(2-naphthyl)methyl-α-D-mannopyranoside (3-8)

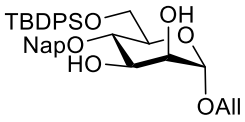

TBDPSCl (0.878 mL, 3.38 mmol) was added to a mixture of triol **3-7** (1.01 g, 2.81 mmol), imidazole (230 mg, 3.38 mmol) and DMAP (68.7 mg, 0.563 mmol) in anhydrous DCM (28 mL) at room temperature. After 1.5 h, the reaction was diluted with DCM, washed with water and brine, dried over Na_2SO_4, filtered, and concentrated under reduced pressure. The crude was purified by flash silica gel column chromatography to afford the diol **3-8** in 80% yield (1.35 g, 2.25 mmol) as a colorless oil; R_f = 0.45 (heptane/EtOAc, 1:1).

^{1}H NMR (400 MHz, $CDCl_3$) δ (ppm) 7.80 – 7.85 (m, 1H, Ar), 7.69 – 7.80 (m, 7H, Ar), 7.46 – 7.51 (m, 2H, Ar), 7.32 – 7.45 (m, 7H, Ar), 5.82 – 5.94 (m, 1H, -C$\underline{H}$= Allyl), 5.27 (dq, *J* = 17.2, 1.6 Hz, 1H, =C$\underline{H}_{2a}$ Allyl), 5.18 (dq, *J* = 10.4, 1.4 Hz, 1H, =C$\underline{H}_{2b}$ Allyl), 4.94 & 4.82 (ABq, *J* = 11.4 Hz, 1H, C$\underline{H}_2$ Nap), 4.90 (d, *J* = 1.6 Hz, 1H, Man-1), 4.18 (ddt, *J* = 12.7, 4.9, 1.4 Hz, 1H, C$\underline{H}_{2a}$- Allyl), 4.00 – 4.07 (m, 1H, Man-3), 3.94 – 4.00 (m, 4H, Man-2, Man-6, C$\underline{H}_{2b}$- Allyl), 3.82 (t, *J* = 9.3 Hz, 1H, Man-4), 3.74 (dt, *J* = 9.8, 3.1 Hz, 1H, Man-5), 2.42 (d, *J* = 6.0 Hz, 1H, O$\underline{H}$-3), 2.20 (d, *J* = 5.4 Hz, 1H, O$\underline{H}$-2), 1.10 (s, 9H, $\underline{C}H_3$ tBu).

^{13}C NMR (101 MHz, $CDCl_3$) δ (ppm) 136.0, 135.79, 135.77 (C_q Ar), 133.76 (-$\underline{C}$H= Allyl), 133.4, 133.2 (C_q Ar), 129.8, 128.5, 128.1, 127.8, 127.7, 126.8, 126.3, 126.1, 125.9 (C Ar), 117.7 (=$\underline{C}H_2$ Allyl), 98.5 (Man-1), 76.1 (Man-4), 75.0 ($\underline{C}H_2$ Nap), 72.3 (Man-5), 72.1 (Man-3), 71.3 (Man-2), 67.9 (-$\underline{C}H_2$- Allyl), 63.3 (Man-6), 27.0 ($\underline{C}H_3$ tBu).

Allyl 6-*O*-*tert*-butyldiphenylsilyl-3,4-di-*O*-(2-naphthyl)methyl-α-D-mannopyranoside (3-9)

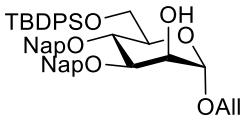

A mixture of diol **3-8** (951 mg, 1.59 mmol), 4 Å MS (2.37 g) and dibutyltin oxide (474 mg, 1.91 mmol) in toluene (18.5 mL) was refluxed at 115 °C for 3.5 h. It was allowed to cool down to 40 °C, filtered and concentrated at 50 °C by rotatory evaporation. The residue was dissolved in DMF (11 mL) and NapBr (421 mg, 1.91 mmol) was added followed by TBAI (587 mg, 1.56 mmol). The

reaction mixture was heated at 60 °C for 2.5 h. It was cooled to room temperature, diluted with EtOAc, and a 5% $Na_2S_2O_3$ aqueous solution was added until the orange color faded. Solvents were removed under reduced pressure, and the remaining was dissolved with ethyl acetate. The solution was washed with water, and the aqueous phase was extracted with ethyl acetate. Organic layers were combined, washed with brine, dried with Na_2SO_4, filtered, and evaporated. The crude compound was purified by silica gel column chromatography to give the alcohol **3-9** in 70% yield (819 mg, 1.11 mmol) as a colorless oil; R_f = 0.35 (hexane/EtOAc, 8:2).

$[\alpha]_D^{20}$**:** 10.24 (c = 1, $CHCl_3$).

IR (ATR) v(cm^{-1}) 3477 (O-H), 3055, 2932, 2859, 1604, 1510, 1473, 1429, 1363, 1272, 1112, 1056, 998, 892, 857, 814, 742, 703, 669.

^{1}H NMR (400 MHz, $CDCl_3$) δ (ppm) 7.78 – 7.86 (m, 4H, Ar), 7.67 – 7.77 (m, 7H, Ar), 7.62 (s, 1H, Ar), 7.45 – 7.52 (m, 5H, Ar), 7.28 – 7.43 (m, 7H, Ar), 5.83 – 5.96 (m, 1H, -C<u>H</u>= Allyl), 5.26 (dd, *J* = 17.2, 1.5 Hz, 1H, =C<u>H</u>$_{2a}$ Allyl), 5.19 (dd, *J* = 10.4, 1.1 Hz, 1H, =C<u>H</u>$_{2b}$ Allyl), 5.05 & 4.77 (ABq, *J* = 11.1 Hz, 2H, C<u>H</u>$_2$ Nap), 4.99 (d, *J* = 1.1 Hz, 1H, Man-1), 4.90 (dd, *J* = 25.9, 11.6 Hz, 2H, C<u>H</u>$_2$ Nap), 4.14 – 4.23 (m, 2H, C<u>H</u>$_{2a}$- Allyl, Man-2), 3.94 – 4.06 (m, 5H, C<u>H</u>$_{2b}$- Allyl, Man-6, Man-4, Man-3), 3.80 (dt, *J* = 9.6, 3.3 Hz, 1H, Man-5), 2.49 (s, 1H, O<u>H</u>), 1.07 (s, 9H, <u>C</u>H$_3$ tBu).

^{13}C NMR (101 MHz, $CDCl_3$) δ (ppm) 136.03, 135.99, 135.9, 135.7, 135.5 (C_q Ar), 133.82 (-<u>C</u>H= Allyl), 133.78, 133.4, 133.1, 133.0 (C_q Ar), 129.7, 128.5, 128.2, 128.1, 127.82, 127.78, 127.7, 126.8, 126.6, 126.3, 126.12, 126.11, 126.06, 125.97, 125.95, 125.9 (C Ar), 117.8 (=<u>C</u>H$_2$ Allyl), 98.2 (Man-1), 80.5 (Man-3), 75.4 (<u>C</u>H$_2$ Nap), 74.4 (Man-4), 72.6 (Man-5), 72.2 (<u>C</u>H$_2$ Nap), 68.7(Man-2), 67.8 (-<u>C</u>H$_2$- Allyl), 63.3 (Man-6), 26.9 (<u>C</u>H$_3$ tBu).

HRMS: $[M+Na]^+$ cald 761.3274; found 761.3331; $[M+K]^+$ cald 777.3014; found 777.3065.

Allyl 2-*O*-acetyl-6-*O*-*tert*-butyldiphenylsilyl-3,4-di-*O*-(2-naphthyl)methyl-α-D-mannopyranoside (3-5)

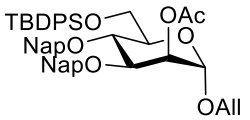

To a solution of alcohol **3-9** (1.37 g, 1.85 mmol) and DMAP (45 mg, 0.37 mmol) in anhydrous DCM (18 mL), pyridine (0.6 mL, 7.40 mmol) was added followed by acetic anhydride (350 µL, 3.70 mmol) at 0 °C. The reaction mixture was stirred at room temperature for 1.5 h before it was quenched with 1 M aq. HCl and extracted with DCM. Organic layers were combined, washed with brine, dried over Na_2SO_4, filtered, and concentrated. The residue was purified by silica gel column chromatography to afford the fully protected mannoside **3-5** in 82% yield (1.19 g, 1.52 mmol) as a colorless oil; R_f = 0.56 (heptane/EtOAc, 7:3).

^{1}H NMR (400 MHz, $CDCl_3$) δ (ppm) 7.70 – 7.87 (m, 11H, Ar), 7.67 (s, 1H, Ar), 7.30 – 7.53 (m, 12H, Ar), 5.82 – 5.97 (m, 1H, -C<u>H</u>= Allyl), 5.51 (app t, *J* = 2.3 Hz, 1H, Man-2), 5.27 (dd, *J* = 17.1, 1.6 Hz, 1H, =C<u>H</u>$_{2a}$ Allyl), 5.20 (dd, *J* = 10.4, 1.6 Hz, 1H, =C<u>H</u>$_{2b}$ Allyl), 5.14 & 4.82 (ABq, *J* = 11.0

Hz, 2H, C$\underline{H}_2$ Nap), 4.95 (d, *J* = 1.8 Hz, 1H, Man-1), 4.95 & 4.77 (ABq, *J* = 11.4 Hz, 2H, C$\underline{H}_2$ Nap), 4.17 – 4.21 (m, 2H, Man-3, -C$\underline{H}_{2a}$- Allyl), 4.14 – 4.16 (m, 1H, Man-4), 4.09 (dd, $J_{6a,6b}$ = 11.2 Hz, $J_{6a,5}$ = 4.0 Hz, 1H, Man-6a), 3.94 – 4.04 (m, 2H, Man-6b,-C$\underline{H}_{2b}$- Allyl), 3.77 – 3.83 (m, 1H, Man-5), 2.21 (s, 3H, C$\underline{H}_3$ Ac), 1.12 (s, 9H, C$\underline{H}_3$ tBu).

^{13}C NMR (101 MHz, CDCl$_3$) δ (ppm) 170.7 (C=O Ac), 136.10, 136.08, 135.7, 135.6, 134.0 (C$_q$ Ar), 133.6 (-C$\underline{H}$= Allyl), 133.40, 133.39, 133.3, 133.1, 133.0 (C$_q$ Ar), 129.7, 128.3, 128.2, 128.09, 128.07, 127.80, 127.78, 127.7, 127.0, 126.5, 126.3, 126.12, 126.10, 126.04, 125.99, 125.9 (C Ar), 117.9 (=C$\underline{H}_2$ Allyl), 96.7 (Man-1), 78.4 (Man-3), 75.5 (C$\underline{H}_2$ Nap), 74.4 (Man-4), 72.9 (Man-5), 72.0 (C$\underline{H}_2$ Nap), 69.2 (Man-2), 68.0 (-C$\underline{H}_2$- Allyl), 63.0 (Man-6), 26.9 (C$\underline{H}_3$ tBu), 21.2 (C$\underline{H}_3$ Ac).

ESI-MS: 803.2 [M+Na]$^+$.

Allyl 2-*O*-acetyl-3,4-di-*O*-(2-naphthyl)methyl-α-D-mannopyranoside (3-10)

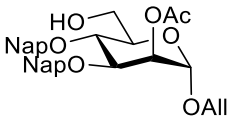

To a solution of mannoside **3-5** (79 mg, 0.101 mmol) in THF (1 mL), TBAF (0.25 mL, 0.253 mmol) was added, and it was stirred at room temperature for 1 h. Solvents were removed under reduced pressure, and the resulting brown oil was purified by silica gel column chromatography to afford the alcohol **3-10** in 91% yield (49.7 mg, 0.0916 mmol) as a colorless oil; R_f = 0.22 (heptane/EtOAc, 6:4).

^{1}H NMR (400 MHz, CDCl$_3$) δ (ppm) 7.79 – 7.86 (m, 5H, Ar), 7.70 – 7.79 (m, 4H, Ar), 7.41 – 7.51 (m, 6H, Ar), 5.83 – 5.95 (m, 1H, -C$\underline{H}$= Allyl), 5.49 – 5.52 (m, 1H, Man-2), 5.28 (dq, *J* = 17.2, 1.6 Hz, 1H, -C$\underline{H}_{2a}$- Allyl), 5.22 (dq, *J* = 10.3, 1.4 Hz, 1H, -C$\underline{H}_{2b}$- Allyl), 5.13 & 4.85 (ABq, *J* = 11.1 Hz, 1H, C$\underline{H}_2$ Nap), 4.92 & 4.73 (ABq, *J* = 11.4 Hz, 1H, C$\underline{H}_2$ Nap), 4.89 (d, *J* = 1.7 Hz, 1H, Man-1), 4.12 – 4.21 (m, 2H, -C$\underline{H}_{2a}$- Allyl, Man-3), 3.97 – 4.03 (m, 1H, -C$\underline{H}_{2b}$- Allyl), 3.84 – 3.95 (m, 3H, Man-4, Man-6), 3.77 – 3.82 (m, 1H, Man-5).

^{13}C NMR (101 MHz, CDCl$_3$) δ (ppm) 170.5, 135.8, 135.5, 133.4, 133.3 (C$_q$ Ar), 133.08 (-C$\underline{H}$= Allyl), 133.06 (C$_q$ Ar), 128.3, 128.05, 128.03, 127.78, 127.76, 126.9, 126.7, 126.2, 126.1, 126.00, 125.97 (C Ar), 118.0 (=C$\underline{H}_2$ Allyl), 97.1 (Man-1), 78.1 (Man-3), 75.4 (C$\underline{H}_2$ Nap), 74.3 (Man-4), 72.0 (C$\underline{H}_2$ Nap), 71.9 (Man-5), 68.8 (Man-2), 68.3 (-C$\underline{H}_2$- Allyl), 62.2 (Man-6), 21.2 (C$\underline{H}_3$ Ac).

2-*O*-Acetyl-6-*O*-*tert*-butyldiphenylsilyl-3,4-di-*O*-(2-naphthyl)methyl-α-D-mannopyranose (3-11)

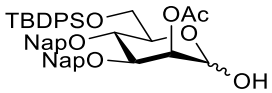

To a solution of the fully protected mannose **3-5** (286 mg, 0.366 mmol) in an anhydrous MeOH:DCM 1:1 mixture (2.4 mL), $PdCl_2$ (13 mg, 0.0732 mmol) was added at room temperature.

After 3.5 h, the mixture was filtered through a pad of Celite, and the volatiles were evaporated *in vacuo*. The resulting oil was purified by flash silica gel column chromatography to obtain alcohol **3-11** in 84% yield (228 mg, 0.308 mmol) as a white solid; R_f = 0.26 (hexane/EtOAc, 8:2).

^{1}H NMR (400 MHz, $CDCl_3$) δ (ppm) 7.64 – 7.86 (m, 12H, Ar), 7.28 – 7.52 (m, 12H, Ar), 5.47 (dd, $J_{2,3}$ = 3.0 Hz, $J_{2,1}$ = 1.9 Hz, 1H, Man-2), 5.27 (d, $J_{1,2}$ = 1.9 Hz, 1H, Man-1), 5.14 & 4.84 (ABq, J = 11.0 Hz, 2H, C$\underline{H}_2$ Nap), 4.92 & 4.75 (ABq, J = 11.6 Hz, 2H, C$\underline{H}_2$ Nap), 4.15 – 4.26 (m, 2H, Man-3, Man-4), 4.10 – 4.15 (dd, $J_{6a,6b}$ = 11.3 Hz, $J_{6b,5}$ = 3.3 Hz, 1H, Man-6a), 3.92 – 3.97 (m, 1H, Man-5), 3.90 (dd, $J_{6b,6a}$ = 11.3 Hz, $J_{6b,5}$ = 1.7 Hz, 1H, Man-6b), 2.68 (s, 1H, O$\underline{H}$-1), 2.19 (s, 3H, C$\underline{H}_3$ Ac), 1.10 (d, J = 2.3 Hz, 9H, C$\underline{H}_3$ tBu).

^{13}C NMR (101 MHz, $CDCl_3$) δ (ppm) 170.8 (C=O Ac), 136.2, 136.1, 135.68, 135.66, 135.6, 134.0, 133.4, 133.4, 133.3, 133.1, 133.1 (C_q Ar), 129.8, 128.3, 128.2, 128.11, 128.08, 127.82, 127.80, 127.79, 127.7, 127.0, 126.4, 126.3, 126.14, 126.12, 126.00, 125.92 (C Ar), 92.6 (Man-1), 77.7 (Man-3), 75.5 (C$\underline{H}_2$ Nap), 74.2 (Man-4), 72.8 (Man-5), 72.0 (C$\underline{H}_2$ Nap), 69.4 (Man-2), 63.0 (Man-6), 26.9 (C$\underline{H}_3$ tBu), 21.3 (C$\underline{H}_3$ Ac).

ESI-MS: 763.2 $[M+Na]^+$.

2-*O*-Acetyl-6-*O*-*tert*-butyldiphenylsilyl-3,4-di-*O*-(2-naphthyl)methyl-α-D-mannopyranosyl trichloroacetimidate (3-12)

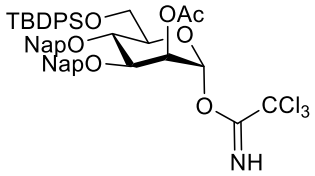

To a solution of the hemiacetal **3-11** (68.3 mg, 0.0922 mmol) in anhydrous DCM (0.75 mL) at 0 °C, trichloroacetonitrile (18.5 µL, 0.184 mmol) was added followed by DBU (2.7 µL, 0.0184 mmol). After 40 min, the solution was slightly concentrated under reduced pressure and immediately purified by flash silica gel column chromatography to give the imidate **3-12** in 87% yield (71.1 mg, 0.0803 mmol) as a white solid; R_f = 0.56 (hexane/EtOAc, 8:2).

^{1}H NMR (400 MHz, $CDCl_3$) δ (ppm) 8.64 (s, 1H, N$\underline{H}$), 7.61 – 7.87 (m, 12H, Ar), 7.26 – 7.56 (m, 12H, Ar), 6.35 (d, $J_{1,2}$ = 2.0 Hz, 1H, Man-1), 5.56 (dd, $J_{2,3}$ = 3.2 Hz, $J_{2,1}$ = 2.0 Hz, 1H, Man-2), 5.15 & 4.84 (ABq, J = 10.8 Hz, 2H, C$\underline{H}_2$ Nap), 4.95 & 4.79 (ABq, J = 11.5 Hz, 2H, C$\underline{H}_2$ Nap), 4.34 (t, J = 9.7 Hz, 1H, Man-4), 4.16 (dd, $J_{3,4}$ = 9.7 Hz, $J_{3,2}$ = 3.2 Hz, 1H, Man-3), 4.08 (dd, $J_{6a,6b}$ = 11.5 Hz, $J_{6b,5}$ = 3.3 Hz, 1H, Man-6a), 3.90 – 3.96 (m, 2H, Man-5, Man-6b), 2.23 (s, 3H, C$\underline{H}_3$ Ac), 1.09 (s, 9H, C$\underline{H}_3$ tBu).

^{13}C NMR (101 MHz, $CDCl_3$) δ (ppm) 170.4 (C=O Ac), 160.1 (C$\underline{}$=NH), 136.1, 135.8, 135.7, 135.1, 133.9, 133.4, 133.3, 133.2, 133.1, 133.0 (C_q Ar), 129.8, 128.5, 128.3, 128.1, 127.84, 127.82, 127.7, 127.6, 126.8, 126.4, 126.3, 126.2, 126.1, 126.0 (C Ar), 95.5 (Man-1), 91.0 (C$\underline{}$$Cl_3$), 77.3 (Man-3), 75.8 (C$\underline{H}_2$ Nap), 75.5 (Man-5), 73.6 (Man-4), 72.4 (C$\underline{H}_2$ Nap), 67.7 (Man-2), 62.4 (Man-6), 26.9 (C$\underline{H}_3$ tBu), 21.2 (C$\underline{H}_3$ Ac).

Allyl 2,3-*O*-isopropylidene-α-D-mannopyranoside (3-14)

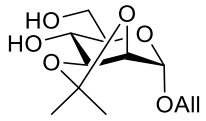

To a solution of allyl 2,3-*O*-isopropylidene-6-*O*-*tert*-butyldiphenylsilyl-α-D-mannopyranoside **3-13** (1.75 g, 3.50 mmol) in THF (35 mL), TBAF (8.8 mL, 8.763 mmol) was added, and it was stirred at room temperature for 2 h. Solvents were removed under reduced pressure, and the resulting brown oil was purified by silica gel column chromatography to afford the diol **3-14** in 86% yield (779 mg, 2.99 mmol) as a colorless oil; R_f = 0.36 (hexane/EtOAc, 2:8).

$[\boldsymbol{\alpha}]_{\boldsymbol{D}}^{\boldsymbol{20}}$**:** 40.62 (c = 1, $CHCl_3$).

IR (ATR) ν(cm^{-1}) 3437 (O-H), 2988, 2930, 1649, 1459, 1374, 1308, 1244, 1220, 1171, 1140, 1075, 1033, 992, 919, 859, 820, 788, 752, 667.

^{1}H NMR (400 MHz, $CDCl_3$) δ (ppm) 5.82 – 5.96 (m, 1H, -C<u>H</u>= Allyl), 5.30 (dq, *J* = 17.2, 1.6 Hz, 1H, =C<u>H</u>$_{2a}$ Allyl), 5.22 (dq, *J* = 10.4, 1.3 Hz, 1H, =C<u>H</u>$_{2b}$ Allyl), 5.07 (s, 1H, Man-1), 4.13 – 4.24 (m, 3H, -C<u>H</u>$_{2a}$- Allyl, Man-2, Man-3), 4.00 (ddt, *J* = 12.7, 6.2, 1.3 Hz, 1H, -C<u>H</u>$_{2b}$- Allyl), 3.84 (br s, 2H, Man-6), 3.69 – 3.78 (m, 1H, Man-4), 3.63 (dt, *J* = 9.6, 3.9 Hz, 1H, Man-5), 3.33 (s, 1H, O<u>H</u>-4), 2.49 (s, 1H, O<u>H</u>-6), 1.52 (s, 3H, CH_3), 1.35 (s, 3H, CH_3).

^{13}C NMR (101 MHz, $CDCl_3$) δ (ppm) 133.4 (-<u>C</u>H= Allyl), 118.2 (=<u>C</u>H$_2$ Allyl), 109.7 (C Acetal), 96.5 (Man-1), 78.4 (Man), 75.7 (Man), 69.8 (Man-5), 69.5 (Man-4), 68.3 (-<u>C</u>H$_2$- Allyl), 62.4 (Man-6), 28.1 (<u>C</u>H$_3$), 26.2 (<u>C</u>H$_3$).

ESI-MS: 283.0 $[M+Na]^+$.

HRMS: $[M+Na]^+$ cald 283.1158; found 283.1111.

Allyl 4,6-di-*O*-(2-naphthyl)methyl-α-D-mannopyranoside (3-16)

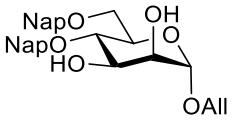

NaH (295 mg, 7.38 mmol, 60% in mineral oil) was added to a solution of **3-14** (0.77 g, 2.96 mmol) in DMF (30 mL) at 0 °C. After 30 min, 2-(Bromomethyl)naphthalene (1.64 g, 7.38 mmol) was added, and the reaction mixture was stirred at room temperature for 8 h. The reaction was quenched with aq. NH_4Cl, and volatiles were removed under reduced pressure. The remaining was dissolved with ethyl acetate, and the solution was extracted with water. The layers were separated, and the aqueous phase was extracted with ethyl acetate. Organic layers were combined, washed with brine, dried with Na_2SO_4, filtered, and evaporated. The crude compound was dissolved in a DCM/MeOH 1:1 mixture (33 mL) and CSA was added (250 mg, 1.076 mmol). The reaction was stirred overnight before it was quenched with Et_3N and concentrated *in vacuo*. The

residue was purified by silica gel column chromatography to give the diol **3-16** in 81% yield (1.20 g, 2.40 mmol) as a white solid; R_f = 0.44 (hexane/EtOAc, 6:4).

$[\alpha]_D^{20}$**:** 56.95 (c = 1, $CHCl_3$).

IR (ATR) v(cm^{-1}) 3428 (O-H), 3057, 2924, 1694, 1603, 1510, 1368, 1273, 1126, 1092, 1064, 1008, 857, 814, 754, 688.

^{1}H NMR (400 MHz, $CDCl_3$) δ (ppm) 7.72 – 7.84 (m, 5H, Ar), 7.58 – 7.67 (m, 2H, Ar), 7.53 (s, 1H, Ar), 7.39 – 7.52 (m, 5H, Ar), 7.20 – 7.26 (m, 1H, Ar), 5.80 – 5.95 (m, 1H, -C<u>H</u>= Allyl), 5.23 – 5.32 (m, 1H, -C<u>H</u>$_{2a}$- Allyl), 5.18 (dd, *J* = 10.3, 1.6 Hz, 1H, -C<u>H</u>$_{2b}$- Allyl), 4.91 (d, *J* = 11.2 Hz, 1H, Man-1), 4.86 (d, *J* = 11.2 Hz, 2H, C<u>H</u>$_2$ Nap), 4.58 – 4.72 (m, 2H, C<u>H</u>$_2$ Nap), 4.14 – 4.23 (m, 1H, -C<u>H</u>$_{2a}$- Allyl), 3.92 – 4.04 (m, 3H, -C<u>H</u>$_{2b}$- Allyl, Man-3, Man-2), 3.73 – 3.90 (m, 4H, Man-6, Man-5, Man-4), 2.46 (s, 2H, O<u>H</u> x 2).

^{13}C NMR (101 MHz, $CDCl_3$) δ (ppm) 135.6, 135.4 (C_q Ar), 133.7 (-<u>C</u>H= Allyl), 133.30, 133.27, 133.1, 133.0 (C_q Ar), 128.4, 128.0, 127.9, 127.7, 127.1, 126.8, 126.3, 126.21, 126.19, 126.1, 126.0, 125.8 (C Ar), 117.6 (=<u>C</u>H$_2$ Allyl), 98.8 (Man-1), 75.8 (Man-4), 74.9 (<u>C</u>H$_2$ Nap), 73.8 (<u>C</u>H$_2$ Nap), 72.1 (Man-3), 71.2 (Man-2), 70.8 (Man-5), 68.8 (Man-6), 68.2 (-<u>C</u>H$_2$- Allyl).

ESI-MS: 523.1 $[M+Na]^+$.

HRMS: $[M+Na]^+$ cald 523.2097; found 523.2091.

Allyl 3,4,6-tri-*O*-(2-naphthyl)methyl-α-D-mannopyranoside (3-17)

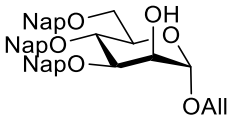

A mixture of diol **3-16** (1 g, 2.00 mmol), 4 Å MS (2.5 g) and dibutyltin oxide (596 mg, 2.40 mmol) in toluene (24 mL) was refluxed at 112 °C for 3 h. It was allowed to cool down to 40 °C, filtered and concentrated at 50 °C by rotatory evaporation. The residue was dissolved in DMF (15 mL) and NapBr (529 mg, 2.40 mmol) was added followed by TBAI (737 mg, 2.00 mmol). The reaction mixture was heated at 60 °C for 3 h. It was cooled to room temperature, diluted with EtOAc, and a 5% $Na_2S_2O_3$ aqueous solution was added until the orange color faded. Solvents were removed under reduced pressure, and the remaining was dissolved with ethyl acetate. The solution was washed with water, and the aqueous phase was extracted with ethyl acetate. Organic layers were combined, washed with brine, dried with Na_2SO_4, filtered, and evaporated. The crude compound was purified by silica gel column chromatography to give the alcohol **3-17** in 67% yield (0.854 g, 1.33 mmol) as a colorless oil; R_f = 0.18 (hexane/EtOAc, 7:3).

$[\alpha]_D^{20}$**:** 24.50 (c = 1, $CHCl_3$).

IR (ATR) v(cm^{-1}) 3446 (O-H), 3056, 2914, 1636, 1603, 1510, 1460, 1367, 1272, 1171, 1125, 1093, 1058, 1020, 893, 856, 814, 752, 684.

^{1}H NMR (400 MHz, $CDCl_3$) δ (ppm) 7.54 – 7.70 (m, 9H, Ar), 7.41 (d, *J* = 8.1 Hz, 2H, Ar), 7.24 – 7.38 (m, 9H, Ar), 7.00 (dd, *J* = 8.4, 1.6 Hz, 1H, Ar), 5.69 – 5.84 (m, 1H, -C<u>H</u>= Allyl), 5.14 (dd, *J* =

17.1, 1.9 Hz, 1H, -C$\underline{H}_{2a}$- Allyl), 5.02 – 5.09 (m, 1H, -C$\underline{H}_{2b}$- Allyl), 4.89 (d, *J* = 1.7 Hz, 1H, Man-1), 4.86 & 4.49 (ABq, *J* = 11.1 Hz, 2H, C$\underline{H}_2$ Nap), 4.75 & 4.68 (ABq, *J* = 11.7 Hz, 2H, C$\underline{H}_2$ Nap), 7.40 & 4.53 (ABq, *J* = 12.3 Hz, 2H, C$\underline{H}_2$ Nap), 4.08 (dd, *J* = 12.9, 5.2 Hz, 1H, -C$\underline{H}_{2a}$- Allyl), 4.01 (s, 1H, Man-2), 3.83 – 3.93 (m, 3H, -C$\underline{H}_{2b}$- Allyl, Man-4, Man-3), 3.69 – 3.78 (m, 2H, Man-6a, Man-5), 3.60 – 3.67 (m, 1H, Man-6b), 2.63 (s, 1H, O$\underline{H}$).

^{13}C NMR (101 MHz, $CDCl_3$) δ (ppm) 135.7, 135.6, 135.4 (C_q Ar), 133.7 (-$\underline{C}$H= Allyl), 133.25, 133.22, 133.18, 133.0, 132.9 (C_q Ar), 128.4, 128.2, 128.01, 127.97, 127.9, 127.8, 127.7, 127.6, 126.8, 126.6, 126.4, 126.2, 126.12, 126.08, 126.04, 125.95, 125.9, 125.83, 125.79 (C Ar), 117.6 (=$\underline{C}H_2$ Allyl), 98.6 (Man-1), 80.3 (Man-3), 75.2 ($\underline{C}H_2$ Nap), 74.4 (Man-4), 73.6 ($\underline{C}H_2$ Nap), 72.0 ($\underline{C}H_2$ Nap), 71.2 (Man-5), 68.8 (Man-6), 68.4 (Man-2), 68.0 (-$\underline{C}H_2$- Allyl).

ESI-MS: 663.2 $[M+Na]^+$.

HRMS: $[M+Na]^+$ cald 663.2723; found 663.2715.

Allyl 2-*O*-levulinyl-3,4,6-tri-*O*-(2-naphthyl)methyl-α-D-mannopyranoside (3-6)

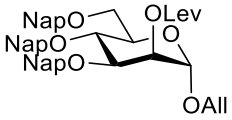

To a solution of alcohol **3-17** (0.880 g, 1.37 mmol) and DMAP (50 mg, 0.411 mmol) in DCM (13.9 mL) was added LevOH (0.197 mL, 1.922 mmol) and DIC (0.3 mL, 1.92 mmol) at room temperature. The reaction mixture was stirred overnight before it was washed with water. The aqueous phase was extracted with DCM. Organic layers were combined, washed with 1 M aq. citric acid followed by brine, dried with Na_2SO_4, filtered, and concentrated. The residue was purified by flash column chromatography on silica gel to afford the protected mannoside **3-6** in 93% yield (949 mg, 1.28 mmol) as a colorless oil; R_f = 0.65 (hexane/EtOAc, 6:4).

$[\alpha]_D^{20}$: 0.02 (c = 1, $CHCl_3$).

IR (ATR) ν(cm^{-1}) 3057, 2924, 1741 (C=O), 1720 (C=O), 1603, 1510, 1460, 1407, 1365, 1253, 1209, 1126, 1138, 1088, 1061, 1020, 991, 857, 818, 752.

^{1}H NMR (400 MHz, $CDCl_3$) δ (ppm) 7.63 – 7.74 (m, 8H, Ar), 7.61 (dd, *J* = 7.6, 1.7 Hz, 1H, Ar), 7.46 (d, *J* = 8.3 Hz, 2H, Ar), 7.28 – 7.43 (m, 9H, Ar), 7.04 (dd, *J* = 8.4, 1.7 Hz, 1H, Ar), 5.72 – 5.84 (m, 1H, -C$\underline{H}$= Allyl), 5.39 (dd, *J* = 3.4, 1.8 Hz, 1H, Man-2), 5.17 (dd, *J* = 17.2, 1.6 Hz, 1H, -C$\underline{H}_{2a}$- Allyl), 5.06 – 5.13 (m, 1H, -C$\underline{H}_{2b}$- Allyl), 4.93 & 4.53 (ABq, *J* = 11.0 Hz, 2H, C$\underline{H}_2$ Nap), 4.85 (d, *J* = 1.8 Hz, 1H, Man-1), 4.79 & 4.59 (ABq, *J* = 5.1 Hz, 2H, C$\underline{H}_2$ Nap), 4.76 & 4.56 (ABq, *J* = 5.9 Hz, 2H, C$\underline{H}_2$ Nap), 4.09 (ddt, *J* = 12.9, 5.2, 1.5 Hz, 1H, -C$\underline{H}_{2a}$- Allyl), 4.01 (dd, *J* = 9.3, 3.4 Hz, 1H, Man-3), 3.85 – 3.94 (m, 2H, -C$\underline{H}_{2b}$- Allyl, Man-4), 3.75 – 3.82 (m, 2H, Man-6a, Man-5), 3.64 – 3.72 (m, 1H, Man-6b), 2.57 – 2.68 (m, 4H, C$\underline{H}_2$-C$\underline{H}_2$ Lev), 1.99 (s, 3H, C$\underline{H}_3$ Lev).

^{13}C NMR (101 MHz, $CDCl_3$) δ (ppm) 206.5 ($\underline{C}$=O Lev), 172.2 ($\underline{C}$=O Lev), 135.8, 135.63 (C_q Ar), 135.57 (-$\underline{C}$H= Allyl), 133.5, 133.32, 133.26, 133.2, 133.05, 133.02, 132.9 (C_q Ar), 128.3, 128.2, 128.02, 127.95, 127.9, 127.8, 127.7, 127.6, 126.9, 126.8, 126.4, 126.2, 126.1, 126.0, 125.92,

125.88, 125.8 (C Ar), 117.9 (=$\underline{C}H_2$ Allyl), 97.0 (Man-1), 78.3 (Man-3), 75.3 ($\underline{C}H_2$ Nap), 74.3 (Man-4), 73.6 ($\underline{C}H_2$ Nap), 71.7 ($\underline{C}H_2$ Nap), 71.4 (Man-5), 69.0 (Man-2), 68.8 (Man-6), 68.3 (-$\underline{C}H_2$- Allyl), 38.0 ($\underline{C}H_2$ Lev), 29.8 ($\underline{C}H_3$ Lev), 28.3 ($\underline{C}H_2$ Lev).

ESI-MS: 761.2 $[M+Na]^+$.

HRMS: $[M+Na]^+$ cald 761.3090; found 761.3076.

2-*O*-levulinyl-3,4,6-tri-*O*-(2-naphthyl)methyl-α,β-D-mannopyranose (3-18)

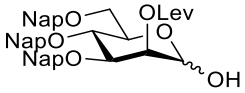

To a solution of the allylated mannoside **3-6** (934 mg, 1.26 mmol) in a 1:1 DCM/MeOH anhydrous mixture (10 mL), $PdCl_2$ (6.7 mg, 0.379 mmol) was added at room temperature. After 4 h, the mixture was filtered through a pad of Celite, and the volatiles were evaporated *in vacuo*. The resulting orange oil was purified by flash silica gel column chromatography to obtain **3-18** in 82% yield (717 mg, 1.03 mmol) as a white solid; R_f = 0.26 (hexane/EtOAc, 1:1).

$[\alpha]_D^{20}$: -9.47 (c = 1, $CHCl_3$).

IR (ATR) v(cm^{-1}) 3413 (O-H), 3057, 2924, 2866, 1740 (C=O), 1719 (C=O), 1603, 1510, 1406, 1365, 1254, 1209, 1158, 1125, 1084, 966, 894, 858, 818, 753, 667.

^{1}H NMR (400 MHz, $CDCl_3$) δ (ppm) 7.70 – 7.84 (m, 10H, Ar), 7.42 – 7.62 (m, 12H, Ar), 7.16 (dd, *J* = 8.5, 1.7 Hz, 1H, Ar), 5.46 – 5.51 (m, 1H, Man-2), 5.26 – 5.32 (m, 1H, Man-1 α-anomer), 5.04 & 4.66 (ABq, *J* = 11.1 Hz, 2H, C$\underline{H}_2$ Nap), 4.87 & 4.66 (ABq, *J* = 11.4 Hz, 2H, C$\underline{H}_2$ Nap), 4.78 & 4.66 (ABq, *J* = 12.1 Hz, 2H, C$\underline{H}_2$ Nap), 4.12 – 4.21 (m, 2H, Man-5, Man-3), 3.75 – 3.89 (m, 3H, Man-6, Man-4), 2.67 – 2.80 (m, 4H, C$\underline{H}_2$-C$\underline{H}_2$ Lev), 2.11 (s, 3H, C$\underline{H}_3$ Lev).

^{13}C NMR (101 MHz, $CDCl_3$) δ (ppm) 206.6 ($\underline{C}$=O Lev), 172.2 ($\underline{C}$=O Lev), 135.8, 135.6, 135.4, 133.4, 133.3, 133.2, 133.1, 133.05, 132.95 (C_q Ar), 128.33, 128.29, 128.2, 128.1, 128.04, 128.00, 127.98, 127.81, 127.75, 127.73, 127.69, 127.0, 126.91, 126.89, 126.5, 126.25, 126.22, 126.15, 126.12, 126.09, 126.07, 126.03, 126.01, 125.92, 125.86 (C_q Ar), 92.5 (Man-1 α-anomer), 77.8 (Man-3), 75.2 ($\underline{C}H_2$ Nap), 74.7 (Man-4), 73.6 ($\underline{C}H_2$ Nap), 71.7 ($\underline{C}H_2$ Nap), 71.1 (Man-5), 69.4 (Man-2), 69.3 (Man-6), 38.1 ($\underline{C}H_2$ Lev), 29.8 ($\underline{C}H_3$ Lev), 28.3 ($\underline{C}H_2$ Lev).

ESI-MS: 721.2 $[M+Na]^+$.

HRMS: $[M+Na]^+$ cald 721.2777; found 721.2756.

2-*O*-levulinyl-3,4,6-tri-*O*-(2-naphthyl)methyl-α-D-mannopyranosyl trichloroimidate (3-19)

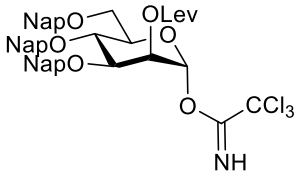

To a solution of the hemiacetal **3-18** (717 mg, 1.02 mmol) in anhydrous DCM (8.5 mL) at 0 °C, trichloroacetonitrile (0.51 mL, 5.13 mmol) was added followed by DBU (15.3 µL, 0.102 mmol). After 1 h, the solution was slightly concentrated under reduced pressure and immediately purified by flash silica gel column chromatography to give the imidate **3-19** in 82% yield (705 mg, 0.835 mmol) as a white solid; R_f = 0.69 (hexane/EtOAc, 1:1).

$[\alpha]_D^{20}$: 32.08 (c = 1, $CHCl_3$).

IR (ATR) v(cm^{-1}) 3339 (N-H), 3058, 2924, 2866, 1746 (C=O), 1720 (C=O), 1675 (C=N), 1603, 1510, 1406, 1355, 1301, 1273, 1154, 1126, 1101, 1049, 973, 858, 819, 796, 754.

^{1}H NMR (400 MHz, $CDCl_3$) δ (ppm) 8.73 (s, 1H, N-H), 7.73 – 7.92 (m, 13H, Ar), 7.63 (dd, *J* = 8.7, 4.6 Hz, 3H, Ar), 7.42 – 7.59 (m, 12H, Ar), 7.21 – 7.31 (m, 1H, Ar), 6.38 (d, *J* = 2.0 Hz, 1H, Man-1), 5.60 (t, *J* = 2.3 Hz, 1H, Man-2), 5.10 & 4.75 (ABq, *J* = 10.9 Hz, 2H, CH_2 Nap), 4.96 & 4.79 (ABq, *J* = 11.5 Hz, 2H, CH_2 Nap), 4.89 & 4.67 (ABq, *J* = 12.2 Hz, 2H, CH_2 Nap), 4.14 – 4.20 (m, 4H, Man-3, Man-5), 4.05 – 4.10 (m, 1H, Man-4), 3.95 (dd, *J* = 11.1, 3.7 Hz, 1H, Man-6a), 3.82 (dd, *J* = 11.1, 1.9 Hz, 1H, Man-6b), 2.74 – 2.84 (m, 4H, CH_2-CH_2 Lev), 2.14 (s, 3H, CH_3 Lev).

^{13}C NMR (101 MHz, $CDCl_3$) δ (ppm) 206.2 (C=O Lev), 172.0 (C=O Lev), 156.0 (C=NH), 135.62, 135.56, 135.1, 133.29, 133.26, 133.2, 133.1, 133.0 (C_q Ar), 128.4, 128.3, 128.3, 128.01, 127.99, 127.96, 127.80, 127.77, 127.7, 127.4, 126.8, 126.4, 126.21, 126.19, 126.1, 126.05, 125.98, 125.9 (C_q Ar), 95.4 (Man-1), 90.8 (CCl_3), 77.2 (Man-1), 75.6 (CH_2 Nap), 74.4 (Man-4), 73.7 (Man-5), 73.6 (CH_2 Nap), 72.1 (CH_2 Nap), 68.4 (Man-6), 67.7 (Man-2), 38.0 (CH_2 Lev), 29.8 (CH_3 Lev), 28.2 (CH_2 Lev).

ESI-MS: 864.1 $[M+Na]^+$.

HRMS: $[M+Na]^+$ cald 864.1874; found 864.1821.

Allyl 2-*O*-levulinyl-3,4,6-tri-*O*-(2-naphthyl)methyl-α-D-mannopyranosyl-(1→6)-2-*O*-acetyl-3,4-di-*O*-(2-naphthyl)methyl-α-D-mannopyranoside (3-20)

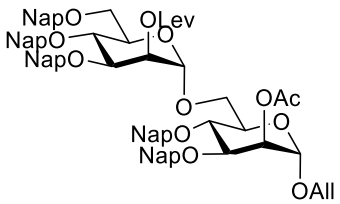

A mixture of donor **3-19** (704.8 mg, 0.836 mmol) and acceptor **3-10** (378 mg, 0.697 mmol) in anhydrous DCM (6.3 mL) was stirred at room temperature for 10 min. TMSOTf (25.2 µL, 0.139

mmol) was added to the mixture at 0 °C, and it was stirred for 1 h. The reaction was quenched with Et_3N, and the solvents were removed under reduced pressure. The residue was purified by flash silica gel column chromatography to give the dimannoside **3-20** in 94% yield (799 mg, 0.653 mmol) as a white foam; R_f = 0.37 (hexane/EtOAc, 6:4).

$[\alpha]_D^{20}$: 24.15 (c = 1, $CHCl_3$).

IR (ATR) v(cm^{-1}) 3057, 2926, 1743 (C=O), 1721 (C=O), 1603, 1510, 1461, 1369, 1236, 1141, 1126, 1087, 982, 894, 858, 819, 754.

^{1}H NMR (400 MHz, $CDCl_3$) δ (ppm) 7.66 – 7.78 (m, 13H, Ar), 7.55 – 7.65 (m, 6H, Ar), 7.35 – 7.52 (m, 16H, Ar), 7.06 (d, *J* = 8.4 Hz, 1H, Ar), 5.76 – 5.88 (m, 1H, -C<u>H</u>= Allyl), 5.56 – 5.60 (m, 1H, ManII-2), 5.45 – 5.49 (m, 1H, ManI-2), 5.23 (dd, *J* = 17.2, 1.5 Hz, 1H, -C<u>H</u>$_{2a}$- Allyl), 5.14 (d, *J* = 10.4 Hz, 1H, -C<u>H</u>$_{2b}$- Allyl), 5.05 (s, 1H, ManII-1), 4.99 (d, *J* = 11.1 Hz, 2H, C<u>H</u>$_2$ Nap), 4.82 – 4.92 (m, 3H, C<u>H</u>$_2$ Nap, ManI-1), 4.75 (d, *J* = 12.3 Hz, 1H, C<u>H</u>$_2$ Nap), 4.68 (d, *J* = 11.2 Hz, 1H, C<u>H</u>$_2$ Nap), 4.63 (d, *J* = 11.6 Hz, 1H, C<u>H</u>$_2$ Nap), 4.54 – 4.62 (m, 2H, C<u>H</u>$_2$ Nap), 4.48 (d, *J* = 12.3 Hz, 1H, C<u>H</u>$_2$ Nap), 4.02 – 4.13 (m, 3H, ManI-3, ManII-3, -C<u>H</u>$_{2a}$- Allyl), 3.74 – 4.01 (m, 8H, -C<u>H</u>$_{2b}$- Allyl, ManI-6, ManI-4, ManII-4, ManI-5, ManII-5), 3.69 (dd, *J* = 10.8, 3.9 Hz, 1H, ManII-6a), 3.58 (dd, *J* = 10.6, 1.3 Hz, 1H, ManII-6b), 2.68 – 2.76 (m, 4H, C<u>H</u>$_2$-C<u>H</u>$_2$ Lev), 2.17 (s, 3H, C<u>H</u>$_3$ Lev), 2.10 (s, 3H, C<u>H</u>$_3$ Ac).

^{13}C NMR (101 MHz, $CDCl_3$) δ (ppm) 206.4 (<u>C</u>=O Lev), 172.0 (<u>C</u>=O Lev), 170.7 (<u>C</u>=O Ac), 135.90, 135.88, 135.6, 135.4, 135.3, 133.33, 133.30, 133.28, 133.26, 133.22 (C_q Ar), 133.18 (-<u>C</u>H= Allyl), 133.1, 133.0, 132.9, 132.9 (C_q Ar), 128.30, 128.26, 128.2, 128.1, 128.05, 127.96, 127.93, 127.91, 127.8, 127.73, 127.72, 127.6, 127.14, 127.10, 126.7, 126.33, 126.30, 126.28, 126.16, 126.12, 126.08, 126.0, 125.94, 125.92, 125.89, 125.80, 125.78, 125.6 (C Ar), 118.2 (=<u>C</u>H$_2$ Allyl), 98.0 (ManII-1), 96.8 (ManI-1), 78.4 (ManI-3), 77.6 (ManII-3), 75.2 (<u>C</u>H$_2$ Nap), 75.1 (<u>C</u>H$_2$ Nap), 74.23 (Man-4), 74.16 (Man-4), 73.4 (<u>C</u>H$_2$ Nap), 72.0 (<u>C</u>H$_2$ Nap), 71.4 (Man-5), 71.3 (Man-5), 71.0 (<u>C</u>H$_2$ Nap), 68.8 (ManI-2), 68.6 (ManII-6), 68.5 (ManII-2), 68.2 (-<u>C</u>H$_2$- Allyl), 66.0 (ManI-6), 38.1 (<u>C</u>H$_2$ Lev), 29.9 (<u>C</u>H$_3$ Lev), 28.3 (<u>C</u>H$_2$ Lev), 21.2 (<u>C</u>H$_3$ Ac).

ESI-MS: 1245.3 $[M+Na]^+$.

HRMS: $[M+Na]^+$ cald 1245.4976; found 1245.4896.

Allyl 3,4,6-tri-*O*-(2-naphthyl)methyl-α-D-mannopyranosyl-(1→6)-2-*O*-acetyl-3,4-di-*O*-(2-naphthyl)methyl-α-D-mannopyranoside (3-21)

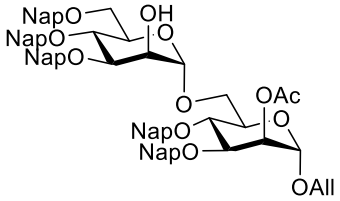

To a solution of dimannose **3-20** (1.09 g, 0.891 mmol) in anhydrous DCM (7.4 mL), hydrazine acetate (148 mg, 1.60 mmol) was added. The reaction mixture was stirred at room temperature

overnight before it was washed with saturated aq. $NaHCO_3$ and brine, dried over Na_2SO_4, filtered, and concentrated *in vacuo*. The crude product was purified by flash silica gel column chromatography to give the alcohol **3-21** in 74% yield (742 mg, 0.659 mmol) as a white foam; R_f = 0.41 (hexane/EtOAc, 4:6).

$[\alpha]_D^{20}$: 38.57 (c = 1, $CHCl_3$).

IR (ATR) v(cm^{-1}) 3457 (O-H), 3056, 2926, 1747 (C=O), 1603, 1510, 1460, 1370, 1236, 1171, 1126, 1064, 982, 894, 857, 816, 753, 673.

^{1}H NMR (400 MHz, $CDCl_3$) δ (ppm) 7.58– 7.83 (m, 19H, Ar), 7.36 – 7.51 (m, 16H, Ar), 7.06 (dd, *J* = 8.4, 1.2 Hz, 1H, Ar), 5.77 – 5.90 (m, 1H, (m, 1H, -C<u>H</u>= Allyl)), 5.47 (dd, *J* = 3.0, 1.8 Hz, 1H, ManI-2), 5.24 (dd, *J* = 17.2, 1.3 Hz, 1H, -C<u>H</u>$_{2a}$- Allyl), 5.12 – 5.19 (m, 2H, -C<u>H</u>$_{2b}$- Allyl, ManII-1), 5.03 (d, *J* = 11.3 Hz, 1H, C<u>H</u>$_2$ Nap), 4.95 (d, *J* = 11.1 Hz, 1H, C<u>H</u>$_2$ Nap), 4.84 – 4.92 (m, 3H, C<u>H</u>$_2$ Nap, ManI-1), 4.79 (d, *J* = 11.8 Hz, 1H, C<u>H</u>$_2$ Nap), 4.73 (d, *J* = 12.4 Hz, 1H, C<u>H</u>$_2$ Nap), 4.69 (d, *J* = 11.2 Hz, 1H, C<u>H</u>$_2$ Nap), 4.63 (d, *J* = 11.4 Hz, 1H, C<u>H</u>$_2$ Nap), 4.56 (d, *J* = 11.1 Hz, 1H, C<u>H</u>$_2$ Nap), 4.48 (d, *J* = 12.4 Hz, 1H, C<u>H</u>$_2$ Nap), 4.23 (s, 1H, ManII-2), 4.07 – 4.15 (m, 2H, ManI-3, -C<u>H</u>$_{2a}$- Allyl), 4.02 (dd, *J* = 11.3, 3.6 Hz, 1H, ManII-6a), 3.91 – 3.98 (m, 3H, -C<u>H</u>$_{2b}$- Allyl, ManII-3, ManI-4), 3.76 – 3.90 (m, 4H, ManII-6b, ManII-5, ManI-5, ManII-4), 3.65 (dd, *J* = 10.8, 3.9 Hz, 1H, ManI-6a), 3.56 – 3.61 (m, 1H, ManI-6b), 2.13 (s, 3H C<u>H</u>$_3$ Ac).

^{13}C NMR (101 MHz, $CDCl_3$) δ (ppm) 170.5 (<u>C</u>=O Ac), 136.0, 135.7, 135.4, 135.3 (C_q Ar), 133.4 (-<u>C</u>H= Allyl), 133.3, 133.2, 133.0 (C_q Ar), 128.5, 128.4, 128.23, 128.16, 128.1, 128.0, 127.8, 127.7, 127.2, 126.9, 126.8, 126.4, 126.2, 126.1, 126.0, 125.9, 125.7 (C Ar), 118.2 (=<u>C</u>H$_2$ Allyl), 99.6 (ManII-1), 96.8 (ManI-1), 79.8 (ManII-3), 78.5 (ManI-3), 75.2 (<u>C</u>H$_2$ Nap x2), 74.4 (Man-4), 74.3 (Man-4), 73.6 (<u>C</u>H$_2$ Nap), 72.0 (<u>C</u>H$_2$ Nap), 71.9 (<u>C</u>H$_2$ Nap), 71.2 (ManII-5, ManI-5), 68.9 (ManI-2), 68.8 (ManII-6), 68.4 (ManII-2), 68.3 (-<u>C</u>H$_2$- Allyl), 66.2 (ManI-6), 21.2 (<u>C</u>H$_3$ Ac).

ESI-MS: 1142.3 $[M+NH_4]^+$.

HRMS: $[M+Na]^+$ cald 1147.4608; found 1147.4554.

Allyl 2-*O*-acetyl-6-*O*-*tert*-butyldiphenylsilyl-3,4-di-*O*-(2-naphthyl)methyl-α-D-mannopyranosyl-(1→2)-3,4,6-tri-*O*-(2-naphthyl)methyl-α-D-mannopyranosyl-(1→6)-2-*O*-acetyl-3,4-di-*O*-(2-naphthyl)methyl-α-D-mannopyranoside (3-4)

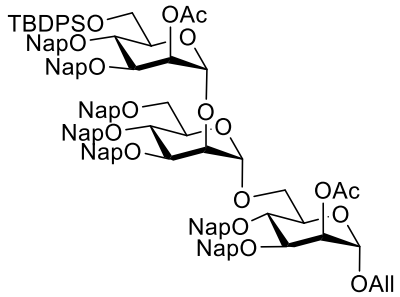

A solution of glycosyl acceptor **3-21** (160 mg, 0.142 mmol) and glycosyl donor **3-12** (151 mg, 0.170 mmol) in anhydrous DCM (1 mL) was stirred at room temperature for 10 min. The mixture

was cooled to -9 °C, and TMSOTf (5.1 µL, 0.0284 mmol) was added. After stirring for 1h, the reaction was quenched with aq. $NaHCO_3$, layers were separated, and the aqueous phase was extracted with DCM. Organic layers were combined, washed with brine, dried over Na_2SO_4, filtered and concentrated. The obtained residue was purified by flash silica gel column chromatography to afford the trimannose **3-4** in 90% yield (236 mg, 0.127 mmol) as a white solid; R_f = 0.28 (hexane/EtOAc, 8:2). Product without the silyl protecting group was also recovered in 8% yield (18.3 mg, 0.0114 mmol); R_f = 0.40 (hexane/EtOAc, 1:1).

^{1}H NMR (400 MHz, $CDCl_3$) δ (ppm) 7.24 – 7.85 (m, 57H, H Ar), 7.17 (dd, *J* = 8.4, 1.6 Hz, 1H, H Ar), 7.07 (dd, *J* = 8.4, 1.7 Hz, 1H, H Ar), 5.70 – 5.84 (m, 1H, -C<u>H</u>= Allyl), 5.69 (t, *J* = 2.5 Hz, 1H, ManIII-2), 5.47 (dd, *J* = 3.4, 1.8 Hz, 1H, ManI-2), 5.35 (d, *J* = 1.9 Hz, 1H, ManIII-1), 5.20 (dd, *J* = 17.2, 1.7 Hz, 1H, =C<u>H</u>$_{2a}$ Allyl), 5.06 – 5.15 (m, 2H, =C<u>H</u>$_{2b}$ Allyl, C<u>H</u>$_2$ Nap), 4.93 – 4.99 (m, 2H, C<u>H</u>$_2$ Nap), 4.96 (d, *J* = 2.3 Hz, 1H, ManII-1), 4.82 – 4.93 (m, 3H, C<u>H</u>$_2$ Nap), 4.75 – 4.81 (m, 2H, C<u>H</u>$_2$ Nap), 4.78 (d, *J* = 1.8 Hz, 1H, ManI-1), 4.59 – 4.67 (m, 3H, C<u>H</u>$_2$ Nap), 4.56 (d, *J* = 10.9 Hz, 2H, C<u>H</u>$_2$ Nap), 4.40 (d, *J* = 12.4 Hz, 1H, C<u>H</u>$_2$ Nap), 4.30 (app t, *J* = 2.4 Hz, 1H, ManII-2), 4.25 (d, *J* = 9.7 Hz, 1H, ManIII-4), 4.19 (dd, *J* = 9.6, 3.0 Hz, 1H, ManIII-3), 4.11 – 4.15 (m, 1H, ManIII-6a), 4.04 – 4.12 (m, 2H, ManII-3, ManI-3), 4.01 – 4.04 (m, 1H, -C<u>H</u>$_{2a}$- Allyl), 3.97 – 4.01 (m, 1H, ManI-6a), 3.89 – 3.95 (m, 3H, ManII-4, ManIII-5, ManIII-6b), 3.85 – 3.89 (m, 1H, -C<u>H</u>$_{2b}$- Allyl), 3.80 – 3.84 (m, 2H, ManI-4, ManI-5), 3.74 – 3.79 (m, 1H, ManII-5), 3.60 (d, *J* = 10.8 Hz, 1H, ManI-6b), 3.46 – 3.56 (m, 2H, ManII-6), 2.13 (s, 3H, C<u>H</u>$_3$ Ac), 2.06 (s, 3H, C<u>H</u>$_3$ Ac), 1.09 (s, 9H, C<u>H</u>$_3$ tBu).

^{13}C NMR (101 MHz, $CDCl_3$) δ (ppm) 170.52 (C=O Ac), 170.50 (C=O Ac), 136.3, 136.1, 136.03, 135.95, 135.7, 135.65, 135.62, 135.3, 133.9, 133.41, 133.36, 133.33, 133.30, 133.25 (C_q Ar), 133.22 (-<u>C</u>H= Allyl), 133.1, 133.04, 133.02, 132.91, 132.89 (C_q Ar), 129.8, 129.7, 128.4, 128.3, 128.2, 128.13, 128.10, 128.08, 128.04, 128.02, 127.96, 127.9, 127.83, 127.77, 127.73, 127.71, 127.66, 127.2, 126.9, 126.6, 126.5, 126.41, 126.35, 126.3, 126.22, 126.19, 126.13, 126.06, 126.02, 125.98, 125.96, 125.94, 125.87, 125.82, 125.77, 125.7, 125.5 (C Ar), 118.3 (=<u>C</u>H$_2$ Allyl), 99.2 (ManIII-1), 99.1 (ManII-1), 96.8 (ManI-1), 79.6 (ManII-3), 78.7 (ManI-3), 78.2 (ManIII-3), 75.5 (<u>C</u>H$_2$ Nap), 75.2 (<u>C</u>H$_2$ Nap), 74.9 (<u>C</u>H$_2$ Nap), 74.5, 74.2 (ManI-4, ManIII-4), 73.4 (ManII-2), 73.3 (<u>C</u>H$_2$ Nap), 72.1 (<u>C</u>H$_2$ Nap), 72.04 (<u>C</u>H$_2$ Nap), 71.95 (ManII-5), 71.7 (<u>C</u>H$_2$ Nap), 70.8 (ManI-5), 69.2 (ManIII-2), 69.0 (ManII-6), 68.8 (ManI-2), 68.1 (ManII-1), 66.3 (ManI-6), 63.0 (ManIII-6), 26.9 (<u>C</u>H$_3$ tBu), 21.25 (<u>C</u>H$_3$ Ac), 21.17 (<u>C</u>H$_3$ Ac).

ESI-MS: 1869.5 $[M+Na]^+$.

2-*O*-Acetyl-6-*O*-*tert*-butyldiphenylsilyl-3,4-di-*O*-(2-naphthyl)methyl-α-D-mannopyranosyl-(1→2)-3,4,6-tri-*O*-(2-naphthyl)methyl-α-D-mannopyranosyl-(1→6)-2-*O*-acetyl-3,4-di-*O*-(2-naphthyl)methyl-α-D-mannopyranose (3-22)

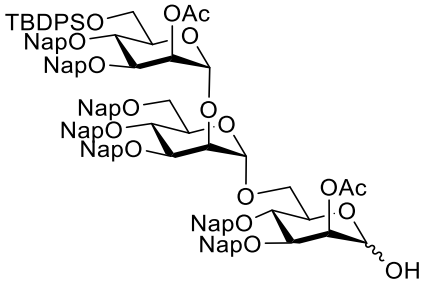

To a solution of the fully protected trimannose **3-4** (207 mg, 0.112 mmol) in a 1:1 DCM/MeOH anhydrous mixture (2.1 mL), $PdCl_2$ (3.9 mg, 0.0224 mmol) was added at room temperature. After 4 h, the mixture was filtered through a pad of Celite, and the volatiles were evaporated *in vacuo*. The resulting oil was purified by flash silica gel column chromatography to obtain **3-22** in 88% yield (179 mg, 0.0990 mmol) as a white solid; R_f = 0.40 (hexane/EtOAc, 7:3).

^{1}H NMR (400 MHz, $CDCl_3$) δ (ppm) 7.61 – 7.81 (m, 35H, H Ar), 7.55 (d, *J* = 8.2 Hz, 2H, H Ar), 7.33 – 7.47 (m, 21H, H Ar), 7.05 (dd, *J* = 8.4, 1.7 Hz, 1H, H Ar), 5.61 (s, 1H, ManIII-2), 5.30 (s, 1H, ManI-2), 5.24 (s, 1H, ManIII-1), 5.11 (d, *J* = 10.8 Hz, 1H, C$\underline{H}_2$ Nap), 4.98 (d, *J* = 11.6 Hz, 1H, C$\underline{H}_2$ Nap), 4.92 (d, *J* = 2.6 Hz, 1H, ManII-1), 4.71 – 4.92 (m, 7H, C$\underline{H}_2$ Nap, ManI-1), 4.46 – 4.67 (m, 5H, C$\underline{H}_2$ Nap), 4.18 – 4.25 (m, 2H, ManII-2), 4.16 – 4.18 (m, 1H, ManIII-3) 4.03 – 4.07 (m, 3H, ManI-3, ManI-5, ManIII-6a), 4.00 (dd, *J* = 8.0, 2.7 Hz, 1H), 3.89 – 3.98 (m, 3H, ManIII-6b, ManI-6a), 3.81 – 3.87 (m, 1H, ManII-5), 3.76 (d, *J* = 8.5 Hz, 1H), 3.75 – 3.64 (m, 2H, ManI-6b), 3.62 (dd, *J* = 10.7, 2.0 Hz, 1H, ManII-6a), 3.48 – 3.59 (m, 2H, ManII-6b), 2.12 (s, 3H, C$\underline{H}_3$ Ac), 2.04 (s, 3H, C$\underline{H}_3$ Ac), 1.08 (s, 9H, C$\underline{H}_3$ tBu).

^{13}C NMR (101 MHz, $CDCl_3$) δ (ppm) 170.5 (C=O Ac), 170.3 (C=O Ac), 136.1, 135.9, 135.71, 135.69, 135.64, 135.60, 135.4, 133.9, 133.41, 133.38, 133.36, 133.33, 133.26, 133.2, 133.11, 133.09, 133.05, 132.96 (C_q Ar), 129.8, 129.7, 128.4, 128.32, 128.26, 128.2, 128.11, 128.09, 128.05, 127.99, 127.9, 127.84, 127.80, 127.75, 127.70, 127.66, 127.1, 127.0, 126.7, 126.6, 126.4, 126.24, 126.18, 126.15, 126.10, 126.07, 126.0, 125.94, 125.89, 125.8, 125.7 (C Ar), 99.5 (ManII-1), 98.1 (ManIII-1), 92.3 (ManI-1), 78.2, 78.1, 77.4, 75.8 (C$\underline{H}_2$ Nap), 75.2, 75.95 (C$\underline{H}_2$ Nap) 74.94 (C$\underline{H}_2$ Nap), 74.8, 74.4, 73.4 (C$\underline{H}_2$ Nap), 73.1, 72.8, 72.2 (C$\underline{H}_2$ Nap), 72.04 (C$\underline{H}_2$ Nap), 71.98 (ManII-5), 71.9 (C$\underline{H}_2$ Nap), 71.0, 69.8 (ManII-6), 69.1 (ManIII-2), 69.0 (ManI-2), 68.6 (ManI-6), 63.0 (ManIII-6), 26.9 (C$\underline{H}_3$ tBu), 21.24 (C$\underline{H}_3$ Ac), 21.18 (C$\underline{H}_3$ Ac).

ESI-MS: 1829.4 $[M+Na]^+$.

2-*O*-Acetyl-6-*O*-*tert*-butyldiphenylsilyl-3,4-di-*O*-(2-naphthyl)methyl-α-D-mannopyranosyl-(1→2)-3,4,6-tri-*O*-(2-naphthyl)methyl-α-D-mannopyranosyl-(1→6)-2-*O*-acetyl-3,4-di-*O*-(2-naphthyl)methyl-α-D-mannopyranosyl trichloroacetimidate (3-23)

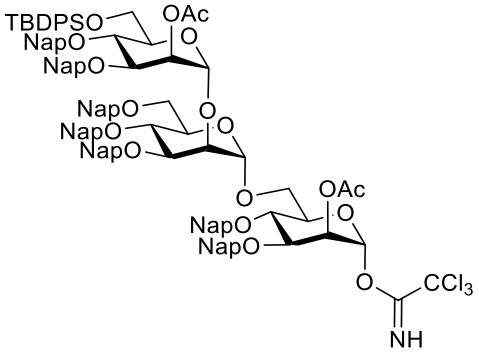

To a solution of **3-22** (179 mg, 0.0988 mmol) in anhydrous DCM (1.2 mL) at 0 °C, trichloroacetonitrile (99 µL, 0.988 mmol) was added followed by DBU (2 µL, 0.0134 mmol). After 45 min, the solution was slightly concentrated under reduced pressure and immediately purified by flash silica gel column chromatography to afford the imidate **3-23** (161 mg, 0.0824 mmol) in 83% yield as a white solid; R_f = 0.58 (hexane/EtOAc, 7:3).

^{1}H NMR (400 MHz, $CDCl_3$) δ (ppm) 8.63 (s, 1H, NH), 7.25 – 7.86 (m, 57H, H Ar), 7.21 (dd, *J* = 8.4, 1.7 Hz, 1H, H Ar), 7.10 (dd, *J* = 8.5, 1.7 Hz, 1H, H Ar), 6.19 (d, *J* = 1.9 Hz, 1H, ManI-1), 5.65 – 5.71 (m, 1H, ManIII-2), 5.55 (dd, *J* = 3.4, 2.0 Hz, 1H, ManI-2), 5.33 (d, *J* = 1.9 Hz, 1H, ManIII-1), 5.11 (d, *J* = 11.1 Hz, 1H, CH_2 Nap), 4.93 – 4.99 (m, 2H, CH_2 Nap), 4.92 (d, *J* = 1.8 Hz, 2H, CH_2 Nap, ManII-1), 4.89 (s, 1H, CH_2 Nap), 4.77 – 4.86 (m, 3H, CH_2 Nap), 4.71 (d, *J* = 11.2 Hz, 1H, CH_2 Nap), 4.66 & 4.43 (ABq, *J* = 12.5 Hz, 2H, CH_2 Nap), 4.52 – 4.65 (m, 3H, CH_2 Nap), 4.25 (d, *J* = 3.2 Hz, 1H, ManII-2), 4.18 (d, *J* = 3.0 Hz, 1H, ManIII-4), 4.15 – 4.17 (m, 1H, ManIII-3), 4.11 – 4.14 (m, 1H, ManIII-6a), 4.06 – 4.13 (m, 1H, ManI-3), 3.98 – 4.01 (m, 1H, ManII-3), 3.87 – 3.97 (m, 6H, ManI-4, ManII-4, ManI-5, ManIII-5, ManIII-6b, ManI-6a), 3.79 – 3.83 (m, 1H, ManII-5), 3.60 – 3.69 (m, 1H, ManI-6b), 3.59 (dd, *J* = 11.2, 4.5 Hz, 1H, ManII-6a), 3.51 (dd, *J* = 11.2, 1.9 Hz, 1H, ManII-6b), 2.12 (s, 3H, CH_3 Ac), 2.08 (s, 3H, CH_3 Ac), 1.07 (s, 9H, CH_3 tBu).

^{13}C NMR (101 MHz, $CDCl_3$) δ (ppm) 170.5 (C=O Ac), 170.1 (C=O Ac), 159.5 (C=NH), 136.3, 136.1, 136.0, 135.8, 135.7, 135.6, 134.8, 133.9, 133.45, 133.41, 133.33, 133.31, 133.27, 133.24, 133.22, 133.1, 133.04, 133.02, 132.97, 132.9 (C_q Ar), 129.7, 128.4, 128.4, 128.2, 128.12, 128.09, 128.01, 127.97, 127.94, 127.91, 127.83, 127.81, 127.76, 127.73, 127.71, 127.67, 127.6, 126.9, 126.6, 126.50, 126.47, 126.4, 126.28, 126.27, 126.2, 126.1, 126.05, 126.01, 125.98, 125.96, 125.93, 125.90, 125.86, 125.8, 125.7, 125.6 (C Ar), 99.1 (ManIII-1), 99.0 (ManII-1), 95.0 (ManI-1), 90.8 (CCl_3), 79.8 (ManII-3), 78.3 (ManIII-3), 77.8 (ManI-3), 75.5 (CH_2 Nap), 75.3 (CH_2 Nap), 75.2 (CH_2 Nap), 74.5, 74.3 (ManIII-4), 73.7, 73.6, 73.41 (ManII-2), 73.35, 73.2 (CH_2 Nap), 72.4 (CH_2 Nap), 72.1 (CH_2 Nap), 72.0 (ManII-5), 71.8 (CH_2 Nap), 69.2 (ManIII-2), 69.0 (ManII-6), 67.6 (ManI-2), 66.1 (ManI-6), 63.0 (ManIII-6), 26.9 (CH_3- tBu), 21.2 (CH_3 Ac), 21.1 (CH_3 Ac).

ESI-MS: 1973.5 $[M+Na]^+$.

2-*O*-Acetyl-6-*O*-*tert*-butyldiphenylsilyl-3,4-di-*O*-(2-naphthyl)methyl-α-D-mannopyranosyl-(1→2)-3,4,6-tri-*O*-(2-naphthyl)methyl-α-D-mannopyranosyl-(1→6)-2-*O*-acetyl-3,4-di-*O*-(2-naphthyl)methyl-α-D-mannopyranosyl-(1→4)-2-azido-2-deoxy-3,6-di-*O*-(2-naphthyl)methyl-α-D-glucopyranosyl-(1→6)-1-*O*-allyl-2,3,4,5-tetra-O-(2-naphthyl)methyl-D-*myo*-inositol (3-24)

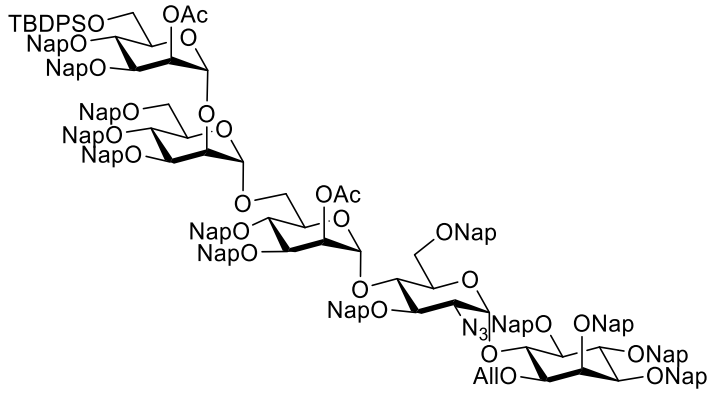

A solution of the pseudodisaccharide glycosyl acceptor **2-46** (25 mg, 0.0200 mmol) and the trimannoside glycosyl donor **3-23** (51 mg, 0.0260 mmol) in a 6:1 Et_2O/DCM anhydrous mixture (2 mL) was stirred at room temperature for 10 min. The mixture was cooled to -10 °C, and TMSOTf (1.1 µL, 6 µmol) was added. After stirring for 1 h, the reaction was quenched with a solution of Et_3N in DCM (1 mL, 0.012 M), and volatiles were removed under reduced pressure. The obtained residue was purified by flash silica gel column chromatography to afford the pseudopentasaccharide **3-24** as a white solid; R_f = 0.45 (hexane/EtOAc, 7:3).

$[\alpha]_D^{20}$**:** 6.05 (c = 1, $CHCl_3$).

IR (ATR) ν(cm^{-1}) 3056, 2931, 2860, 2107 (N=N=N), 1738 (C=O), 1603, 1510, 1462, 1429, 1368, 1237, 1125, 1088, 1051, 983, 894, 856, 816, 753, 704.

^{1}H NMR (400 MHz, $CDCl_3$) δ (ppm) 7.02 – 7.79 (m, 101H, H Ar), 5.79 – 5.93 (m, 1H, -C<u>H</u>= Allyl), 5.77 (d, *J* = 3.7 Hz, 1H, Glc-1), 5.56 (t, *J* = 2.5 Hz, 1H, ManI-2), 5.36 – 5.42 (m, 1H, ManIII-2), 5.35 (s, 1H, ManIII-1), 5.12 – 5.20 (m, 2H, =C<u>H</u>$_{2a}$ Allyl, ManI-1), 4.93 – 5.11 (m, 10H, =C<u>H</u>$_{2b}$ Allyl, C<u>H</u>$_2$ Nap), 4.62 – 4.87 (m, 15H, C<u>H</u>$_2$ Nap), 4.59 (s, 1H, ManII-1), 4.54 (d, *J* = 11.8 Hz, 1H, C<u>H</u>$_2$ Nap), 4.27 – 4.46 (m, 9H, C<u>H</u>$_2$ Nap, Ino-6), 4.04 – 4.25 (m, 9H, C<u>H</u>$_2$ Nap, ManII-2, ManI-3, Ino-2, Ino-4, Glc-5), 4.03 (dd, *J* = 9.7, 2.8 Hz, 1H), 3.92 – 3.99 (m, 7H, C<u>H</u>$_2$ Nap, -C<u>H</u>$_2$- Allyl, Glc-3, ManIII-6a), 3.88 (dd, *J* = 9.5, 2.4 Hz, 1H, ManII-3), 3.64 – 3.82 (m, 4H, ManI-6a, ManIII-6b), 3.61 (dd, *J* = 9.2, 3.1 Hz, 1H, ManIII-3), 3.34 – 3.56 (m, 6H, Ino-1, Ino-3, Ino-5, ManI-5, ManII-5, Glc-6a), 3.17 – 3.31 (m, 3H, Glc-2, ManII-6), 3.15 (dd, *J* = 11.5, 3.0 Hz, 1H, Glc-6b), 3.02 (d, *J* = 10.6 Hz, 1H, ManI-6b), 2.00 (s, 3H, C<u>H</u>$_3$ Ac), 1.64 (s, 3H, C<u>H</u>$_3$ Ac), 0.97 (s, 9H, C<u>H</u>$_3$ tBu).

^{13}C NMR (101 MHz, $CDCl_3$) δ (ppm) 170.4 (C=O Ac), 170.1 (C=O Ac), 136.5, 136.3, 136.09, 136.06, 136.00, 135.8, 135.69, 135.67, 135.5, 135.3, 135.2 (C_q Ar), 134.30 (-<u>C</u>H= Allyl), 134.0, 133.42, 133.38, 133.34, 133.30, 133.27, 133.25, 133.22, 133.18, 133.16, 133.13, 133.07, 133.00, 132.95, 132.9, 132.85, 132.83, 132.6 (C_q Ar), 129.8, 129.7, 128.33, 128.26, 128.21, 128.16,

128.1, 128.04, 127.98, 127.94, 127.90, 127.86, 127.83, 127.80, 127.77, 127.71, 127.67, 127.64, 127.61, 127.2, 126.85, 126.75, 126.72, 126.67, 126.45, 126.40, 126.36, 126.3, 126.25, 126.16, 126.11, 126.07, 126.04, 126.01, 125.97, 125.93, 125.86, 125.8, 125.74, 125.68, 125.65, 125.60, 125.55, 125.5, 124.9 (C Ar), 117.4 (=$\underline{C}H_2$ Allyl), 99.2 (ManI-1), 99.1 (ManIII-1), 98.9 (ManII-1), 97.8 (Glc-1), 82.1 (Ino-4), 82.0 (Ino-1), 81.6 (Ino-5), 80.8 (Ino-3), 80.6 (Glc-3), 79.5 (ManII-3), 78.8 (ManIII-3), 78.2 (ManI-3), 76.0 ($\underline{C}H_2$ Nap), 75.52 (Ino-6), 75.47 ($\underline{C}H_2$ Nap), 75.2 ($\underline{C}H_2$ Nap), 75.1 ($\underline{C}H_2$ Nap), 74.7 ($\underline{C}H_2$ Nap), 74.6, 74.2 ($\underline{C}H_2$ Nap x3), 74.01, 73.45 (Ino-2), 73.41 ($\underline{C}H_2$ Nap), 73.3 ($\underline{C}H_2$ Nap), 73.2 (ManII-2), 73.1 ($\underline{C}H_2$ Nap), 72.8, 72.1 (ManII-5), 72.0 ($\underline{C}H_2$ Nap), 71.8 ($\underline{C}H_2$ Nap), 71.4 ($\underline{C}H_2$ Nap, C-5), 71.1 (-$\underline{C}H_2$- Allyl), 69.9 (Glc-5), 69.2 (ManI-2), 69.0, 68.9 (Glc-6), 68.8 (ManIII-2), 66.0 (ManI-6), 63.6 (Glc-2), 62.7 (ManIII-6), 26.9 ($\underline{C}H_3$ tBu), 21.2 ($\underline{C}H_3$ Ac), 20.9 ($\underline{C}H_3$ Ac).

HRMS: $[M+2Na]^{2+}$ cald 1541.1224; found 1541.6324. $[M+Na+K]^{2+}$ cald 1549.1093; found 1549.1146.

400 MHz NMR Data		Glc-1	ManI-1	ManII-1	ManIII-1
Chemical shift (ppm)	^{13}C	97.8	99.2	98.9	99.1
	^{1}H	5.77	5.15	4.59	5.35

6-*O*-*Tert*-butyldiphenylsilyl-3,4-di-*O*-(2-naphthyl)methyl-α-D-mannopyranosyl-(1→2)-3,4,6-tri-*O*-(2-naphthyl)methyl-α-D-mannopyranosyl-(1→6)-3,4-di-*O*-(2-naphthyl)methyl-α-D-mannopyranosyl-(1→4)-2-azido-2-deoxy-3,6-di-*O*-(2-naphthyl)methyl-α-D-glucopyranosyl-(1→6)-1-*O*-allyl-2,3,4,5-tetra-O-(2-naphthyl)methyl-D-*myo*-inositol (3-25)

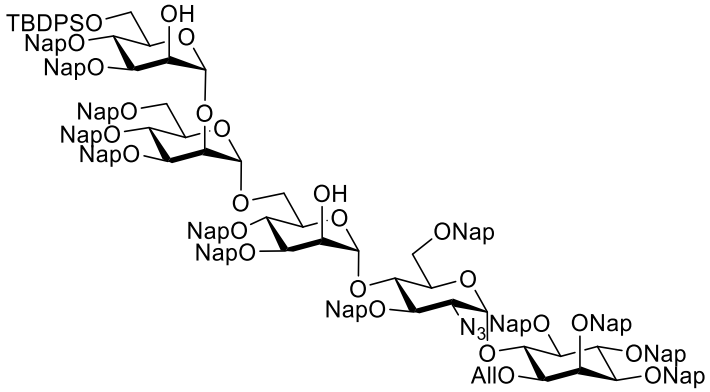

To a solution of the pseudopentasaccharide **3-24** (0.0200 mmol) in an 8:5 MeOH/DCM (2.4 mL) anhydrous mixture, NaOMe (43 mg, 0.8 mmol) was added and it was heated at 50 °C for 6 h. The reaction was cooled to room temperature, neutralized with Amberlite IR 120 H^+ resin, filtered and concentrated *in vacuo*. The resulting residue was purified by flash silica gel column chromatography to obtain **3-25** in 94% yield over two steps (55 mg, 0.0186 mmol) as a white solid; R_f = 0.42 (hexane/EtOAc, 7:3).

$[\boldsymbol{\alpha}]_{\boldsymbol{D}}^{\boldsymbol{20}}$**:** 7.69 (c = 1, $CHCl_3$).

IR (ATR) v(cm^{-1}) 3480 (O-H), 3056, 2930, 2106 (N=N=N), 1603, 1510, 1462, 1428, 1366, 1272, 1125, 1049, 893, 856, 815, 752, 704.

^{1}H NMR (400 MHz, $CDCl_3$) δ (ppm) 7.06 – 7.80 (m, 101H, Ar), 5.79 – 5.93 (m, 1H, -C<u>H</u>= Allyl), 5.74 (d, *J* = 3.6 Hz, 1H, Glc-1), 5.33 (s, 1H, ManIII-1), 5.05 – 5.22 (m, 3H, =C<u>H</u>$_2$ Allyl, ManI-1), 4.63 – 5.04 (m, 17H, C<u>H</u>$_2$ Nap, ManII-1), 4.29 – 4.63 (m, 8H, C<u>H</u>$_2$ Nap), 4.25 (d, *J* = 10.7 Hz, 2H, C<u>H</u>$_2$ Nap), 4.10 – 4.20 (m, 5H, ManII-2, ManIII-2), 3.98 – 4.10 (m, 5H), 3.81 – 3.94 (m, 5H, -C<u>H</u>$_2$-Allyl), 3.69 – 3.83 (m, 4H,), 3.53 – 3.62 (m, 3H, ManI-2), 3.32 – 3.53 (m, 6H), 3.13 – 3.18 (m, 2H, Glc-2), 2.97 – 3.09 (m, 2H), 2.27 (s, 1H, ManIII O<u>H</u>-2), 1.87 (s, 1H, ManI O<u>H</u>-2), 0.97 (s, 9H, C<u>H</u>$_3$ tBu).

^{13}C NMR (101 MHz, $CDCl_3$) δ (ppm) 136.4, 136.3, 136.11, 136.08, 135.82, 135.76, 135.2 (C_q Ar), 134.3 (-<u>C</u>H= Allyl), 133.4, 133.34, 133.31, 133.27, 133.2, 133.13, 133.07, 133.0, 132.9 (C_q Ar), 129.73, 129.68, 128.32, 128.30, 128.25, 128.20, 128.16, 128.12, 128.10, 128.06, 128.03, 127.98, 127.92, 127.89, 127.83, 127.81, 127.77, 127.75, 127.71, 127.68, 127.66, 127.6, 126.8, 126.41, 126.38, 126.36, 126.31, 126.26, 126.2, 126.13, 126.09, 126.03, 126.00, 125.94, 125.91, 125.87, 125.8, 125.74, 125.68 (C Ar), 117.3 (=<u>C</u>H$_2$ Allyl), 101.8 (ManI-1), 100.4 (ManIII-1), 99.1 (ManII-1), 97.6 (Glc-1), 82.1, 82.0, 81.8, 80.8, 80.2, 80.0, 79.6, 79.5, 77.4, 77.2, 76.0 (<u>C</u>H$_2$ Nap), 75.4 (<u>C</u>H$_2$ Nap), 75.22, 75.18 (<u>C</u>H$_2$ Nap), 75.1 (<u>C</u>H$_2$ Nap), 75.0 (<u>C</u>H$_2$ Nap), 74.7, 74.2 (<u>C</u>H$_2$ Nap), 74.1, 73.5, 73.4 (<u>C</u>H$_2$ Nap), 73.3 (<u>C</u>H$_2$ Nap), 73.0 (<u>C</u>H$_2$ Nap), 72.8, 72.6, 72.4 (ManII-2), 72.23, 72.17 (<u>C</u>H$_2$ Nap), 71.7 (<u>C</u>H$_2$ Nap), 71.6, 71.4 (<u>C</u>H$_2$), 71.1 (-<u>C</u>H$_2$- Allyl), 70.0, 69.2 (<u>C</u>H$_2$), 68.4 (ManI-2), 65.3 (<u>C</u>H$_2$), 63.2 (Glc-2), 63.0 (<u>C</u>H$_2$), 27.0 (<u>C</u>H$_3$ tBu).

HRMS: $[M+2Na]^{2+}$ cald 1499.1118; found 1499.1119.

400 MHz NMR Data		**Glc-1**	**ManI-1**	**ManII-1**	**ManIII-1**
Chemical shift (ppm)	^{13}C	97.6	101.8	99.1	100.4
	^{1}H	5.74	5.14	4.77	5.33

Allyl 6-*O*-*tert*-butyldiphenylsilyl-2-*O*-levulinyl-3,4-di-*O*-(2-naphthyl)methyl-α-D-mannopyranoside (3-26)

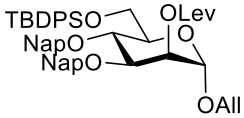

To a solution of alcohol **3-9** (804 mg, 1.09 mmol) and DMAP (39.9 mg, 0.326 mmol) in DCM (10.9 mL), LevOH (0.156 mL, 1.52 mmol) and DIC (0.238 mL, 1.52 mmol) were added at room temperature. The reaction mixture was stirred overnight before it was washed with water. The aqueous phase was extracted with DCM. Organic layers were combined, washed with 1 M aq. citric acid followed by brine, dried with Na_2SO_4, filtered, and concentrated. The residue was purified by flash column chromatography on silica gel to afford the fully protected mannoside **3-26** in 99% yield (912 mg, 1.09 mmol) as a colorless oil; R_f = 0.32 (hexane/EtOAc, 8:2).

$[\alpha]_D^{20}$**:** -12.56 (c = 1, $CHCl_3$).

IR (ATR) v(cm^{-1}) 3054, 2932, 2859, 1742 (C=O), 1722 (C=O), 1604, 1510, 1473, 1429, 1363, 1256, 1139, 1106, 1061, 998, 933, 858, 822, 743, 704.

^{1}H NMR (400 MHz, $CDCl_3$) δ (ppm) 7.75 – 7.92 (m, 11H, Ar), 7.72 (s, 1H, Ar), 7.35 – 7.58 (m, 12H, Ar), 5.89 – 6.01 (m, 1H, -C<u>H</u>= Allyl), 5.59 (d, *J* = 1.7 Hz, 1H, Man-2), 5.32 (dd, *J* = 17.2, 1.5 Hz, 1H, -C<u>H</u>$_{2a}$- Allyl), 5.25 (d, *J* = 10.3 Hz, 1H, -C<u>H</u>$_{2b}$- Allyl), 5.19 & 4.88 (ABq, *J* = 11.0 Hz, 2H, C<u>H</u>$_2$ Nap), 4.94 – 5.03 (m, 2H, C<u>H</u>$_2$ Nap, Man-1), 4.79 (d, *J* = 11.4 Hz, 1H, C<u>H</u>$_2$ Nap), 4.20 – 4.28 (m, 2H, -C<u>H</u>$_{2a}$- Allyl, Man-3), 4.10 – 4.20 (m, 2H, Man-6a, Man-4), 4.00 – 4.10 (m, 2H, -C<u>H</u>$_{2b}$- Allyl, Man-6b), 3.84 – 3.91 (m, 1H, Man-5), 2.71 – 2.88 (m, 4H, C<u>H</u>$_2$-C<u>H</u>$_2$ Lev), 2.18 (s, 3H, C<u>H</u>$_3$ Lev), 1.18 (s, 9H, <u>C</u>H$_3$ tBu).

^{13}C NMR (101 MHz, $CDCl_3$) δ (ppm) 206.3 (<u>C</u>=O Lev), 172.3 (<u>C</u>=O Lev), 136.04, 136.00, 135.7, 135.6, 133.9 (C_q Ar), 133.6 (-<u>C</u>H= Allyl), 133.4, 133.2, 133.06, 133.01 (C_q Ar), 129.7, 128.2, 128.1, 128.04, 128.01, 127.8, 127.7, 127.6, 126.9, 126.5, 126.3, 126.05, 126.02, 125.92, 125.87 (C Ar), 117.9 (=<u>C</u>H$_2$ Allyl), 96.7 (Man-1), 78.4 (Man-3), 75.4 (<u>C</u>H$_2$ Nap), 74.3 (Man-4), 72.8 (Man-5), 71.8 (<u>C</u>H$_2$ Nap), 69.2 (Man-2), 68.0 (-<u>C</u>H$_2$- Allyl), 63.0 (Man-6), 38.1 (<u>C</u>H$_2$ Lev), 29.9 (<u>C</u>H$_2$ Lev), 28.2 (<u>C</u>H$_3$ Lev), 26.9 (<u>C</u>H$_3$ tBu).

HRMS: $[M+Na]^+$ cald 859.3681; found 859.3681; $[M+K]^+$ cald 875.3382; found 875.3418.

6-*O*-*tert*-butyldiphenylsilyl-2-*O*-levulinyl-3,4-di-*O*-(2-naphthyl)methyl-α-D-mannopyranose (3-27)

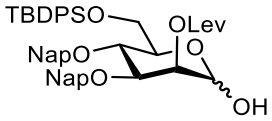

To a solution of the allyl mannoside **3-26** (905 mg, 1.08 mmol) in a 1:1 DCM/MeOH anhydrous mixture (9 mL), $PdCl_2$ (77 mg, 0.432 mmol) was added at room temperature. After 3.5 h, the mixture was filtered through a pad of Celite, and the volatiles were evaporated *in vacuo*. The crude was purified by flash silica gel column chromatography to obtain hemiacetal **3-27** in 60% yield (516 mg, 0.648 mmol) as a white solid; R_f = 0.25 (hexane/EtOAc, 7:3).

$[\alpha]_D^{20}$**:** -29.68 (c = 1, $CHCl_3$).

IR (ATR) v(cm^{-1}) 3396 (O-H), 3054, 2933, 2859, 1742 (C=O), 1721 (C=O), 1510, 1473, 1429, 1363, 1158, 1126, 1112, 1060, 893, 859, 822, 746, 704.

^{1}H NMR (400 MHz, $CDCl_3$) δ (ppm) 7.69 – 7.87 (m, 14H, Ar), 7.67 (s, 1H, Ar), 7.29 – 7.52 (m, 15H, Ar), 5.50 (app s, 1H, Man-2), 5.27 (d, *J* = 2.0 Hz, 1H, Man-1 α-anomer), 5.15 & 4.85 (ABq, *J* = 11.0 Hz, 2H, C<u>H</u>$_2$ Nap), 4.91 & 4.73 (ABq, *J* = 11.5 Hz, 2H, C<u>H</u>$_2$ Nap), 4.16 – 4.21 (m, 2H, Man-4, Man-3), 4.12 (dd, *J* = 11.1, 3.6 Hz, 1H, Man-6a), 3.94 – 4.00 (m, 1H, Man-5), 3.92 (dd, *J* = 11.2, 1.6 Hz, 1H, Man-6b), 2.96 (s, 1H, O<u>H</u>), 2.69 – 2.79 (m, 4H, C<u>H</u>$_2$-C<u>H</u>$_2$ Lev), 2.13 (s, 3H, C<u>H</u>$_3$ Lev), 1.11 (s, 9H, <u>C</u>H$_3$ tBu).

^{13}C NMR (101 MHz, $CDCl_3$) δ (ppm) 206.6 (C=O Lev), 172.4 (C=O Lev), 136.2, 136.1, 136.0, 135.69, 135.67, 134.0, 133.42, 133.39, 133.3, 133.1, 133.0 (C_q Ar), 129.8, 128.23, 128.15, 128.09, 128.06, 127.83, 127.81, 127.78, 127.76, 127.71, 127.67, 127.0, 126.4, 126.3, 126.1, 126.01, 125.98, 125.95, 125.94, 125.89 (C_q Ar), 92.6 (Man-1 α-anomer), 77.7 (Man-3), 75.4 (CH_2 Nap), 74.2 (Man-4), 72.7 (Man-5), 71.8 (CH_2 Nap), 69.4 (Man-2), 63.1 (Man-6), 38.1 (CH_2 Lev), 29.9 (CH_2 Lev), 28.3 (CH_3 Lev), 27.0 (CH_3 tBu).

HRMS: $[M+NH_4]^+$ cald 814.3775; found 814.3815; $[M+Na]^+$ cald 819.3329; found 819.3370; $[M+K]^+$ cald 835.3068; found 835.3103.

6-*O*-*tert*-butyldiphenylsilyl-2-*O*-levulinyl-3,4-di-*O*-(2-naphthyl)methyl-α-D-mannopyranosyl (3-28)

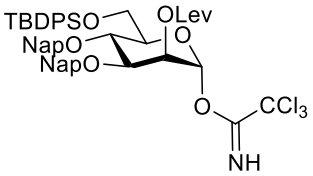

The hemiacetal **3-27** (439 mg, 0.551 mmol) was combined with CCl_3CN (0.28 mL, 2.756 mmol) and DBU (8.2 µL, 0.0551 mmol) in anhydrous DCM (4.6 mL) at 0 °C. The reaction mixture was stirred for 1 h before it was slightly concentrated under reduced pressure and immediately purified by flash silica gel column chromatography to give the imidate **3-28** in 87% yield (450 mg, 0.478 mmol) as a white foam; R_f = 0.50 (hexane/EtOAc, 7:3).

$[\alpha]_D^{20}$: 6.44 (c = 1, $CHCl_3$).

IR (ATR) ν(cm^{-1}) 3344 (N-H), 3055, 2933, 2859, 1746 (C=O), 1721 (C=O), 1675 (C=N), 1604, 1510, 1473, 1428, 1361, 1301, 1273, 1152, 1105, 1048, 972, 936, 858, 822, 796, 754, 703.

^{1}H NMR (400 MHz, $CDCl_3$) δ (ppm) 8.69 (s, 1H, NH), 7.85 (m, 5H, Ar), 7.81 – 7.70 (m, 9H, Ar), 7.69 (s, 1H, Ar), 7.58 – 7.44 (m, 6H, Ar), 7.47 – 7.31 (m, 10H, Ar), 6.39 (d, *J* = 1.9 Hz, 1H, Man-1), 5.61 (dd, *J* = 3.2, 2.0 Hz, 1H, Man-2), 5.18 & 4.88 (ABq, *J* = 10.9 Hz, 2H, CH_2 Nap), 4.97 & 4.81 (ABq, *J* = 11.4 Hz, 2H, CH_2 Nap), 4.33 (t, *J* = 9.7 Hz, 1H, Man-4), 4.19 (dd, *J* = 9.7, 3.2 Hz, 1H, Man-3), 4.11 (dd, *J* = 11.6, 3.4 Hz, 1H, Man-6a), 4.03 – 3.93 (m, 2H, Man-6b, Man-5), 2.84 – 2.77 (m, 4H, CH_2-CH_2 Lev), 2.18 (s, 3H, CH_3 Lev), 1.13 (s, 9H, CH_3 tBu).

^{13}C NMR (101 MHz, $CDCl_3$) δ (ppm) 206.2 (C=O Lev), 172.1 (C=O Lev), 160.0 (C=NH), 136.0, 135.8, 135.7, 135.6, 135.1, 133.8, 133.4, 133.3, 133.2, 133.1, 133.0 (C_q Ar), 129.8, 129.7, 128.4, 128.3, 128.1, 128.0, 127.83, 127.80, 127.78, 127.74, 127.71, 127.5, 126.8, 126.5, 126.21, 126.18, 126.15, 126.12, 126.08, 126.0 (C Ar), 95.5 (Man-1), 90.9 (CCl_3), 77.2 (Man-3), 75.8 (CH_2 Nap), 75.4 (Man-5), 73.6 (Man-4), 72.1 (CH_2 Nap), 67.8 (Man-2), 62.5 (Man-6), 38.0 (CH_2 Lev), 30.0 (CH_2 Lev), 28.2 (CH_3 Lev), 26.9 (CH_3 tBu).

HRMS: $[M+Na]^+$ cald 962.2425; found 962.2471.

Allyl 2-*O*-levulinyl-6-*O*-*tert*-butyldiphenylsilyl-3,4-di-*O*-(2-naphthyl)methyl-α-D-mannopyranosyl-(1→2)-3,4,6-tri-*O*-(2-naphthyl)methyl-α-D-mannopyranosyl-(1→6)-2-*O*-acetyl-3,4-di-*O*-(2-naphthyl)methyl-α-D-mannopyranoside (3-29)

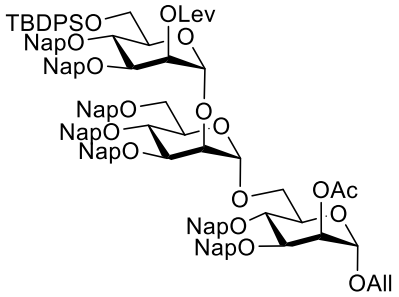

A solution of glycosyl acceptor **3-21** (362 mg, 0.322 mmol) and glycosyl donor **3-28** (364 mg, 0.387 mmol) in anhydrous Et_2O (6 mL) was stirred at room temperature for 5 min. The mixture was cooled to -10 °C, and TMSOTf (11.6 µL, 0.0644 mmol) was added. After stirring for 1.5 h, the reaction was quenched with Et_3N and concentrated. The obtained residue was purified by flash silica gel column chromatography to afford the trimannoside **3-29** in quantitative yield (613 mg, 0.322 mmol) as a white solid; R_f = 0.47 (hexane/EtOAc, 7:3).

$[\alpha]_D^{20}$: -7.74 (c = 1, $CHCl_3$).

IR (ATR) ν(cm^{-1}) 3296, 3056, 2932, 2859, 1738 (C=O), 1603, 1510, 1472, 1429, 1366, 1236, 1140, 1126, 1088, 1056, 894, 857, 820, 753, 705.

^{1}H NMR (400 MHz, $CDCl_3$) δ (ppm) 7.62 – 7.87 (m, 32H, H Ar), 7.29 – 7.59 (m, 45H, H Ar), 7.16 – 7.22 (m, 1H, H Ar), 7.04 – 7.12 (m, 1H, H Ar), 5.72 – 5.87 (m, 1H, -C<u>H</u>= Allyl), 5.71 (s, 1H, ManIII-2), 5.50 (s, 1H, ManI-2), 5.36 (s, 1H, ManIII-1), 5.17 – 5.26 (m, 1H, =C<u>H</u>$_{2a}$ Allyl), 5.08 – 5.17 (m, 2H, =C<u>H</u>$_{2b}$ Allyl, C<u>H</u>$_2$ Nap), 4.93 – 5.04 (m, 4H, ManII-1, C<u>H</u>$_2$ Nap), 4.84 – 4.95 (m, 3H, C<u>H</u>$_2$ Nap), 4.74 – 4.86 (m, 4H, ManI-1, C<u>H</u>$_2$ Nap), 4.53 – 4.71 (m, 6H, C<u>H</u>$_2$ Nap), 4.42 (d, *J* = 12.4 Hz, 1H, C<u>H</u>$_2$ Nap), 4.32 (s, 1H, ManII-2), 4.18 – 4.27 (m, 2H, ManIII-3), 4.13 – 4.18 (m, 1H, ManIII-6a), 4.03 – 4.18 (m, 4H, ManII-3, ManI-3, -C<u>H</u>$_{2a}$- Allyl), 3.90 – 4.03 (m, 6H, ManIII-6b, ManI-6a, ManII-4), 3.88 (d, *J* = 6.8 Hz, 1H, -C<u>H</u>$_{2b}$- Allyl), 3.83 – 3.87 (m, 2H), 3.76 – 3.82 (m, 1H, ManII-5), 3.63 (d, *J* = 10.8 Hz, 1H, ManI-6b), 3.47 – 3.60 (m, 2H, ManII-6), 2.60 – 2.78 (m, 4H, C<u>H</u>$_2$-C<u>H</u>$_2$ Lev), 2.10 (s, 3H, C<u>H</u>$_3$ Lev), 2.09 (s, 3H, C<u>H</u>$_3$ Ac), 1.12 (s, 11H, C<u>H</u>$_3$ tBu).

^{13}C NMR (101 MHz, $CDCl_3$) δ (ppm) 206.4 (<u>C</u>=O Lev), 172.2 (<u>C</u>=O Lev), 170.5 (<u>C</u>=O Ac), 163.6, 136.2, 136.1, 136.0, 135.9, 135.7, 135.6, 135.3 (C_q Ar), 133.8 (-<u>C</u>H= Allyl), 133.4, 133.34, 133.31, 133.28, 133.26, 133.24, 133.22, 133.19, 133.1, 133.03, 133.00, 132.89, 132.87 (C_q Ar), 129.77, 129.75, 128.4, 128.3, 128.24, 128.15, 128.11, 128.09, 128.06, 128.03, 128.00, 127.95, 127.90, 127.84, 127.81, 127.75, 127.72, 127.70, 127.6, 127.2, 126.9, 126.7, 126.5, 126.44, 126.39, 126.34, 126.30, 126.23, 126.20, 126.14, 126.11, 126.07, 126.05, 126.00, 125.97, 125.9, 125.85, 125.81, 125.75, 125.7, 125.4 (C Ar), 118.3 (=<u>C</u>H$_2$ Allyl), 99.14 (ManIII-1), 99.06 (ManII-1), 96.8 (ManI-1), 79.5 (ManII-3), 78.7 (ManI-3), 78.2 (ManIII-3), 75.4 (<u>C</u>H$_2$ Nap), 75.2 (<u>C</u>H$_2$ Nap), 74.9 (<u>C</u>H$_2$ Nap), 74.5, 74.2 (ManII-2), 73.6, 73.3, 73.2 (<u>C</u>H$_2$ Nap), 72.0 (<u>C</u>H$_2$ Nap), 71.91 (ManII-5),

71.90 (CH$_2$ Nap), 71.6 (CH$_2$ Nap), 70.8, 69.3 (ManIII-2), 69.0 (ManII-6), 68.8 (ManI-2), 68.1 (-CH$_2$- Allyl), 66.3 (ManI-6), 63.1 (ManIII-6), 38.1 (CH$_2$ Lev), 29.9 (CH$_3$ Lev), 28.3 (CH$_2$ Lev), 26.9 (CH$_3$- tBu), 21.2 (CH$_3$ Ac).

HRMS: [M+Na]$^+$ cald 1925.7934; found 1925.8235.

Allyl 6-*O*-*tert*-butyldiphenylsilyl-3,4-di-*O*-(2-naphthyl)methyl-α-D-mannopyranosyl-(1→2)-3,4,6-tri-*O*-(2-naphthyl)methyl-α-D-mannopyranosyl-(1→6)-2-*O*-acetyl-3,4-di-*O*-(2-naphthyl)methyl-α-D-mannopyranoside (3-30)

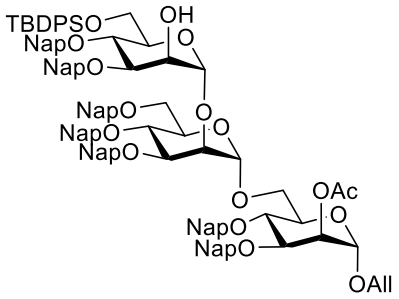

To a solution of trimannoside **3-29** (178 mg, 0.0936 mmol) in anhydrous DCM (0.85 mL), hydrazine acetate (17.2 mg, 0.1872 mmol) was added. The reaction mixture was stirred at room temperature overnight before it was washed with saturated aq. $NaHCO_3$ and brine, dried over Na_2SO_4, filtered, and concentrated *in vacuo*. The crude product was purified by flash silica gel column chromatography to give the alcohol **3-30** in 66% yield (112 mg, 0.0621 mmol) as a white foam; R_f = 0.4 (hexane/EtOAc, 7:3).

$[\alpha]_D^{20}$**:** 4.05 (c = 1, $CHCl_3$).

IR (ATR) v(cm^{-1}) 3055, 2932, 1747 (C=O), 1603, 1510, 1472, 1429, 1369, 1272, 1236, 1125, 1086, 1051, 982, 893, 857, 815, 753,705.

^{1}H NMR (400 MHz, $CDCl_3$) δ (ppm) 7.27 – 7.84 (m, 77H, H Ar), 7.15 – 7.20 (m, 2H, H Ar), 7.07 – 7.12 (m, 1H, H Ar), 5.72 – 5.84 (m, 1H, -CH= Allyl), 5.48 (s, 1H, ManI-2), 5.43 (s, 1H, ManIII-1), 5.20 (d, *J* = 17.3 Hz, 1H, =CH$_{2a}$ Allyl), 4.52 – 5.13 (m, 22H, =CH$_{2b}$ Allyl, ManII-1, ManI-1, CH$_2$ Nap), 4.45 (d, *J* = 12.4 Hz, 1H, CH$_2$ Nap), 4.34 (s, 1H, ManII-2), 4.30 (s, 1H, ManIII-2), 3.91 – 4.17 (m, 13H, ManIII-3, ManII-3, ManI-3, ManIII-6, ManI-6a, ManII-4, -CH$_{2a}$- Allyl), 3.76 – 3.91 (m, 5H, ManII-5, -CH$_{2b}$- Allyl), 3.57 – 3.65 (m, 2H, ManI-6b, ManII-6a), 3.52 (d, *J* = 10.8 Hz, 1H, ManII-6b), 2.07 (s, 3H, CH$_3$ Ac), 1.09 (s, 11H, CH$_3$ tBu).

^{13}C NMR (101 MHz, $CDCl_3$) δ (ppm) 170.5 (C=O Ac), 136.2, 136.1, 136.05, 136.03, 135.8, 135.6, 135.4, 133.8 (C$_q$ Ar), 133.41 (-CH= Allyl), 133.38, 133.3, 133.25, 133.23, 133.14, 133.07, 133.04, 132.92, 132.90 (C$_q$ Ar), 129.7, 128.4, 128.31, 128.29, 128.17, 128.14, 128.11, 128.08, 128.06, 128.02, 127.97, 127.92, 127.89, 127.84, 127.77, 127.73, 127.70, 127.2, 126.8, 126.7, 126.45, 126.42, 126.35, 126.21, 126.19, 126.13, 126.08, 126.04, 126.01, 125.98, 125.96, 125.9, 125.8, 125.7, 125.4 (C Ar), 118.3 (=CH$_2$ Allyl), 100.9 (ManIII-1), 99.2 (ManII-1), 96.8 (ManI-1), 80.2 (Man-3), 79.6 (Man-3), 78.8 (Man-3), 75.3, 75.1, 74.9, 74.7, 74.3, 74.3, 73.5 (ManII-2), 73.3, 73.2, 72.3

(ManII-5), 72.1, 71.7, 70.8, 69.1 (ManII-6), 69.0 (ManIII-2), 68.8 (ManI-2), 68.1 (-$\underline{C}H_2$- Allyl), 66.3 (ManI-6), 63.4 (ManIII-6), 27.0 ($\underline{C}H_3$- tBu), 21.2 ($\underline{C}H_3$ Ac).

HRMS: $[M+Na]^+$ cald 1827.7566; found 1827.7845.

Allyl 6-*O*-*tert*-butyldiphenylsilyl-3,4-di-*O*-(2-naphthyl)methyl-α-D-mannopyranosyl-(1→2)-3,4,6-tri-*O*-(2-naphthyl)methyl-α-D-mannopyranosyl-(1→6)-3,4-di-*O*-(2-naphthyl)methyl-α-D-mannopyranoside (3-35)

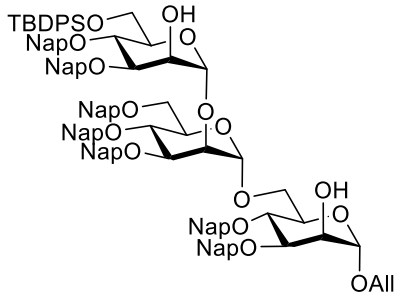

A solution of the trimannoside **3-4** (75.4 mg, 0.0396 mmol) and NaOMe (0.5 M in MeOH, 222 µL, 0.111 mmol) in anhydrous MeOH/DCM 8:2 (1 mL) was stirred at room temperature for 48 h. The reaction was neutralized with Amberlite IR 120 H^+ resin, filtered, and concentrated *in vacuo*. The resulting residue was purified by flash silica gel column chromatography to give the diol **3-35** in 87% yield (61.1 mg, 0.0346 mmol) as a white foam; R_f = 0.40 (hexane/EtOAc, 4:6).

$[\boldsymbol{\alpha}]_{\boldsymbol{D}}^{\boldsymbol{20}}$**:** 16.15 (c = 1, $CHCl_3$).

IR (ATR) v(cm^{-1}) 3474 (O-H), 3056, 2931, 1603, 1510, 1462, 1429, 1365, 1272, 1125, 1104, 1052, 893, 857, 814, 753, 705.

^{1}H NMR (400 MHz, $CDCl_3$) δ (ppm) 7.52 – 7.77 (m, 30H, H Ar), 7.41 – 7.50 (m, 10H, H Ar), 7.13 – 7.39 (m, 33H, H Ar), 5.56 – 5.71 (m, 1H, -C$\underline{H}$= Allyl), 5.37 (s, 1H, ManIII-1), 5.06 (d, *J* = 17.2 Hz, 1H, =C$\underline{H}_{2a}$ Allyl), 4.59 – 5.02 (m, 15H, =C$\underline{H}_{2b}$ Allyl, ManII-1, ManI-1, C$\underline{H}_2$ Nap), 4.55 – 4.60 (m, 1H, C$\underline{H}_2$ Nap), 4.45 – 4.53 (m, 2H, C$\underline{H}_2$ Nap), 4.39 (d, *J* = 12.4 Hz, 1H, C$\underline{H}_2$ Nap), 4.23 (s, 1H, ManII-2), 4.21 (s, 1H, ManIII-2), 4.09 – 4.11 (m, 1H), 3.79 – 4.03 (m, 11H, ManIII-3, ManII-3, ManI-3, ManIII-6, ManI-6a, ManI-2, -C$\underline{H}_{2a}$- Allyl), 3.68 – 3.75 (m, 2H, C$\underline{H}_{2b}$- Allyl), 3.61 – 3.66 (m, 2H), 3.46 – 3.60 (m, 4H, ManI-6b, ManII-6), 0.99 (s, 10H, C$\underline{H}_3$ tBu).

^{13}C NMR (101 MHz, $CDCl_3$) δ (ppm) 136.23, 136.19, 136.15, 136.1, 136.0, 135.8, 135.7, 135.6, 135.3, 133.9 (C_q Ar), 133.5 (-$\underline{C}$H= Allyl), 133.41, 133.35, 133.32, 133.31, 133.28, 133.26, 133.13, 133.06, 133.0, 132.93, 132.92 (C_q Ar), 129.7, 128.5, 128.4, 128.3, 128.2, 128.14, 128.08, 128.05, 128.01, 127.99, 127.96, 127.9, 127.82, 127.80, 127.77, 127.75, 127.72, 127.68, 126.9, 126.8, 126.7, 126.45, 126.40, 126.3, 126.19, 126.16, 126.12, 126.08, 126.03, 125.98, 125.93, 125.88, 125.79, 125.7, 125.6 (C Ar), 118.0 (=$\underline{C}H_2$ Allyl), 100.6 (ManIII-1), 99.4 (ManII-1), 98.1 (ManI-1), 80.5 (ManI-3), 80.2 (ManIII-3), 79.5 (ManII-3), 75.4, 75.2, 75.0, 74.8, 74.3, 74.1, 73.4, 73.0 (ManII-2), 72.9, 72.3, 72.1, 71.8, 70.8, 69.2 (ManII-6), 68.9 (ManIII-2), 68.3 (ManI-2), 67.8 (-$\underline{C}H_2$- Allyl), 66.1 (ManI-6), 63.2 (ManIII-6), 27.0 ($\underline{C}H_3$- tBu).

HRMS: $[M+NH_4]^+$ cald 1780.7907; found 1780.8054; $[M+Na]^+$ cald 1785.7461; found 1785.7626; $[M+K]^+$ cald 1801.7200; found 1801.7349.

Allyl 6-*O*-*tert*-butyldiphenylsilyl-2-*O*-levulinyl-3,4-di-*O*-(2-naphthyl)methyl-α-D-mannopyranosyl-(1→2)-3,4,6-tri-*O*-(2-naphthyl)methyl-α-D-mannopyranosyl-(1→6)-2-*O*-levulinyl-3,4-di-*O*-(2-naphthyl)methyl-α-D-mannopyranoside (3-36)

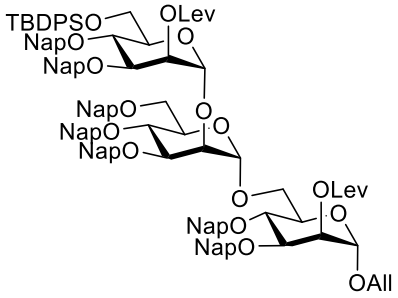

To a solution of diol **3-35** (54.5 mg, 0.0309 mmol) and DMAP (2.3 mg, 0.0185 mmol) in DCM (1.1 mL) LevOH (7.6 µL, 0.0741 mmol) and DIC (11.6 µL, 0.0741 mmol) were added at room temperature. The reaction mixture was stirred 60 h before it was washed with water. The aqueous phase was extracted with DCM. Organic layers were combined, washed with 1 M aq. citric acid followed by brine, dried with Na_2SO_4, filtered, and concentrated. The residue was purified by flash column chromatography on silica gel to afford the protected mannoside **3-36** in 93% yield (56 mg, 0.0287 mmol) as a white foam; R_f = 0.26 (hexane/EtOAc, 7:3).

$[\alpha]_D^{20}$**:** -7.13 (c = 1, $CHCl_3$).

IR (ATR) v(cm^{-1}) 3055, 2931, 1742 (C=O), 1721 (C=O), 1603, 1510, 1462, 1429, 1364, 1272, 1140, 1126, 1088, 1057, 895, 858, 817, 753, 706.

^{1}H NMR (400 MHz, $CDCl_3$) δ (ppm) 7.62 – 7.64 (m, 27H, H Ar), 7.52 – 7.59 (m, 7H, H Ar), 7.29 – 7.50 (m, 28H, H Ar), 7.19 (d, *J* = 8.4 Hz, 1H, H Ar), 7.09 (d, *J* = 8.4 Hz, 1H, H Ar), 5.71 – 5.81 (m, 1H, -C<u>H</u>= Allyl), 5.69 (s, 1H, ManIII-2), 5.45 (s, 1H, ManI-2), 5.35 (s, 1H, ManIII-1), 5.18 (d, *J* = 17.1 Hz, 1H, =C<u>H</u>$_{2a}$ Allyl), 5.09 (dd, *J* = 13.2, 10.7 Hz, 2H, =C<u>H</u>$_{2b}$ Allyl, C<u>H</u>$_2$ Nap), 4.75 – 5.02 (m, 10H, ManII-1, ManI-1, C<u>H</u>$_2$ Nap), 4.52 – 4.68 (m, 5H, C<u>H</u>$_2$ Nap), 4.42 (d, *J* = 12.4 Hz, 1H, C<u>H</u>$_2$ Nap), 4.31 (d, *J* = 2.8 Hz, 1H, ManII-2), 4.16 – 4.23 (m, 2H, ManIII-3), 4.13 (dd, *J* = 11.3, 3.4 Hz, 1H, ManIII-6a), 3.99 – 4.09 (m, 4H, ManII-3, ManI-3, -C<u>H</u>$_{2a}$- Allyl), 3.89 – 3.98 (m, 4H, ManIII-6b, ManI-6a), 3.76 – 3.88 (m, 4H, ManI-5, -C<u>H</u>$_{2b}$- Allyl), 3.50 – 3.64 (m, 3H, ManII-6, ManI-6b), 2.45 – 2.68 (m, 8H, C<u>H</u>$_2$-C<u>H</u>$_2$ Lev x2), 2.07 (s, 3H, C<u>H</u>$_3$ Lev), 2.02 (s, 3H, C<u>H</u>$_3$ Lev), 1.08 (s, 9H, C<u>H</u>$_3$ tBu).

^{13}C NMR (101 MHz, $CDCl_3$) δ (ppm) 206.4 (<u>C</u>=O Lev), 206.2 (<u>C</u>=O Lev), 172.3 (<u>C</u>=O Lev), 172.2 (<u>C</u>=O Lev), 136.3, 136.1, 136.05, 136.01, 135.9, 135.8, 135.73, 135.69, 135.5 (C_q Ar), 133.8 (-<u>C</u>H= Allyl), 133.42, 133.36, 133.33, 133.30, 133.28, 133.24, 133.22, 133.1, 133.0, 132.92, 132.90 (C_q Ar), 129.8, 128.3, 128.23, 128.17, 128.12, 128.09, 128.06, 128.03, 127.98, 127.92, 127.91, 127.85, 127.81, 127.76, 127.74, 127.71, 127.66, 127.2, 126.9, 126.51, 126.45, 126.4, 126.3,

126.22, 126.16, 126.11, 126.05, 126.01, 125.97, 125.93, 125.91, 125.84, 125.80, 125.76, 125.70, 125.6 (C Ar), 118.3 (=$\underline{C}H_2$ Allyl), 99.2 (ManIII-1), 99.1 (ManII-1), 96.7 (ManI-1), 79.7 (ManI-3), 78.7 (ManII-3), 78.2 (ManIII-3), 75.4, 75.2, 75.0, 74.6, 74.2 (ManII-2), 73.7, 73.3, 71.9, 71.8, 71.7, 70.7, 69.3 (ManIII-2), 69.0 (ManII-6), 68.9 (ManI-2), 68.0 (-$\underline{C}H_2$- Allyl), 66.5 (ManI-6), 63.1 (ManIII-6), 38.2 ($\underline{C}H_2$ Lev), 37.9 ($\underline{C}H_2$ Lev), 29.9 ($\underline{C}H_3$ Lev), 29.8 ($\underline{C}H_3$ Lev), 28.3 ($\underline{C}H_2$ Lev), 28.1 ($\underline{C}H_2$ Lev), 26.9 ($\underline{C}H_3$- tBu).

HRMS: $[M+NH_4]^+$ cald 1976.8642; found 1976.8684; $[M+Na]^+$ cald 1981.8196; found 1981.8271.

6-*O*-*tert*-butyldiphenylsilyl-2-*O*-levulinyl-3,4-di-*O*-(2-naphthyl)methyl-α-D-mannopyranosyl-(1→2)-3,4,6-tri-*O*-(2-naphthyl)methyl-α-D-mannopyranosyl-(1→6)-2-*O*-levulinyl-3,4-di-*O*-(2-naphthyl)methyl-α-D-mannopyranose (3-37)

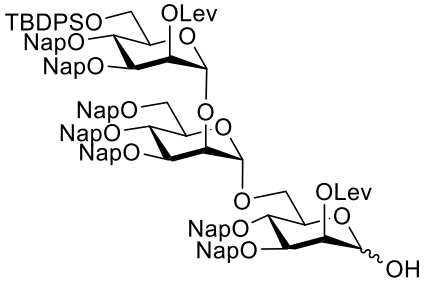

To a solution of the fully protected trimannose **3-36** (55.8 mg, 0.0285 mmol) in a 1:1 DCM/MeOH anhydrous mixture (0.8 mL), $PdCl_2$ (2.5 mg, 0.0142 mmol) was added at room temperature. After 6 h, the mixture was filtered through a pad of Celite, and the volatiles were evaporated *in vacuo*. The resulting oil was purified by flash silica gel column chromatography to obtain the hemiacetal **3-37** in 74% yield (40.3 mg, 0.0210 mmol) as a white solid; R_f = 0.32 (hexane/EtOAc, 6:4).

$[\alpha]_D^{20}$**:** -12.99 (c = 1, $CHCl_3$).

IR (ATR) v(cm^{-1}) 3429 (O-H), 3056, 2930, 1742 (C=O), 1721 (C=O), 1603, 1510, 1472, 1429, 1364, 1272, 1126, 1105, 1054, 896, 858, 818, 753, 706.

^{1}H NMR (400 MHz, $CDCl_3$) δ (ppm) 7.58 – 7.86 (m, 53H, H Ar), 7.26 – 7.50 (m, 51H, H Ar), 5.62 (s, 1H, ManIII-2), 5.31 (s, 1H, ManI-2), 5.26 (s, 1H, ManIII-1), 5.11 (d, *J* = 10.9 Hz, 2H, C$\underline{H}_2$ Nap), 4.71 – 5.03 (m, 17H, C$\underline{H}_2$ Nap, ManII-1, ManI-1), 4.52 – 4.67 (m, 9H, C$\underline{H}_2$ Nap), 4.50 (d, *J* = 11.1 Hz, 1H, C$\underline{H}_2$ Nap), 4.31 (s, 1H), 4.10 – 4.15 (m, 6H, ManII-2), 3.83 – 4.13 (m, 16H, ManI-3,ManII-3, ManIII-3 ManII-5, ManIII-6, ManI-6a), 3.73 – 3.80 (m, 1H), 3.60 – 3.74 (m, 4H, ManI-6b, ManII-6a), 3.48 – 3.60 (m, 3H, ManII-6b), 2.63 – 2.69 (m, 5H, C$\underline{H}_2$-C$\underline{H}_2$ Lev), 2.58 (d, *J* = 4.9 Hz, 5H, C$\underline{H}_2$-C$\underline{H}_2$ Lev), 2.08 (s, 3H, C$\underline{H}_3$ Lev), 2.06 (s, 3H, C$\underline{H}_3$ Lev), 1.08 (s, 10H, C$\underline{H}_3$ tBu).

^{13}C NMR (101 MHz, $CDCl_3$) δ (ppm) 206.4 ($\underline{C}$=O Lev), 206.3 ($\underline{C}$=O Lev), 172.2 ($\underline{C}$=O Lev), 172.1 ($\underline{C}$=O Lev), 136.0, 135.9, 135.8, 135.7, 135.6, 135.4, 133.9, 133.40, 133.36, 133.34, 133.32, 133.25, 133.21, 133.09, 133.05, 133.01, 132.96, 132.9 (C_q Ar), 129.79, 129.76, 128.4, 128.3, 128.24, 128.16, 128.11, 128.07, 128.04, 127.99, 127.96, 127.9, 127.83, 127.79, 127.74, 127.70, 127.67, 127.01, 126.95, 126.8, 126.65, 126.62, 126.57, 126.4, 126.31, 126.28, 126.18, 126.16,

126.13, 126.11, 126.07, 126.04, 126.02, 125.98, 125.95, 125.89, 125.86, 125.83, 125.78 (C Ar), 99.61 (ManII-1), 99.2 (ManIII-1), 92.2 (ManI-1), 78.1 (ManI-3, ManII-3), 78.0 (ManIII-3), 75.7, 75.5, 75.2, 74.9, 74.7, 74.4, 74.2, 73.4 (ManII-2), 73.1, 72.0, 71.9 (ManII-5), 71.7, 71.0, 69.8 (ManII-6), 69.2 (ManIII-2), 69.1 (ManI-2), 68.8 (ManI-6), 63.0 (ManIII-6), 38.1 ($\underline{C}H_2$ Lev), 38.0 ($\underline{C}H_2$ Lev), 29.91 ($\underline{C}H_3$ Lev), 29.87 ($\underline{C}H_3$ Lev), 28.3 ($\underline{C}H_2$ Lev), 28.1 ($\underline{C}H_2$ Lev), 26.9 ($\underline{C}H_3$- tBu).
HRMS: $[M+NH_4]^+$ cald 1936.8329; found 1936.8326; $[M+Na]^+$ cald 1941.7883; found 1941.7937.

6-*O*-*tert*-butyldiphenylsilyl-2-*O*-levulinyl-3,4-di-*O*-(2-naphthyl)methyl-α-D-mannopyranosyl-(1→2)-3,4,6-tri-*O*-(2-naphthyl)methyl-α-D-mannopyranosyl-(1→6)-2-*O*-levulinyl-3,4-di-*O*-(2-naphthyl)methyl-α-D-mannopyranosyl trichloroacetimidate (3-38)

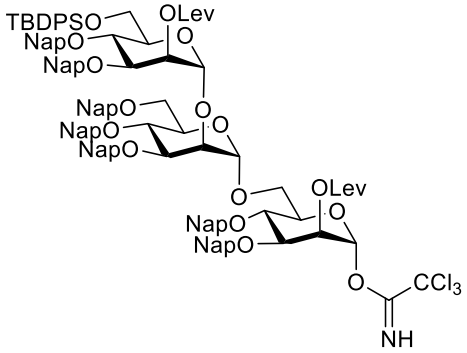

To a solution of hemiacetal **3-37** (38 mg, 0.0198 mmol) in anhydrous DCM (1 mL) at 0 °C, trichloroacetonitrile (19.8 µL, 0.198 mmol) was added followed by DBU (0.3 µL, 0.00198 mmol). After 50 min, the solution was slightly concentrated under reduced pressure and immediately purified by flash silica gel column chromatography to afford the imidate **3-38** in 82% yield (33.5 mg, 0.0162 mmol) as a white solid; R_f = 0.47 (hexane/EtOAc, 6:4).
$[\alpha]_D^{20}$**:** -4.48 (c = 1, $CHCl_3$).
IR (ATR) ν(cm^{-1}) 3056, 2931, 1743 (C=O), 1721 (C=O), 1677, 1603, 1510, 1472, 1429, 1364, 1273, 1153, 1126, 1105, 1055, 975, 895, 858, 818, 797, 754, 706.
^{1}H NMR (400 MHz, $CDCl_3$) δ (ppm) 8.62 (s, 1H, N$\underline{H}$), 7.59 – 7.84 (m, 31H, H Ar), 7.26 – 7.54 (m, 37H, H Ar), 7.11 (dd, *J* = 8.4, 1.7 Hz, 1H, H Ar), 6.19 (s, 1H, ManI-1), 5.68 (s, 1H, ManIII-2), 5.53 (s, 1H, ManI-2), 5.32 (s, 1H, ManIII-1), 5.10 (d, *J* = 11.1 Hz, 1H, C$\underline{H}_2$ Nap), 4.75 – 5.02 (m, 10H, C$\underline{H}_2$ Nap, ManII-1), 4.60 – 4.73 (m, 3H, C$\underline{H}_2$ Nap), 4.50 – 4.60 (m, 2H, C$\underline{H}_2$ Nap), 4.45 (d, *J* = 12.4 Hz, 1H, C$\underline{H}_2$ Nap), 4.26 (s, 1H, ManII-2), 4.14 – 4.21 (m, 1H, ManIII-3), 4.13 (dd, *J* = 11.3, 3.2 Hz, 1H, ManIII-6a), 4.08 (dd, *J* = 9.2, 3.3 Hz, 1H, ManI-3), 3.86 – 4.04 (m, 8H, ManII-3, ManIII-6b, ManI-6a), 3.81 – 3.88 (m, 2H, ManI-4, ManII-5), 3.58 – 3.70 (m, 2H, ManI-6b, ManII-6a), 3.54 (d, *J* = 10.1 Hz, 1H, ManII-6b), 2.49 – 2.68 (m, 8H, C$\underline{H}_2$-C$\underline{H}_2$ Lev x2), 2.06 (s, 3H, C$\underline{H}_3$ Lev), 2.03 (d, *J* = 5.9 Hz, 3H, C$\underline{H}_3$ Lev), 1.07 (s, 9H, C$\underline{H}_3$ tBu).
^{13}C NMR (101 MHz, $CDCl_3$) δ (ppm) 206.4 ($\underline{C}$=O Lev), 206.0 ($\underline{C}$=O Lev), 172.2 ($\underline{C}$=O Lev), 172.1 ($\underline{C}$=O Lev), 159.4 ($\underline{C}$=NH), 136.3, 136.2, 136.08, 136.06, 135.94, 135.74, 135.67, 135.5, 134.9, 133.9, 133.5, 133.4, 133.33, 133.31, 133.27, 133.23, 133.19, 133.04, 133.01, 132.9 (C_q Ar),

129.8, 128.4, 128.3, 128.21, 128.16, 128.12, 128.08, 128.05, 128.01, 127.98, 127.9, 127.84, 127.80, 127.75, 127.70, 127.66, 127.6, 126.9, 126.6, 126.5, 126.41, 126.36, 126.3, 126.23, 126.16, 126.13, 126.07, 126.04, 126.00, 125.96, 125.9, 125.84, 125.76, 125.7 (C Ar), 99.2 (ManIII-1), 99.0 (ManII-1), 95.0 (ManI-1), 90.8 (CCl_3), 80.0 (ManII-3), 78.2 (ManIII-3), 77.7 (ManI-3), 75.5, 75.3, 75.2, 74.5, 74.2 (ManII-2), 73.7, 73.6, 73.5, 73.2, 72.2 (ManII-5, 71.9, 71.8, 69.3 (ManIII-2), 69.1 (ManII-6), 67.8 (ManI-2), 66.2 (ManI-6), 63.1 (ManIII-6), 38.2 ($\underline{C}H_2$ Lev), 37.8 ($\underline{C}H_2$ Lev), 29.9 ($\underline{C}H_3$ Lev), 29.8 ($\underline{C}H_3$ Lev), 28.3 ($\underline{C}H_2$ Lev), 28.0 ($\underline{C}H_2$ Lev), 26.9 ($\underline{C}H_3$- tBu).
HRMS: $[M+Na]^+$ cald 2084.6980; found 2084.6948.

2-*O*-levulinyl-6-*O*-*tert*-butyldiphenylsilyl-3,4-di-*O*-(2-naphthyl)methyl-α-D-mannopyranosyl-(1→2)-3,4,6-tri-*O*-(2-naphthyl)methyl-α-D-mannopyranosyl-(1→6)-2-*O*-levulinyl-3,4-di-*O*-(2-naphthyl)methyl-α-D-mannopyranosyl-(1→4)-2-azido-2-deoxy-3,6-di-*O*-(2-naphthyl)methyl-α-D-glucopyranosyl-(1→6)-1-*O*-allyl-2,3,4,5-tetra-O-(2-naphthyl)methyl-D-*myo*-inositol (3-39)

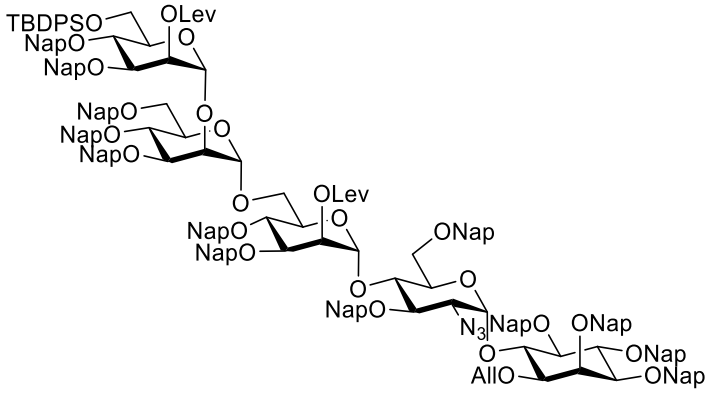

A solution of the pseudodisaccharide glycosyl acceptor **2-46** (105 mg, 0.0839 mmol) and the trimannoside glycosyl donor **3-38** (225 mg, 0.109 mmol) in a 6:1 Et_2O/DCM anhydrous mixture (1.4 mL) was stirred at room temperature for 8 min. The mixture was cooled to -11 °C, and TMSOTf (4.6 µL, 0.0252 mmol) was added. After stirring for 1.5 h, the reaction was quenched with Et_3N (5 µL), and volatiles were removed under reduced pressure. The obtained residue was purified by flash silica gel column chromatography to afford the pseudopentasaccharide **3-39** (252 mg, 0.0801 mmol) as a white foam in 96% yield; R_f = 0.38 (heptane/EtOAc, 6:4).

Alternatively, to a solution of diol **3-25** (27.3 mg, 9.24 µmol) and DMAP (1 mg, 8.18 µmol) in DCM (0.2 mL), LevOH (2.6 µL, 25.9 µmol) and DIC (4 µL, 25.9 µmol) were added at room temperature. The reaction mixture was stirred overnight before it was washed with water. The aqueous phase was extracted with DCM. Organic layers were combined, washed with 1 M aq. citric acid followed by brine, dried with Na_2SO_4, filtered, and concentrated. The residue was purified by flash column chromatography on silica gel to afford the fully protected pseudopentasaccharide **3-39** in 69% yield (20.0 mg, 6.41 µmol) as a white residue.

^{1}H NMR (400 MHz, $CDCl_3$) δ (ppm) 7.06 – 7.80 (m, 112H, Ar), 6.98 (t, *J* = 7.5 Hz, 1H, Ar), 6.89 (d, *J* = 8.0 Hz, 2H, Ar), 5.78 – 5.92 (m, 1H, -C<u>H</u>= Allyl), 5.76 (d, *J* = 3.7 Hz, 1H, Glc-1), 5.57 (s, 1H, ManI-2), 5.29 – 5.36 (m, 2H, ManIII-2, ManIII-1), 5.10 – 5.19 (m, 2H, ManI-1, =C<u>H</u>$_{2a}$ Allyl), 5.00 – 5.09 (m, 2H, =C<u>H</u>$_{2b}$ Allyl, C<u>H</u>$_2$ Nap), 4.93 – 5.03 (m, 5H, C<u>H</u>$_2$ Nap), 4.68 – 4.90 (m, 10H, C<u>H</u>$_2$ Nap), 4.64 (d, *J* = 11.4 Hz, 1H, C<u>H</u>$_2$ Nap), 4.62 (s, 1H, ManII-1), 4.58 (d, *J* = 11.9 Hz, 1H, C<u>H</u>$_2$ Nap), 4.39 – 4.48 (m, 2H C<u>H</u>$_2$ Nap), 4.29 – 4.40 (m, 4H, C<u>H</u>$_2$ Nap), 4.27 (d, *J* = 12.3 Hz, 1H, C<u>H</u>$_2$ Nap), 4.09 – 4.23 (m, 5H, ManII-2), 3.99 – 4.10 (m, 4H, ManI-3, ManIII-6a), 3.85 – 4.02 (m, 7H, C<u>H</u>$_2$ Nap, -C<u>H</u>$_2$- Allyl, ManII-3), 3.73 – 3.85 (m, 3H, ManIII-6b), 3.53 – 3.72 (m, 4H, ManI-6a, ManIII-3), 3.33 – 3.50 (m, 5H, ManII-6a), 3.32 (dd, *J* = 11.1, 4.1 Hz, 1H, Glc-6a), 3.22 – 3.20 (m, 2H, ManII-6b, Glc-2), 3.15 (dd, 1H, Glc-6b), 3.06 (d, *J* = 10.6 Hz, 1H, ManI-6b), 2.44 – 2.60 (m, 4H, C<u>H</u>$_2$-C<u>H</u>$_2$ Lev), 2.25 – 2.38 (m, 1H, CH$_2$-C<u>H</u>$_2$ Lev), 1.96 – 2.17 (m, 3H, C<u>H</u>$_2$-C<u>H</u>$_2$ Lev), 1.94 (s, 3H, C<u>H</u>$_3$ Lev), 1.72 (s, 3H, C<u>H</u>$_3$ Lev), 0.98 (s, 10H, C<u>H</u>$_3$ tBu).

^{13}C NMR (101 MHz, $CDCl_3$) δ (ppm) 206.3 (<u>C</u>=O Lev), 205.8 (<u>C</u>=O Lev), 172.0 (<u>C</u>=O Lev), 171.8 (<u>C</u>=O Lev), 163.4, 136.4, 136.25, 136.21, 136.05, 136.00, 135.97, 135.95, 135.88, 135.72, 135.68, 135.66, 135.60, 135.49, 135.17 (C_q Ar), 134.21 (-<u>C</u>H= Allyl), 133.82, 133.34, 133.32, 133.30, 133.26, 133.22, 133.16, 133.12, 133.10, 133.06, 133.00, 132.96, 132.92, 132.88, 132.84, 132.79, 132.77, 132.54 (C_q Ar), 129.74, 129.69, 128.35, 128.26, 128.14, 128.11, 128.08, 128.01, 127.96, 127.93, 127.91, 127.89, 127.85, 127.81, 127.75, 127.69, 127.63, 127.60, 127.58, 127.52, 127.08, 126.82, 126.76, 126.68, 126.59, 126.56, 126.44, 126.38, 126.33, 126.27, 126.24, 126.22, 126.19, 126.16, 126.10, 126.08, 126.04, 125.96, 125.93, 125.89, 125.86, 125.84, 125.79, 125.73, 125.62, 125.54, 125.46, 125.32, 124.83 (C Ar), 117.3 (=<u>C</u>H$_2$ Allyl), 99.1 (ManI-1), 98.9 (ManII-1, ManIII-1), 97.6 (Glc-1), 91.8, 82.0, 81.9, 81.6, 80.7, 80.5, 79.7, 78.4, 78.1, 75.9, 75.4, 75.1, 75.0, 74.9, 74.7, 74.2, 74.0, 73.9, 73.6 (ManII-2), 73.5, 73.3, 73.2, 73.1, 73.0, 72.6, 72.0, 71.8, 71.7, 71.6, 71.5 (-<u>C</u>H$_2$- Allyl), 71.3, 71.0, 69.8, 69.2 (ManI-2), 68.99 (ManII-6), 68.98 (ManIII-2), 68.8 (Glc-6), 66.1 (ManI-6), 63.4 (Glc-2), 62.8 (ManIII-6), 38.1 (<u>C</u>H$_2$ Lev), 37.5 (<u>C</u>H$_2$ Lev), 29.8 (<u>C</u>H$_3$ Lev), 29.6 (<u>C</u>H$_3$ Lev), 28.2 (<u>C</u>H$_2$ Lev), 27.8 (<u>C</u>H$_2$ Lev), 26.9 (<u>C</u>H$_3$- tBu).

HRMS: $[M+Na]^+$ cald 3171.3073; found 3171.3130.

400 MHz NMR Data		**Glc-1**	**ManI-1**	**ManII-1**	**ManIII-1**
Chemical shift (ppm)	^{13}C	97.6	99.2	98.9	98.9
	^{1}H	5.76	5.13	4.62	5.33

2-*O*-levulinyl-6-*O*-*tert*-butyldiphenylsilyl-3,4-di-*O*-(2-naphthyl)methyl-α-D-mannopyranosyl-(1→2)-3,4,6-tri-*O*-(2-naphthyl)methyl-α-D-mannopyranosyl-(1→6)-2-*O*-levulinyl-3,4-di-*O*-(2-naphthyl)methyl-α-D-mannopyranosyl-(1→4)-2-azido-2-deoxy-3,6-di-*O*-(2-naphthyl)methyl-α-D-glucopyranosyl-(1→6)-2,3,4,5-tetra-O-(2-naphthyl)methyl-D-*myo*-inositol (3-40)

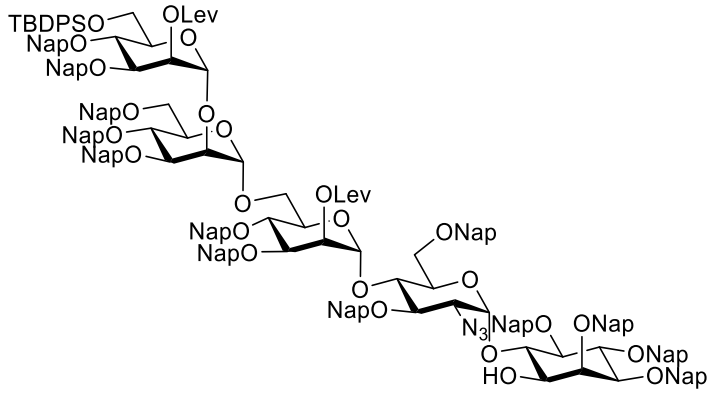

A solution of $[IrCOD(PPh_2Me)_2]PF_6$ (6.8 mg, 0.008 mmol) in THF (3 mL) was stirred under hydrogen at room temperature until it changed from red to colorless to pale yellow. The hydrogen atmosphere was exchanged with Ar. This solution was then added into a THF (3 mL) solution of pseudopentasaccharide **3-39** (0.252 g, 0.08 mmol). The reaction was stirred at room temperature for 3 h before the solvent was removed and the residue was dissolved in acetone/water 9:1 (3 mL). Mercury(II) chloride (0.130 g, 0.480 mmol) and mercury(II) oxide (3.5 mg, 0.016 mmol) were added. After 2 h, the solvent was removed. The residue was dissolved in DCM and washed with saturated $NaHCO_3$, dried over Na_2SO_4, filtered, and concentrated. The obtained crude was purified by flash silica gel column chromatography to give the alcohol **3-40** (233 mg, 0.0750 mmol) as a white foam in 94% yield; R_f = 0.36 (heptane/EtOAc, 6:4).

Alternatively, to a solution of the allylated pseudopentasaccharide **3-39** (0.107 mg, 0.0341 mmol) in a 1:1 DCM/MeOH anhydrous mixture (1.4 mL), $PdCl_2$ (3.4 mg, 0.0194 mmol) was added at room temperature. After 5 h, the mixture was filtered through a pad of Celite, and the volatiles were evaporated *in vacuo*. The crude residue was purified by flash silica gel column chromatography to obtain alcohol **3-40** in 82% yield (87 mg, 0.028 mmol) as a white foam.

^{1}H NMR (400 MHz, $CDCl_3$) δ (ppm) 7.62 – 7.88 (m, 42H, Ar), 7.50 – 7.62 (m, 22H, Ar), 7.28 – 7.50 (m, 54H, Ar), 7.08 – 7.24 (m, 16H, Ar), 6.98 – 7.02 (m, 1H, Ar), 5.62 – 5.68 (m, 1H, ManI-2), 5.41 – 5.49 (m, 3H, ManIII-1, ManIII-2, Glc-1), 5.21 (d, *J* = 1.8 Hz, 1H, ManI-1), 5.18 (d, *J* = 11.8 Hz, 1H, C$\underline{H}_2$ Nap), 4.92 – 5.16 (m, 9H, C$\underline{H}_2$ Nap), 4.84 – 4.94 (m, 7H, C$\underline{H}_2$ Nap), 4.75 – 4.85 (m, 4H, C$\underline{H}_2$ Nap), 4.75 (s, 1H, ManII-1), 4.64 – 4.74 (m, 2H, C$\underline{H}_2$ Nap), 4.42 – 4.57 (m, 6H, C$\underline{H}_2$ Nap), 4.17 – 4.33 (m, 10H, ManII-2, C$\underline{H}_2$ Nap), 4.02 – 4.18 (m, 8H, ManI-3, ManIII-6a), 3.97 – 4.05 (m, 4H,), 3.81 – 3.94 (m, 6H, ManI-6a, ManIII-6b, ManIII-3), 3.63 – 3.80 (m, 6H), 3.59 (dd, *J* = 9.8, 2.3 Hz, 1H), 3.44 – 3.54 (m, 3H, Glc-2), 3.25 – 3.45 (m, 5H, ManI-6b, ManII-6, Glc-6), 3.22 (d, *J*

= 6.3 Hz, 1H), 2.54 – 2.64 (m, 4H, $C\underline{H}_2$-$C\underline{H}_2$ Lev), 2.36 – 2.46 (m, 1H, CH_2-$C\underline{H}_2$ Lev), 2.17 – 2.25 (m, 2H, $C\underline{H}_2$-$C\underline{H}_2$ Lev), 2.01 – 2.08 (m, 5H, $C\underline{H}_2$-$C\underline{H}_2$ Lev, $C\underline{H}_3$ Lev), 1.82 (s, 3H, $C\underline{H}_3$ Lev), 1.06 (s, 12H, $C\underline{H}_3$ tBu).

^{13}C NMR (101 MHz, $CDCl_3$) δ (ppm) 206.3 (C=O Lev), 205.8 (C=O Lev), 172.0 (C=O Lev), 171.8 (C=O Lev), 136.4, 136.13, 136.06, 136.03, 135.7, 135.6, 135.3, 135.2, 133.9, 133.42, 133.36, 133.32, 133.28, 133.19, 133.1, 133.0, 132.9 (C_q Ar), 129.8, 128.4, 128.2, 128.1, 128.03, 128.00, 127.85, 127.77, 127.70, 127.1, 127.0, 126.8, 126.64, 126.59, 126.5, 126.32, 126.27, 126.1, 126.02, 125.96, 125.9, 125.85, 125.79, 125.69, 125.4, 125.2 (C Ar), 99.2 (ManI-1), 99.0 (ManII-1), 98.8 (ManIII-1), 98.2 (Glc-1), 82.0, 81.5, 81.2, 80.9, 80.7, 80.0, 78.2, 75.9, 75.4, 75.2, 75.1, 74.8, 74.6, 74.1, 73.7 (ManII-2), 73.4, 73.2, 72.0, 71.8, 71.6, 70.7, 69.0 (ManI-2, ManII-6, ManIII-2, Glc-6), 66.4 (ManI-6), 64.5 (Glc-2), 62.9 (ManIII-6), 38.2 ($C\underline{H}_2$ Lev), 37.6 ($C\underline{H}_2$ Lev), 29.9 ($C\underline{H}_3$ Lev), 29.6 ($C\underline{H}_3$ Lev), 28.3 ($C\underline{H}_2$ Lev), 27.9 ($C\underline{H}_2$ Lev), 27.0 ($C\underline{H}_3$- tBu).

HRMS: $[M+2Na]^{2+}$ cald 1577.1329; found 1577.1335; $[M+Na]^{+}$ cald 3131.276080; found 3131.3054.

400 MHz NMR Data		Glc-1	ManI-1	ManII-1	ManIII-1
Chemical shift (ppm)	^{13}C	98.2	99.2	99.0	98.8
	^{1}H	5.45	5.21	4.75	5.45

2-*O*-levulinyl-3,4-di-*O*-(2-naphthyl)methyl-α-D-mannopyranosyl-(1→2)-3,4,6-tri-*O*-(2-naphthyl)methyl-α-D-mannopyranosyl-(1→6)-2-*O*-levulinyl-3,4-di-*O*-(2-naphthyl)methyl-α-D-mannopyranosyl-(1→4)-2-azido-2-deoxy-3,6-di-*O*-(2-naphthyl)methyl-α-D-glucopyranosyl-(1→6)-1-*O*-(2-oleoyl-1-stearoyl-*sn*-glycero-3-phosphonate)-2,3,4,5-tetra-O-(2-naphthyl)methyl-D-*myo*-inositol (3-42)

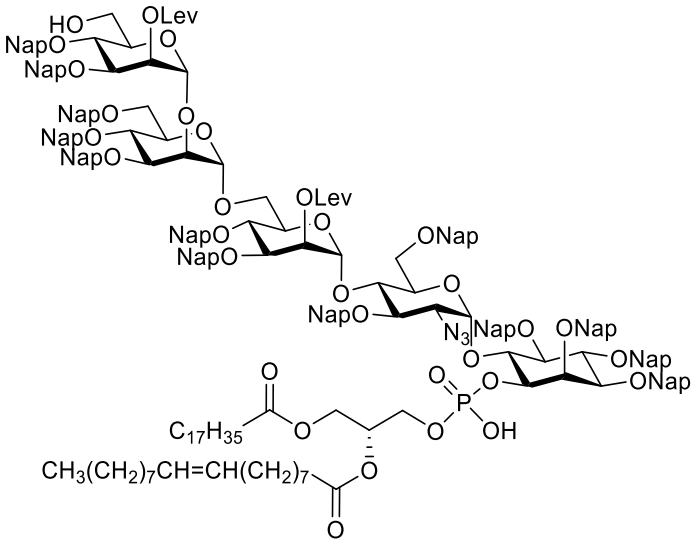

Alcohol **3-40** (98 mg, 0.0315 mmol) and H-phosphonate **2-8** (87% purity, 45.7 mg, 0.0504 mmol) were co-evaporated with anhydrous pyridine (4 x 4 mL) and placed under high vacuum for 1 h. The residue was dissolved in anhydrous pyridine (2 mL) and PivCl (10 µL, 0.0819 mmol) was

added. The reaction mixture was stirred for 2 h at room temperature before water (136 µL) and iodine (24 mg, 0.0945 mmol) were added. The reaction mixture was stirred for an additional hour, and solid $Na_2S_2O_3$ was added until the color of the reaction changed from orange to yellow. Volatiles were removed under reduced pressure. The remaining was triturated with DCM to remove $Na_2S_2O_3$, and concentrated. Purification was performed by flash silica gel column chromatography (eluting with MeOH/DCM 1:90 and gradually increasing the polarity to 1:10). The obtained compound was dissolved in chloroform, and Amberlite IR 120 (Na^+) form resin was added. After stirring for 5 min, the solution was filtered and concentrated to afford the lipidated pseudopentasaccharide **3-41** in 92% yield (0.111 mg, 0.0291 mmol) as a white foam; R_f = 0.46 (MeOH/DCM, 1:10). **HRMS:** $[M+Na+H]^{2+}$ cald 1908.3966; found 1908.3983; $[M+Na]^+$ cald 3815.7855; found 3815.9348.

In a 2 mL Eppendorf, the fully protected lipidated pseudopentasaccharide **3-41** (73.5 mg, 0.0192 mmol) was dissolved in THF (200 µL) and 27.8 µL (0.212 mmol) of 70 % HF·Pyridine complex was added. The reaction mixture was stirred at room temperature for 24 h before it was slowly quenched with aq. sat. $NaHCO_3$, diluted with brine and water, and extracted with DCM. The organic layer was dried over Na_2SO_4, filtered and concentrated. The crude material was purified by flash silica gel column chromatography followed by LH-20 size exclusion chromatography eluting with MeOH/$CHCl_3$ 1:2 to furnish the alcohol **3-42** (62 mg, 0.0174 mmol) in 90% yield as a white foam; R_f = 0.33 (MeOH/DCM, 1:20).

^{1}H NMR (400 MHz, $CDCl_3$) δ (ppm) 7.86 – 7.93 (m, 3H, Ar), 7.28 – 7.86 (m, 162H, Ar), 7.05 – 7.24 (m, 25H, Ar), 6.93 – 7.01 (m, 2H, Ar), 6.03 (d, *J* = 3.8 Hz, 1H, Glc-1), 5.54 – 5.61 (m, 1H, ManI-2), 5.24 – 5.39 (m, 10H, ManIII-1, ManIII-2, -C<u>H</u>=C<u>H</u>- Oleoyl, C<u>H</u> sn-2), 5.15 – 5.25 (m, 4H, C<u>H</u>$_2$ Nap), 4.78 – 5.07 (m, 23H, C<u>H</u>$_2$ Nap, ManI-1, ManII-1), 4.61 – 4.80 (m, 13H, C<u>H</u>$_2$ Nap), 4.25 – 4.62 (m, 23H, C<u>H</u>$_2$ Nap, C<u>H</u>$_{2a}$ sn-1), 4.79 – 3.28 (m, 32H, C<u>H</u>$_2$ Nap, C<u>H</u>$_{2b}$ sn-1, C<u>H</u>$_2$ sn-3, Glc-3, ManI-3, ManII-2), 3.35 – 3.81 (m, 27H, Glc-6, ManI-6a, ManII-6, ManIII-6), 3.17 – 3.34 (m, 3H, ManI-6b, Glc-2), 2.51 – 2.63 (m, 5H), 2.13 – 2.38 (m, 19H, 2 x O-COC<u>H</u>$_2$-CH_2 lipid), 1.92 – 2.09 (m, 19H, C<u>H</u>$_3$ Lev, -C<u>H</u>$_2$-CH=CH-C<u>H</u>$_2$- Oleoyl), 1.84 (s, 3H, C<u>H</u>$_3$ Lev), 1.58 – 1.71 (m, 16H), 1.46 – 1.55 (m, 9H, 2 x O-COCH_2-C<u>H</u>$_2$ lipid), 1.15 – 1.38 (m, 191H, -C<u>H</u>$_2$- lipid), 0.84 – 0.97 (m, 47H, 2 x C<u>H</u>$_3$ lipid).

^{13}C NMR (101 MHz, $CDCl_3$) δ (ppm) complemented with HSQC 206.4 (<u>C</u>=O Lev), 206.2 (<u>C</u>=O Lev), 171.9 (<u>C</u>=O), 136.1, 133.43, 133.40, 133.31, 133.26, 132.99, 132.92 (C_q Ar), 130.06 (-<u>C</u>H=CH- Oleoyl), 129.88 (-CH=<u>C</u>H- Oleoyl), 128.11, 128.06, 128.03, 128.01, 127.91, 127.86, 127.76, 127.73, 127.70, 127.10, 126.65, 126.54, 126.37, 126.16, 126.09, 126.06, 125.99, 125.95, 125.84, 125.76, 125.73, 125.61 (C Ar), 99.8 (ManI-1 ManIII-1), 99.5 (ManII-1), 97.2 (Glc-1), 80.1 (Glc-3), 78.1, 75.5 (ManII-2),75.3, 74.3, 73.4, 72.5, 71.8, 70.7 (<u>C</u>H sn-2), 69.4 (ManI-2, ManIII-2), 69.2 (Glc-6, ManII-6), 65.8 (ManI-6), 63.2 (Glc-2), 62.9 (<u>C</u>H_2 sn-1), 61.9 (ManIII-6), 38.1, 37.7,

34.3, 34.1, 32.1, 32.0, 29.91, 29.86, 29.84, 29.80, 29.71, 29.67, 29.6, 29.51, 29.46, 29.4, 29.3, 29.3, 28.25, 27.4, 27.3, 27.0, 25.2, 25.0, 22.83, 22.82, 20.2.

^{31}P NMR (400 MHz, $CDCl_3$) δ (ppm) -1.69.

HRMS: $[M+Na2]^{2+}$ cald 1800.3287; found 1800.3247; $[M+H]^+$ cald 3555.6858; found 3555.7234.

400 MHz NMR Data		Glc-1	ManI-1	ManII-1	ManIII-1
Chemical shift (ppm)	^{13}C	97.2	99.8	99.5	98.8
	^{1}H	6.03	5.01	4.93	5.37

2-Hydroxyethyl 4-methylbenzenesulfonate (3-44)

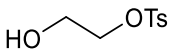

P-toluenesulfonyl chloride (1 g, 5.24 mmol) was added to ethylene glycol **3-43** (18 mL, 328 mmol), and the suspension was stirred at room temperature for 5 min before triethylamine (0.73 mL, 5.24 mmol) was added dropwise. After 1 h, the reaction was quenched with water (40 mL) and extracted with DCM. The organic layers were combined, washed with brine, dried over Na_2SO_4, filtered, and concentrated under reduced pressure. The resulting yellow oil was purified by flash silica gel column chromatography to afford the alcohol **3-44** in 93% yield (1.06 g, 4.90 mmol) as a turbid oil; R_f = 0.30 (heptane/EtOAc, 1:1).

^{1}H NMR (400 MHz, $CDCl_3$) δ (ppm) 7.83 – 7.79 (m, 2H, Ar), 7.38 – 7.33 (m, 2H, Ar), 4.18 – 4.11 (m, 2H, -C$\underline{H}_2$-CH_2-OH), 3.86 – 3.77 (m, 2H, -CH_2-C$\underline{H}_2$-OH), 2.45 (s, 3H, C$\underline{H}_3$), 2.09 – 2.01 (m, 1H, $\underline{H}$O).

^{13}C NMR (101 MHz, $CDCl_3$) δ (ppm) 145.25 (C_q Ar), 132.79 (C_q Ar), 130.09 (C Ar), 128.11 (C Ar), 71.74 (-$\underline{C}H_2$-CH_2-OH), 60.90 (-CH_2-$\underline{C}H_2$-OH), 21.79 ($\underline{C}H_3$).

2-Azidoethanol (3-45)

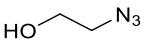

A mixture of 2-Hydroxyethyl 4-methylbenzenesulfonate **3-44** (1.05 g, 4.85 mmol) and sodium azide (631 mg, 9.70 mmol) in water/acetone 1:1 (3.66 mL) was stirred at 65 °C overnight. The reaction was diluted with aq. sat. $NaHCO_3$ and extracted with diethyl ether. The solvent was removed under reduced pressure to give **3-45** as a slightly yellow liquid in 79% yield (334 mg, 3.83 mmol), which was used in the next step without further purification.

^{1}H NMR (400 MHz, $CDCl_3$) δ (ppm) 3.74 – 3.83 (m, 2H, -C$\underline{H}_2$-OH), 3.42 – 3.48 (m, 2H, -C$\underline{H}_2$-N_3).

HSQC (101 MHz, $CDCl_3$) δ (ppm) 61.6 (-$\underline{C}H_2$-OH), 53.5 (-$\underline{C}H_2$-N_3).

2-Azidoethyl H-phosphonate (3-3)

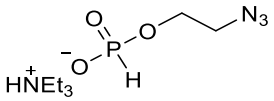

To a mixture of phosphonic acid (139 mg, 1.69 mmol) and 2-azidoethanol **3-45** (123 mg, 1.41 mmol) in anhydrous pyridine (9.4 mL), pivaloyl chloride (0.207 mL, 1.69 mmol) was added, and the mixture was stirred at room temperature overnight. Volatiles were removed under reduced pressure and the crude product was purified by column using silica gel deactivated with triethylamine (elution with MeOH/DCM 1:90 and gradually increasing the polarity to 1:10) to afford the H-phosphonate **3-3** in 80% yield (348 mg, 1.13 mmol, 82% purity; excess triethylammonium salt) as a white solid; R_f = 0.24 (MeOH/DCM, 1:10).

^{1}H NMR (400 MHz, $CDCl_3$) δ (ppm) 11.61 (s, 1H, H-NEt_3), 7.47 (s, 0.5H, H-P), 5.87 (s, 0.5H, H-P), 3.80 – 3.96 (m, 2H, -CH_2-O-), 3.29 (t, *J* = 5.0 Hz, 2H, -CH_2-N_3), 2.80 – 3.11 (m, 6H, CH_2 Et_3N), 1.20 (t, *J* = 7.3 Hz, 9H, CH_3 Et_3N).

^{13}C NMR (101 MHz, $CDCl_3$) δ (ppm) 62.4 (-CH_2-O-), 51.3 (-CH_2-N_3), 45.6 (CH_2 Et_3N), 8.4 (CH_3 Et_3N).

^{31}P NMR (162 MHz, $CDCl_3$) δ (ppm) 3.23.

6-*O*-(2-azidoethylphosphonato)-2-*O*-levulinyl-3,4-di-*O*-(2-naphthyl)methyl-α-D-mannopyranosyl-(1→2)-3,4,6-tri-*O*-(2-naphthyl)methyl-α-D-mannopyranosyl-(1→6)-2-*O*-levulinyl-3,4-di-*O*-(2-naphthyl)methyl-α-D-mannopyranosyl-(1→4)-2-azido-2-deoxy-3,6-di-*O*-(2-naphthyl)methyl-α-D-glucopyranosyl-(1→6)-1-*O*-(2-oleoyl-1-stearoyl-*sn*-glycero-3-phosphonate)-2,3,4,5-tetra-O-(2-naphthyl)methyl-D-*myo*-inositol (3-46)

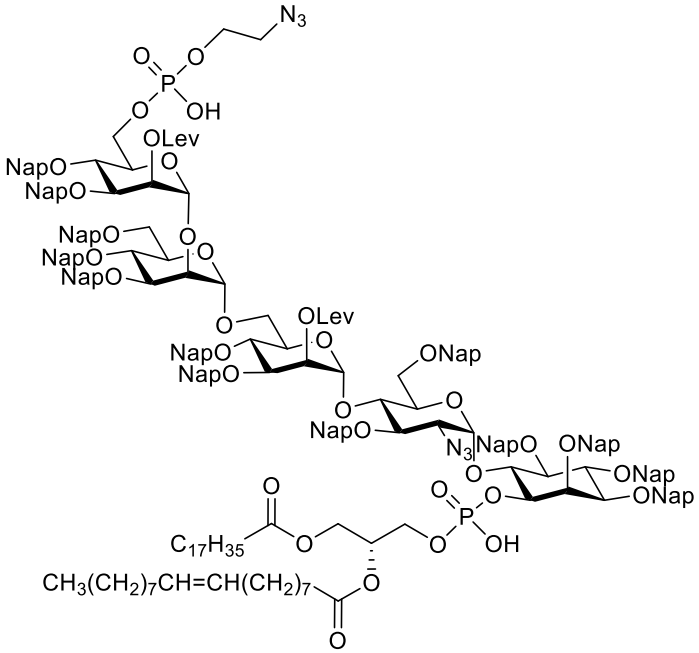

Alcohol **3-42** (94.3 mg, 0.0265 mmol) and H-phosphonate **3-3** (36.7 mg, 0.119 mmol) were co-evaporated with anhydrous pyridine (3 x 1 mL) and placed under high vacuum for 1 h. The residue

was dissolved in anhydrous pyridine (1.6 mL) and PivCl (24.3 µL, 0.199 mmol) was added. The reaction mixture was stirred for 3 h at room temperature before water (174 µL) and iodine (40.4 mg, 0.159 mmol) were added. It was stirred overnight, and solid $Na_2S_2O_3$ was added until the color of the reaction changed from orange to yellow. Volatiles were removed under reduced pressure. The remaining was triturated with DCM to remove $Na_2S_2O_3$, and concentrated. Purification was performed by flash silica gel column chromatography (eluting with MeOH/DCM 1:90 and gradually increasing the polarity to 1:20) followed by LH-20 size exclusion chromatography eluting with MeOH/$CHCl_3$ 1:2 to give the fully protected *fp*GPI **3-46** in 98% yield (97.5 mg, 0.026 mmol) as a white foam; R_f = 0.66 (MeOH/DCM, 1:10).

^{1}H NMR (400 MHz, $CDCl_3$) δ (ppm) 7.26 – 7.88 (m, 302H, Ar), 6.01 – 6.10 (m, 1H, Glc-1), 5.63 (s, 1H, ManI-2), 3.11 – 5.43 (m, 272H), 2.49 – 2.64 (m, 10H), 1.67 – 2.36 (m, 76H), 1.45 – 1.65 (m, 22H), 1.07 – 1.34 (m, 301H), 0.84 – 0.91 (m, 49H).

^{13}C NMR (101 MHz, $CDCl_3$) δ (ppm) complemented with HSQC 206.6 (C=O Lev), 205.9 (C=O Lev), 173.5 (C=O), 173.5 (C=O), 171.9 (C=O Lev), 136.32, 136.16, 135.91, 135.74, 135.32, 133.47, 133.41, 133.37, 133.31, 133.24, 133.00, 132.95, 132.91, 132.88 (C_q Ar), 130.08 (-CH=CH- Oleoyl), 129.88 (-CH=CH- Oleoyl), 128.15, 128.10, 128.03, 127.97, 127.90, 127.85, 127.81, 127.77, 127.74, 127.72, 127.67, 127.62, 126.45, 126.16, 126.11, 126.01, 125.95, 125.89, 125.82, 125.70, 125.60 (C Ar), 99.6 (ManI-1 ManIII-1), 98.9 (ManII-1), 96.6 (Glc-1), 82.2, 81.0, 75.8, 75.3, 74.4, 73.4, 72.6, 71.7, 70.7 (CH sn-2), 69.8, 69.3 (ManI-2, ManIII-2), 69.1 (Glc-6, ManII-6), 66.2 (ManI-6), 64.2, 63.0 (Glc-2), 45.4, 38.2, 37.7, 37.5, 34.4, 34.2, 33.8, 32.1, 32.0, 30.3, 30.2, 29.91, 29.86, 29.84, 29.81, 29.72, 29.67, 29.6, 29.51, 29.46, 29.4, 29.30, 29.28, 29.22, 29.1, 28.3, 28.0, 27.4, 27.3, 27.0, 26.8, 25.1, 25.00, 24.98, 23.3, 22.84, 22.82, 20.2, 14.33, 14.27, 13.8, 8.5.

^{31}P NMR (400 MHz, $CDCl_3$) δ (ppm) -0.15, -1.37.

HRMS: $[M-2H]^{2-}$ cald 1850.8306; found 1850.8174.

400 MHz NMR Data		**Glc-1**	**ManI-1**	**ManII-1**	**ManIII-1**
Chemical shift (ppm)	^{13}C	96.6	99.6	98.9	99.6
	^{1}H	6.06	5.10	4.81	5.40

6-*O*-(2-aminoethylphosphonato)-α-D-mannopyranosyl-(1→2)-α-D-mannopyranosyl-(1→6)-α-D-mannopyranosyl-(1→4)-2-amino-2-deoxy-α-D-glucopyranosyl-(1→6)-1-*O*-(2-oleoyl-1-stearoyl-*sn*-glycero-3-phosphonate)-D-*myo*-inositol (3-1)

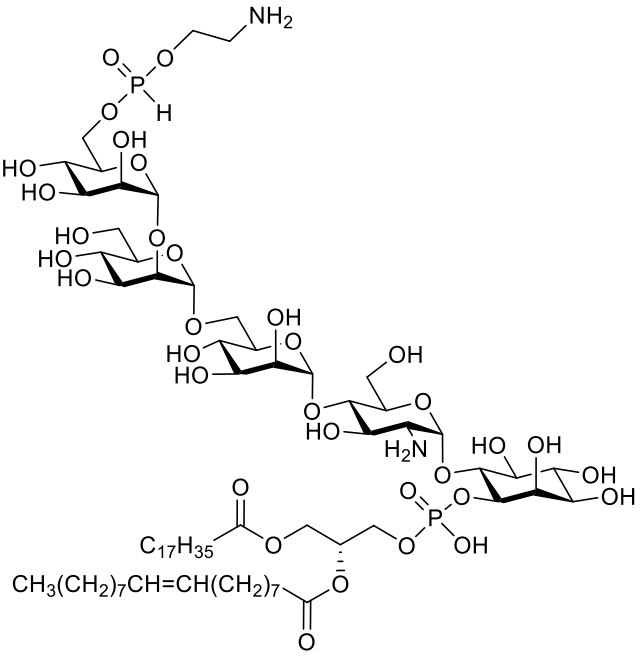

DDQ (100 mg, 0.441 mmol) was added to a solution of the protected GPI **3-46** (91.9 mg, 0.0245 mmol) in a 4:1 DCM/MeOH mixture (1.1 mL). The reaction mixture was stirred at room temperature overnight before volatiles were removed under reduced pressure. The residue was purified by LH-20 size exclusion chromatography eluting with MeOH/$CHCl_3$/H_2O 3:3:1. It was dissolved in anhydrous THF (0.5 mL) and pyridine (95.3 µL, 1.18 mmol) was added followed by AcOH (63.3 µL, 1.11 mmol) and hydrazine acetate (13.5 mg, 0.147 mmol). The reaction mixture was stirred overnight before it was quenched with acetone, and volatiles were removed under reduced pressure. To the obtained *O*-deprotected glycolipid, 0.49 mL of a 1 M solution of $P(CH_3)_3$ in THF were added followed by water (200 µL). After 2 h, the brown oily solid formed during the reaction was removed from the mixture and triturated with MeOH to afford the final *fp*GPI **3-1** in 89% yield (35.7 mg, 0.0218 mmol) as a slightly pink solid. For the NMR sample, the compound was dissolved in a 3:3:1 CD_3OD/$CDCl_3$/D_2O mixture.

^{1}H NMR (400 MHz, CD_3OD) δ (ppm) 5.21 (d, *J* = 3.9 Hz, 1H, Glc-1), 5.02 – 5.07 (m, 2H, -C<u>H</u>=C<u>H</u>- Oleoyl), 4.97 (d, *J* = 5.3 Hz, 1H, C<u>H</u> sn-2), 4.88 (s, 1H, Man-1), 4.83 (d, *J* = 8.6 Hz, 1H, Man-1), 4.67 (s, 1H, Man-1), 4.13 (d, *J* = 12.3 Hz, 1H, C<u>H</u>$_{2a}$ sn-1), 3.67 – 3.93 (m, 14H, C<u>H</u>$_{2b}$ sn-1, C<u>H</u>$_2$ sn-3), 3.26 – 3.66 (m, 28H), 3.15 (d, *J* = 9.6 Hz, 1H), 2.89 – 2.99 (m, 3H, Glc-2), 1.99 – 2.08 (m, 4H, 2 x O-COC<u>H</u>$_2$-CH$_2$- lipid), 1.69 – 1.76 (m, 4H, -C<u>H</u>$_2$-CH=CH-C<u>H</u>$_2$- Oleoyl), 1.27 – 1.35 (m, 5H, 2 x O-COCH$_2$-C<u>H</u>$_2$- lipid), 0.93 – 1.04 (m, 67H, C<u>H</u>$_2$ lipid), 0.55 – 0.62 (m, 7H, 2 x C<u>H</u>$_3$ lipid).

^{13}C NMR (101 MHz, CD_3OD) δ (ppm) complemented with HSQC 174.0 (<u>C</u>=O), 129.6 (-<u>C</u>H=CH- Oleoyl), 129.3 (-CH=<u>C</u>H- Oleoyl), 102.3, 101.3, 98.0, 95.1 (Glc-1), 79.1, 78.4, 76.7, 76.4, 72.9, 72.6, 72.3, 71.7, 70.2 (<u>C</u>H sn-2), 66.8, 66.6, 66.4, 64.8, 63.7, 62.8 (<u>C</u>H$_2$ sn-1), 61.4, 60.7, 54.2

(Glc-2), 40.0,33.7 (2 x O-CO<u>C</u>H$_2$-CH$_2$- lipid), 31.5, 29.32, 29.27, 29.22, 29.1, 28.93, 28.89 (<u>C</u>H$_2$ lipid), 26.8 (-<u>C</u>H$_2$-CH=CH-<u>C</u>H$_2$- Oleoyl), 24.5, (2 x O-COCH$_2$-<u>C</u>H$_2$- lipid), 22.2 (<u>C</u>H$_2$ lipid), 13.5 (2 x <u>C</u>H$_3$ lipid).

^{31}P NMR (400 MHz, CD$_3$OD) δ (ppm) -0.27, -0.04.

HRMS: [M-H]$^-$ cald 1633.8007; found 1633.8046.

Triethylammonium 2-(N-(*tert*-butyloxycarbonyl)-2,2-dimethylthiazolidine-L-cysteinyl)aminoethyl H-phosphonate (3-49)

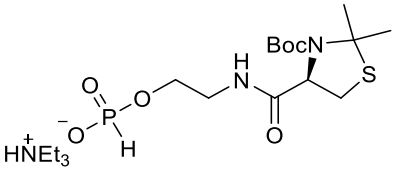

This compound was already available in our laboratory.

^{1}H NMR (400 MHz, CDCl$_3$) δ (ppm) 12.25 (s, 1H, <u>H</u>-NEt$_3$), 7.62 (s, 0.5H, <u>H</u>-P), 6.03 (s, 0.5H, <u>H</u>-P), 4.73 (s, 1H, α-C<u>H</u> cysteine), 3.91 – 4.01 (m, 2H, -C<u>H</u>$_2$-O-), 3.49 – 3.58 (m, 2H, -C<u>H</u>$_2$-NH-), 3.13 – 3.30 (m, 1H, C<u>H</u>$_2$ cysteine), 3.01 – 3.12 (m, 6H, C<u>H</u>$_2$ Et$_3$N), 1.87 (s, 3H, C<u>H</u>$_3$), 1.76 (s, 3H, C<u>H</u>$_3$), 1.45 (s, 9H, C<u>H</u>$_3$ tBu), 1.34 (t, *J* = 7.3 Hz, 9H, C<u>H</u>$_3$ Et$_3$N).

^{13}C NMR (101 MHz, CDCl$_3$) δ (ppm) 67.4 (α-<u>C</u>H cysteine), 63.0 (-<u>C</u>H$_2$-O-), 45.7 (<u>C</u>H$_2$ Et$_3$N), 40.7 (-<u>C</u>H$_2$-NH-), 31.2 (<u>C</u>H$_2$ cysteine), 28.5 (<u>C</u>H$_3$ tBu, <u>C</u>H$_3$ x2), 8.7 (C<u>H</u>$_3$ Et$_3$N).

^{31}P NMR (162 MHz, CDCl$_3$) δ (ppm) 4.93.

6-*O*-(2-(N-(*tert*-butyloxycarbonyl)-2,2-dimethylthiazolidine-L-cysteinyl)aminoethylphosphonato)-α-D-mannopyranosyl-(1→2)-α-D-mannopyranosyl-(1→6)-α-D-mannopyranosyl-(1→4)-2-amino-2-deoxy-α-D-glucopyranosyl-(1→6)-1-*O*-(2-oleoyl-1-stearoyl-*sn*-glycero-3-phosphonate)-D-*myo*-inositol (3-51)

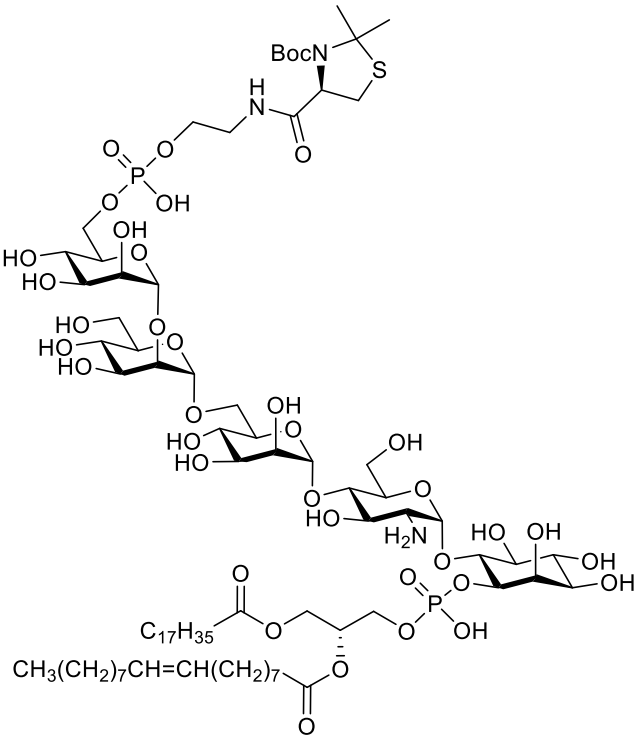

Alcohol **3-42** (90.8 mg, 0.0255 mmol) and H-phosphonate **3-49** (53.9 mg, 0.115 mmol) were co-evaporated with anhydrous pyridine (3 x 1 mL) and placed under high vacuum for 40 min. The residue was dissolved in anhydrous pyridine (1.5 mL) and PivCl (23.4 µL, 0.191 mmol) was added. The reaction mixture was stirred for 1.5 h at room temperature before iodine (35.0 mg, 0.138 mmol) and water (169 µL) were added. The reaction mixture was stirred overnight, and solid $Na_2S_2O_3$ was added until the color of the reaction changed from orange to yellow. Volatiles were removed under reduced pressure. The remaining was triturated with DCM to remove $Na_2S_2O_3$, and concentrated. Purification was performed by flash silica gel column chromatography (eluting with MeOH/DCM 1:90 and gradually increasing the polarity to 1:10). to afford the fully protected *fp*GPI **3-50** (94.8 mg, 0.0242 mmol).

DDQ (45 mg, 0.199 mmol) was added to a solution of the protected GPI **3-50** (43.3 mg, 0.0110 mmol) in a 4:1 DCM/MeOH mixture (1.1 mL). The reaction mixture was stirred at room temperature overnight before volatiles were removed under reduced pressure. The residue was purified by LH-20 size exclusion chromatography eluting with MeOH/$CHCl_3$ 9:1. It was dissolved in anhydrous THF (1 mL), and pyridine (43 µL) was added followed by AcOH (28 µL) and hydrazine acetate (6.1 mg, 0.066 mmol). The reaction mixture was stirred overnight before it was quenched with acetone, and volatiles were removed under reduced pressure. To the obtained *O*-deprotected glycolipid, 0.22 mL of a 1 M solution of $P(CH_3)_3$ in THF were added followed by water (40.5 µL). After 2 h, the mixture was concentrated and triturated with MeOH to give the GPI **3-51**

as a slightly yellow solid in 48% yield over four steps (10 mg, 0.00561 mmol). For the NMR sample, the compound was dissolved in a 3:3:1 $CD_3OD/CDCl_3/D_2O$ mixture.

^{1}H NMR (400 MHz, CD_3OD) δ (ppm) 5.22 (s, 1H, Glc-1), 5.03 – 5.09 (m, 2H, -C<u>H</u>=C<u>H</u>- Oleoyl), 4.97 (s, 1H, C<u>H</u> sn-2), 4.89 (s, 1H, Man-1), 4.84 (s, 1H, Man-1), 4.67 (s, 1H, Man-1), 4.13 (d, *J* = 12.0 Hz, 1H, C<u>H</u>$_{2a}$ sn-1), 3.84 – 3.97 (m, 3H, C<u>H</u>$_{2b}$ sn-1, C<u>H</u>$_2$ sn-3), 3.28 – 3.84 (m, 34H), 3.11 – 3.22 (m, 3H), 2.74 – 2.86 (m, 1H), 2.00 – 2.09 (m, 5H, 2 x O-COC<u>H</u>$_2$-CH$_2$- lipid), 1.69 – 1.77 (m, 5H, -C<u>H</u>$_2$-CH=CH-C<u>H</u>$_2$- Oleoyl), 1.44 – 1.58 (m, 6H, 2 x C<u>H</u>$_3$ *N,S*-acetal), 1.26 – 1.37 (m, 6H, 2 x O-COCH$_2$-C<u>H</u>$_2$- lipid), 1.11 – 1.22 (m, 10H, C<u>H</u>$_3$ Boc), 0.94 – 1.07 (m, 77H, C<u>H</u>$_2$ lipid), 0.56 – 0.62 (m, 10H, 2 x C<u>H</u>$_3$ lipid).

^{31}P NMR (400 MHz, CD_3OD) δ (ppm) -0.05.

HRMS: $[M+H]^+$ cald 1878.9093; found 1878.8553.

6-*O*-(2-L-cysteinylaminoethylphosphonato)-α-D-mannopyranosyl-(1→2)-α-D-mannopyranosyl-(1→6)-α-D-mannopyranosyl-(1→4)-2-amino-2-deoxy-α-D-glucopyranosyl-(1→6)-1-*O*-(2-oleoyl-1-stearoyl-*sn*-glycero-3-phosphonate)-D-*myo*-inositol (3-48)

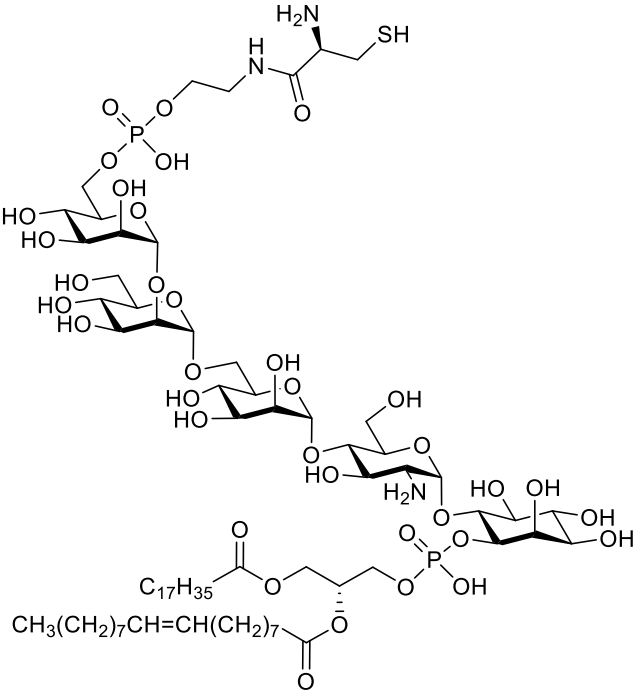

To a solution of *O*-deprotected GPI **3-51** (5.2 mg, 2.77 µmol) in toluene (0.4 mL), TFA (0.1 mL) was added at room temperature. After 35 min, volatiles were removed under reduced pressure at 30 °C, and it was left under high vacuum for 1 h before the residue was mixed with a MeOH/water 1:1 mixture (0.5 mL). It was stirred 5 min before it was concentrated at 45 °C. The procedure with MeOH/water was repeated two more times to ensure complete opening of the *N,S*-acetal. The crude material was triturated with MeOH to furnish the final *Pf*-GPI **3-48** as a white solid (1.9 mg). For the NMR sample, the compound was dissolved in a 3:3:1 $CD_3OD/CDCl_3/D_2O$ mixture.

^{1}H NMR (400 MHz, CD_3OD) 5.18 – 5.25 (m, 1H, Glc-1), 5.00 – 5.07 (m, 2H, -CH=CH- Oleoyl), 4.93 – 5.00 (m, 1H, CH sn-2), 4.84 – 4.93 (m, 1H, Man-1), 4.78 – 4.84 (m, 1H, Man-1), 4.62 – 4.68 (m, 1H, Man-1), 4.12 (d, *J* = 12.3 Hz, 1H, CH_{2a} sn-1), 3.85 – 3.93 (m, 2H, CH_{2b} sn-1), 3.25 – 3.84 (m, 28H), 1.98 – 2.07 (m, 4H, 2 x O-$COCH_2$-CH_2- lipid), 1.66 – 1.76 (m, 4H, -CH_2-CH=CH-CH_2- Oleoyl), 1.24 – 1.36 (m, 7H, 2 x O-$COCH_2$-CH_2- lipid), 0.92 – 1.09 (m, 69H, CH_2 lipid), 0.75 (s, 4H), 0.51 – 0.61 (m, 11H, 2 x CH_3 lipid).

^{31}P NMR (400 MHz, CD_3OD) δ (ppm) -0.059, -0.03.

HRMS: $[M-H]^-$ cald 1736.8100; found 1749.8604.

Allyl 3,4,6-tri-*O*-benzyl-2-*O*-(2-(N-(*tert*-butyloxycarbonyl)-2,2-dimethylthiazolidine-L-cysteinyl)aminoethylphosphonato)-α-D-mannopyranoside (3-53)

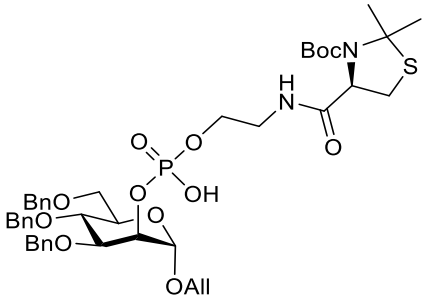

Alcohol **3-52** (80 mg, 0.163 mmol) and H-phosphonate **2-49** (153 mg, 0.326 mmol) were co-evaporated with anhydrous pyridine (3 x 2 mL) and placed under high vacuum for 1.5 h. The residue was dissolved in anhydrous pyridine (4 mL) and PivCl (60 µL, 0.489 mmol) was added. The reaction mixture was stirred for 1.5 h at room temperature before iodine (166 mg, 0.652 mmol) and water (500 µL) were added. The reaction mixture was stirred for 1 h, and solid $Na_2S_2O_3$ was added until the color of the reaction changed from orange to yellow. Volatiles were removed under reduced pressure. The remaining was triturated with DCM to remove $Na_2S_2O_3$, and concentrated. Purification was performed by flash silica gel column chromatography (eluting with MeOH/DCM 1:90 and gradually increasing the polarity to 1:10) followed by LH-20 size exclusion chromatography eluting with MeOH/$CHCl_3$ 1:2 to afford the fully protected mannose **3-53** (124 mg, 0.134 mmol) in 84% yield as a colorless oil.

^{1}H NMR (400 MHz, $CDCl_3$) δ (ppm) 12.50 (s, 1H, H-NEt_3), 7.38 – 7.47 (m, 2H), 7.17 – 7.38 (m, 15H, Ar), 5.82 – 5.96 (m, 1H, -CH= Allyl), 5.24 (d, *J* = 17.2 Hz, 1H, =CH_{2a} Allyl), 5.11 – 5.20 (m, 2H, =CH_{2b} Allyl, Man-1), 4.85 – 4.95 (m, 2H, CH_2 Bn), 4.64 – 4.79 (m, 2H, Man-2, α-CH cysteine), 4.48 – 4.64 (m, 4H, CH_2 Bn), 4.15 (dd, *J* = 12.9, 5.2 Hz, 1H, -CH_{2a}- Allyl), 3.94 – 4.07 (m, 4H, -CH_{2b}- Allyl, Man-3, -CH_2-O-), 3.70 – 3.94 (m, 4H, Man-4, Man-5, Man-6), 3.34 – 3.51 (m, 2H, -CH_2-NH-), 3.12 – 3.28 (m, 2H, CH_2 cysteine), 2.80 – 2.93 (m, 6H, CH_2 Et_3N), 1.89 (s, 3H, CH_3 *N,S*-acetal), 1.78 (s, 3H CH_3 *N,S*-acetal), 1.40 – 1.52 (m, 9H, CH_3 Boc), 1.18 (t, *J* = 7.3 Hz, 9H, CH_3 Et_3N).

^{13}C NMR (101 MHz, $CDCl_3$) δ (ppm) 170.9 (C=O), 138.8, 138.6, 138.4 (C_q Ar), 134.1 (-CH= Allyl), 128.5, 128.5, 128.4, 128.23, 128.17, 128.0, 127.94, 127.86, 127.8, 127.5 (C Ar), 117.1 (=CH_2 Allyl), 98.6 (Man-1), 80.9, 78.9 (Man-3), 75.2 (CH_2 Bn), 74.6 (Man-4), 73.5 (CH_2 Bn), 71.39 (CH_2 Bn), 71.36 (Man-2, Man-5), 69.5 (Man-6), 68.3 (-CH_2- Allyl), 67.3 (α-CH cysteine), 64.5 (-CH_2-O-), 45.4 (CH_2 Et_3N), 40.9 (-CH_2-NH-), 31.2 (CH_2 cysteine), 28.5 (CH_3 Boc, 2 x CH_3 *N,S*-acetal), 8.6 (CH_3 Et_3N).

^{31}P NMR (400 MHz, $CDCl_3$) δ (ppm) 0.12.

ESI-MS: $[M+H]^+$ cald 857.3; found 857.7.

Allyl 3,4,6-tri-*O*-benzyl-2-*O*-(2-L-cysteinylaminoethylphosphonato)-α-D-mannopyranoside (3-54)

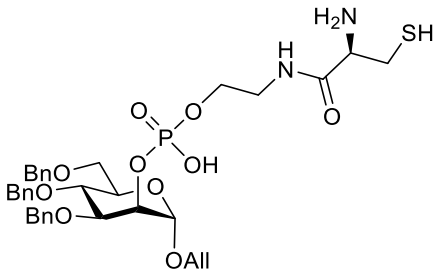

To a solution of fully protected mannose **3-53** (16.5 mg, 0.0192 mmol) in toluene (0.224 mL), TFA (0.224 mL) was added at room temperature. After 1 h, volatiles were removed under reduced pressure at 30 °C, and it was left under high vacuum for 2 h before the residue was mixed with a MeOH/water 1:1 mixture (0.5 mL). It was stirred 5 min and concentrated at 45 °C. The procedure with MeOH/water was repeated two more times to ensure complete opening of the *N,S*-acetal, thereby furnishing the mannose **3-54** as a white solid (12.8 mg, 0.0178 mmol).

Alternatively, to a solution of fully protected mannose **3-53** (24.7 mg, 0.0288 mmol) in toluene (0.335 mL), TFA (0.335 mL) was added at room temperature. After 1 h, volatiles were removed under reduced pressure at 30 °C, and it was left under high vacuum for 2 h. The residue was dissolved in a MeOH/H_2O/$CHCl_3$ 3:3:1 mixture (0.3 mL), and a 1 M $AgNO_3$ aq. solution (43.3 µL) was added. After 1 h, mercaptoethanol (3 µL, 0.0432) was added, and the reaction mixture was stirred before the solvents were removed under reduced pressure. The crude was purified by LH-20 size exclusion chromatography eluting with MeOH/$CHCl_3$ 9:1 to furnish the mannose **3-54** (16.1 mg, 0.0225 mmol) in 78% yield.

^{1}H NMR (400 MHz, MeOD) δ (ppm) 7.38 – 7.46 (m, 2H, Ar), 7.22 – 7.38 (m, 12H, Ar), 7.15 – 7.23 (m, 2H, Ar), 5.86 – 6.01 (m, 1H, -CH= Allyl), 5.22 – 5.32 (m, 1H, =CH_{2a} Allyl), 5.16 (dd, *J* = 10.4, 1.7 Hz, 1H, =CH_{2b} Allyl), 5.08 – 5.14 (m, 1H, Man-1), 4.79 – 4.86 (m, 2H, CH_2 Bn), 4.44 – 4.69 (m, 5H, CH_2 Bn, Man-2), 4.20 (dd, *J* = 13.0, 5.1 Hz, 1H, -CH_{2a}- Allyl), 3.81 – 4.07 (m, 6H, -CH_{2b}- Allyl, -CH_2-O-, α-CH cysteine, Man-4, Man-3), 3.61 – 3.77 (m, 3H, Man-5, Man-6), 3.33 – 3.51 (m, 1H, -CH_{2a}-NH-), 3.22 – 3.30 (m, 1H, -CH_{2b}-NH-), 2.76 – 3.11 (m, 2H, CH_2 cysteine).

^{13}C NMR (101 MHz, MeOD) δ (ppm) 168.4 (C=O), 139.8, 139.7, 139.5 (C_q Ar), 135.3 (-CH= Allyl), 129.5, 129.44, 129.39, 129.34, 129.31, 129.28, 129.15, 129.1, 128.8, 128.68, 128.66 (C Ar), 117.4 (=CH_2 Allyl), 99.4 (Man-1), 79.7 (Man-3), 76.0 (CH_2 Bn), 75.6 (Man-4), 74.3 (CH_2 Bn), 72.9 (Man-2, Man-5), 72.4 (CH_2 Bn), 70.3 (Man-6), 69.3 (-CH_2- Allyl), 65.2 (-CH_2-O-), 56.4 (α-CH cysteine), 41.6 (-CH_2-NH-), 26.2 (CH_2 cysteine).

^{31}P NMR (400 MHz, $CDCl_3$) δ (ppm) -0.26.

ESI-MS: $[M+H]^+$ cald 717.3; found 717.3.

5.4 Methods for chapter 4

2-Azido-2-deoxy-4,6-*O*-(p-methoxybenzylidene)-α-D-glucopyranosyl-(1→6)-1-*O*-allyl-2,3,4,5-tetra-*O*-(2-naphthyl)methyl-D-*myo*-inositol (4-8)

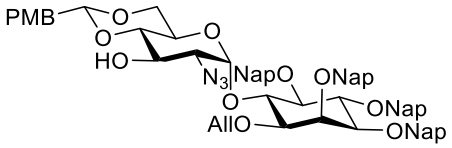

A mixture of triol **2-32** (135 mg, 0.139 mmol), *p*-anisaldehyde dimethyl acetal (0.071 mL, 0.418 mmol) and CSA (8.1 mg, 0.0349 mmol) in anhydrous ACN (3.5 mL) was stirred at room temperature for 40 min. the reaction was quenched with aq. $NaHCO_3$, and layers were separated. The aqueous phase was extracted with DCM. Organic layers were combined, washed with brine, dried over Na_2SO_4, filtered, and concentrated under reduced pressure. The crude was purified by silica gel column chromatography to afford the desired alcohol **4-8** in 88% yield (132 mg, 0.122 mmol) as a white solid; R_f = 0.19 (hexane/EtOAc, 3:1).

^{1}H NMR (400 MHz, $CDCl_3$) δ (ppm) 7.73 – 7.89 (m, 11H, Ar), 7.61 – 7.70 (m, 3H, Ar), 7.59 (d, *J* = 8.5 Hz, 1H, Ar), 7.33 – 7.52 (m, 12H, Ar), 7.28 (dd, *J* = 8.4, 1.7 Hz, 1H, Ar), 6.78 (d, *J* = 8.7 Hz, 2H, CH Ar PMB), 6.54 (d, *J* = 8.8 Hz, 2H, CH Ar PMB), 5.90 – 6.04 (m, 1H, -CH= Allyl), 5.82 (d, *J* = 3.8 Hz, 1H, Glc-1), 5.31 (s, 1H, CH PMB), 5.25 (dd, *J* = 17.3, 1.7 Hz, 1H, =CH_{2a} Allyl), 5.05 – 5.22 (m, 6H, =CH_{2b} Allyl, CH_2 Nap), 4.94 (d, *J* = 10.7 Hz, 1H, CH_2 Nap), 4.89 & 4.82 (ABq, *J* = 11.9 Hz, 2H, CH_2 Nap), 4.43 (t, *J* = 9.6 Hz, 1H, Ino-6), 4.33 (t, *J* = 9.6 Hz, 1H, Ino-4), 4.10 – 4.29 (m, 4H, Ino-2, Glc-3, Glc-5, Glc-6a), 3.97 – 4.12 (m, 2H, -CH_2- Allyl), 3.73 (s, 3H, CH_3-O), 3.51 – 3.64 (m, 3H, Glc-6b, Ino-3, Ino-5), 3.45 (dd, *J* = 9.8, 2.2 Hz, 1H, Ino-1), 3.41 (t, *J* = 9.4 Hz, 1H, Glc-4), 3.23 (dd, *J* = 10.1, 3.8 Hz, 1H, Glc-2), 2.60 (s, 1H, OH-3').

^{13}C NMR (101 MHz, $CDCl_3$) δ (ppm) 136.3, 136.23, 136.05, 135.8 (C_q Ar), 134.3 (-CH= Allyl), 133.6, 133.3, 133.3, 133.1, 133.1, 133.0, 132.9 (C_q Ar), 128.3, 128.23, 128.17, 128.0, 127.84, 127.82, 127.77 (C Ar), 127.6 (CH Ar PMB), 126.82, 126.75, 126.5, 126.4, 126.3, 126.25, 126.17, 126.1, 125.98, 125.95, 125.90, 125.86, 125.8, 125.6, 125.2, 125.1 (C Ar), 117.5 (=CH_2 Allyl), 113.4 (CH Ar PMB), 101.9 (CH PMB), 98.1 (Glc-1), 82.1, 82.04, 81.99, 81.7 (Ino-5), 80.8 (Ino-3),

76.0 (<u>C</u>H$_2$ Nap), 75.4 (<u>C</u>H$_2$ Nap), 75.2 (Ino-6), 74.3 (<u>C</u>H$_2$ Nap), 73.2 (<u>C</u>H$_2$ Nap), 73.1 (Ino-2), 71.2 (-<u>C</u>H$_2$- Allyl), 68.84 (Glc-6), 68.81 (Glc-3), 63.3 (Glc-2), 62.3 (Glc-5), 55.4 (<u>C</u>H$_3$-O).
ESI-MS: 1086.3 $[M+H]^+$, 1109.3 $[M+Na]^+$.

2-Azido-2-deoxy-3-*O*-(2-naphthyl)methyl-4,6-*O*-(*p*-methoxybenzylidene)-α-D-glucopyranosyl-(1→6)-1-*O*-allyl-2,3,4,5-tetra-*O*-(2-naphthyl)methyl-D-*myo*-inositol (4-9)

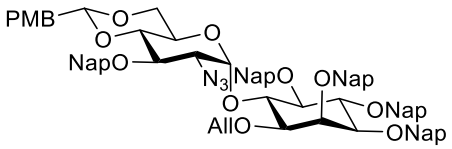

To a mixture of alcohol **4-8** (80.3 mg, 0.0739 mmol) and TBAI (40.9 mg, 0.111 mmol), NaH (5.9 mg, 0.148 mmol, 60% in mineral oil) was added at 0 °C. After 20 min, NapBr (24.5 mg, 0.111 mmol) was added, and the mixture was stirred for additional 1.5 h. The reaction was quenched with water, and volatiles were removed under reduced pressure. The remaining was dissolved with ethyl acetate, and the solution was extracted with water. The layers were separated, and the aqueous phase was extracted with ethyl acetate. Organic layers were collected, washed with brine, dried over Na_2SO_4, filtered, and concentrated *in vacuo*. The crude was purified by flash silica gel column chromatography to obtain the fully protected pseudodisaccharide **4-9** in 88% yield (80.2 mg, 0.0654 mmol) as a white solid; R_f = 0.45 (hexane/EtOAc, 8:2).
^{1}H NMR (400 MHz, $CDCl_3$) δ (ppm) 7.72 – 7.85 (m, 14H, Ar), 7.65 – 7.69 (m, 1H, Ar), 7.60 – 7.65 (m, 4H, Ar), 7.58 (d, *J* = 8.1 Hz, 1H, Ar), 7.41 – 7.52 (m, 14H, Ar), 7.29 (dd, *J* = 8.4, 1.6 Hz, 1H, Ar), 6.97 (d, *J* = 8.7 Hz, 2H, C<u>H</u> Ar PMB), 6.66 (d, *J* = 8.8 Hz, 2H, C<u>H</u> Ar PMB), 5.89 – 6.01 (m, 1H, -C<u>H</u>= Allyl), 5.78 (d, *J* = 3.8 Hz, 1H, Glc-1), 5.41 (s, 1H, C<u>H</u> PMB), 5.23 (dd, *J*= 17.2, 1.7 Hz, 1H, =C<u>H</u>$_{2a}$ Allyl), 5.14 – 5.18 (m, 1H, =C<u>H</u>$_{2b}$ Allyl), 5.14 & 4.94 (ABq, *J* = 10.9 Hz, 2H, C<u>H</u>$_2$ Nap), 5.07 & 5.05 (ABq, *J* = 12.2 Hz, 4H, C<u>H</u>$_2$ Nap), 5.00 & 4.88 (ABq, *J* = 11.4 Hz, 2H, C<u>H</u>$_2$ Nap), 4.86 & 4.79 (ABq, *J* = 11.8 Hz, 2H, C<u>H</u>$_2$ Nap), 4.38 (t, *J* = 9.5 Hz, 1H, Ino-6), 4.24 – 4.33 (m, 2H, Ino-4, Glc-5), 4.18 (dd, *J* = 10.1, 4.9 Hz, 1H, Glc-6a), 4.13 (app t, *J* = 2.3 Hz, 1H, Ino-2), 3.99 – 4.08 (m, 3H, -C<u>H</u>$_2$- Allyl, Glc-3), 3.79 (s, 3H, C<u>H</u>$_3$-O), 3.65 (t, *J* = 9.4 Hz, 1H, Glc-4), 3.53 – 3.62 (m, 2H, Glc-6b, Ino-5), 3.51 (dd, *J* = 9.9, 2.3 Hz, 1H, Ino-3), 3.42 (dd, *J* = 9.7, 2.1 Hz, 1H, Ino-1), 3.36 (dd, *J* = 10.0, 3.8 Hz, 1H, Glc-2).
^{13}C NMR (101 MHz, $CDCl_3$) δ (ppm) 136.4, 136.2, 136.0, 135.8, 135.6 (C_q Ar), 134.4 (-<u>C</u>H= Allyl), 133.5, 133.4, 133.34, 133.30, 133.12, 133.08, 133.0, 130.0 (C_q Ar), 128.34, 128.28, 128.23, 128.19, 128.16, 128.1, 128.0, 127.84, 127.82, 127.75, 127.71, 127.68 (C Ar), 127.5 (C<u>H</u> Ar PMB), 127.1, 126.73, 126.69, 126.5, 126.4, 126.30, 126.28, 126.19, 126.15, 126.1, 126.04, 125.96, 125.94, 125.89, 125.85, 125.82, 125.80, 125.62, 125.60 (C Ar), 117.5 (=<u>C</u>H$_2$ Allyl), 113.4 (C<u>H</u> Ar PMB), 101.4 (C<u>H</u> PMB), 98.1 (Glc-1), 83.0 (Glc-4), 82.1 (Ino), 82.0 (Ino), 81.4 (Ino-5), 80.8 (Ino-3), 76.0 (<u>C</u>H$_2$ Nap), 75.9 (Glc-3), 75.5 (<u>C</u>H$_2$ Nap), 75.3 (Ino-6), 74.9 (<u>C</u>H$_2$ Nap), 74.3 (<u>C</u>H$_2$ Nap),

73.2 (CH_2 Nap), 73.0 (Ino-2), 71.2 (-CH_2- Allyl), 68.9 (Glc-6), 63.3 (Glc-2), 62.7 (Glc-5), 55.4 (CH_3-O).

ESI-MS: 1249.3 $[M+Na]^+$.

2-Azido-2-deoxy-3-*O*-(2-naphthyl)methyl-6-*O*-(p-methoxybenzyl)-α-D-glucopyranosyl-(1→6)-1-*O*-allyl-2,3,4,5-tetra-*O*-(2-naphthyl)methyl-D-*myo*-inositol (4-6)

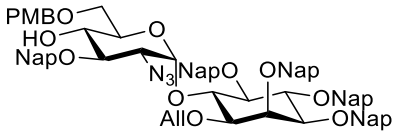

A mixture of the fully protected pseudodisaccharide **4-9** (50 mg, 0.0408 mmol), 4 Å molecular sieves (150 mg), and $NaBH_3CN$ (25.6 mg, 0.408 mmol) in a 1:1 THF/DCM anhydrous mixture (1 mL) was stirred for 40 min at room temperature. TFA (0.062 mL, 0.815 mmol) was added dropwise, and it was stirred at the same temperature for 6 h. The reaction was quenched with aq. $NaHCO_3$ and filtered through a pad of Celite. The aqueous phase was extracted with DCM, and organic layers were collected, washed with brine, dried over Na_2SO_4, filtered, and concentrated by rotatory evaporation. The resulting crude was purified by silica gel column chromatography to give the final pseudodisaccharide acceptor **4-6** in 89% yield (44.1 mg, 0.0361 mmol) as a white solid; R_f = 0.37 (hexane/EtOAc, 3:1).

^{1}H NMR (400 MHz, $CDCl_3$) δ (ppm) 7.75 – 7.87 (m, 17H, Ar), 7.62 – 7.70 (m, 6H, Ar), 7.40 – 7.52 (m, 12H, Ar), 6.90 (d, *J* = 8.6 Hz, 2H, CH Ar PMB), 6.72 (d, *J* = 8.6 Hz, 2H, CH Ar PMB), 5.89 – 6.03 (m, 1H, -CH= Allyl), 5.78 (d, *J* = 3.8 Hz, 1H, Glc-1), 5.26 (dd, *J* = 17.2 Hz, 1.7 Hz, 1H, =CH_{2a} Allyl), 5.15 – 5.23 (m, 3H, =CH_{2b} Allyl, CH_2 Nap), 5.02 (d, *J* = 11.1 Hz, 2H, CH_2 Nap), 5.00 – 5.01 (m, 3H, CH_2 Nap), 4.91 (d, *J* = 11.6 Hz, 1H, CH_2 Nap), 4.86 & 4.81 (ABq, *J* = 11.9 Hz, 2H, CH_2 Nap), 4.38 (t, *J* = 9.5 Hz, 1H, Ino-6), 4.32 (t, *J* = 9.5 Hz, 1H, Ino-4), 4.14 – 4.19 (m, 1H, Ino-2), 4.13 (d, *J* = 3.1 Hz, 1H, CH_{2a} PMB), 4.00 – 4.10 (m, 3H, Glc-5, -CH_2- Allyl), 3.86 – 3.96 (m, 2H, Glc-3, CH_{2b} PMB), 3.75 (s, 3H, CH_3-O), 3.71 (td, *J* = 9.3, 2.9 Hz, 1H, Glc-4), 3.57 (t, *J* = 8.2 Hz, 1H, Ino-5), 3.52 – 3.55 (m, 1H, Ino-3), 3.45 (dd, *J* = 9.8, 2.1 Hz, 1H, Ino-1), 3.30 (dd, *J* = 10.3 Hz, 3.8 Hz, 1H, Glc-2), 3.25 (dd, *J*= 10.3 Hz, *J*= 4.5 Hz, 1H, Glc-6a), 3.09 (dd, *J* = 10.3 Hz, *J* = 3.5 Hz, 1H, Glc-6b), 2.19 (d, *J* = 3.1 Hz, 1H, OH-4').

^{13}C NMR (101 MHz, $CDCl_3$) δ (ppm) 136.4, 136.2, 136.0, 135.84, 135.78 (C_q Ar), 134.4 (-CH= Allyl), 133.44, 133.40, 133.35, 133.30, 133.2, 133.12, 133.08, 133.0, 132.9 (C_q Ar), 129.9 (C Ar), 129.4 (CH Ar PMB), 128.4, 128.3, 128.2, 128.14, 128.10, 128.07, 128.0, 127.9, 127.83, 127.79, 127.73, 127.70, 127.0, 126.72, 126.70, 126.5, 126.4, 126.30, 126.27, 126.20, 126.19, 126.17, 126.13, 126.10, 126.05, 126.03, 125.99, 125.94, 125.89, 125.84, 125.79, 125.6 (C Ar), 117.2 (=CH_2 Allyl), 113.7 (CH Ar PMB), 97.8 (Glc-1), 82.12 (Ino), 82.10 (Ino), 81.7 (Ino-5), 80.9 (Ino-3), 79.4 (Glc-3), 76.0 (CH_2 Nap), 75.6 (CH_2 Nap), 75.4 (Ino-6), 75.0 (CH_2 Nap), 74.3 (CH_2 Nap), 73.1

(CH_2 Nap), 72.93 (CH_2 PMB), 72.91 (Ino-2), 72.6 (Glc-4), 71.2 (-CH_2- Allyl), 69.4 (Glc-5), 69.0 (Glc-6), 63.0 (Glc-2), 55.3 (CH_3-O).

ESI-MS: 1251.4 $[M+Na]^+$.

Allyl 2,3,4,6-tetra-*O*-(2-naphthyl)methyl-α-D-mannopyranosyl-(1→2)-6-*O*-*tert*-butyldiphenylsilyl-3,4-di-*O*-(2-naphthyl)methyl-α-D-mannopyranoside (4-11)

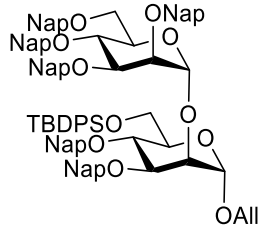

To a mixture of alcohol **4-10** (473 mg, 0.358 mmol) and TBAI (172 mg, 0.465 mmol), NaH (28.6 mg, 0.716 mmol, 60% in mineral oil) was added at 0 °C. After 20 min, NapBr (103 mg, 0.465 mmol) was added, and the mixture was stirred overnight at 50 °C. The reaction was quenched with water, and volatiles were removed under reduced pressure. The remaining was dissolved with ethyl acetate, and the solution was extracted with water. The layers were separated, and the aqueous phase was extracted with ethyl acetate. Organic layers were collected, washed with brine, dried over Na_2SO_4, filtered, and concentrated *in vacuo*. The crude was purified by flash silica gel column chromatography to obtain the fully protected dimannoside **4-11** in 88% yield (460 mg, 0.315 mmol) as a white solid; R_f = 0.59 (hexane/EtOAc, 7:3).

$[\boldsymbol{\alpha}]_{\boldsymbol{D}}^{\boldsymbol{20}}$**:** -33.9 (c = 1, $CHCl_3$).

IR (ATR) ν(cm^{-1}) 3058, 3015, 2926, 1602, 1510, 1459, 1427, 1358, 1347, 1269, 1215, 1163, 1105, 1086, 1055, 895, 854, 814, 751, 704.

^{1}H NMR (400 MHz, $CDCl_3$) δ (ppm) 7.82 (d, *J* = 6.4 Hz, 2H, Ar), 7.65 – 7.81 (m, 16H, Ar), 7.63 (m, 4H, Ar), 7.47 – 7.61 (m, 9H, Ar), 7.36 – 7.50 (m, 10H, Ar), 7.26 – 7.39 (m, 13H, Ar), 7.21 (dd, *J* = 8.4, 1.6 Hz, 1H, Ar), 5.69 – 5.83 (m, 1H, -C$\underline{H}$= Allyl), 5.40 (d, *J* = 1.9 Hz, 1H, ManIV-1), 5.13 (dd, *J* = 17.2, 1.7 Hz, 1H, -C$\underline{H}_{2a}$- Allyl), 5.02 – 5.11 (m, 1H, -C$\underline{H}_{2b}$- Allyl), 5.07 & 4.93 (ABq, *J* = 11.2 Hz, 2H, C$\underline{H}_2$ Nap), 5.02 (d, *J* = 1.7 Hz, 1H, ManIII-1), 4.90 & 4.73 (ABq, *J* = 12.1 Hz, 2H, C$\underline{H}_2$ Nap), 4.80 (s, 2H, C$\underline{H}_2$ Nap), 4.77 – 4.63 (m, 4H), 4.71 & 4.54 (ABq, *J* = 11.1 Hz, 2H, C$\underline{H}_2$ Nap), 4.20 – 4.26 (m, 1H, ManIII-2), 4.12 – 4.17 (m, 1H, ManIV-4), 4.01 – 4.10 (m, 4H, -C$\underline{H}_{2a}$- Allyl, ManIV-5, ManIV-3, ManIII-3), 3.96 – 3.99 (m, 1H, ManIV-2), 3.88 – 3.94 (m, 4H, ManIV-6, ManIII-6), 3.78 – 3.85 (m, 2H, -C$\underline{H}_{2b}$- Allyl, ManIII-4), 3.73 (dt, *J* = 10.0, 3.3 Hz, 1H, ManIII-5), 1.01 (s, 9H, C$\underline{H}_3$ tBu).

^{13}C NMR (101 MHz, $CDCl_3$) δ (ppm) 136.3, 136.21, 136.17, 136.0, 135.94, 135.90, 135.8, 134.0 (C_q Ar), 133.9 (-C$\underline{H}$= Allyl), 133.45, 133.41, 133.35, 133.3, 133.2, 133.1, 133.0 (C_q Ar), 129.7, 128.4, 128.3, 128.2, 128.1, 128.0, 127.83, 127.80, 127.78, 127.73, 127.70, 126.73, 126.5, 126.4, 126.3, 126.2, 126.1, 126.02, 125.99, 125.95, 125.9, 125.8 (C Ar), 117.2 (=C$\underline{H}_2$ Allyl), 99.9 (ManIV-

1), 98.2 (ManIII-1), 80.5 (ManIII-3), 80.1 (ManIV-3), 75.5 (ManIV-2), 75.4 (ManIV-4), 75.2 (CH$_2$ Nap x2), 75.1 (ManIII-4), 74.7 (ManIII-2), 73.8 (CH$_2$ Nap), 73.1 (ManIII-5), 72.7 (CH$_2$ Nap), 72.6 (CH$_2$ Nap), 72.54 (CH$_2$ Nap), 72.48 (ManIV-5), 69.7 (ManIV-6), 67.8 (-CH$_2$- Allyl), 63.5 (ManIII-6), 27.0 (CH$_3$ tBu).

HRMS: $[M+NH_4]^+$ cald 1478.6752; found 1478.6774; $[M+Na]^+$ cald 1483.6307; found 1483.6332.

2,3,4,6-tetra-*O*-(2-naphthyl)methyl-α-D-mannopyranosyl-(1→2)-6-*O*-*tert*-butyldiphenylsilyl-3,4-di-*O*-(2-naphthyl)methyl-α,β-D-mannopyranose (4-12)

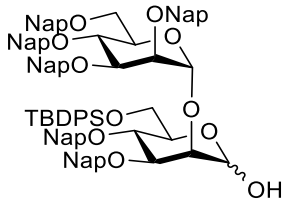

To a solution of the fully protected dimannoside **4-11** (301 mg, 0.206 mmol) in an anhydrous MeOH:DCM 1:1 mixture (3.6 mL), $PdCl_2$ (21.9 mg, 0.124 mmol) was added at room temperature. After 7 h, the mixture was filtered through a pad of Celite, and the volatiles were evaporated *in vacuo*. The resulting orange oil was purified by flash silica gel column chromatography to obtain alcohol **4-12** in 80% yield (236 mg, 0.166 mmol) as a white foam; R_f = 0.39 (hexane/EtOAc, 7:3). $[\alpha]_D^{20}$**:** -43.41 (c = 1, $CHCl_3$).

IR (ATR) ν(cm^{-1}) 3400 (O-H), 3056, 2931, 2859, 1603, 1510, 1472, 1429, 1364, 1272, 1216, 1104, 1059, 954, 894, 856, 815, 753, 705, 668.

^{1}H NMR (400 MHz, $CDCl_3$) δ (ppm) 7.80 – 7.86 (m, 2H, Ar), 7.60 – 7.80 (m, 27H, Ar), 7.47 – 7.63 (m, 12H, Ar), 7.35 – 7.50 (m, 16H, Ar), 7.24 – 7.38 (m, 14H, Ar), 7.21 (dd, *J* = 8.5, 1.7 Hz, 1H, Ar), 5.42 – 5.38 (m, 2H, ManIV-1, ManIII-1 α-anomer), 5.06 (d, *J* = 11.3 Hz, 1H, CH$_2$ Nap), 5.00 (d, *J* = 11.0 Hz, 1H, CH$_2$ Nap), 4.82 – 4.91 (m, 2H, CH$_2$ Nap), 4.79 (s, 2H, CH$_2$ Nap), 4.62 – 4.76 (m, 9H, CH$_2$ Nap), 4.21 – 4.26 (m, 1H, ManIII-2), 4.03 – 4.15 (m, 5H, ManIV-5, ManIV-4, ManIV-3, ManIII-3), 3.94 – 4.04 (m, 4H, ManIV-2, ManIII-6a, ManIII-4), 3.87 – 3.95 (m, 4H, ManIV-6, ManIII-5), 3.82 – 3.88 (m, 1H, ManIII-6b), 1.00 (s, 9H, CH$_3$ tBu).

^{13}C NMR (101 MHz, $CDCl_3$) δ (ppm) 136.3, 136.2, 136.11, 136.08, 135.99, 135.97, 135.9, 135.84, 135.81, 135.7, 133.9, 133.41, 133.39, 133.34, 133.30, 133.28, 133.24, 133.20, 133.1, 133.05, 133.03, 133.00, 132.93, 132.89 (C_q Ar), 129.7, 128.44, 128.40, 128.31, 128.26, 128.22, 128.15, 128.08, 128.05, 128.02, 127.9, 127.84, 127.82, 127.79, 127.73, 127.69, 126.89, 126.75, 126.7, 126.59, 126.55, 126.5, 126.42, 126.38, 126.34, 126.30, 126.27, 126.22, 126.20, 126.17, 126.15, 126.12, 126.09, 126.07, 126.04, 126.01, 125.98, 125.95, 125.9, 125.84, 125.78 (C Ar), 99.9 (ManIV-1), 93.9 (ManIII-1), 80.2 (ManIII-3), 79.7 (ManIV-3), 75.4 (ManIV-4), 75.22 (ManIV-2), 75.17 (CH$_2$ Nap), 75.10 (CH$_2$ Nap), 74.85 (ManIII-4), 74.82 (ManIII-2), 73.6 (CH$_2$ Nap), 72.8 (ManIII-5), 72.7 (CH$_2$ Nap), 72.6 (CH$_2$ Nap), 72.5 (CH$_2$ Nap), 72.3 (ManIV-5), 69.7 (ManIV-6), 63.4 (ManIII-6), 27.0 (CH$_3$ tBu).

HRMS: $[M+NH_4]^+$ cald 1438.6440; found 1438.6682; $[M+Na]^+$ cald 1443.5994; found 1443.61961; $[M+K]^+$ cald 1459.5733; found 1459.5872.

2,3,4,6-tetra-*O*-(2-naphthyl)methyl-α-D-mannopyranosyl-(1→2)-6-*O*-*tert*-butyldiphenylsilyl-3,4-di-*O*-(2-naphthyl)methyl-α-D-mannopyranosyl trichloroacetimidate (4-7)

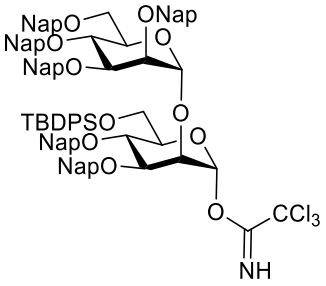

To a solution of the hemiacetal **4-12** (228 mg, 0.160 mmol) in anhydrous DCM (1 mL) at 0 °C, trichloroacetonitrile (160 µL, 1.60 mmol) was added followed by DBU (2.4 µL, 0.016 mmol). After 1.3 h, the solution was transferred to the column for purification by flash silica gel column chromatography to afford the imidate **4-7** in 83% yield (208 mg, 0.133 mmol) as a white solid; R_f = 0.62 (hexane/EtOAc, 7:3).

$[\alpha]_D^{20}$**:** -11.57 (c = 1, $CHCl_3$).

IR (ATR) v(cm^{-1}) 3058, 2930, 2859, 1674 (N=O), 1603, 1510, 1472, 1429, 1346, 1273, 1216, 1170, 1106, 1085, 1054, 967, 926, 894, 856, 815, 796, 750, 703, 667.

^{1}H NMR (400 MHz, $CDCl_3$) δ (ppm) 8.44 (s, 1H, NH), 7.80 – 7.85 (m, 2H, Ar), 7.61 – 7.78 (m, 22H, Ar), 7.49 – 7.58 (m, 6H, Ar), 7.36 – 7.49 (m, 14H, Ar), 7.27 – 7.36 (m, 8H, Ar), 7.17 (dd, *J* = 8.4, 1.6 Hz, 1H, Ar), 6.41 (d, *J* = 2.0 Hz, 1H, ManIII-1), 5.47 (d, *J* = 1.8 Hz, 1H, ManIV-1), 5.06 & 4.70 (ABq, *J* = 11.2 Hz, 2H, CH_2 Nap), 4.97 & 4.64 (ABq, *J* = 10.9 Hz, 2H, CH_2 Nap), 4.93 & 4.70 (ABq, *J* = 12.1 Hz, 2H, CH_2 Nap), 4.75 – 4.85 (m, 2H, CH_2 Nap), 4.67 – 4.74 (m, 4H, CH_2 Nap), 4.30 (s, 1H, ManIII-2), 4.23 (t, *J* = 9.4 Hz, 1H, ManIV-4), 4.02 – 4.72 (m, 5H, ManIV-5, ManIV-3, ManIV-2, ManIII-4, ManIII-3), 3.99 (dd, *J* = 10.9, 4.4 Hz, 1H, ManIV-6a), 3.95 (dd, *J* = 11.5, 4.2 Hz, 1H, ManIII-6a), 3.88 – 3.93 (m, 3H, ManIV-6b, ManIII-6b, ManIII-5), 0.98 (s, 9H, CH_3 tBu).

^{13}C NMR (101 MHz, $CDCl_3$) δ (ppm) 160.0 (C=NH), 136.3, 136.2, 136.1, 136.0, 135.9, 135.8, 135.4, 133.8, 133.44, 133.39, 133.37, 133.34, 133.32, 133.2, 133.14, 133.12, 133.09, 132.99, 132.97 (C_q Ar), 129.78, 129.76, 128.6, 128.3, 128.24, 128.15, 128.1, 128.03, 127.98, 127.9, 127.83, 127.81, 127.77, 127.75, 127.69, 127.2, 126.74, 126.66, 126.6, 126.40, 126.35, 126.23, 126.21, 126.11, 126.08, 126.03, 126.00, 125.91, 125.89, 125.86, 125.7 (C Ar), 100.0 (ManIV-1), 97.3 (ManIII-1), 91.1 (CCl_3), 80.3 (ManIV-3), 79.4 (ManIII-3), 75.8 (ManIII-5), 75.5 (CH_2 Nap), 75.3 (ManIV-2), 75.2 (ManIV-4), 75.1 (CH_2 Nap), 74.3 (ManIII-4), 73.7 (CH_2 Nap), 73.1 (CH_2 Nap), 72.72 (CH_2 Nap), 72.69 (CH_2 Nap), 72.56 (ManIV-5, ManIII-2), 69.2 (ManIV-6), 62.9 (ManIII-6), 27.0 (CH_3 tBu).

HRMS: $[M+Na]^+$ cald 1586.5090; found 1586.5453.

2,3,4,6-tetra-*O*-(2-naphthyl)methyl-α-D-mannopyranosyl-(1→2)-6-*O*-*tert*-butyldiphenylsilyl-3,4-di-*O*-(2-naphthyl)methyl-α-D-mannopyranosyl-(1→2)-3,4,6-tri-*O*-(2-naphthyl)methyl-α-D-mannopyranosyl-(1→6)-2-*O*-acetyl-3,4-di-*O*-(2-naphthyl)methyl-α-D-mannopyranose (4-13)

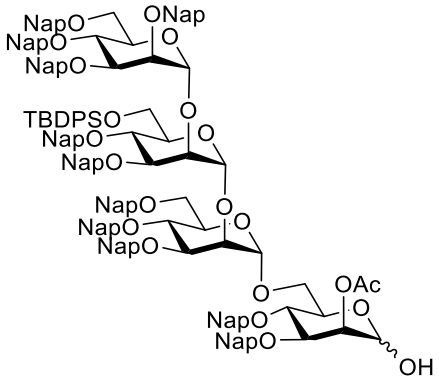

A solution of glycosyl acceptor **3-21** (51.8 mg, 0.0460 mmol) and glycosyl donor **4-7** (86.5 mg, 0.0552 mmol) in anhydrous Et_2O (1 mL) was stirred at room temperature for 5 min. The mixture was cooled to -10 °C, and TMSOTf (1.6 µL, 0.0092 mmol) was added. After stirring for 1 h, the reaction was quenched with Et_3N and concentrated. The obtained white foam was dissolved in a 5:4 DCM/MeOH anhydrous mixture (0.9 mL), and $PdCl_2$ (4.7 mg, 0.0046 mmol) was added at room temperature. After 3.5 h, the mixture was filtered through a pad of Celite, and the volatiles were evaporated *in vacuo*. The residue was purified by flash silica gel column chromatography to obtain **4-13** in 98% yield (112 mg, 0.045 mmol) as a white foam; R_f = 0.29 (hexane/EtOAc, 7:3).
$[\alpha]_D^{20}$**:** -17.34 (c = 1, $CHCl_3$).

IR (ATR) ν(cm^{-1}) 3347 (O-H), 3055, 2929, 1731 (C=O), 1603, 1510, 1462, 1429, 1368, 1238, 1125, 1086, 1053, 893, 856, 816, 752, 704, 667.

^{1}H NMR (400 MHz, $CDCl_3$) δ (ppm) 7.27 – 7.85 (m, 120H, H Ar), 5.48 (s, 1H, ManIII-1), 5.44 (s, 1H, ManIV-1), 5.32 (s, 1H, ManI-2), 5.03 (d, J = 11.2 Hz, 1H, CH2 Nap), 4.90 – 5.00 (m, 4H, CH2 Nap, ManII-1), 4.89 (s, 1H, ManI-1), 4.78 – 4.87 (m, 5H, CH2 Nap), 4.50 – 4.73 (m, 20H, CH2 Nap), 4.31 – 4.46 (m, 5H, ManIII-2), 4.17 – 4.29 (m, 3H, ManII-2), 3.80 – 4.11 (m, 20H, ManIV-3, ManIII-3, ManII-3, ManI-3, ManIV-2, ManIII-6, ManI-6a), 3.62 – 3.77 (m, 5H, ManIV-6, ManI-6b), 3.49 – 3.64 (m, 4H, ManII-6), 2.01 (s, 3H, CH3 Ac), 0.99 (s, 11H, CH3 tBu).

^{13}C NMR (101 MHz, $CDCl_3$) complemented with HSQC (400 MHz, 101 MHz, $CDCl_3$) δ (ppm) 171.3 (C=O Ac), 136.01, 135.8, 135.5, 133.3, 133.0 (C_q Ar), 129.8, 128.2, 128.0, 127.8, 127.1, 127.0, 126.5, 126.2, 126.0, 125.9 (C Ar), 99.9 (ManIV-1), 99.8 (ManIII-1, ManII-1), 92.2 (ManI-1), 80.2 (ManIV-3, ManIII-3), 79.4 (ManII-3), 78.3 (ManI-3), 75.4 (ManIV-2), 74.8 (ManIII-2), 72.7 (ManII-2), 69.9 (ManII-6), 69.3 (ManIV-6), 69.1 (ManI-2), 68.8 (ManI-6), 63.5 (ManIII-6), 27.1 ($\underline{C}H_3$ tBu), 21.2 ($\underline{C}H_3$ Ac).

HRMS: $[M+H]^+$ cald 2488.0466; found 2488.0322; $[M+Na]^+$ cald 2510.0286; found 2510.0154.

2,3,4,6-tetra-*O*-(2-naphthyl)methyl-α-D-mannopyranosyl-(1→2)-6-*O*-*tert*-butyldiphenylsilyl-3,4-di-*O*-(2-naphthyl)methyl-α-D-mannopyranosyl-(1→2)-3,4,6-tri-*O*-(2-naphthyl)methyl-α-D-mannopyranosyl-(1→6)-2-*O*-acetyl-3,4-di-*O*-(2-naphthyl)methyl-α-D-mannopyranosyl trichloroacetimidate (4-14)

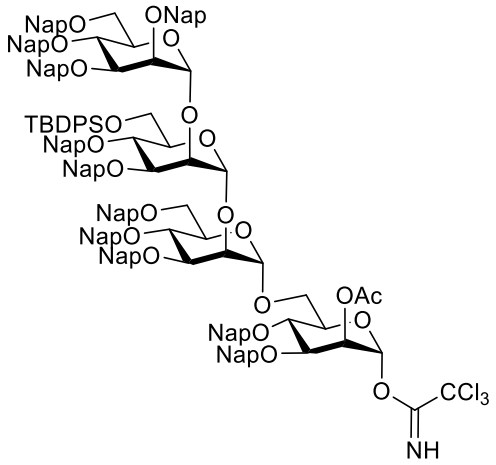

To a solution of hemiacetal **4-13** (112 mg, 0.0448 mmol) in anhydrous DCM (1 mL) at 0 °C, trichloroacetonitrile (45 µL, 0.448 mmol) was added followed by DBU (0.68 µL, 0.00448 mmol). After 1 h, the reaction mixture was directly purified by flash silica gel column chromatography to afford the imidate **4-14** (90.9 mg, 0.0345 mmol) in 77% yield as a white foam; R_f = 0.49 (hexane/EtOAc, 8:2).

$[\alpha]_D^{20}$**:** -1.82 (c = 1, $CHCl_3$).

IR (ATR) ν(cm^{-1}) 3056, 2929, 2859, 1751 (C=O), 1675 (C=N), 1603, 1510, 1472, 1429, 1365, 1273, 1229, 1125, 1088, 1052, 973, 894, 856, 816, 753, 705.

^{1}H NMR (400 MHz, $CDCl_3$) δ (ppm) 8.60 (s, 1H, NH), 7.62 – 7.86 (m, 30H, H Ar), 7.28 – 7.61 (m, 69H, H Ar), 7.15 – 7.20 (m, 4H, H Ar), 7.08 (dd, *J* = 8.4, 1.6 Hz, 1H, H Ar), 6.18 (s, 1H, ManI-1), 5.55 (s, 2H, ManI-2, ManIII-1), 5.48 (s, 1H, ManIV-1), 5.06 (d, *J* = 11.2 Hz, 1H, CH_2 Nap), 4.94 – 5.01 (m, 4H, ManII-1, CH_2 Nap), 4.90 (dd, *J* = 11.5, 2.1 Hz, 2H, CH_2 Nap), 4.54 – 4.78 (m, 17H, CH_2 Nap), 4.43 – 4.50 (m, 2H, ManIII-2, CH_2 Nap), 4.39 (d, *J* = 12.4 Hz, 1H, CH_2 Nap), 4.32 – 4.35 (m, 1H, ManII-2), 4.28 (t, *J* = 9.5 Hz, 1H), 4.07 – 4.15 (m, 5H, ManIII-3, ManI-3, ManIII-6a), 3.90 – 4.05 (m, 11H, ManIV-2, ManII-3, ManIII-6b, ManI-6a), 3.62 – 3.86 (m, 6H, ManI-6b), 3.53 (d, *J* = 11.2 Hz, 1H), 2.01 (s, 3H, CH_3 Ac), 1.01 (s, 10H, CH_3 tBu).

^{13}C NMR (101 MHz, $CDCl_3$) δ (ppm) 170.1 (C=O Ac), 159.5 (C=NH), 136.33, 136.31, 136.2, 136.1, 136.01, 135.95, 135.9, 135.83, 135.75, 135.7, 135.6, 134.9, 133.7, 133.43, 133.39, 133.34, 133.32, 133.28, 133.26, 133.22, 133.1, 133.03, 133.00, 132.97, 132.92, 132.91 (C_q Ar), 129.8, 128.6, 128.5, 128.20, 128.17, 128.11, 128.08, 128.04, 128.02, 127.99, 127.96, 127.93, 127.88, 127.82, 127.80, 127.73, 127.69, 127.66, 127.6, 126.9, 126.6, 126.51, 126.46, 126.42, 126.36, 126.3, 126.25, 126.19, 126.14, 126.12, 126.10, 126.08, 126.06, 126.01, 125.98, 125.93, 125.87, 125.82, 125.80, 125.76, 125.74, 125.70, 125.61 (C Ar), 100.6 (ManIII-1), 99.8 (ManIV-1), 99.1 (ManII-1), 95.1 (ManI-1), 90.8 (CCl_3), 80.3 (Man-3), 80.1 (Man-3), 79.9 (ManII-3), 77.9 (Man-

3), 75.2 (ManVI-2), 75.0 (ManIII-2), 74.8, 74.6, 73.6, 73.5, 73.3 (ManII-2), 73.1, 72.8, 72.6, 72.5, 72.4, 72.3, 72.0, 71.6, 69.1 (ManII-6, ManIV-6), 67.6 (ManI-2), 66.1 (ManI-6), 63.5 (ManIII-6), 27.0 ($\underline{C}H_3$- tBu), 21.0 ($\underline{C}H_3$ Ac).

HRMS: $[M+Na]^+$ cald 2652.9382; found 2652.9351.

3-(p-methoxybenzyl)-2-linoleyl-1-octadecanoyl-*sn*-glycerol (4-15)

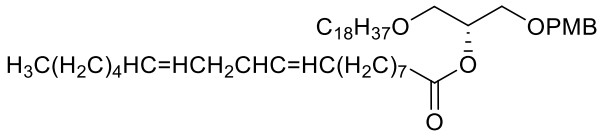

DMAP (290 mg, 2.38 mmol) and DIC (372 µL, 2.38 mmol) were added to a solution of 3-(p-methoxybenzyl)-1-octadecanoyl-*sn*-glycerol **2-56** (850 mg, 1.83 mmol) and linoleic acid (741 µL, 2.38 mmol) in anhydrous DCM (7.6 mL). After 1.5 h, the reaction was quenched with water, and the layers were separated. The aqueous phase was extracted with DCM. Organic layers were dried over Na_2SO_4, filtered, and concentrated. Crude was purified by flash silica gel column chromatography to afford **4-15** (1.23 g, 1.69 mmol) in 92% yield as a colorless oil; R_f = 0.58 (hexane/EtOAc, 7:3).

^{1}H NMR (400 MHz, $CDCl_3$) δ (ppm) 7.21 – 7.26 (m, 2H, Ar of PMB), 6.84 – 6.89 (m, 2H, Ar of PMB), 5.28 – 5.43 (m, 5H, -C$\underline{H}$=C$\underline{H}$-CH_2-C$\underline{H}$=C$\underline{H}$- Linoleyl), 5.16 (p, J = 5.1 Hz, 1H, C$\underline{H}$ sn-2), 4.41 – 4.53 (m, 2H, C$\underline{H}_2$ PMB), 3.80 (s, 3H, C$\underline{H}_3$ PMB), 3.52 – 3.63 (m, 4H, C$\underline{H}_2$ sn-1, C$\underline{H}_2$ sn-3), 3.45 – 3.47 (m, 2H, O-C$\underline{H}_2$-CH_2 Octadecanoyl), 2.77 (t, J = 6.4 Hz, 2H, -CH=CH-C$\underline{H}_2$-CH=CH- Linoleyl), 2.32 (t, J = 7.5 Hz, 2H, O-COC$\underline{H}_2$-CH_2 Linoleyl), 2.0 – 2.09 (m, 5H, -C$\underline{H}_2$-CH=CH-CH_2-CH=CH-C$\underline{H}_2$- Linoleyl), 1.67 – 1.67 (m, 2H, O-$COCH_2$-C$\underline{H}_2$ Linoleyl), 1.48 – 1.57 (m, 2H, O-CH_2-C$\underline{H}_2$ Octadecanoyl), 1.21 – 1.39 (m, 53H, C$\underline{H}_2$ lipid), 0.85 – 0.93 (m, 7H, 2 x C$\underline{H}_3$ lipid).

^{13}C NMR (101 MHz, $CDCl_3$) δ (ppm) 173.5 (C=O Linoleyl), 159.4 (C_q Ar of PMB), 130.4 (-$\underline{C}$H=CH-CH_2-CH=CH- Linoleyl), 130.3 (-CH=$\underline{C}$H-CH_2-CH=CH- Linoleyl), 130.2 (C_q Ar of PMB), 129.39 ($\underline{C}$H Ar of PMB), 128.2 (-CH=CH-CH_2-CH=$\underline{C}$H- Linoleyl), 128.1 (-CH=CH-CH_2-$\underline{C}$H=CH- Linoleyl), 113.9 ($\underline{C}$H Ar of PMB), 73.0 ($\underline{C}H_2$ PMB), 71.8 (O-$\underline{C}H_2$-CH_2 Octadecanoyl), 71.4 ($\underline{C}$H sn-2), 69.4 ($\underline{C}H_2$ sn-1), 68.6 ($\underline{C}H_2$ sn-3), 55.4 ($\underline{C}H_3$ PMB), 34.6 (O-CO$\underline{C}H_2$-CH_2 Linoleyl), 32.1, 31.7, 29.9, 29.81, 29.78, 29.7, 29.6, 29.52, 29.50, 29.4, 29.3, 29.2 ($\underline{C}H_2$ lipid), 27.4 (-$\underline{C}H_2$-CH=CH-CH_2-CH=CH-$\underline{C}H_2$- Linoleyl), 26.2 ($\underline{C}H_2$ lipid), 25.8 (-CH=CH-$\underline{C}H_2$-CH=CH- Linoleyl), 25.2 (O-$COCH_2$-$\underline{C}H_2$ Linoleyl), 22.8 ($\underline{C}H_2$ lipid), 22.7 ($\underline{C}H_2$ lipid), 14.3 ($\underline{C}H_3$ lipid), 14.2 ($\underline{C}H_3$ lipid).

2-Linoleyl-1-octadecanoyl-*sn*-glycerol (4-16)

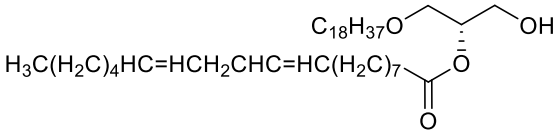

TFA (2.4 mL) was added to a solution of 3-(*p*-methoxybenzyl)-2-linoleyl-1-octadecanoyl-*sn*-glycerol **4-15** (400 mg, 0.756 mmol) in anhydrous DCM (23 mL) at -20 °C, and it was stirred for 20 min. The reaction was quenched with Et_3N and concentrated under reduced pressure. The crude product was purified by flash silica gel column chromatography to obtain the alcohol **4-16** in 63% (288 mg, 0.474 mmol) yield as a white solid; Rf = 0.5 (hexane/EtOAc, 7:3).

^{1}H NMR (400 MHz, $CDCl_3$) δ (ppm) 5.28 – 5.43 (m, 5H, -C<u>H</u>=C<u>H</u>-CH_2-C<u>H</u>=C<u>H</u>- Linoleyl), 5.00 (p, J = 4.8 Hz, 1H, C<u>H</u> sn-2), 3.77 – 3.85 (m, 2H, C<u>H_2</u> sn-3), 3.56 – 3.67 (m, 2H, C<u>H_2</u> sn-1), 3.39 – 3.51 (m, 2H, O-C<u>H_2</u>-CH_2 Octadecanoyl), 2.73 – 2.81 (m, 2H, -CH=CH-C<u>H_2</u>-CH=CH- Linoleyl), 2.35 (t, J = 7.5 Hz, 2H, O-COC<u>H_2</u>-CH_2 Linoleyl), 2.20 (s, 1H, O<u>H</u>-sn3), 2.05 (q, J = 6.9 Hz, 4H, -C<u>H_2</u>-CH=CH-CH_2-CH=CH-C<u>H_2</u>- Linoleyl), 1.60 – 1.66 (m, 2H, O-COCH_2-C<u>H_2</u> Linoleyl), 1.51 – 1.58 (m, 2H, O-CH_2-C<u>H_2</u> Octadecanoyl), 1.21 – 1.38 (m, 46H, C<u>H_2</u> lipid), 0.85 – 0.91 (m, 6H, 2 x C<u>H_3</u> lipid).

^{13}C NMR (101 MHz, $CDCl_3$) δ (ppm) 173.8 (C=O Linoleyl), 130.4 (-CH=<u>C</u>H-CH_2-CH=CH- Linoleyl), 130.2 (-<u>C</u>H=CH-CH_2-CH=CH- Linoleyl), 128.2 (-CH=CH-CH_2-CH=<u>C</u>H- Linoleyl), 128.0 (-CH=CH-CH_2-<u>C</u>H=CH- Linoleyl), 73.0 (<u>C</u>H sn-2), 72.1 (O-<u>C</u>H_2-CH_2 Octadecanoyl), 70.2 (<u>C</u>H_2 sn-1), 63.2 (<u>C</u>H_2 sn-3), 34.5 (O-CO<u>C</u>H_2-CH_2 Linoleyl), 32.1, 31.7, 29.85, 29.83, 29.81, 29.78, 29.75, 29.7, 29.6, 29.51, 29.49, 29.33, 29.26, 29.2 (<u>C</u>H_2 lipid), 27.4 (-<u>C</u>H_2-CH=CH-CH_2-CH=CH-<u>C</u>H_2-Linoleyl), 26.2 (<u>C</u>H_2 lipid), 25.8 (-CH=CH-<u>C</u>H_2-CH=CH- Linoleyl), 25.1 (O-COCH_2-<u>C</u>H_2 Linoleyl), 22.8 (<u>C</u>H_2 lipid), 22.7 (<u>C</u>H_2 lipid), 14.3 (<u>C</u>H_3 lipid), 14.2 (<u>C</u>H_3 lipid).

Triethylammonium 2-linoleyl-1-octadecanoyl-*sn*-glycero-3-H-phosphonate (4-4)

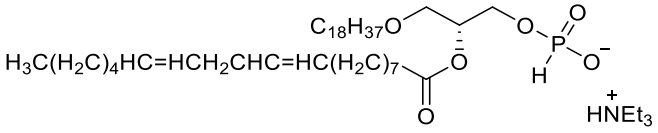

A mixture of 2-linoleyl-1-octadecanoyl-*sn*-glycerol **4-16** (75 mg, 0.123 mmol) and phosphonic acid (25.3 mg, 0.309 mmol) was co-evaporated with anhydrous pyridine (3 x 1 mL of pyridine; last removal of pyridine was carried out for 2 h). The solid residue was dissolved in anhydrous pyridine (3 mL). Pivaloyl chloride (37.8 µL, 0.309 mmol) was added, and the mixture was stirred 1.5 h. Volatiles were removed under reduced pressure and the crude product was purified on a column of silica gel deactivated with triethylamine (eluting with MeOH/DCM 1:90 and gradually increasing the polarity to 2:10). Product was further purified by size exclusion on a LH-20 column eluting with $CHCl_3$:MeOH 2:1 to afford the H-phosphonate **4-4** in 41% yield (39 mg, 0.0505 mmol) as a slightly yellow oil; R_f = 0.19 (MeOH/DCM, 2:10).

^{1}H NMR (400 MHz, $CDCl_3$) δ (ppm) 12.36 (s, 1H, H-NEt_3), 7.45 (s, 0.5H, H-P), 5.85 (s, 0.5H, H-P), 5.16 – 5.33 (m, 4H, -CH=CH-CH_2-CH=CH- Linoleyl), 5.04 (p, J = 5.2 Hz, 1H, CH sn-2), 3.82 – 3.98 (m, 2H, CH_2 sn-3), 3.41 – 3.51 (m, 2H, CH_2 sn-1), 3.23 – 3.36 (m, 2H, O-CH_2-CH_2 Octadecanoyl), 2.98 (qd, J = 7.2, 3.9 Hz, 6H, CH_2 Et_3N), 2.66 (t, J = 6.7 Hz, 2H, -CH=CH-CH_2-CH=CH- Linoleyl), 2.21 (t, J = 7.6 Hz, 2H, O-$COCH_2$-CH_2 Linoleyl), 1.90 – 1.98 (m, 4H, -CH_2-CH=CH-CH_2-CH=CH-CH_2- Linoleyl), 1.47 – 1.54 (m, 2H, O-$COCH_2$-CH_2 Linoleyl), 1.37 – 1.45 (m, 2H, O-CH_2-CH_2 Octadecanoyl), 1.12 – 1.18 (m, 64H, CH_3 Et_3N, CH_2 lipid), 0.75 – 0.81 (m, 7H, 2 x CH_3 lipid).
^{13}C NMR (101 MHz, $CDCl_3$) δ (ppm) 173.4 (C=O Linoleyl), 130.4 (-CH=CH-CH_2-CH=CH- Linoleyl), 130.2 (-CH=CH-CH_2-CH=CH- Linoleyl), 128.2 (-CH=CH-CH_2-CH=CH- Linoleyl), 128.0 (-CH=CH-CH_2-CH=CH- Linoleyl), 71.8 (CH sn-2, O-CH_2-CH_2 Octadecanoyl), 69.3 (CH_2 sn-1), 62.7 (CH_2 sn-3), 45.6 (CH_2 Et_3N), 34.5 (O-$COCH_2$-CH_2 Linoleyl), 32.1, 31.7, 29.89, 29.87, 29.8, 29.7, 29.51, 29.49, 29.44, 29.35, 29.3 (CH_2 lipid), 27.4 (-CH_2-CH=CH-CH_2-CH=CH-CH_2- Linoleyl), 27.3 (-CH_2-CH=CH-CH_2-CH=CH-CH_2- Linoleyl), 26.2 (CH_2 lipid), 25.8 (-CH=CH-CH_2-CH=CH- Linoleyl), 25.1 (O-$COCH_2$-CH_2 Linoleyl), 22.8 (CH_2 lipid), 22.7 (CH_2 lipid), 14.3 (CH_3 lipid), 14.2 (CH_3 lipid), 8.6 (CH_3 Et_3N).
^{31}P NMR (162 MHz, $CDCl_3$) δ (ppm) 4.04.
HRMS: $[M+Na]^+$ 669.5223cald; found 669.5248.

2,3,4,6-tetra-*O*-(2-naphthyl)methyl-α-D-mannopyranosyl-(1→2)-6-O-*tert*-butyldiphenylsilyl-3,4-di-*O*-(2-naphthyl)methyl-α-D-mannopyranosyl-(1→2)-3,4,6-tri-*O*-(2-naphthyl)methyl-α-D-mannopyranosyl-(1→6)-2-*O*-acetyl-3,4-di-*O*-(2-naphthyl)methyl-α-D-mannopyranosyl-(1→4)-2-azido-3-*O*-(2-naphthyl)methyl-6-*O*-(p-methoxybenzyl)-2-deoxy-α-D-glucopyranosyl-(1→6)-1-*O*-allyl-2,3,4,5-tetra-*O*-(2-naphthyl)methyl-D-myo-inositol (4-17)

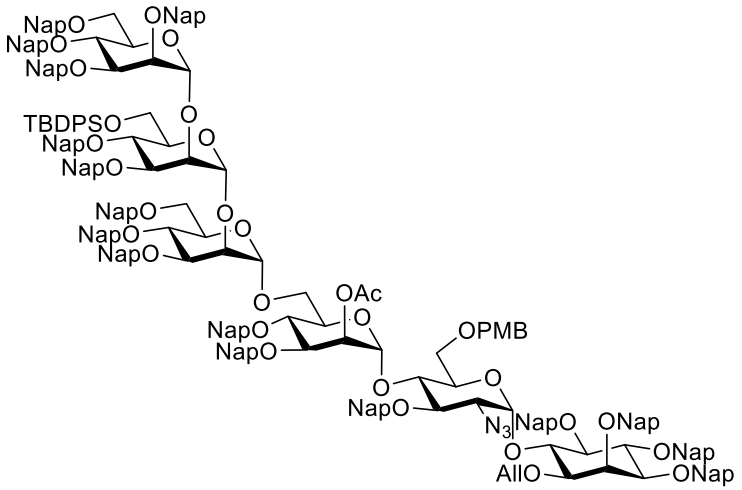

A solution of the pseudodisaccharide glycosyl acceptor **4-6** (34.8 mg, 0.0283 mmol) and the tetra-mannoside glycosyl donor **4-14** (89.5 mg, 0.0340 mmol) in a 10:1 Et_2O/DCM anhydrous mixture (1.1 mL) was stirred at room temperature for 10 min. The mixture was cooled to 0 °C, and TMSOTf (1.5 µL, 0.00850 mmol) was added. After stirring for 1.5 h, the reaction was quenched with Et_3N

(6 µL), and volatiles were removed under reduced pressure. The pseudohexasaccharide **4-17** was obtained as a white foam and used without further purification in the next step.

^{1}H NMR (400 MHz, $CDCl_3$) δ (ppm) 7.63 – 7.89 (m, 44H, Ar), 7.10 – 7.62 (m, 110H, Ar), 7.01 (d, *J* = 8.1 Hz, 2H, Ar PMB), 6.89 – 6.99 (m, 4H, Ar), 6.63 (d, *J* = 8.2 Hz, 2H, Ar PMB), 5.91 – 6.03 (m, 1H, -C<u>H</u>= Allyl), 5.84 (d, *J* = 3.6 Hz, 1H, Glc-1), 5.46 – 5.56 (m, 3H, ManIV-1, ManIII-1, ManI-2), 5.41 (s, 1H, ManI-1), 5.27 (d, *J* = 17.3 Hz, 1H, =C<u>H</u>$_{2a}$ Allyl), 5.19 (d, *J* = 10.4 Hz, 1H, =C<u>H</u>$_{2b}$ Allyl), 5.00 – 5.17 (m, 8H, C<u>H</u>$_2$ Nap), 4.78 – 4.98 (m, 11H, C<u>H</u>$_2$ Nap, ManII-1), 4.53 – 4.78 (m, 15H, C<u>H</u>$_2$ Nap), 4.23 – 4.53 (m, 14H, C<u>H</u>$_2$ Nap, ManIV-2), 3.99 – 4.23 (m, 17H, C<u>H</u>$_2$ Nap, -C<u>H</u>$_2$- Allyl, Glc-3, ManIII-2, ManIII-6a), 3.87 – 3.99 (m, 5H, ManIII-6b), 3.77 – 3.87 (m, 4H, ManI-6a), 3.67 – 3.72 (m, 3H, ManI-3), 3.49 – 3.64 (m, 6H), 3.47 (s, 3H, -OC<u>H</u>$_3$ PMB), 3.34 – 3.45 (m, 1H), 3.30 (dd, *J* = 10.1, 3.6 Hz, 1H, Glc-2), 3.17 (dd, *J* = 11.5, 3.2 Hz, 1H), 3.08 (d, *J* = 10.7 Hz, 1H, ManI-6b), 1.69 (s, 3H, C<u>H</u>$_3$ Ac), 1.00 (s, 10H, C<u>H</u>$_3$ tBu).

^{13}C NMR (101 MHz, $CDCl_3$) δ (ppm) 170.0 (C=O Ac), 159.0, 136.5, 136.4, 136.3, 136.1, 136.0, 135.84, 135.76, 135.3, 135.2 (C_q Ar), 134.3 (-<u>C</u>H= Allyl), 133.8, 133.43, 133.35, 133.3, 133.24, 133.19, 133.13, 133.07, 132.97, 132.92, 132.8, 132.6, 130.2 (C_q Ar), 129.7, 129.2, 128.5, 128.3, 128.2, 128.1, 128.05, 128.02, 127.97, 127.88, 127.84, 127.80, 127.77, 127.73, 127.69, 127.62, 127.61, 127.3, 126.7, 126.6, 126.51, 126.46, 126.4, 126.3, 126.2, 126.14, 126.08, 126.04, 125.97, 125.92, 125.88, 125.84, 125.78, 125.7, 125.6, 125.5, 125.0 (C Ar), 117.3 (=<u>C</u>H$_2$ Allyl), 113.66 (C Ar), 100.5 (ManIII-1), 99.6 (ManIV-1), 99.1 (ManI-1, ManII-1), 97.7 (Glc-1), 82.1, 81.7, 80.8, 80.6, 80.4, 80.2, 79.4, 78.9, 76.0, 75.5, 75.1, 74.9, 74.6, 74.3, 73.6, 73.5, 73.3, 73.1, 72.8, 72.7, 72.6, 72.4, 72.2, 71.9, 71.3, 71.1, 69.9 (-<u>C</u>H$_2$- Allyl), 69.0 (ManI-2), 68.9, 68.5, 65.9 (ManI-6), 63.6 (Glc-2), 63.2 (ManIII-6), 55.0 (-O<u>C</u>H$_3$ PMB), 27.1 (<u>C</u>H$_3$ tBu), 20.8 (<u>C</u>H$_3$ Ac), 19.4.

400 MHz NMR Data		**Glc-1**	**ManI-1**	**ManII-1**	**ManIII-1**	**ManIV-1**
Chemical shift (ppm)	^{13}C	97.7	99.1	99.1	100.5	99.6
	^{1}H	5.83	5.40	4.80	5.51	5.51

2,3,4,6-tetra-*O*-(2-naphthyl)methyl-α-D-mannopyranosyl-(1→2)-6-O-*tert*-butyldiphenylsilyl-3,4-di-*O*-(2-naphthyl)methyl-α-D-mannopyranosyl-(1→2)-3,4,6-tri-*O*-(2-naphthyl)methyl-α-D-mannopyranosyl-(1→6)-3,4-di-*O*-(2-naphthyl)methyl-α-D-mannopyranosyl-(1→4)-2-azido-3-*O*-(2-naphthyl)methyl-6-*O*-(p-methoxybenzyl)-2-deoxy-α-D-glucopyranosyl-(1→6)-1-*O*-allyl-2,3,4,5-tetra-*O*-(2-naphthyl)methyl-D-myo-inositol (4-18)

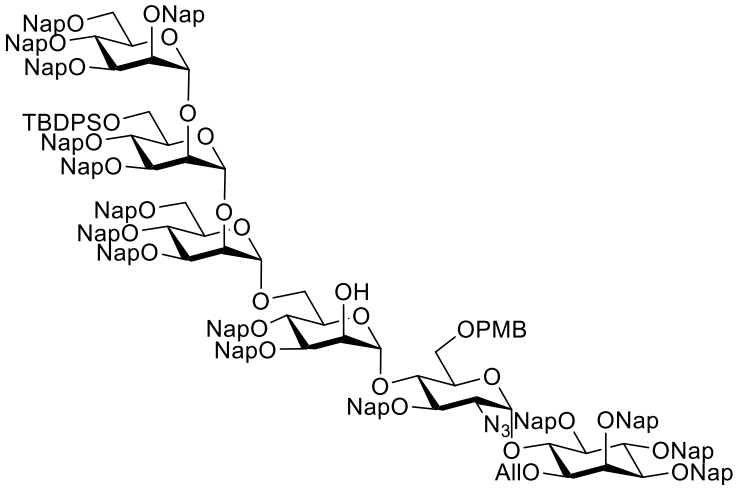

To a solution of the pseudohexasaccharide **4-17** (0.0283 mmol) in an 8:2 MeOH/DCM (1 mL) anhydrous mixture, NaOMe (30 mg, 0.555 mmol) was added, and it was heated at 50 °C for 2 d. The reaction was cooled to room temperature, neutralized with Amberlite IR 120 H^+ resin, filtered and concentrated *in vacuo.* The resulting residue was purified by flash silica gel column chromatography to obtain **4-18** in 57% yield over two steps (59 mg, 0.0161 mmol) as a white greasy solid.

^{1}H NMR (400 MHz, $CDCl_3$) δ (ppm) 6.82 – 7.76 (m, 134H, Ar), 6.47 – 6.55 (m, 2H, Ar PMB), 5.78 – 5.92 (m, 1H, -C<u>H</u>= Allyl), 5.70 (d, *J* = 3.5 Hz, 1H, Glc-1), 5.52 (s, 1H, ManIV-1), 5.39 (s, 1H, ManIII-1), 5.15 (d, *J* = 17.2 Hz, 1H, =C<u>H</u>$_{2a}$ Allyl), 4.84 – 5.12 (m, 10H, =C<u>H</u>$_{2b}$ Allyl, C<u>H</u>$_2$ Nap, ManI-1), 4.42 – 4.84 (m, 23H, C<u>H</u>$_2$ Nap, ManII-1), 4.06 – 4.41 (m, 13H, C<u>H</u>$_2$ Nap, ManII-2, ManIV-2), 3.83 – 4.09 (m, 15H, C<u>H</u>$_2$ Nap, -C<u>H</u>$_2$- Allyl, ManIII-6, ManIII-2), 3.69 – 3.78 (m, 2H, Glc-3), 3.55 – 3.69 (m, 6H, ManI-2), 3.34 – 3.53 (m, 7H, ManI-6a), 3.33 (s, 3H, -OC<u>H</u>$_3$ PMB), 3.28 (d, *J* = 10.8 Hz, 1H), 3.11 (d, *J* = 9.7 Hz, 1H), 3.05 (dd, *J* = 10.2, 3.6 Hz, 1H, Glc-2), 2.88 – 2.98 (m, 2H, ManI-6b), 0.89 (s, 9H, C<u>H</u>$_3$ tBu).

^{13}C NMR (101 MHz, $CDCl_3$) δ (ppm) 159.0, 136.5, 136.38, 136.35, 136.3, 136.2, 136.12, 136.06, 135.98, 135.96, 135.89, 135.83, 135.77, 135.70, 135.6, 135.20, 135.17 (C_q Ar), 134.3 (-<u>C</u>H= Allyl), 133.9, 133.41, 133.36, 133.32, 133.27, 133.24, 133.21, 133.18, 133.1, 133.04, 133.03, 132.97, 132.95, 132.90, 132.86, 132.82, 132.6, 130.2 (C_q Ar), 129.8, 129.7, 129.4, 128.5, 128.3, 128.25, 128.19, 128.17, 128.11, 128.05, 128.00, 127.97, 127.95, 127.91, 127.81, 127.78, 127.76, 127.73, 127.71, 127.68, 127.66, 127.64, 127.62, 127.58, 127.0, 126.74, 126.69, 126.64, 126.54, 126.50, 126.40, 126.35, 126.26, 126.22, 126.18, 126.16, 126.09, 126.06, 126.04, 126.02, 126.00, 125.96, 125.94, 125.90, 125.88, 125.83, 125.80, 125.76, 125.70, 125.65, 125.56, 125.3, 124.7 (C Ar), 117.3 (=<u>C</u>H$_2$ Allyl), 113.6 (C Ar), 101.8 (ManI-1), 100.1 (ManIV-1), 99.7 (ManIII-1), 99.1

(ManII-1), 97.6 (Glc-1), 82.1, 82.0, 81.9, 80.7, 80.5, 80.2, 79.9, 79.7, 79.6, 76.0, 75.2, 75.0, 74.9, 74.7, 74.5 (ManIV-2), 74.2, 74.0, 73.52, 73.47, 73.4, 73.0, 72.9, 72.7, 72.5, 72.4, 72.2, 71.7, 71.6, 71.5, 71.3, 71.0 (-$\underline{C}H_2$- Allyl), 69.8, 69.2, 68.9, 68.4, 65.1 (ManI-6), 63.2 (ManIII-6, Glc-2), 55.0 (-O$\underline{C}H_3$ PMB), 27.1 ($\underline{C}H_3$ Ac).

MALDI-TOF: $[M+Na]^+$ cald 3677.532; found 3678.888.

400 MHz NMR Data		Glc-1	ManI-1	ManII-1	ManIII-1	ManIV-1
Chemical shift (ppm)	^{13}C	97.6	101.8	99.1	99.7	100.1
	^{1}H	5.70	5.04	4.81	5.40	5.52

Allyl 2,3,4,6-tetra-*O*-(2-naphthyl)methyl-α-D-mannopyranosyl-(1→2)-6-*O*-*tert*-butyldiphenylsilyl-3,4-di-*O*-(2-naphthyl)methyl-α-D-mannopyranosyl-(1→2)-3,4,6-tri-*O*-(2-naphthyl)methyl-α-D-mannopyranosyl-(1→6)-2-*O*-levulinyl-3,4-di-*O*-(2-naphthyl)methyl-α-D-mannopyranoside (4-20)

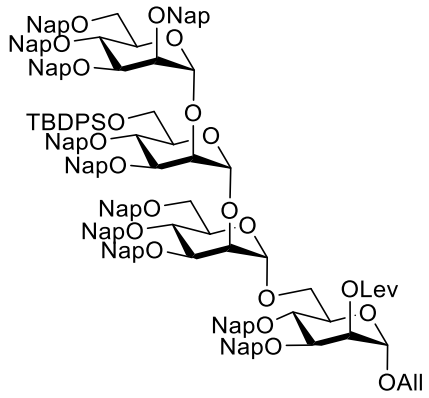

A solution of glycosyl acceptor **3-21** (260.7 mg, 0.231 mmol) and glycosyl donor **4-7** (435.5 mg, 0.278 mmol) in anhydrous Et_2O (2.4 mL) was stirred at room temperature for 10 min. The mixture was cooled to 0 °C, and TMSOTf (8.4 µL, 0.0463 mmol) was added. After stirring for 1 h, the reaction was quenched with Et_3N and concentrated. The resulting white foam was dissolved in anhydrous MeOH/DCM 6:5 (4.2 mL), and NaOMe (25% wt in MeOH, 233 µL) was added. The mixture was stirred at 40 °C for 30 min. The reaction was neutralized with Amberlite IR 120 H^+ resin, filtered, and concentrated *in vacuo*. The resulting residue was purified by flash silica gel column chromatography to give the alcohol **4-19** in quantitative yield (574 mg, 0.231 mmol) as a white foam; R_f = 0.37 (hexane/EtOAc, 3:7). It was dissolved in anhydrous DCM (3.9 mL), and DMAP (14.1 mg, 0.116 mmol) was added followed by LevOH (35.6 µL, 0.348 mmol) and DIC (54.4 µL, 0.348 mmol). The reaction mixture was stirred overnight before it was washed with water. The aqueous phase was extracted with DCM. Organic layers were combined, washed with 1 M aq. citric acid followed by brine, dried with Na_2SO_4, filtered, and concentrated. The residue was purified by flash column chromatography on silica gel to afford the protected tetramannose **4-20** in 85% yield (511 mg, 0.198 mmol) as a white foam; R_f = 0.37 (hexane/EtOAc, 7:3).

$[\boldsymbol{\alpha}]_D^{20}$**:** -3.04 (c = 1, $CHCl_3$).

IR (ATR) ν(cm^{-1}) 3055, 2926, 1743 (C=O), 1721 (C=O), 1603, 1510, 1472, 1429, 1364, 1272, 1125, 1088, 1055, 894, 856, 815, 752, 705.

^{1}H NMR (400 MHz, $CDCl_3$) δ (ppm) 7.60 – 7.87 (m, 29H, H Ar), 7.25 – 7.60 (m, 62H, H Ar), 7.23 – 7.11 (m, 5H, H Ar), 7.03 – 7.10 (m, 1H, H Ar), 5.62 – 5.76 (m, 1H, -C<u>H</u>= Allyl), 5.57 (d, J = 3.0 Hz, 1H, ManIII-1), 5.46 – 5.51 (m, 1H, ManIV-1), 5.43 (s, 1H, ManI-2), 5.13 (d, J = 17.2 Hz, 1H, =C<u>H</u>$_{2a}$ Allyl), 4.80 – 5.09 (m, 9H, ManII-1, =C<u>H</u>$_{2b}$ Allyl, C<u>H</u>$_2$ Nap), 4.53 – 4.79 (m, 17H, ManI-1, C<u>H</u>$_2$ Nap), 4.42 – 4.50 (m, 2H, ManIII-2, C<u>H</u>$_2$ Nap), 4.34 – 4.43 (m, 2H, ManII-2, C<u>H</u>$_2$ Nap), 4.23 – 4.33 (m, 1H), 4.01 – 4.16 (m, 6H, ManI-3, ManII-3, ManIII-3, ManIII-6a), 3.90 – 4.04 (m, 8H, ManIV-2, ManI-6a, ManIII-6b, -C<u>H</u>$_{2a}$- Allyl), 3.68 – 3.86 (m, 7H, ManII-5, ManIV-6, -C<u>H</u>$_{2b}$- Allyl), 3.59 – 3.68 (m, 2H, ManI-6b, ManII-6a), 3.54 (d, J = 11.0 Hz, 1H, ManII-6b), 2.41 – 2.59 (m, 4H, C<u>H</u>$_2$-C<u>H</u>$_2$ Lev), 1.98 (s, 3H, C<u>H</u>$_3$ Lev), 0.96 – 1.05 (m, 10H, C<u>H</u>$_3$ tBu).

^{13}C NMR (101 MHz, $CDCl_3$) δ (ppm) 206.0 (<u>C</u>=O Lev), 172.2 (<u>C</u>=O Lev), 136.2, 136.05, 135.98, 135.90, 135.85, 135.75, 135.67, 135.6, 135.4, 133.6, 133.34, 133.28, 133.24, 133.21, 133.19 (C$_q$ Ar), 133.16 (-<u>C</u>H= Allyl), 133.05, 133.01, 132.97, 132.93, 132.92, 132.88, 132.84, 132.81 (C$_q$ Ar), 129.7, 128.4, 128.14, 128.11, 128.04, 128.02, 127.99, 127.95, 127.90, 127.84, 127.80, 127.75, 127.71, 127.66, 127.62, 127.57, 127.1, 126.8, 126.5, 126.43, 126.38, 126.3, 126.22, 126.15, 126.05, 126.01, 125.96, 125.91, 125.87, 125.82, 125.78, 125.73, 125.69, 125.66, 125.63, 125.4 (C Ar), 118.2 (=<u>C</u>H$_2$ Allyl), 100.5 (ManIII-1), 99.6 (ManIV-1), 99.0 (ManII-1), 96.5 (ManI-1), 80.2 (ManIII-3), 80.0, 79.7, 78.6, 75.1 (ManIV-2), 74.9, 74.8 (ManIII-2), 74.6, 74.2, 73.5, 73.4, 73.2, 73.0 (ManII-2), 72.7, 72.4, 72.1, 71.9 (ManII-5), 71.7, 71.5, 70.6, 69.0 (ManII-6, ManIV-6), 68.8 (ManI-2), 67.9 (-<u>C</u>H$_2$- Allyl), 66.3 (ManI-6), 63.4 (ManIII-6), 37.8 (<u>C</u>H$_2$ Lev), 29.7 (<u>C</u>H$_3$ Lev), 28.0 (<u>C</u>H$_2$ Lev), 26.9 (<u>C</u>H$_3$- tBu).

HRMS: [M+Na]$^+$ cald 2606.0861; found 2606.0603; [M+NH$_4$]$^+$ cald 2601.1307; found 2601.0979.

2,3,4,6-tetra-*O*-(2-naphthyl)methyl-α-D-mannopyranosyl-(1→2)-6-*O*-*tert*-butyldiphenylsilyl-3,4-di-*O*-(2-naphthyl)methyl-α-D-mannopyranosyl-(1→2)-3,4,6-tri-*O*-(2-naphthyl)methyl-α-D-mannopyranosyl-(1→6)-2-*O*-levulinyl-3,4-di-*O*-(2-naphthyl)methyl-α-D-mannopyranose (4-21)

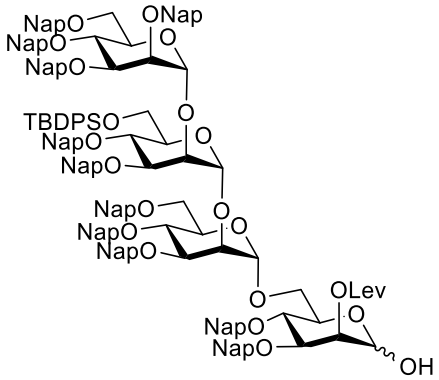

To a solution of the fully protected tetramannose **4-20** (511 mg, 0.198 mmol) in a 5:4 DCM/MeOH anhydrous mixture (4.6 mL), $PdCl_2$ (20 mg, 0.113 mmol) was added at room temperature. After

5 h, the mixture was filtered through a pad of Celite, and the volatiles were evaporated *in vacuo*. The resulting oil was purified by flash silica gel column chromatography to obtain **4-21** in 85% yield (426 mg, 0.167 mmol) as a white foam; R_f = 0.31 (hexane/EtOAc, 6:4).

$[\alpha]_D^{20}$**:** -11.75 (c = 1, $CHCl_3$).

IR (ATR) v(cm^{-1}) 3054, 2930, 1743 (C=O), 1722 (C=O), 1510, 1363, 1363, 1103, 1054, 896, 857, 815, 753, 705.

^{1}H NMR (400 MHz, $CDCl_3$) δ (ppm) 7.60 – 7.82 (m, 53H, H Ar), 7.27 – 7.57 (m, 84H, H Ar), 7.15 – 7.19 (m, 2H, H Ar), 7.03 (dd, J = 8.5, 1.7 Hz, 1H, H Ar), 5.53 (s, 1H, ManIII-1), 5.44 – 5.49 (m, 1H, ManIV-1), 5.31 – 5.37 (m, 1H, ManI-2), 4.91 – 5.10 (m, 8H, ManI-1, ManII-1, C$\underline{H}_2$ Nap), 4.78 – 4.90 (m, 5H, C$\underline{H}_2$ Nap), 4.55 – 4.76 (m, 23H, C$\underline{H}_2$ Nap), 4.33 – 4.49 (m, 5H, ManIII-2, C$\underline{H}_2$ Nap), 4.27 – 4.33 (m, 1H, ManII-2), 4.20 – 4.29 (m, 2H), 3.85 – 4.18 (m, 23H, ManIV-3, ManIII-3, ManII-3, ManI-3, ManII-5, ManIV-2, ManIII-6, ManI-6a), 3.50 – 3.81 (m, 12H, ManIV-6, ManII-6, ManI-6b), 2.52 – 2.64 (m, 5H, C$\underline{H}_2$-C$\underline{H}_2$ Lev), 2.04 (s, 3H, C$\underline{H}_3$ Lev), 1.02 (s, 11H, C$\underline{H}_3$ tBu).

^{13}C NMR (101 MHz, CDCl3) δ (ppm) 206.2 (C=O Lev), 172.1 (C=O Lev), 136.3, 136.0, 135.93, 135.89, 135.83, 135.79, 135.75, 135.6, 135.4, 133.8, 133.4, 133.33, 133.28, 133.2, 133.09, 133.07, 133.05, 132.97, 132.9 (Cq Ar), 129.8, 128.5, 128.34, 128.27, 128.2, 128.1, 128.03, 128.00, 127.97, 127.9, 127.83, 127.78, 127.74, 127.70, 127.0, 126.87, 126.7, 126.50, 126.47, 126.44, 126.37, 126.3, 126.22, 126.15, 126.12, 126.04, 126.03, 125.93, 125.90, 125.81, 125.76 (C Ar), 99.78 (ManIII-1), 99.76 (ManIV-1, ManII-1), 92.3 (ManI-1), 80.2 (ManIV-3, ManIII-3), 78.2 (ManII-3, ManI-3), 75.3, 75.2 (ManIV-2), 74.9, 74.8 (ManIII-2), 73.4, 72.7, 72.5 (ManII-2), 72.3, 72.1 (ManII-5), 71.7, 71.0, 69.9 (ManII-6), 69.2 (ManI-2, ManI-6, ManIV-6), 63.4 (ManIII-6), 38.0 (C$\underline{H}_2$ Lev), 29.8 (C$\underline{H}_3$ Lev), 28.1 (C$\underline{H}_2$ Lev), 27.0 (C$\underline{H}_3$ tBu).

HRMS: $[M+NH_4]^+$ cald 2561.0994; found 2561.0978; $[M+Na]^+$ cald 2566.0548; found 2566.0698.

2,3,4,6-tetra-*O*-(2-naphthyl)methyl-α-D-mannopyranosyl-(1→2)-6-*O*-*tert*-butyldiphenylsilyl-3,4-di-*O*-(2-naphthyl)methyl-α-D-mannopyranosyl-(1→2)-3,4,6-tri-*O*-(2-naphthyl)methyl-α-D-mannopyranosyl-(1→6)-2-*O*-levulinyl-3,4-di-*O*-(2-naphthyl)methyl-α-D-mannopyranosyl trichloroacetimidate (4-22)

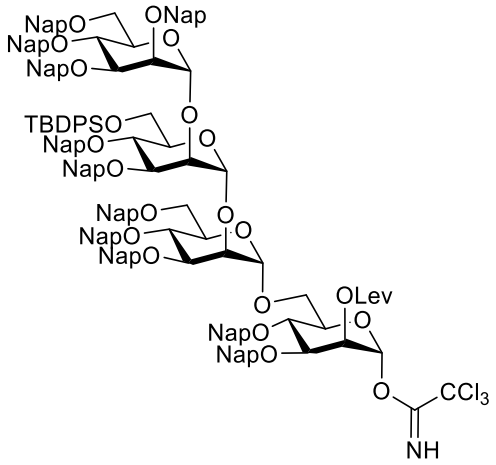

To a solution of hemiacetal **4-21** (426 mg, 0.167 mmol) in anhydrous DCM (4.4 mL) at 0 °C, trichloroacetonitrile (168 µL, 1.67 mmol) was added followed by DBU (2.5 µL, 0.0167 mmol). After 1 h, the reaction mixture was directly purified by flash silica gel column chromatography to afford the imidate **4-22** (412 mg, 0.153 mmol) in 91% yield as a white foam; R_f = 0.34 (hexane/EtOAc, 6:4).

$[\alpha]_D^{20}$**:** -3.28 (c = 1, $CHCl_3$).

IR (ATR) ν(cm^{-1}) 3057, 2931, 1747 (C=O), 1721 (C=O), 1677 (C=N), 1603, 1510, 1471, 1429, 1364, 1273, 1125, 1105, 1055, 975, 895, 857, 816, 753, 705.

^{1}H NMR (400 MHz, $CDCl_3$) δ (ppm) 8.62 (s, 1H, NH), 7.15 – 7.89 (m, 142H, H Ar), 6.21 (s, 1H, ManI-1), 5.58 (s, 1H, ManIII-1), 5.51 – 5.57 (m, 1H, ManI-2), 5.48 (s, 1H, ManIV-1), 4.86 – 5.11 (m, 12H, ManII-1, CH_2 Nap), 4.55 – 4.82 (m, 22H, CH_2 Nap), 4.44 – 4.52 (m, 4H, ManIII-2, CH_2 Nap), 4.33 – 4.42 (m, 3H, ManII-2, CH_2 Nap), 4.24 – 4.33 (m, 2H), 4.04 – 4.18 (m, 7H, ManIV-3, ManIII-3, ManI-3), 3.84 – 4.07 (m, 15H, ManIV-2, ManII-3, ManII-5, ManI-6a, ManIII-6), 3.67 – 3.84 (m, 7H, ManI-6b, ManII-6a, ManIV-6), 3.59 (d, J = 11.2 Hz, 1H, ManII-6b), 2.44 – 2.67 (m, 5H, CH_2-CH_2 Lev), 2.01 (s, 3H, CH_3 Lev), 1.02 (s, 10H, CH_3 tBu).

^{13}C NMR (101 MHz, $CDCl_3$) δ (ppm) 205.8 (C=O Lev), 171.9 (C=O Lev), 159.3 (C=NH), 136.2, 136.13, 136.11, 135.91, 135.86, 135.8, 135.6, 135.5, 134.9, 133.7, 133.34, 133.26, 133.23, 133.19, 133.11, 133.0, 132.94, 132.91, 132.88, 132.83 (C_q Ar), 129.7, 128.4, 128.3, 128.11, 128.08, 128.04, 128.00, 127.94, 127.90, 127.84, 127.78, 127.73, 127.70, 127.65, 127.60, 127.57, 127.49, 126.7, 126.5, 126.4, 126.3, 126.24, 126.19, 126.1, 126.05, 125.99, 125.97, 125.93, 125.89, 125.81, 125.78, 125.73, 125.69, 125.6 (C Ar), 100.5 (ManIII-1), 99.7 (ManIV-1), 98.9 (ManII-1), 94.9 (ManI-1), 90.7 (CCl_3), 80.2 (ManIII-3, ManIV-3), 80.0 (ManII-3), 77.7 (ManI-3), 75.1 (ManIV-2, ManIII-2), 74.6, 73.6, 73.4, 73.2 (ManII-2), 72.7, 72.4, 72.2 (ManII-5), 72.0, 71.9,

71.7, 69.1 (ManII-6, ManIV-6), 67.7 (ManI-2), 66.1 (ManI-6), 63.4 (ManIII-6), 37.7 ($\underline{C}H_2$ Lev), 29.7 ($\underline{C}H_3$ Lev), 27.9 ($\underline{C}H_2$ Lev), 26.9 ($\underline{C}H_3$- tBu).

HRMS: $[M+NH_4]^+$ cald 2704.0090; found 2703.9824; $[M+Na]^+$ cald 2708.9644; found 2708.9356.

2,3,4,6-tetra-*O*-(2-naphthyl)methyl-α-D-mannopyranosyl-(1→2)-6-O-*tert*-butyldiphenylsilyl-3,4-di-*O*-(2-naphthyl)methyl-α-D-mannopyranosyl-(1→2)-3,4,6-tri-*O*-(2-naphthyl)methyl-α-D-mannopyranosyl-(1→6)-2-*O*-levulinyl-3,4-di-*O*-(2-naphthyl)methyl-α-D-mannopyranosyl-(1→4)-2-azido-3-*O*-(2-naphthyl)methyl-6-*O*-(p-methoxybenzyl)-2-deoxy-α-D-glucopyranosyl-(1→6)-1-*O*-allyl-2,3,4,5-tetra-*O*-(2-naphthyl)methyl-D-myo-inositol (4-23)

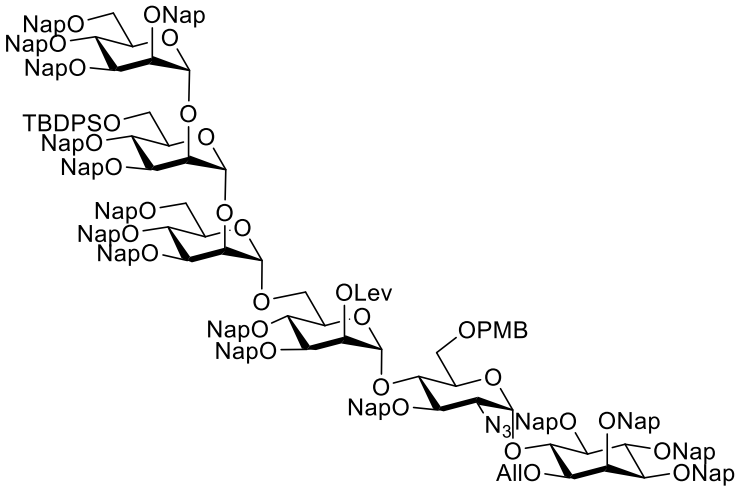

A solution of the pseudodisaccharide glycosyl acceptor **4-6** (153 mg, 0.124 mmol) and the tetra-mannoside glycosyl donor **4-22** (418 mg, 0.155 mmol) in a 10:1 Et_2O/DCM anhydrous mixture (3.1 mL) was stirred at room temperature for 10 min. The mixture was cooled to 0 °C, and TMSOTf (6.7 µL, 0.0373 mmol) was added. After stirring for 1.5 h, the reaction was quenched with Et_3N, and volatiles were removed under reduced pressure. The crude product was purified by flash silica gel column chromatography to obtain the fully protected pseudohexasaccharide **4-23** in quantitative yield as a white foam; R_f = 0.54 (heptane/EtOAc, 6:4).

^{1}H NMR (400 MHz, $CDCl_3$) δ (ppm) 7.26 – 7.85 (m, 260H, Ar), 6.94 – 7.00 (m, 6H, Ar), 6.57 – 6.61 (m, 2H, Ar PMB), 5.86 – 5.99 (m, 1H, -C$\underline{H}$= Allyl), 5.79 (d, *J* = 3.7 Hz, 1H, Glc-1), 5.49 – 5.51 (m, 1H, ManIII-1), 5.46 – 5.48 (m, 1H, ManIV-1), 5.36 – 5.39 (m, 1H, ManI-2), 5.33 – 5.36 (m, 1H, ManI-1), 5.10 – 5.26 (m, 6H, C$\underline{H}_2$ Nap, =C$\underline{H}_2$ Allyl), 4.73 – 5.09 (m, 37H, C$\underline{H}_2$ Nap, ManII-1), 4.52 – 4.73 (m, 31H, C$\underline{H}_2$ Nap), 4.18 – 4.52 (m, 27H, C$\underline{H}_2$ Nap), 3.83 – 4.10 (m, 36H, -C$\underline{H}_2$- Allyl, ManIII-6), 3.59 – 3.82 (m, 18H, ManI-6a), 3.35 – 3.57 (m, 18H), 3.19 – 3.28 (m, 2H, Glc-2), 3.04 – 3.18 (m, 3H, ManI-6b), 2.31 – 2.59 (m, 4H, C$\underline{H}_2$-C$\underline{H}_2$ Lev), 1.92 – 1.98 (m, 2H, C$\underline{H}_2$-C$\underline{H}_2$ Lev), 1.73 (s, 3H, C$\underline{H}_3$ Lev), 0.96 – 1.02 (m, 18H, C$\underline{H}_3$ tBu).

^{13}C NMR (101 MHz, $CDCl_3$) δ (ppm) 205.5 (C=O Lev), 171.8 (C=O Lev), 163.3, 159.0, 136.5, 136.44, 136.38, 136.21, 136.15, 136.11, 136.00, 135.88, 135.82, 135.77, 135.6, 135.5, 135.32 (C_q Ar), 134.33 (-$\underline{C}$H= Allyl), 133.8, 133.5, 133.40, 133.38, 133.33, 133.27, 133.24, 133.17,

133.11, 133.07, 133.02, 133.00, 132.96, 132.92, 132.89, 132.7, 130.2 (C_q Ar), 129.8, 129.3, 128.5, 128.3, 128.21, 128.16, 128.13, 128.09, 128.06, 128.03, 128.00, 127.97, 127.94, 127.91, 127.86, 127.83, 127.79, 127.74, 127.71, 127.66, 127.64, 127.2, 127.1, 126.72, 126.66, 126.57, 126.52, 126.48, 126.39, 126.33, 126.31, 126.27, 126.17, 126.15, 126.10, 126.07, 126.05, 126.02, 125.98, 125.94, 125.88, 125.82, 125.79, 125.74, 125.70, 125.63, 125.40 (C Ar), 117.3 (=$\underline{C}H_2$ Allyl), 113.7 (C Ar), 100.6 (ManIII-1), 99.6 (ManIV-1), 99.2 (ManI-1, ManII-1), 97.7 (Glc-1), 92.0, 82.1, 81.7, 80.9, 80.6, 80.4, 79.8, 78.6, 76.0, 75.4, 75.2, 75.1, 74.6, 74.4, 74.3, 74.0, 73.6, 73.4, 73.1, 73.0, 72.9, 72.7, 72.6, 72.4, 72.2, 71.7, 71.5, 71.3, 71.1 (-$\underline{C}H_2$- Allyl), 69.9, 69.2, 66.1 (ManI-6), 63.5 (Glc-2, ManII-6), 55.0 (-O$\underline{C}H_3$ PMB), 37.5, 35.6, 32.9, 32.5, 32.0, 29.5 ($\underline{C}H_3$ Lev), 29.2, 27.0 ($\underline{C}H_3$ tBu), 26.6, 26.8, 25.4, 23.1, 22.8, 19.4, 14.3.

HRMS: $[M+2Na]^{2+}$ cald 1899.2792; found 1899.2741.

400 MHz NMR Data		Glc-1	ManI-1	ManII-1	ManIII-1	ManIV-1
Chemical shift (ppm)	^{13}C	97.6	99.2	99.2	100.6	99.6
	^{1}H	5.79	5.34	4.79	5.49	5.47

2,3,4,6-tetra-*O*-(2-naphthyl)methyl-α-D-mannopyranosyl-(1→2)-6-O-*tert*-butyldiphenylsilyl-3,4-di-*O*-(2-naphthyl)methyl-α-D-mannopyranosyl-(1→2)-3,4,6-tri-*O*-(2-naphthyl)methyl-α-D-mannopyranosyl-(1→6)-2-*O*-levulinyl-3,4-di-*O*-(2-naphthyl)methyl-α-D-mannopyranosyl-(1→4)-2-azido-3-*O*-(2-naphthyl)methyl-6-*O*-(p-methoxybenzyl)-2-deoxy-α-D-glucopyranosyl-(1→6)-2,3,4,5-tetra-*O*-(2-naphthyl)methyl-D-myo-inositol (4-24)

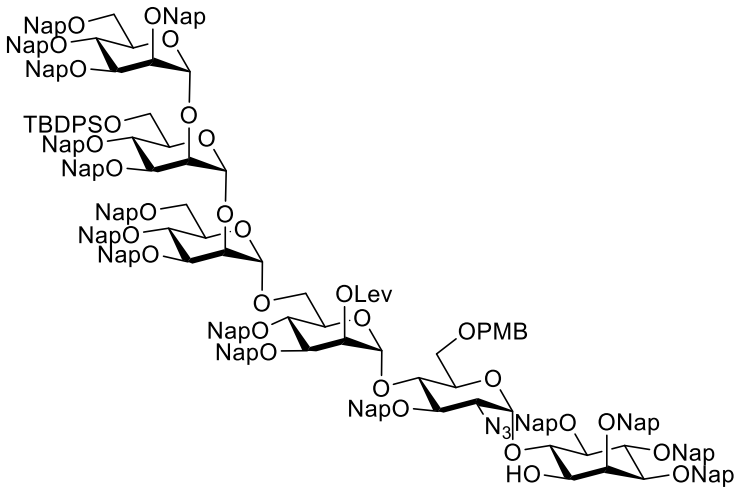

A solution of $[IrCOD(PPh_2Me)_2]PF_6$ (8 mg, 0.0095 mmol) in THF (3.5 mL) was stirred under hydrogen at room temperature until it changed from red to colorless to pale yellow. The hydrogen atmosphere was exchanged with Ar. This solution was then added into a THF (3.5 mL) solution of pseudohexasaccharide **4-23** (0.356 g, 0.0948 mmol). The reaction was stirred at room temperature for 3 h before the solvent was removed and the residue was dissolved in acetone/water 9:1 (3.5 mL). Mercury(II) chloride (0.154 g, 0.569 mmol) and mercury(II) oxide (4.1 mg, 0.0190 mmol) were added. After 2 h, the solvent was removed. The residue was dissolved in DCM and washed

with saturated $NaHCO_3$, dried over Na_2SO_4, filtered, and concentrated. The obtained crude was purified by flash silica gel column chromatography to give the alcohol **4-24** (299 mg, 0.0805 mmol) as a white foam in 85% yield; R_f = 0.48 (heptane/EtOAc, 6:4).

^{1}H NMR (400 MHz, $CDCl_3$) δ (ppm) 7.24 – 7.85 (m, 165H, Ar), 7.07 – 7.24 (m, 18H, Ar), 6.91 – 7.03 (m, 4H, Ar), 6.85 (d, *J* = 8.5 Hz, 1H, Ar PMB), 6.51 (d, *J* = 8.6 Hz, 1H, Ar PMB), 5.47 – 5.51 (m, 1H, ManIII-1), 5.42 – 5.47 (m, 1H, ManIV-1), 5.39 – 5.43 (m, 1H, ManI-2), 5.39 (d, *J* = 3.5 Hz, 1H, Glc-1), 5.33 – 5.37 (m, 1H, ManI-1), 5.17 (d, *J* = 11.9 Hz, 1H, C$\underline{H}_2$ Nap), 5.12 (d, *J* = 10.9 Hz, 1H, C$\underline{H}_2$ Nap), 4.72 – 5.07 (m, 19H, C$\underline{H}_2$ Nap, ManII-1), 4.40 – 4.72 (m, 24H, C$\underline{H}_2$ Nap), 4.14 – 4.39 (m, 9H, C$\underline{H}_2$ Nap), 3.14 – 4.48 (m, 37H, C$\underline{H}_2$ Nap, ManIII-6, ManI-6a), 3.33 – 3.50 (m, 7H, Glc-2, -OC$\underline{H}_3$ PMB), 3.15 – 3.29 (m, 3H, ManI-6b), 2.29 – 2.60 (m, 2H, C$\underline{H}_2$-C$\underline{H}_2$ Lev), 1.87 – 2.21 (m, 4H, C$\underline{H}_2$-C$\underline{H}_2$ Lev), 1.75 (s, 3H, C$\underline{H}_3$ Lev), 0.97 (s, 9H, C$\underline{H}_3$ tBu).

^{13}C NMR (101 MHz, $CDCl_3$) δ (ppm) 205.6 (C=O Lev), 171.8 (C=O Lev), 159.0, 136.4, 136.2, 136.1, 136.0, 135.9, 135.8, 135.3, 133.5, 133.4, 133.32, 133.27, 133.2, 133.1, 133.0, 132.9 (C_q Ar), 129.8, 129.2, 128.4, 128.2, 128.1, 128.04, 127.97, 127.9, 127.7, 127.6, 127.1, 127.0, 126.6, 126.4, 126.51, 126.46, 126.3, 126.14, 126.07, 126.0, 125.9, 125.8, 125.7, 125.4, 113.6 (C_q Ar), 100.6 (ManIII-1), 99.7 (ManIV-1), 99.2 (ManI-1, ManII-1), 98.1 (Glc-1), 82.0, 81.5, 80.9, 80.7, 80.4, 75.9, 75.1, 74.7, 74.5, 73.5, 73.4, 73.2, 73.0, 72.7, 72.6, 72.5, 72.2, 71.6, 70.7, 69.1, 66.3 (ManI-6), 64.5 (Glc-2), 63.4 (ManIII-6), 55.0 (-O$\underline{C}H_3$ PMB), 53.6, 51.0, 37.5, 29.8, 29.5 ($\underline{C}H_3$ Lev), 27.1 ($\underline{C}H_3$ tBu), 19.4.

HRMS: $[M+2Na]^{2+}$ cald 1879.2636; found 1879.2512; $[M+Na+K]^{2+}$ cald 1887.25055; found 1887.2352.

400 MHz NMR Data		**Glc-1**	**ManI-1**	**ManII-1**	**ManIII-1**	**ManIV-1**
Chemical shift (ppm)	^{13}C	98.1	99.2	99.2	100.6	99.7
	^{1}H	5.39	5.35	4.83	5.49	5.44

2,3,4,6-tetra-*O*-(2-naphthyl)methyl-α-D-mannopyranosyl-(1→2)-6-O-*tert*-butyldiphenylsilyl-3,4-di-*O*-(2-naphthyl)methyl-α-D-mannopyranosyl-(1→2)-3,4,6-tri-*O*-(2-naphthyl)methyl-α-D-mannopyranosyl-(1→6)-2-*O*-levulinyl-3,4-di-*O*-(2-naphthyl)methyl-α-D-mannopyranosyl-(1→4)-2-azido-3-*O*-(2-naphthyl)methyl-2-deoxy-α-D-glucopyranosyl-(1→6)-1-*O*-(2-linoleyl-1-stearoyl-*sn*-glycero-3-phosphonate)-2,3,4,5-tetra-*O*-(2-naphthyl)methyl-D-myo-inositol (4-26)

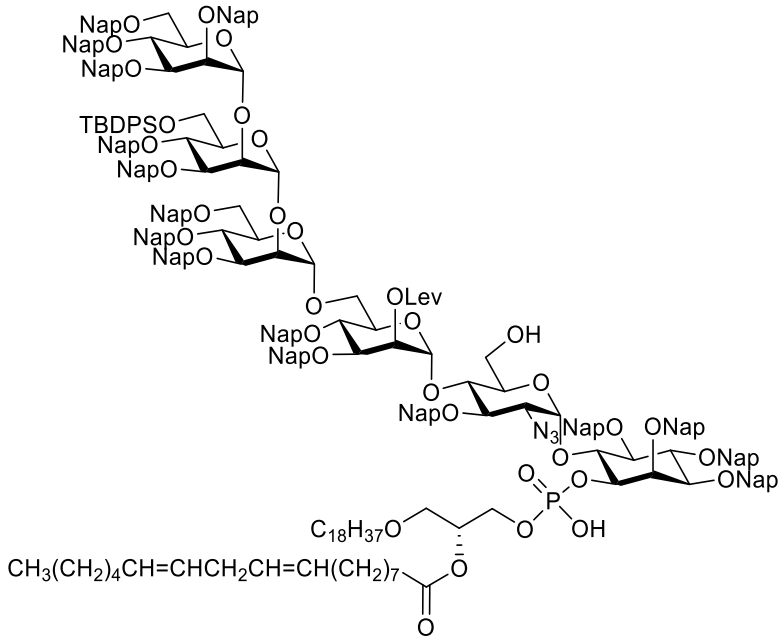

Alcohol **4-24** (189 mg, 0.0508 mmol) and H-phosphonate **4-4** (62.7 mg, 0.0812 mmol) were co-evaporated with anhydrous pyridine (3 x 1 mL) and placed under high vacuum for 1 h. The residue was dissolved in anhydrous pyridine (3.9 mL) and PivCl (16.2 µL, 0.132 mmol) was added. The reaction mixture was stirred for 2 h at room temperature before water (117 µL) and iodine (38.6 mg, 0.152 mmol) were added. The reaction mixture was stirred for an additional hour, and solid $Na_2S_2O_3$ was added until the color of the reaction changed from orange to yellow. Volatiles were removed under reduced pressure. The remaining was triturated with DCM to remove $Na_2S_2O_3$, and concentrated. Purification was performed by flash silica gel column chromatography (eluting with MeOH/DCM 1:90 and gradually increasing the polarity to 1:20) to afford the lipidated pseudohexasaccharide **4-25** in 82% yield (183 mg, 0.0418 mmol) as a white foam; R_f = 0.29 (MeOH/DCM, 1:20). **HRMS:** $[M+2Na]^{2+}$ cald 2213.5208; found 2213.5317.

TFA (0.1 mL) was added to a solution of pseudohexasaccharide **4-25** (56.5 mg, 0.0129 mmol) in anhydrous DCM (0.9 mL) at -20 °C, and it was stirred for 15 min. The reaction was quenched with Et_3N and concentrated under reduced pressure. The crude product was purified by flash silica gel column chromatography followed by size exclusion on a LH-20 column eluting with $CHCl_3$:MeOH 2:1 to afford alcohol **4-26** in 96% yield (52.8 mg, 0.0124 mmol) as a white foam; R_f = 0.23 (MeOH/DCM, 1:20)

^{1}H NMR (400 MHz, $CDCl_3$) δ (ppm) 6.92 – 7.87 (m, 156H), 5.95 (s, 1H), 5.41 – 5.61 (m, 3H), 5.10 – 5.41 (m, 8H), 2.99 – 5.06 (m, 90H), 2.65 – 2.79 (m, 2H), 2.42 – 2.61 (m, 3H), 2.12 – 2.40 (m, 7H), 1.86 – 2.10 (m, 6H), 1.77 (s, 3H), 1.05 – 1.35 (m, 62H), 0.82 – 1.03 (m, 32H).

^{13}C NMR (101 MHz, $CDCl_3$) δ (ppm) 205.8, 171.4, 136.4, 136.1, 136.03, 135.96, 135.91, 135.85, 135.7, 133.45, 133.40, 133.37, 133.32, 133.28, 133.25, 133.21, 133.03, 133.00, 132.95, 132.92, 132.90, 130.3, 130.19, 128.21, 128.16, 128.08, 128.04, 128.01, 127.99, 127.94, 127.91, 127.86, 127.83, 127.78, 127.72, 127.69, 127.63, 126.56, 126.4, 126.3, 126.24, 126.18, 126.09, 126.06, 126.04, 125.98, 125.94, 125.91, 125.87, 125.83, 125.81, 125.76, 125.7, 100.4, 99.7, 81.9, 80.4, 75.8, 75.1, 73.4, 72.8, 72.6, 72.5, 72.2, 71.7, 69.0, 64.4, 63.4, 45.5, 37.5, 34.5, 32.04, 31.6, 29.88, 29.86, 29.81, 29.77, 29.72, 29.67, 29.55, 29.50, 29.47, 29.4, 29.3, 29.2, 27.8, 27.4, 27.3, 27.09, 27.06, 26.1, 25.8, 25.0, 22.8, 22.7, 19.4, 14.3, 8.47.

^{31}P NMR (400 MHz, $CDCl_3$) δ (ppm) -1.46.

HRMS: $[M+H+Na]^{2+}$ cald 2142.5011; found 2142.4877; $[M+2Na]^{2+}$ cald 2153.4921; found 2153.4986.

400 MHz NMR Data		**Glc-1**	**ManI-1**	**ManII-1**	**ManIII-1**	**ManIV-1**
Chemical shift (ppm)	^{13}C	96.6	100	99.2	100.2	99.6
	^{1}H	5.94	5.28	4.94	5.60	5.51

6 References

(1) Walsh, C. T.; Garneau-Tsodikova, S.; Gatto, G. J. Protein Posttranslational Modifications: The Chemistry of Proteome Diversifications. *Angew. Chem. Int. Ed.* **2005**, *44* (45), 7342–7372.

(2) Peter, O.; Menon, A. K. Thematic Review Series: Lipid Posttranslational Modifications. GPI Anchoring of Protein in Yeast and Mammalian Cells, or: How We Learned to Stop Worrying and Love Glycophospholipids. *J. Lipid. Res.* **2007**, *48* (5), 993–1011.

(3) McConville, M. J.; Ferguson, M. A. J. The Structure, Biosynthesis and Function of Glycosylated Phosphatidylinositols in the Parasitic Protozoa and Higher Eukaryotes. *Biochem. J.* **1993**, *294* (2), 305–324.

(4) Futerman, A. H.; Low, M. G.; Ackermann, K. E.; Sherman, W. R.; Silman, I. Identification of Covalently Bound Inositol in the Hydrophobic Membrane-Anchoring Domain of Torpedo Acetylcholinesterase. *Biochem. Biophys. Res. Commun.* **1985**, *129* (1), 312–317.

(5) Tse, A. G. D.; Barclay, A. N.; Watts, A.; Williams, A. F. A Glycophospholipid Tail at the Carboxyl Terminus of the Thy-1 Glycoprotein of Neurons and Thymocytes. *Science.* **1985**, *230* (4729), 1003–1008.

(6) Tsai, Y.-H.; Liu, X.; Seeberger, P. H. Chemical Biology of Glycosylphosphatidylinositol Anchors. *Angew. Chem. Int. Ed.* **2012**, *51* (46), 11438–11456.

(7) Singh, N.; Liang, L.-N.; Tykocinski, M. L.; Tartakoff, A. M. A Novel Class of Cell Surface Glycolipids of Mammalian Cells. *J. Biol. Chem.* **1996**, *271* (22), 12879–12884.

(8) Garg, M.; Seeberger, P. H.; Varón Silva, D. Glycosylphosphatidylinositols: Occurrence, Synthesis, and Properties. In *Reference Module in Chemistry, Molecular Sciences and Chemical Engineering*; Elsevier, 2016; p B9780124095472116000.11657-9.

(9) Vilotijevic, I.; Götze, S.; Seeberger, P. H.; Varón Silva, D. Chemical Synthesis of GPI Anchors and GPI-Anchored Molecules. In *Modern Synthetic Methods in Carbohydrate Chemistry*; Werz, D. B., Vidal, S., Eds.; Wiley-VCH Verlag GmbH & Co. KGaA: Weinheim, Germany, 2013; pp 335–372.

(10) Paulick, M. G.; Bertozzi, C. R. The Glycosylphosphatidylinositol Anchor: A Complex Membrane-Anchoring Structure for Proteins. *Biochemistry.* **2008**, *47* (27), 6991–7000.

(11) Almeida, I. C.; Gazzinelli, R. T. Proinflammatory Activity of Glycosylphosphatidylinositol Anchors Derived from *Trypanosoma cruzi*: Structural and Functional Analyses. *J. Leukoc. Biol.* **2001**, *70* (4), 467–477.

(12) Kinoshita, T. Biosynthesis and Deficiencies of Glycosylphosphatidylinositol. *Proc. Jpn. Acad., Ser. B.* **2014**, *90* (4), 130–143.

(13) Naik, R. S.; Branch, O. H.; Woods, A. S.; Vijaykumar, M.; Perkins, D. J.; Nahlen, B. L.; Lal, A. A.; Cotter, R. J.; Costello, C. E.; Ockenhouse, C. F.; Davidson, E. A.; Gowda, D.

C. Glycosylphosphatidylinositol Anchors of *Plasmodium falciparum*. *J. Exp. Med.* **2000**, *192* (11), 1563–1576.

(14) Simons, K.; Vaz, W. L. C. Model Systems, Lipid Rafts, and Cell Membranes. *Annu. Rev. Biophys. Biomol. Struct.* **2004**, *33* (1), 269–295.

(15) Schmitz, G.; Orsó, E. CD14 Signalling in Lipid Rafts: New Ligands and Co-Receptors: *Curr. Opin. Lipidol.* **2002**, *13* (5), 513–521.

(16) Simons, K.; Toomre, D. Lipid Rafts and Signal Transduction. *Nat. Rev. Mol. Cell. Biol.* **2000**, *1* (1), 31–39.

(17) Müller, G. A.; Tschöp, M. H.; Müller, T. D. Chip-Based Sensing of the Intercellular Transfer of Cell Surface Proteins: Regulation by the Metabolic State. *Biomedicines.* **2021**, *9* (10), 1452.

(18) Cross, B.; Ronzon, F.; Roux, B.; Rieu, J.-P. Measurement of the Anchorage Force between GPI-Anchored Alkaline Phosphatase and Supported Membranes by AFM Force Spectroscopy. *Langmuir.* **2005**, *21* (11), 5149–5153.

(19) Medof, M. E.; Kinoshita, T.; Nussenzweig, V. Inhibition of Complement Activation on the Surface of Cells after Incorporation of Decay-Accelerating Factor (DAF) into Their Membranes. *J. Exp. Med.* **1984**, *160* (5), 1558–1578.

(20) Walter, E. I.; Ratnoff, W. D.; Long, K. E.; Kazura, J. W.; Medof, M. E. Effect of Glycoinositolphospholipid Anchor Lipid Groups on Functional Properties of Decay-Accelerating Factor Protein in Cells. *J. Biol. Chem.* **1992**, *267* (2), 1245–1252.

(21) Suzuki, K.; Okumura, Y.; Sato, T.; Sunamoto, J. Membrane Protein Transfer from Human Erythrocyte Ghosts to Liposomes Containing an Artificial Boundary Lipid. *Proc. Jpn. Acad. Ser. B*. **1995**, *71* (3), 93–97.

(22) Suzuki, K.; Okumura, Y. GPI-Linked Proteins Do Not Transfer Spontaneously from Erythrocytes to Liposomes. New Aspects of Reorganization of the Cell Membrane. *Biochemistry.* **2000**, *39* (31), 9477–9485.

(23) Ronzon, F.; Morandat, S.; Roux, B.; Bortolato, M. Insertion of a Glycosylphosphatidylinositol-Anchored Enzyme into Liposomes. *J. Membr. Biol.* **2004**, *197* (3), 169–177.

(24) Müller, G. A.; Lechner, A.; Tschöp, M. H.; Müller, T. D. Interaction of Full-Length Glycosylphosphatidylinositol-Anchored Proteins with Serum Proteins and Their Translocation to Cells In Vitro Depend on the (Pre-)Diabetic State in Rats and Humans. *Biomedicines.* **2021**, *9* (3), 277.

(25) Müller, G. A. Membrane Insertion and Intercellular Transfer of Glycosylphosphatidylinositol-Anchored Proteins: Potential Therapeutic Applications. *Arch. Physiol. Biochem*. **2020**, *126* (2), 139–156.

(26) Brunschwig, E. B.; Levine, E.; Trefzer, U.; Tykocinski, M. L. Glycosylphosphatidylinositol-Modified Murine B7-1 and B7-2 Retain Costimulator Function. *J. Immunol.* **1995**, *155* (12), 5498–5505.

(27) Brunschwig, E. B.; Fayen, J. D.; Medof, M. E.; Tykocinski, M. L. Protein Transfer of Glycosyl-Phosphatidylinositol (GPI)-Modified Murine B7–1 and B7–2 Costimulators: *J. Immunother.* **1999**, *22* (5), 390–400.

(28) Barboni, E.; Rivero, B. P.; George, A. J.; Martin, S. R.; Renoup, D. V.; Hounsell, E. F.; Barber, P. C.; Morris, R. J. The Glycophosphatidylinositol Anchor Affects the Conformation of Thy-1 Protein. *J. Cell. Sci.* **1995**, *108* (2), 487–497.

(29) Sharom, F. J.; Lehto, M. T. Glycosylphosphatidylinositol-Anchored Proteins: Structure, Function, and Cleavage by Phosphatidylinositol-Specific Phospholipase C. *Biochem. Cell Biol.* **2002**, *80* (5), 535–549.

(30) Sharom, F. J.; Radeva, G. GPI-Anchored Protein Cleavage in the Regulation of Transmembrane Signals. In *Membrane Dynamics and Domains*; Quinn, P. J., Ed.; Harris, J. R., Biswas, B. B., Series Eds.; Subcellular Biochemistry; Springer US: Boston, MA, 2004; Vol. 37, pp 285–315.

(31) Seong, J.; Wang, Y.; Kinoshita, T.; Maeda, Y. Implications of Lipid Moiety in Oligomerization and Immunoreactivities of GPI-Anchored Proteins. *J. Lipid Res.* **2013**, *54* (4), 1077–1091.

(32) Scheckel, C.; Aguzzi, A. Prions, Prionoids and Protein Misfolding Disorders. *Nat. Rev. Genet.* **2018**, *19* (7), 405–418.

(33) Puig, B.; Altmeppen, H. C.; Linsenmeier, L.; Chakroun, K.; Wegwitz, F.; Piontek, U. K.; Tatzelt, J.; Bate, C.; Magnus, T.; Glatzel, M. GPI-Anchor Signal Sequence Influences PrPC Sorting, Shedding and Signalling, and Impacts on Different Pathomechanistic Aspects of Prion Disease in Mice. *PLOS. Pathog.* **2019**, *15* (1), e1007520.

(34) Becker, C. F. W.; Liu, X.; Olschewski, D.; Castelli, R.; Seidel, R.; Seeberger, P. H. Semisynthesis of a Glycosylphosphatidylinositol-Anchored Prion Protein. *Angew. Chem. Int. Ed.* **2008**, *47* (43), 8215–8219.

(35) Abbasnia, T.; Asoodeh, A.; Habibi, G.; Haghparast, A. Isolation and Purification of Glycosylphosphatidylinositols (GPIs) in the Schizont Stage of Theileria Annulata and Determination of Antibody Response to GPI Anchors in Vaccinated and Infected Animals. *Parasites Vectors.* **2018**, *11* (1), 82.

(36) Morotti, A. L. M.; Martins-Teixeira, M. B.; Carvalho, I. Protozoan Parasites Glycosylphosphatidylinositol Anchors: Structures, Functions and Trends for Drug Discovery. *CMC.* **2019**, *26* (23), 4301–4322.

(37) Tachado, S. D.; Schofield, L. Glycosylphosphatidylinositol Toxin of *Trypanosoma brucei* Regulates IL-1α and TNF-α Expression in Macrophages by Protein Tyrosine Kinase-Mediated Signal Transduction. *Biochem. Biophys. Res. Commun.* **1994**, *205* (2), 984–991.

(38) Guha-Niyogi, A.; Sullivan, D. R.; Turco, S. J. Glycoconjugate Structures of Parasitic Protozoa. *Glycobiology.* **2001**, *11* (4), 45R-59R.

(39) Low, M. G. Glycosyl-phosphatidylinositol: A Versatile Anchor for Cell Surface Proteins. *FASEB j.* **1989**, *3* (5), 1600–1608.

(40) Low, M. G.; Saltiel, A. R. Structural and Functional Roles of Glycosyl-Phosphatidylinositol in Membranes. *Science.* **1988**, *239* (4837), 268–275.

(41) Brown, D. A.; Rose, J. K. Sorting of GPI-Anchored Proteins to Glycolipid-Enriched Membrane Subdomains during Transport to the Apical Cell Surface. *Cell.* **1992**, *68* (3), 533–544.

(42) Lipardi, C.; Nitsch, L.; Zurzolo, C. Detergent-Insoluble GPI–Anchored Proteins Are Apically Sorted in Fischer Rat Thyroid Cells, but Interference with Cholesterol or Sphingolipids Differentially Affects Detergent Insolubility and Apical Sorting. *MBoC.* **2000**, *11* (2), 531–542.

(43) Kinoshita, T.; Fujita, M.; Maeda, Y. Biosynthesis, Remodelling and Functions of Mammalian GPI-Anchored Proteins: Recent Progress. *J. Biochem.* **2008**, *144* (3), 287–294.

(44) Wu, T.; Yin, F.; Guang, S.; He, F.; Yang, L.; Peng, J. The Glycosylphosphatidylinositol Biosynthesis Pathway in Human Diseases. *Orphanet. J. Rare. Dis.* **2020**, *15* (1), 129.

(45) Kinoshita, T. Biosynthesis and Biology of Mammalian GPI-Anchored Proteins. *Open Biol.* **2020**, *10* (3), 190290.

(46) Almeida, A.; Layton, M.; Karadimitris, A. Inherited Glycosylphosphatidyl Inositol Deficiency: A Treatable CDG. *Biochim. Biophys. Acta. Mol. Basis. Dis.* **2009**, *1792* (9), 874–880.

(47) Guerrero, P. A.; Murakami, Y.; Malik, A.; Seeberger, P. H.; Kinoshita, T.; Varón Silva, D. Rescue of Glycosylphosphatidylinositol-Anchored Protein Biosynthesis Using Synthetic Glycosylphosphatidylinositol Oligosaccharides. *ACS Chem. Biol.* **2021**, *16* (11), 2297–2306.

(48) Bellai-Dussault, K.; Nguyen, T. T. M.; Baratang, N. V.; Jimenez-Cruz, D. A.; Campeau, P. M. Clinical Variability in Inherited Glycosylphosphatidylinositol Deficiency Disorders. *Clin. Genet.* **2019**, *95* (1), 112–121.

(49) Murakata, C.; Ogawa, T. Synthetic Study on Glycophosphatidyl Inositol (GPI) Anchor of *Trypanosoma brucei*: Glycoheptaosyl Core. *Tetrahedron Lett.* **1990**, *31* (17), 2439–2442.

(50) Baeschlin, D. K.; Chaperon, A. R.; Green, L. G.; Hahn, M. G.; Ince, S. J.; Ley, S. V. 1,2-Diacetals in Synthesis: Total Synthesis of a Glycosylphosphatidylinositol Anchor of *Trypanosoma brucei*. *Chem. Eur. J.* **2000**, *6* (1), 172–186.

(51) Shao, N.; Xue, J.; Guo, Z. Chemical Synthesis of a Skeleton Structure of Sperm CD52—A GPI-Anchored Glycopeptide. *Angew. Chem. Int. Ed.* **2004**, *43* (12), 1569–1573.

(52) Wu, X.; Guo, Z. Convergent Synthesis of a Fully Phosphorylated GPI Anchor of the CD52 Antigen. *Org. Lett.* **2007**, *9* (21), 4311–4313.

(53) Campbell, A. S.; Fraser-Reid, B. First Synthesis of a Fully Phosphorylated GPI Membrane Anchor: Rat Brain Thy-1. *J. Am. Chem. Soc.* **1995**, *117* (41), 10387–10388.

(54) Baeschlin, D. K.; Chaperon, A. R.; Charbonneau, V.; Green, L. G.; Ley, S. V.; Lücking, U.; Walther, E. Rapid Assembly of Oligosaccharides: Total Synthesis of a Glycosylphosphatidylinositol Anchor of *Trypanosoma brucei*. *Angew. Chem. Int. Ed.* **1998**, *37* (24), 3423–3428.

(55) Mayer, T. G.; Kratzer, B.; Schmidt, R. R. Synthesis of a GPI Anchor of Yeast (Saccharomyces Cerevisiae). *Angew. Chem. Int. Ed. Engl.* **1994**, *33* (21), 2177–2181.

(56) Lu, J.; Jayaprakash, K. N.; Schlueter, U.; Fraser-Reid, B. Synthesis of a Malaria Candidate Glycosylphosphatidylinositol (GPI) Structure: A Strategy for Fully Inositol Acylated and Phosphorylated GPIs. *J. Am. Chem. Soc.* **2004**, *126* (24), 7540–7547.

(57) Kwon, Y.-U.; Liu, X.; Seeberger, P. H. Total Syntheses of Fully Lipidated Glycosylphosphatidylinositol Anchors of *Toxoplasma gondii*. *Chem. Commun.* **2005**, No. 17, 2280.

(58) Tsai, Y.-H.; Götze, S.; Vilotijevic, I.; Grube, M.; Silva, D.; Seeberger, P. H. A General and Convergent Synthesis of Diverse Glycosylphosphatidylinositol Glycolipids. *Chem. Sci.* **2013**, *4* (1), 468–481.

(59) Tsai, Y.-H.; Götze, S.; Azzouz, N.; Hahm, H. S.; Seeberger, P. H.; Varón Silva, D. A General Method for Synthesis of GPI Anchors Illustrated by the Total Synthesis of the Low-Molecular-Weight Antigen from *Toxoplasma gondii*. *Angew. Chem. Int. Ed.* **2011**, *50* (42), 9961–9964.

(60) Nikolaev, A. V.; Al-Maharik, N. Synthetic Glycosylphosphatidylinositol (GPI) Anchors: How These Complex Molecules Have Been Made. *Nat. Prod. Rep.* **2011**, *28* (5), 970.

(61) Lahmann, M.; Garegg, P.; Konradsson, P.; Oscarson, S. Synthesis of a Polyphosphorylated GPI-Anchor Core Structure. *Can. J. Chem.* **2002**, *80* (8), 1105–1111.

(62) Lindberg, J.; Öhberg, L.; Garegg, P. J.; Konradsson, P. Efficient Routes to Glucosamine-Myo-Inositol Derivatives, Key Building Blocks in the Synthesis of Glycosylphosphatidylinositol Anchor Substances. *Tetrahedron.* **2002**, *58* (7), 1387–1398.

(63) Lu, J.; Jayaprakash, K. N.; Fraser-Reid, B. First Synthesis of a Malarial Prototype: A Fully Lipidated and Phosphorylated GPI Membrane Anchor. *Tetrahedron Lett.* **2004**, *45* (4), 879–882.

(64) Schofield, L.; Hewitt, M. C.; Evans, K.; Siomos, M.-A.; Seeberger, P. H. Synthetic GPI as a Candidate Anti-Toxic Vaccine in a Model of Malaria. *Nature.* **2002**, *418* (6899), 785–789.

(65) Hewitt, M. C.; Snyder, D. A.; Seeberger, P. H. Rapid Synthesis of a Glycosylphosphatidylinositol-Based Malaria Vaccine Using Automated Solid-Phase Oligosaccharide Synthesis. *J. Am. Chem. Soc.* **2002**, *124* (45), 13434–13436.

(66) Reichardt, N.-C.; Martín-Lomas, M. A Practical Solid-Phase Synthesis of Glycosylphosphatidylinositol Precursors. *Angew. Chem. Int. Ed.* **2003**, *42* (38), 4674–4677.

(67) Murakata, C.; Ogawa, T. Stereoselective Total Synthesis of the Glycosyl Phosphatidylinositol (GPI) Anchor of *Trypanosoma brucei*. *Carbohydr. Res.* **1992**, *235*, 95–114.

(68) Murakata, C.; Ogawa, T. A Total Synthesis of GPI Anchor of *Trypanosoma brucei*. *Tetrahedron Lett.* **1991**, *32* (5), 671–674.

(69) Udodong, U. E.; Madsen, R.; Roberts, C.; Fraser-Reid, B. A Ready, Convergent Synthesis of the Heptasaccharide GPI Membrane Anchor of Rat Brain Thy-1 Glycoprotein. *J. Am. Chem. Soc.* **1993**, *115* (17), 7886–7887.

(70) Almeida, I. C. Highly Purified Glycosylphosphatidylinositols from *Trypanosoma cruzi* Are Potent Proinflammatory Agents. *The EMBO Journal.* **2000**, *19* (7), 1476–1485.

(71) Yashunsky, D. V.; Borodkin, V. S.; Ferguson, M. A. J.; Nikolaev, A. V. The Chemical Synthesis of Bioactive Glycosylphosphatidylinositols from *Trypanosoma cruzi* Containing an Unsaturated Fatty Acid in the Lipid. *Angew. Chem. Int. Ed.* **2006**, *45* (3), 468–474.

(72) Swarts, B. M.; Guo, Z. Synthesis of a Glycosylphosphatidylinositol Anchor Bearing Unsaturated Lipid Chains. *J. Am. Chem. Soc.* **2010**, *132* (19), 6648–6650.

(73) Swarts, B. M.; Guo, Z. Chemical Synthesis and Functionalization of Clickable Glycosylphosphatidylinositol Anchors. *Chem. Sci.* **2011**, *2* (12), 2342.

(74) Lee, B.-Y.; Seeberger, P. H.; Varón Silva, D. Synthesis of Glycosylphosphatidylinositol (GPI)-Anchor Glycolipids Bearing Unsaturated Lipids. *Chem. Commun.* **2016**, *52* (8), 1586–1589.

(75) Ding, N.; Li, X.; Chinoy, Z. S.; Boons, G.-J. Synthesis of a Glycosylphosphatidylinositol Anchor Derived from *Leishmania Donovani* That Can Be Functionalized by Cu-Catalyzed Azide–Alkyne Cycloadditions. *Org. Lett.* **2017**, *19* (14), 3827–3830.

(76) Chiyonobu, T.; Inoue, N.; Morimoto, M.; Kinoshita, T.; Murakami, Y. Glycosylphosphatidylinositol (GPI) Anchor Deficiency Caused by Mutations in *PIGW* Is Associated with West Syndrome and Hyperphosphatasia with Mental Retardation Syndrome. *J. Med. Genet.* **2014**, *51* (3), 203–207.

(77) Murakami, Y.; Kinoshita, T. [Inherited GPI deficiencies: a new disease with intellectual disability and epilepsy]. *No To Hattatsu.* **2015**, *47* (1), 5–13.

(78) Baratang, N. V.; Jimenez Cruz, D. A.; Ajeawung, N. F.; Nguyen, T. T. M.; Pacheco-Cuéllar, G.; Campeau, P. M. Inherited Glycophosphatidylinositol Deficiency Variant Database and Analysis of Pathogenic Variants. *Mol. Genet. Genomic. Med.* **2019**, *7* (7).

(79) Zunich, J.; Esterly, N. Chime Syndrome (Zunich Syndrome). In *Neurocutaneous Disorders Phakomatoses and Hamartoneoplastic Syndromes*; Ruggieri, M., Pascual-Castroviejo, I., Di Rocco, C., Eds.; Springer Vienna: Vienna, 2008; pp 949–955.

(80) Murakami, Y.; Siripanyapinyo, U.; Hong, Y.; Kang, J. Y.; Ishihara, S.; Nakakuma, H.; Maeda, Y.; Kinoshita, T. PIG-W Is Critical for Inositol Acylation but Not for Flipping of Glycosylphosphatidylinositol-Anchor. *MBoC.* **2003**, *14* (10), 4285–4295.

(81) Hill, A.; DeZern, A. E.; Kinoshita, T.; Brodsky, R. A. Paroxysmal Nocturnal Haemoglobinuria. *Nat. Rev. Dis. Primers.* **2017**, *3* (1), 17028.

(82) Takeda, J.; Miyata, T.; Kawagoe, K.; Iida, Y.; Endo, Y.; Fujita, T.; Takahashi, M.; Kitani, T.; Kinoshita, T. Deficiency of the GPI Anchor Caused by a Somatic Mutation of the PIG-A Gene in Paroxysmal Nocturnal Hemoglobinuria. *Cell.* **1993**, *73* (4), 703–711.

(83) Kinoshita, T.; Inoue, N.; Takeda, J. Defective Glycosyl Phosphatidylinositol Anchor Synthesis and Paroxysmal Nocturnal Hemoglobinuria. In *Advances in Immunology*; Elsevier, 1995; Vol. 60, pp 57–103.

(84) Lazo-Langner, A.; Chin-Yee, I.; Al-Ani, F. Eculizumab in the Management of Paroxysmal Nocturnal Hemoglobinuria: Patient Selection and Special Considerations. *TCRM.* **2016**, *Volume 12*, 1161–1170.

(85) Lee, J. W.; Sicre de Fontbrune, F.; Wong Lee Lee, L.; Pessoa, V.; Gualandro, S.; Füreder, W.; Ptushkin, V.; Rottinghaus, S. T.; Volles, L.; Shafner, L.; Aguzzi, R.; Pradhan, R.; Schrezenmeier, H.; Hill, A. Ravulizumab (ALXN1210) vs Eculizumab in Adult Patients with PNH Naive to Complement Inhibitors: The 301 Study. *Blood.* **2019**, *133* (6), 530–539.

(86) Brodsky, R. A. Stem Cell Transplantation for Paroxysmal Nocturnal Hemoglobinuria. *Haematologica.* **2010**, *95* (6), 855–856.

(87) Nakasone, H.; Iijima, K.; Asano, H.; Nakamura, F.; Kida, M.; Izutsu, K.; Urabe, A.; Usuki, K. Immunosuppressive therapy with antithymocyte globulin and cyclosporine for paroxysmal nocturnal hemoglobinuria. *Rinsho Ketsuek.i* **2008**, *49* (7), 498–504.

(88) Knaus, A.; Pantel, J. T.; Pendziwiat, M.; Hajjir, N.; Zhao, M.; Hsieh, T.-C.; Schubach, M.; Gurovich, Y.; Fleischer, N.; Jäger, M.; Köhler, S.; Muhle, H.; Korff, C.; Møller, R. S.; Bayat, A.; Calvas, P.; Chassaing, N.; Warren, H.; Skinner, S.; Louie, R.; Evers, C.; Bohn, M.; Christen, H.-J.; van den Born, M.; Obersztyn, E.; Charzewska, A.; Endziniene, M.; Kortüm, F.; Brown, N.; Robinson, P. N.; Schelhaas, H. J.; Weber, Y.; Helbig, I.; Mundlos, S.; Horn, D.; Krawitz, P. M. Characterization of Glycosylphosphatidylinositol Biosynthesis Defects by Clinical Features, Flow Cytometry, and Automated Image Analysis. *Genome Med.* **2018**, *10* (1), 3.

(89) Kuki, I.; Takahashi, Y.; Okazaki, S.; Kawawaki, H.; Ehara, E.; Inoue, N.; Kinoshita, T.; Murakami, Y. Vitamin B6-Responsive Epilepsy Due to Inherited GPI Deficiency. *Neurology.* **2013**, *81* (16), 1467–1469.

(90) Houjou, T.; Hayakawa, J.; Watanabe, R.; Tashima, Y.; Maeda, Y.; Kinoshita, T.; Taguchi, R. Changes in Molecular Species Profiles of Glycosylphosphatidylinositol Anchor Precursors in Early Stages of Biosynthesis. *J. Lipid Res.* **2007**, *48* (7), 1599–1606.

(91) Niemietz, M.; Perkams, L.; Hoffman, J.; Eller, S.; Unverzagt, C. Selective Oxidative Debenzylation of Mono- and Oligosaccharides in the Presence of Azides. *Chem. Commun.* **2011**, *47* (37), 10485.

(92) Lee, S.-U.; Li, C. F.; Mortales, C.-L.; Pawling, J.; Dennis, J. W.; Grigorian, A.; Demetriou, M. Increasing Cell Permeability of N-Acetylglucosamine via 6-Acetylation Enhances Capacity to Suppress T-Helper 1 (TH1)/TH17 Responses and Autoimmunity. *PLOS ONE.* **2019**, *14* (3), e0214253.

(93) Wang, Y.; Menon, A. K.; Maki, Y.; Liu, Y.-S.; Iwasaki, Y.; Fujita, M.; Guerrero, P. A.; Varón Silva, D.; Seeberger, P. H.; Murakami, Y.; Kinoshita, T. Genome-Wide CRISPR Screen Reveals CLPTM1L as a Lipid Scramblase Required for Efficient Glycosylphosphatidylinositol Biosynthesis. *Proc. Natl. Acad. Sci. U.S.A.* **2022**, *119* (14), e2115083119.

(94) Phillips, M. A.; Burrows, J. N.; Manyando, C.; van Huijsduijnen, R. H.; Van Voorhis, W. C.; Wells, T. N. C. Malaria. *Nat. Rev. Dis. Primers.* **2017**, *3* (1), 17050.

(95) Ashley, E. A.; Pyae Phyo, A.; Woodrow, C. J. Malaria. *The Lancet.* **2018**, *391* (10130), 1608–1621.

(96) Talapko; Škrlec; Alebić; Jukić; Včev. Malaria: The Past and the Present. *Microorganisms.* **2019**, *7* (6), 179.

(97) Idro, R.; Marsh, K.; John, C. C.; Newton, C. R. J. Cerebral Malaria: Mechanisms of Brain Injury and Strategies for Improved Neurocognitive Outcome. *Pediatr. Res.* **2010**, *68* (4), 267–274.

(98) Ghazanfari, N.; Mueller, S. N.; Heath, W. R. Cerebral Malaria in Mouse and Man. *Front. Immunol.* **2018**, *9*, 2016.

(99) World malaria report 2021. Geneva: World Health Organization; 2021.

(100) Hay, S. I.; Guerra, C. A.; Tatem, A. J.; Noor, A. M.; Snow, R. W. The Global Distribution and Population at Risk of Malaria: Past, Present, and Future. *Lancet Infect. Dis.* **2004**, *4* (6), 327–336.

(101) Greenwood, B. M.; Fidock, D. A.; Kyle, D. E.; Kappe, S. H. I.; Alonso, P. L.; Collins, F. H.; Duffy, P. E. Malaria: Progress, Perils, and Prospects for Eradication. *J. Clin. Invest.* **2008**, *118* (4), 1266–1276.

(102) PATH Washington DC. Malaria Parasite Life Cycle. *mvi PATH Malaria Vaccine Initiative*. Available online: https://www.malariavaccine.org/malaria-and-vaccines/vaccine-development/life-cycle-malaria-parasite. (Accessed June 15, 2022).

(103) Dini, S.; Zaloumis, S.; Cao, P.; Price, R. N.; Fowkes, F. J. I.; van der Pluijm, R. W.; McCaw, J. M.; Simpson, J. A. Investigating the Efficacy of Triple Artemisinin-Based Combination Therapies for Treating *Plasmodium falciparum* Malaria Patients Using Mathematical Modeling. *Antimicrob. Agents Chemother.* **2018**, *62* (11), e01068-18.

(104) Clinical Trials Register—Clinical Trials for Malaria 2019. Available Online: https://www.clinicaltrialsregister.eu/ctr-search/search?query=malaria (Accessed on June 15, 2022).

(105) Draper, S. J.; Sack, B. K.; King, C. R.; Nielsen, C. M.; Rayner, J. C.; Higgins, M. K.; Long, C. A.; Seder, R. A. Malaria Vaccines: Recent Advances and New Horizons. *Cell Host & Microbe.* **2018**, *24* (1), 43–56.

(106) Rénia, L.; Goh, Y. S.; Peng, K.; Mauduit, M.; Snounou, G. Assessing Malaria Vaccine Efficacy. In *Towards Malaria Elimination - A Leap Forward*; Manguin, S., Dev, V., Eds.; InTech, 2018.

(107) Greenwood, B. M.; Targett, G. A. T. Malaria Vaccines and the New Malaria Agenda. *Clin. Microbiol. Infect.* **2011**, *17* (11), 1600–1607.

(108) Hoffman, S. L.; Vekemans, J.; Richie, T. L.; Duffy, P. E. The March toward Malaria Vaccines. *Vaccine.* **2015**, *33*, D13–D23.

(109) Gowda, D. C.; Gupta, P.; Davidson, E. A. Glycosylphosphatidylinositol Anchors Represent the Major Carbohydrate Modification in Proteins of Intraerythrocytic Stage *Plasmodium falciparum*. *J. Biol. Chem.* **1997**, *272* (10), 6428–6439.

(110) Naik, R. S.; Davidson, E. A.; Gowda, D. C. Developmental Stage-Specific Biosynthesis of Glycosylphosphatidylinositol Anchors in Intraerythrocytic *Plasmodium falciparum* and Its Inhibition in a Novel Manner by Mannosamine. *J. Biol. Chem.* **2000**, *275* (32), 24506–24511.

(111) Schofield, L.; Grau, G. E. Immunological Processes in Malaria Pathogenesis. *Nat. Rev. Immunol.* **2005**, *5* (9), 722–735.

(112) de Souza, J. B.; Todd, J.; Krishegowda, G.; Gowda, D. C.; Kwiatkowski, D.; Riley, E. M. Prevalence and Boosting of Antibodies to *Plasmodium falciparum* Glycosylphosphatidylinositols and Evaluation of Their Association with Protection from Mild and Severe Clinical Malaria. *Infect. Immun.* **2002**, *70* (9), 5045–5051.

(113) Schofield, L.; Hackett, F. Signal Transduction in Host Cells by a Glycosylphosphatidylinositol Toxin of Malaria Parasites. *J. Exp. Med.* **1993**, *177* (1), 145–153.

(114) Elased, K. M.; Gumaa, K. A.; de Souza, J. B.; Rahmoune, H.; Playfair, J. H. L.; Rademacher, T. W. Reversal of Type 2 Diabetes in Mice by Products of Malaria Parasites. *Mol. Genet. Metab.* **2001**, *73* (3), 248–258.

(115) Boutlis, C. S.; Gowda, D. C.; Naik, R. S.; Maguire, G. P.; Mgone, C. S.; Bockarie, M. J.; Lagog, M.; Ibam, E.; Lorry, K.; Anstey, N. M. Antibodies to *Plasmodium falciparum* Glycosylphosphatidylinositols: Inverse Association with Tolerance of Parasitemia in Papua New Guinean Children and Adults. *Infect. Immun.* **2002**, *70* (9), 5052–5057.

(116) Hudson Keenihan, S. N.; Ratiwayanto, S.; Soebianto, S.; Krisin, null; Marwoto, H.; Krishnegowda, G.; Gowda, D. C.; Bangs, M. J.; Fryauff, D. J.; Richie, T. L.; Kumar, S.; Baird, J. K. Age-Dependent Impairment of IgG Responses to Glycosylphosphatidylinositol with Equal Exposure to *Plasmodium falciparum* among Javanese Migrants to Papua, Indonesia. *Am. J. Trop. Med. Hyg.* **2003**, *69* (1), 36–41.

(117) Perraut, R.; Diatta, B.; Marrama, L.; Garraud, O.; Jambou, R.; Longacre, S.; Krishnegowda, G.; Dieye, A.; Gowda, D. C. Differential Antibody Responses to *Plasmodium falciparum* Glycosylphosphatidylinositol Anchors in Patients with Cerebral and Mild Malaria. *Microbes Infect.* **2005**, *7* (4), 682–687.

(118) Naik, R. S.; Krishnegowda, G.; Ockenhouse, C. F.; Gowda, D. C. Naturally Elicited Antibodies to Glycosylphosphatidylinositols (GPIs) of *Plasmodium falciparum* Require Intact GPI Structures for Binding and Are Directed Primarily against the Conserved Glycan Moiety. *Infect. Immun.* **2006**, *74* (2), 1412–1415.

(119) Schmidt, A.; Schwarz, R. T.; Gerold, P. *Plasmodium falciparum*: Asexual Erythrocytic Stages Synthesize Two Structurally Distinct Free and Protein-Bound Glycosylphosphatidylinositols in a Maturation-Dependent Manner. *Exp. Parasitol.* **1998**, *88* (2), 95–102.

(120) Malik, A.; Steinbeis, F.; Carillo, M. A.; Seeberger, P. H.; Lepenies, B.; Varón Silva, D. Immunological Evaluation of Synthetic Glycosylphosphatidylinositol Glycoconjugates as Vaccine Candidates against Malaria. *ACS Chem. Biol.* **2020**, *15* (1), 171–178.

(121) Kamena, F.; Tamborrini, M.; Liu, X.; Kwon, Y.-U.; Thompson, F.; Pluschke, G.; Seeberger, P. H. Synthetic GPI Array to Study Antitoxic Malaria Response. *Nat. Chem. Biol.* **2008**, *4* (4), 238–240.

(122) Dijkman, P. M.; Marzluf, T.; Zhang, Y.; Chang, S.-Y. S.; Helm, D.; Lanzer, M.; Bujard, H.; Kudryashev, M. Structure of the Merozoite Surface Protein 1 from *Plasmodium falciparum*. *Sci. Adv.* **2021**, *7* (23), eabg0465.

(123) Das, S.; Hertrich, N.; Perrin, A. J.; Withers-Martinez, C.; Collins, C. R.; Jones, M. L.; Watermeyer, J. M.; Fobes, E. T.; Martin, S. R.; Saibil, H. R.; Wright, G. J.; Treeck, M.; Epp, C.; Blackman, M. J. Processing of *Plasmodium falciparum* Merozoite Surface Protein MSP1 Activates a Spectrin-Binding Function Enabling Parasite Egress from RBCs. *Cell Host & Microbe.* **2015**, *18* (4), 433–444.

(124) Waisberg, M.; Cerqueira, G. C.; Yager, S. B.; Francischetti, I. M. B.; Lu, J.; Gera, N.; Srinivasan, P.; Miura, K.; Rada, B.; Lukszo, J.; Barbian, K. D.; Leto, T. L.; Porcella, S. F.; Narum, D. L.; El-Sayed, N.; Miller, L. H.; Pierce, S. K. *Plasmodium falciparum* Merozoite Surface Protein 1 Blocks the Proinflammatory Protein S100P. *Proc. Natl. Acad. Sci. U.S.A.* **2012**, *109* (14), 5429–5434.

(125) Mazumdar, S.; Mukherjee, P.; Yazdani, S. S.; Jain, S. K.; Mohmmed, A.; Chauhan, V. S. *Plasmodium falciparum* Merozoite Surface Protein 1 (MSP-1)-MSP-3 Chimeric Protein: Immunogenicity Determined with Human-Compatible Adjuvants and Induction of Protective Immune Response. *Infect. Immun.* **2010**, *78* (2), 872–883.

(126) Holder, A. A.; Riley, E. M. Human Immune Response to MSP-1. *Parasitol. Today.* **1996**, *12* (5), 173–174.

(127) Cowan, G. J. M.; Creasey, A. M.; Dhansarnsombut, K.; Thomas, A. W.; Remarque, E. J.; Cavanagh, D. R. A Malaria Vaccine Based on the Polymorphic Block 2 Region of MSP-1 That Elicits a Broad Serotype-Spanning Immune Response. *PLOS ONE.* **2011**, *6* (10), e26616.

(128) Chang, S. P.; Nikaido, C. M.; Hashimoto, A. C.; Hashiro, C. Q.; Yokota, B. T.; Hui, G. S. Regulation of Antibody Specificity to *Plasmodium falciparum* Merozoite Surface Protein-1 by Adjuvant and MHC Haplotype. *J. Immunol*. **1994**, *152* (7), 3483–3490.

(129) Roller, R. F.; Malik, A.; Carillo, M. A.; Garg, M.; Rella, A.; Raulf, M.; Lepenies, B.; Seeberger, P. H.; Varón Silva, D. Semisynthesis of Functional Glycosylphosphatidylinositol-Anchored Proteins. *Angew. Chem. Int. Ed.* **2020**, *59* (29), 12035–12040.

(130) Becker, C. F. W.; Liu, X.; Olschewski, D.; Castelli, R.; Seidel, R.; Seeberger, P. H. Semisynthesis of a Glycosylphosphatidylinositol-Anchored Prion Protein. *Angew. Chem. Int. Ed.* **2008**, *47* (43), 8215–8219.

(131) Conibear, A. C.; Watson, E. E.; Payne, R. J.; Becker, C. F. W. Native Chemical Ligation in Protein Synthesis and Semi-Synthesis. *Chem. Soc. Rev.* **2018**, *47* (24), 9046–9068.

(132) Ito, H.; Imai, N.; Takao, K.; Kobayashi, S. Enantioselective Synthesis of Curacin A. 2. Total Synthesis of Curacin A by Condensation of C1–C7, C8–C17, and C18–C22 Segments. *Tetrahedron Lett.* **1996**, *37* (11), 1799–1800.

(133) Lidani, K. C. F.; Andrade, F. A.; Bavia, L.; Damasceno, F. S.; Beltrame, M. H.; Messias-Reason, I. J.; Sandri, T. L. Chagas Disease: From Discovery to a Worldwide Health Problem. *Front. Public Health.* **2019**, *7*, 166.

(134) Chatelain, E. Chagas Disease Drug Discovery: Toward a New Era. *SLAS Discovery.* **2015**, *20* (1), 22–35.

(135) Tarleton, R. L. *Trypanosoma cruzi* and Chagas Disease: Cause and Effect. In *American Trypanosomiasis*; Tyler, K. M., Miles, M. A., Eds.; Black, S. J., Seed, J. R., Series Eds.; World Class Parasites; Springer US: Boston, MA, 2003; Vol. 7, pp 107–115.

(136) Álvarez-Hernández, D.-A.; García-Rodríguez-Arana, R.; Ortiz-Hernández, A.; Álvarez-Sánchez, M.; Wu, M.; Mejia, R.; Martínez-Juárez, L.-A.; Montoya, A.; Gallardo-Rincon, H.; Vázquez-López, R.; Fernández-Presas, A.-M. A Systematic Review of Historical and Current Trends in Chagas Disease. *Ther. Adv. Infect. Dis.* **2021**, *8*, 204993612110337.

(137) Álvarez-Hernández, D.-A.; Franyuti-Kelly, G.-A.; Díaz-López-Silva, R.; González-Chávez, A.-M.; González-Hermosillo-Cornejo, D.; Vázquez-López, R. Chagas Disease: Current Perspectives on a Forgotten Disease. Rev. Medica *del* Hosp. Gen. de Mex. **2018**, *81* (3), 154–164.

(138) Pan American Health Organization. *Chagas Disease*. Available online: https://www.paho.org/en/topics/chagas-disease. (Accessed June 23, 2022).

(139) World Health Orgamization. Chagas Disease (Also Known as American Trypanosomiasis). Available online: https://www.who.int/news-room/fact-sheets/detail/chagas-disease-(american-trypanosomiasis). (Accessed June 23, 2022).

(140) Ribeiro, A. L.; Nunes, M. P.; Teixeira, M. M.; Rocha, M. O. C. Diagnosis and Management of Chagas Disease and Cardiomyopathy. *Nat. Rev. Cardiol.* **2012**, *9* (10), 576–589.

(141) Urbina, J. A.; Docampo, R. Specific Chemotherapy of Chagas Disease: Controversies and Advances. *Trends Parasitol.* **2003**, *19* (11), 495–501.

(142) C. Onyekwelu, K. Life Cycle of *Trypanosoma cruzi* in the Invertebrate and the Vertebrate Hosts. In *Biology of Trypanosoma cruzi*; De Souza, W., Ed.; IntechOpen, 2019.

(143) Teixeira, D. E.; Benchimol, M.; Crepaldi, P. H.; de Souza, W. Interactive Multimedia to Teach the Life Cycle of *Trypanosoma cruzi*, the Causative Agent of Chagas Disease. *PLOS. Negl. Trop. Dis.* **2012**, *6* (8), e1749.

(144) MacRae, J. I.; Acosta-Serrano, A.; Morrice, N. A.; Mehlert, A.; Ferguson, M. A. J. Structural Characterization of NETNES, a Novel Glycoconjugate in *Trypanosoma cruzi* Epimastigotes. *J. Biol. Chem.* **2005**, *280* (13), 12201–12211.

(145) Silva, J. S.; Vespa, G. N.; Cardoso, M. A.; Aliberti, J. C.; Cunha, F. Q. Tumor Necrosis Factor Alpha Mediates Resistance to *Trypanosoma cruzi* Infection in Mice by Inducing Nitric Oxide Production in Infected Gamma Interferon-Activated Macrophages. *Infect. Immun.* **1995**, *63* (12), 4862–4867.

(146) Vespa, G. N.; Cunha, F. Q.; Silva, J. S. Nitric Oxide Is Involved in Control of *Trypanosoma cruzi*-Induced Parasitemia and Directly Kills the Parasite in Vitro. *Infect. Immun.* **1994**, *62* (11), 5177–5182.

7 List of publications

- **P. A. Guerrero**, Y. Murakami, A. Malik, P. H. Seeberger, T. Kinoshita, and D. Varón Silva, *ACS Chem. Biol*. 2021, 16, 11, 2297–2306. Rescue of Glycosylphosphatidylinositol-Anchored Protein Biosynthesis Using Synthetic Glycosylphosphatidylinositol Oligosaccharides.

- Y. Wang, A. K. Menon, Y. Maki, Y. Liu, Y. Iwasaki, M. Fujita, **P. A. Guerrero**, D. Varón Silva, P. H. Seeberger, Y. Murakami, T. Kinoshita, *PNAS USA*, 2022, 119, 14, e2115083119. CLPTM1L is a Lipid Scramblase Involved in Glycosylphosphatidylinositol Biosynthesis.

Appendix

^{1}H NMR spectrum of compound 2-14

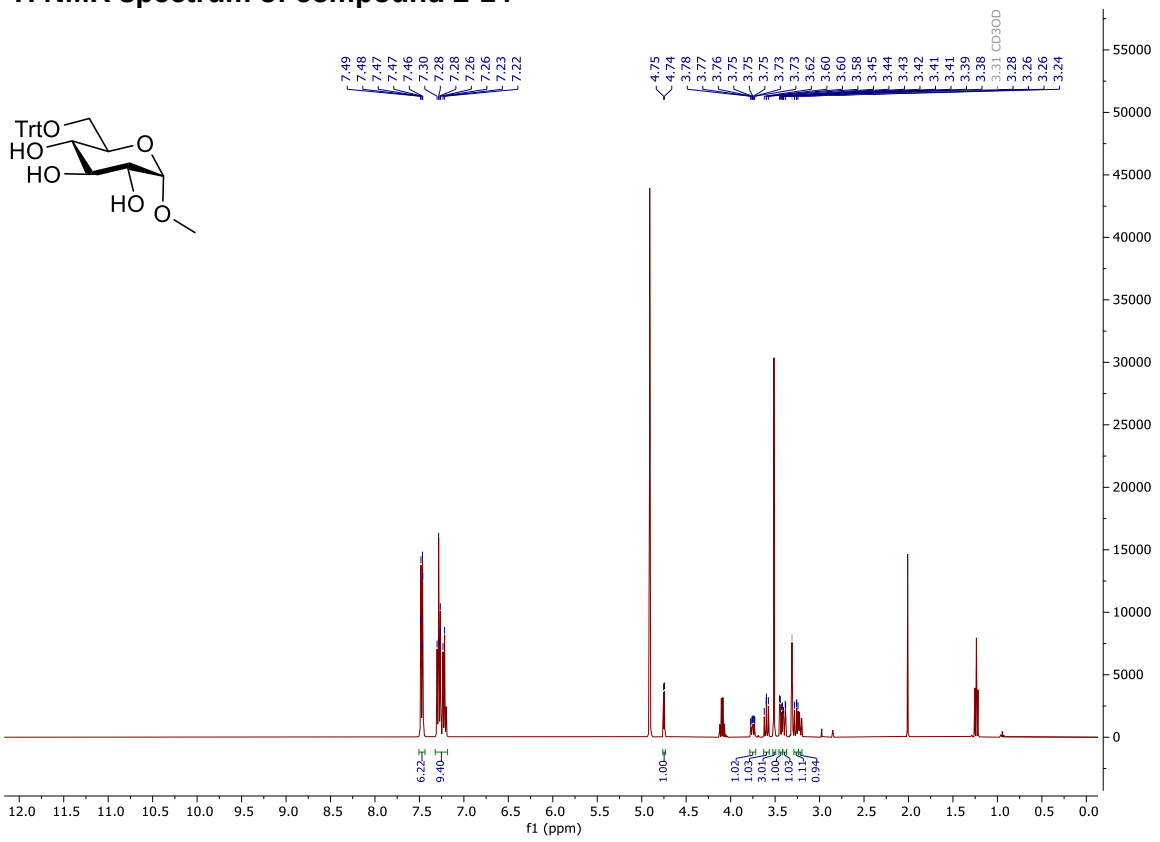

COSY NMR spectrum of compound 2-14

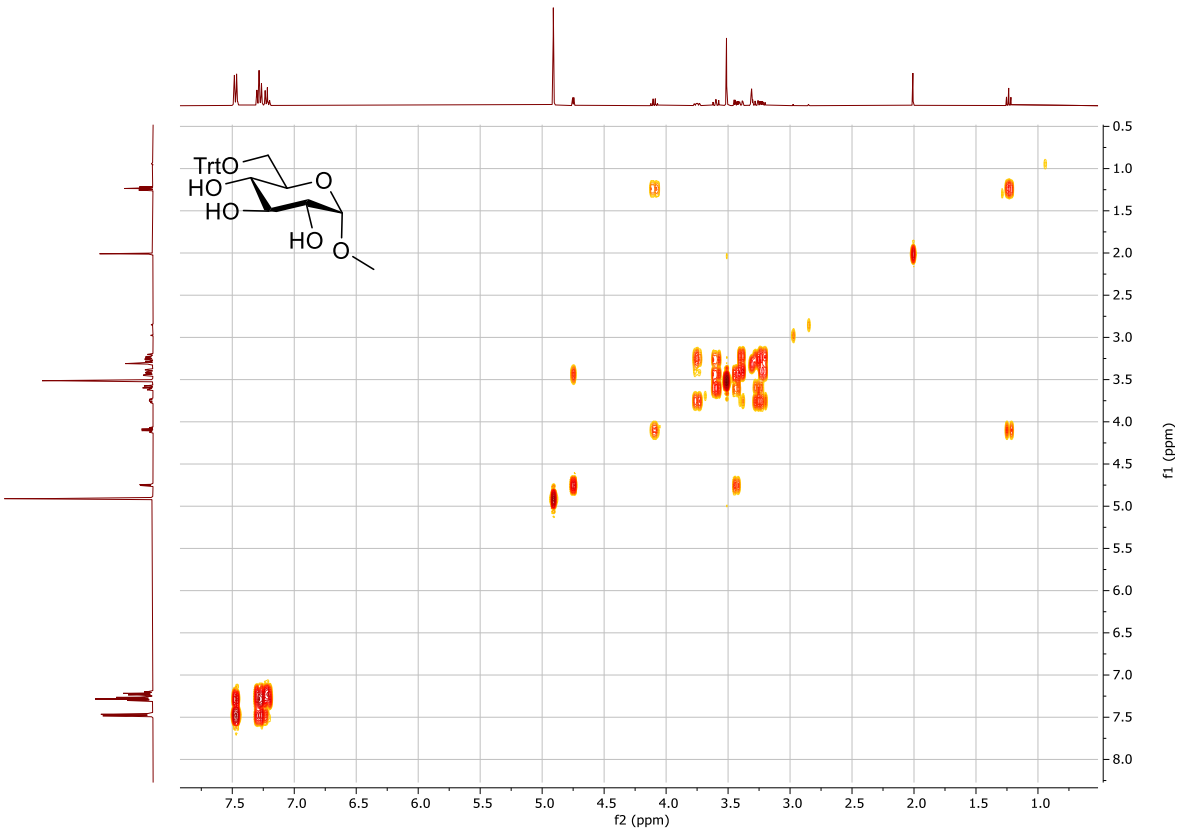

^{1}H NMR spectrum of compound 2-15

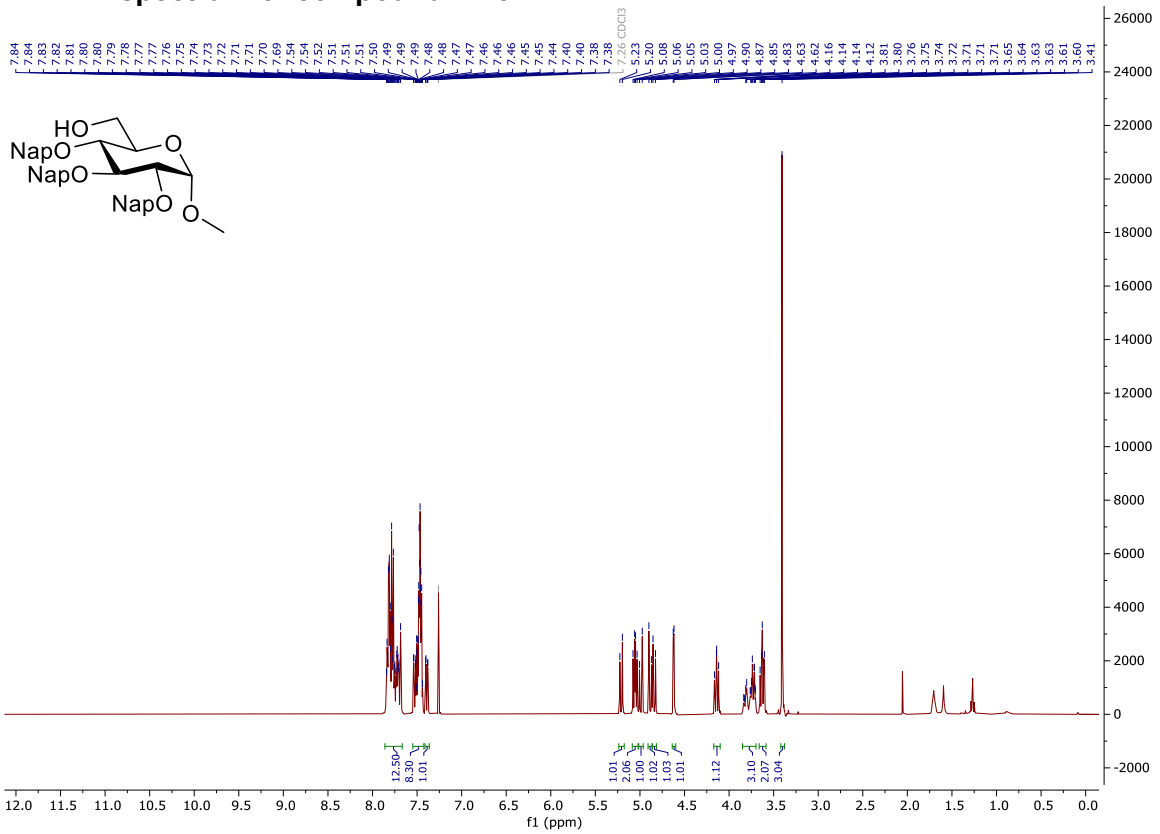

^{13}C NMR spectrum of compound 2-15

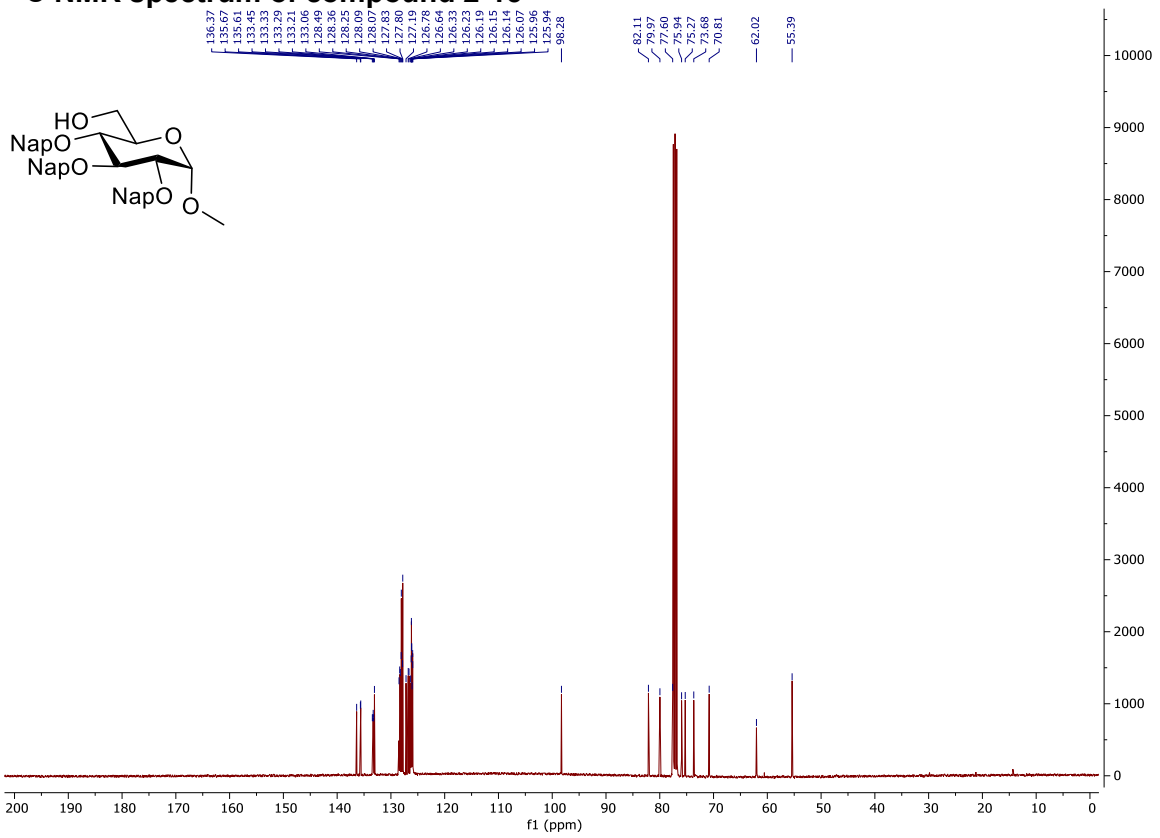

COSY NMR spectrum of compound 2-15

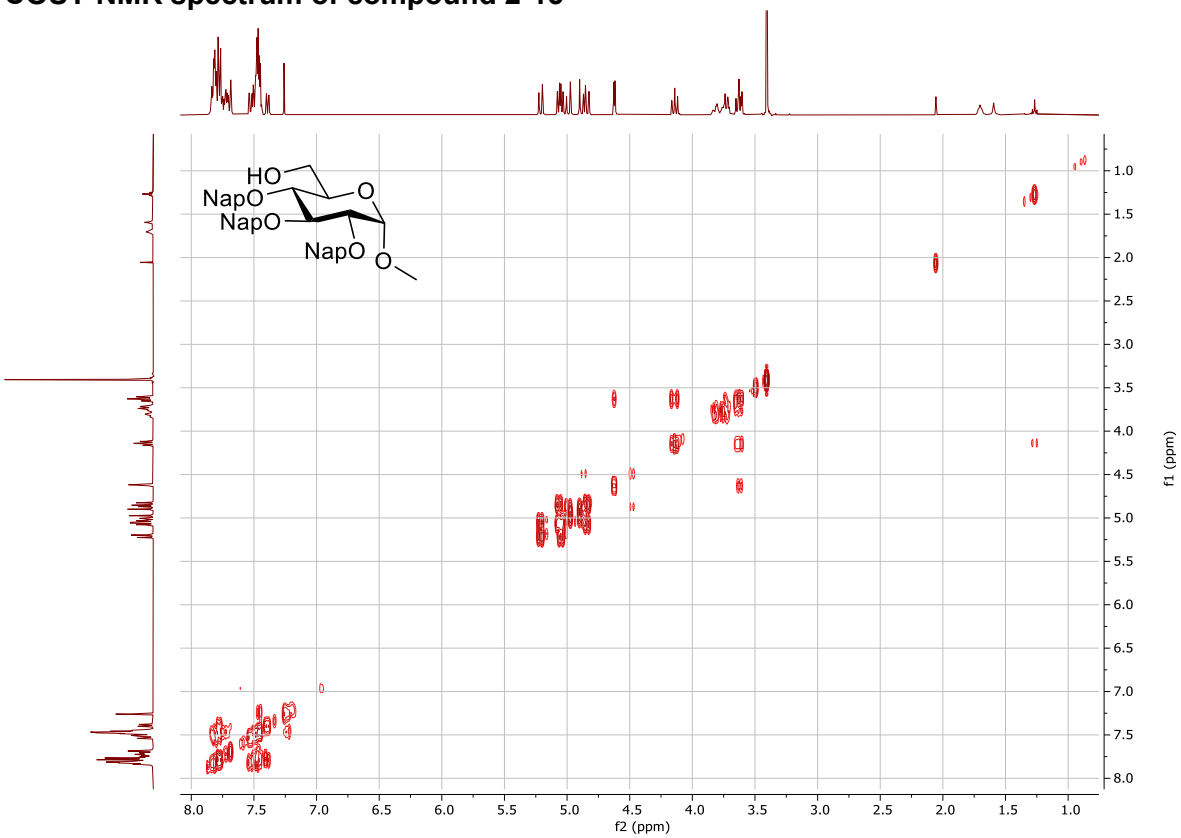

HSQC NMR spectrum of compound 2-15

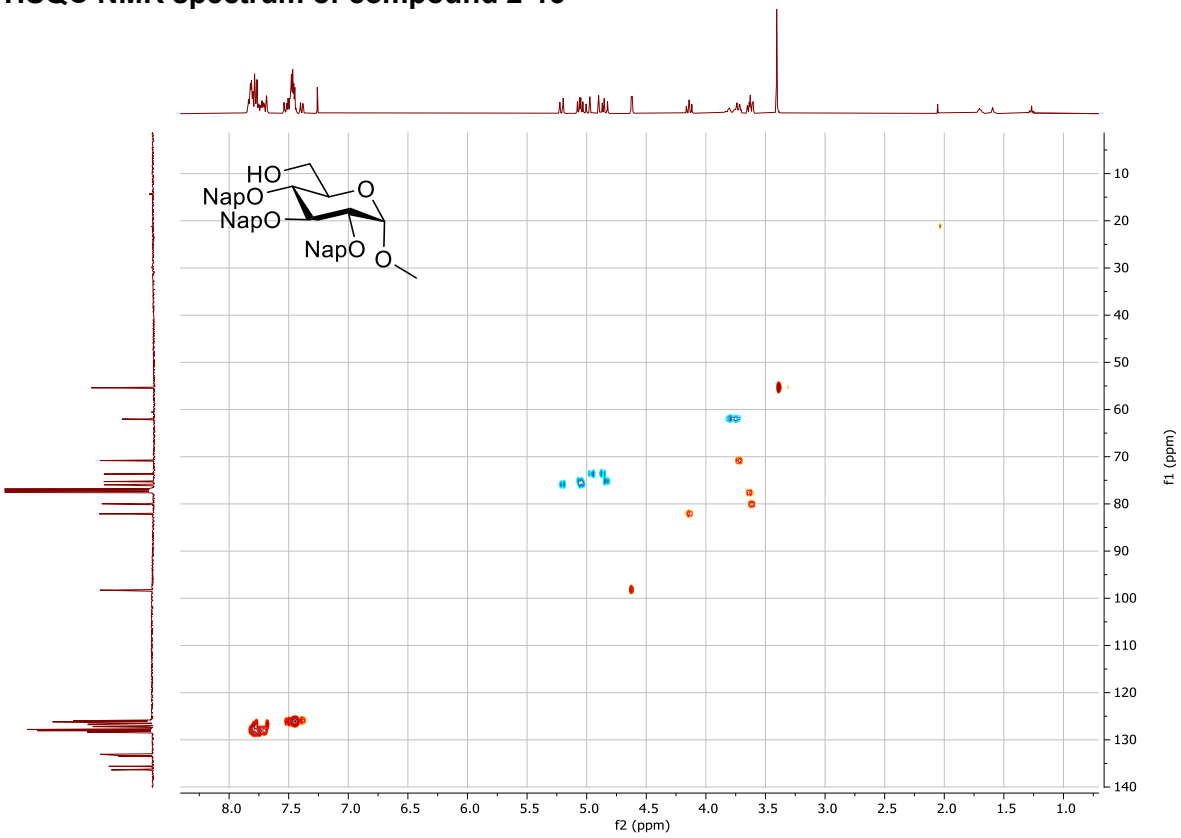

^{1}H NMR spectrum of compound 2-16

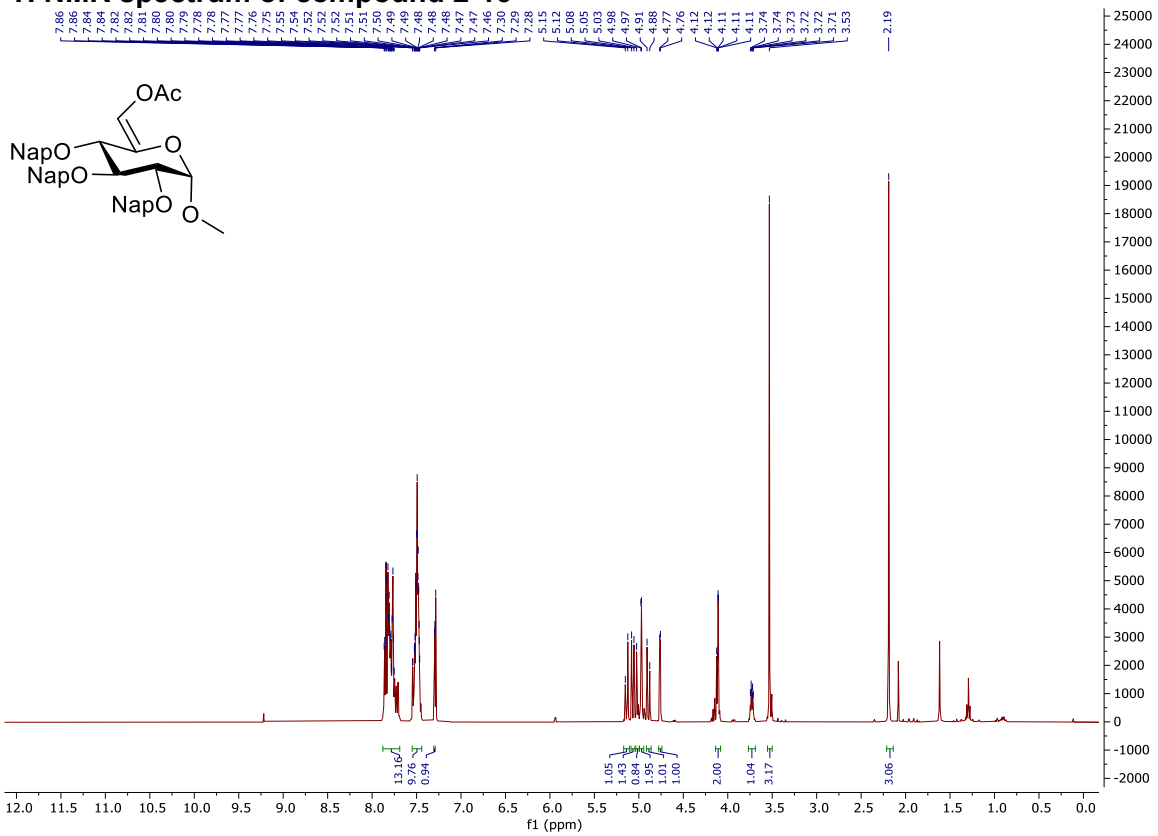

^{13}C NMR spectrum of compound 2-16

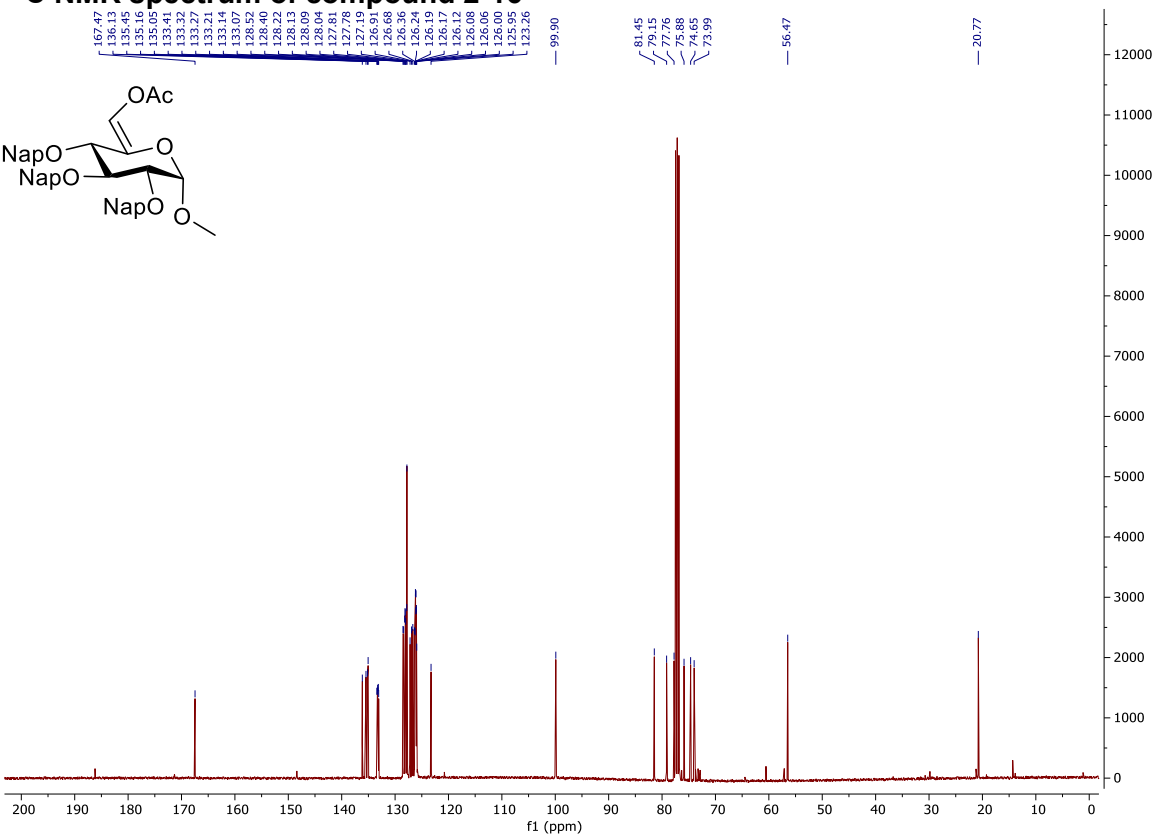

COSY NMR spectrum of compound 2-16

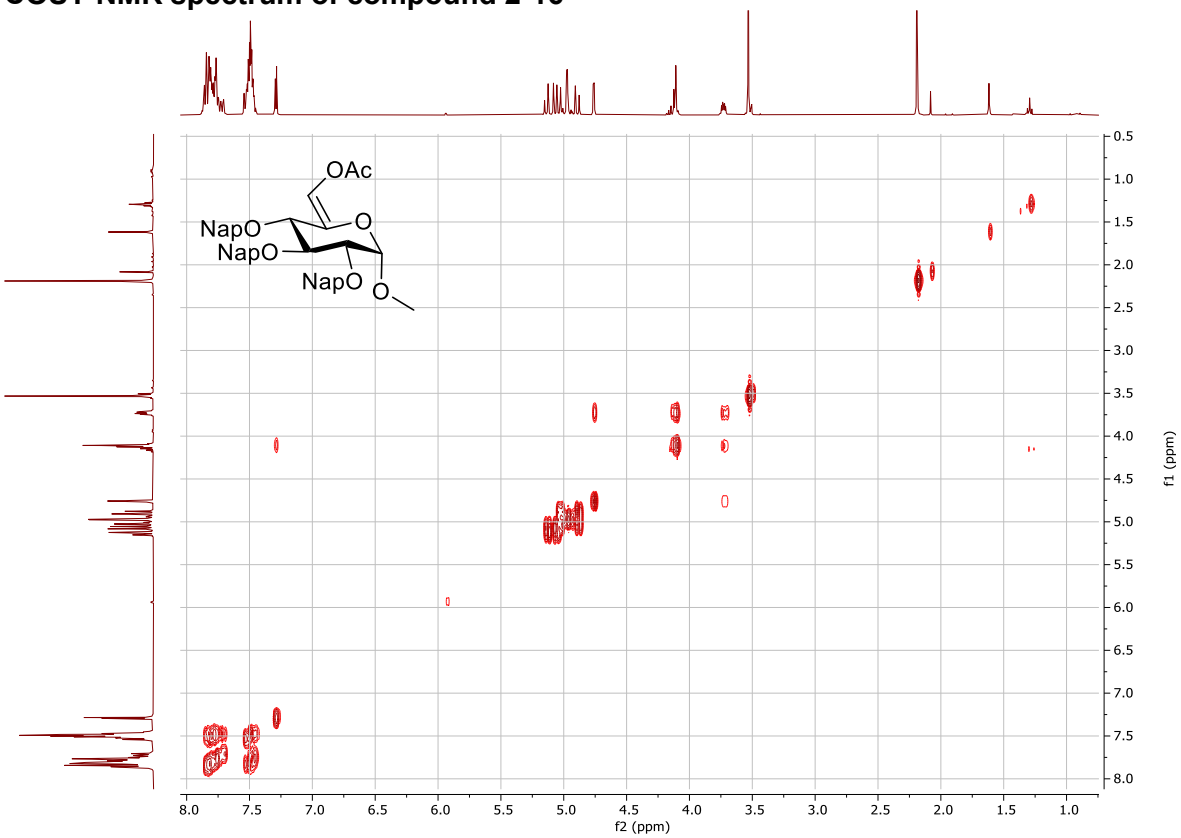

HSQC NMR spectrum of compound 2-16

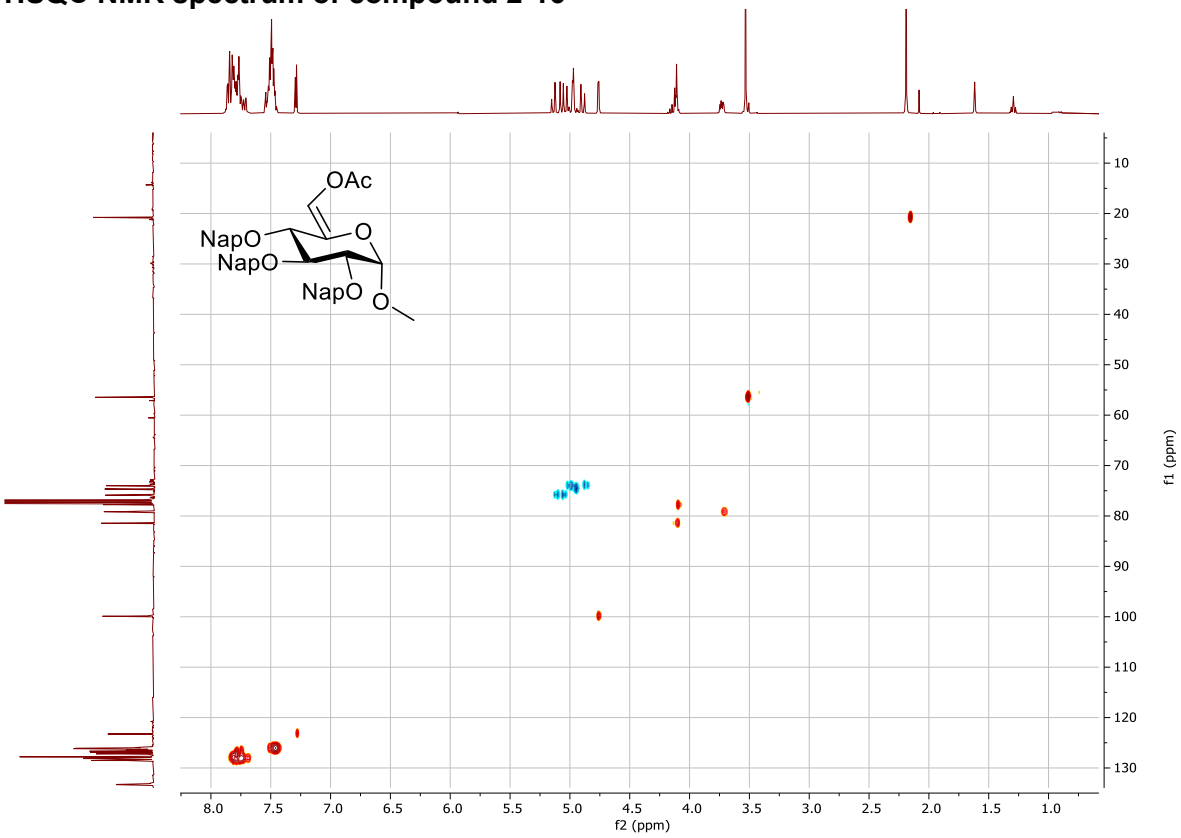

^{1}H NMR spectrum of compound 2-17

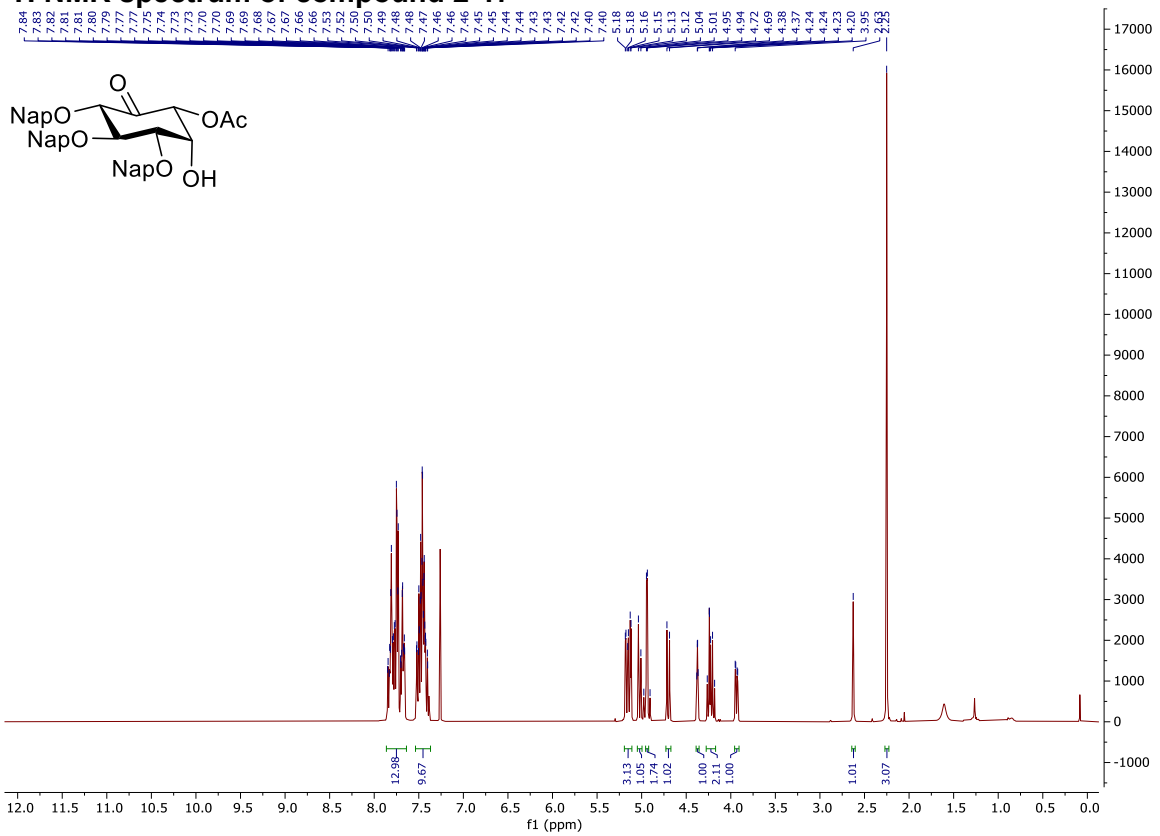

^{13}C NMR spectrum of compound 2-17

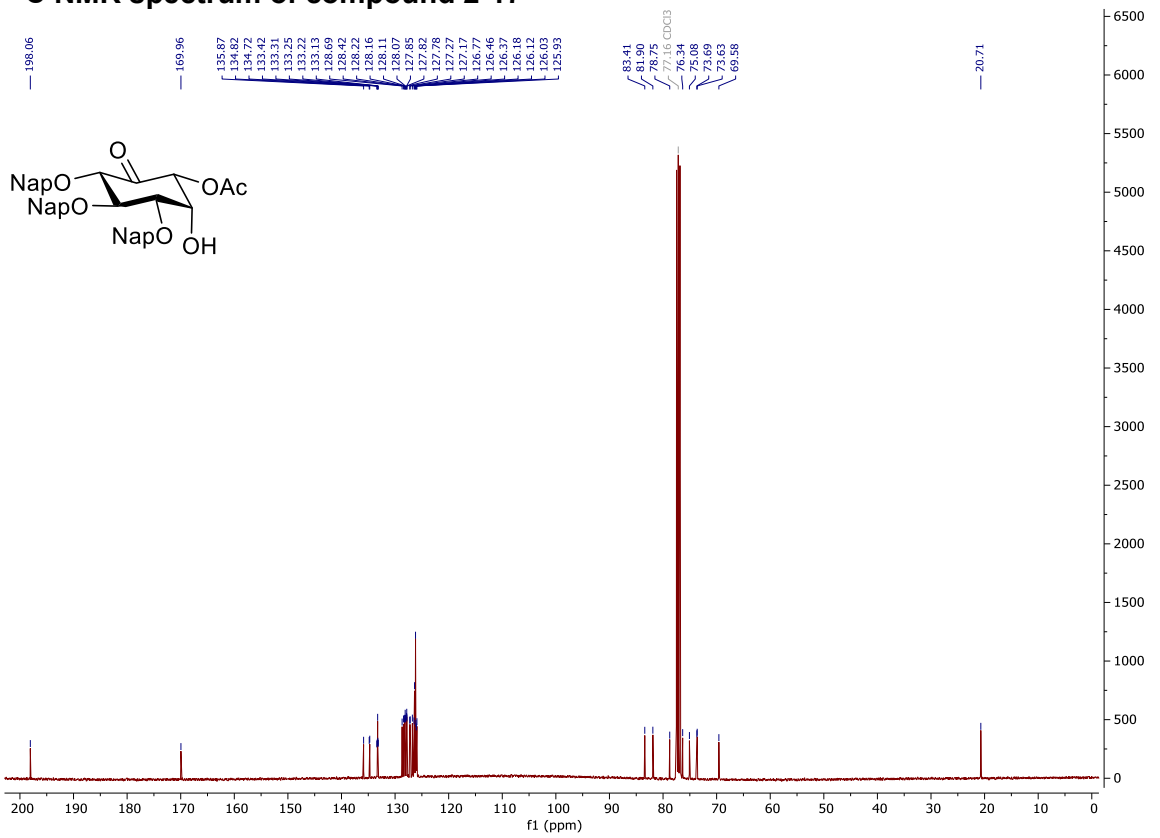

COSY NMR spectrum of compound 2-17

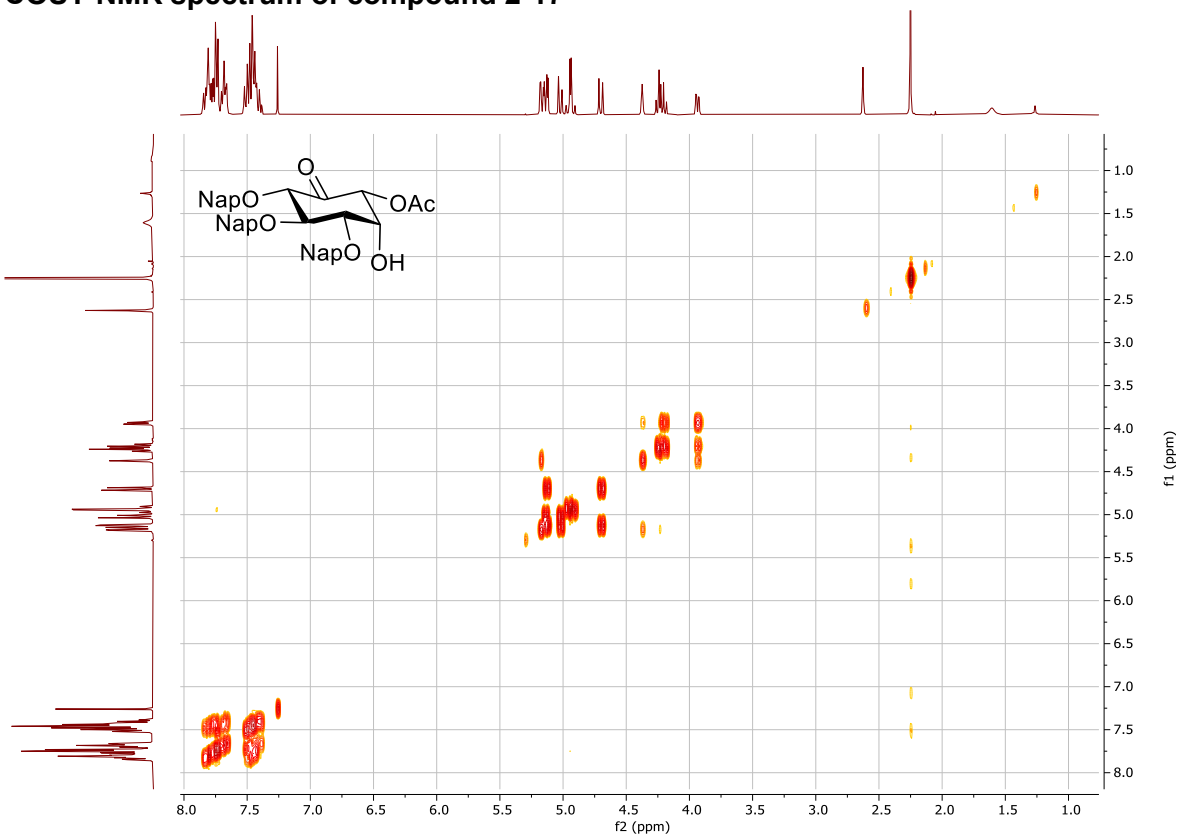

HSQC NMR spectrum of compound 2-17

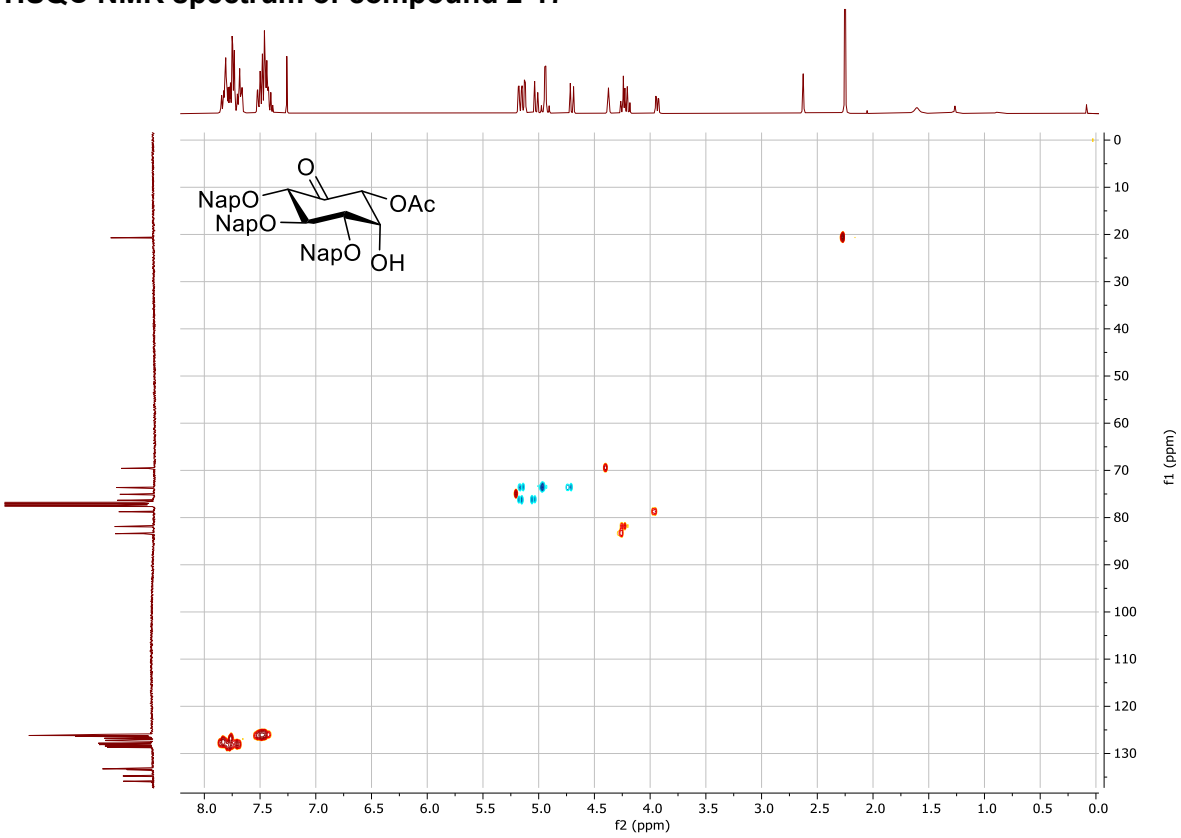

^{1}H NMR spectrum of compound 2-18

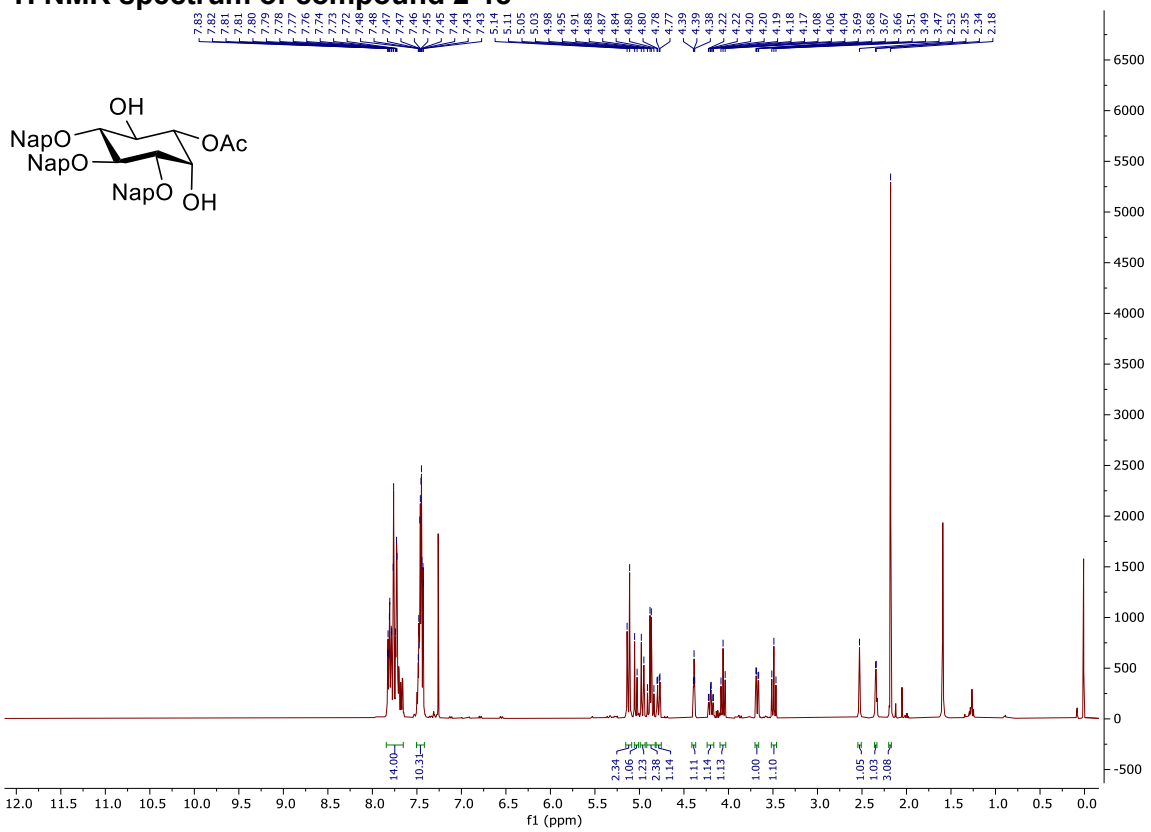

^{13}C NMR spectrum of compound 2-18

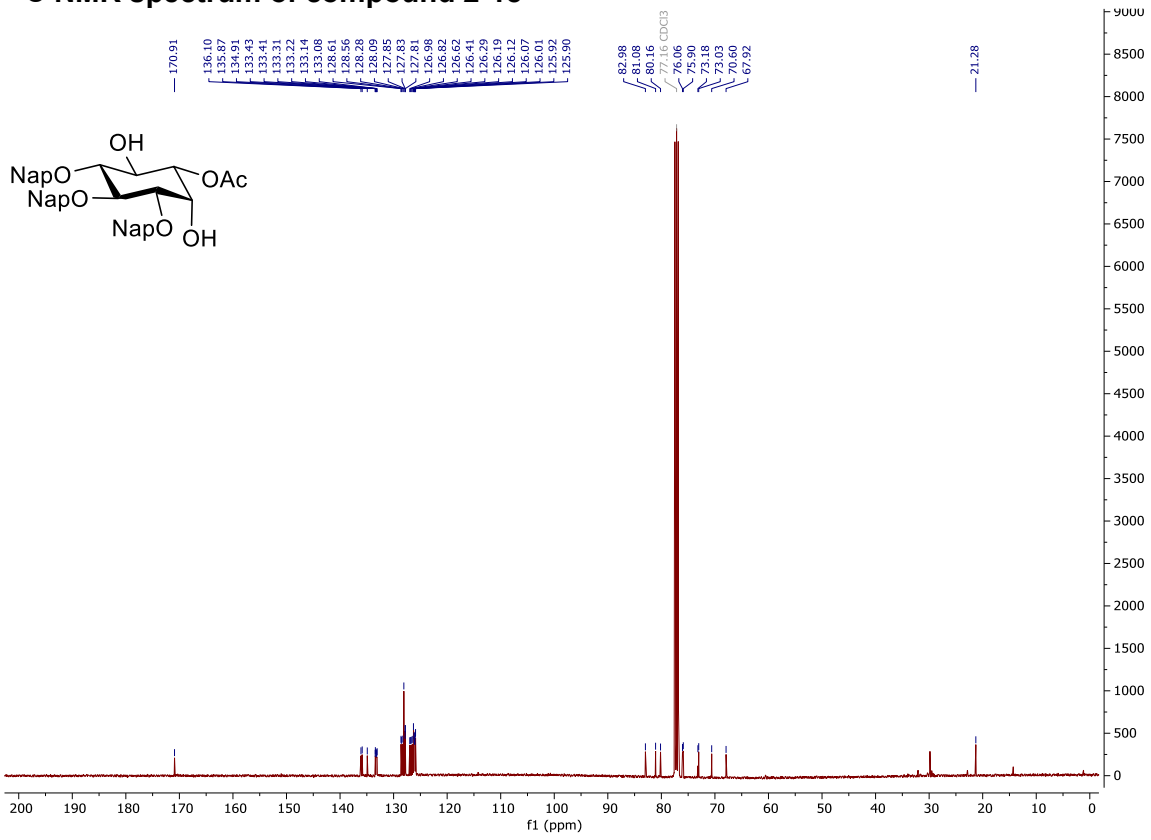

COSY NMR spectrum of compound 2-18

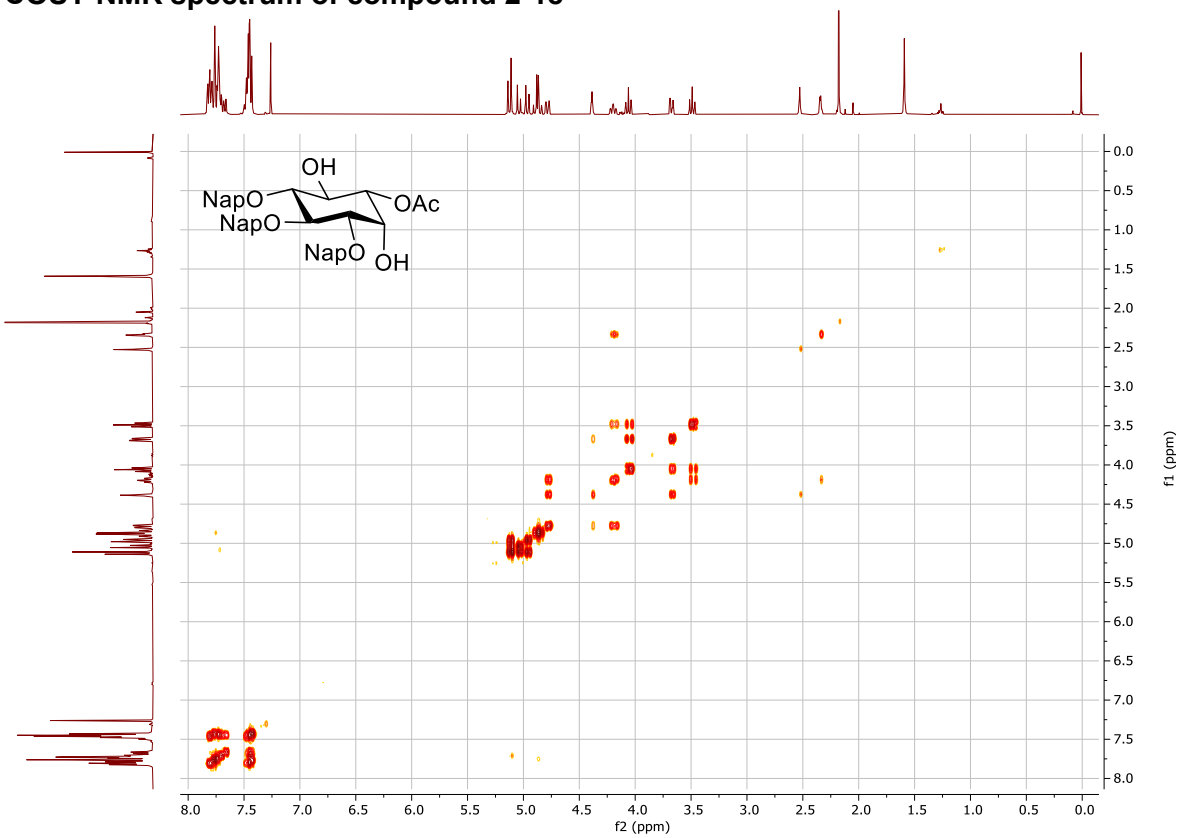

HSQC NMR spectrum of compound 2-18

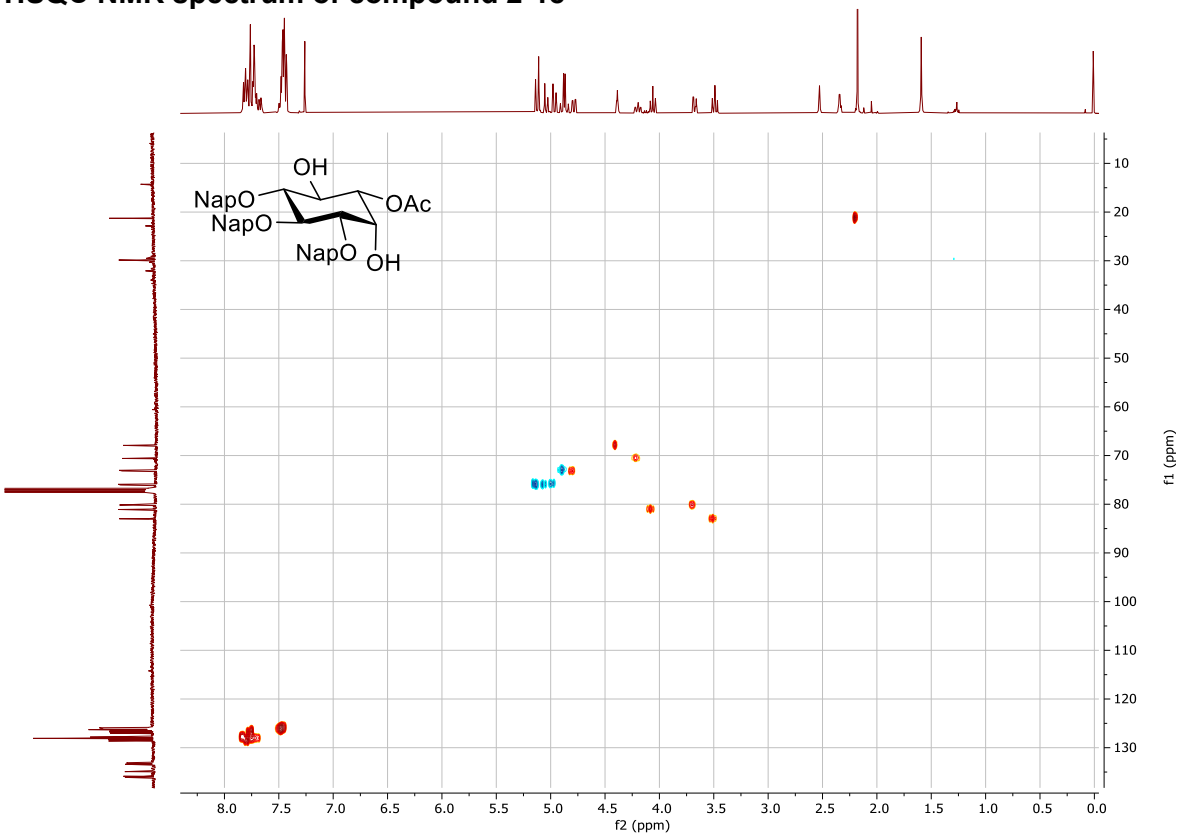

^{1}H NMR spectrum of compound 2-19

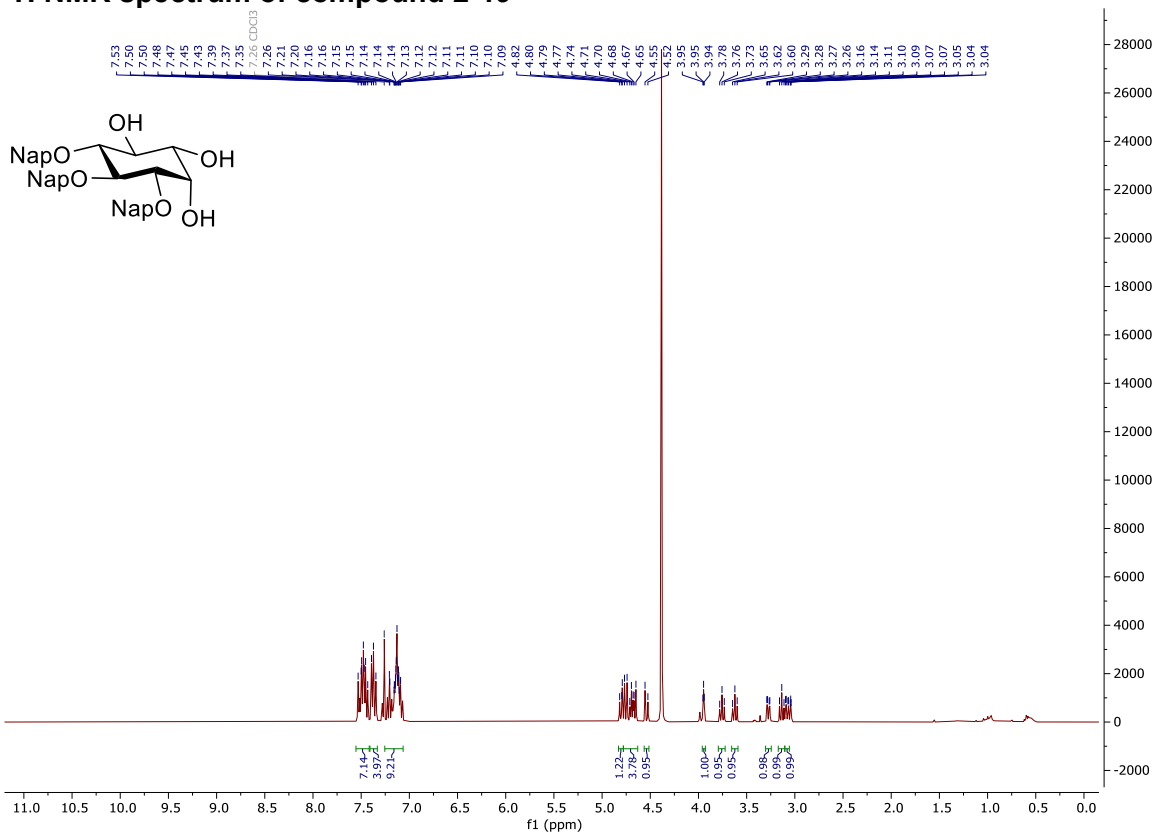

^{13}C NMR spectrum of compound 2-19

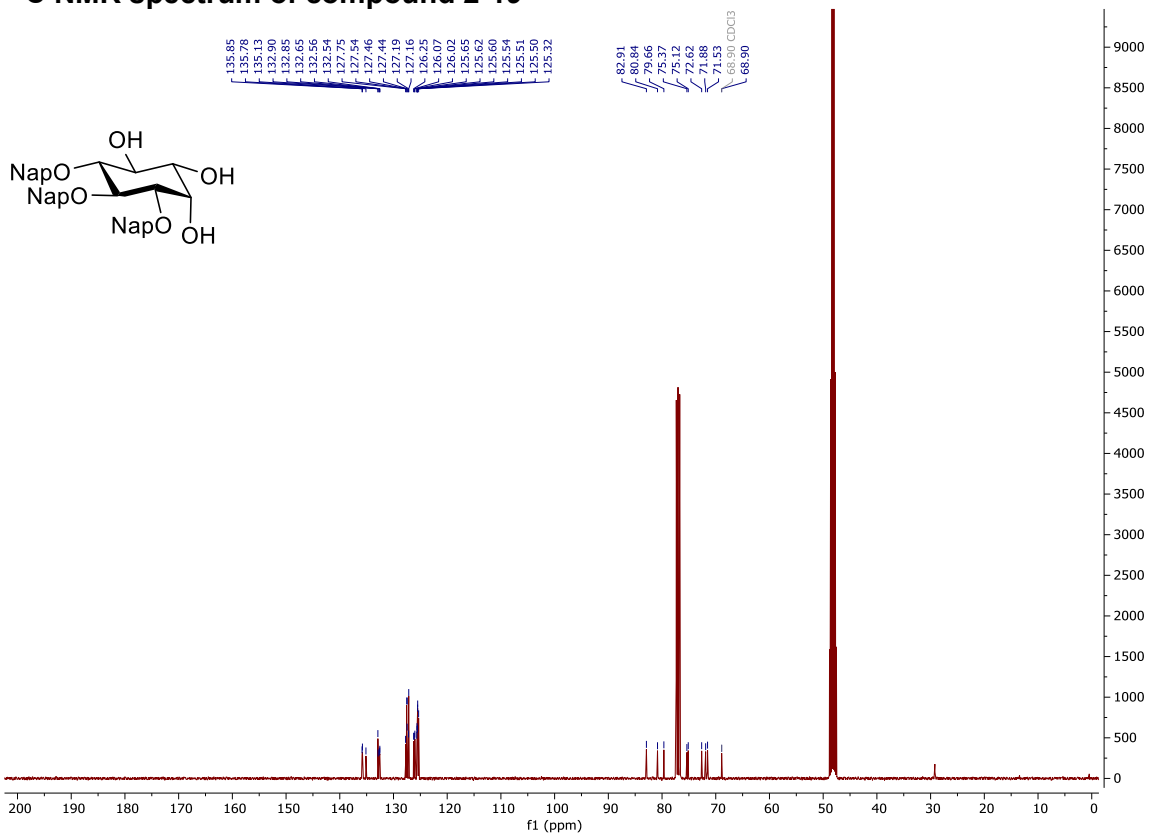

COSY NMR spectrum of compound 2-19

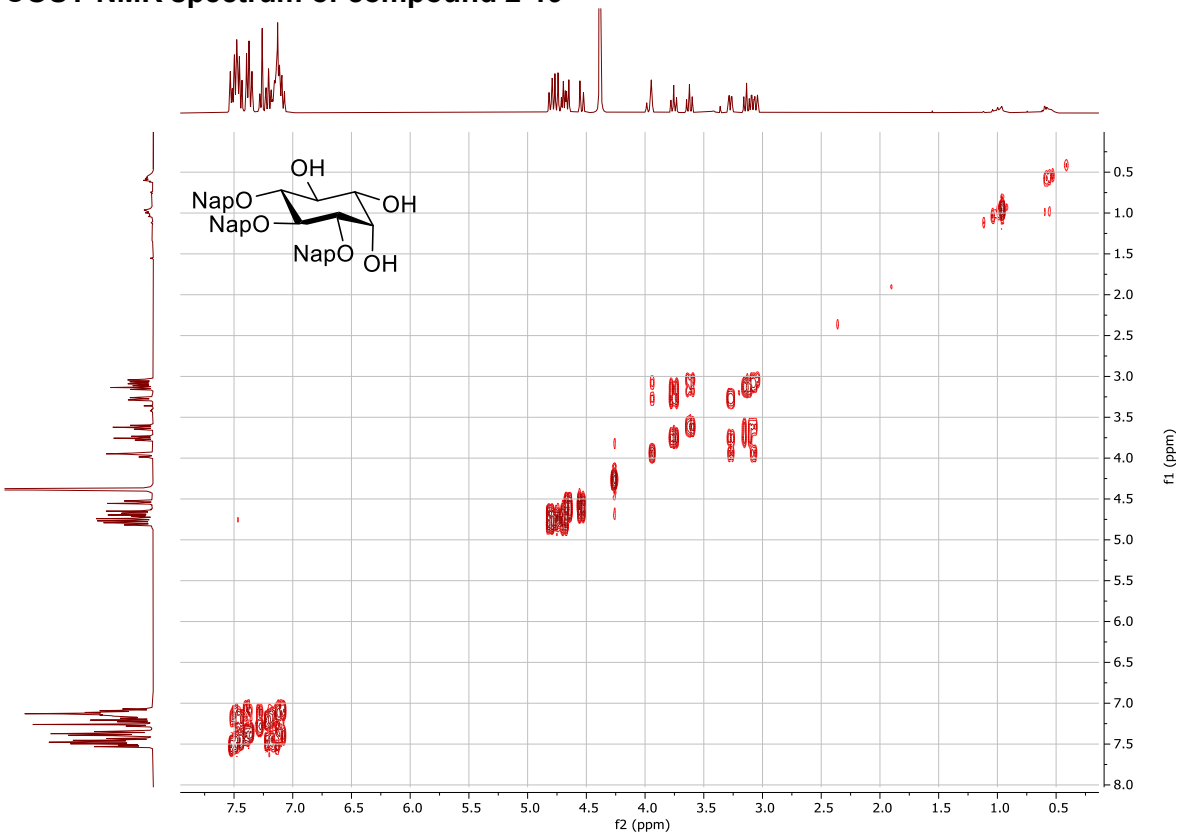

HSQC NMR spectrum of compound 2-19

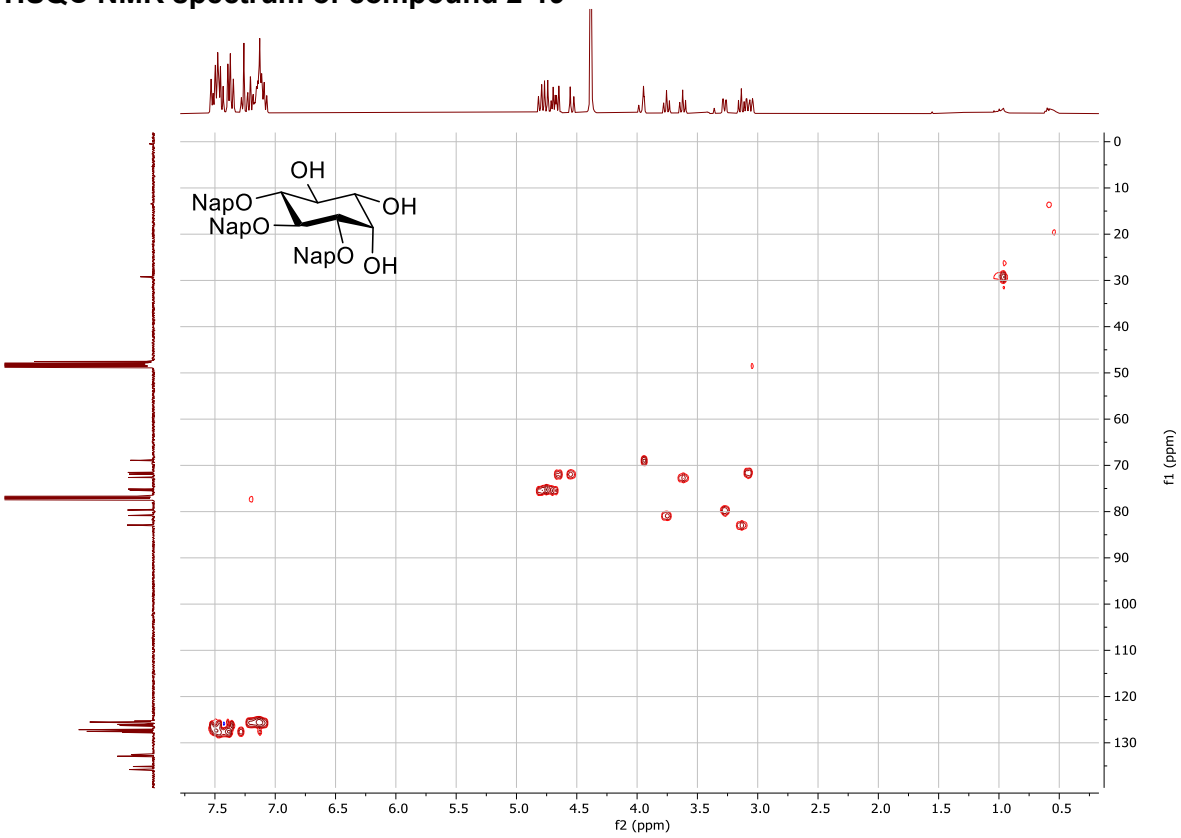

^{1}H NMR spectrum of compound 2-20

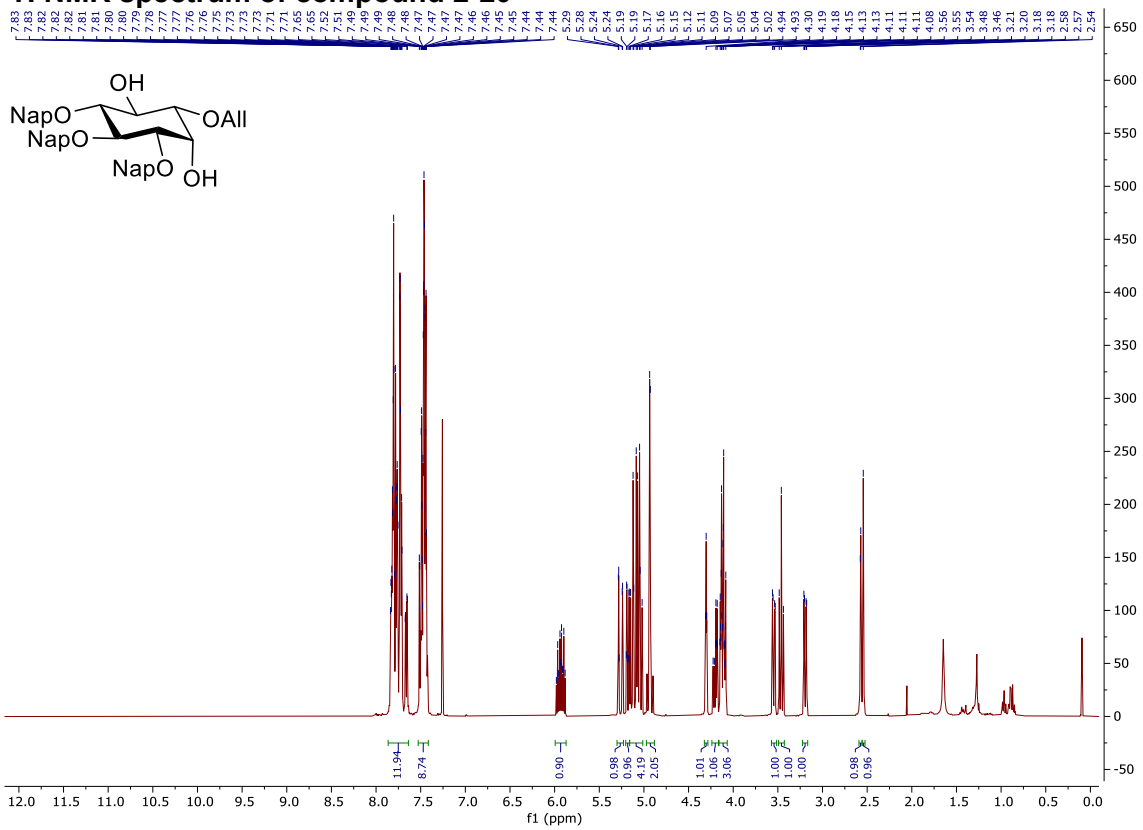

^{13}C NMR spectrum of compound 2-20

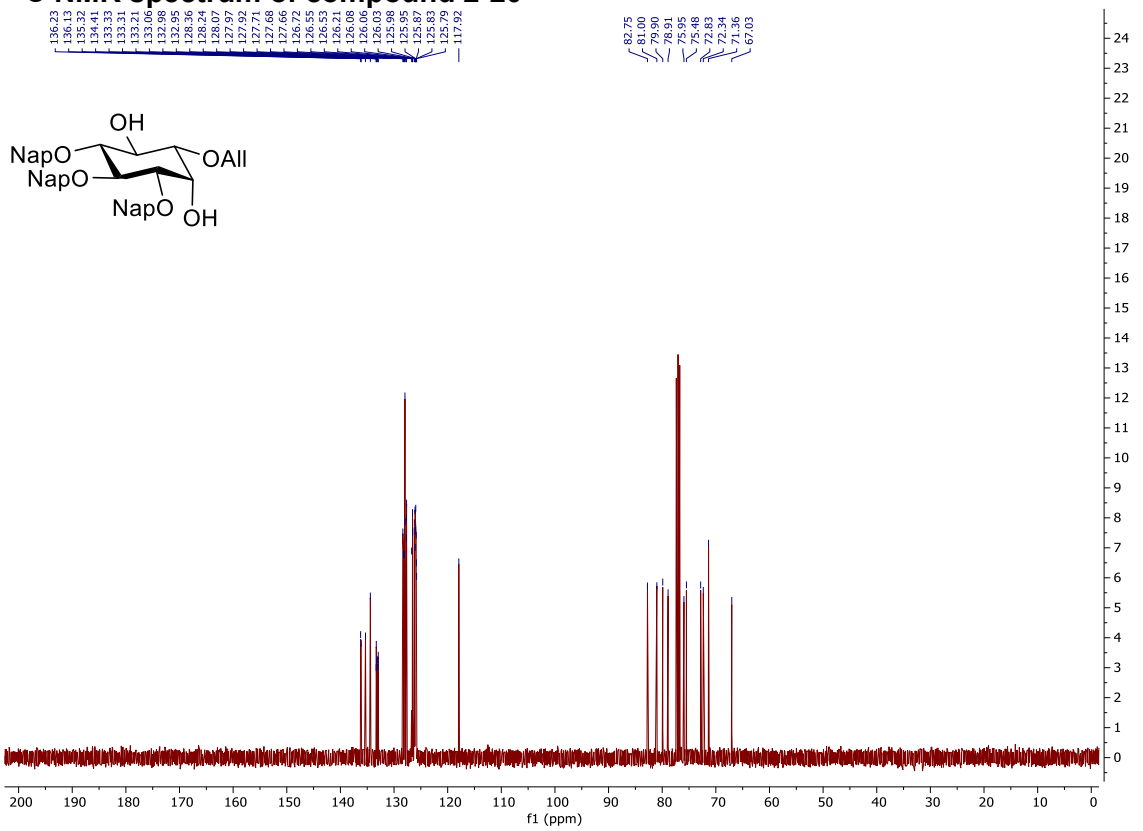

COSY NMR spectrum of compound 2-20

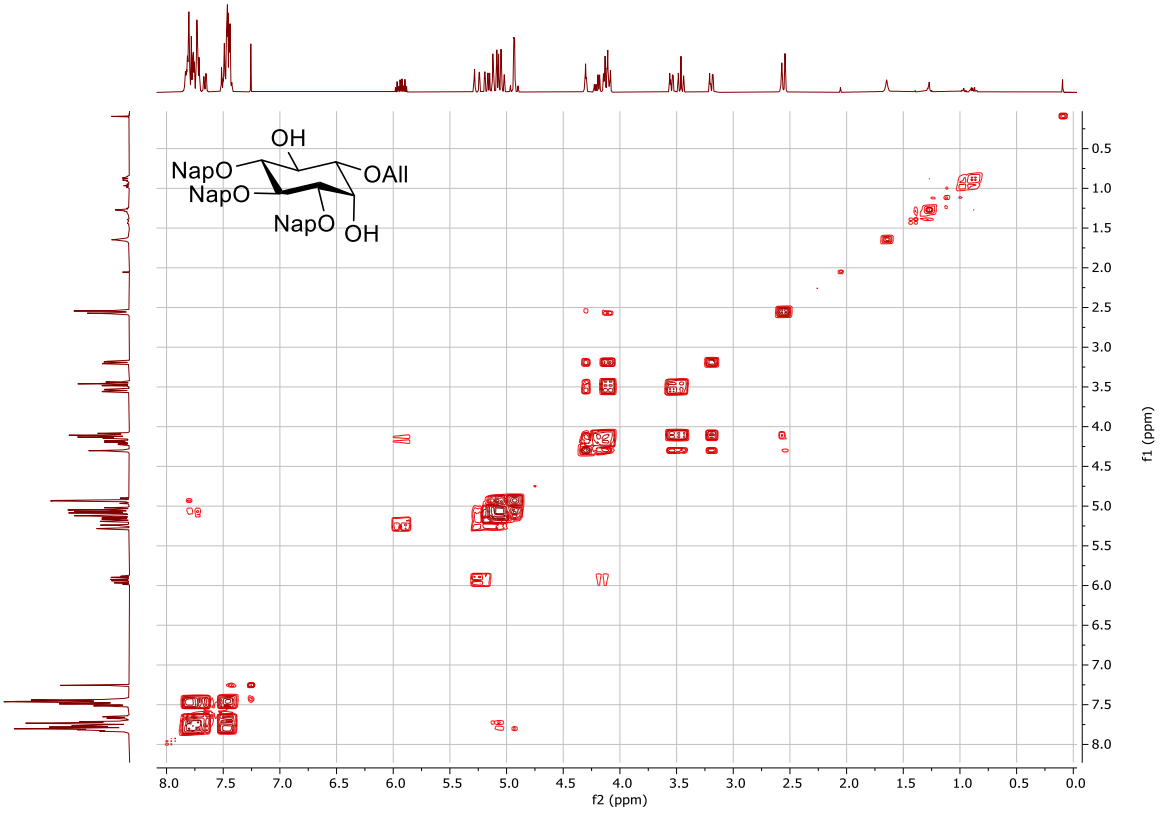

HSQC NMR spectrum of compound 2-20

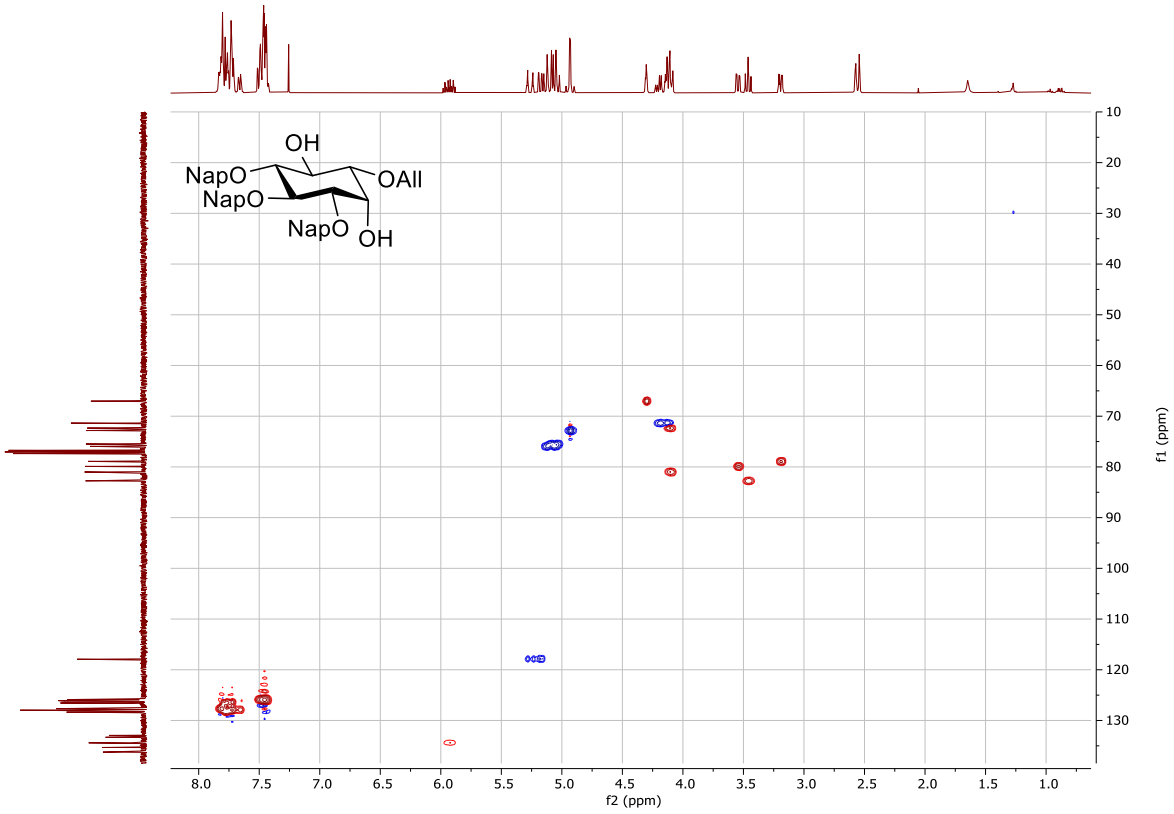

^{1}H NMR spectrum of compound 2-9

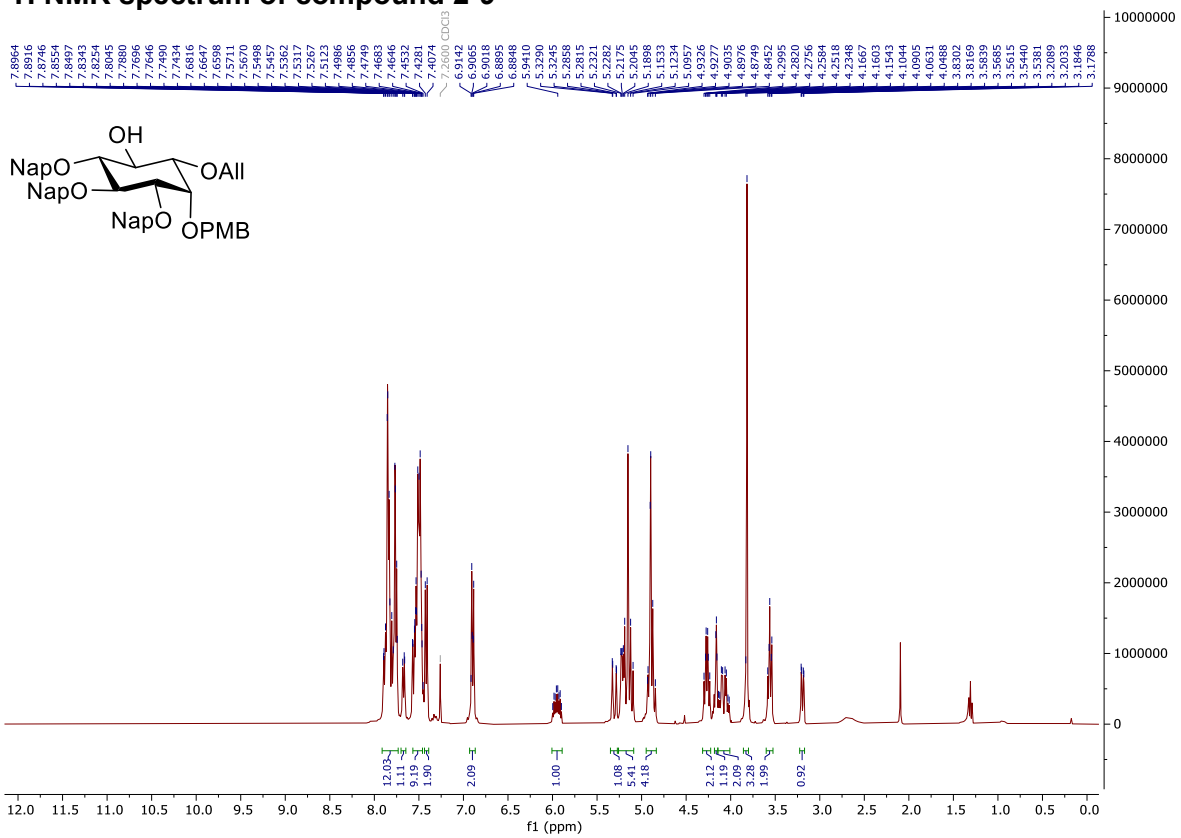

^{13}C NMR spectrum of compound 2-9

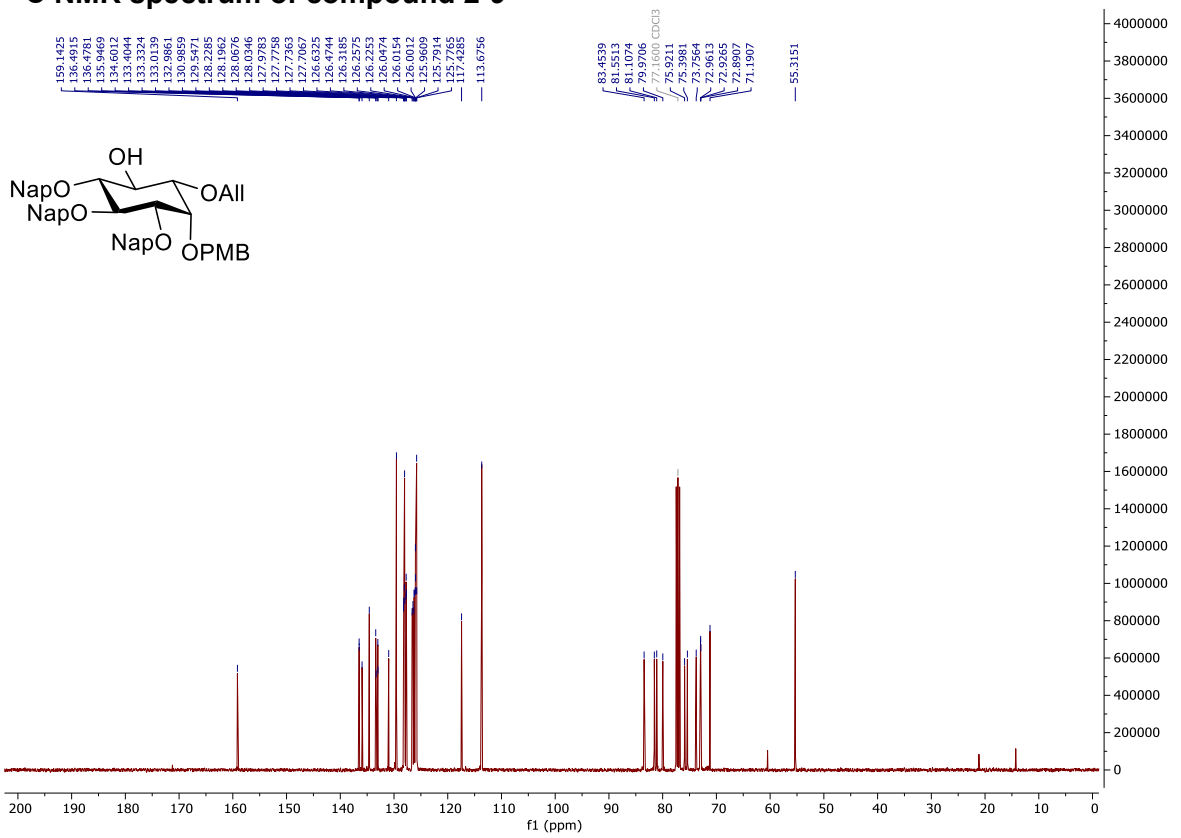

COSY NMR spectrum of compound 2-9

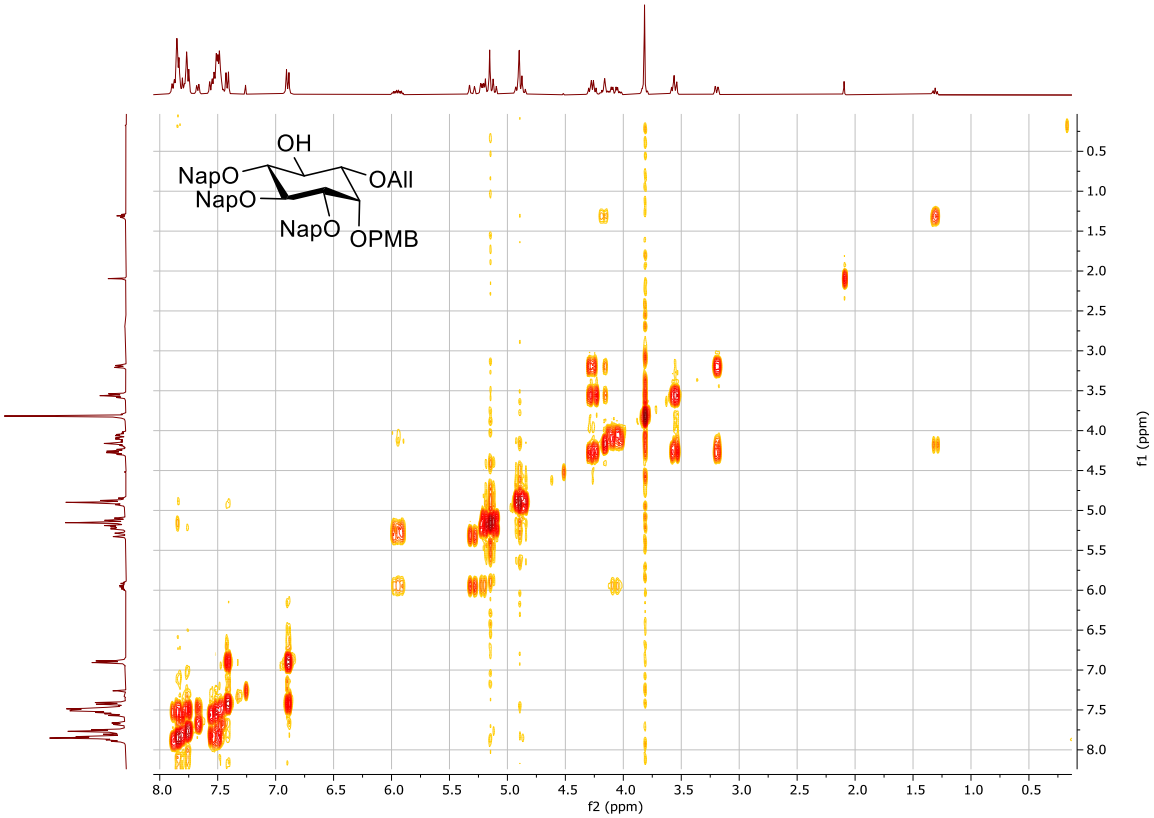

HSQC NMR spectrum of compound 2-9

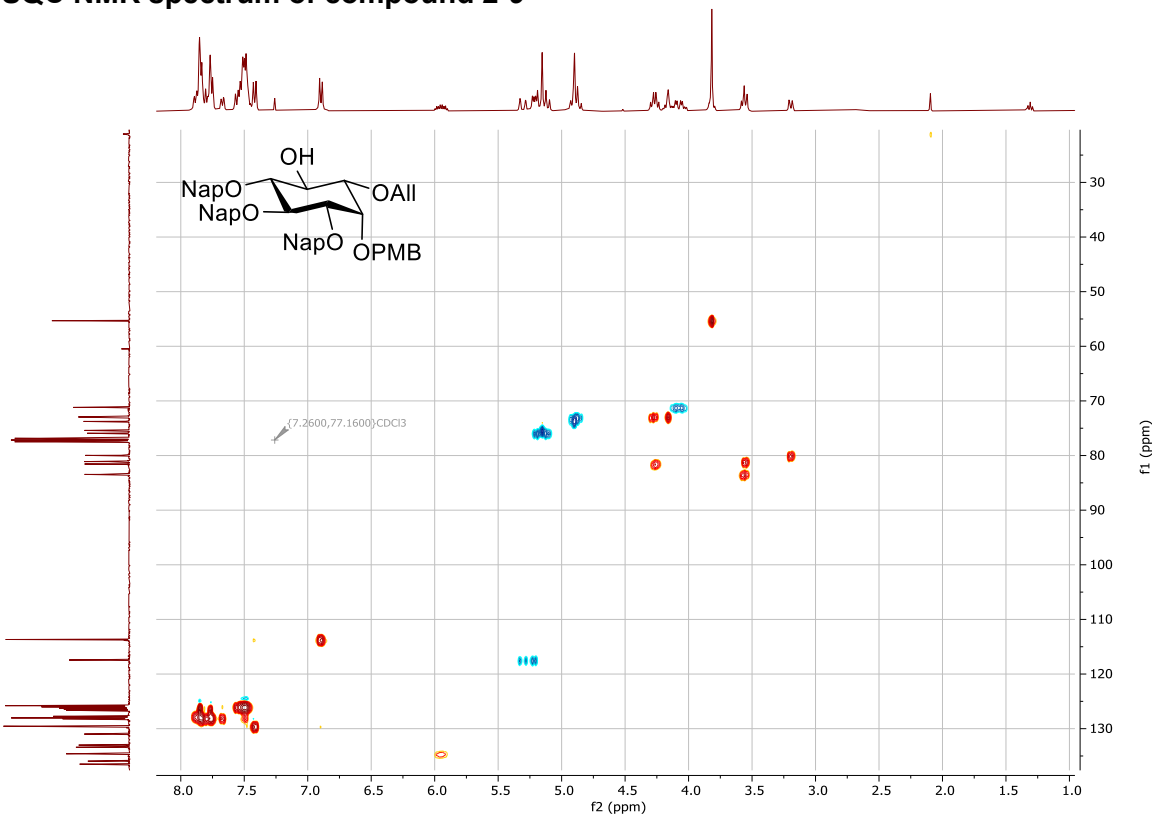

^{1}H NMR spectrum of compound 2-10

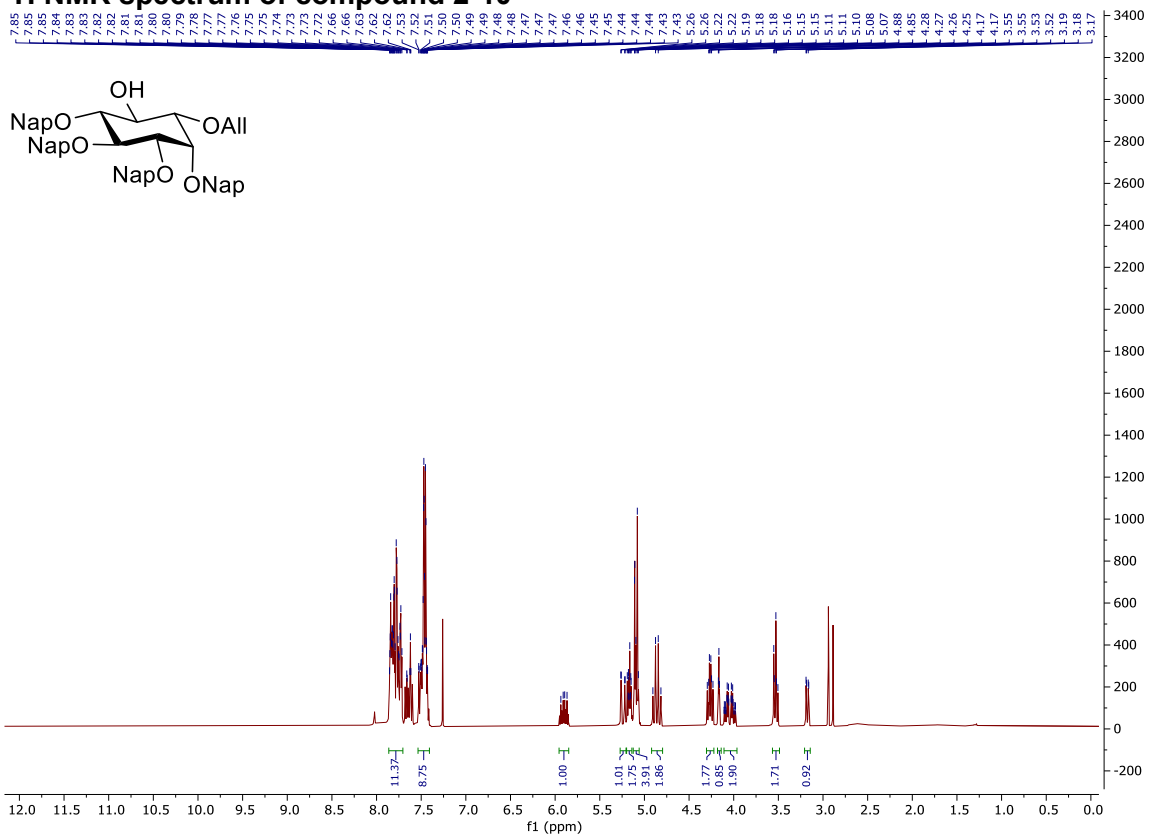

^{13}C NMR spectrum of compound 2-10

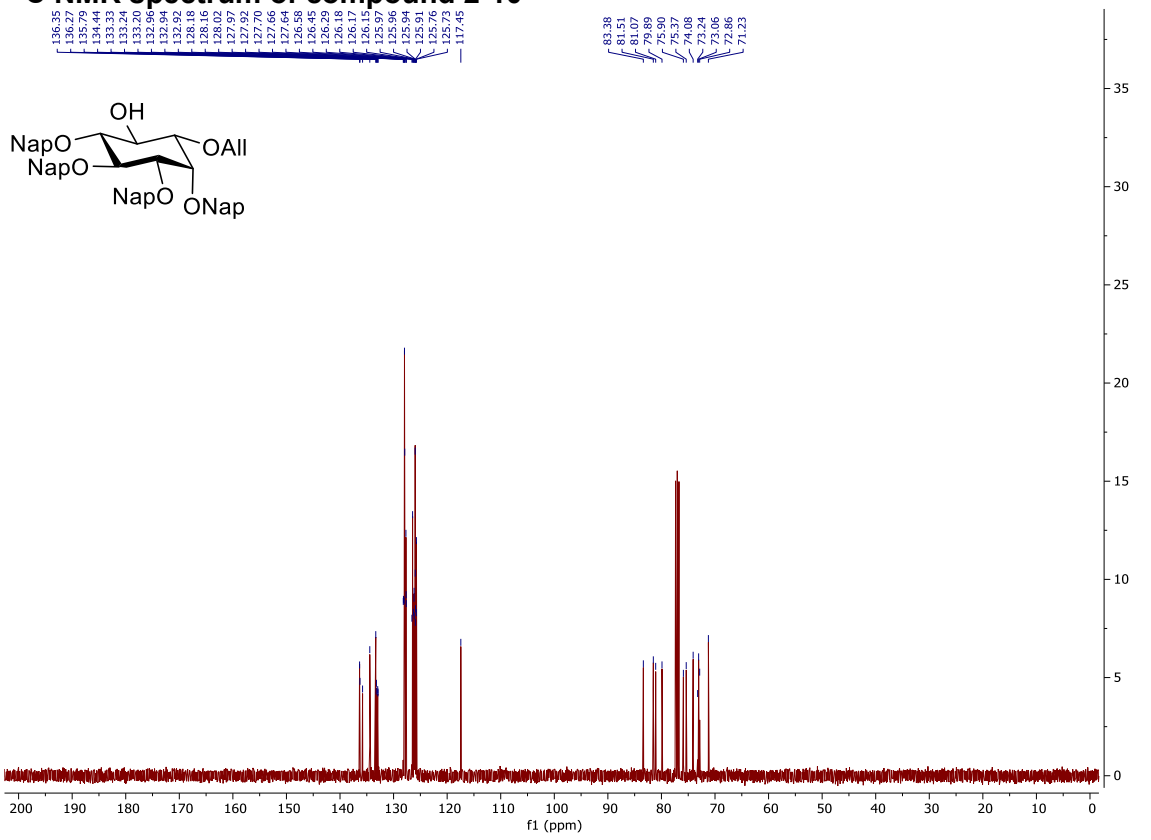

COSY NMR spectrum of compound 2-10

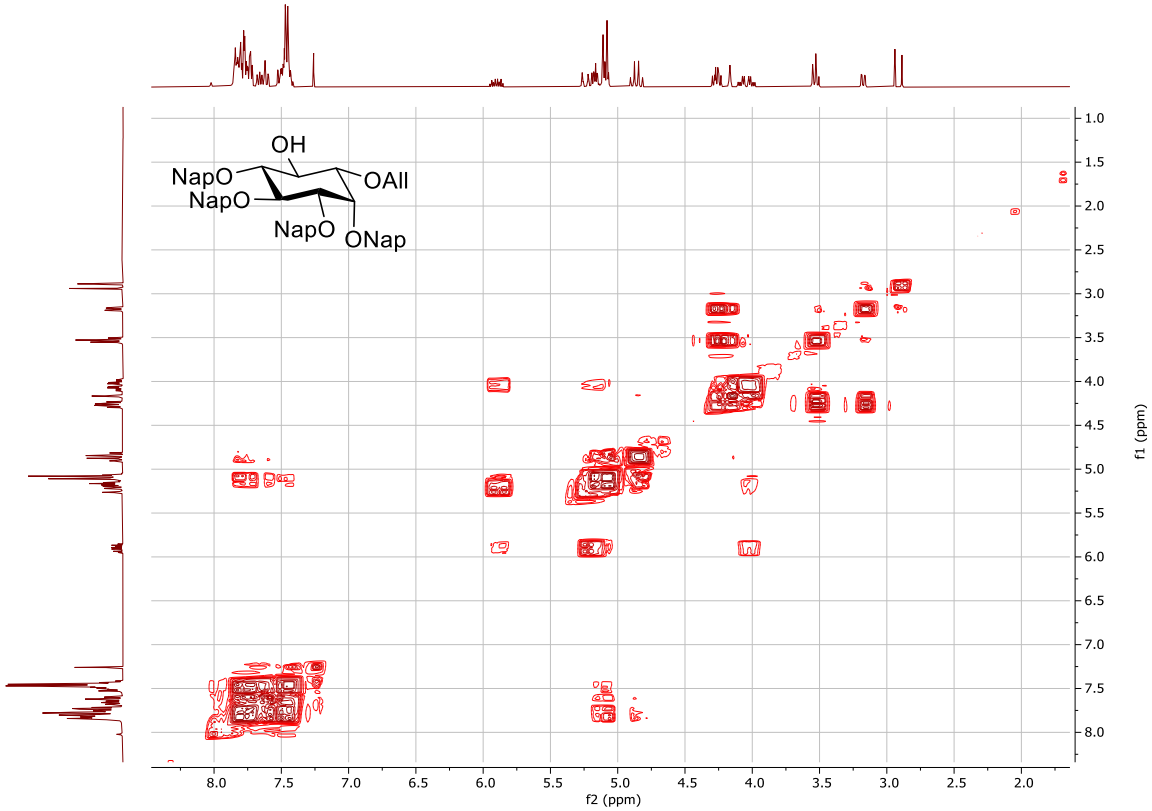

HSQC NMR spectrum of compound 2-10

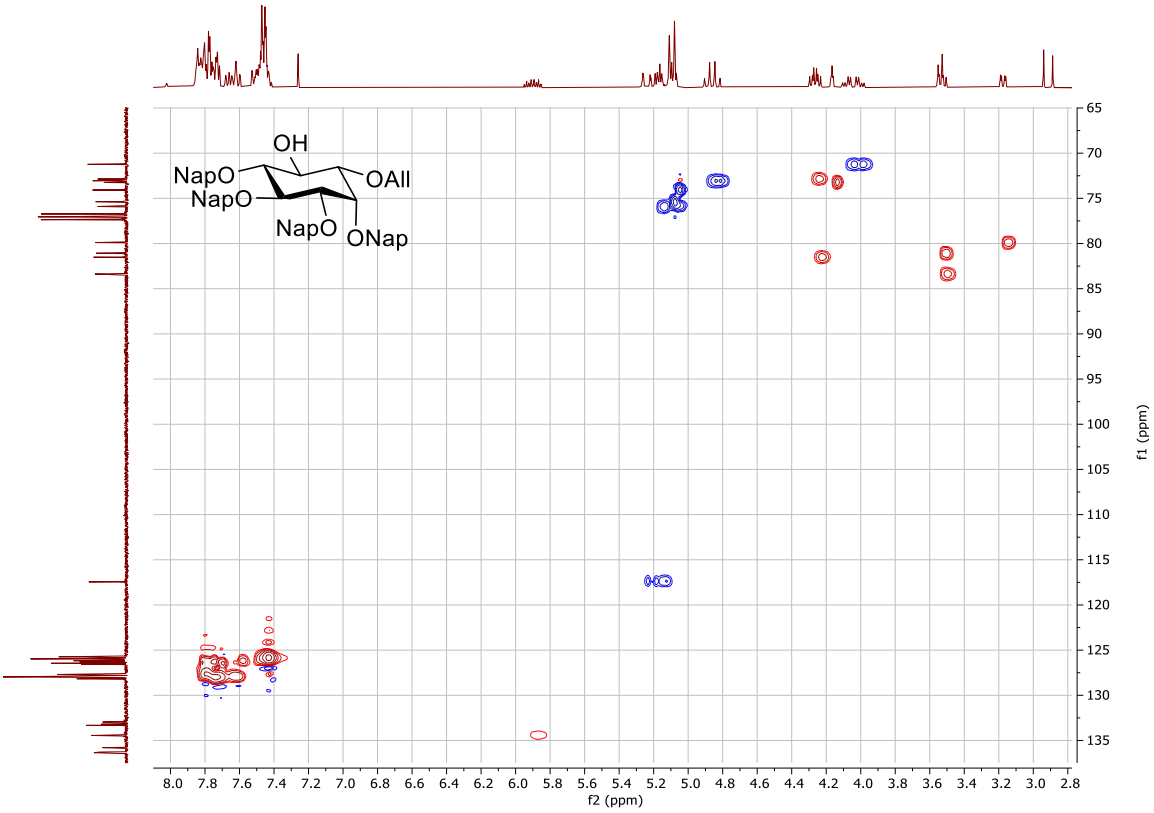

^{1}H NMR spectrum of compound 2-22

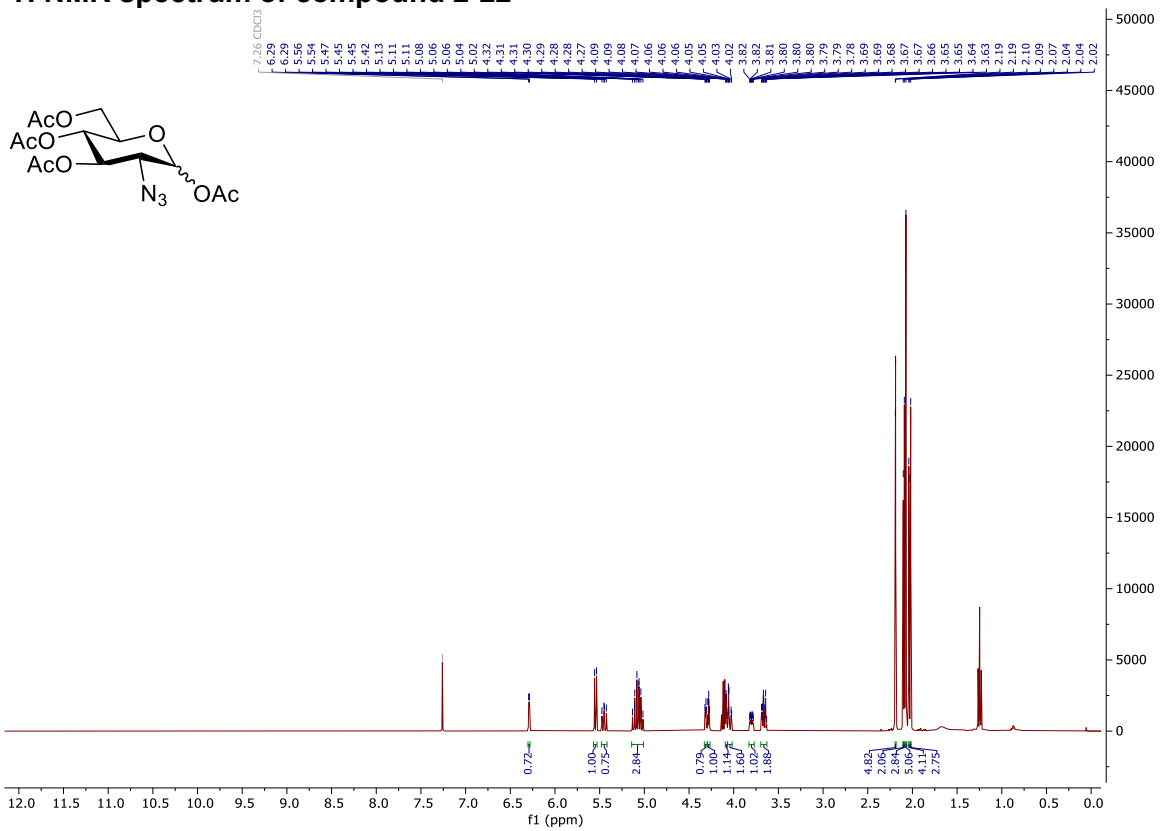

^{13}C NMR spectrum of compound 2-22

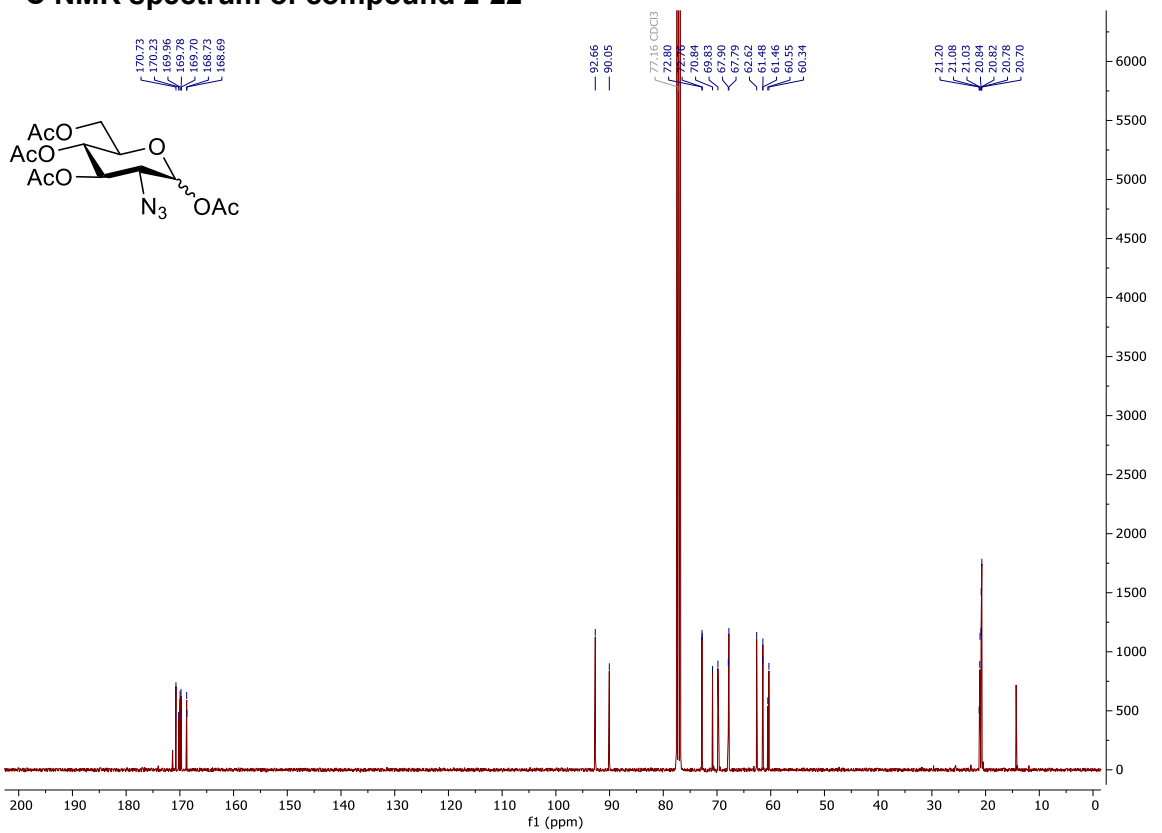

COSY NMR spectrum of compound 2-22

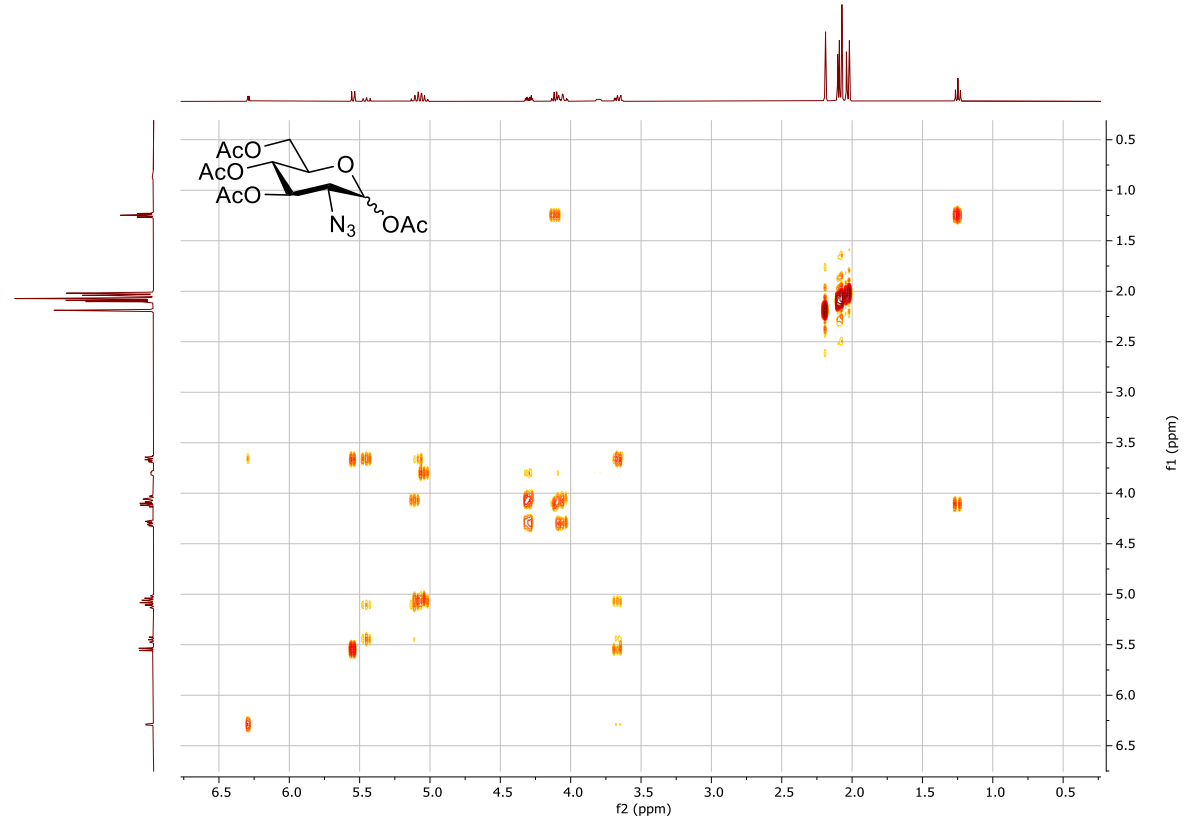

HSQC NMR spectrum of compound 2-22

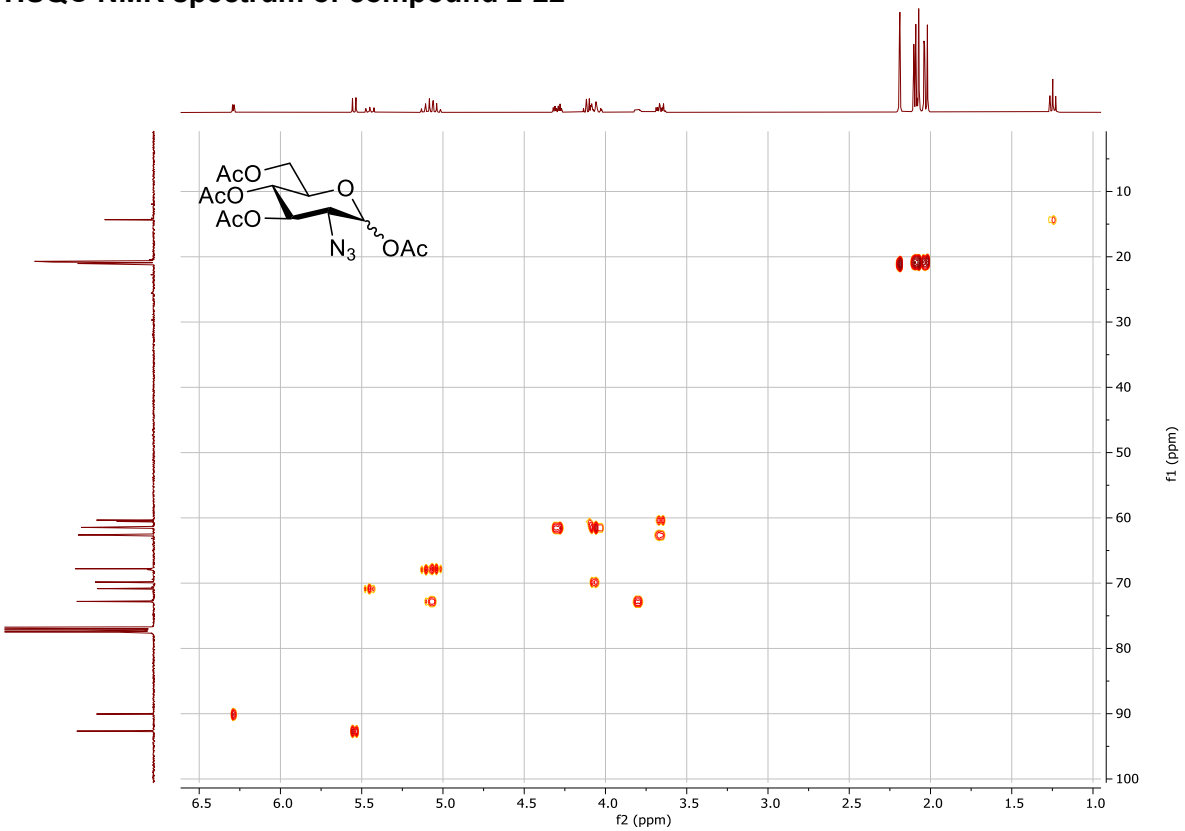

^{1}H NMR spectrum of compound 2-23 (β-anomer)

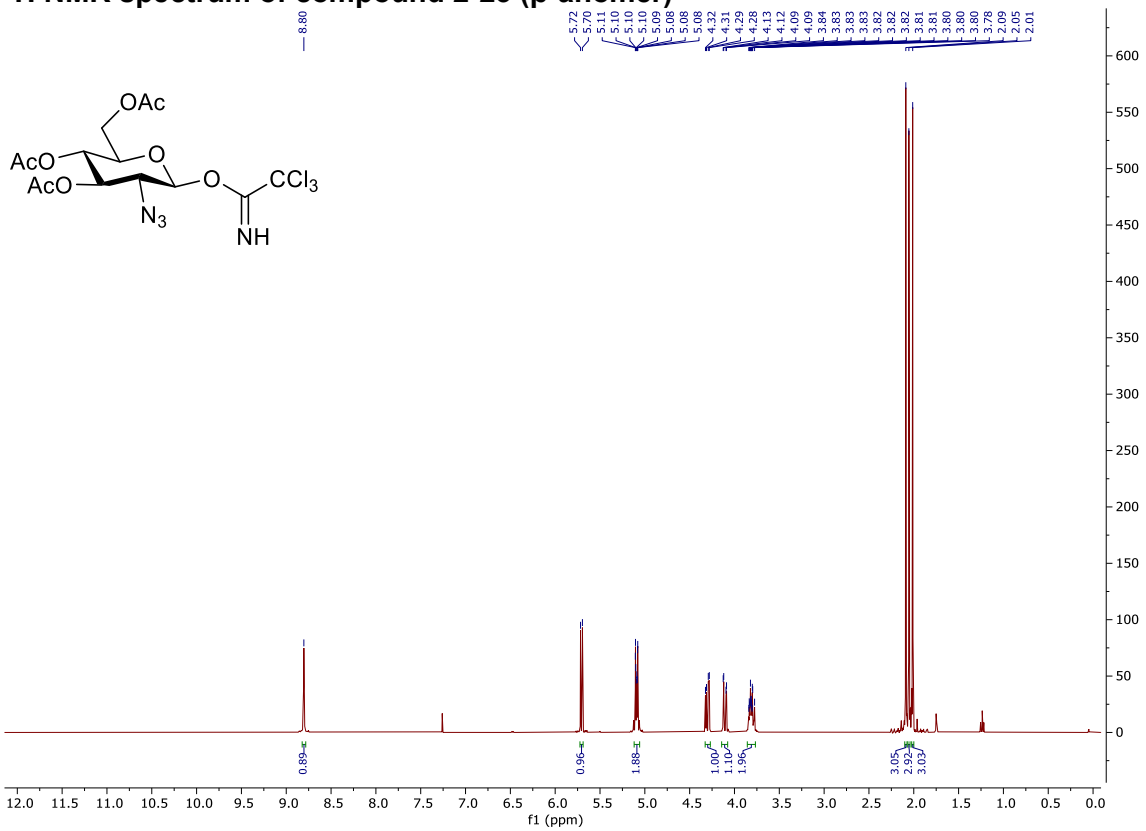

^{13}C NMR spectrum of compound 2-23 (β-anomer)

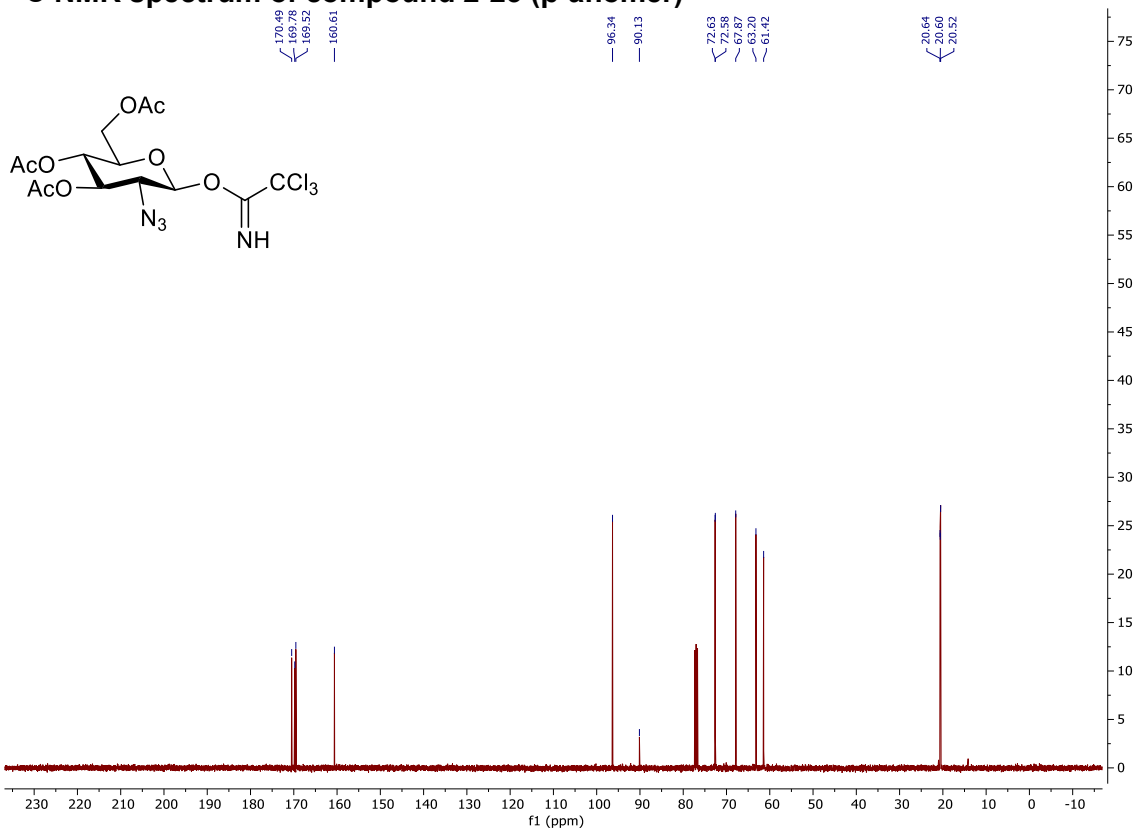

COSY NMR spectrum of compound 2-23 (β-anomer)

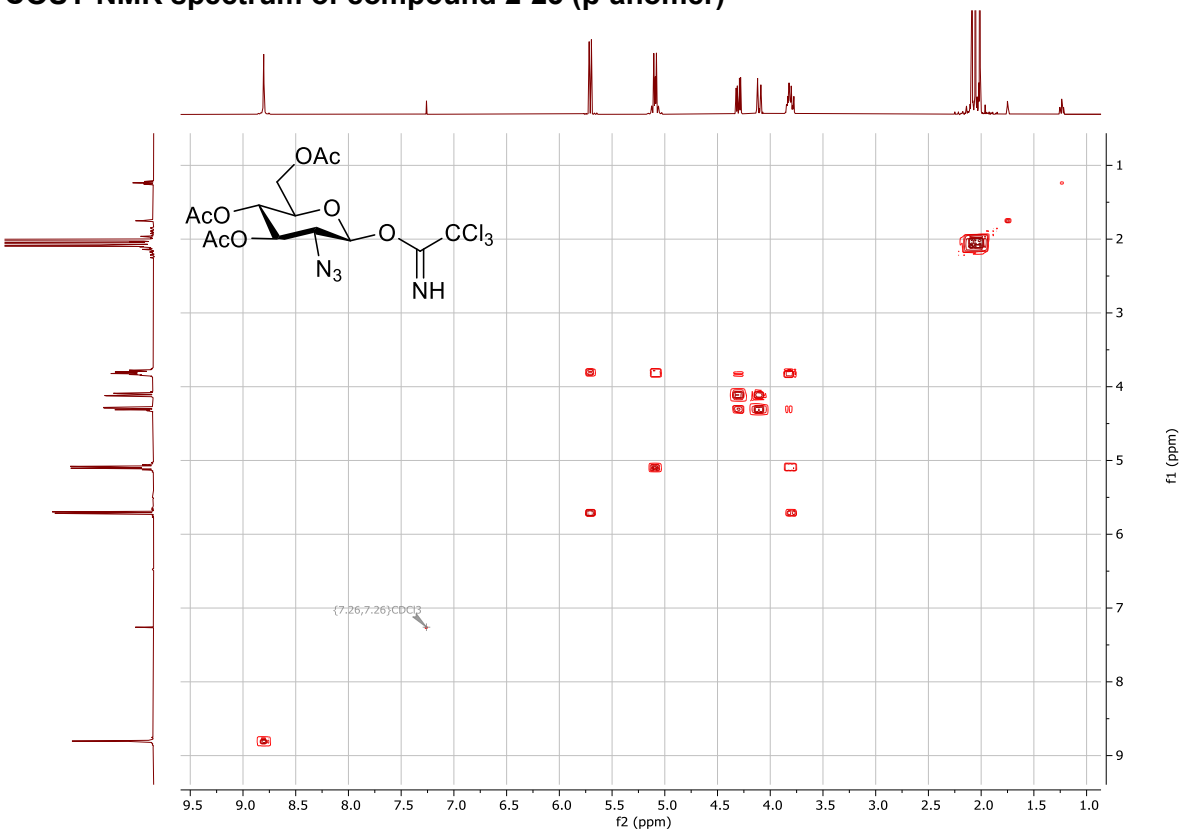

HSQC NMR spectrum of compound 2-23 (β-anomer)

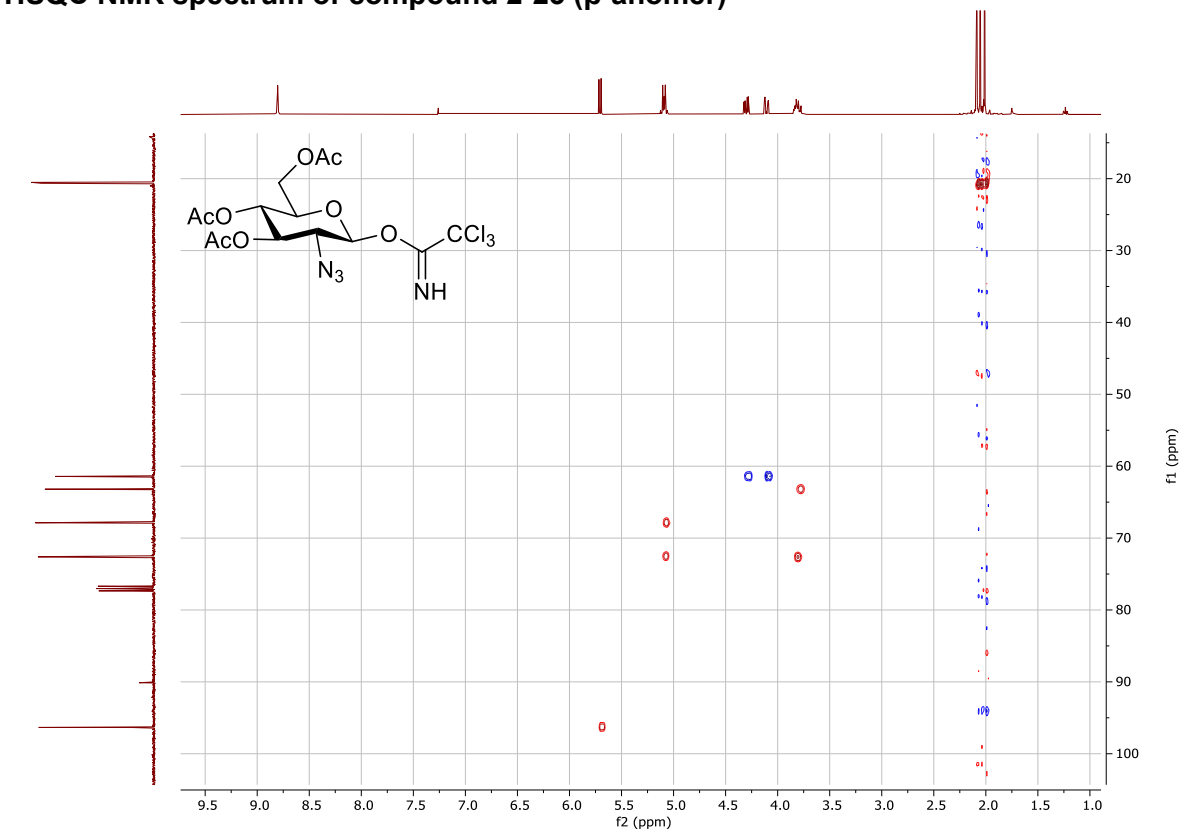

^{1}H NMR spectrum of compound 2-12

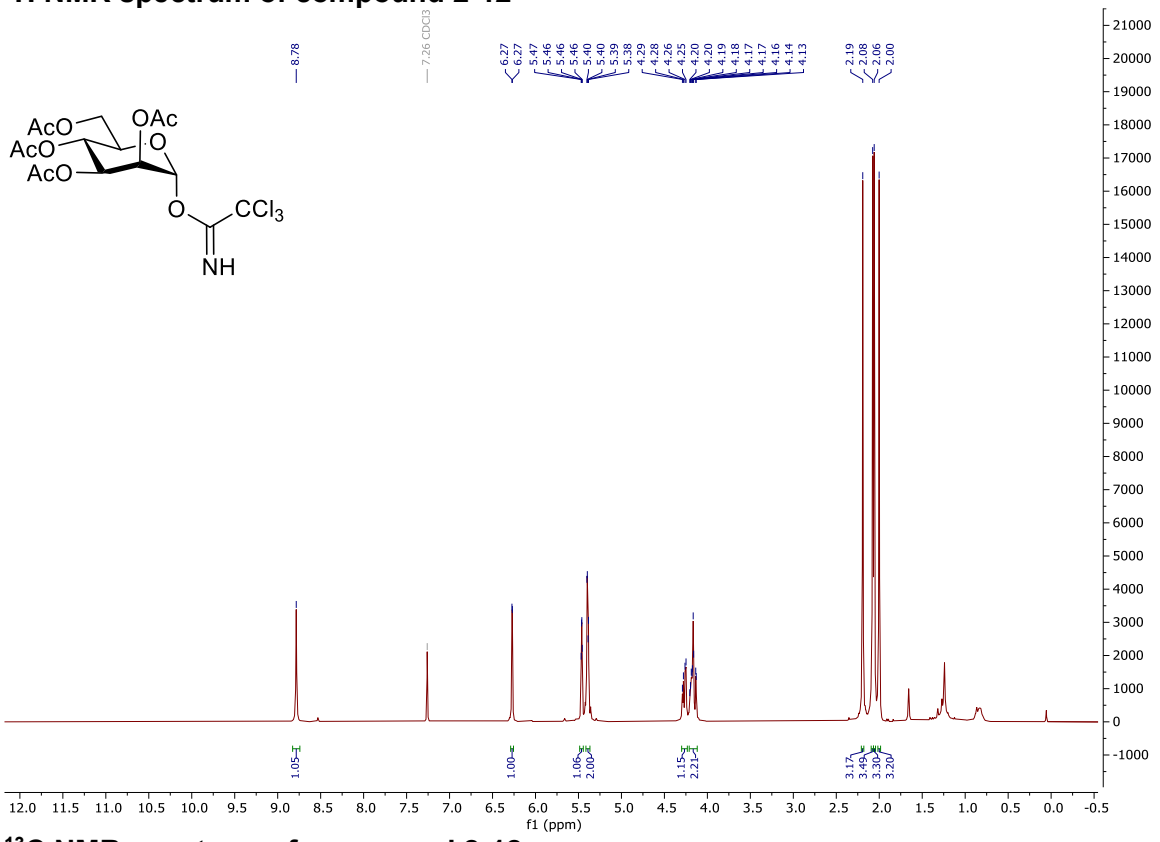

^{13}C NMR spectrum of compound 2-12

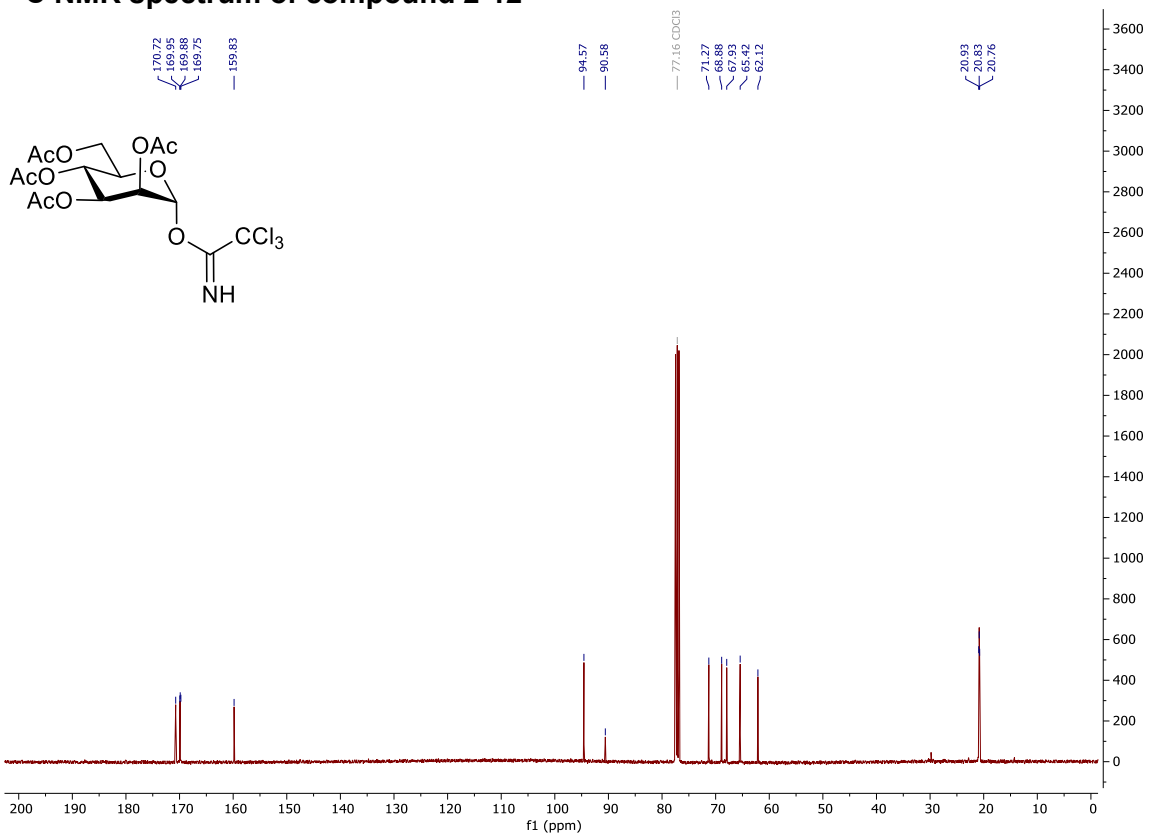

COSY NMR spectrum of compound 2-12

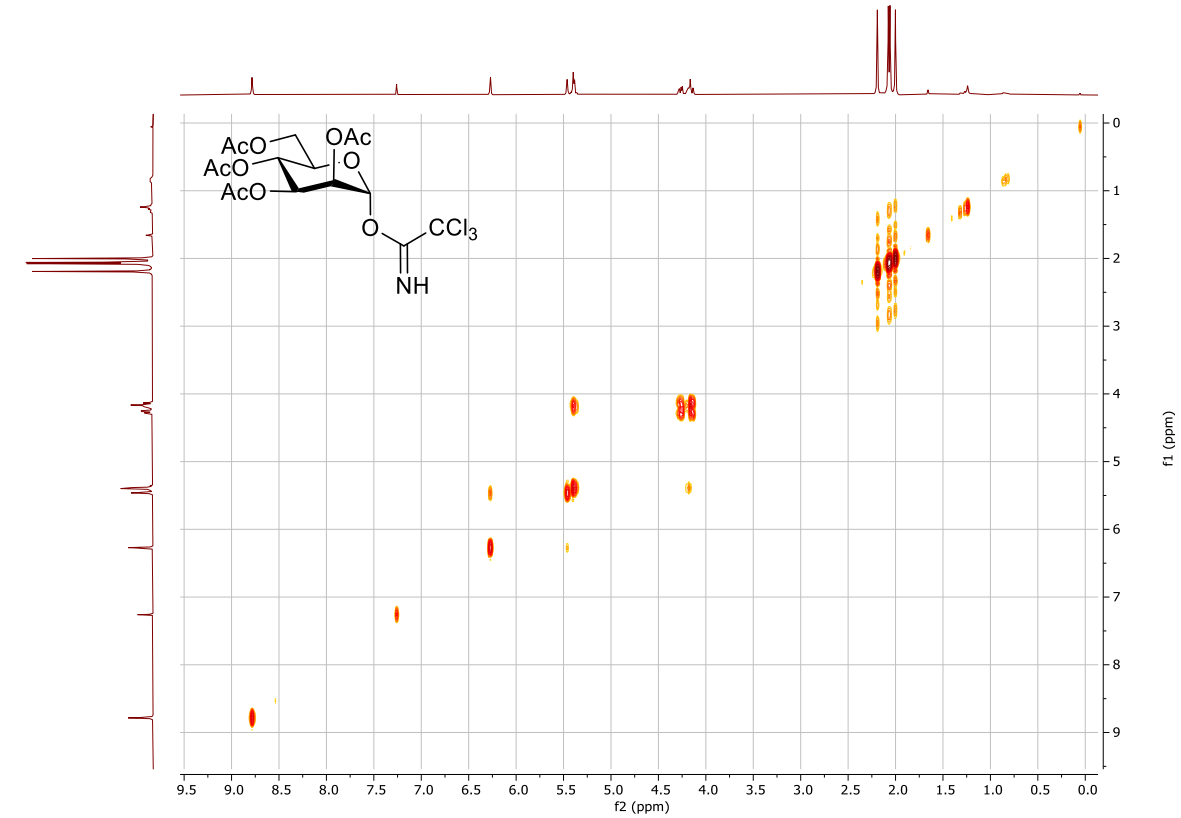

HSQC NMR spectrum of compound 2-12

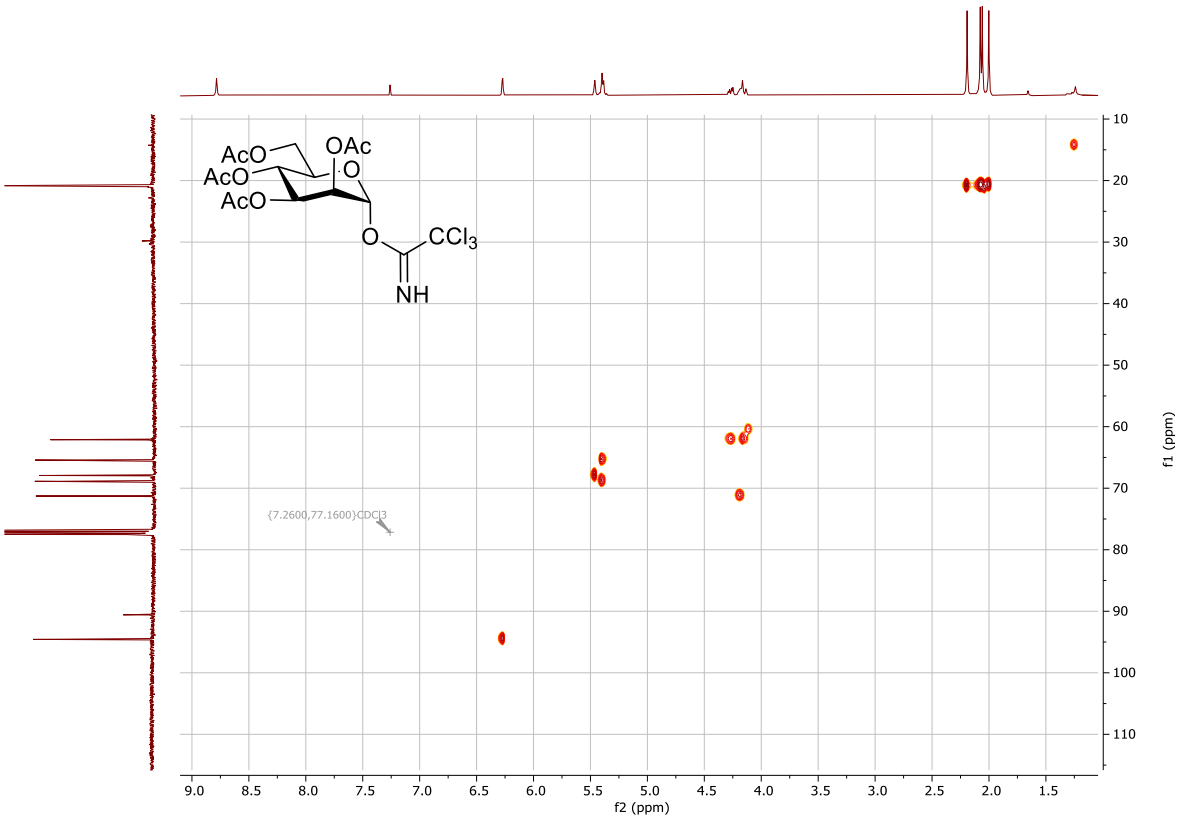

^{1}H NMR spectrum of compound 2-27

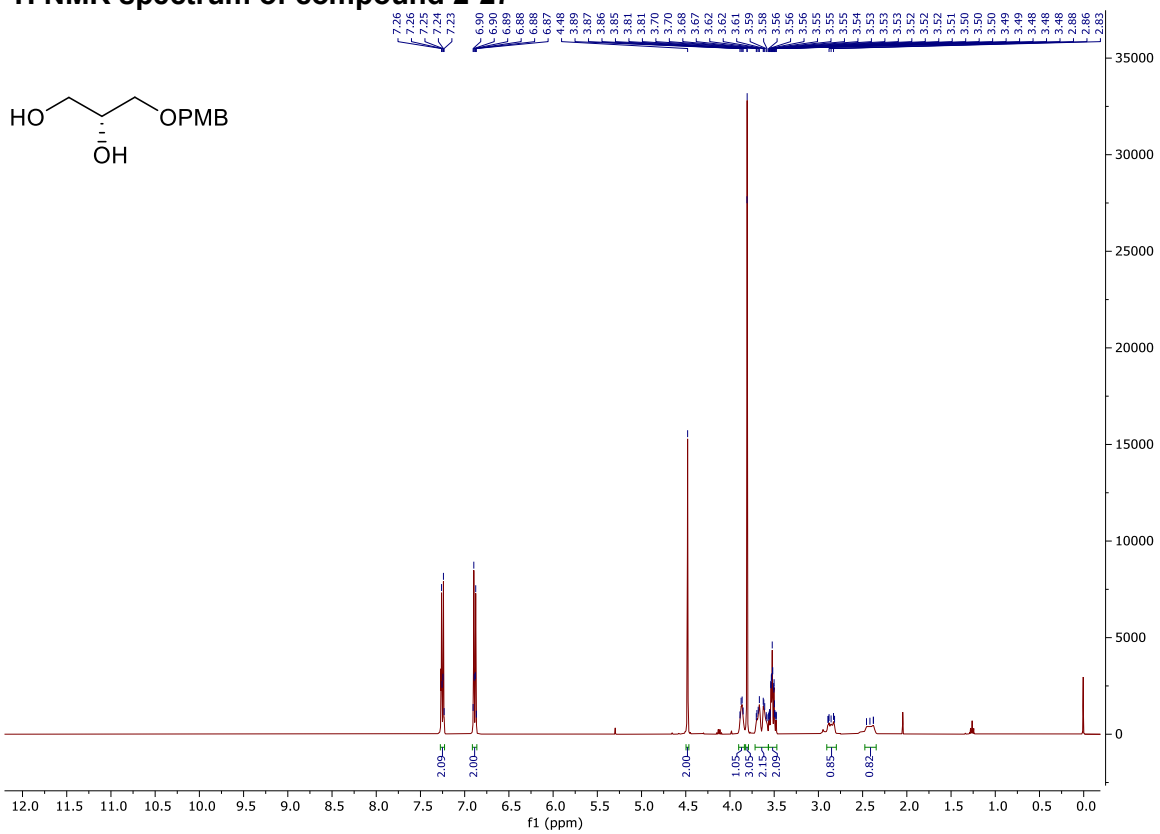

^{13}C NMR spectrum of compound 2-27

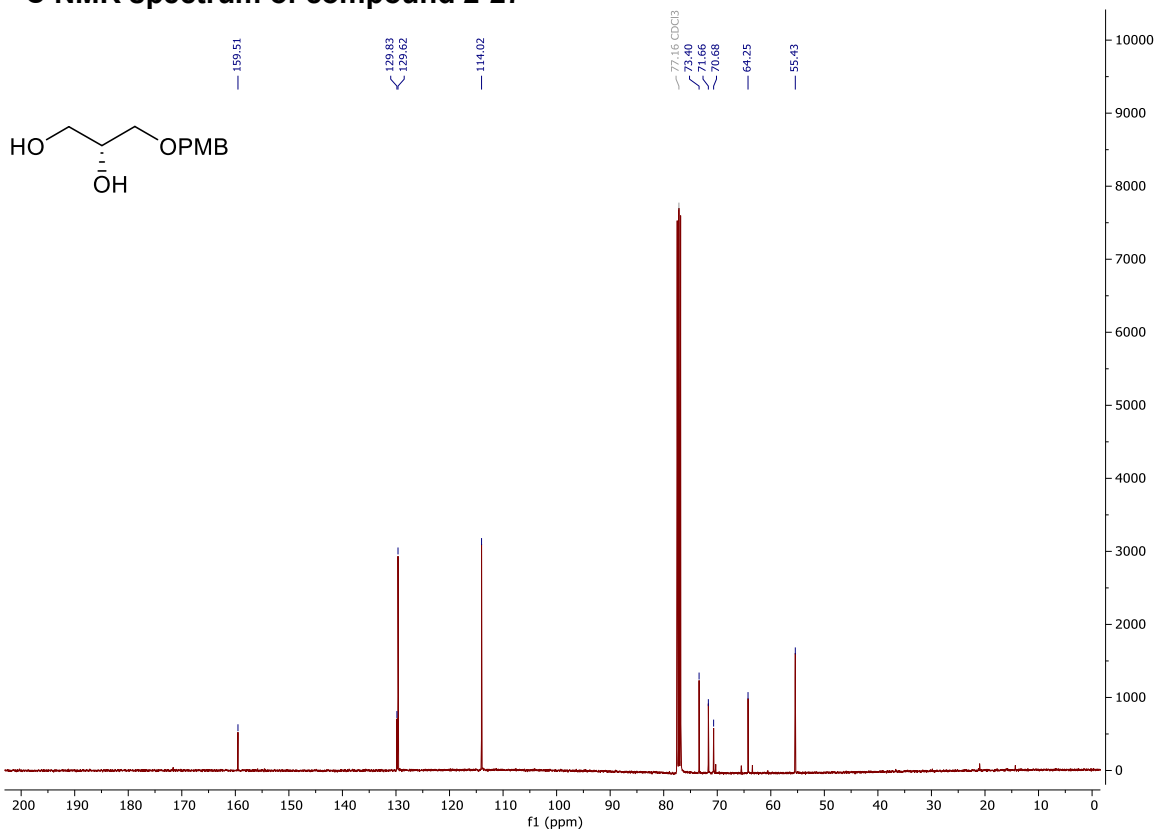

COSY NMR spectrum of compound 2-27

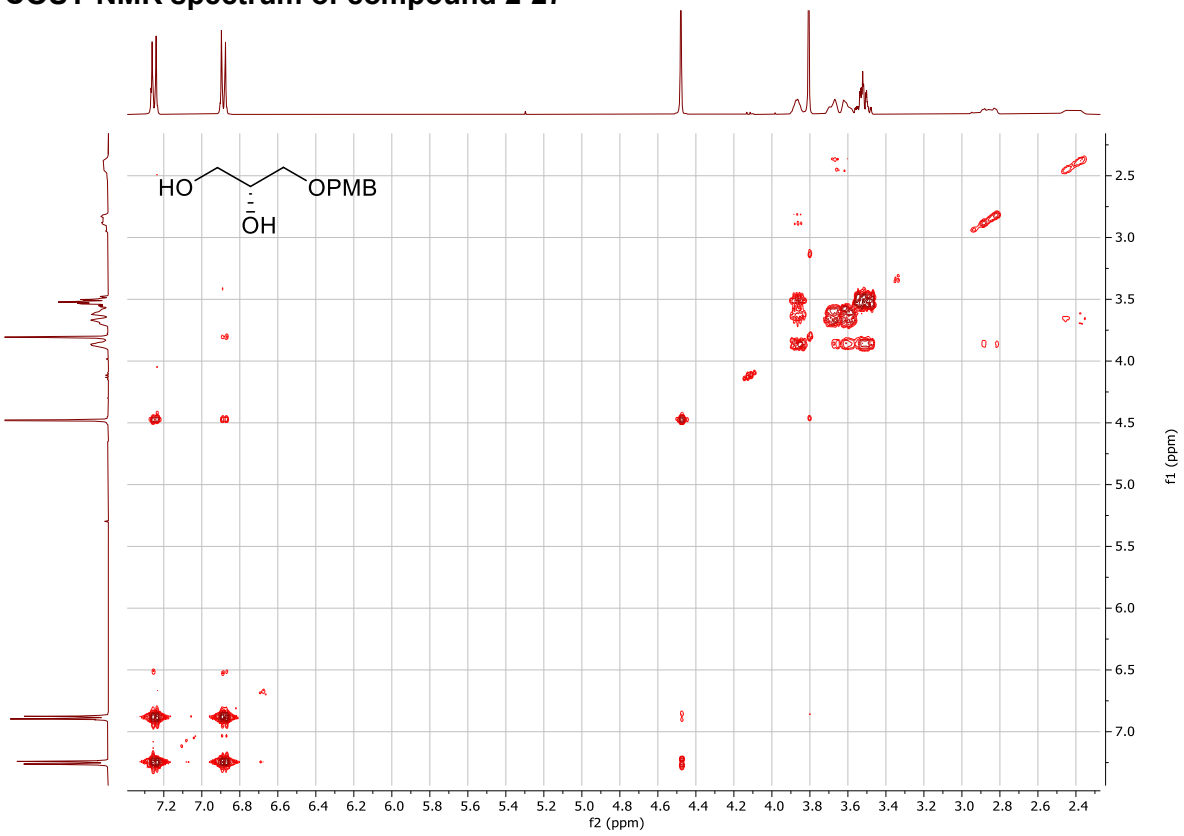

HSQC NMR spectrum of compound 2-27

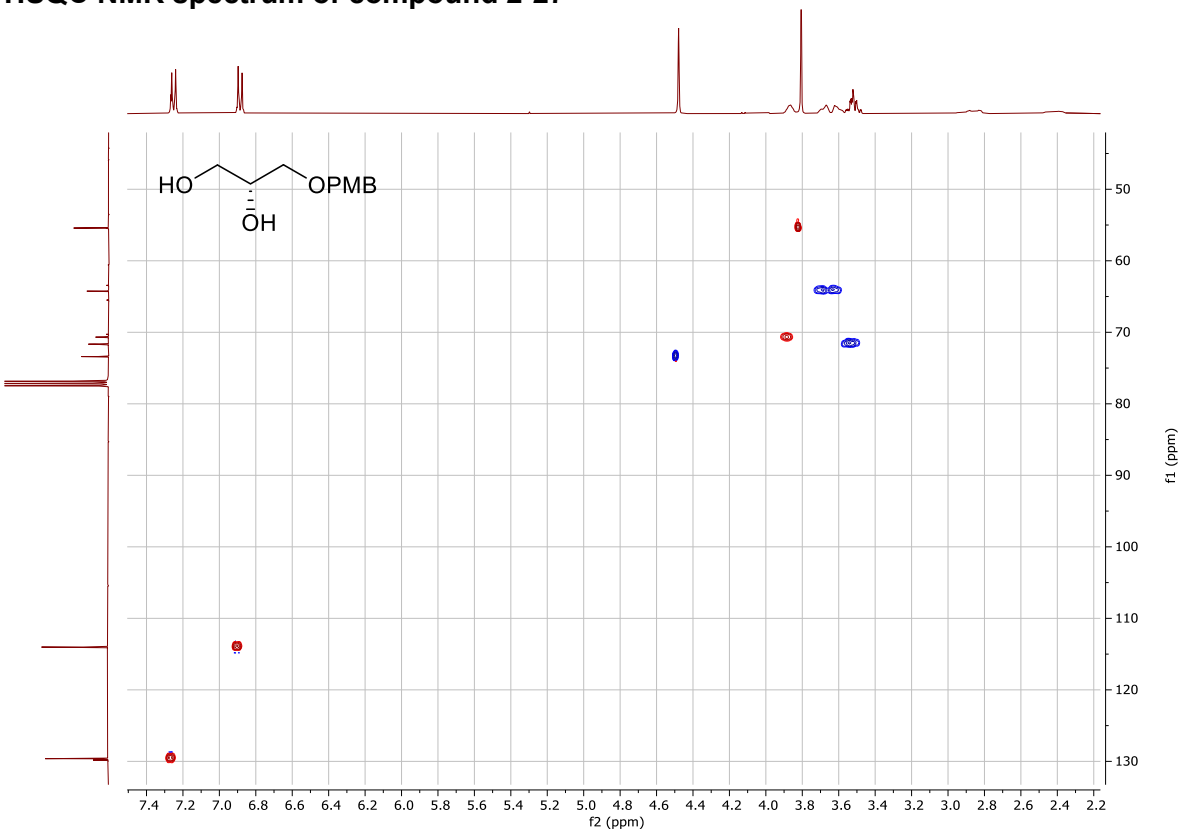

^{1}H NMR spectrum of compound 2-28

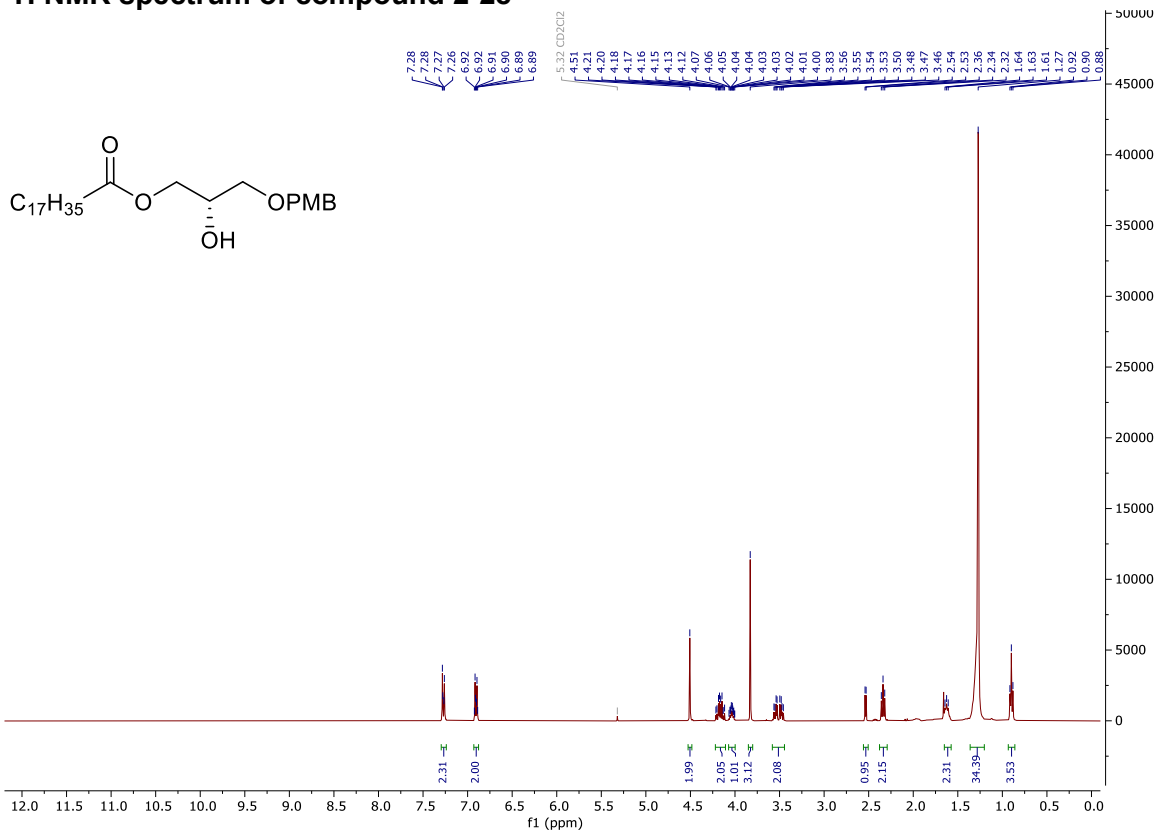

^{13}C NMR spectrum of compound 2-28

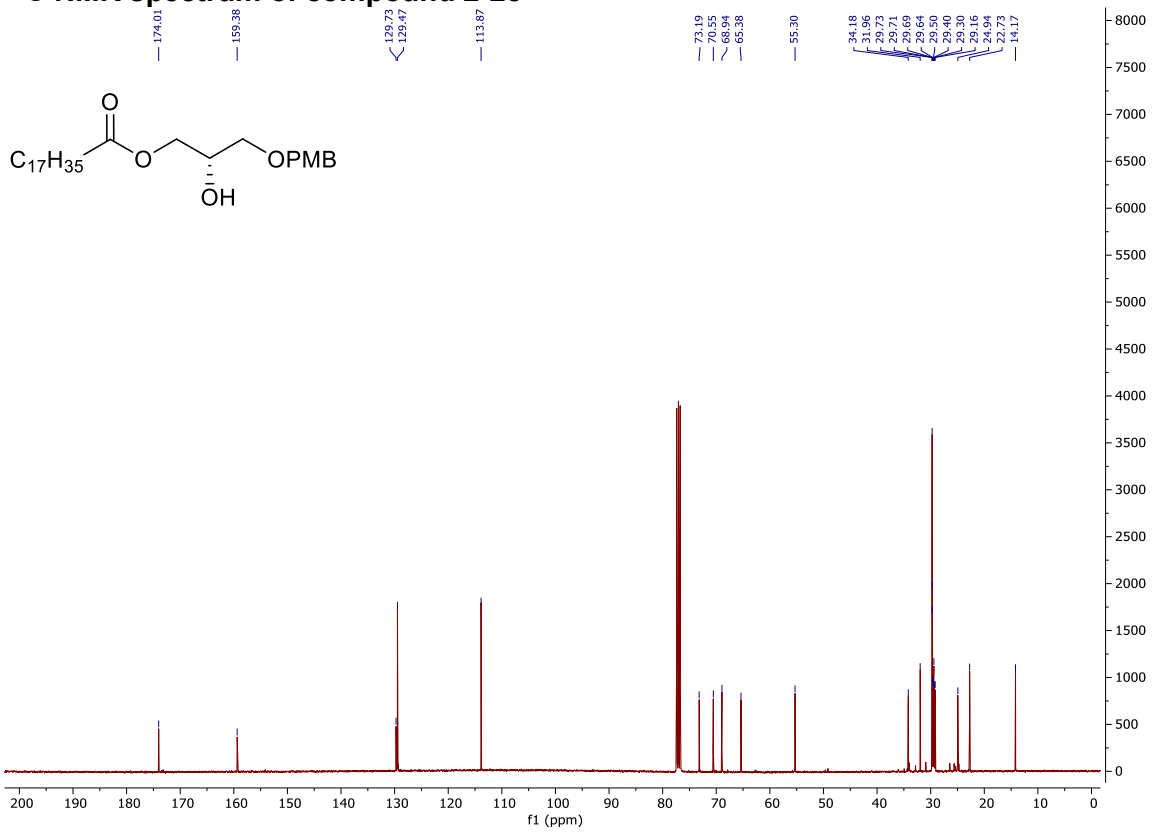

COSY NMR spectrum of compound 2-28

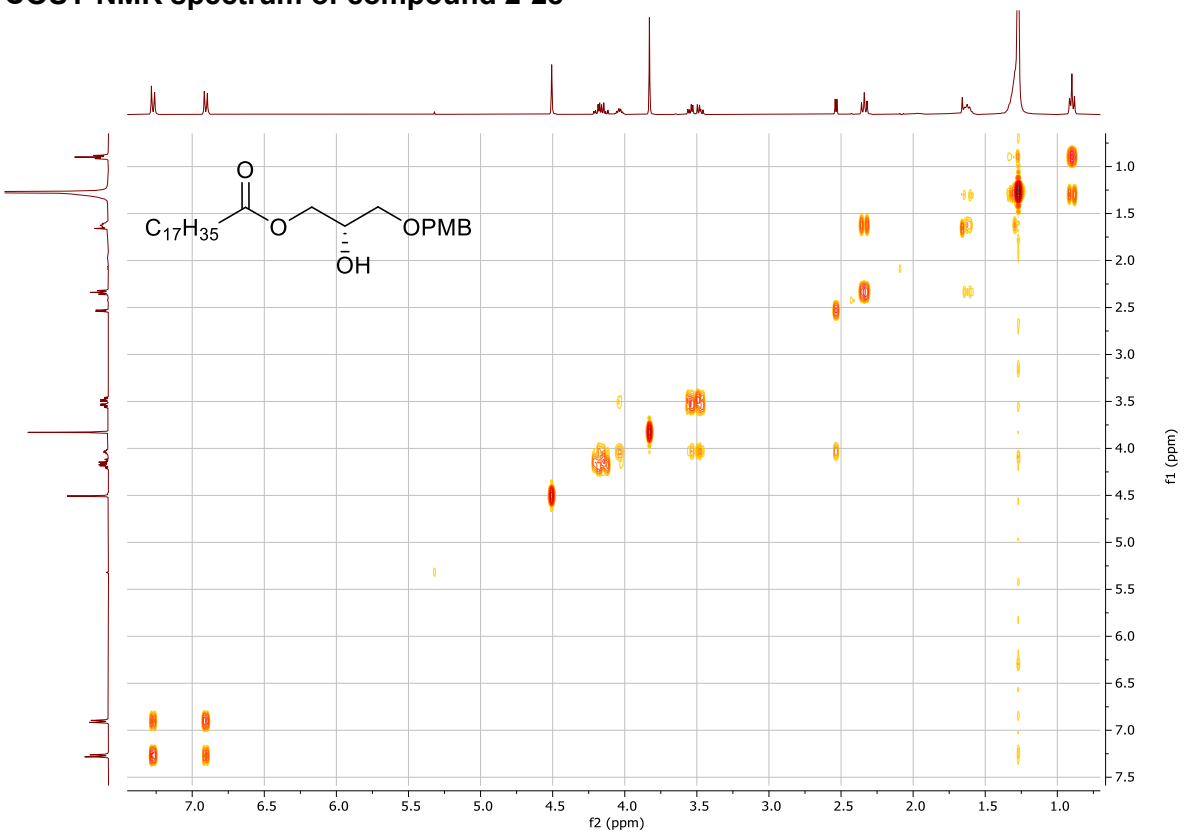

HSQC NMR spectrum of compound 2-28

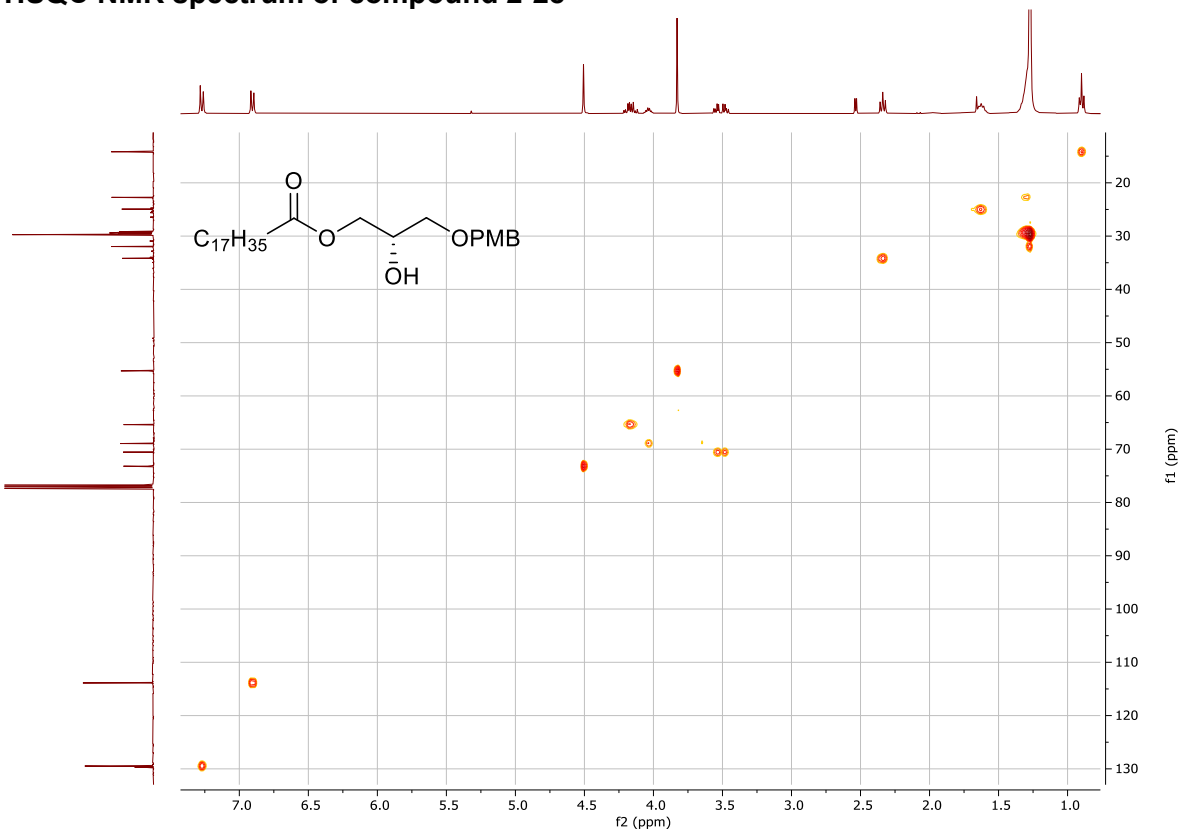

^{1}H NMR spectrum of compound 2-29

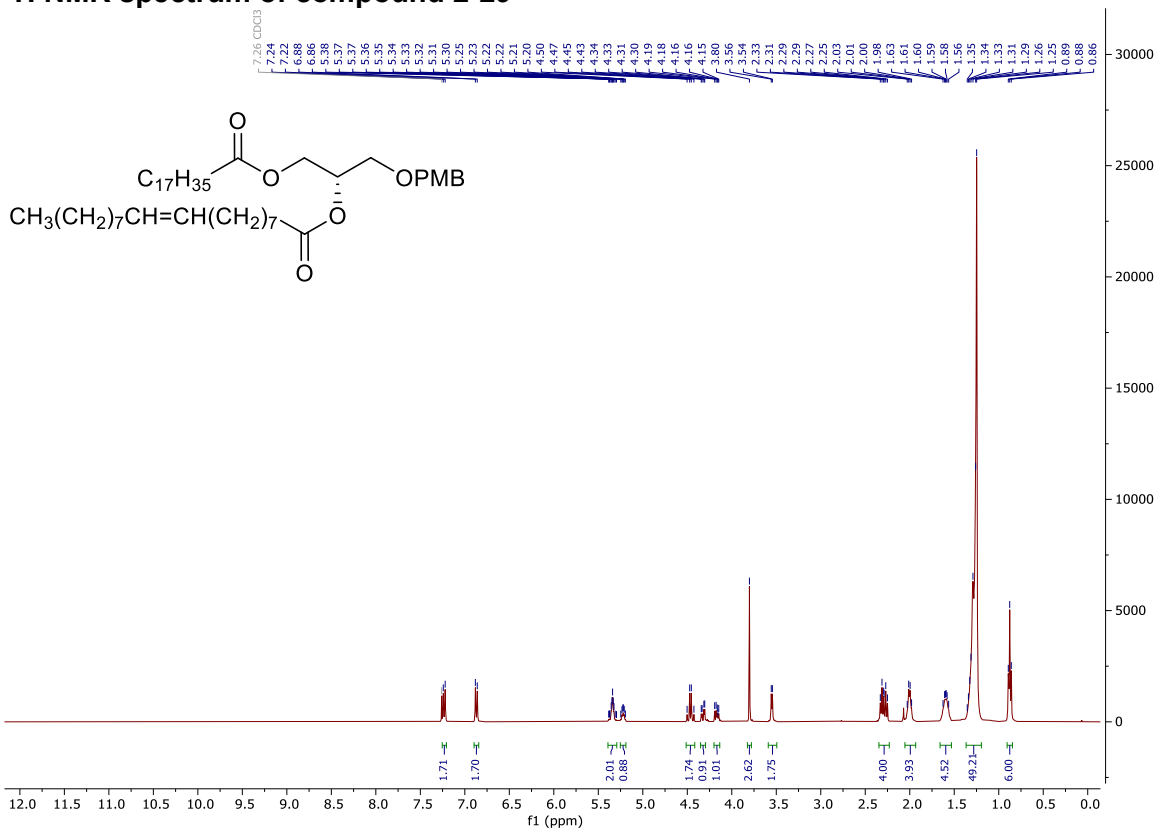

^{13}C NMR spectrum of compound 2-29

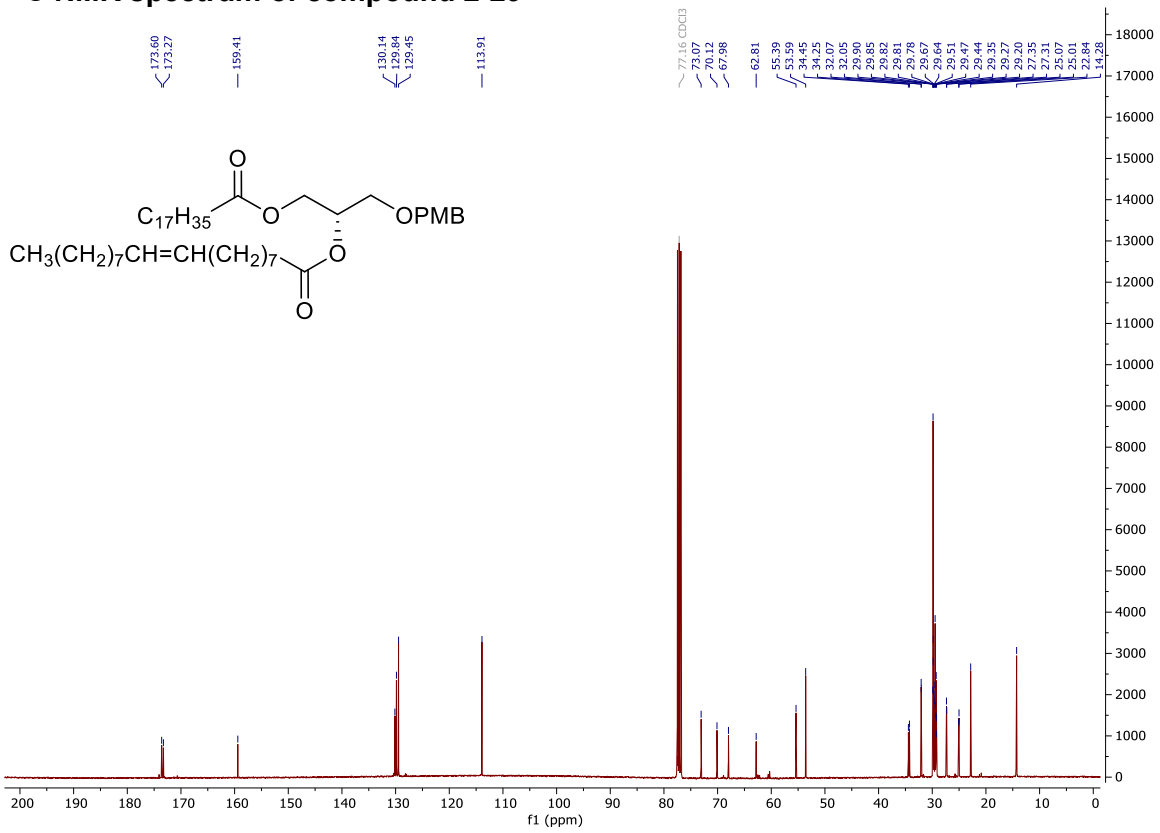

COSY NMR spectrum of compound 2-29

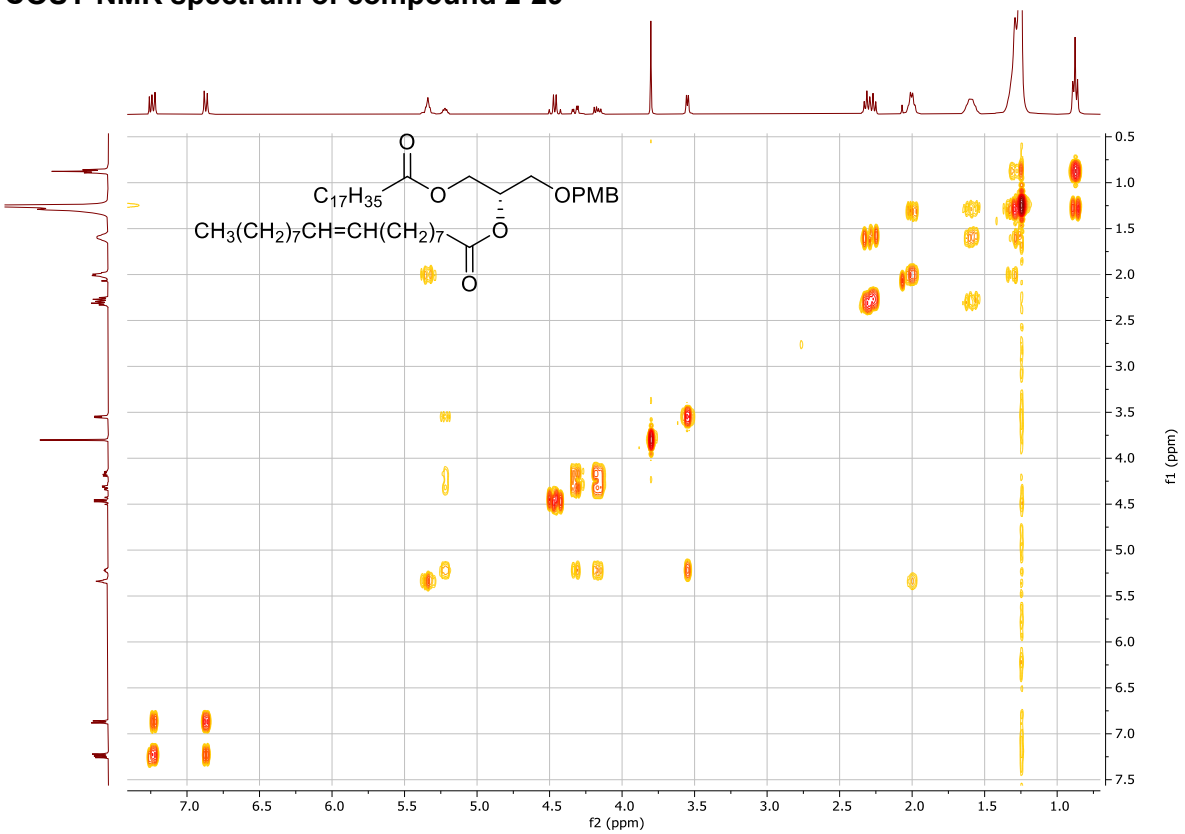

HSQC NMR spectrum of compound 2-29

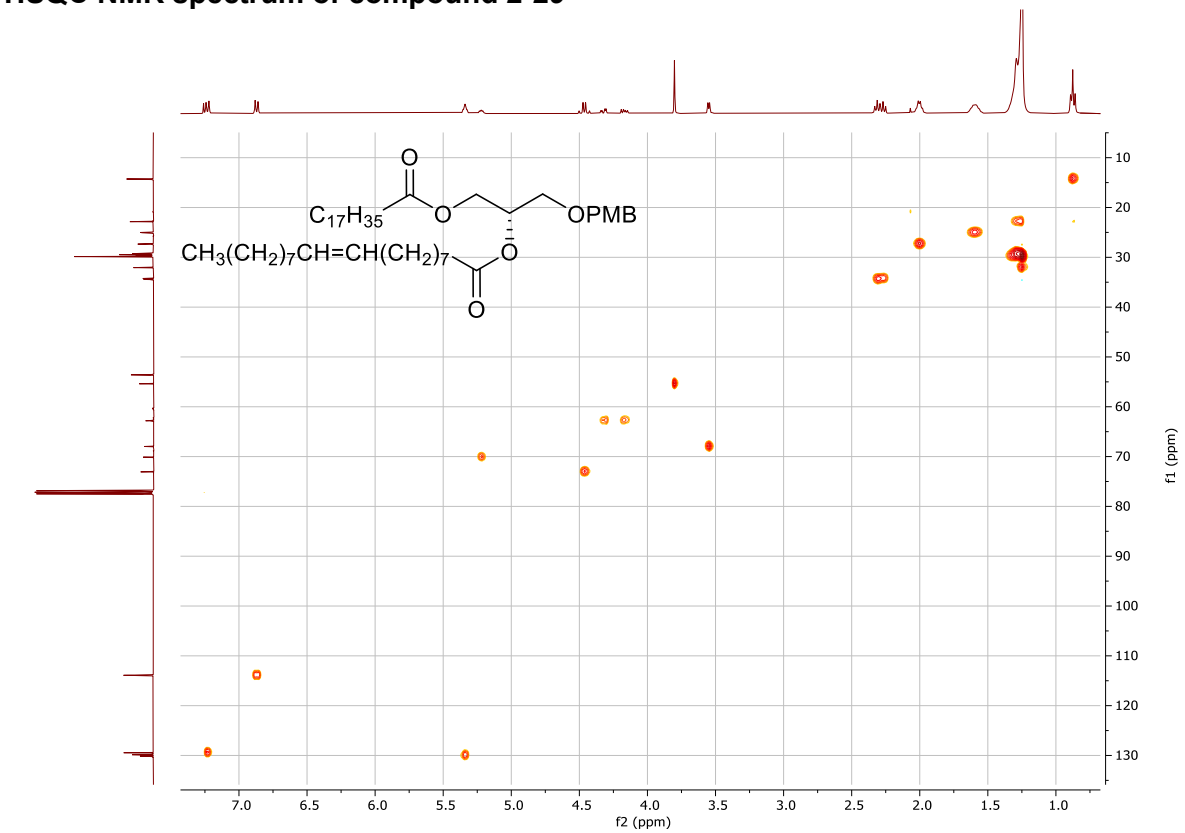

^{1}H NMR spectrum of compound 2-30

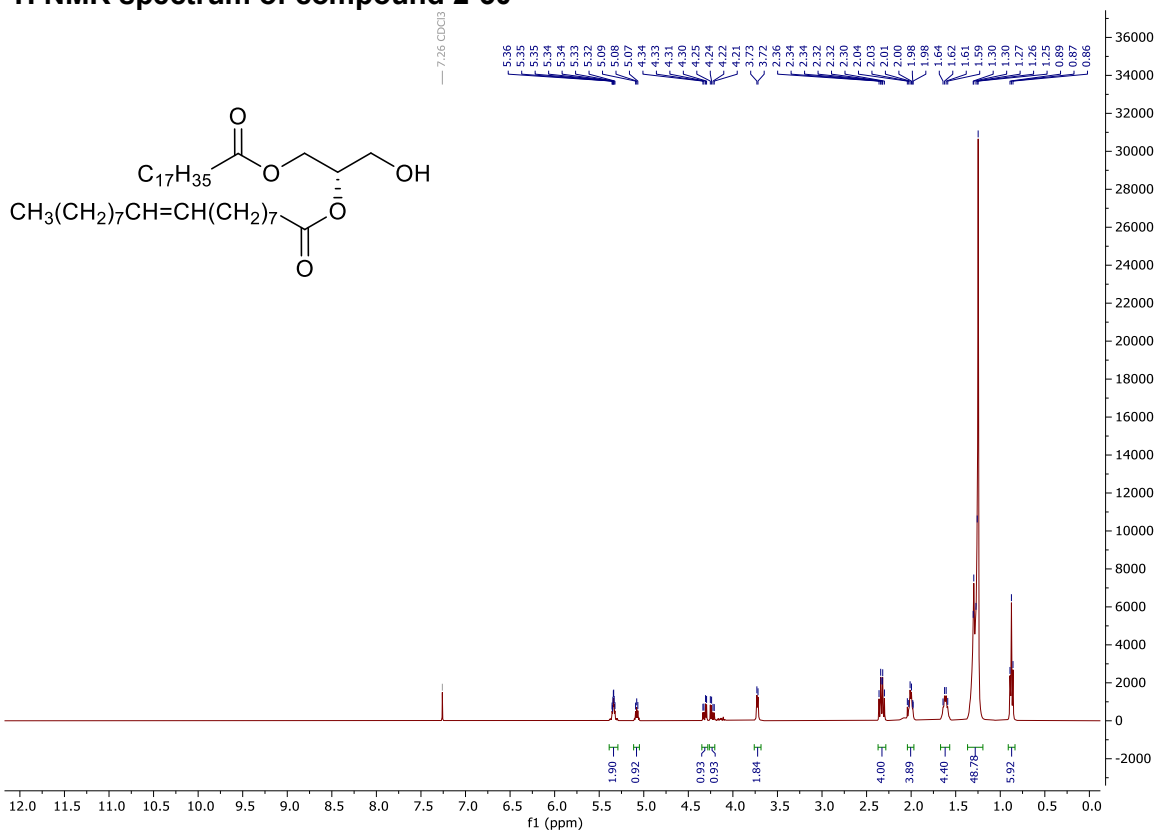

^{13}C NMR spectrum of compound 2-30

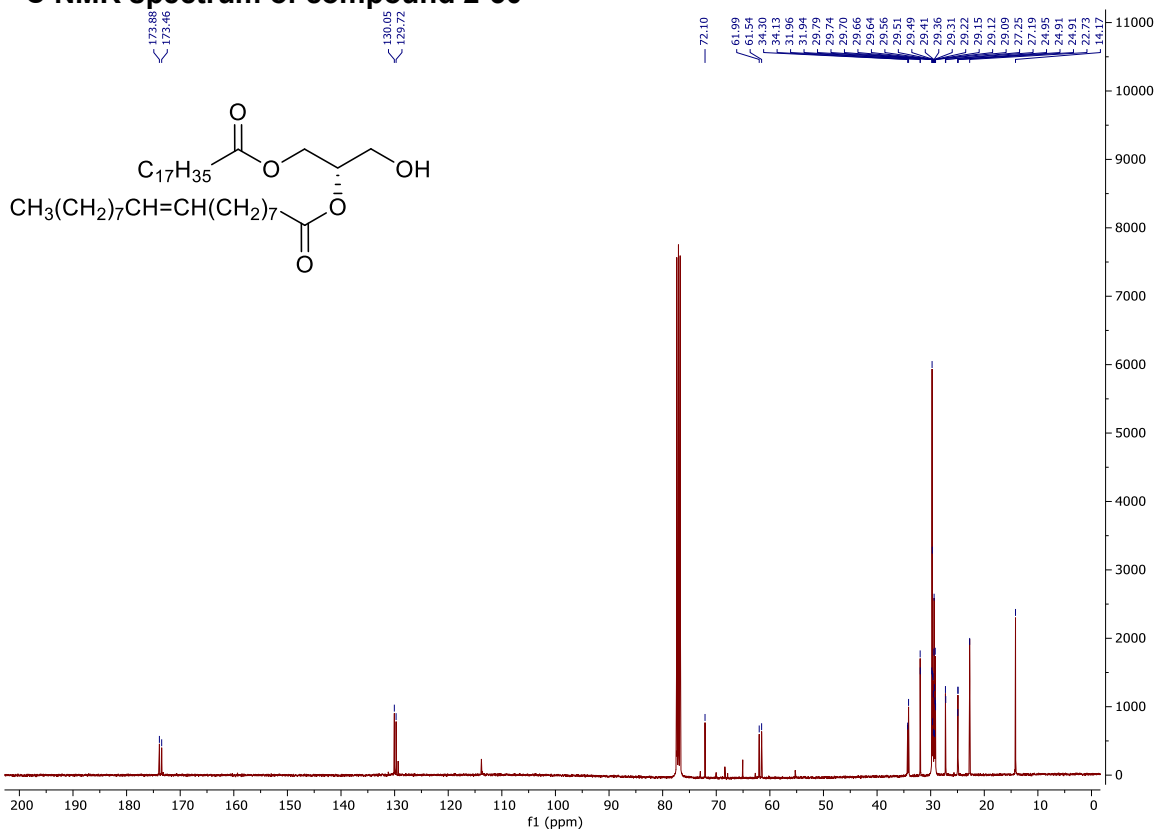

COSY NMR spectrum of compound 2-30

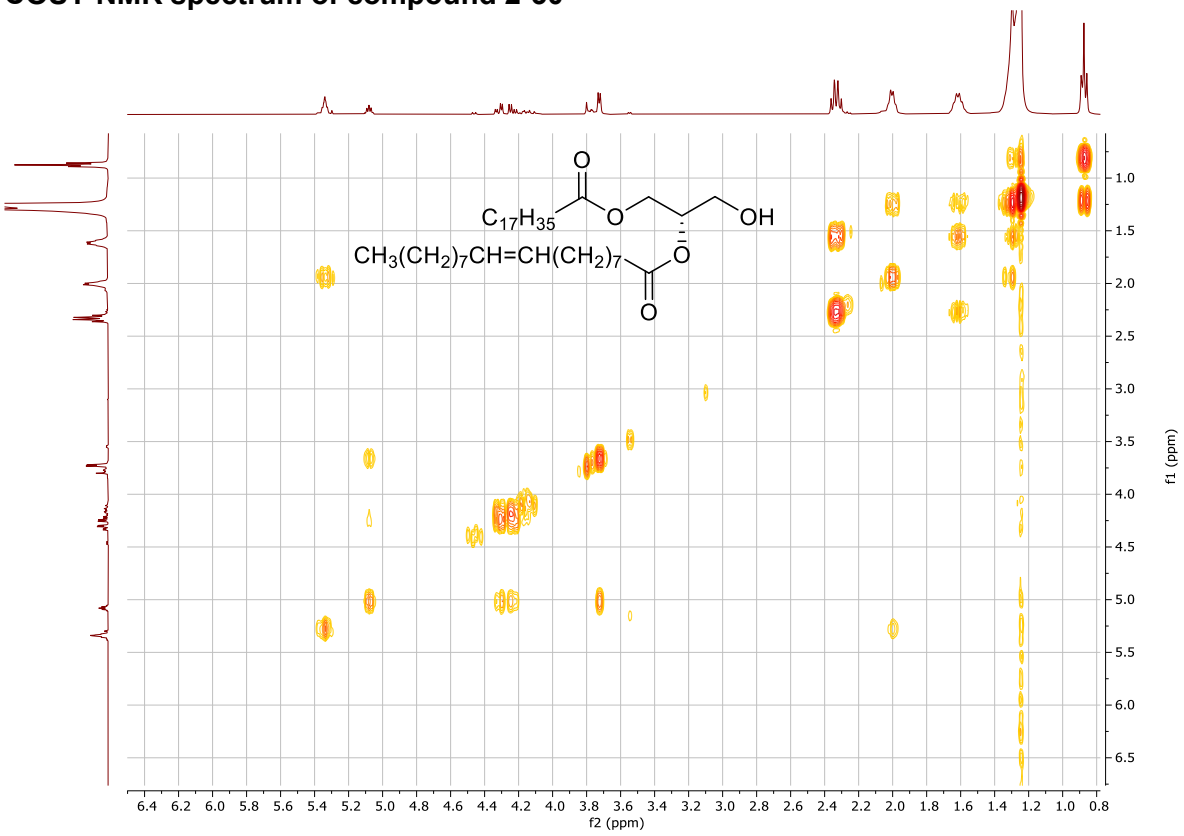

HSQC NMR spectrum of compound 2-30

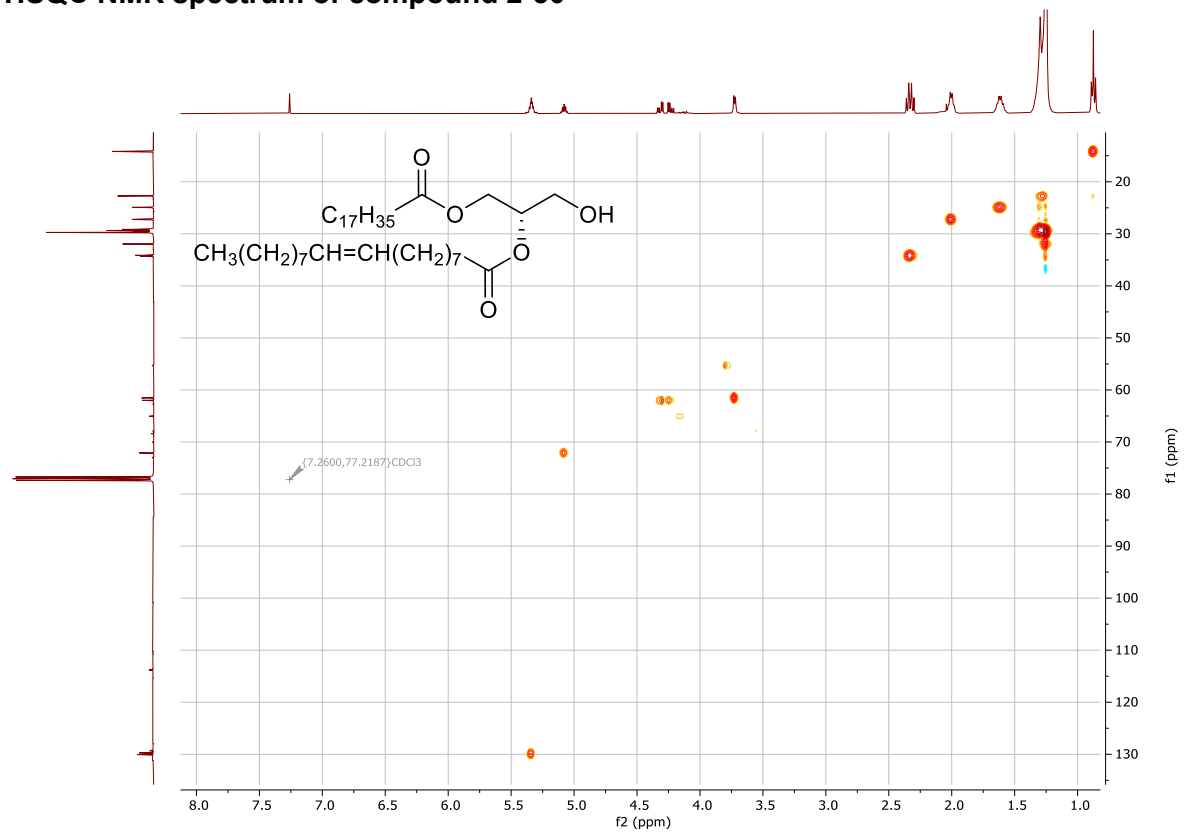

^{1}H NMR spectrum of compound 2-8

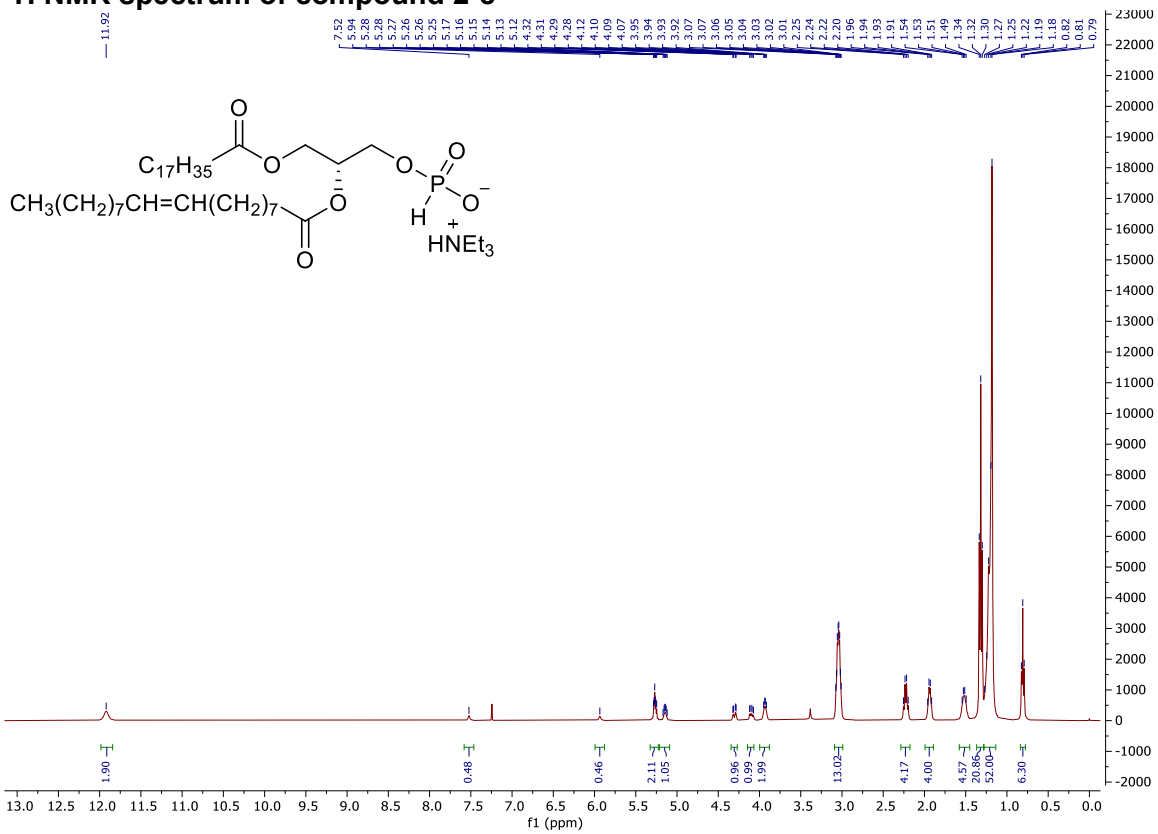

^{13}C NMR spectrum of compound 2-8

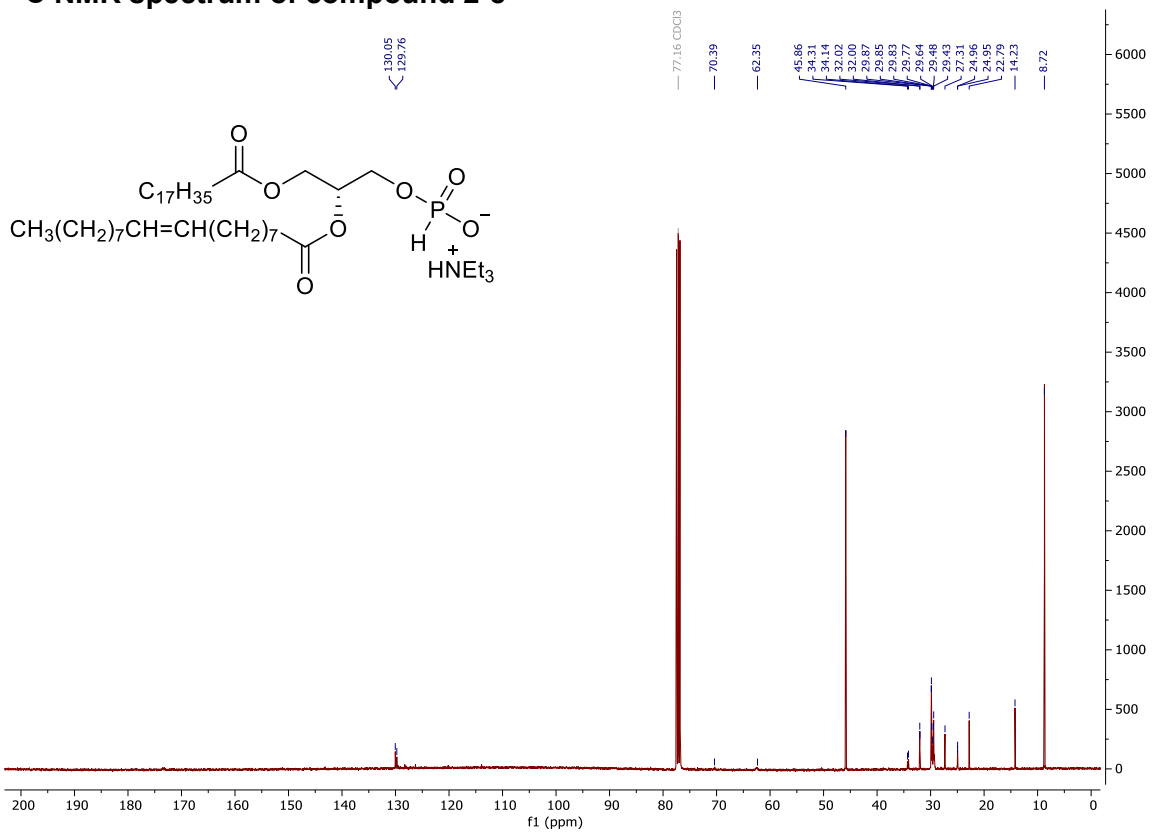

COSY NMR spectrum of compound 2-8

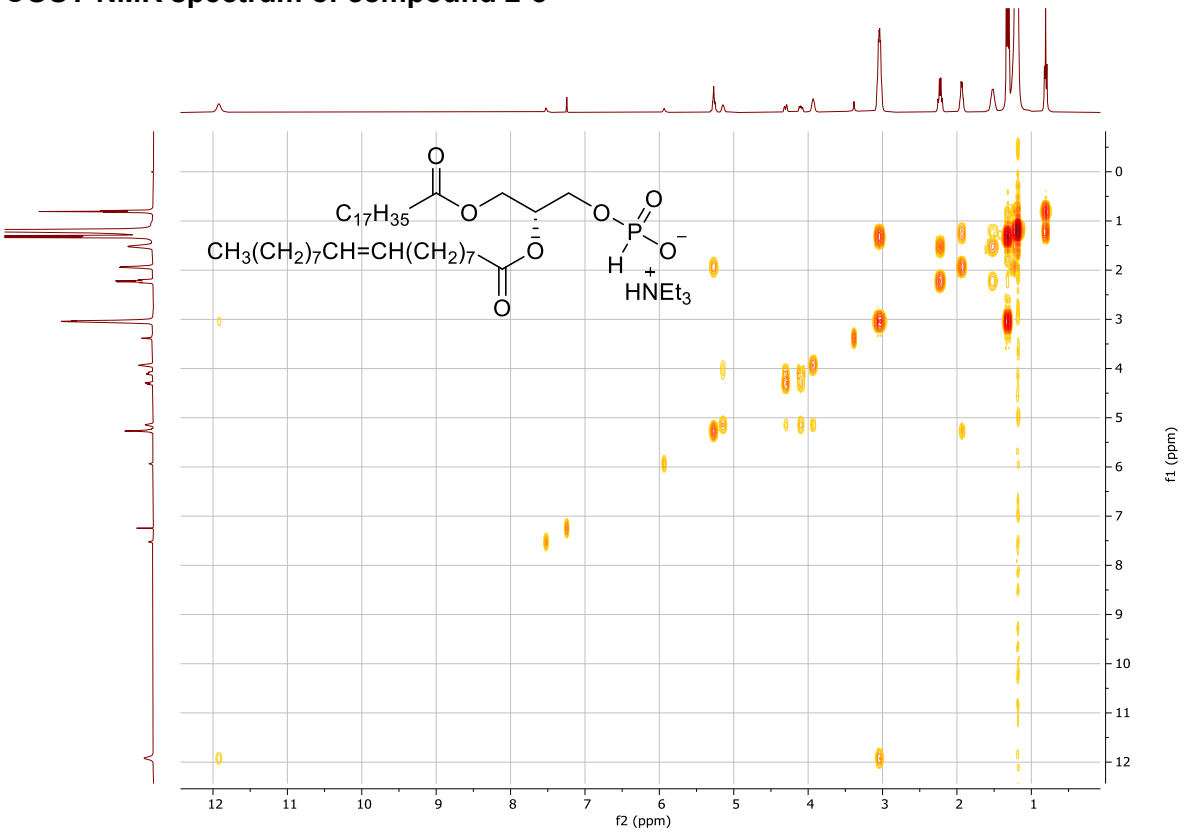

HSQC NMR spectrum of compound 2-8

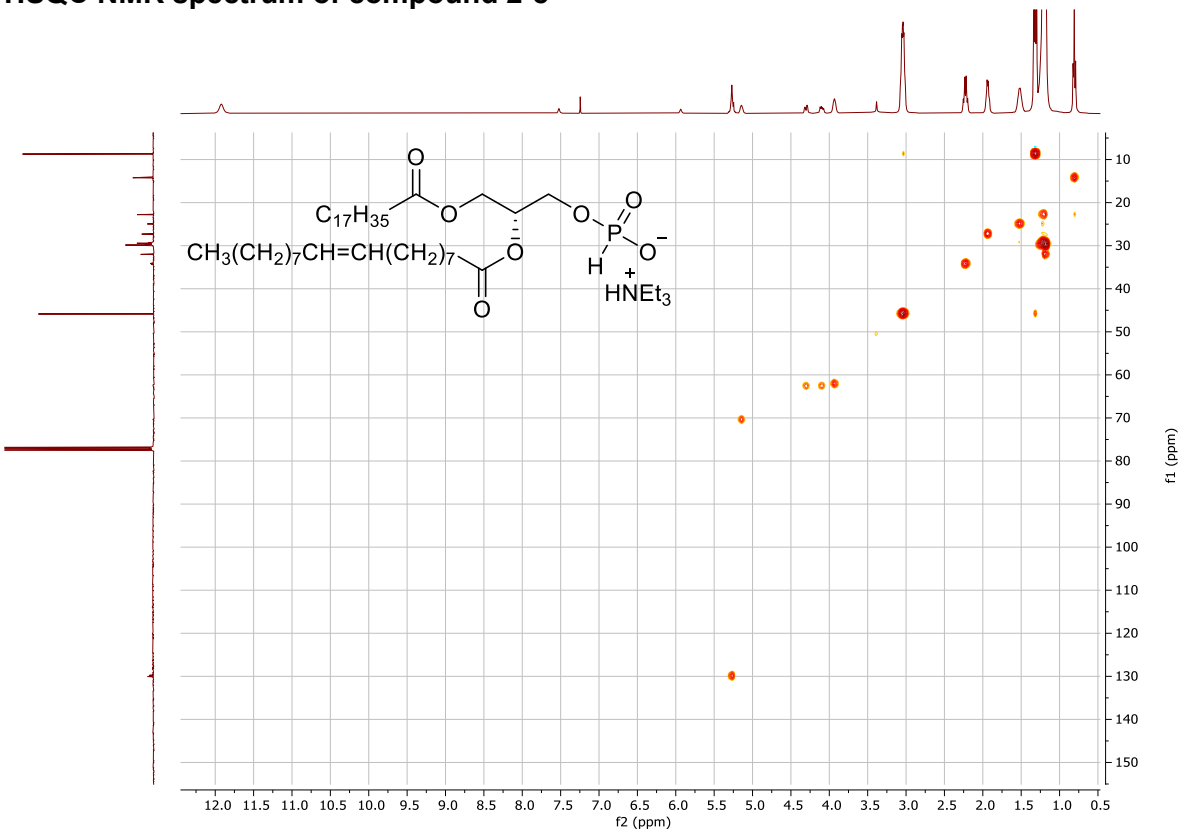

^{31}P NMR spectrum of compound 2-8

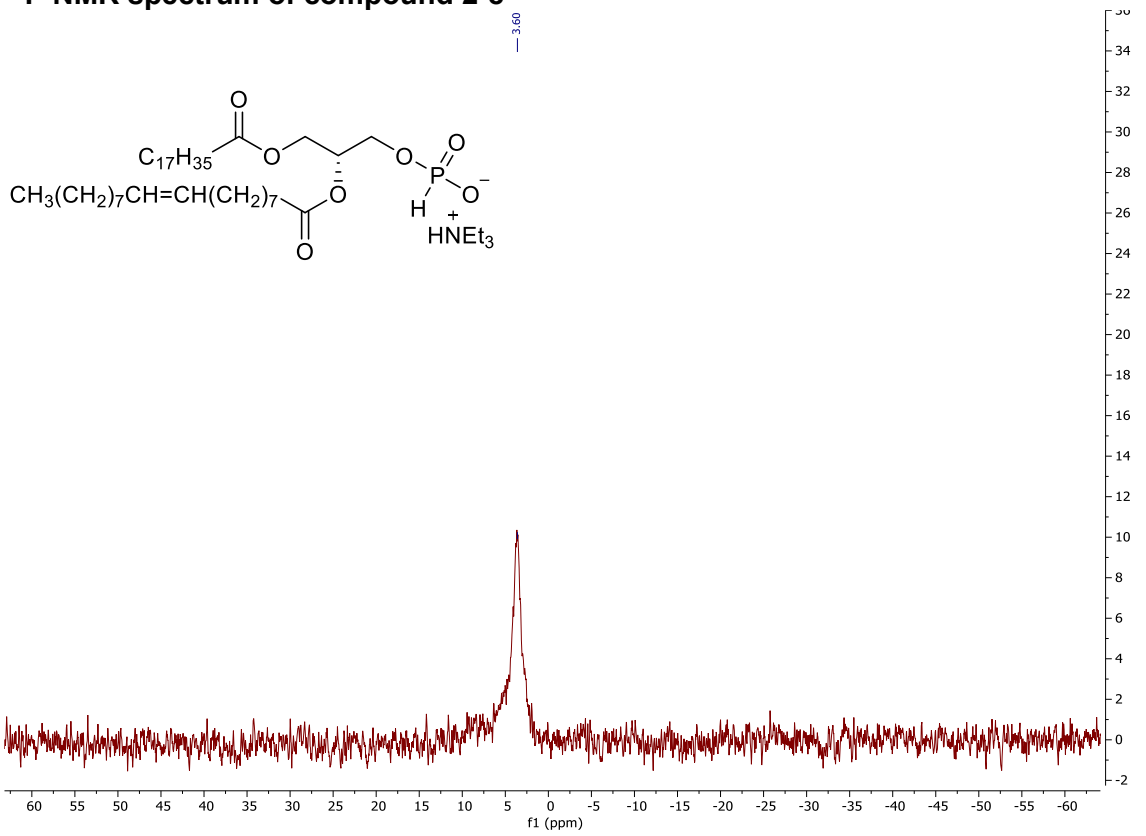

^{1}H NMR spectrum of compound 2-55

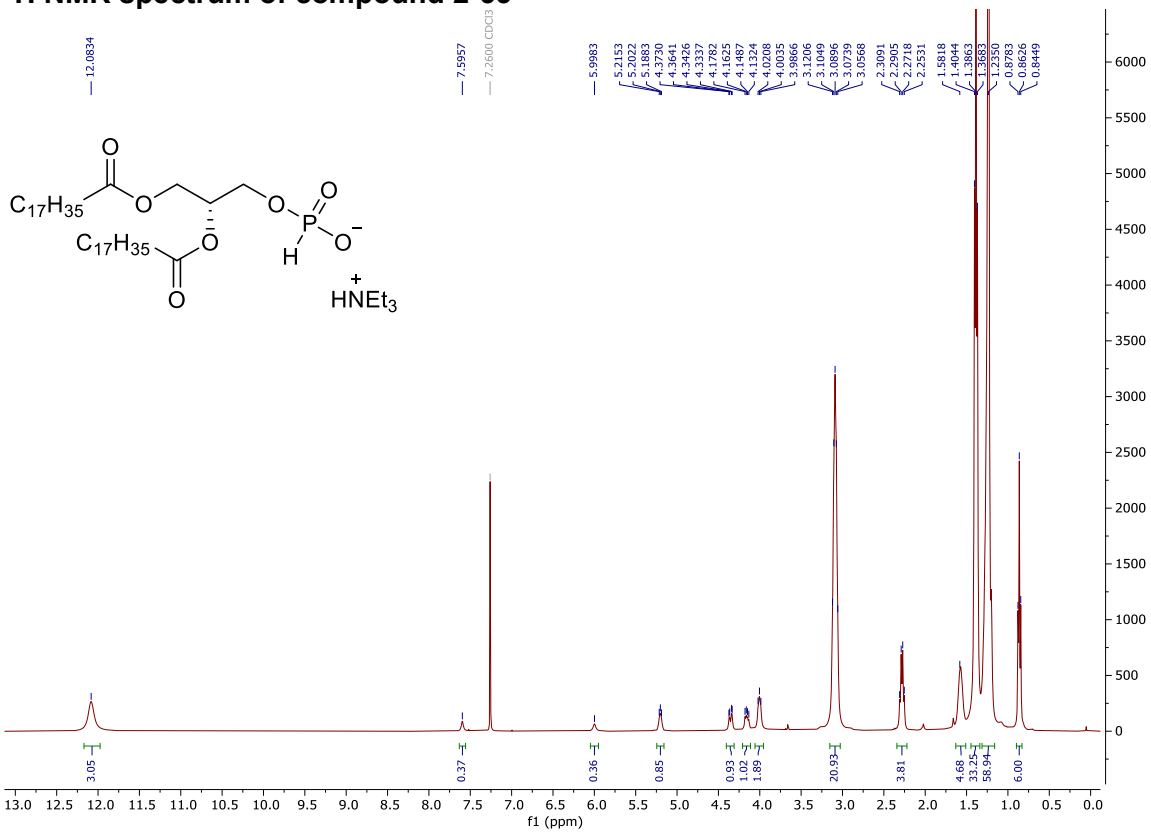

^{13}C NMR spectrum of compound 2-55

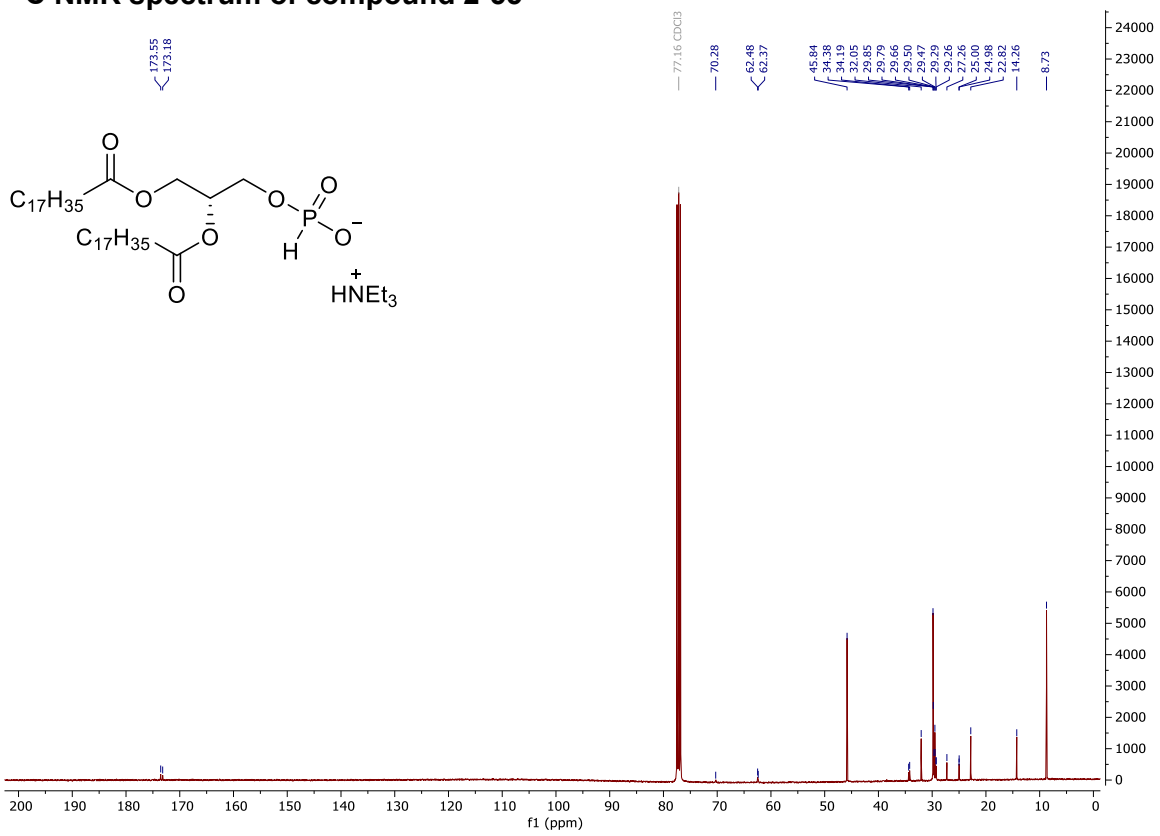

COSY NMR spectrum of compound 2-55

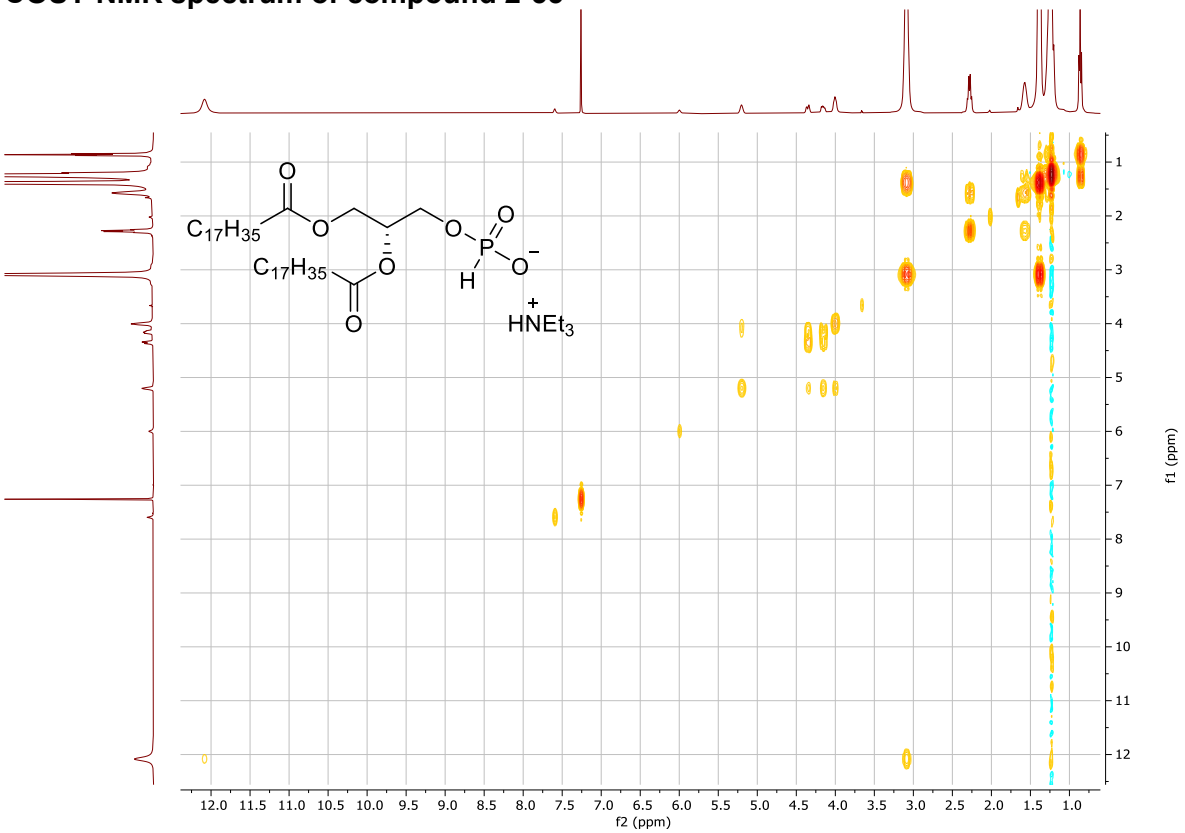

HSQC NMR spectrum of compound 2-55

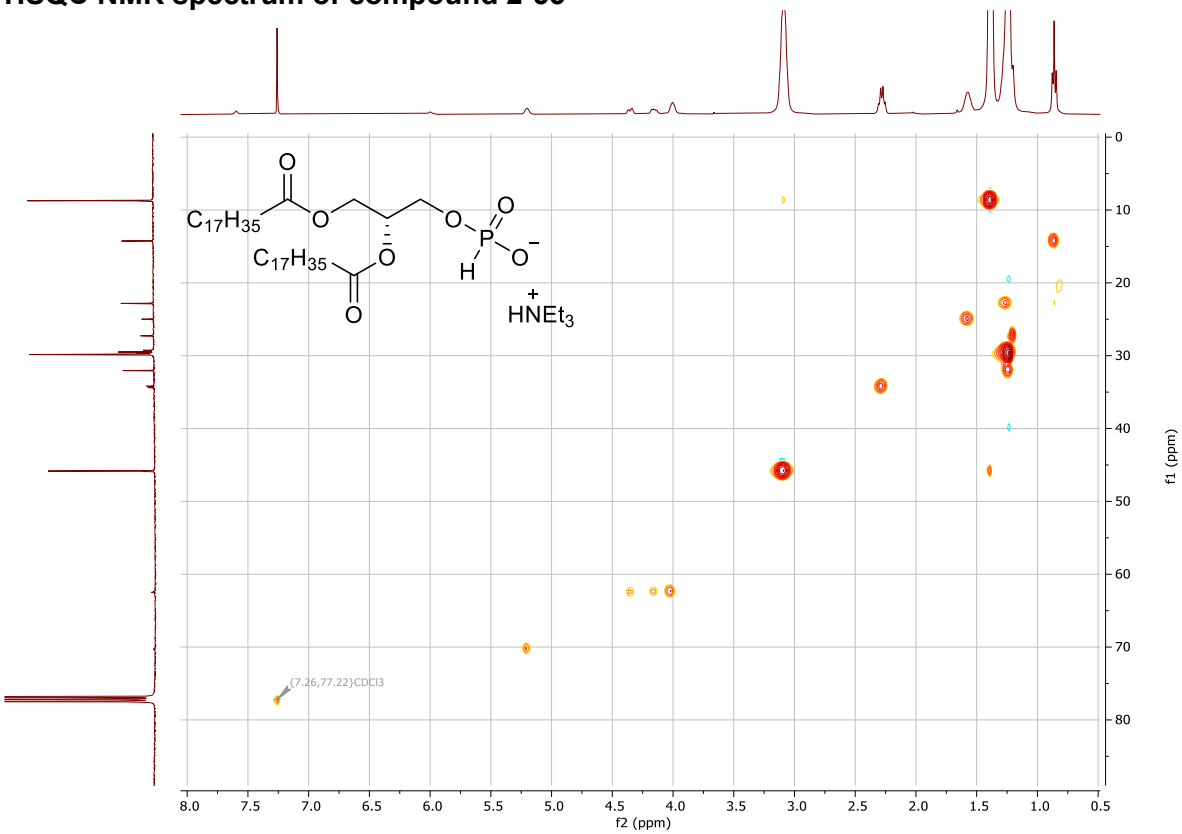

^{31}P NMR spectrum of compound 2-55

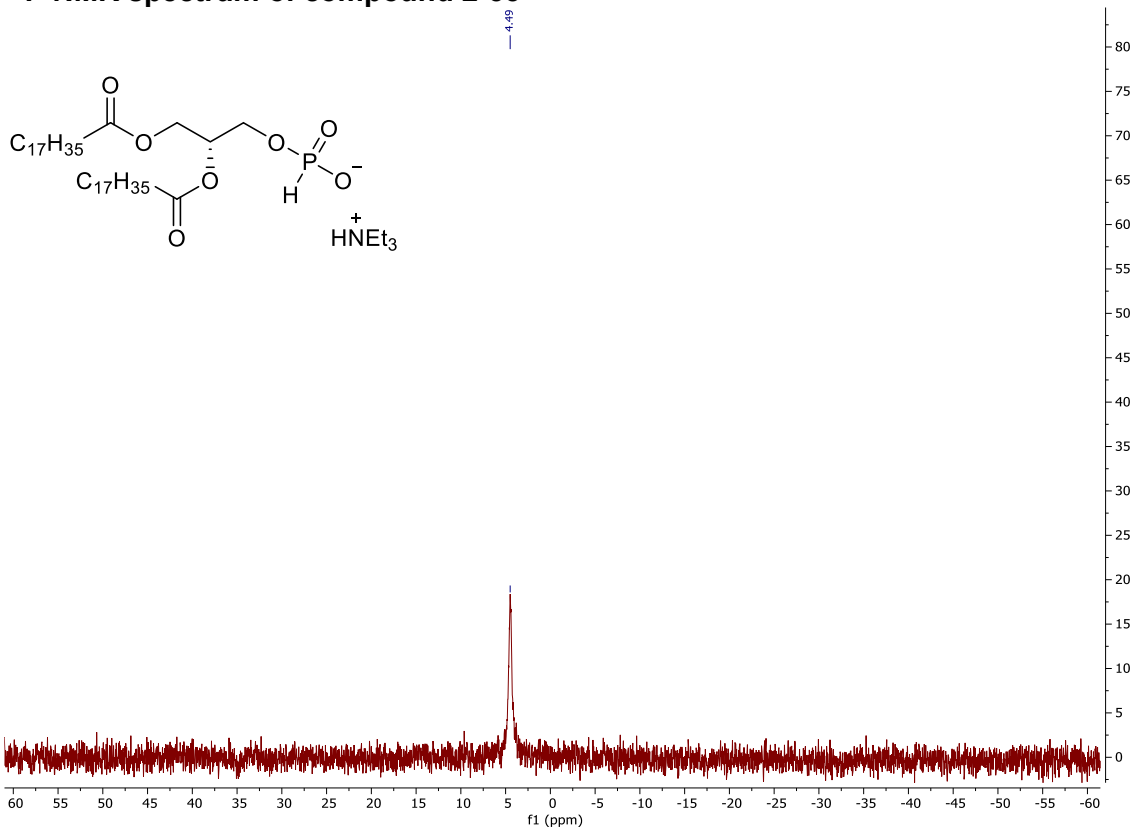

^{1}H NMR spectrum of compound 2-56

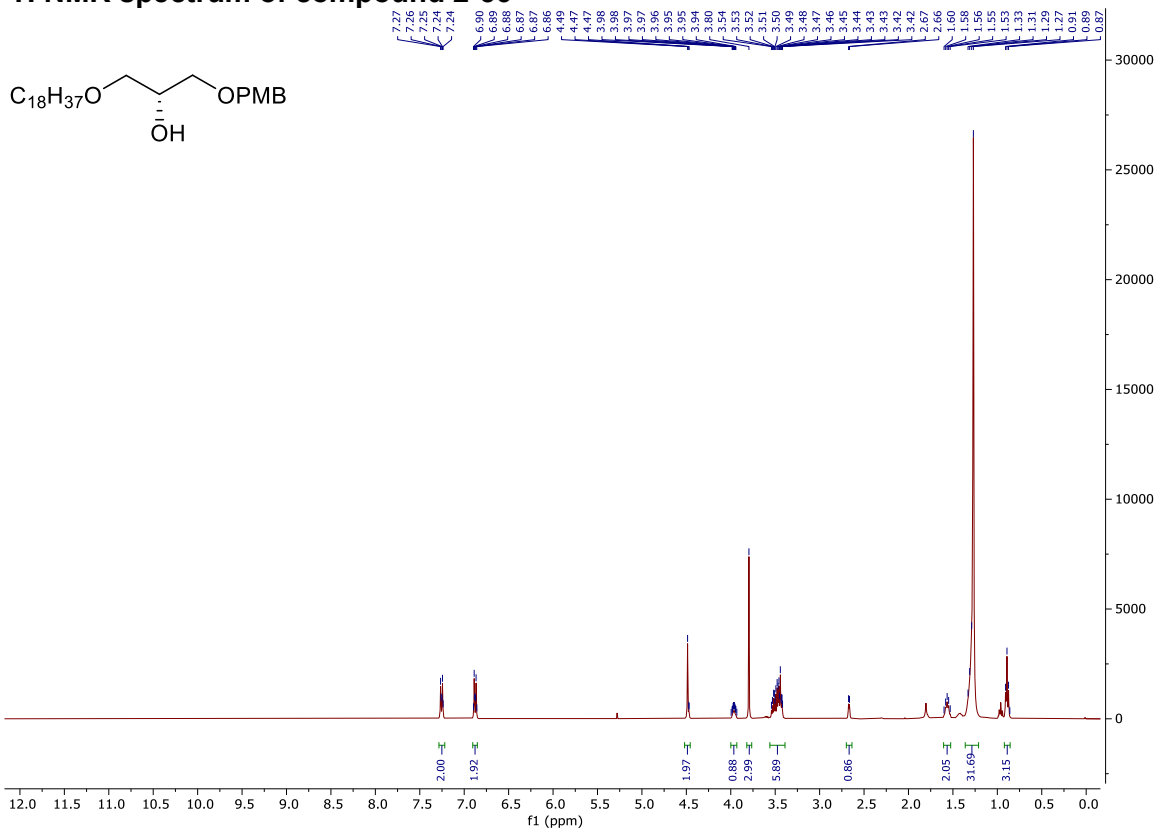

^{13}C NMR spectrum of compound 2-56

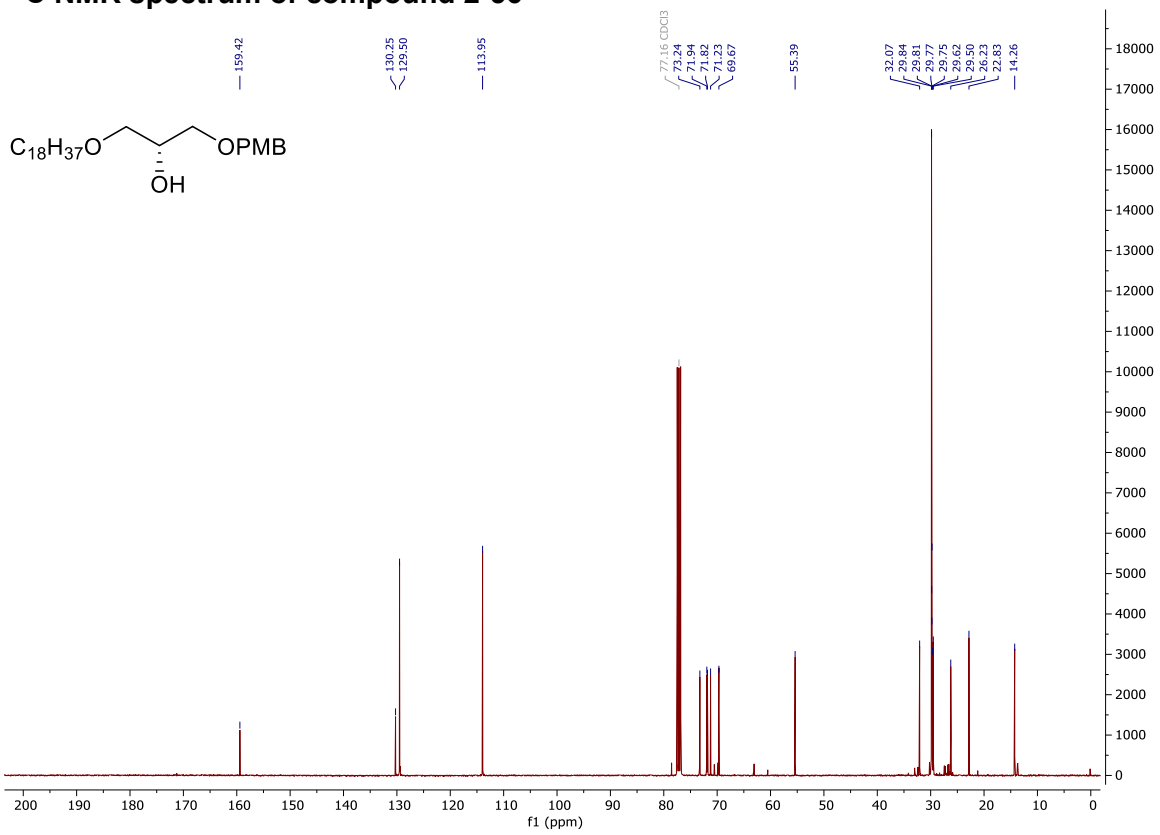

COSY NMR spectrum of compound 2-56

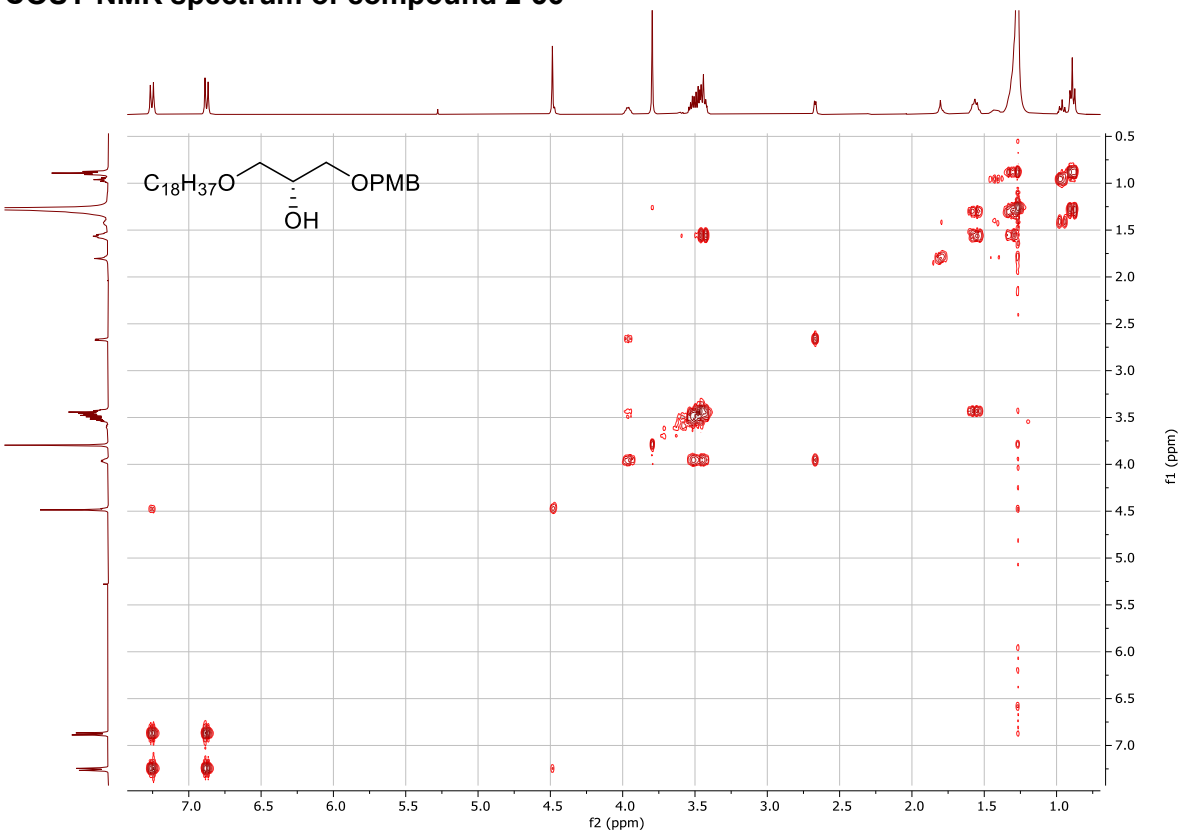

HSQC NMR spectrum of compound 2-56

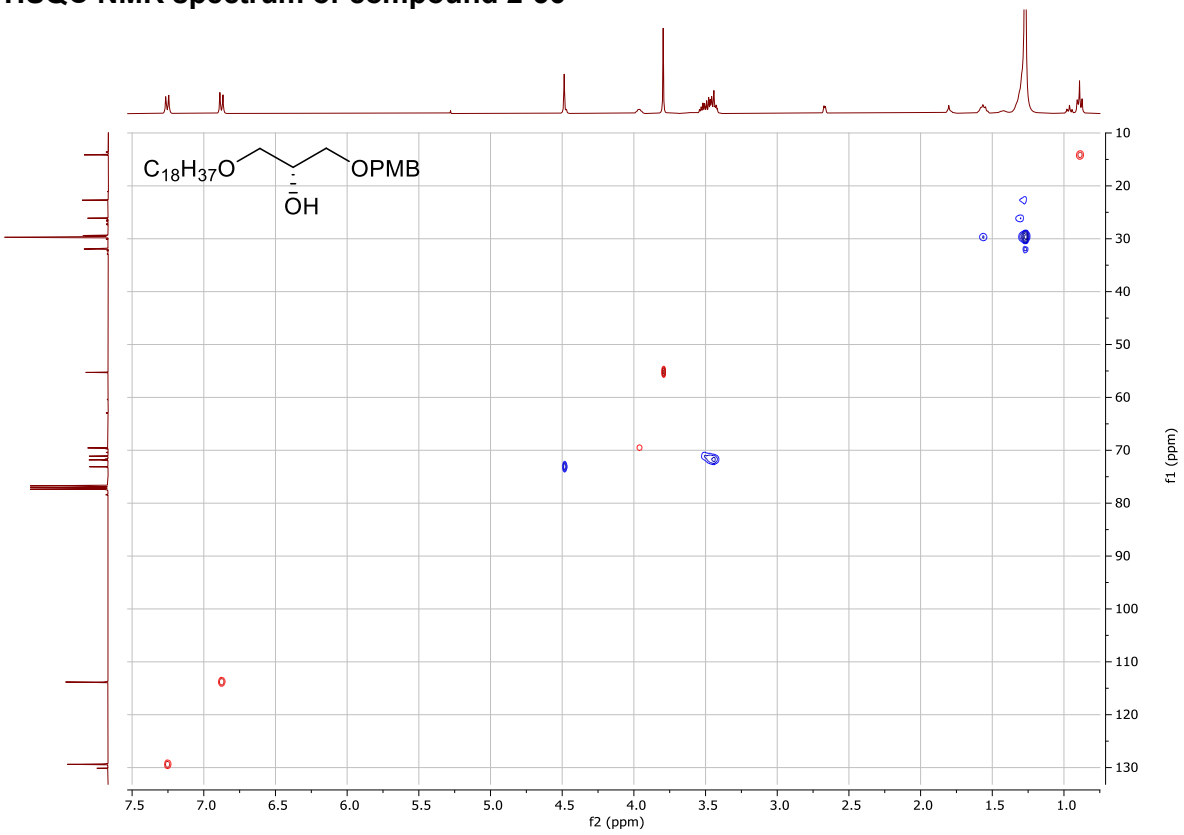

HMBC NMR spectrum of lipid compound 2-56

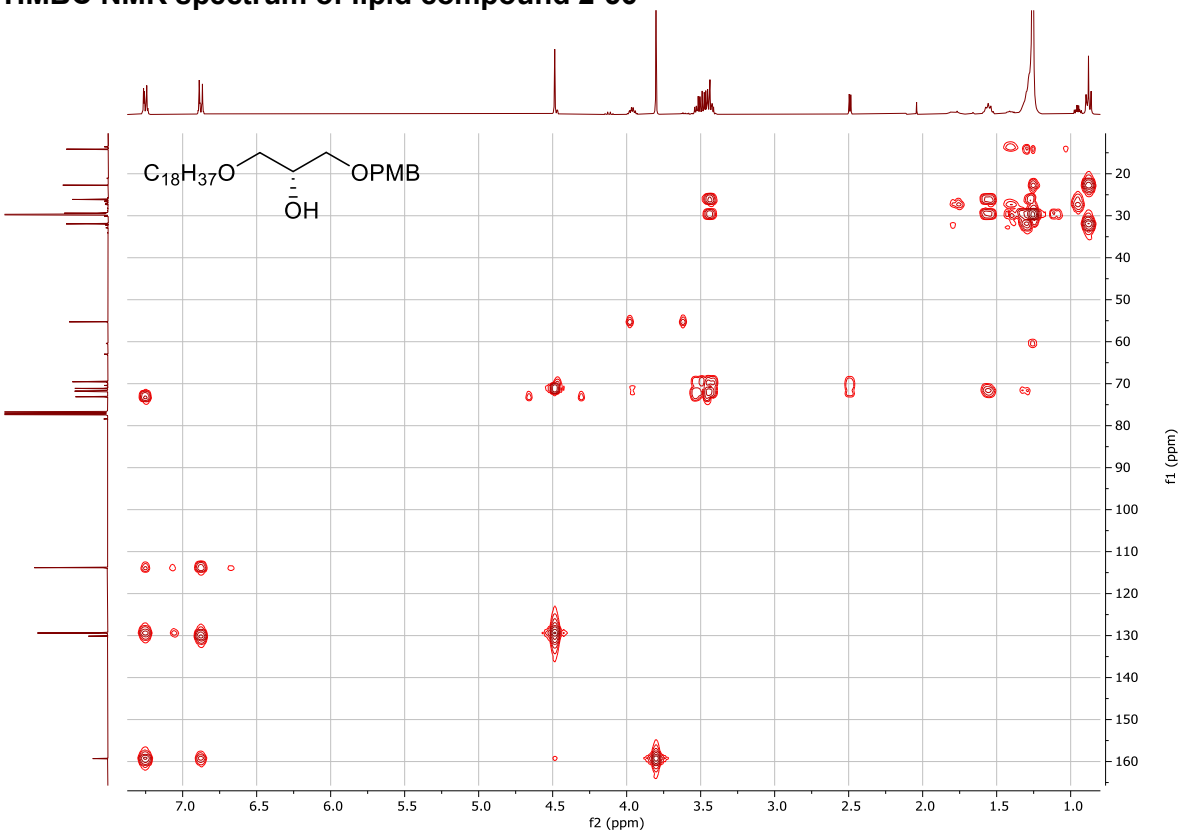

^{1}H NMR spectrum of compound 2-57

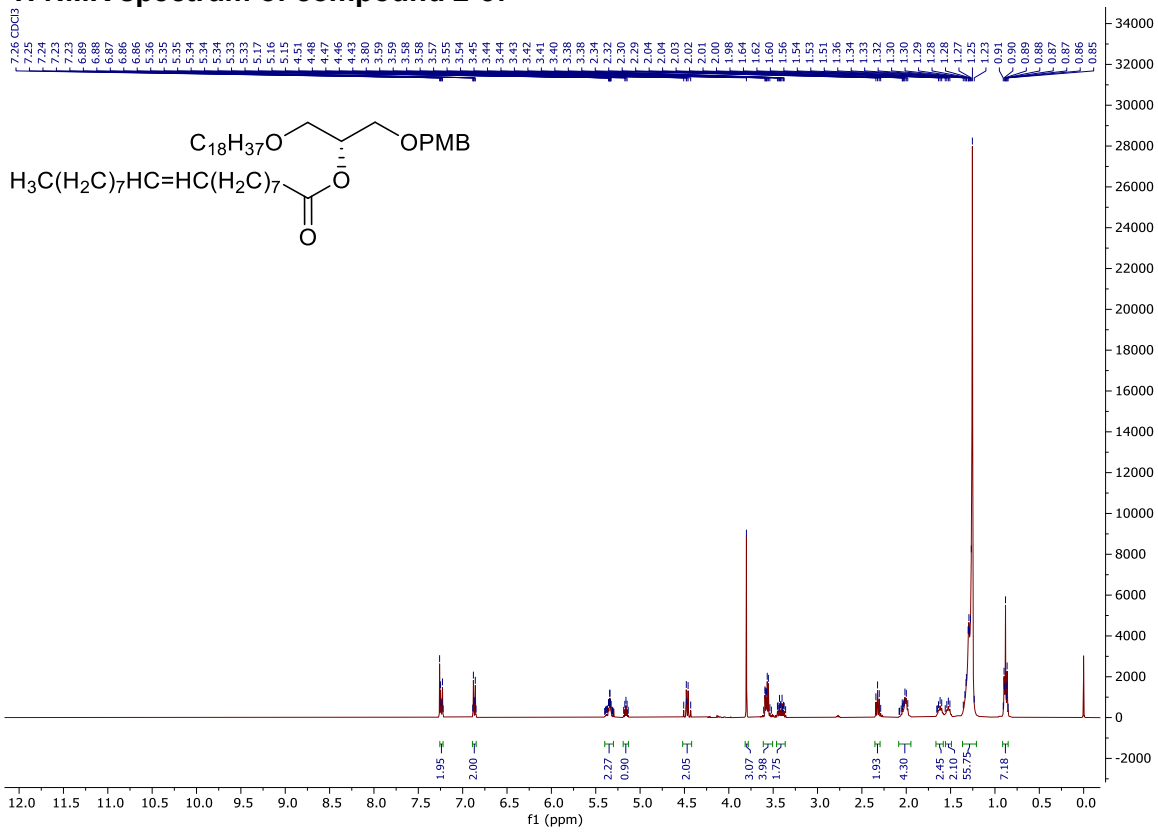

^{13}C NMR spectrum of compound 2-57

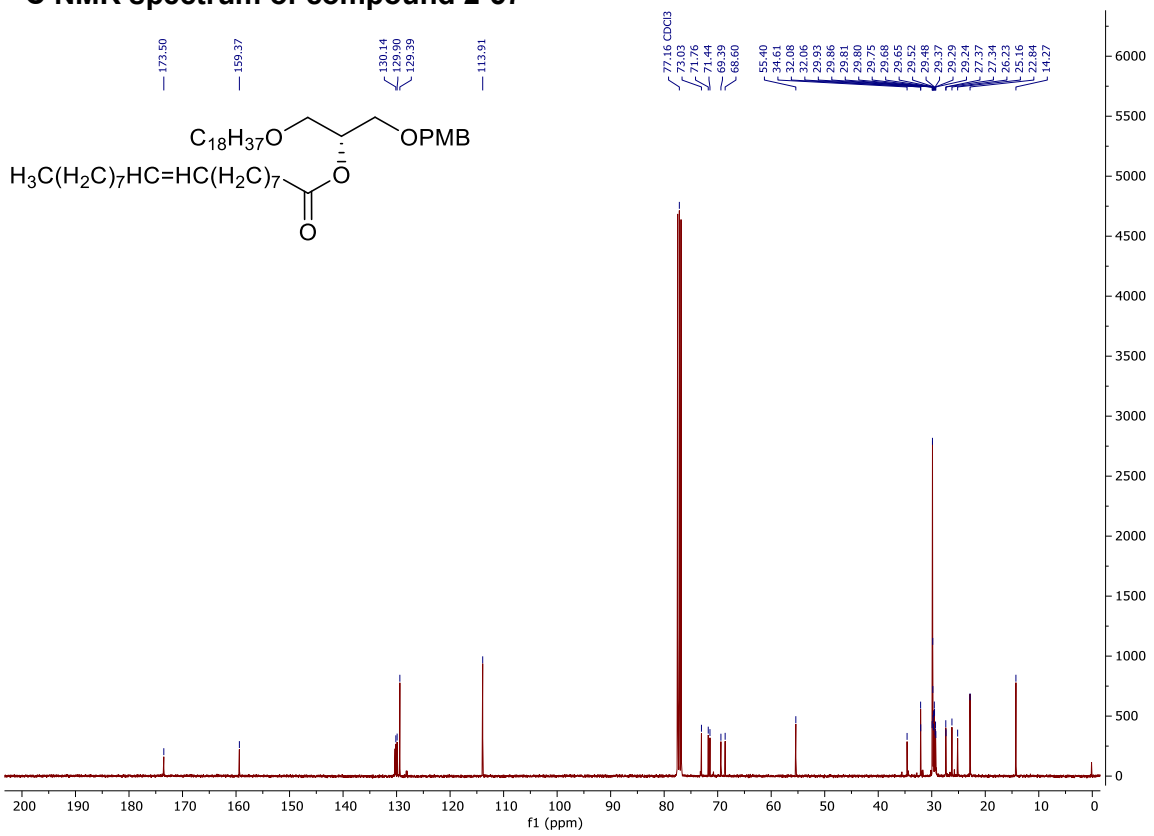

COSY NMR spectrum of compound 2-57

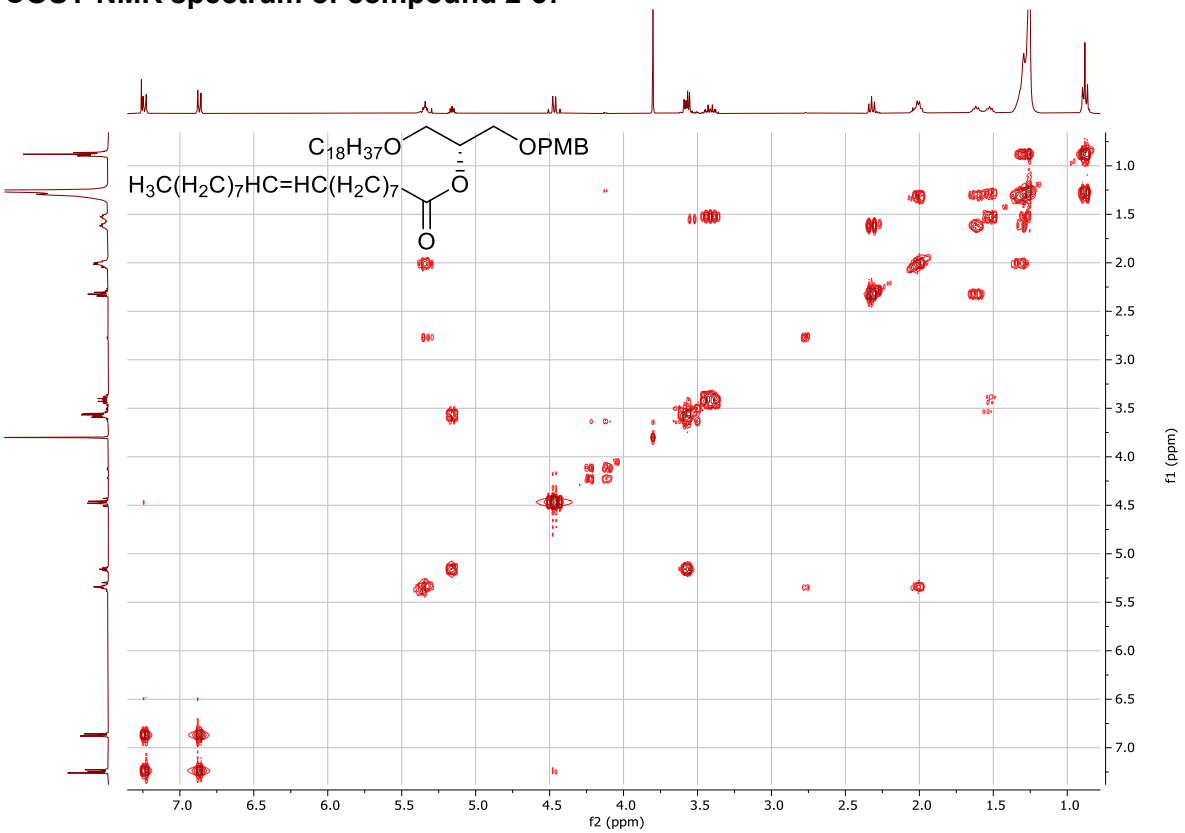

HSQC NMR spectrum of compound 2-57

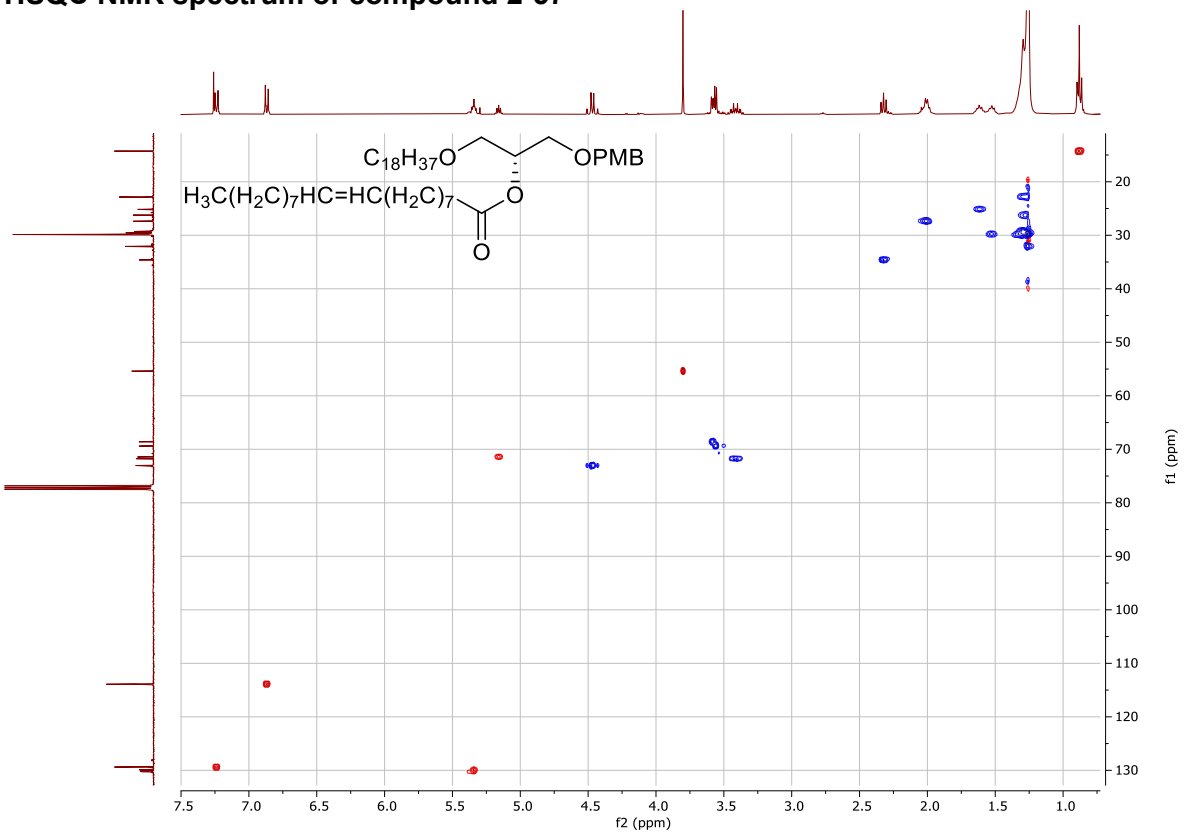

HMBC NMR spectrum of compound 2-57

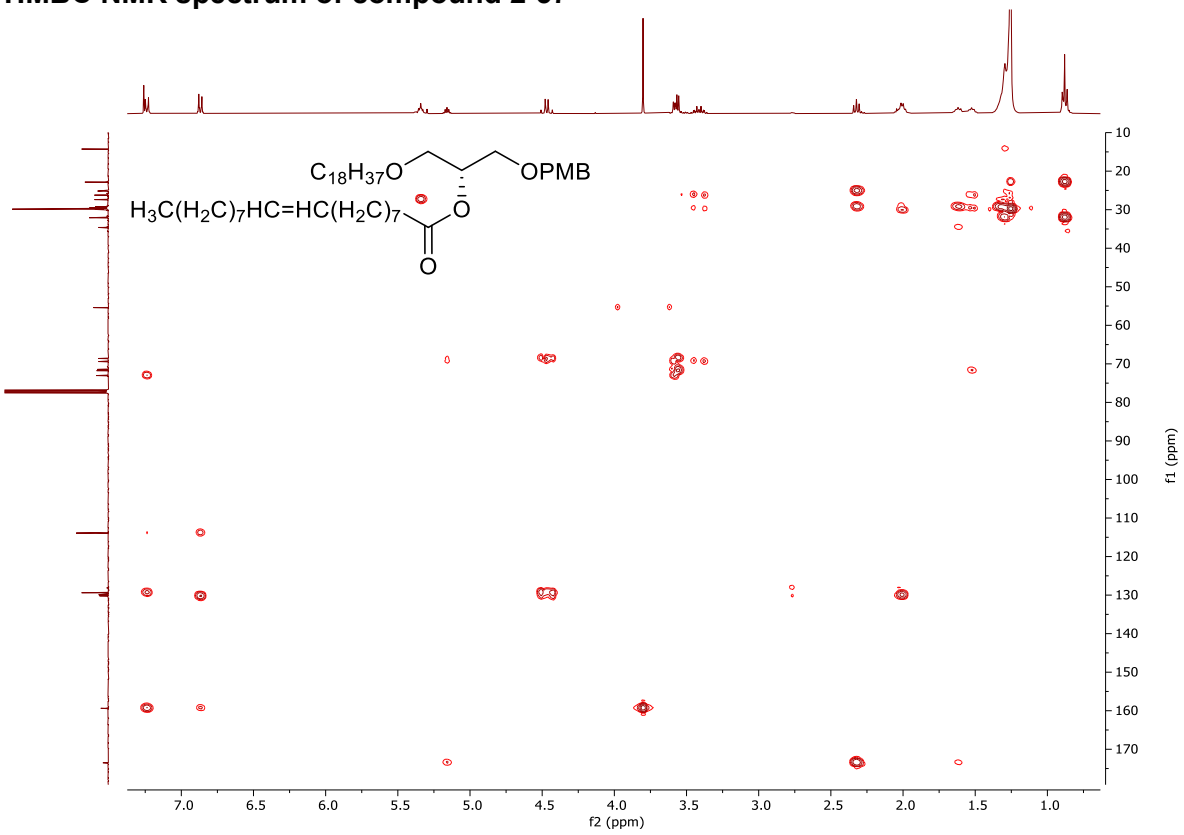

^{1}H NMR spectrum of compound 2-58

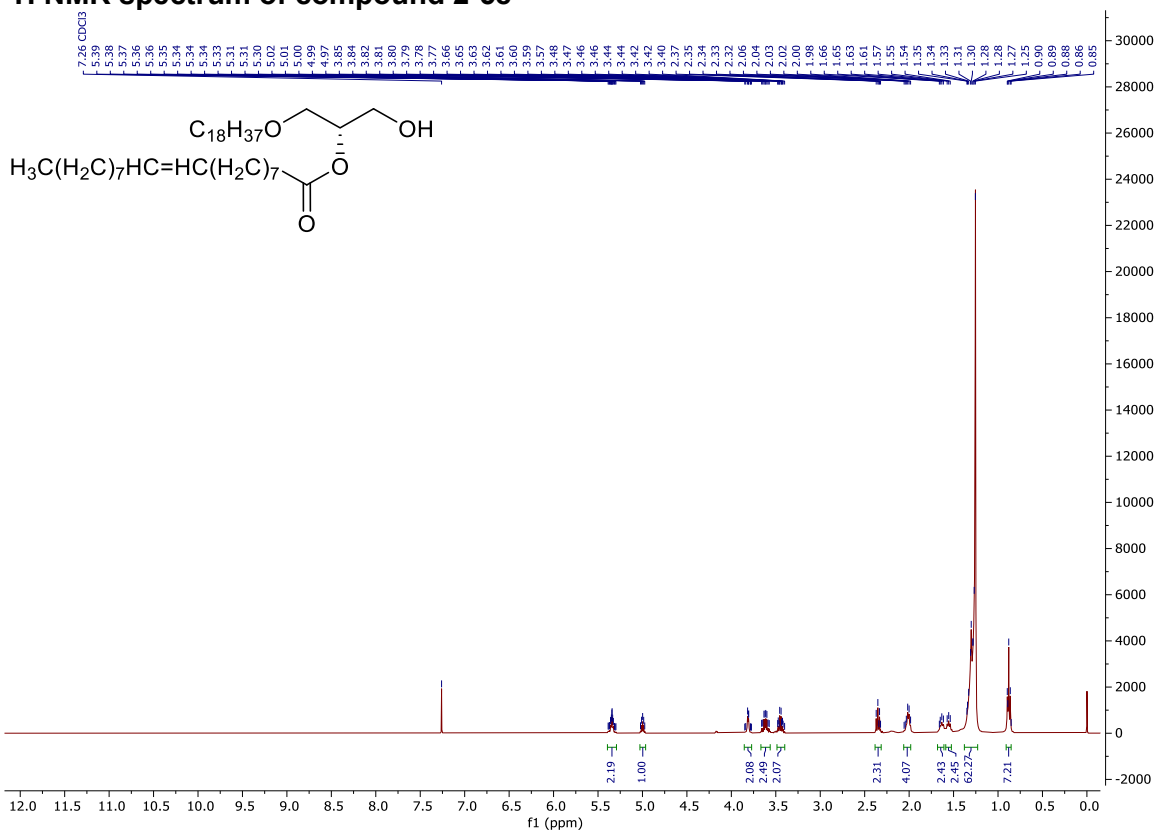

^{13}C NMR spectrum of compound 2-58

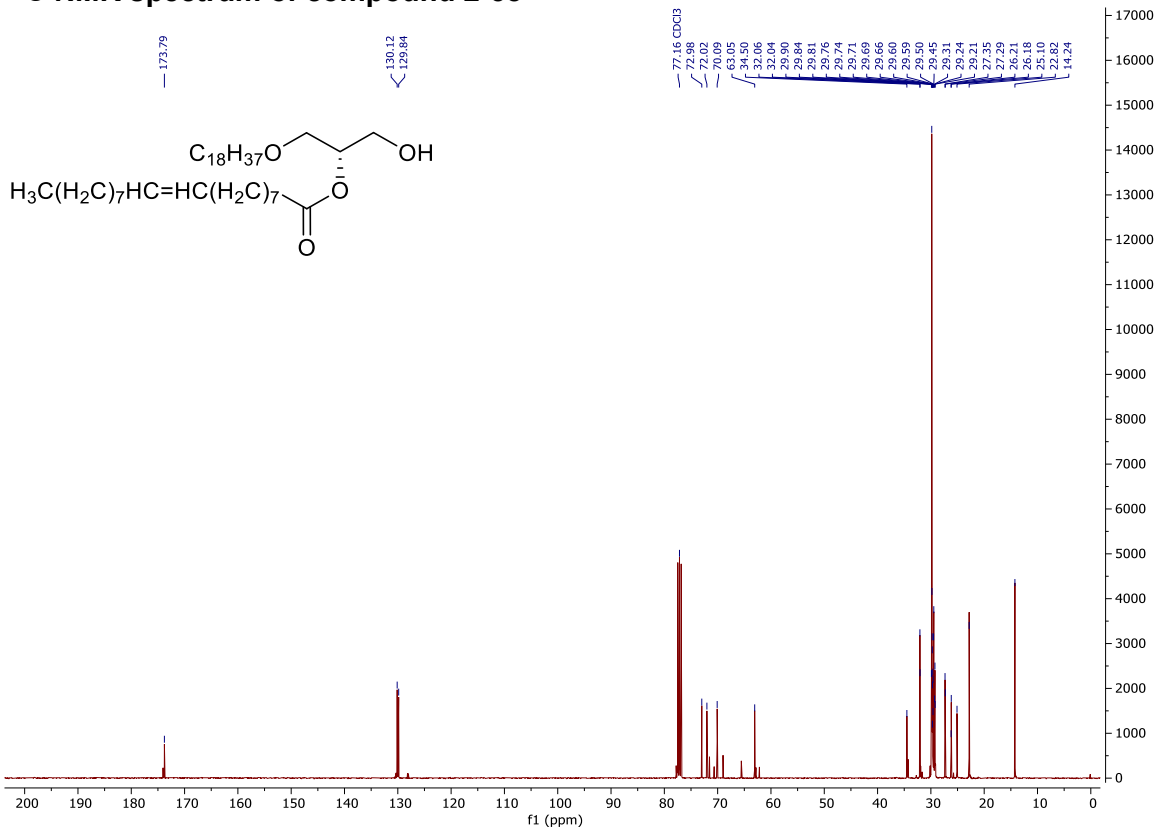

COSY NMR spectrum of compound 2-58

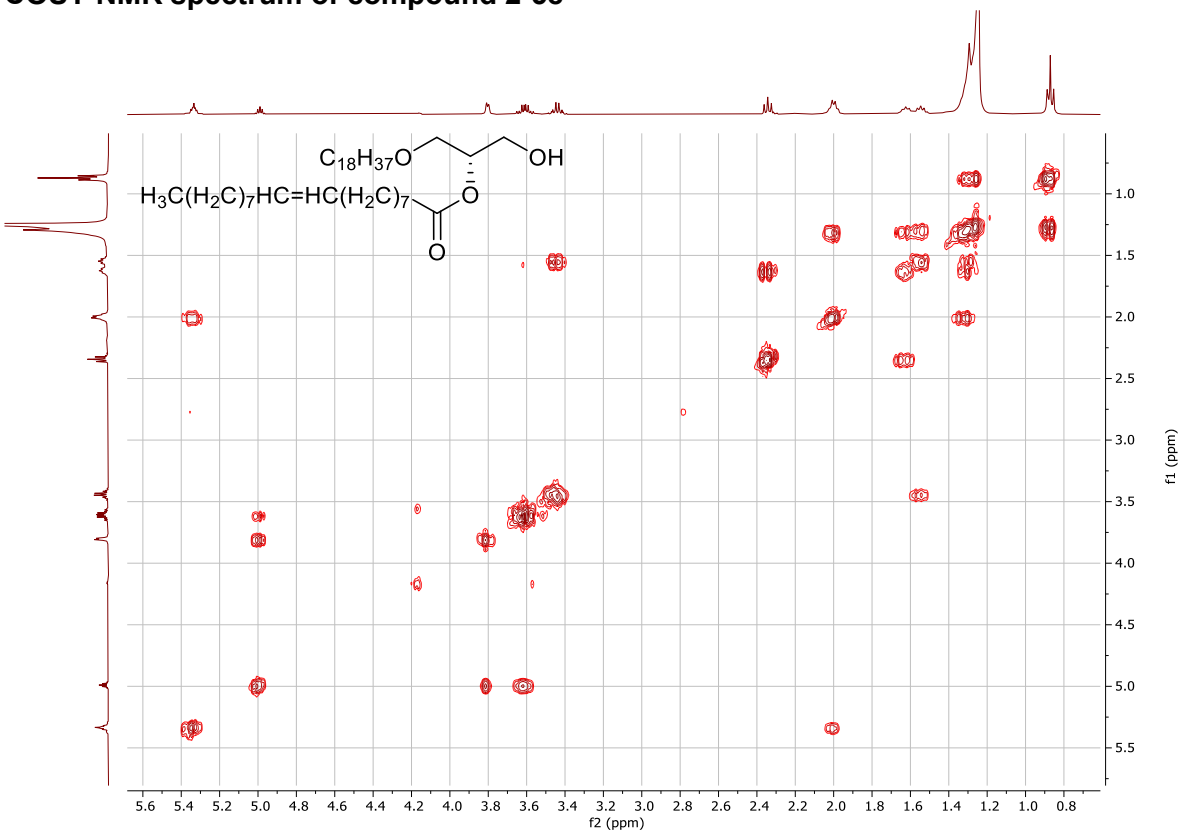

HSQC NMR spectrum of compound 2-58

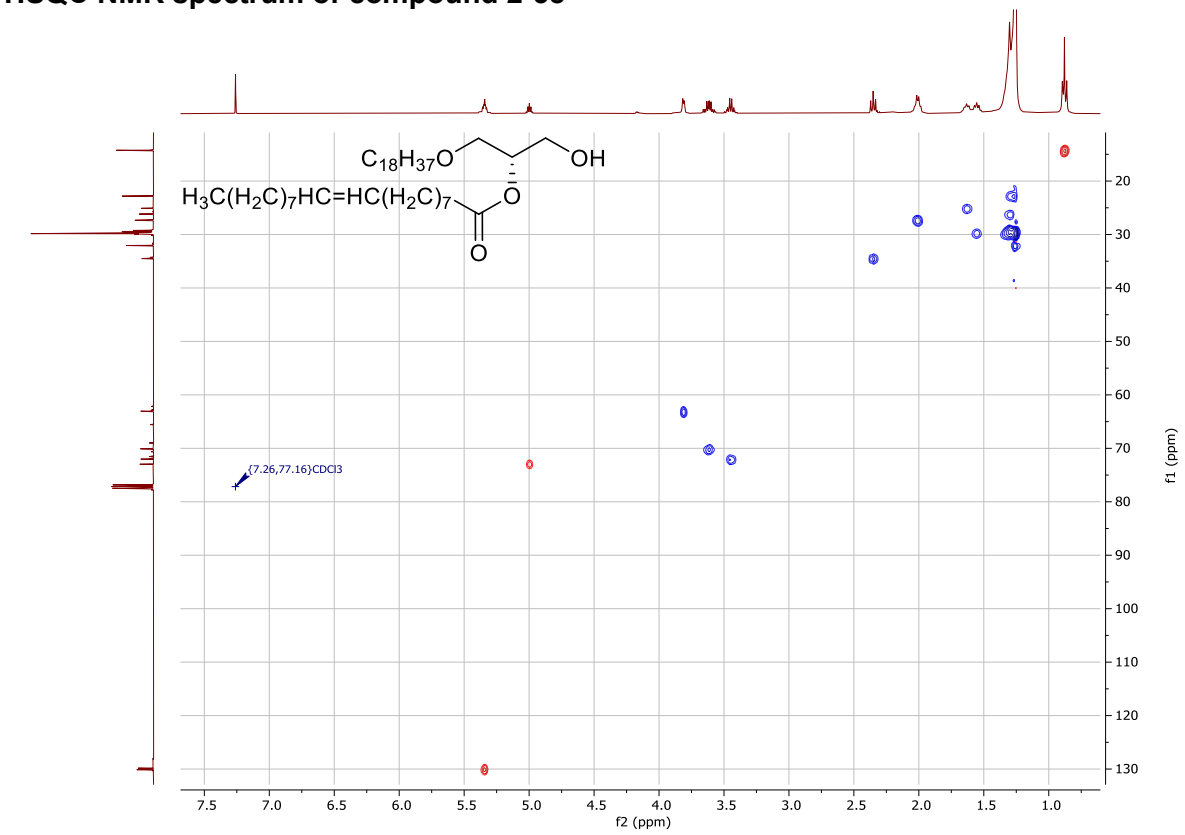

HMBC NMR spectrum of compound 2-58

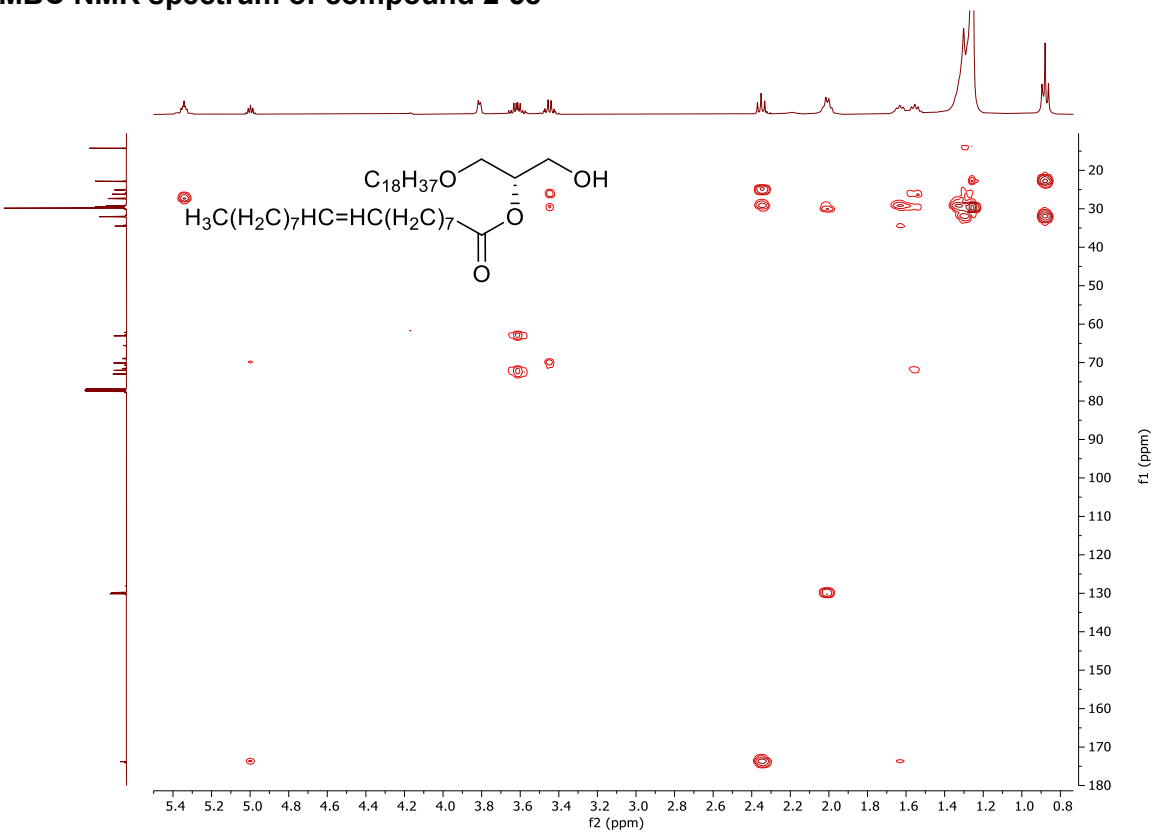

^{1}H NMR spectrum of compound 2-59

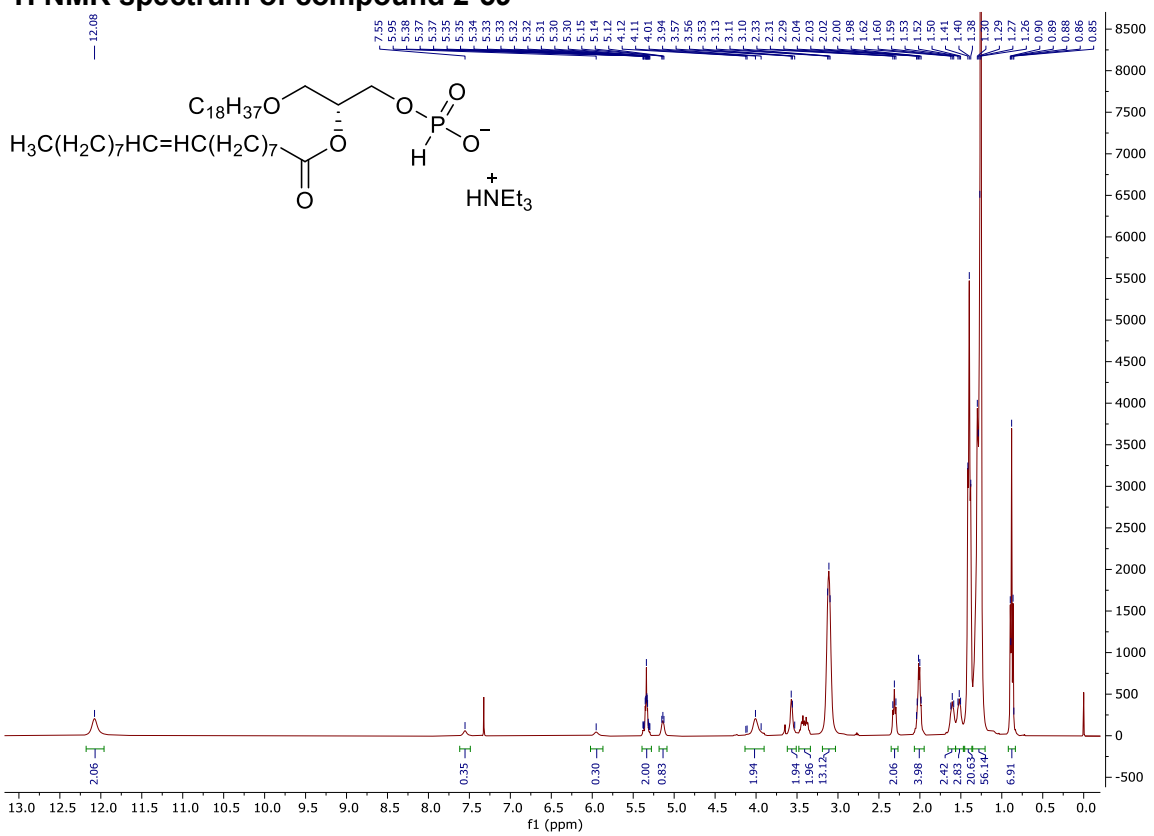

^{13}C NMR spectrum of compound 2-59

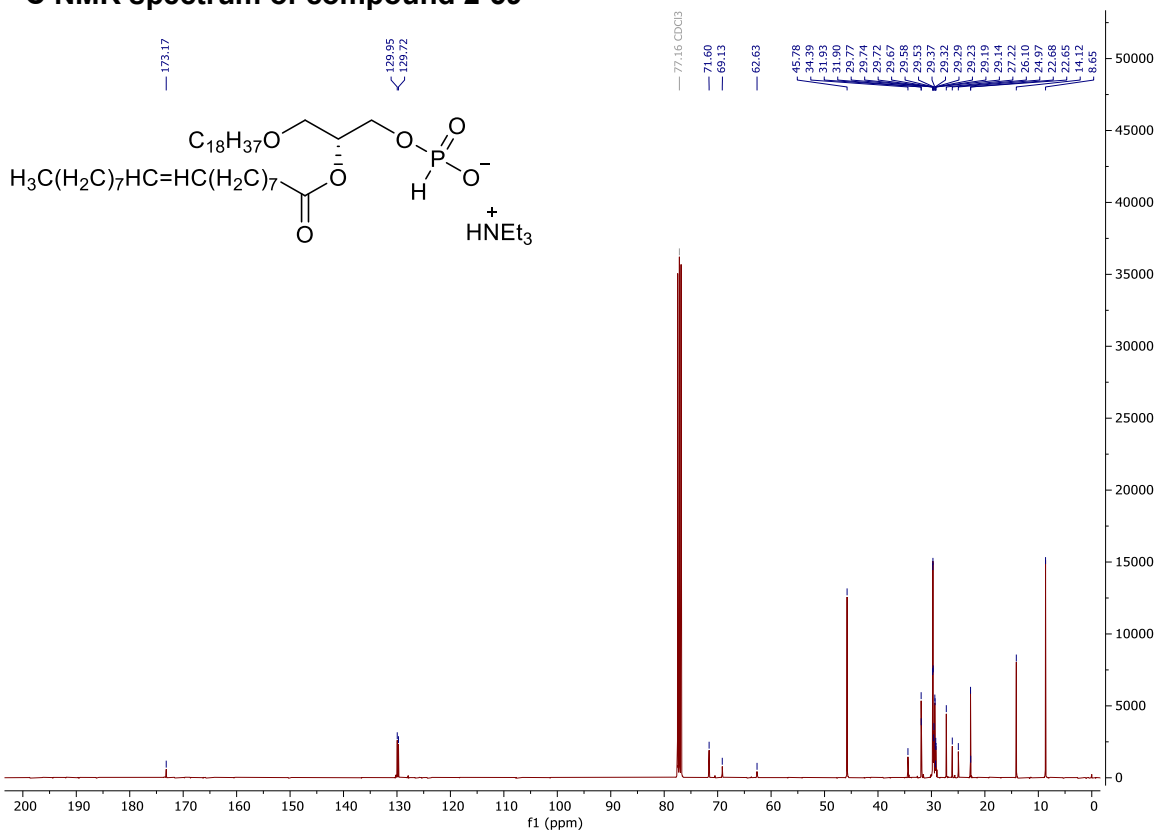

COSY NMR spectrum of compound 2-59

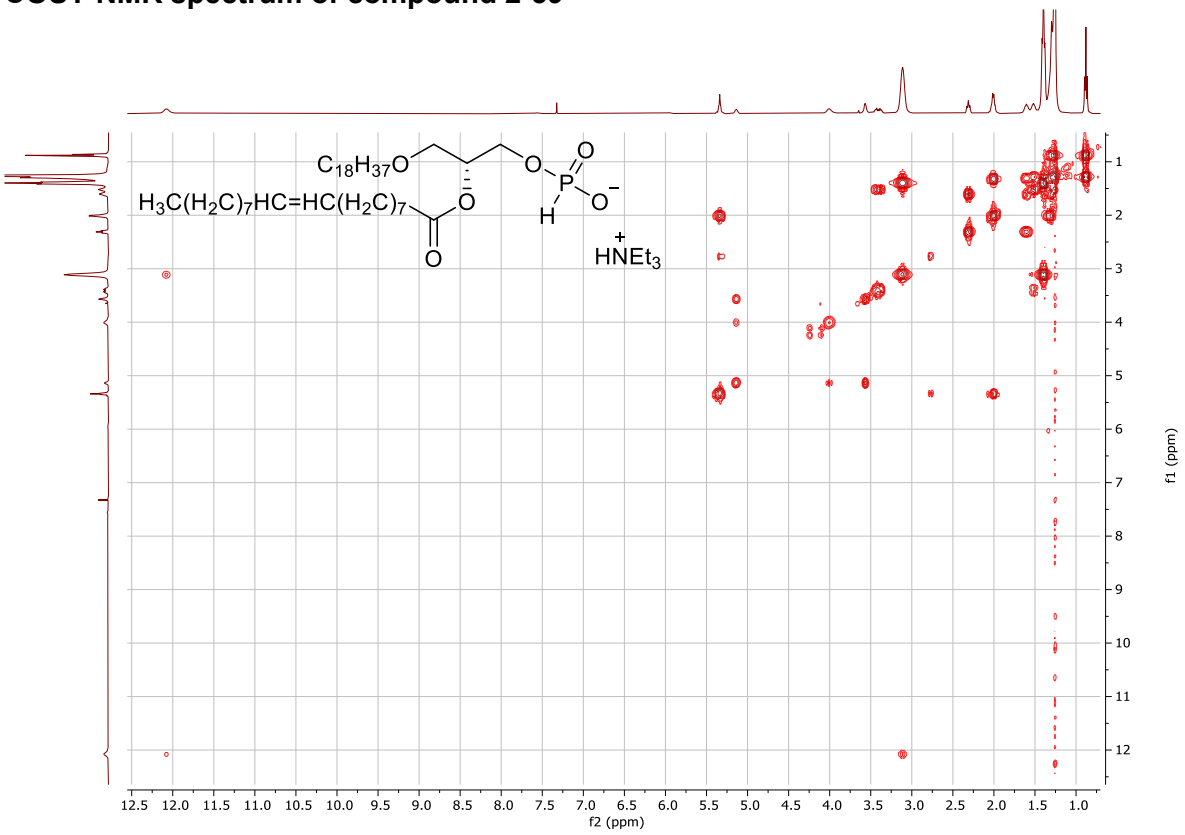

HSQC NMR spectrum of compound 2-59

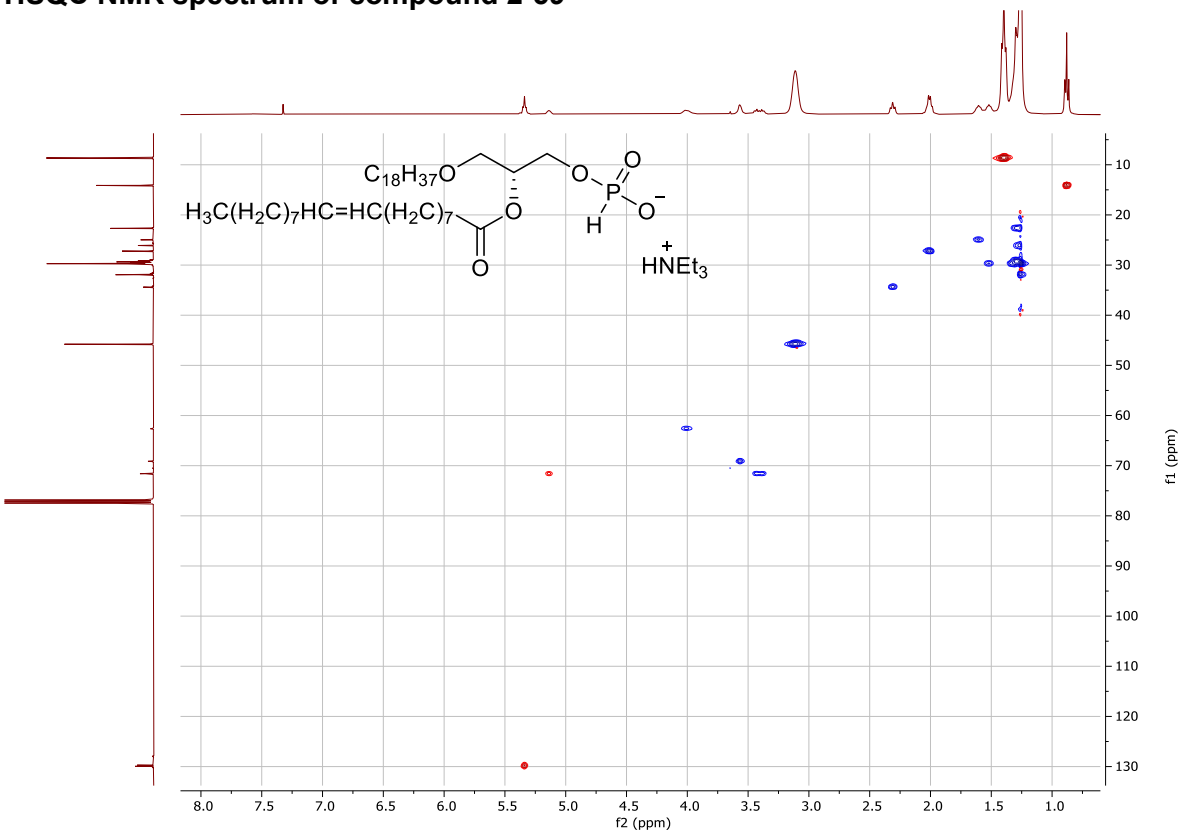

^{31}P NMR spectrum of compound 2-59

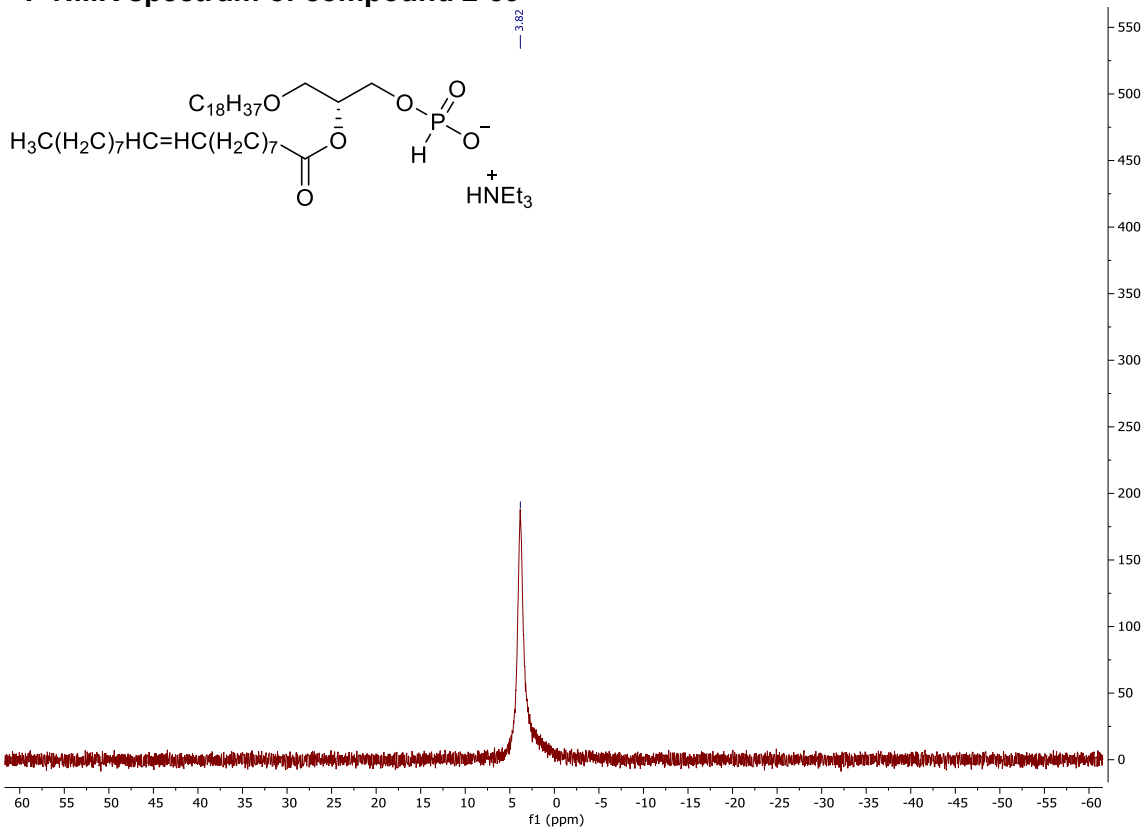

^{1}H NMR spectrum of compound 2-32

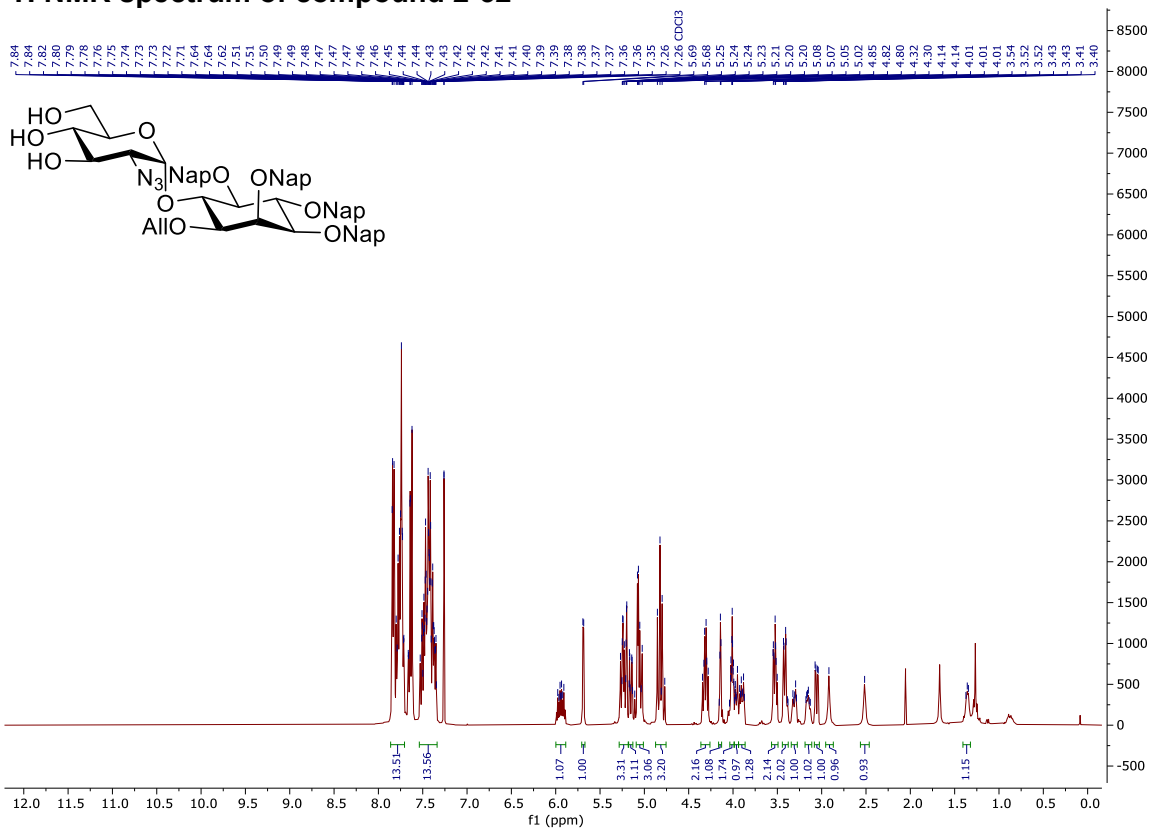

^{13}C NMR spectrum of compound 2-32

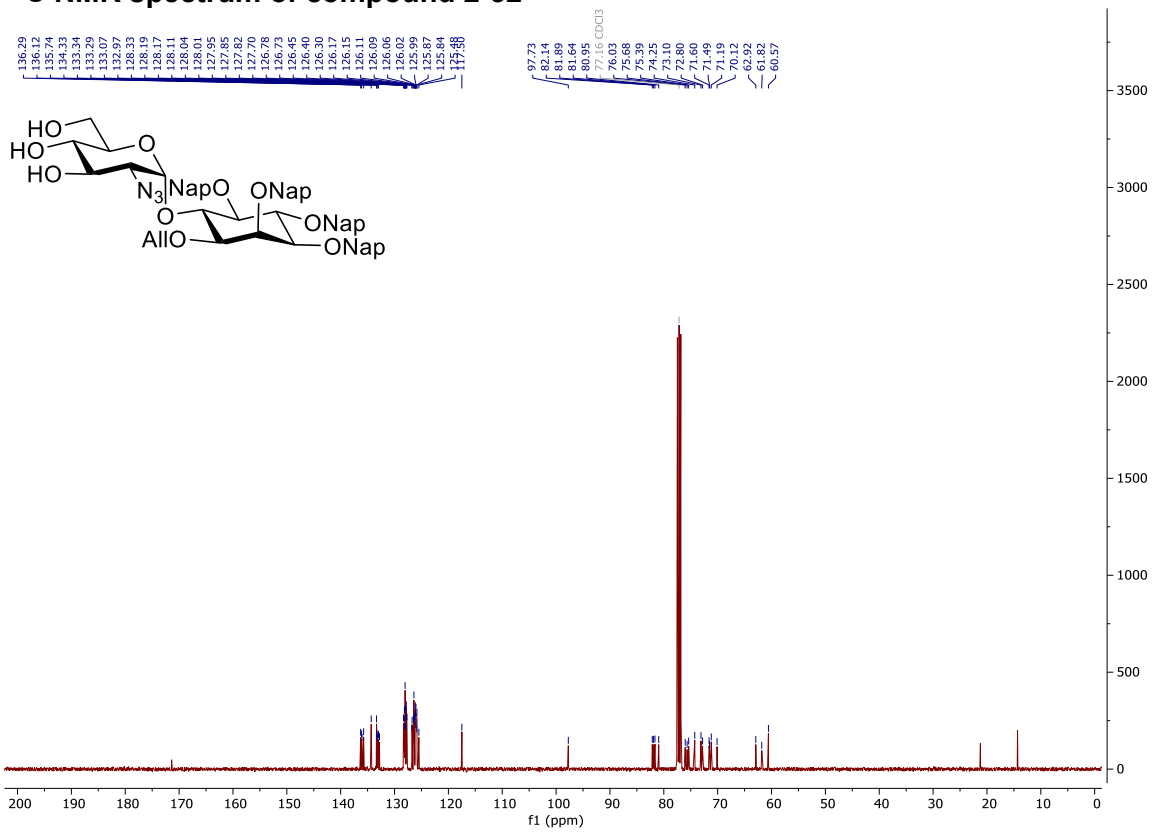

COSY-NMR spectrum of compound 2-32

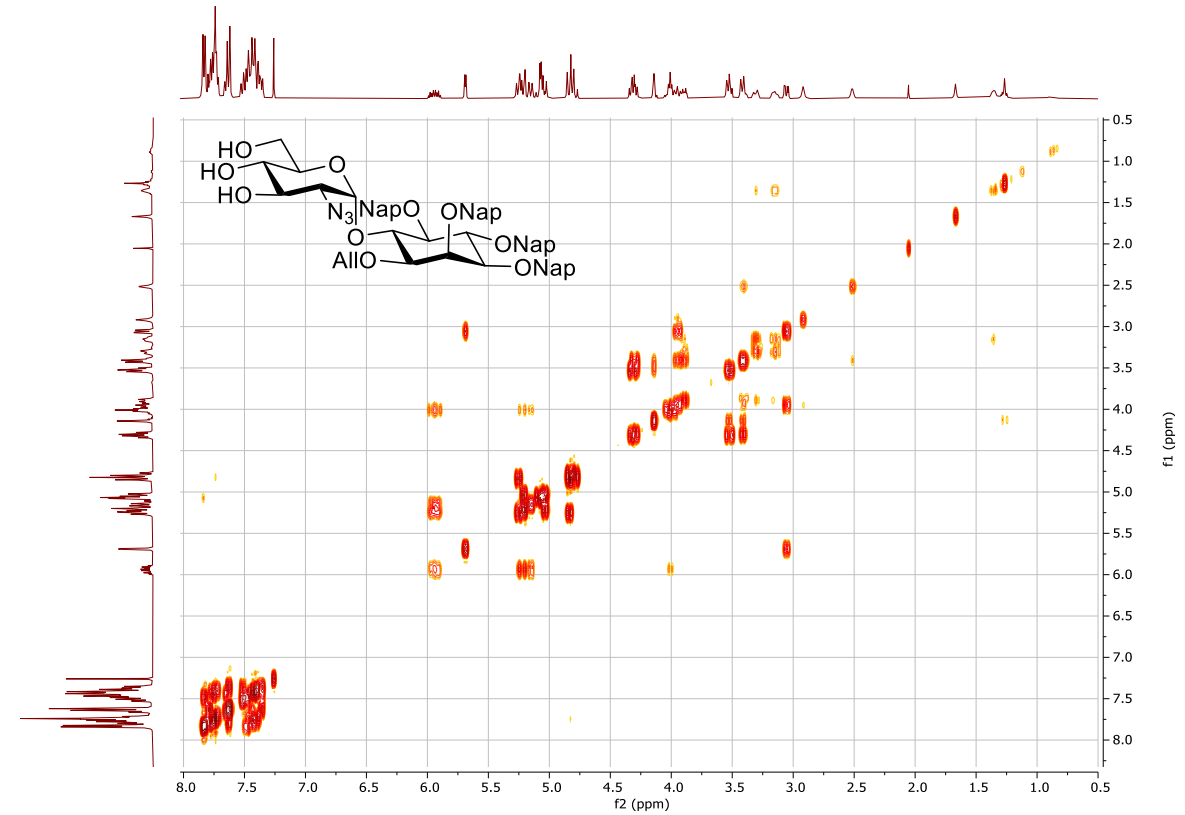

HSQC-NMR spectrum of compound 2-32

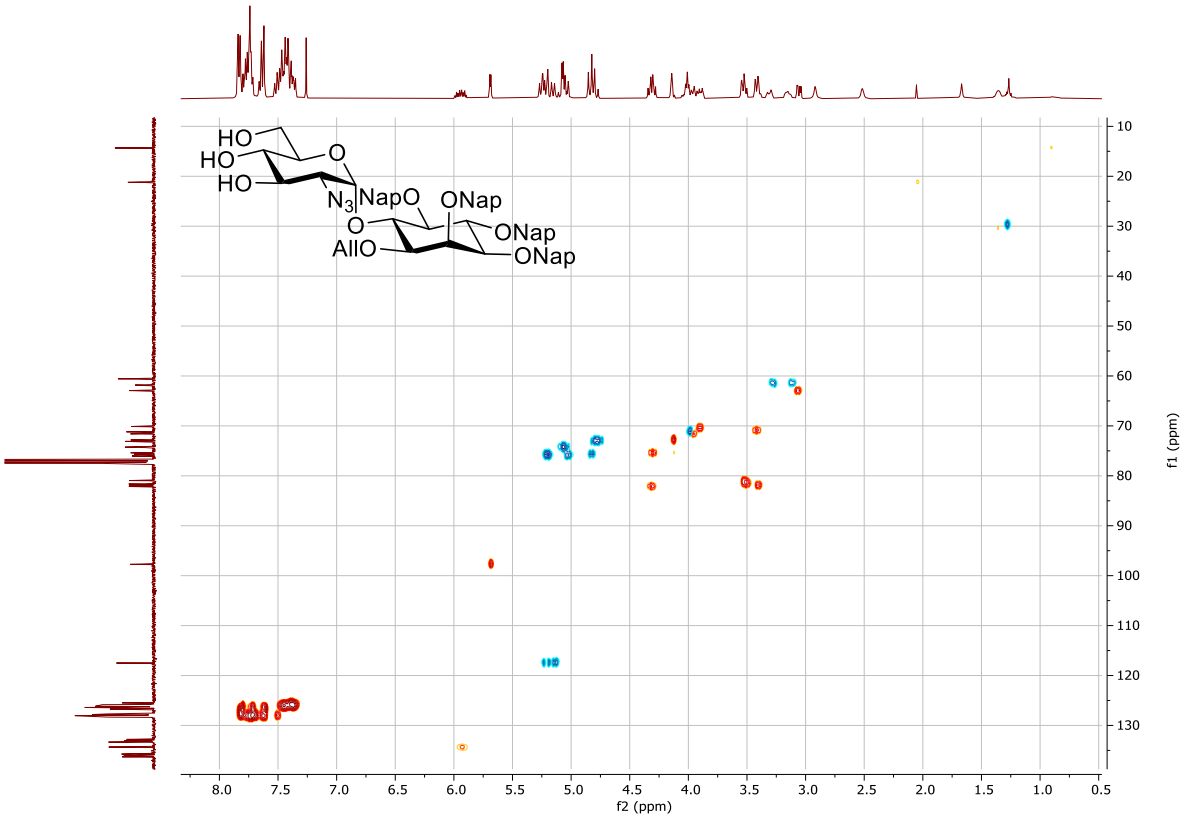

^{1}H NMR spectrum of compound 2-5

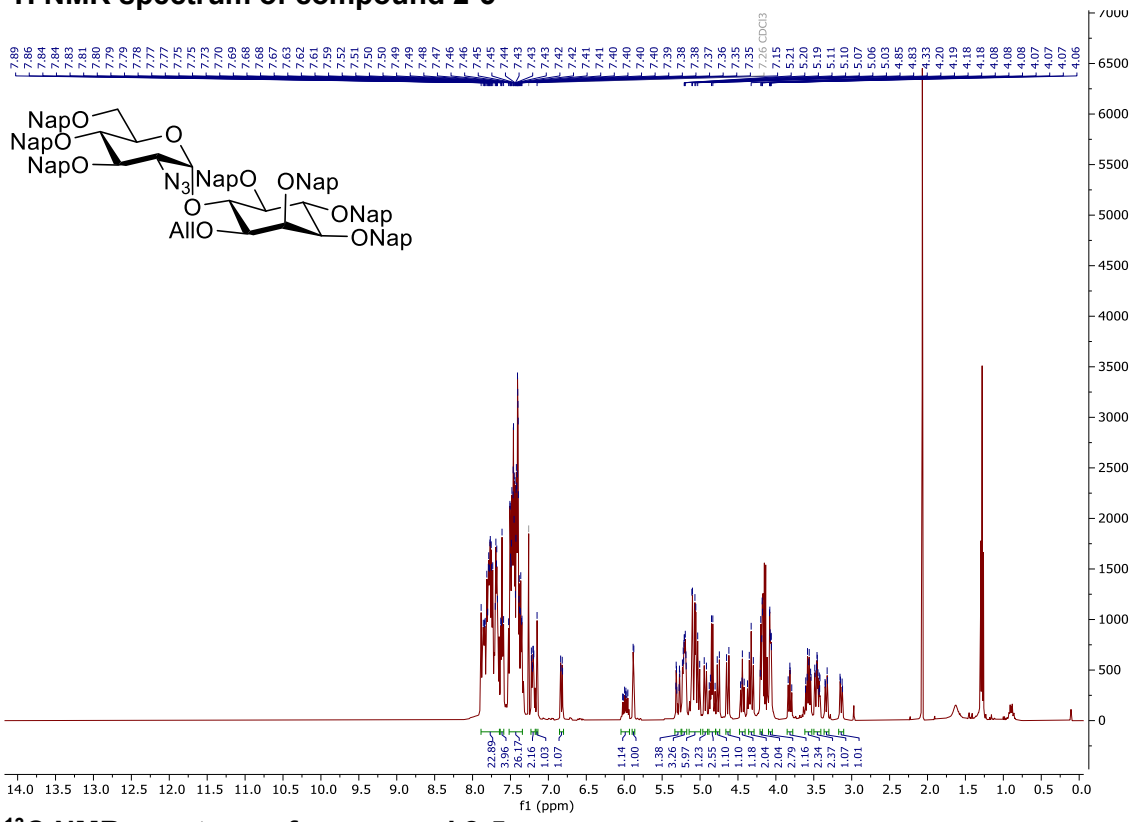

^{13}C NMR spectrum of compound 2-5

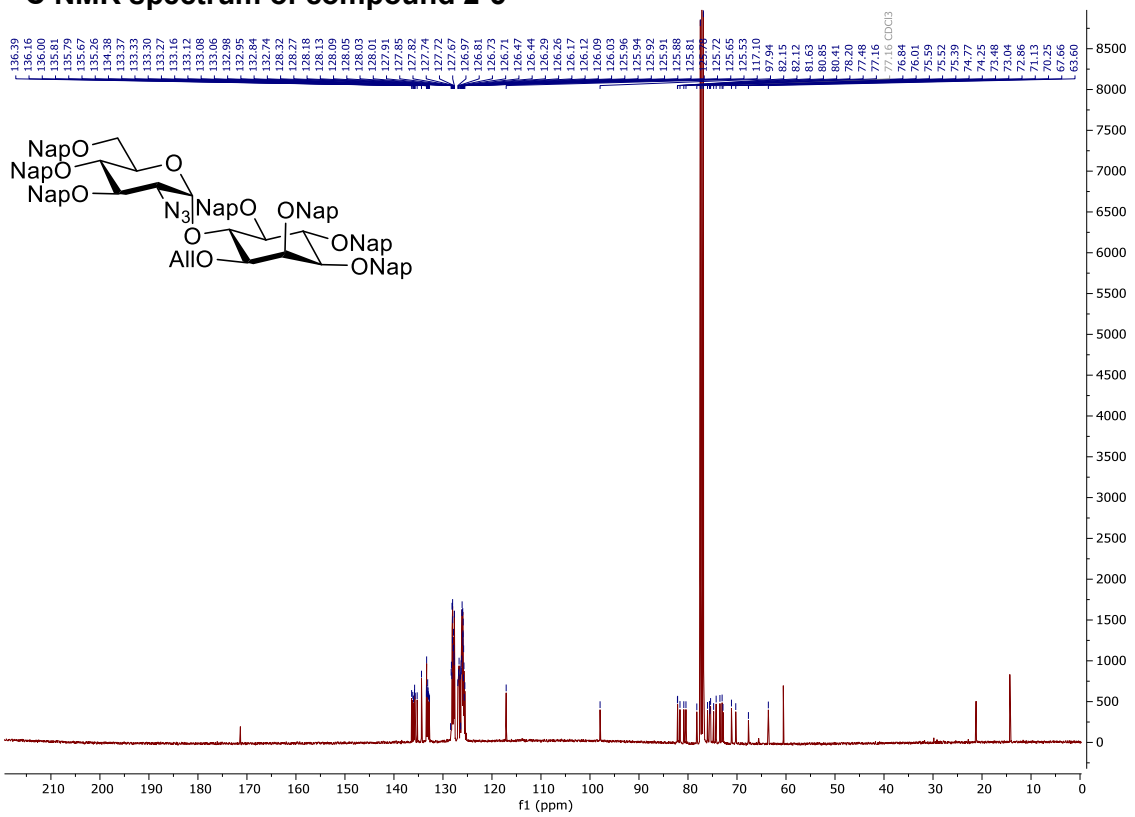

^{1}H NMR spectrum of compound 2-33

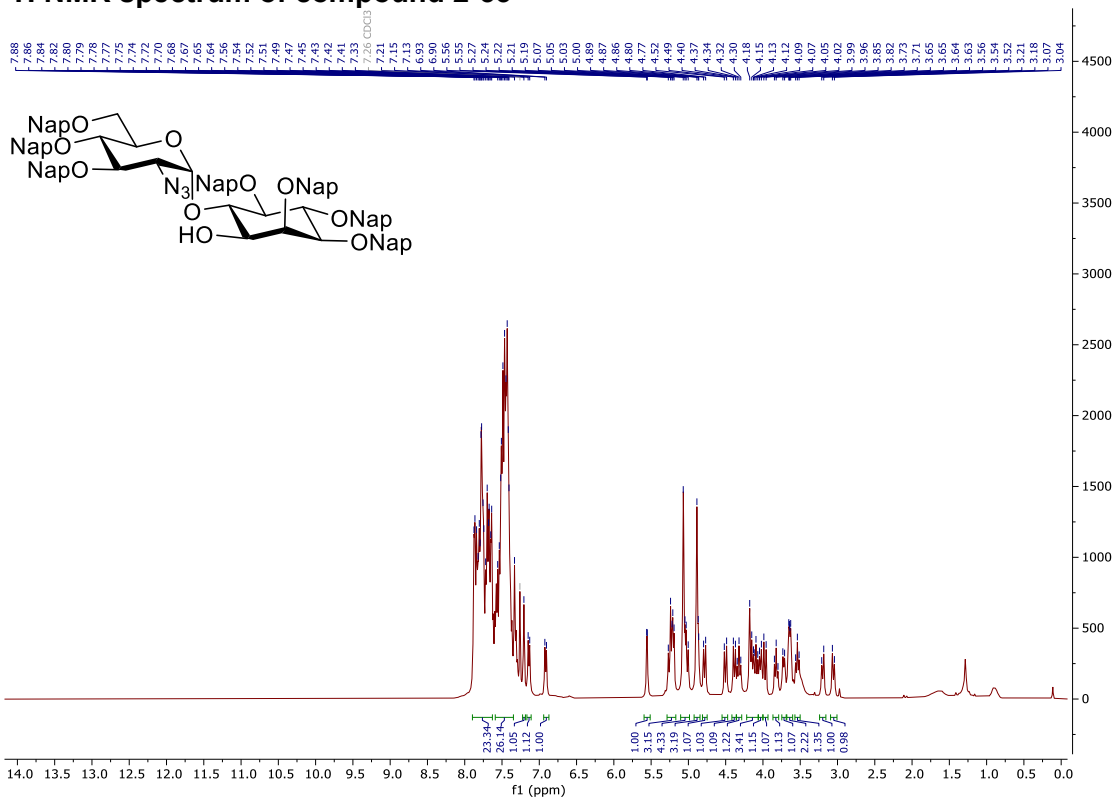

^{13}C NMR spectrum of compound 2-33

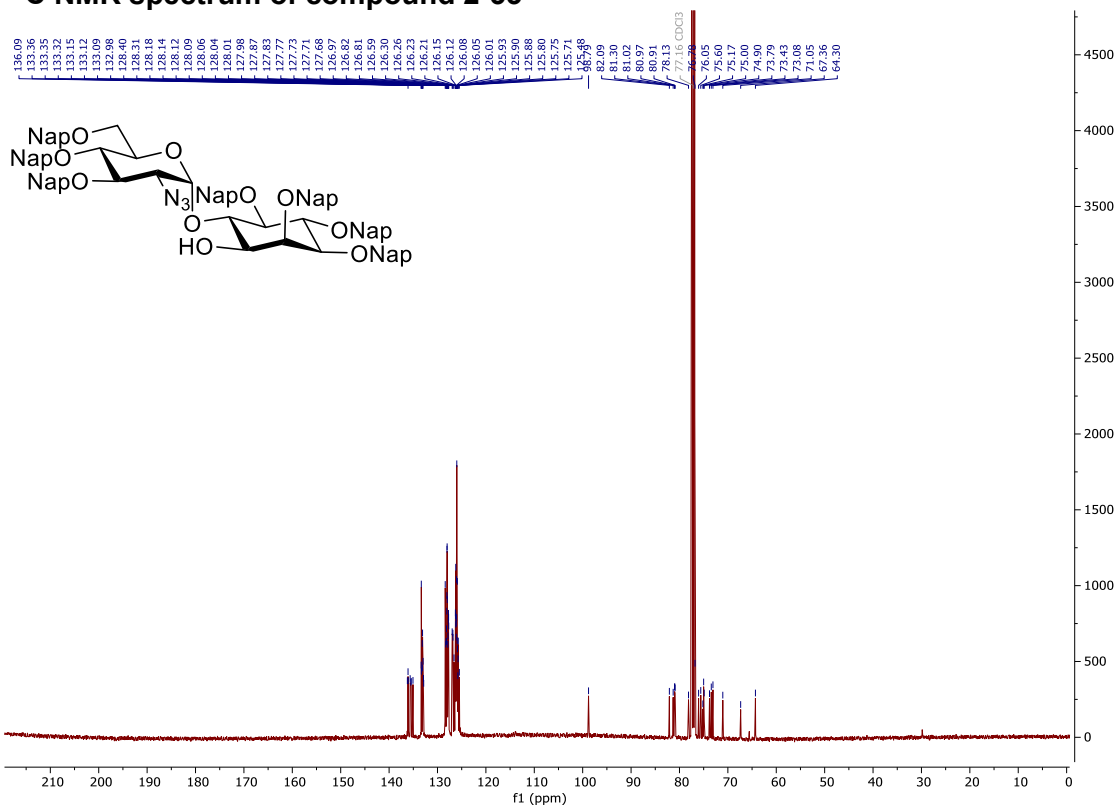

^{1}H NMR spectrum of compound 2-34

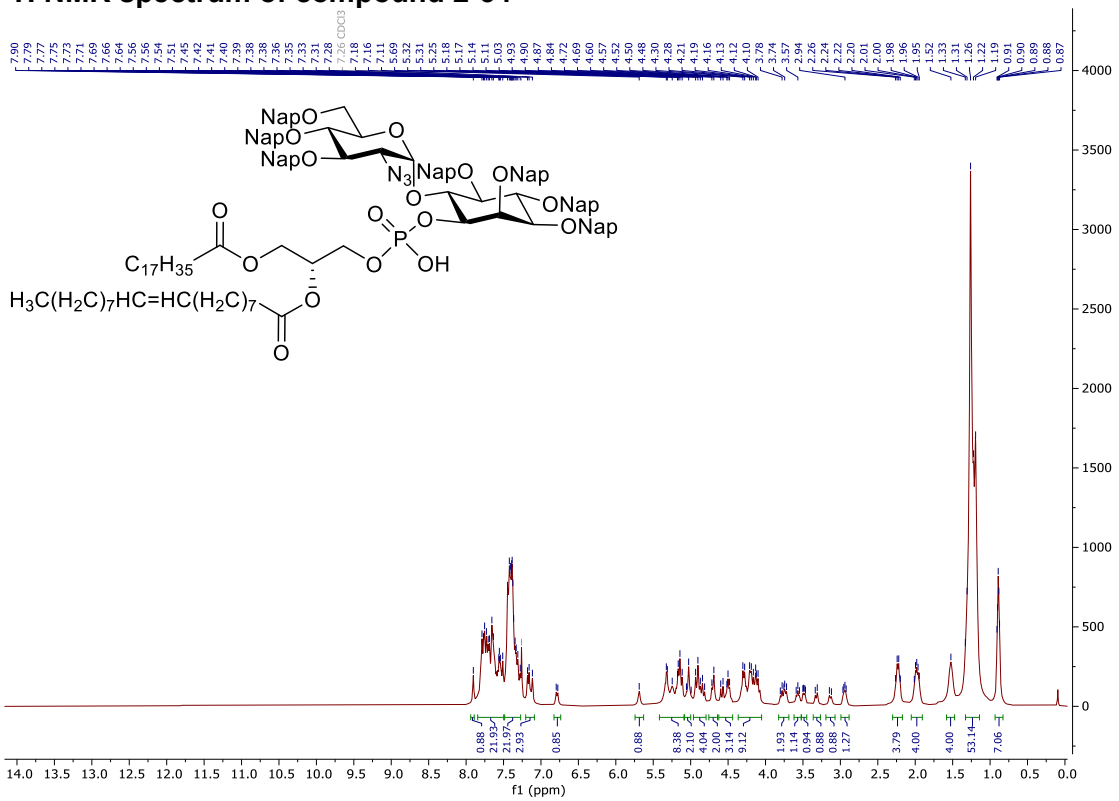

^{13}C NMR spectrum of compound 2-34

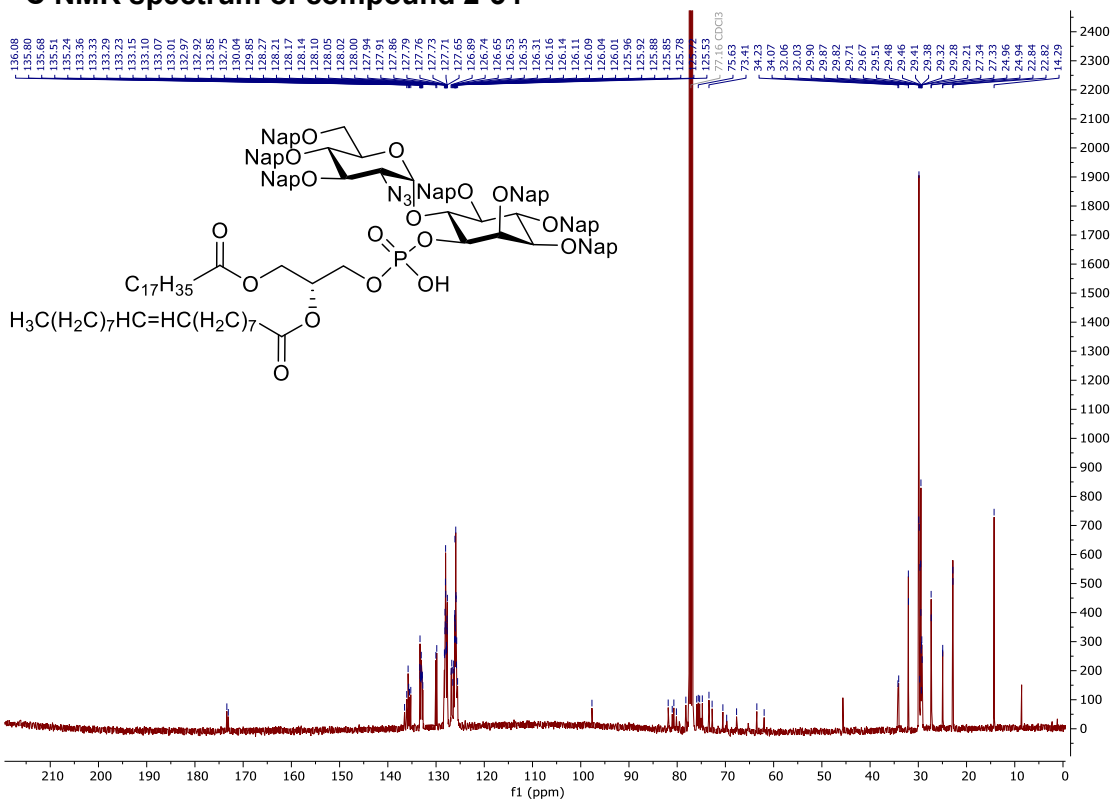

COSY-NMR spectrum of compound 2-34

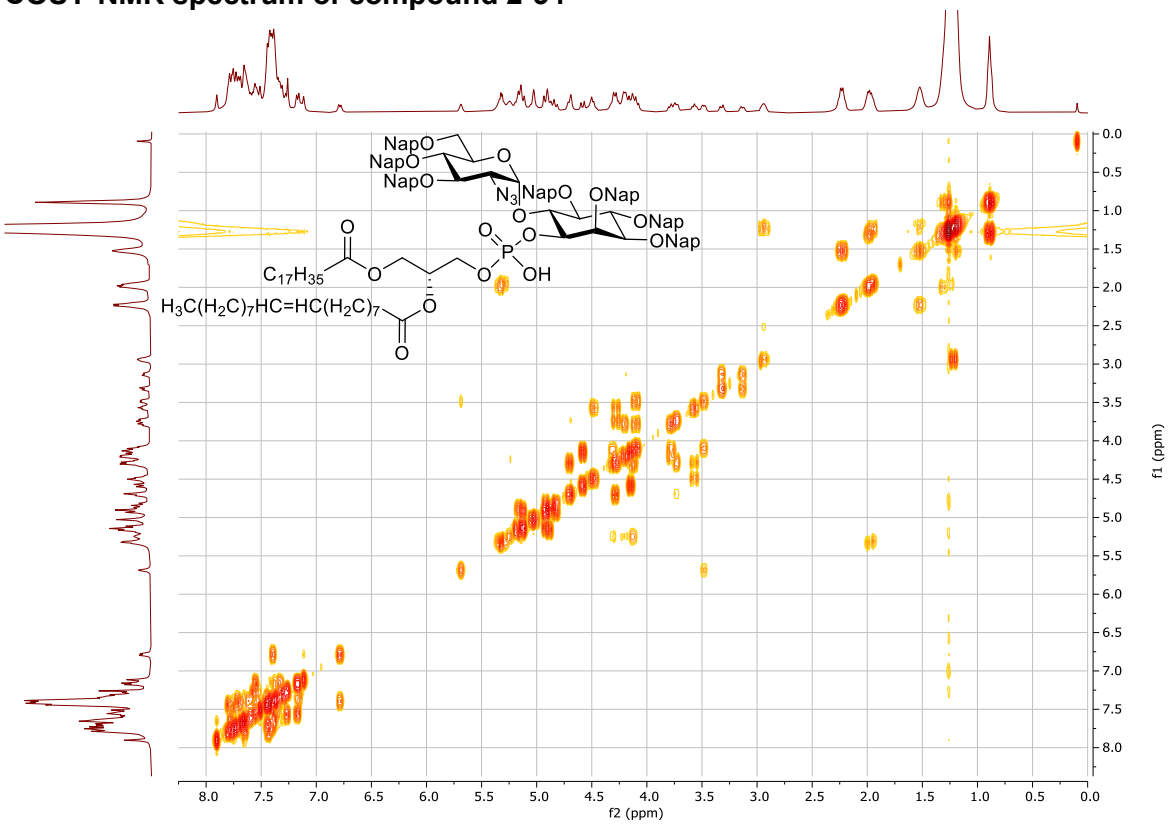

HSQC-NMR spectrum of compound 2-34

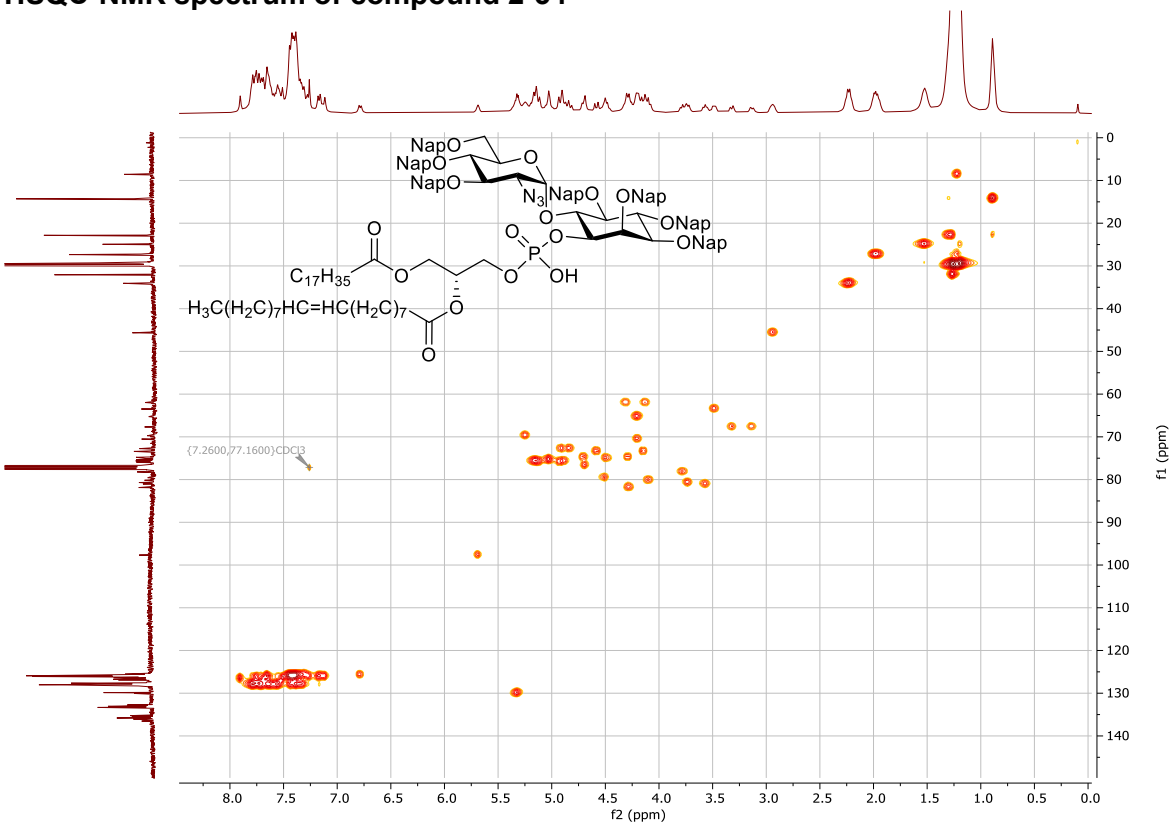

^{31}P NMR spectrum of compound 2-34

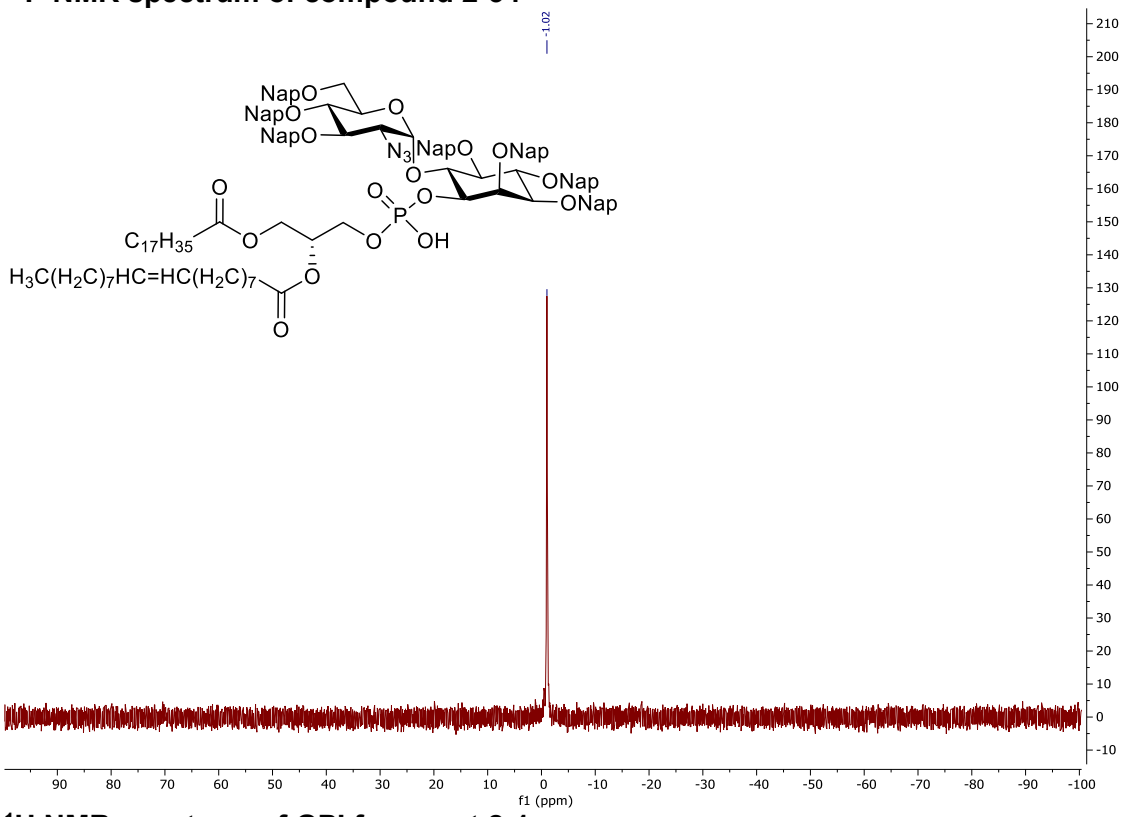

^{1}H NMR spectrum of GPI fragment 2-1

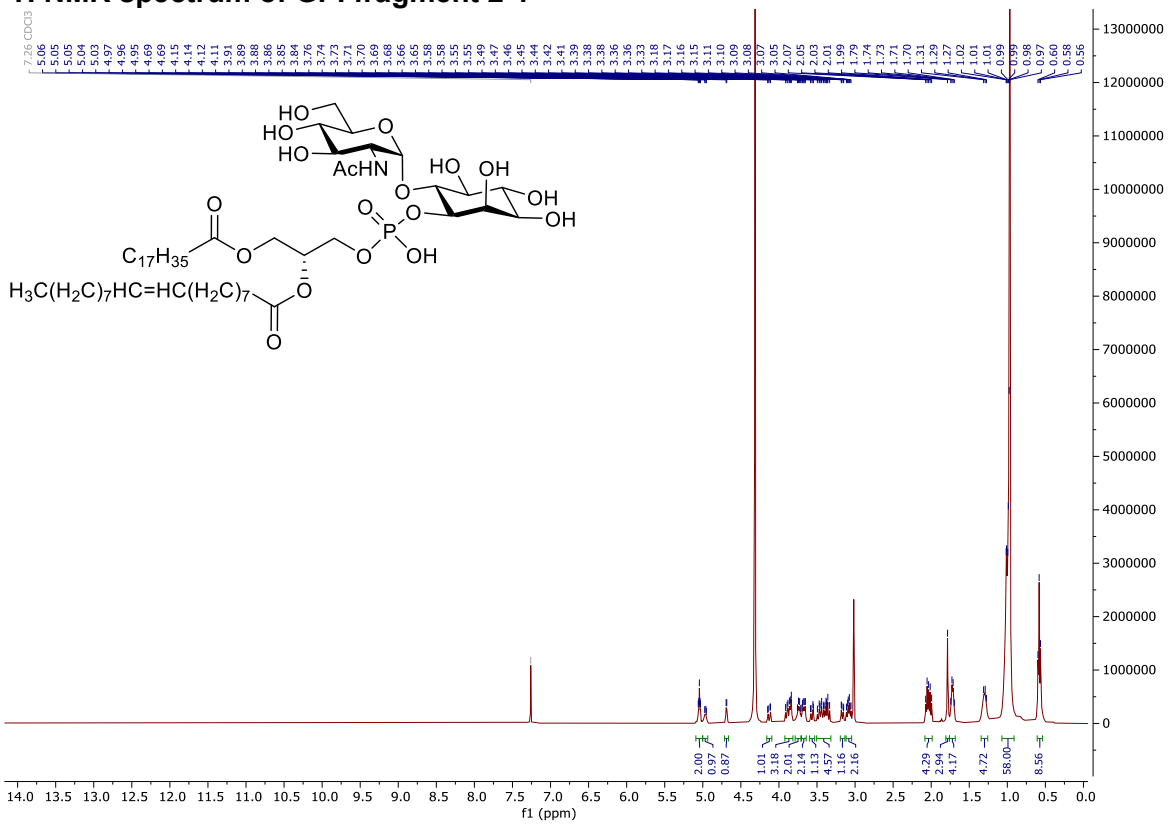

^{13}C NMR spectrum of GPI fragment 2-1

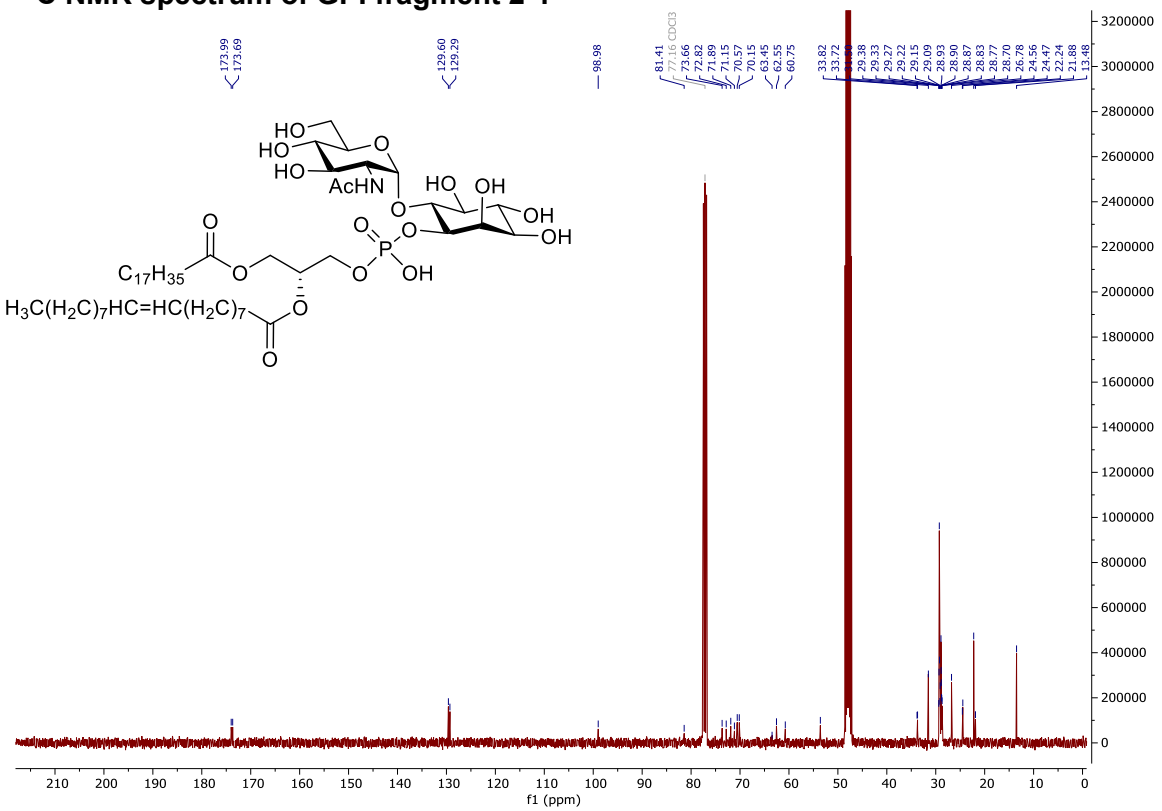

COSY-NMR spectrum of GPI fragment 2-1

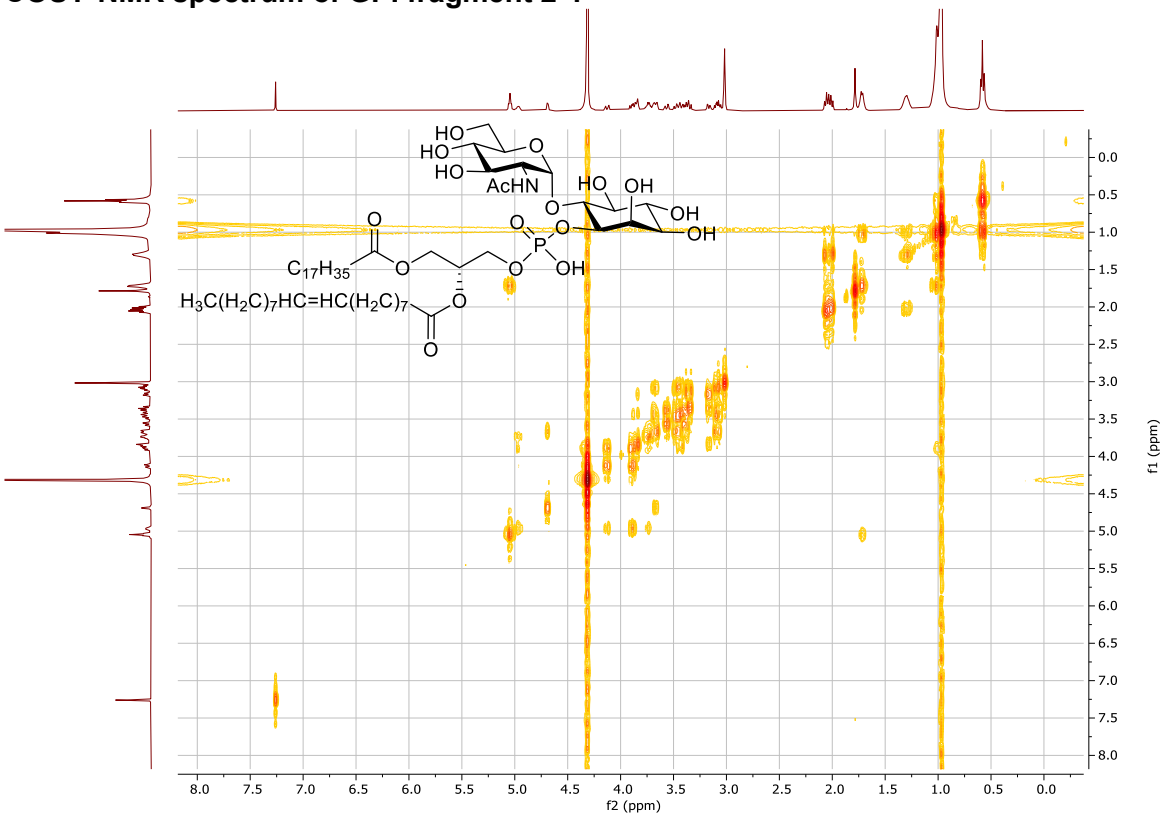

HSQC-NMR spectrum of GPI fragment 2-1

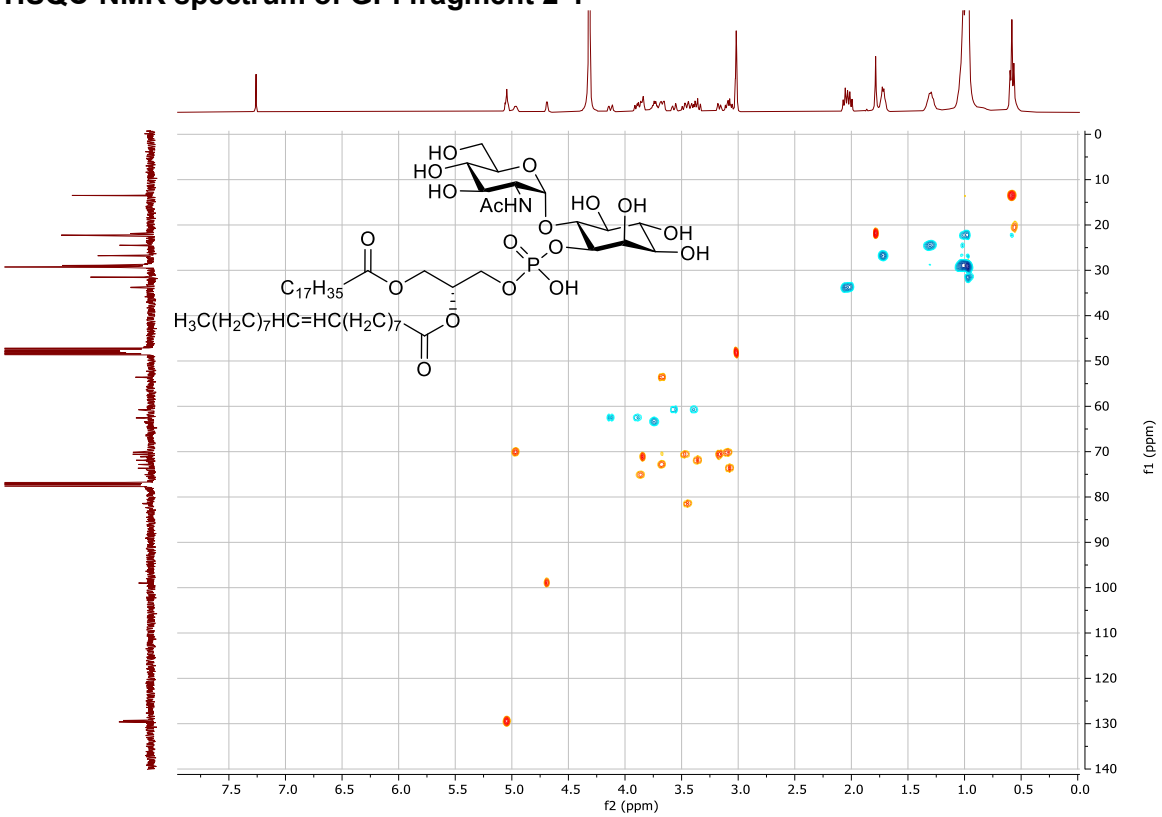

^{31}P-NMR spectrum of GPI fragment 2-1

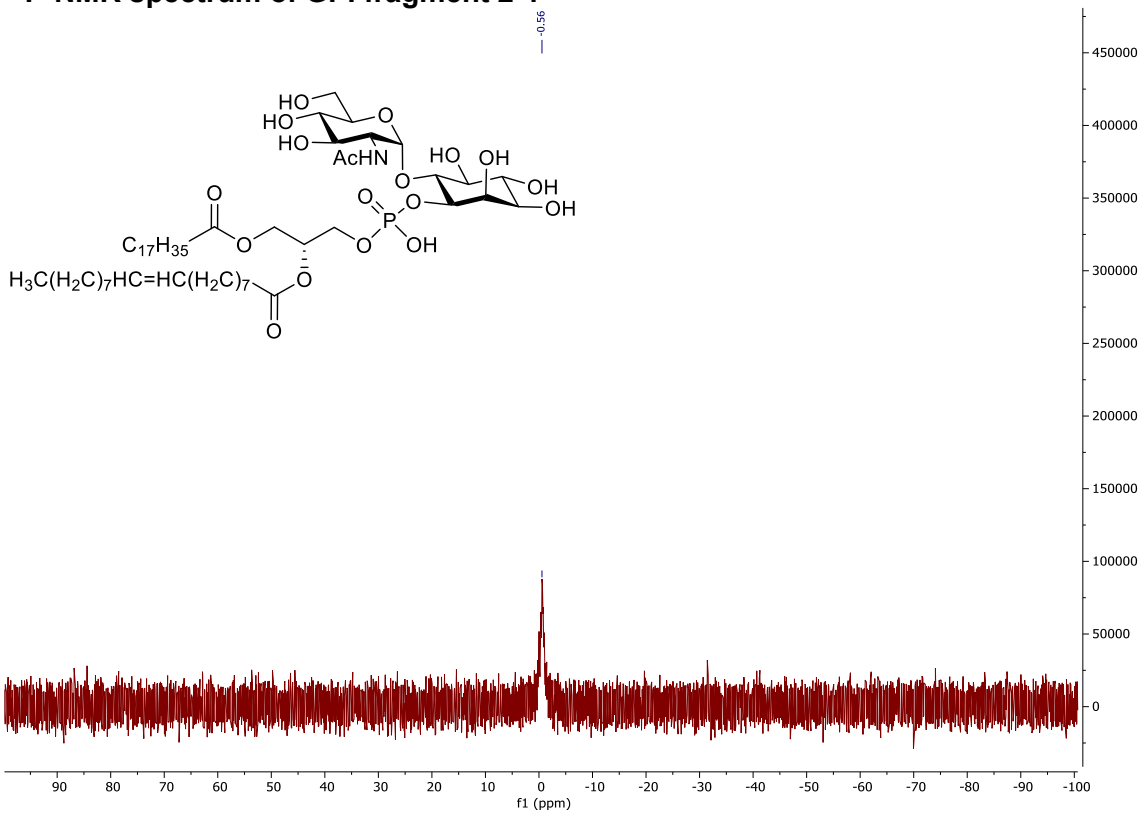

^{1}H NMR spectrum of GPI fragment 2-2

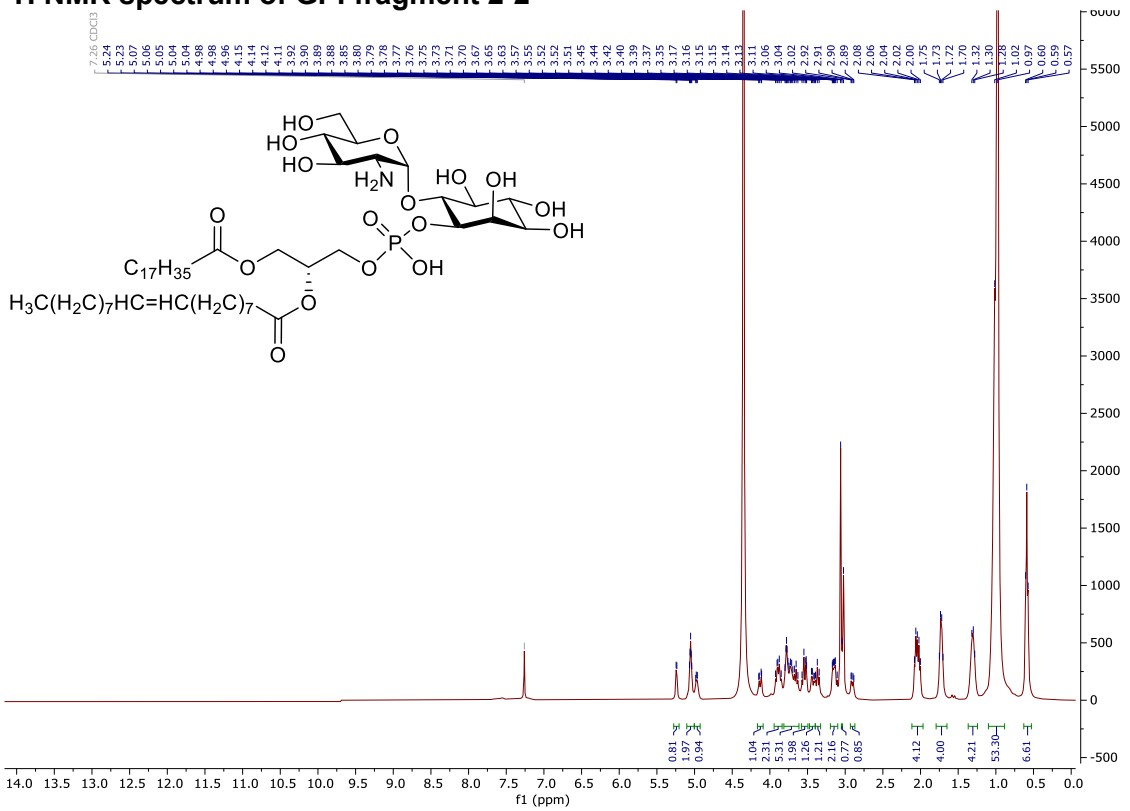

^{13}C-NMR spectrum of GPI fragment 2-2

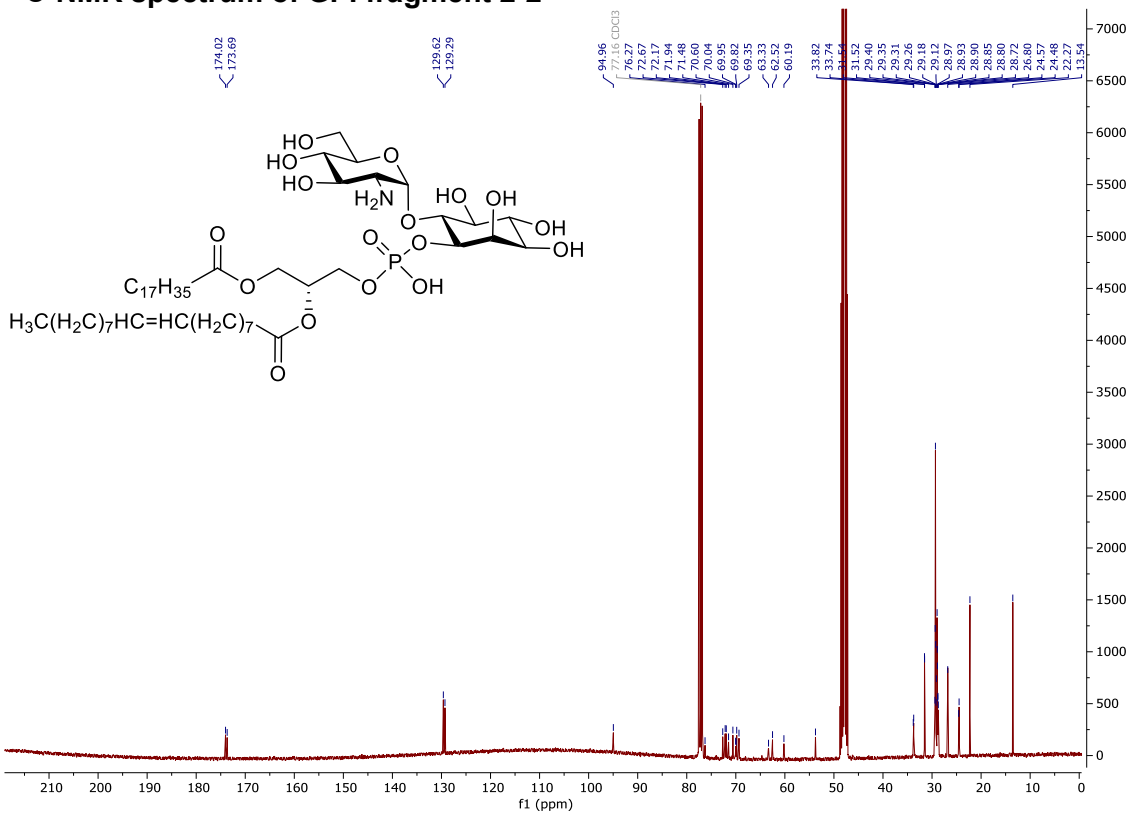

COSY-NMR spectrum of GPI fragment 2-2

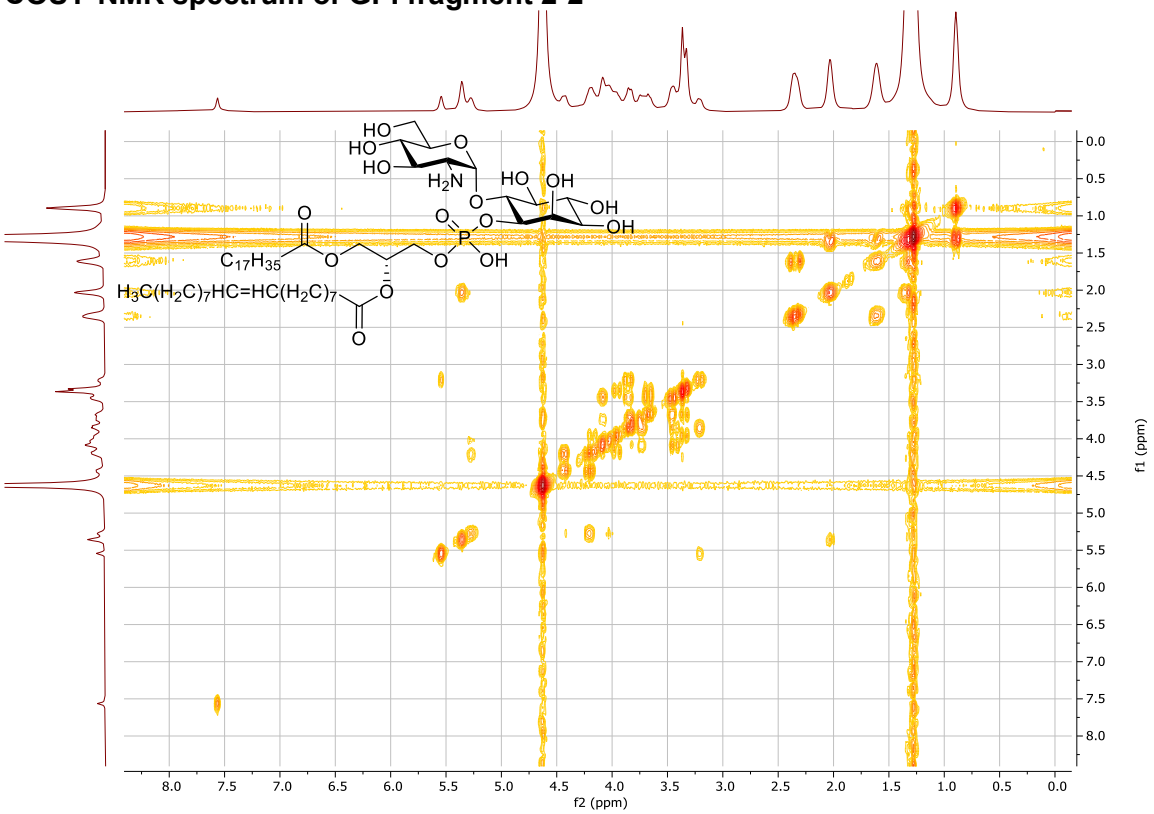

HSQC-NMR spectrum of GPI fragment 2-2

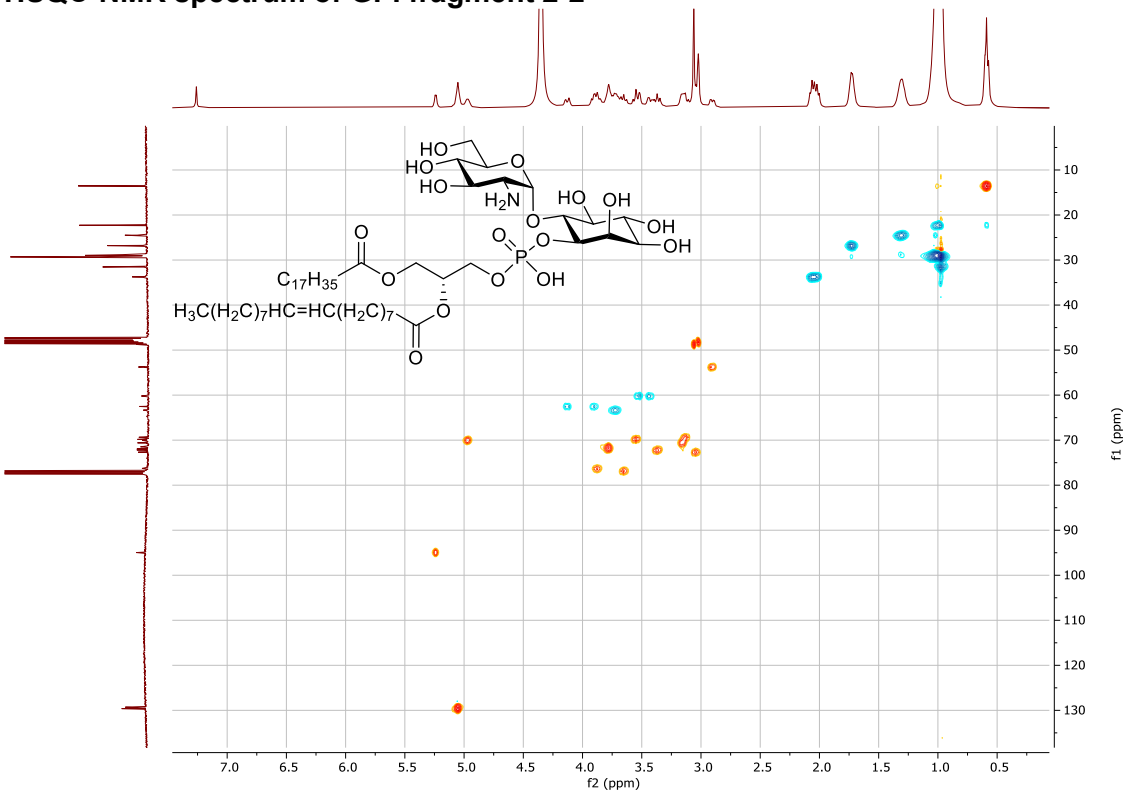

^{31}P-NMR spectrum of GPI fragment 2-2

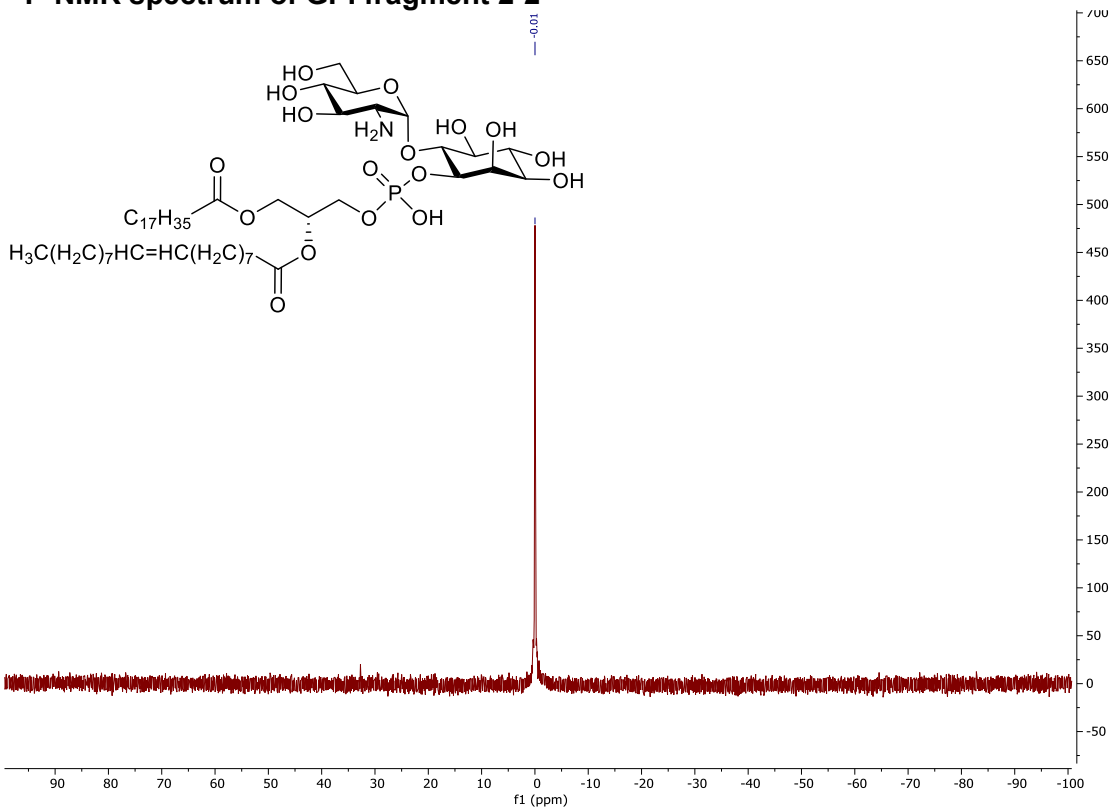

^{1}H NMR spectrum of compound 2-40

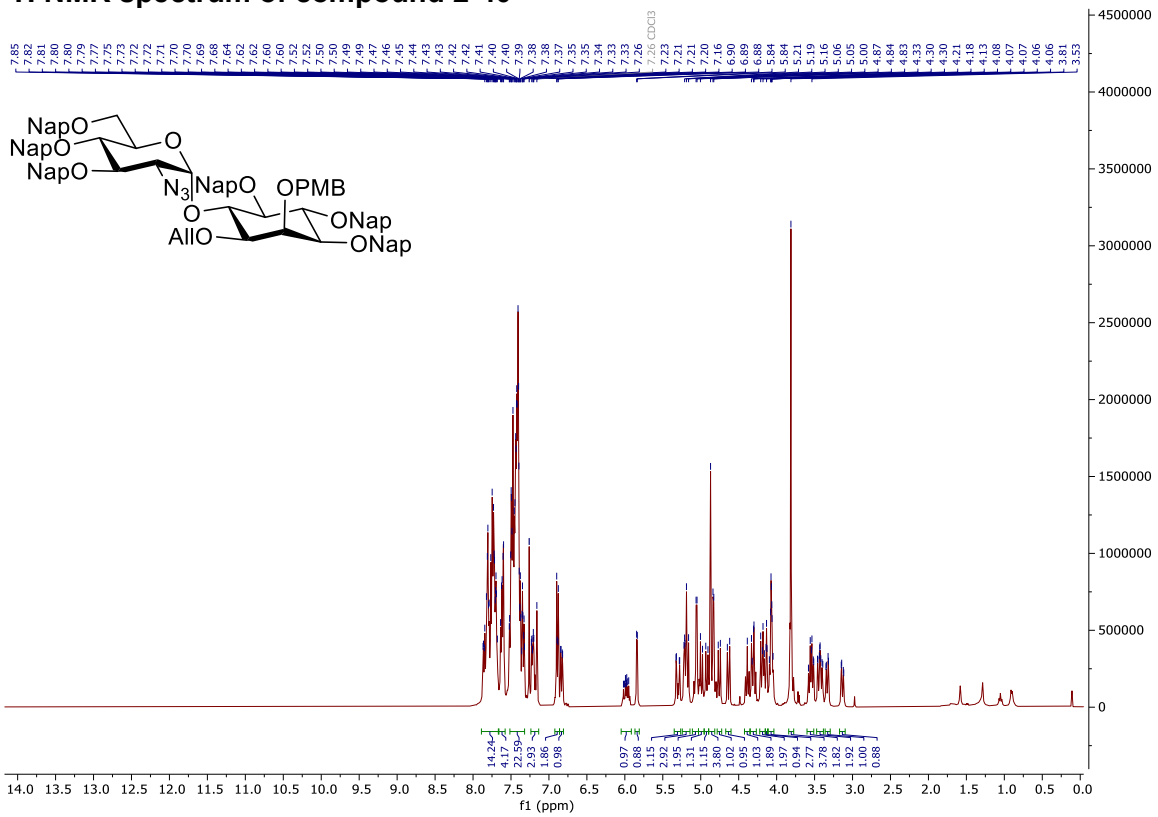

^{13}C NMR spectrum of compound 2-40

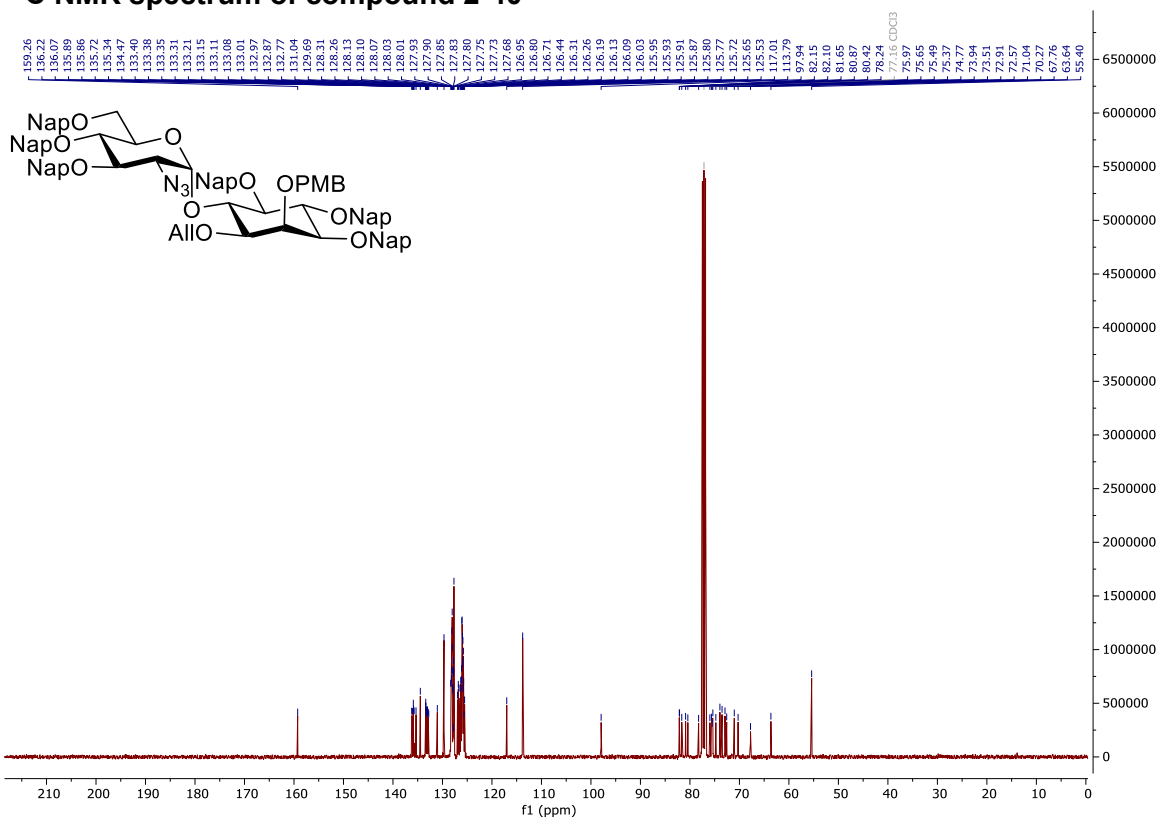

COSY-NMR spectrum of compound 2-40

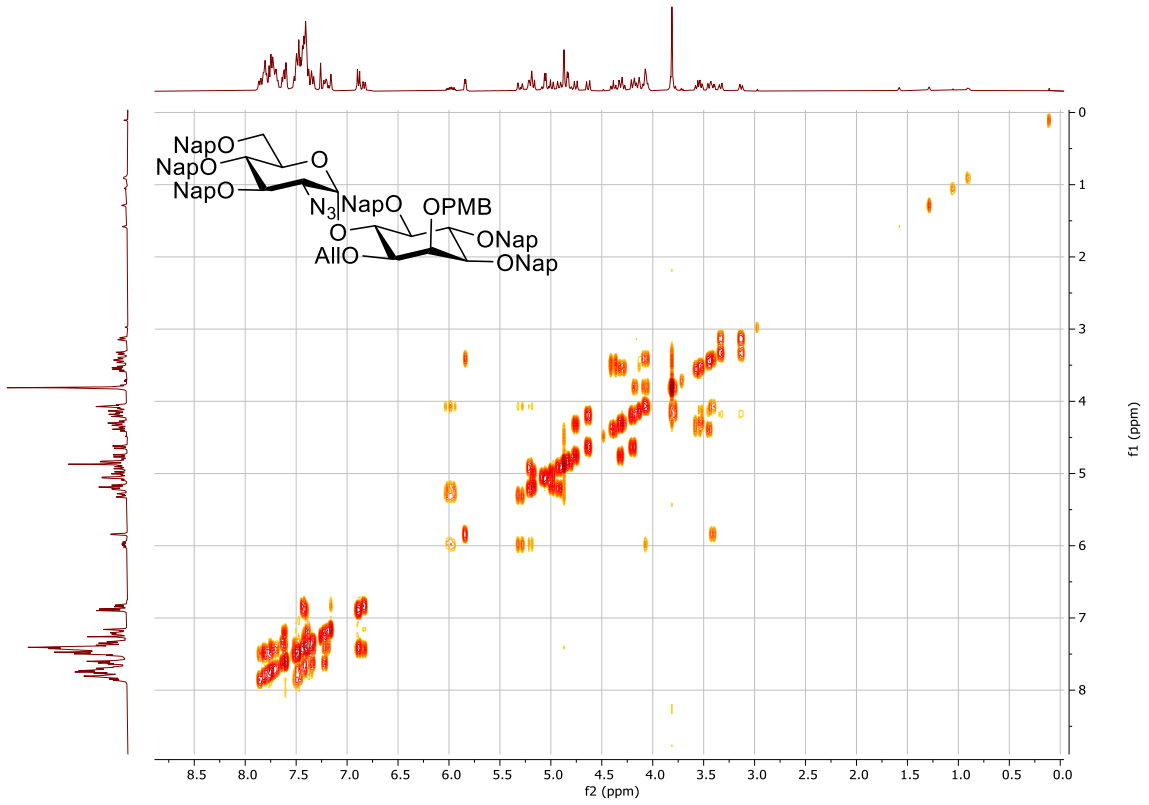

HSQC-NMR spectrum of compound 2-40

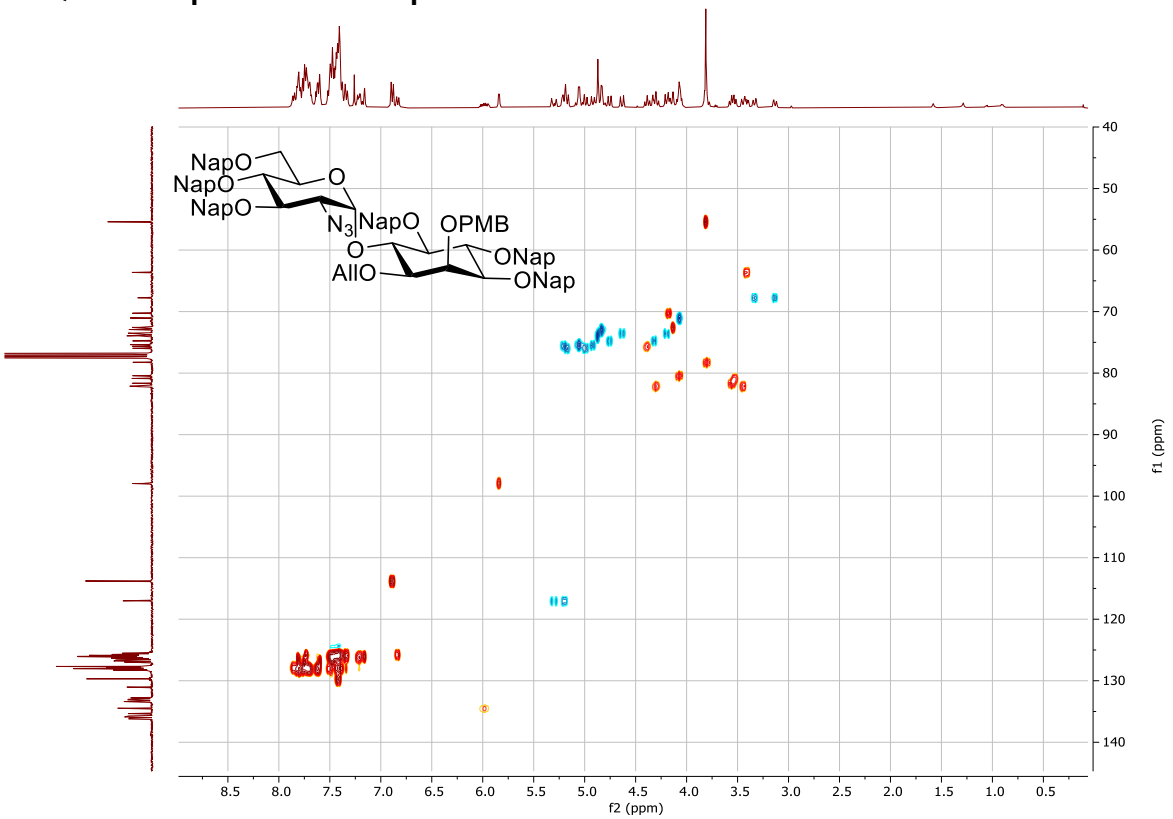

^{1}H NMR spectrum of compound 2-41

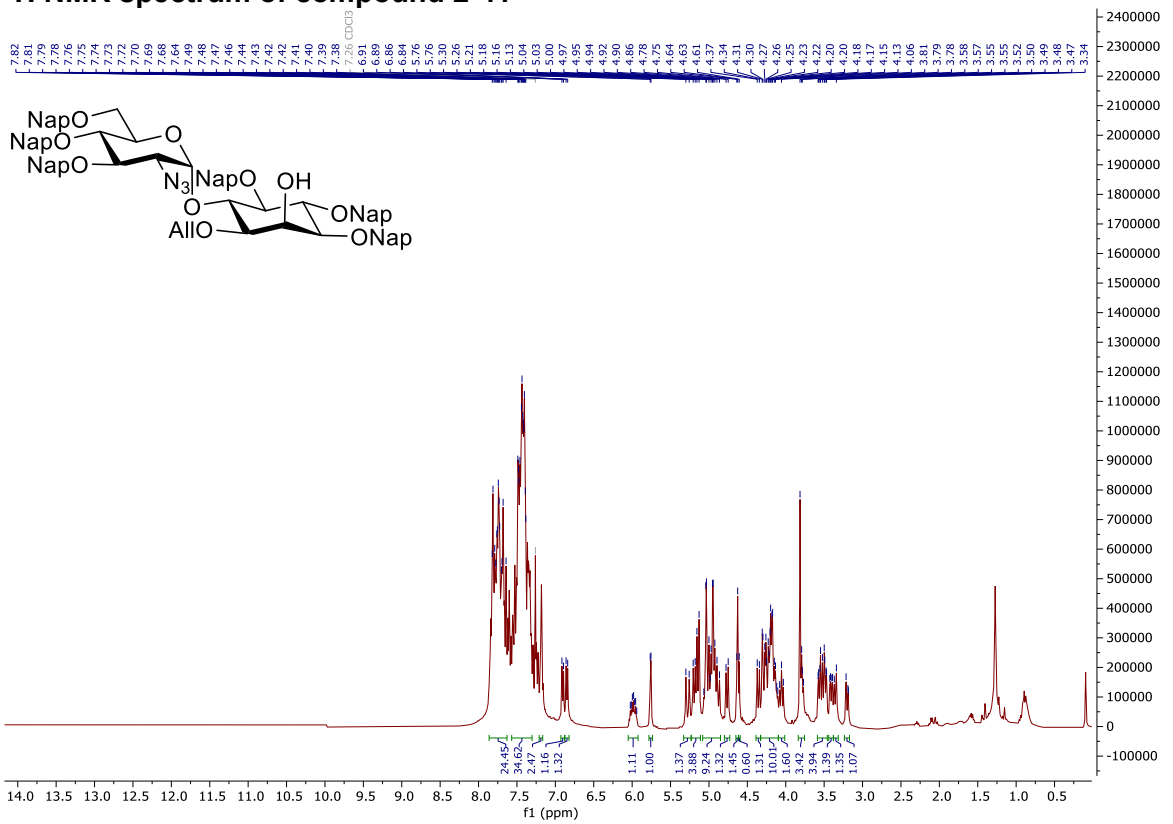

^{13}C NMR spectrum of compound 2-41

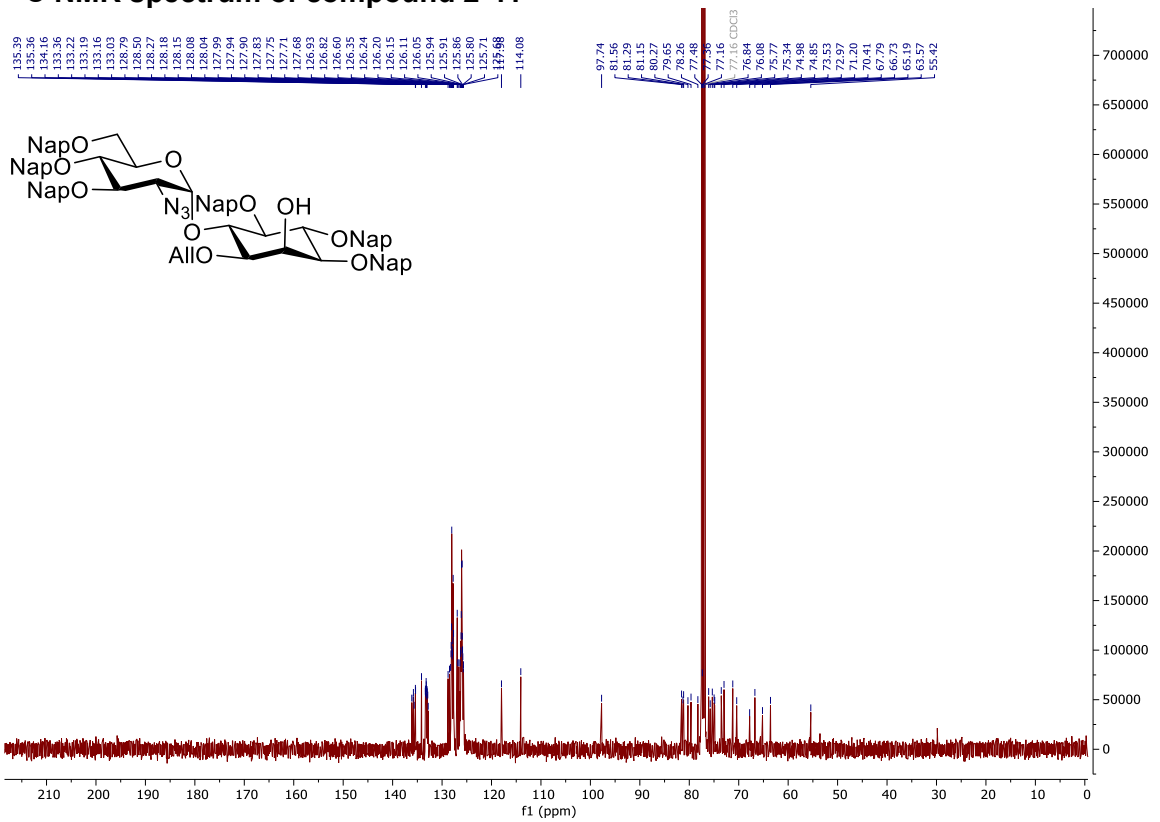

^{1}H NMR spectrum of compound 2-6

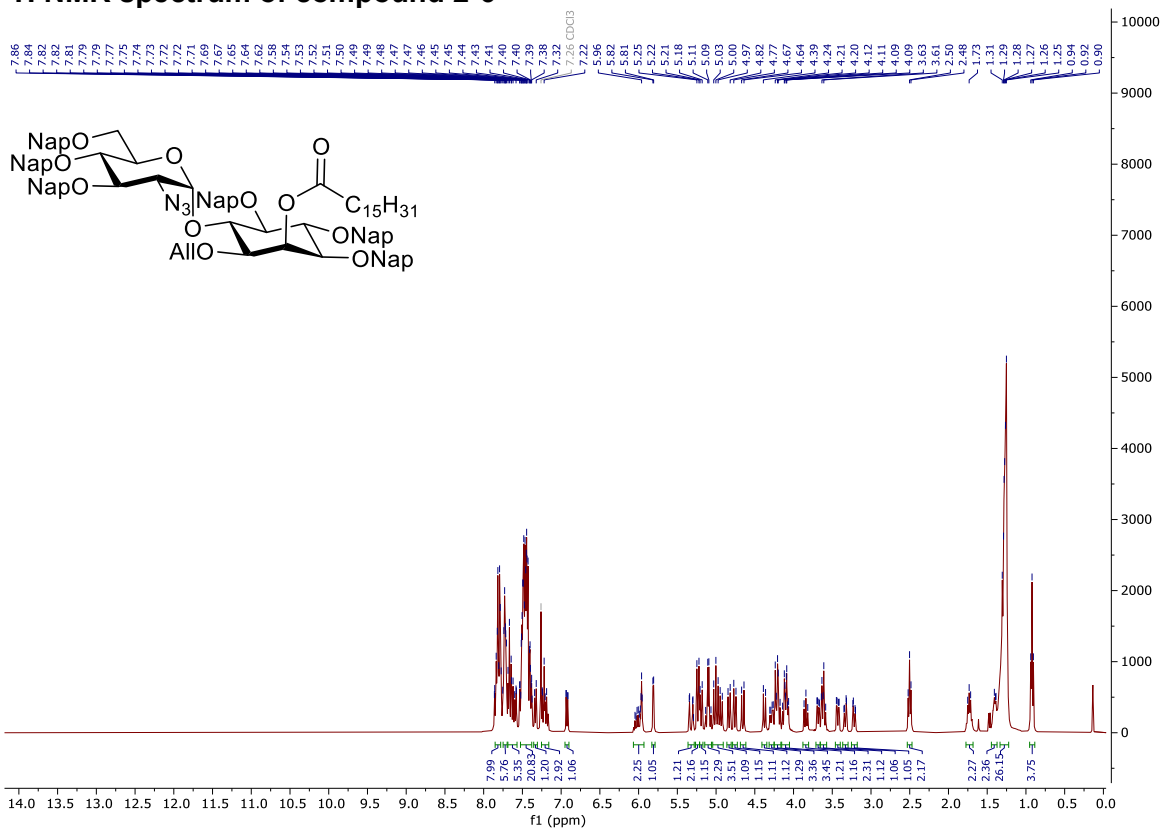

^{13}C NMR spectrum of compound 2-6

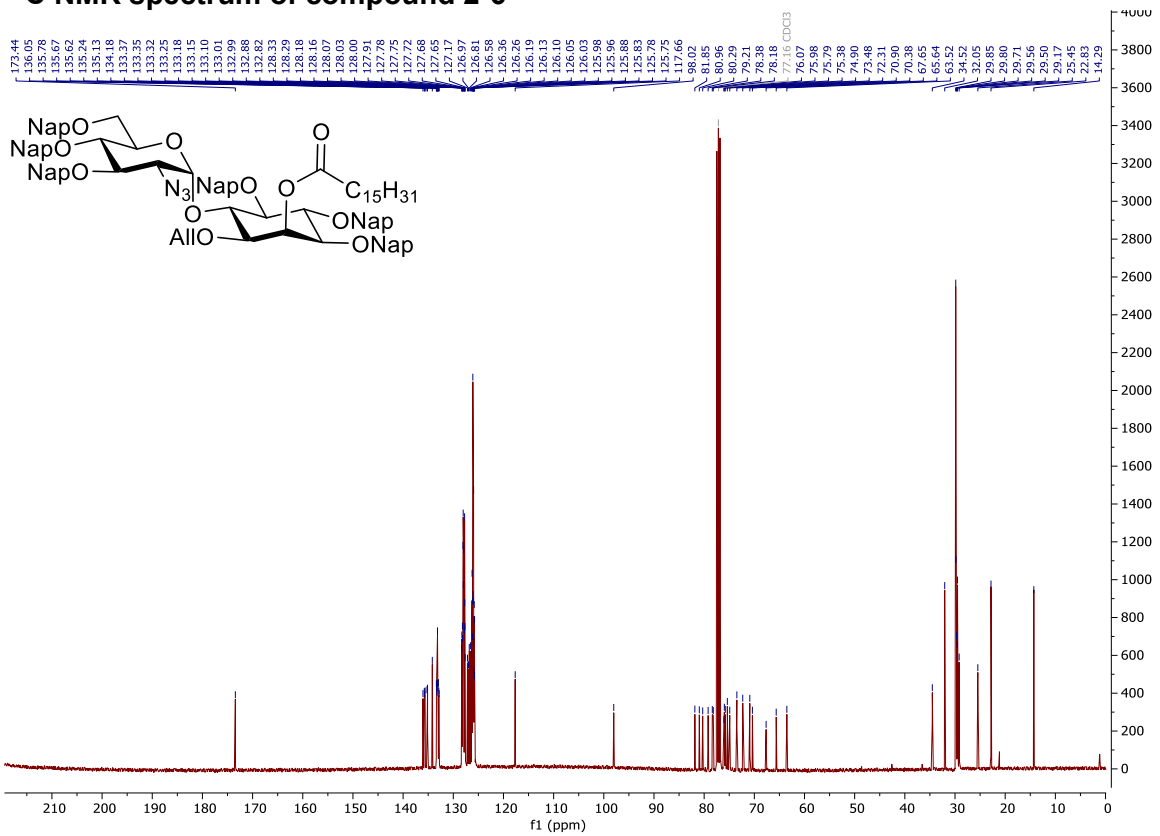

COSY-NMR spectrum of compound 2-6

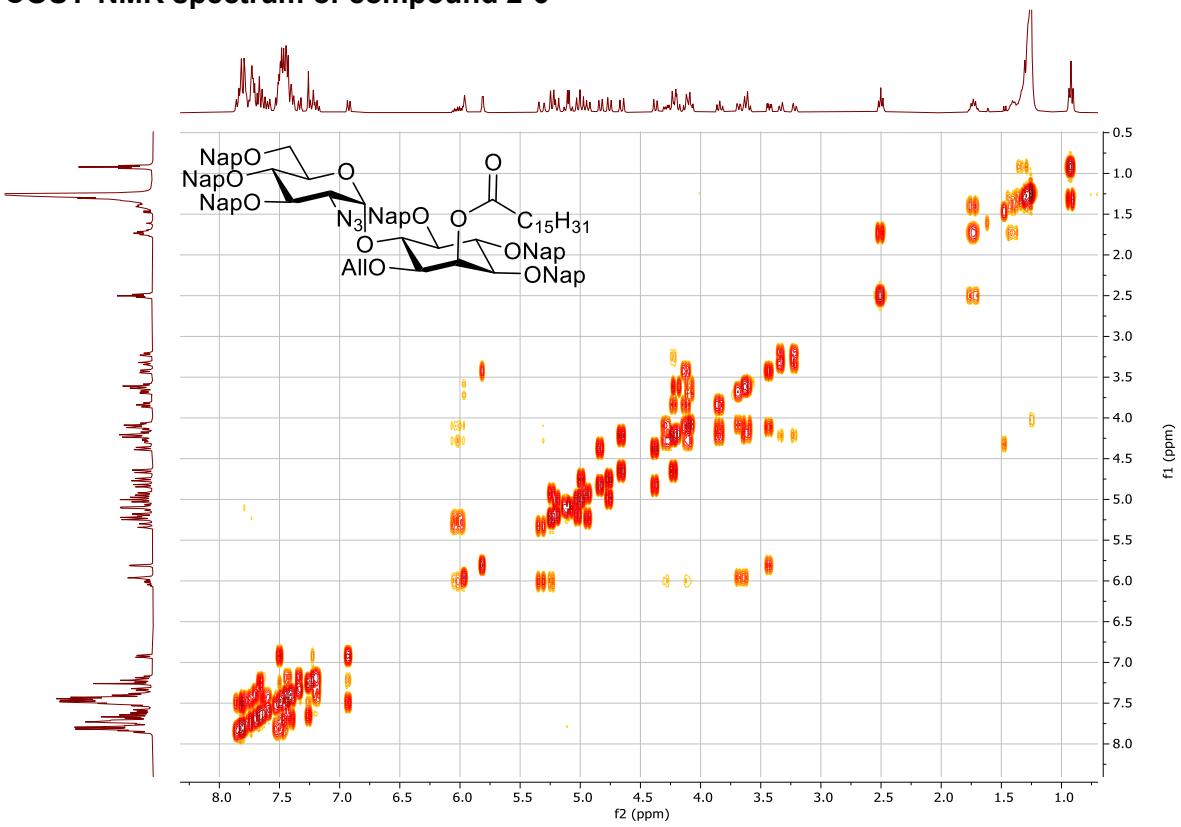

HSQC-NMR spectrum of compound 2-6

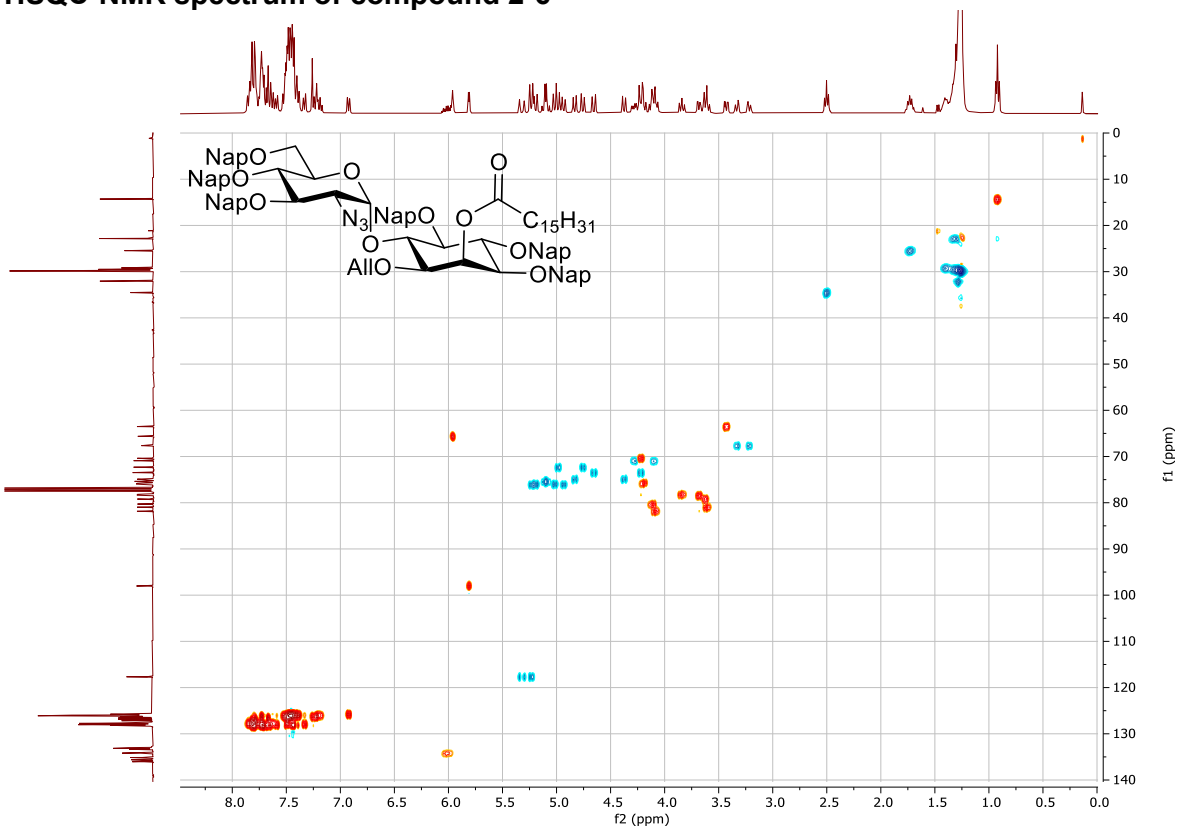

^{1}H NMR spectrum of compound 2-42

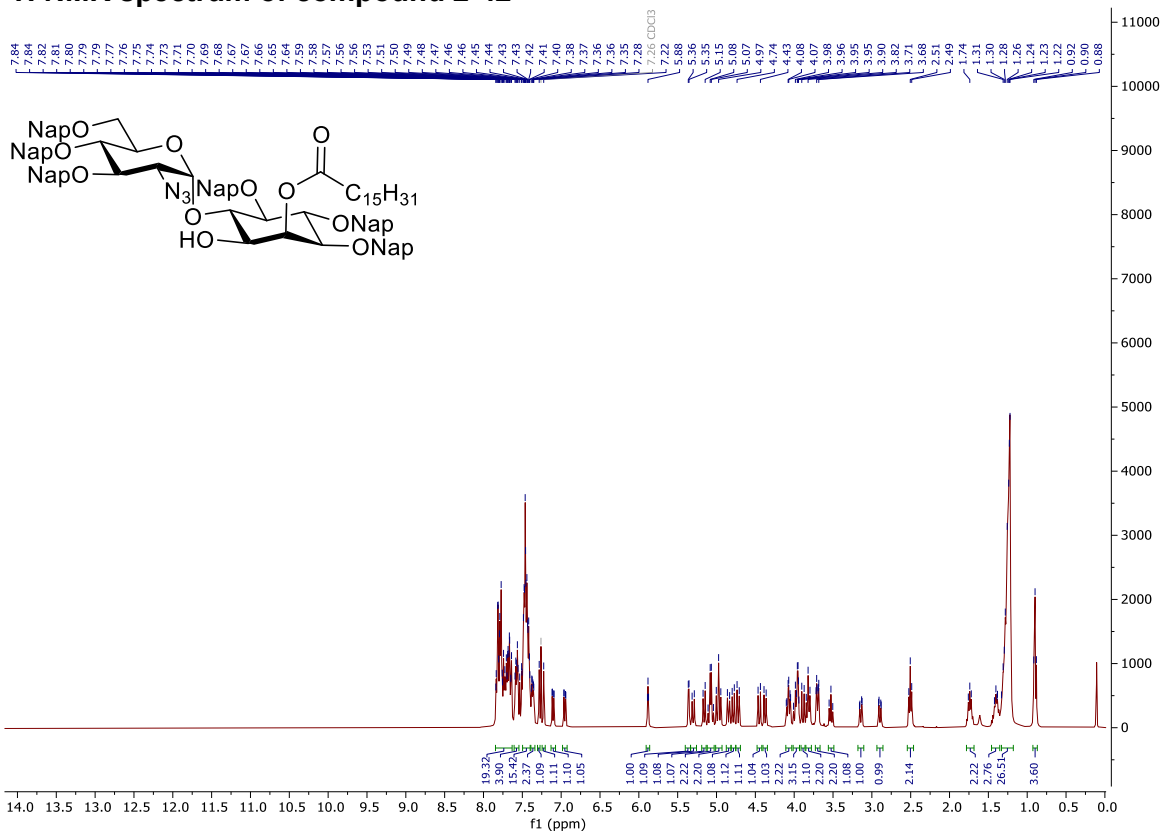

^{13}C NMR spectrum of compound 2-42

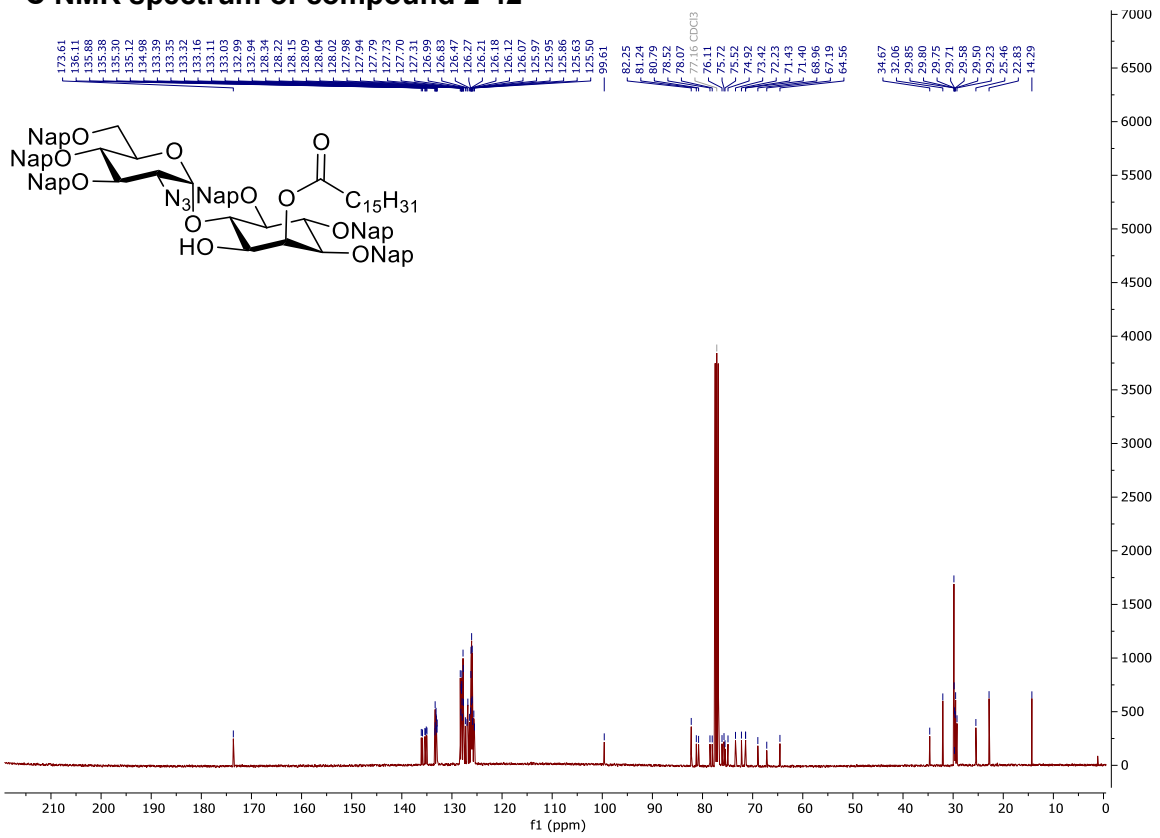

COSY-NMR spectrum of compound 2-42

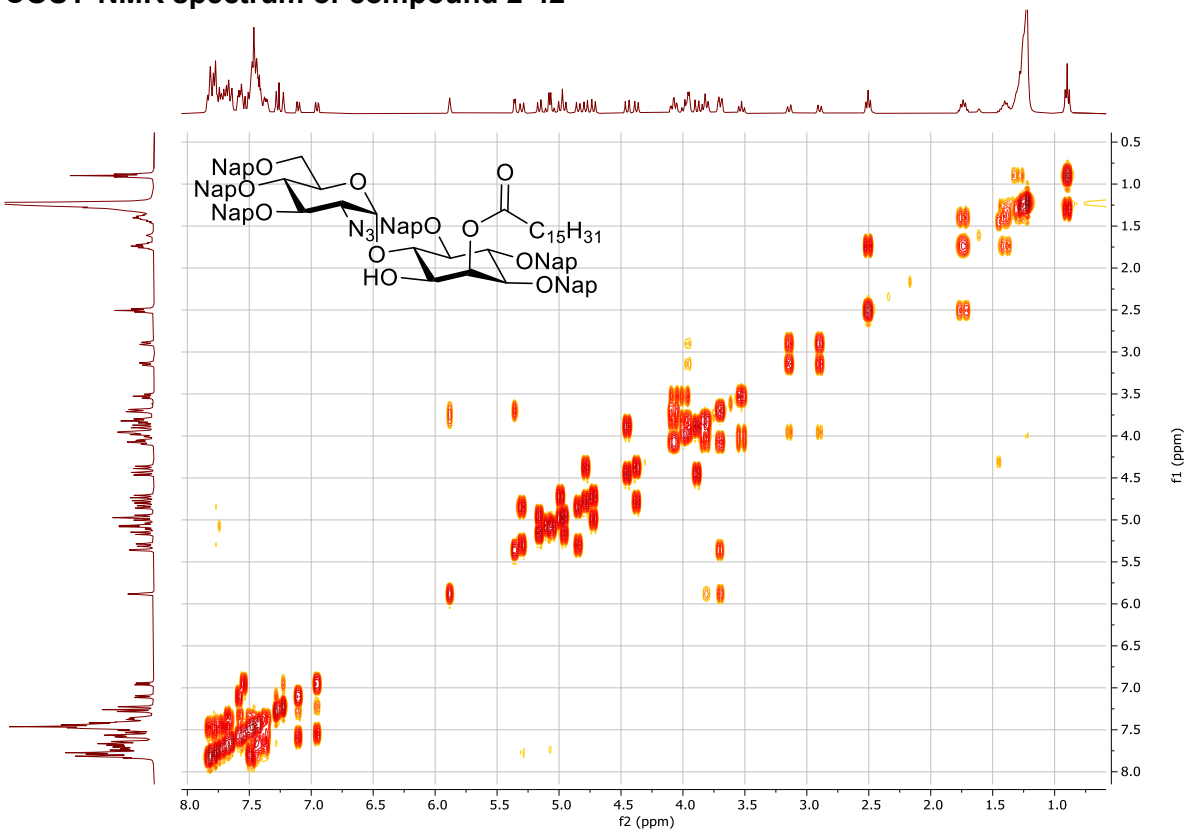

HSQC-NMR spectrum of compound 2-42

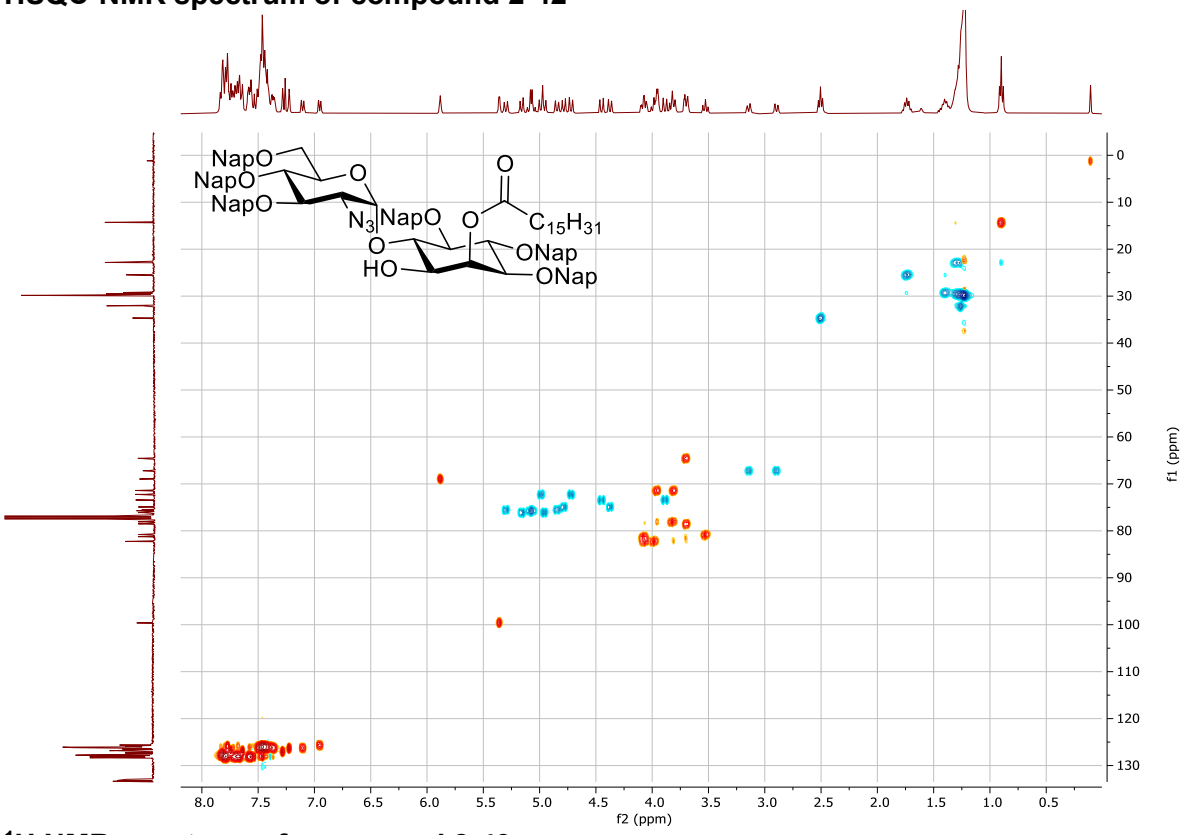

^{1}H NMR spectrum of compound 2-43

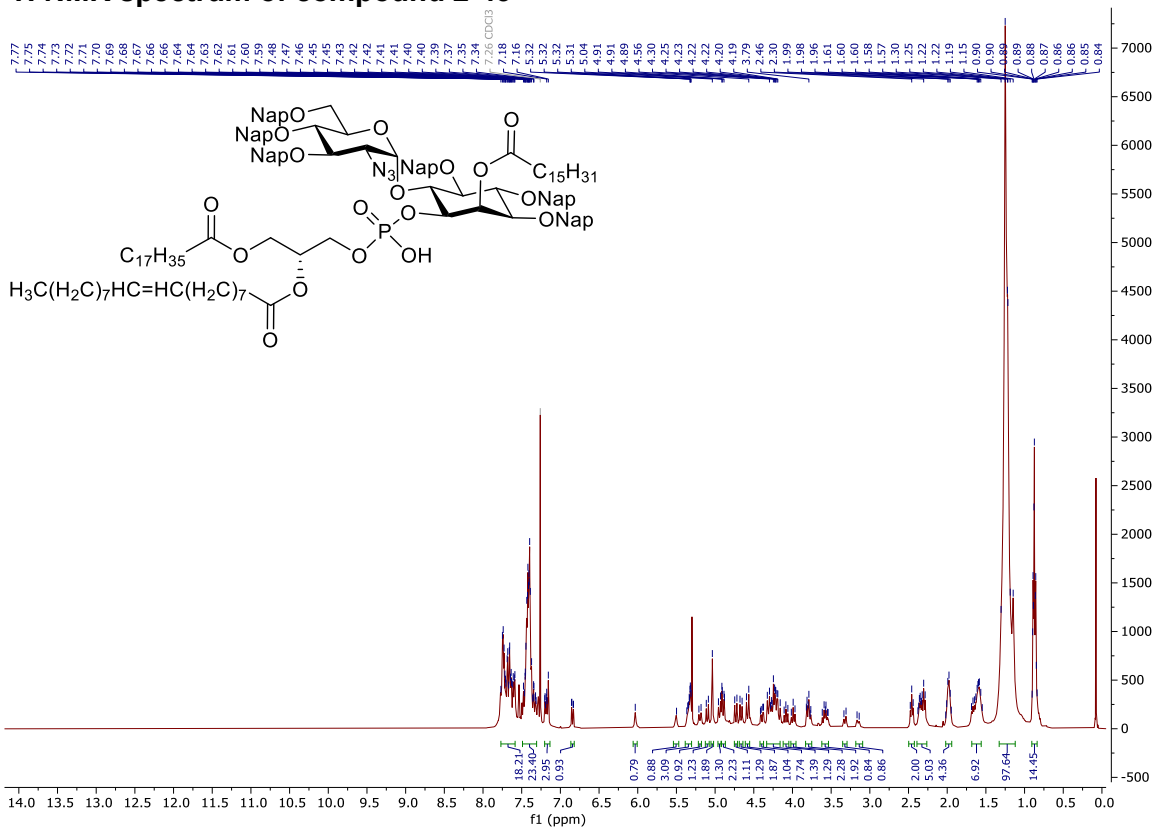

^{13}C NMR spectrum of compound 2-43

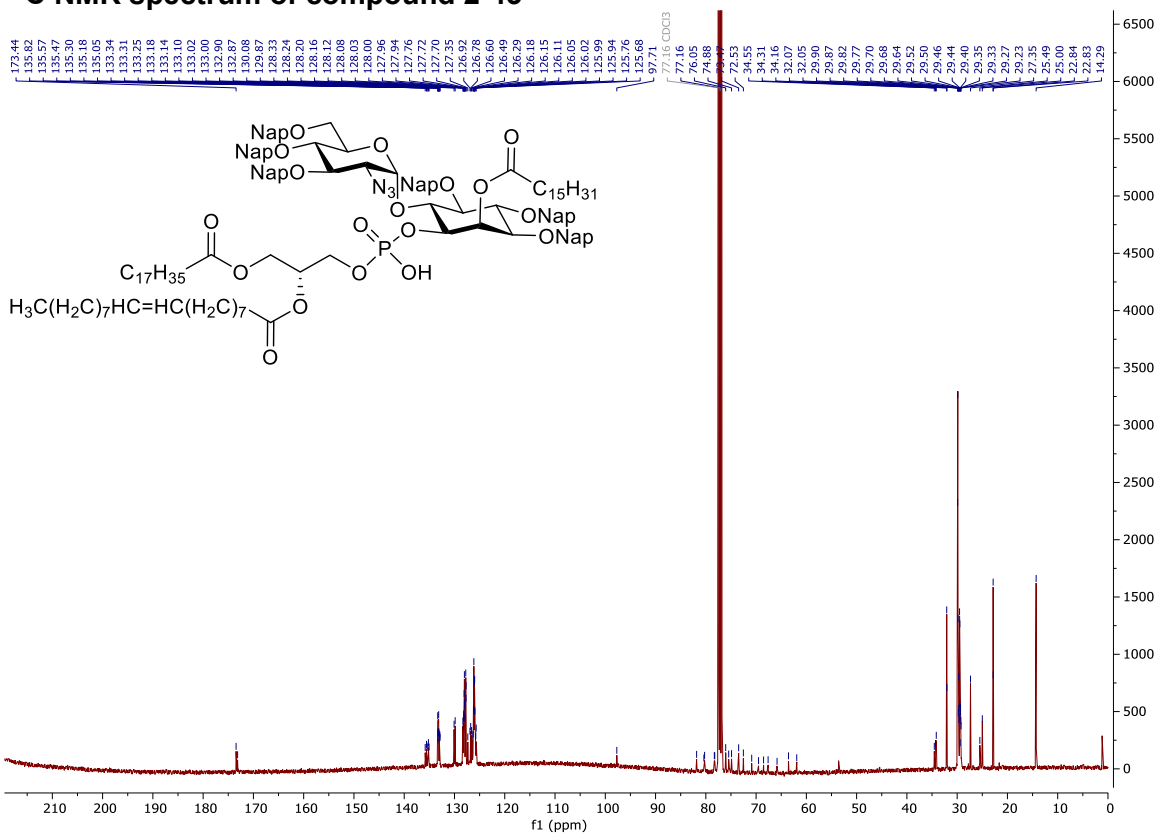

COSY-NMR spectrum of compound 2-43

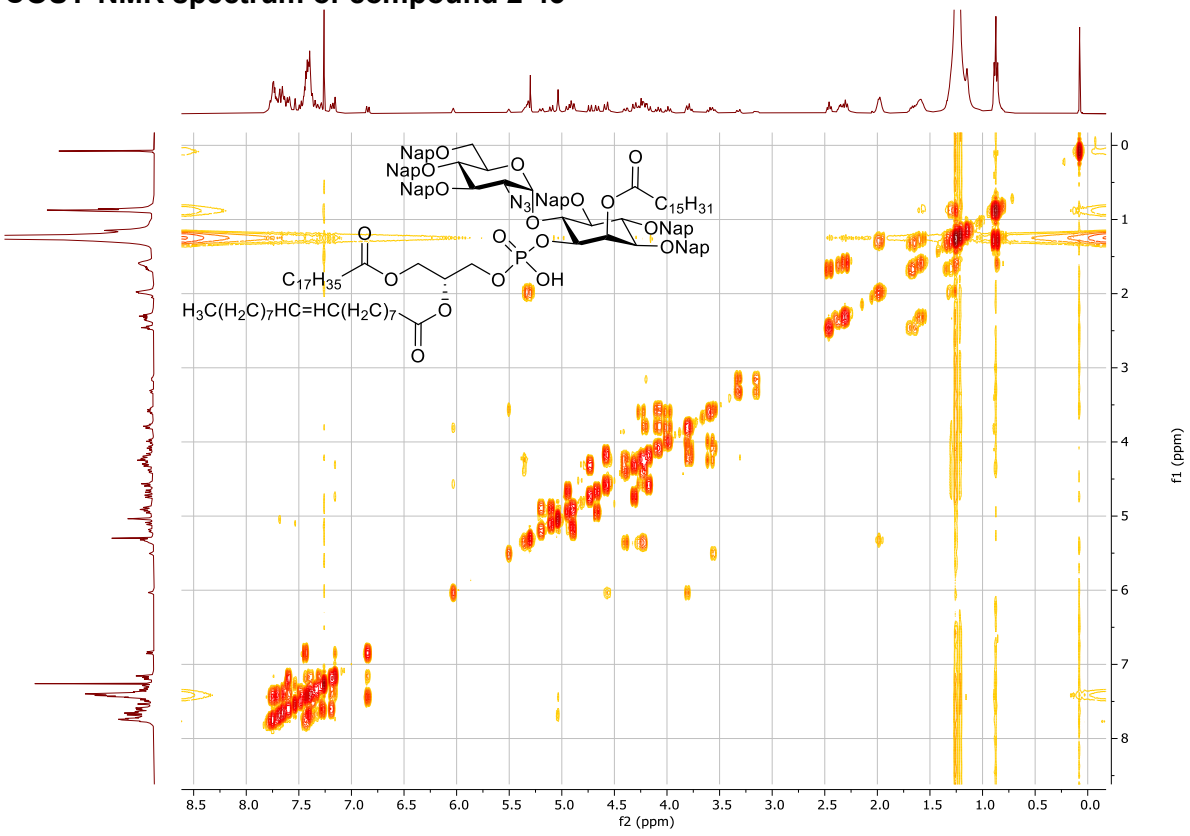

HSQC-NMR spectrum of compound 2-43

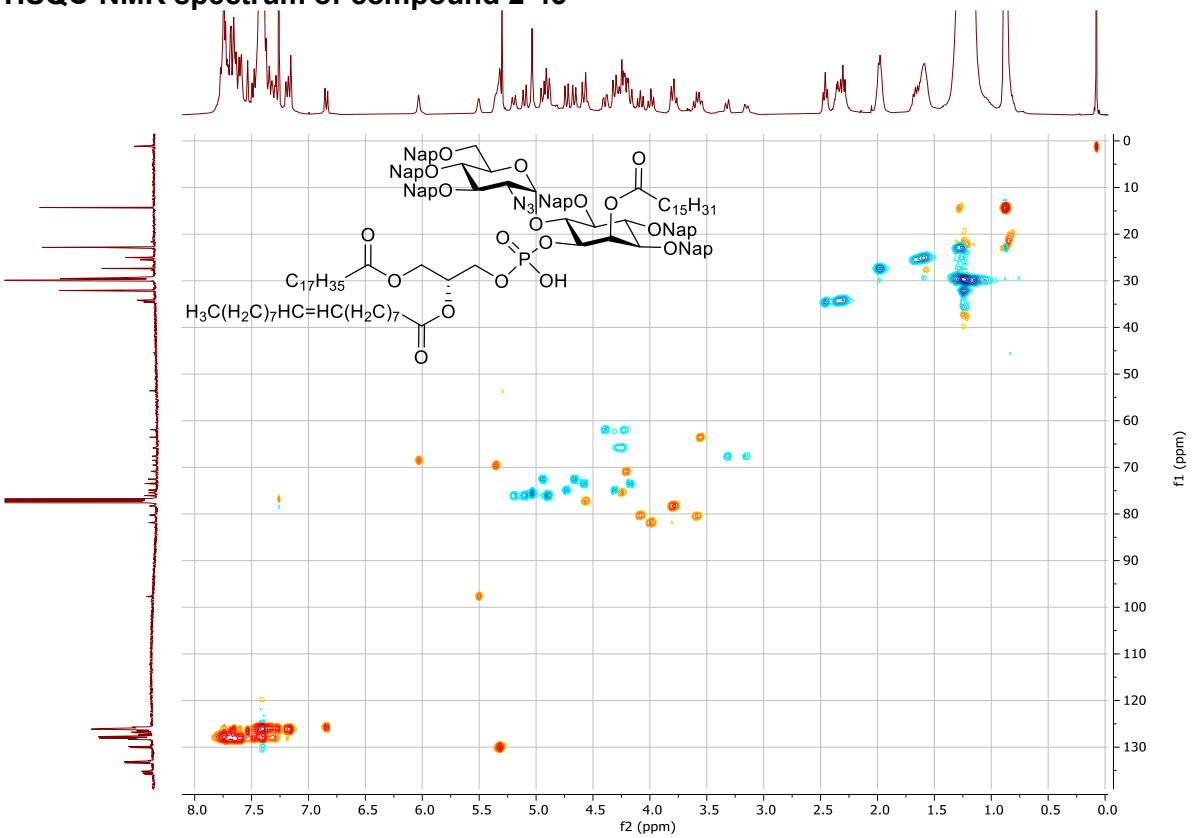

^{31}P NMR spectrum of compound 2-43

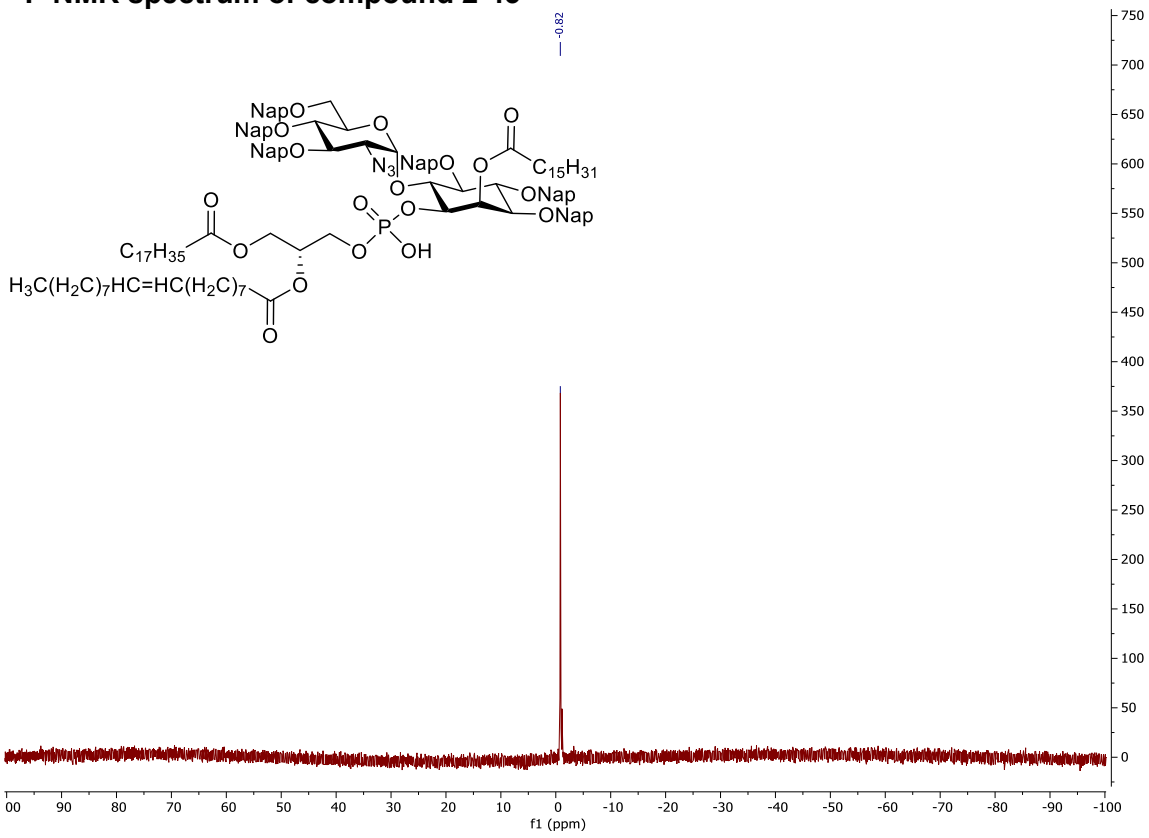

^{1}H NMR spectrum of GPI fragment 2-3

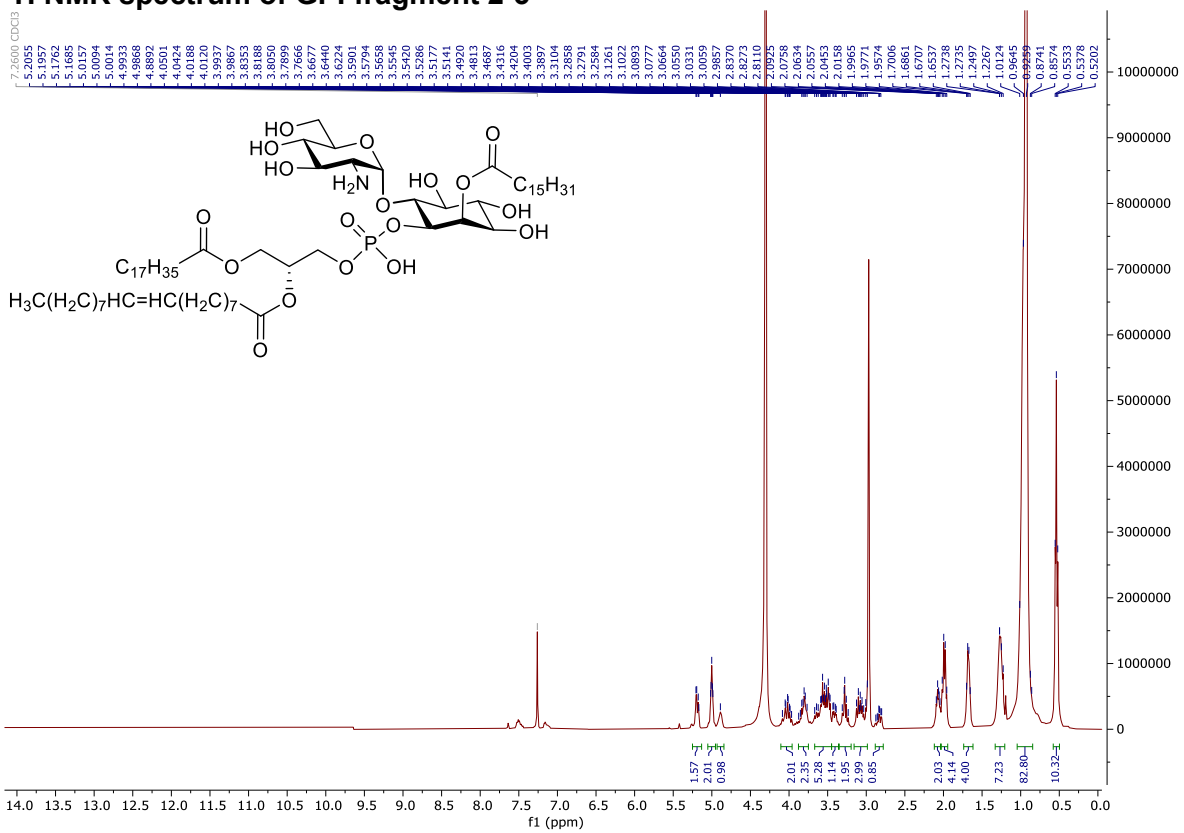

^{13}C-NMR spectrum of GPI fragment 2-3

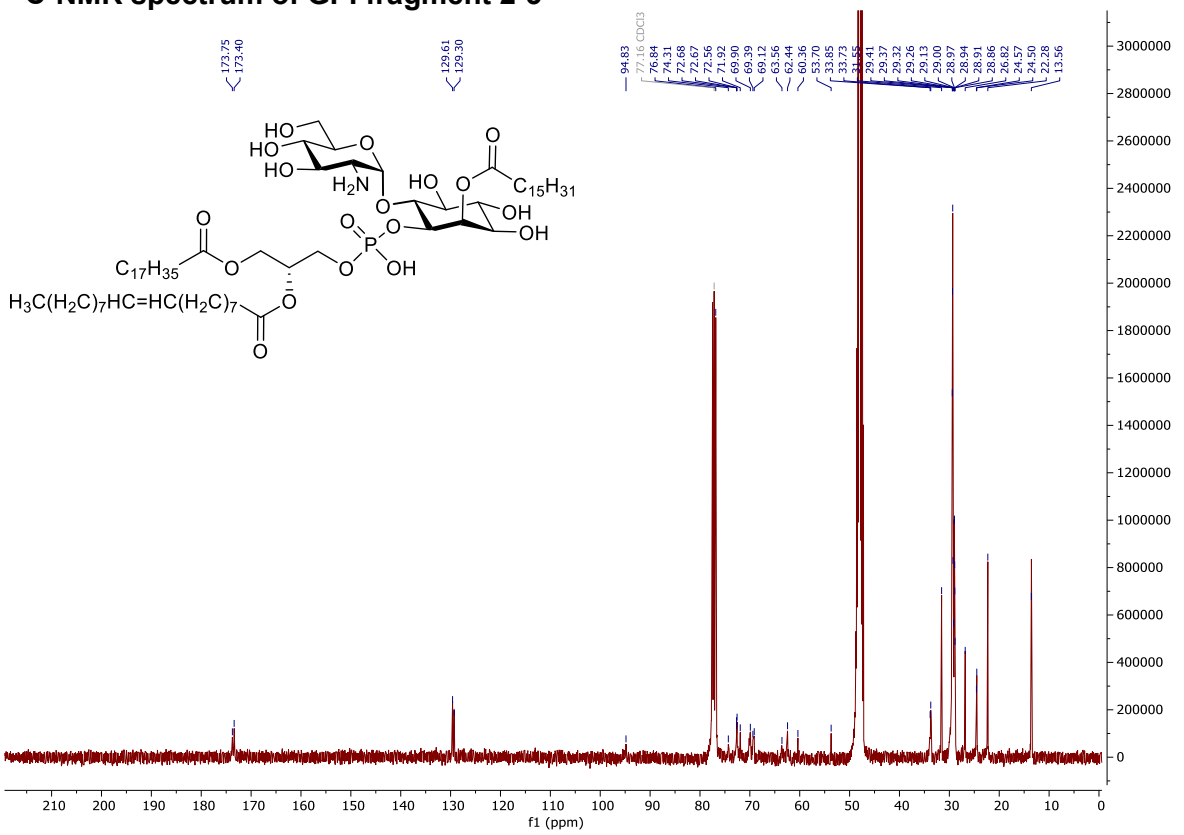

COSY-NMR spectrum of GPI fragment 2-3

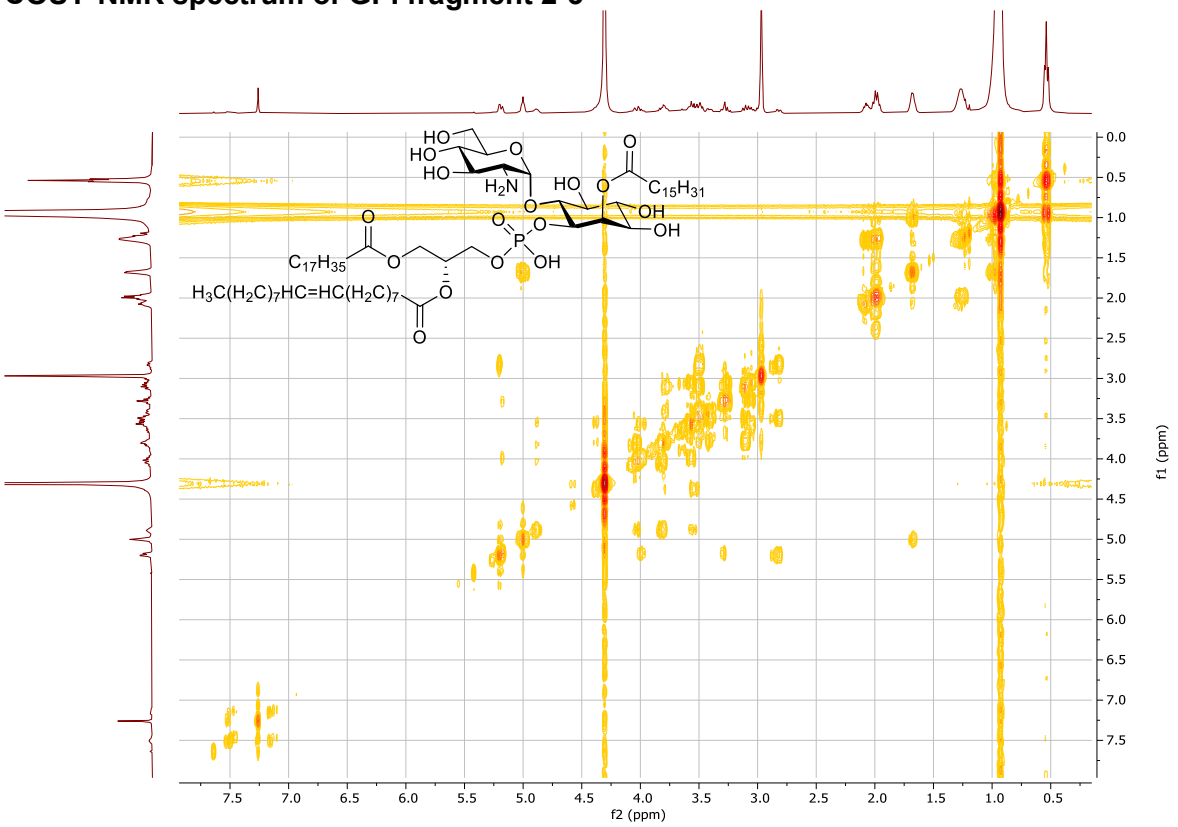

HSQC-NMR spectrum of GPI fragment 2-3

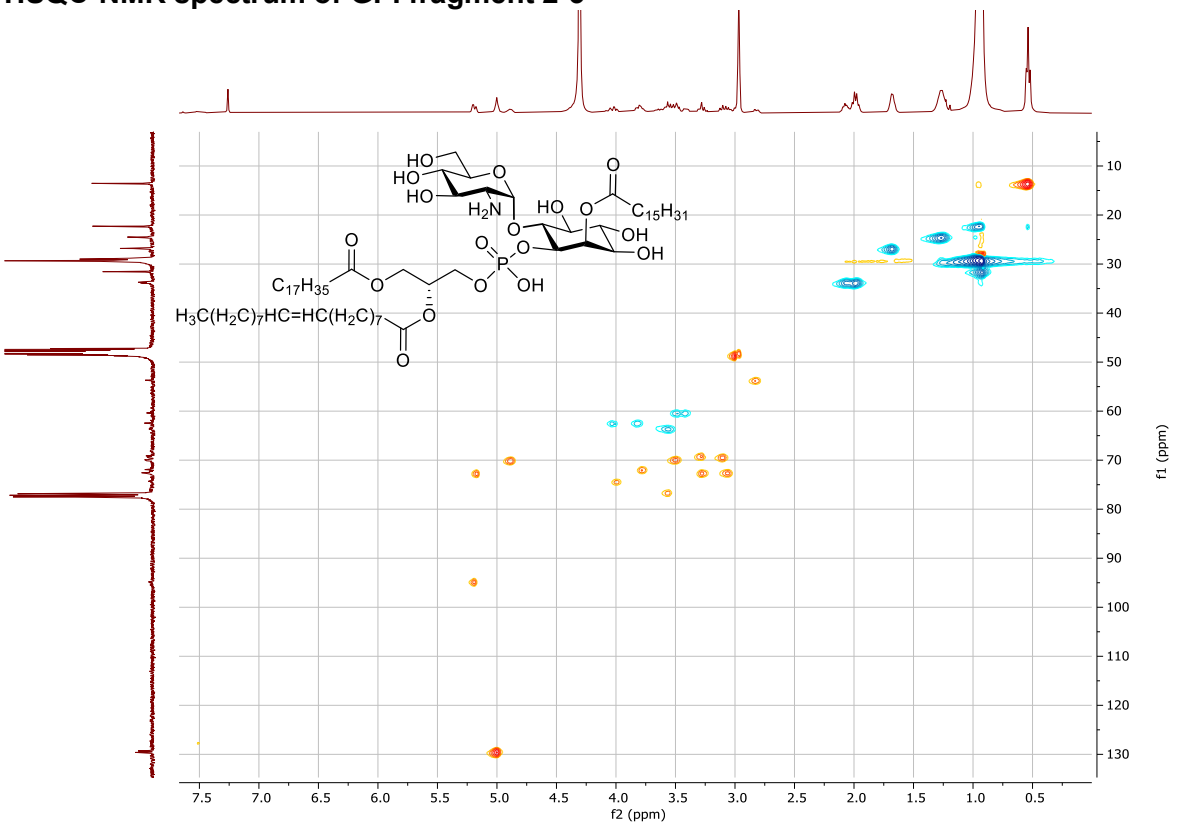

^{31}P-NMR spectrum of GPI fragment 2-3

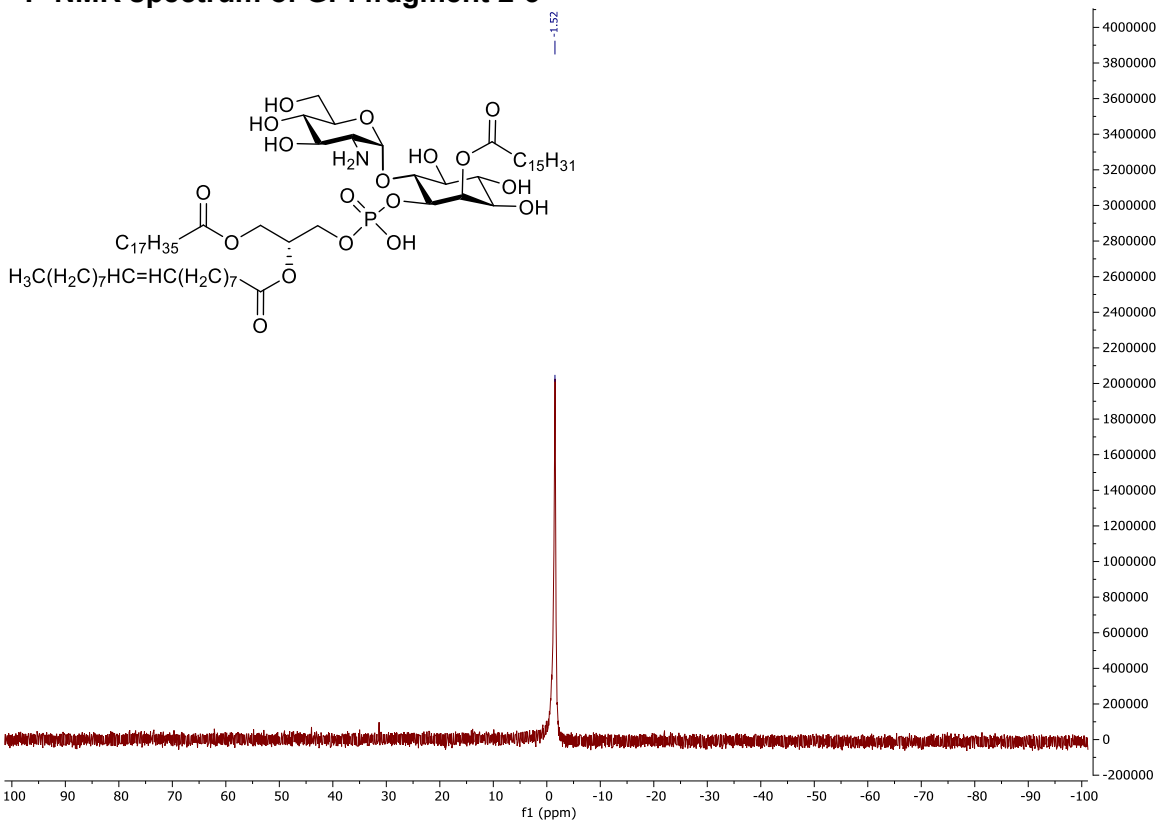

^{1}H NMR spectrum of 2-(Dimethoxymethyl)naphthalene

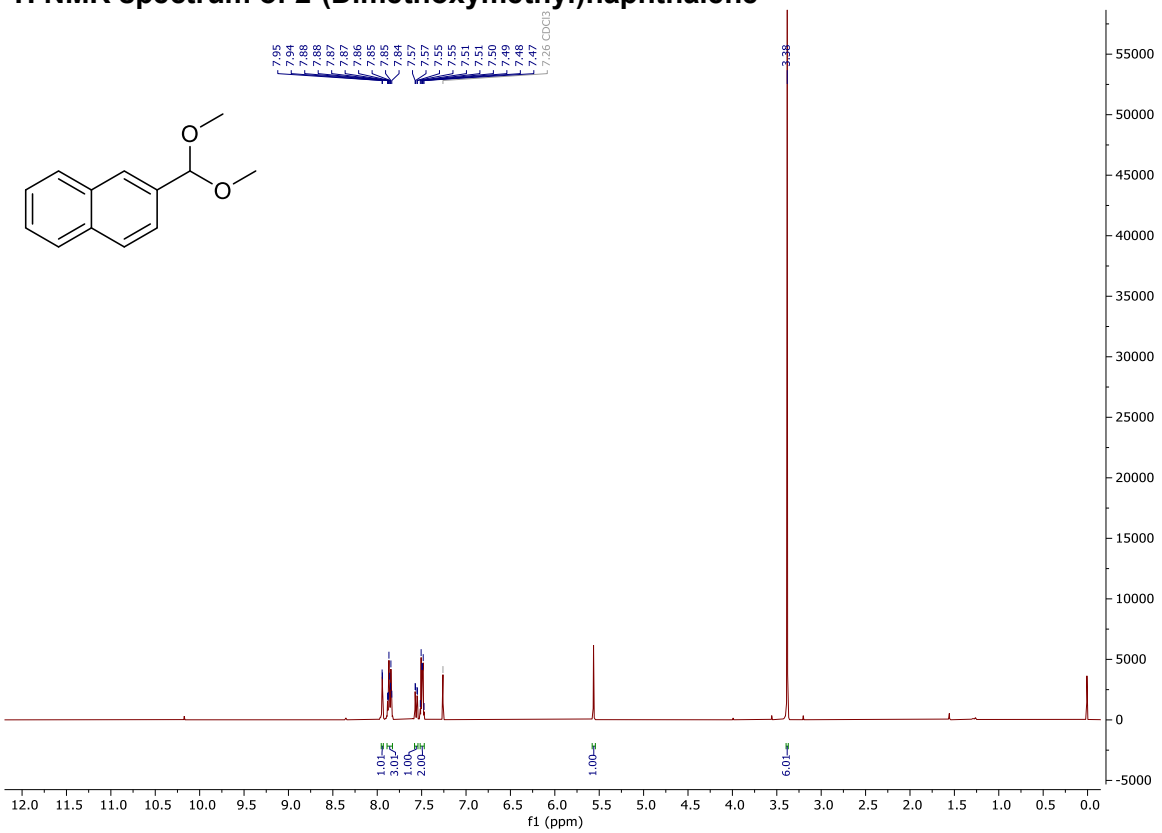

^{13}C NMR spectrum of 2-(Dimethoxymethyl)naphthalene

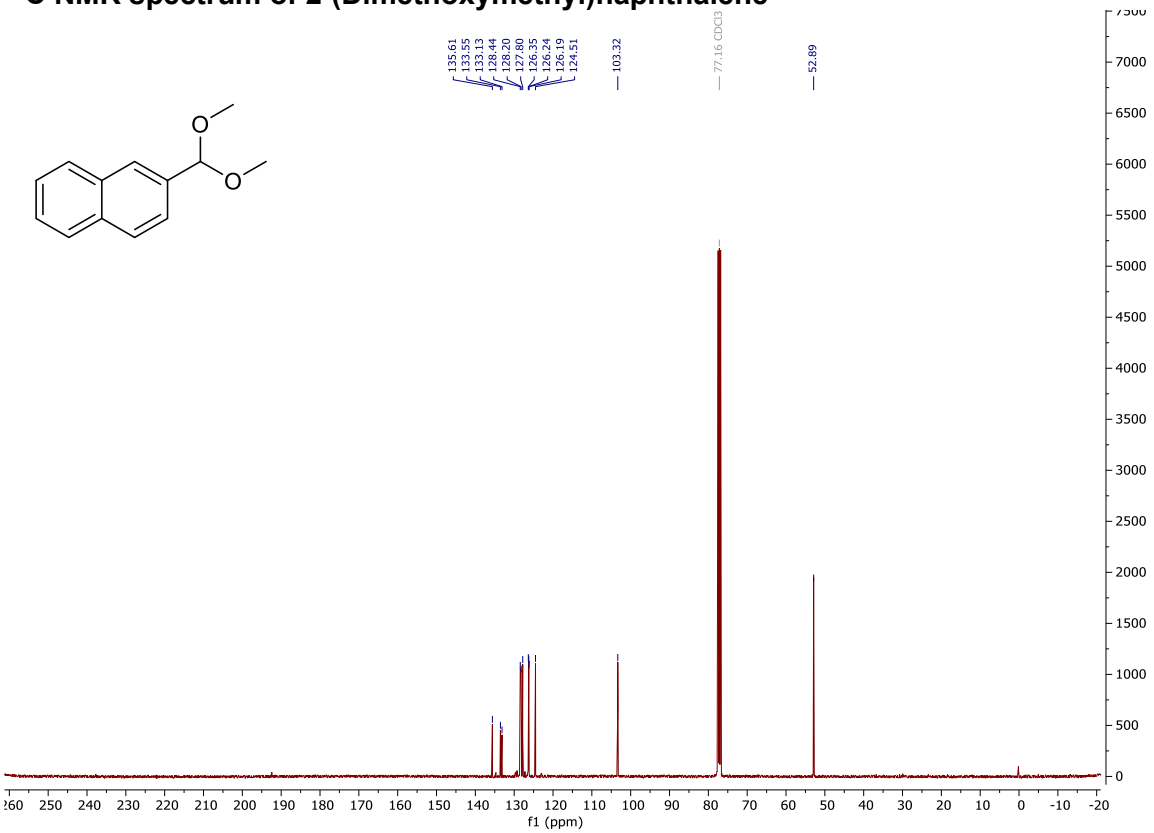

COSY NMR spectrum of 2-(Dimethoxymethyl)naphthalene

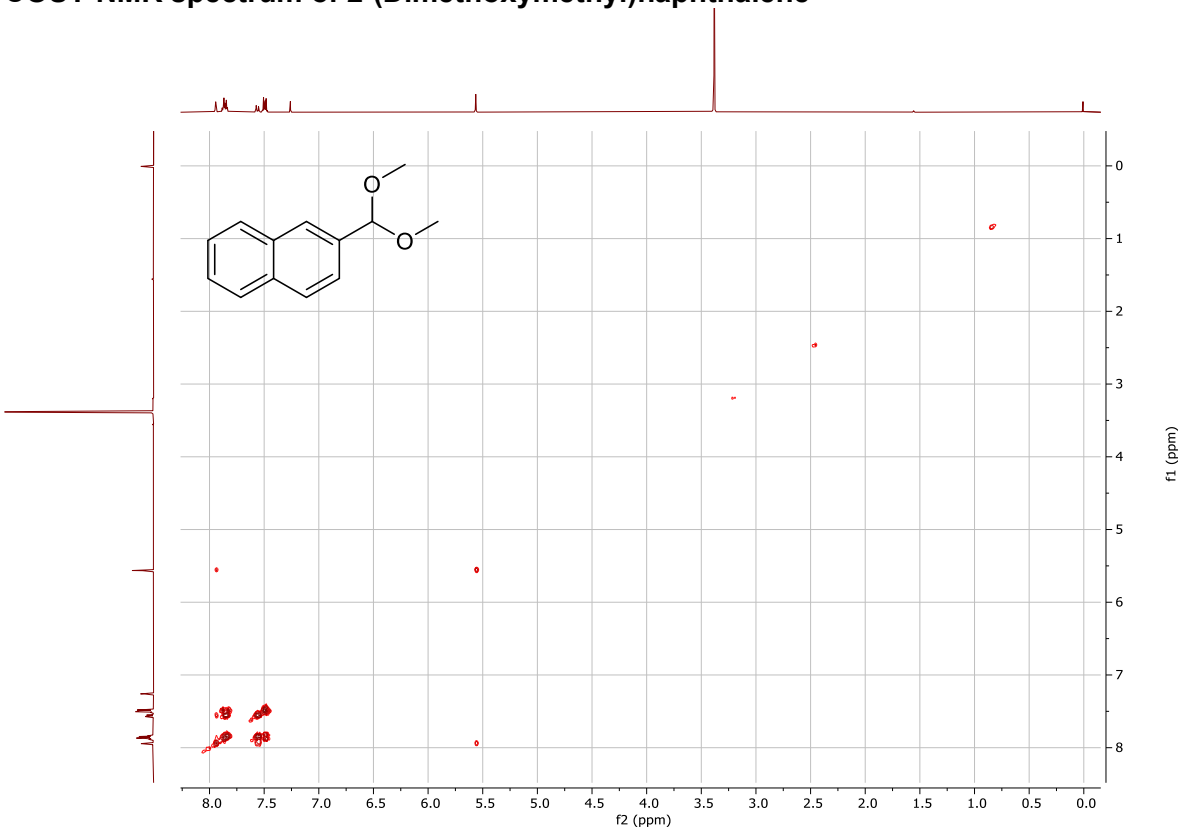

HSQC NMR spectrum 2-(Dimethoxymethyl)naphthalene

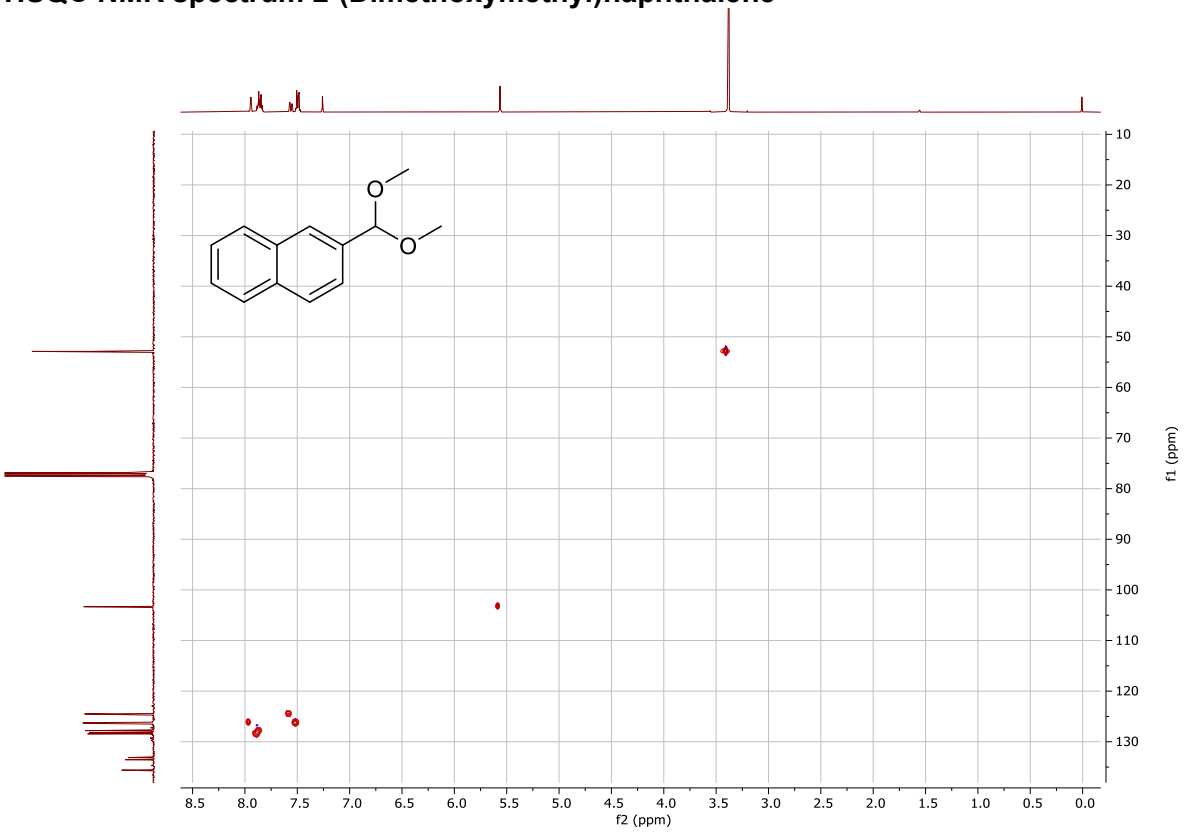

^{1}H NMR spectrum of compound 2-44

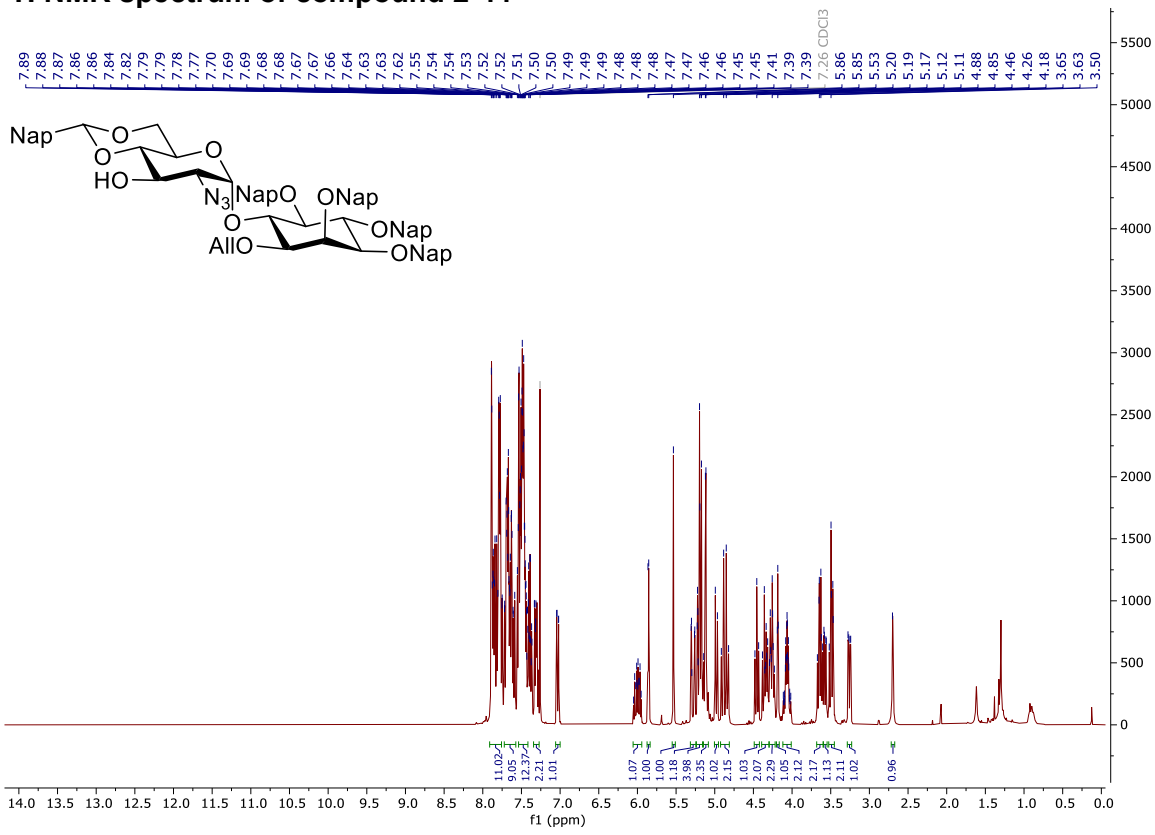

^{13}C NMR spectrum of compound 2-44

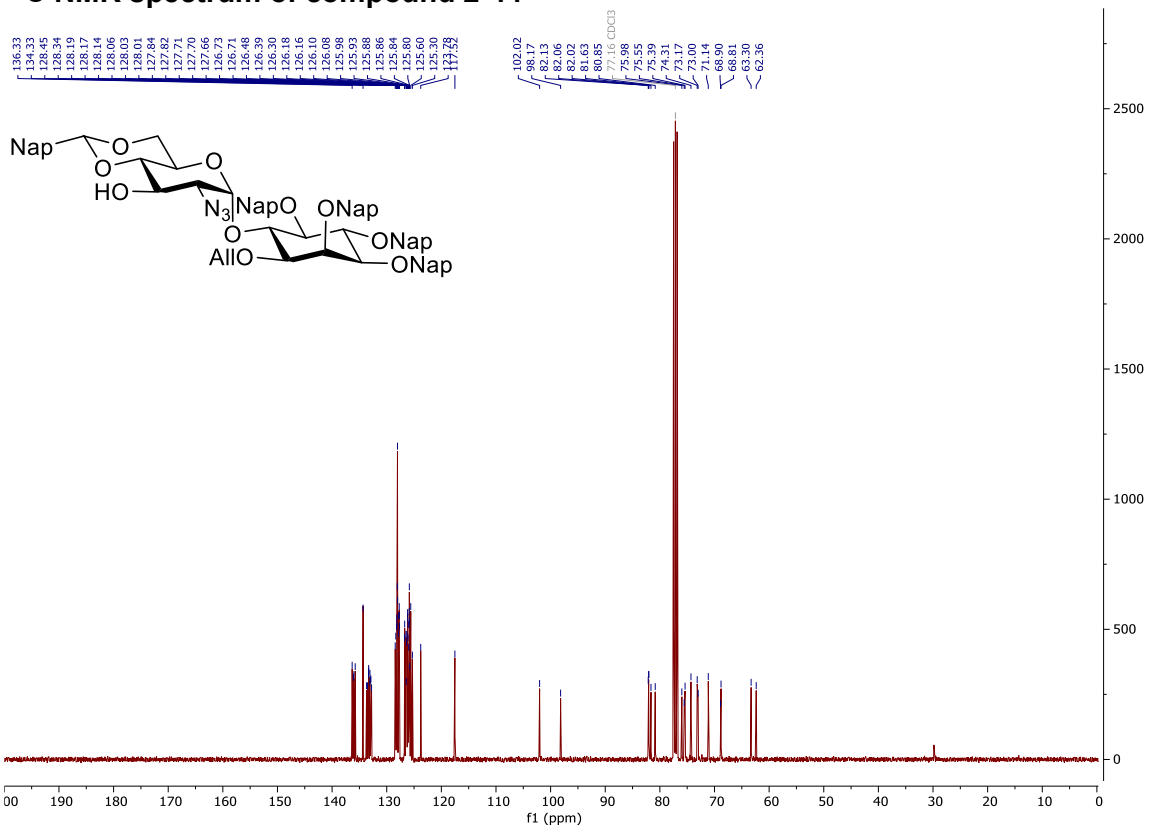

COSY-NMR spectrum of compound 2-44

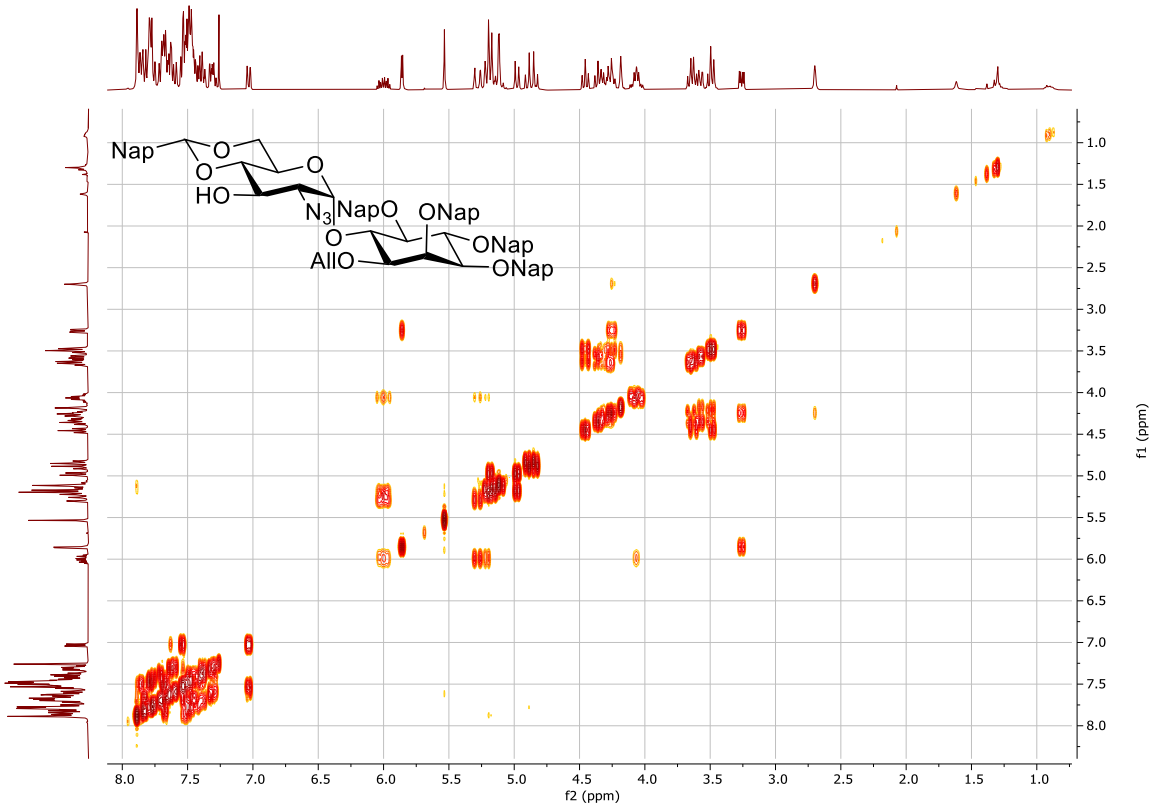

HSQC-NMR spectrum of compound 2-44

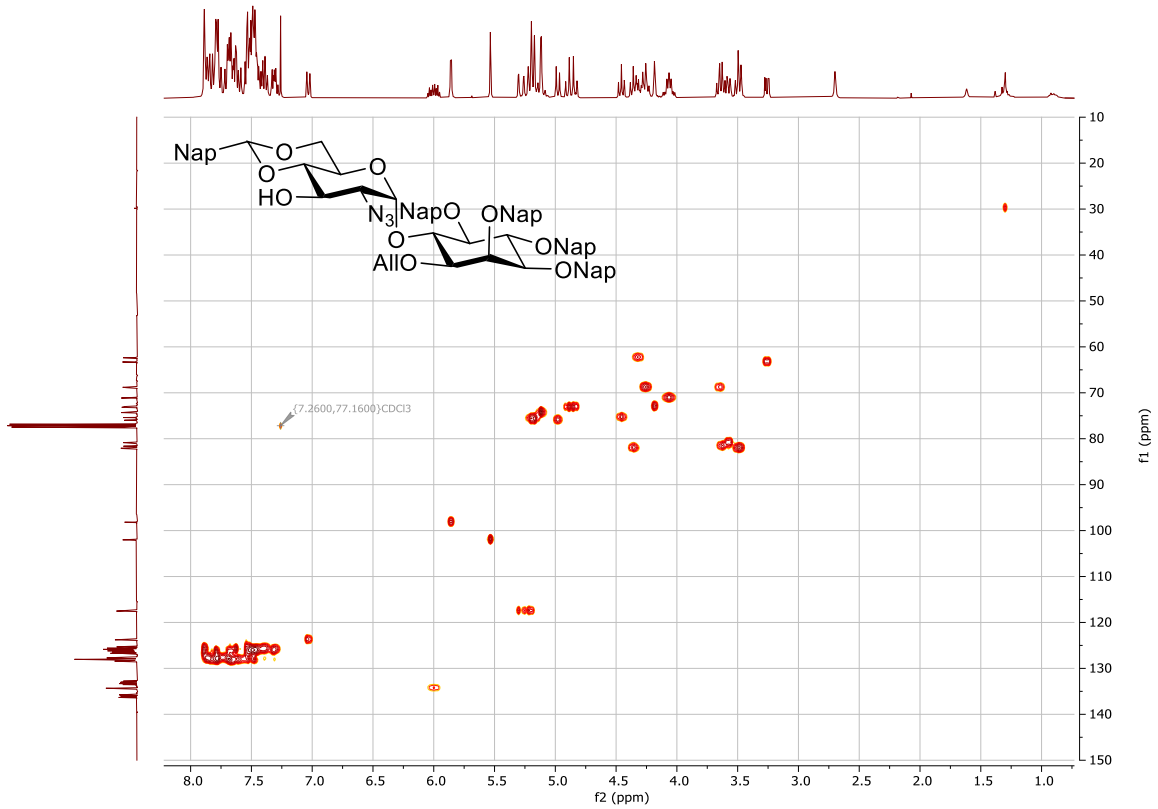

^{1}H NMR spectrum of compound 2-45

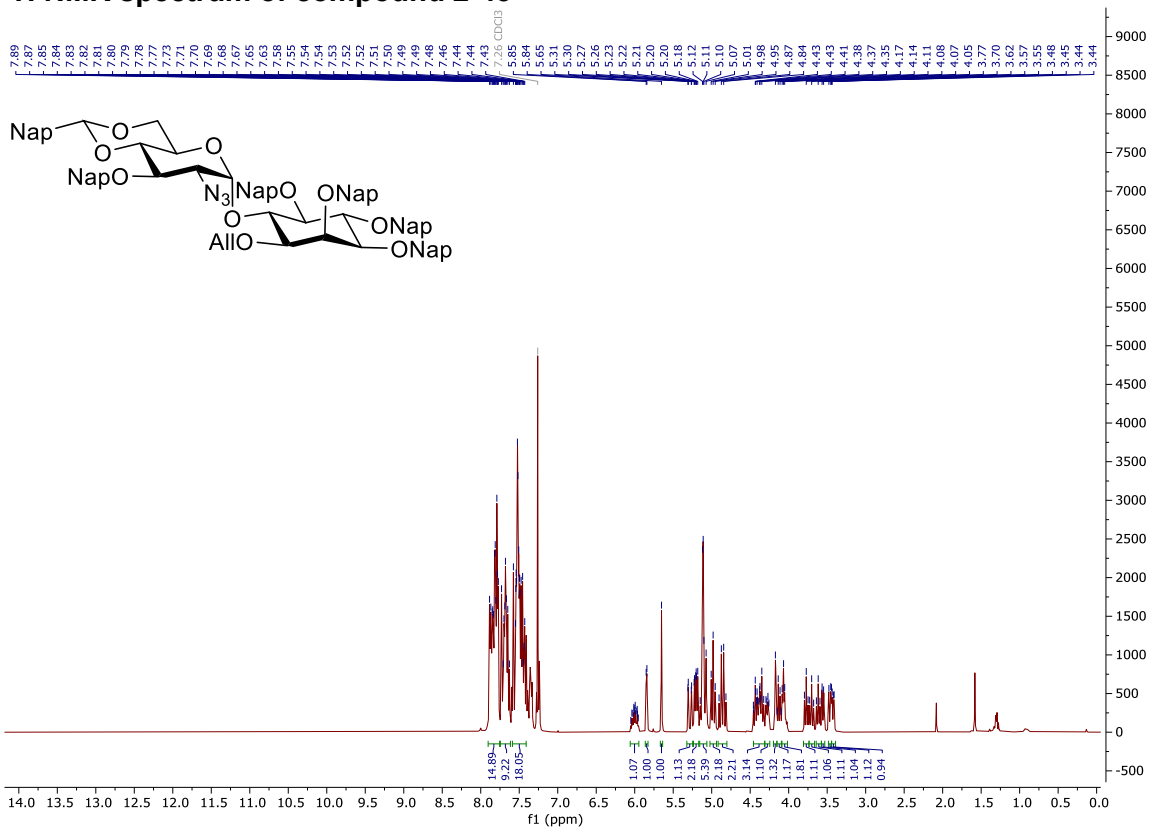

^{13}C NMR spectrum of compound 2-45

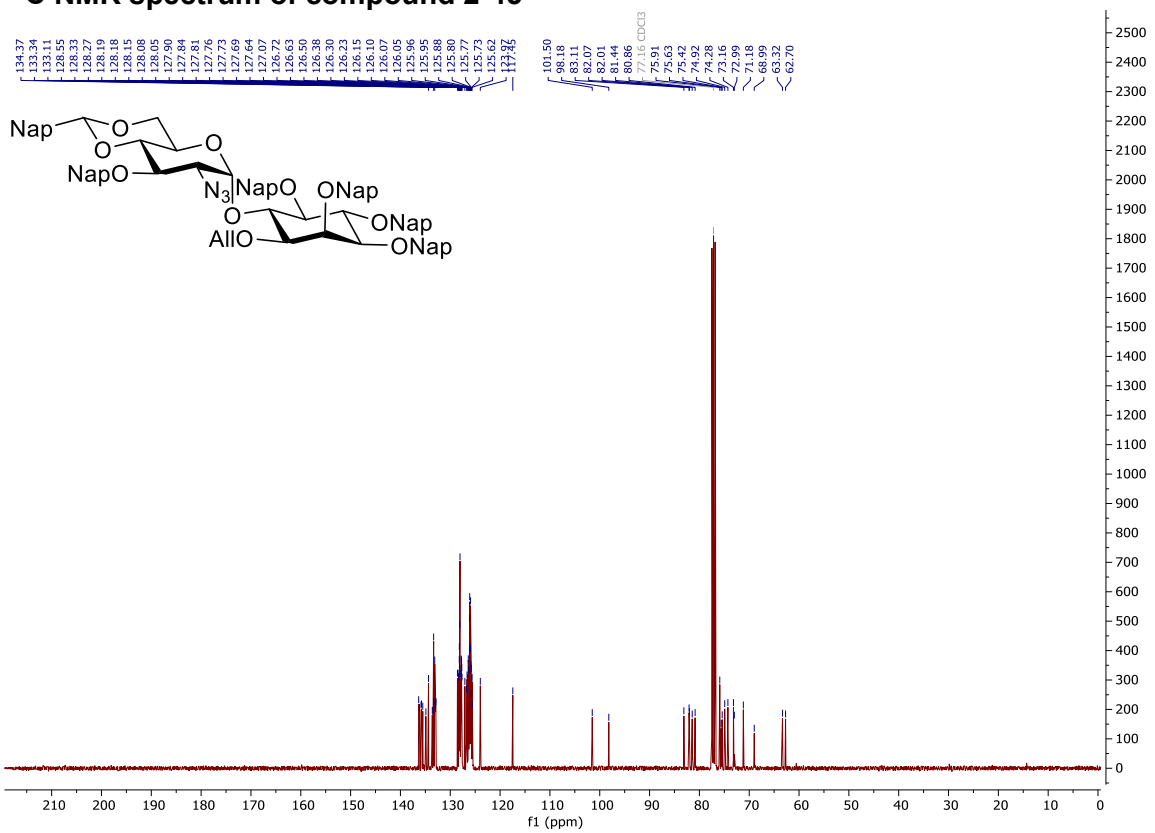

COSY-NMR spectrum of compound 2-45

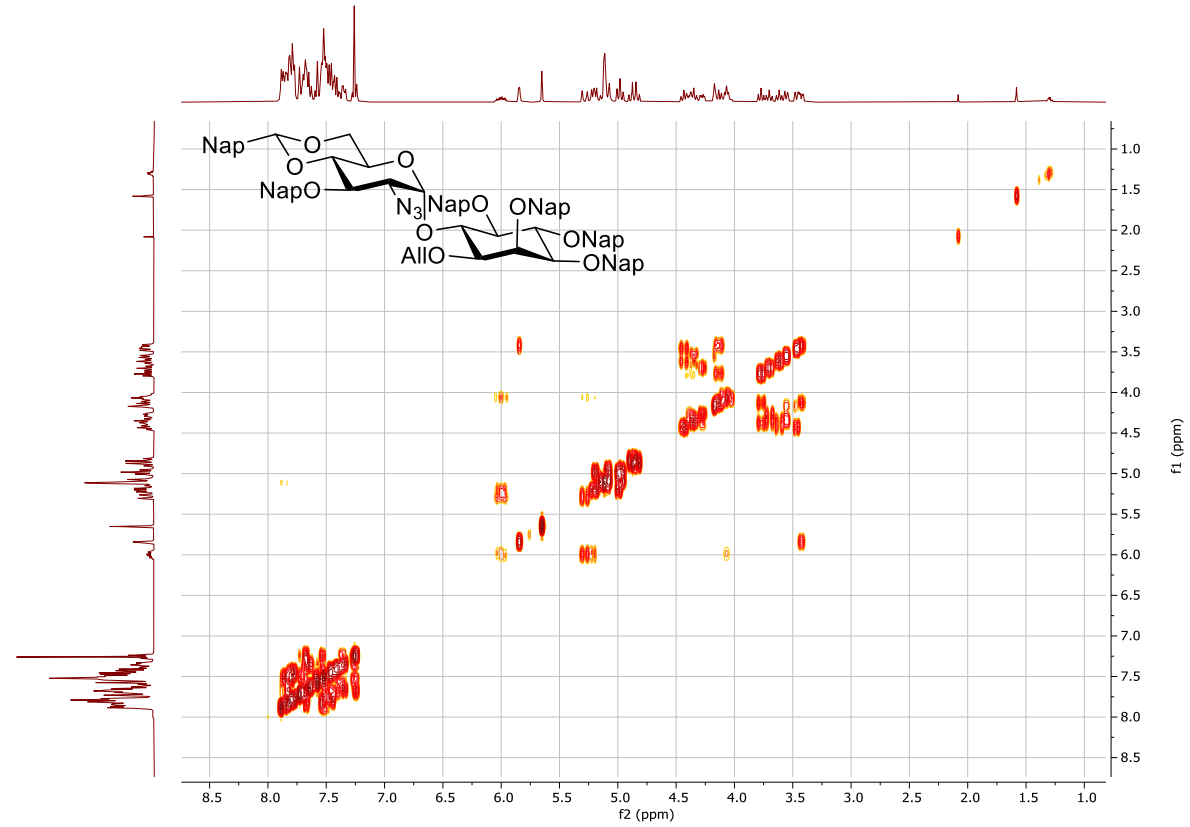

HSQC-NMR spectrum of compound 2-45

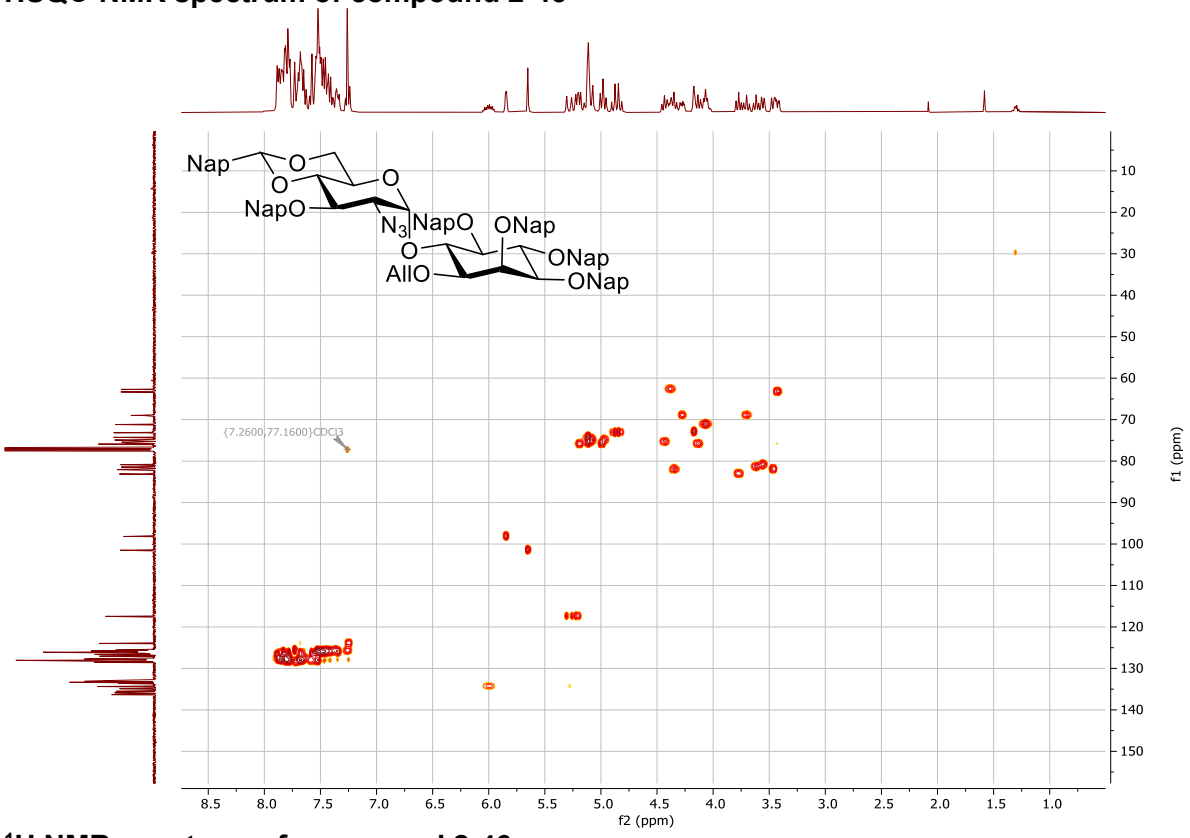

^{1}H NMR spectrum of compound 2-46

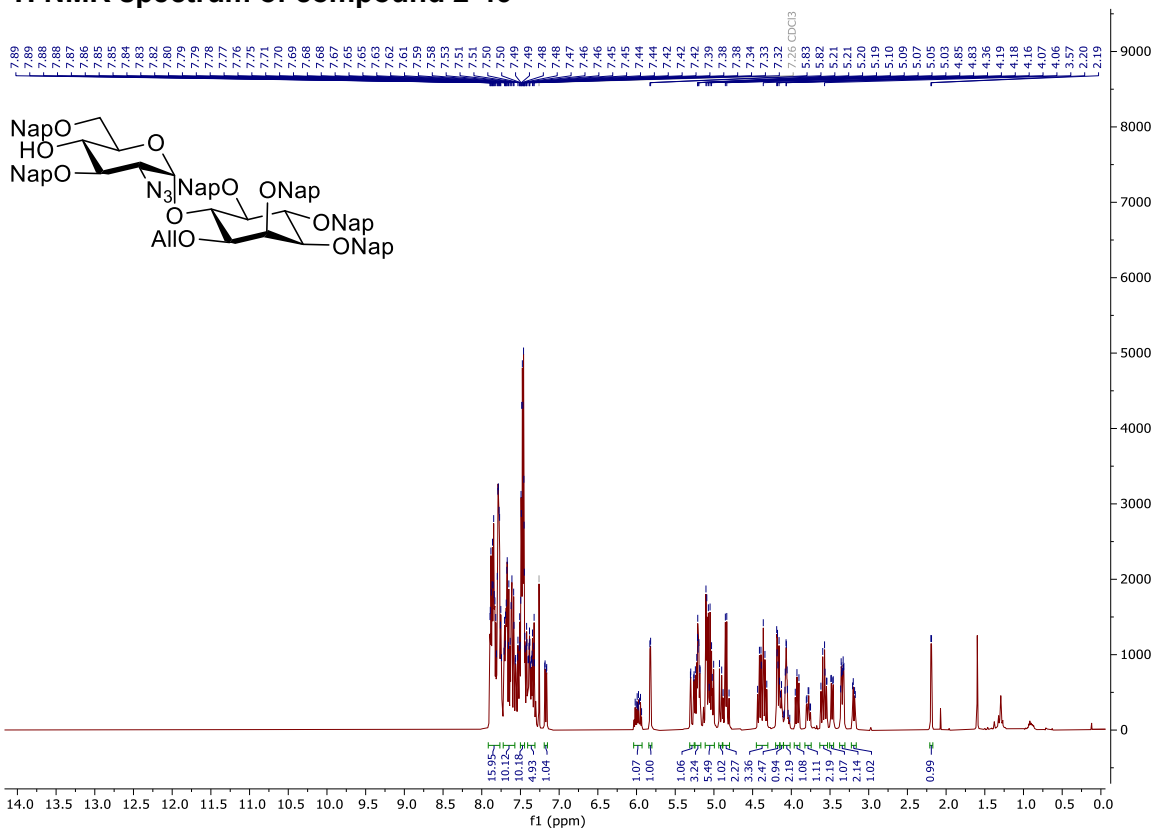

^{13}C NMR spectrum of compound 2-46

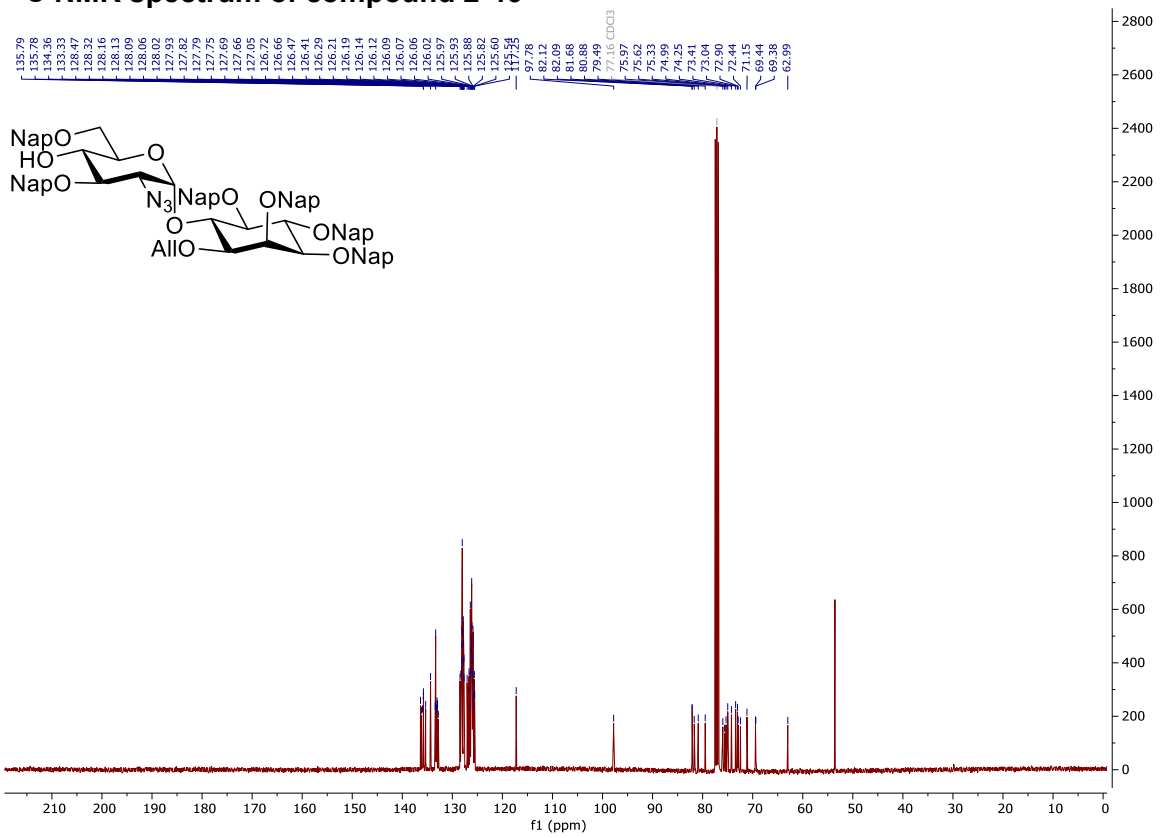

COSY-NMR spectrum of compound 2-46

HSQC-NMR spectrum of compound 2-46

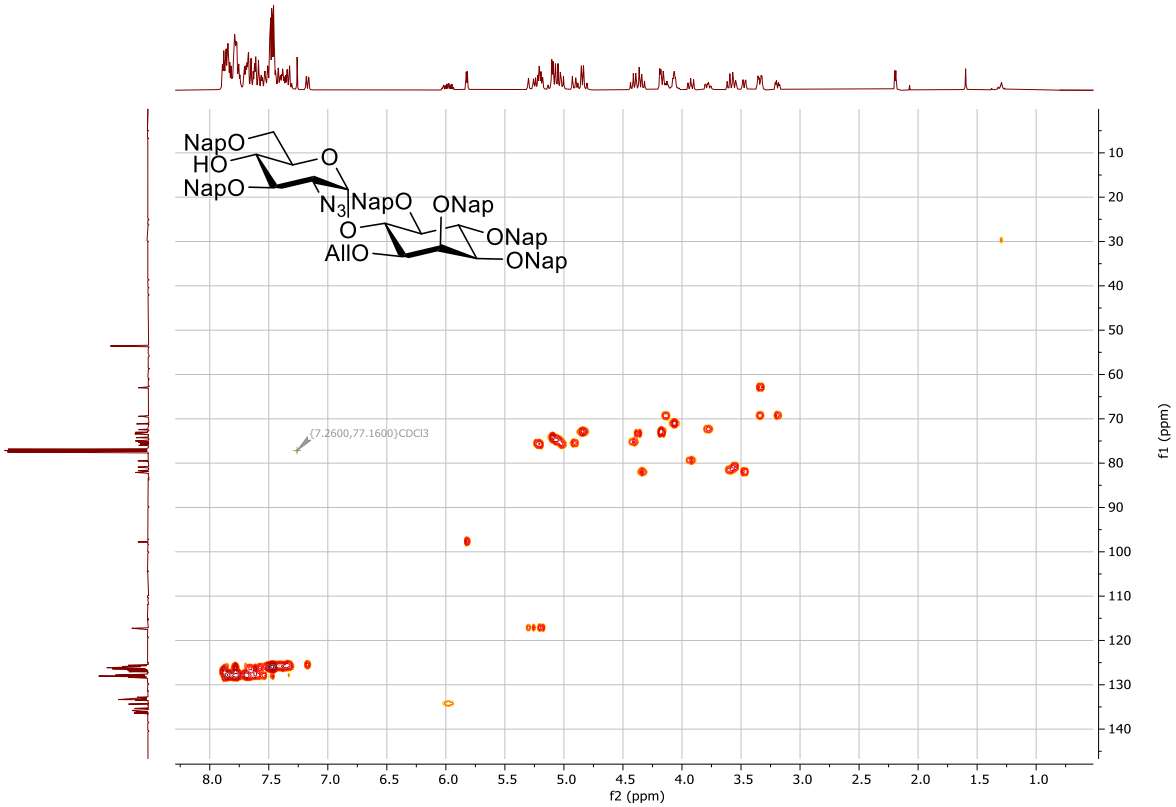

^{1}H NMR spectrum of compound 2-7

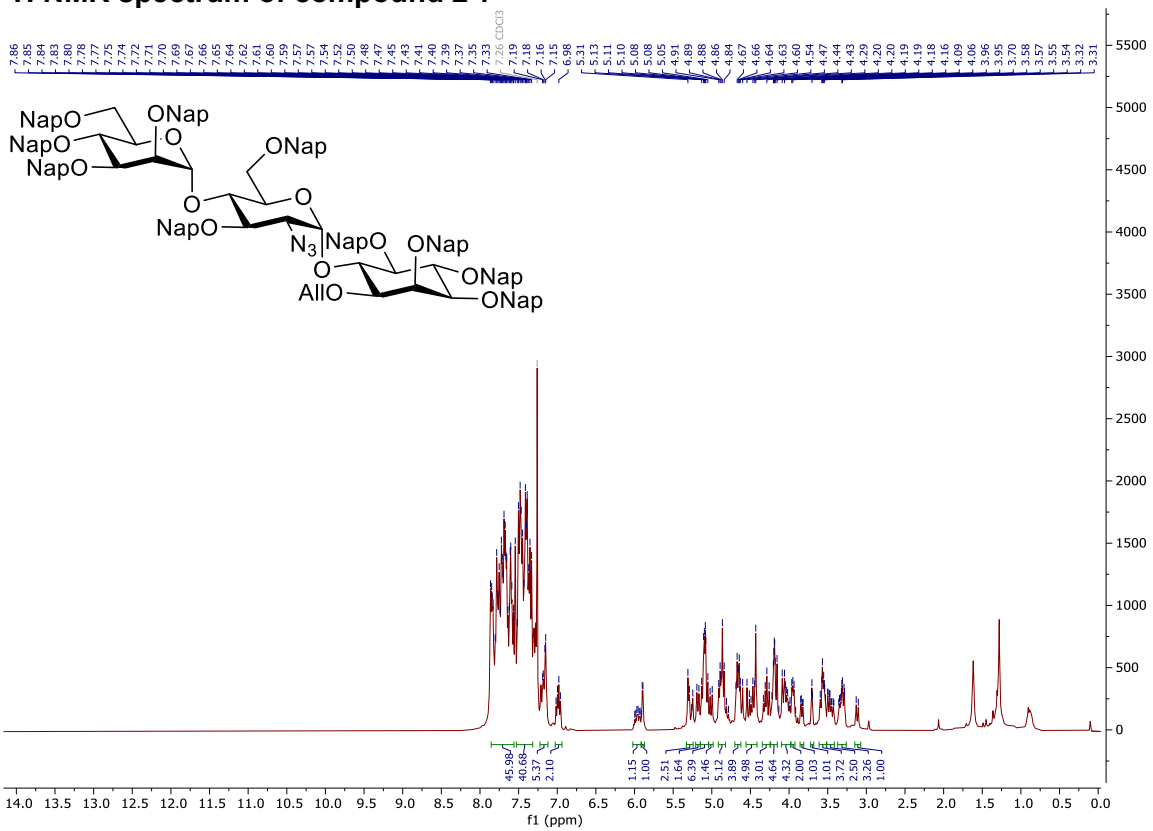

^{13}C NMR spectrum of compound 2-7

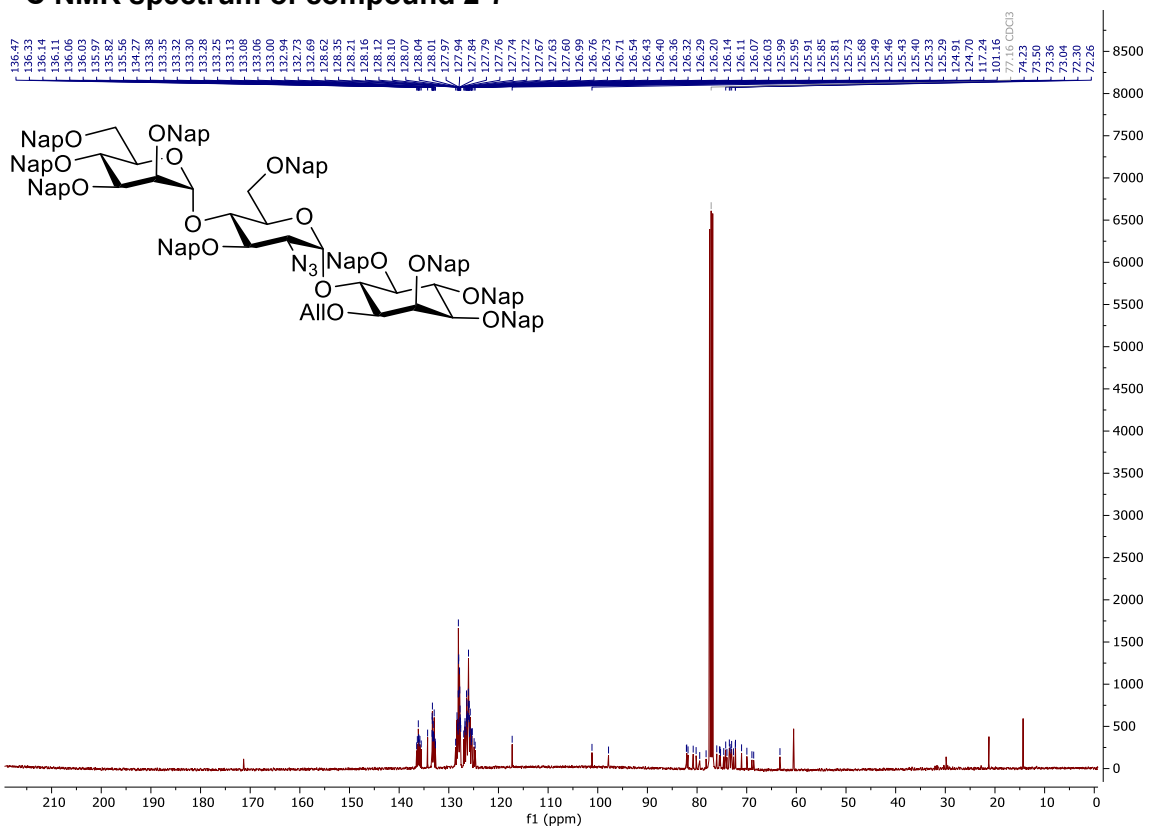

COSY-NMR spectrum of compound 2-7

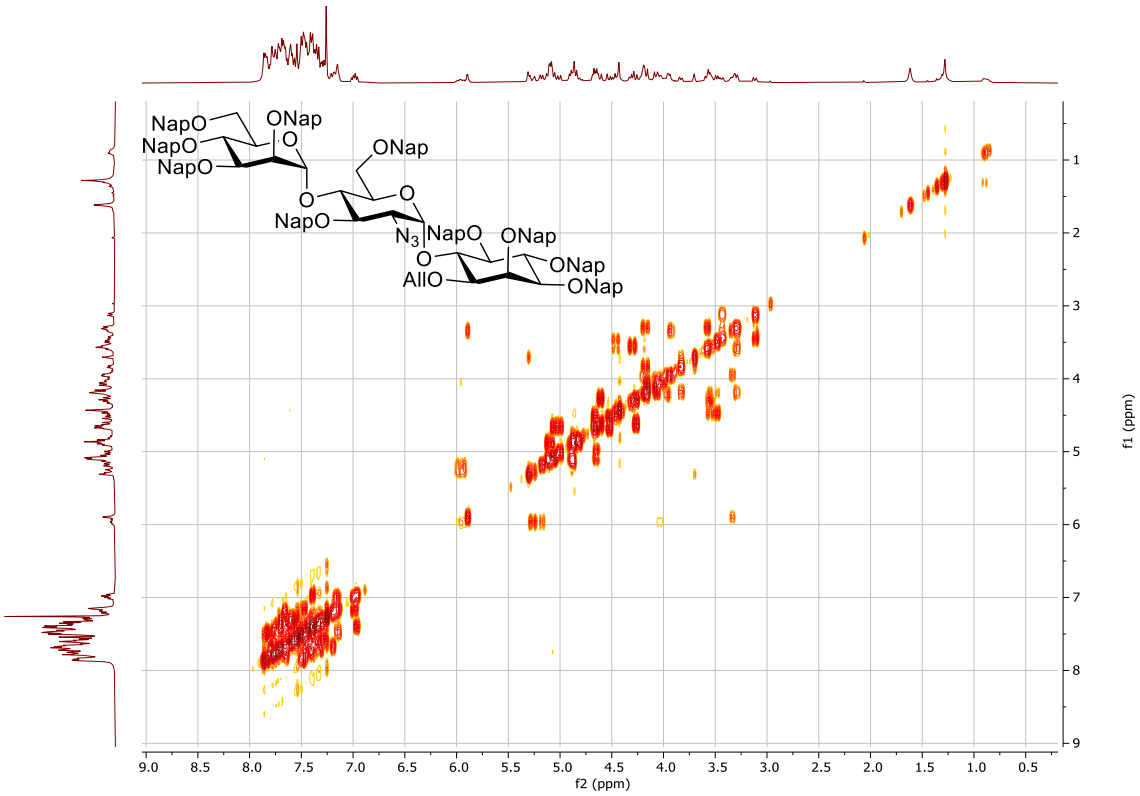

HSQC-NMR spectrum of compound 2-7

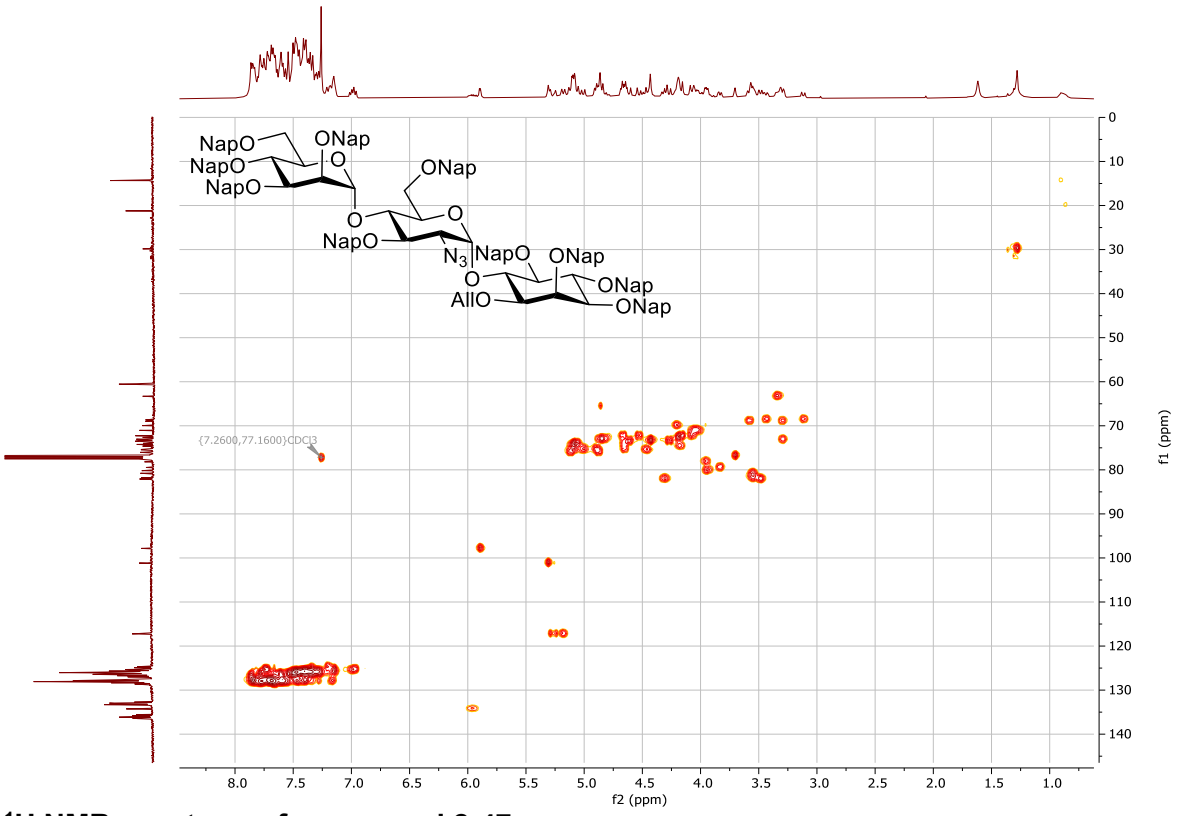

^{1}H NMR spectrum of compound 2-47

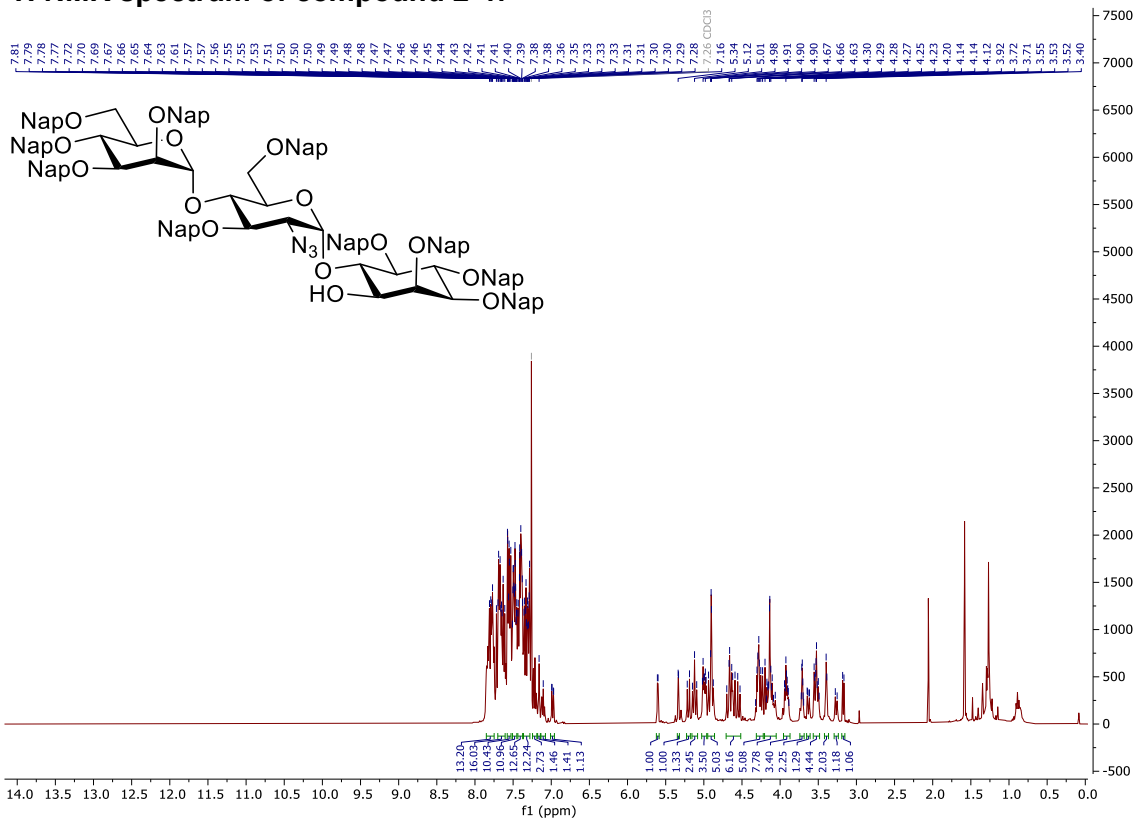

^{13}C NMR spectrum of compound 2-47

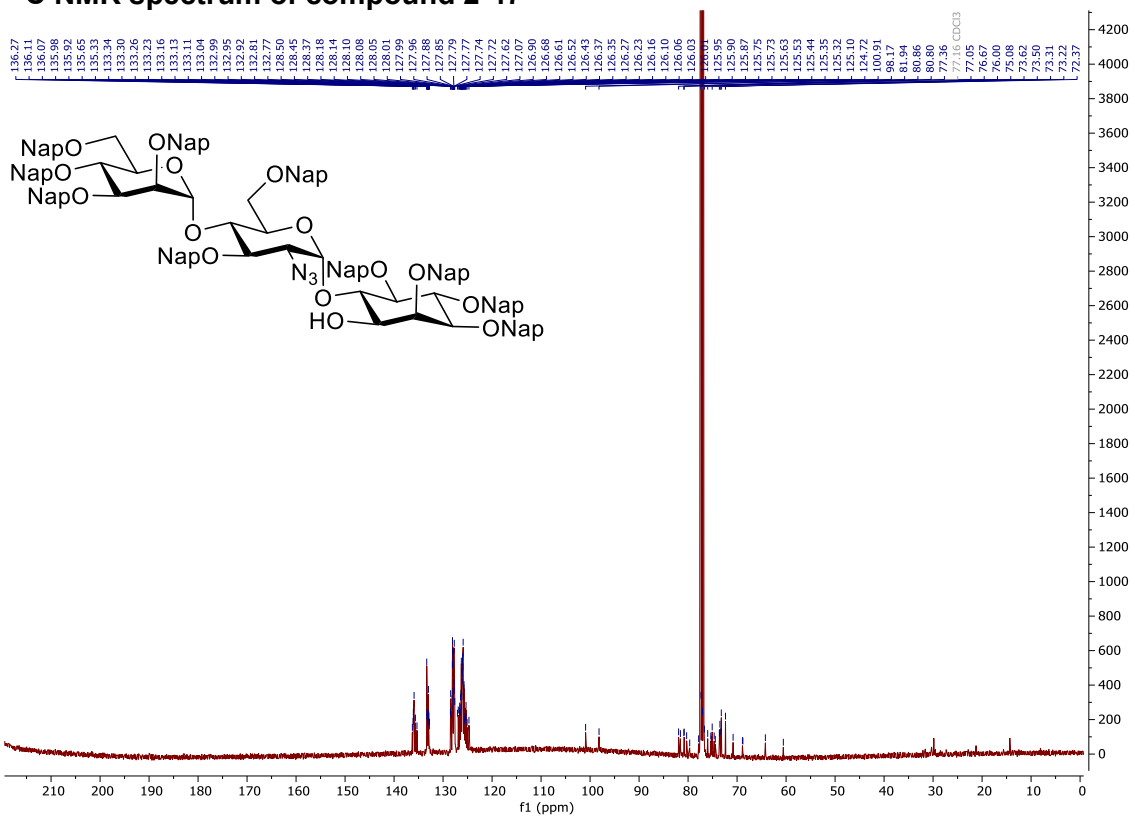

COSY-NMR spectrum of compound 2-47

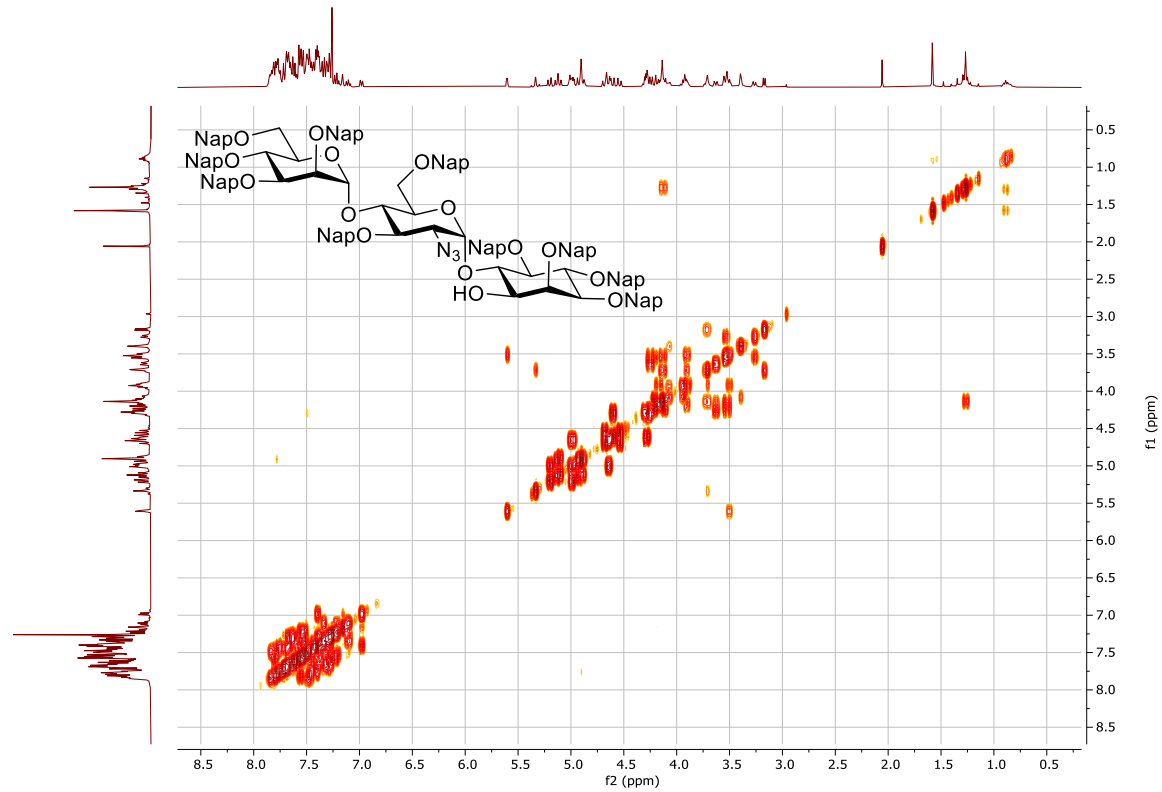

HSQC-NMR spectrum of compound 2-47

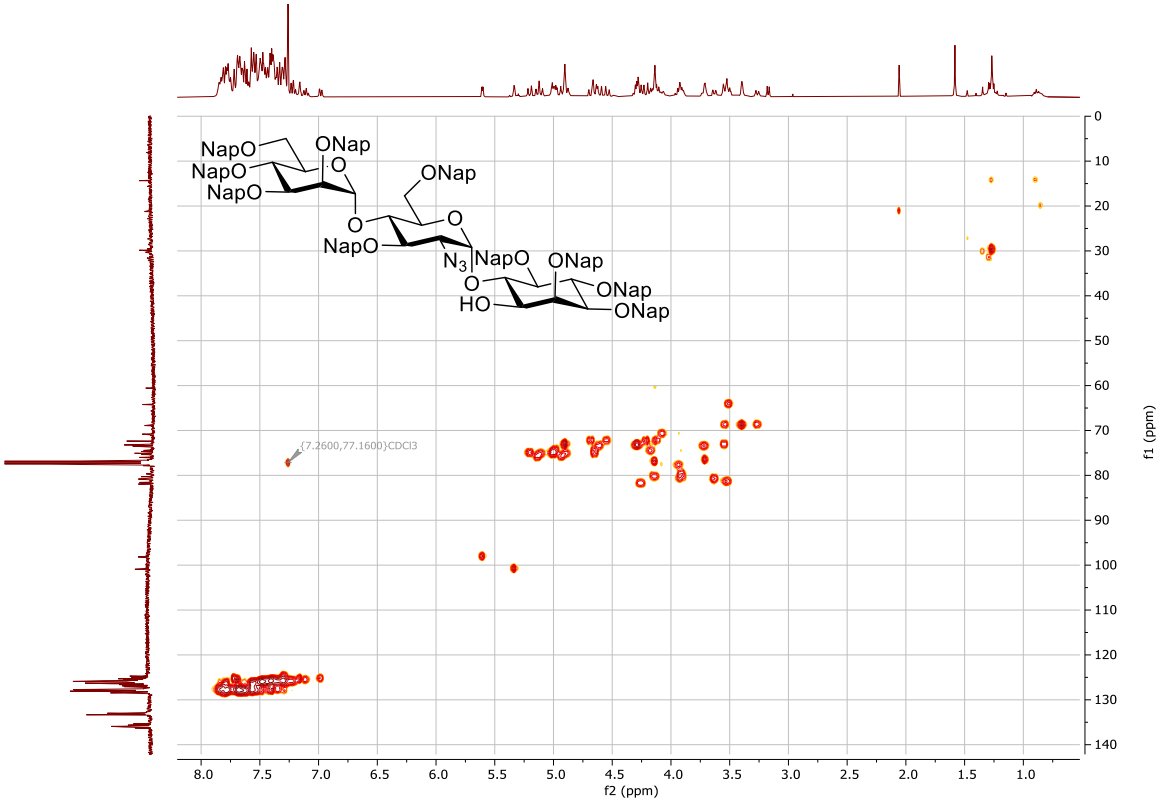

^{1}H NMR spectrum of compound 2-48

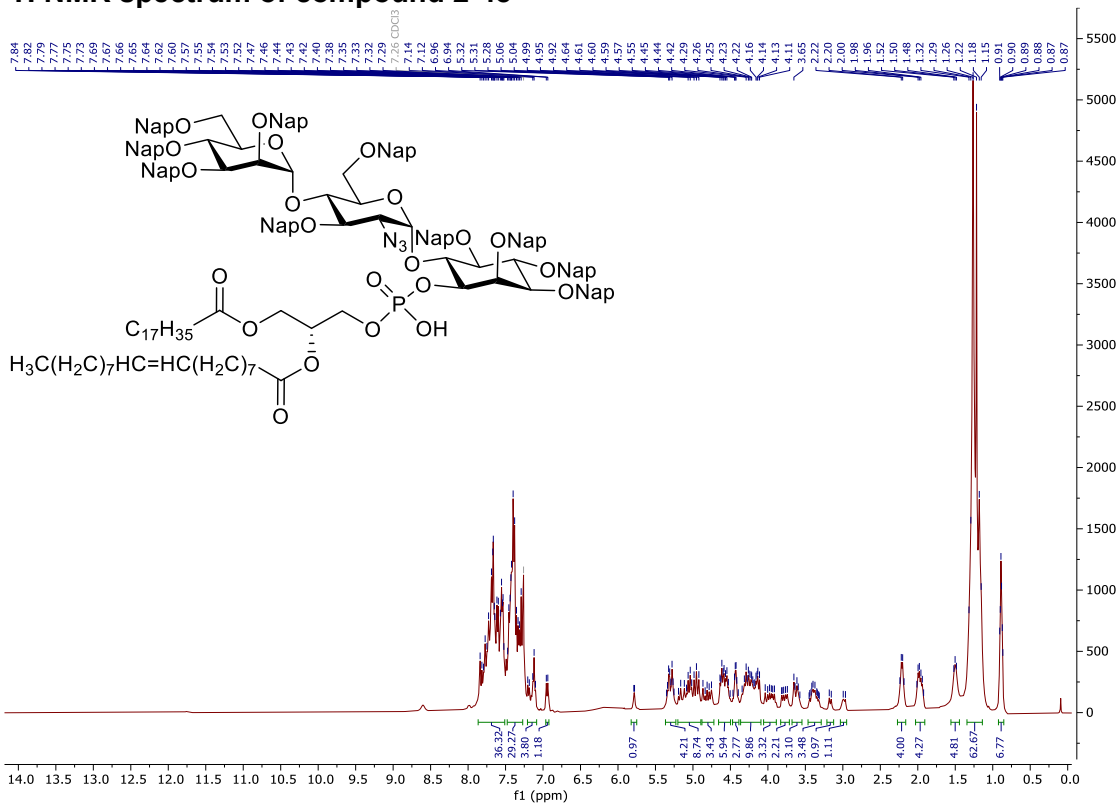

^{13}C NMR spectrum of compound 2-48

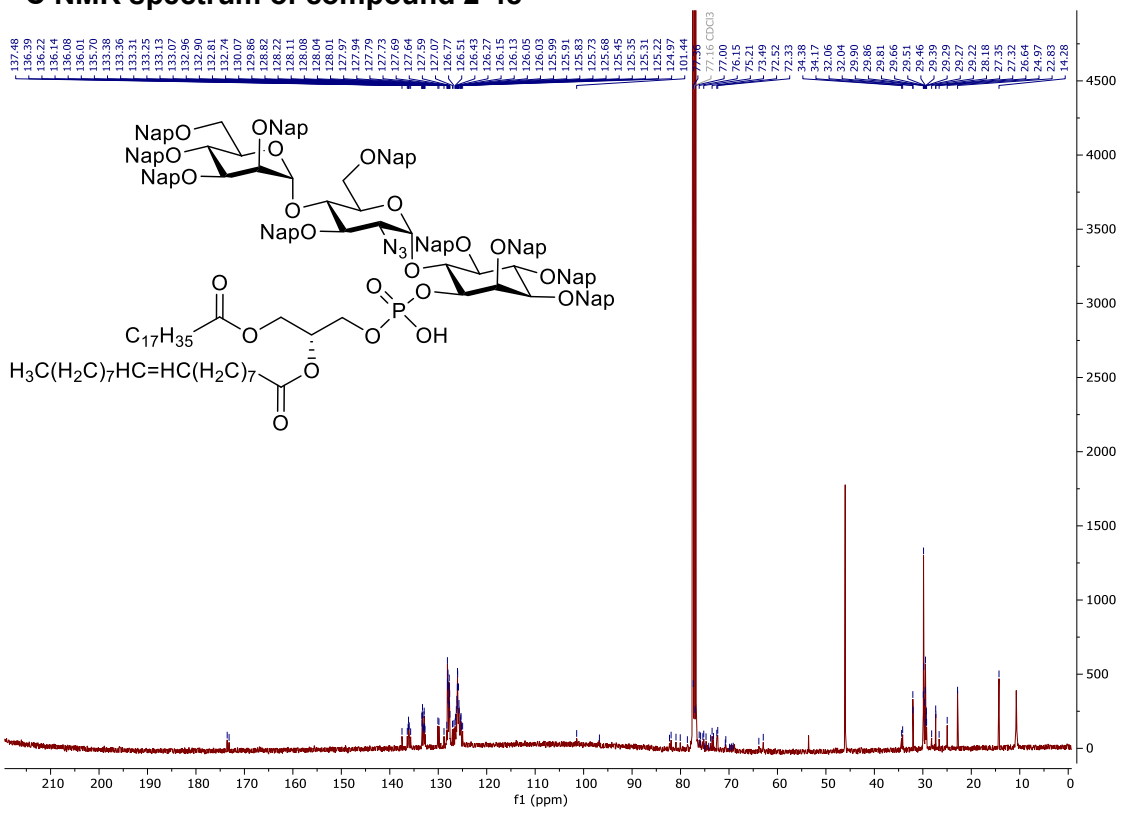

COSY-NMR spectrum of compound 2-48

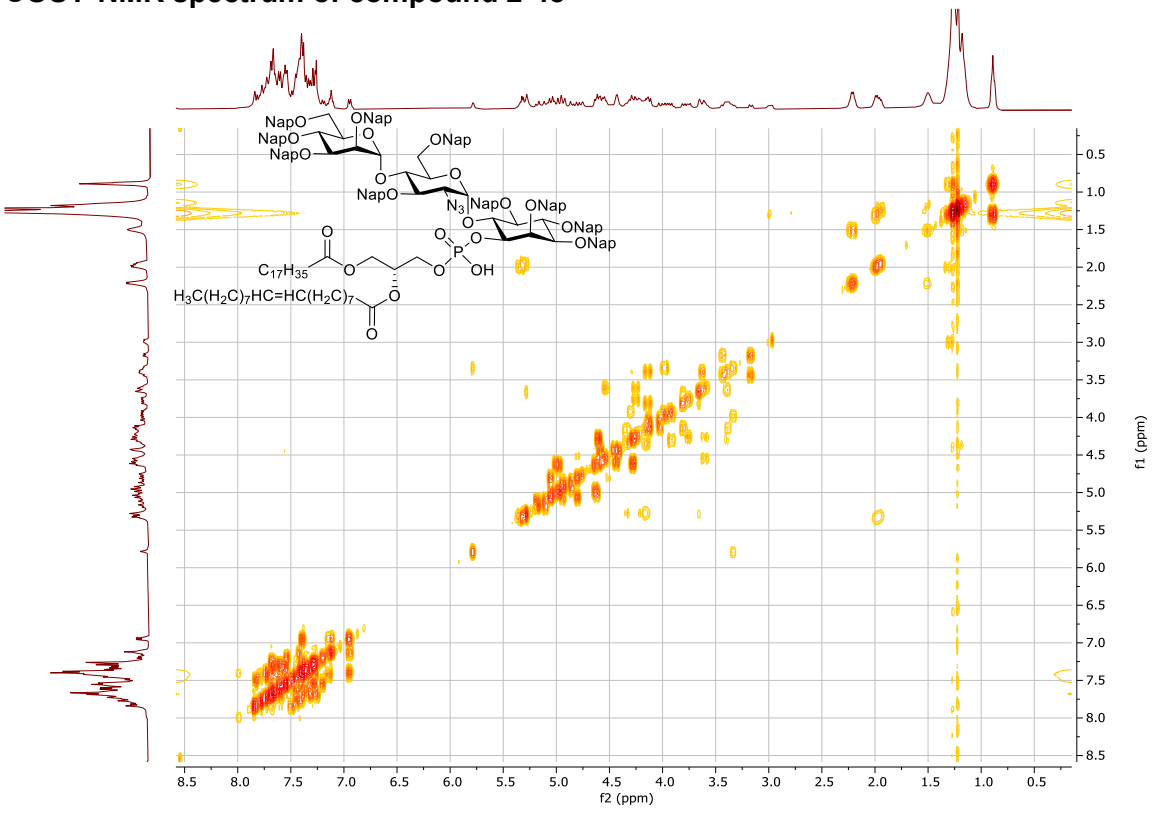

HSQC-NMR spectrum of compound 2-48

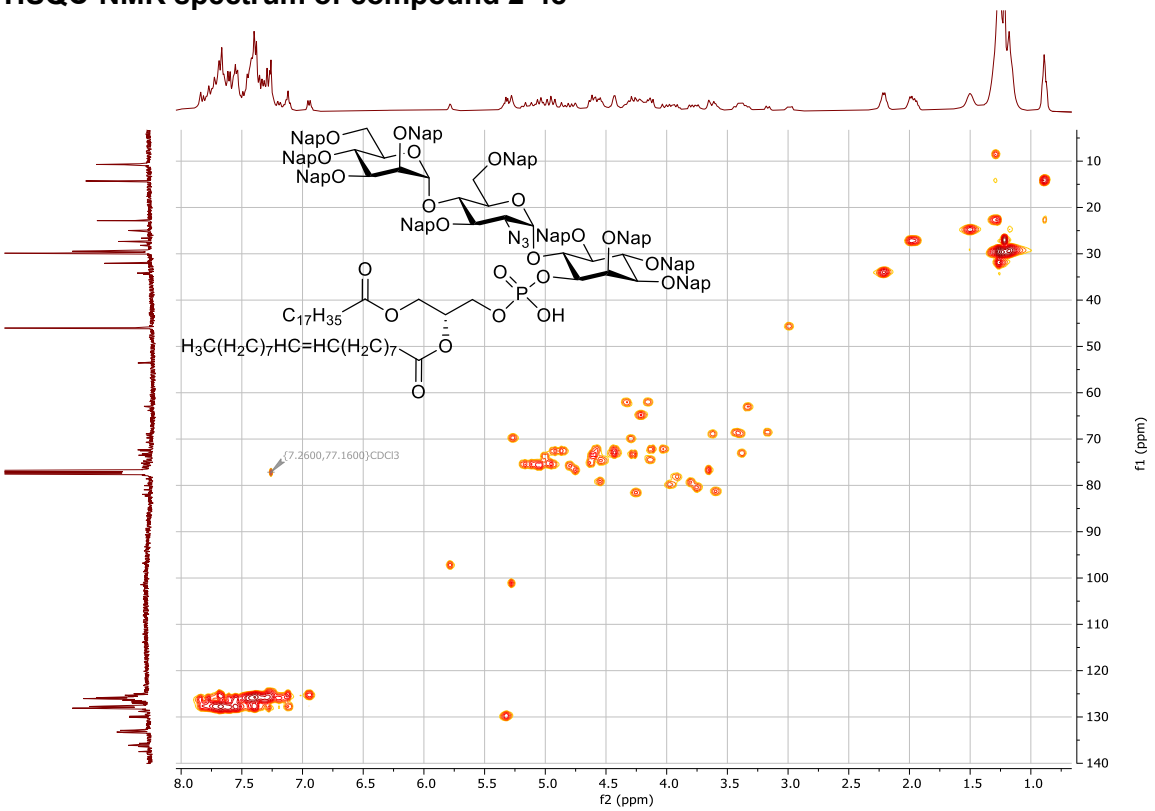

^{31}P NMR spectrum of compound 2-48

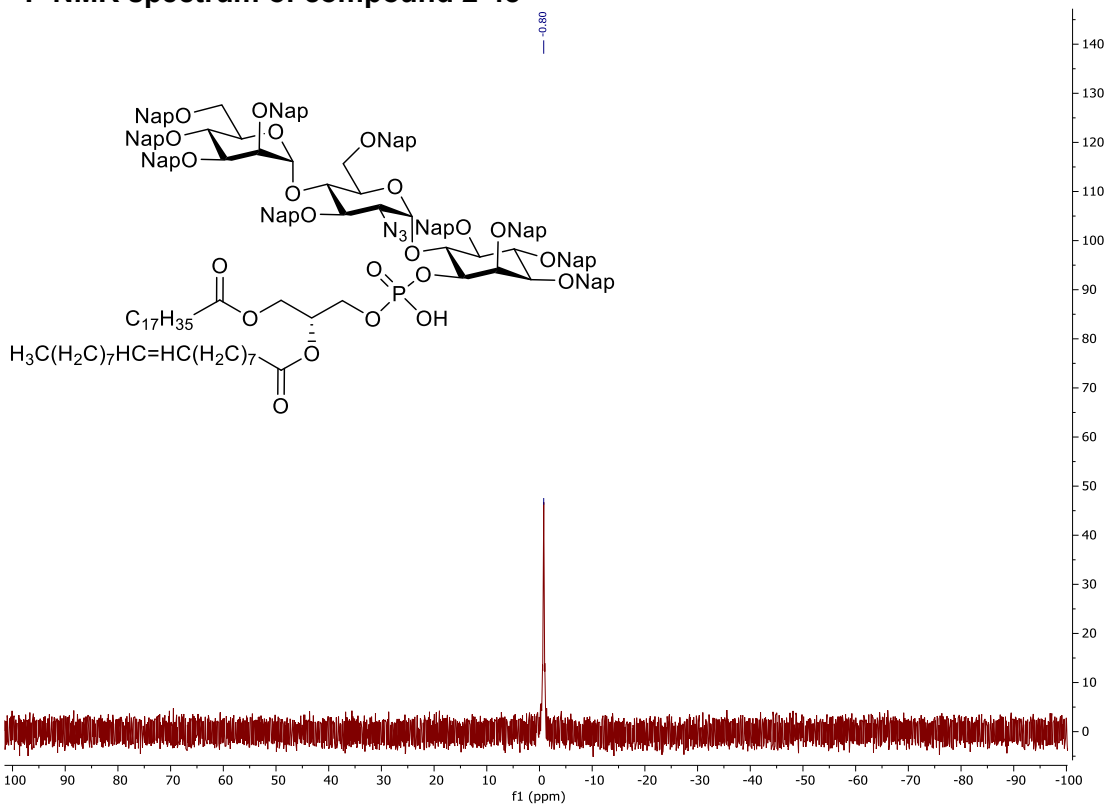

^{1}H NMR spectrum of GPI fragment 2-4

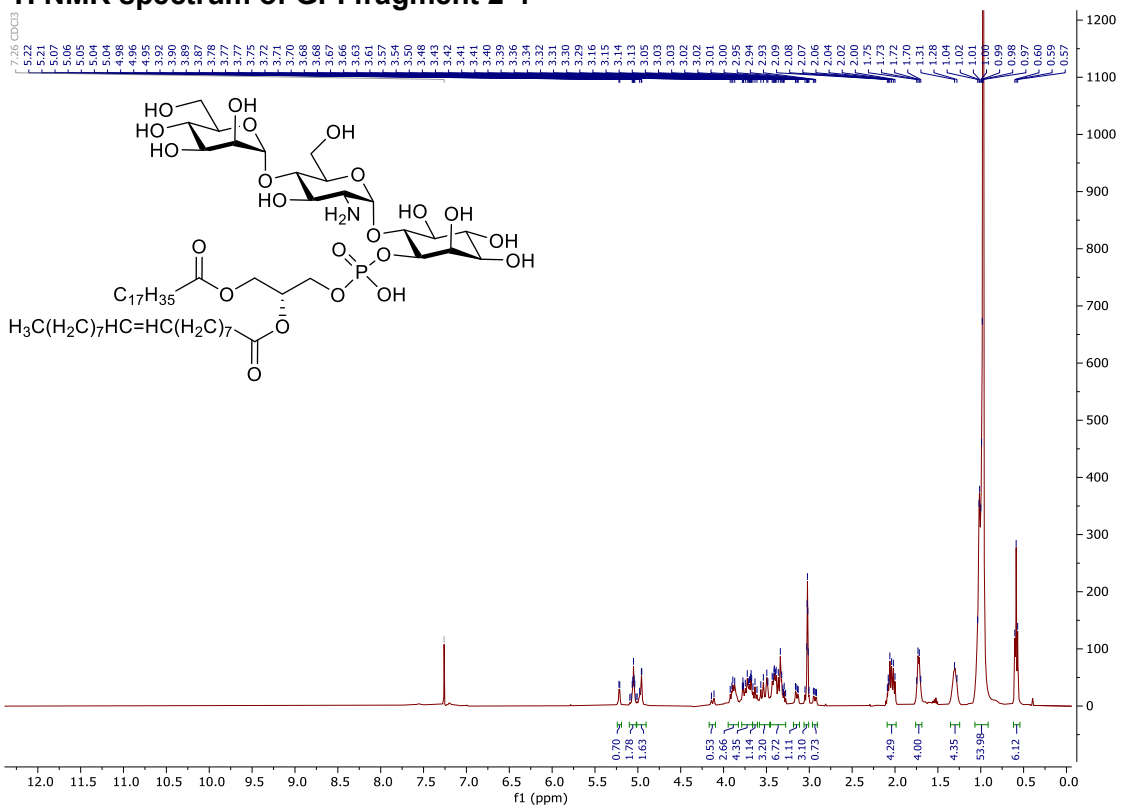

^{13}C NMR spectrum of GPI fragment 2-4

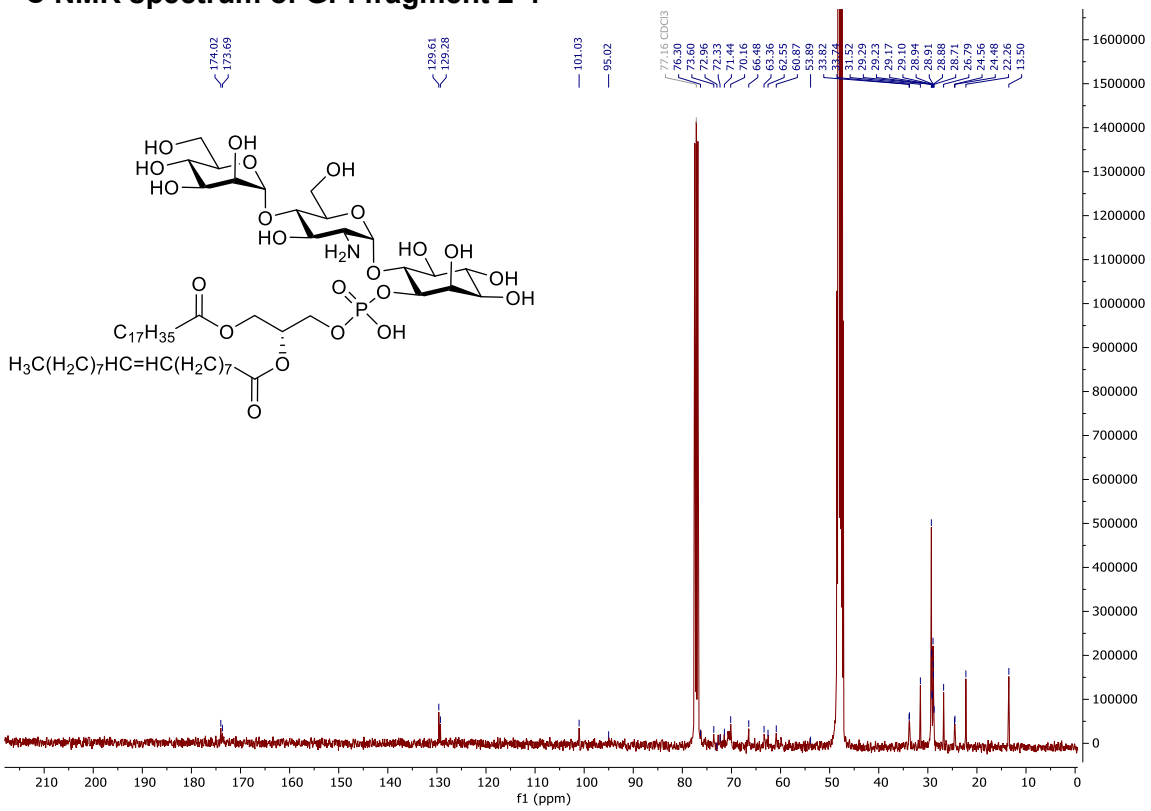

COSY-NMR spectrum of GPI fragment 2-4

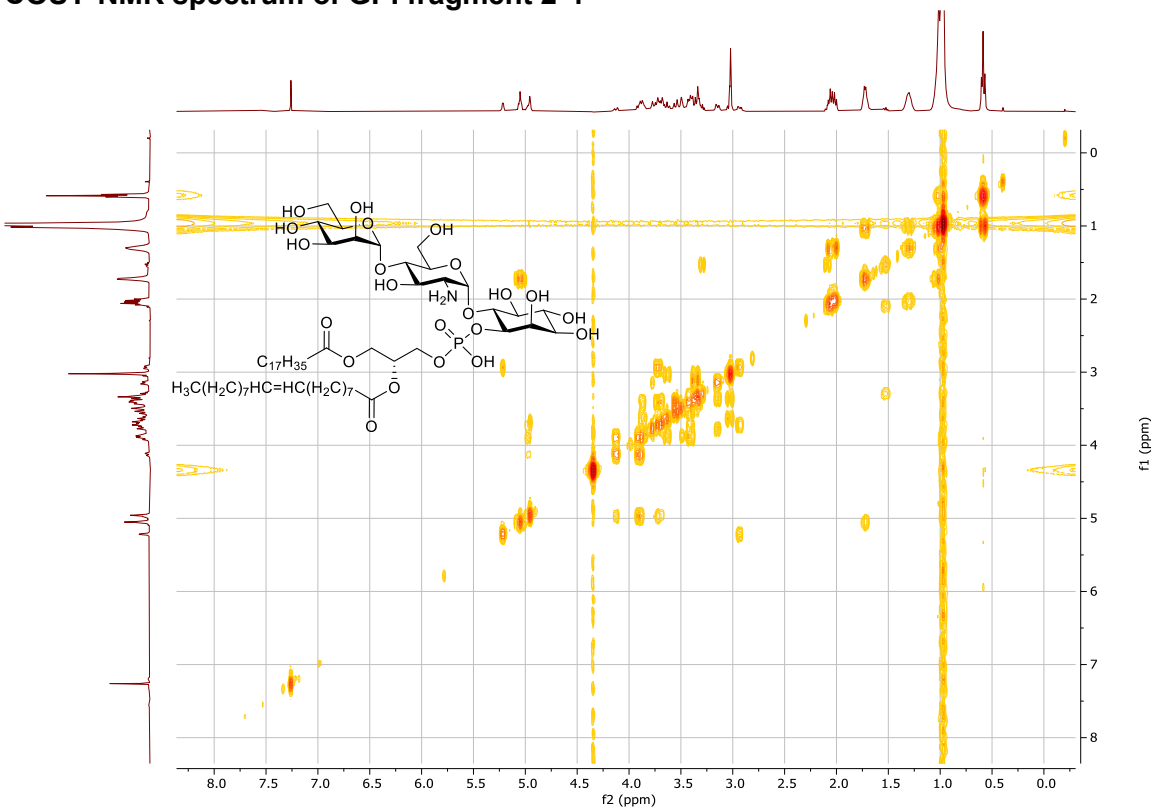

HSQC-NMR spectrum of GPI fragment 2-4

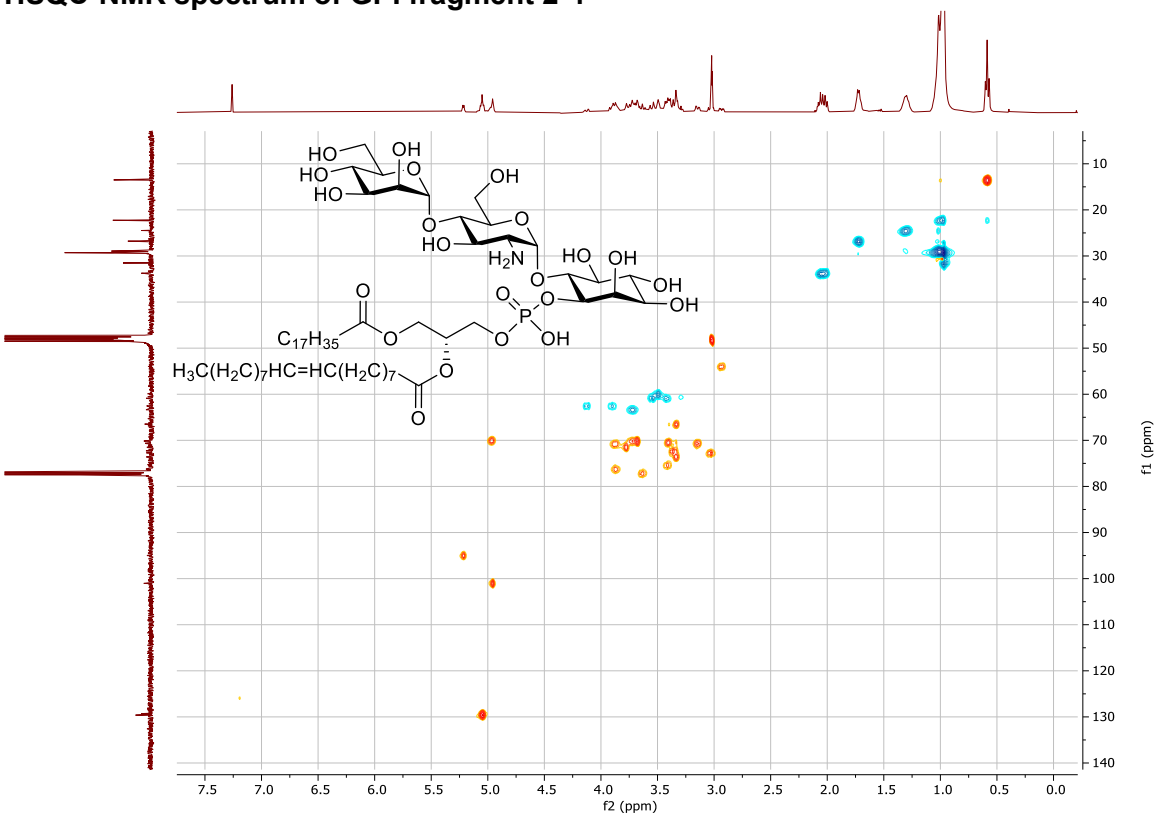

^{31}P-NMR spectrum of GPI fragment 2-4

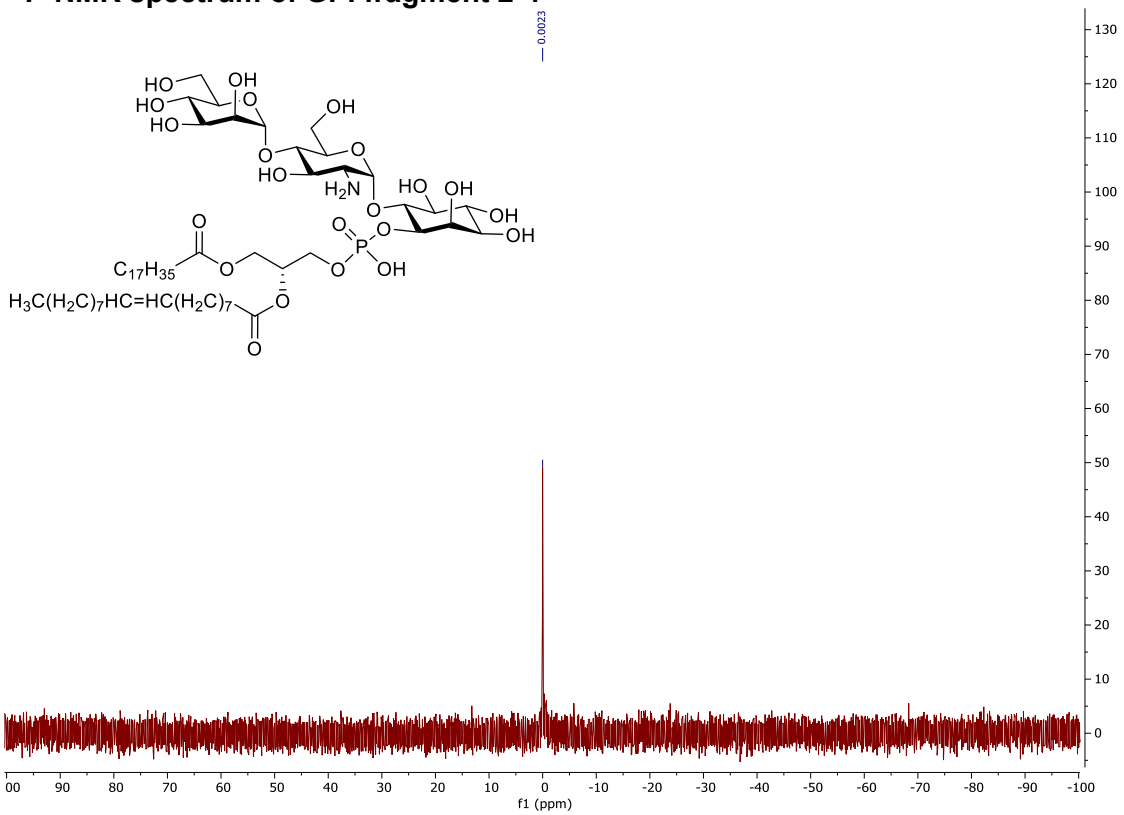

^{1}H NMR spectrum of compound 2-60

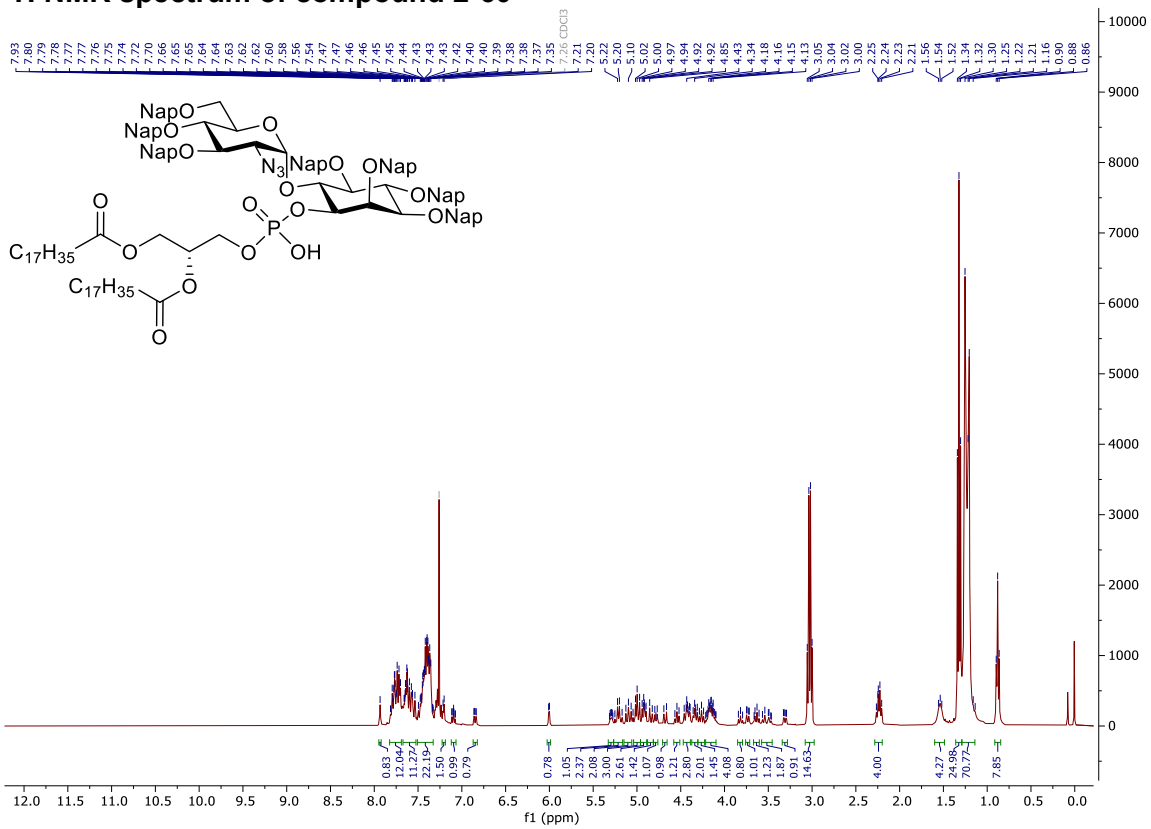

^{13}C NMR spectrum of compound 2-60

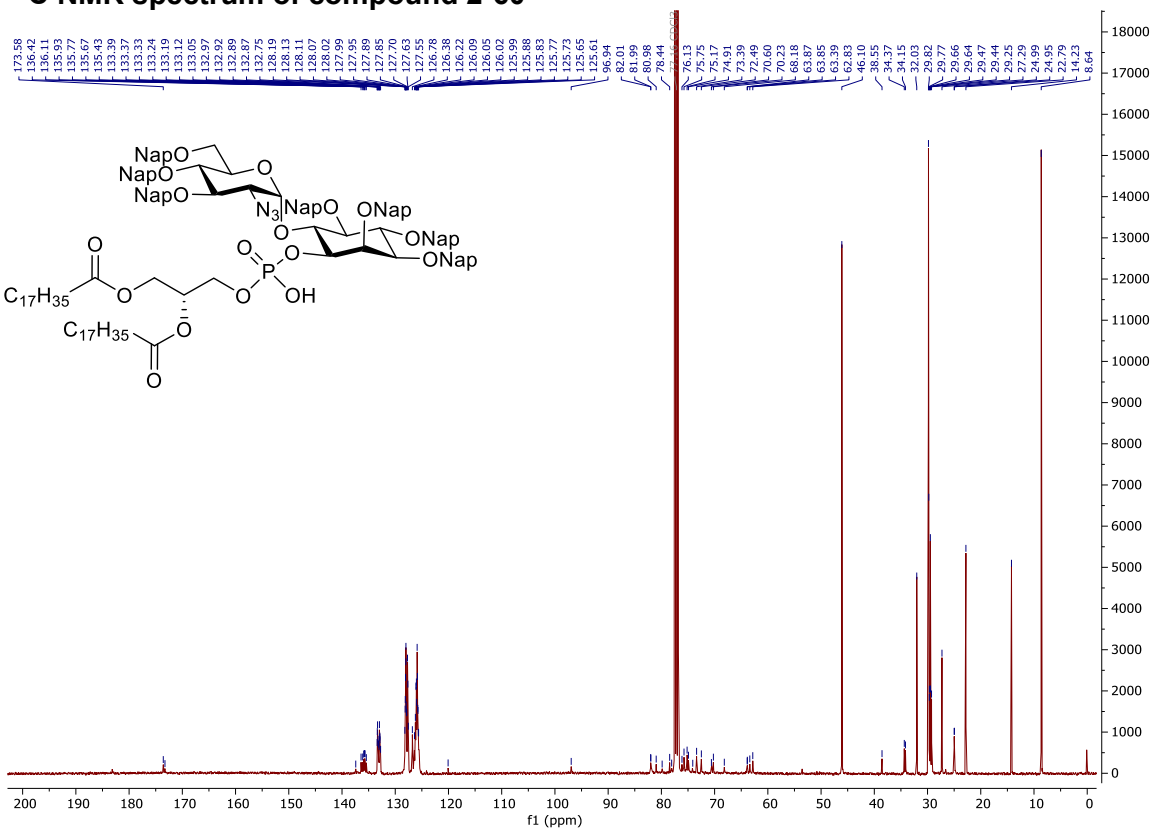

COSY-NMR spectrum of compound 2-60

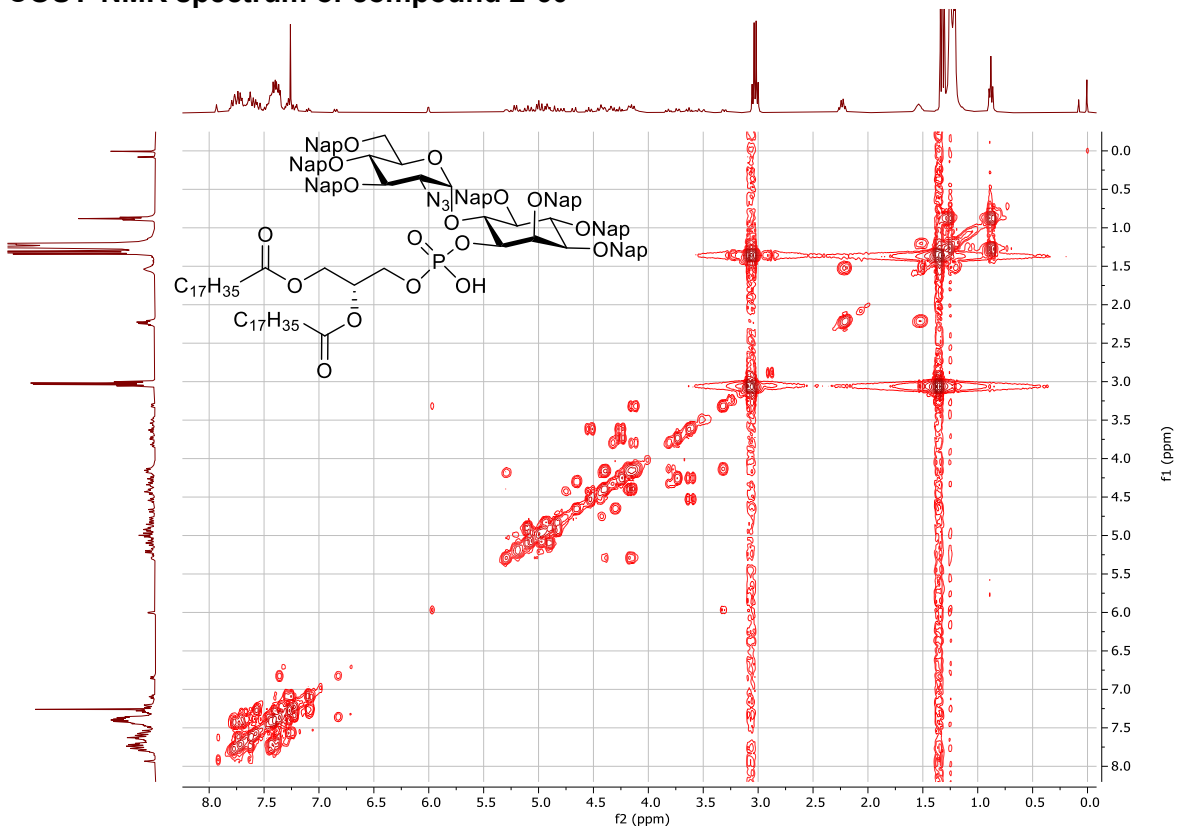

HSQC-NMR spectrum of compound 2-60

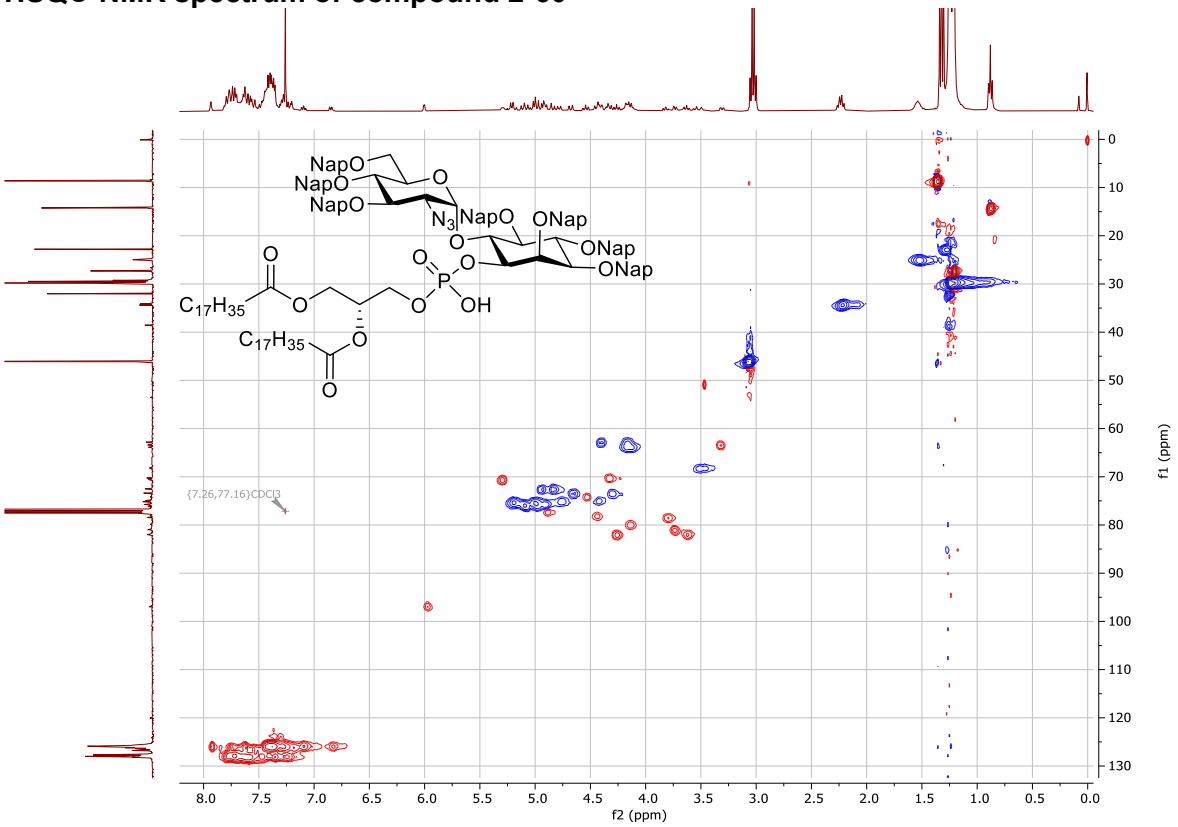

^{31}P-NMR spectrum of compound 2-60

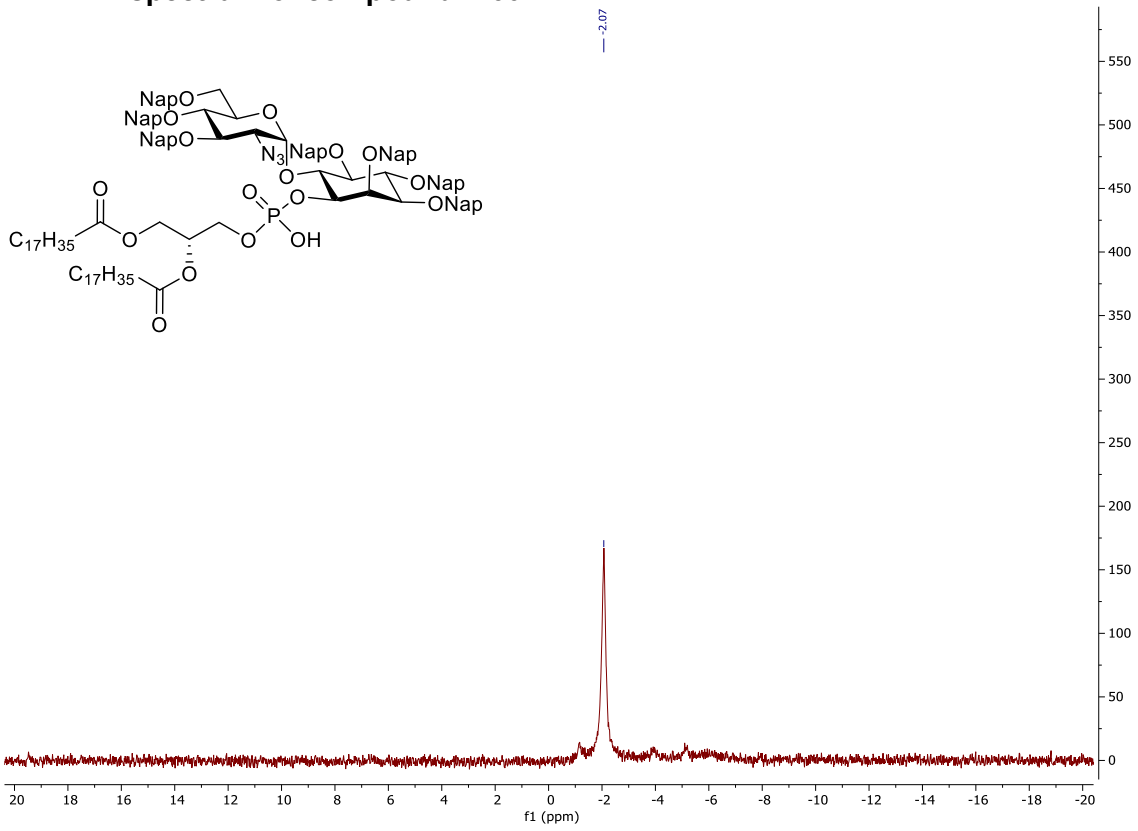

^{1}H NMR spectrum of GPI fragment 2-49

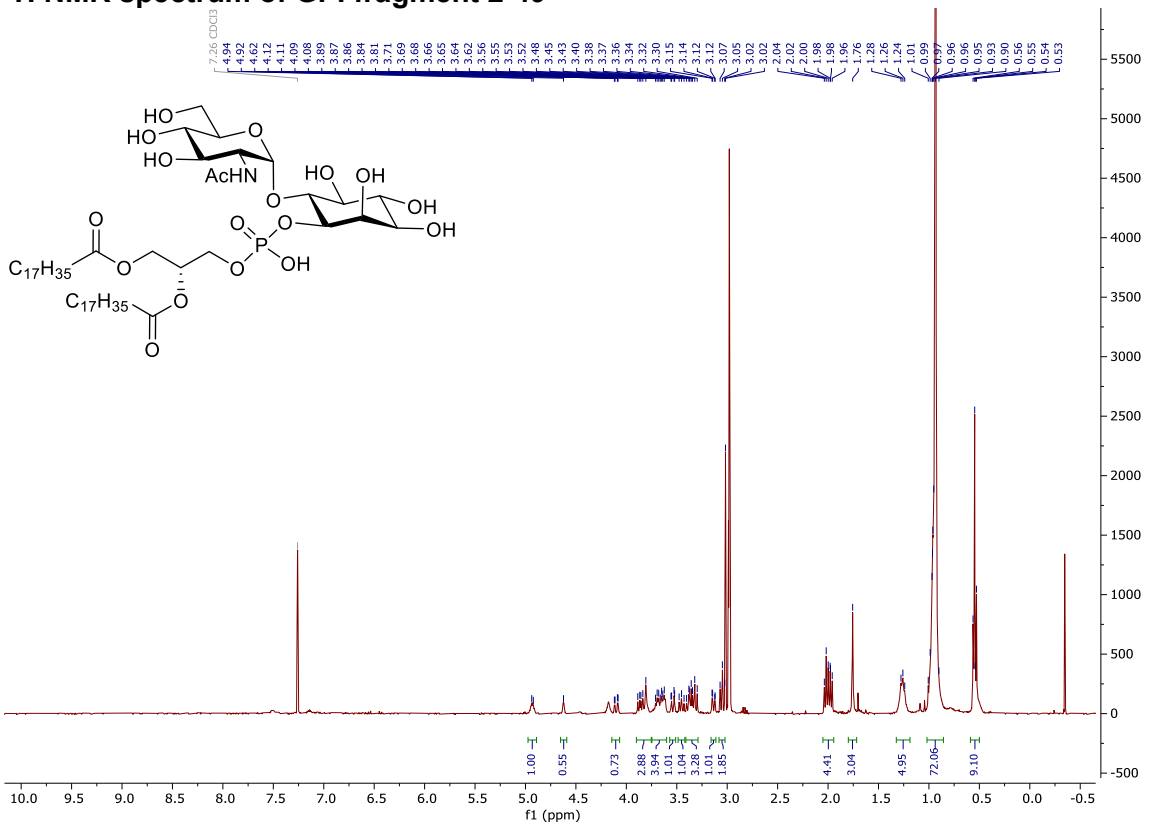

^{13}C NMR spectrum of GPI fragment 2-49

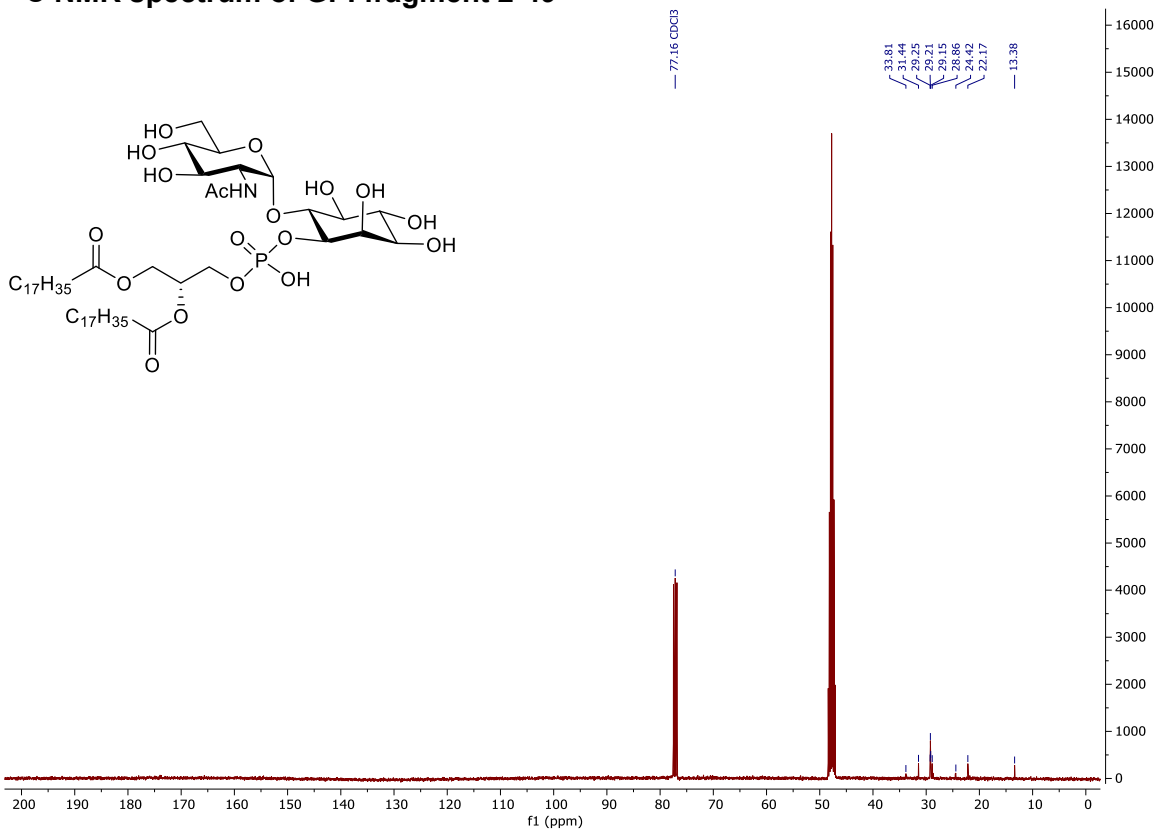

COSY-NMR spectrum of GPI fragment 2-49

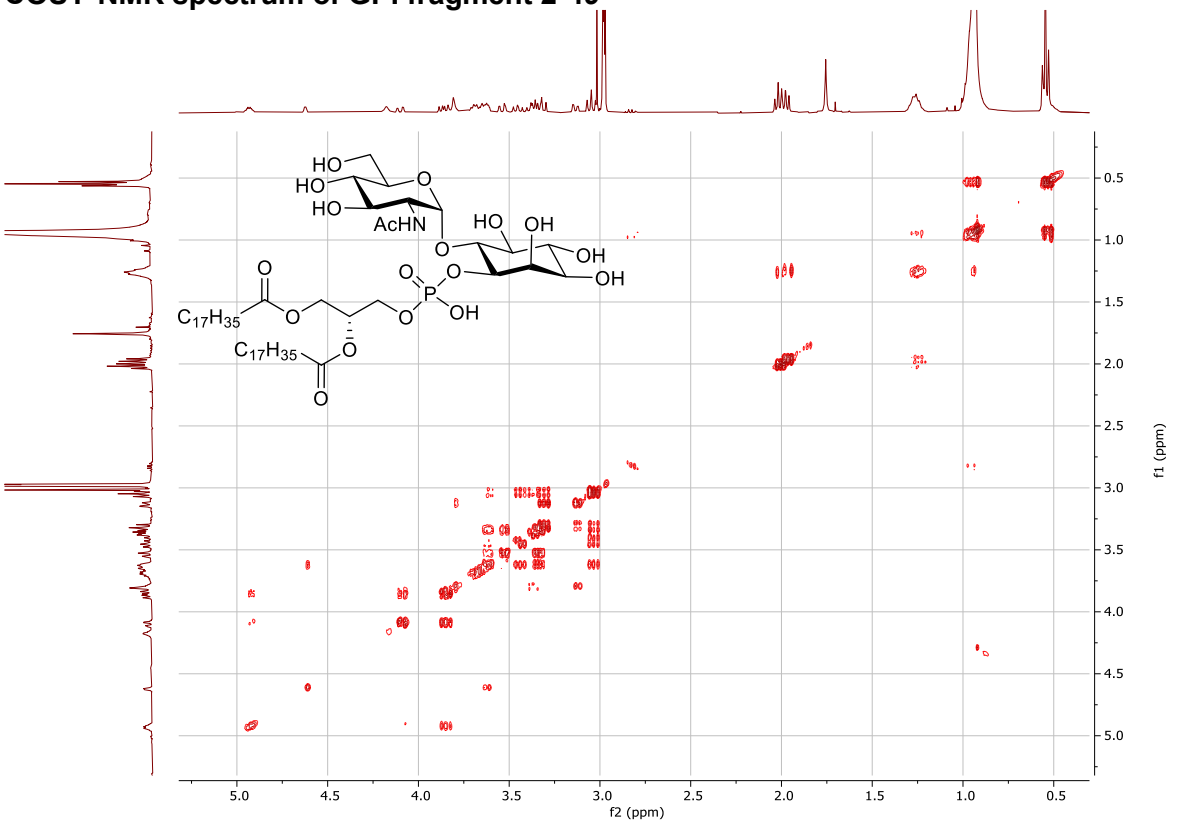

HSQC-NMR spectrum of GPI fragment 2-49

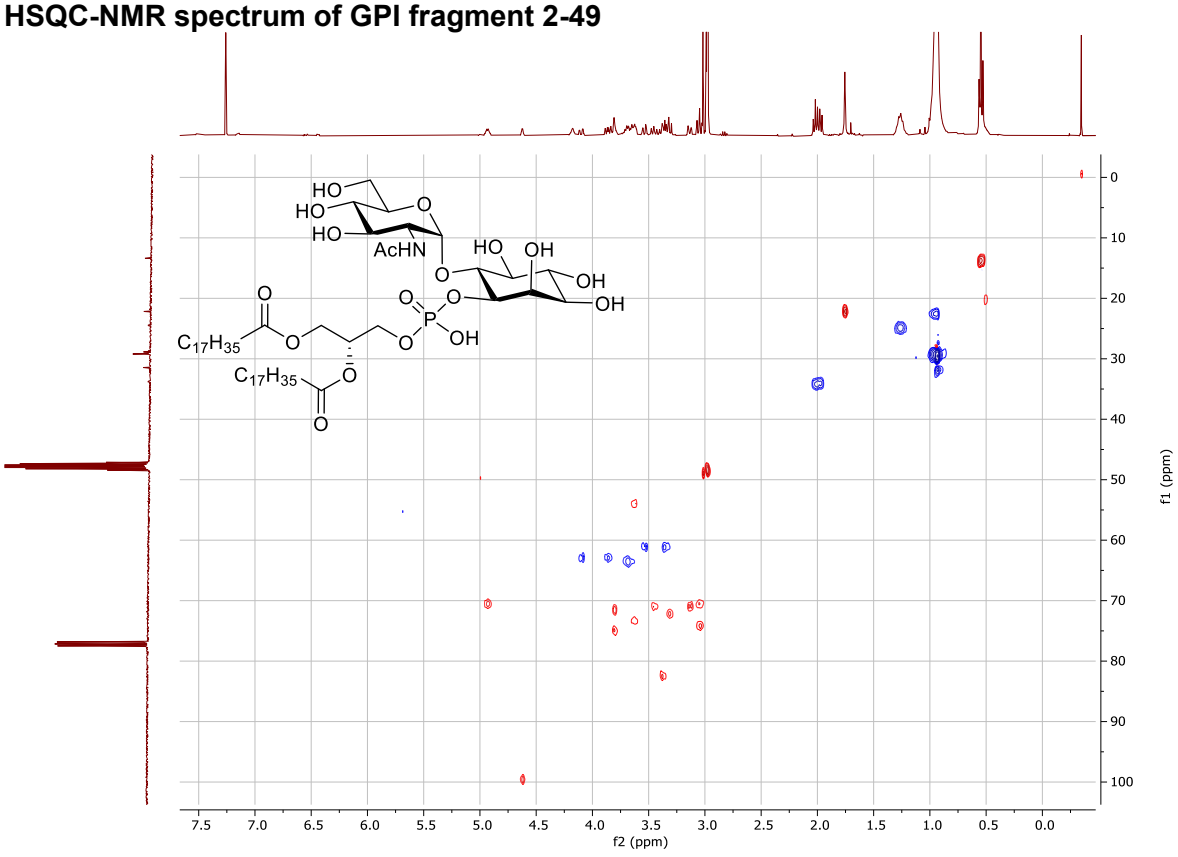

^{31}P-NMR spectrum of GPI fragment 2-49

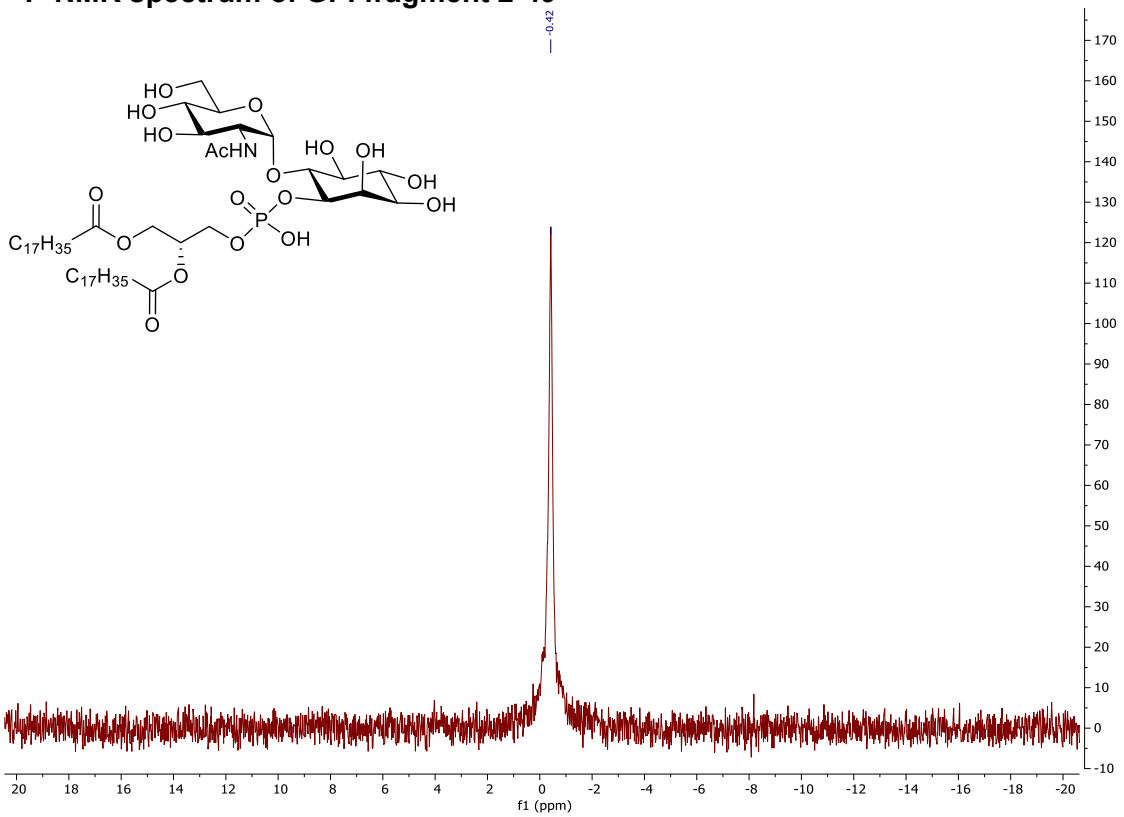

^{1}H NMR spectrum of GPI fragment 2-50

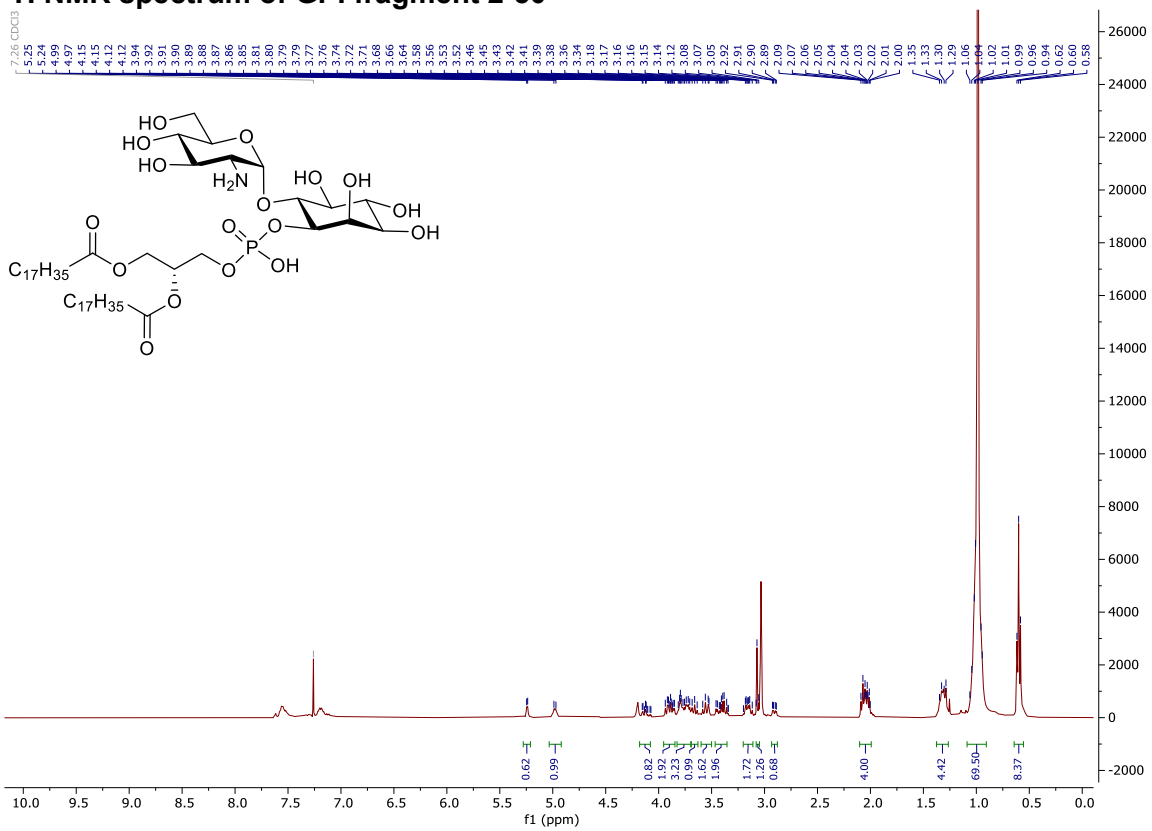

^{13}C NMR spectrum of GPI fragment 2-50

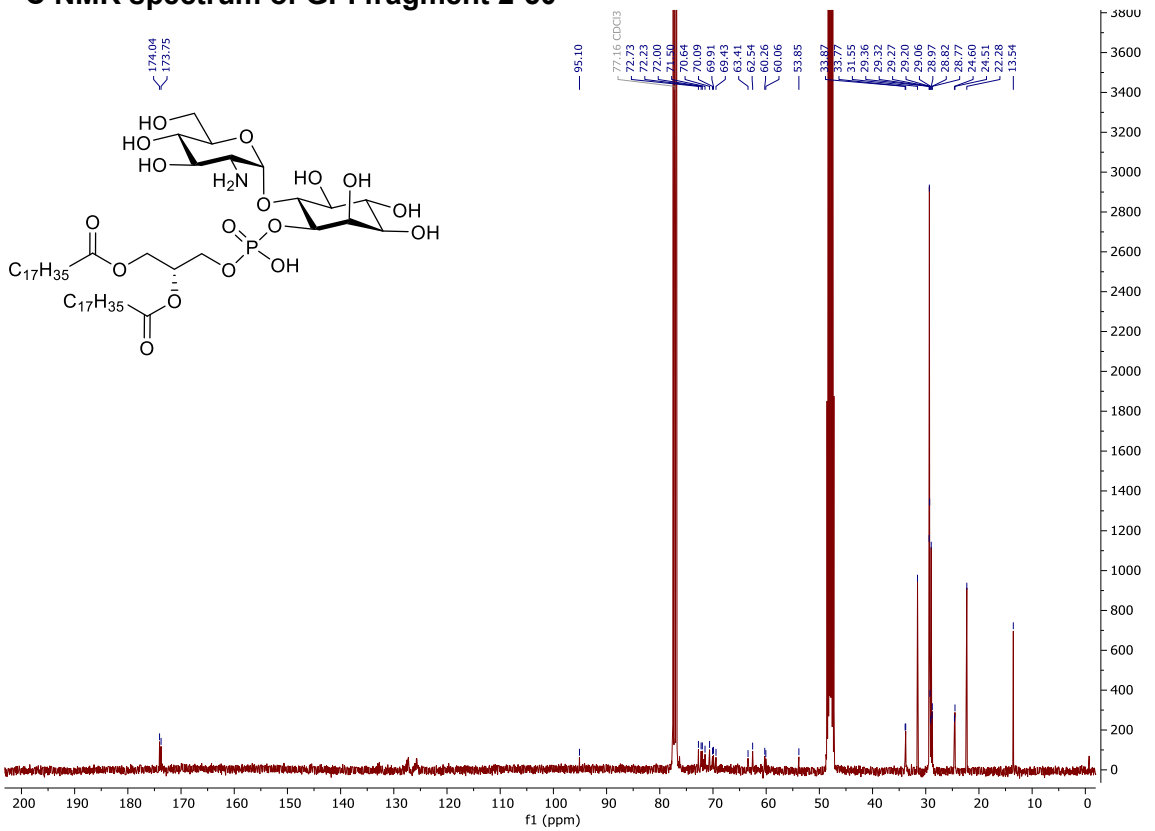

COSY-NMR spectrum of GPI fragment 2-50

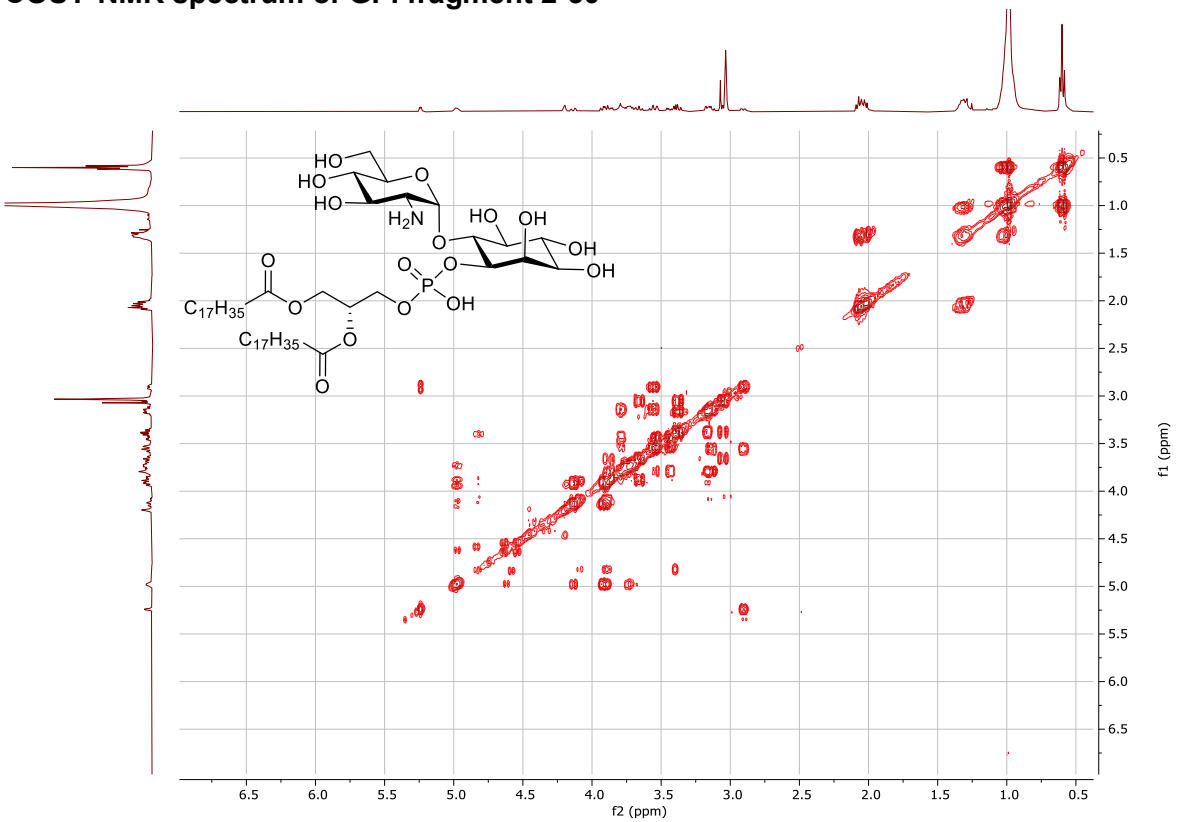

HSQC-NMR spectrum of GPI fragment 2-50

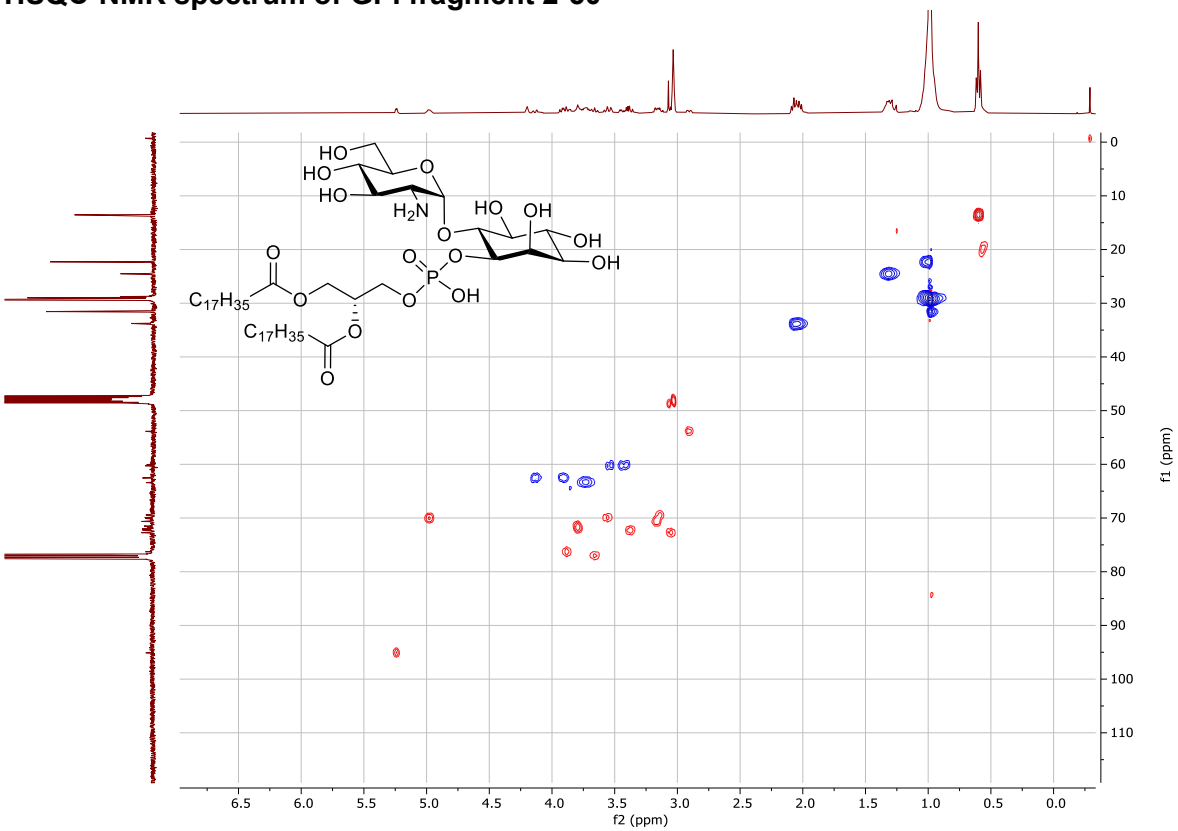

^{31}P-NMR spectrum of GPI fragment 2-50

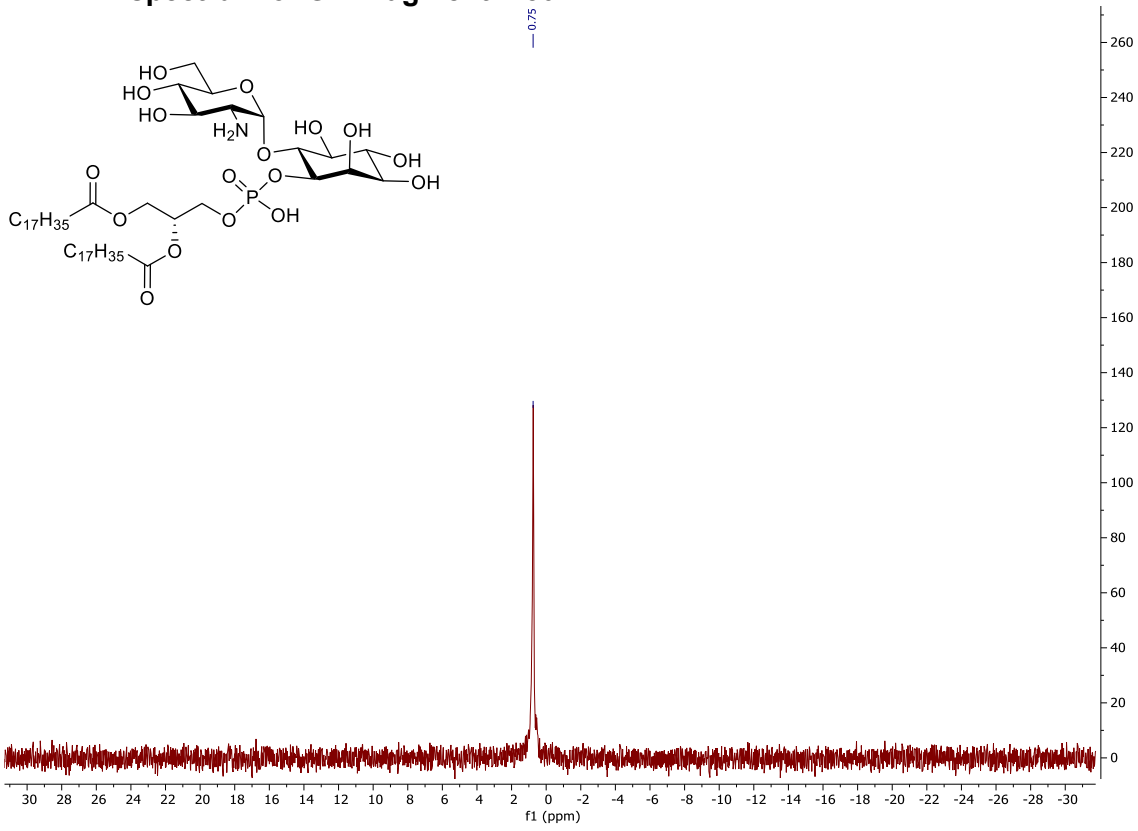

^{1}H NMR spectrum of compound 2-62

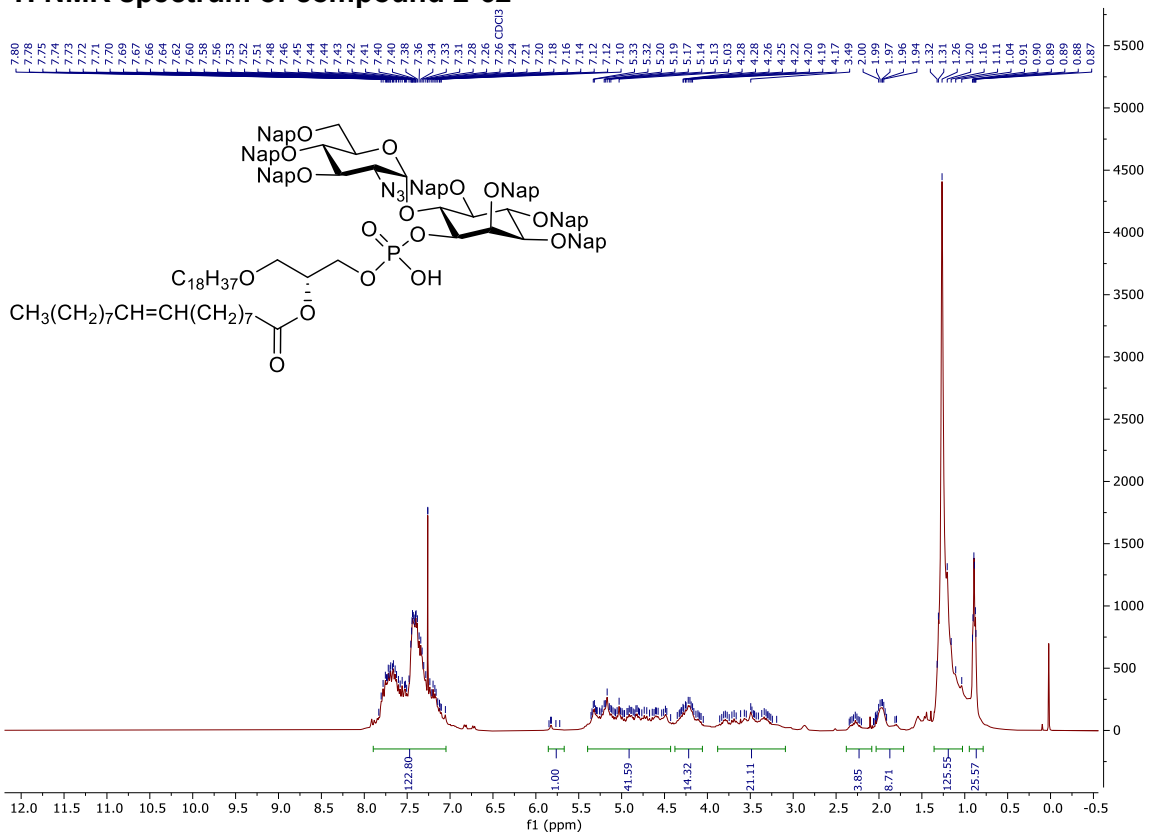

^{13}C NMR spectrum of compound 2-62

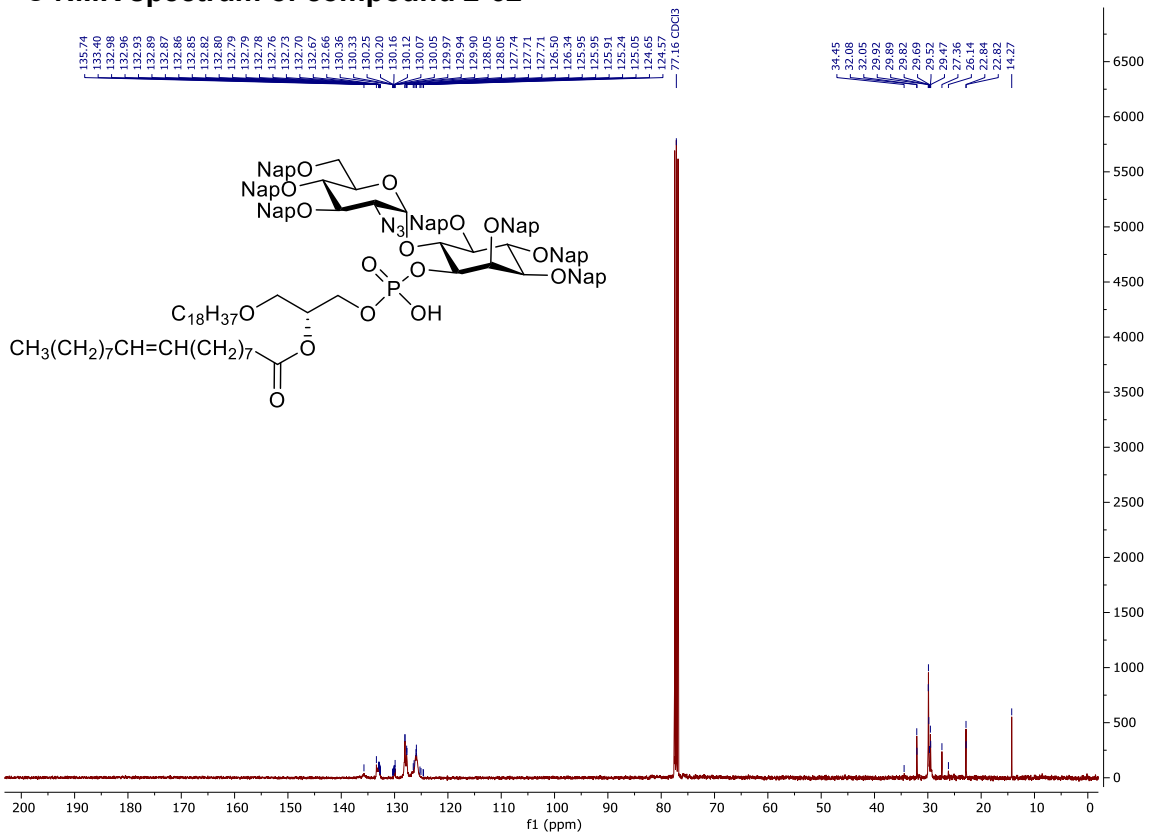

COSY-NMR spectrum of compound 2-62

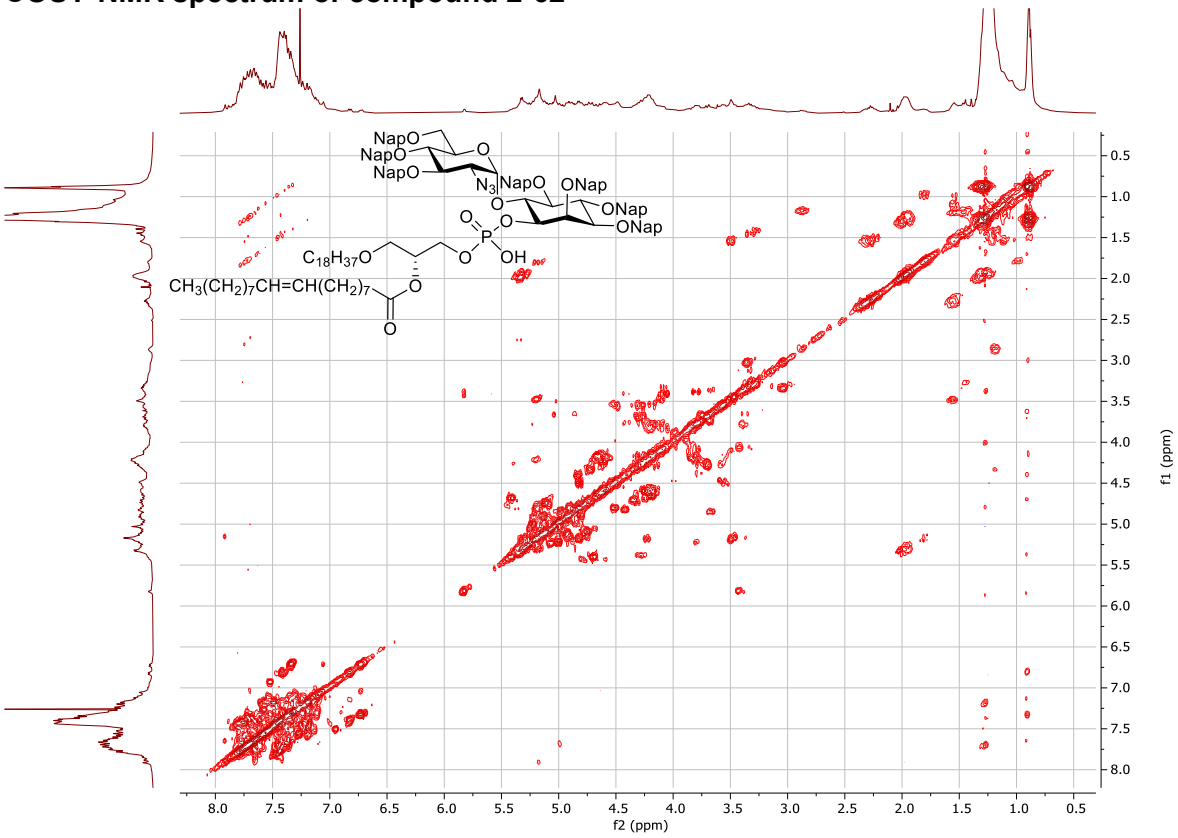

HSQC-NMR spectrum of compound 2-62

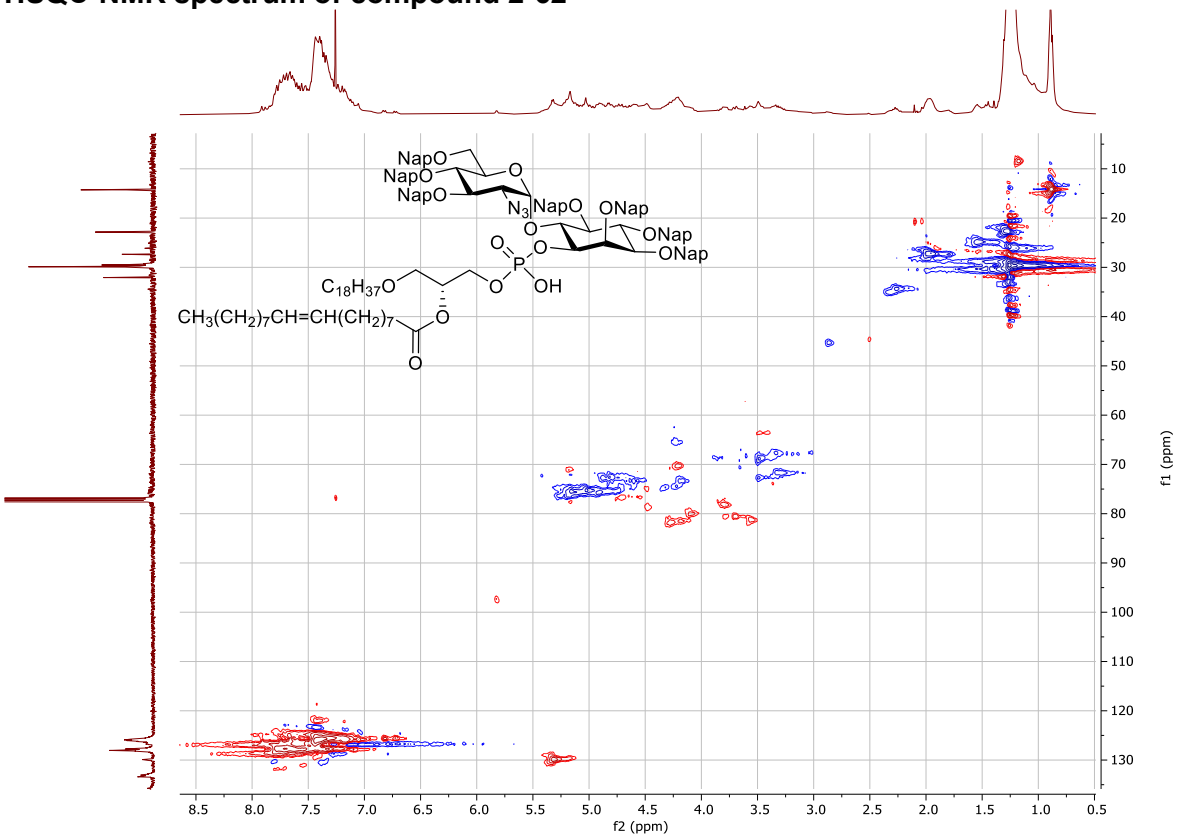

^{31}P-NMR spectrum of compound 2-62

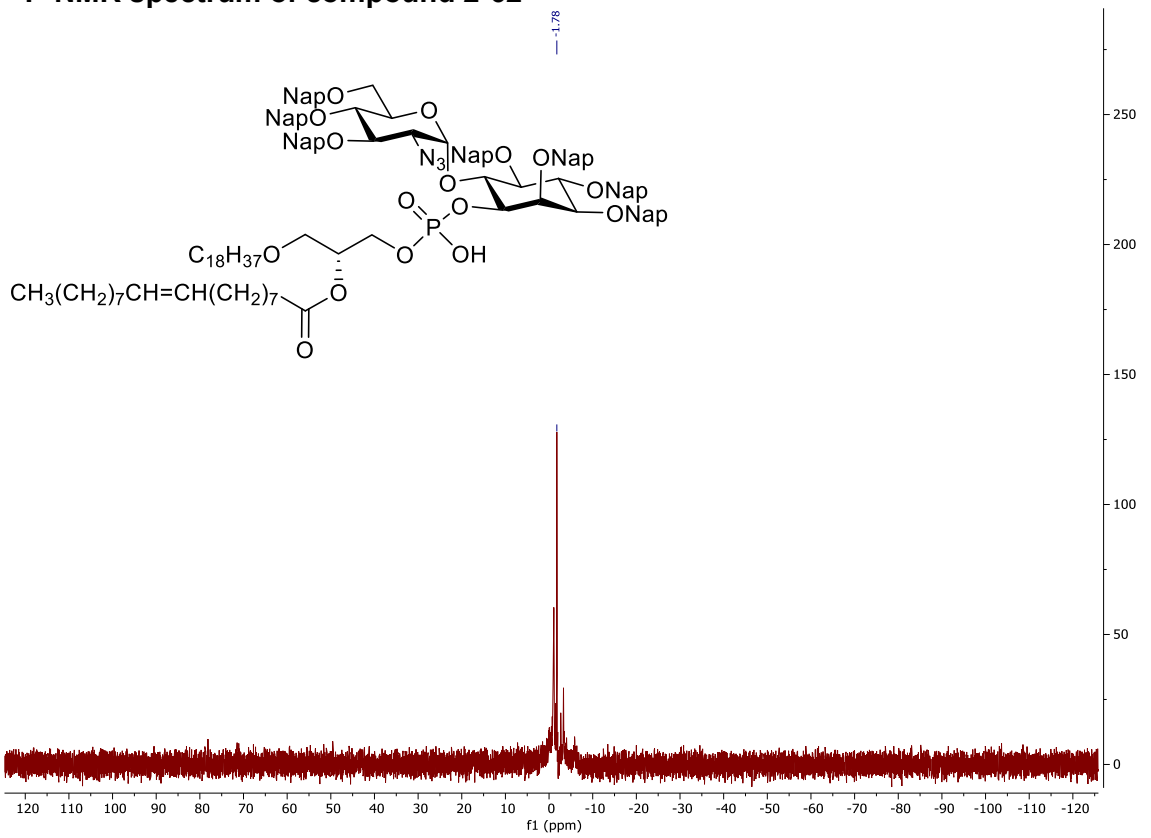

^{1}H NMR spectrum of GPI fragment 2-51

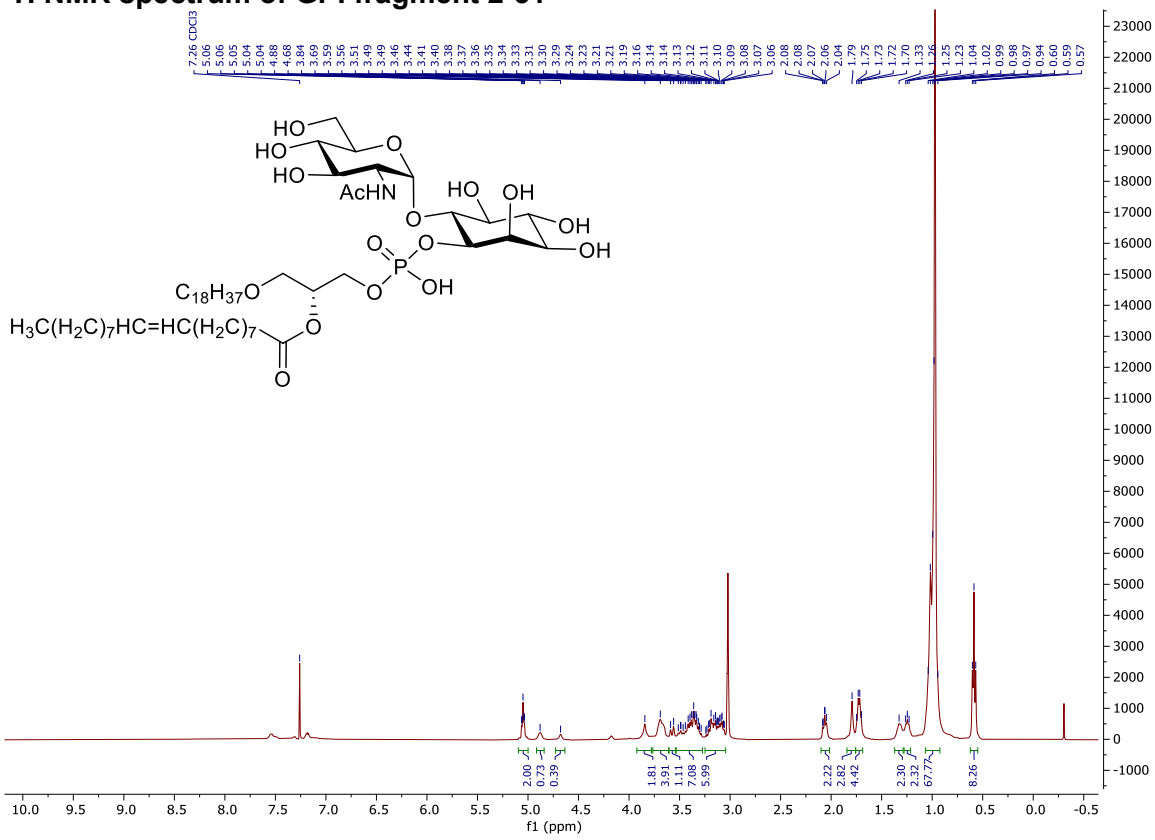

^{13}C NMR spectrum of GPI fragment 2-51

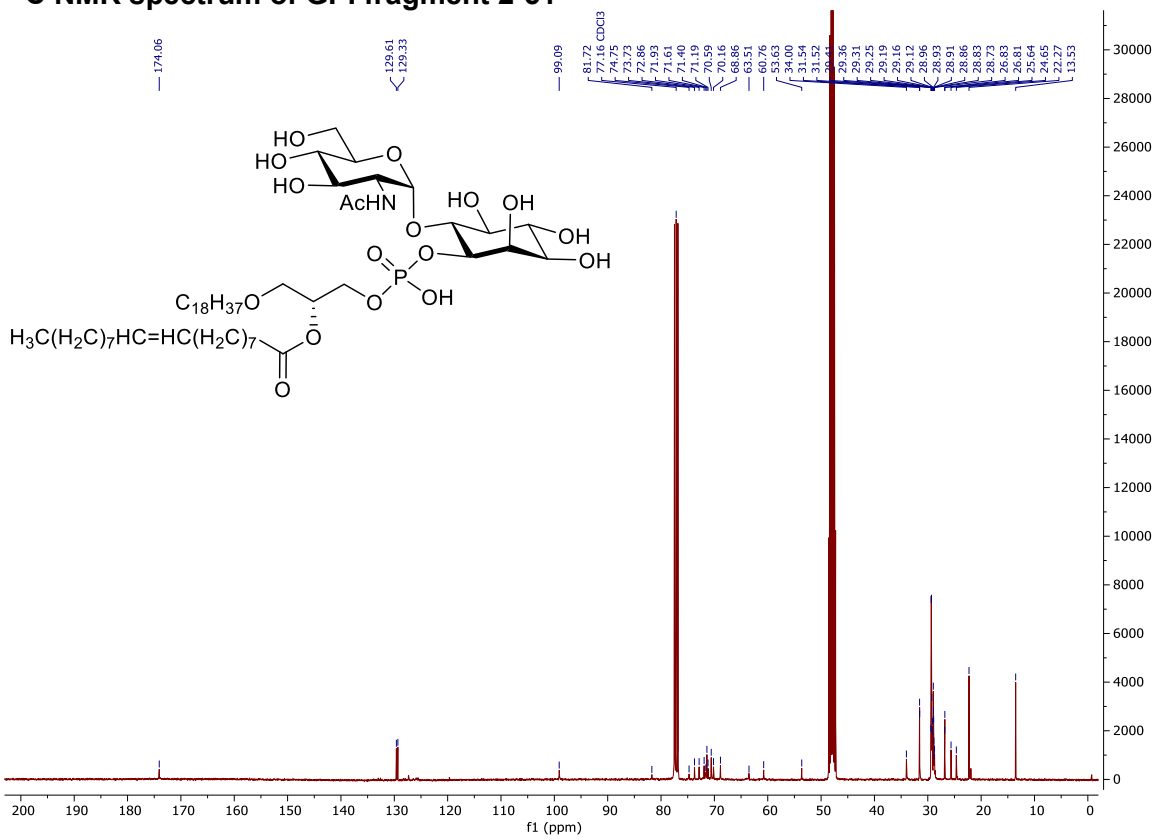

COSY-NMR spectrum of GPI fragment 2-51

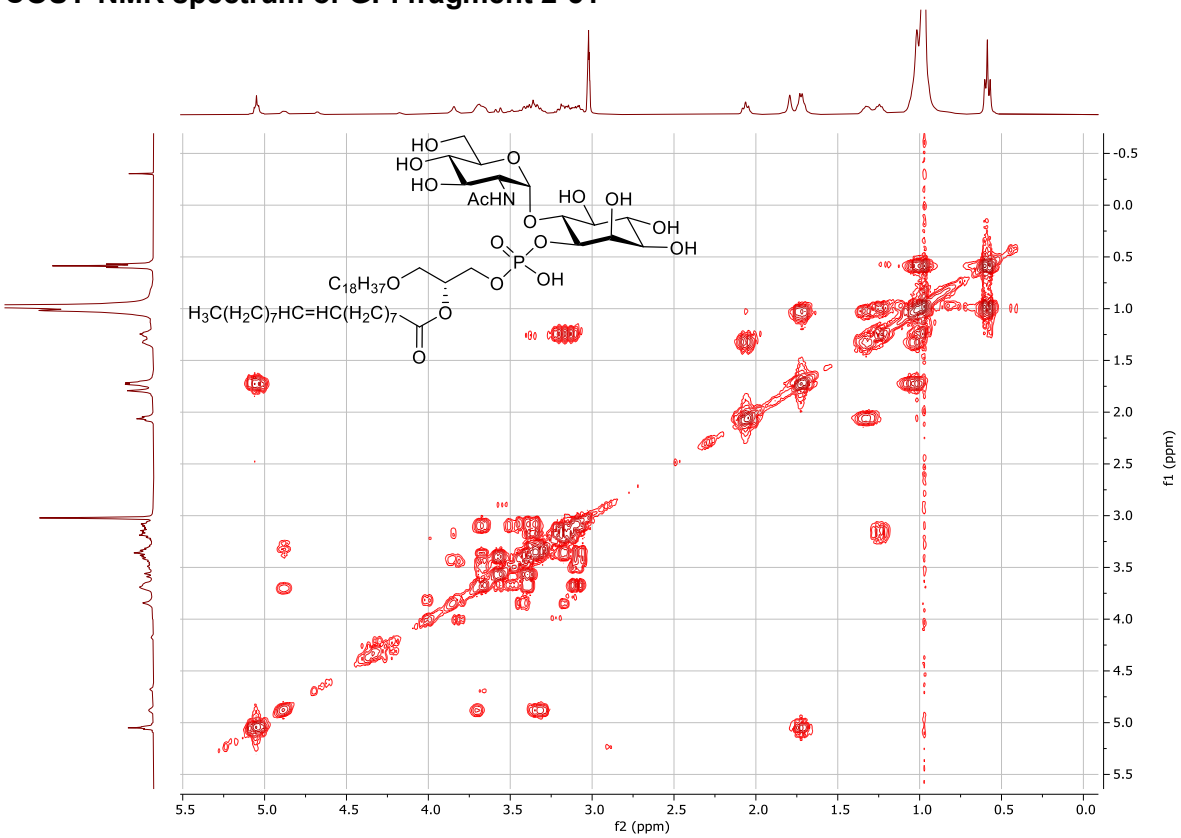

HSQC-NMR spectrum of GPI fragment 2-51

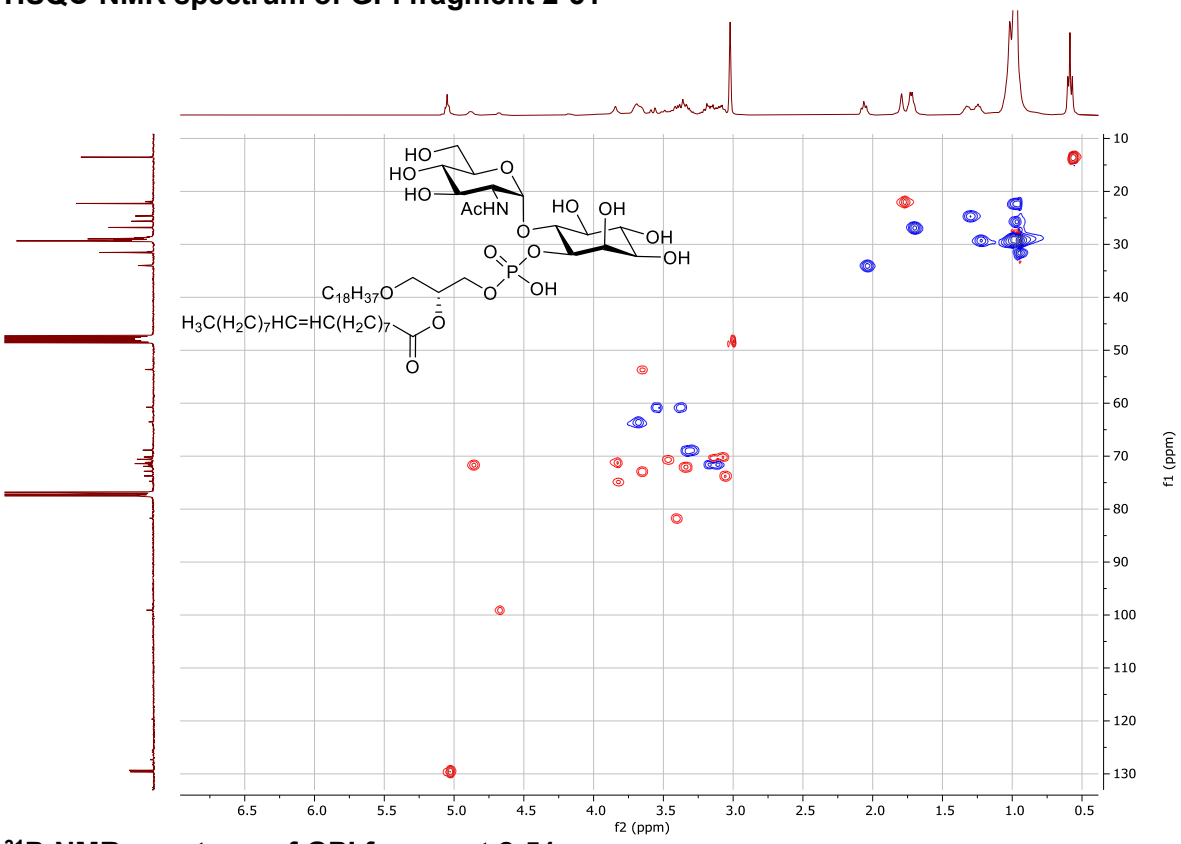

^{31}P-NMR spectrum of GPI fragment 2-51

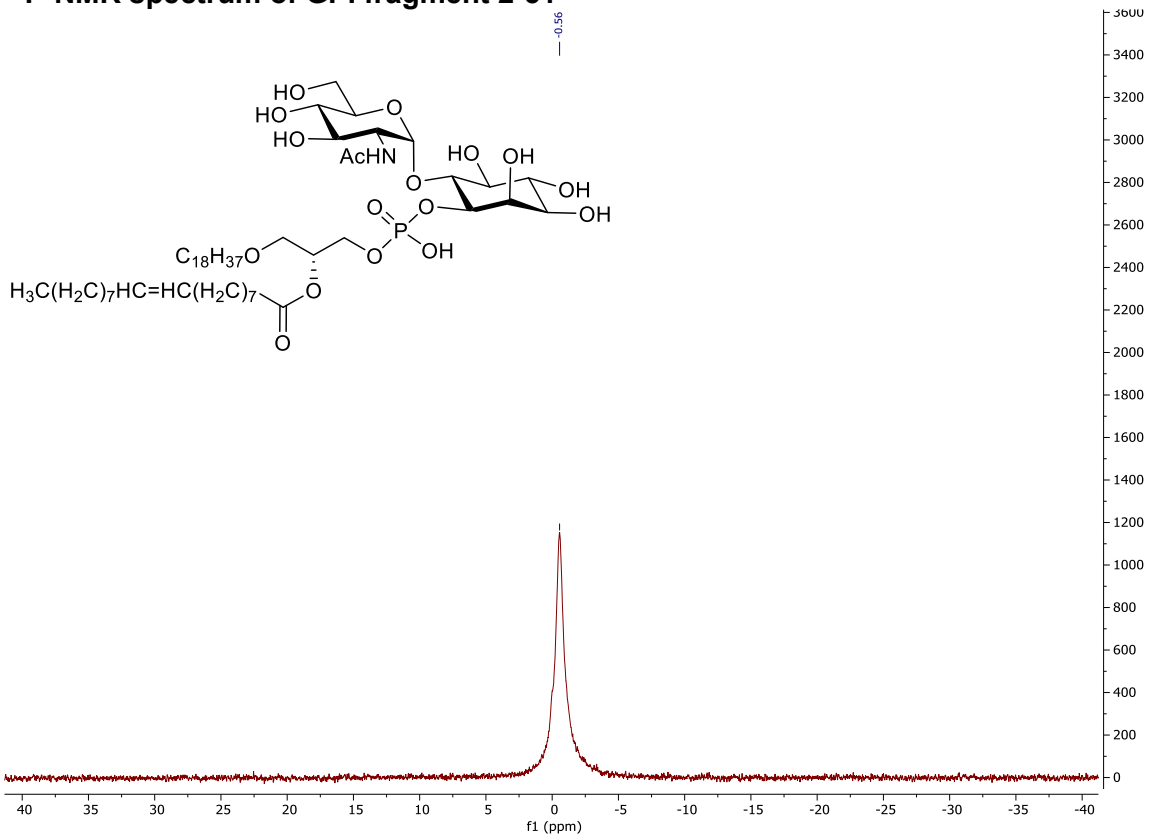

^{1}H NMR spectrum of GPI fragment 2-52

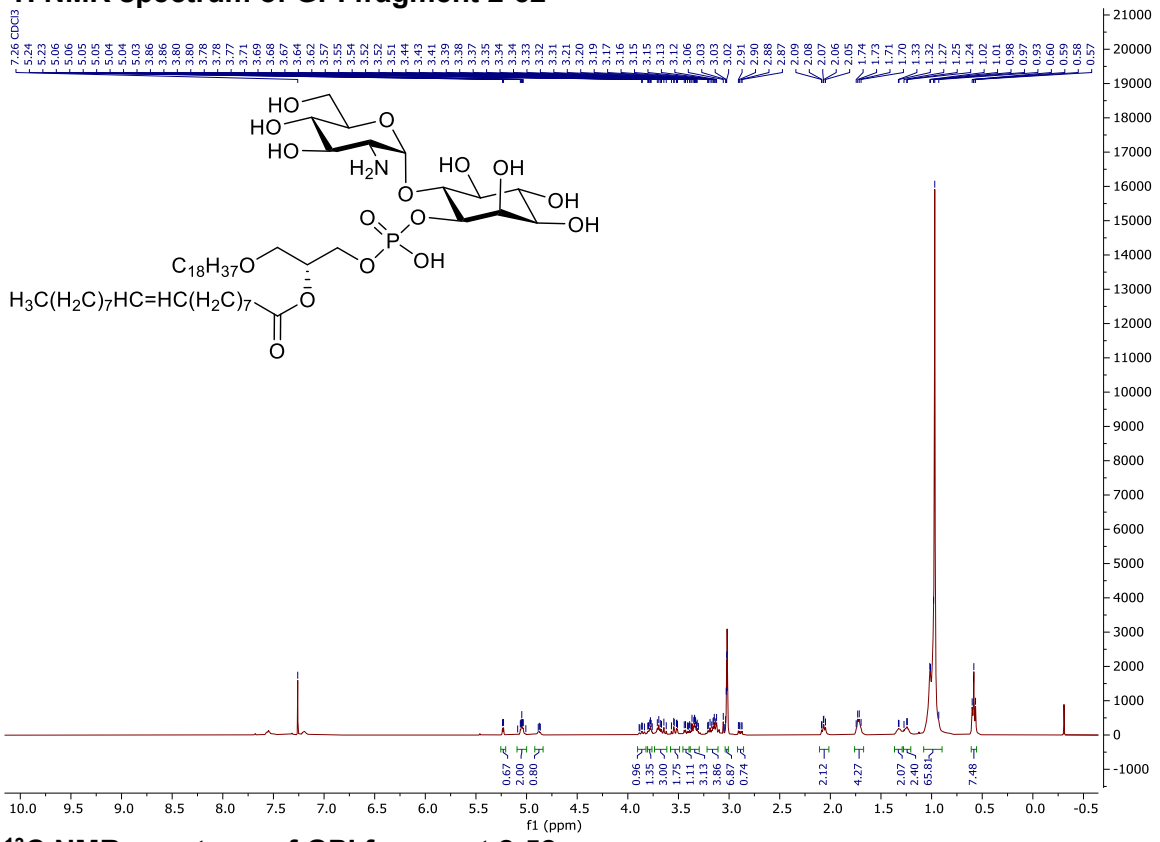

^{13}C NMR spectrum of GPI fragment 2-52

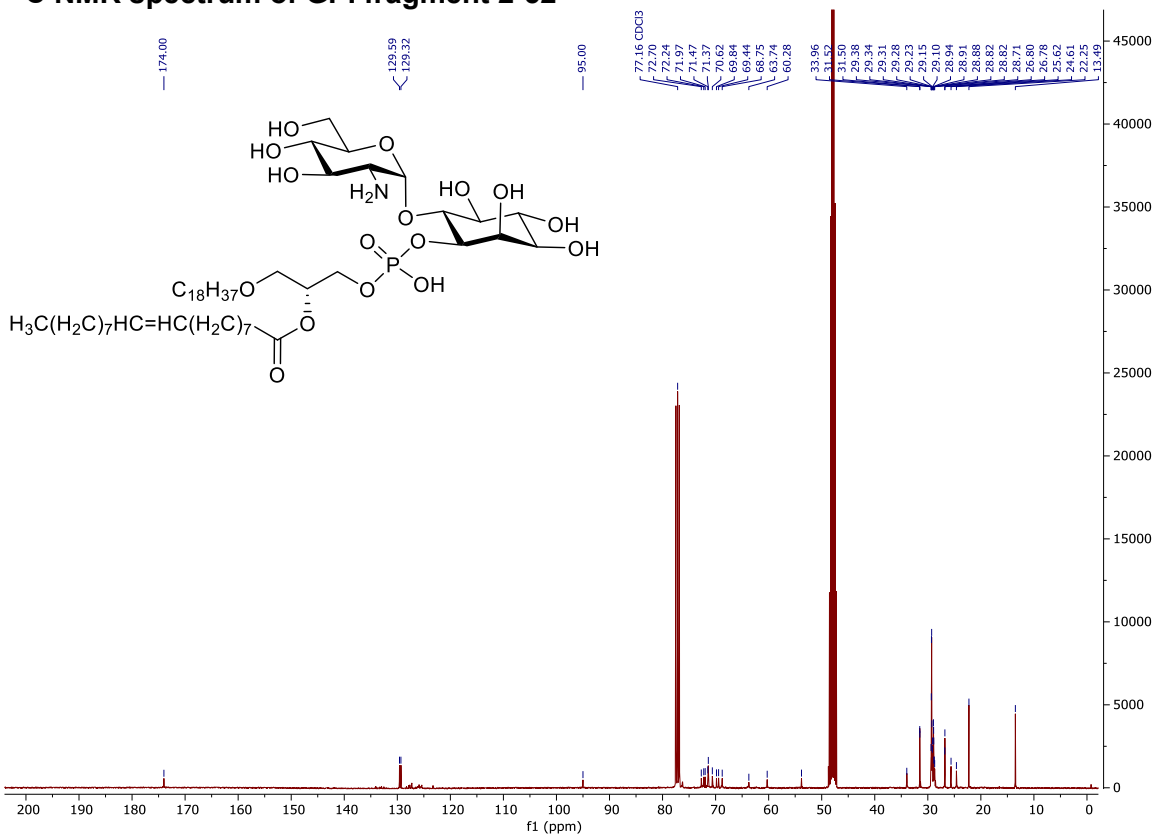

COSY-NMR spectrum of GPI fragment 2-52

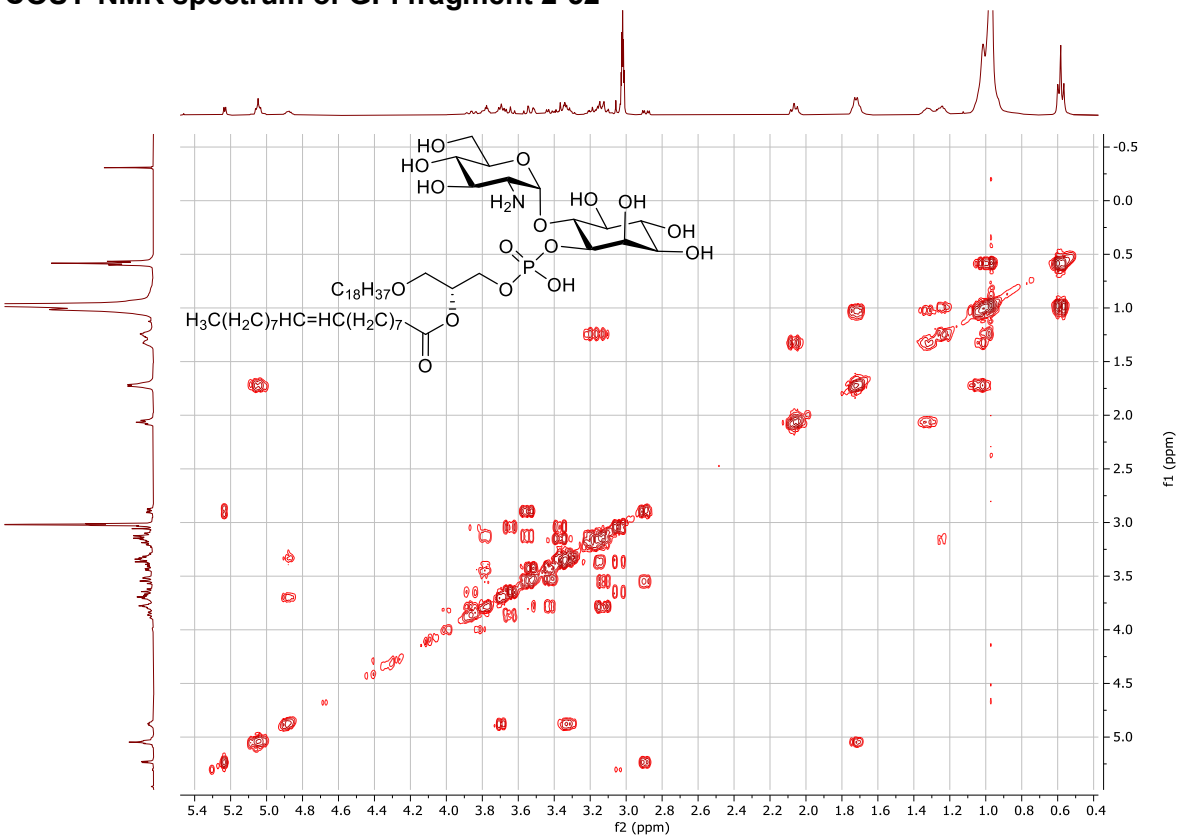

HSQC-NMR spectrum of GPI fragment 2-52

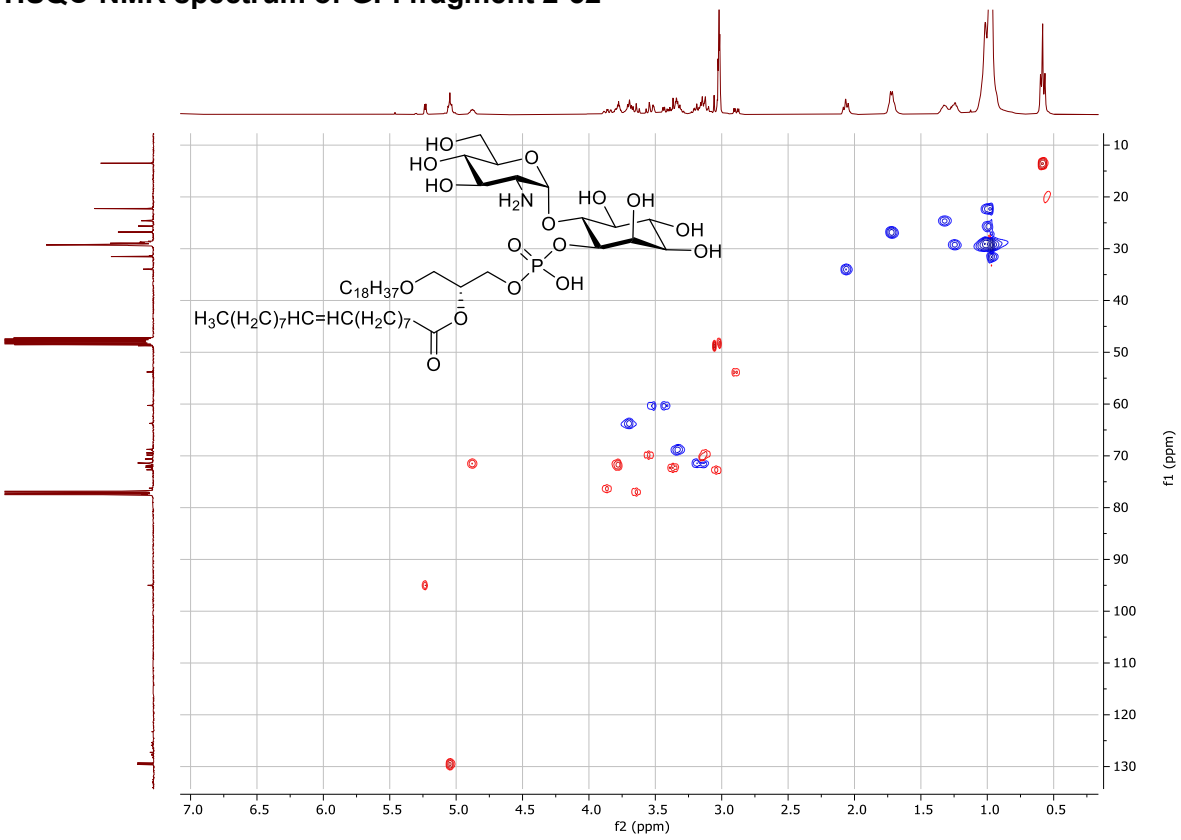

^{31}P-NMR spectrum of GPI fragment 2-52

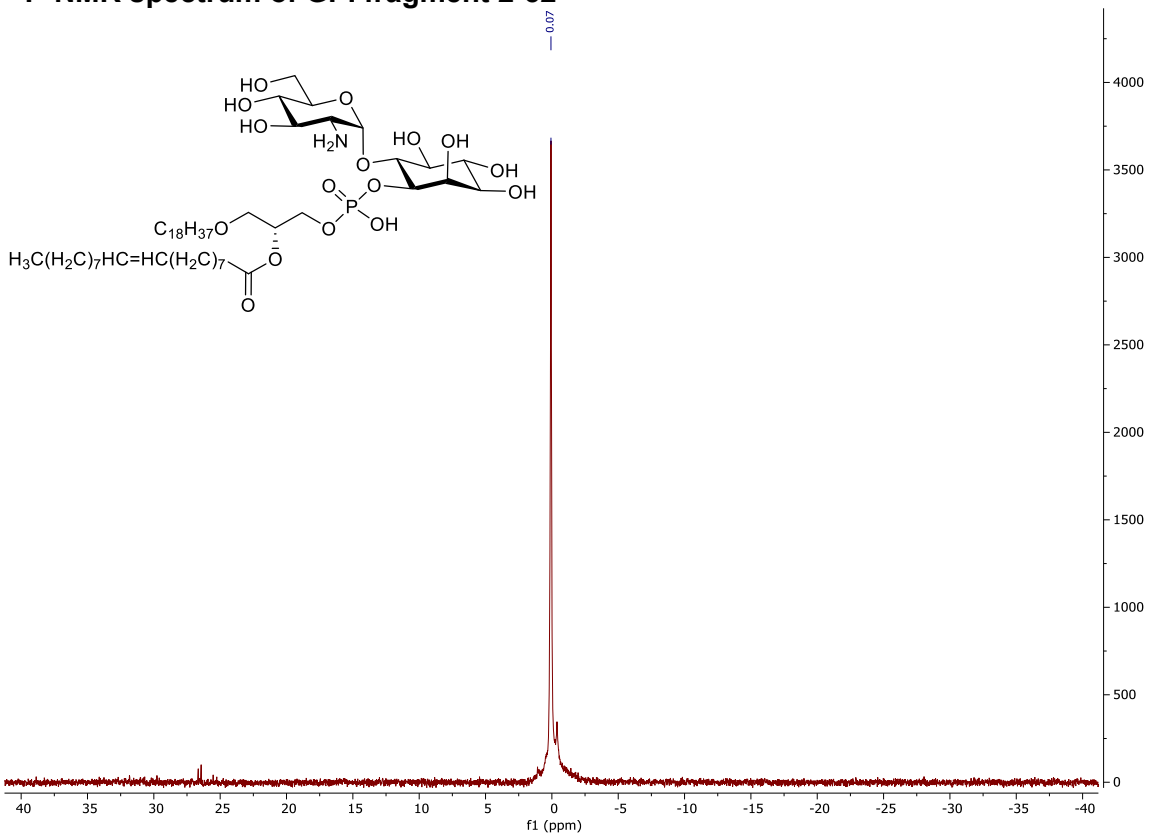

^{1}H NMR spectrum of compound 2-64

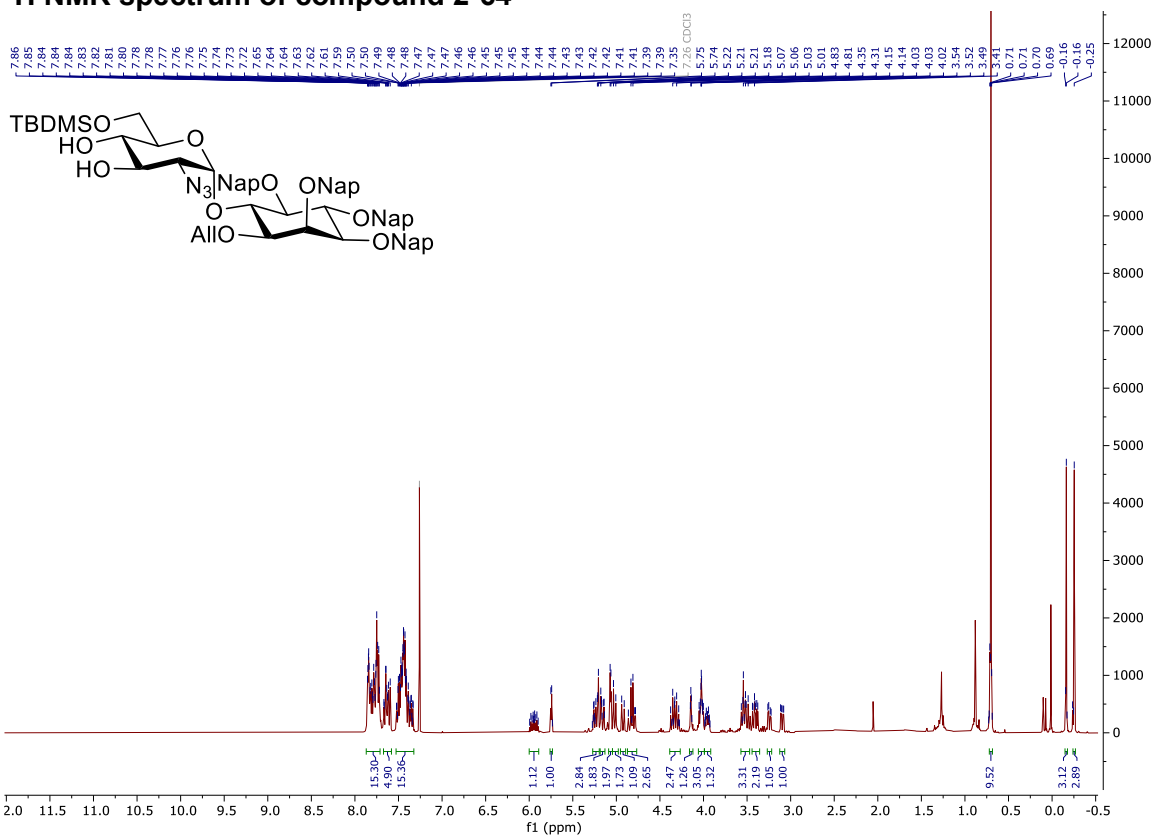

^{13}C NMR spectrum of compound 2-64

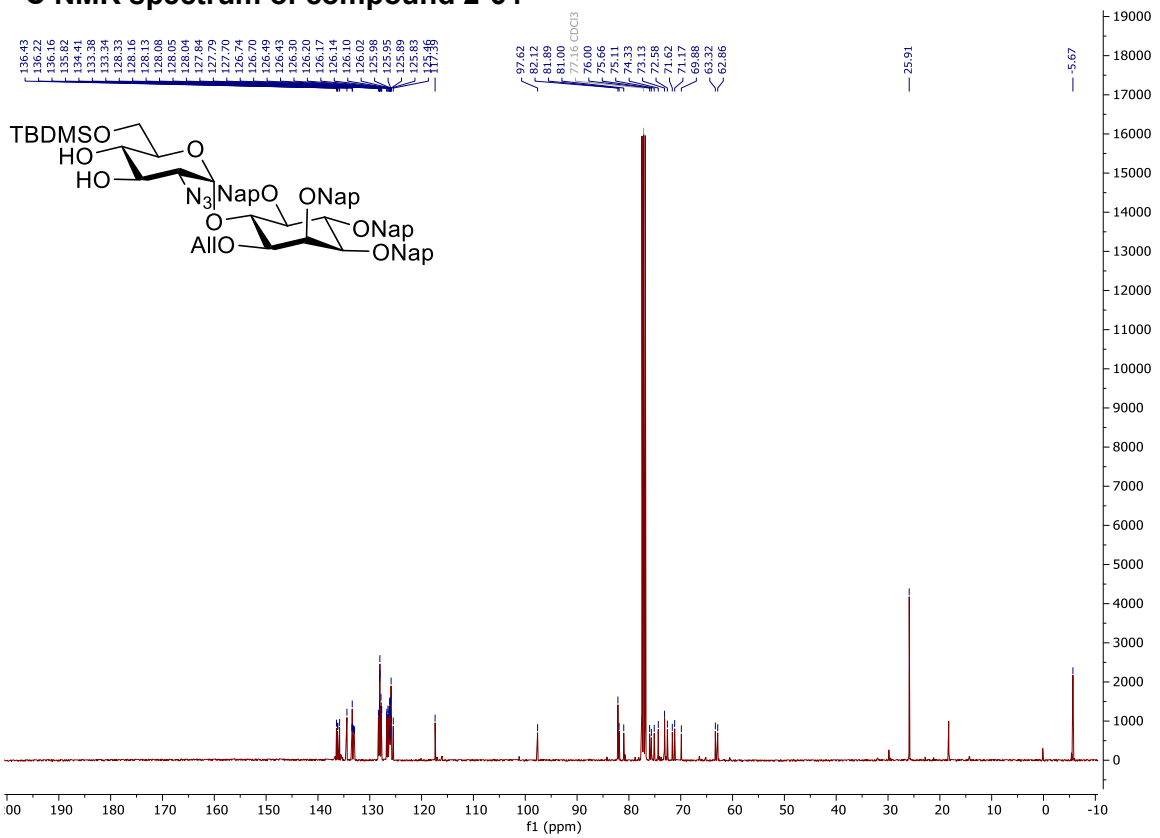

COSY-NMR spectrum of compound 2-64

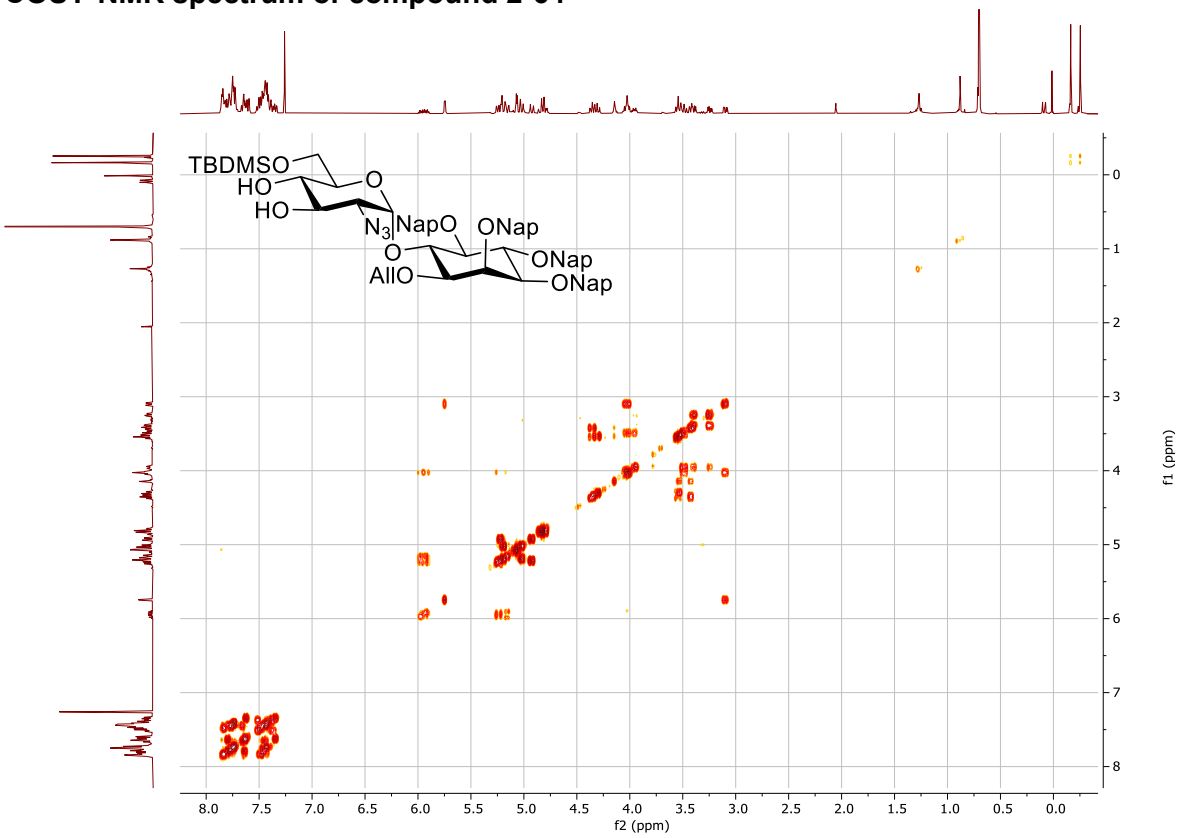

HSQC-NMR spectrum of compound 2-64

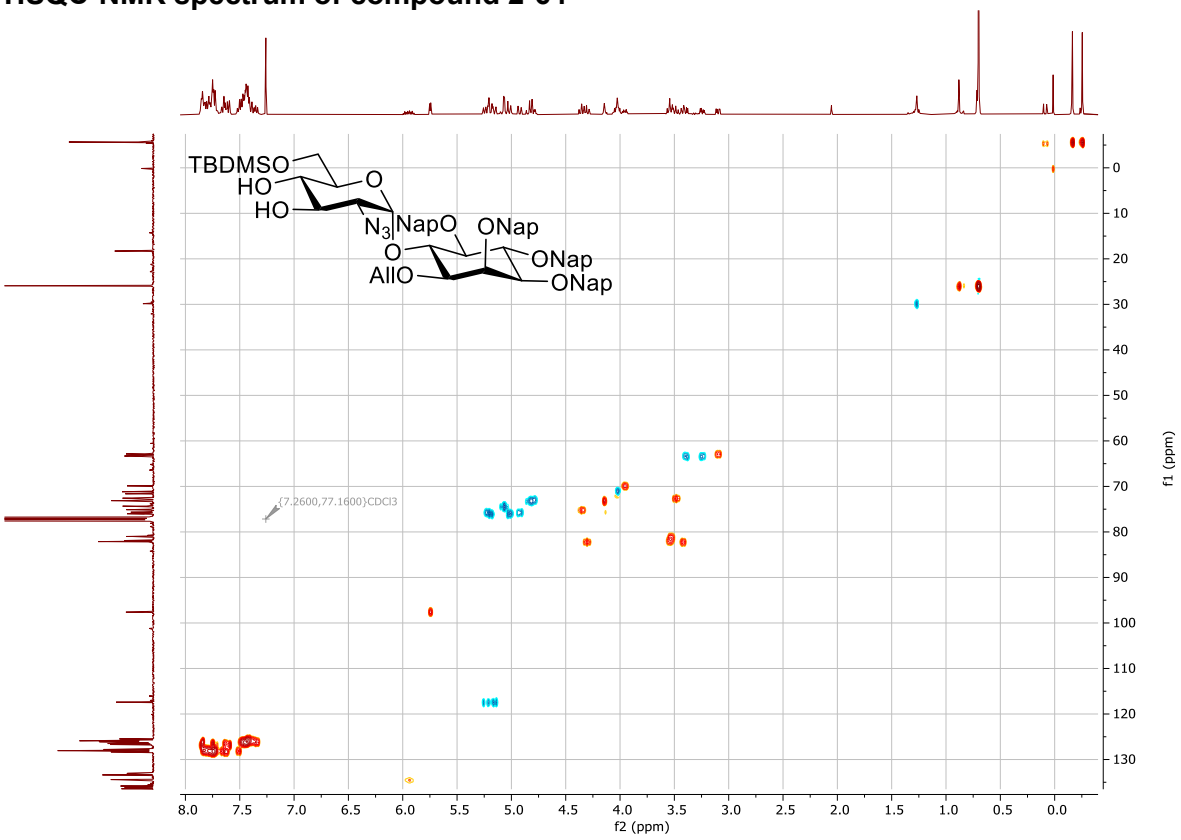

^{1}H NMR spectrum of compound 2-65

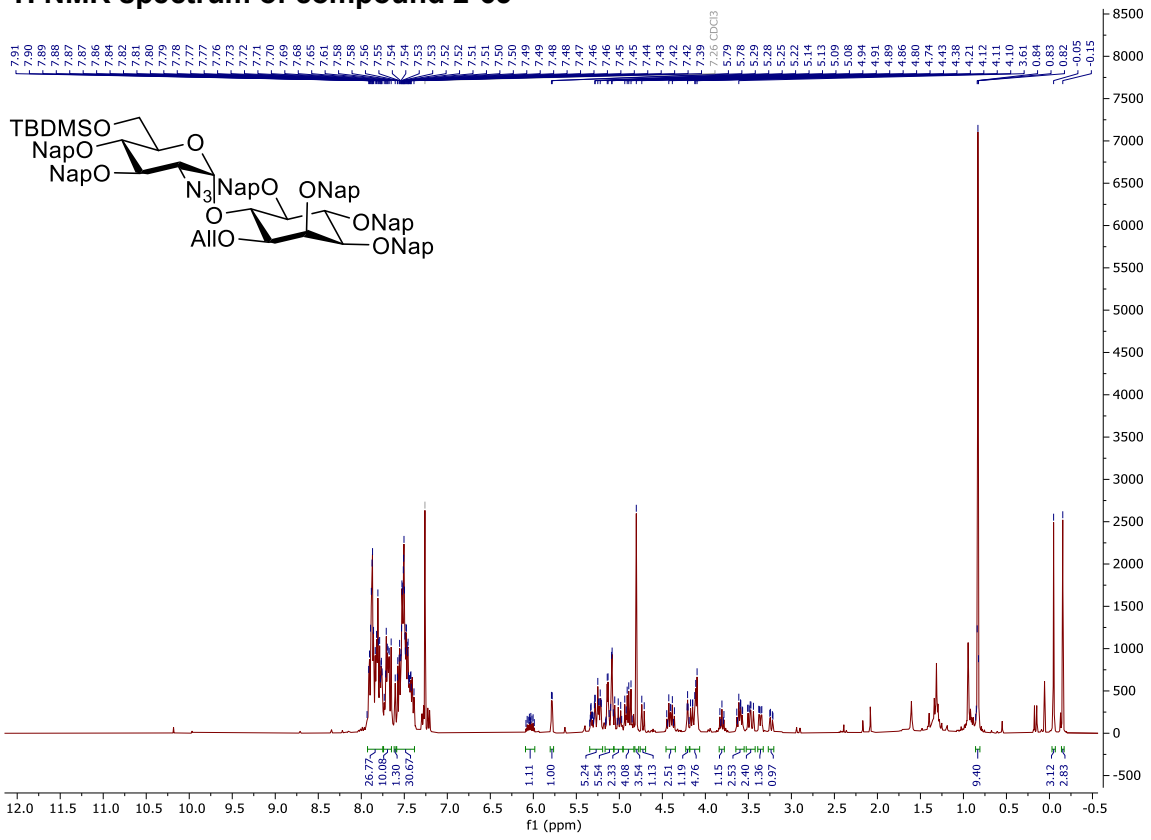

^{13}C NMR spectrum of compound 2-65

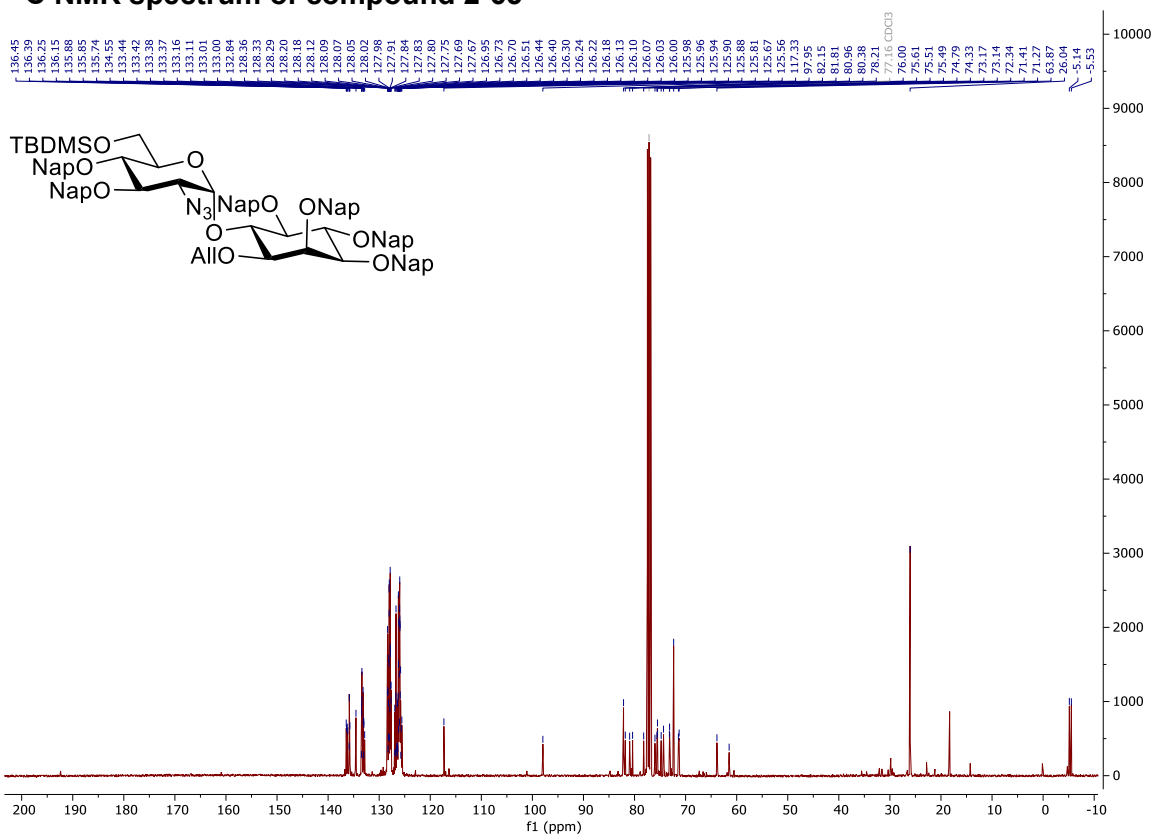

COSY-NMR spectrum of compound 2-65

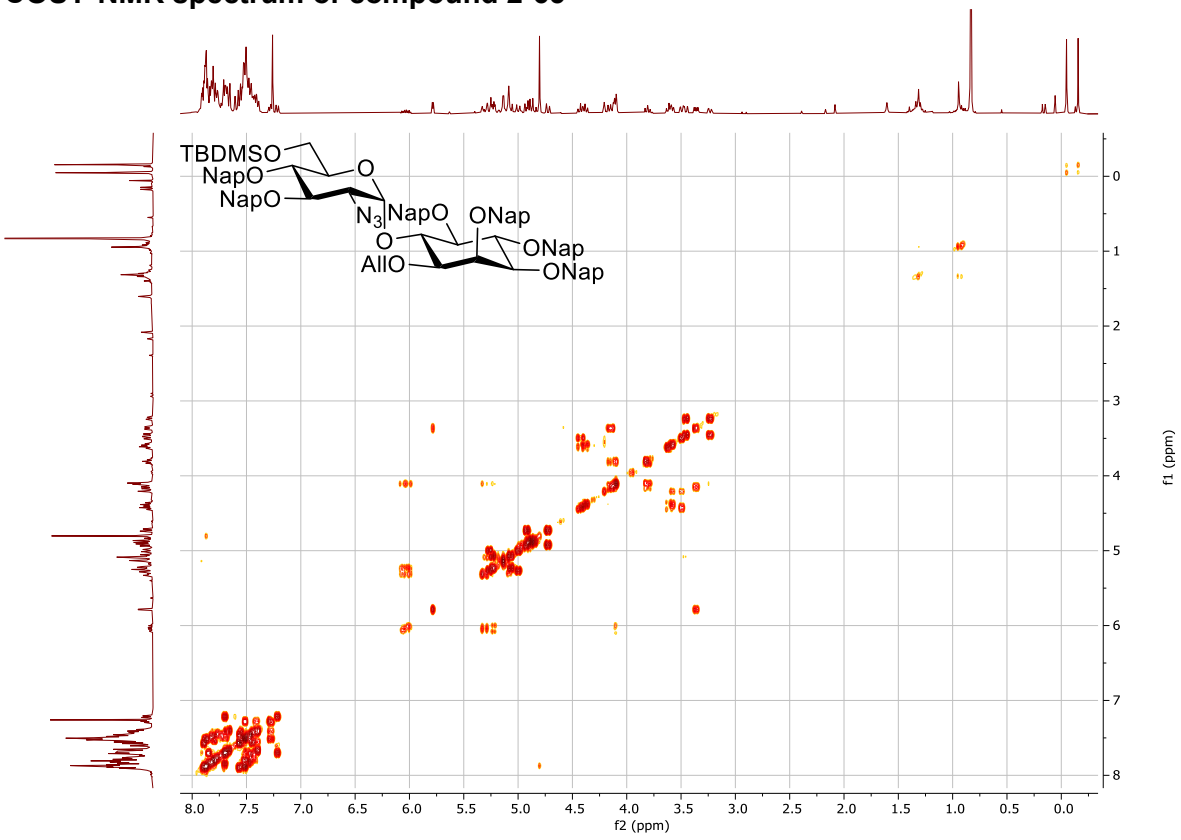

HSQC-NMR spectrum of compound 2-65

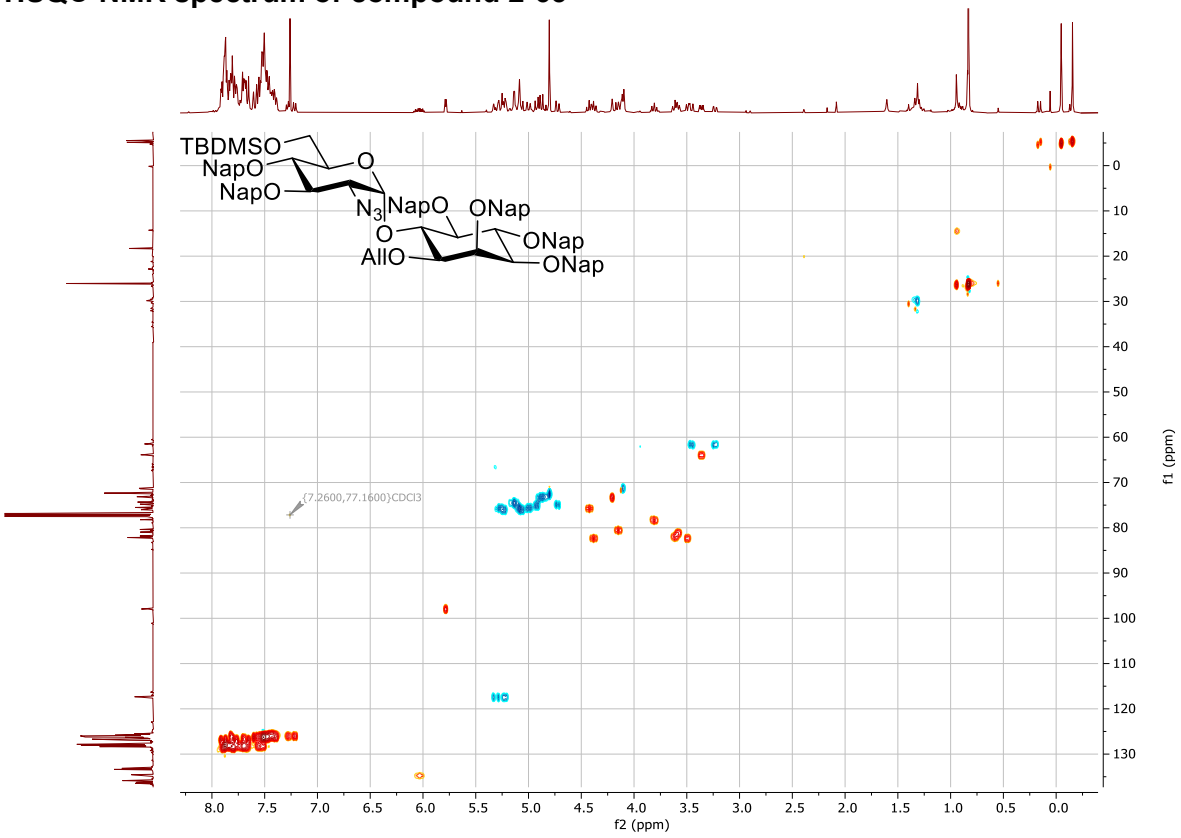

^{1}H NMR spectrum of compound 2-66

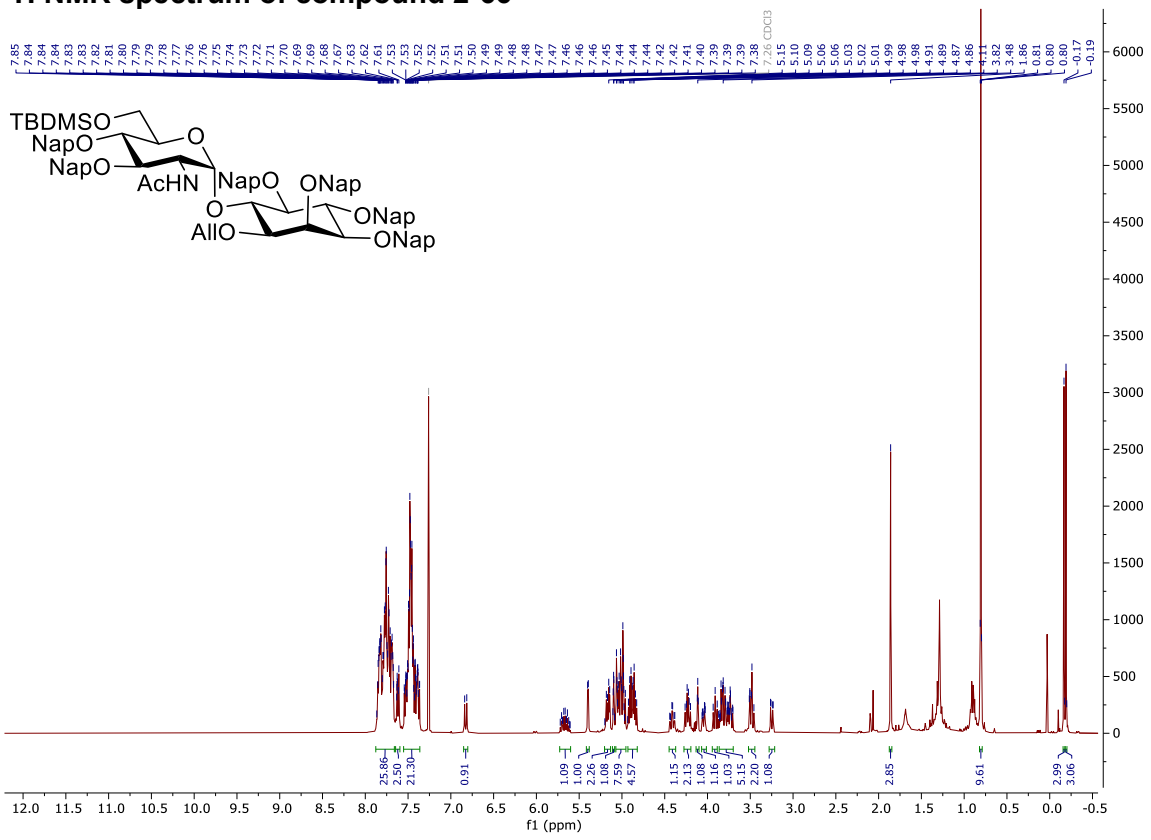

^{13}C NMR spectrum of compound 2-66

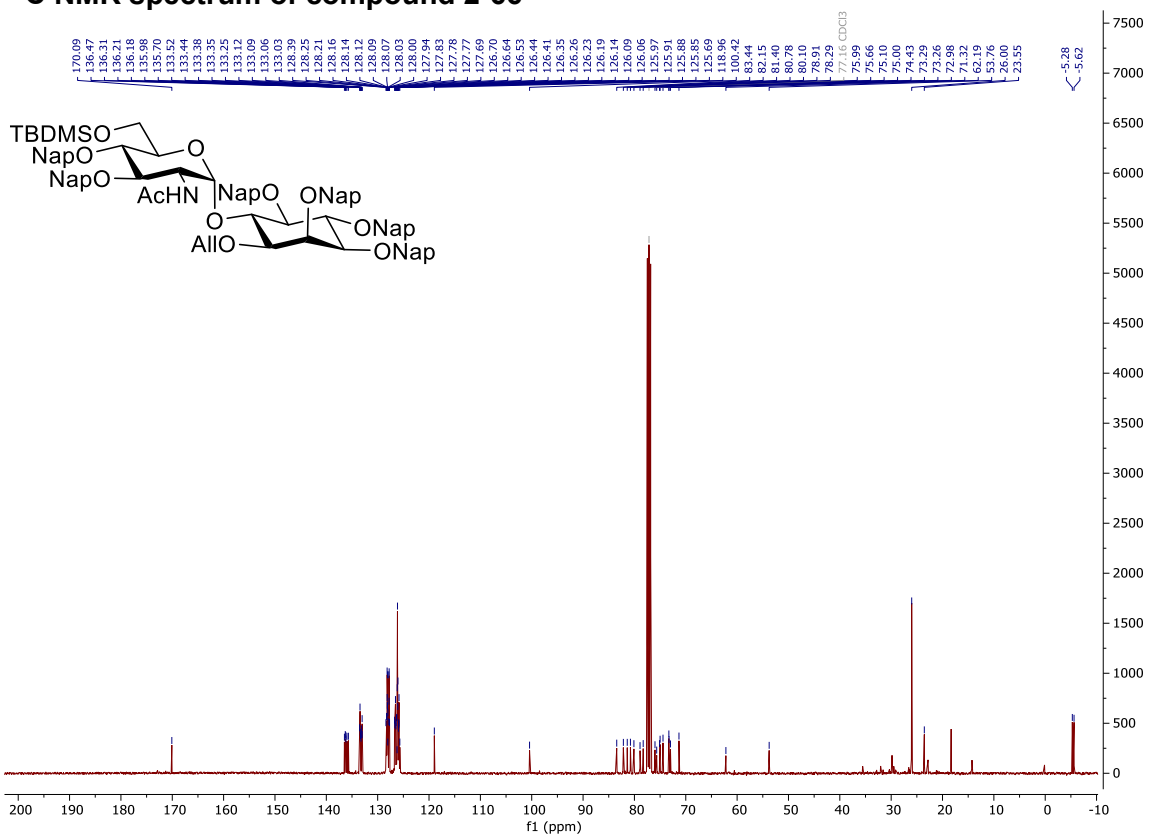

COSY-NMR spectrum of compound 2-66

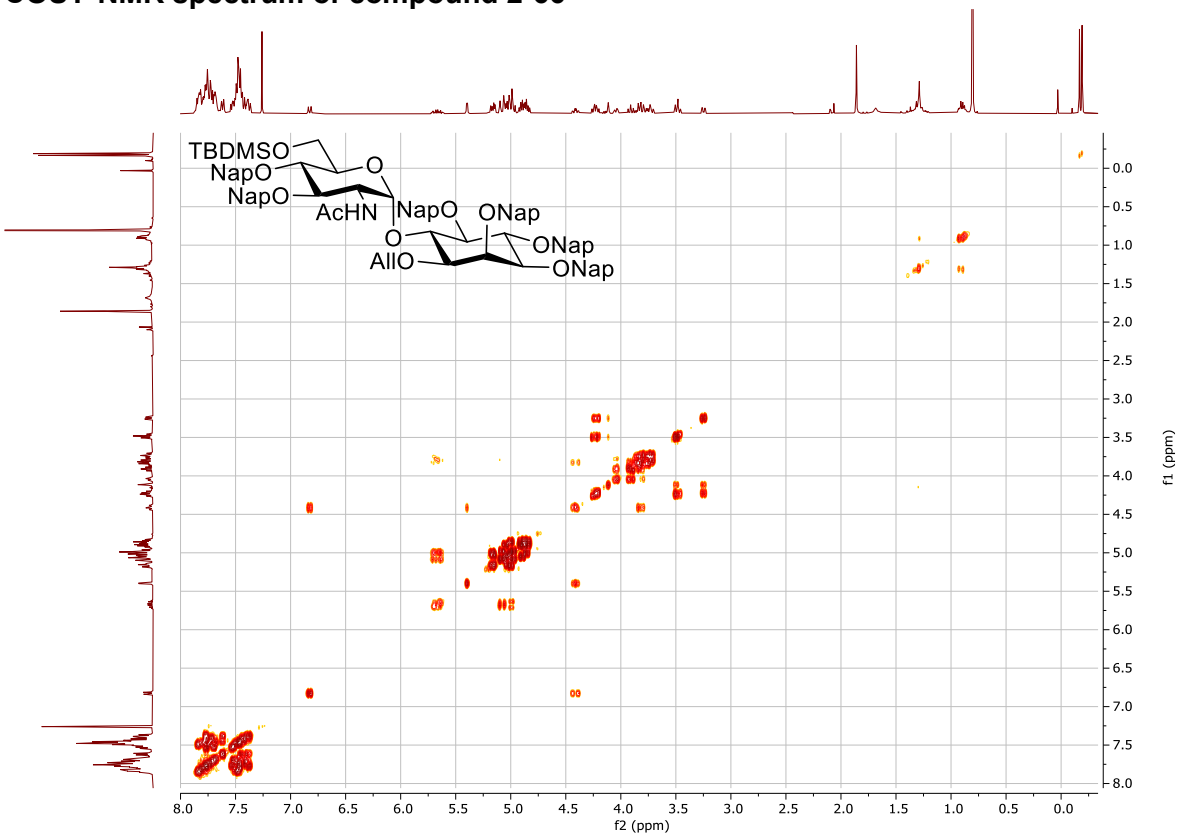

HSQC-NMR spectrum of compound 2-66

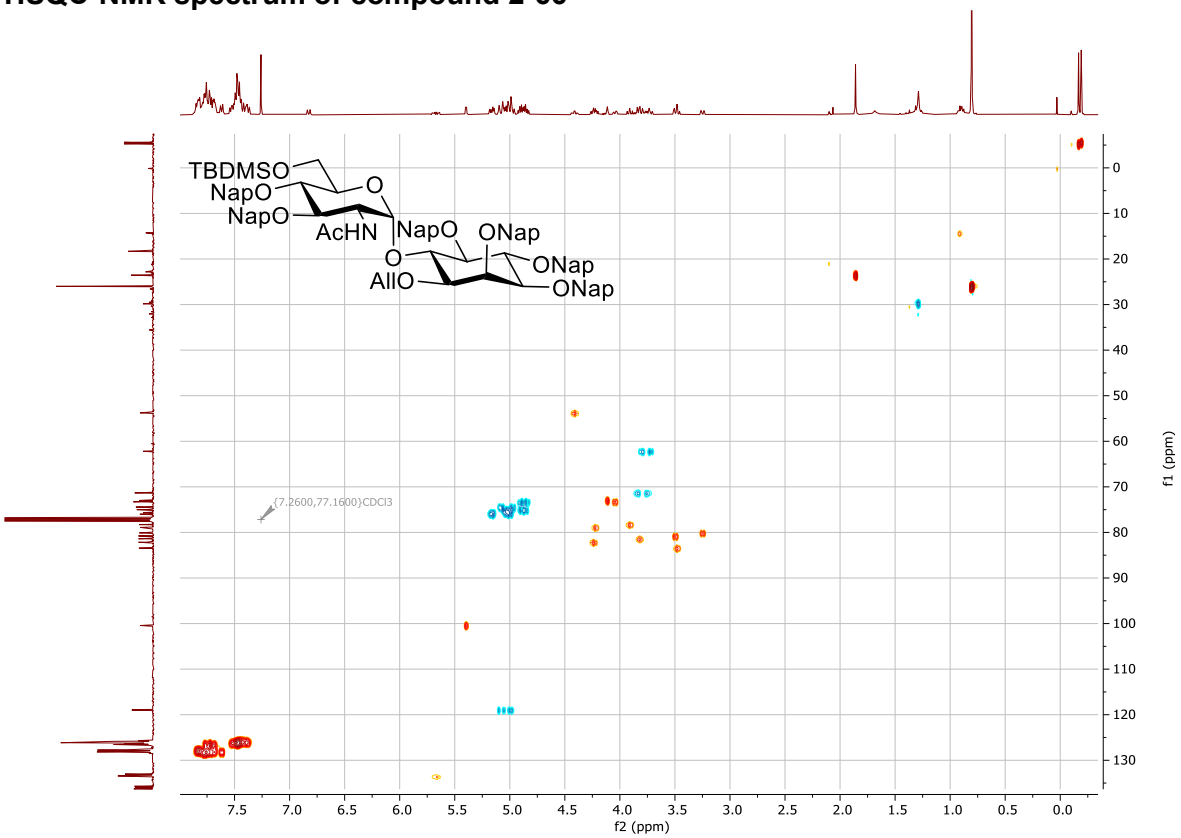

^{1}H NMR spectrum of compound 2-67

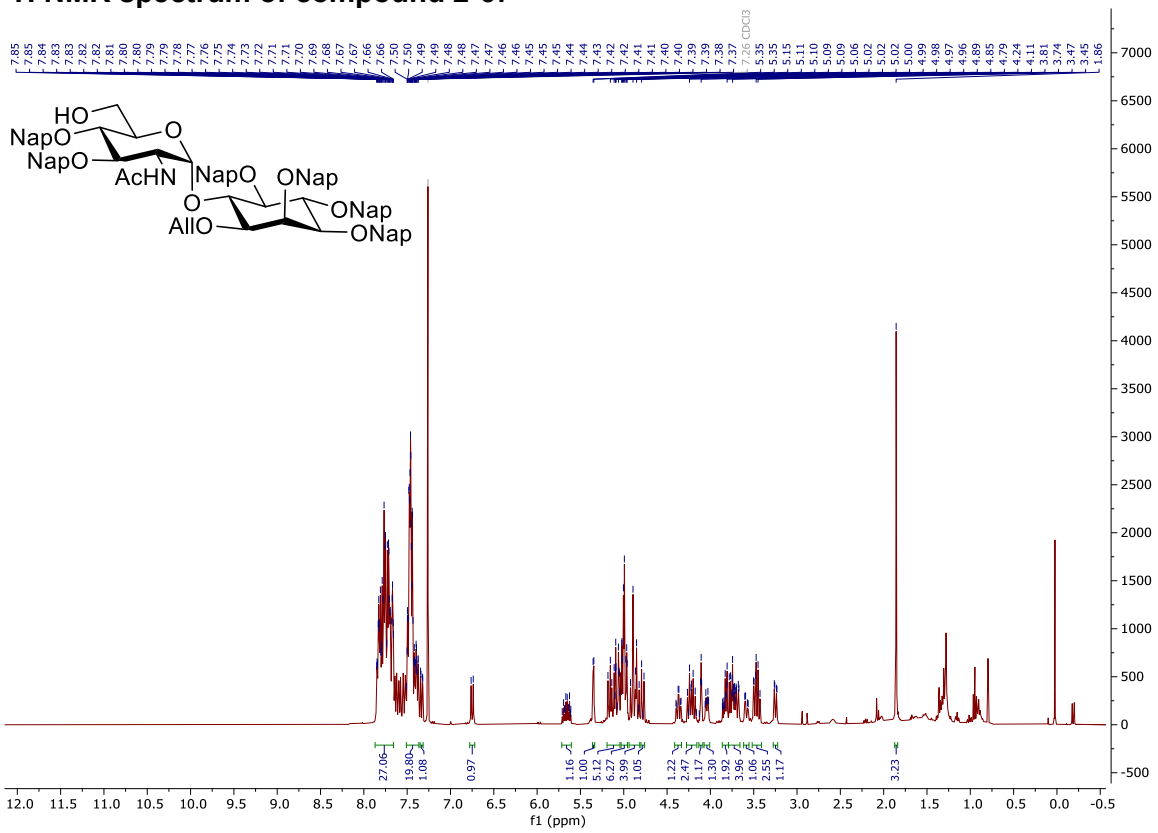

^{13}C NMR spectrum of compound 2-67

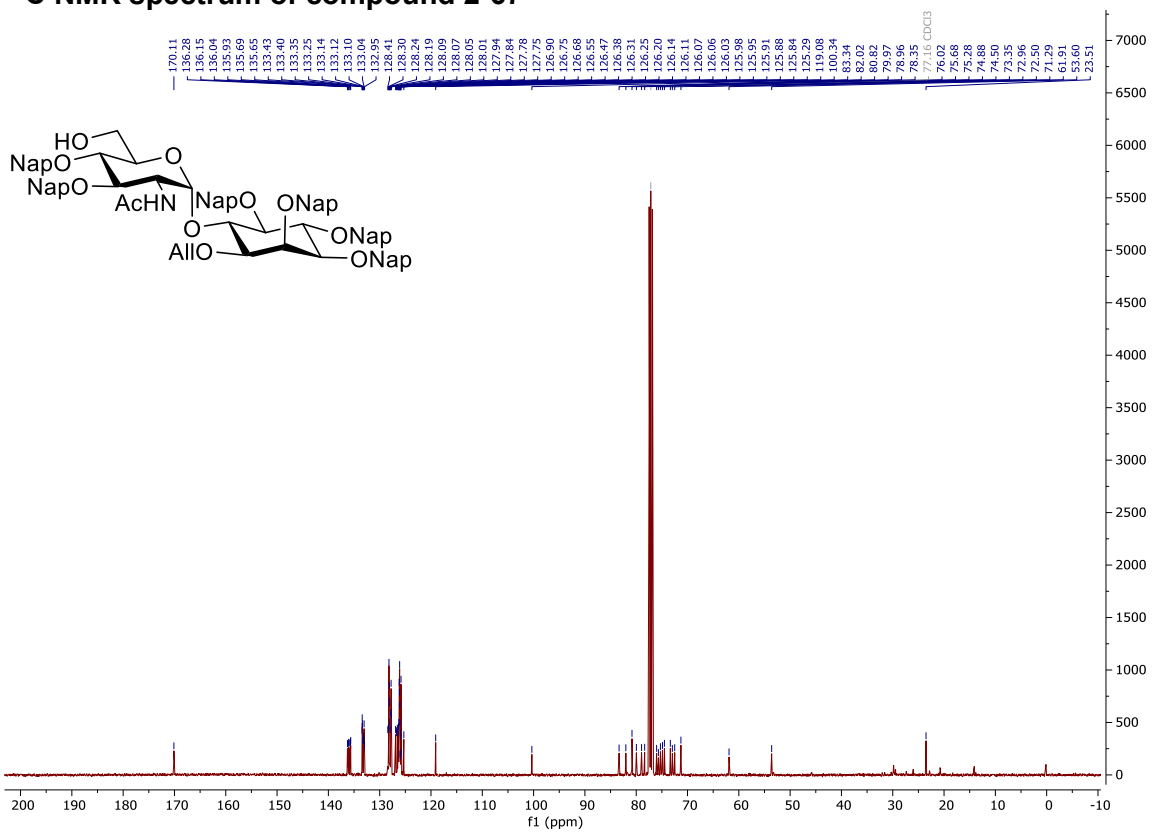

COSY-NMR spectrum of compound 2-67

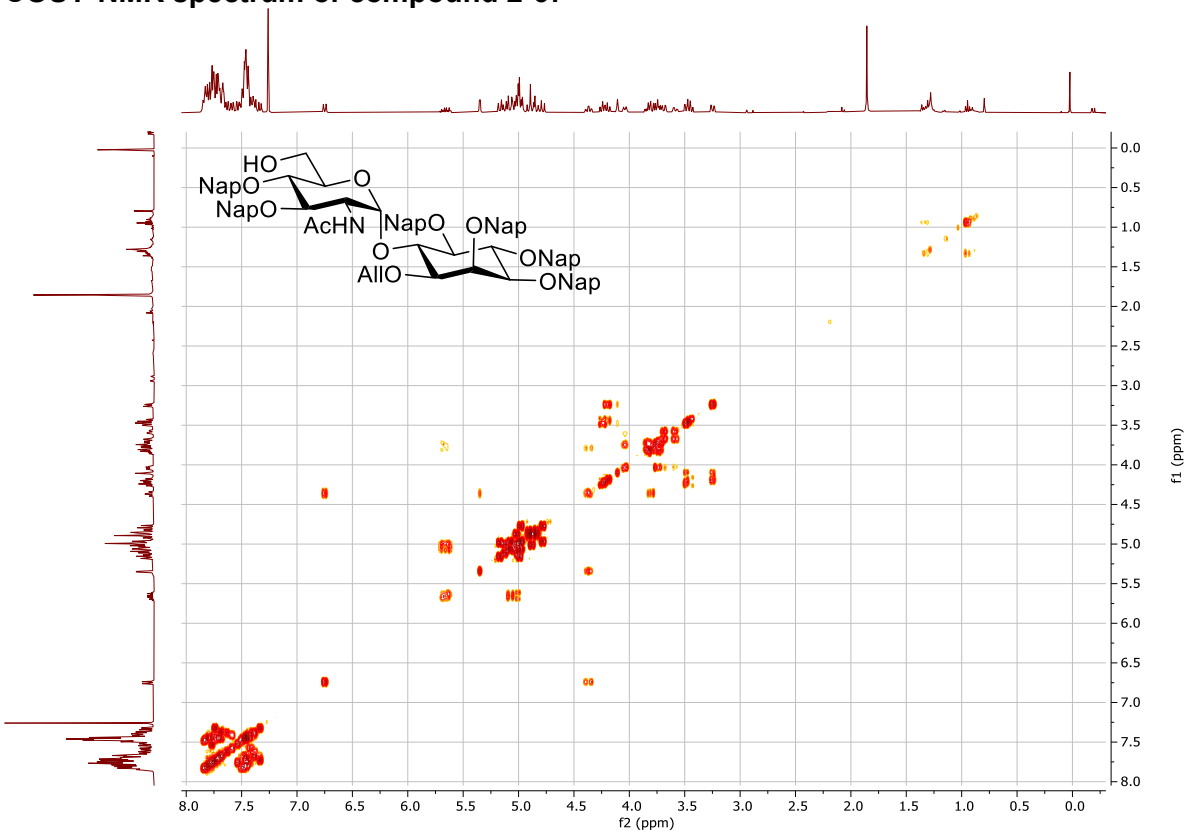

HSQC-NMR spectrum of compound 2-67

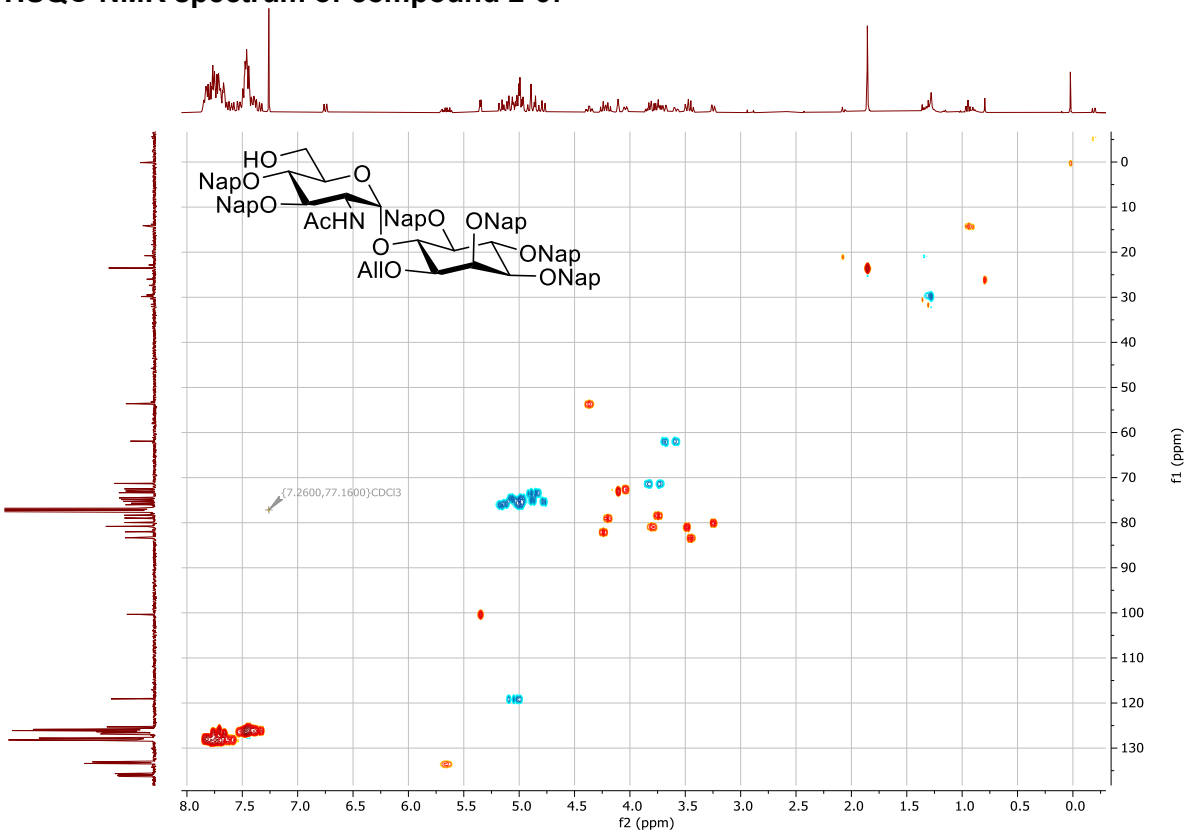

^{1}H NMR spectrum of 3-Azidopropan-1-ol

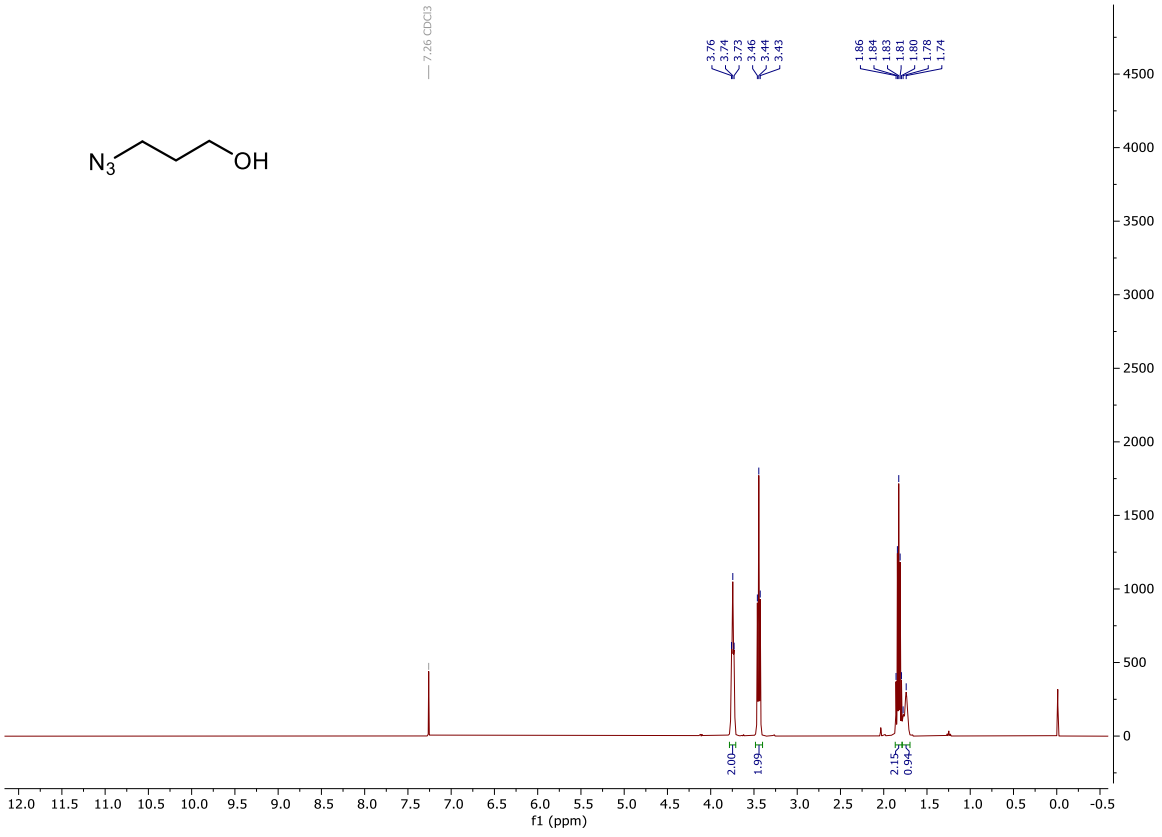

^{13}C NMR spectrum of 3-Azidopropan-1-ol

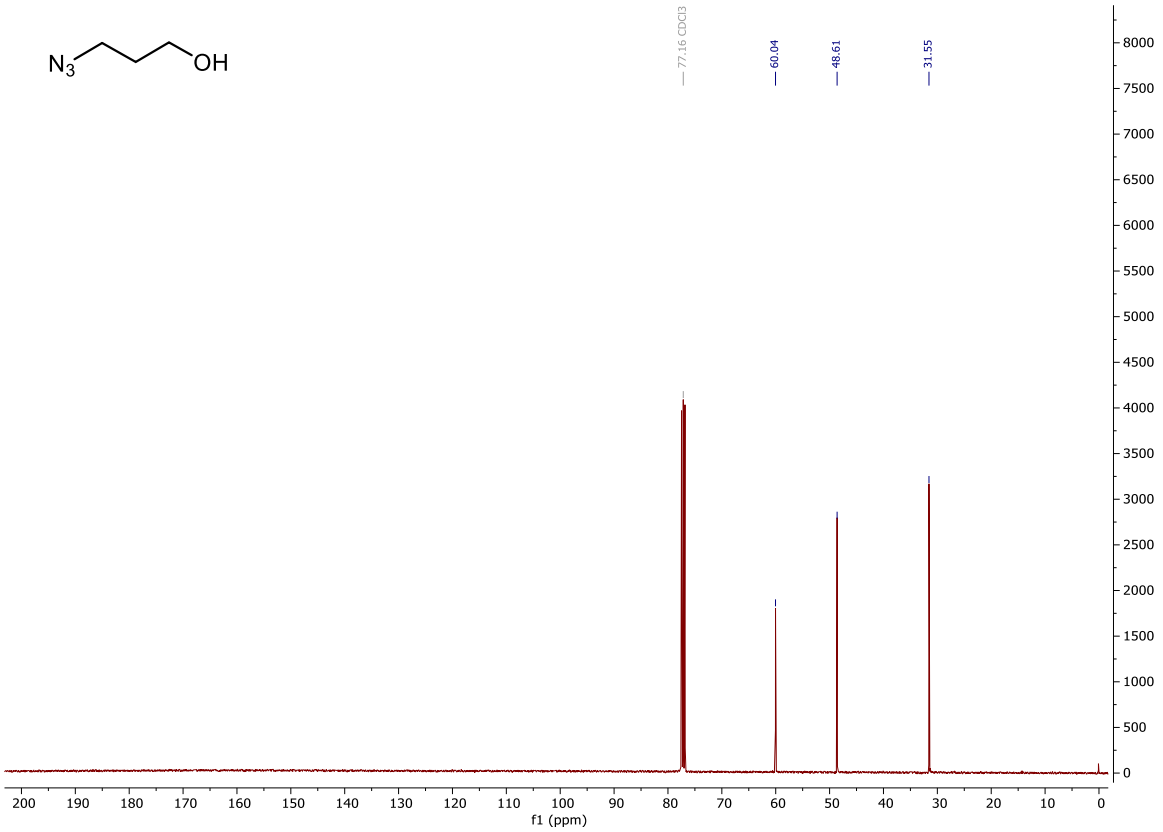

COSY-NMR spectrum of 3-Azidopropan-1-ol

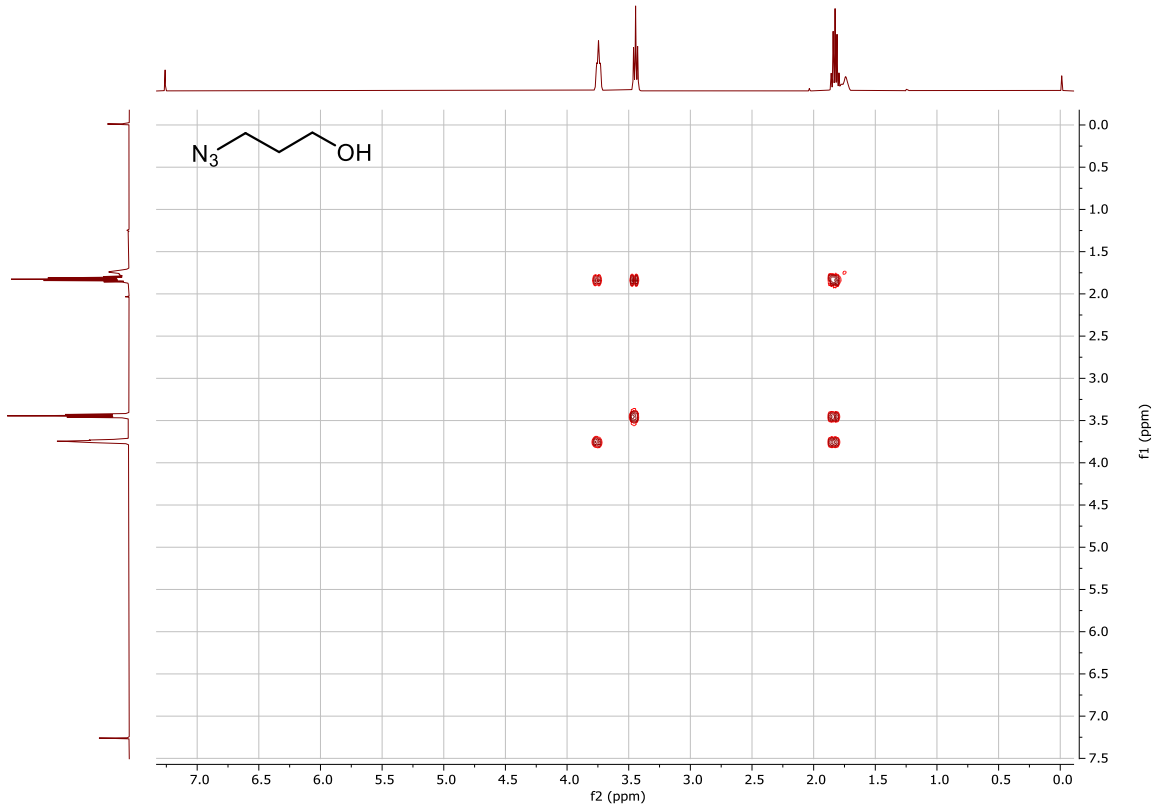

HSQC-NMR spectrum of 3-Azidopropan-1-ol

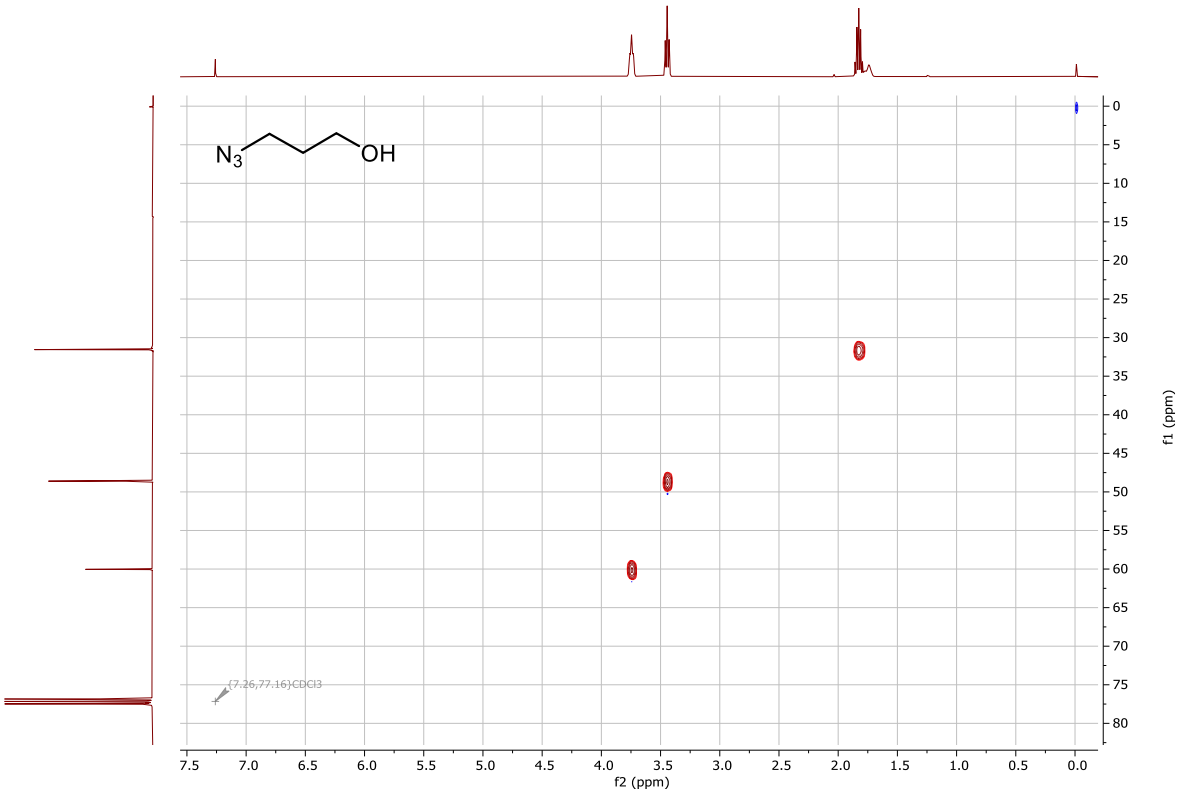

^{1}H NMR spectrum of compound 2-68

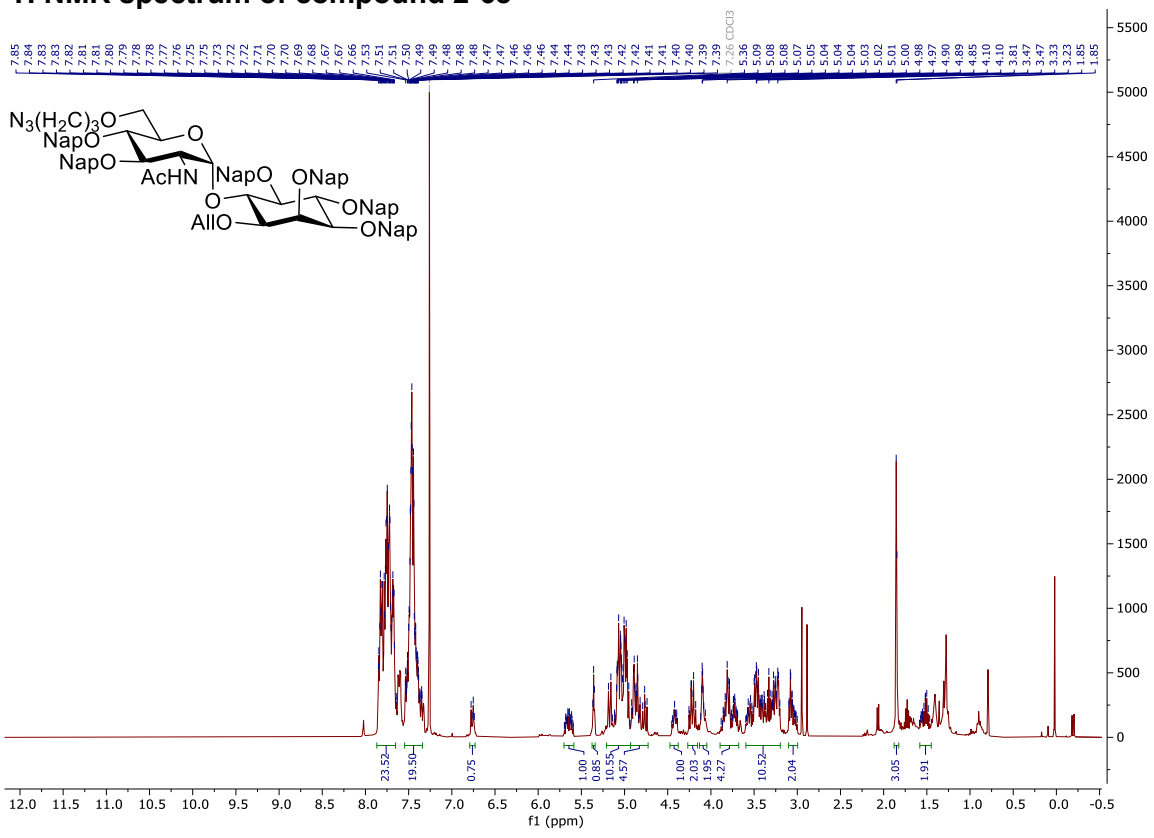

^{13}C NMR spectrum of compound 2-68

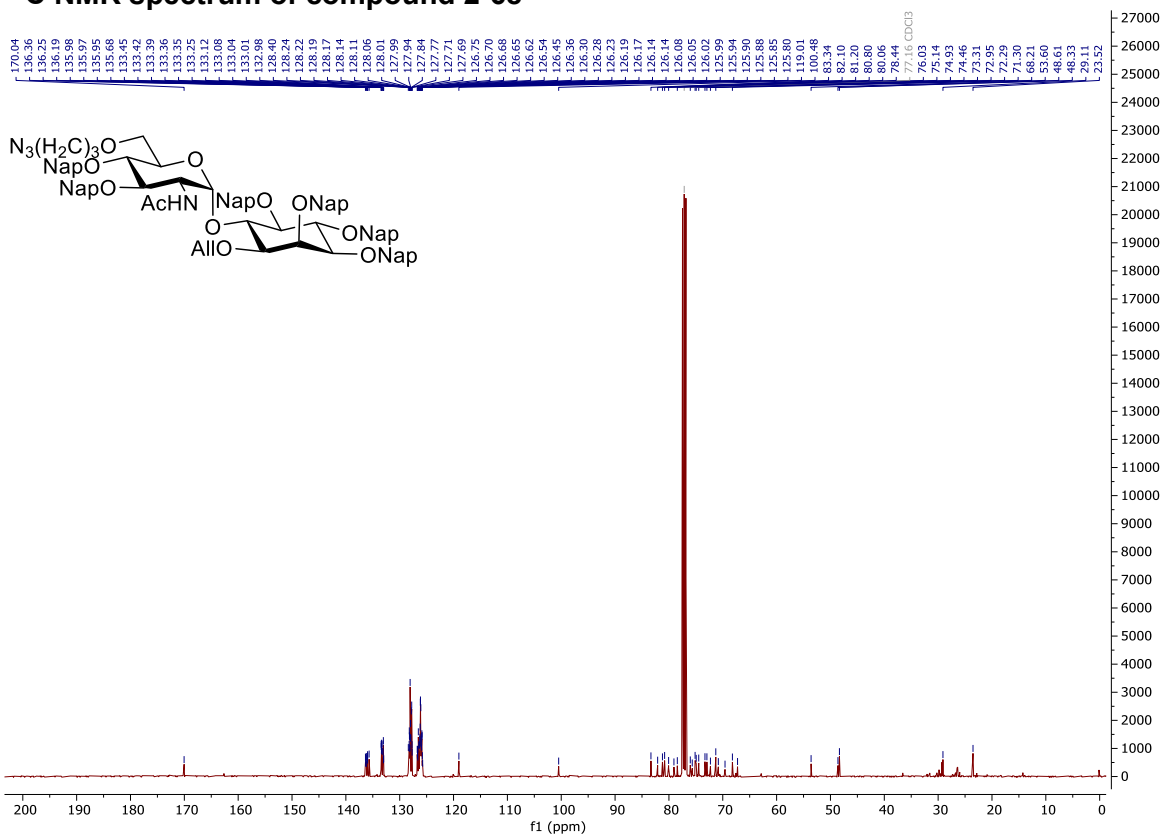

COSY-NMR spectrum of compound 2-68

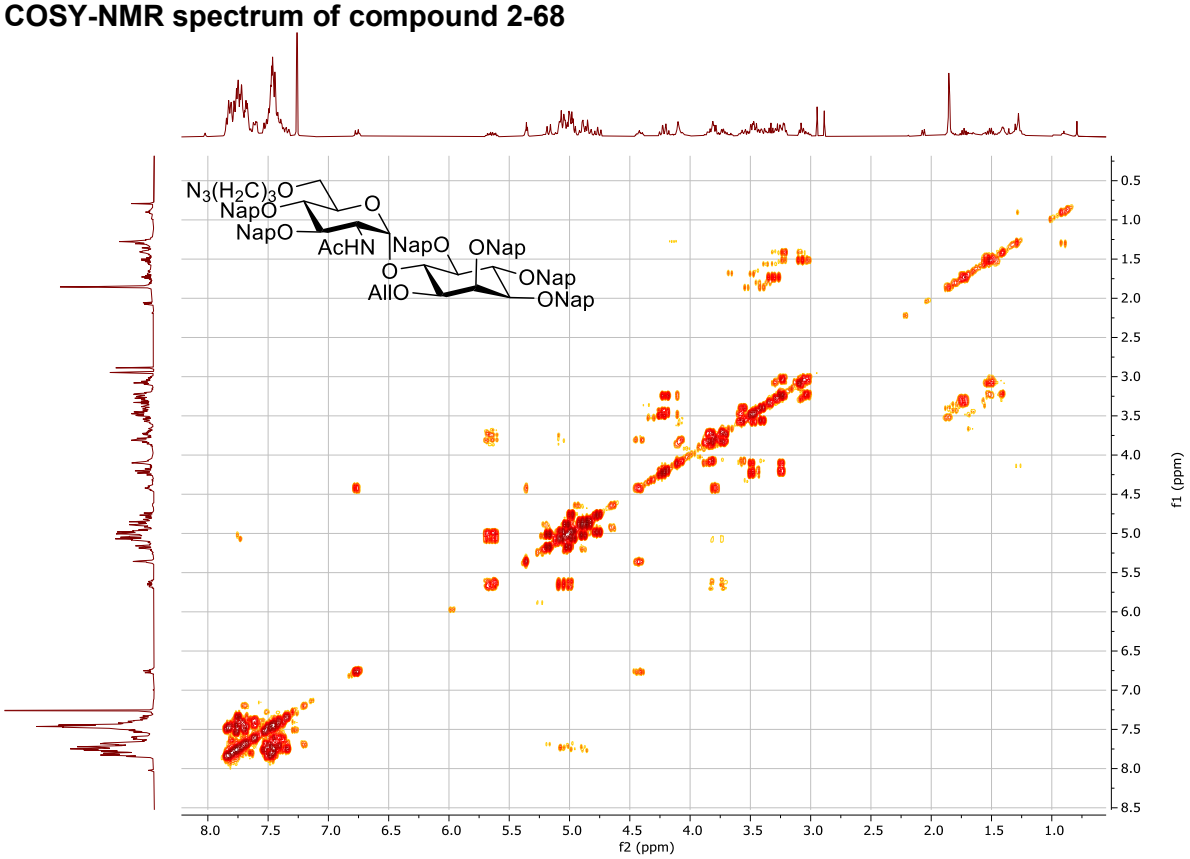

HSQC-NMR spectrum of compound 2-68

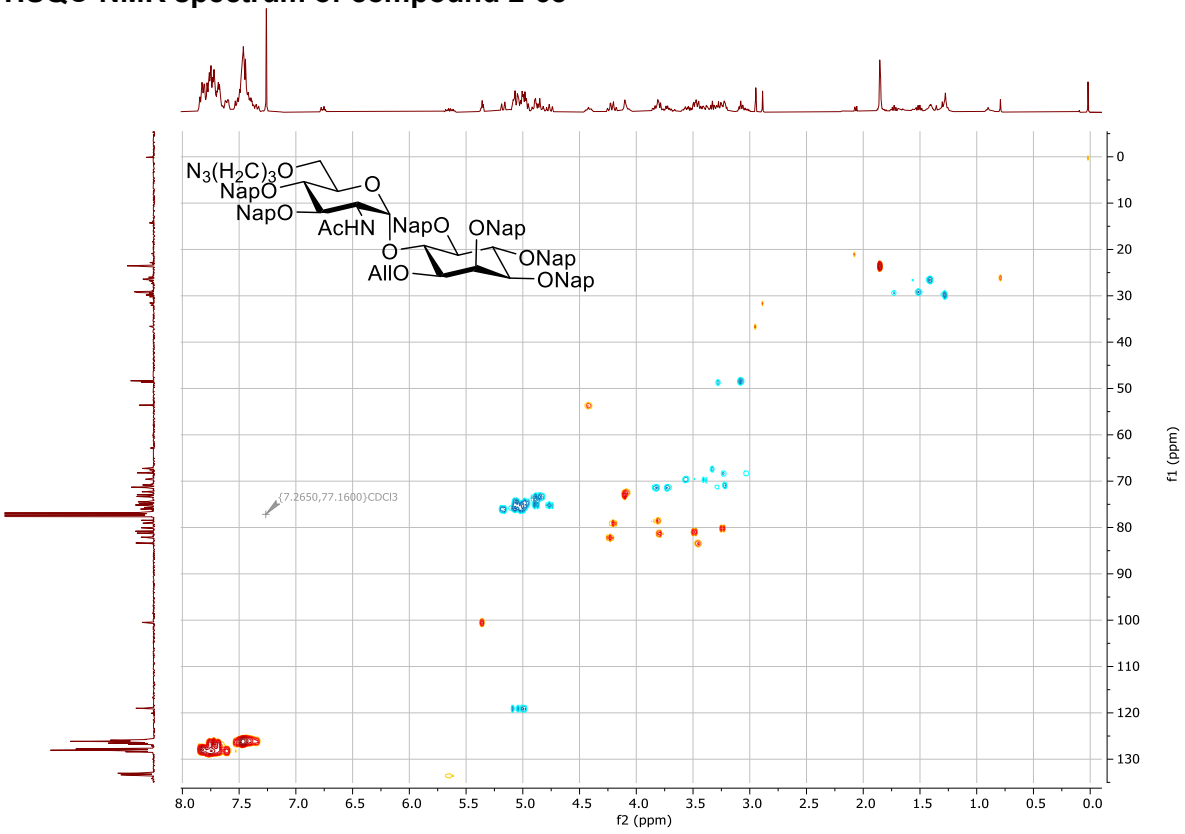

^{1}H NMR spectrum of compound 2-69

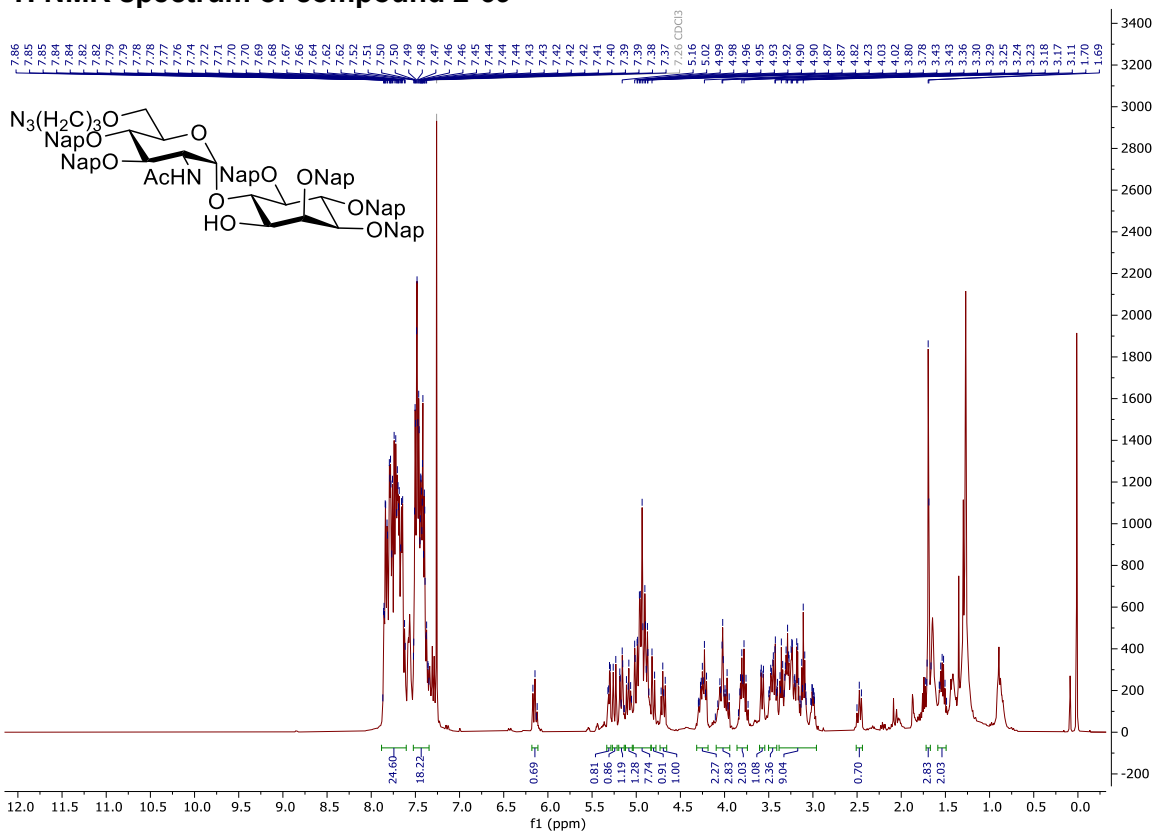

^{13}C NMR spectrum of compound 2-69

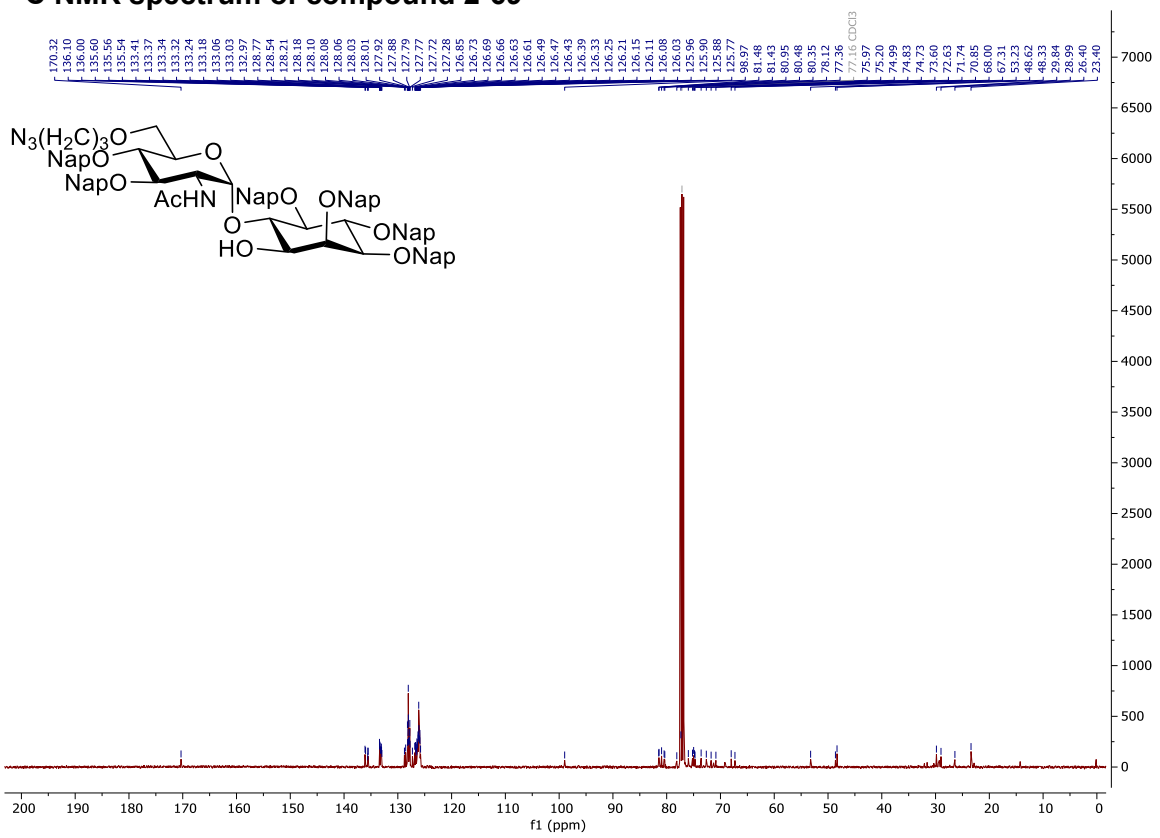

COSY-NMR spectrum of compound 2-69

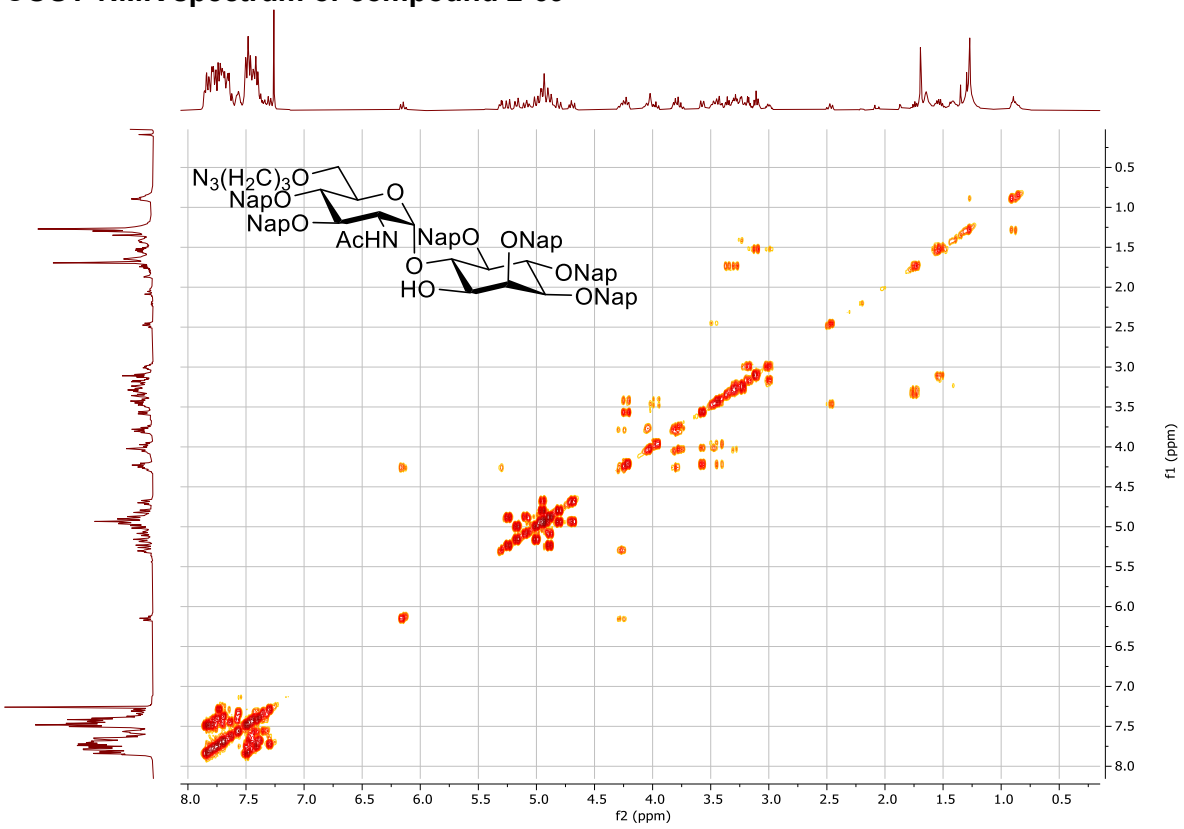

HSQC-NMR spectrum of compound 2-69

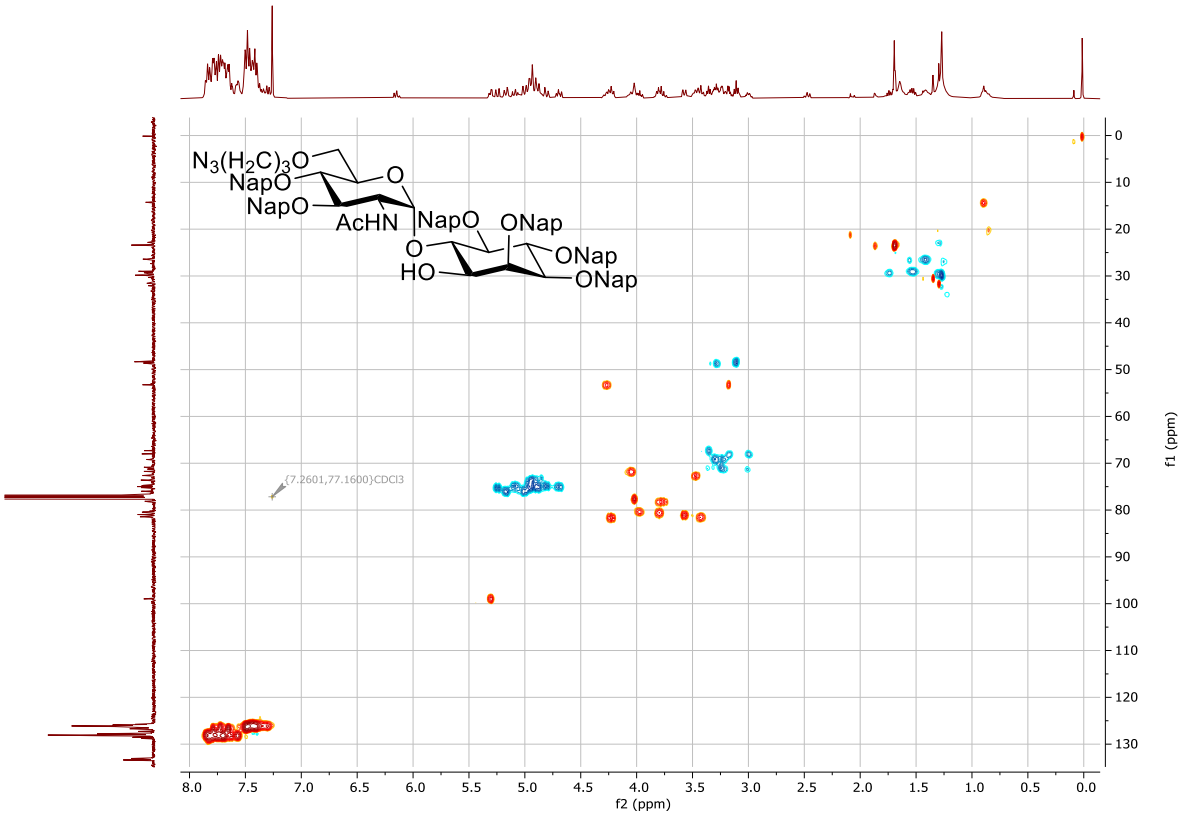

^{1}H NMR spectrum of GPI fragment 2-53

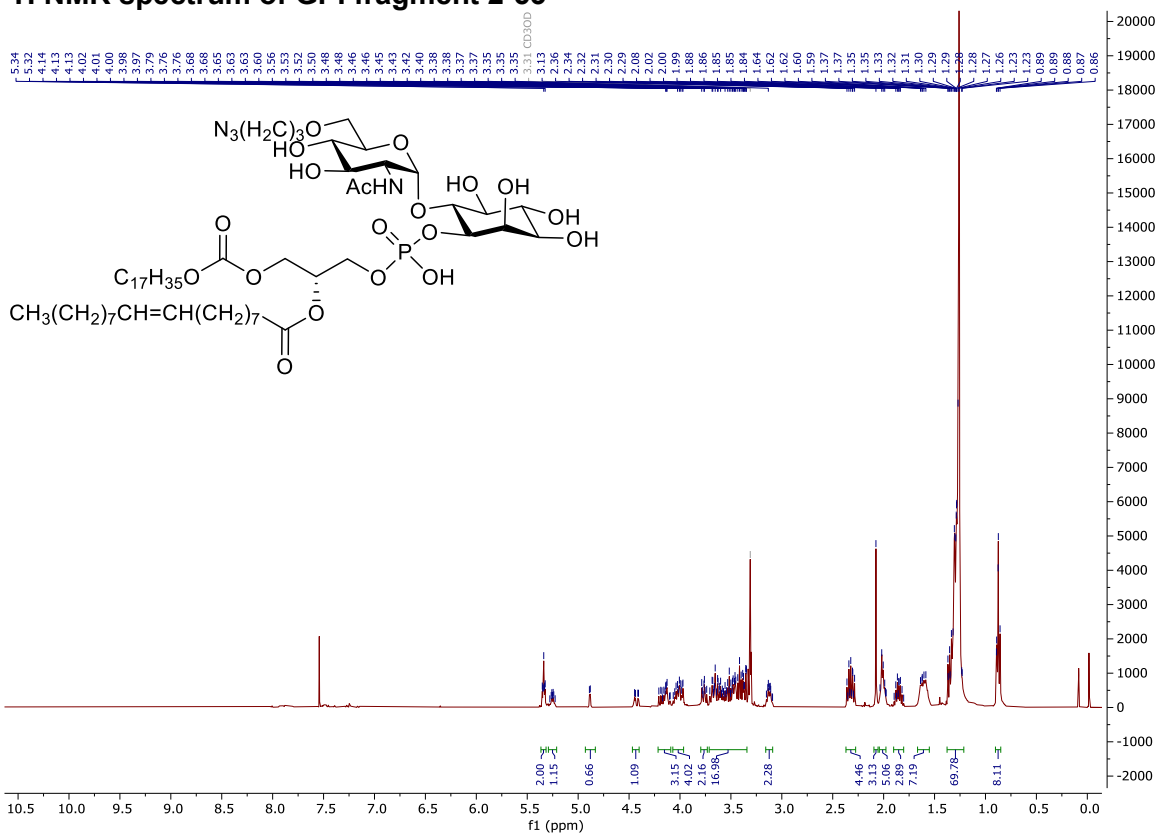

^{13}C NMR spectrum of GPI fragment 2-53

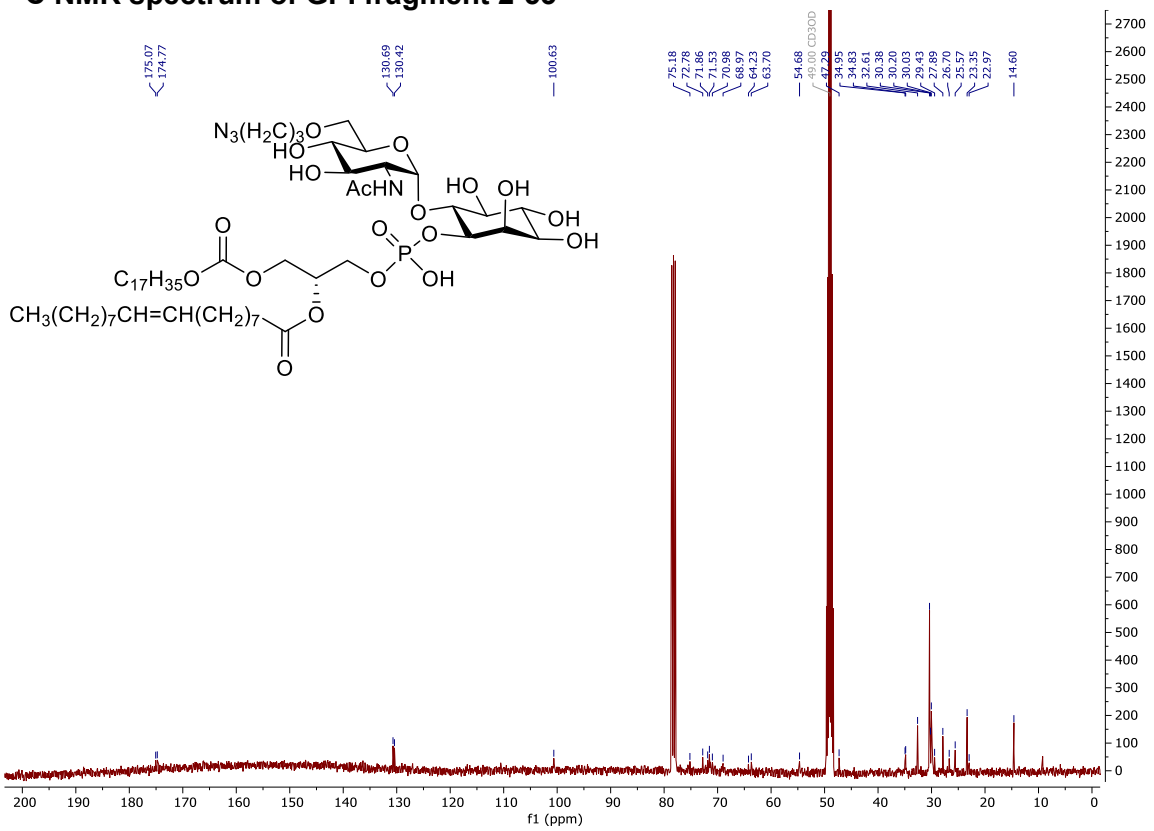

COSY-NMR spectrum of GPI fragment 2-53

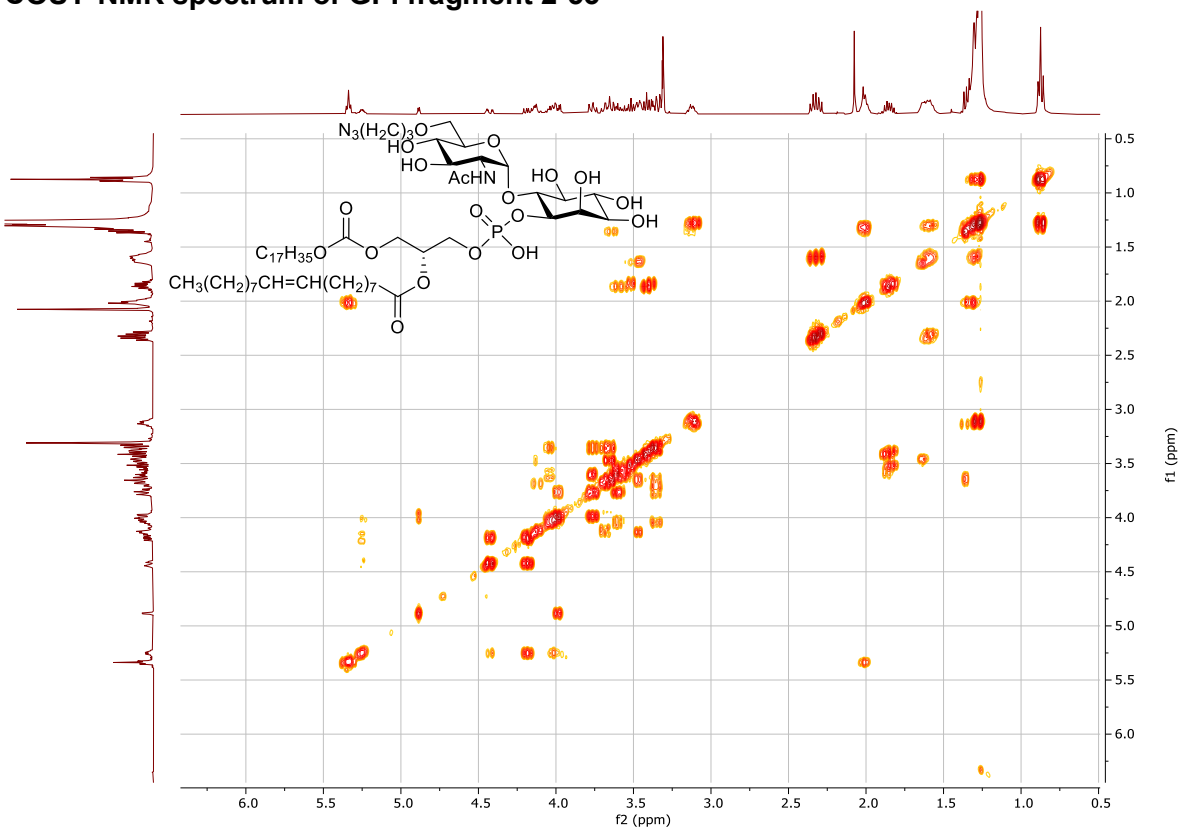

HSQC-NMR spectrum of GPI fragment 2-53

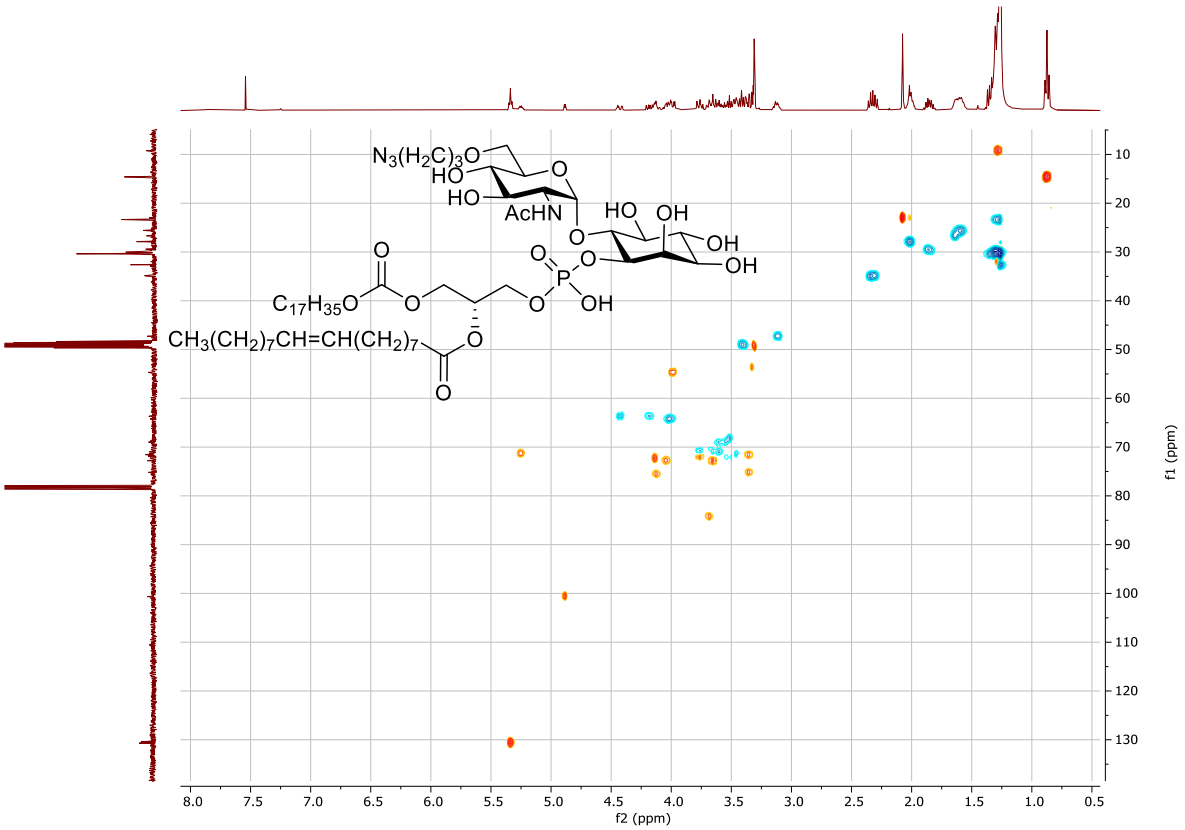

^{31}P-NMR spectrum of GPI fragment 2-53

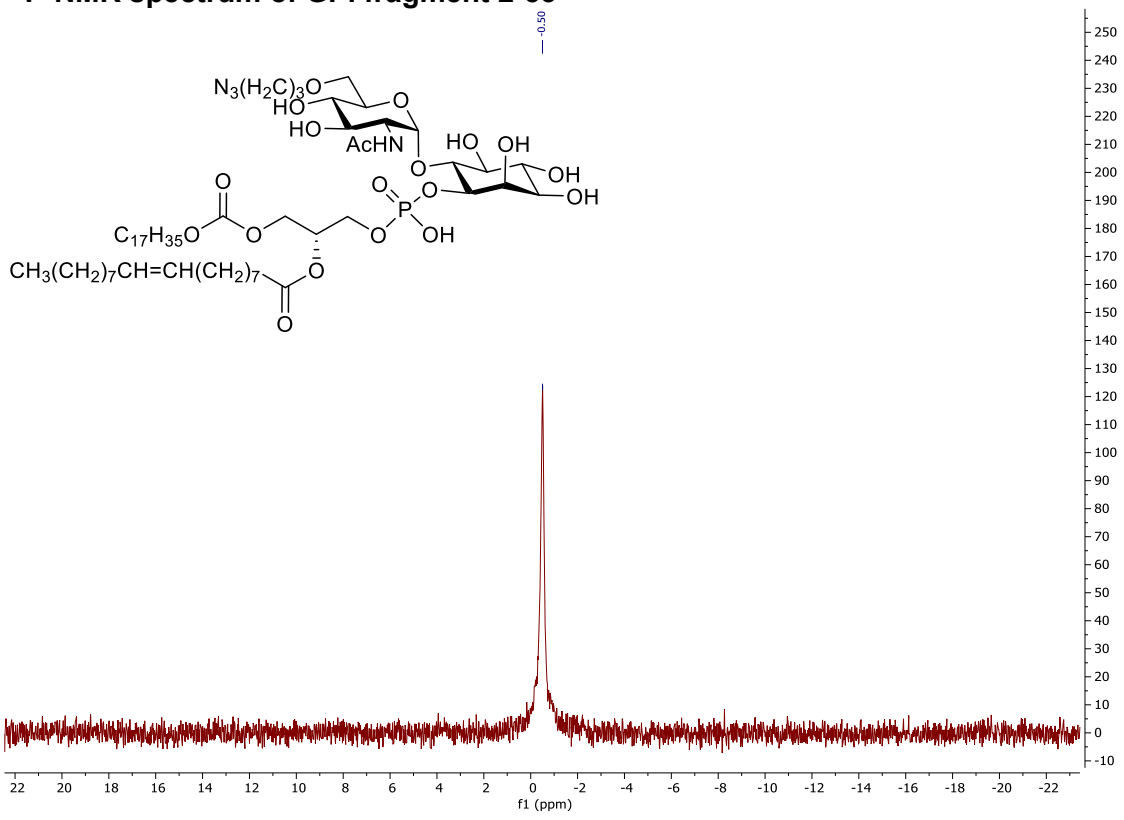

^{1}H NMR spectrum of compound 3-8

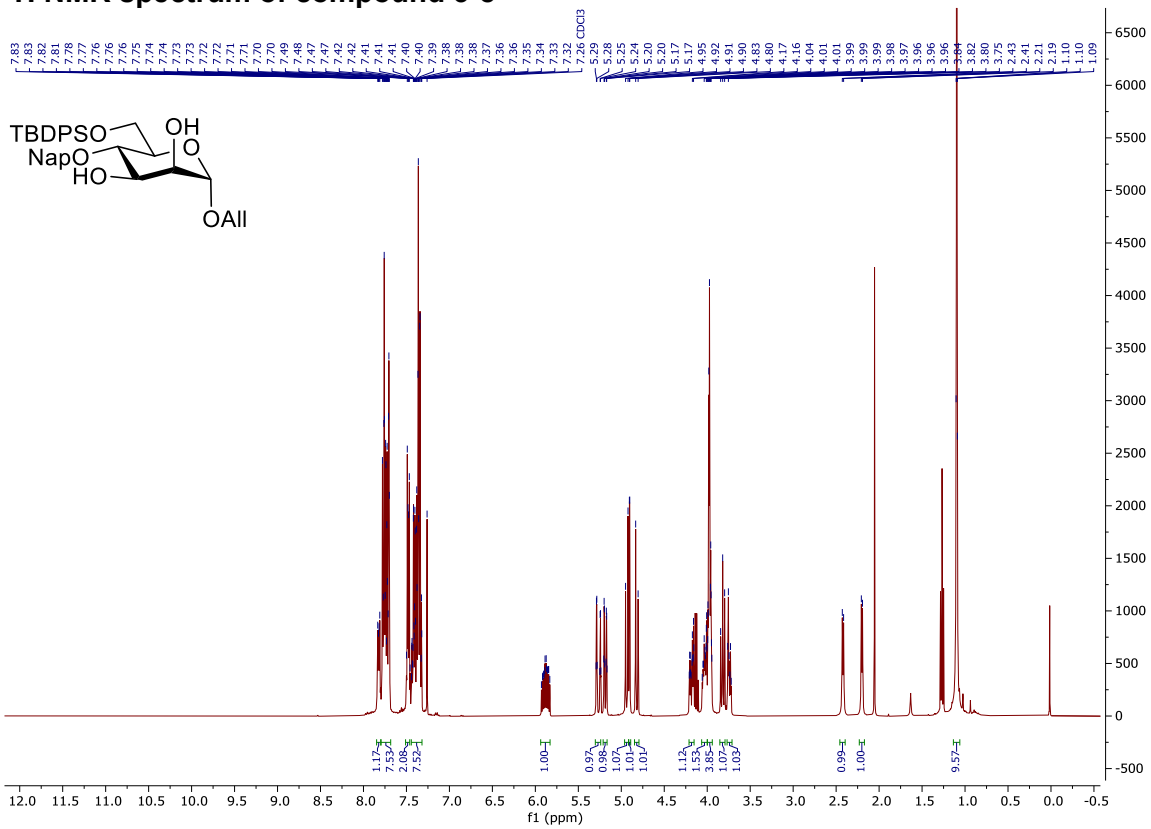

^{13}C NMR spectrum of compound 3-8

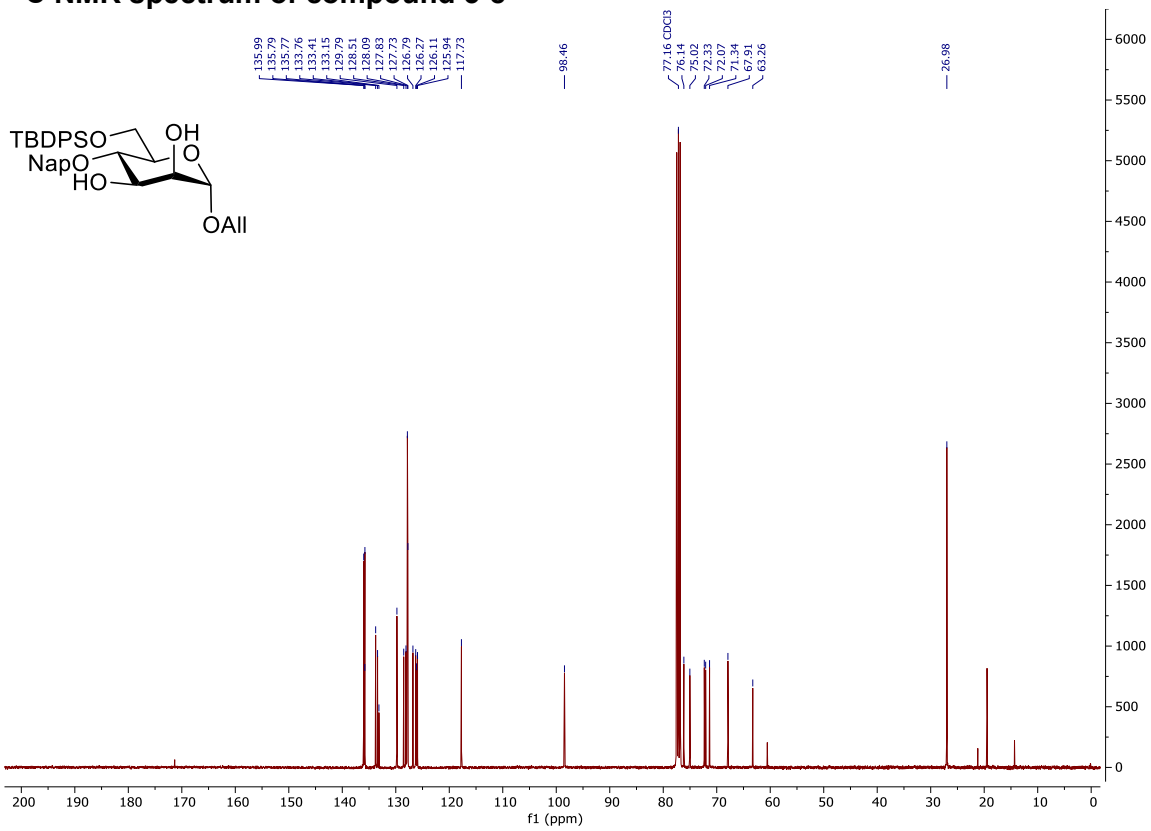

COSY NMR spectrum of compound 3-8

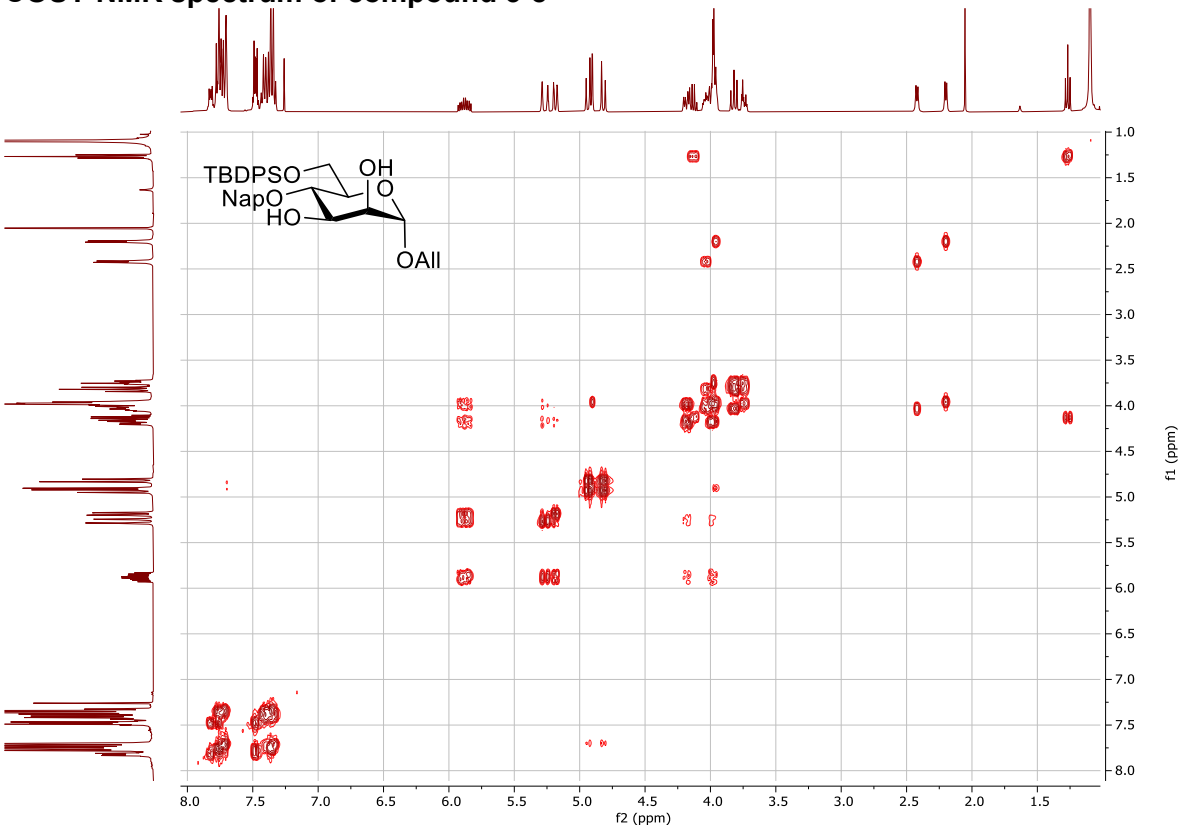

HSQC NMR spectrum of compound 3-8

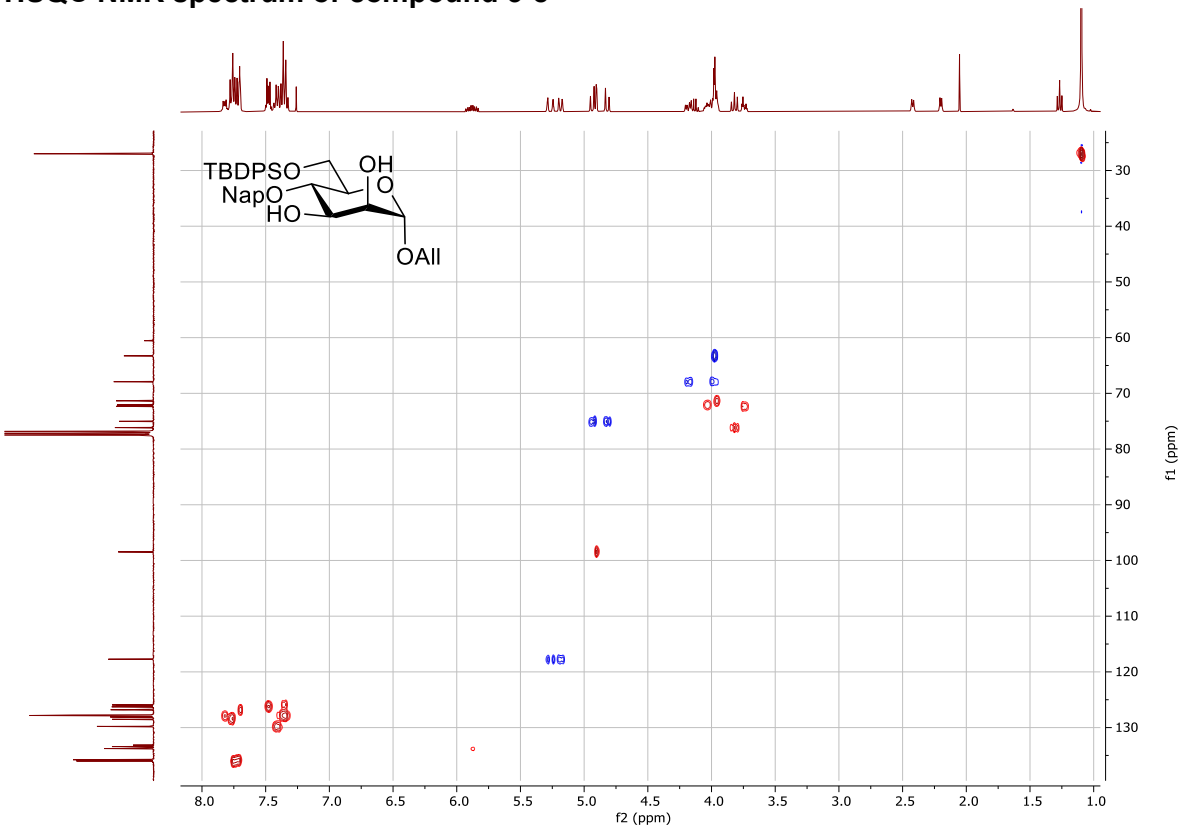

^{1}H NMR spectrum of compound 3-9

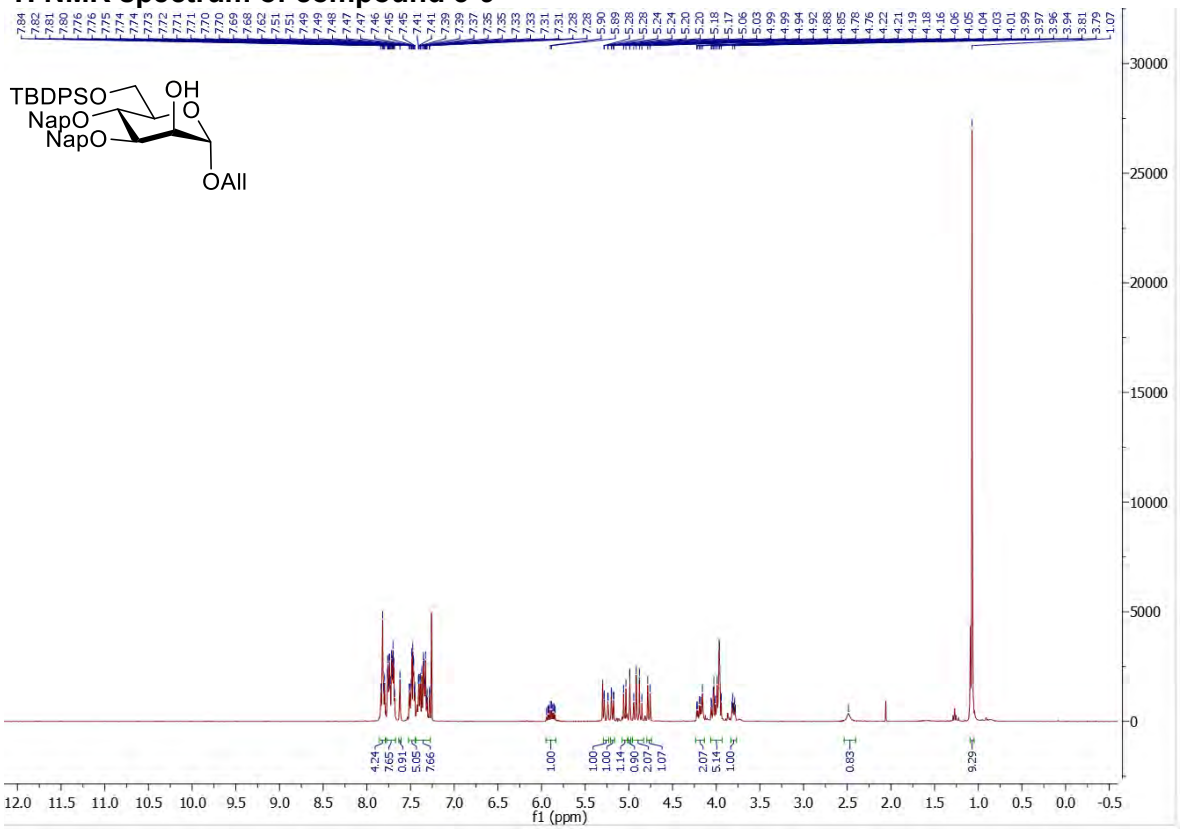

^{13}C NMR spectrum of compound 3-9

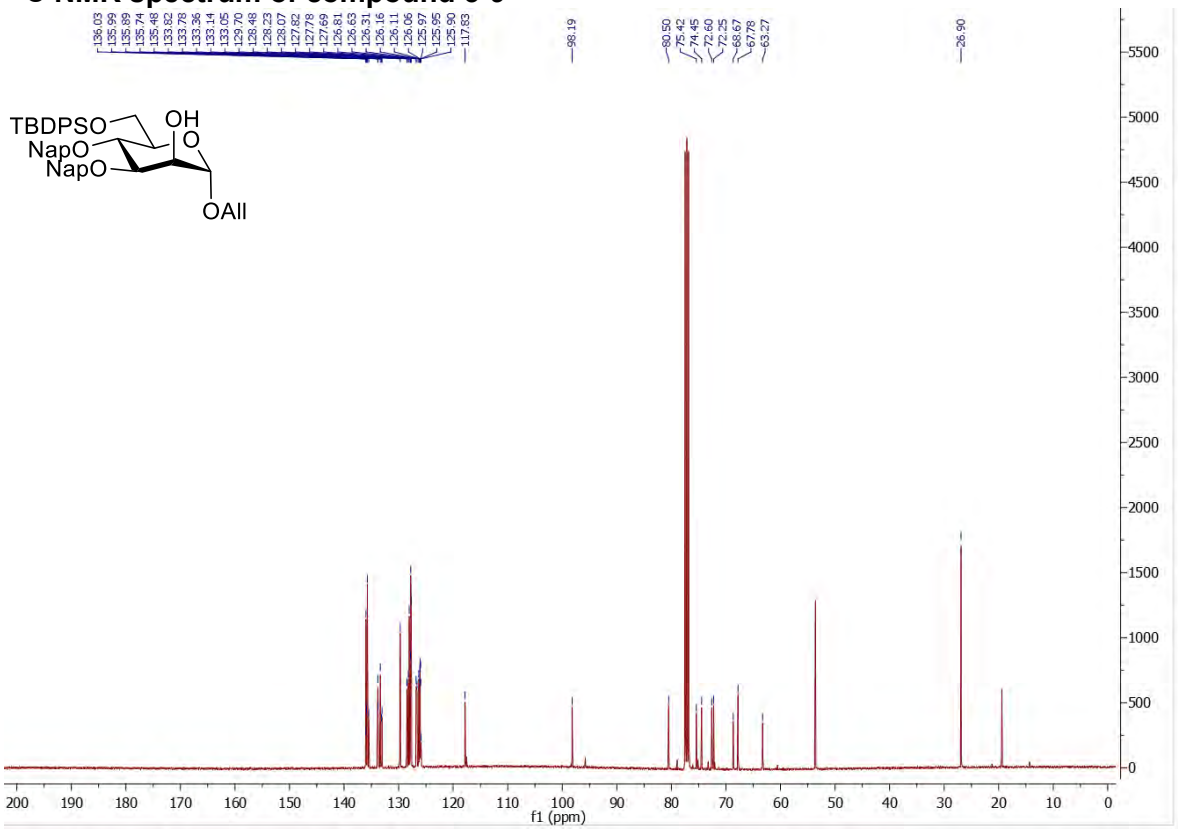

COSY NMR spectrum of compound 3-9

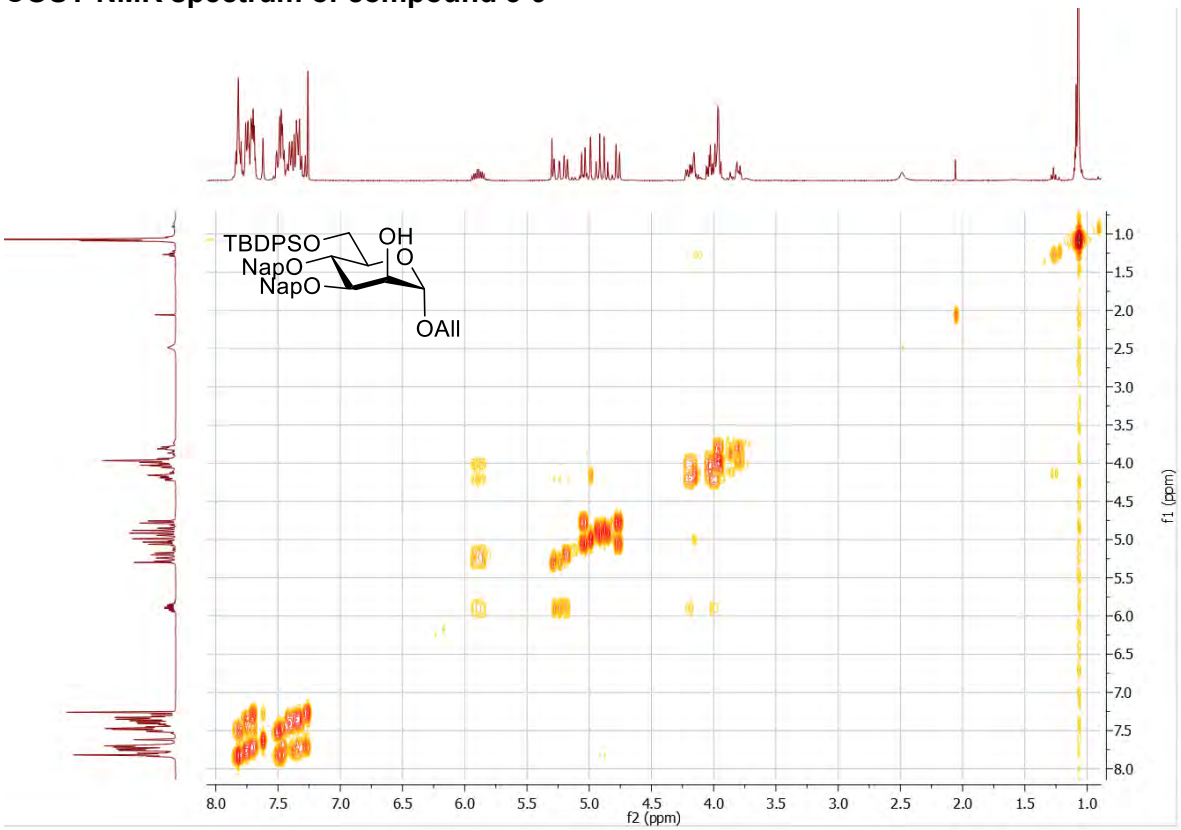

HSQC NMR spectrum of compound 3-9

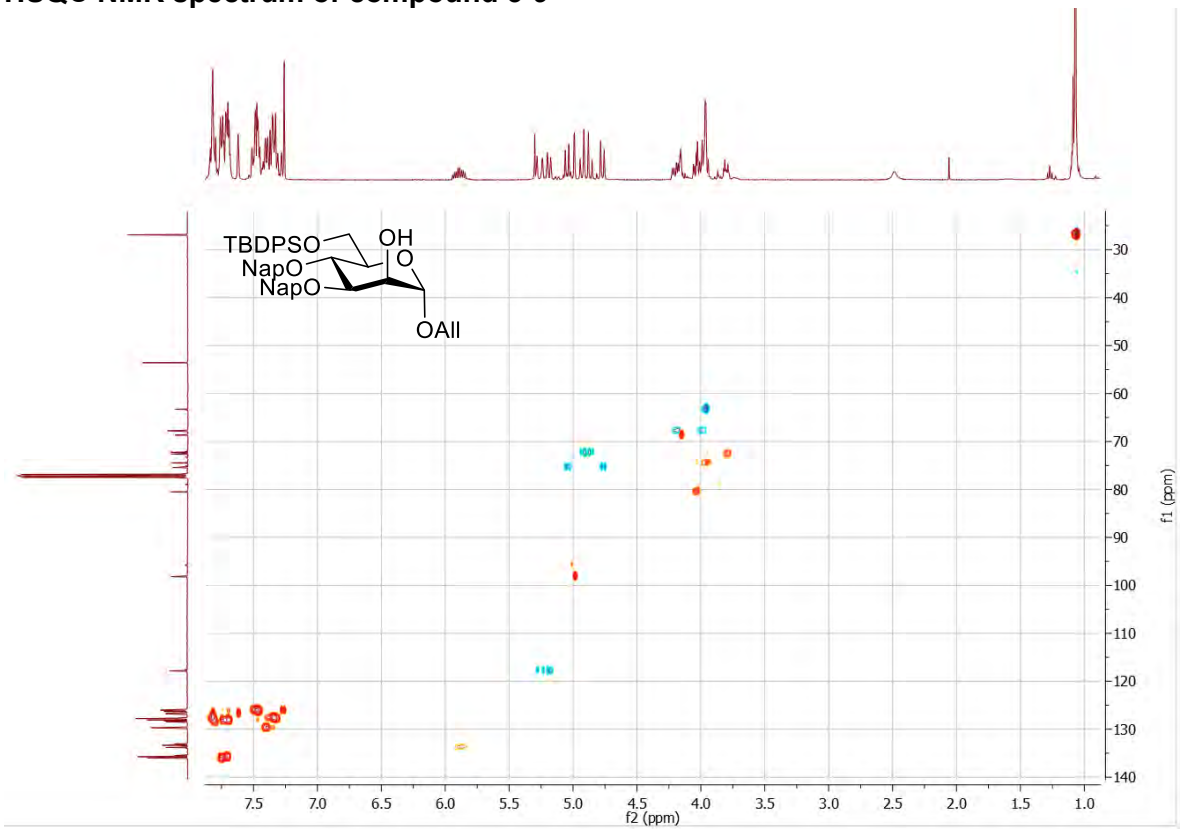

^{1}H NMR spectrum of compound 3-5

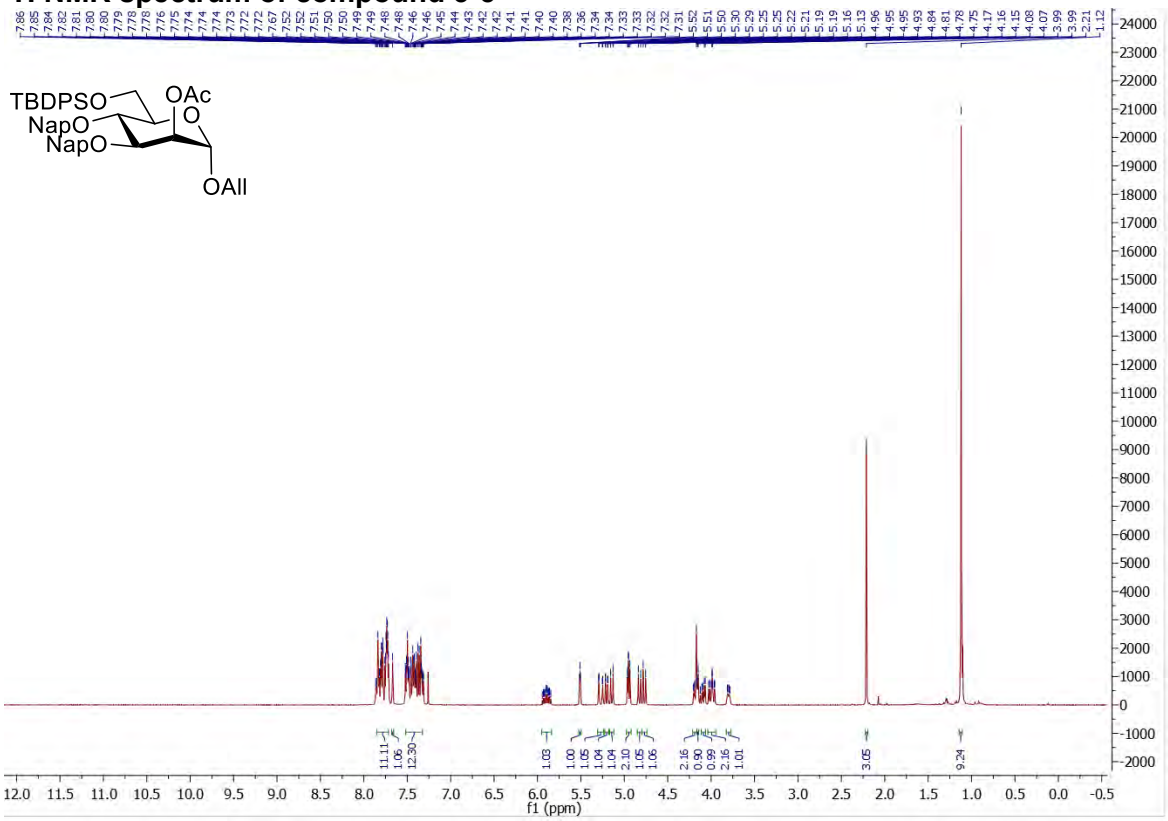

^{13}C NMR spectrum of compound 3-5

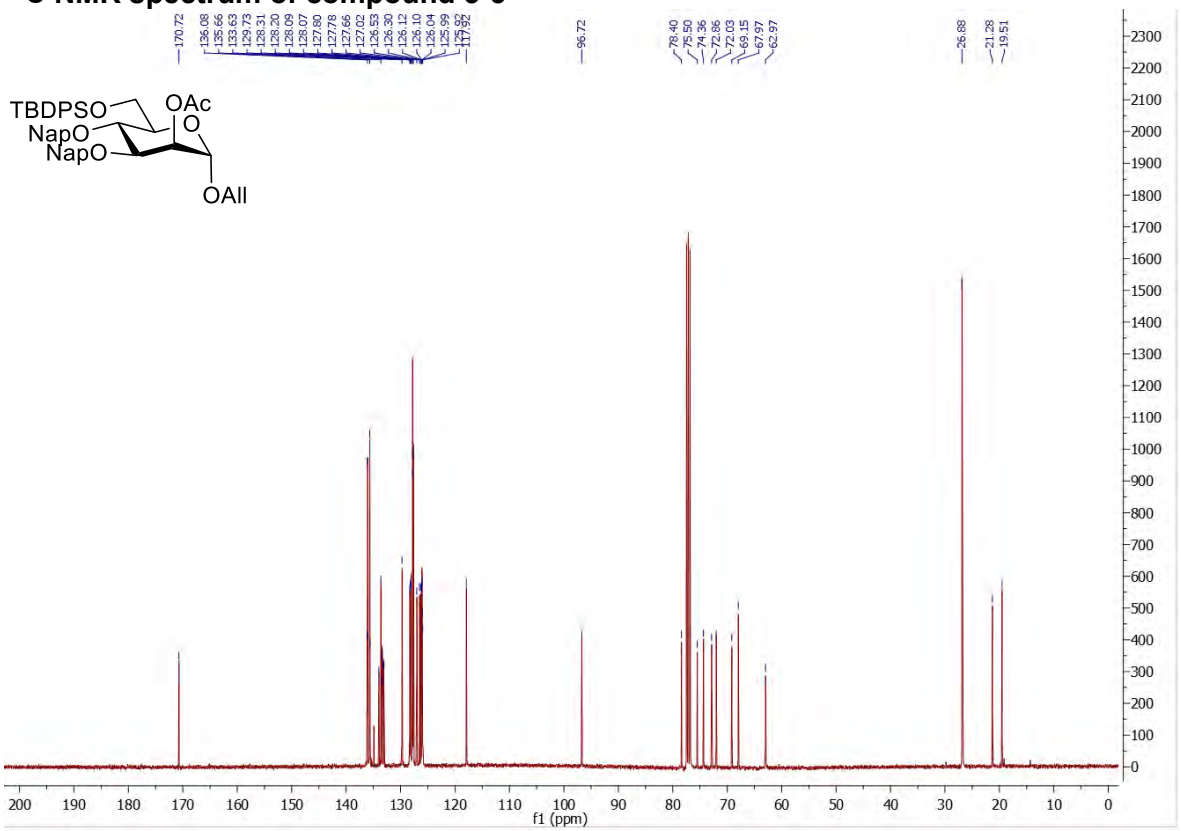

COSY NMR spectrum of compound 3-5

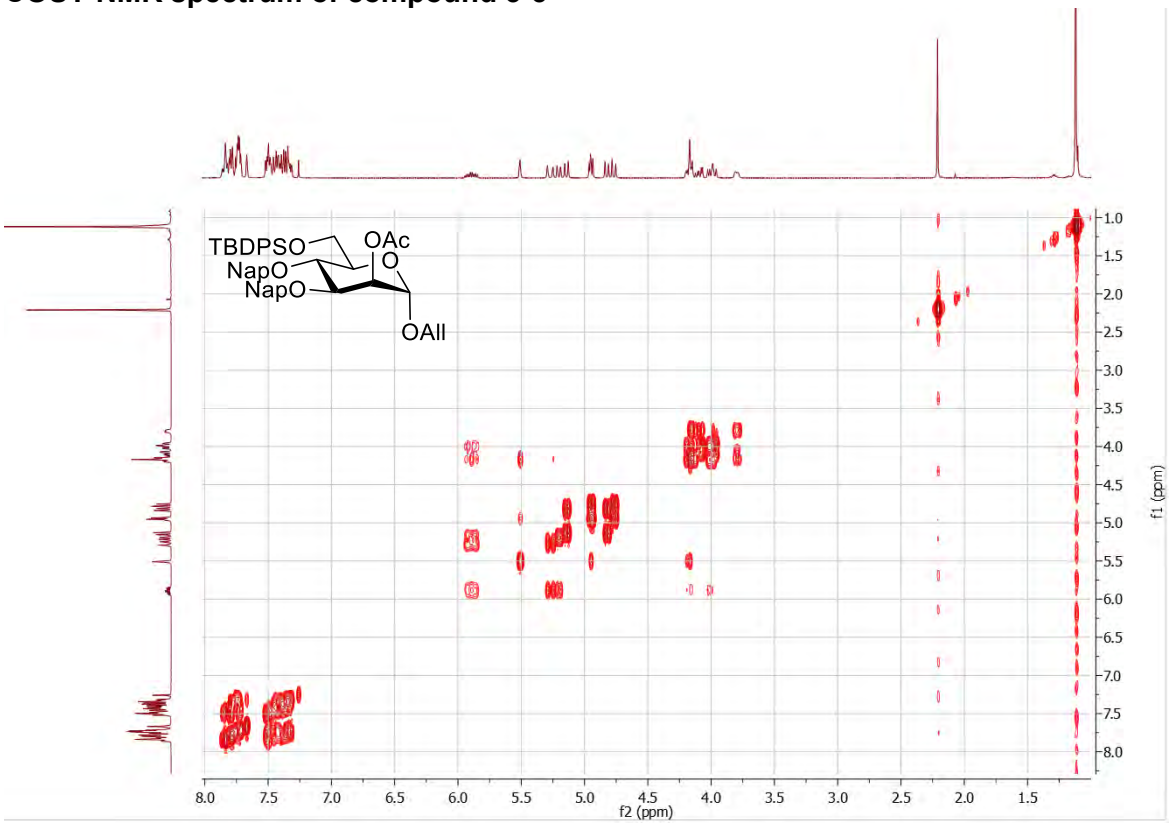

HSQC NMR spectrum of compound 3-5

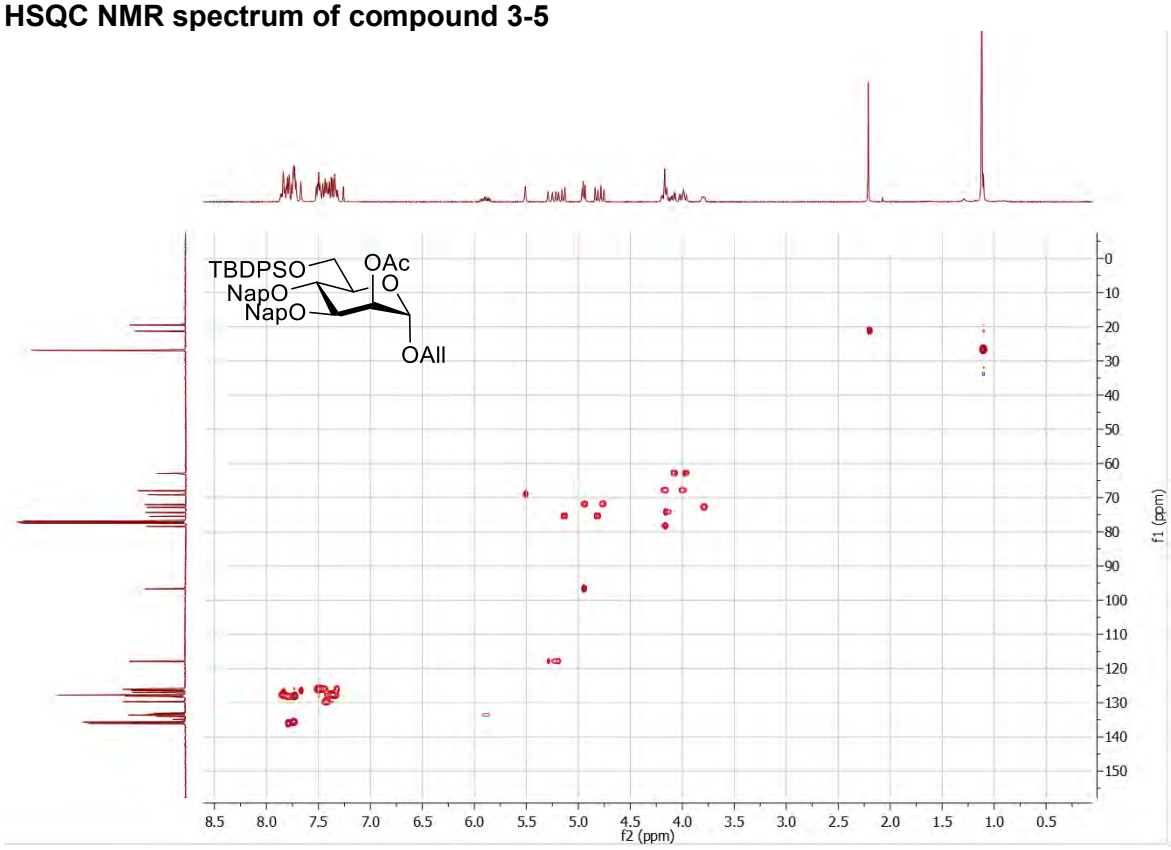

^{1}H NMR spectrum of compound 3-10

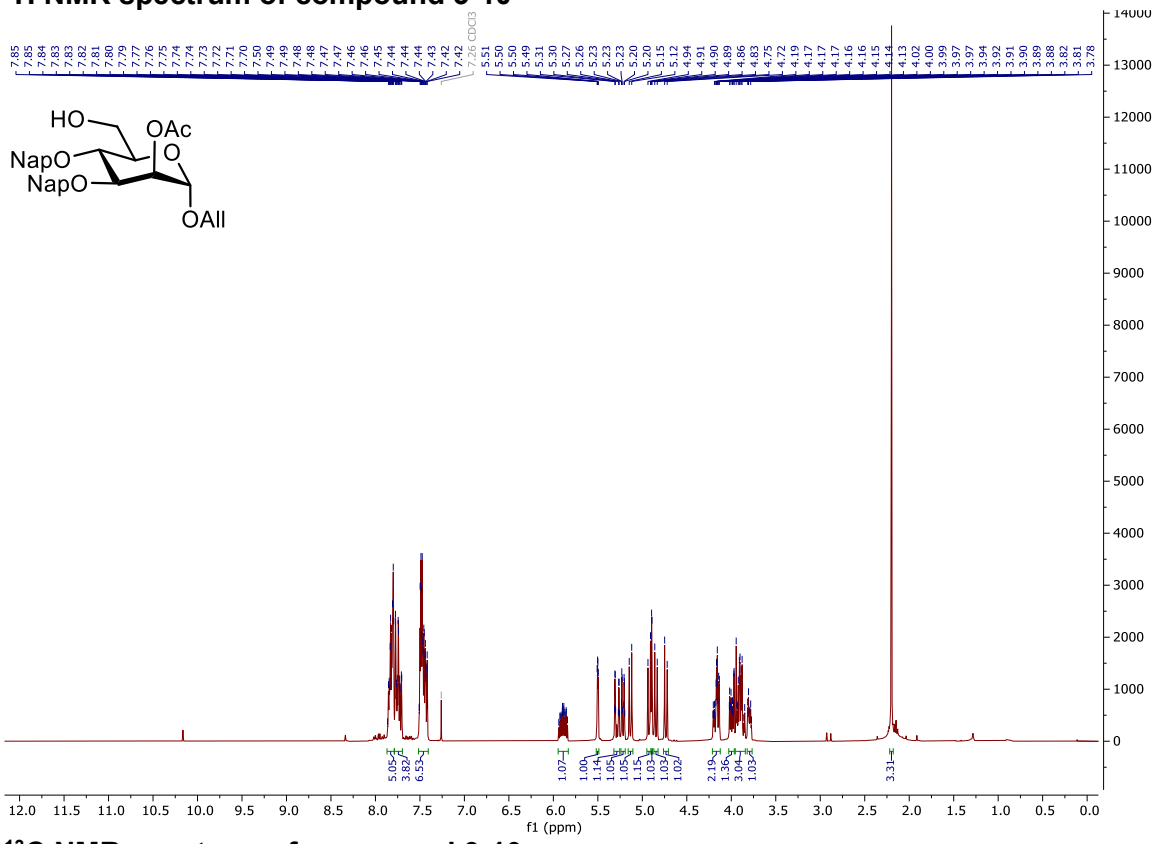

^{13}C NMR spectrum of compound 3-10

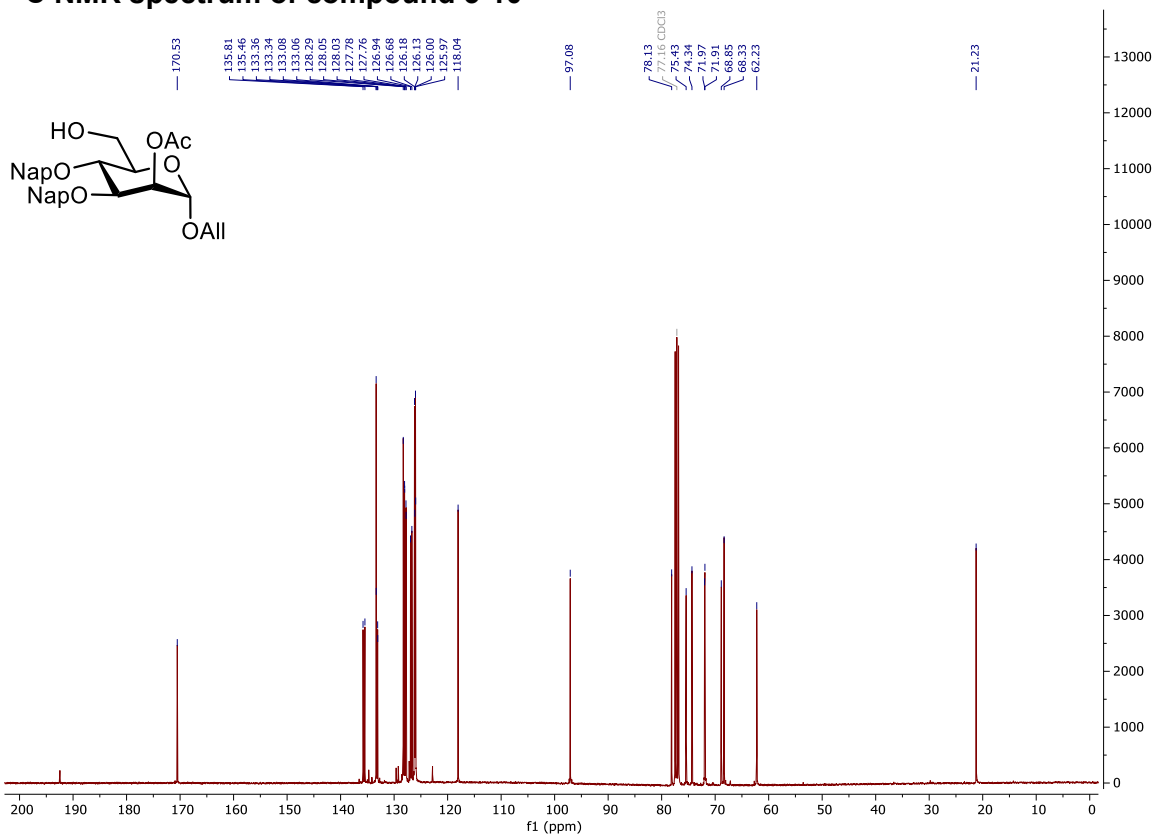

COSY NMR spectrum of compound 3-10

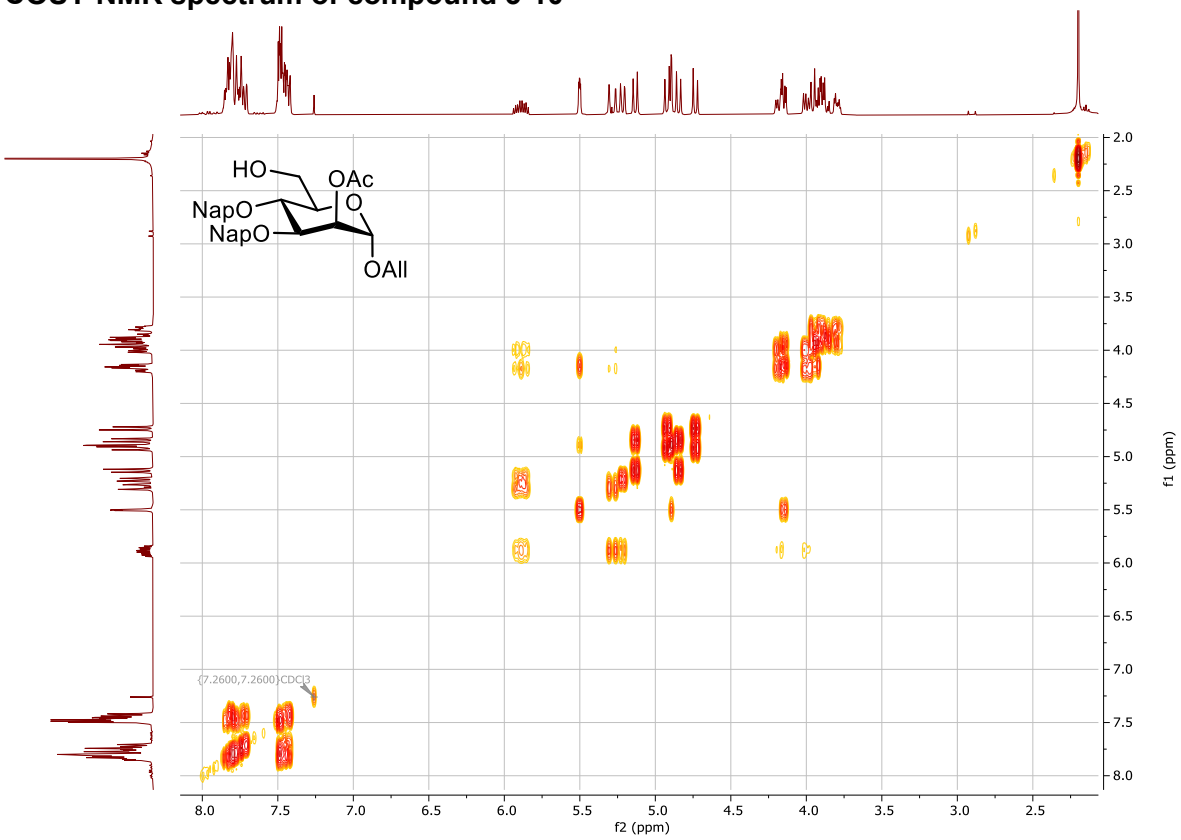

HSQC NMR spectrum of compound 3-10

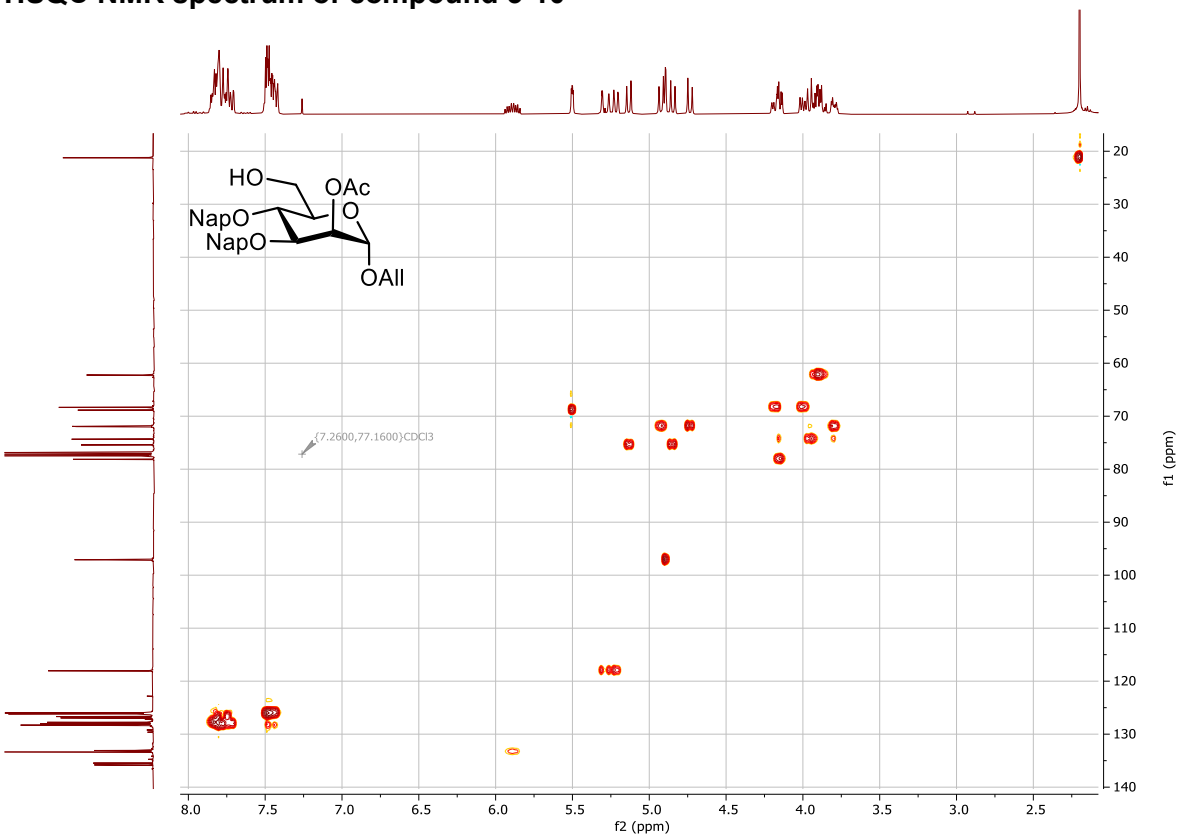

^{1}H NMR spectrum of compound 3-11

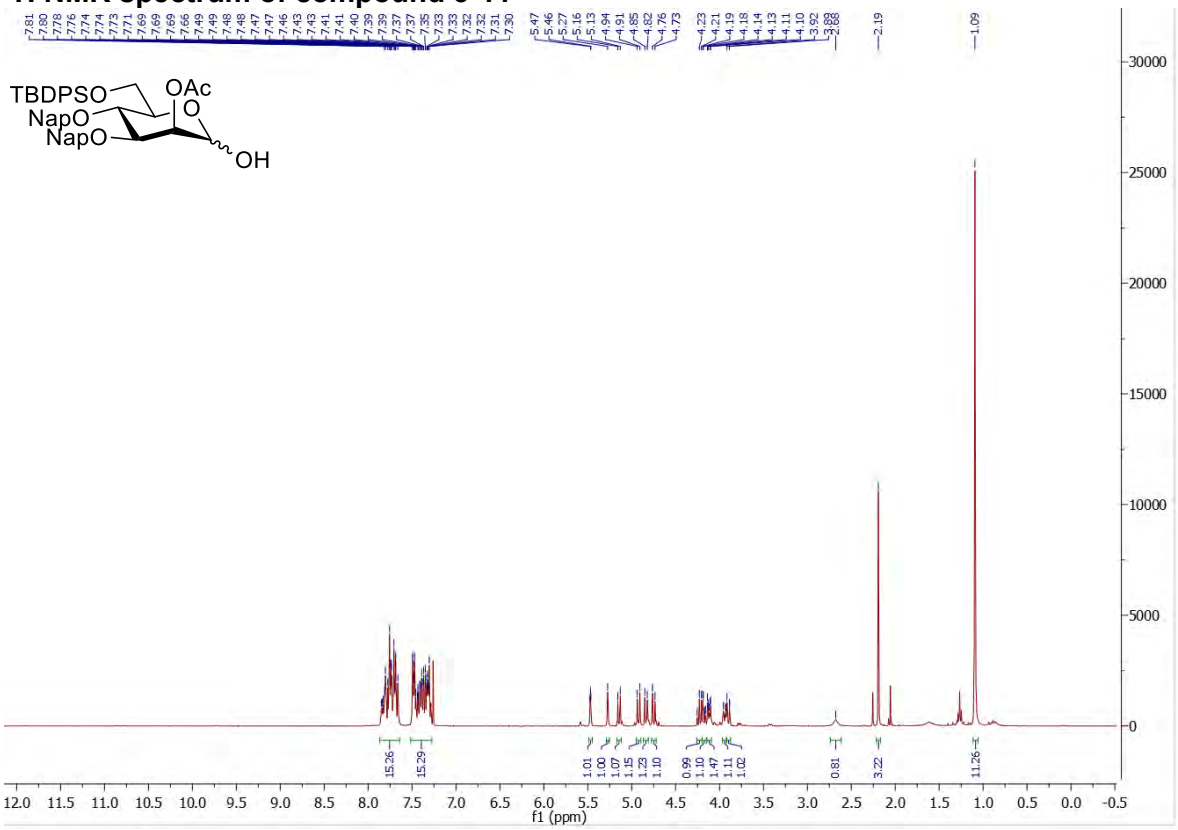

^{13}C NMR spectrum of compound 3-11

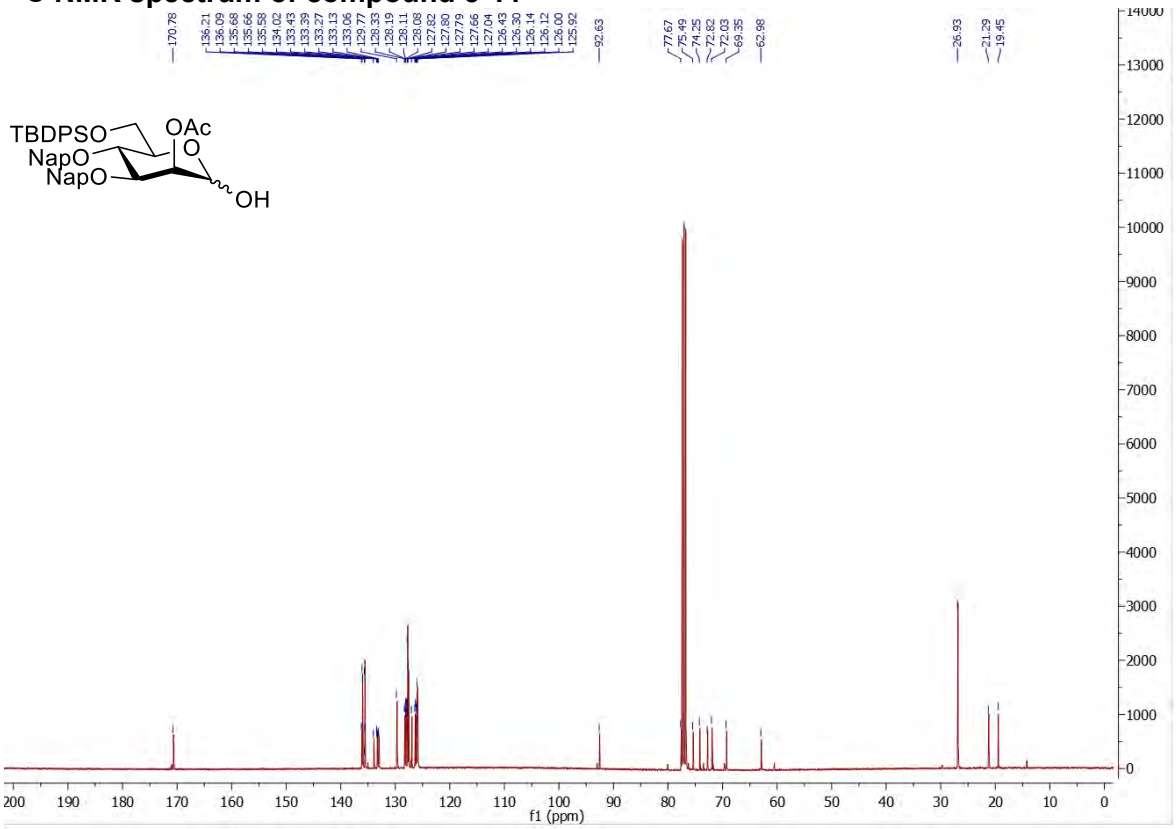

COSY NMR spectrum of compound 3-11

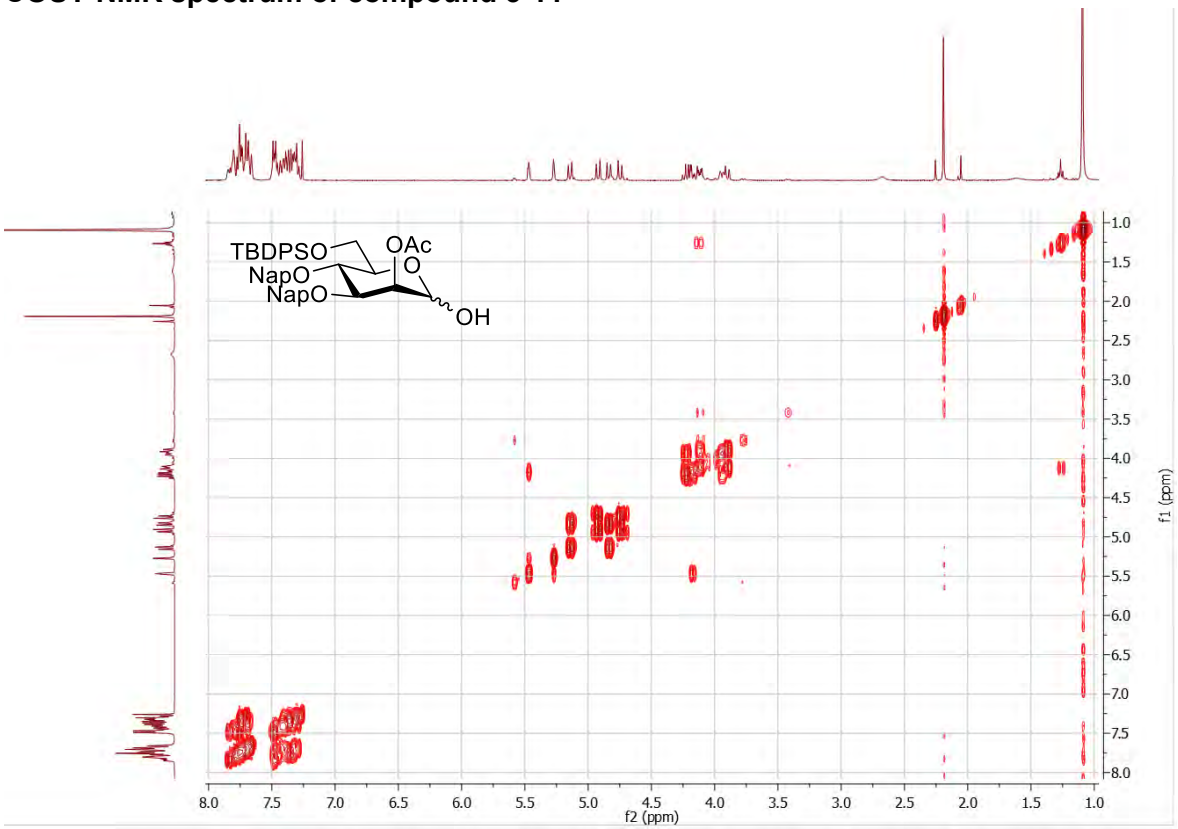

HSQC NMR spectrum of compound 3-11

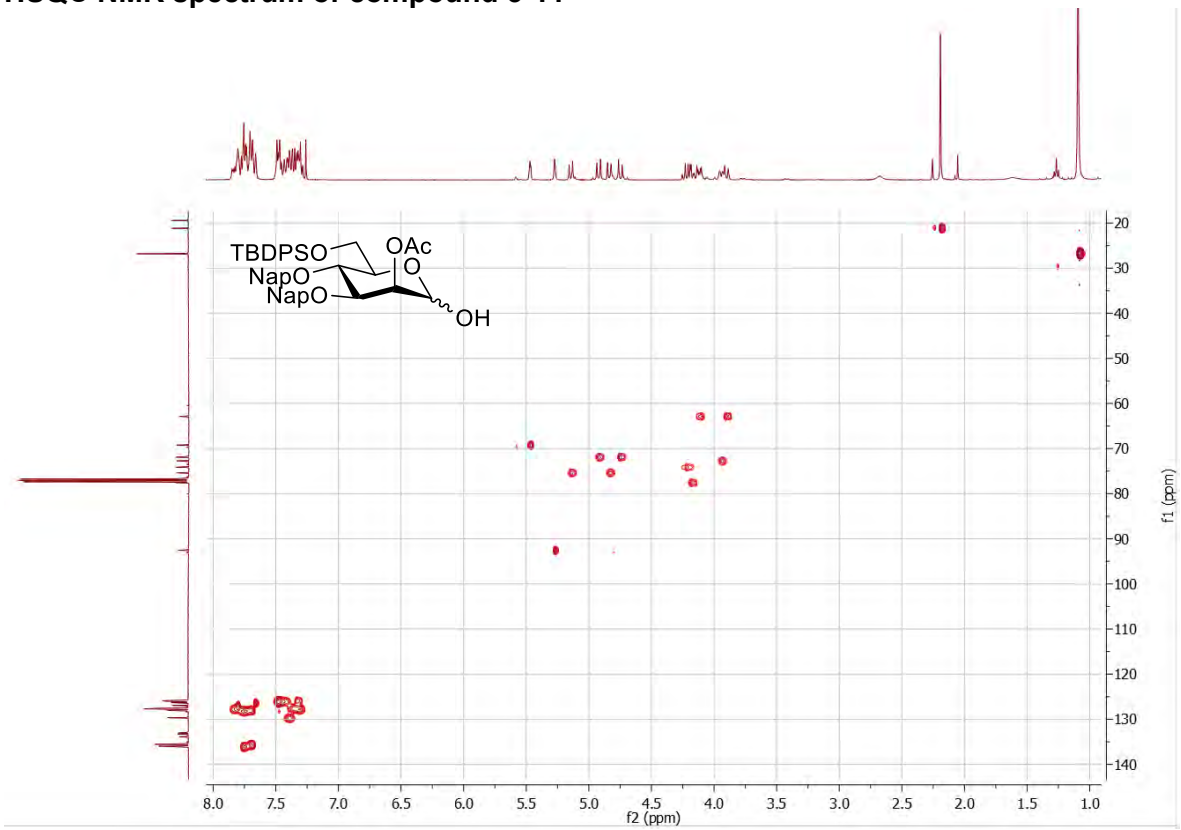

^{1}H NMR spectrum of compound 3-12

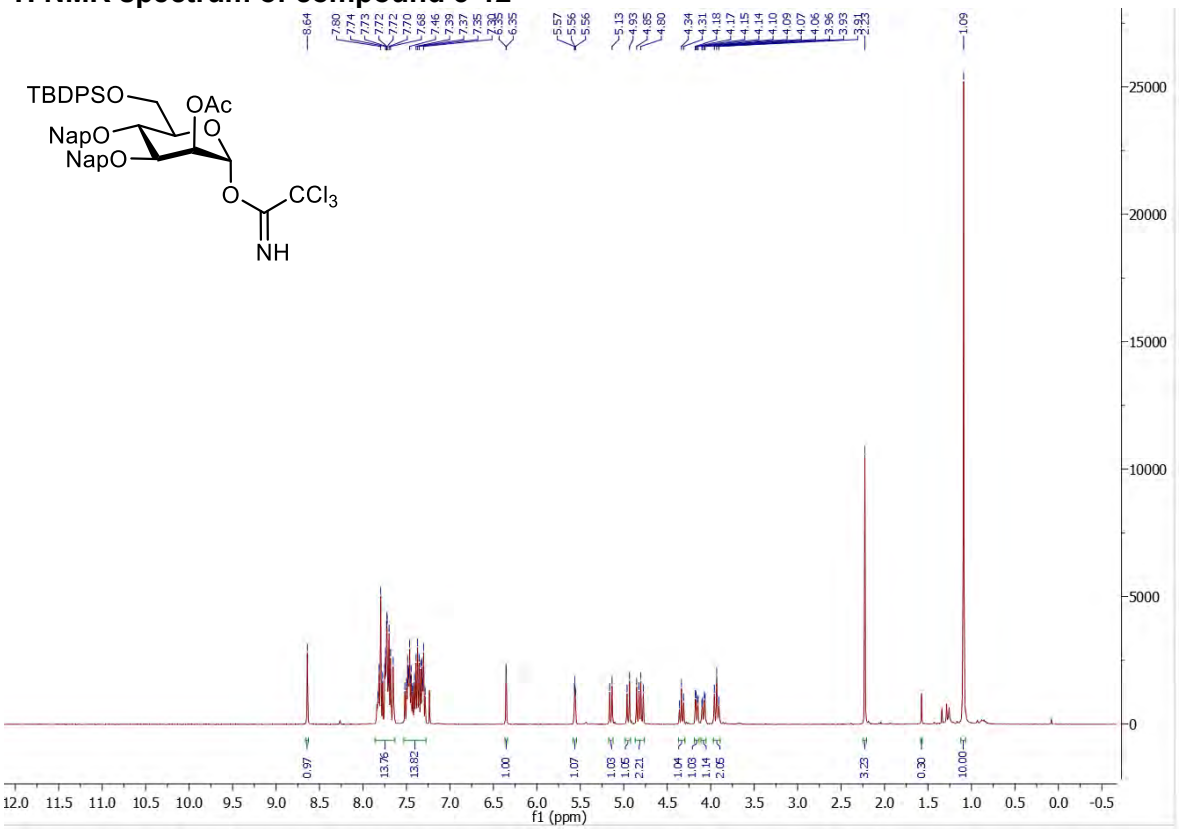

^{13}C NMR spectrum of compound 3-12

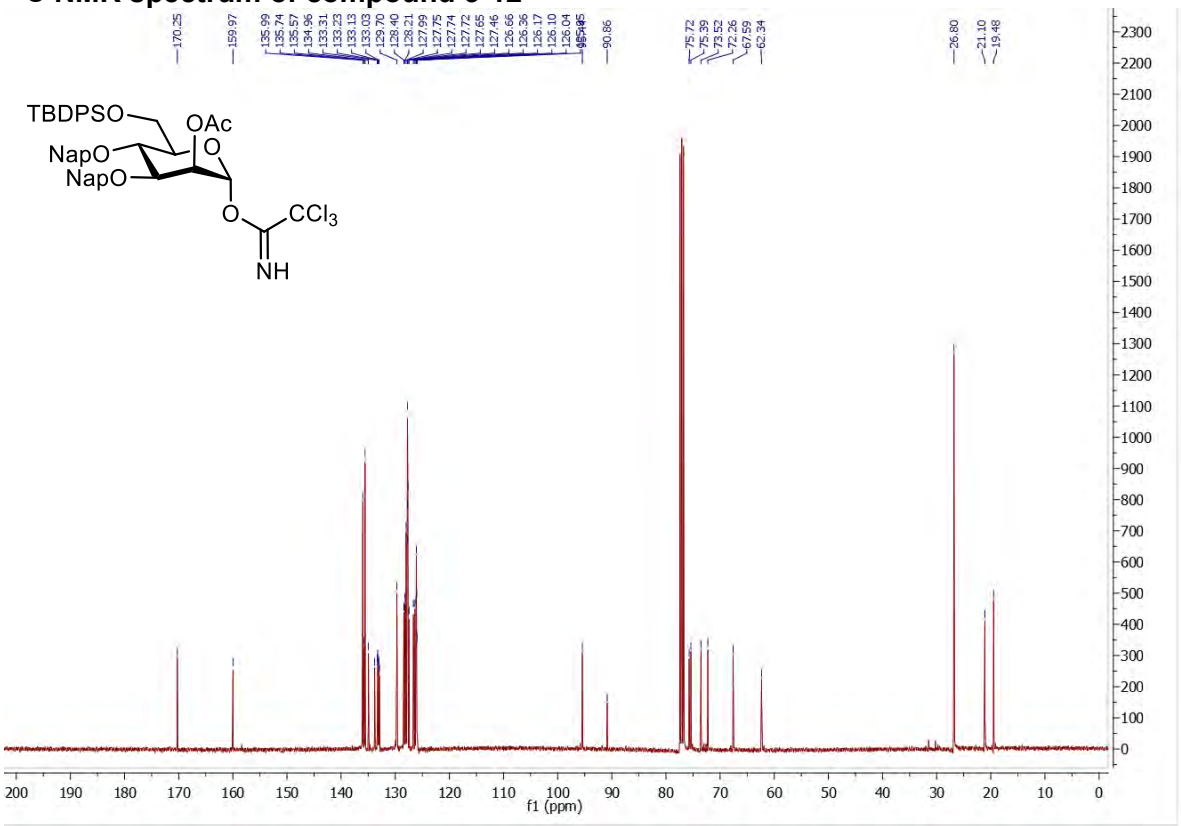

COSY NMR spectrum of compound 3-12

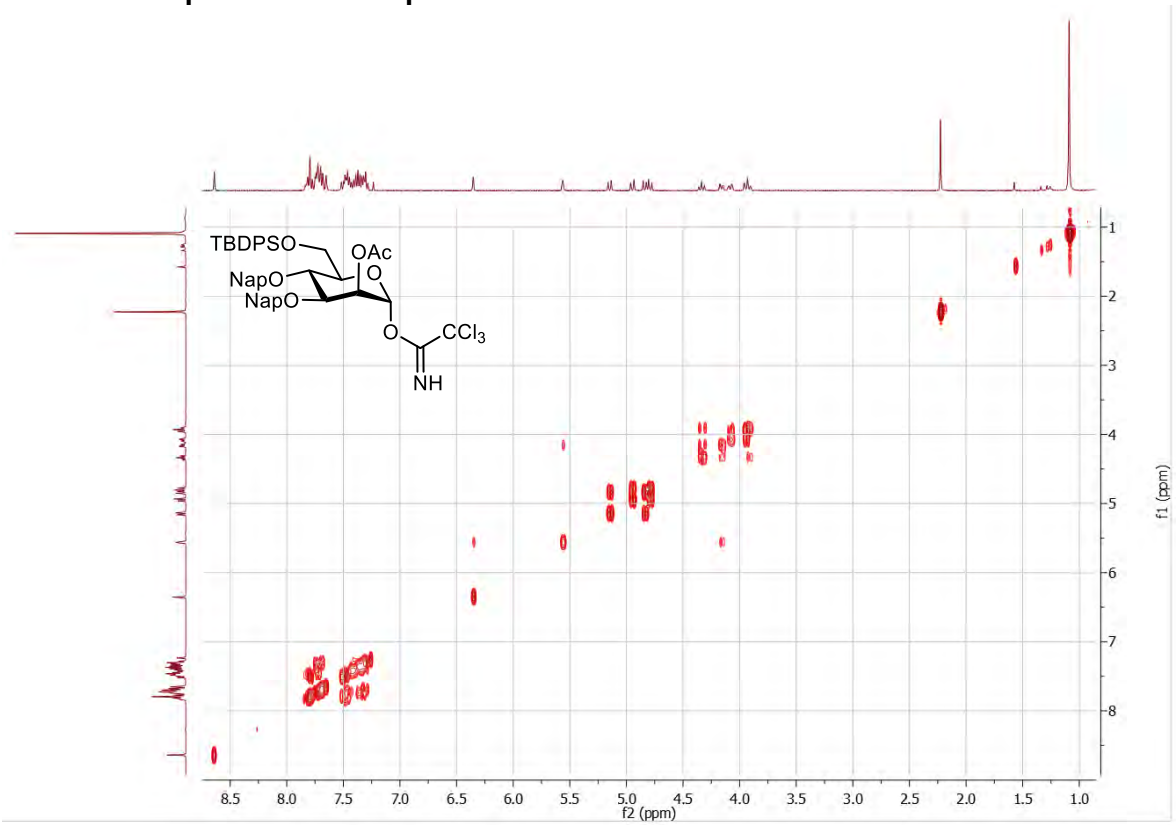

HSQC NMR spectrum of compound 3-12

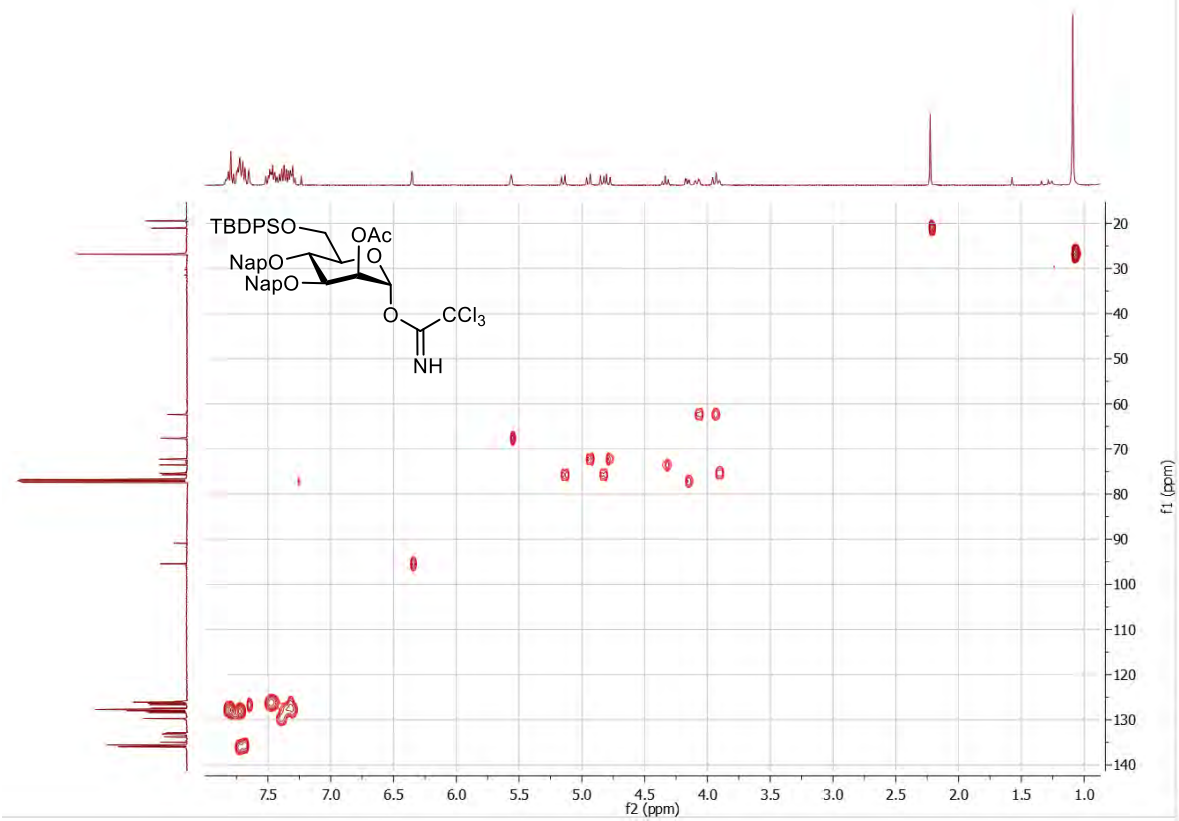

^{1}H NMR spectrum of compound 3-14

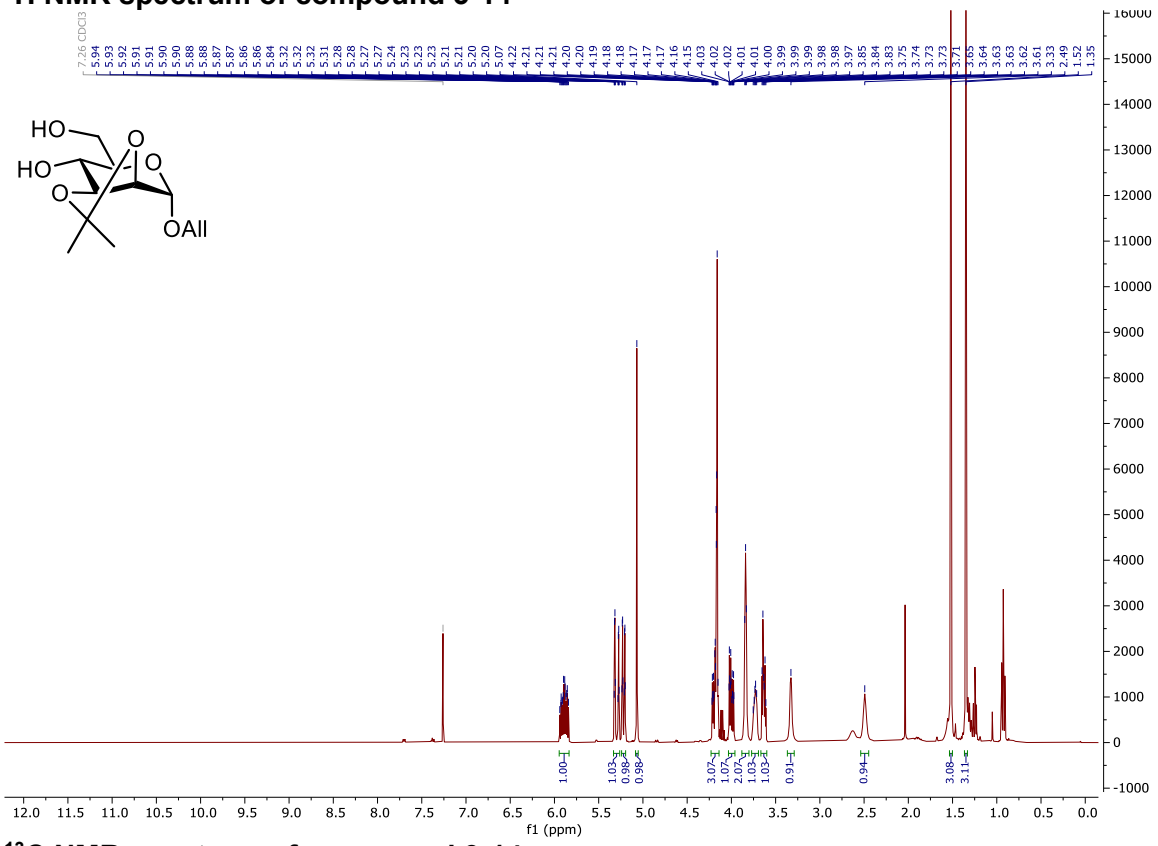

^{13}C NMR spectrum of compound 3-14

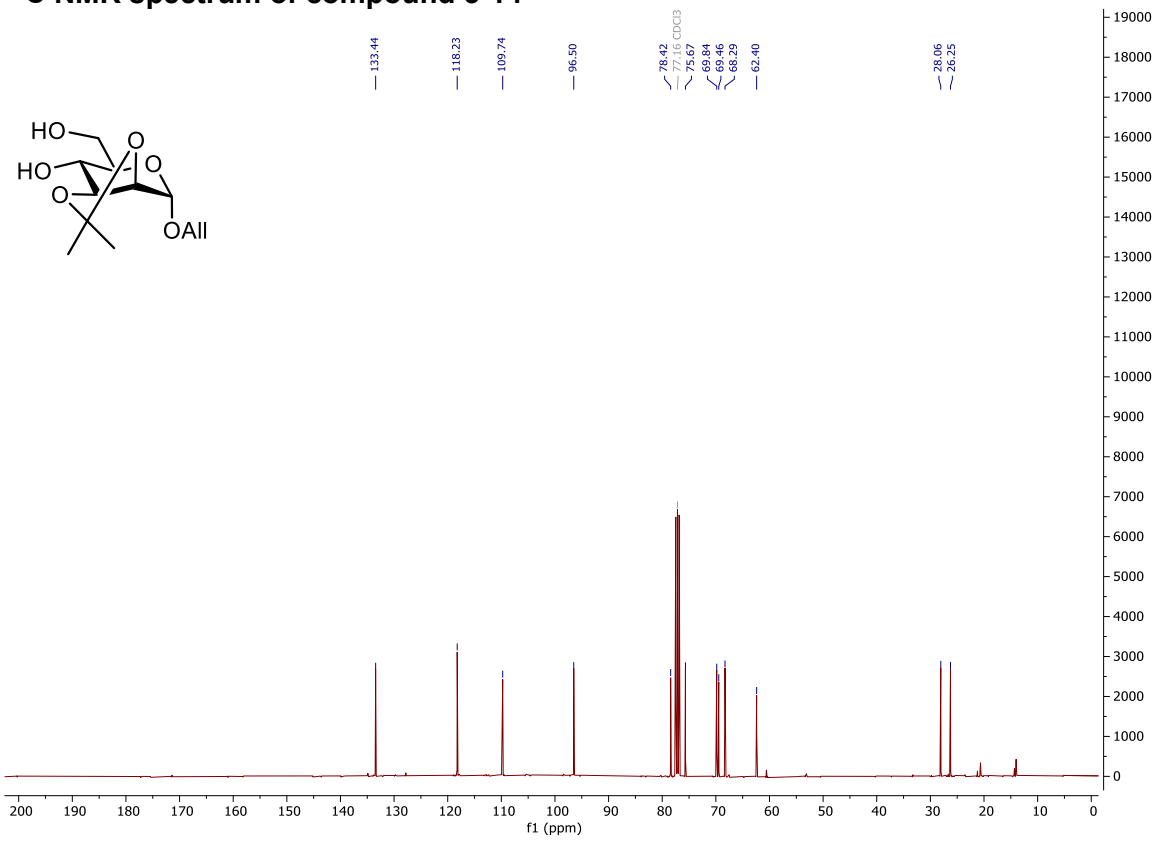

COSY NMR spectrum of compound 3-14

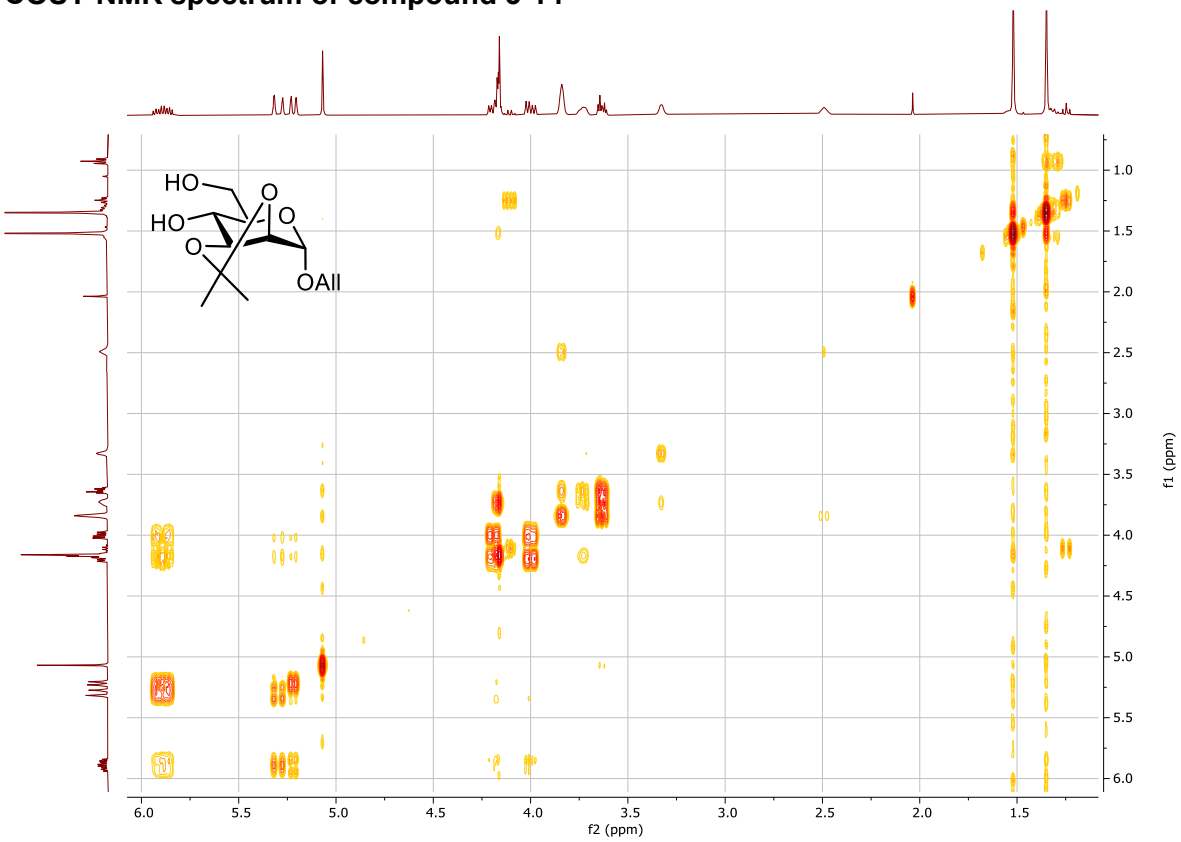

HSQC NMR spectrum of compound 3-14

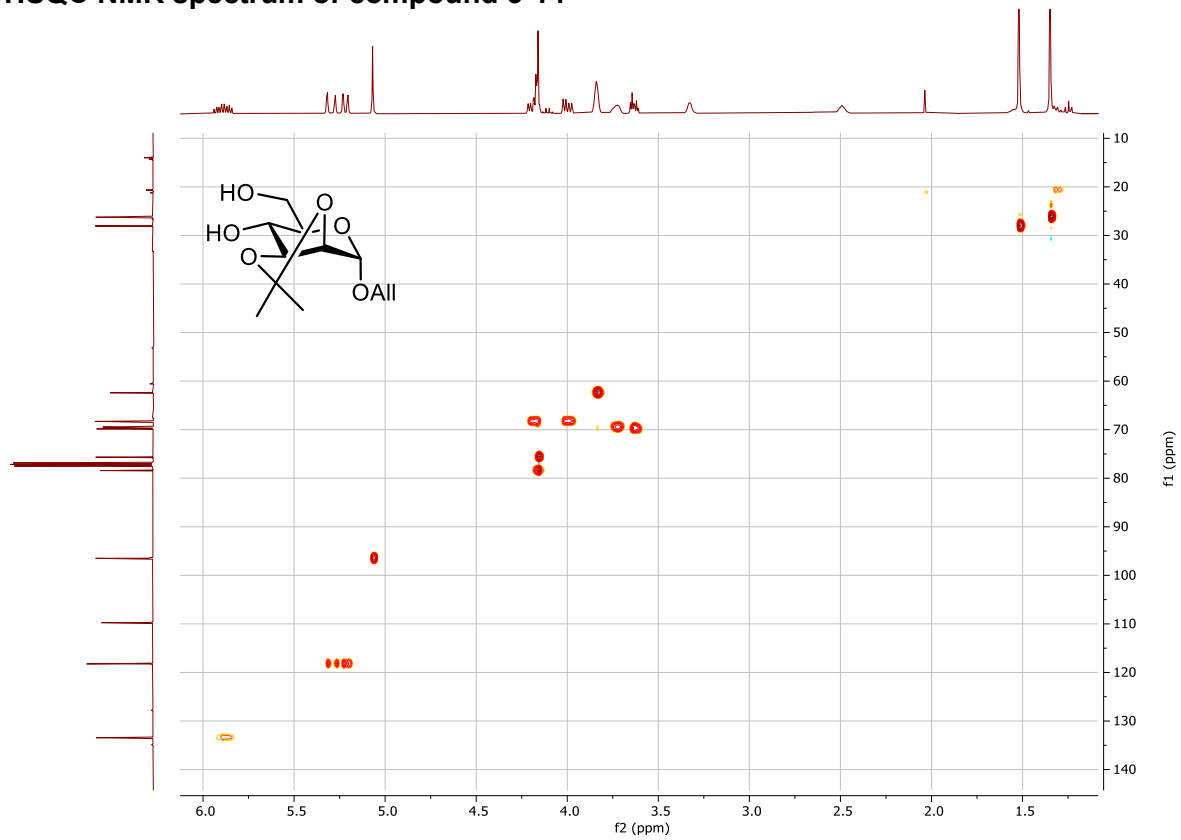

^{1}H NMR spectrum of compound 3-16

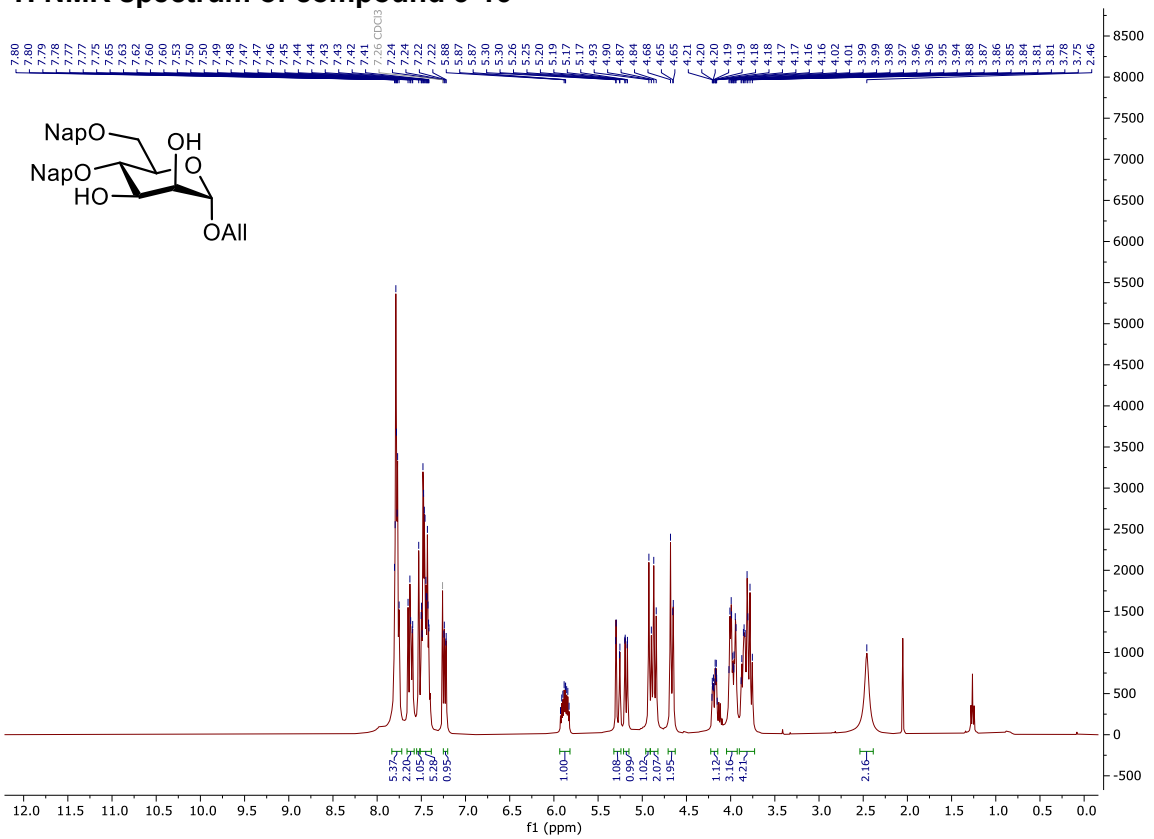

^{13}C NMR spectrum of compound 3-16

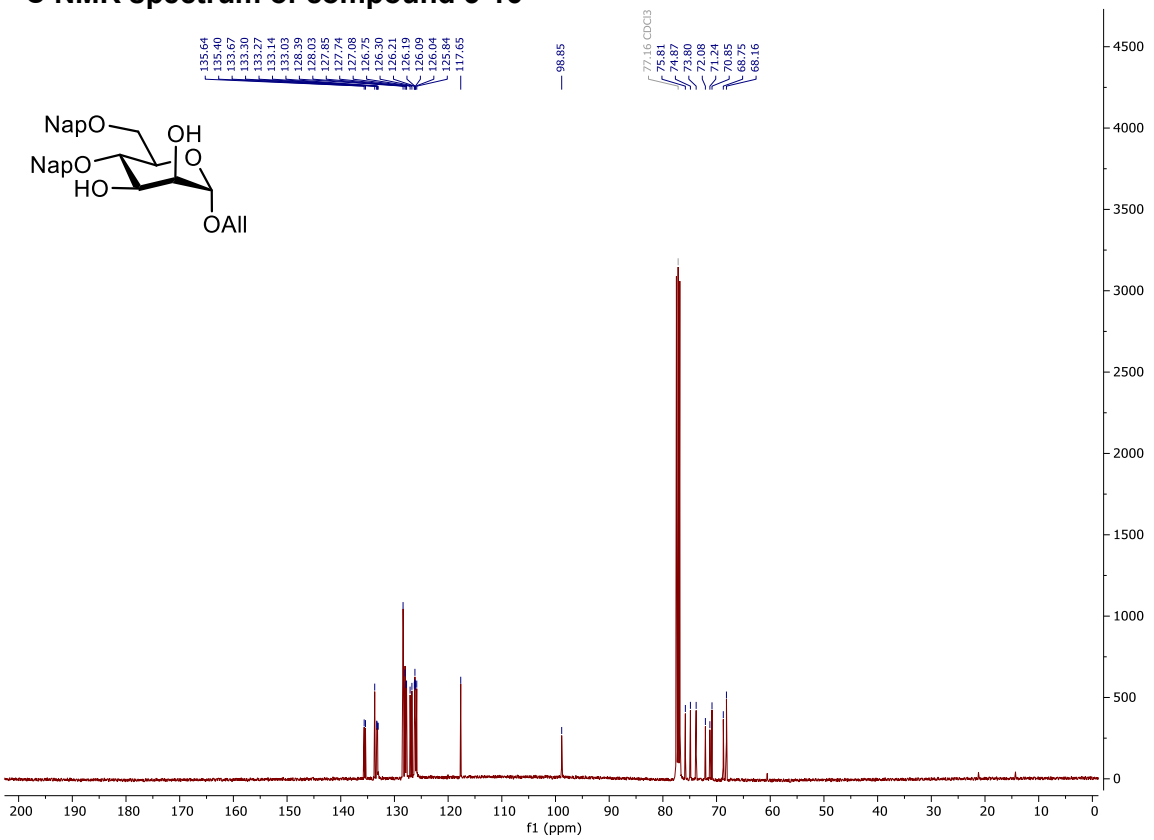

COSY NMR spectrum of compound 3-16

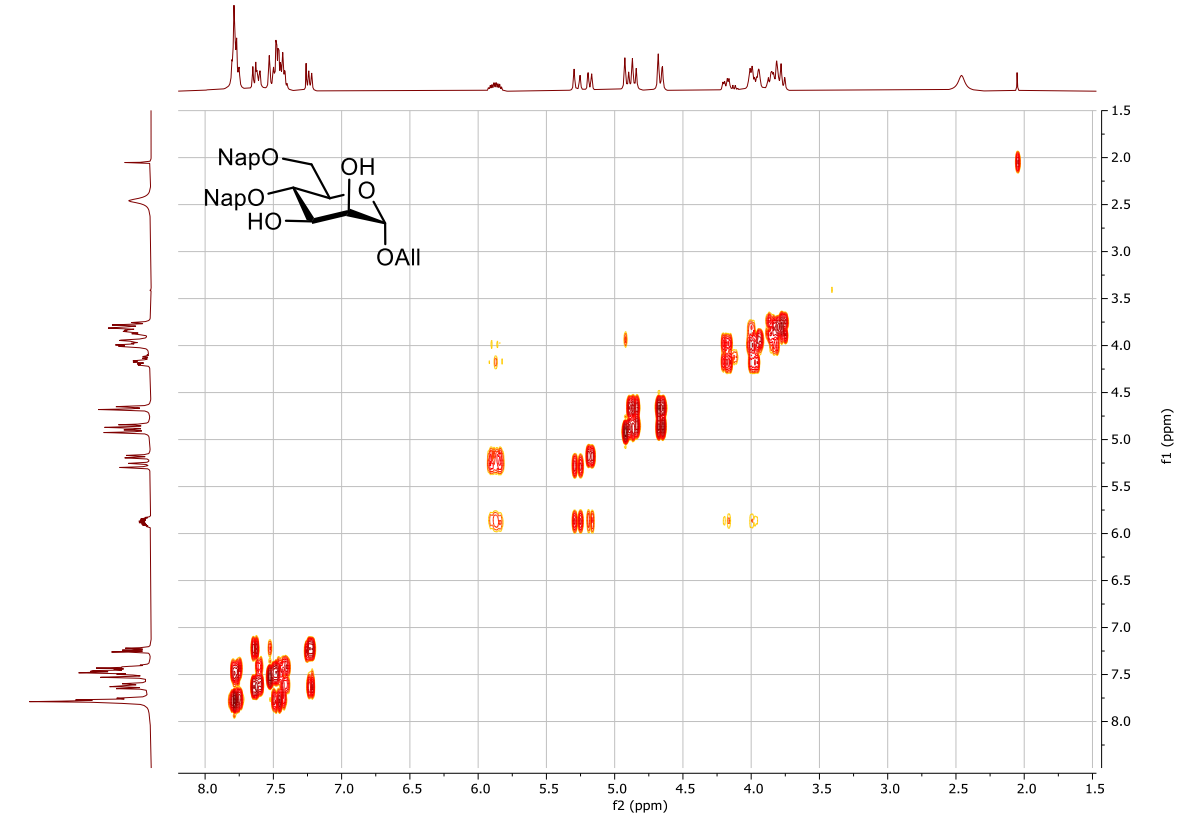

HSQC NMR spectrum of compound 3-16

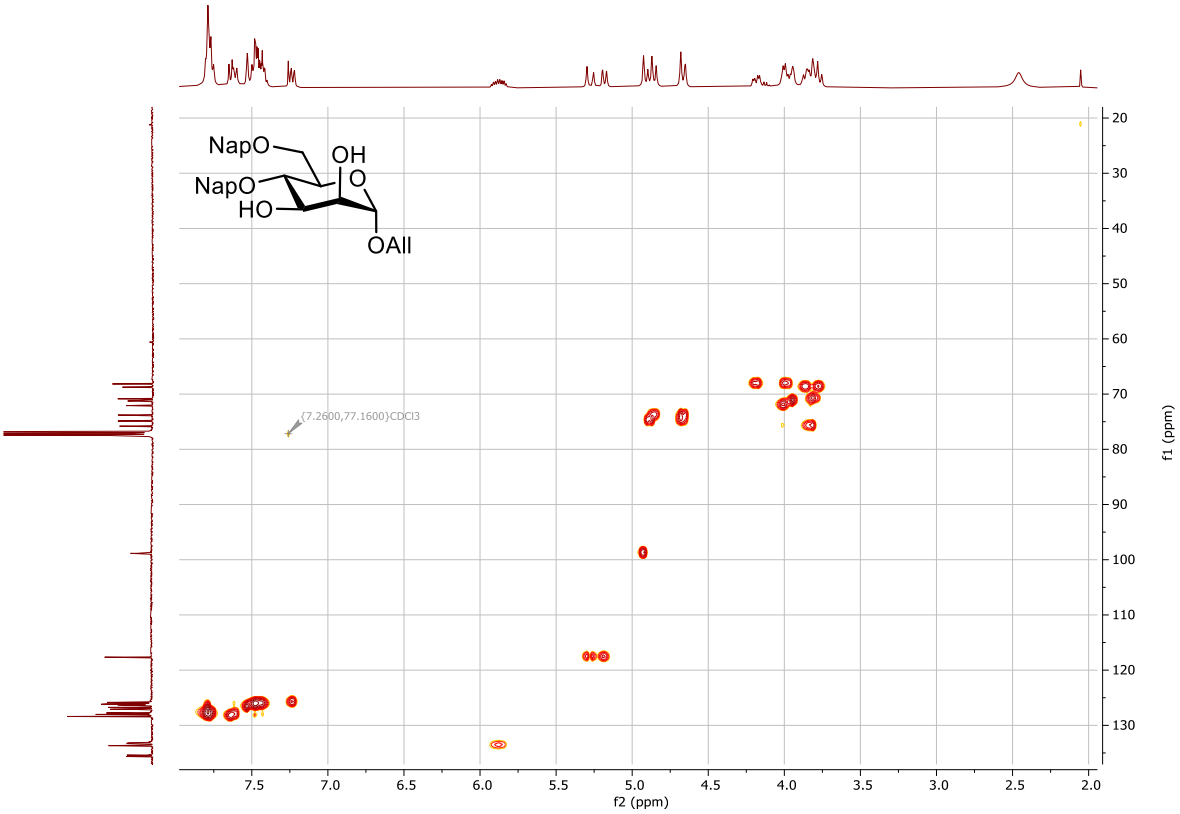

^{1}H NMR spectrum of compound 3-17

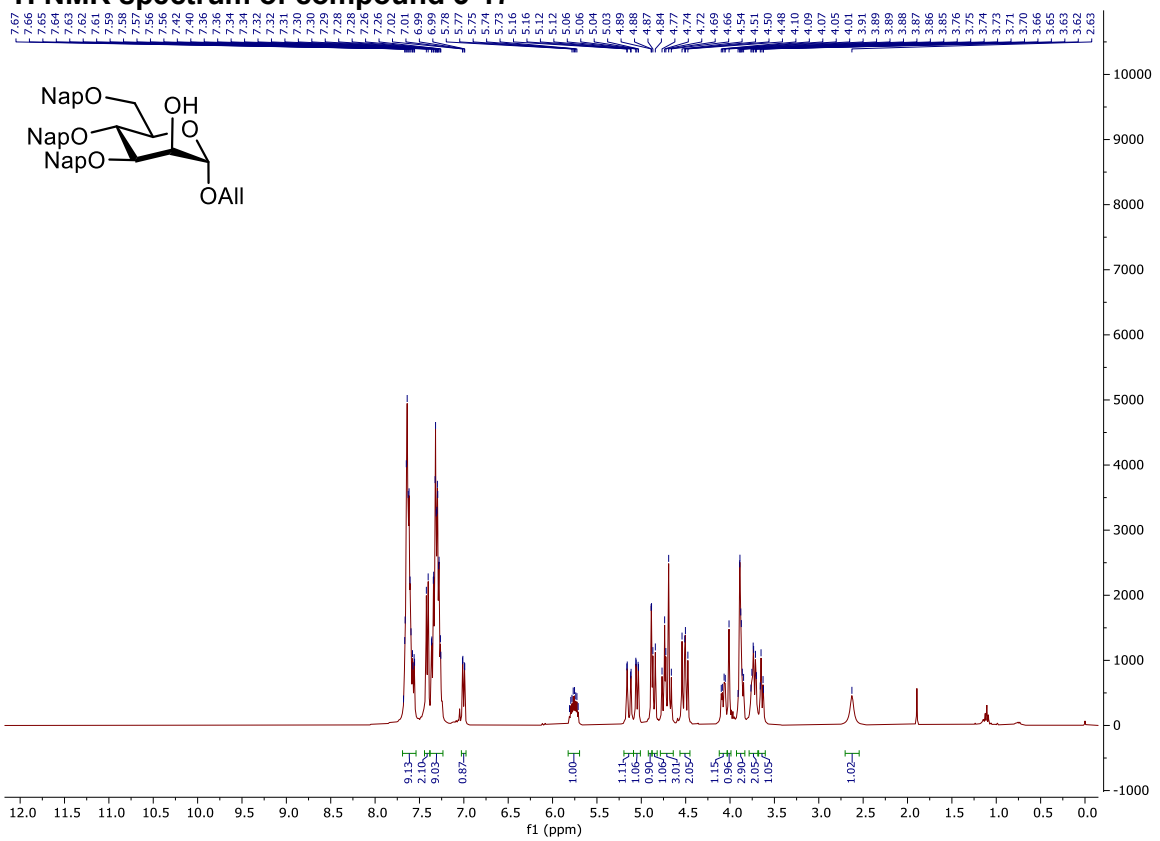

^{13}C NMR spectrum of compound 3-17

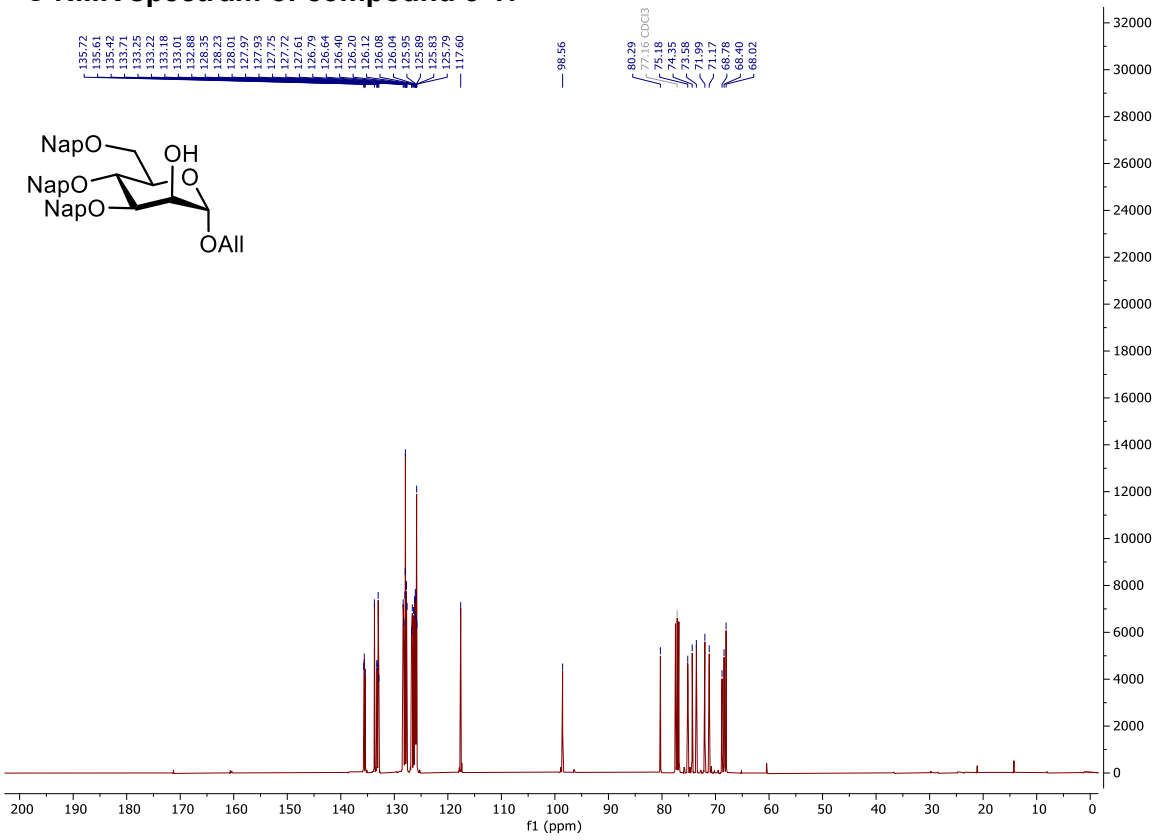

COSY NMR spectrum of compound 3-17

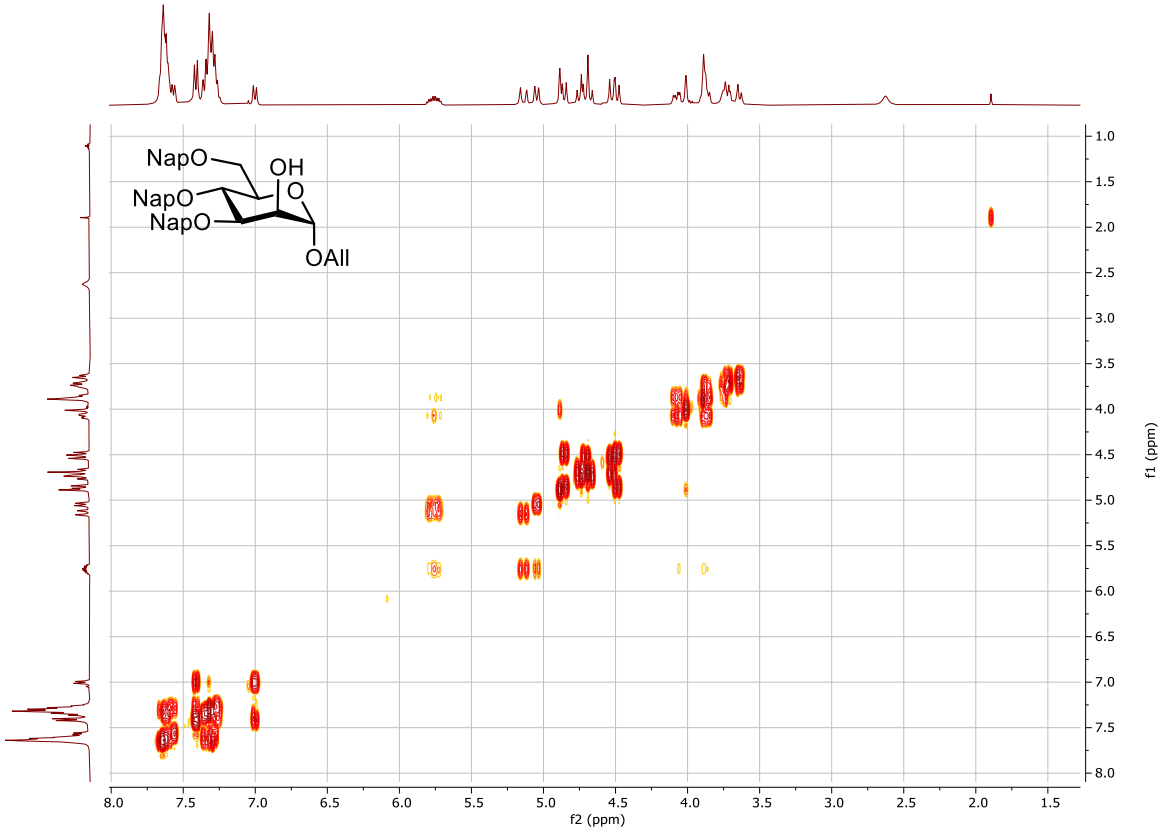

HSQC NMR spectrum of compound 3-17

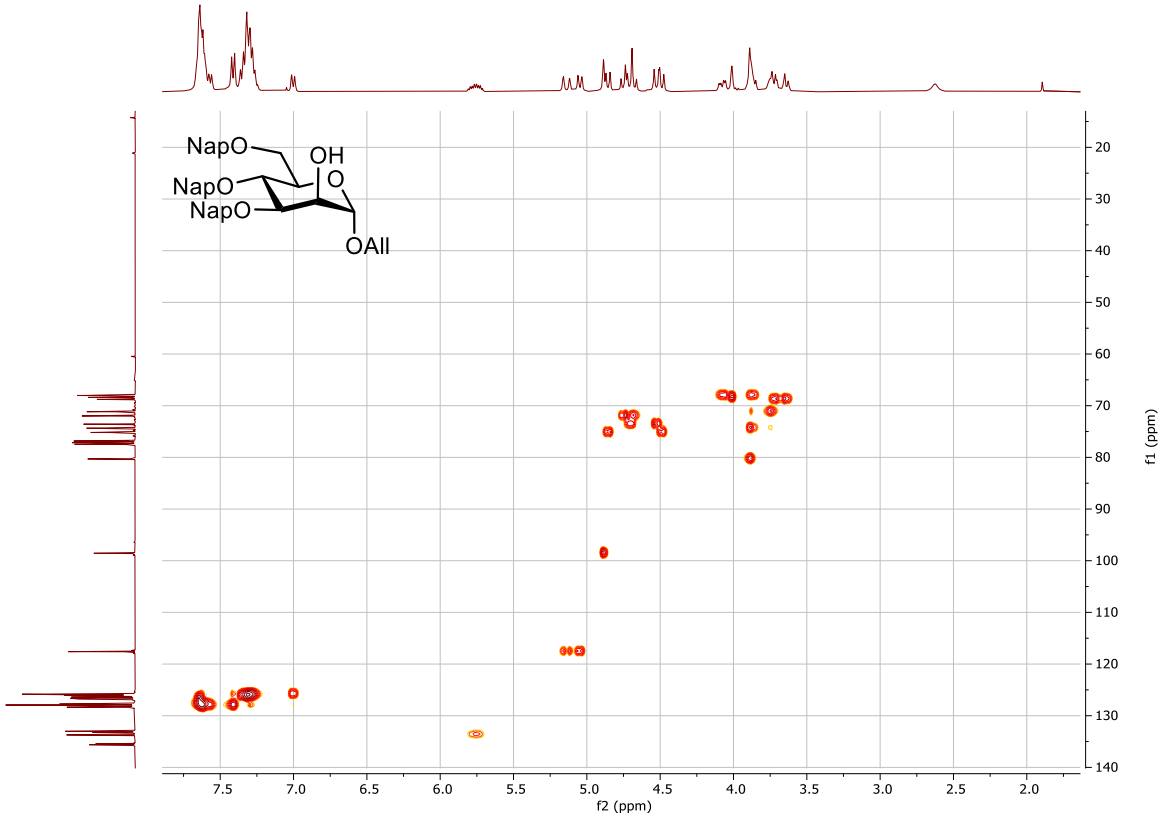

^{1}H NMR spectrum of compound 3-6

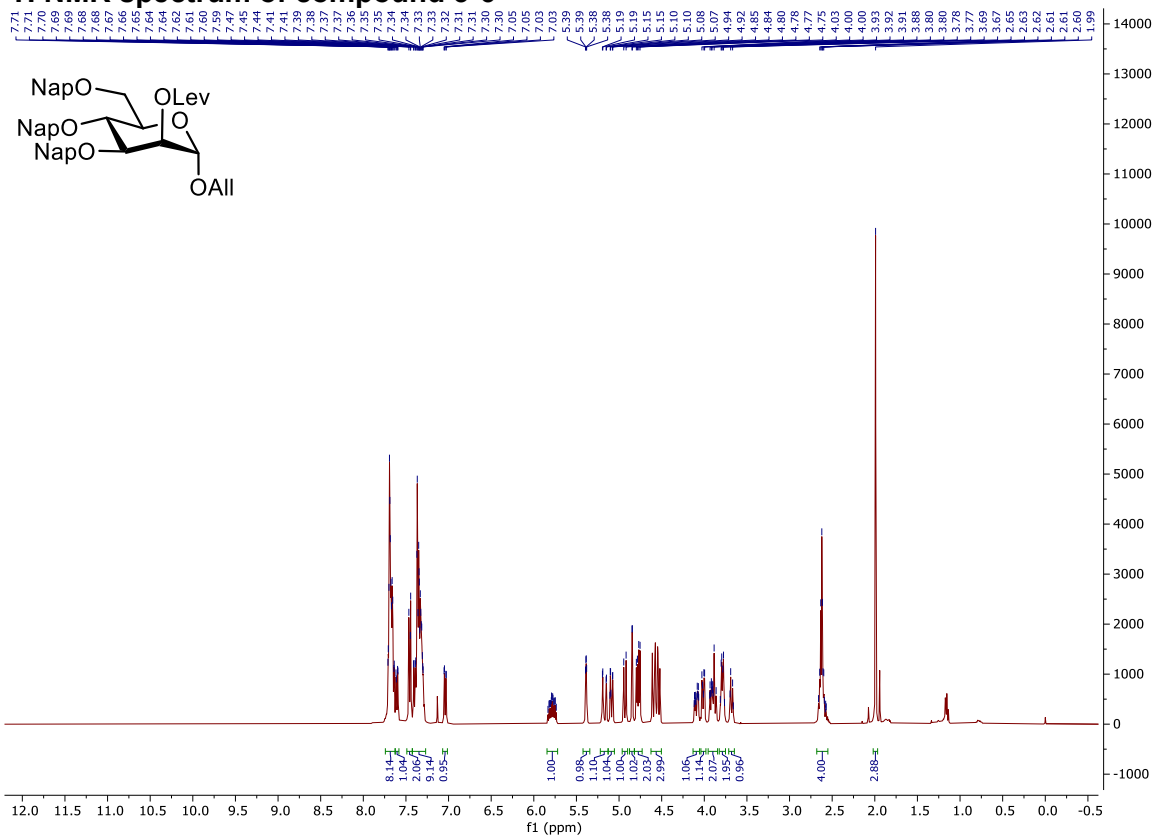

^{13}C NMR spectrum of compound 3-6

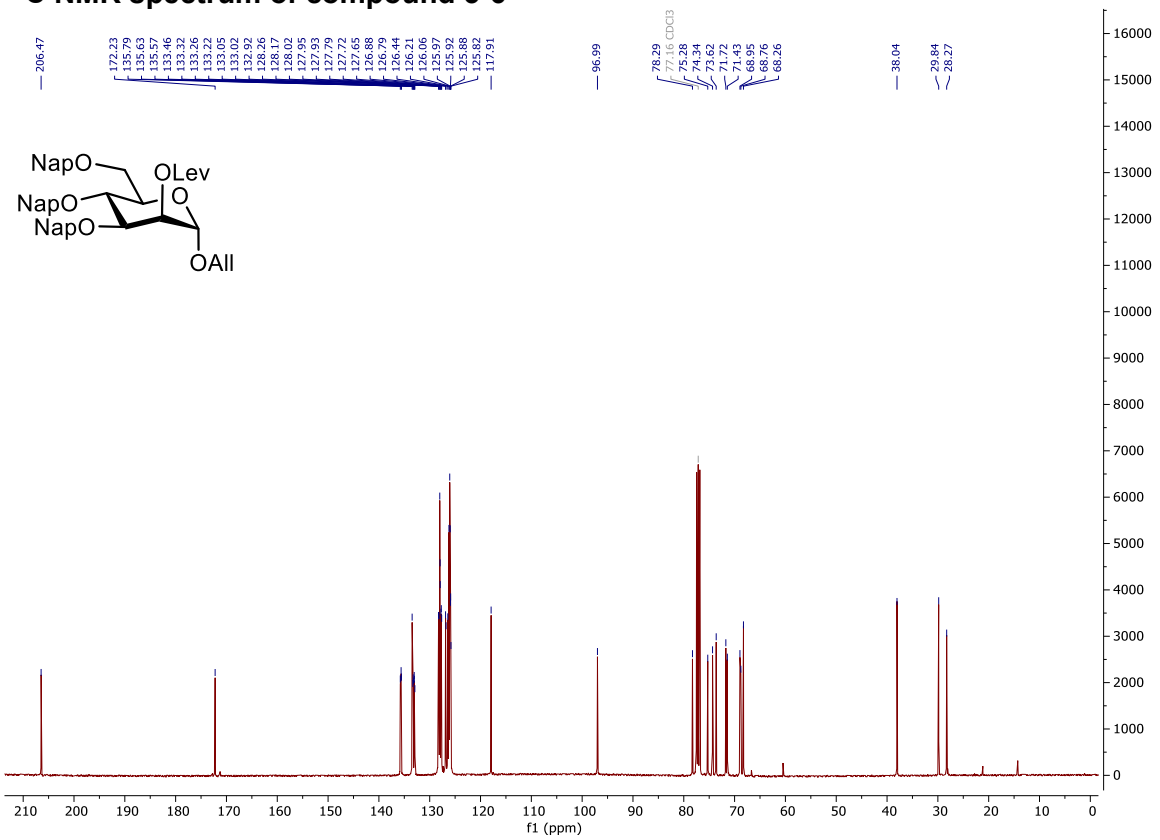

COSY NMR spectrum of compound 3-6

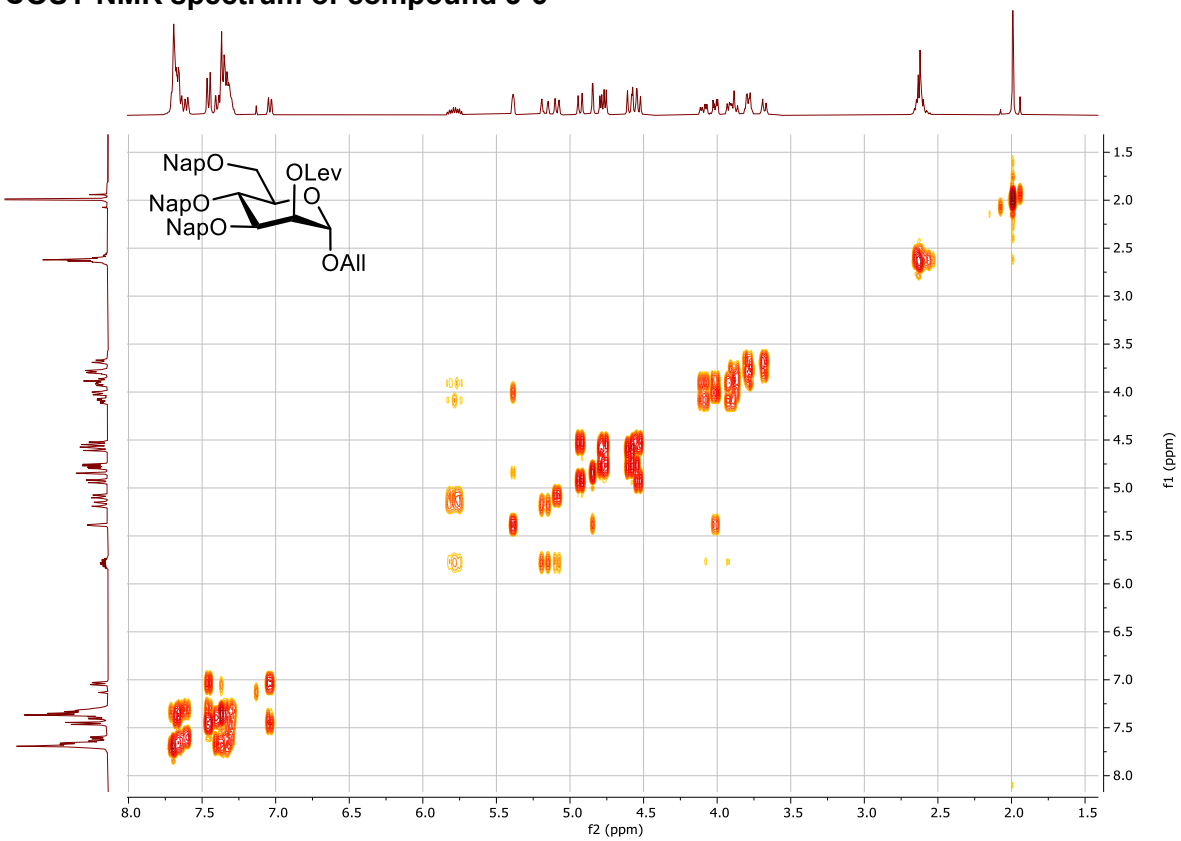

HSQC NMR spectrum of compound 3-6

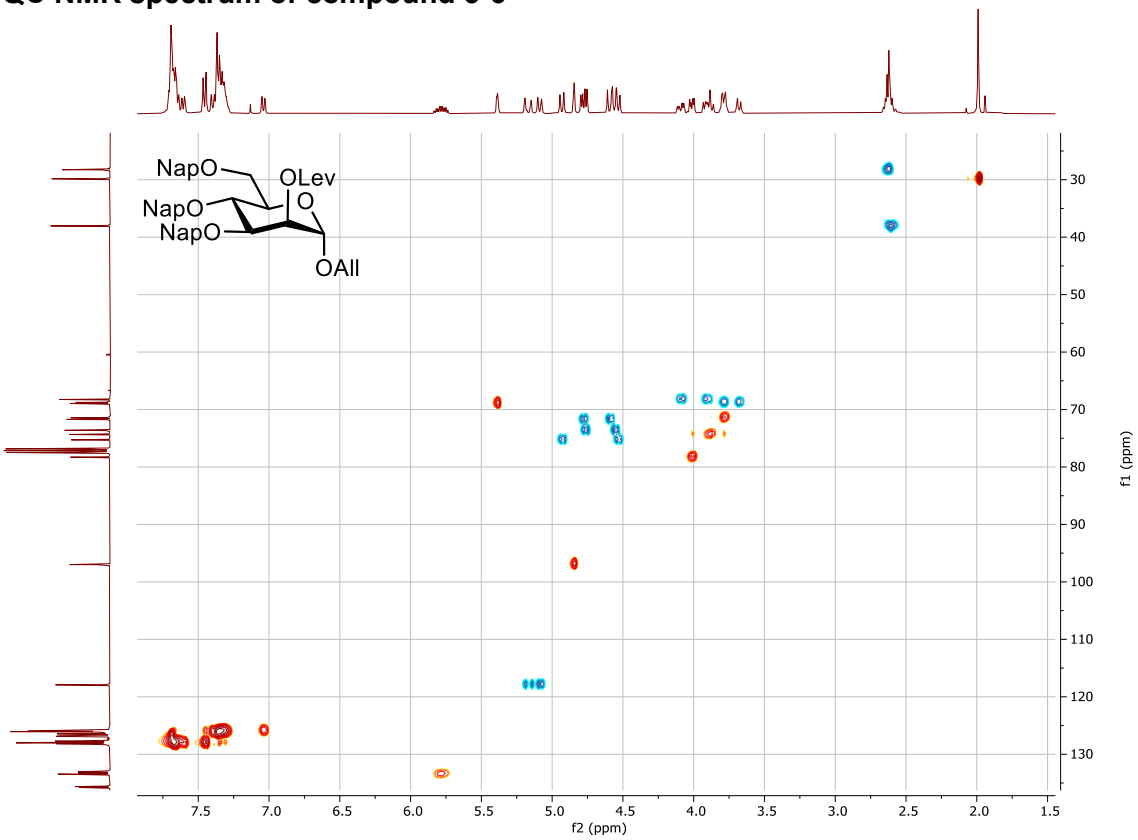

^{1}H NMR spectrum of compound 3-18

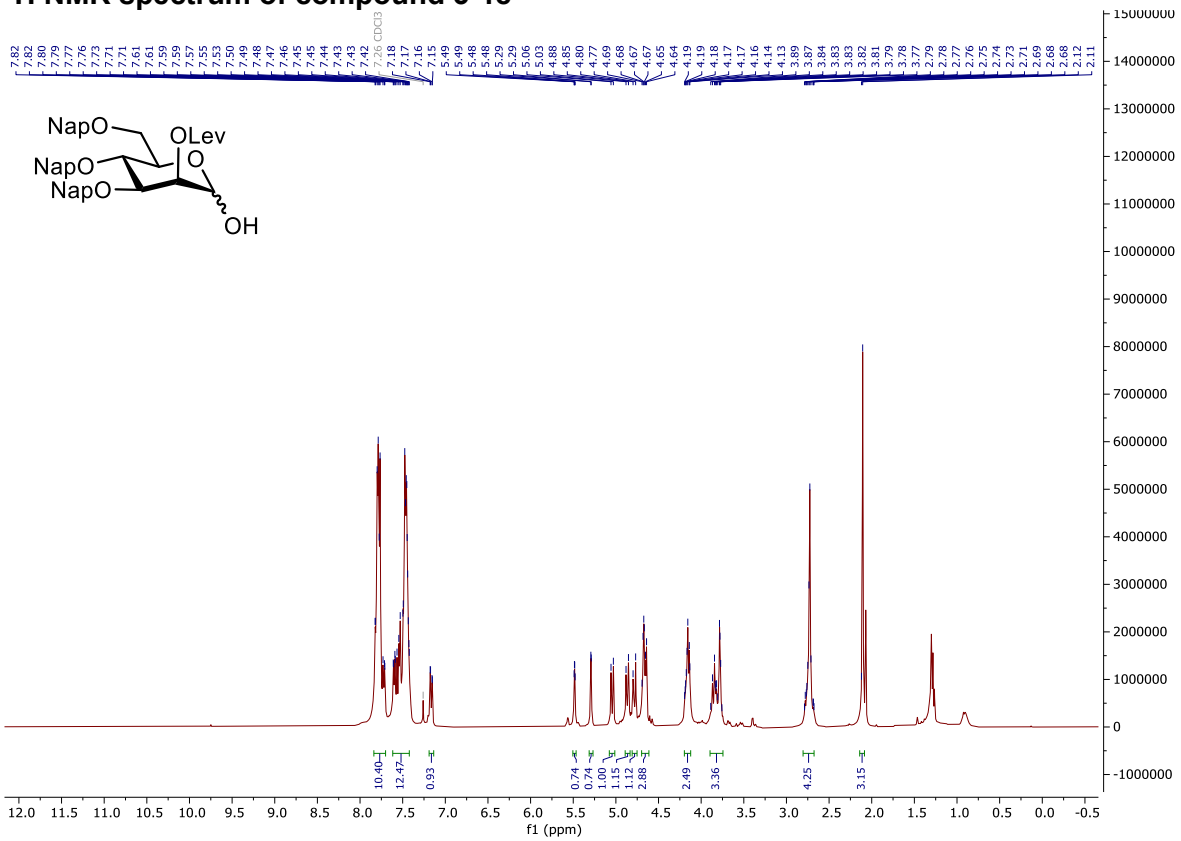

^{13}C NMR spectrum of compound 3-18

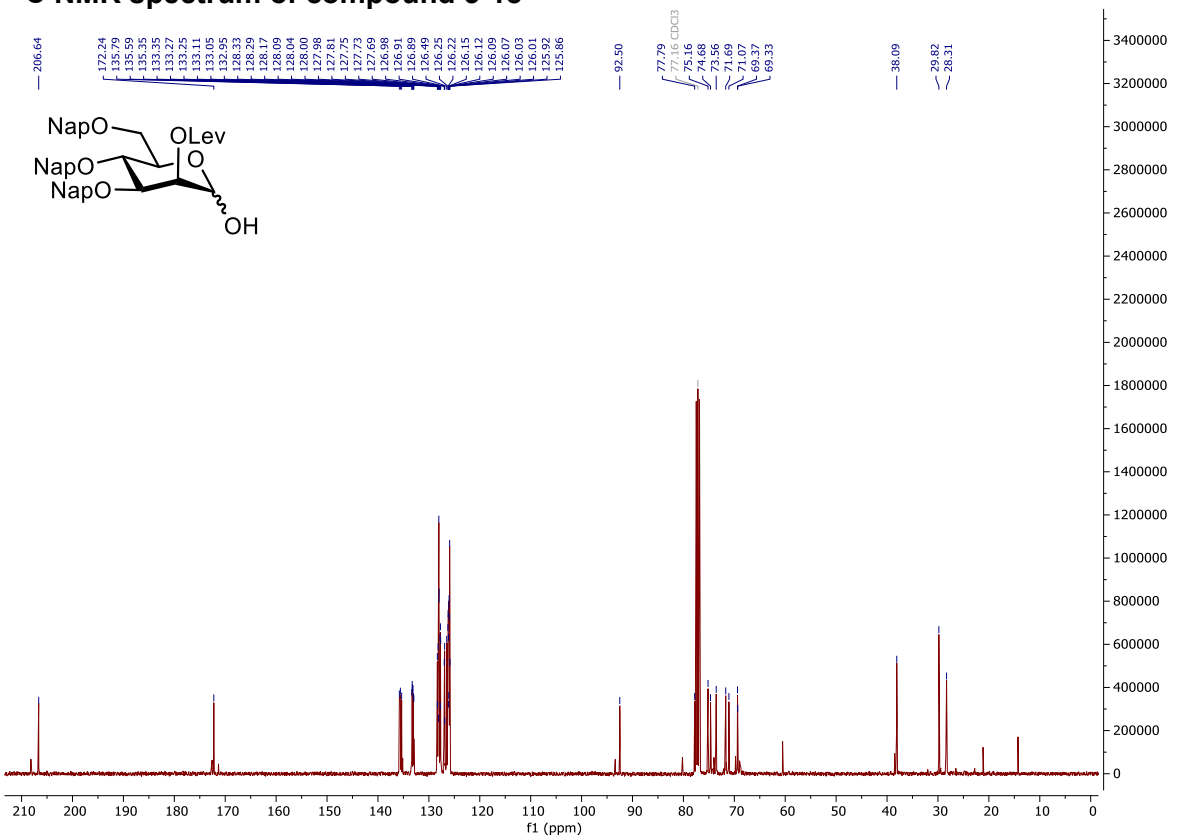

COSY NMR spectrum of compound 3-18

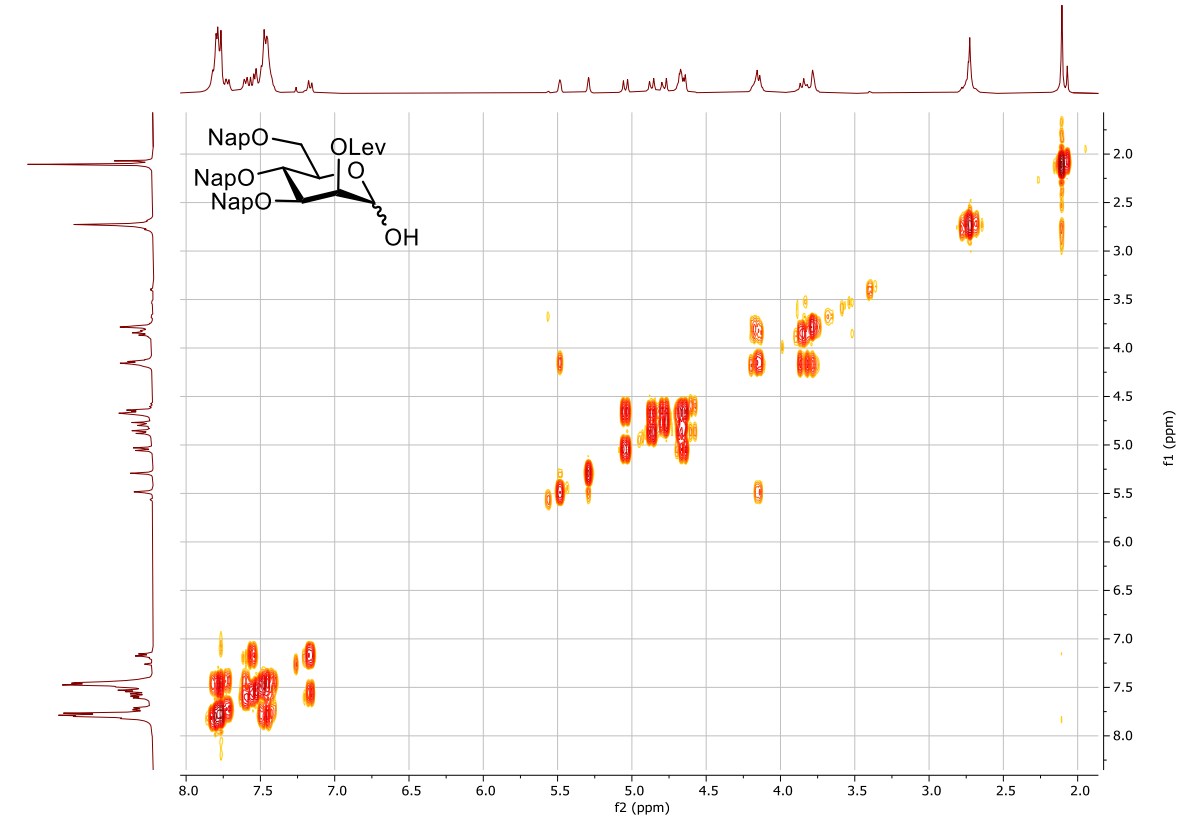

HSQC NMR spectrum of compound 3-18

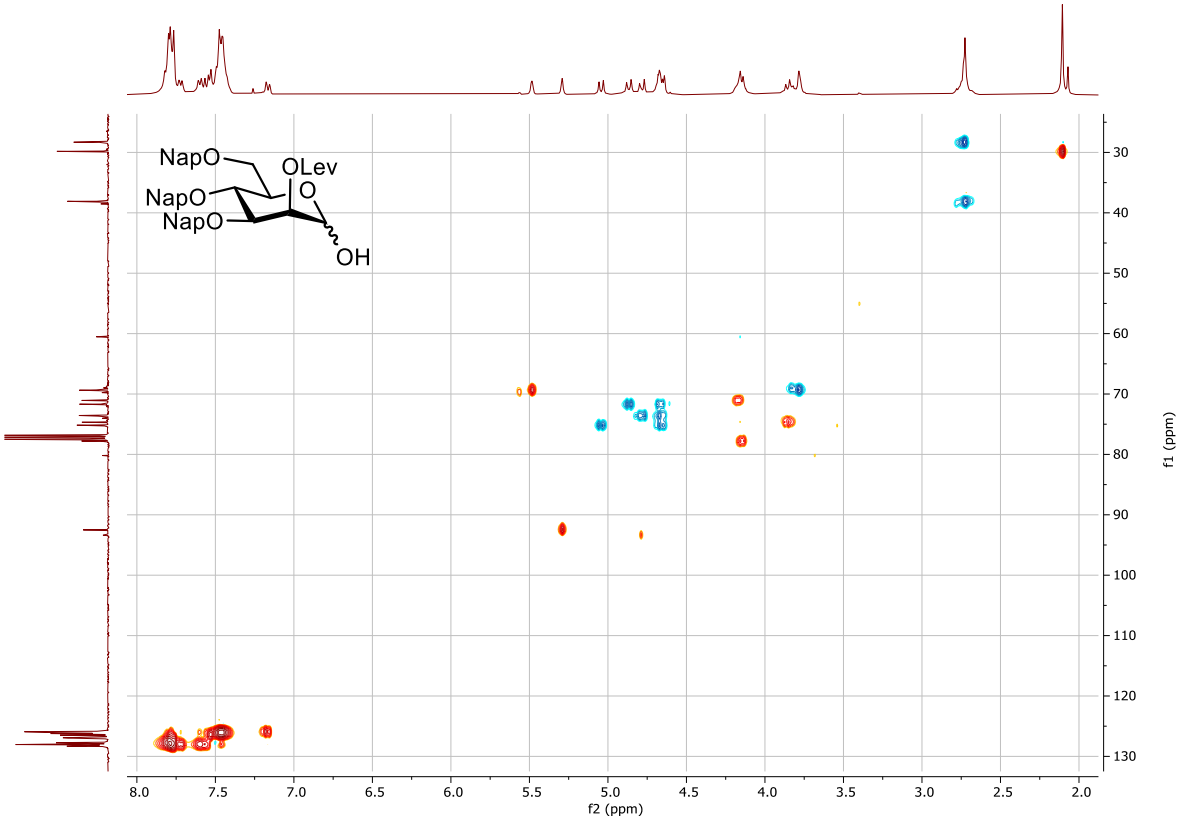

^{1}H NMR spectrum of compound 3-19

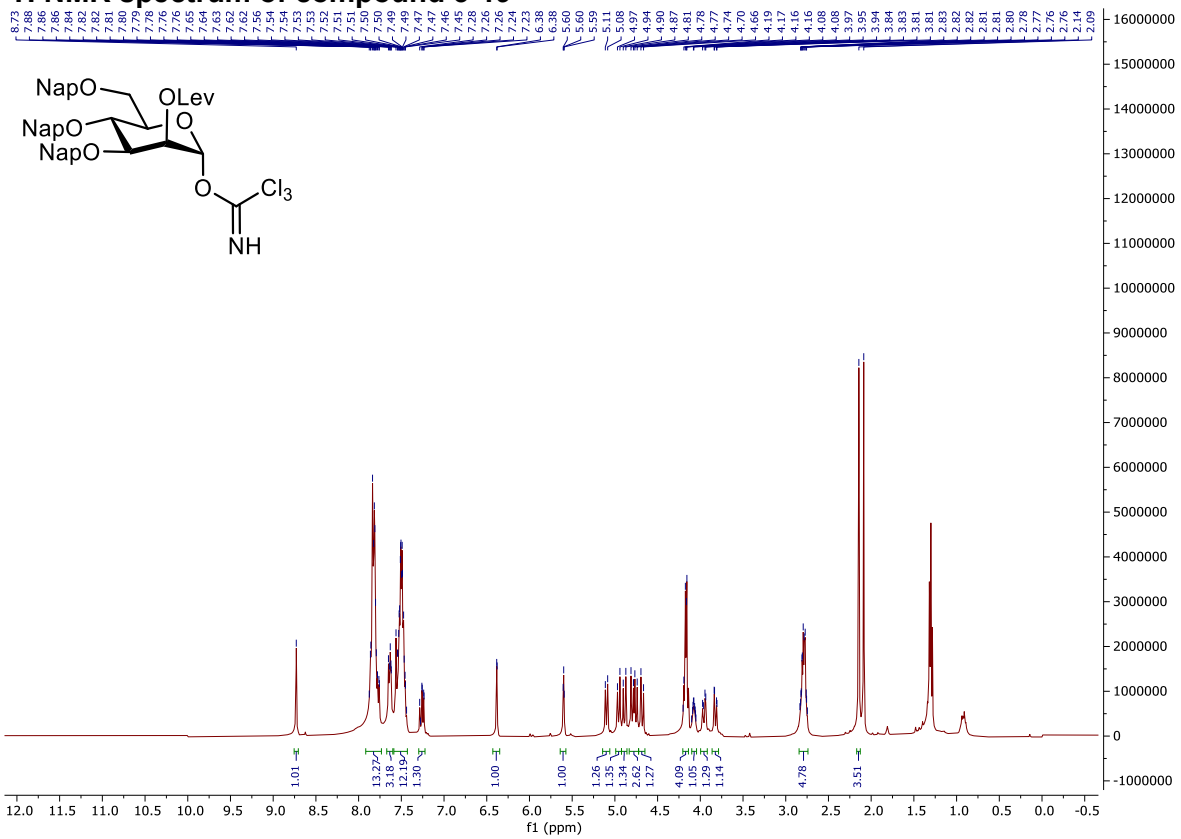

^{13}C NMR spectrum of compound 3-19

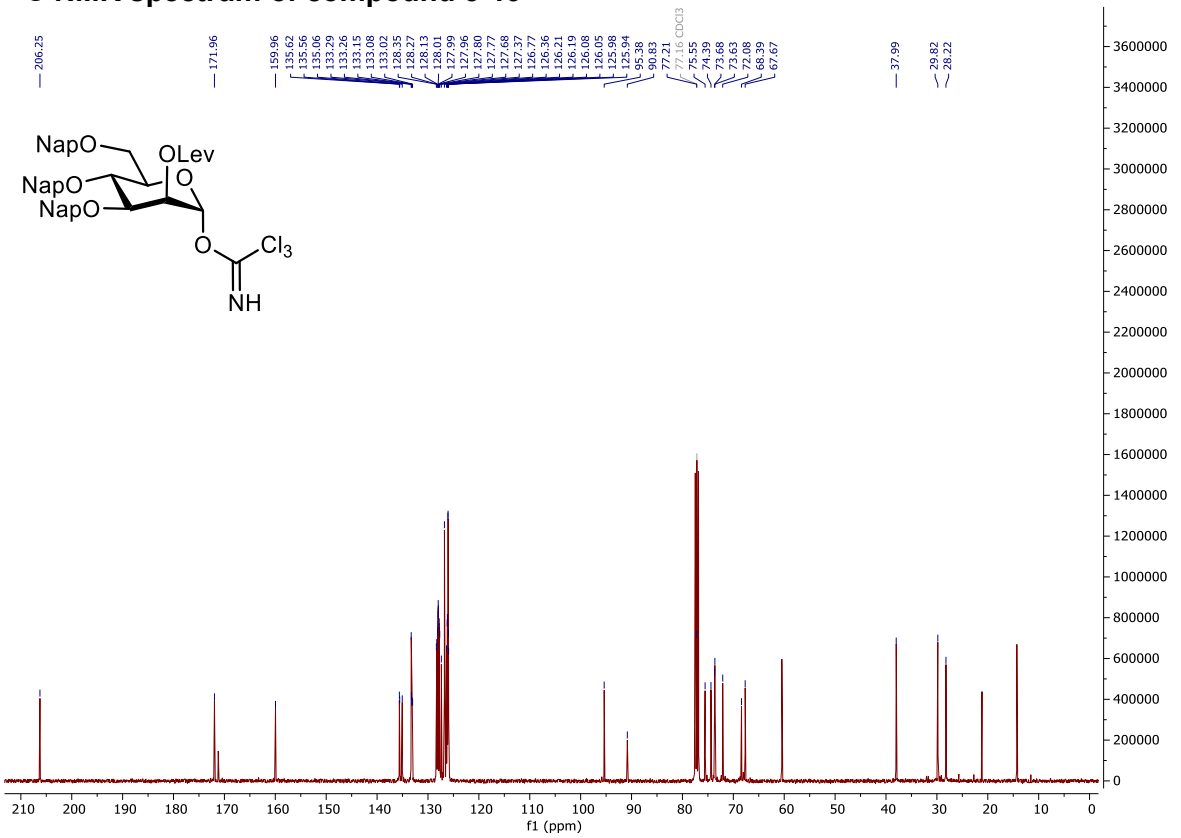

COSY NMR spectrum of compound 3-19

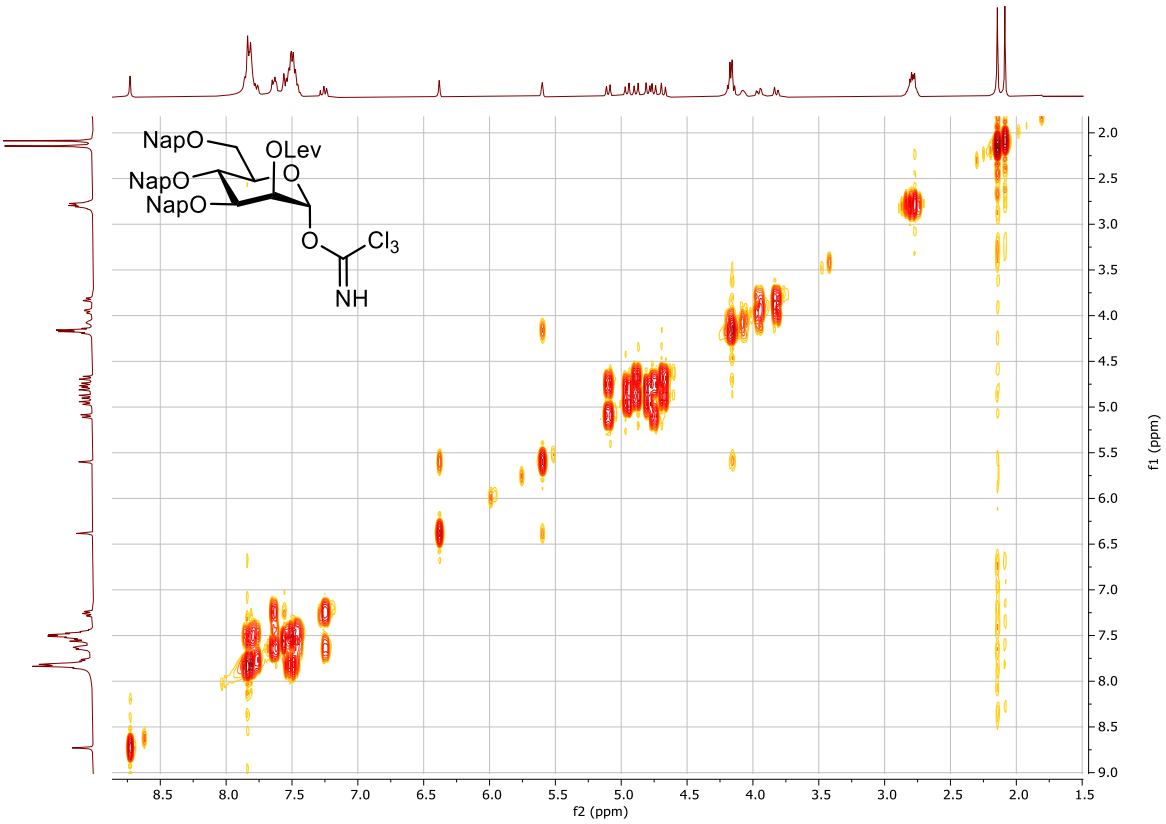

HSQC NMR spectrum of compound 3-19

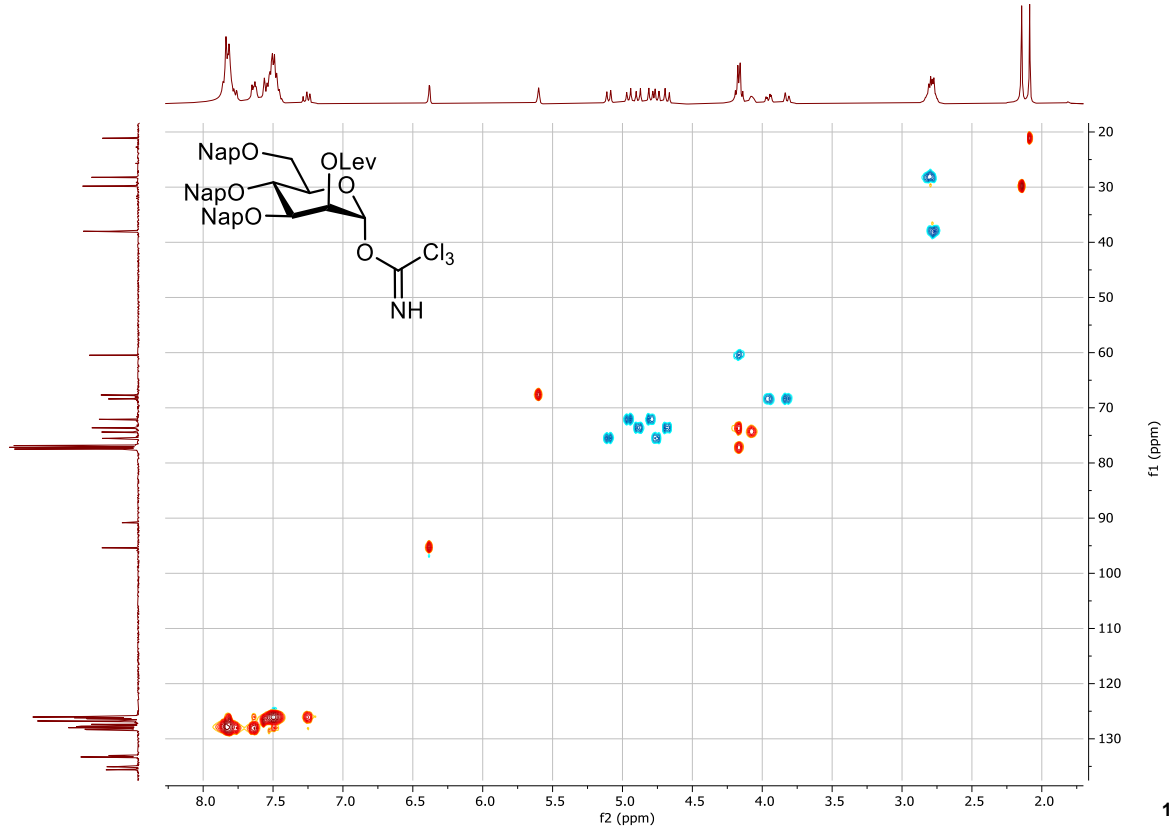

^{1}H

NMR spectrum of compound 3-20

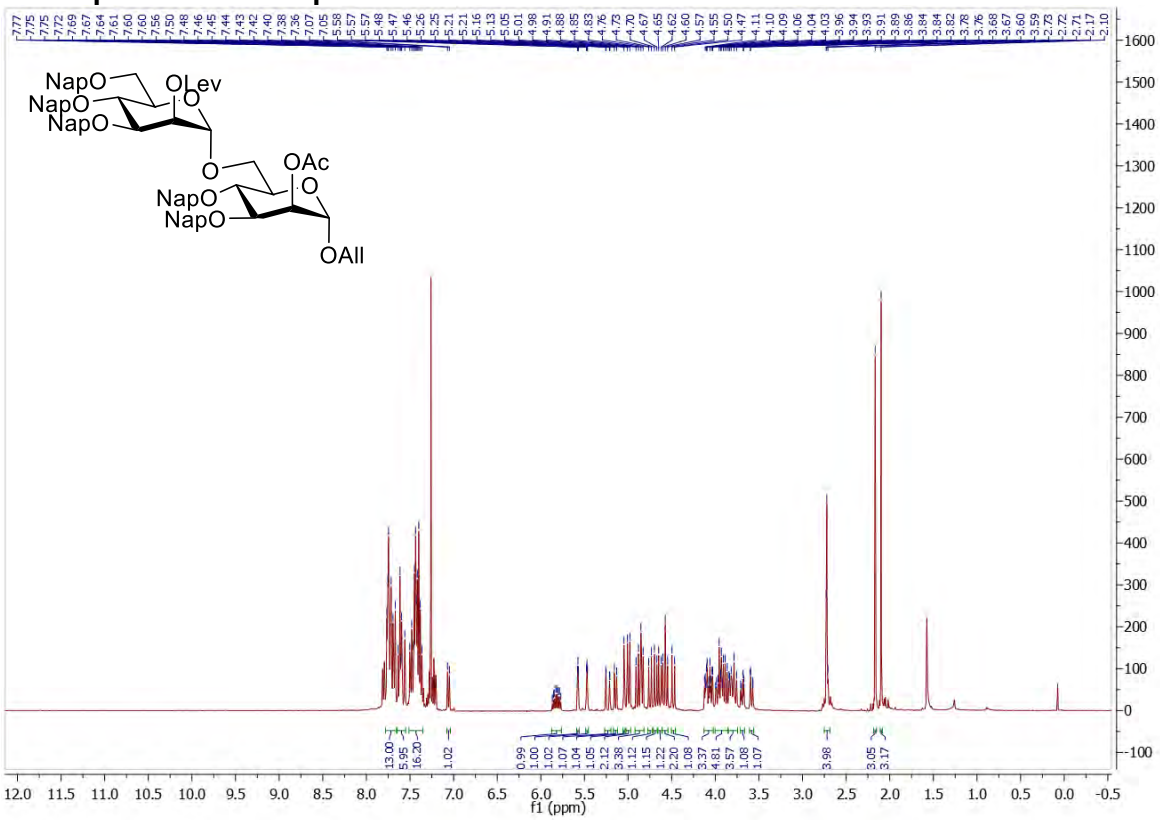

^{13}C NMR spectrum of compound 3-20

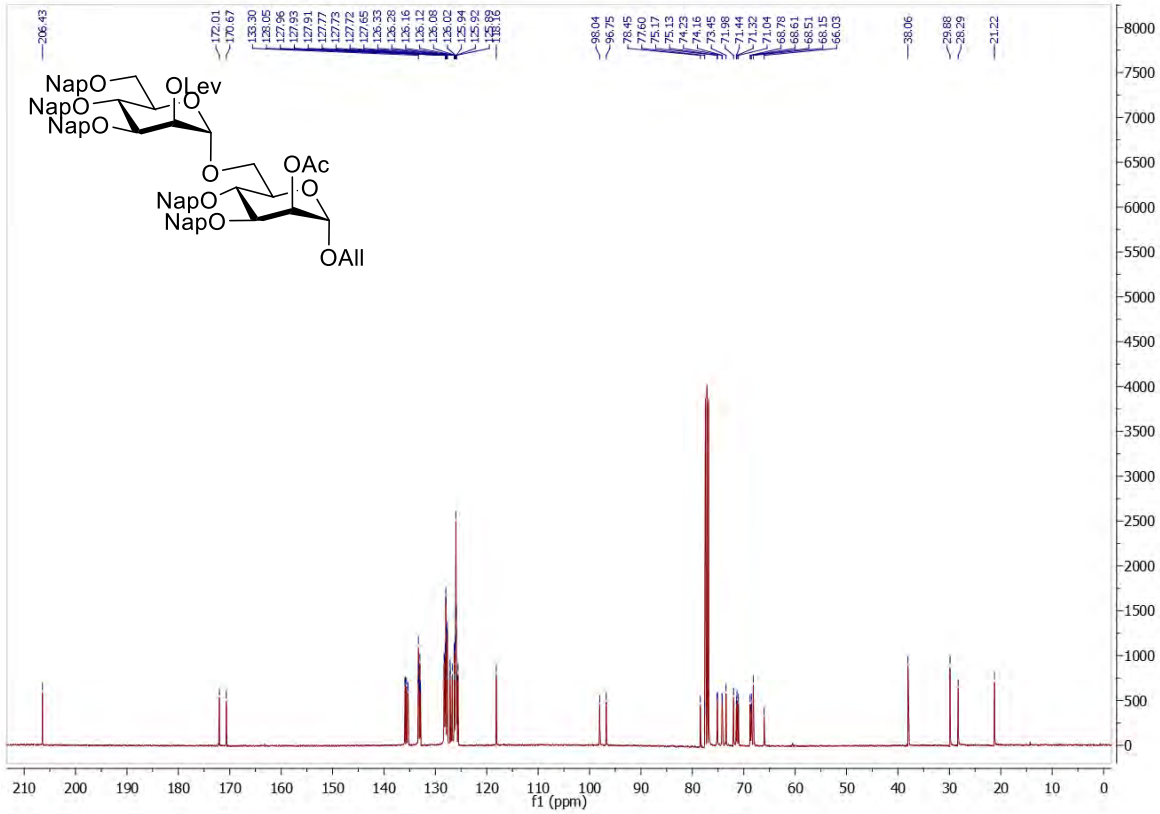

COSY NMR spectrum of compound 3-20

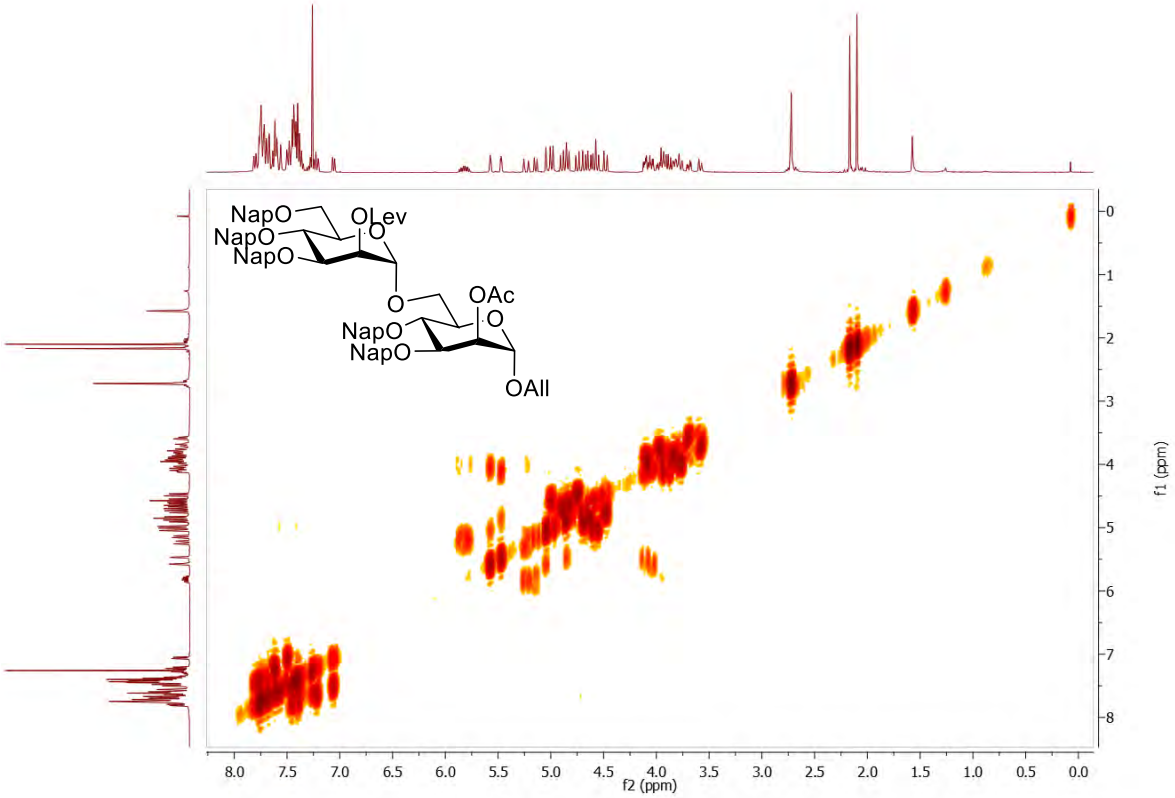

HSQC NMR spectrum of compound 3-20

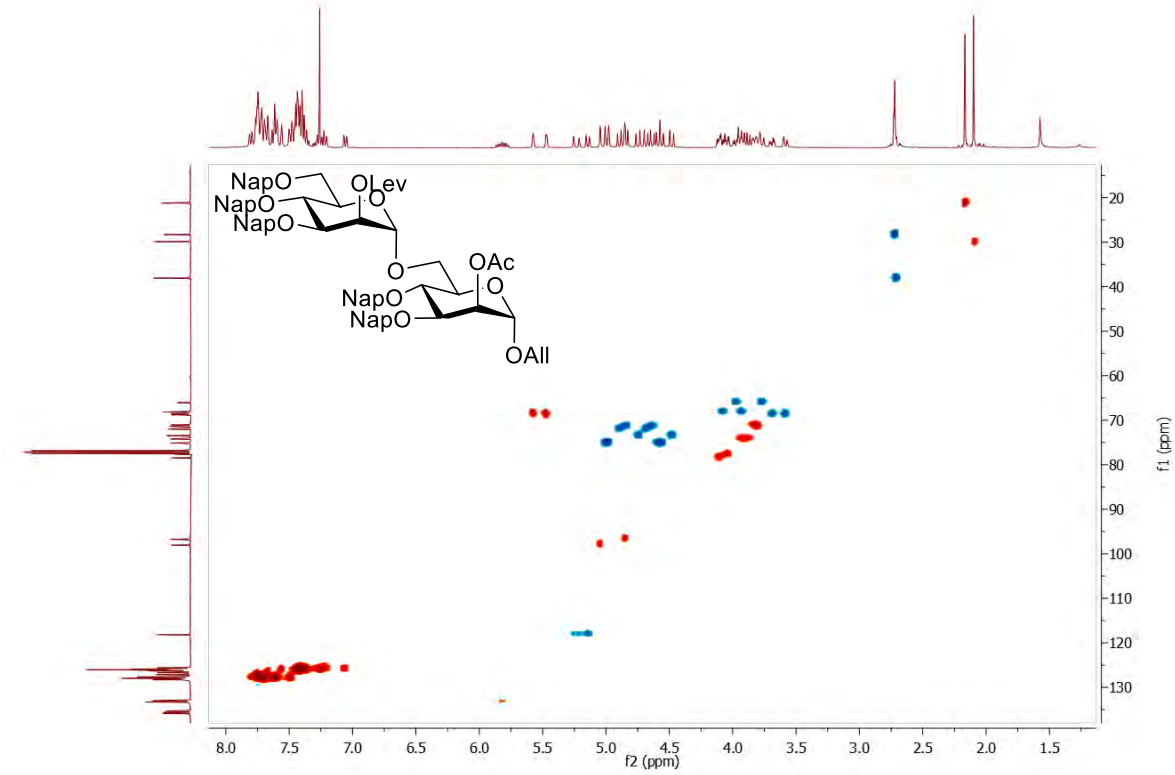

^{1}H NMR spectrum of compound 3-21

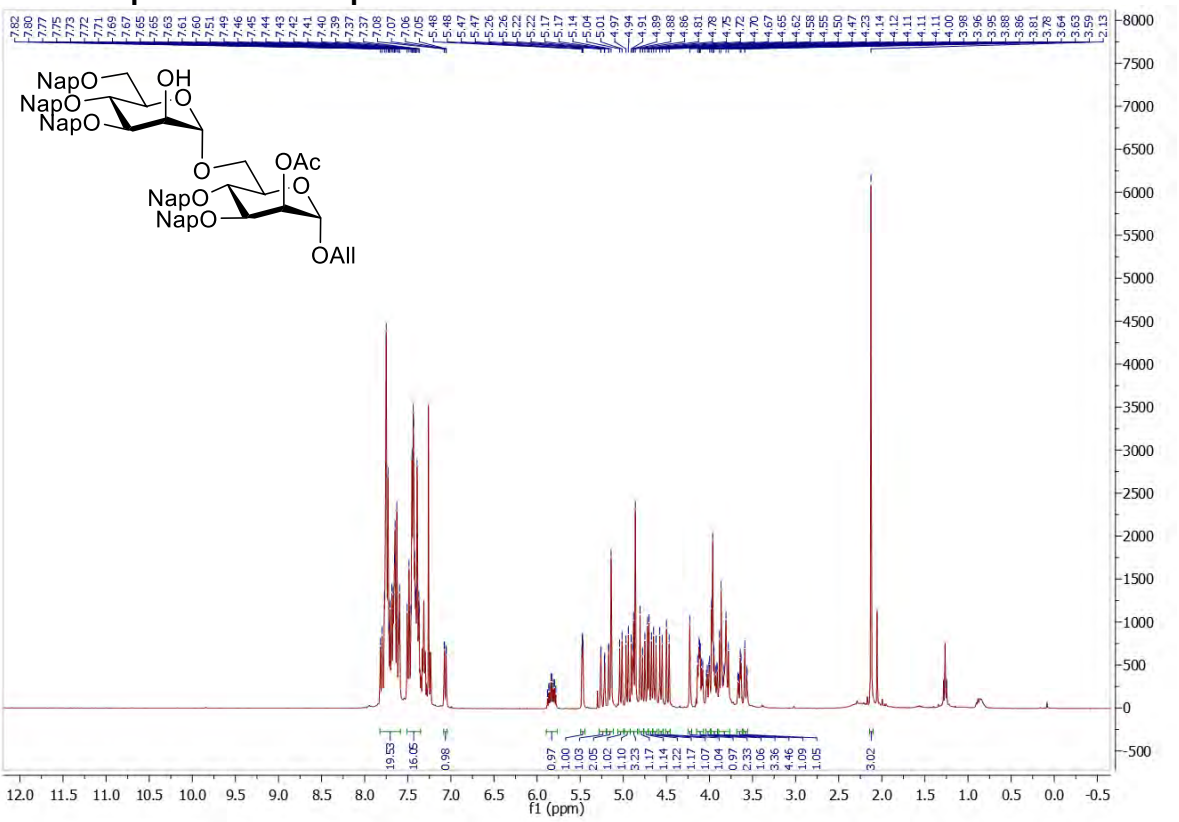

^{13}C NMR spectrum of compound 3-21

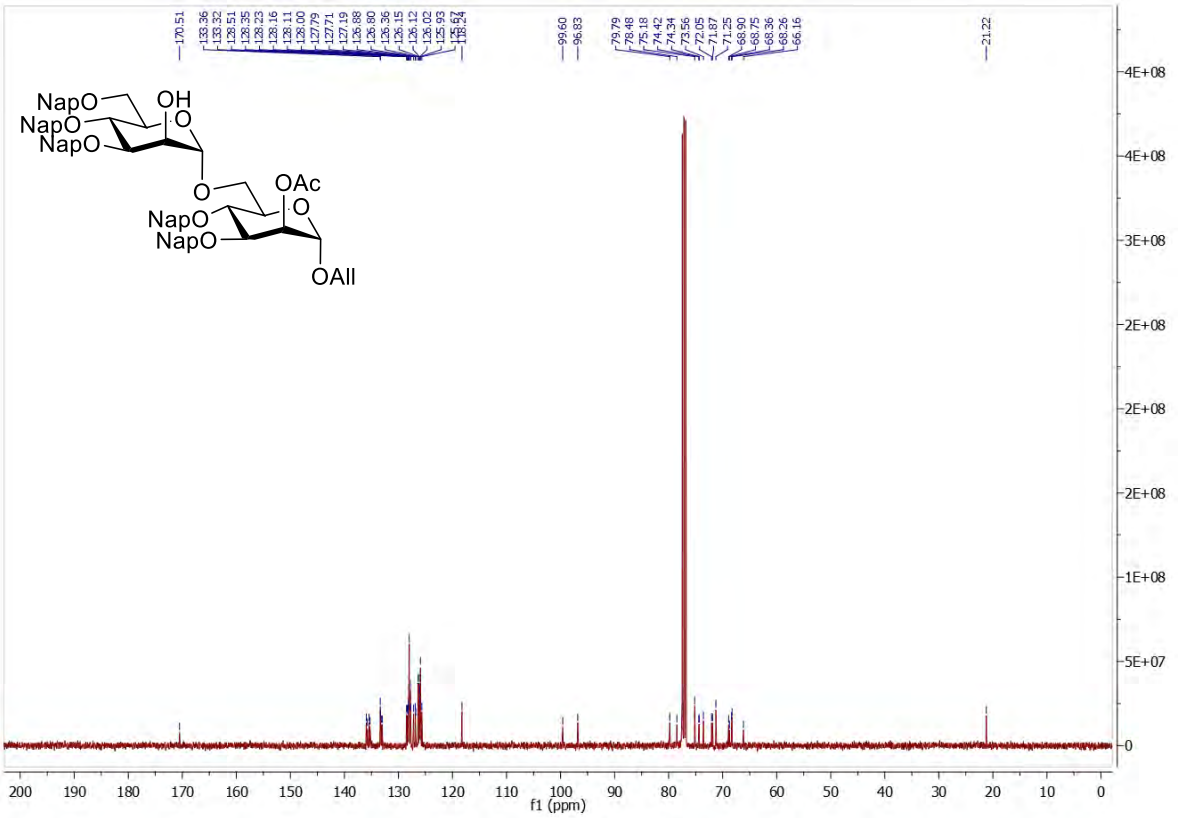

COSY NMR spectrum of compound 3-21

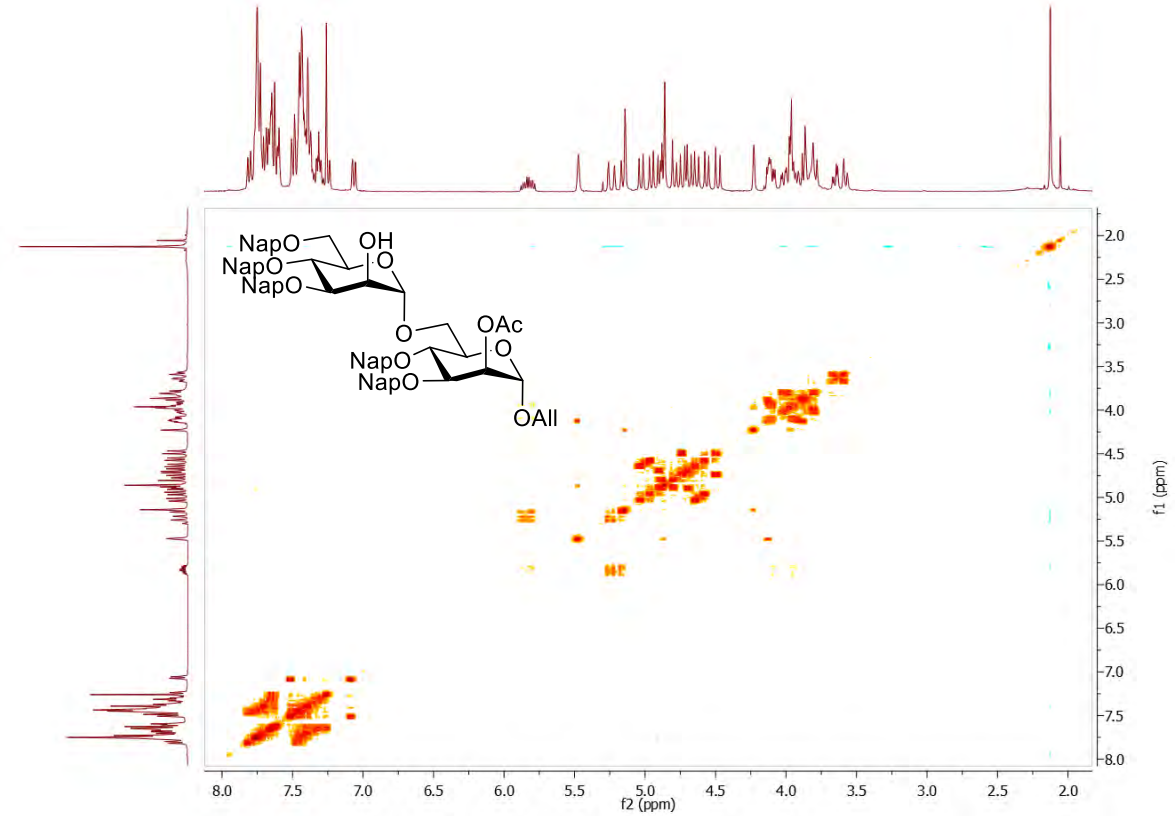

HSQC NMR spectrum of compound 3-21

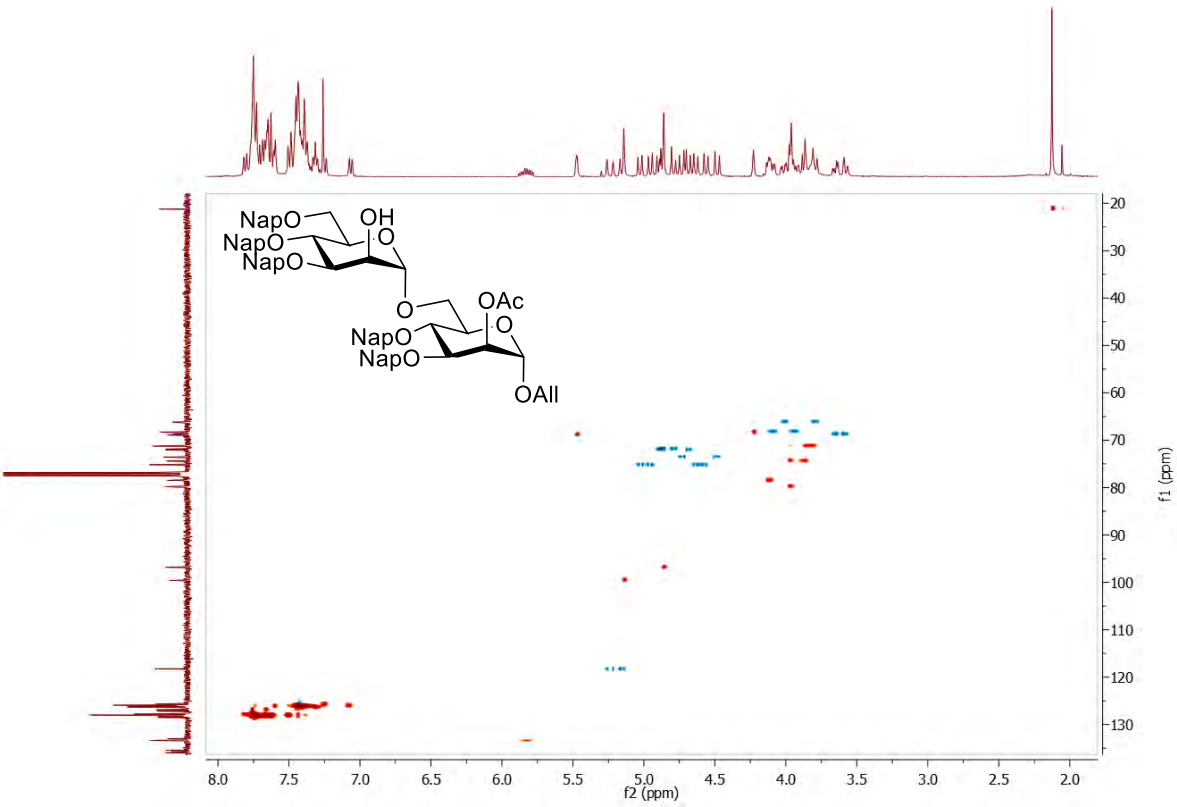

^{1}H NMR spectrum of compound 3-4

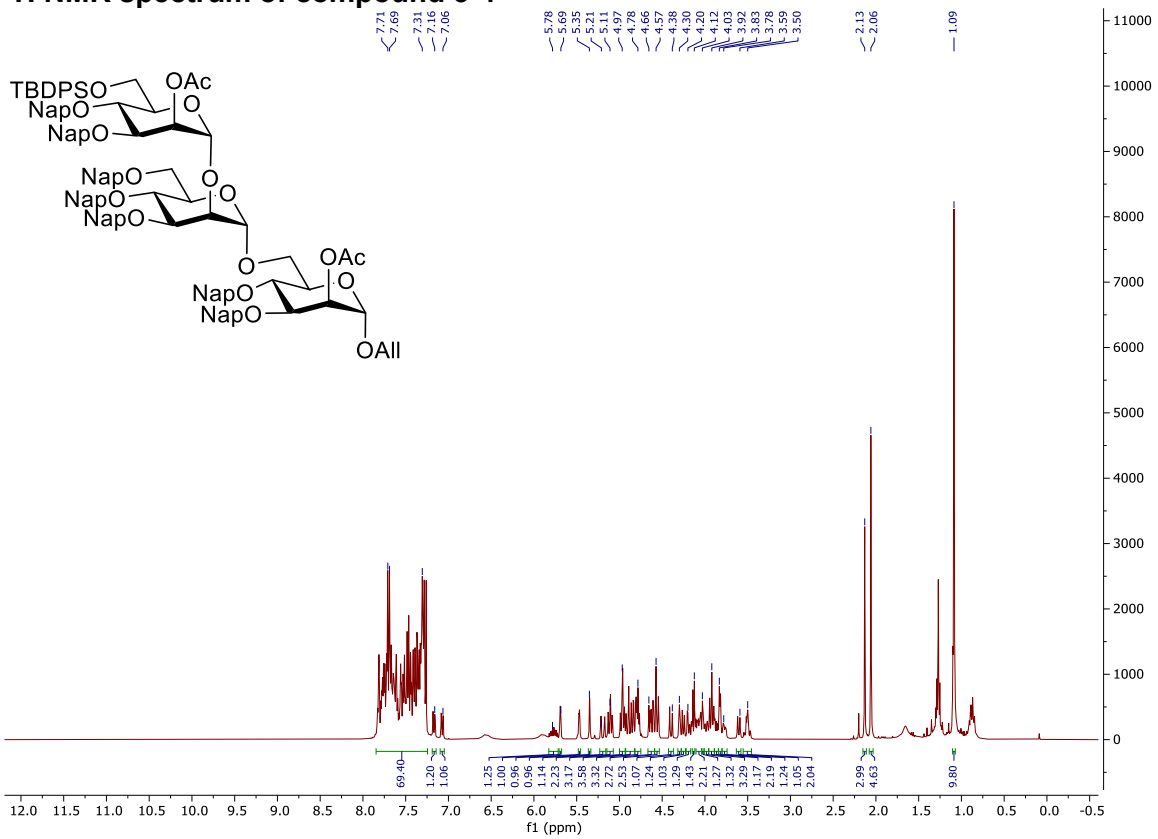

^{13}C NMR spectrum of compound 3-4

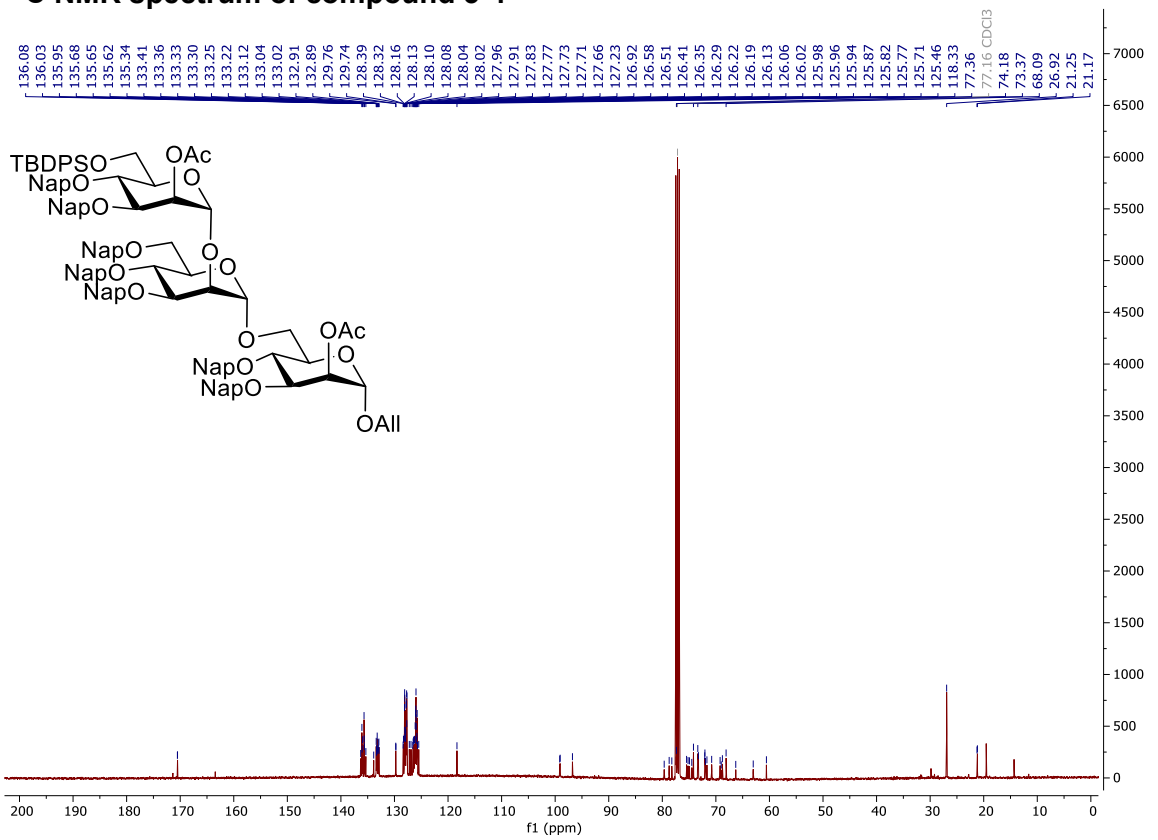

COSY NMR spectrum of compound 3-4

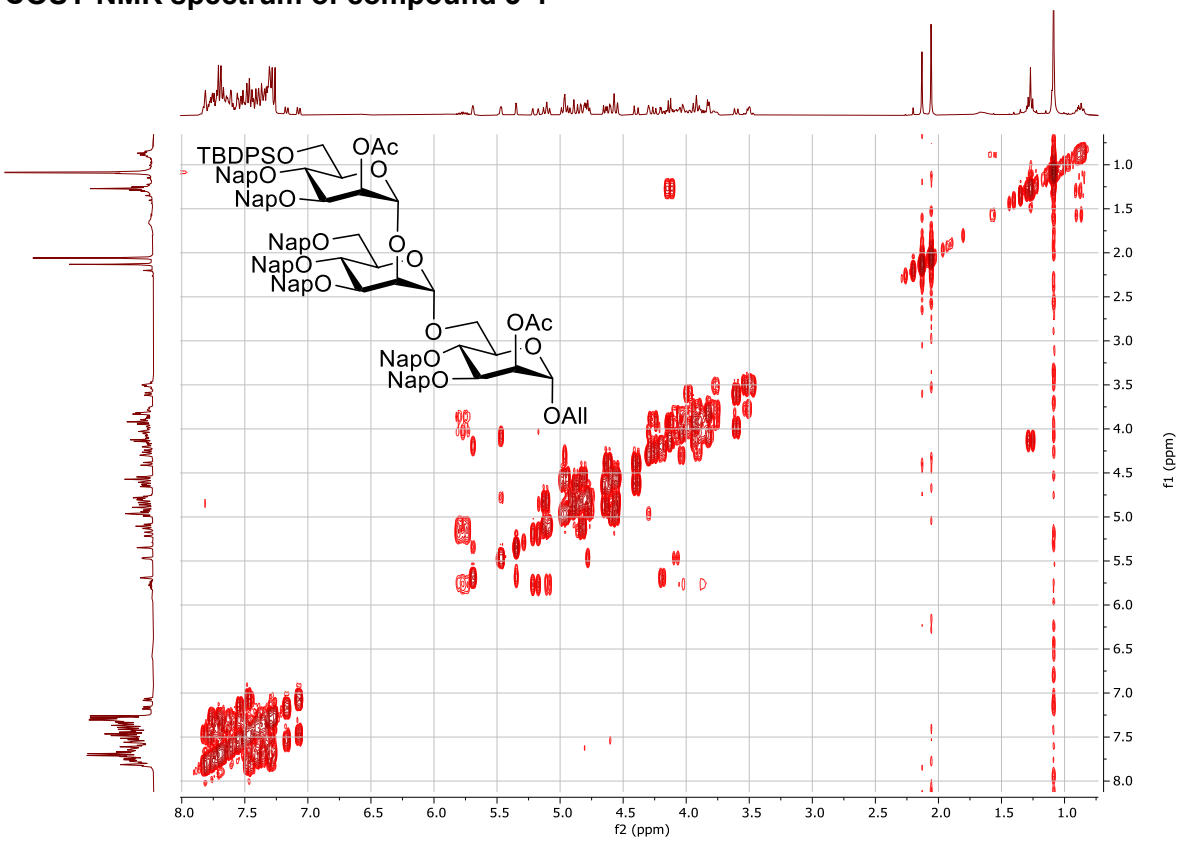

HSQC NMR spectrum of compound 3-4

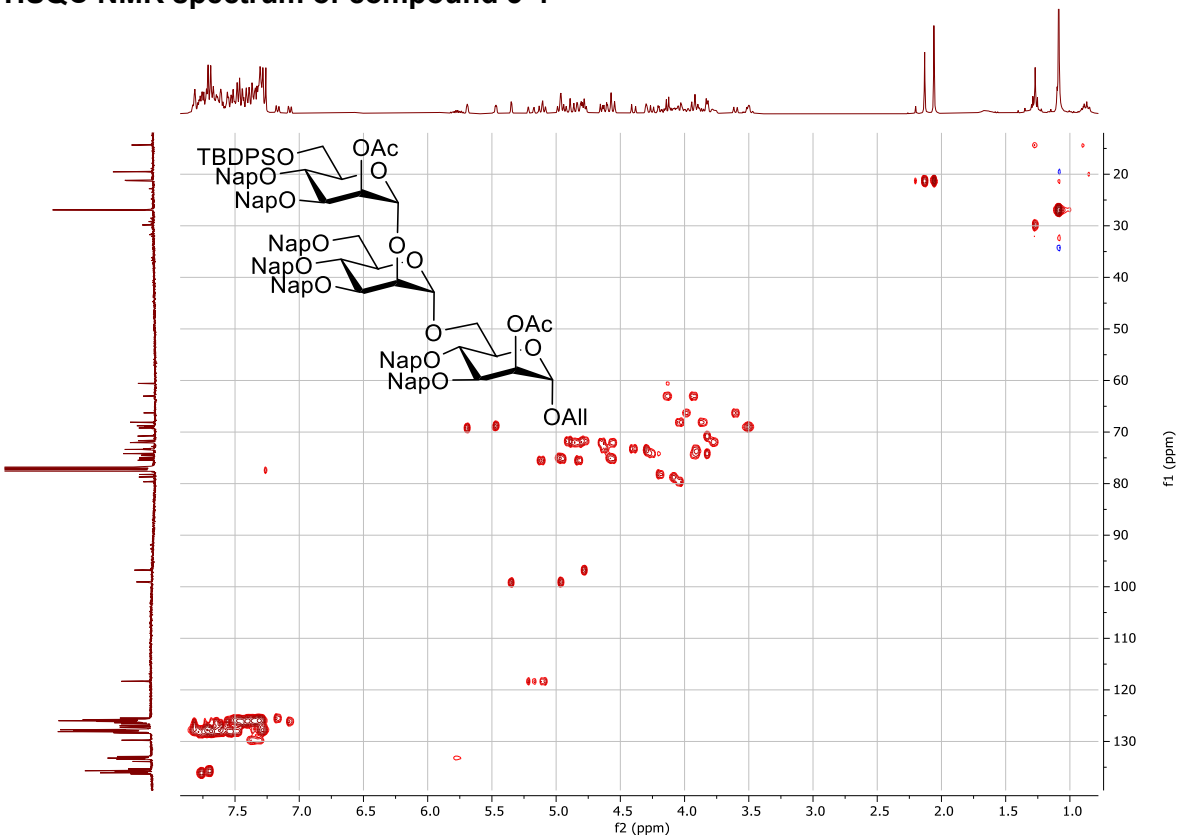

^{1}H NMR spectrum of compound 3-22

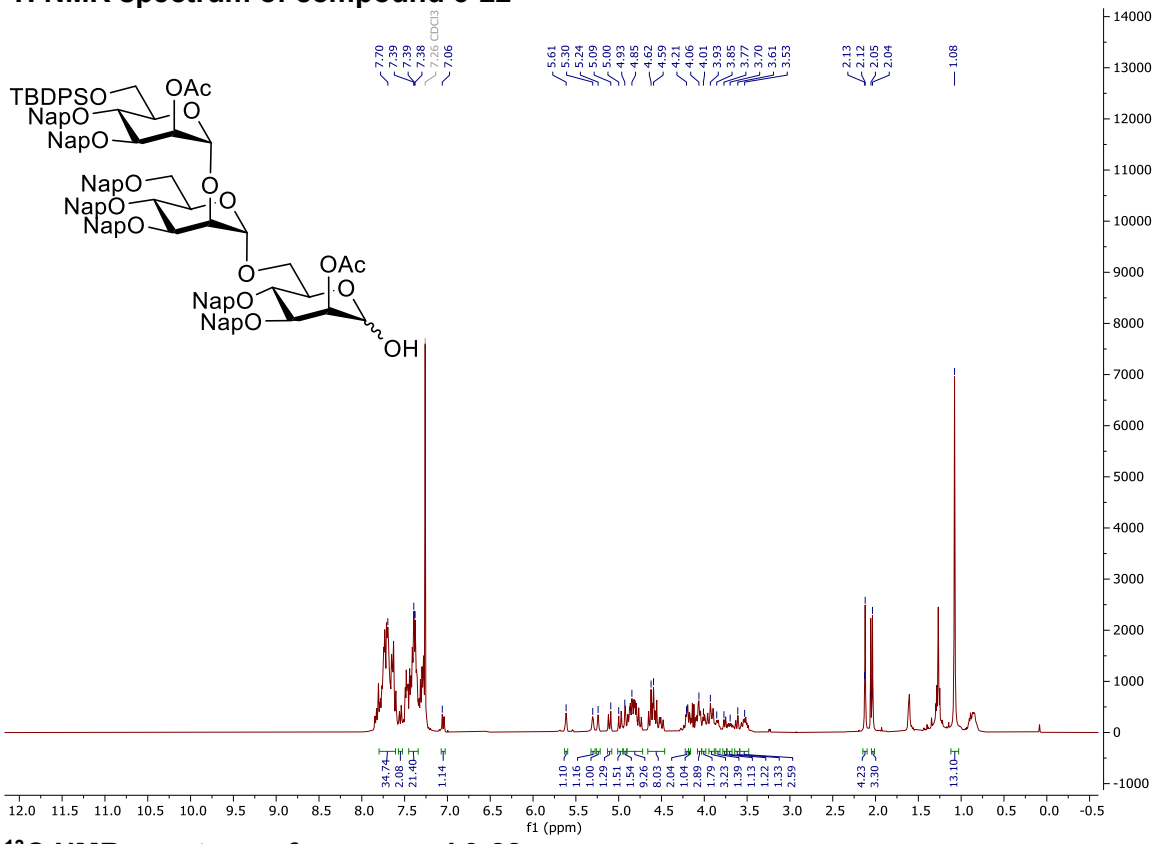

^{13}C NMR spectrum of compound 3-22

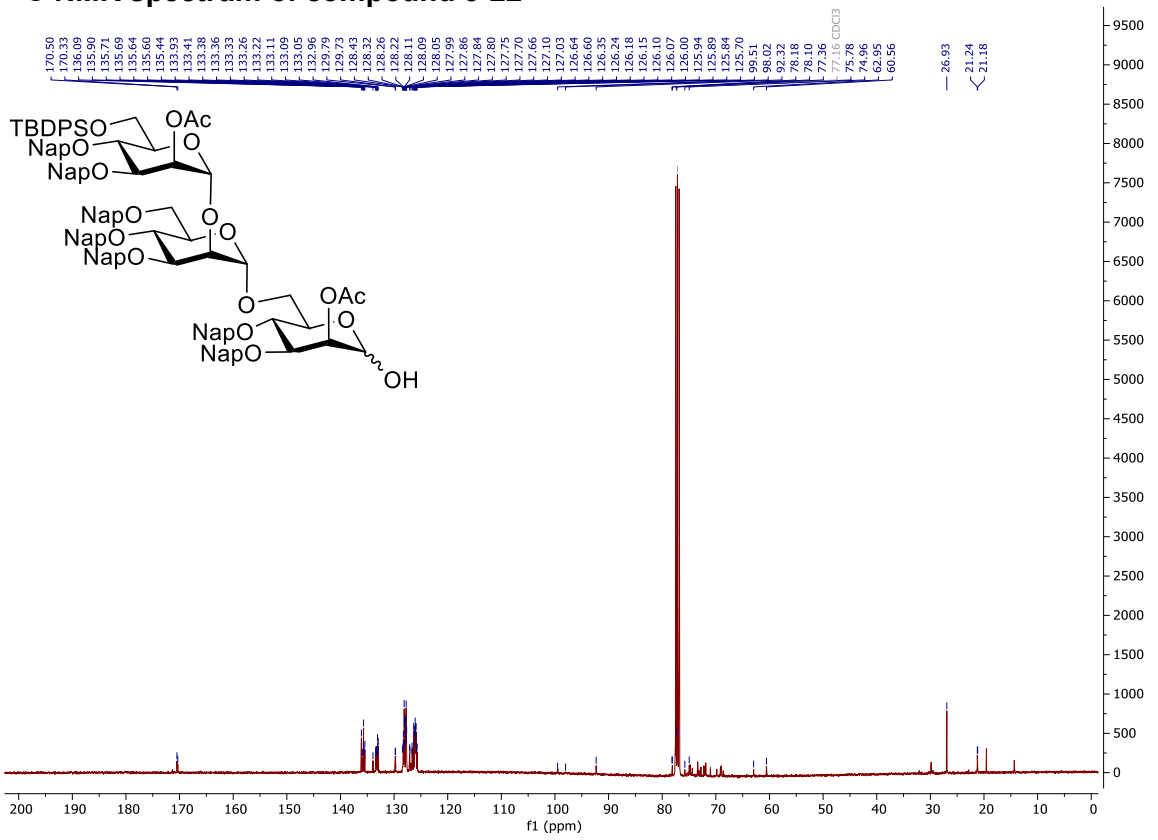

COSY NMR spectrum of compound 3-22

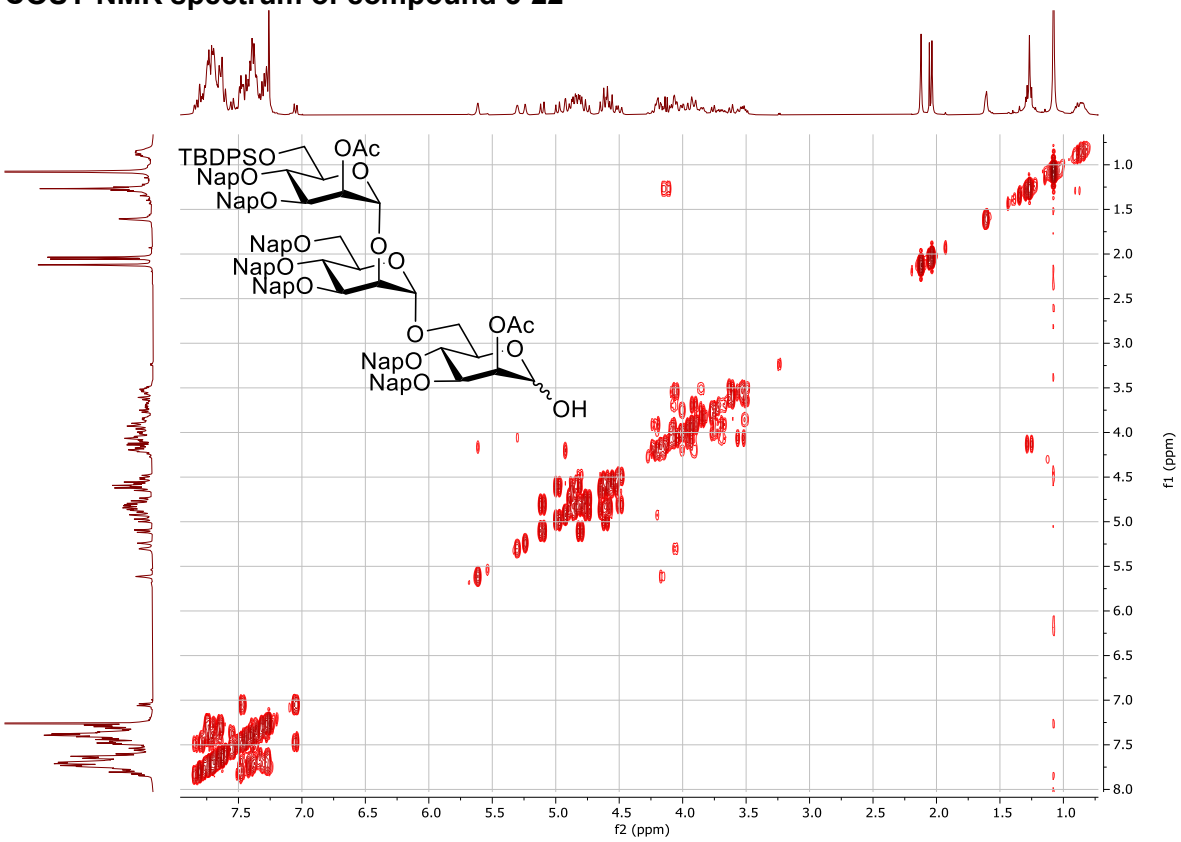

HSQC NMR spectrum compound 3-22

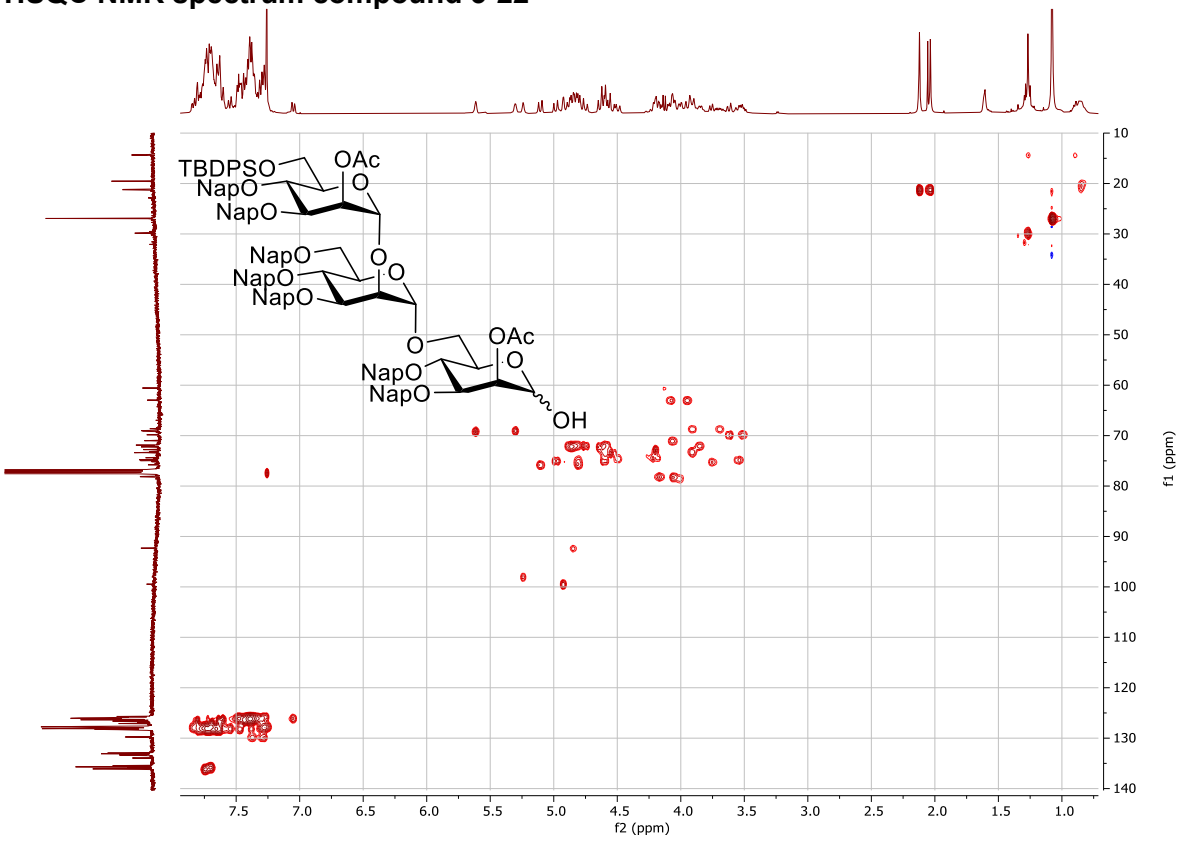

^{1}H NMR spectrum of compound 3-23

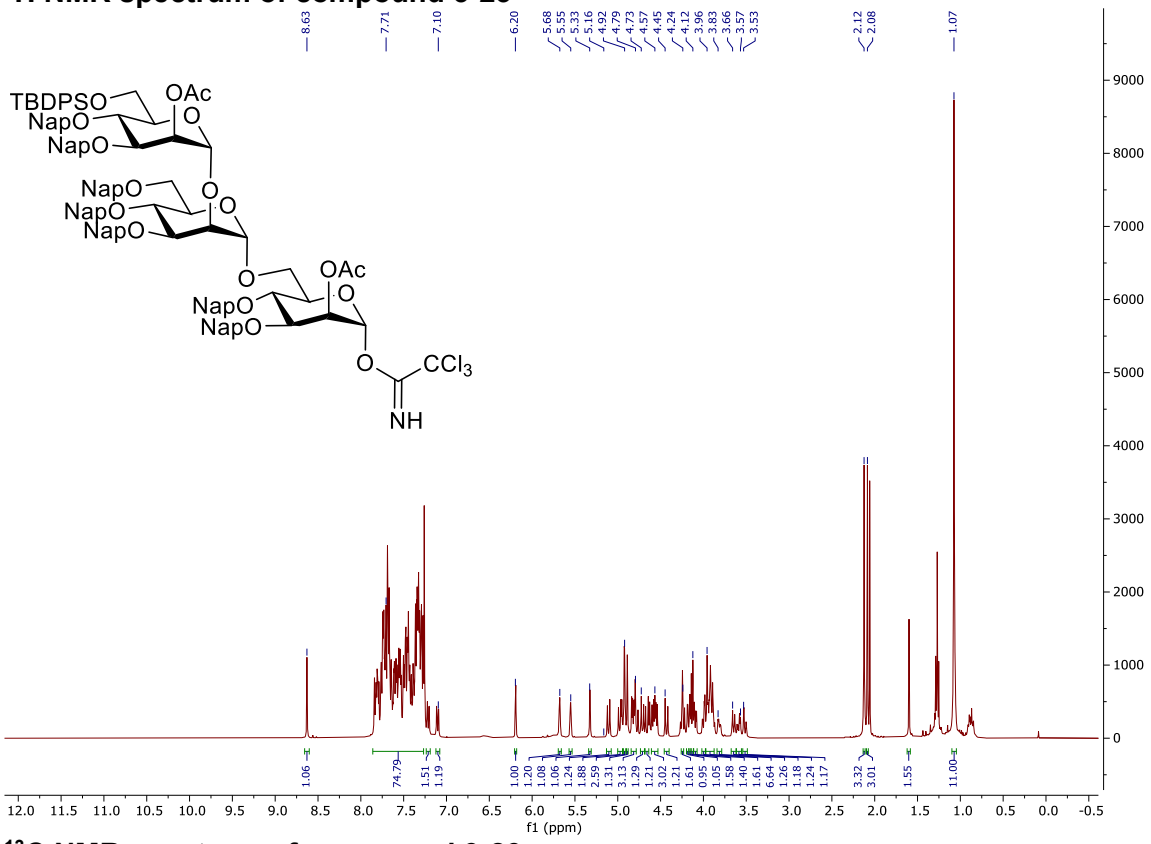

^{13}C NMR spectrum of compound 3-23

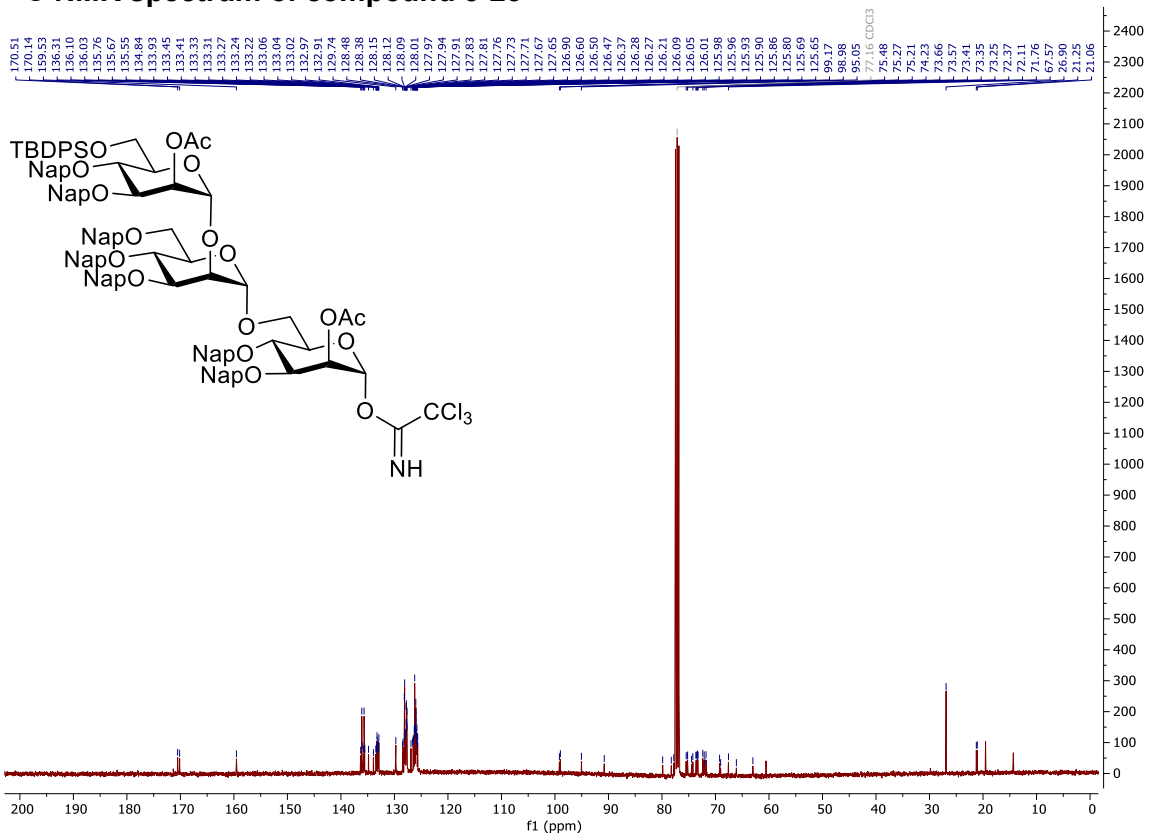

COSY NMR spectrum of compound 3-23

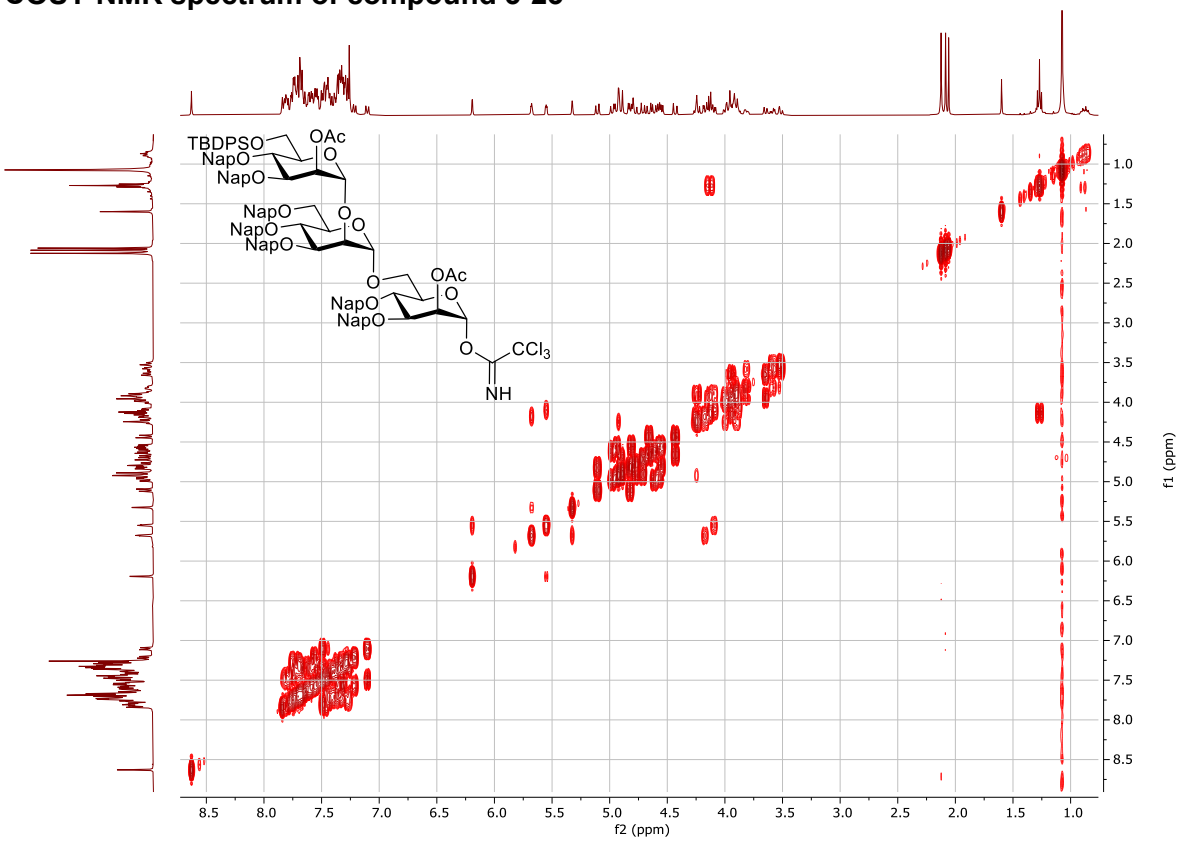

HSQC NMR spectrum of compound 3-23

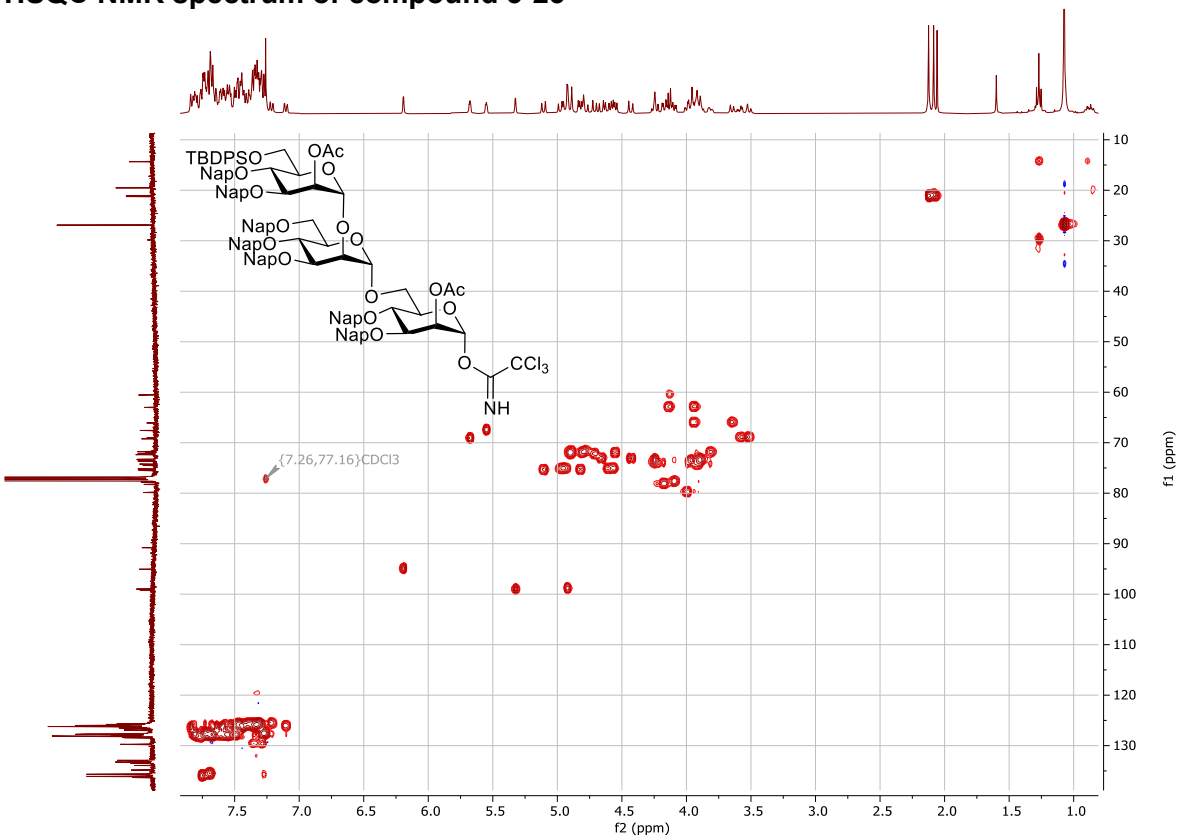

^{1}H NMR spectrum of compound 3-24

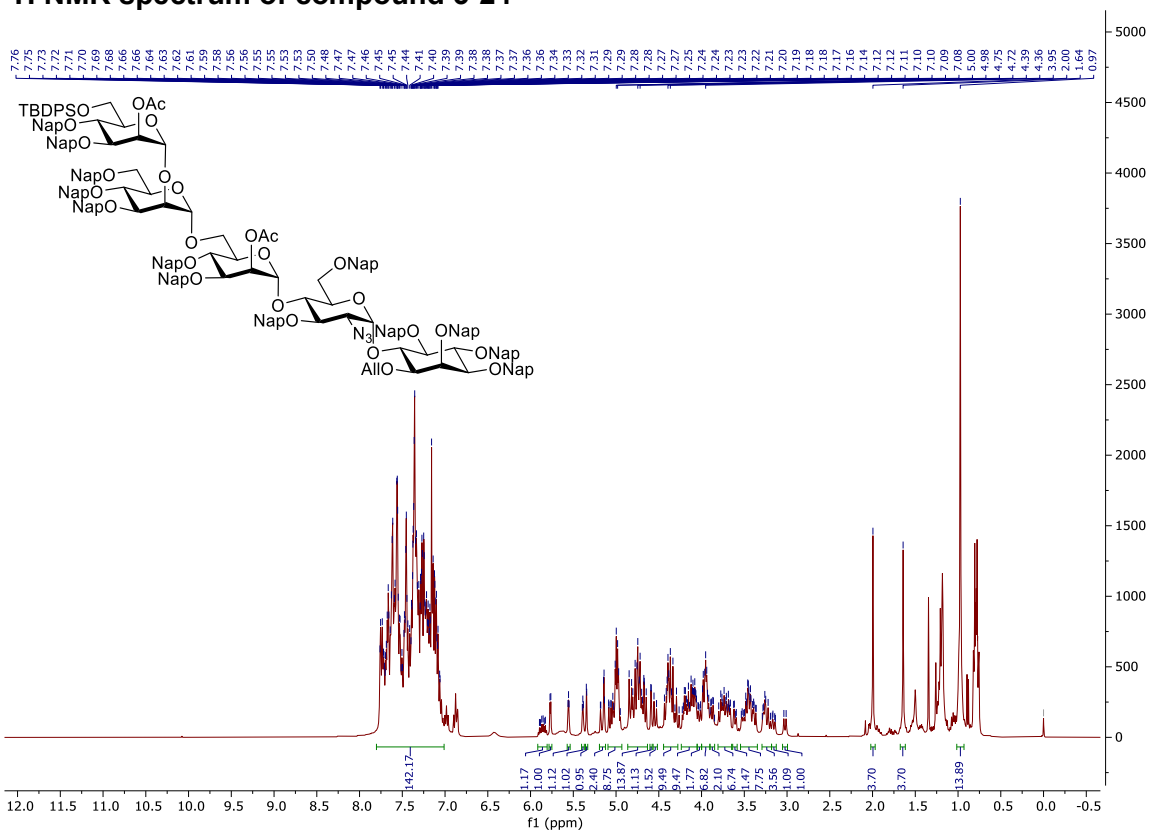

^{13}C NMR spectrum of compound 3-24

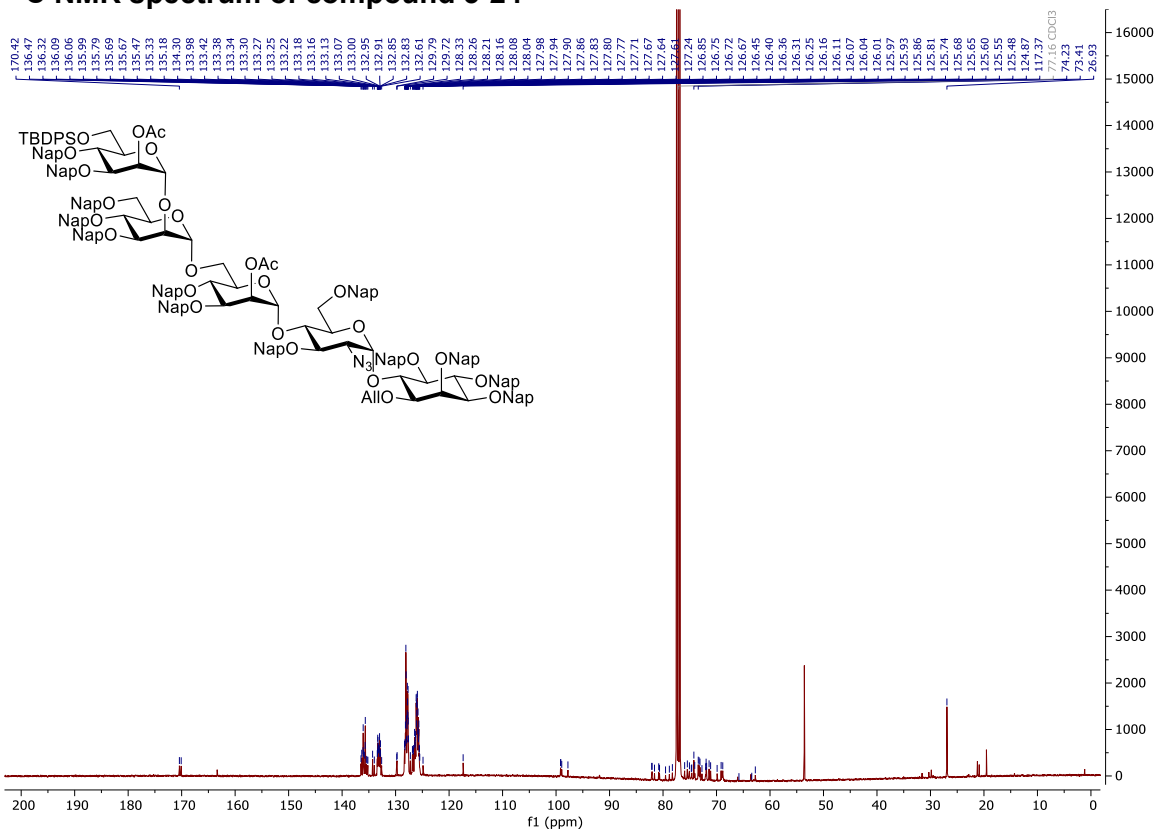

COSY-NMR spectrum of compound 3-24

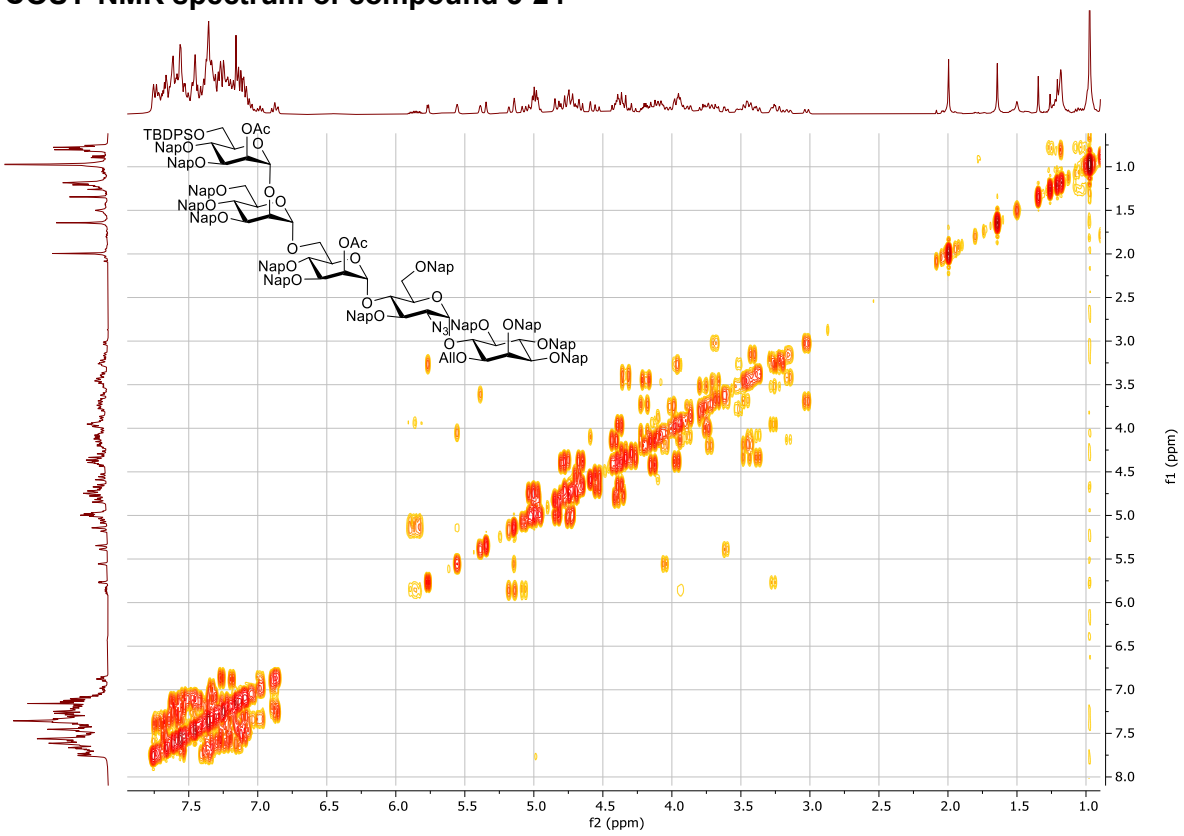

HSQC-NMR spectrum of compound 3-24

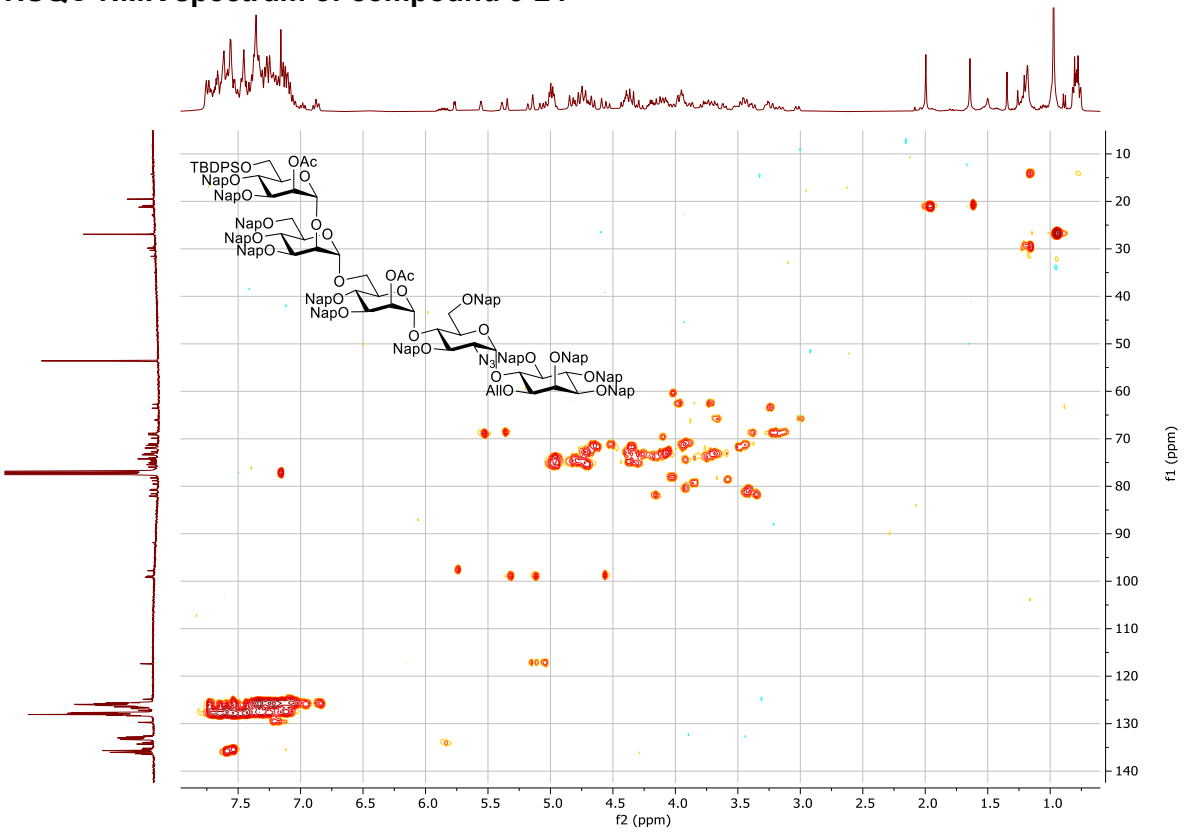

^{1}H NMR spectrum of compound 3-25

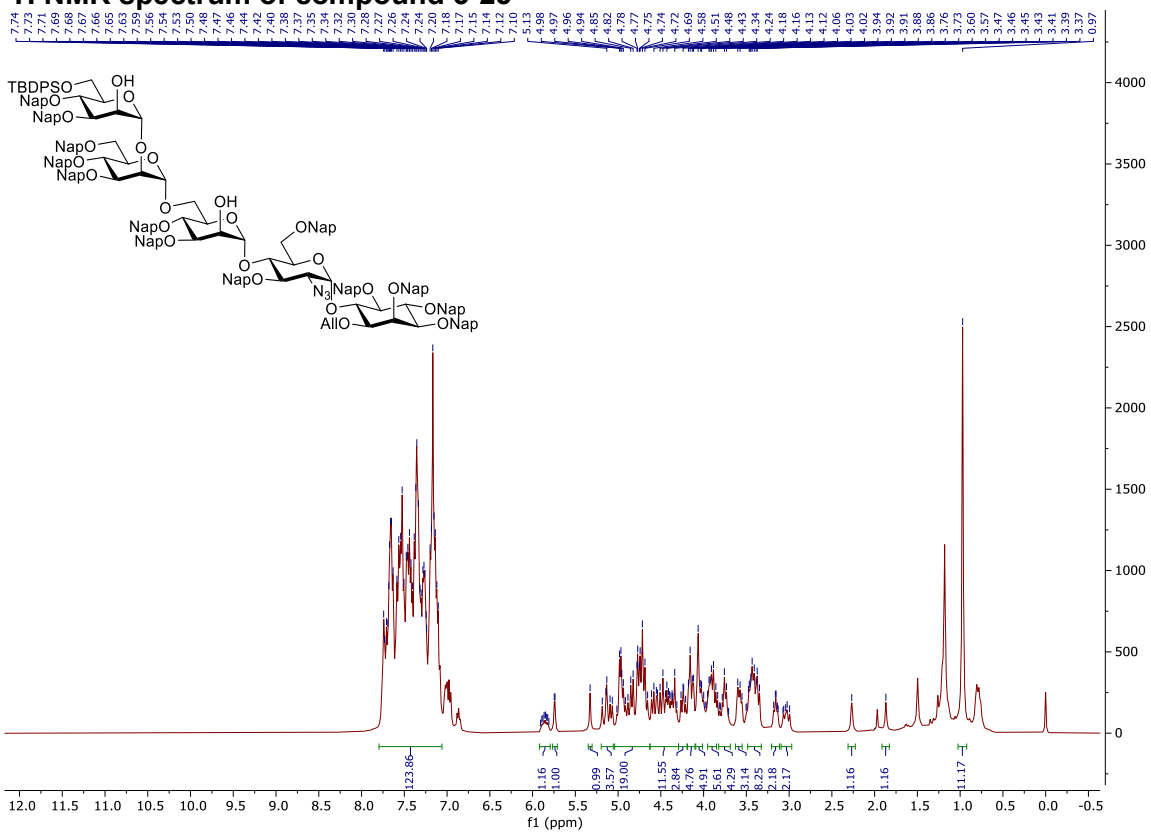

^{13}C NMR spectrum of compound 3-25

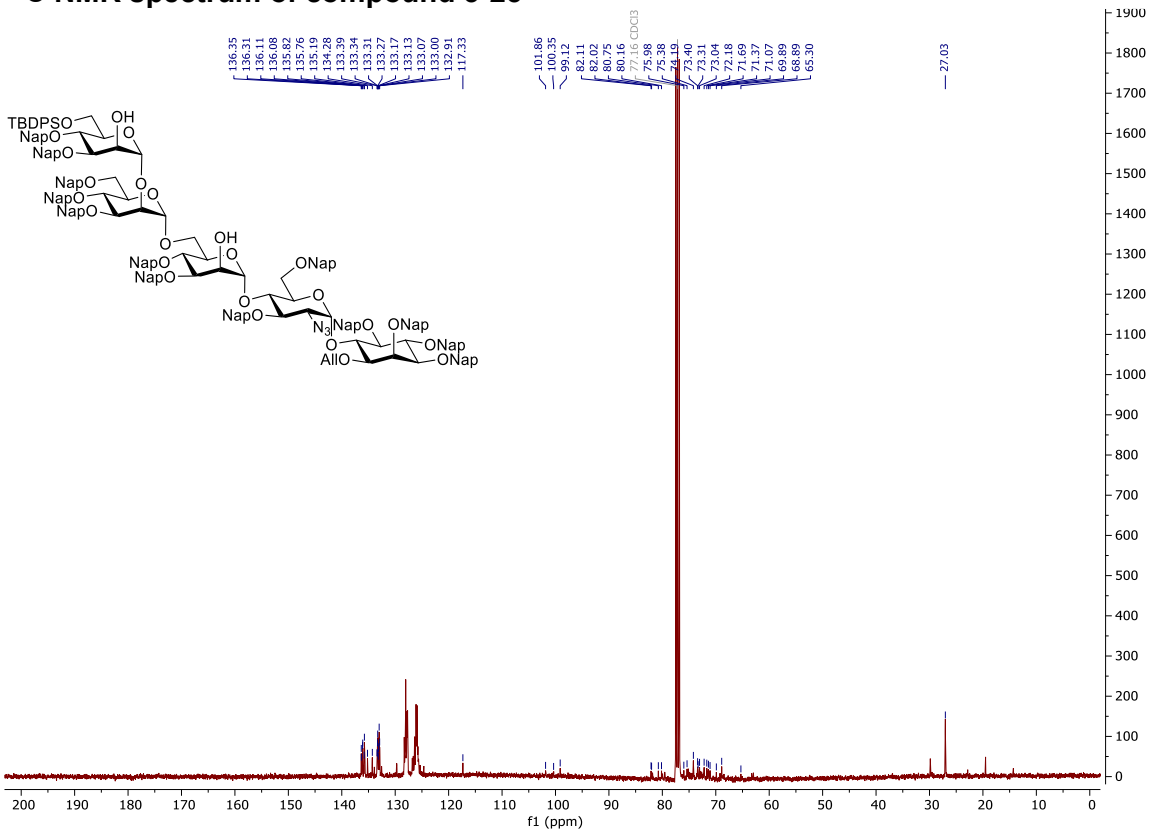

COSY-NMR spectrum of compound 3-25

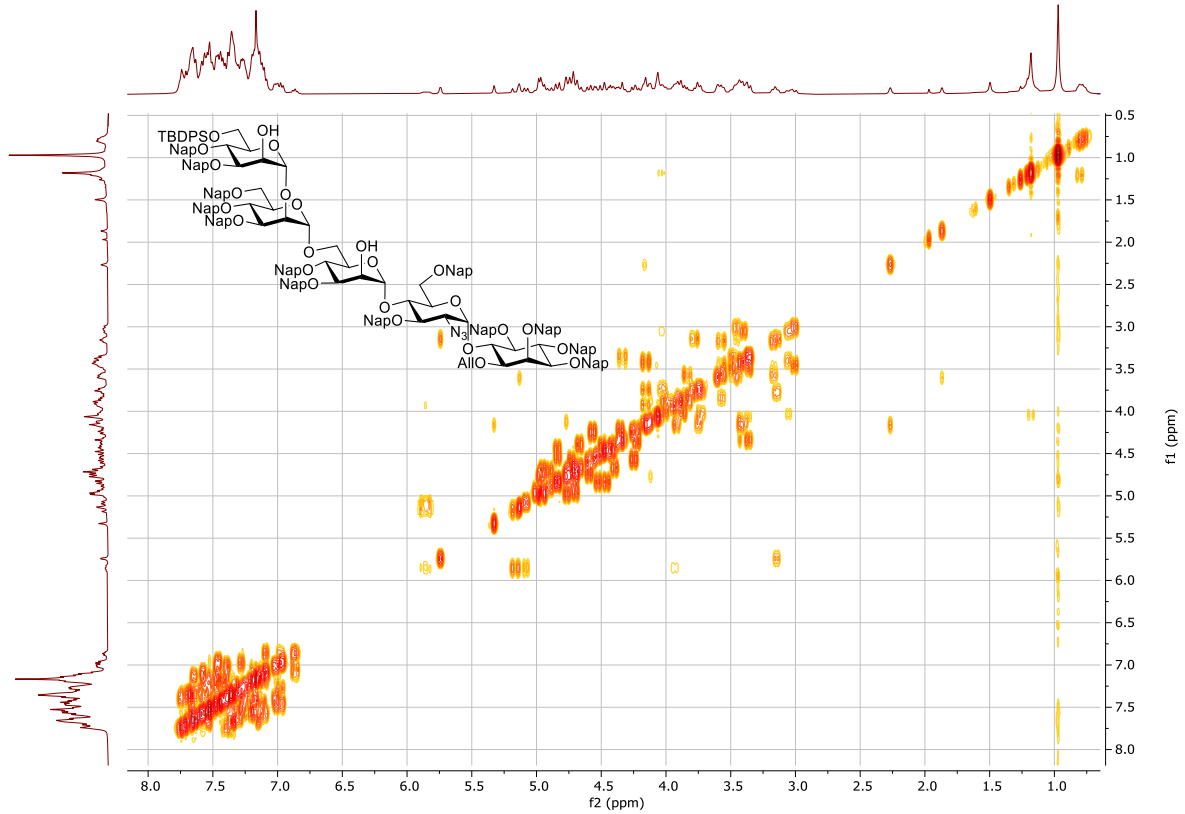

HSQC-NMR spectrum of compound 3-25

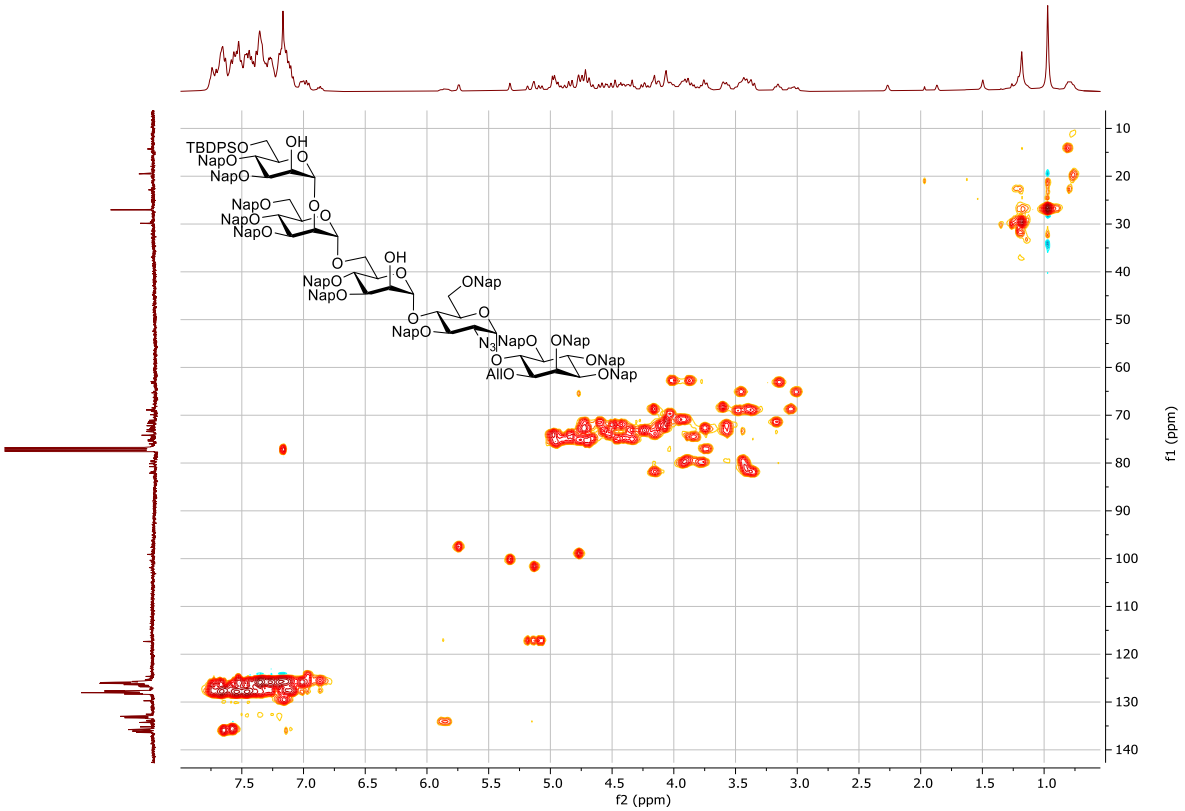

^{1}H NMR spectrum of compound 3-26

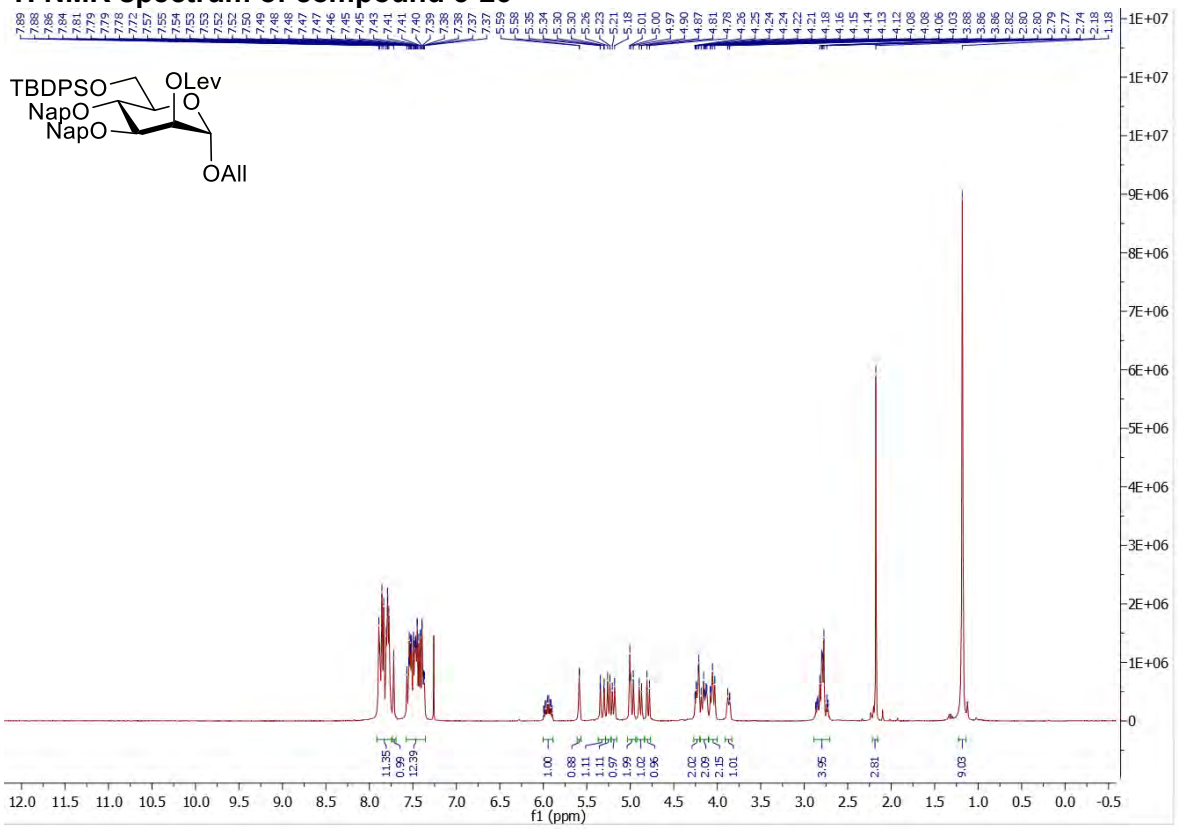

^{13}C NMR spectrum of compound 3-26

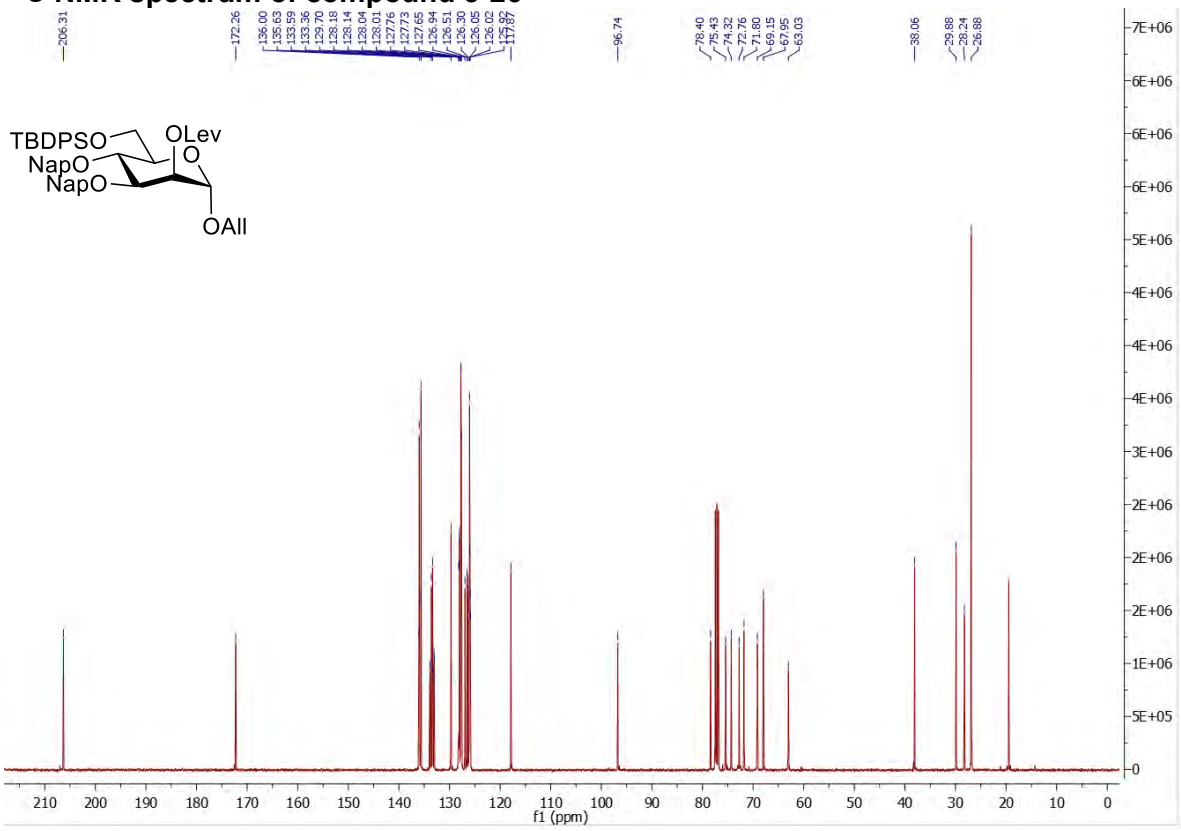

COSY NMR spectrum of compound 3-26

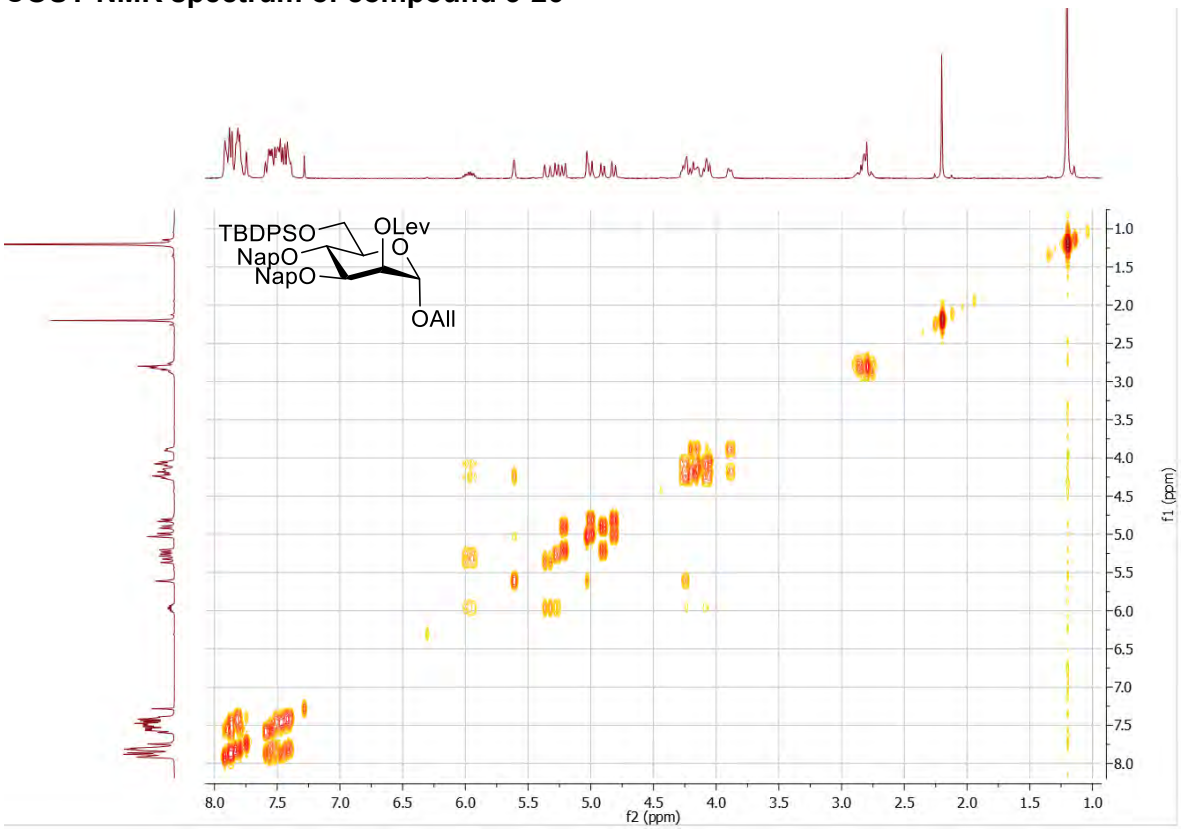

HSQC NMR spectrum of compound 3-26

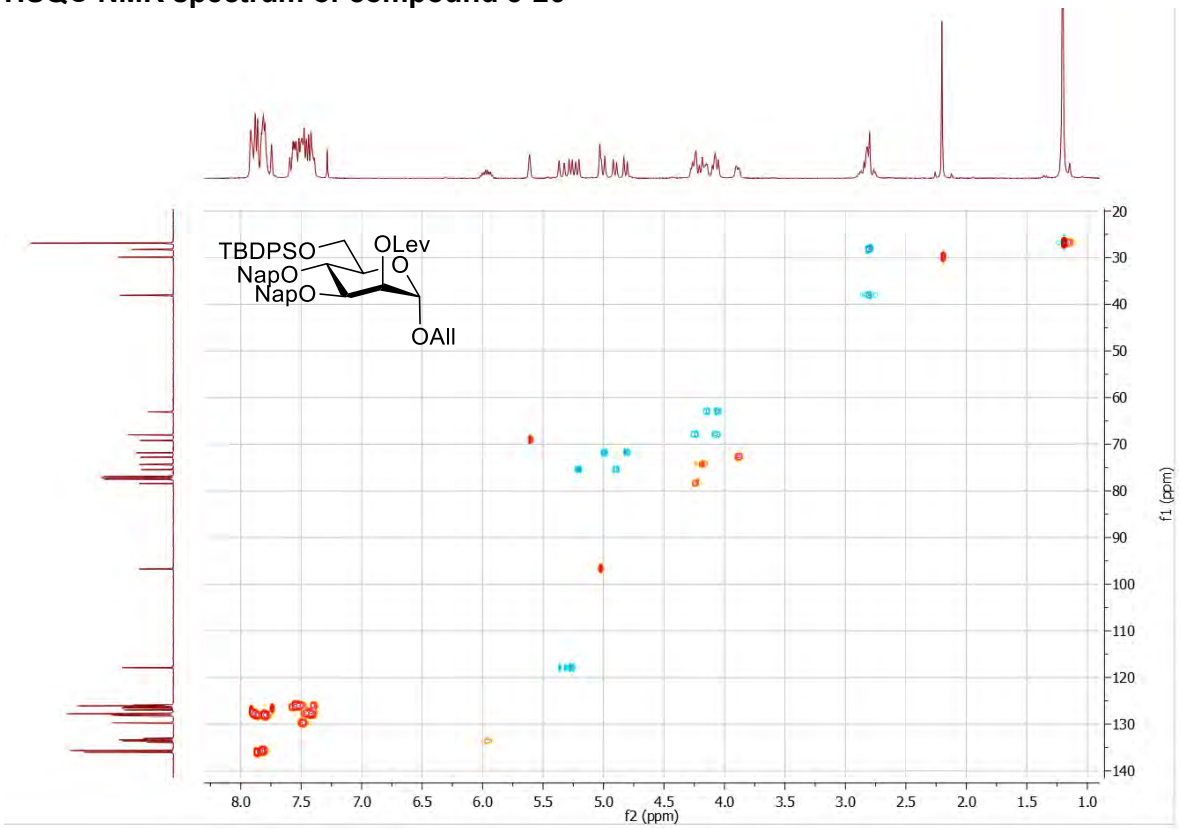

^{1}H NMR spectrum of compound 3-27

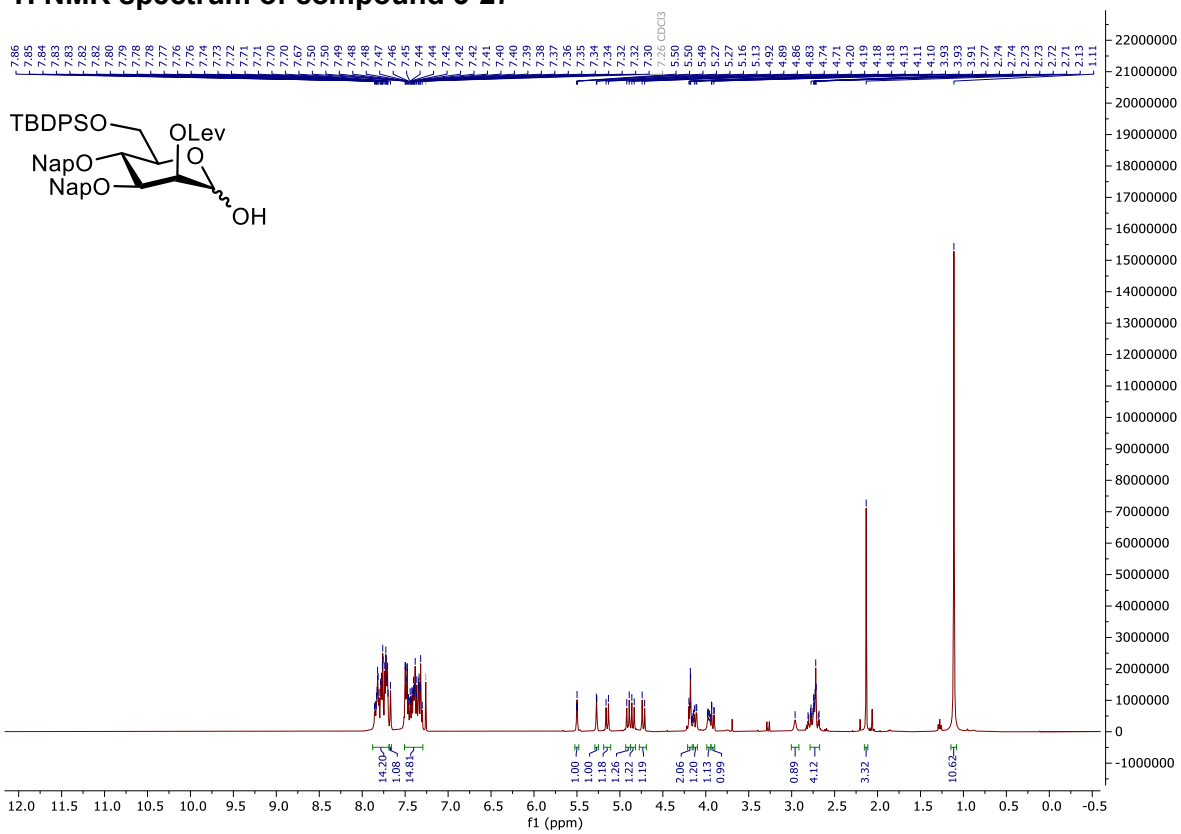

^{13}C NMR spectrum of compound 3-27

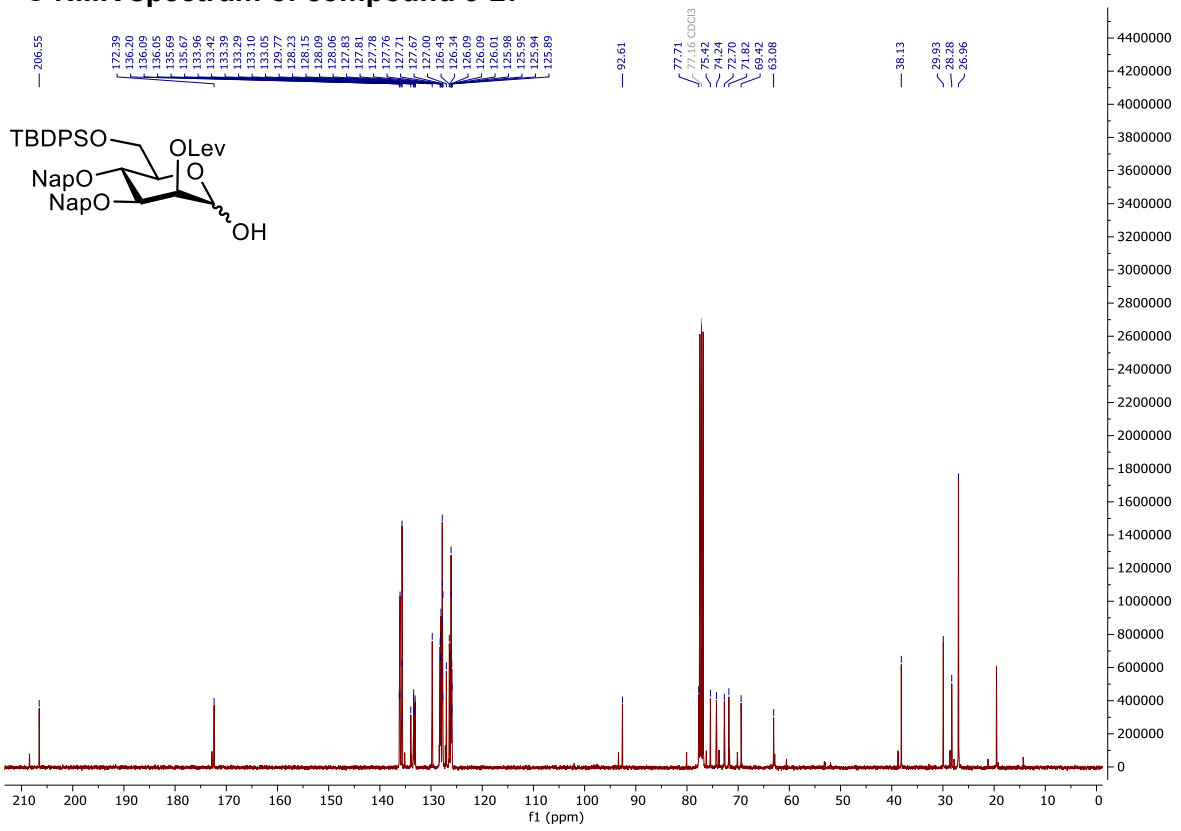

COSY NMR spectrum of compound 3-27

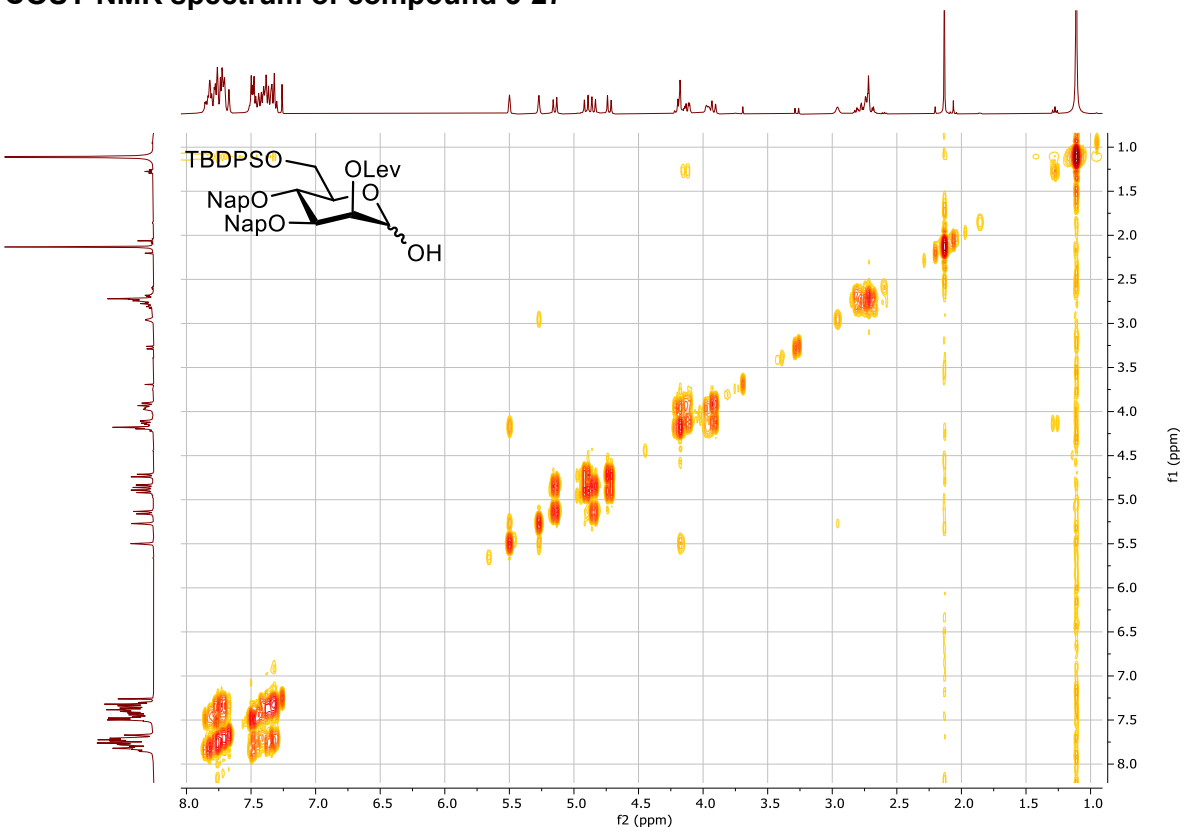

HSQC NMR spectrum of compound 3-27

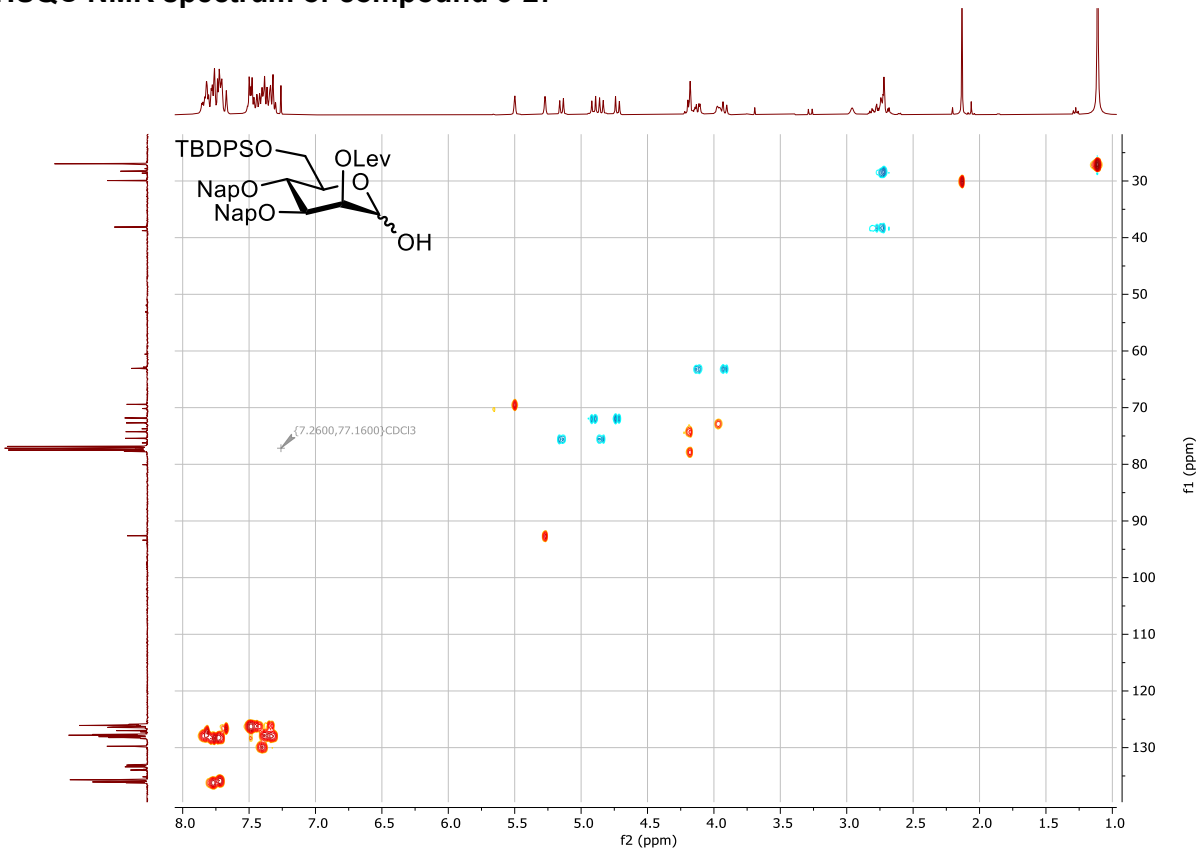

^{1}H NMR spectrum of compound 3-28

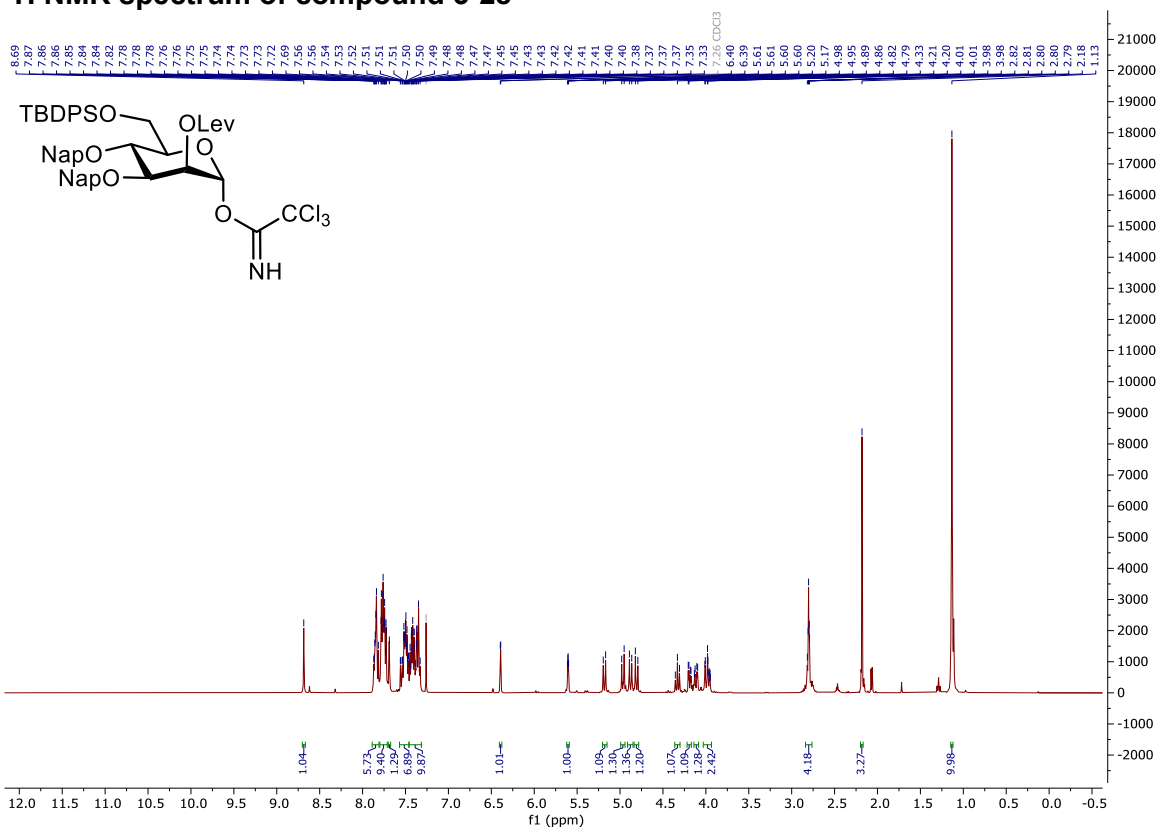

^{13}C NMR spectrum of compound 3-28

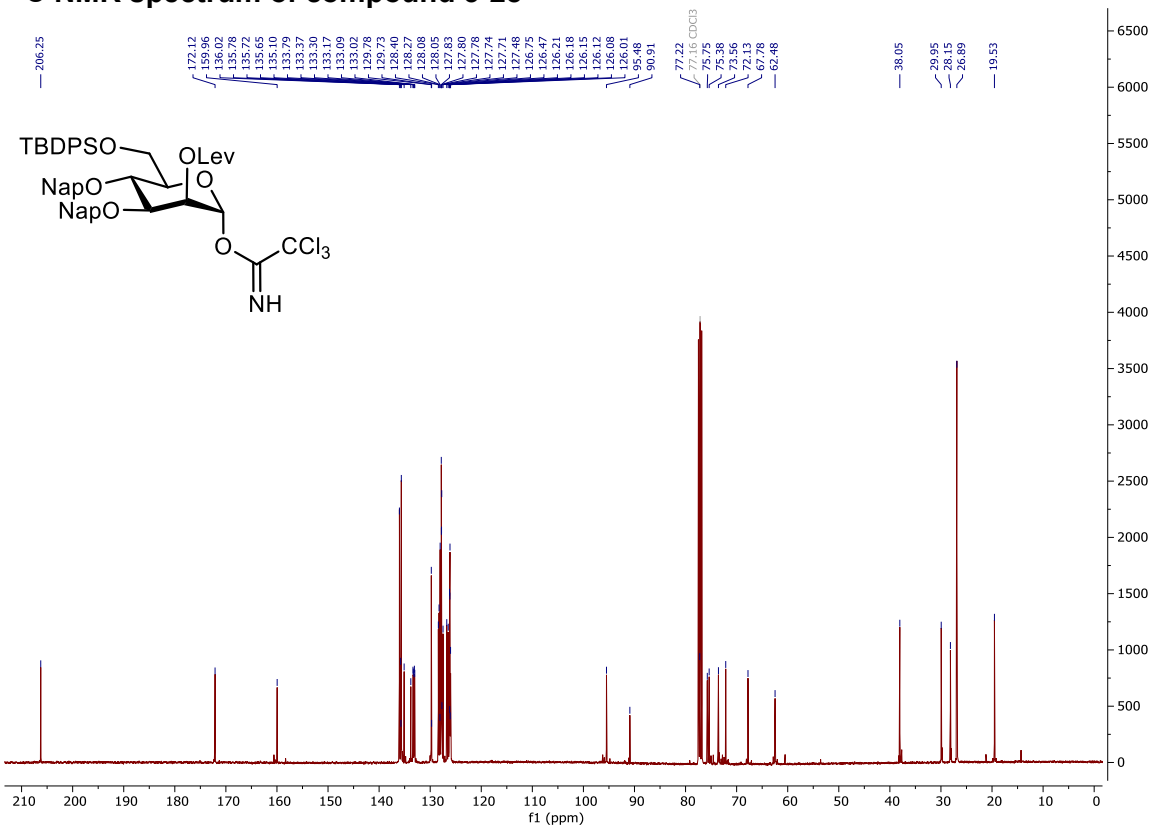

COSY NMR spectrum of compound 3-28

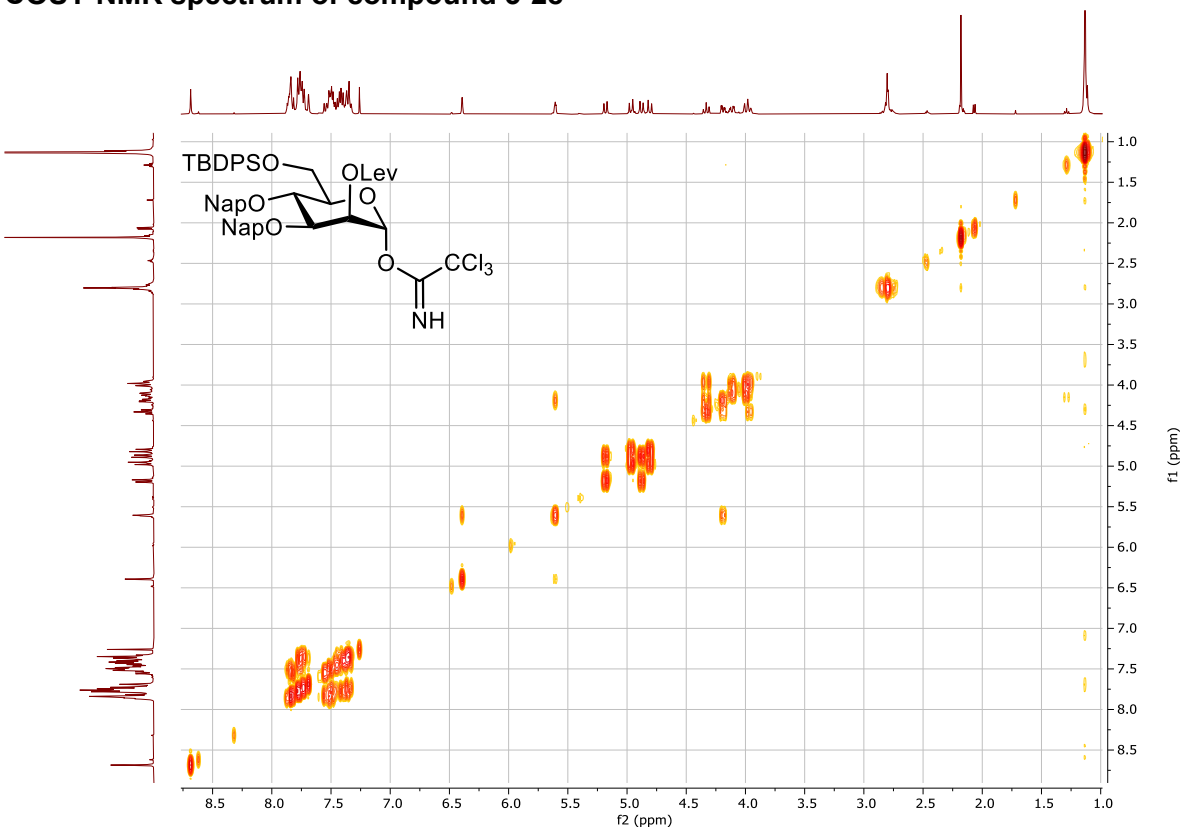

HSQC NMR spectrum of compound 3-28

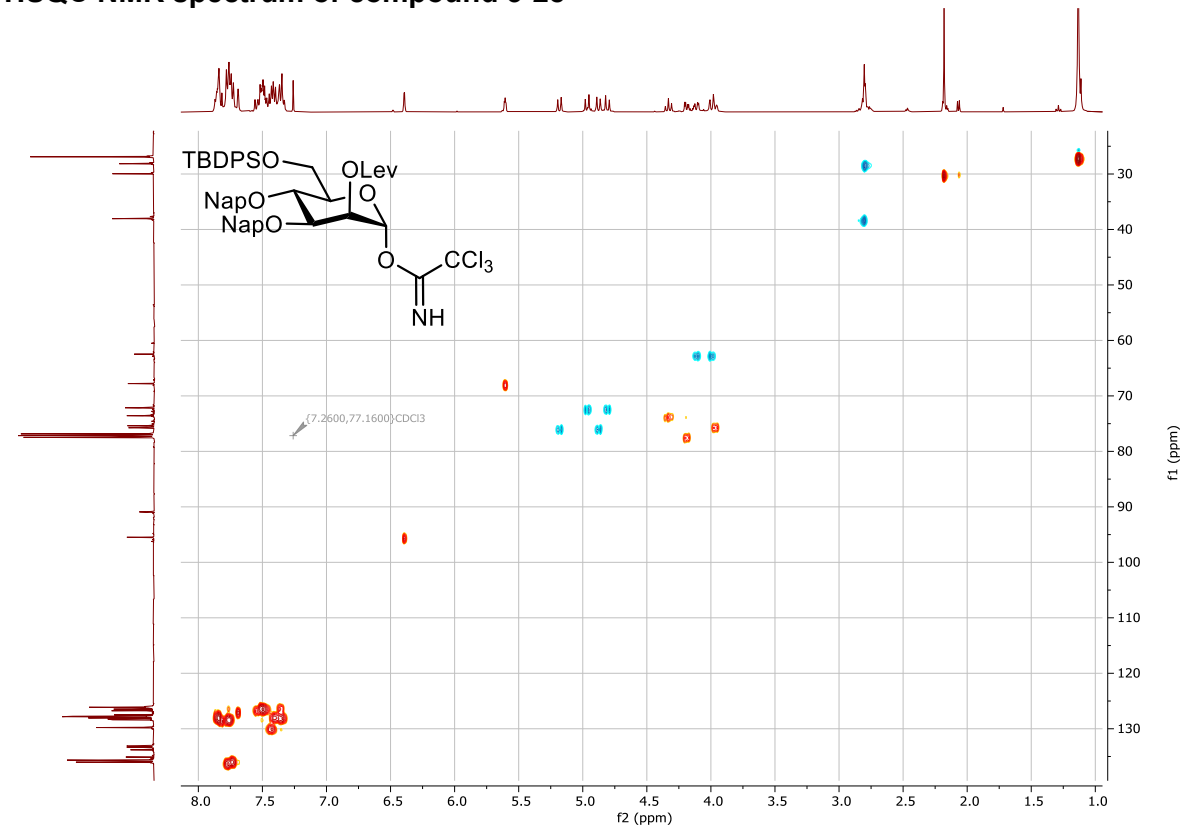

^{1}H NMR spectrum of compound 3-29

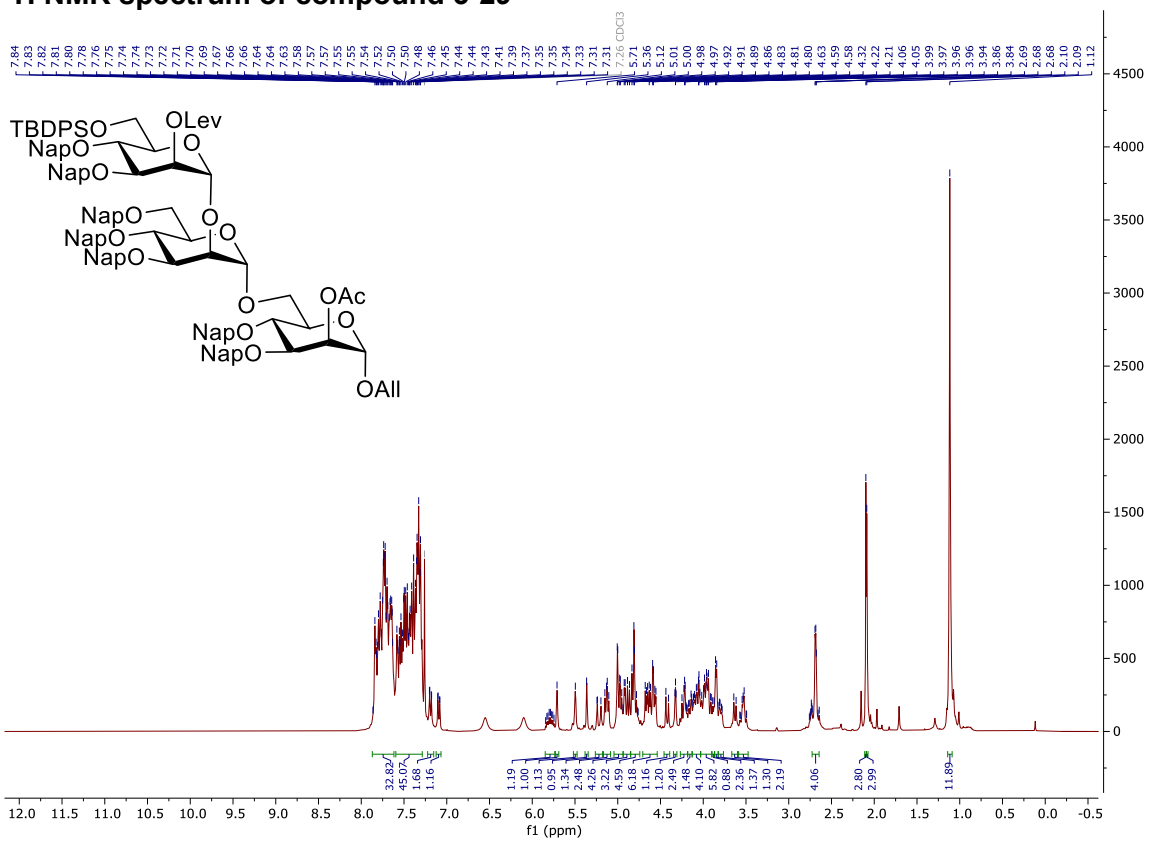

^{13}C NMR spectrum of compound 3-29

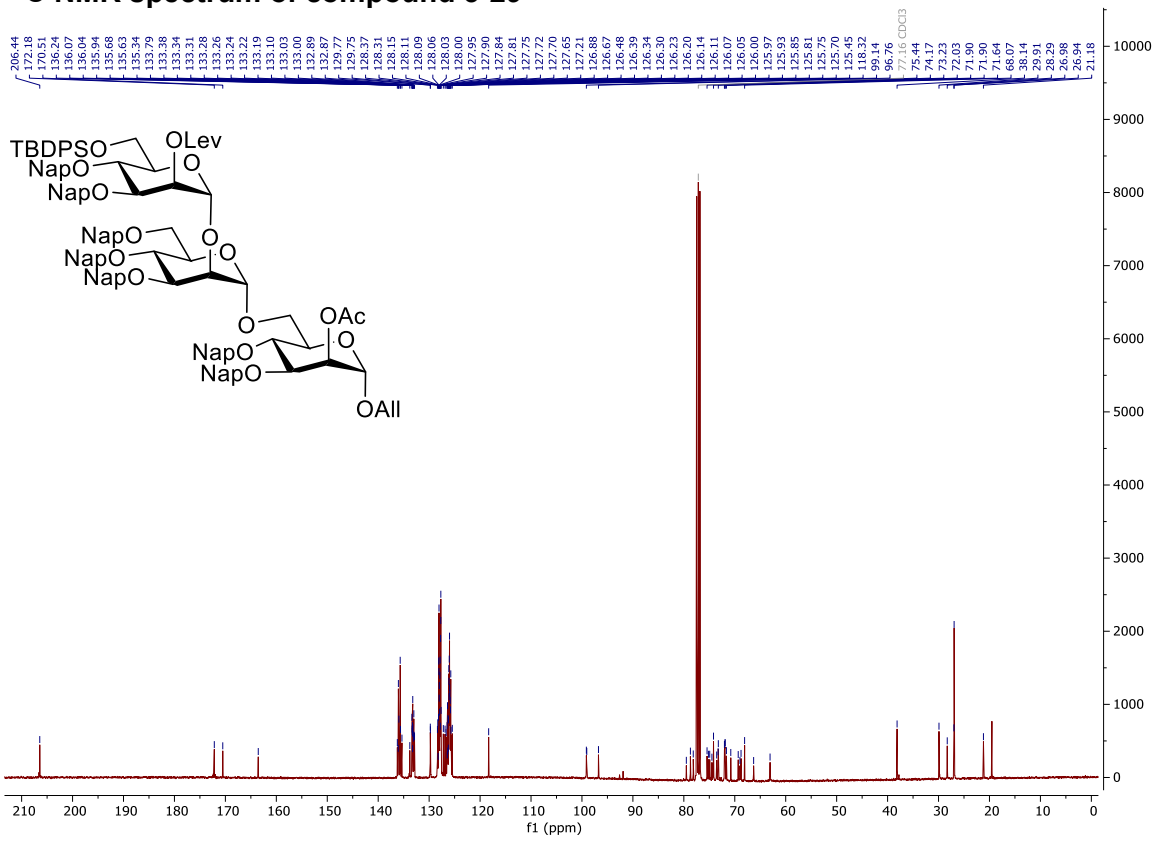

COSY NMR spectrum of compound 3-29

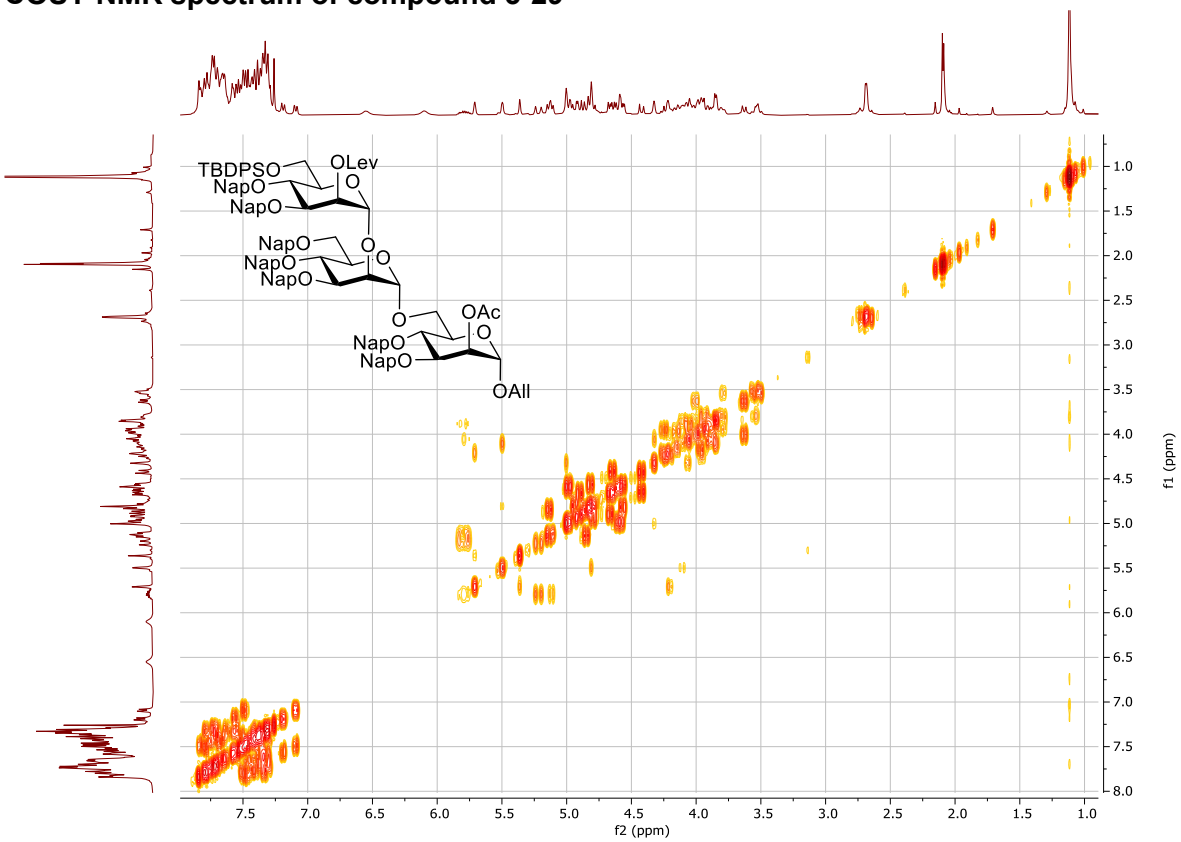

HSQC NMR spectrum of compound 3-29

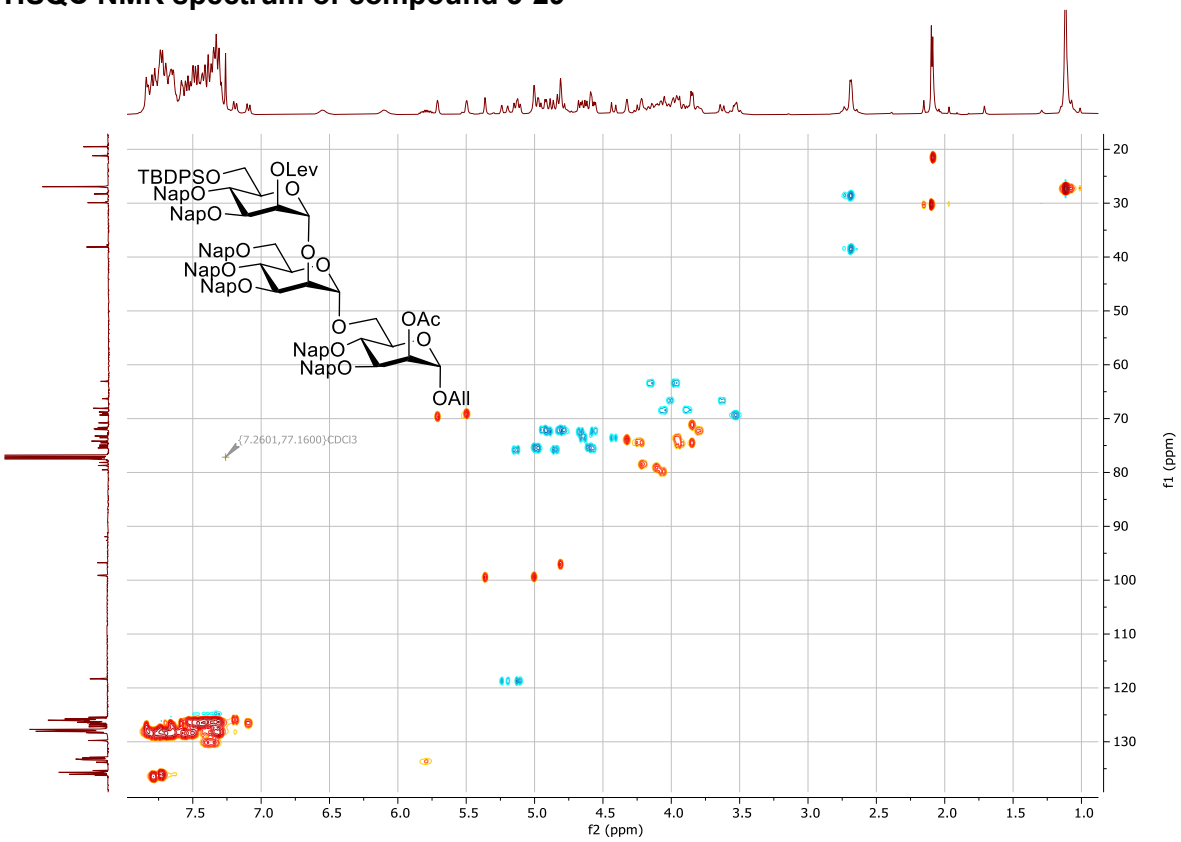

^{1}H NMR spectrum of compound 3-30

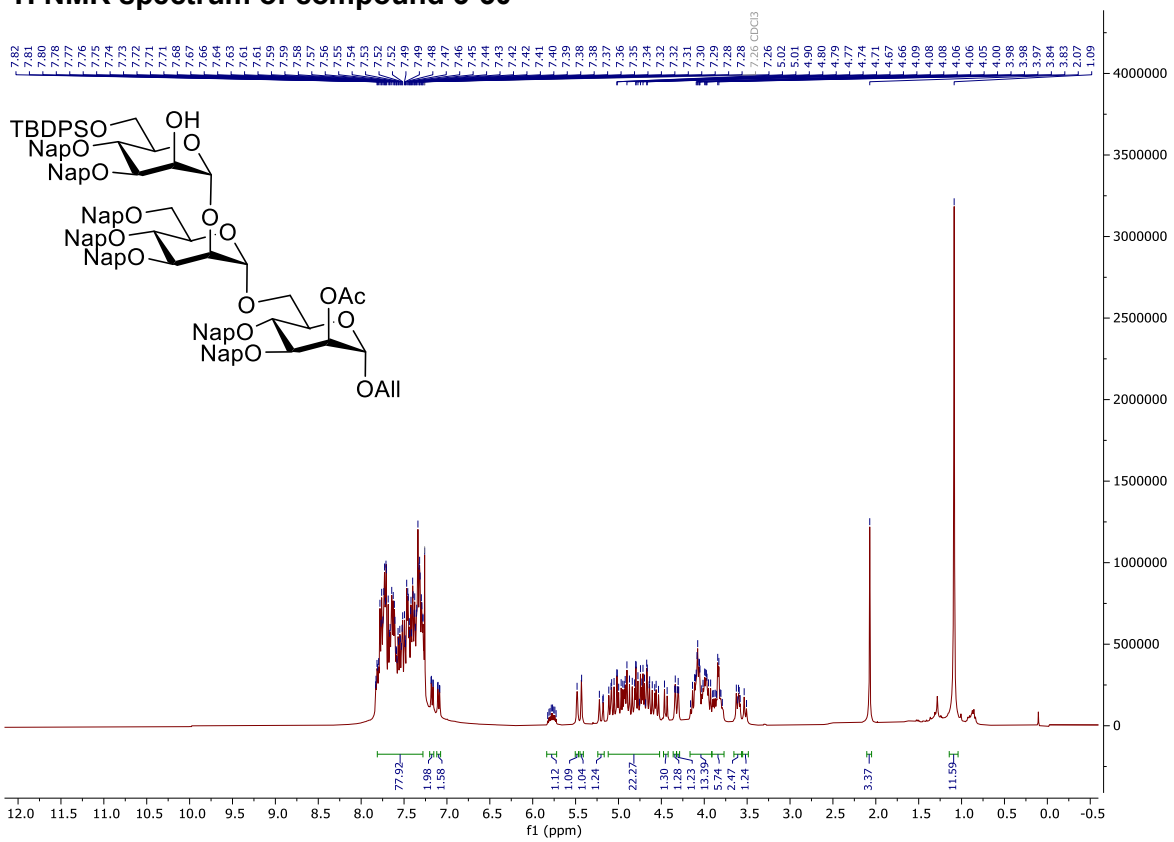

^{13}C NMR spectrum of compound 3-30

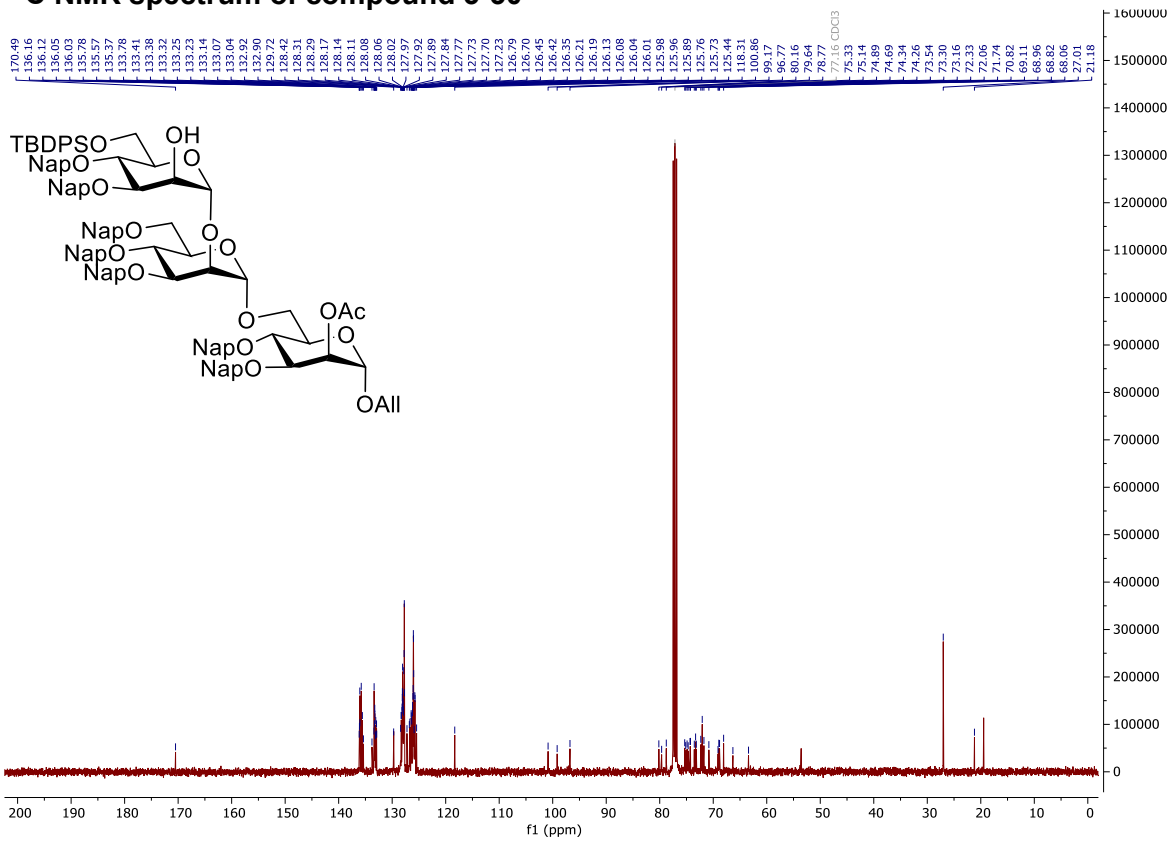

COSY NMR spectrum of compound 3-30

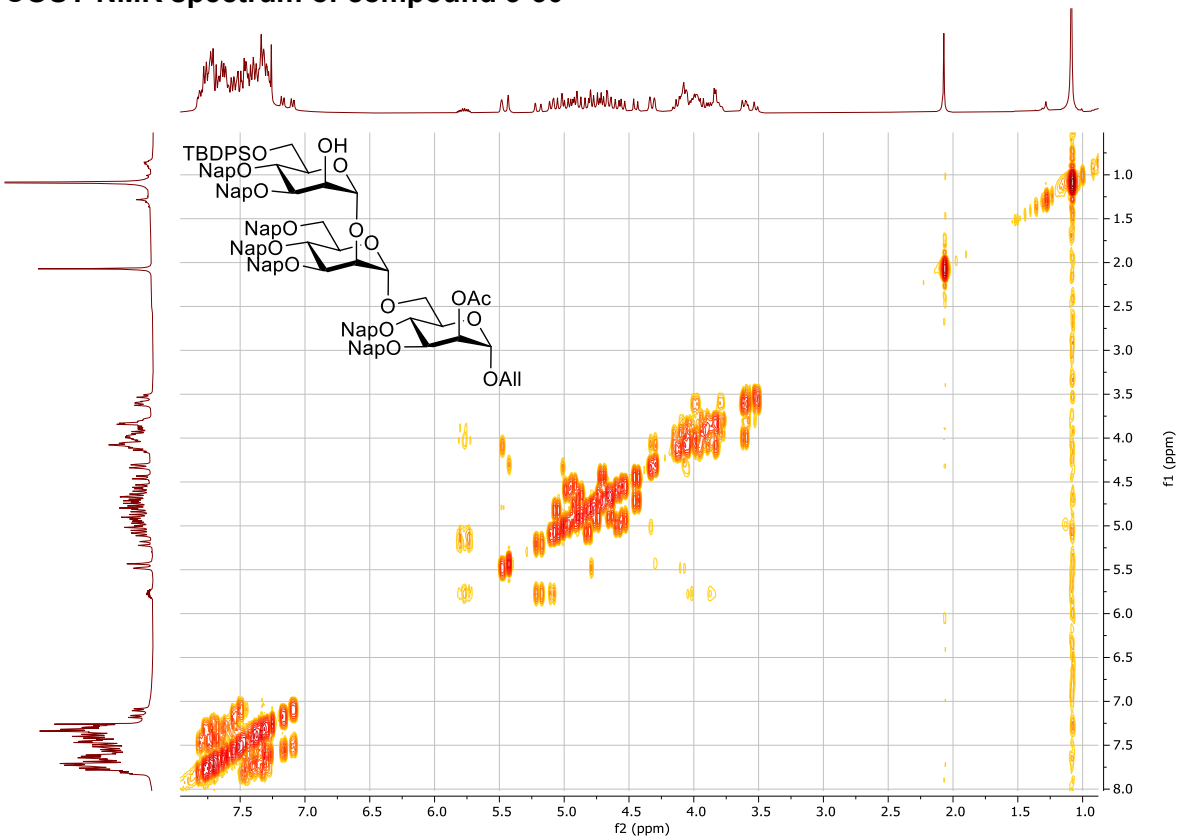

HSQC NMR spectrum of compound 3-30

^{1}H NMR spectrum of compound 3-35

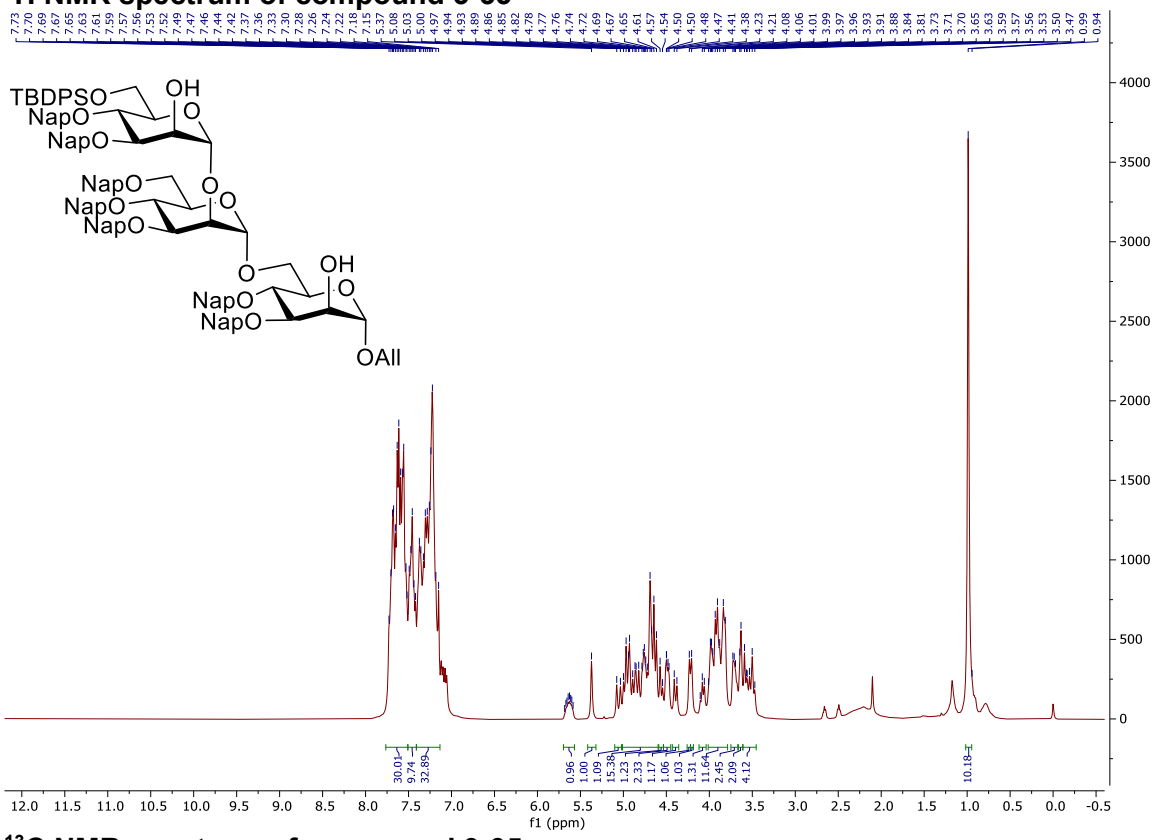

^{13}C NMR spectrum of compound 3-35

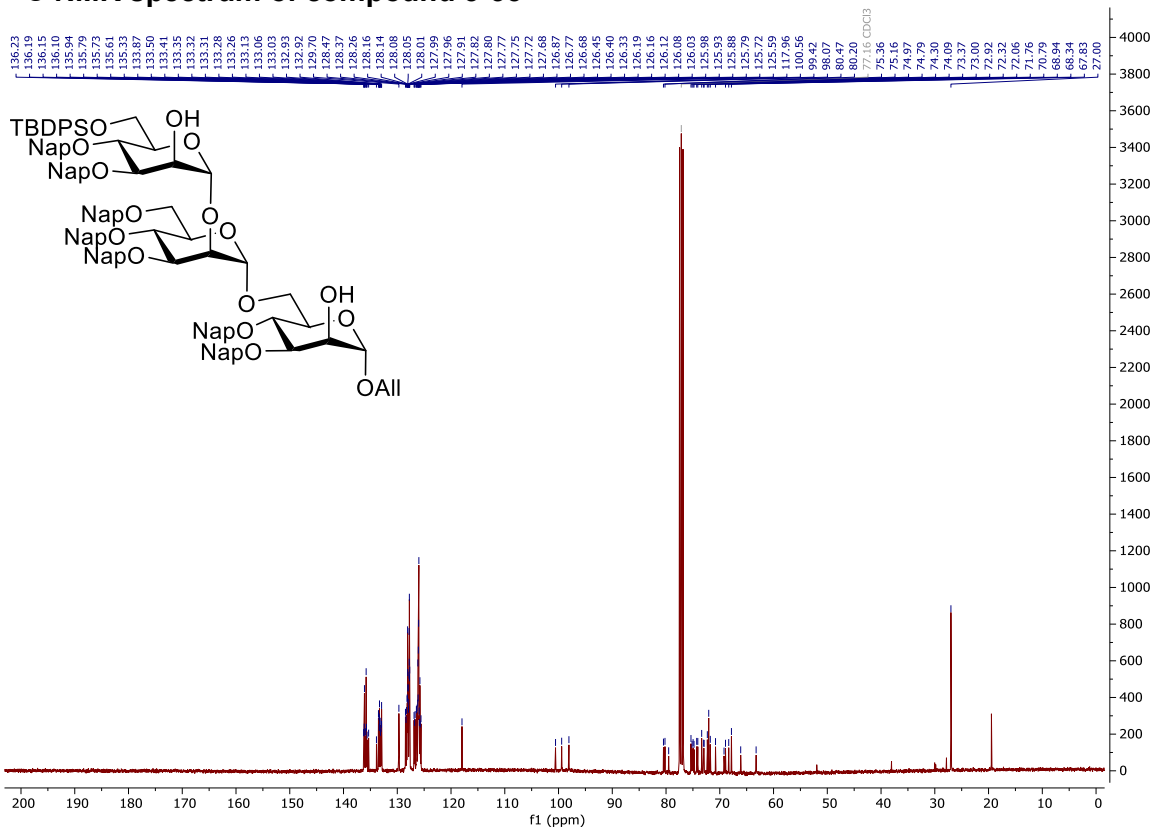

COSY NMR spectrum of compound 3-35

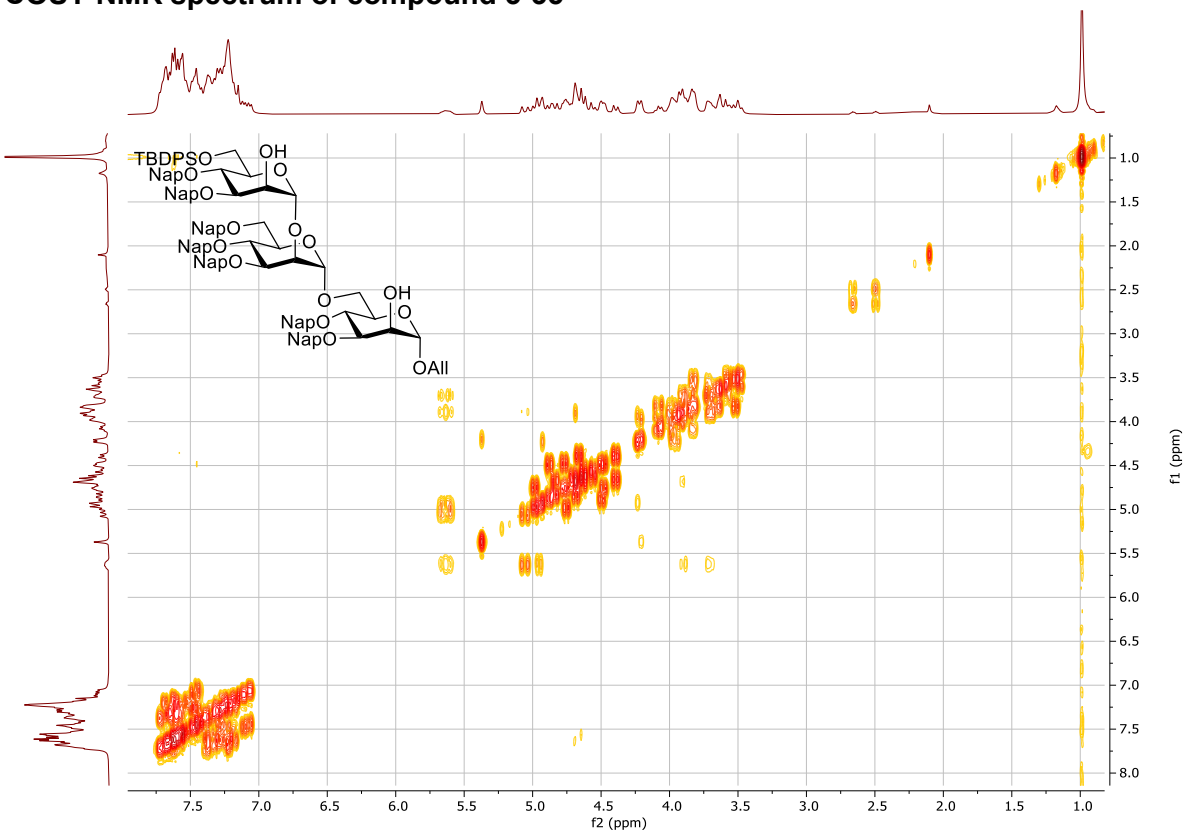

HSQC NMR spectrum of compound 3-35

^{1}H NMR spectrum of compound 3-36

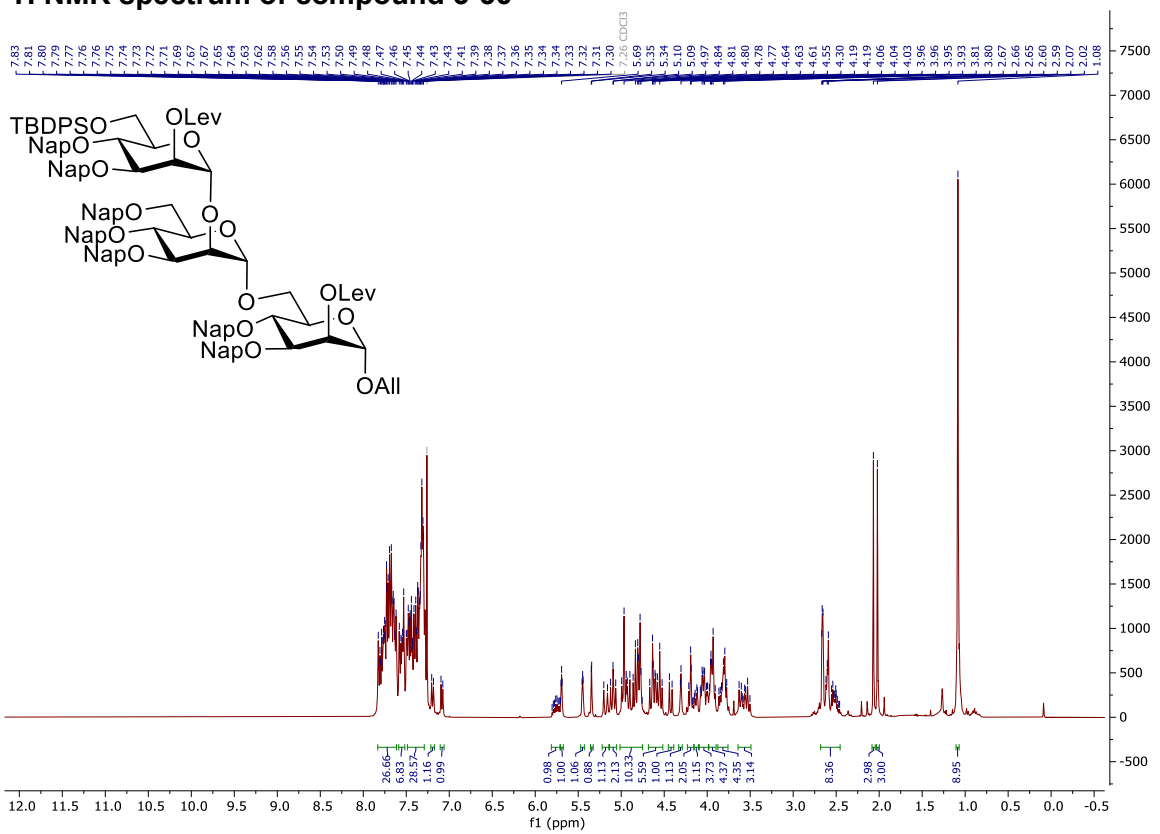

^{13}C NMR spectrum of compound 3-36

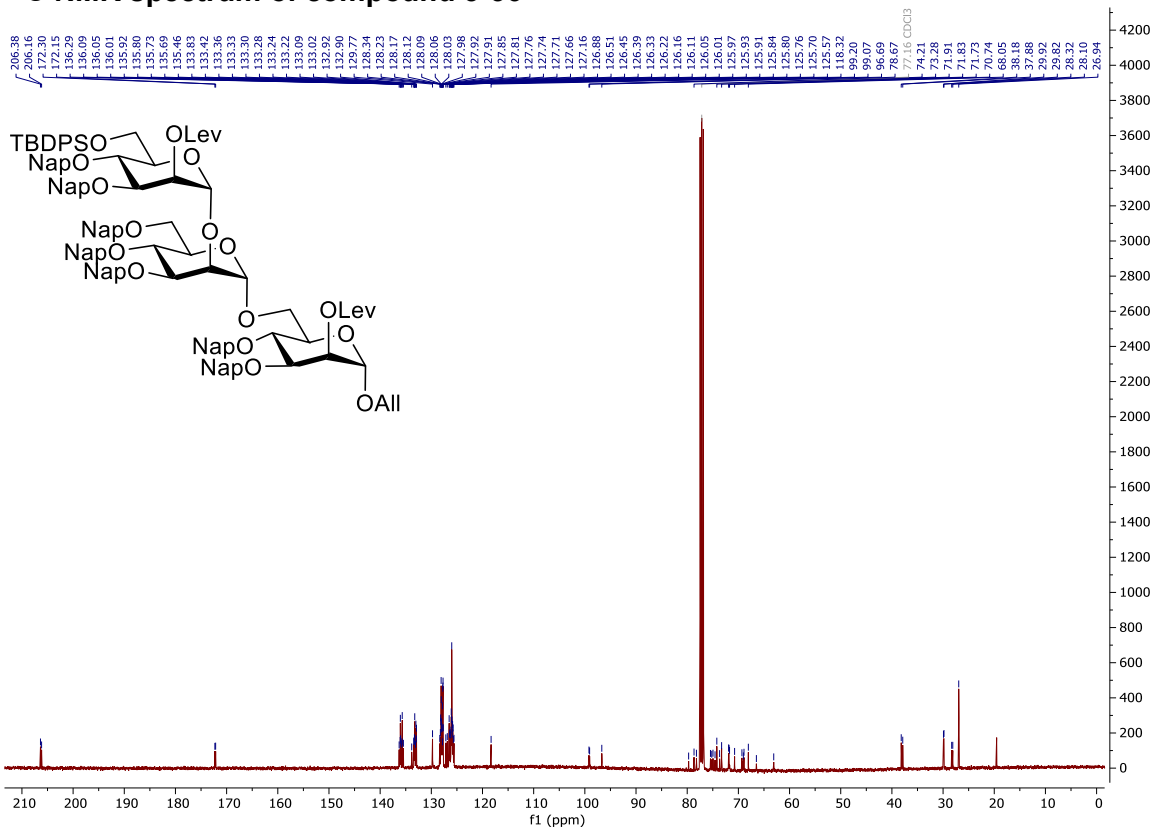

COSY NMR spectrum of compound 3-36

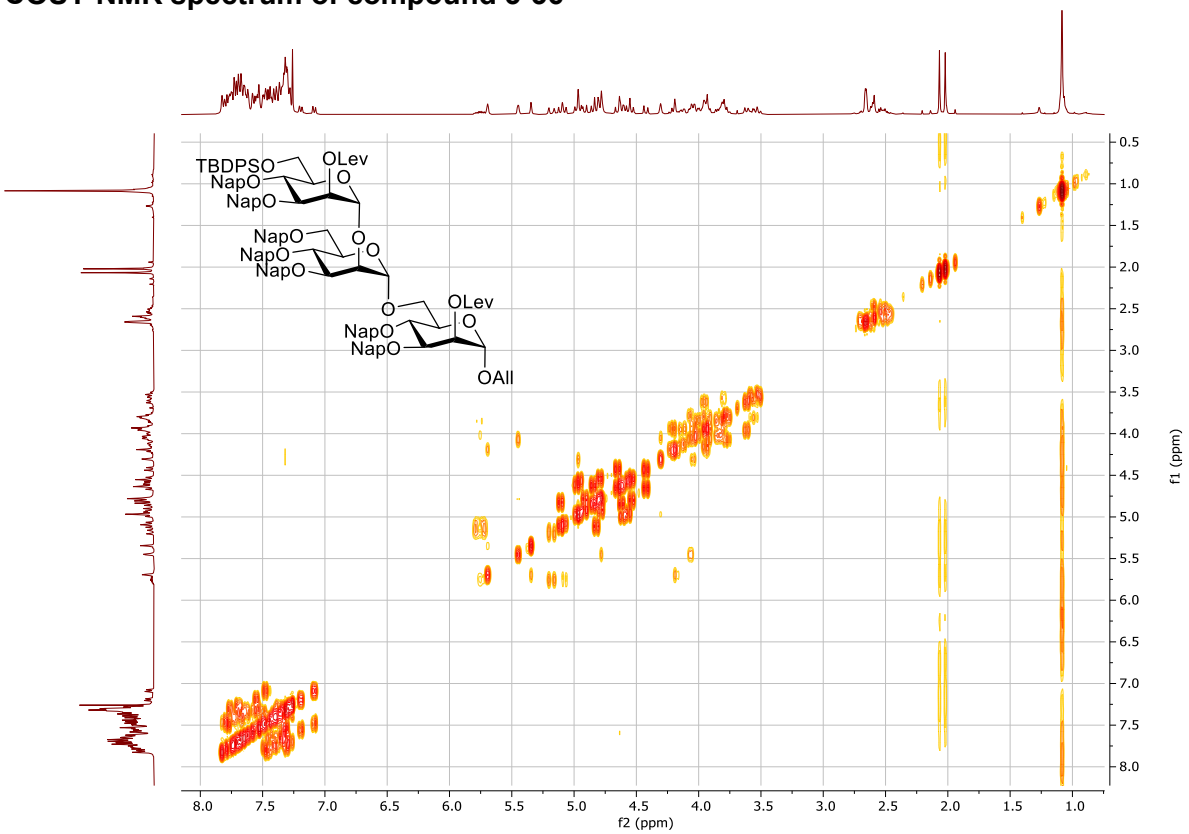

HSQC NMR spectrum of compound 3-36

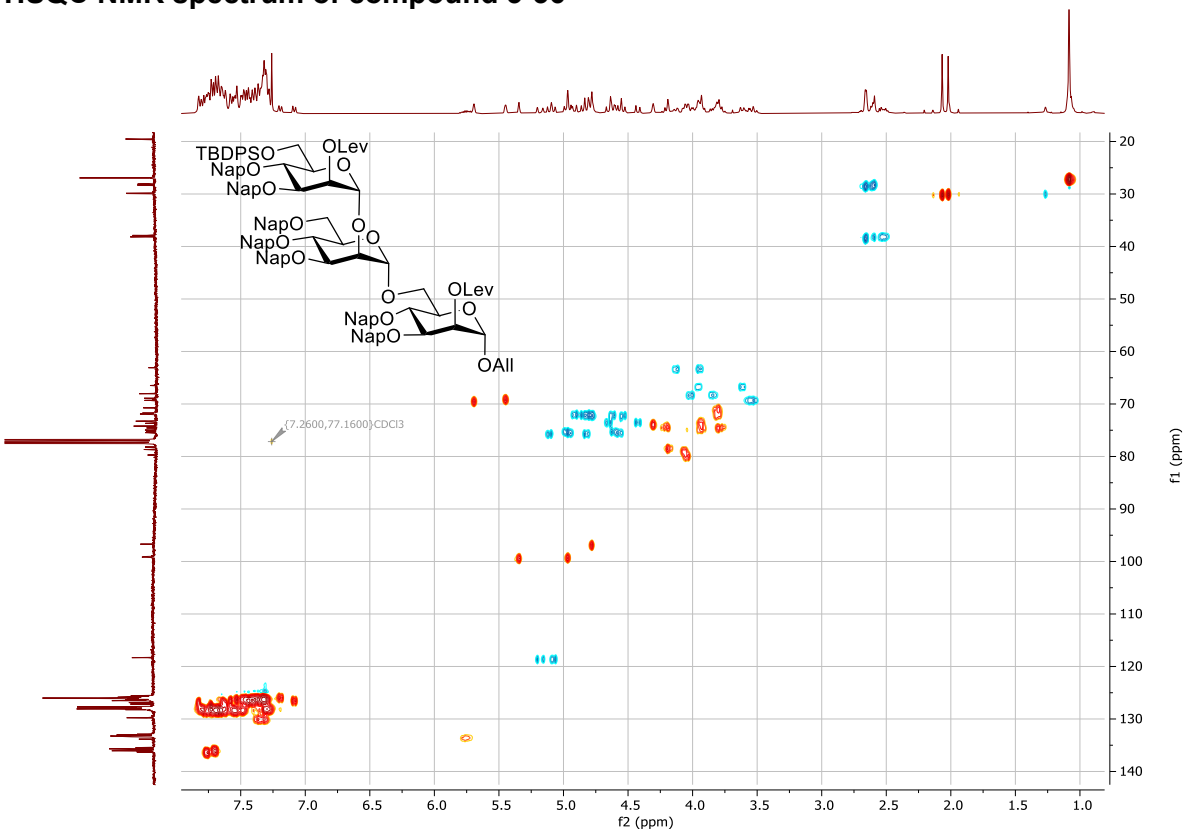

^{1}H NMR spectrum of compound 3-37

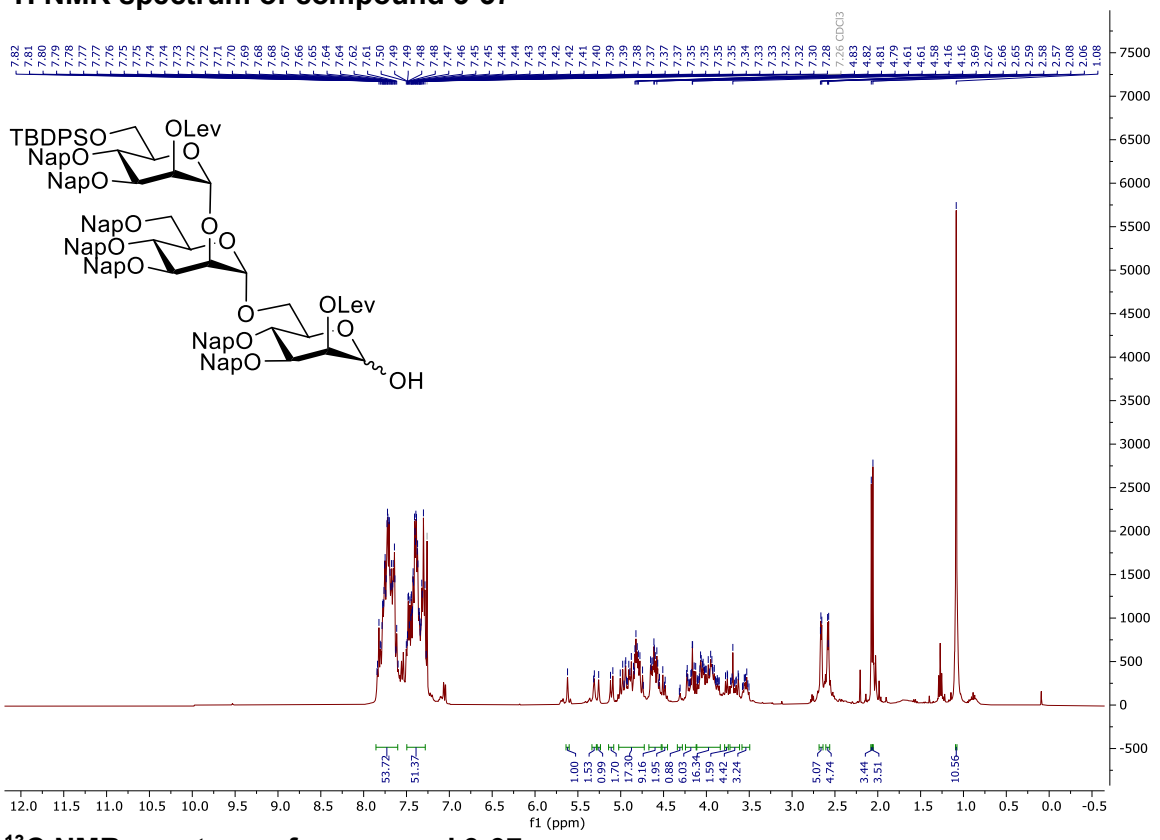

^{13}C NMR spectrum of compound 3-37

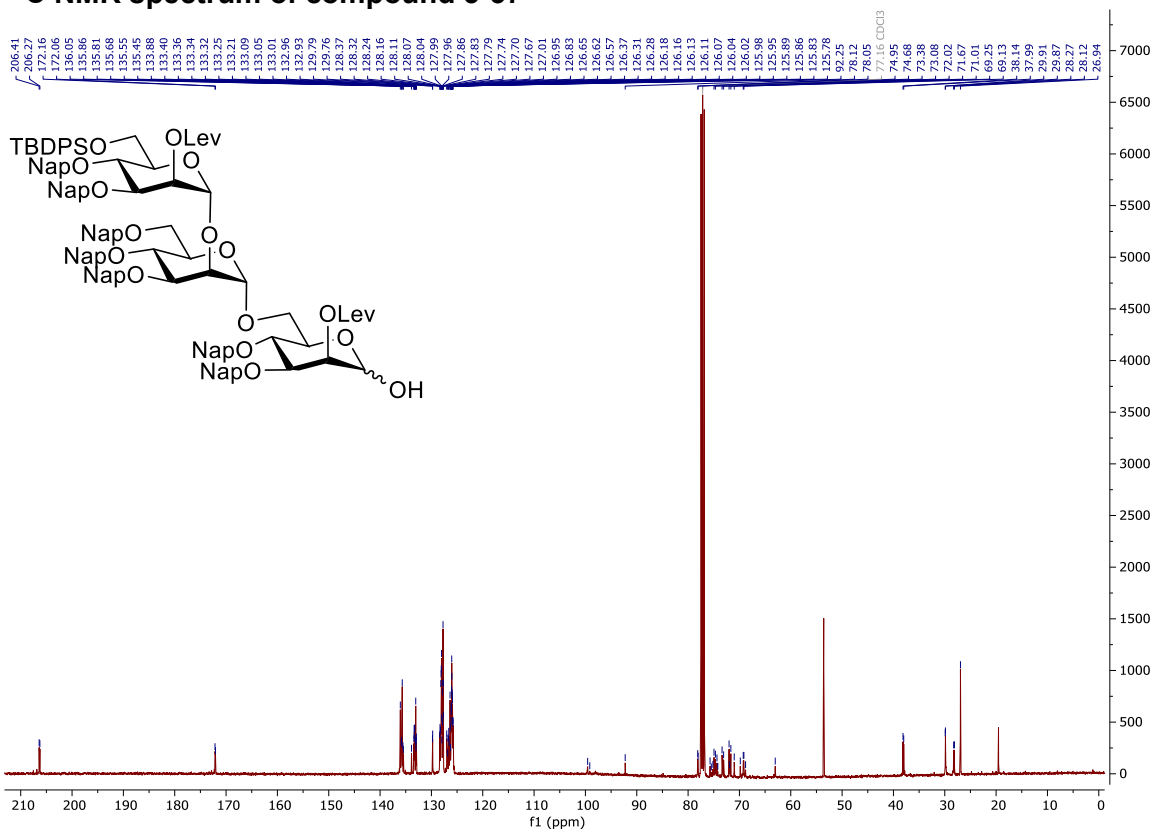

COSY NMR spectrum of compound 3-37

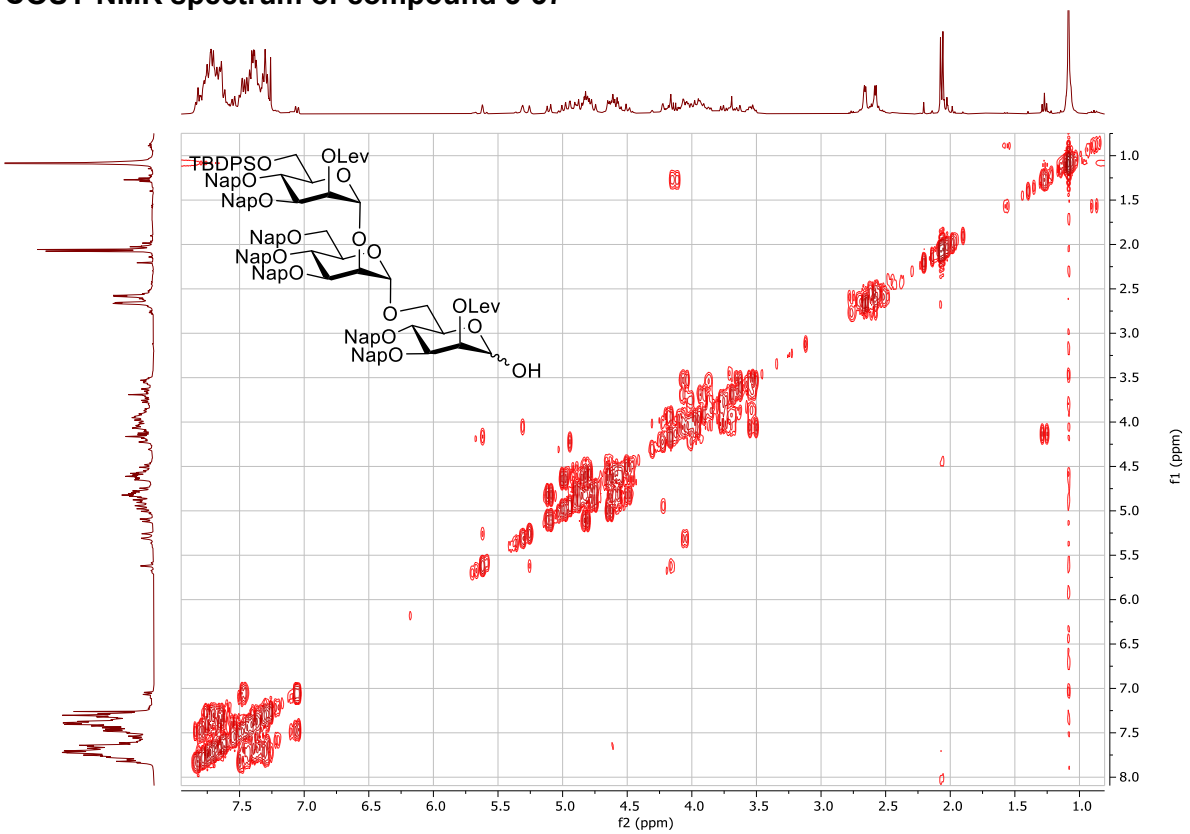

HSQC NMR spectrum of compound 3-37

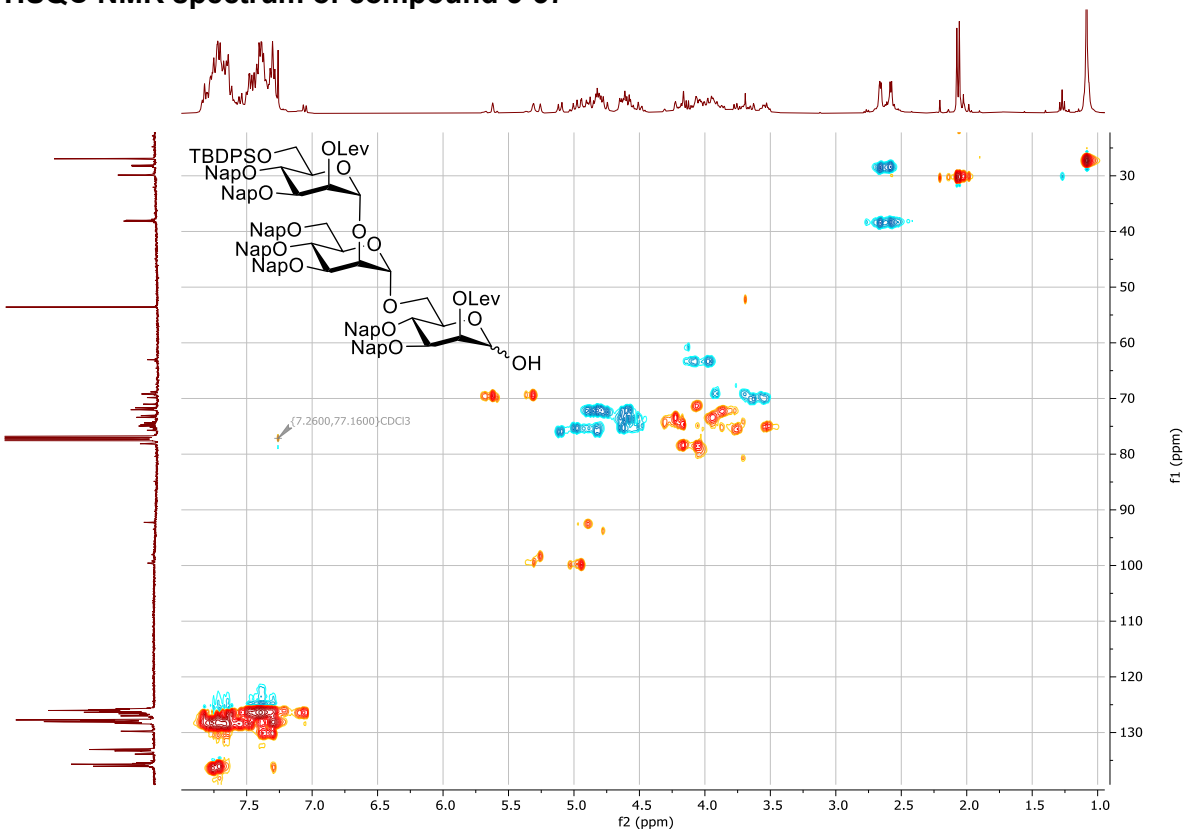

^{1}H NMR spectrum of compound 3-38

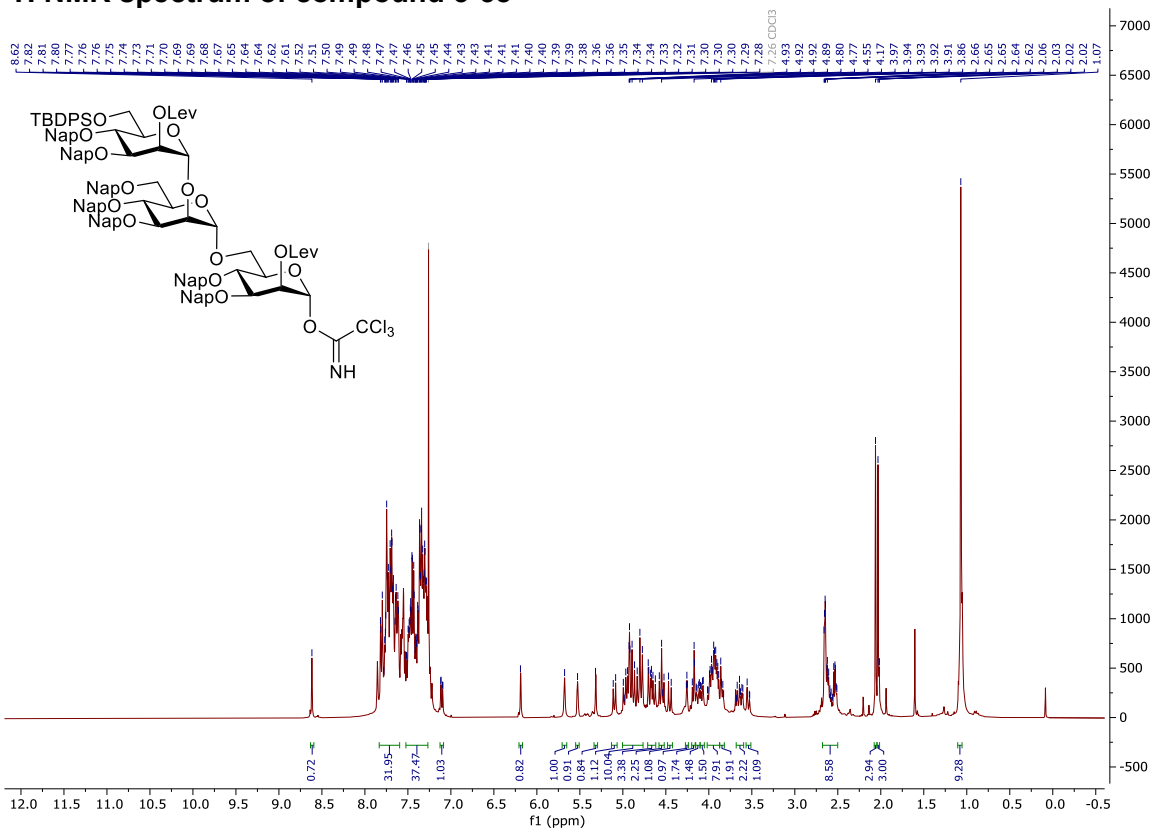

^{13}C NMR spectrum of compound 3-38

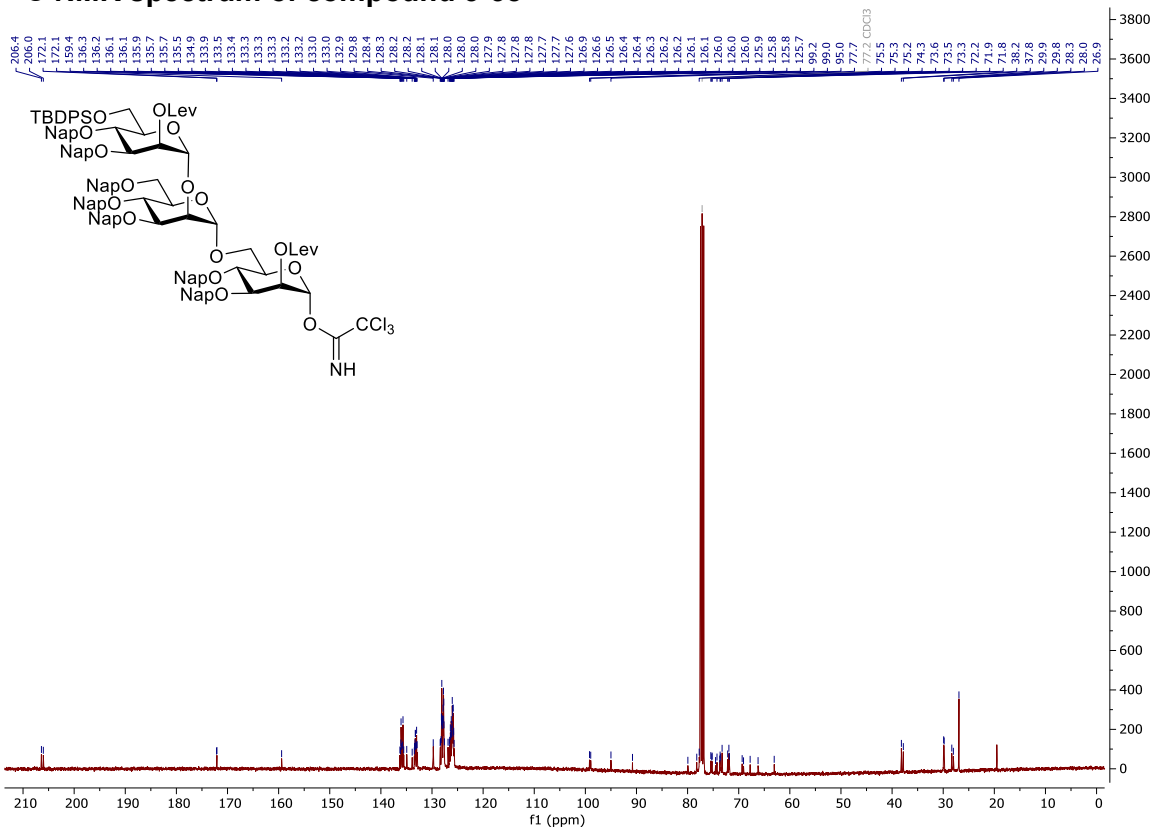

COSY NMR spectrum of compound 3-38

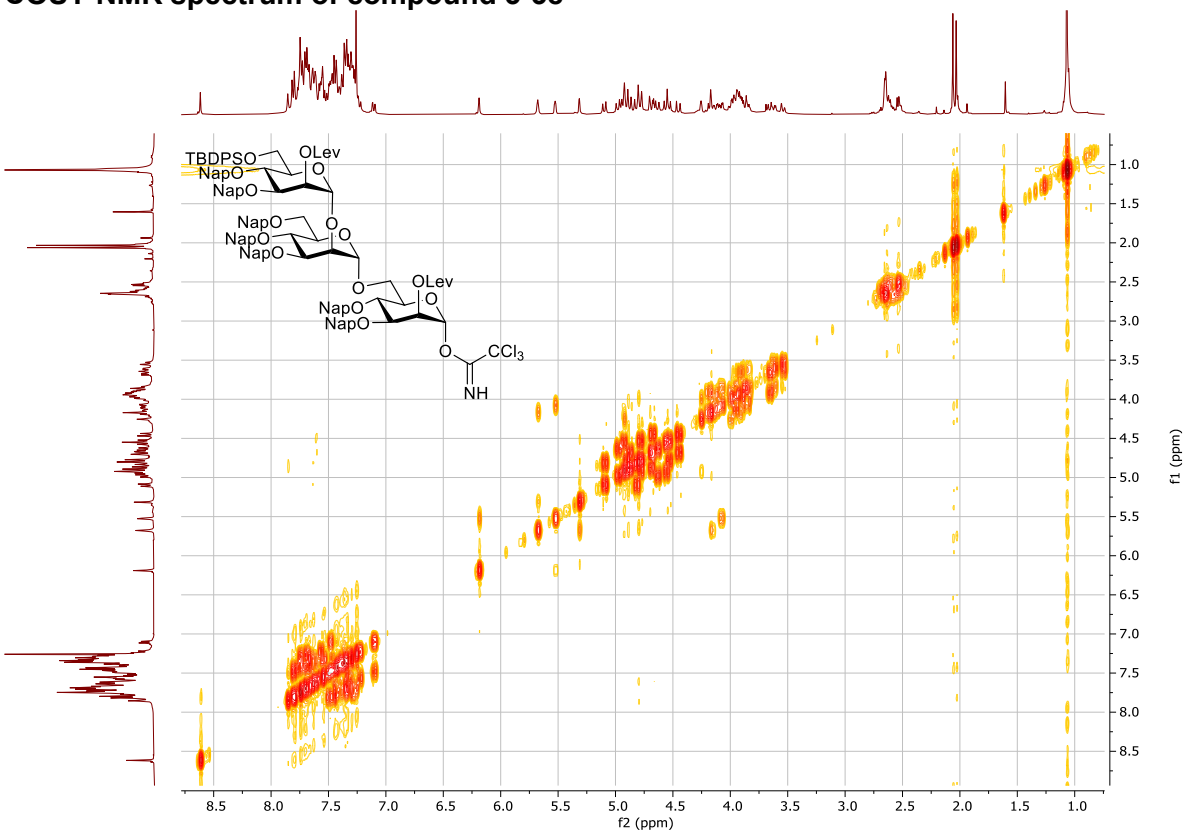

HSQC NMR spectrum of compound 3-38

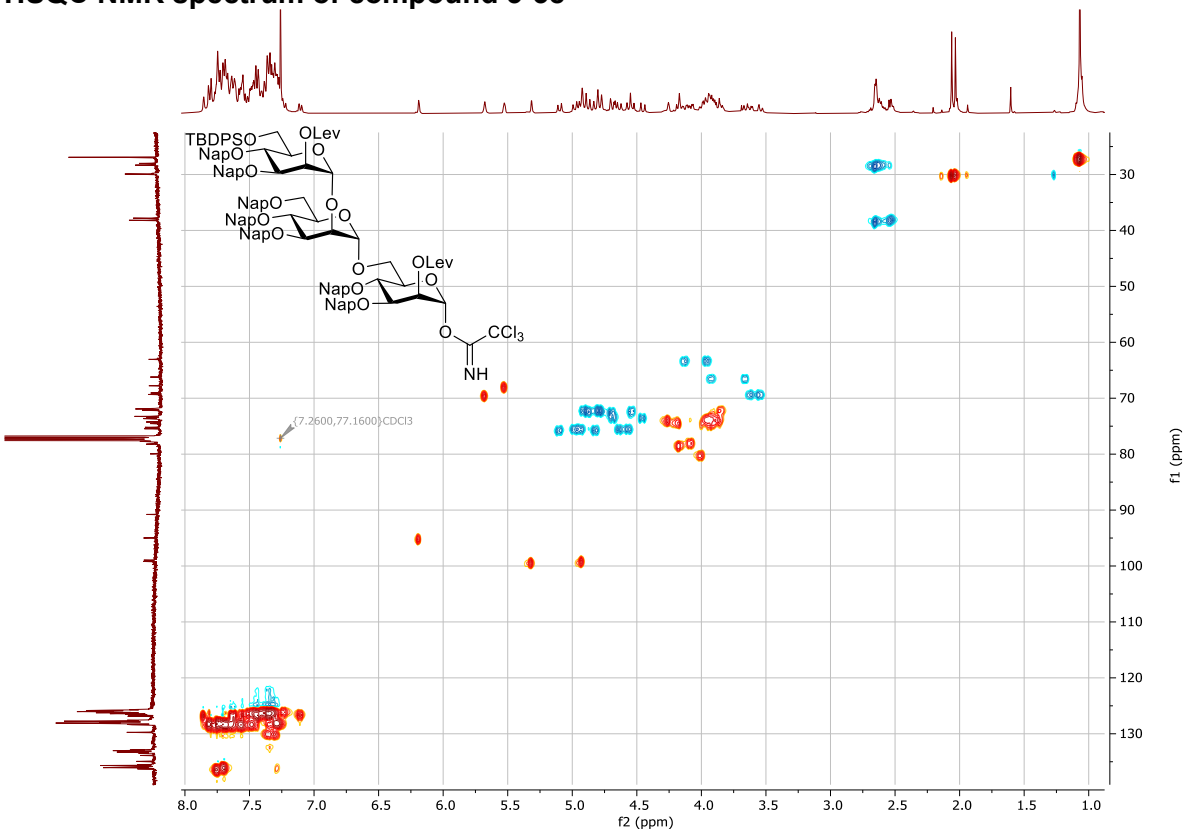

^{1}H NMR spectrum of compound 3-39

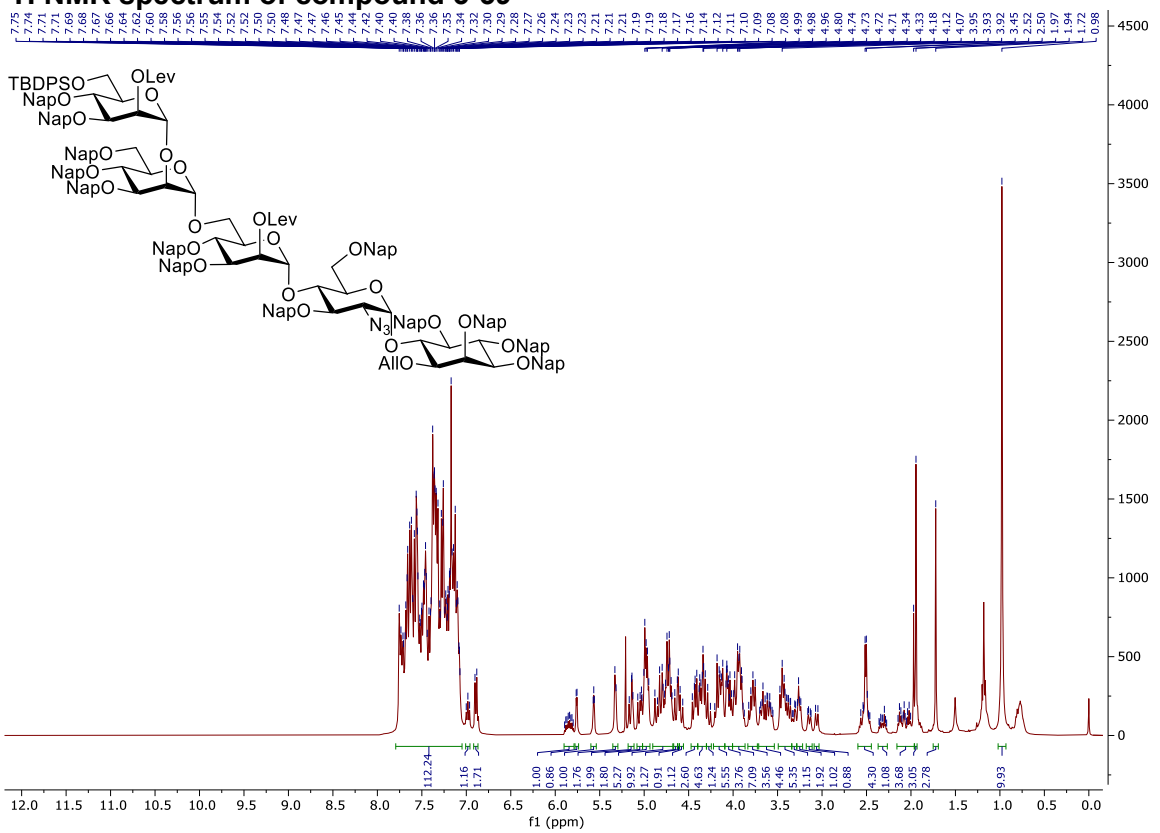

^{13}C NMR spectrum of compound 3-39

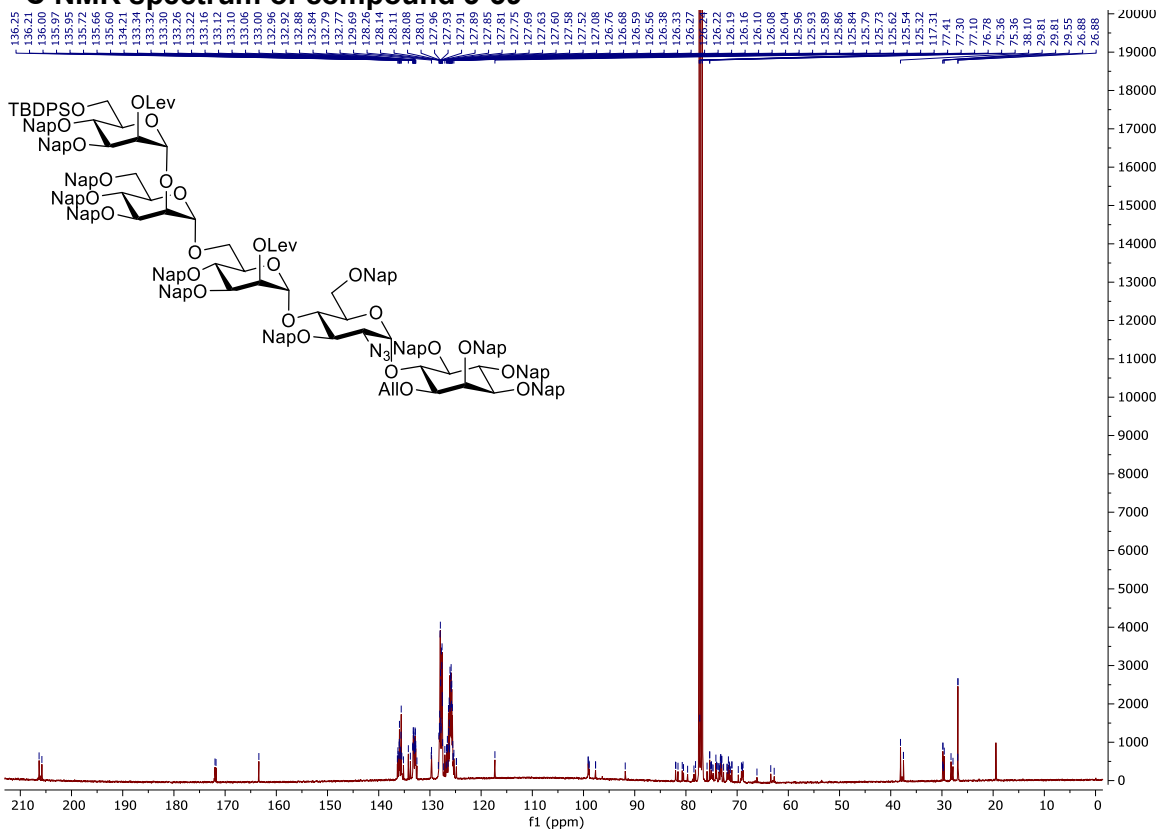

COSY-NMR spectrum of compound 3-39

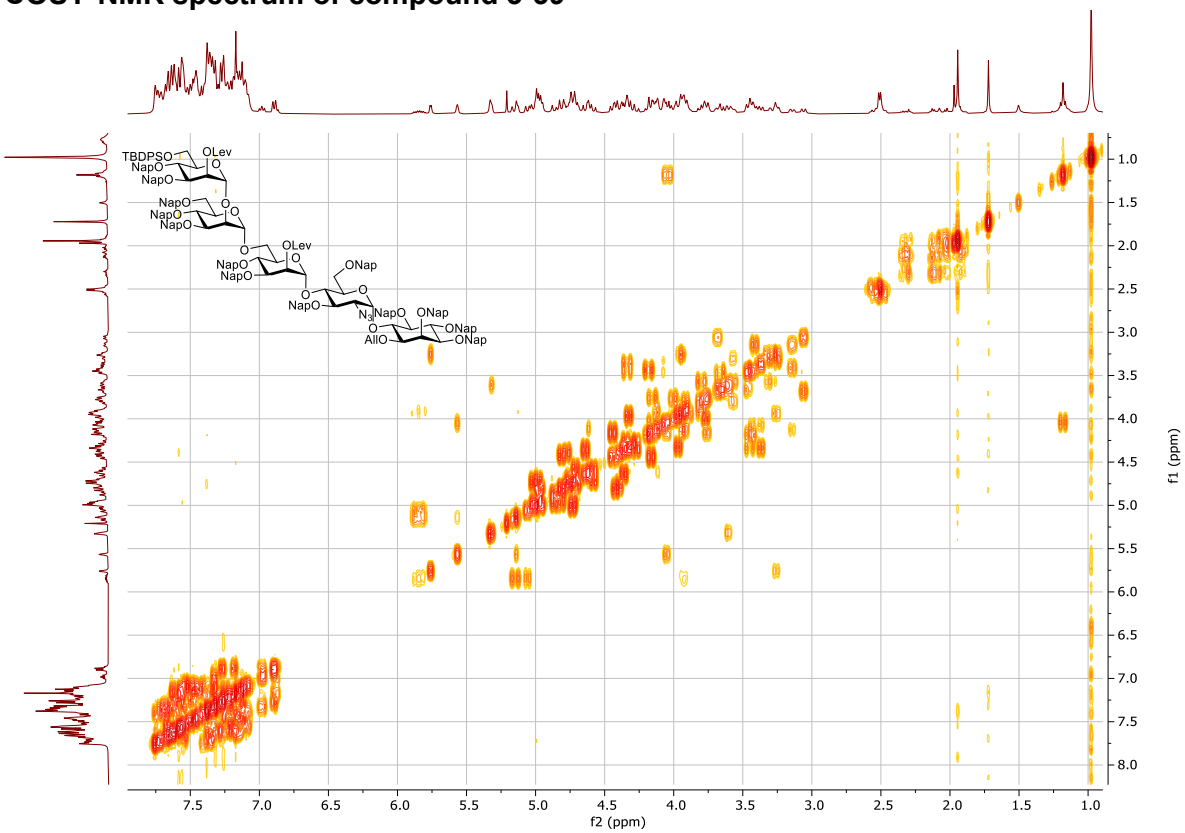

HSQC-NMR spectrum of compound 3-39

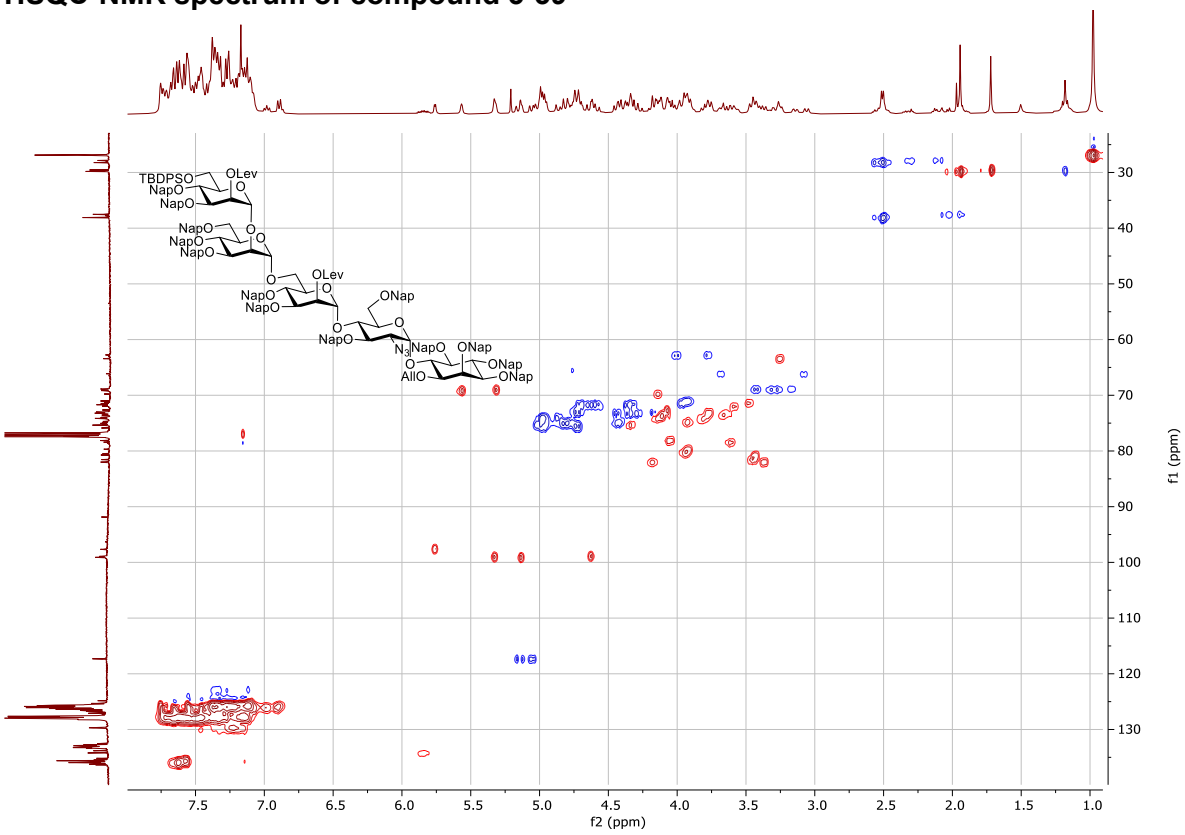

^{1}H NMR spectrum of compound 3-40

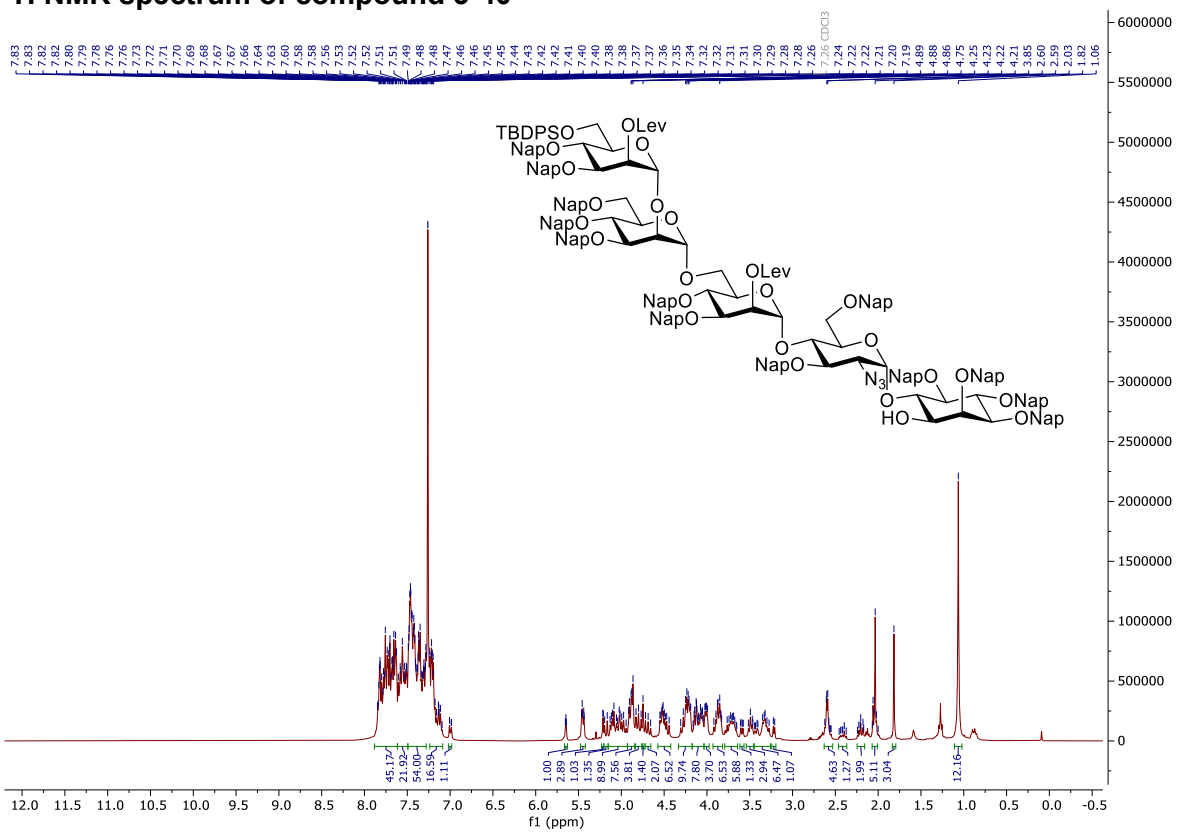

^{13}C NMR spectrum of compound 3-40

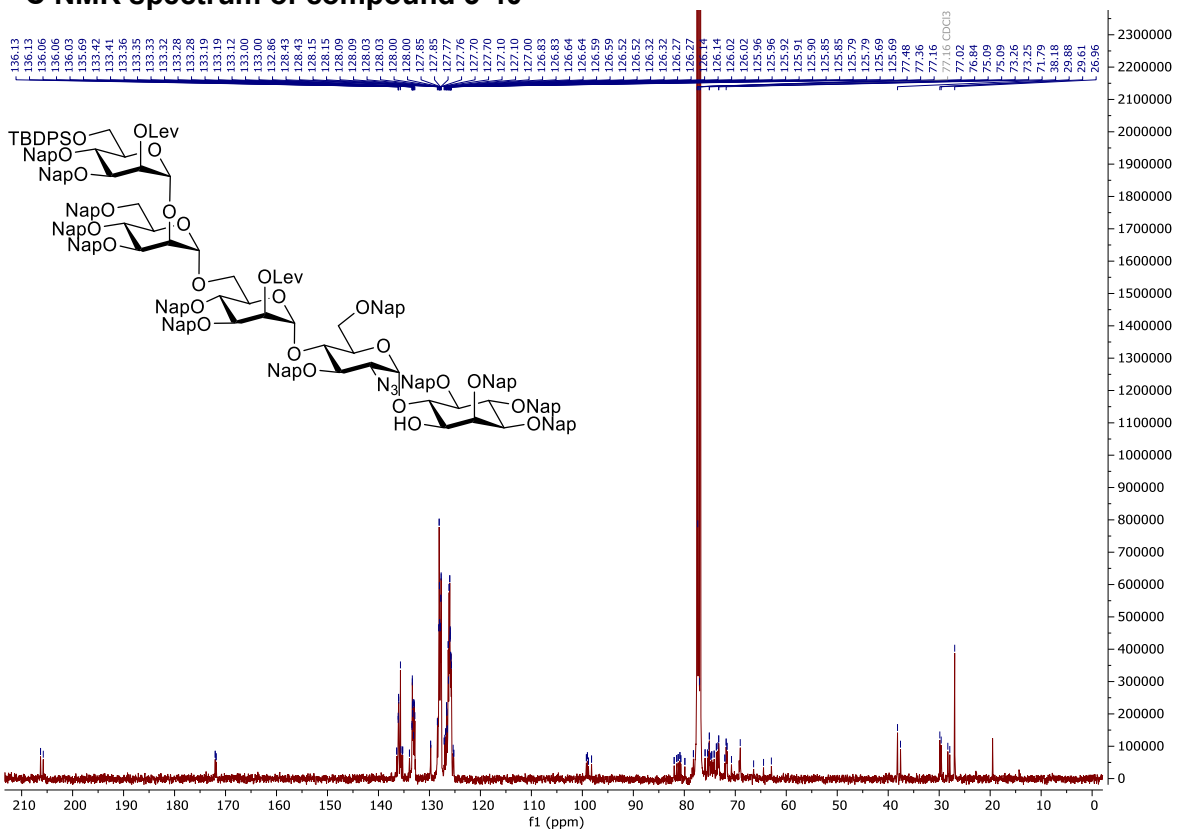

COSY-NMR spectrum of compound 3-40

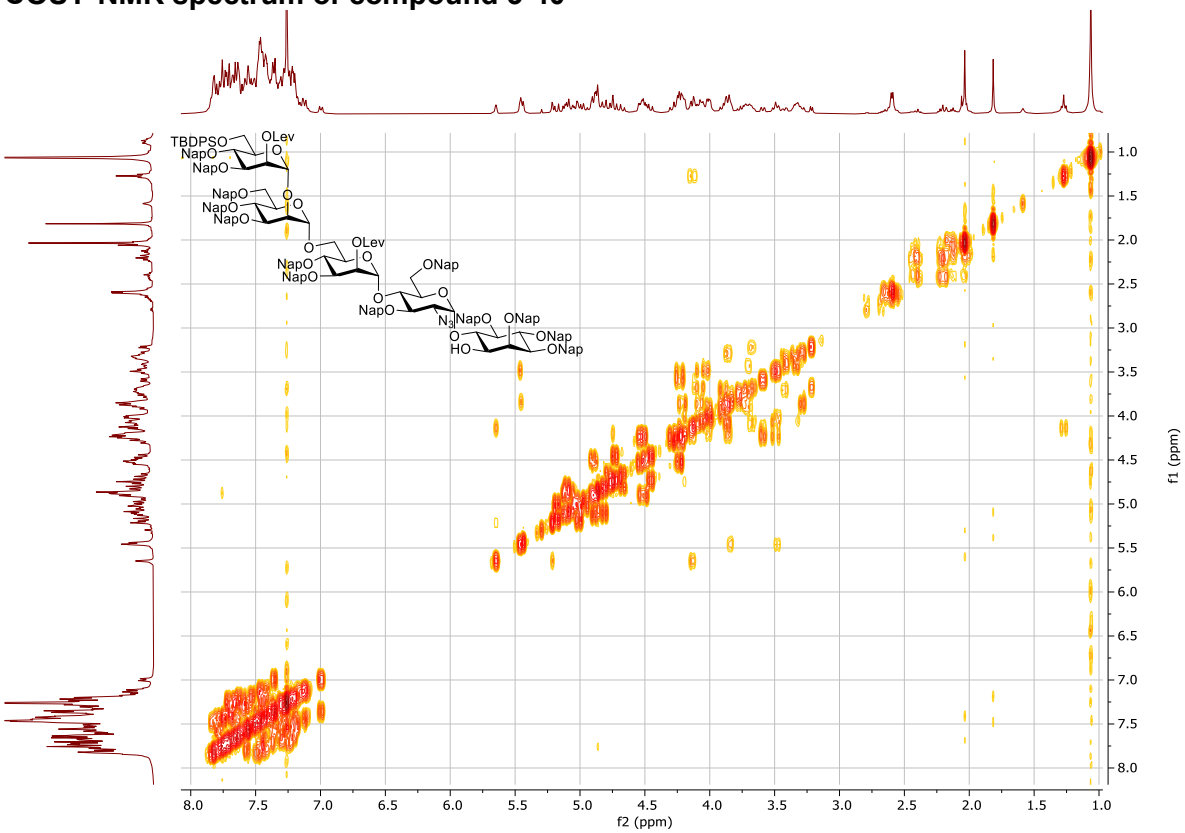

HSQC-NMR spectrum of compound 3-40

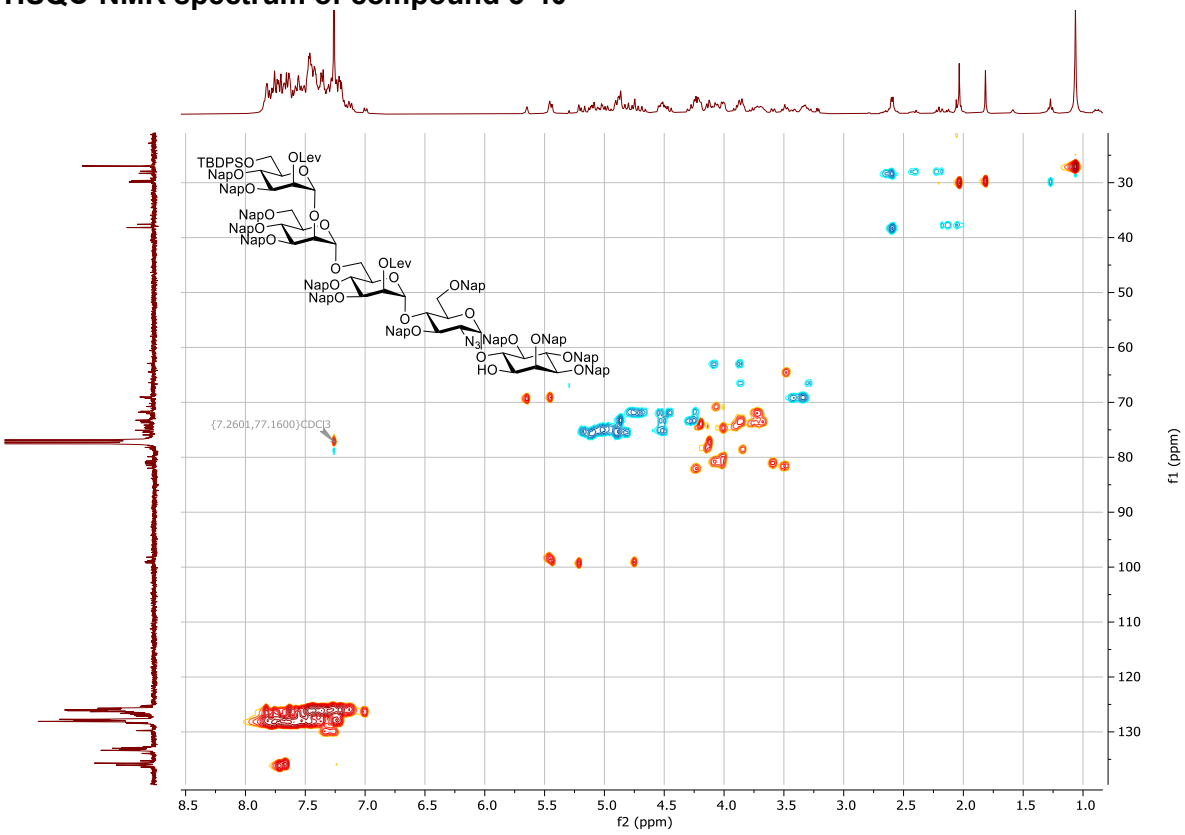

^{1}H NMR spectrum of compound 3-42

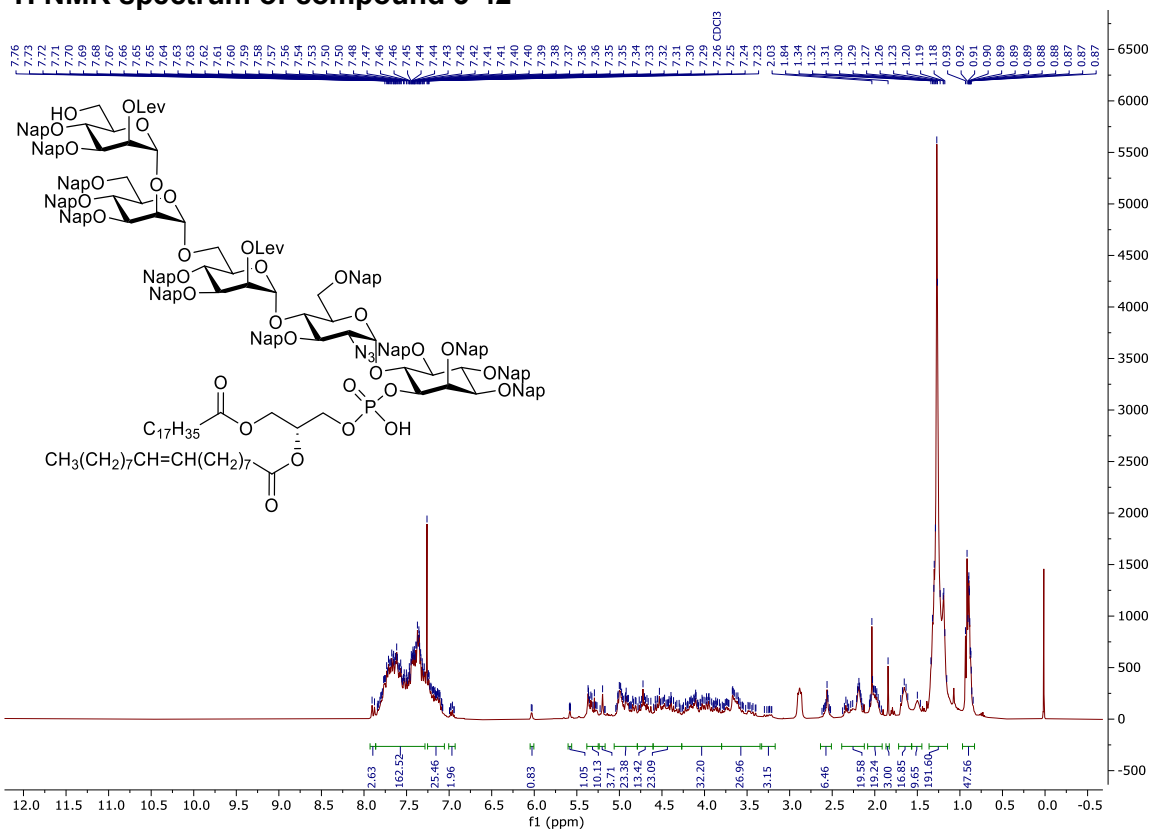

^{13}C NMR spectrum of compound 3-42

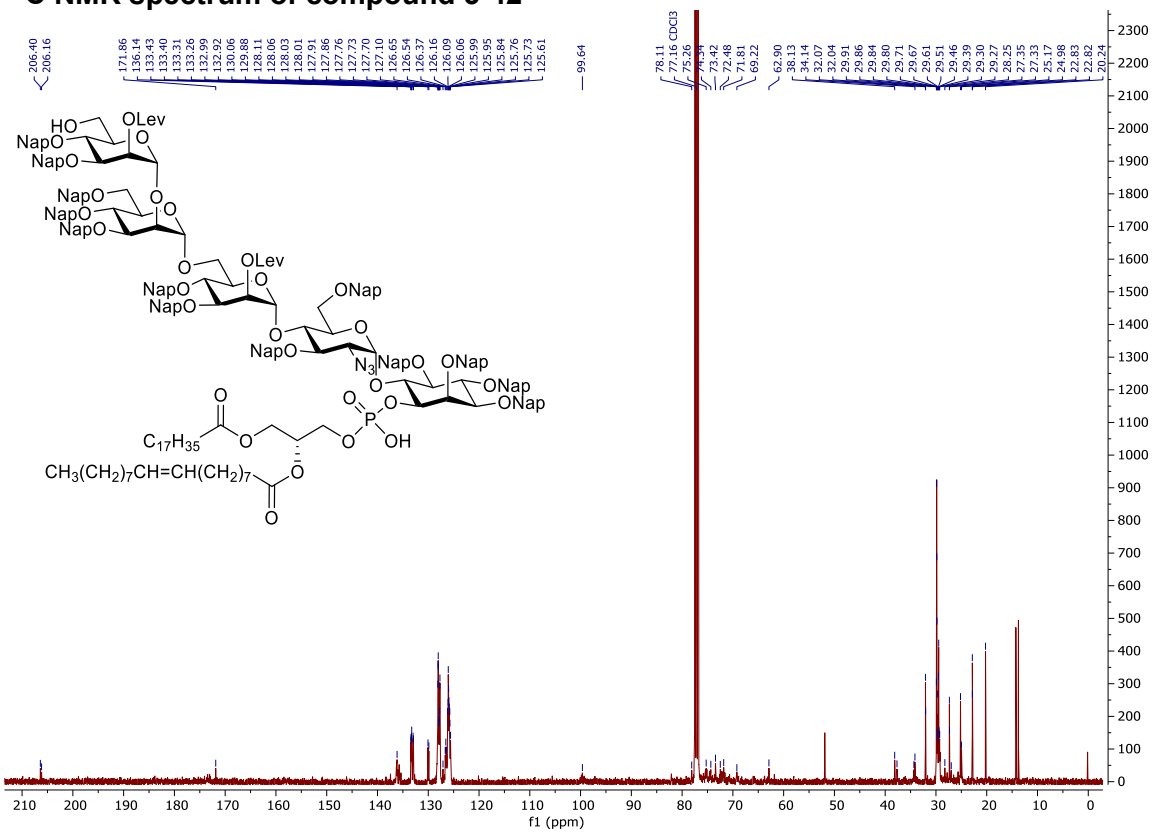

COSY-NMR spectrum of compound 3-42

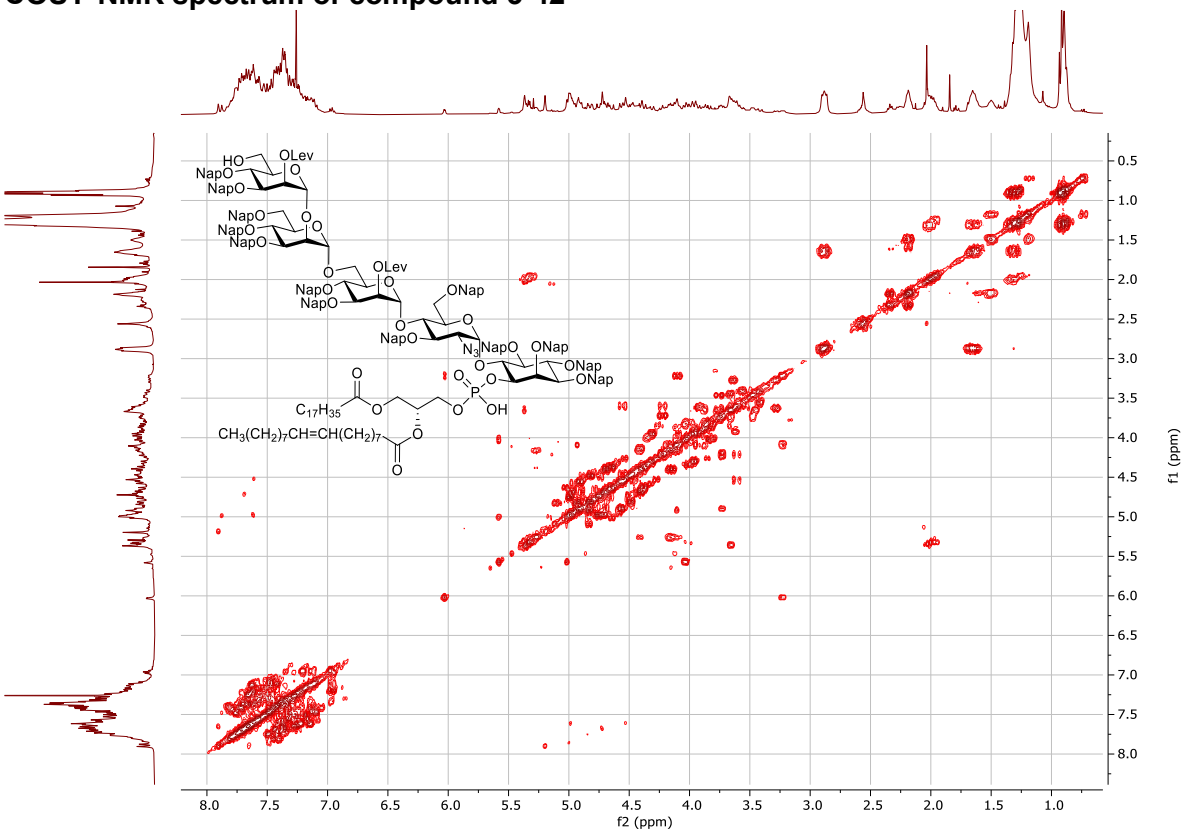

HSQC-NMR spectrum of compound 3-42

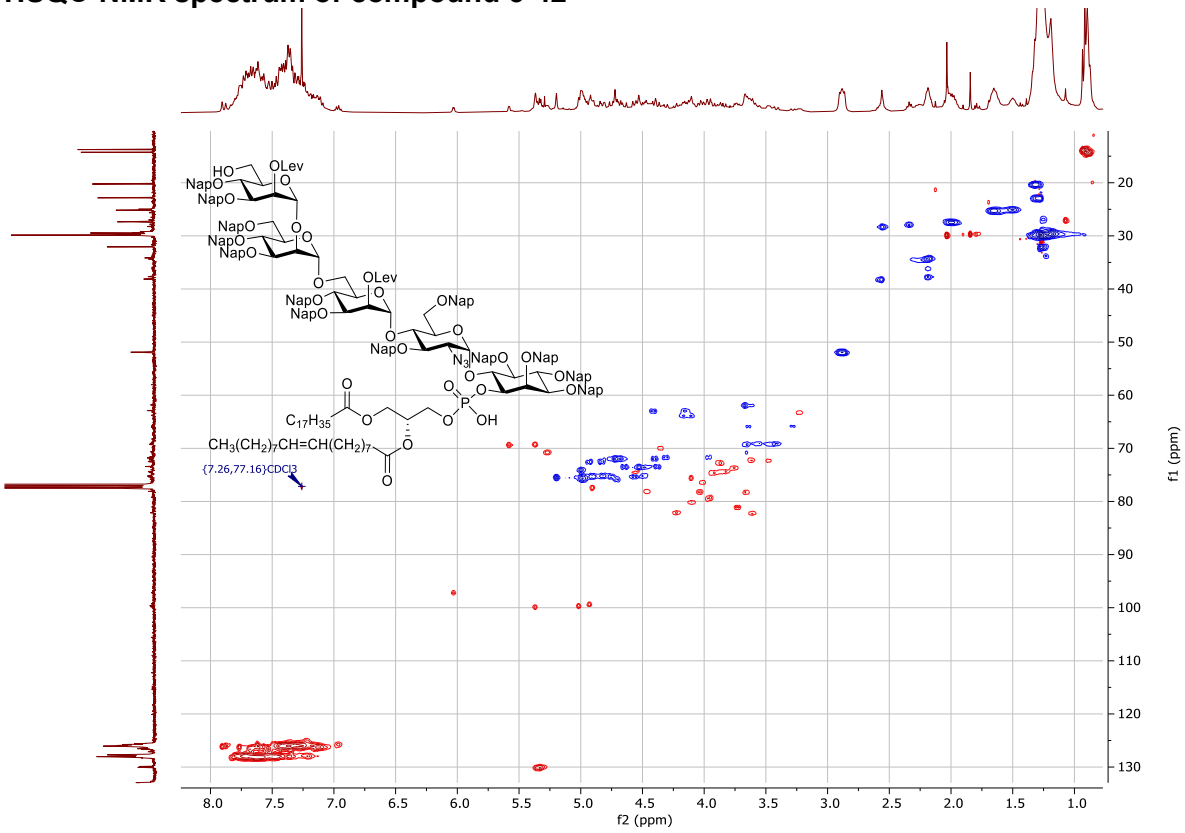

^{31}P NMR spectrum of compound 3-42

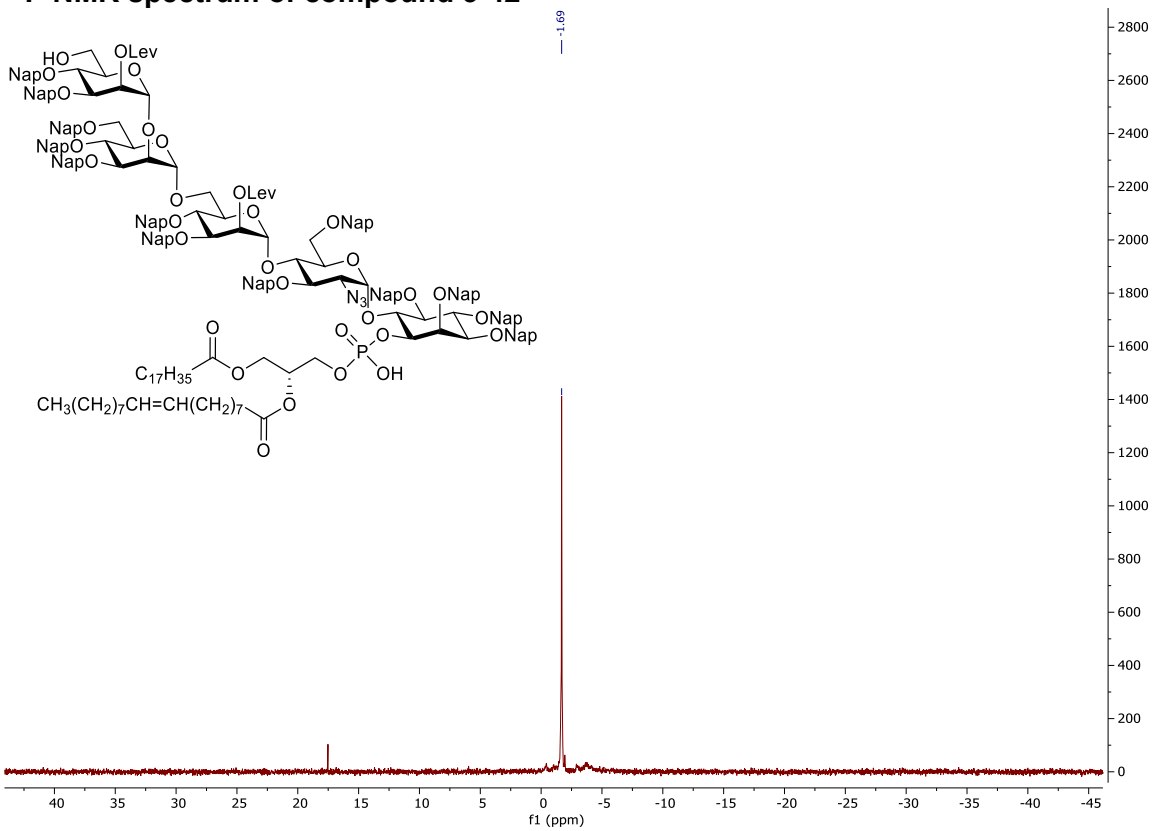

^{1}H NMR spectrum of compound 3-44

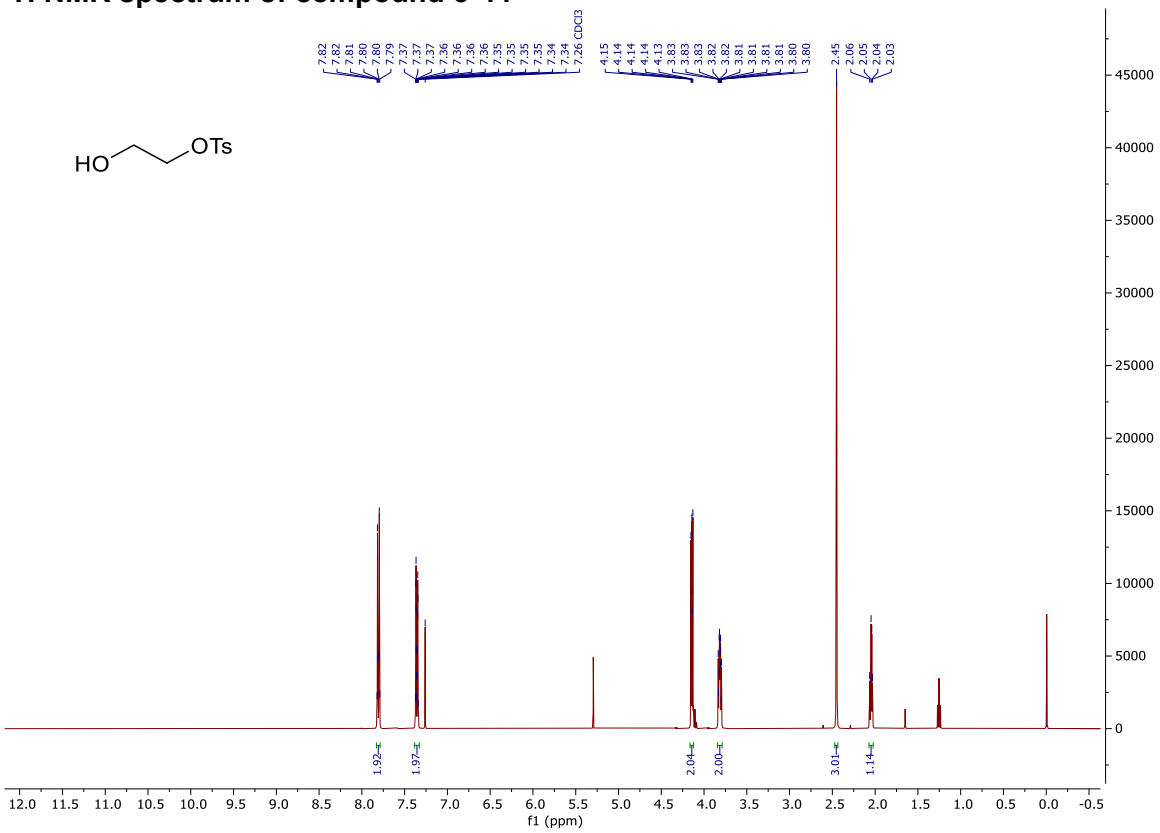

^{13}C NMR spectrum of compound 3-44

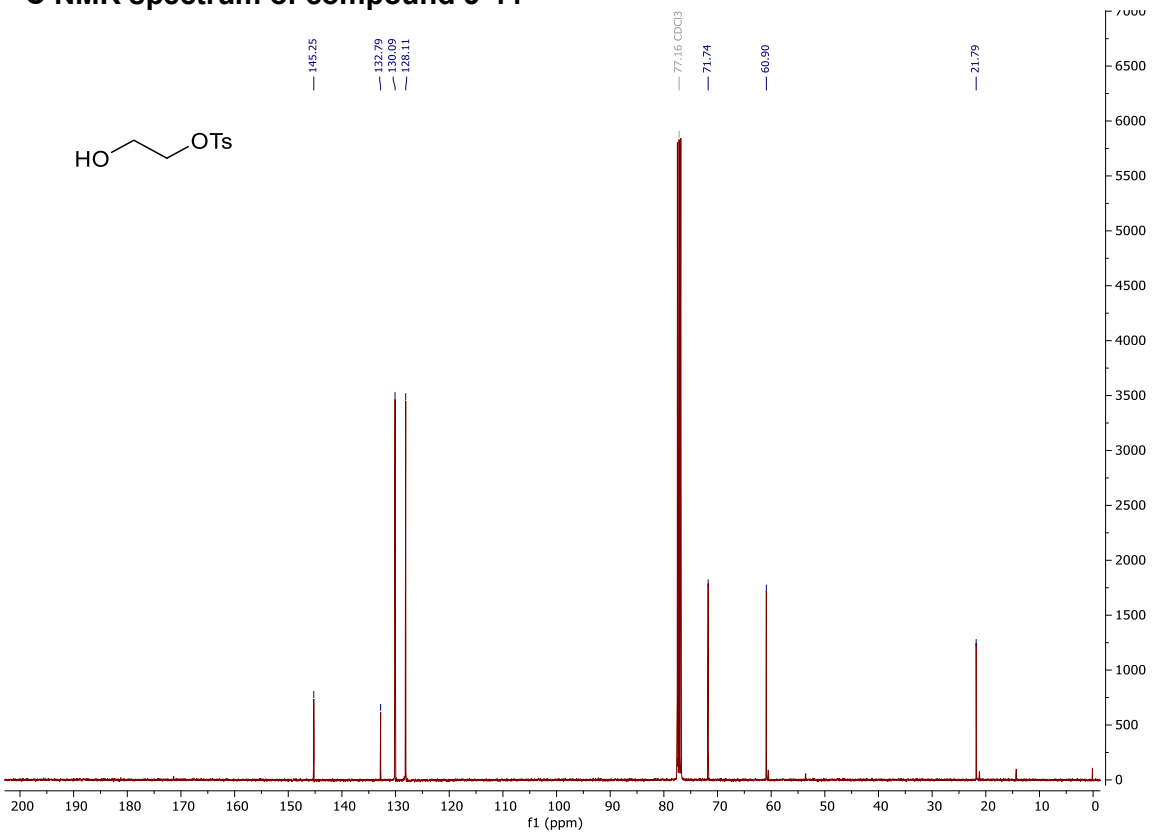

COSY NMR spectrum of compound 3-44

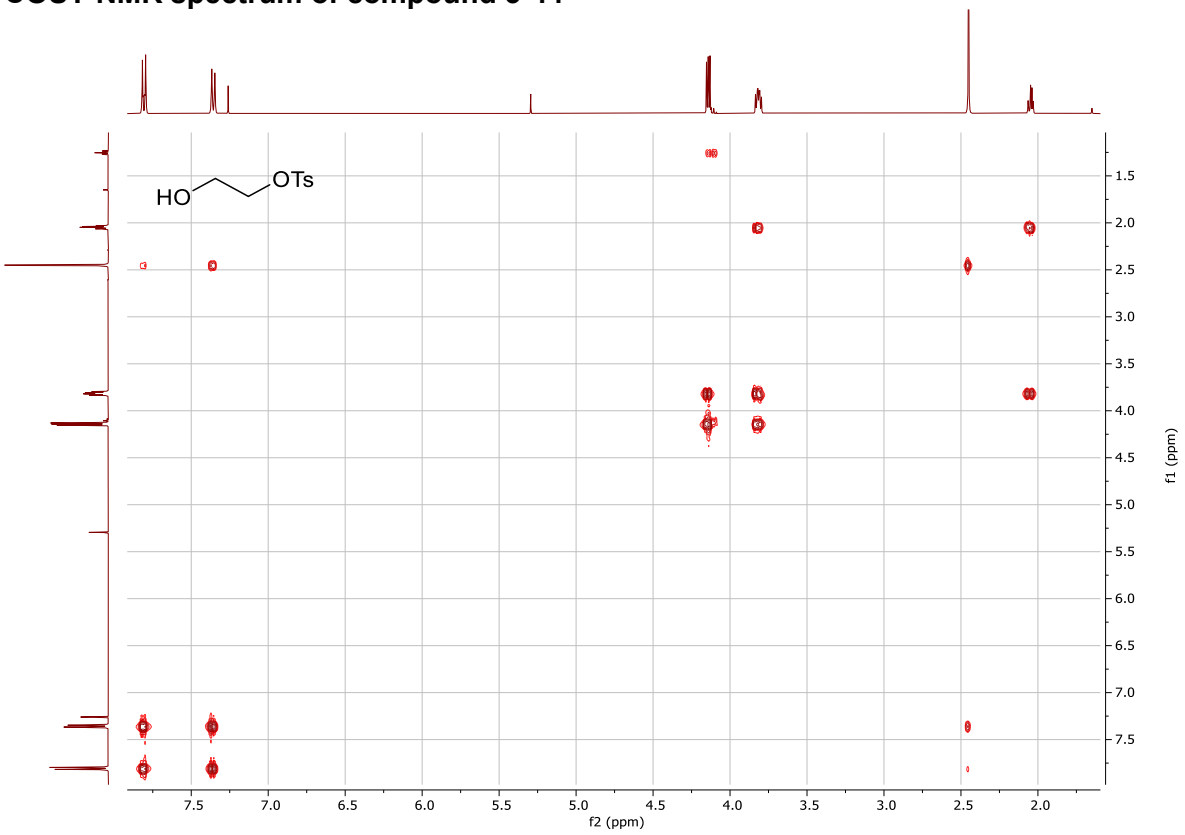

HSQC NMR spectrum of compound 3-44

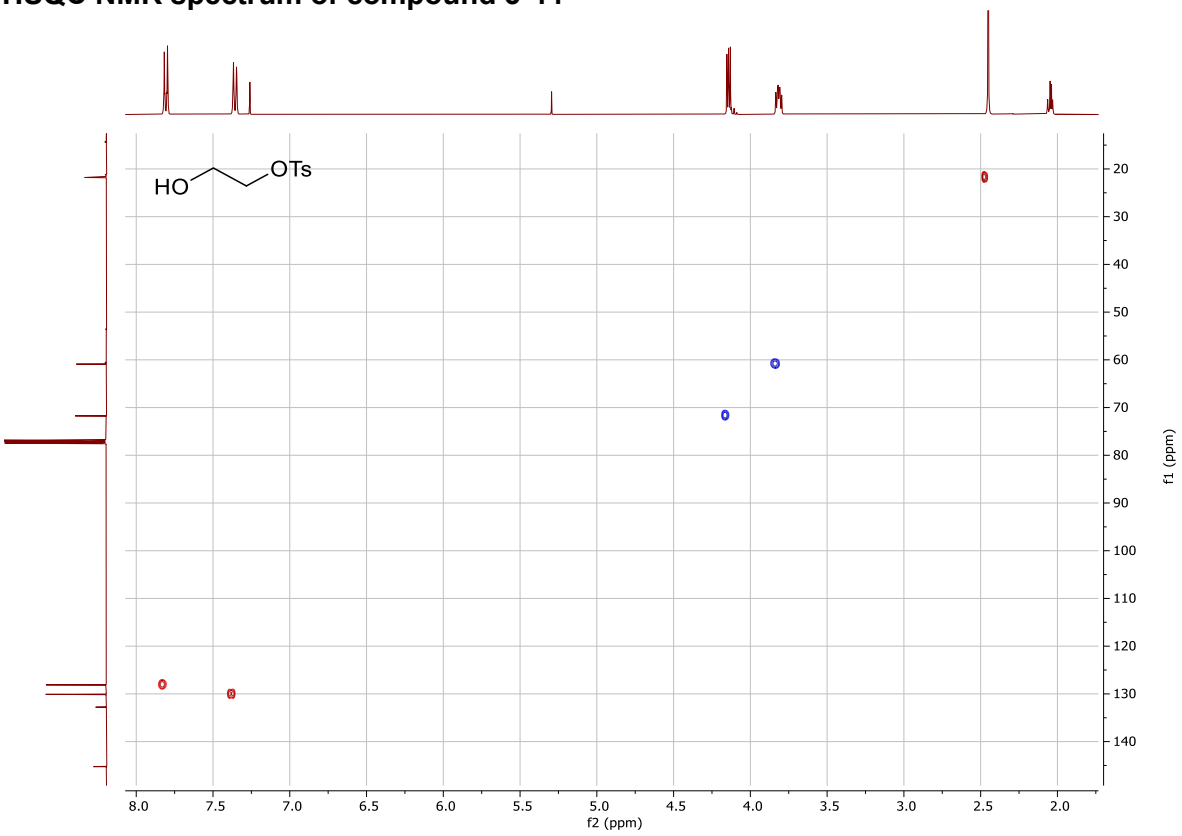

^{1}H NMR spectrum of compound 3-45

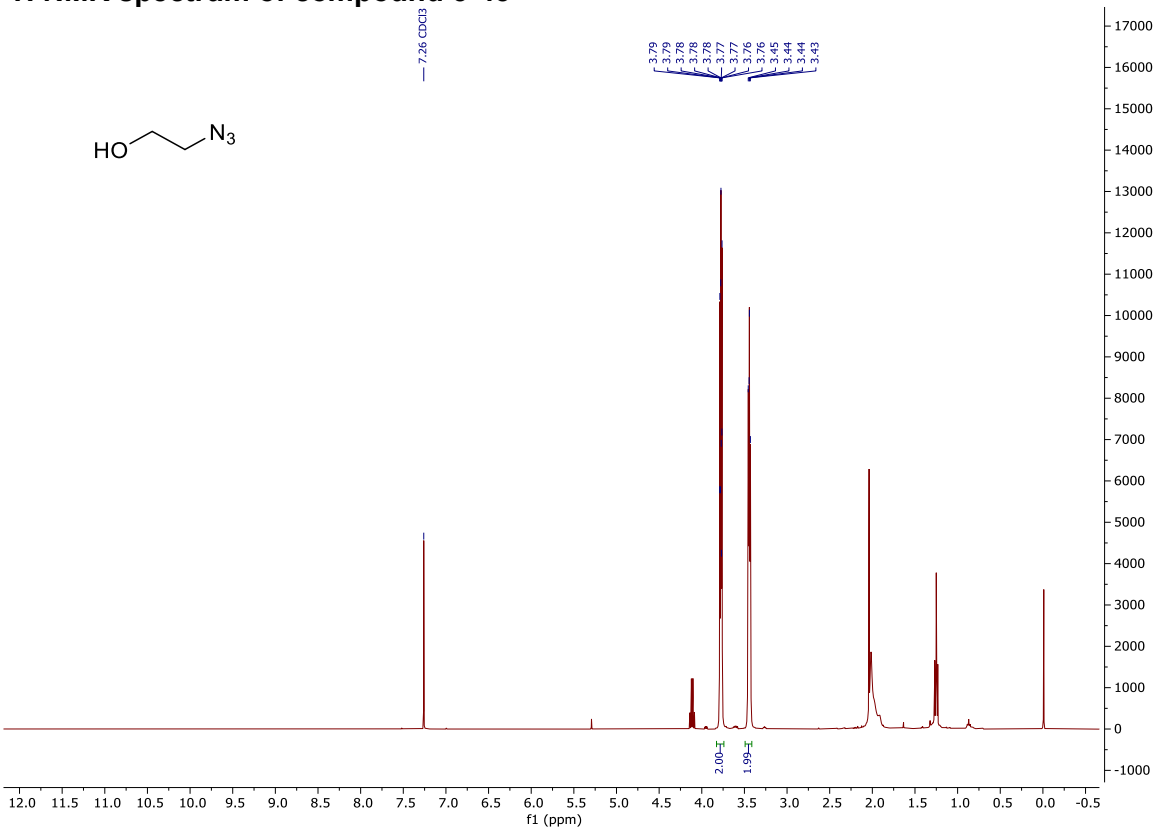

COSY NMR spectrum of compound 3-45

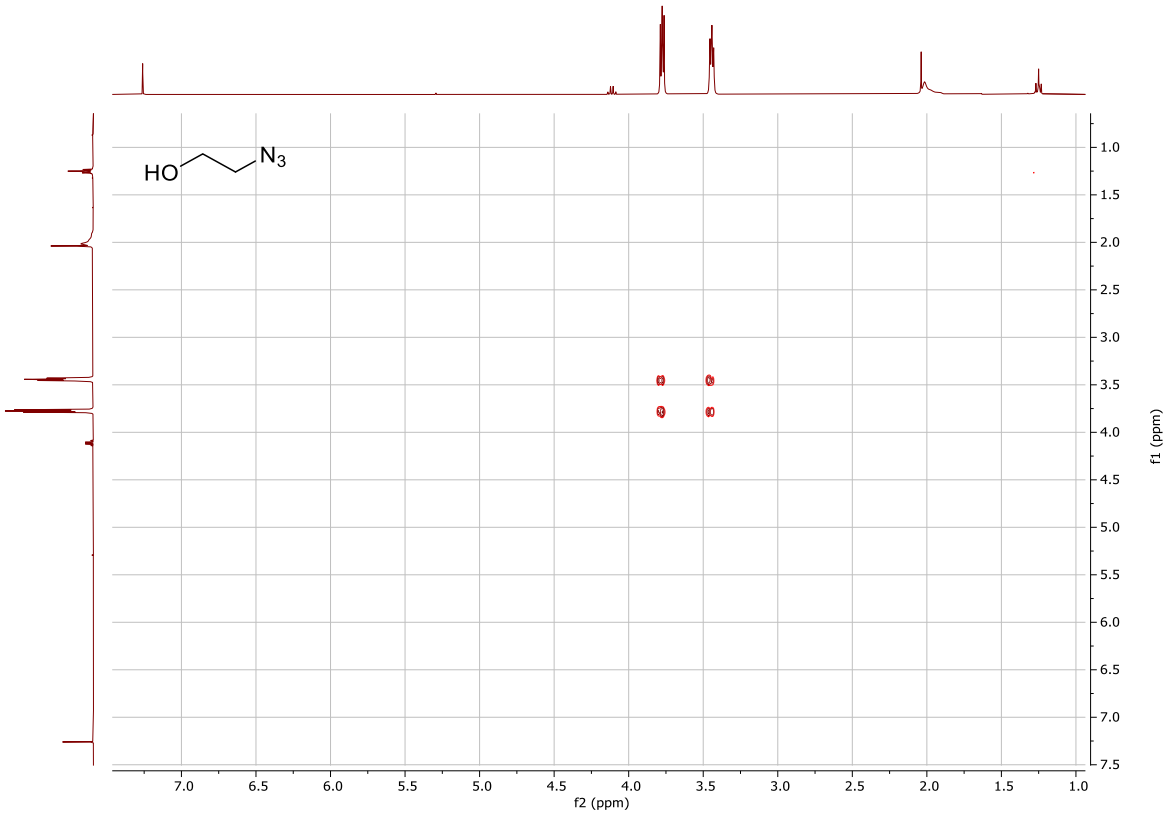

HSQC NMR spectrum of compound 3-45

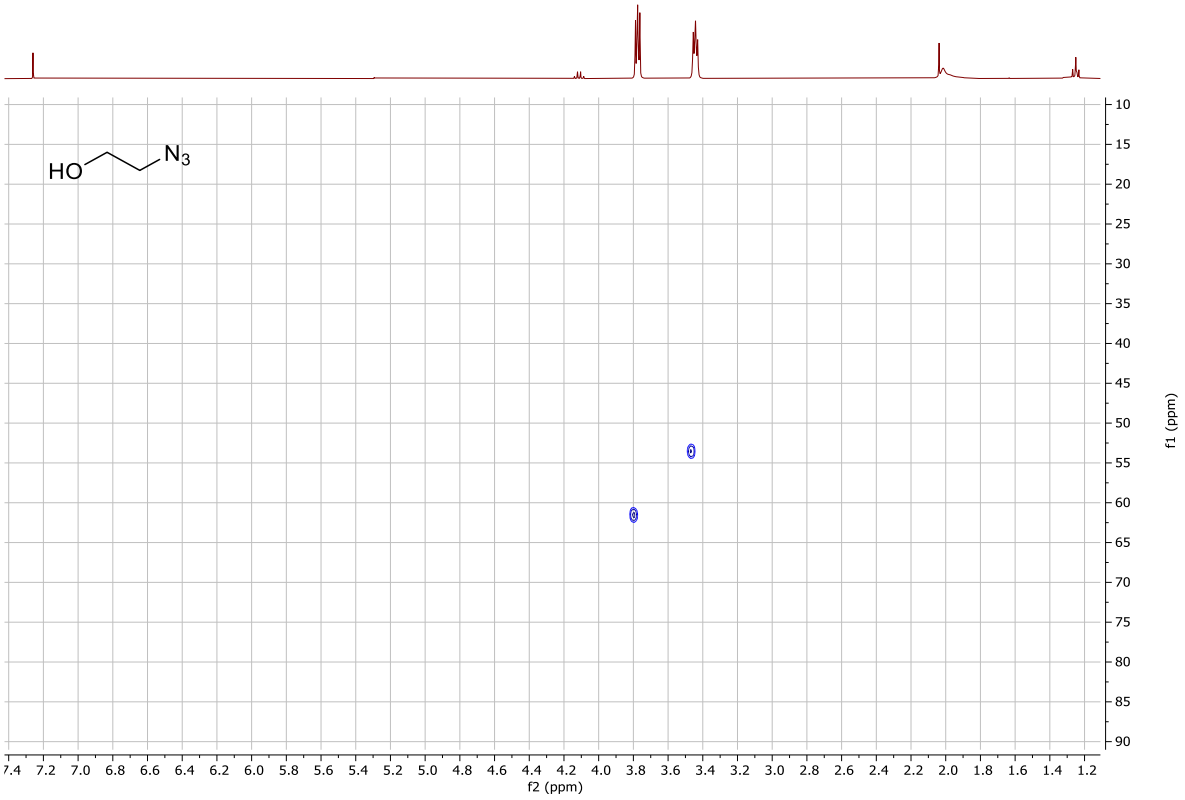

^{1}H NMR spectrum of compound 3-3

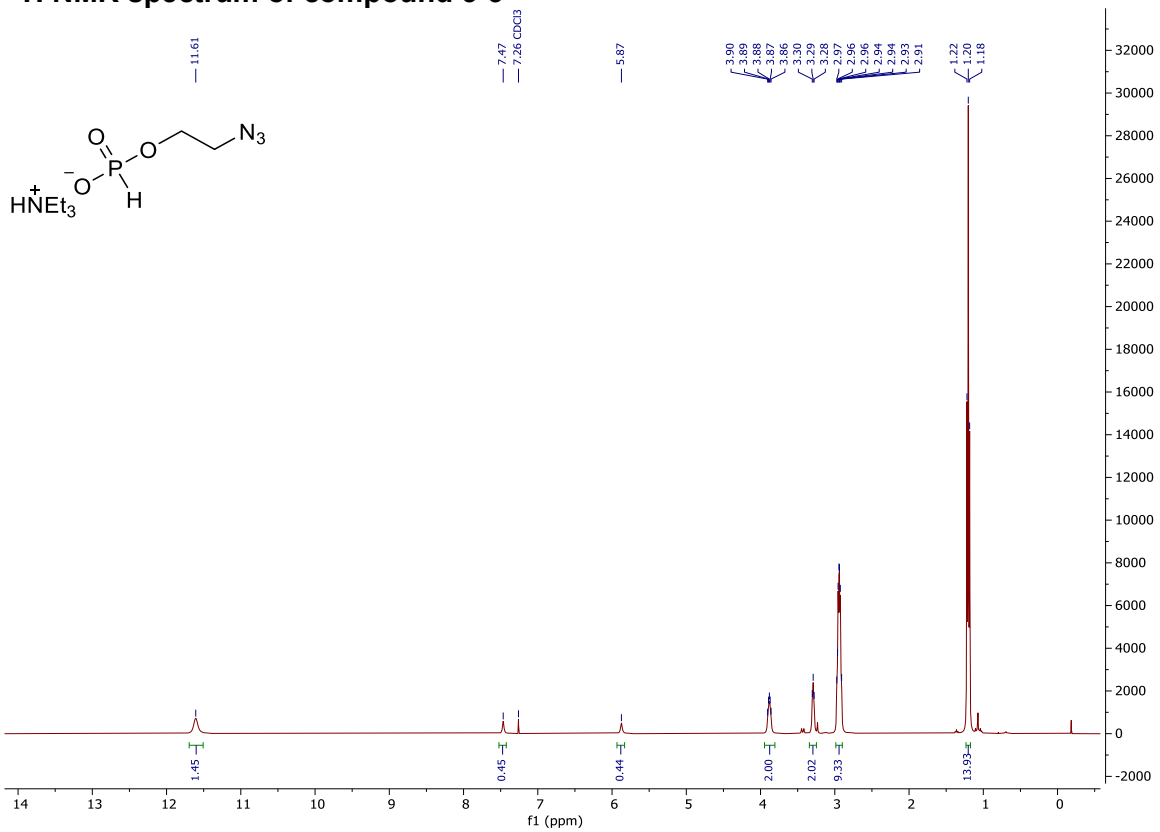

^{13}C NMR spectrum of compound 3-3

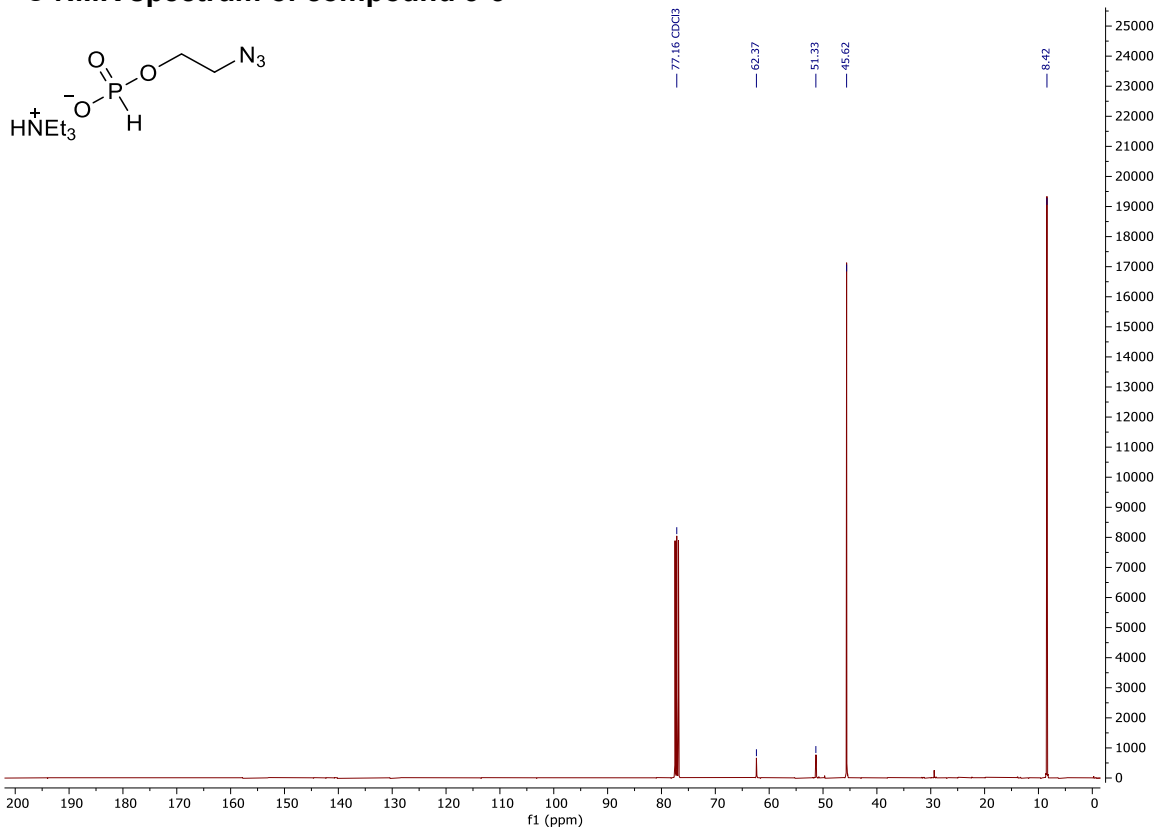

COSY NMR spectrum of compound 3-3

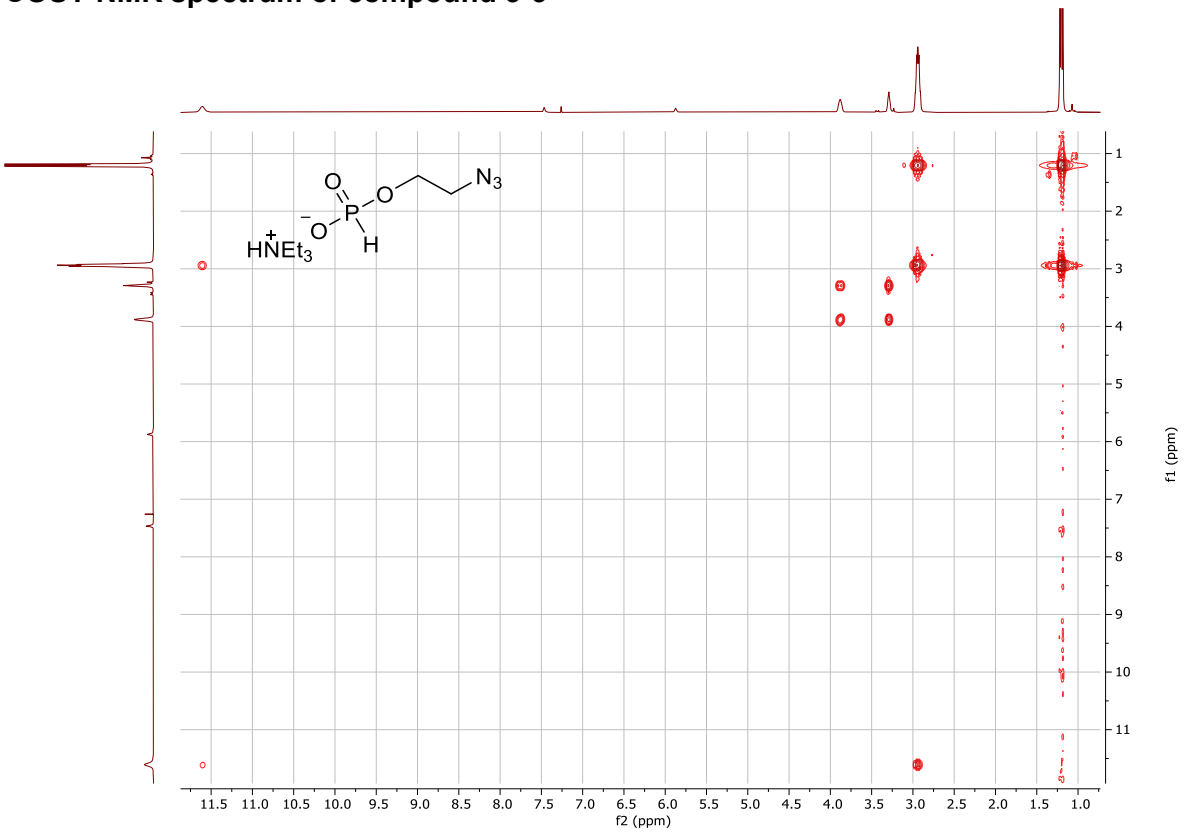

HSQC NMR spectrum of compound 3-3

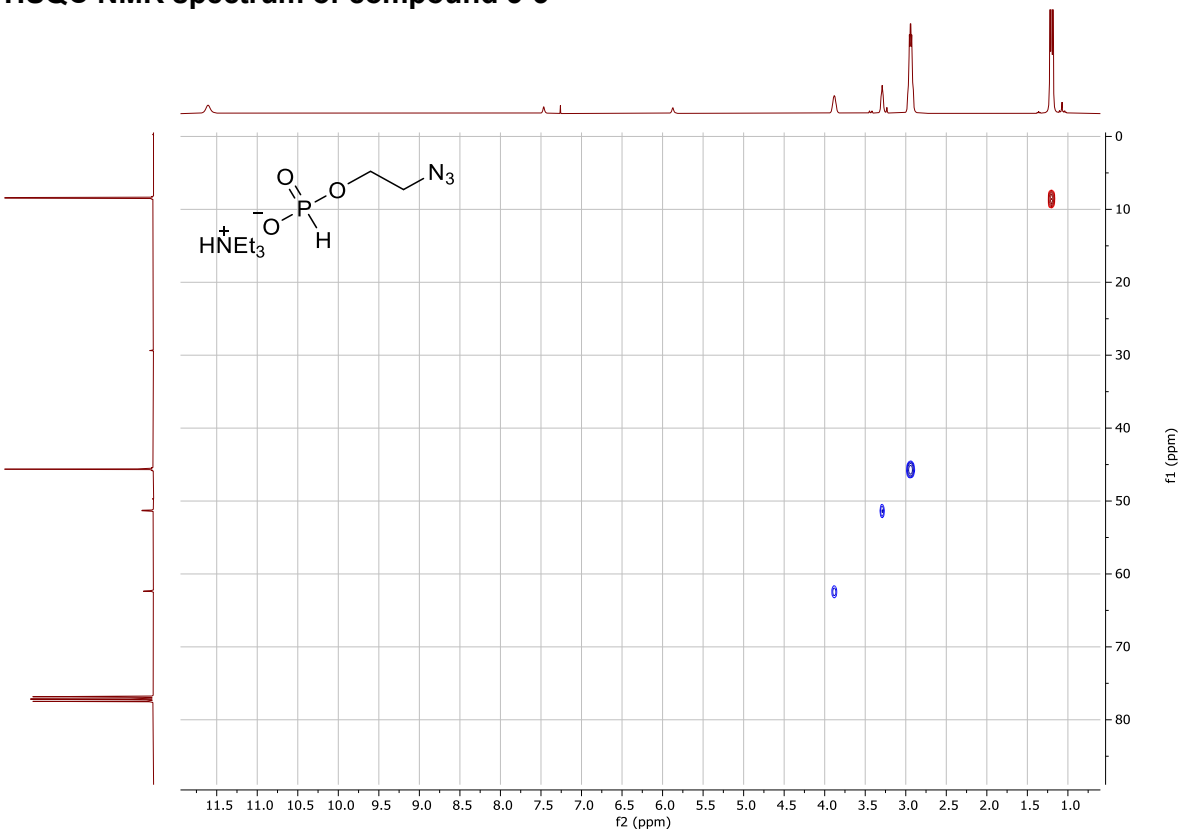

^{31}P NMR spectrum of compound 3-3

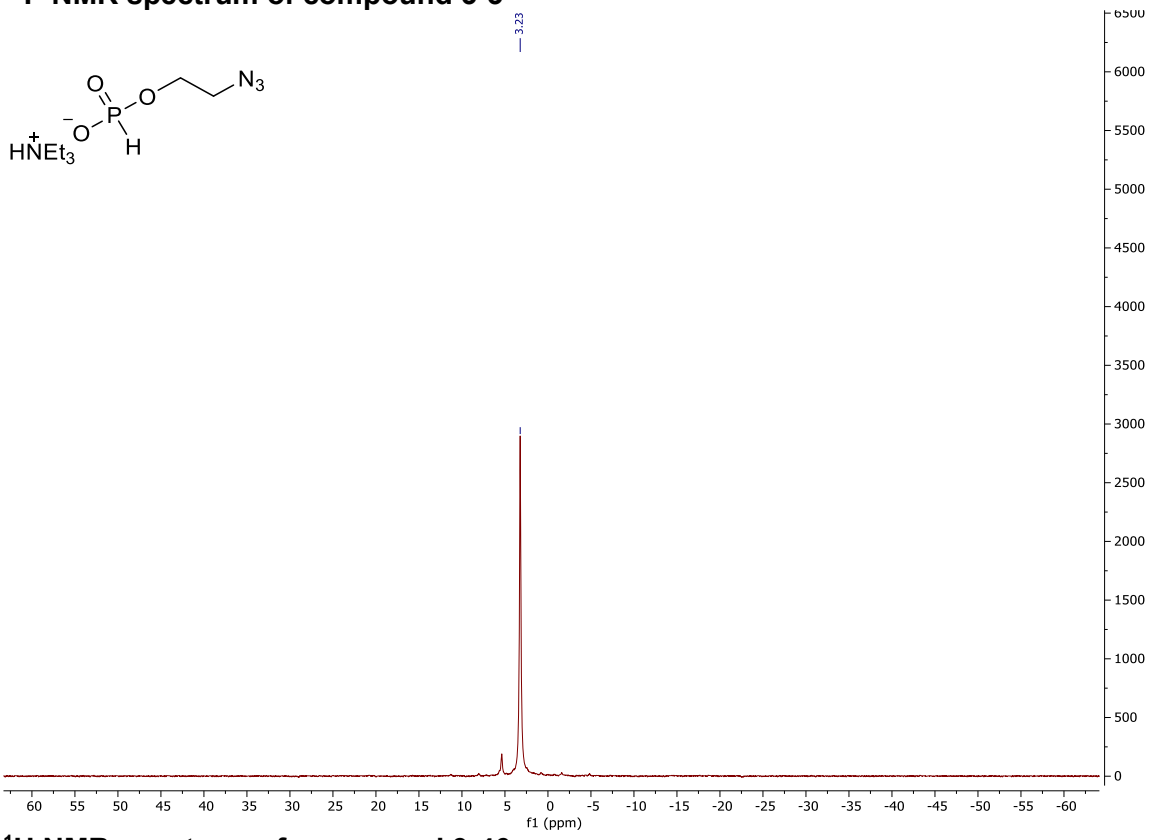

^{1}H NMR spectrum of compound 3-46

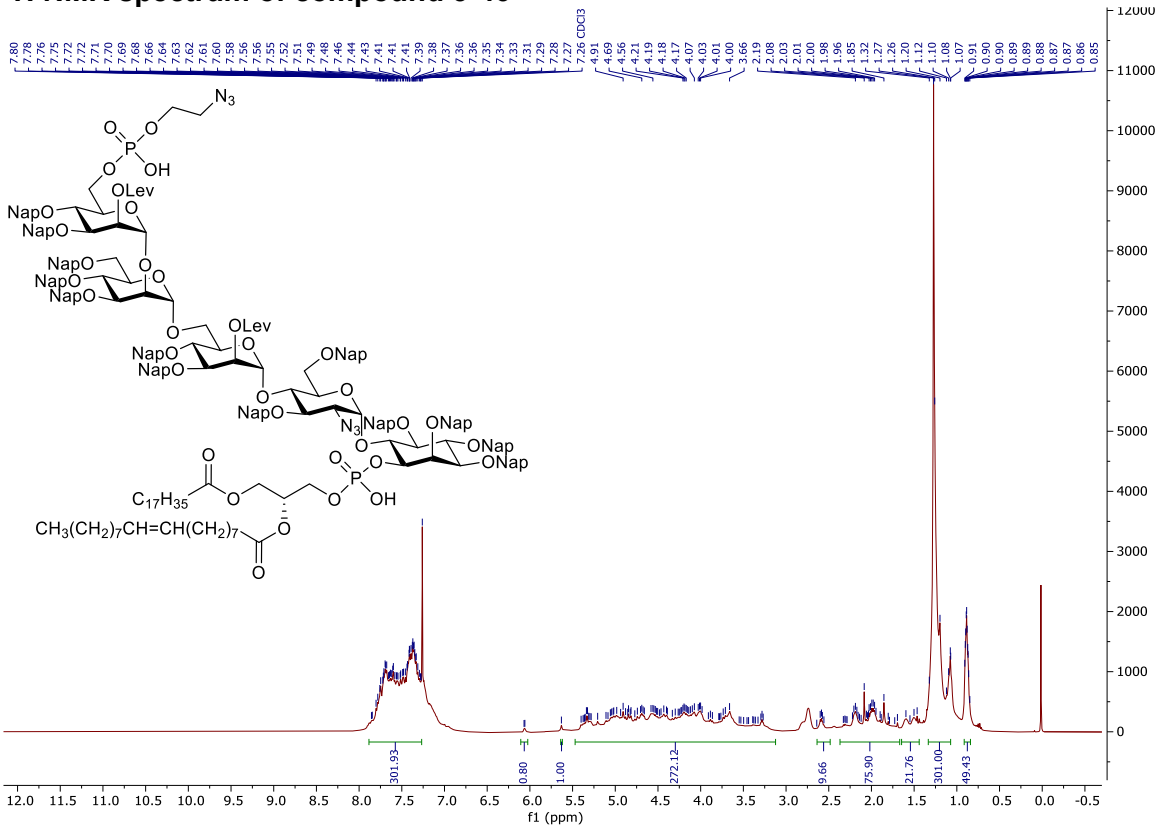

^{13}C NMR spectrum of compound 3-46

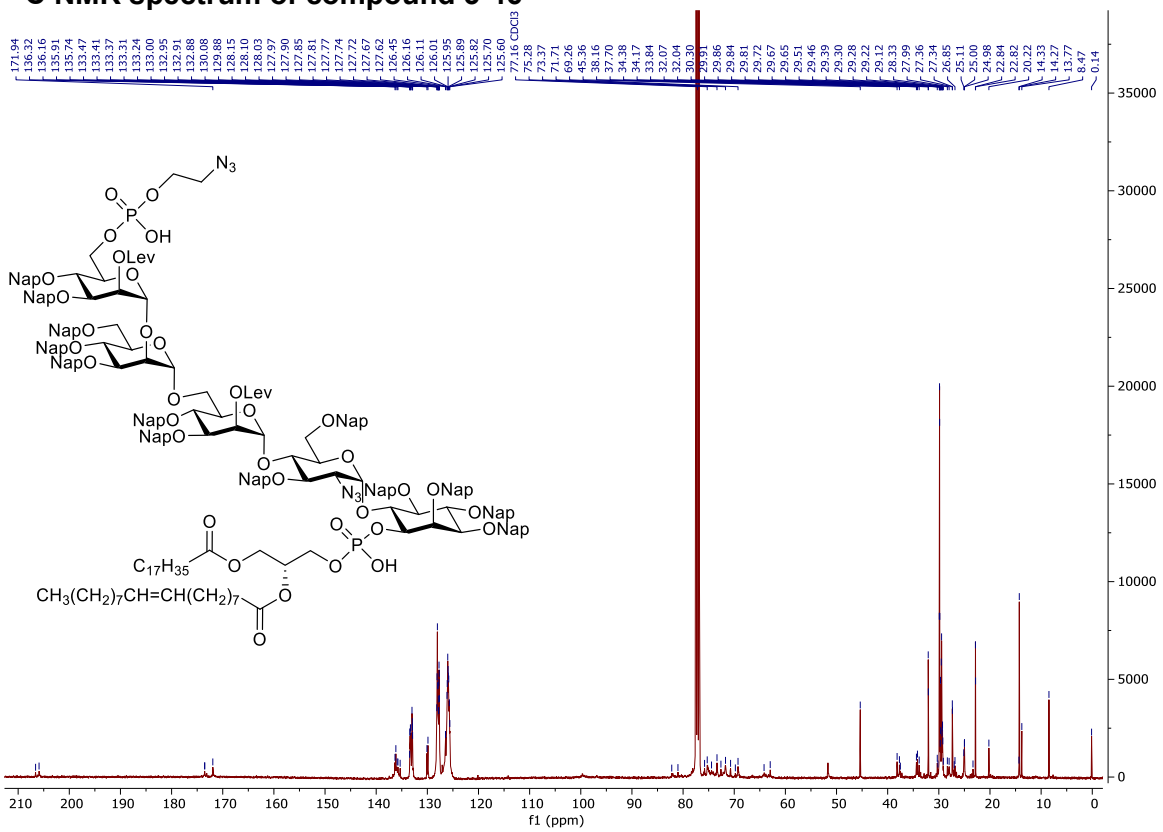

COSY-NMR spectrum of compound 3-46

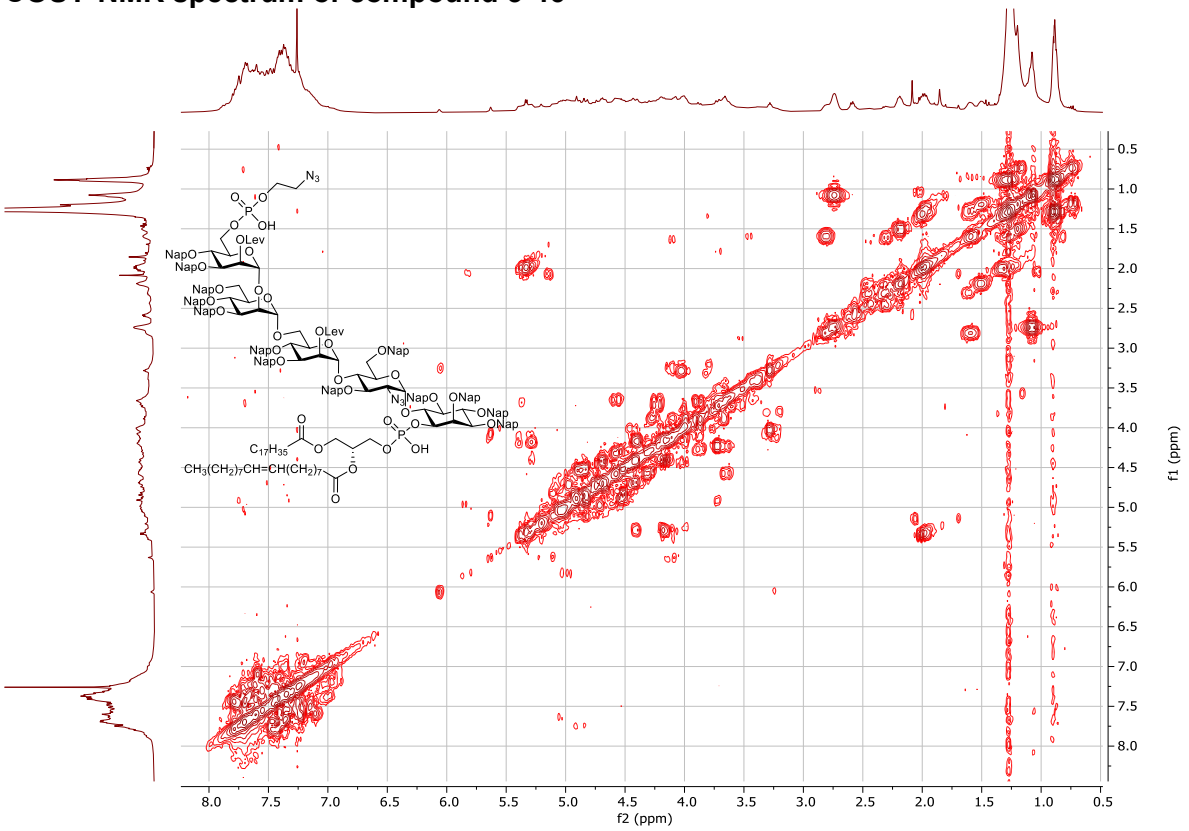

HSQC-NMR spectrum of compound 3-46

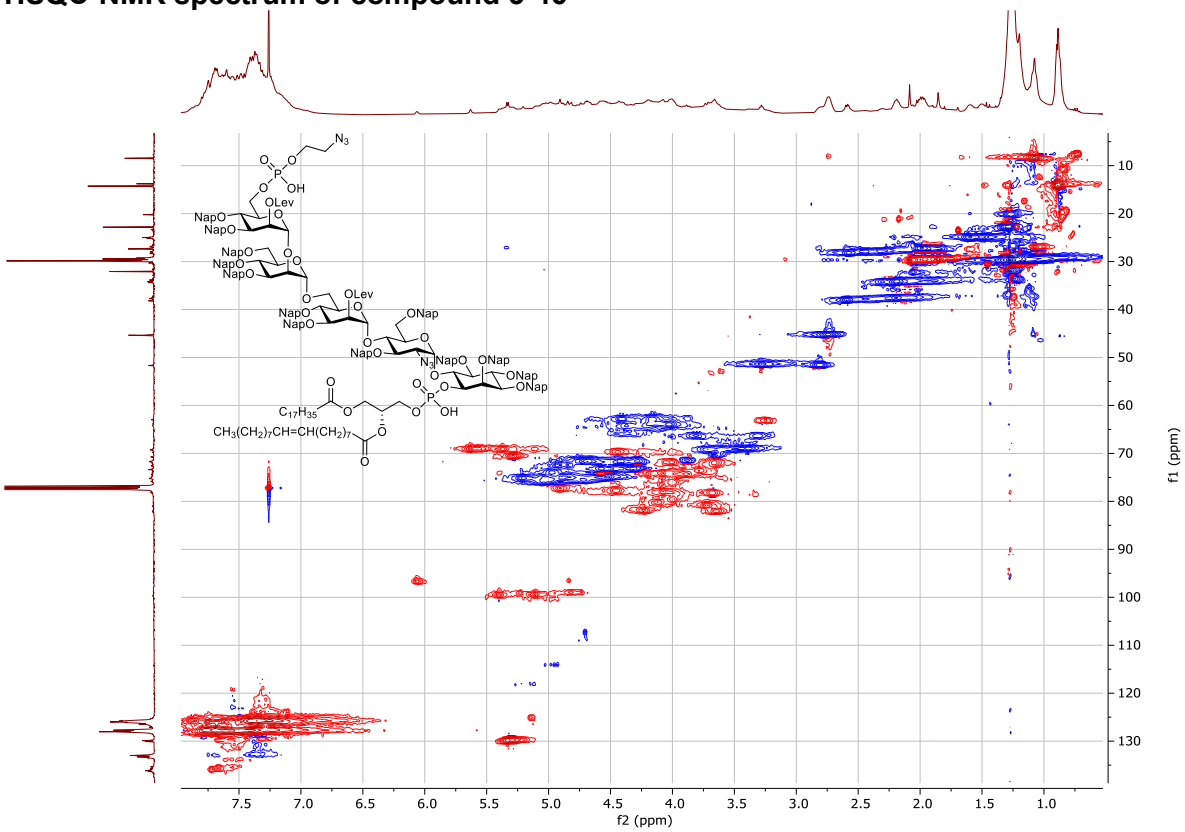

^{31}P NMR spectrum of compound 3-46

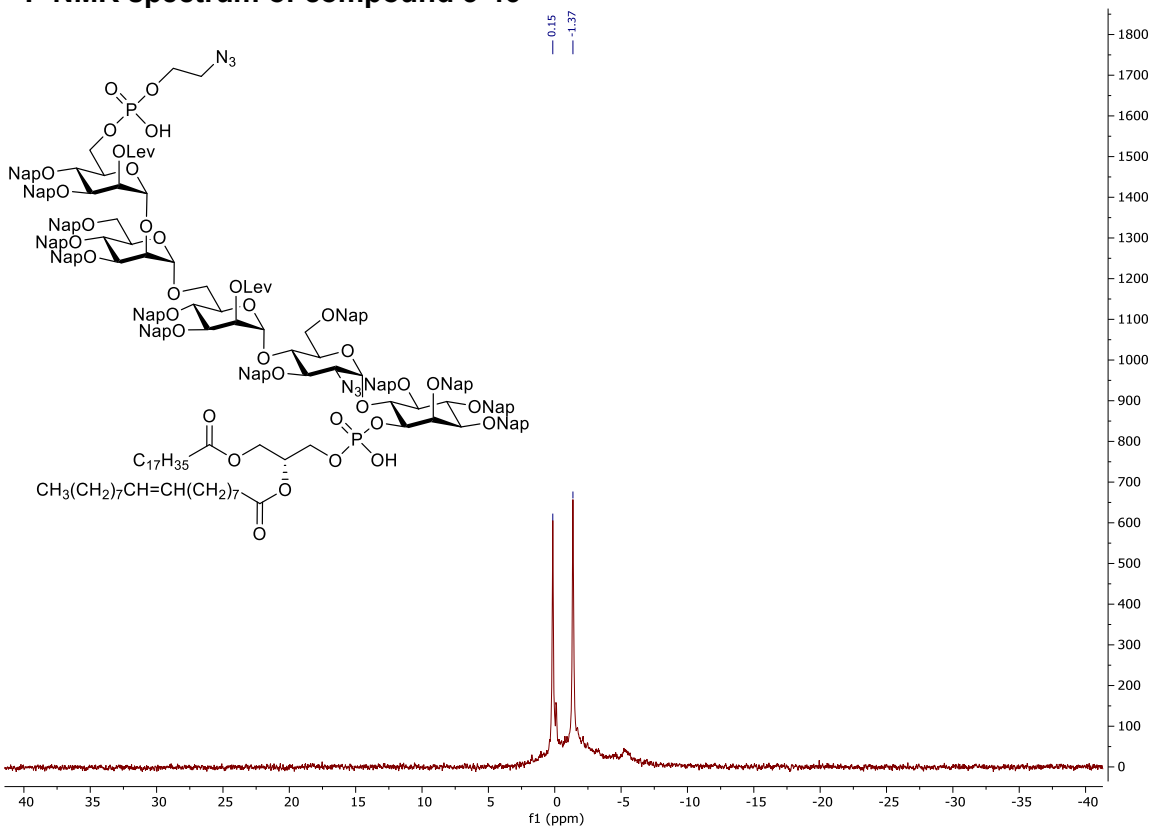

^{1}H NMR spectrum of GPI 3-1

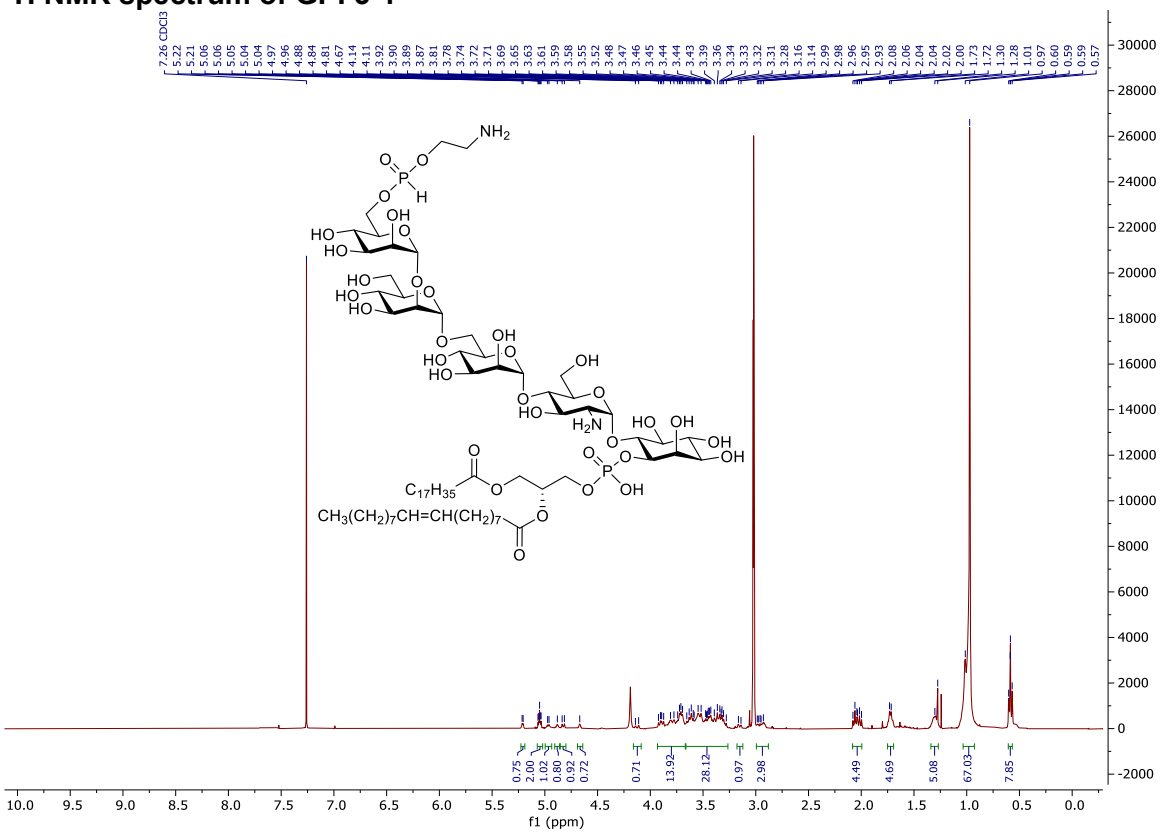

^{13}C NMR spectrum of GPI 3-1

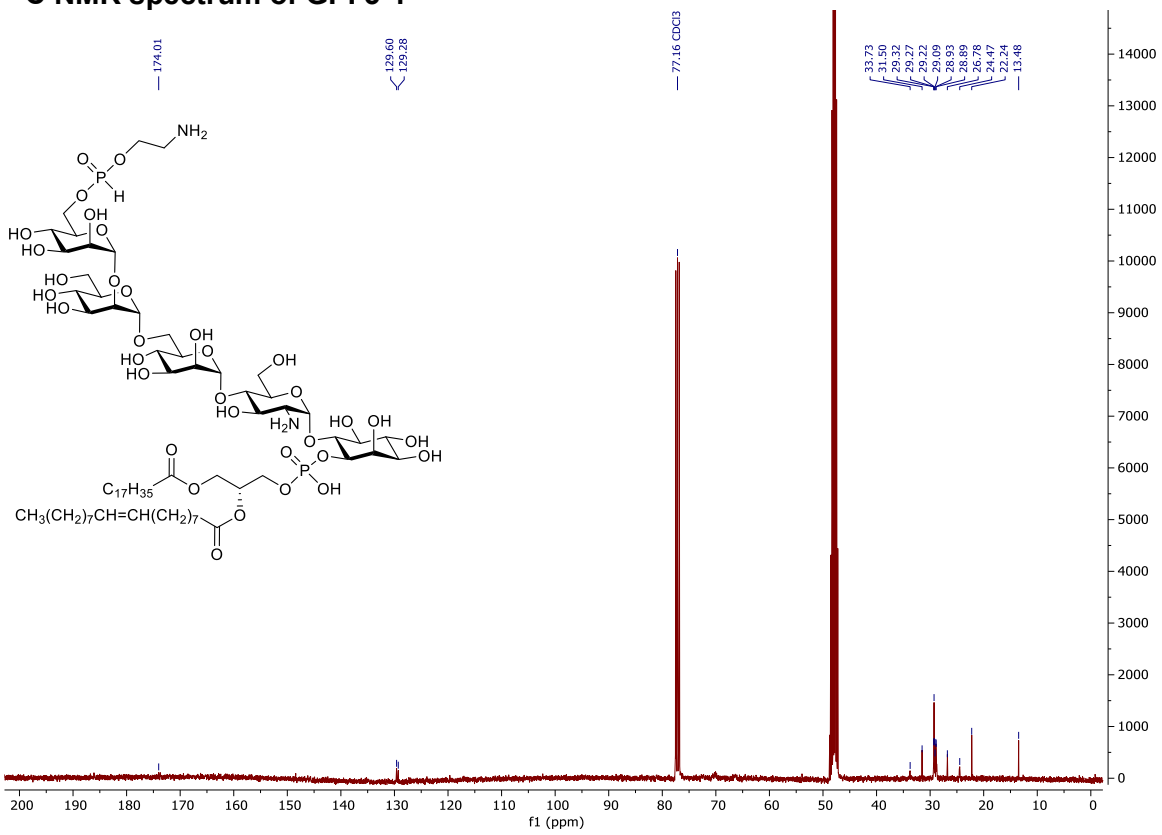

COSY-NMR spectrum of GPI 3-1

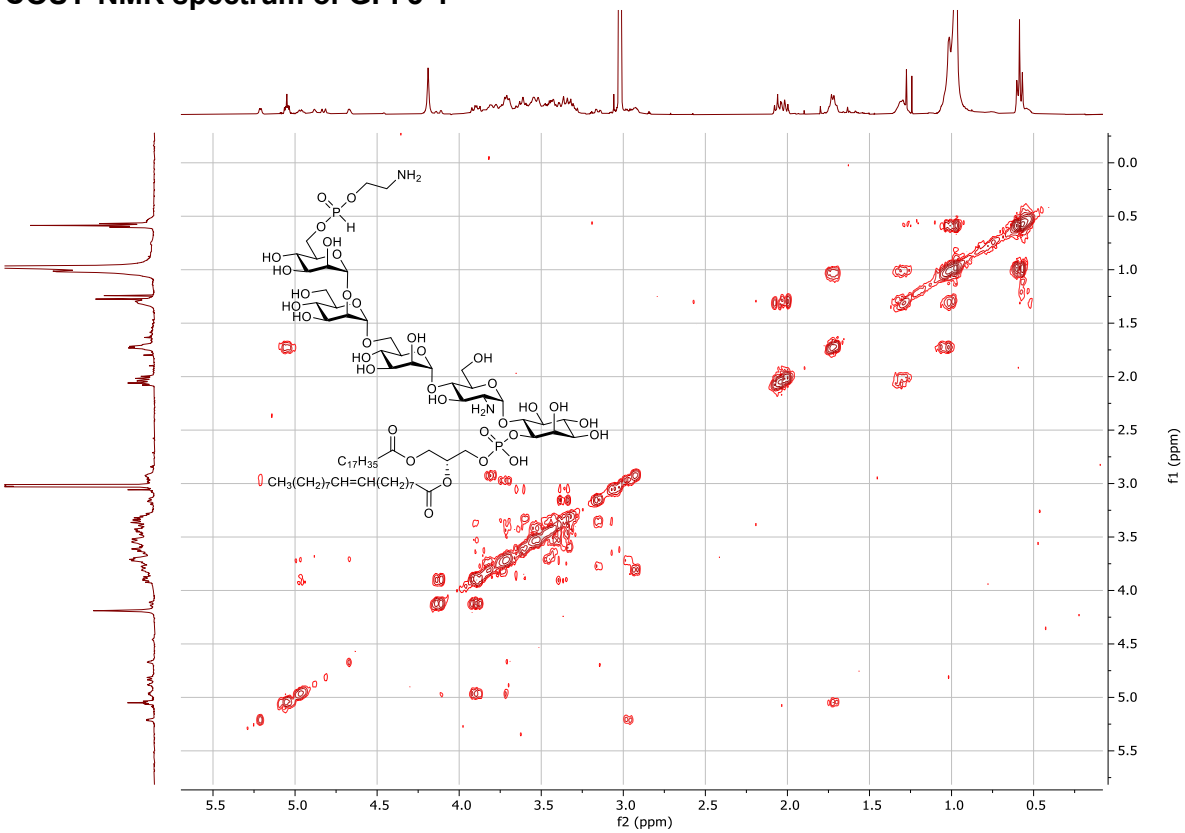

HSQC-NMR spectrum of GPI 3-1

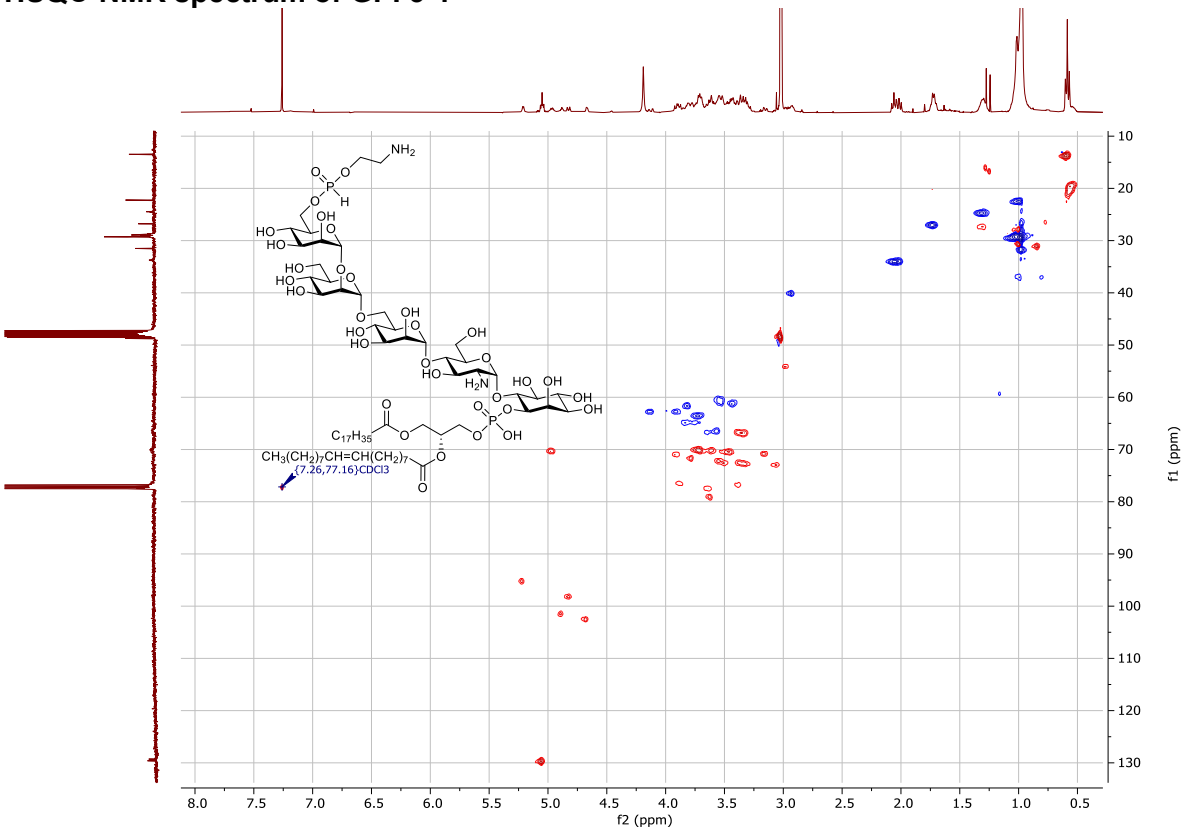

^{31}P NMR spectrum of GPI 3-1

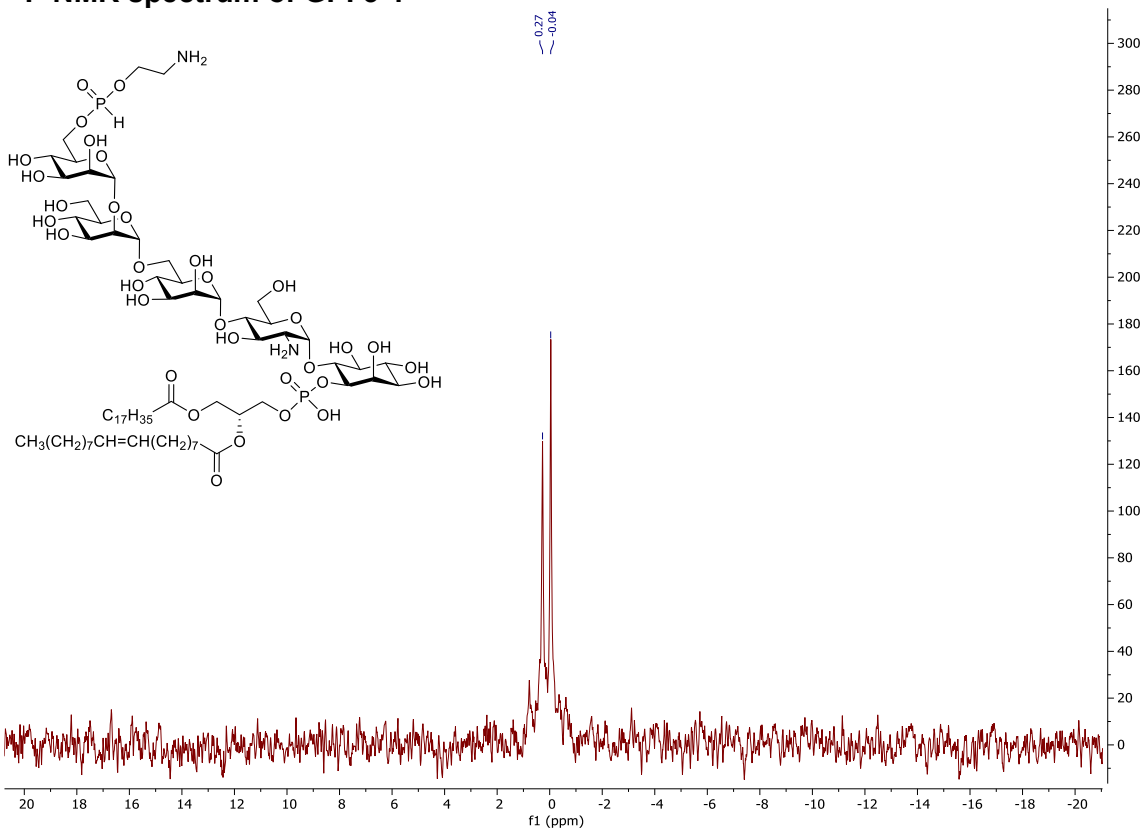

^{1}H NMR spectrum of compound 3-49

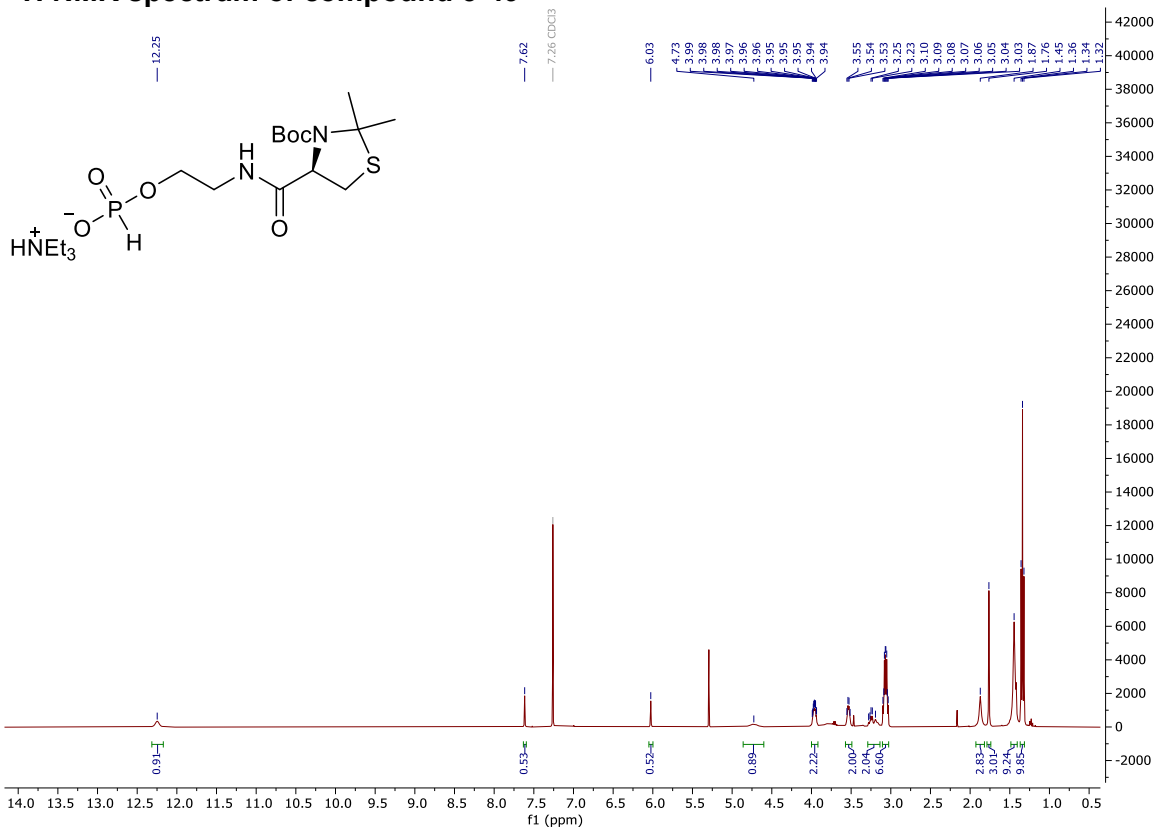

^{13}C NMR spectrum of compound 3-49

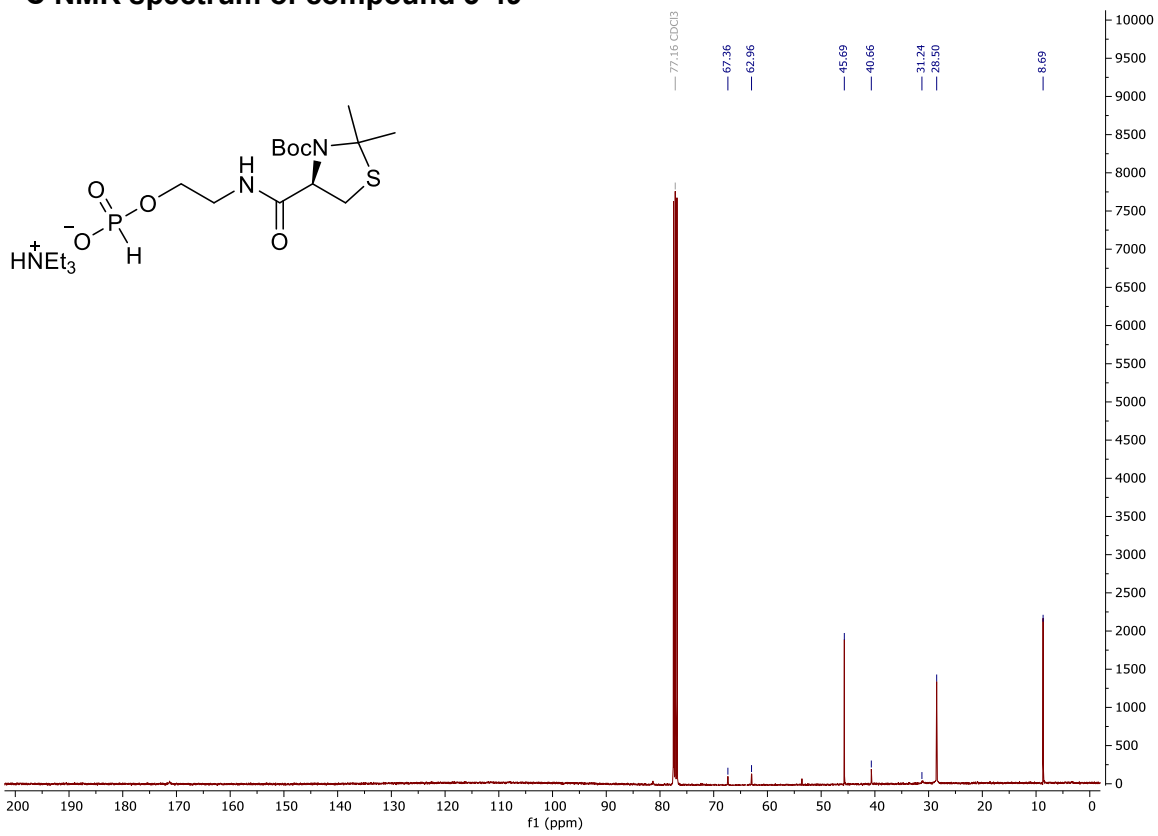

COSY NMR spectrum of compound 3-49

HSQC NMR spectrum of compound 3-49

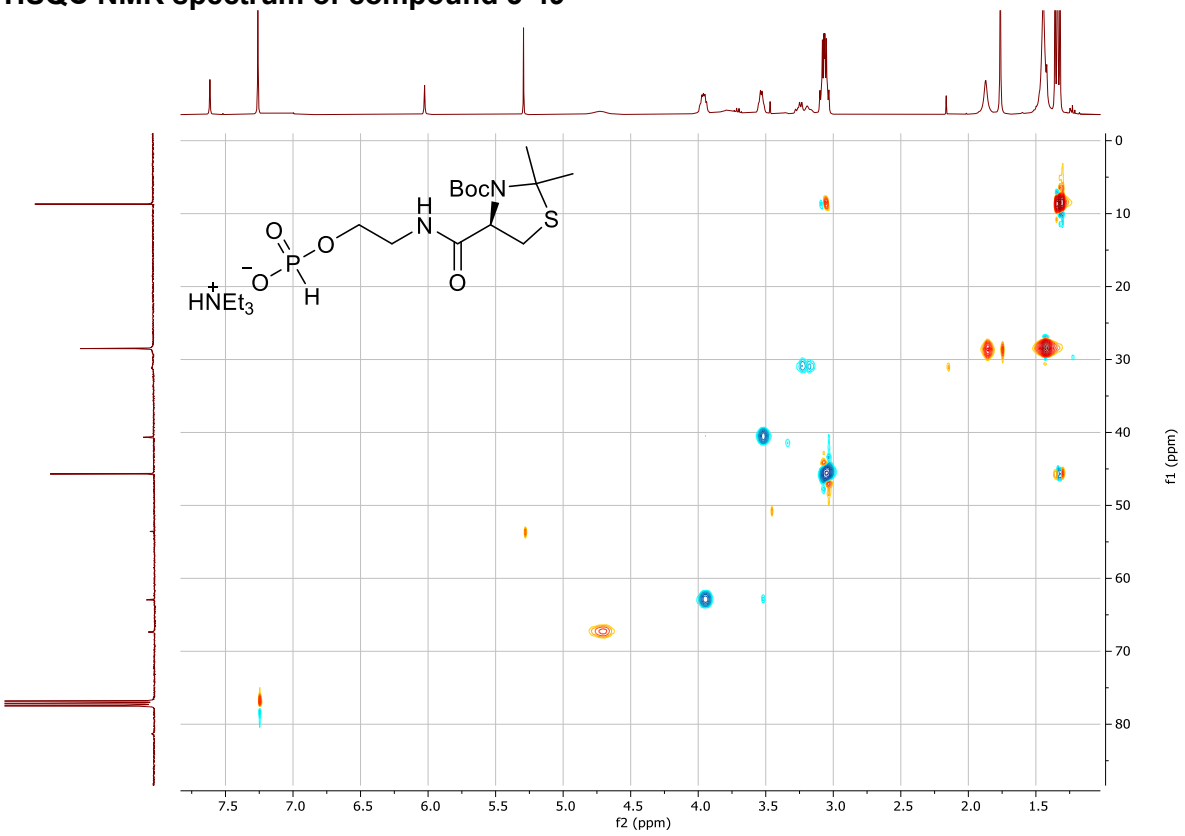

^{31}P NMR spectrum of GPI 3-49

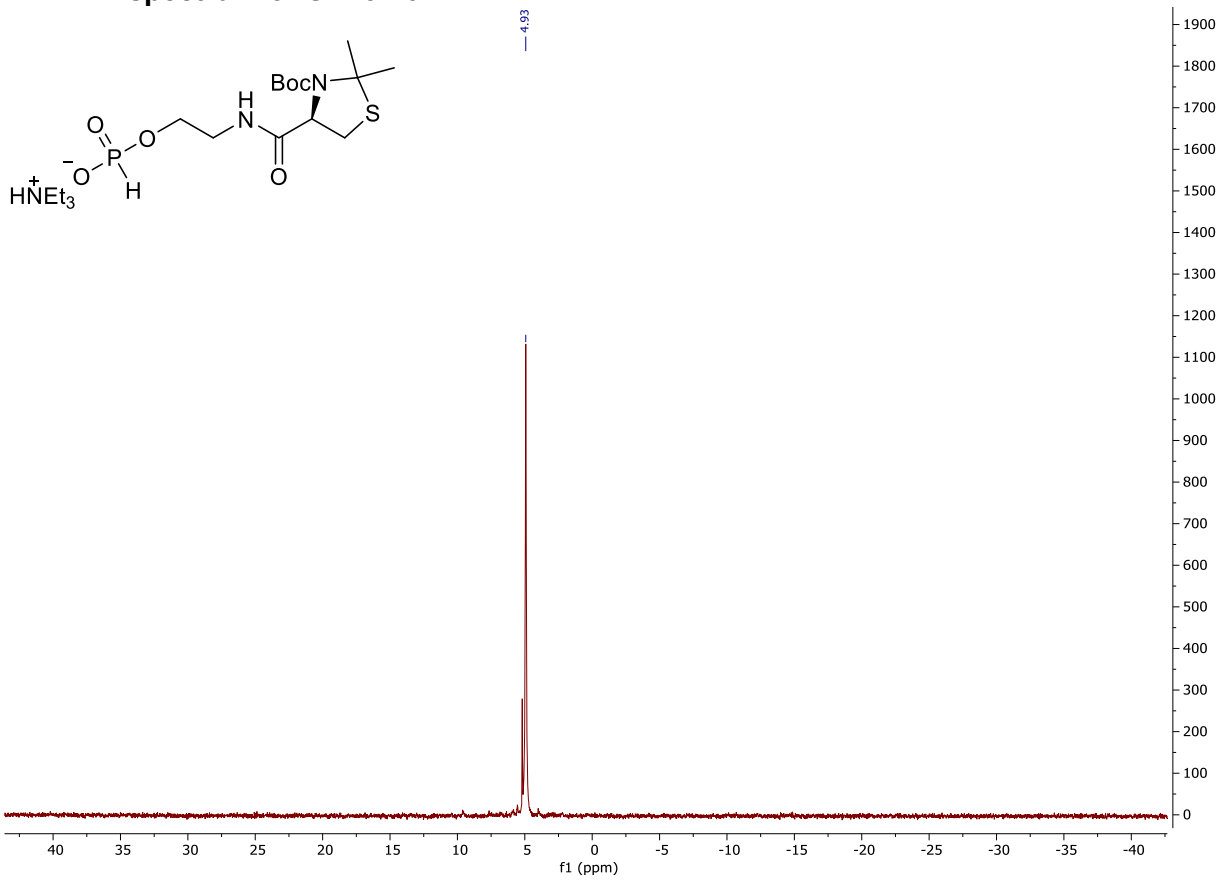

^{1}H NMR spectrum of GPI 3-51

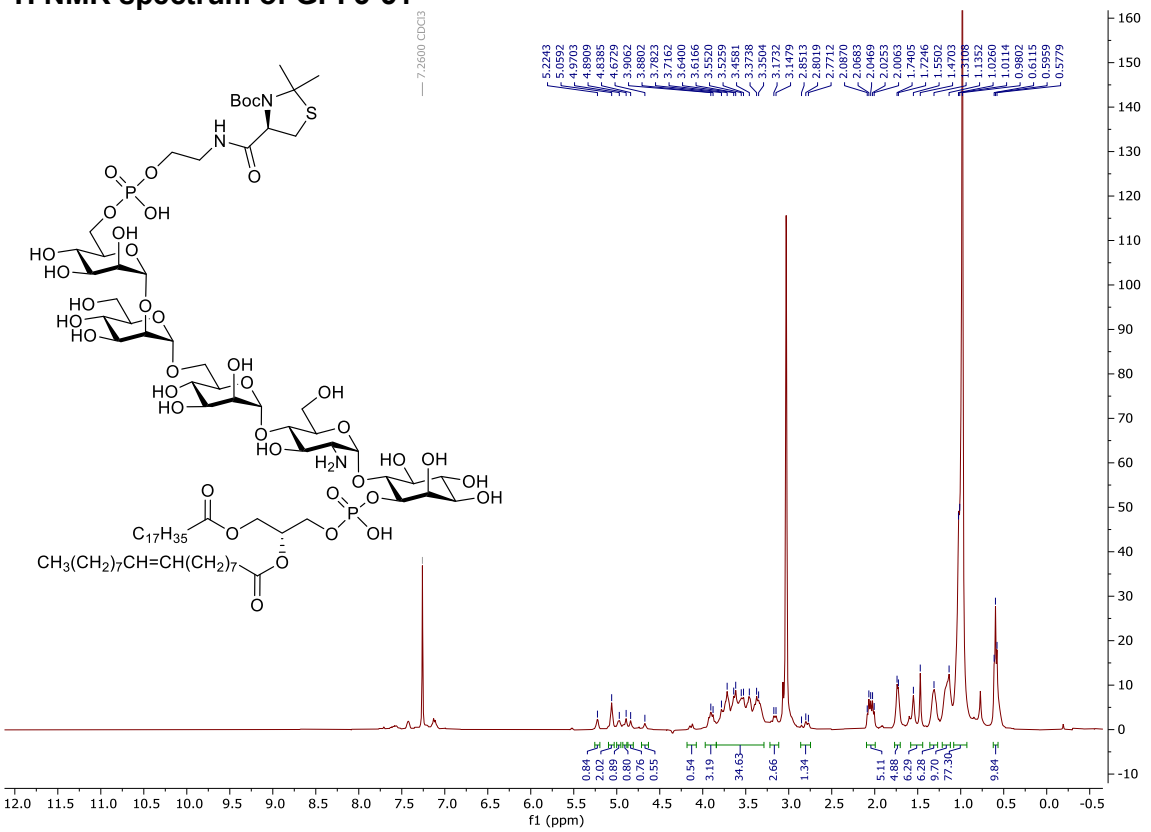

^{13}C NMR spectrum of GPI 3-51

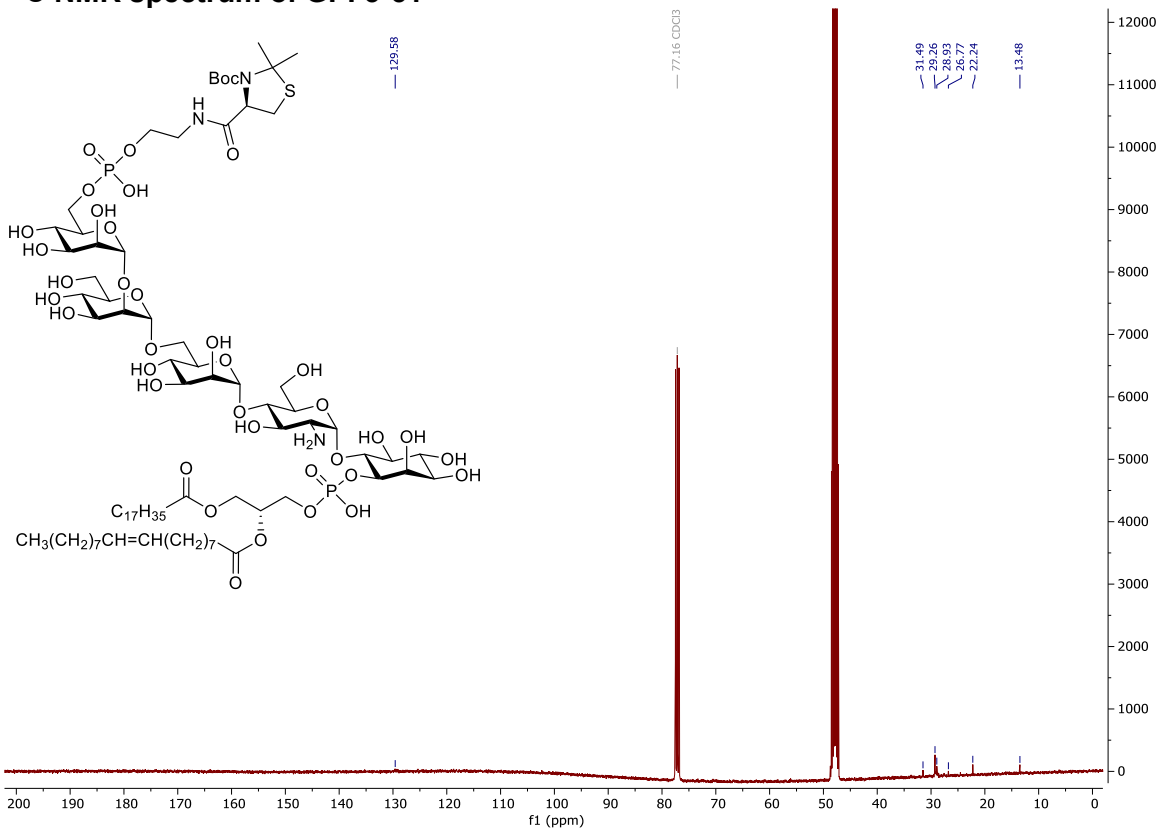

COSY-NMR spectrum of GPI 3-51

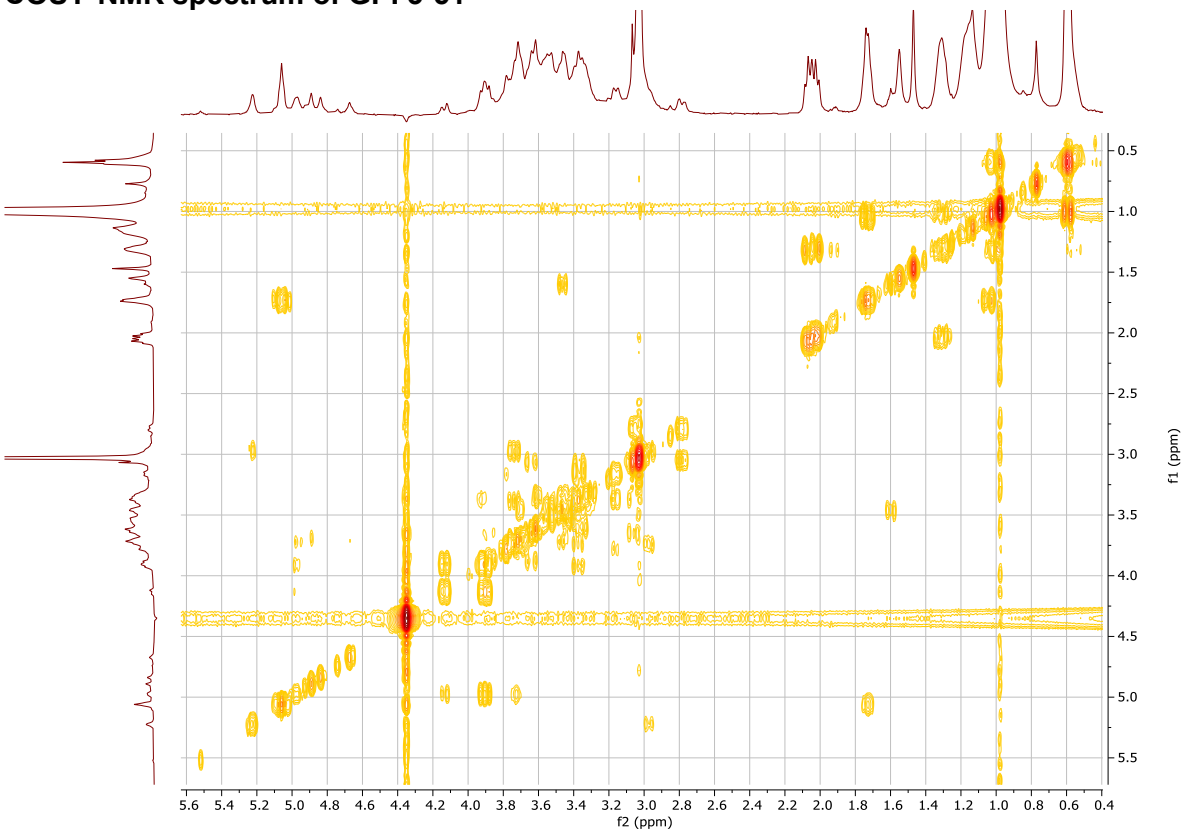

HSQC-NMR spectrum of GPI 3-51

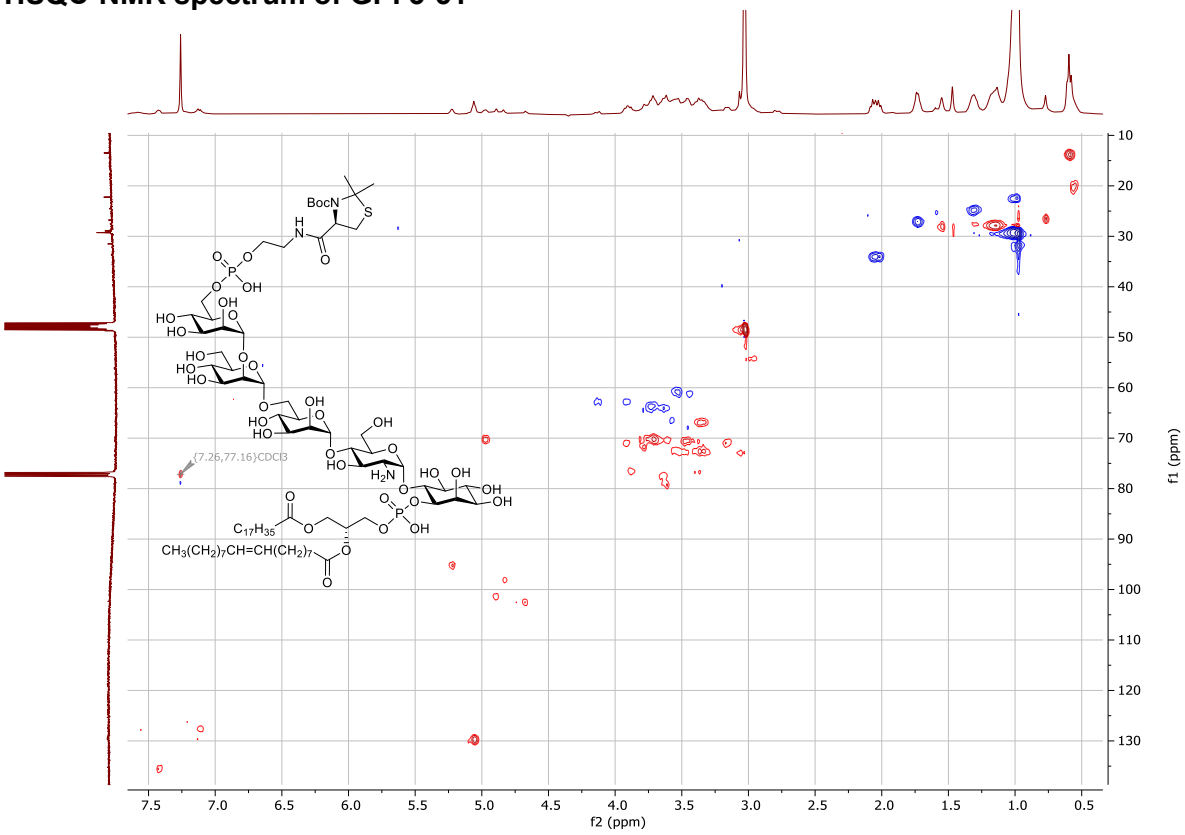

^{31}P NMR spectrum of GPI 3-51

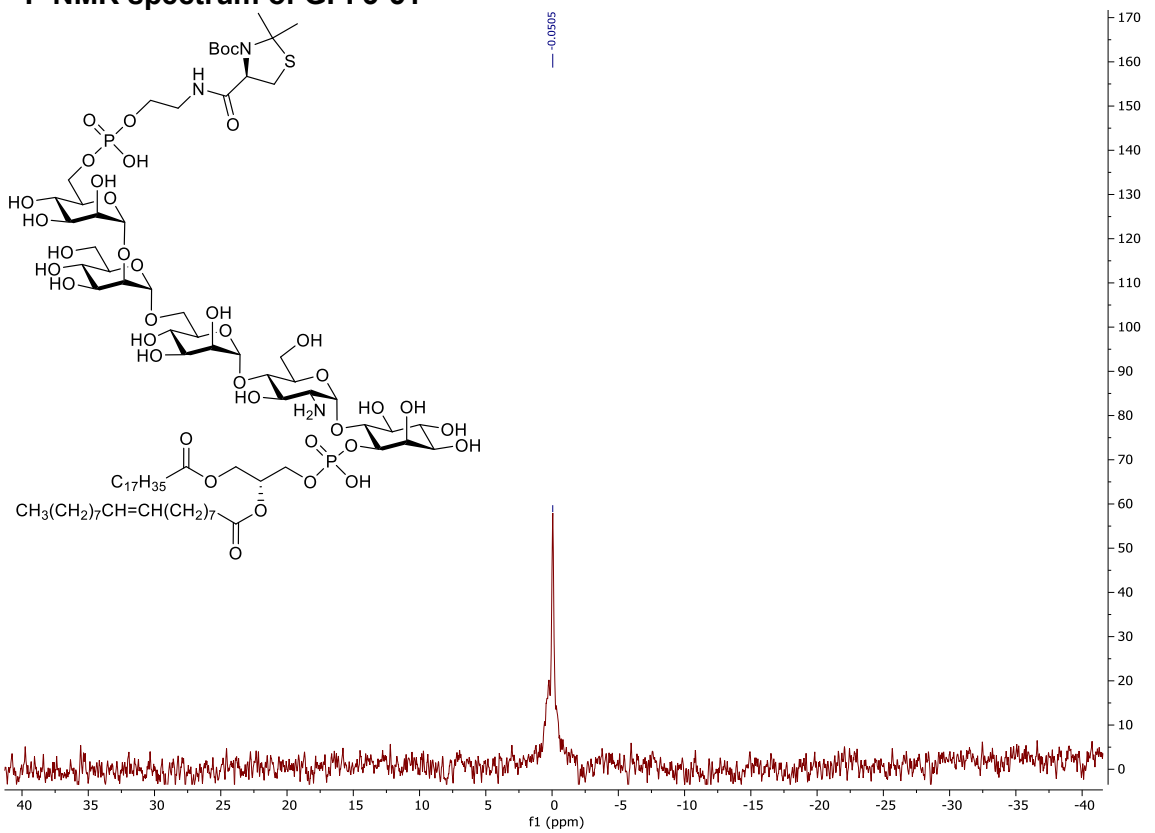

^{1}H NMR spectrum of GPI 3-48

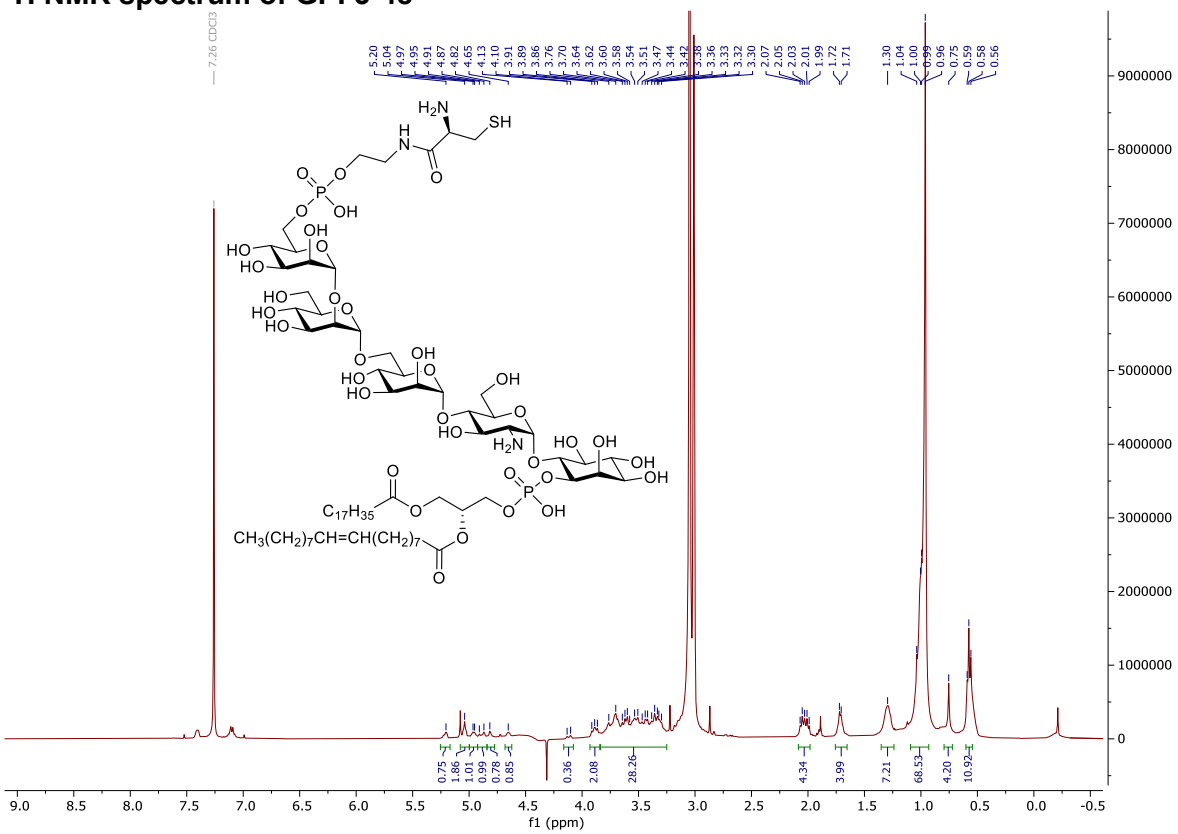

COSY-NMR spectrum of GPI 3-48

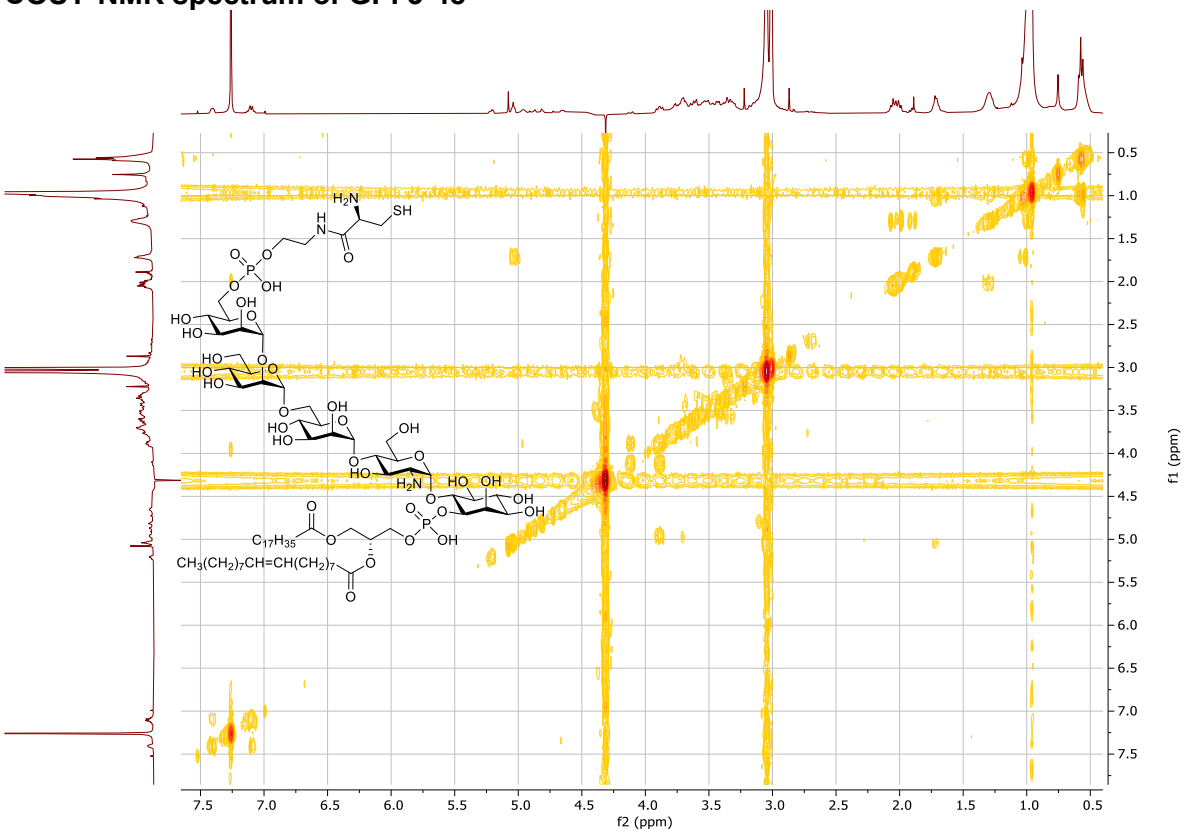

HSQC-NMR spectrum of GPI 3-48

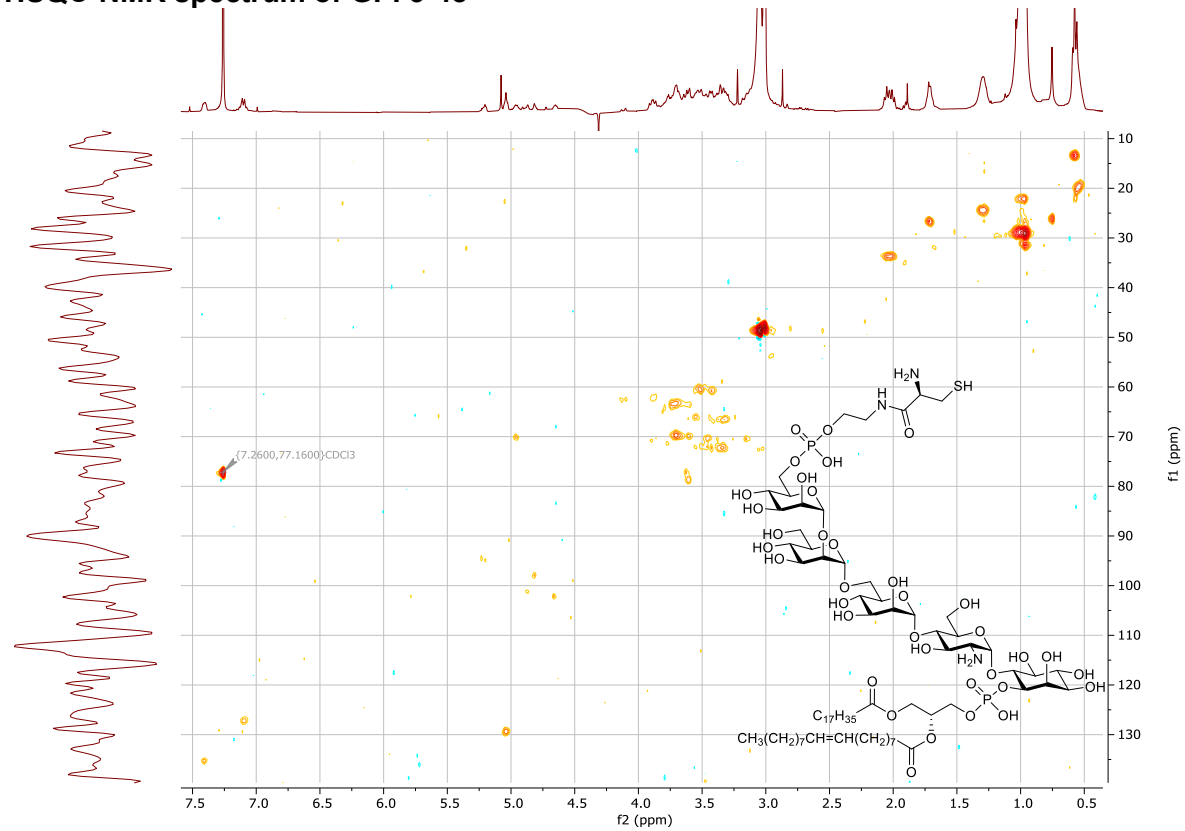

^{31}P NMR spectrum of GPI 3-48

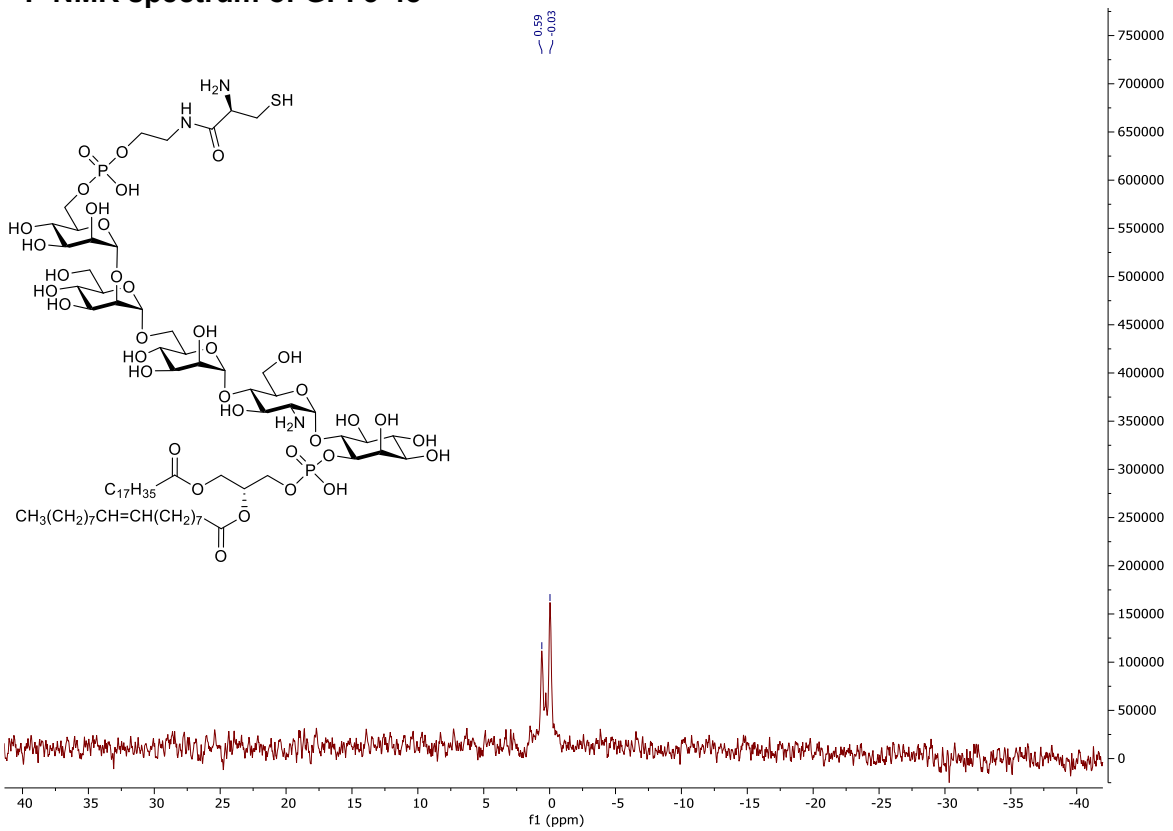

^{1}H NMR spectrum of compound 3-53

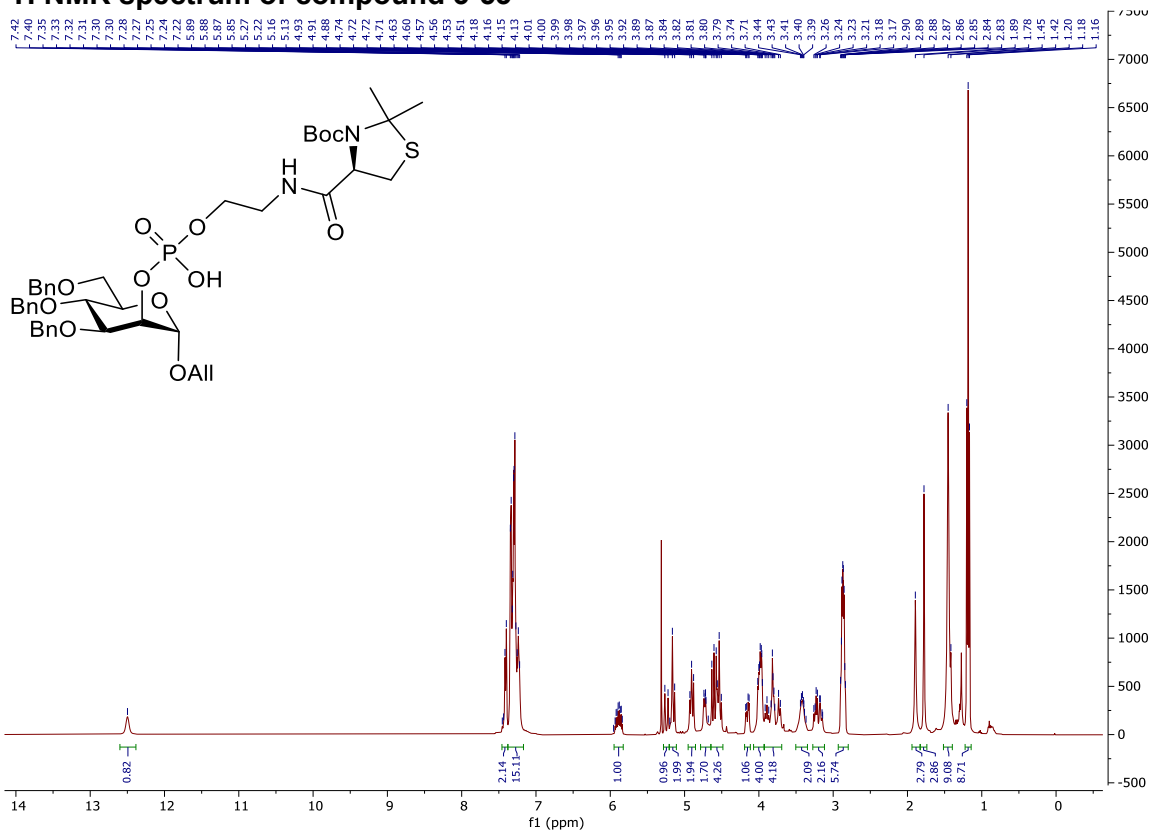

^{13}C NMR spectrum of compound 3-53

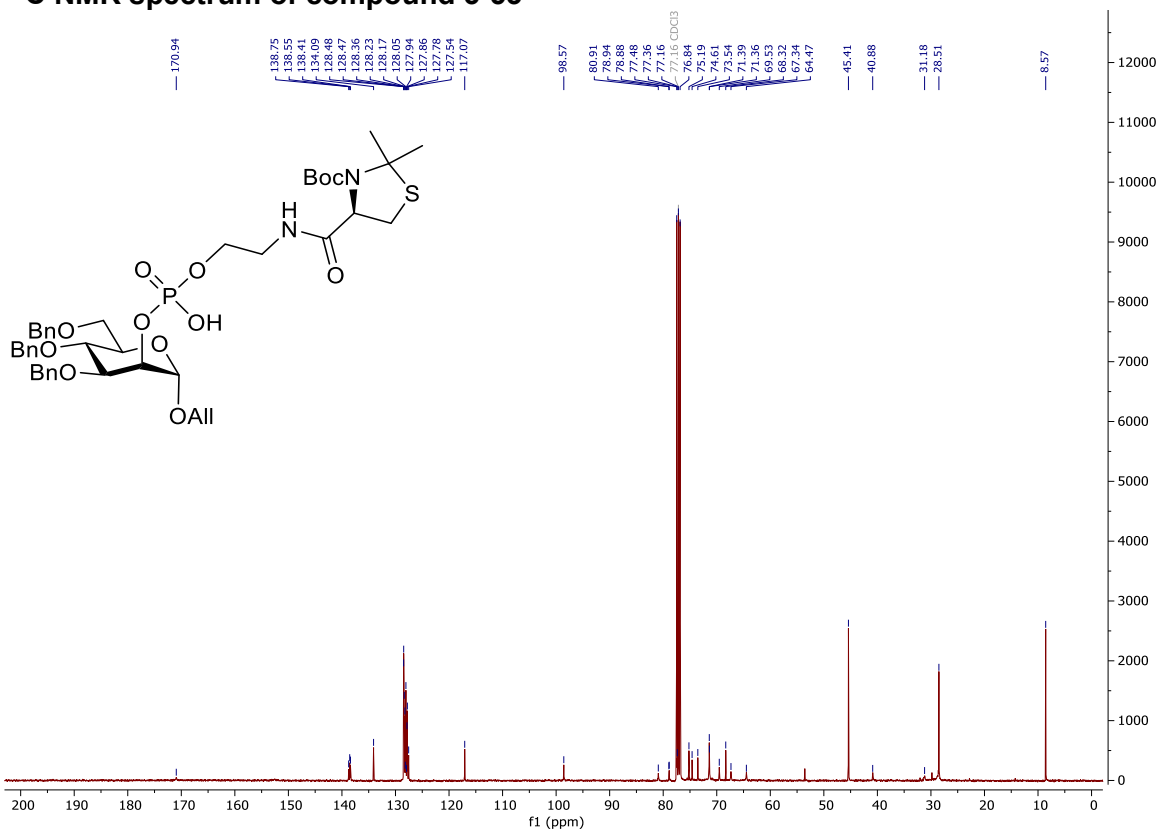

COSY-NMR spectrum of compound 3-53

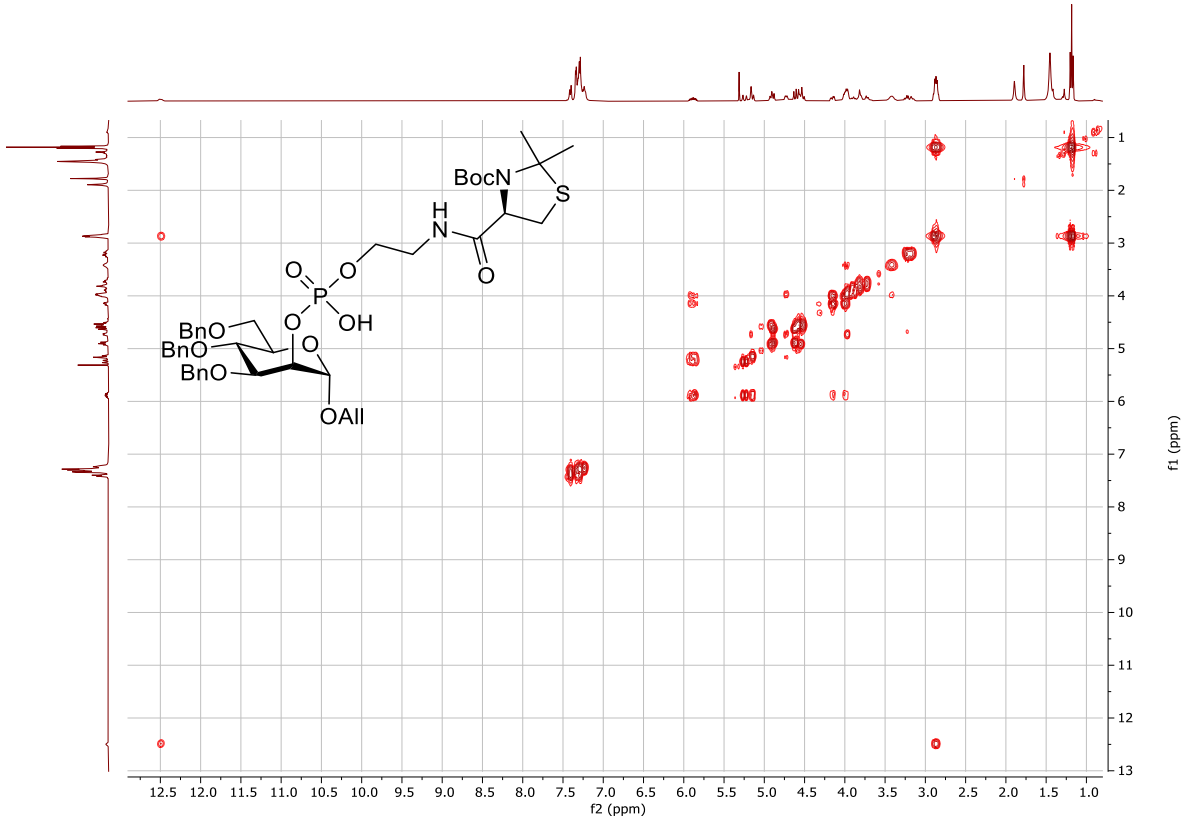

HSQC-NMR spectrum of compound 3-53

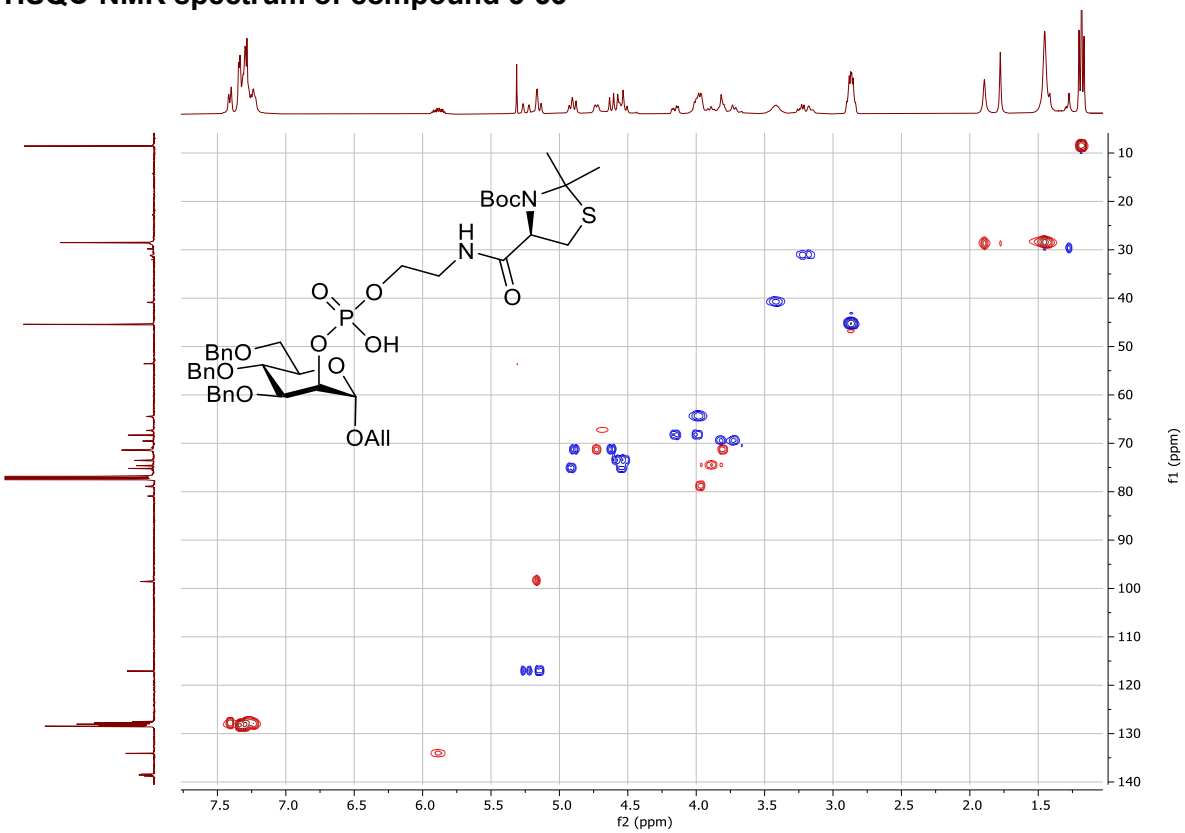

^{31}P NMR spectrum of compound 3-53

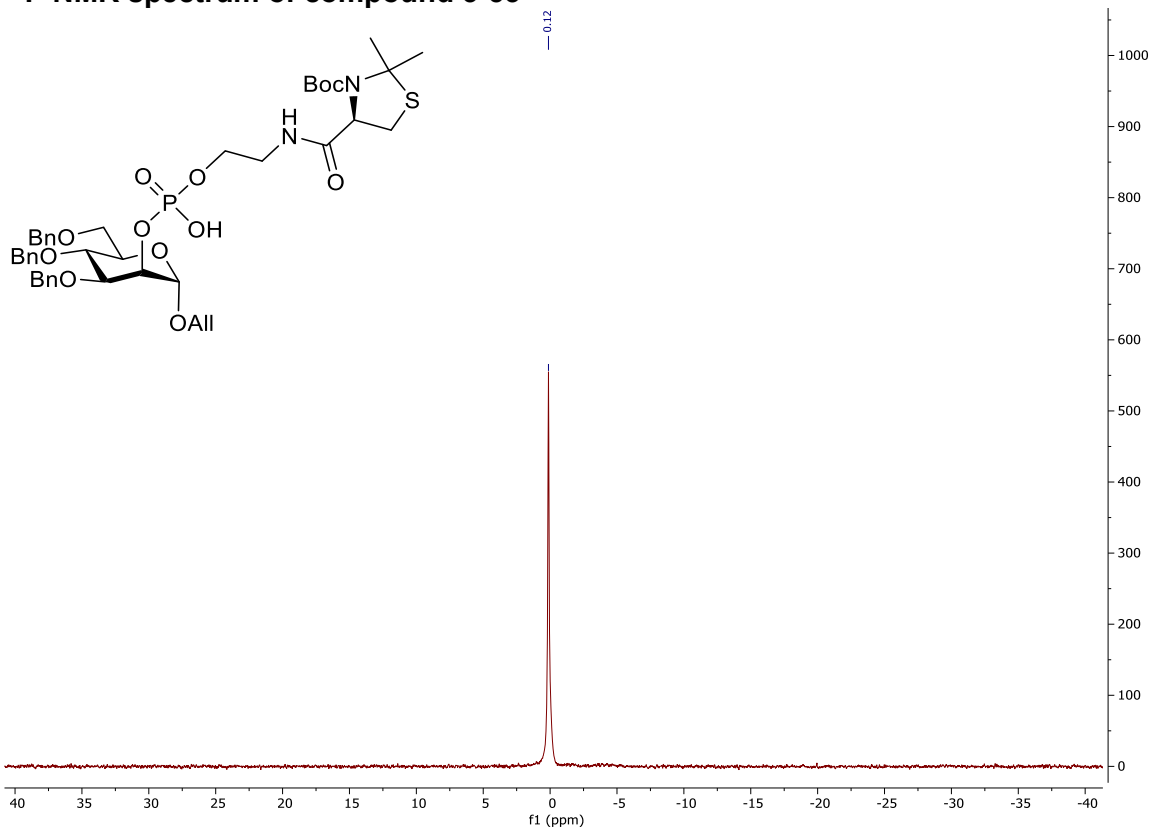

^{1}H NMR spectrum of compound 3-54

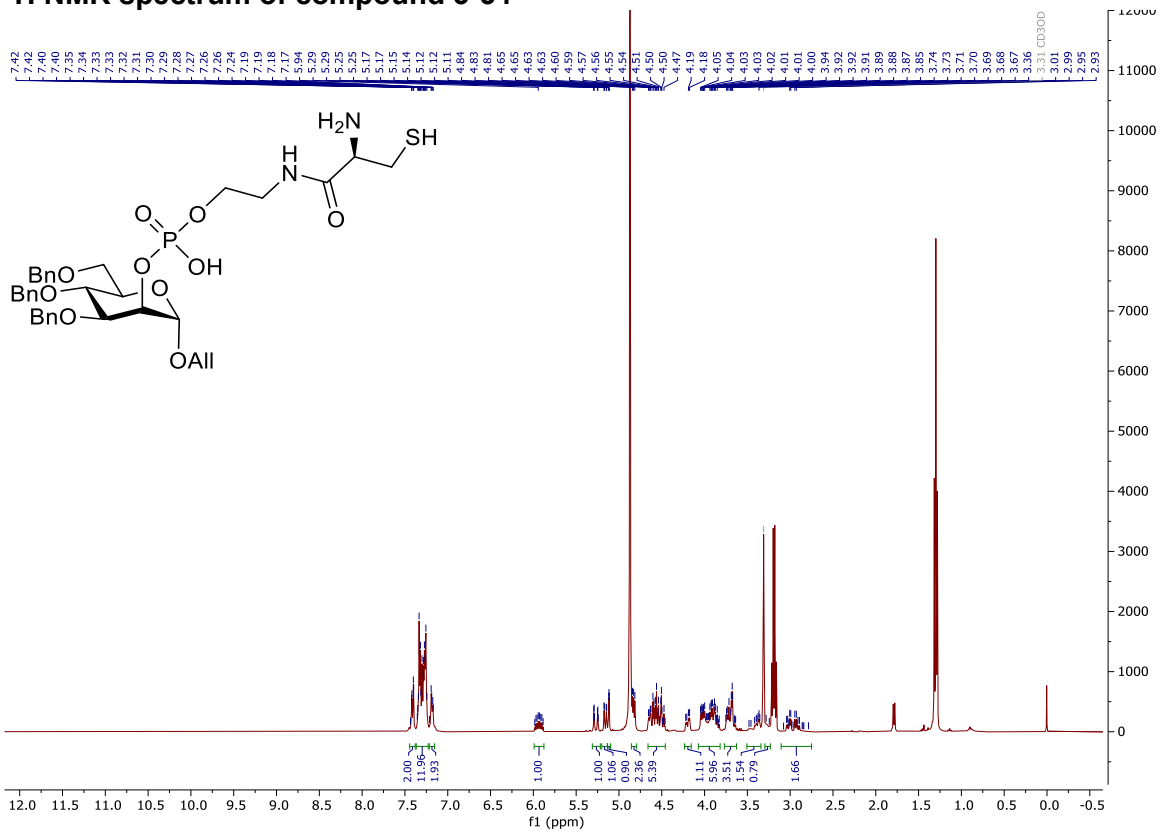

^{13}C NMR spectrum of compound 3-54

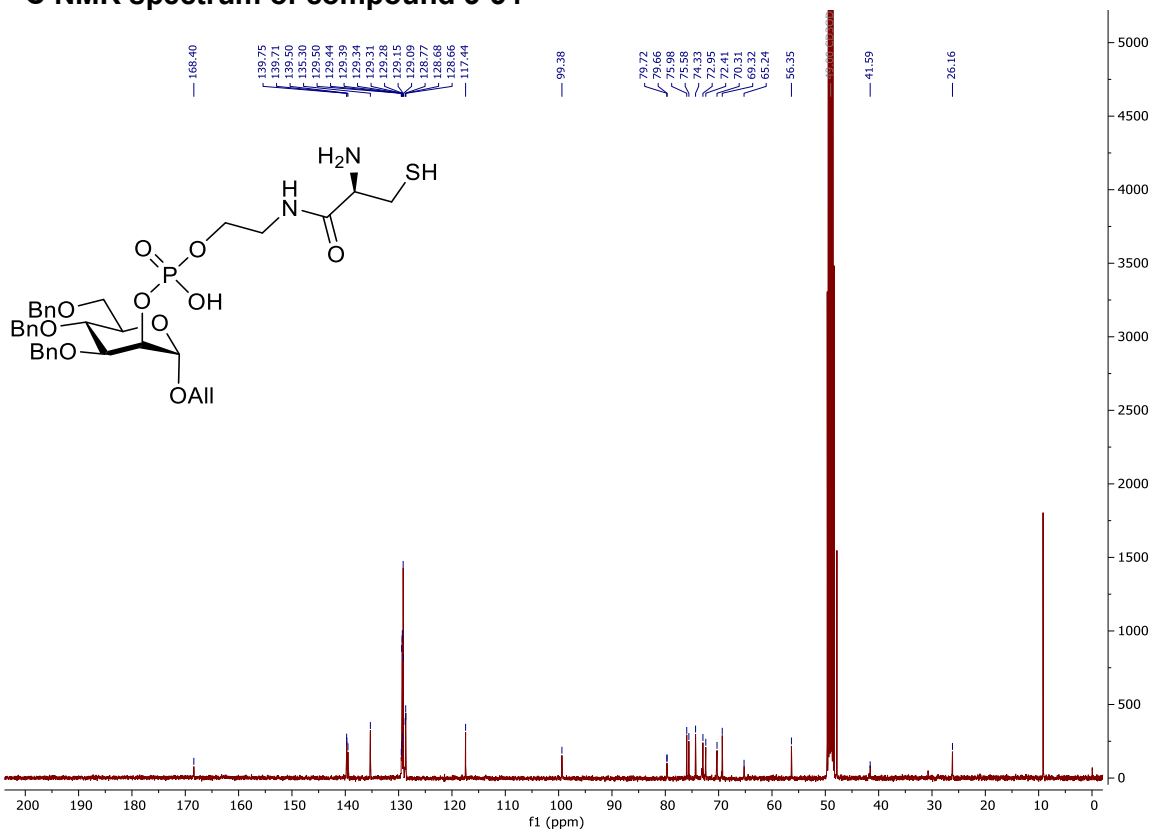

COSY-NMR spectrum of compound 3-54

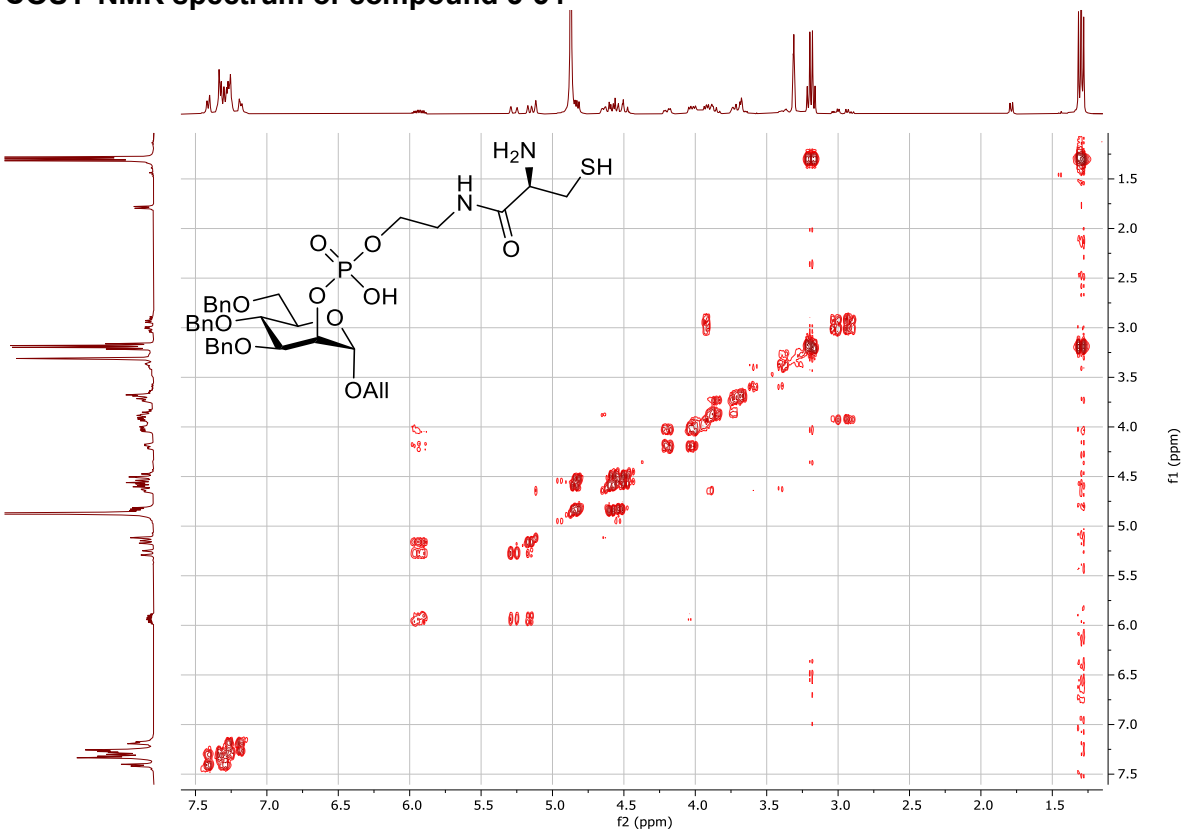

HSQC-NMR spectrum of compound 3-54

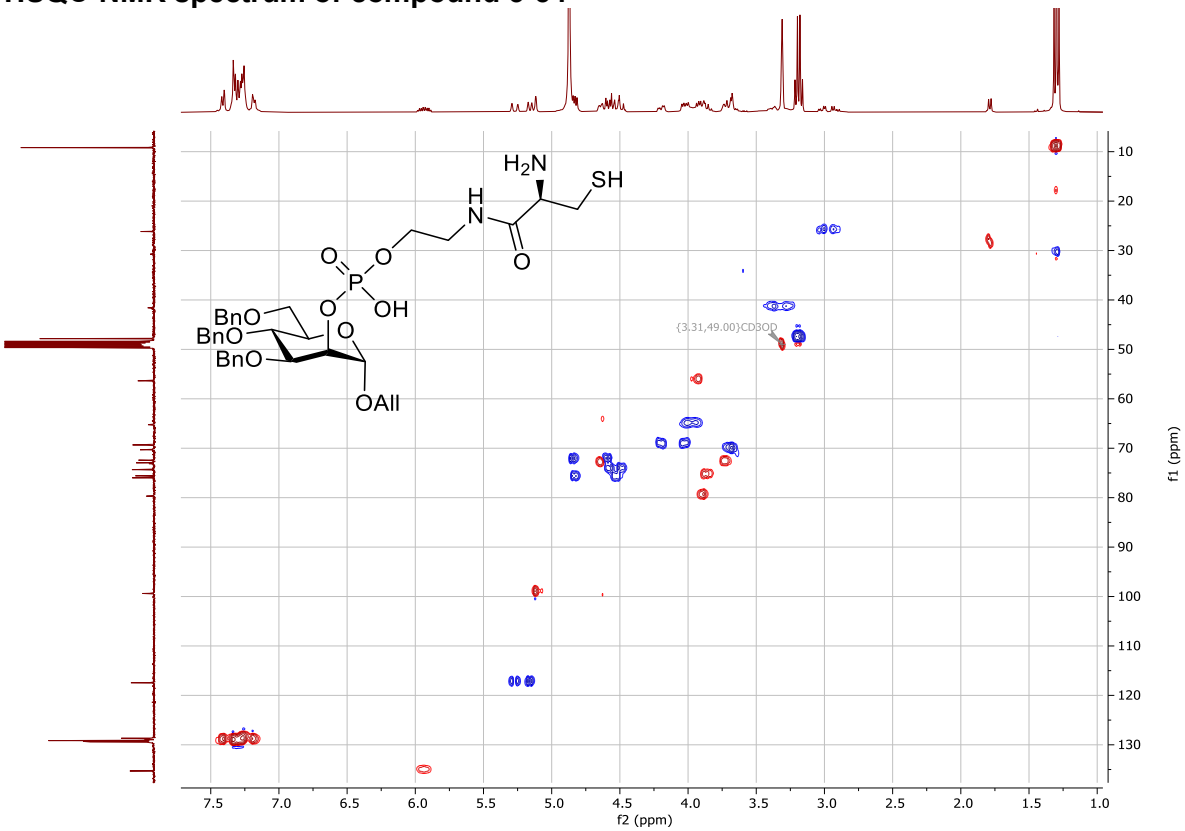

^{31}P NMR spectrum of compound 3-54

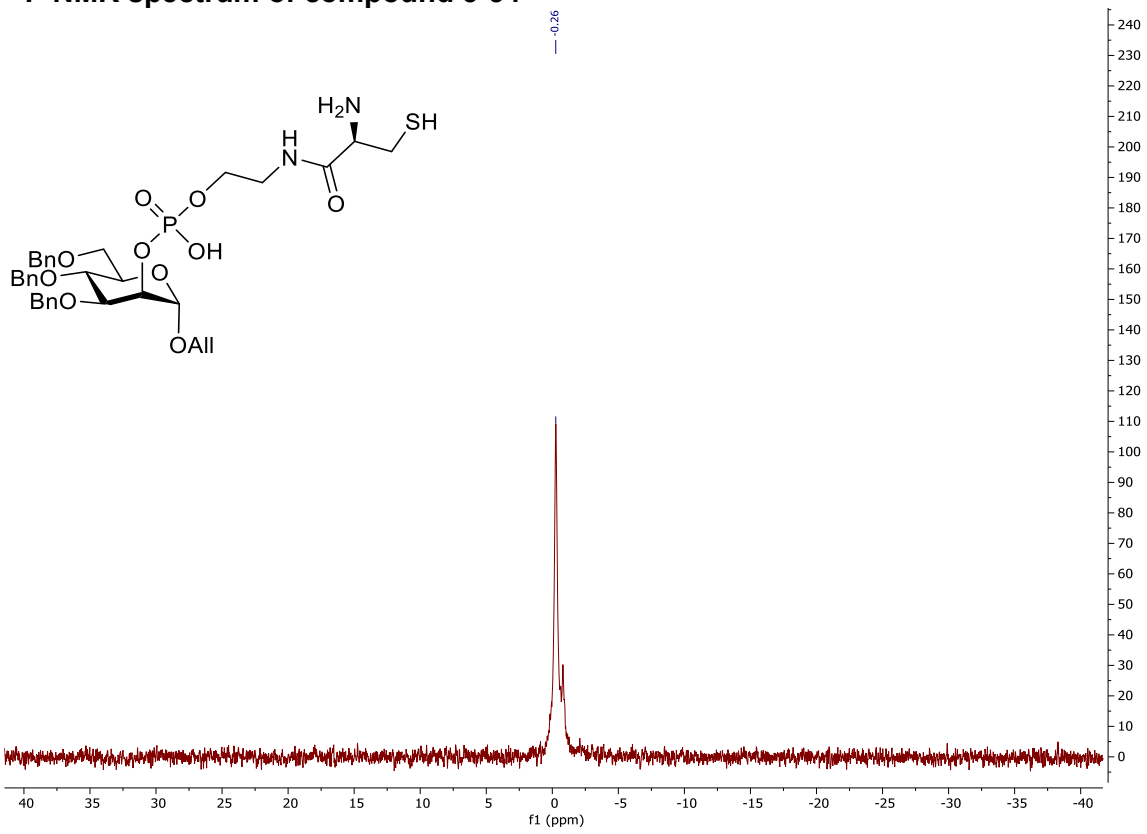

^{1}H NMR spectrum of compound 4-8

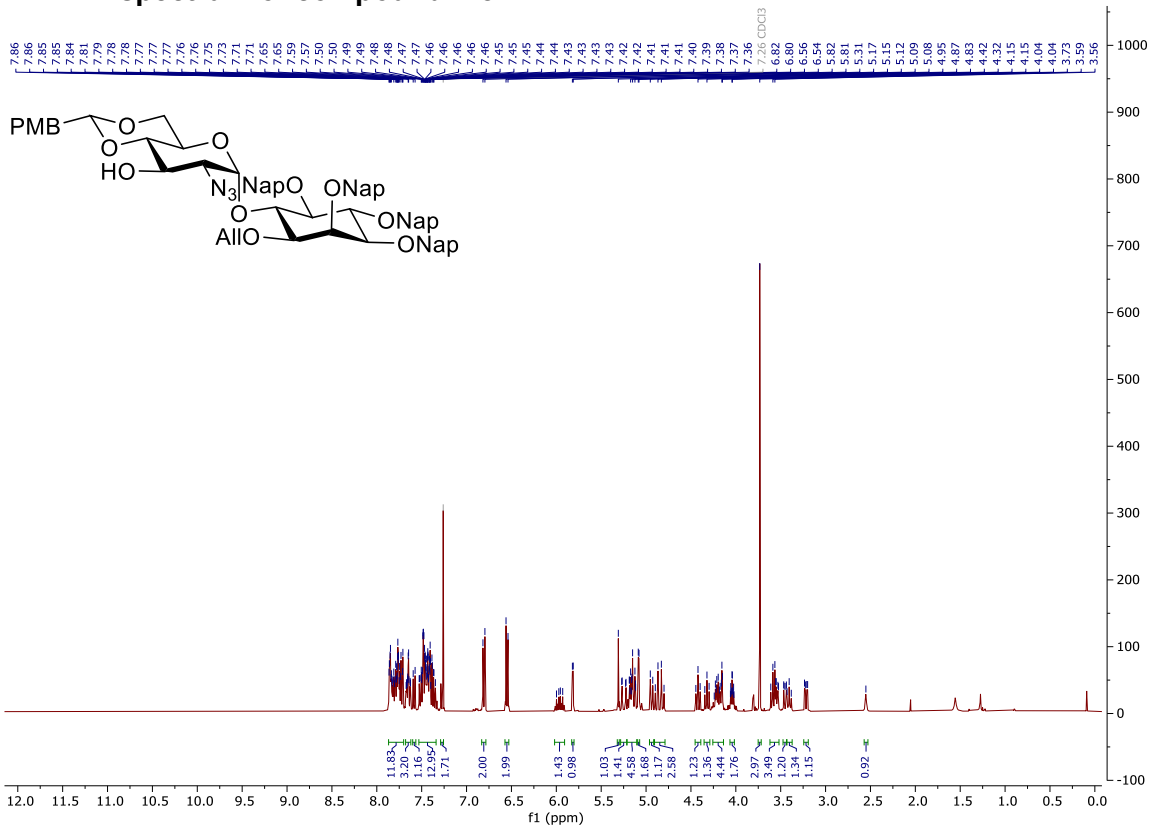

^{13}C NMR spectrum of compound 4-8

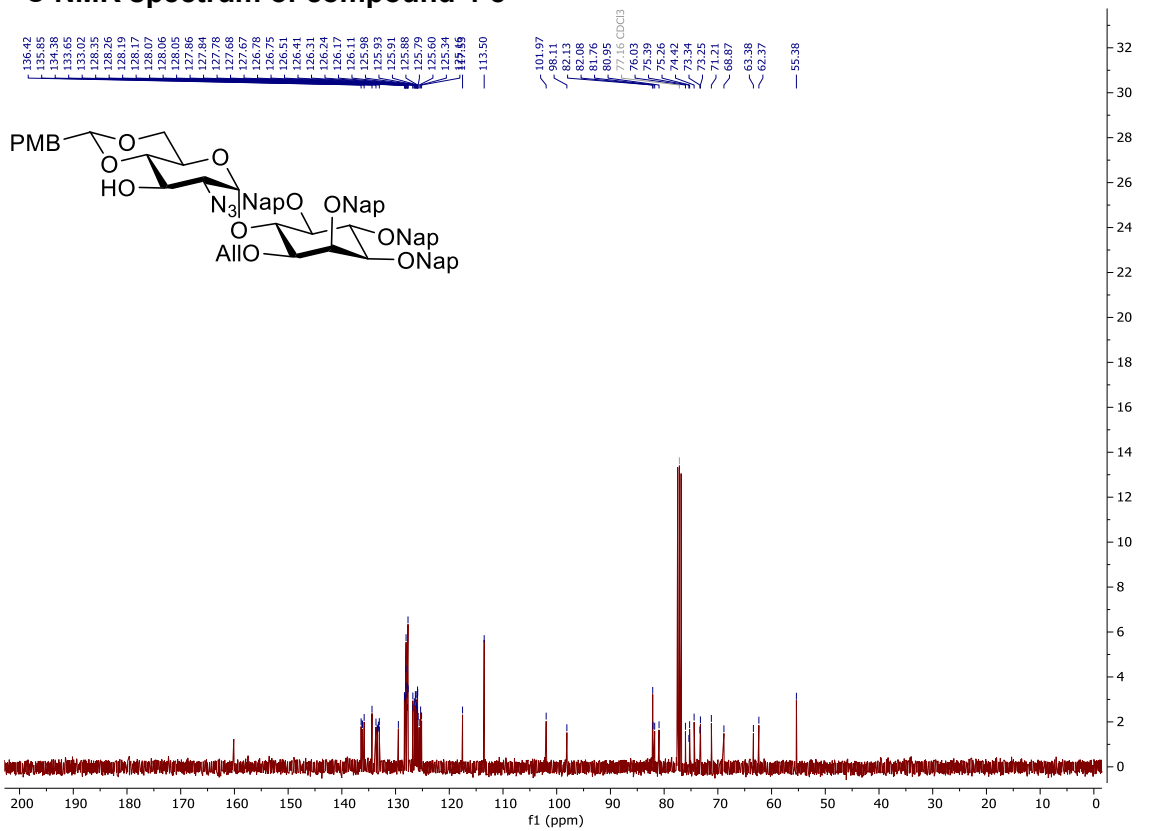

COSY-NMR spectrum of compound 4-8

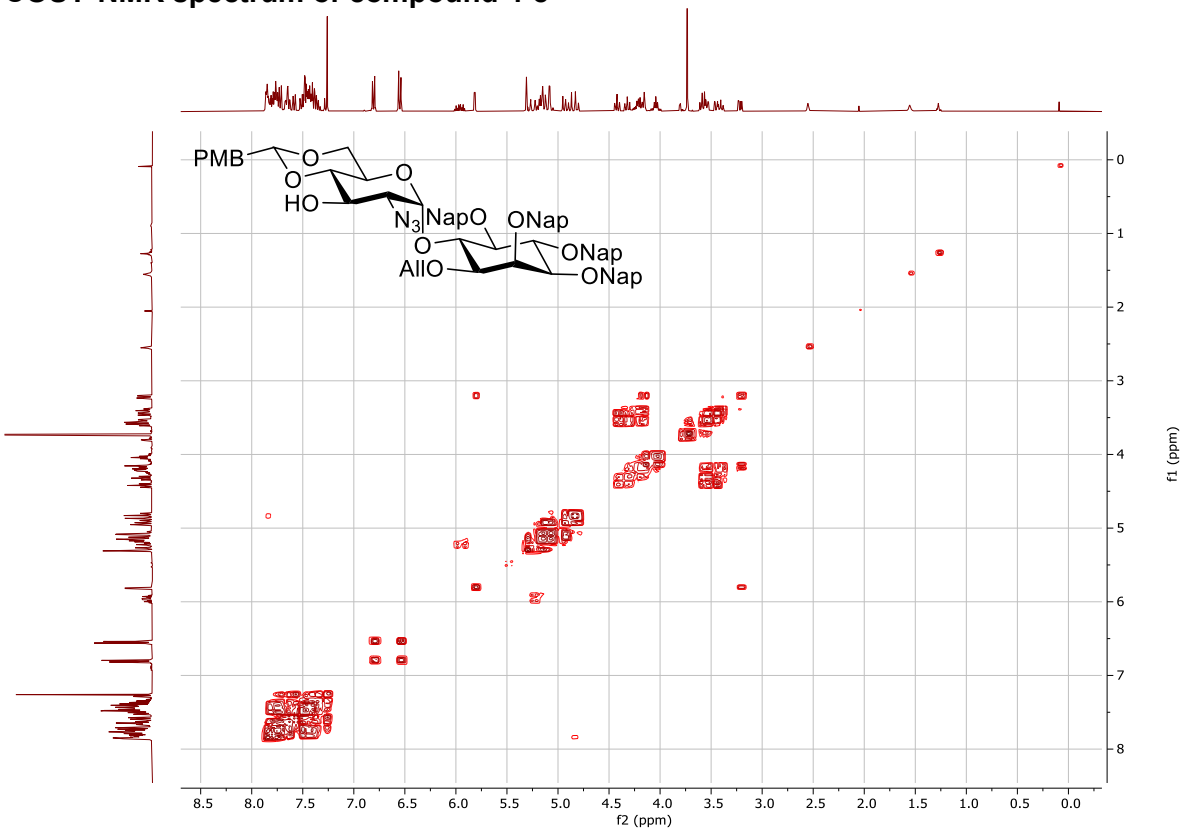

HSQC-NMR spectrum of compound 4-8

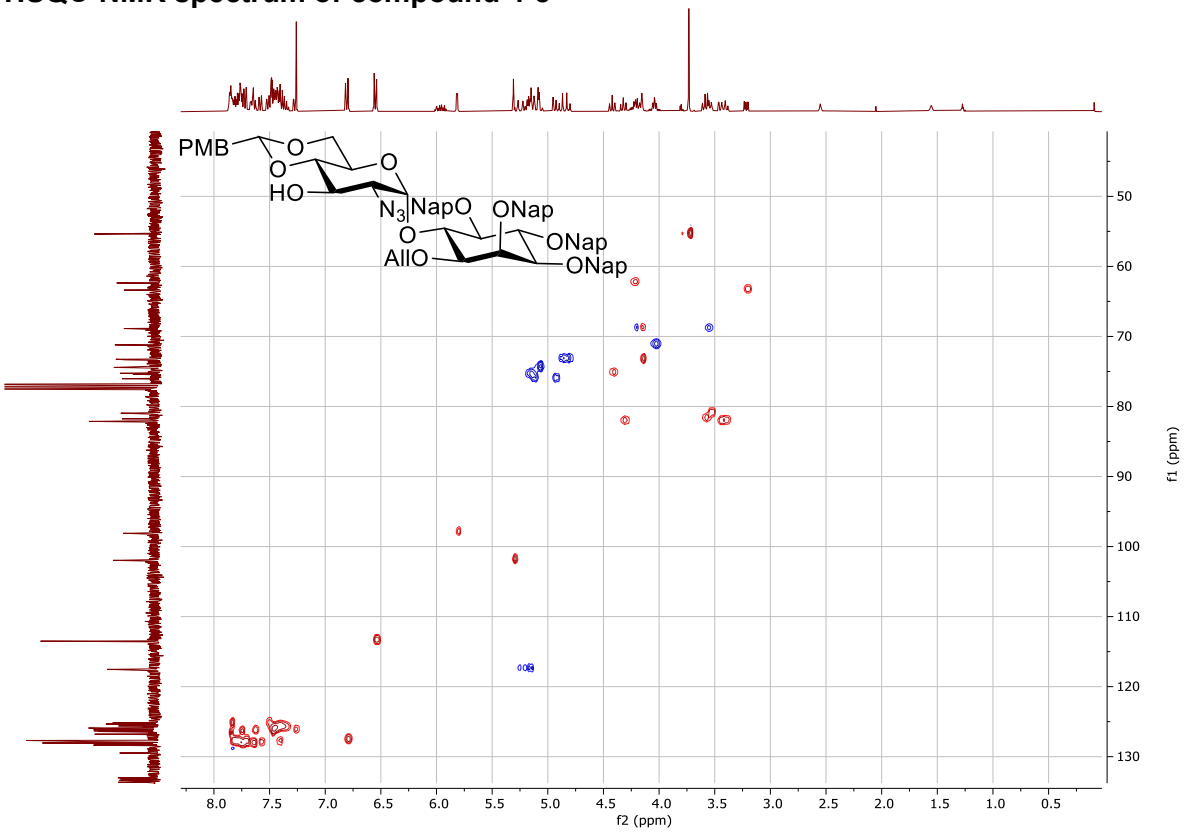

^{1}H NMR spectrum of compound 4-9

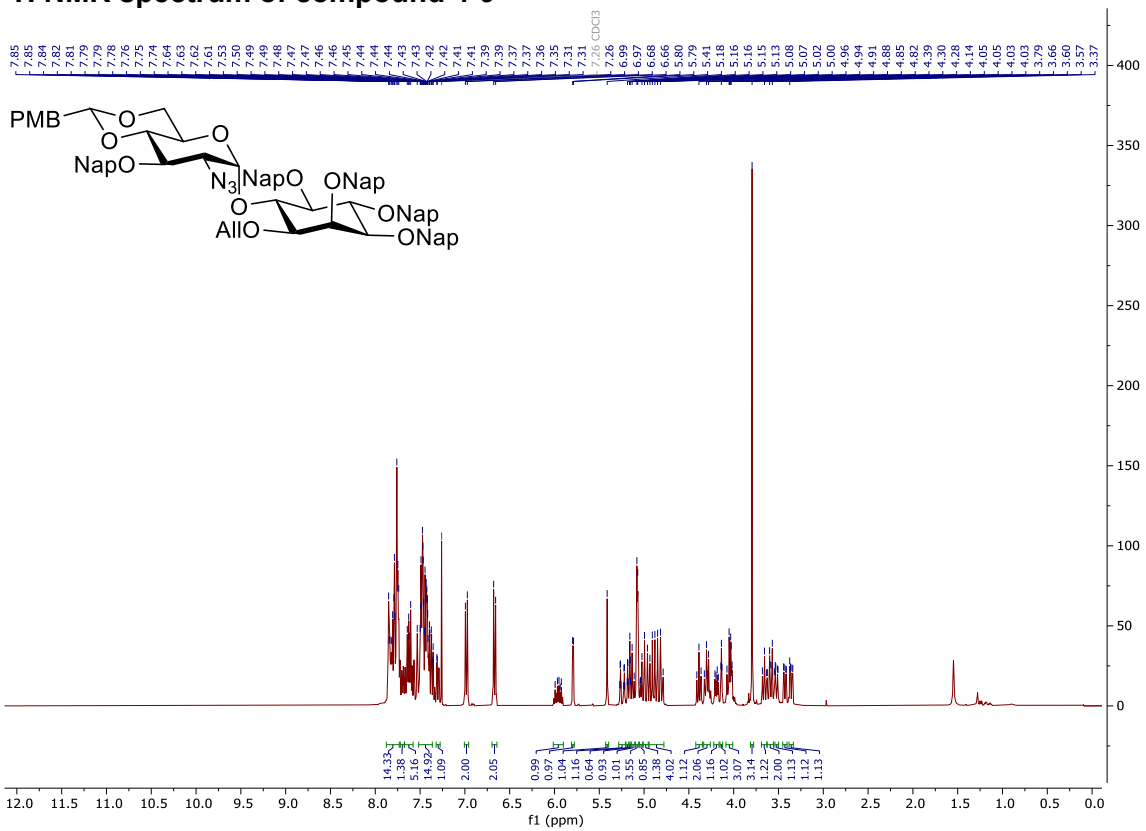

^{13}C NMR spectrum of compound 4-9

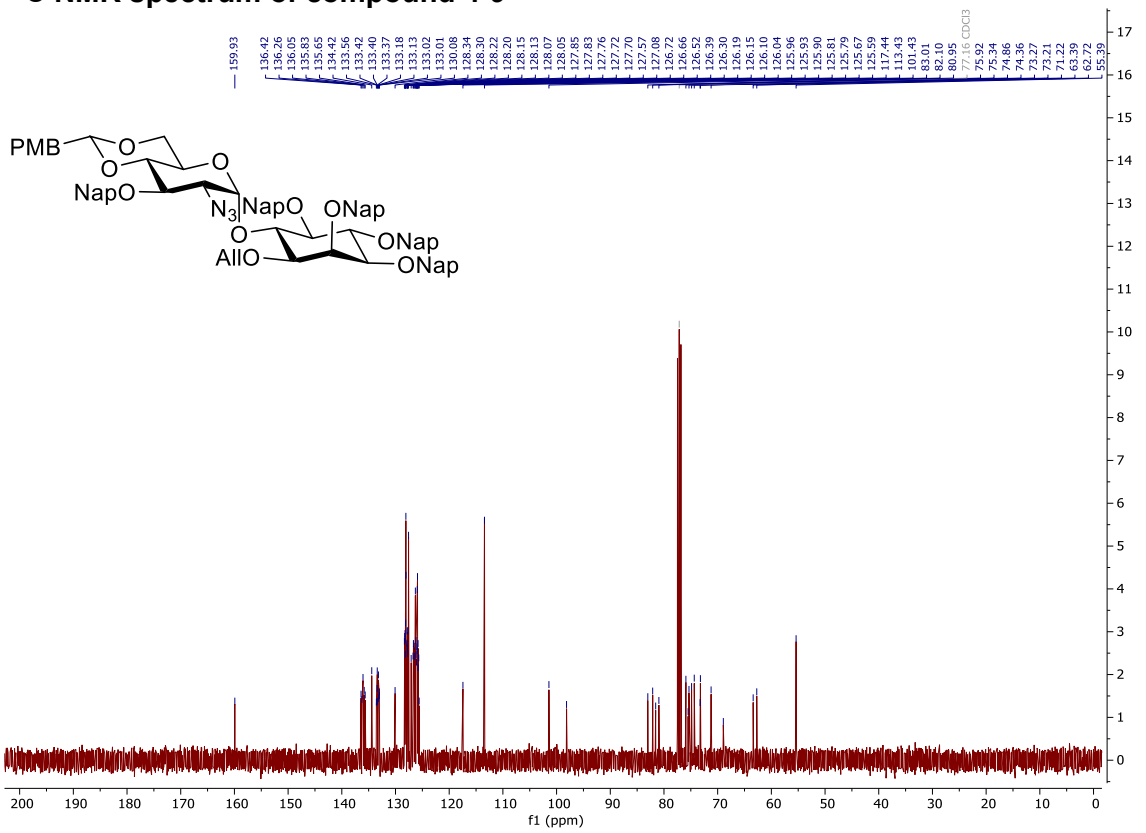

COSY-NMR spectrum of compound 4-9

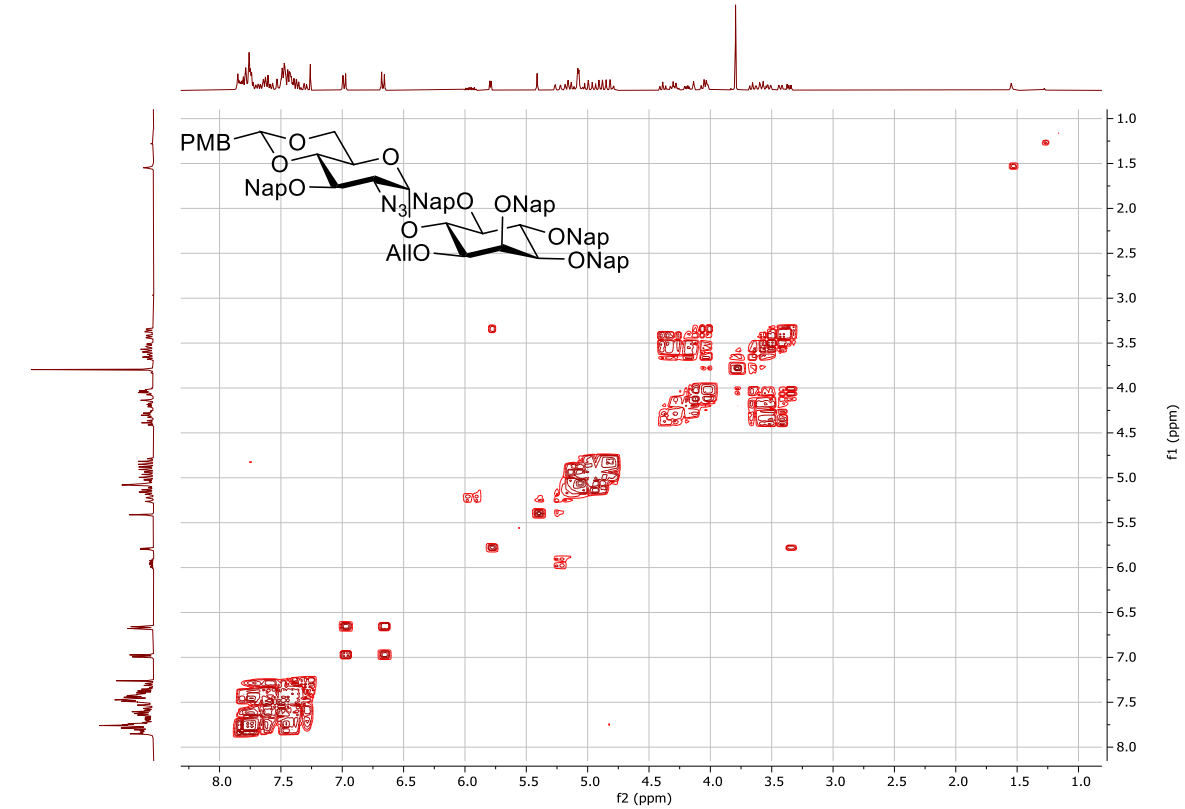

HSQC-NMR spectrum of compound 4-9

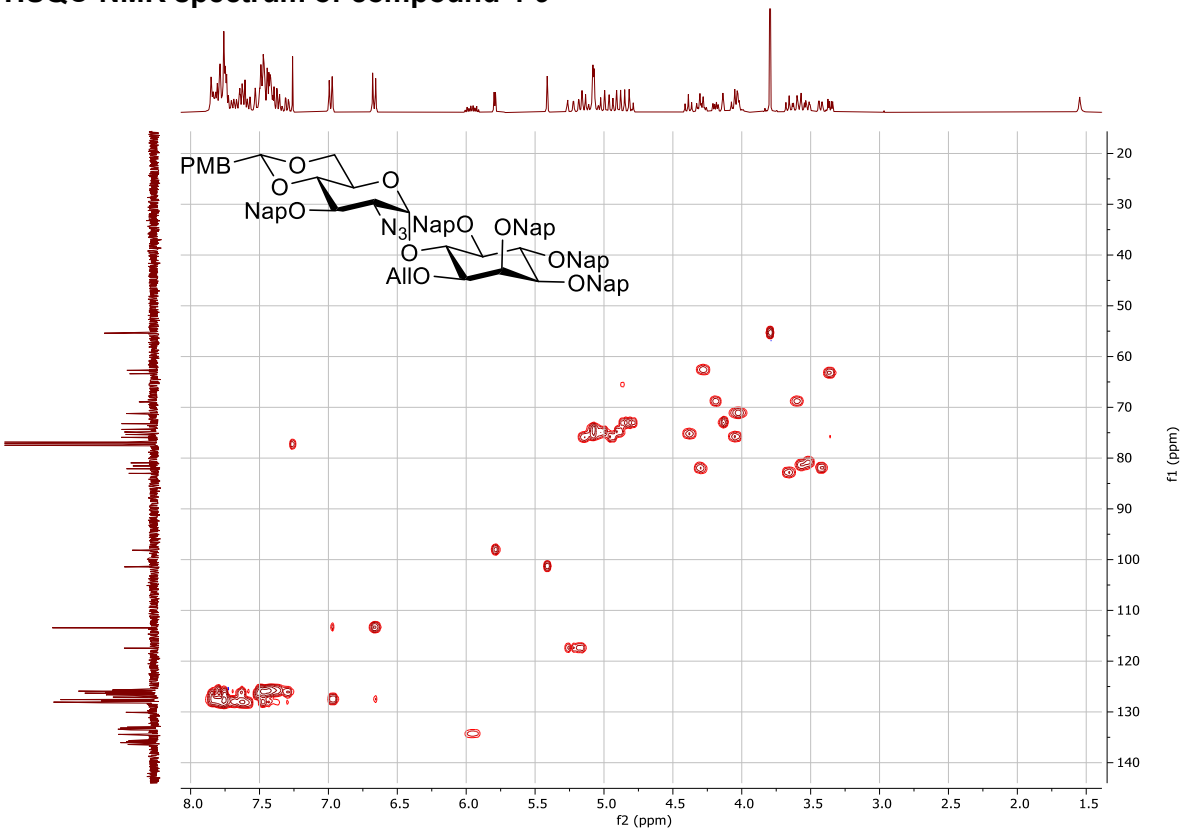

^{1}H NMR spectrum of compound 4-6

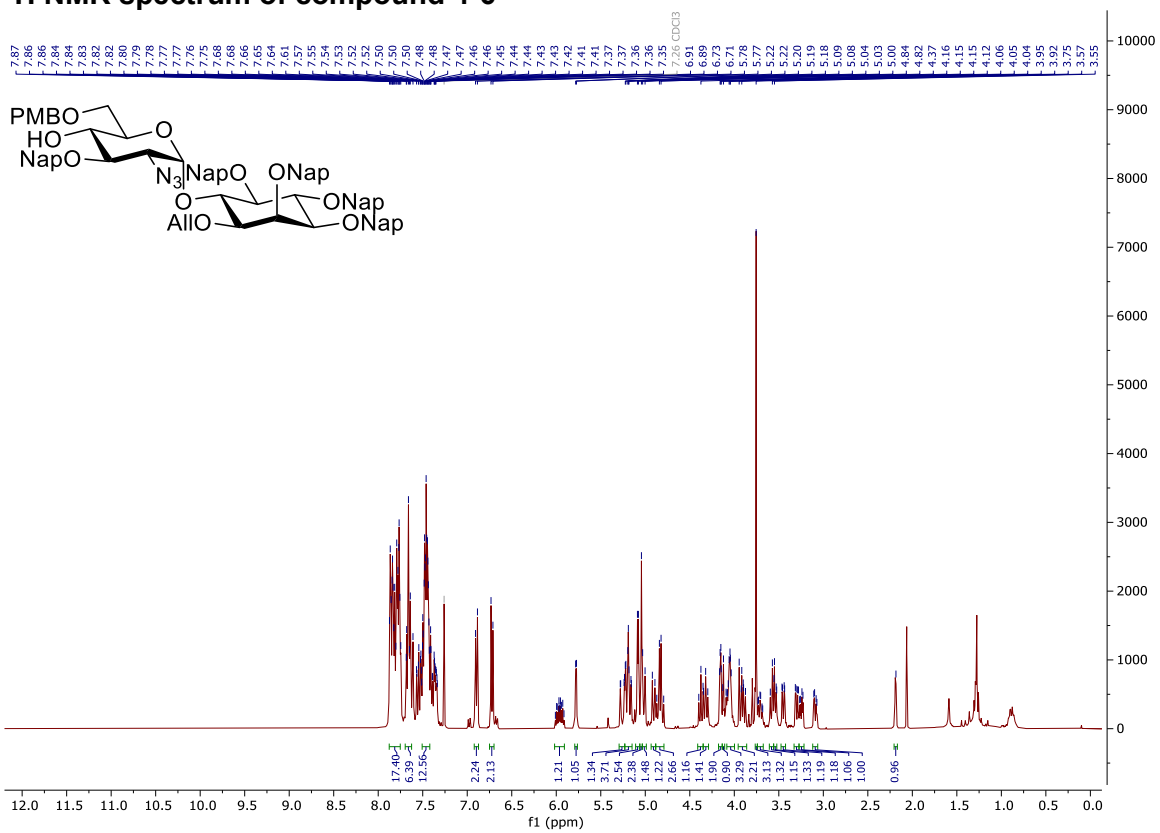

^{13}C NMR spectrum of compound 4-6

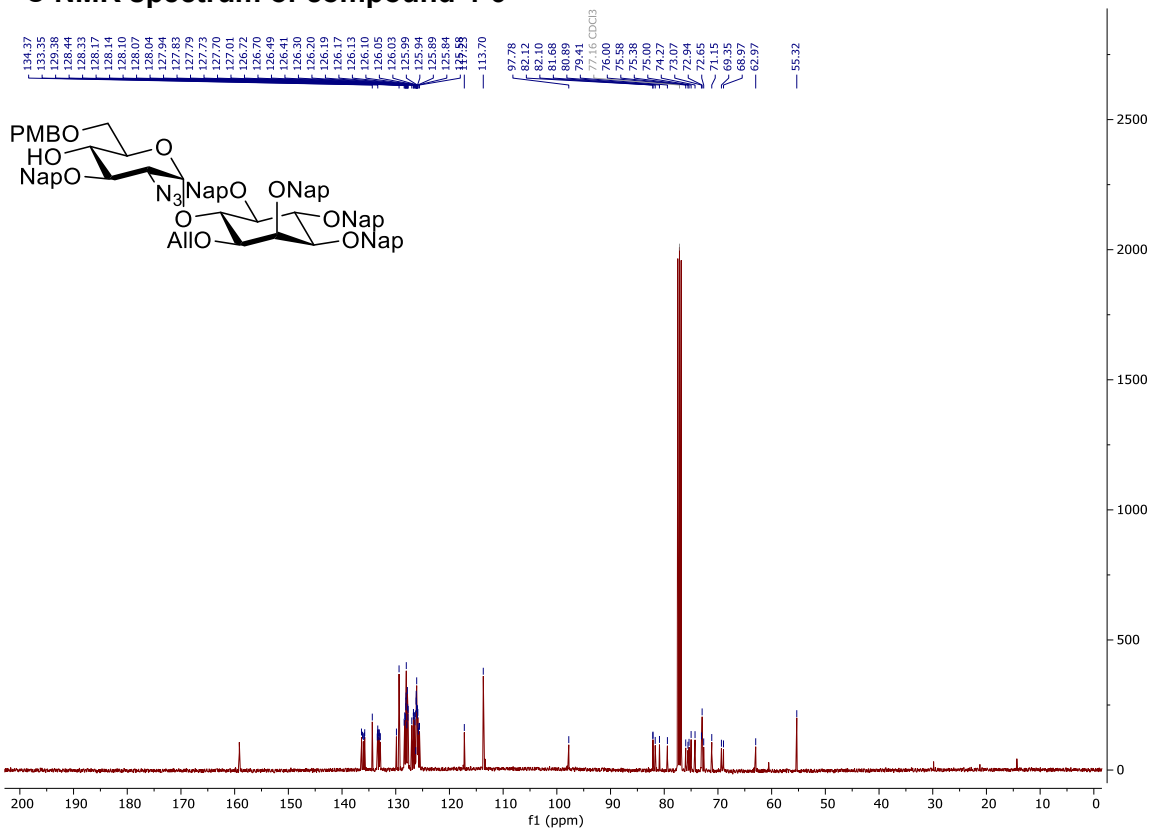

COSY-NMR spectrum of compound 4-6

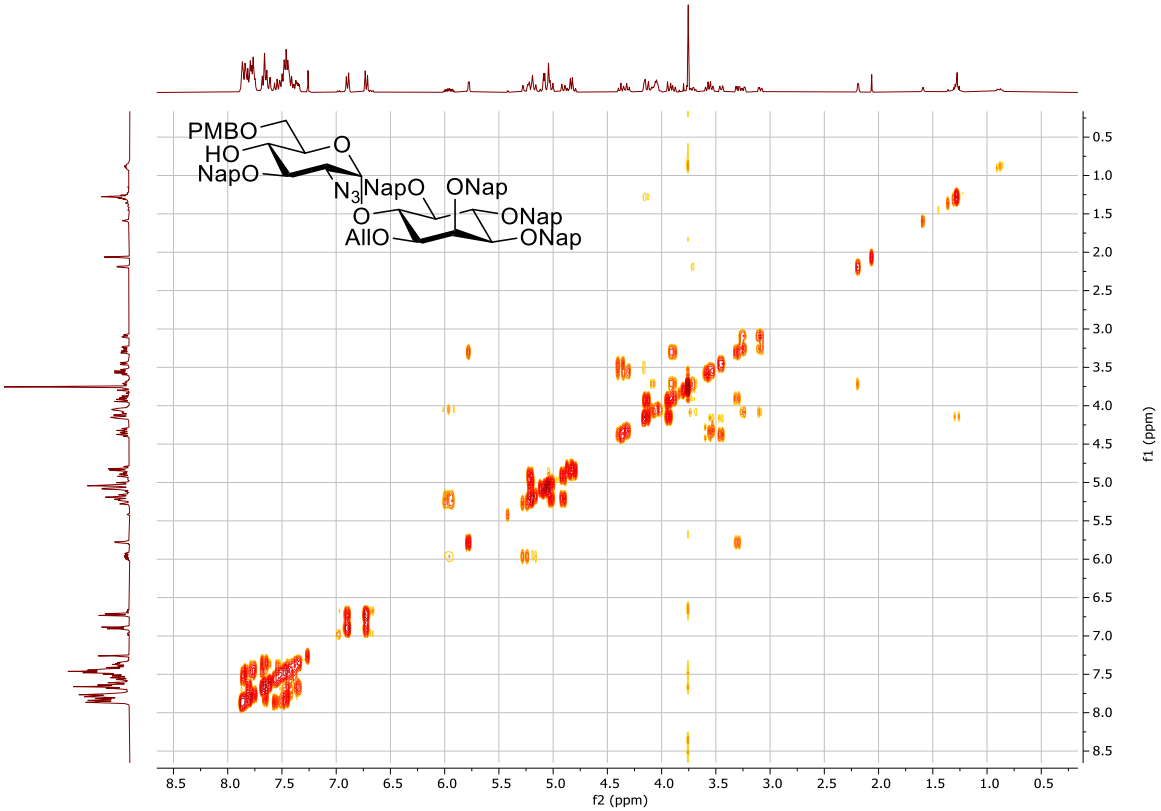

HSQC-NMR spectrum of compound 4-6

^{1}H NMR spectrum of compound 4-11

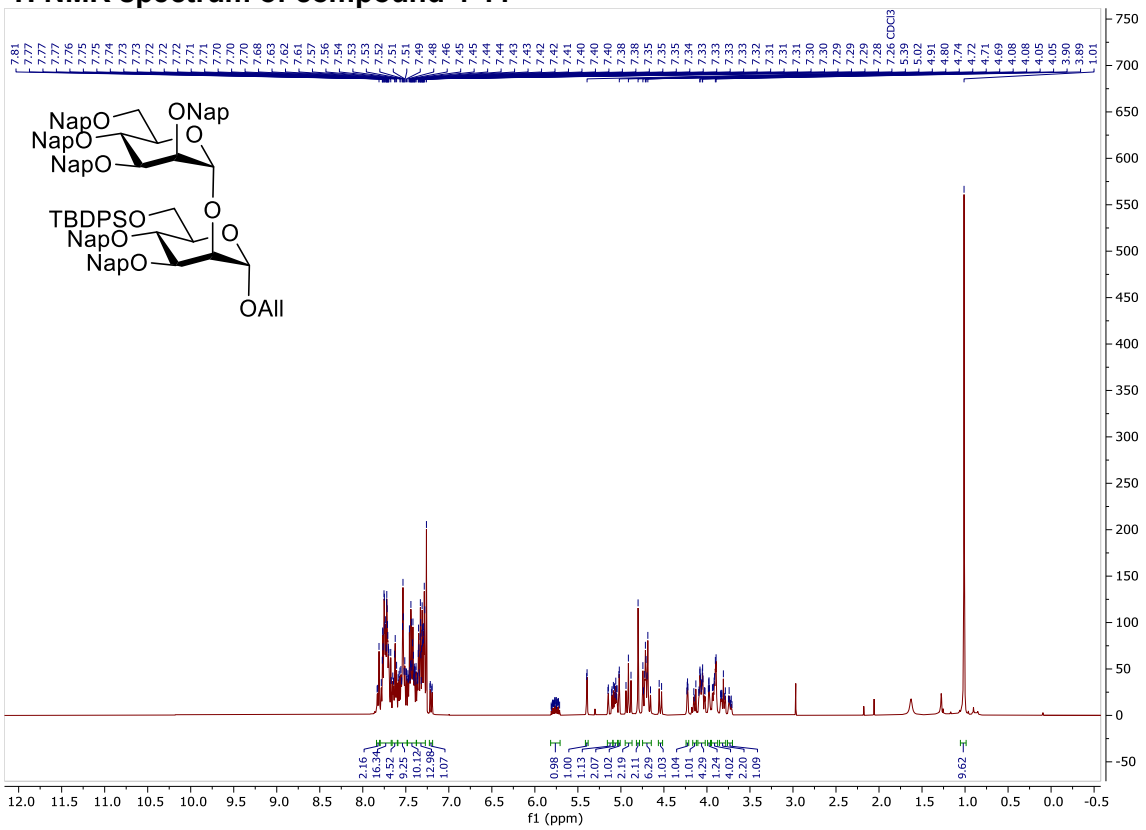

^{13}C NMR spectrum of compound 4-11

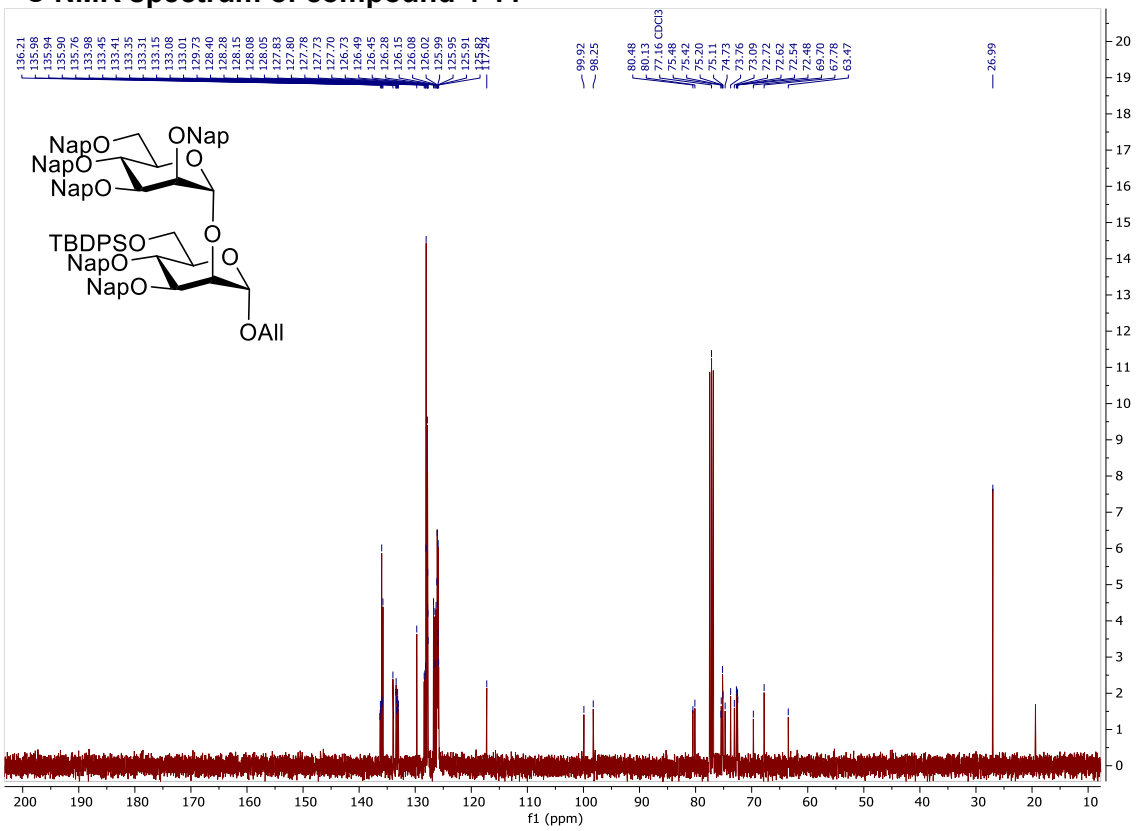

COSY NMR spectrum of compound 4-11

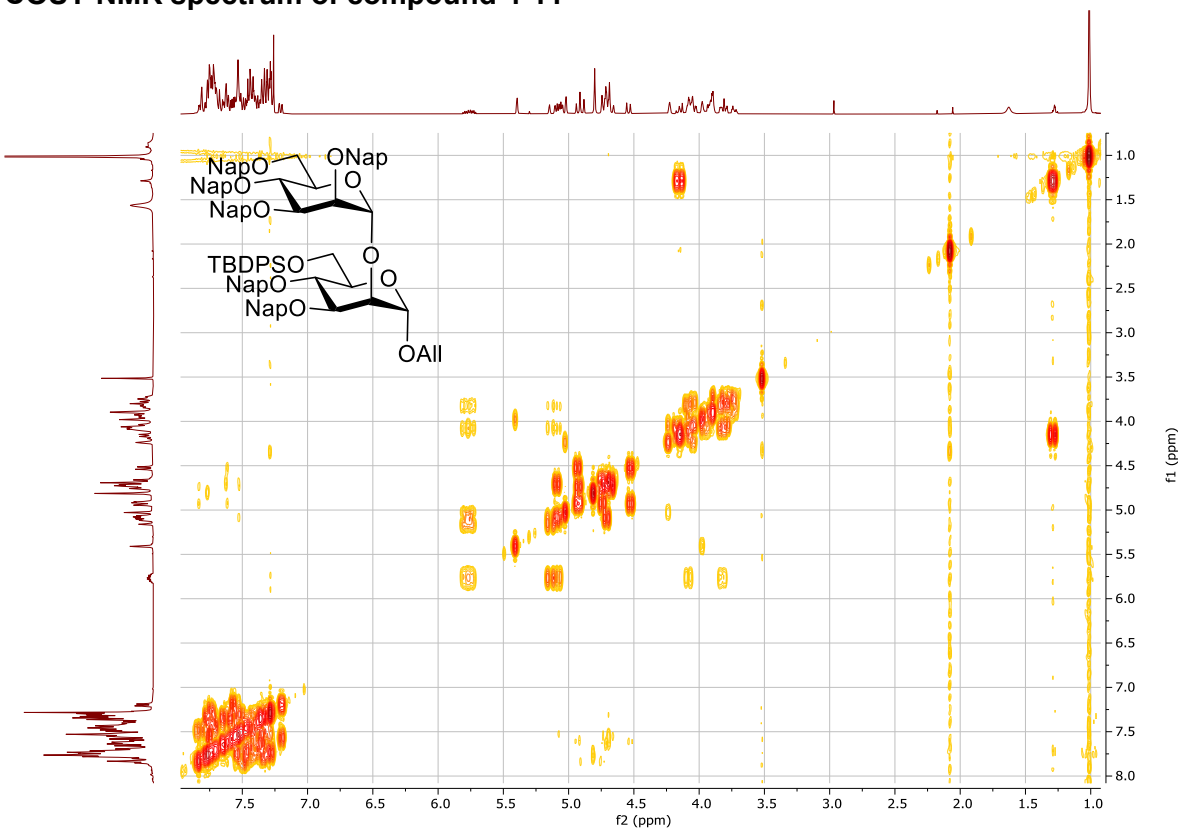

HSQC NMR spectrum of compound 4-11

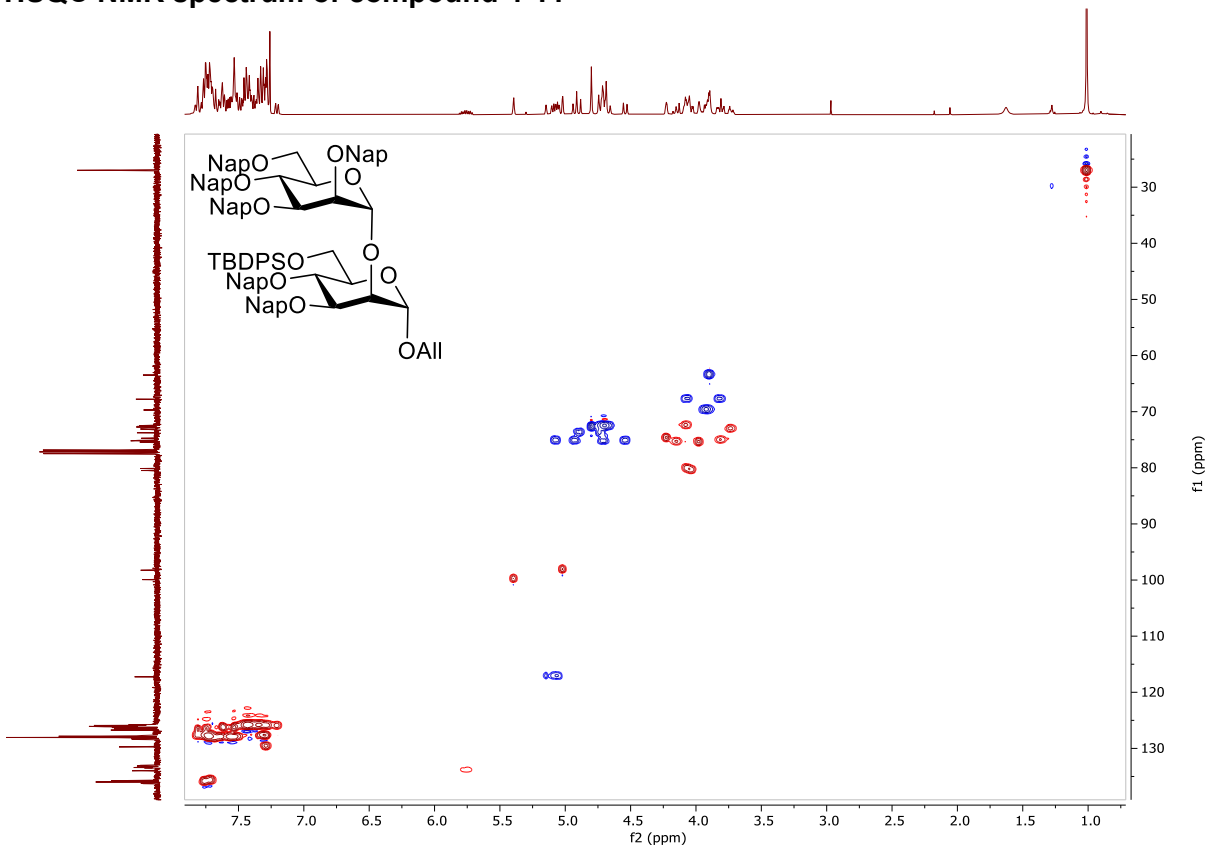

^{1}H NMR spectrum of compound 4-12

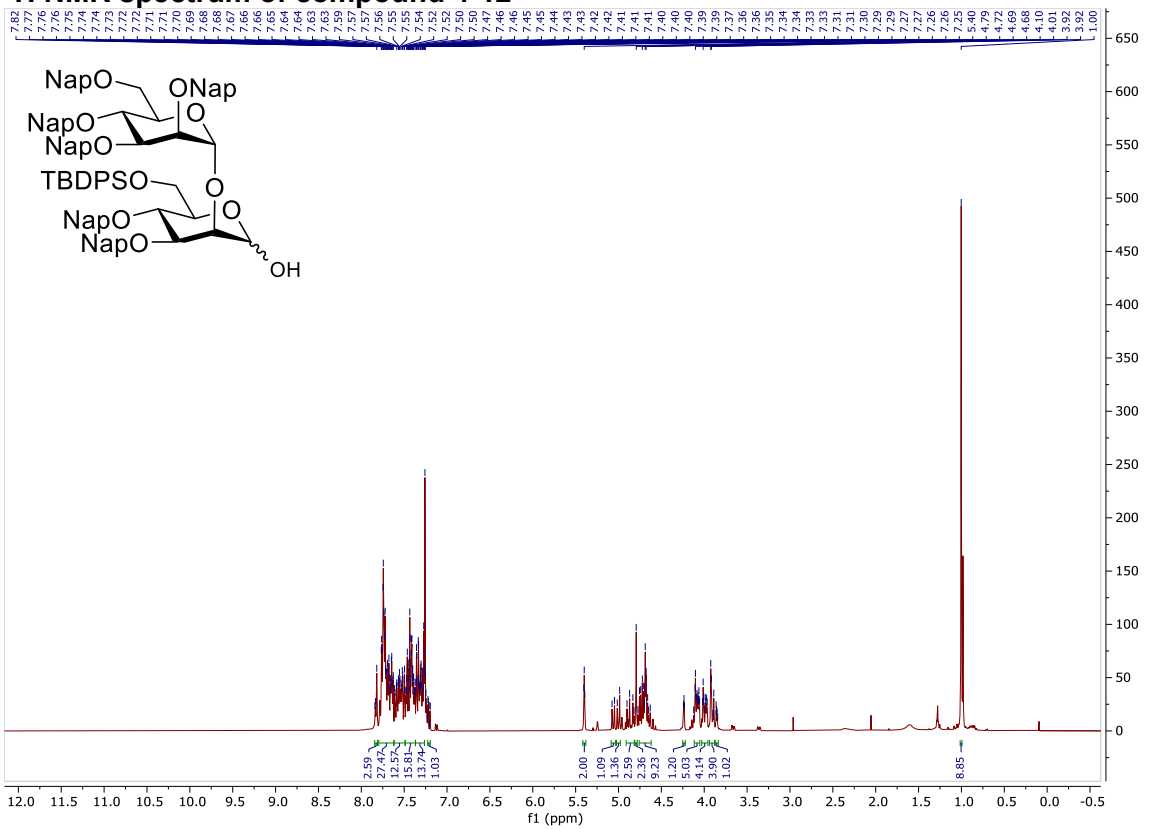

^{13}C NMR spectrum of compound 4-12

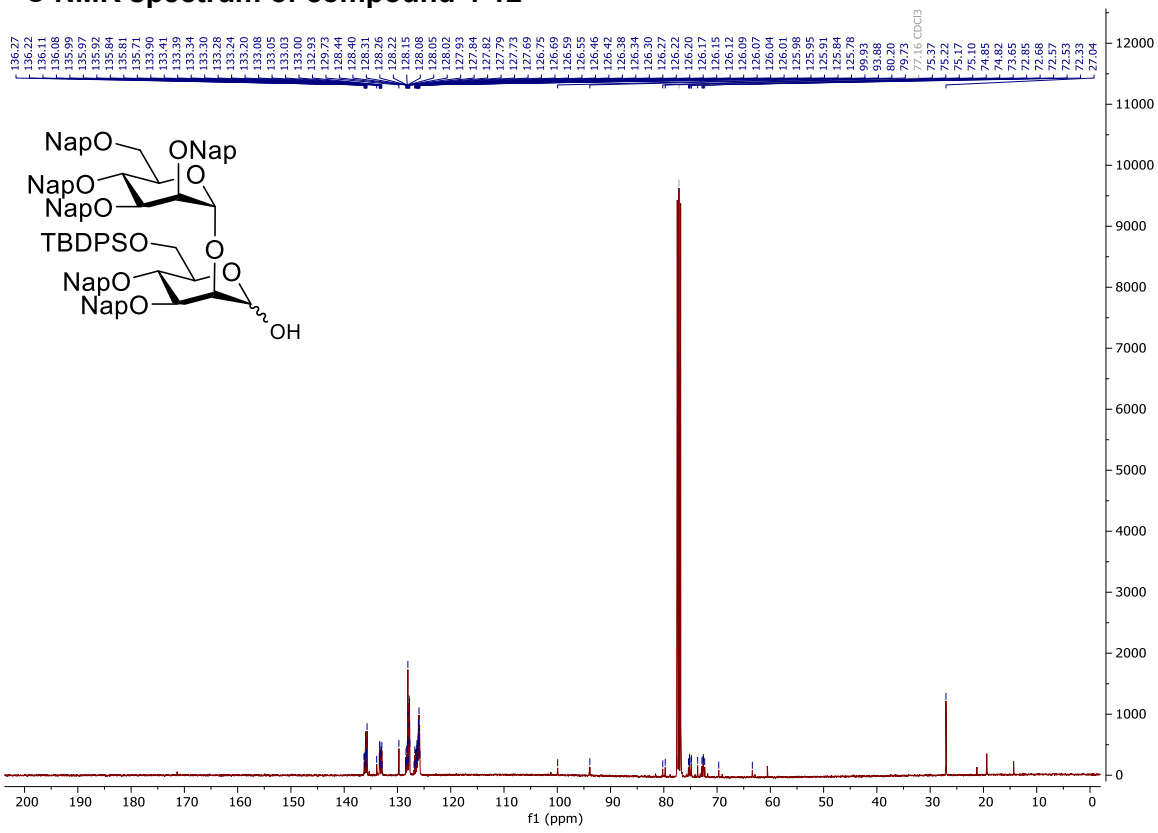

COSY NMR spectrum of compound 4-12

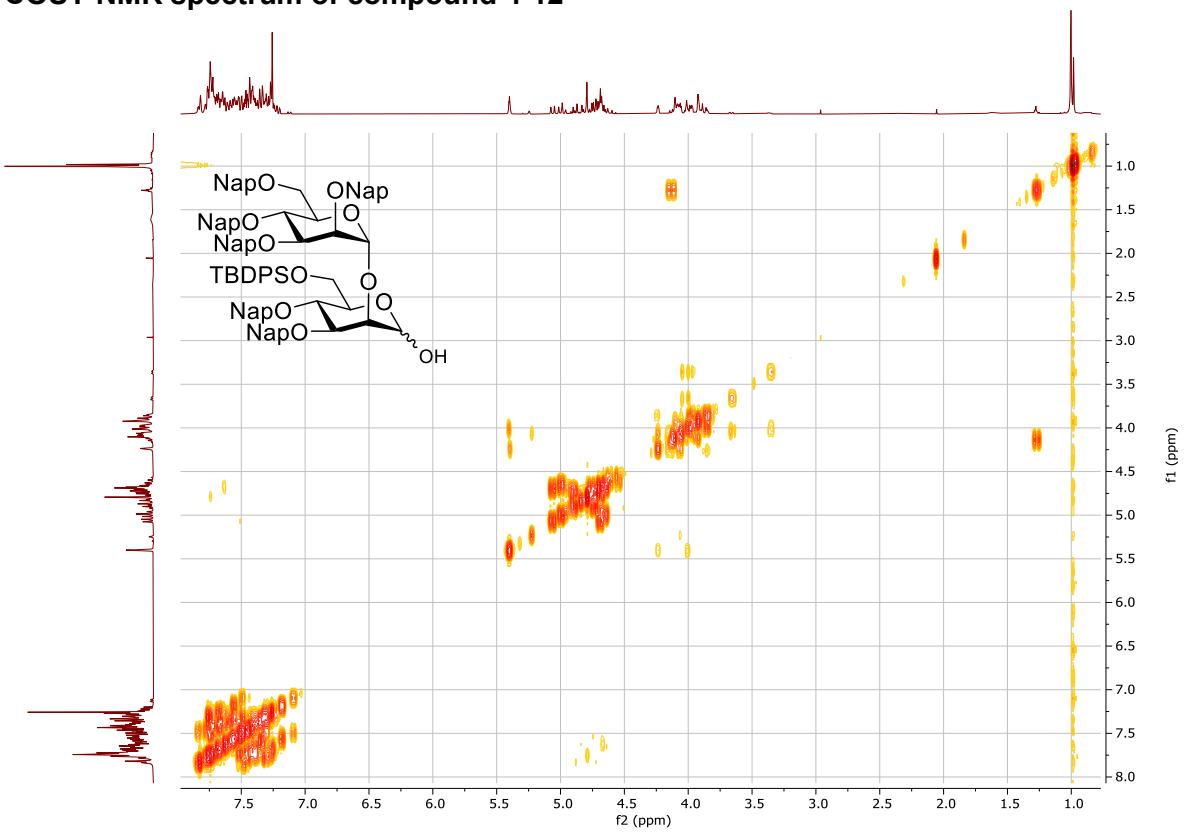

HSQC NMR spectrum of compound 4-12

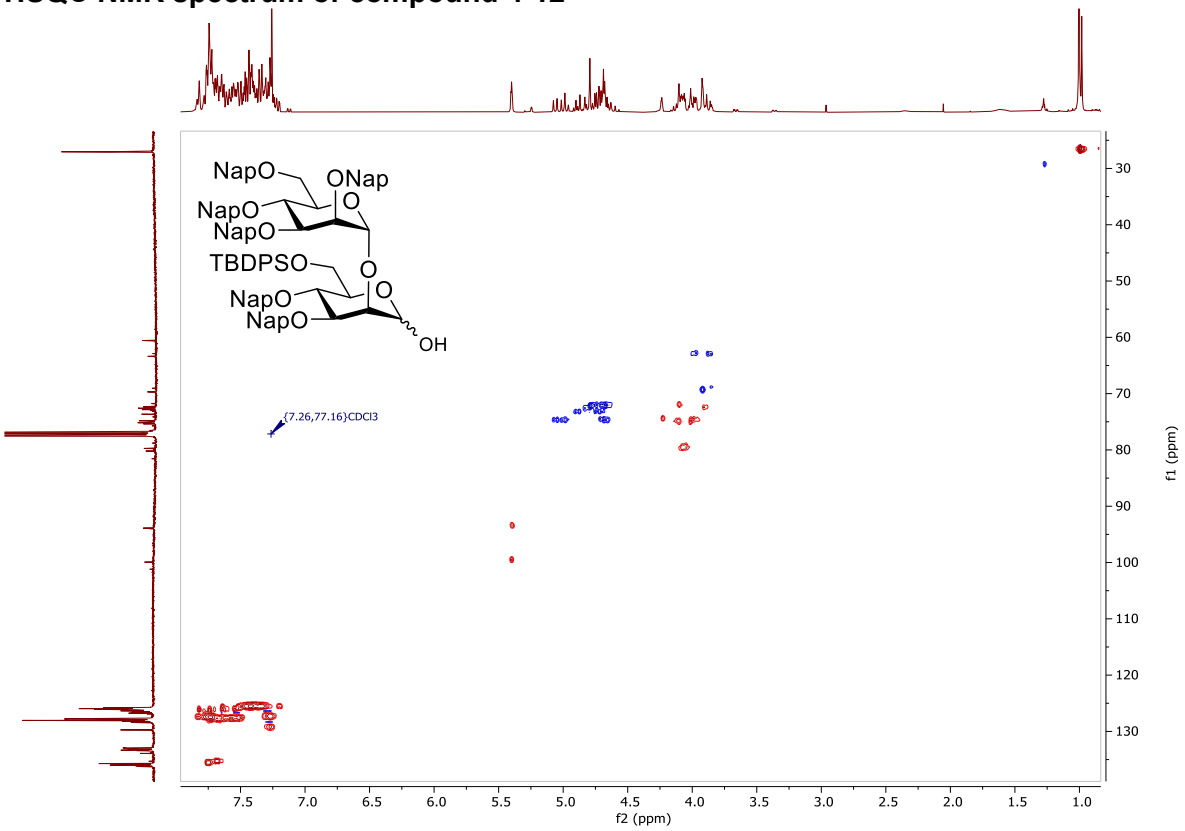

^{1}H NMR spectrum of compound 4-7

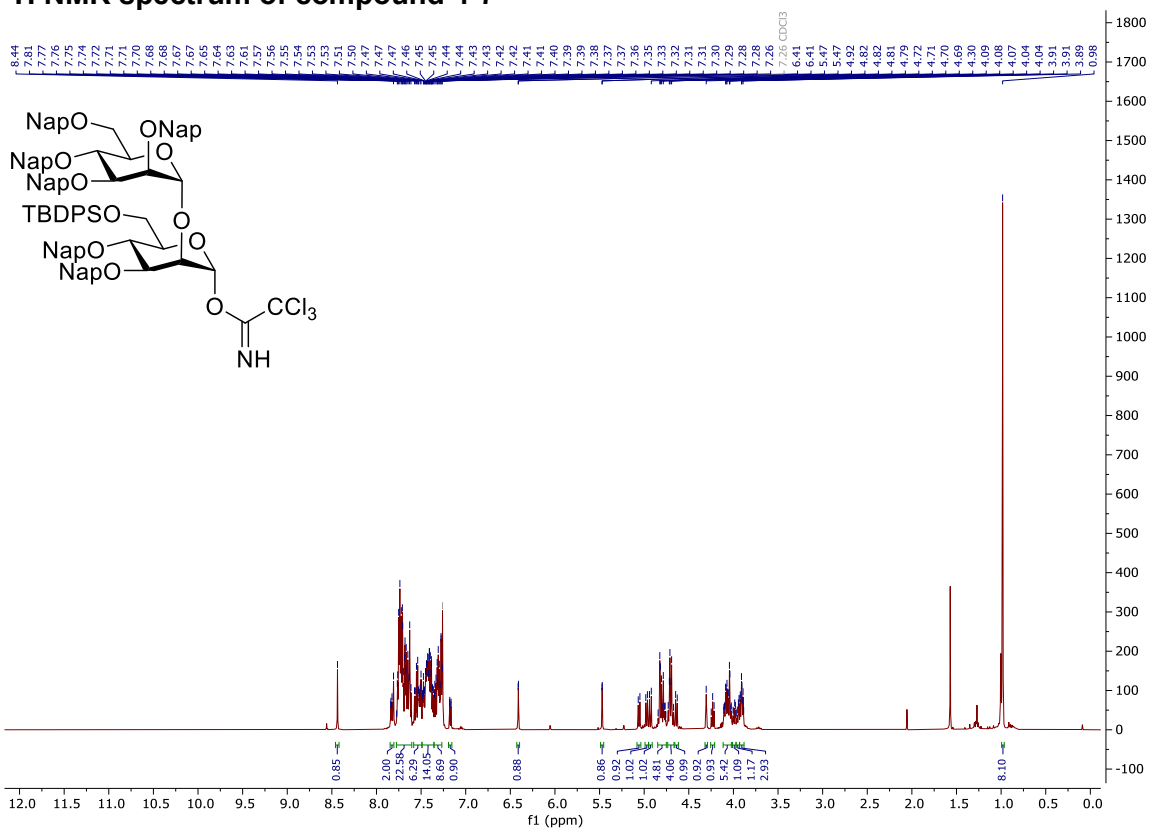

^{13}C NMR spectrum of compound 4-7

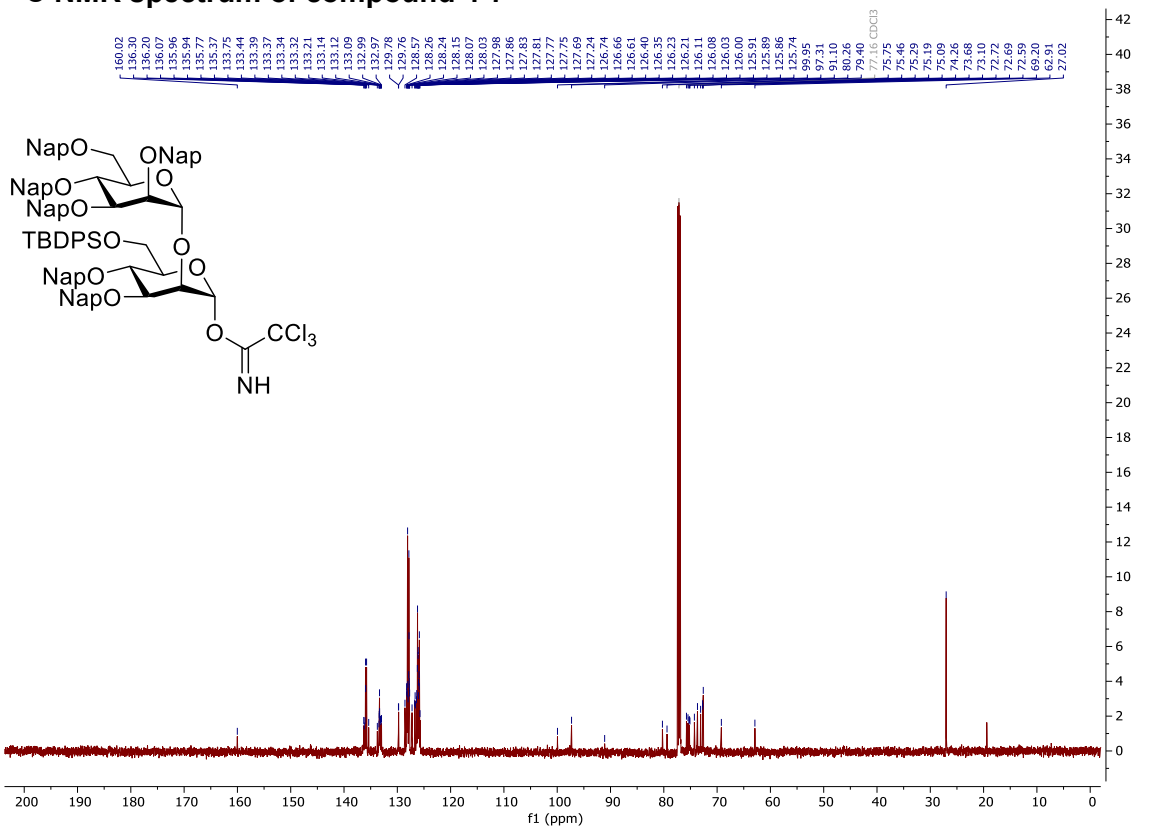

COSY NMR spectrum of compound 4-7

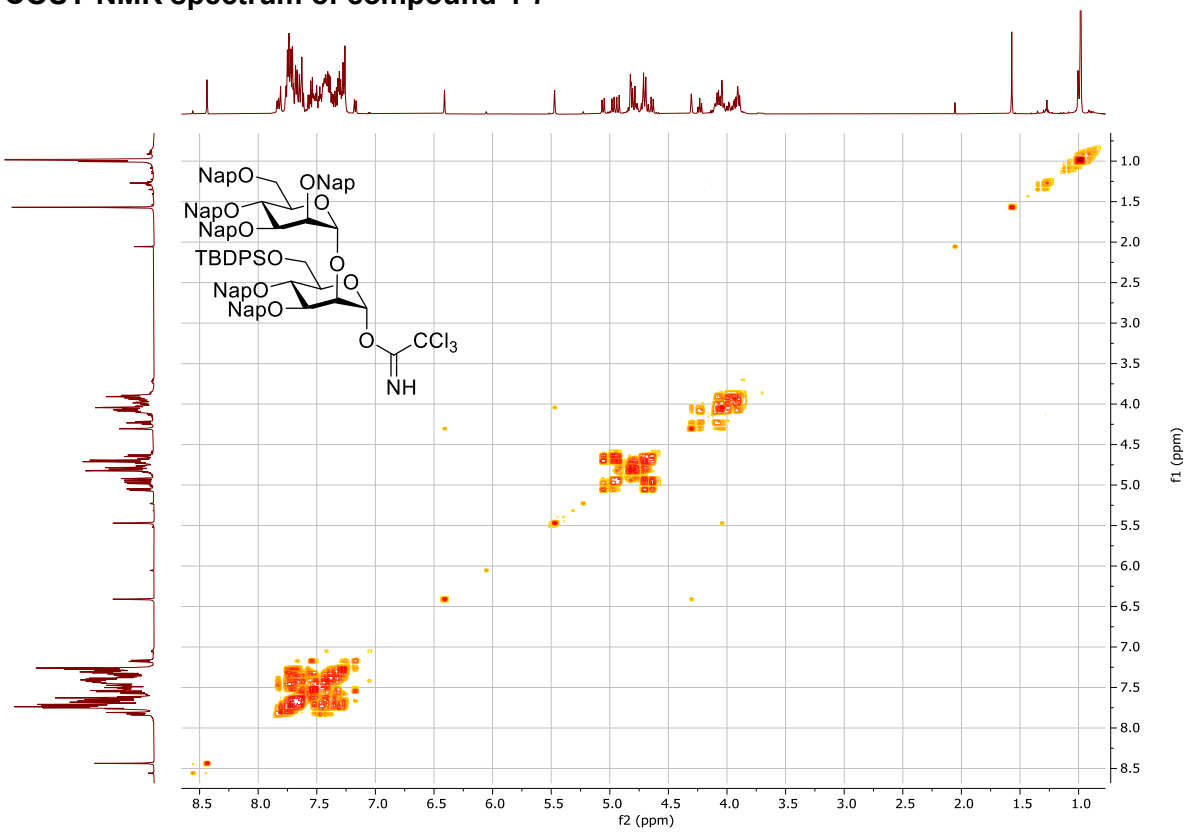

HSQC NMR spectrum of compound 4-7

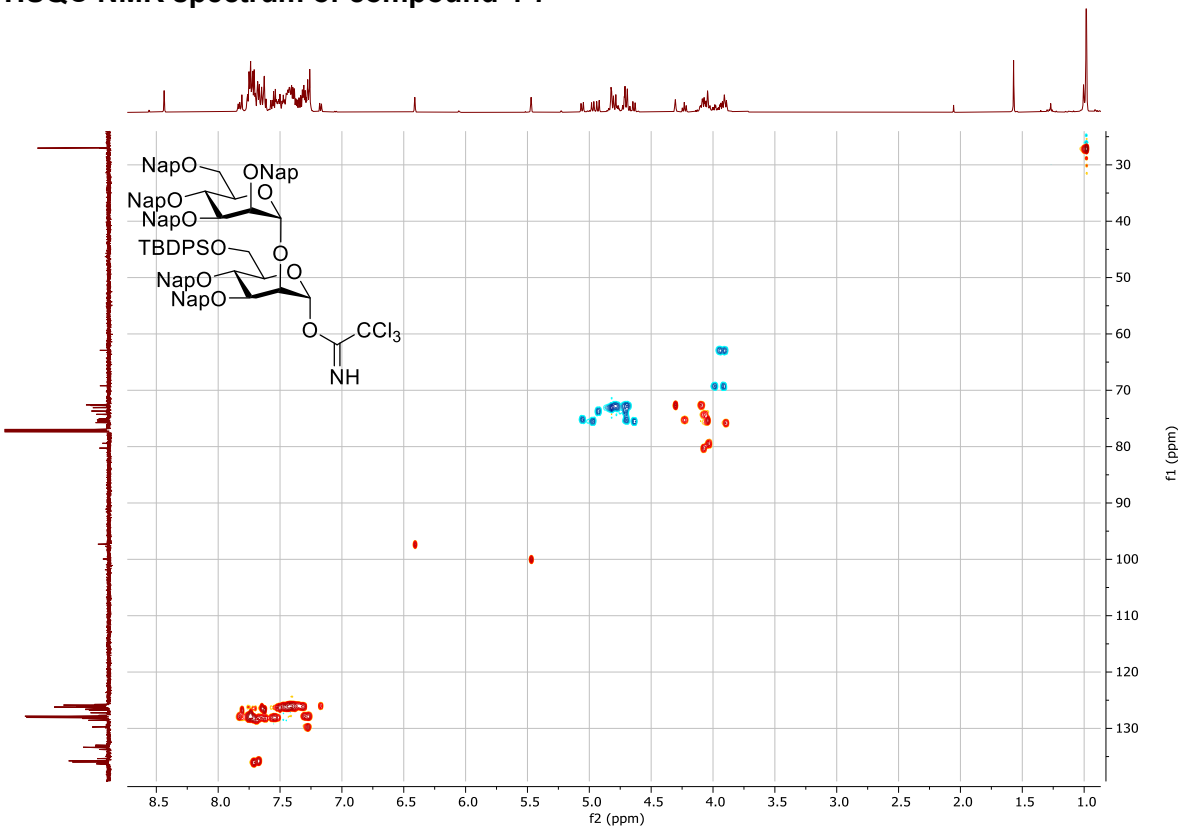

^{1}H NMR spectrum of compound 4-13

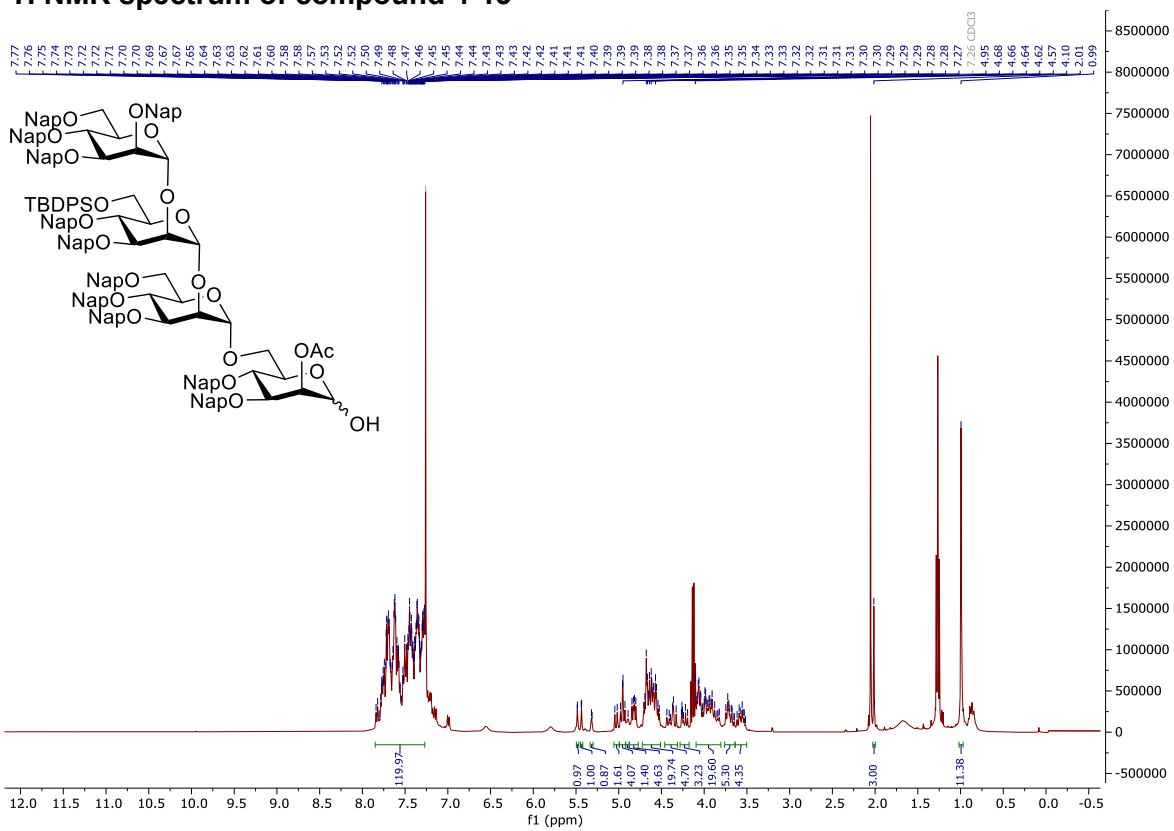

^{13}C NMR spectrum of compound 4-13

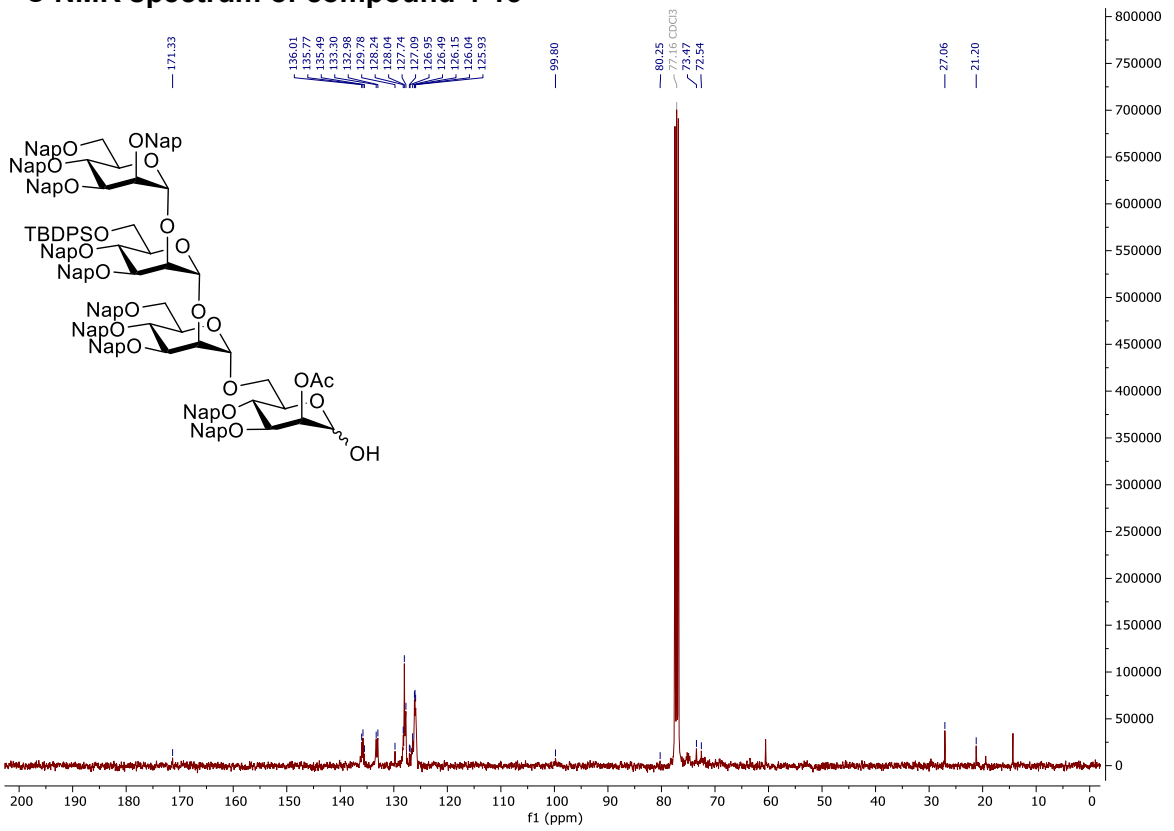

COSY NMR spectrum of compound 4-13

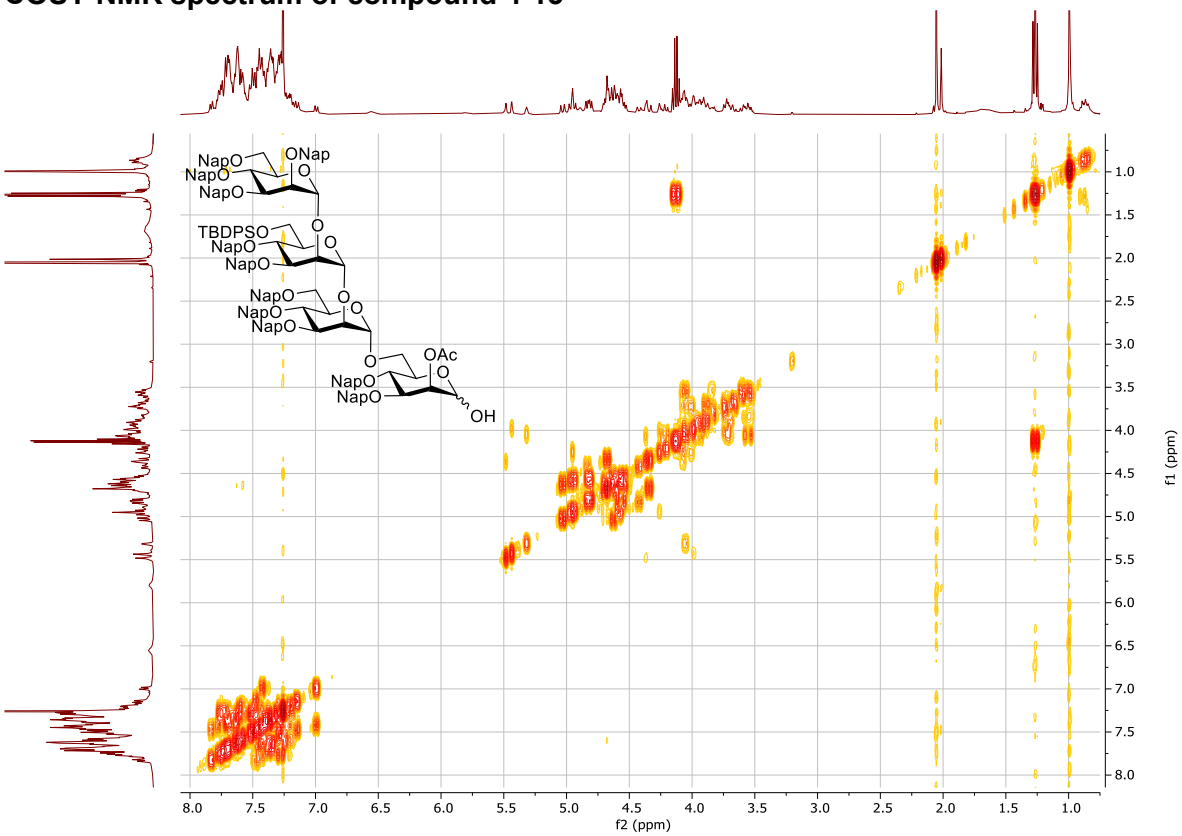

HSQC NMR spectrum of compound 4-13

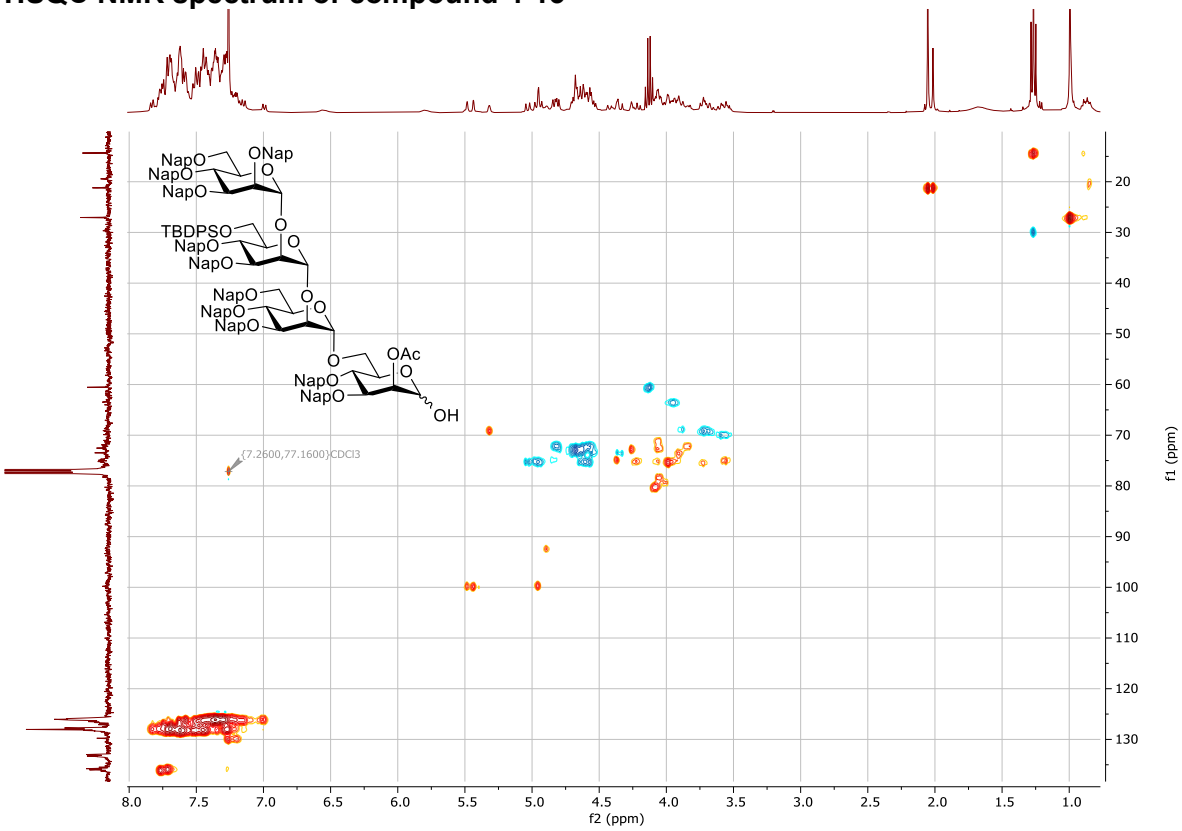

^{1}H NMR spectrum of compound 4-14

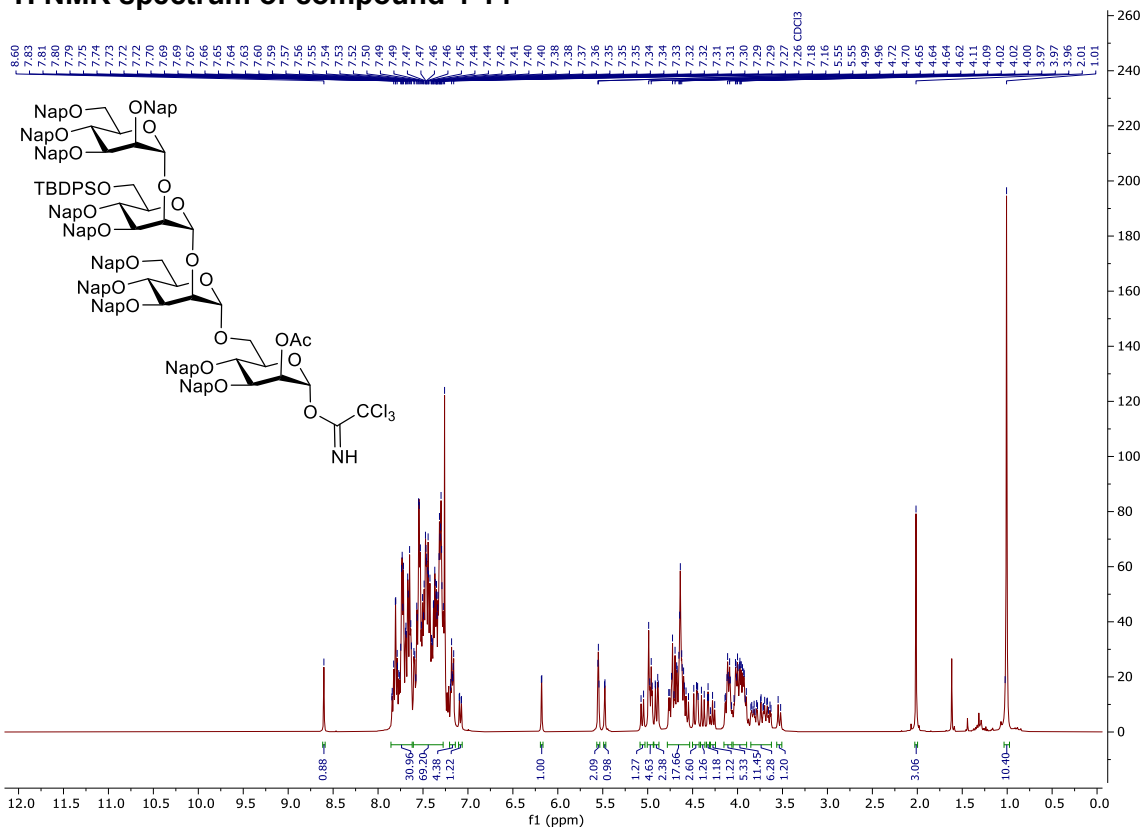

^{13}C NMR spectrum of compound 4-14

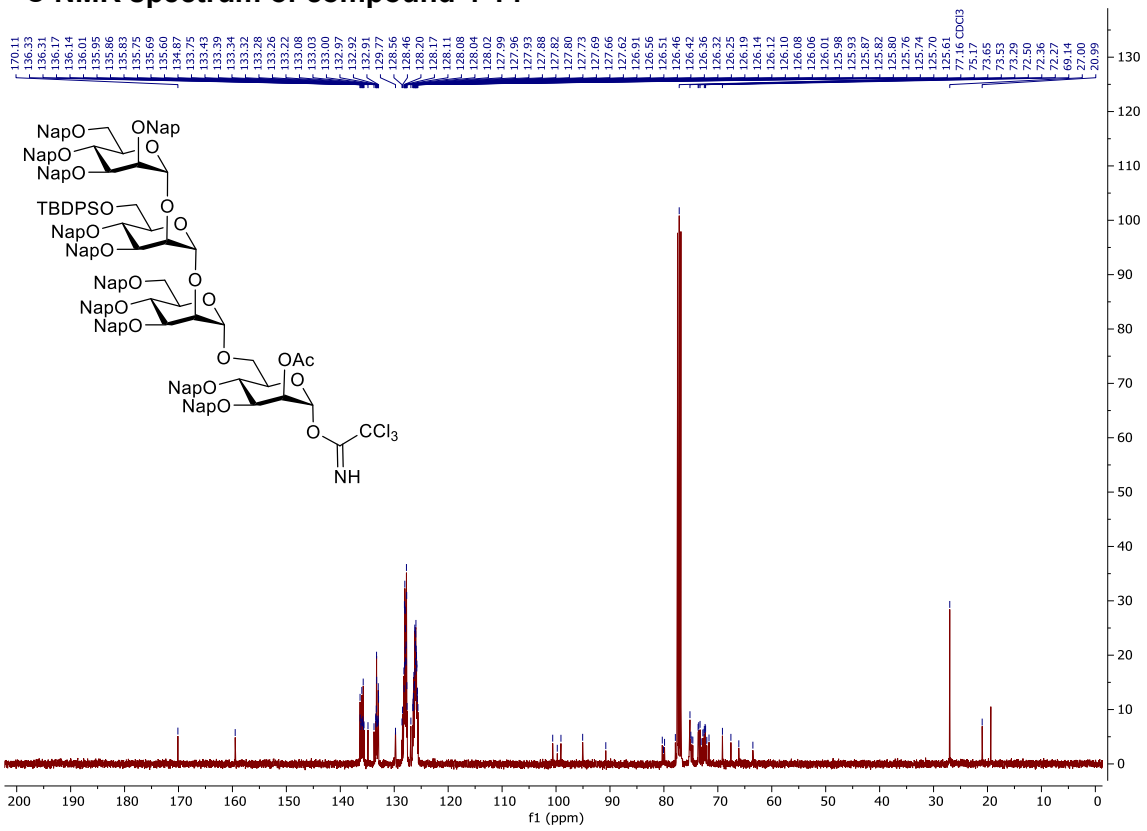

COSY NMR spectrum of compound 4-14

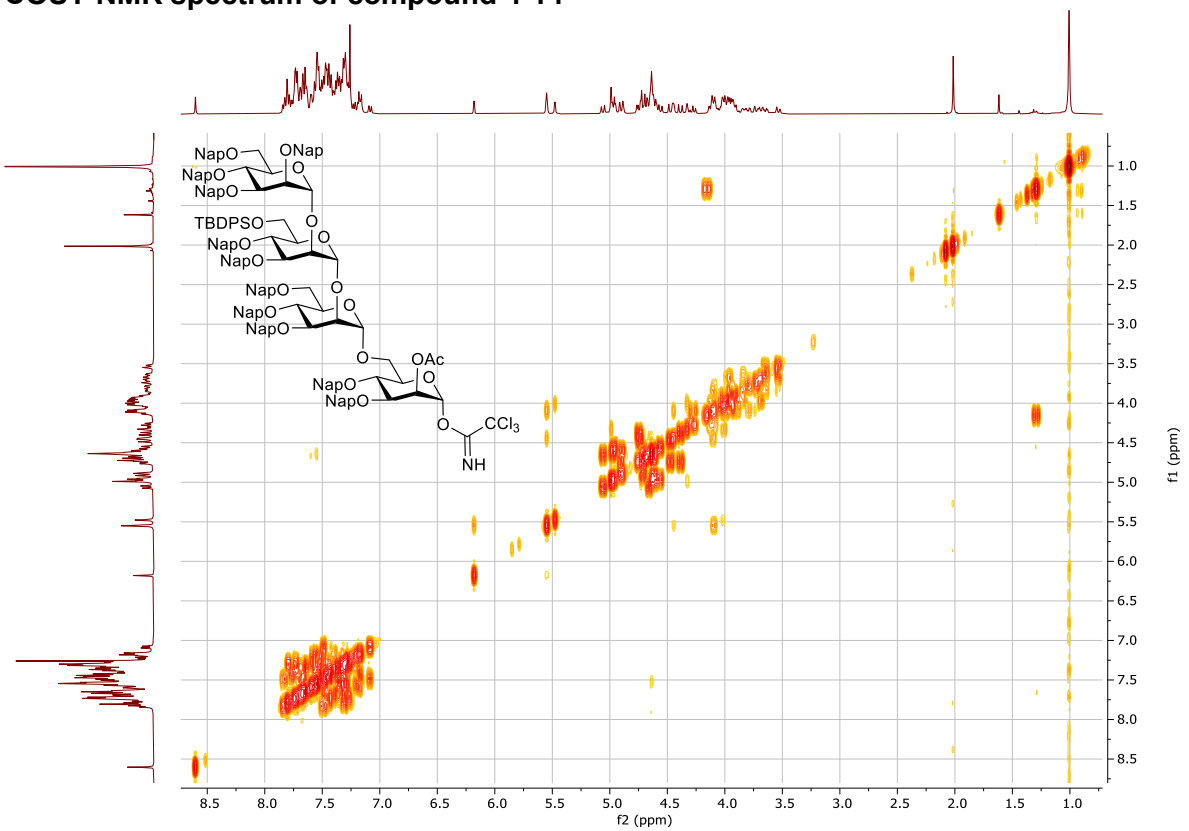

HSQC NMR spectrum of compound 4-14

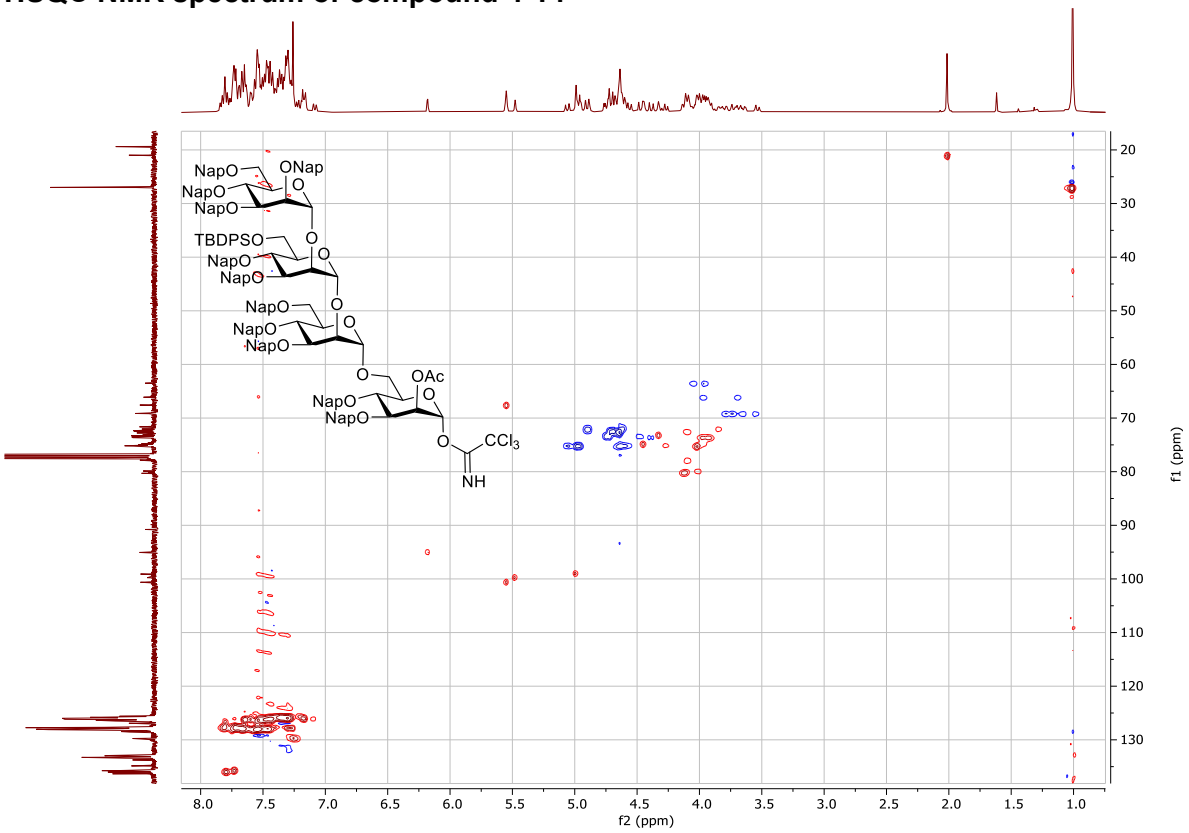

^{1}H NMR spectrum of compound 4-15

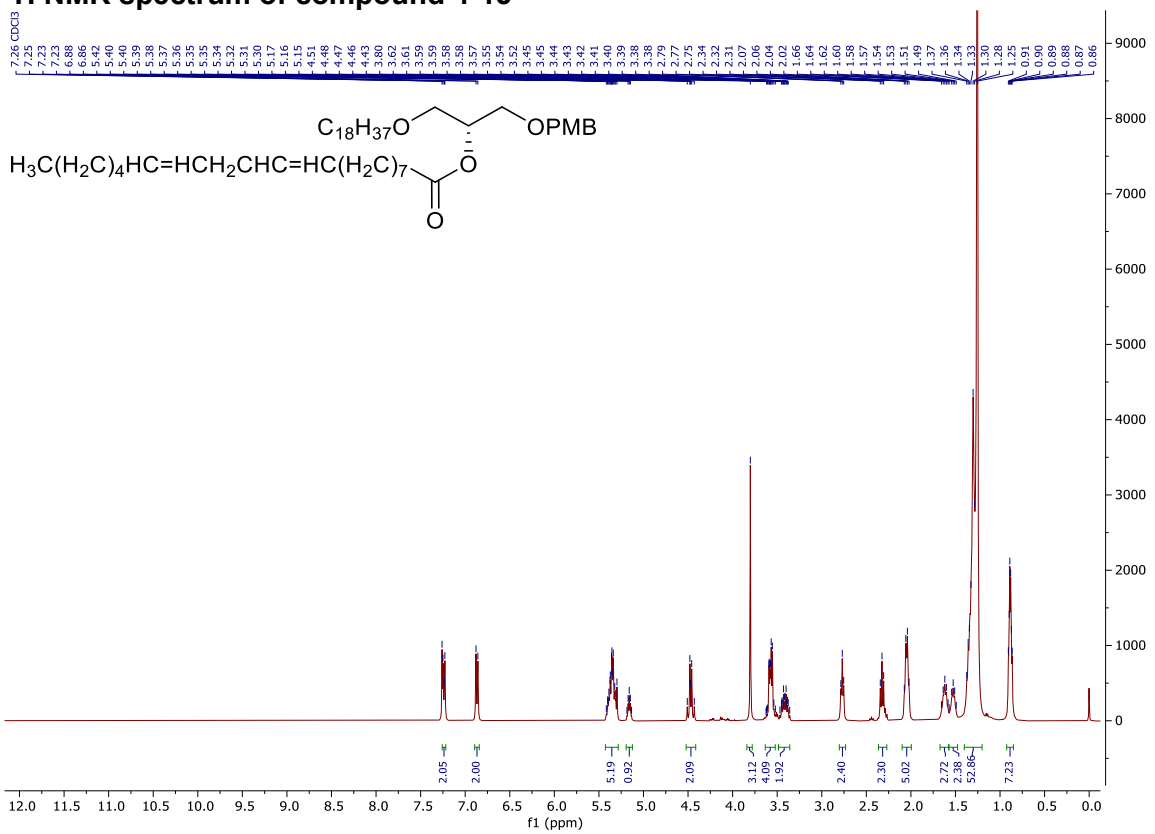

^{13}C NMR spectrum of compound 4-15

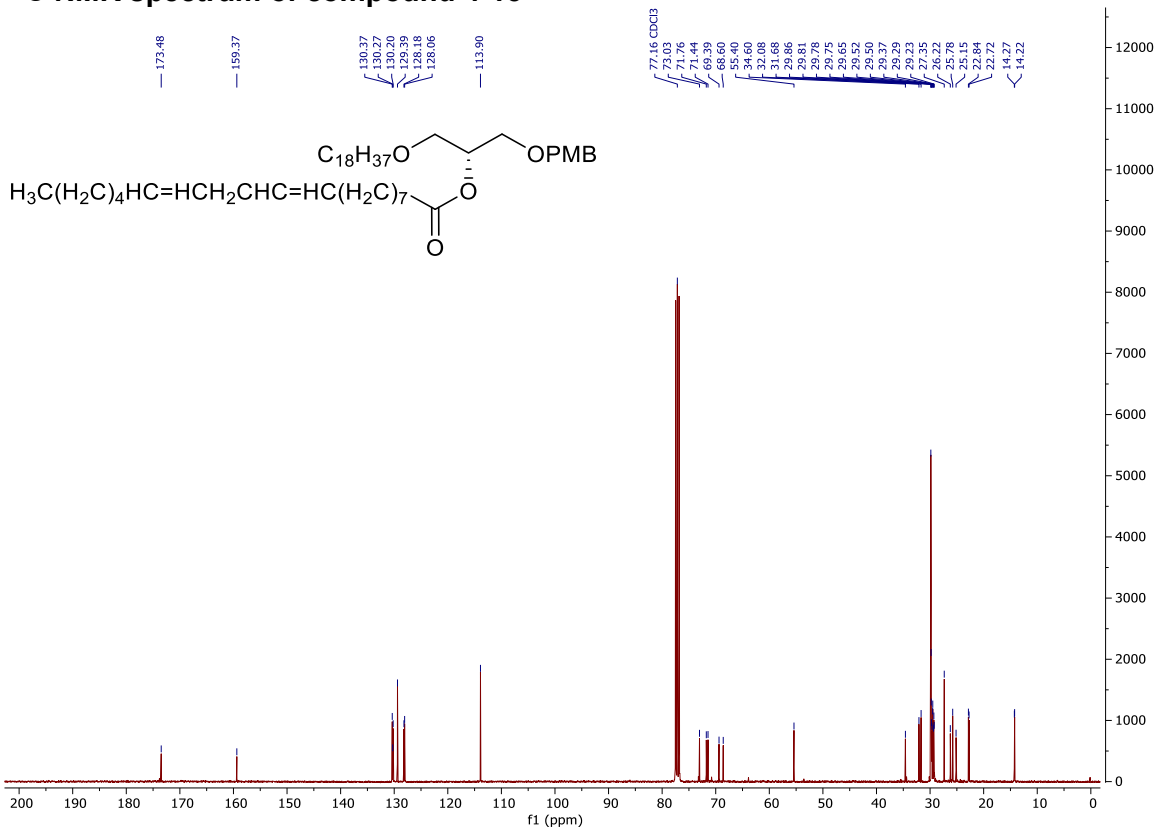

COSY NMR spectrum of compound 4-15

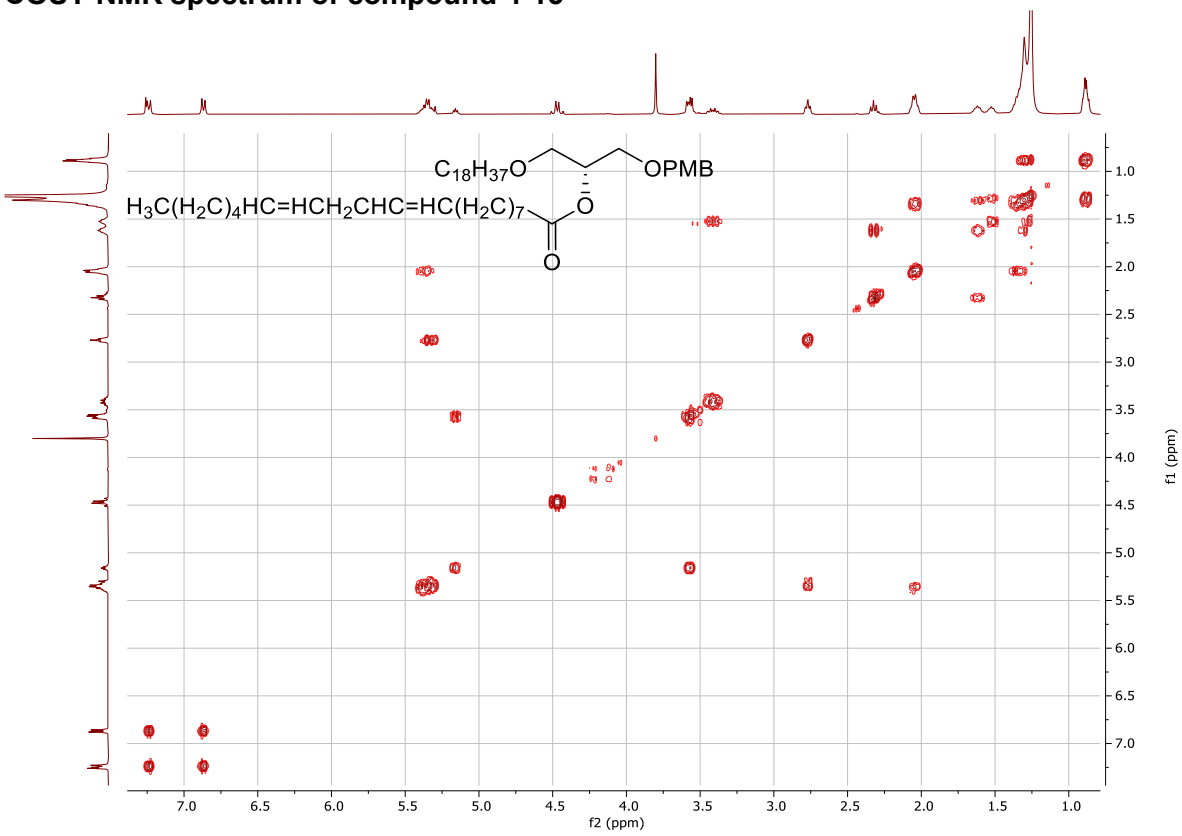

HSQC NMR spectrum of compound 4-15

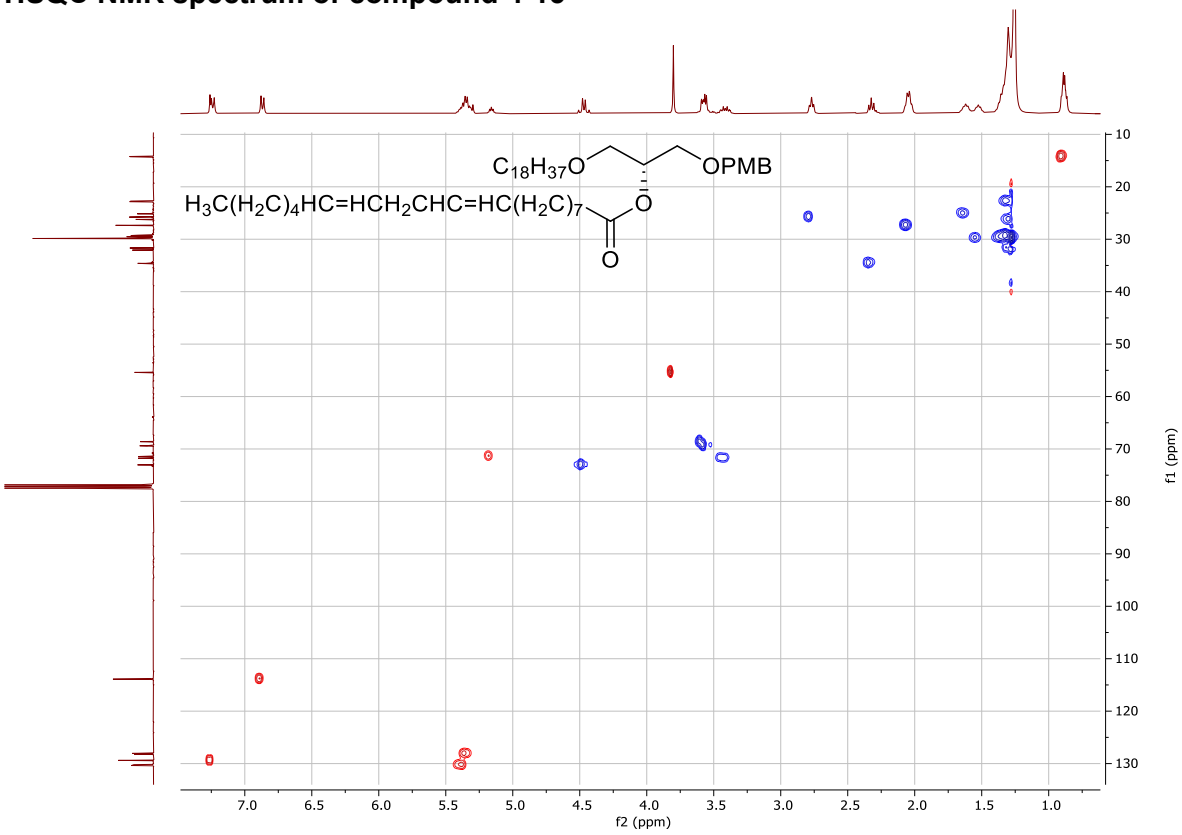

HMBC NMR spectrum of compound 4-15

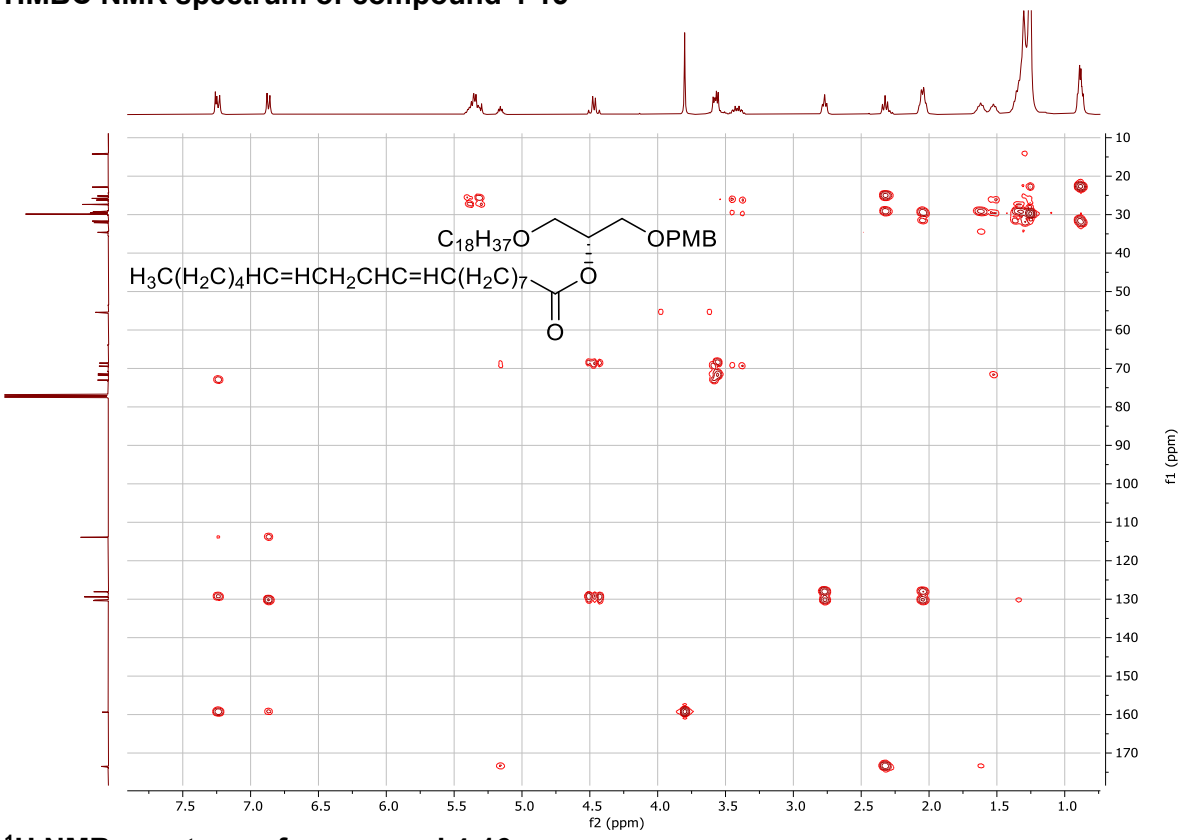

^{1}H NMR spectrum of compound 4-16

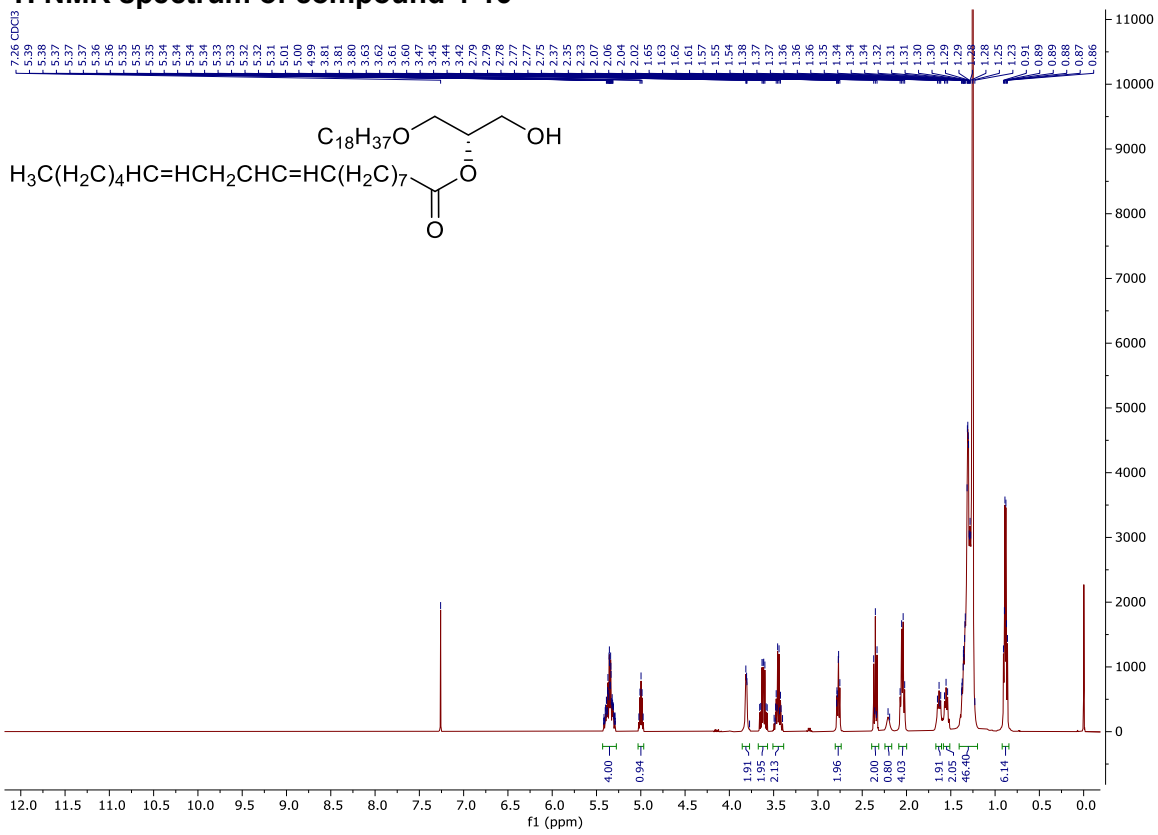

^{13}C NMR spectrum of compound 4-16

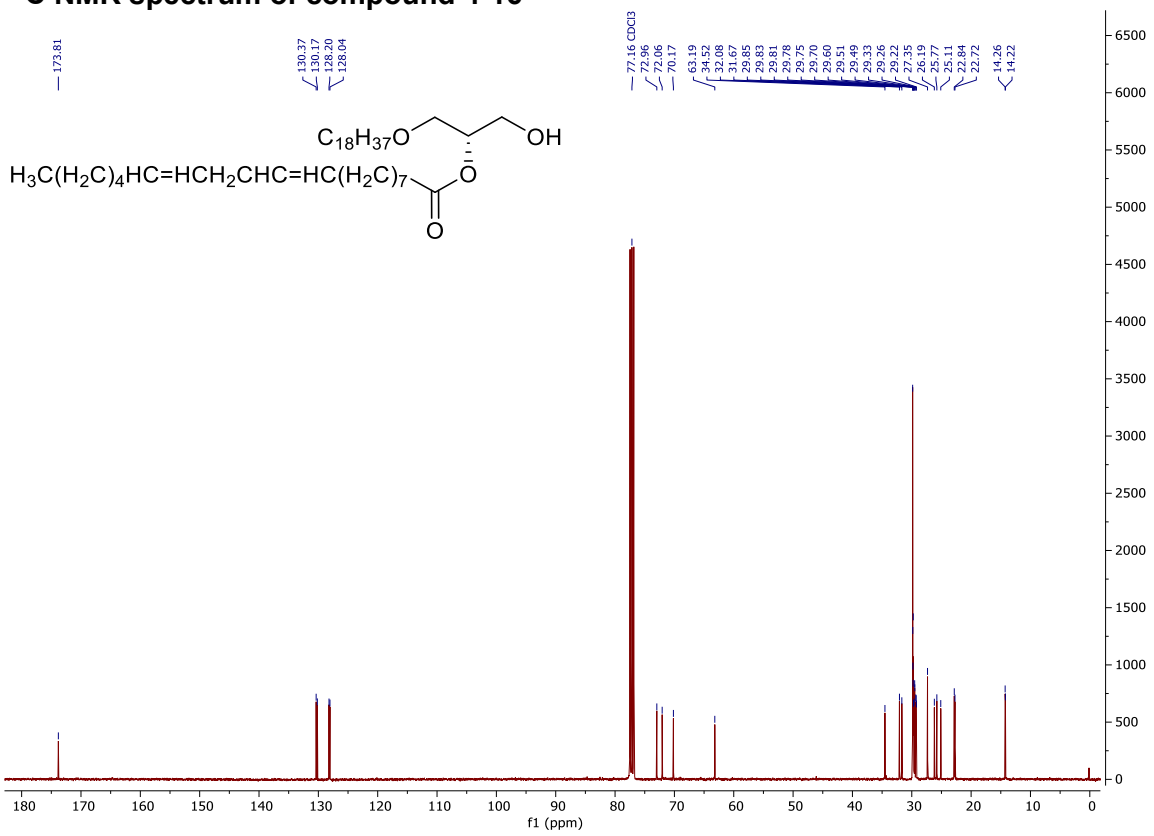

COSY NMR spectrum of compound 4-16

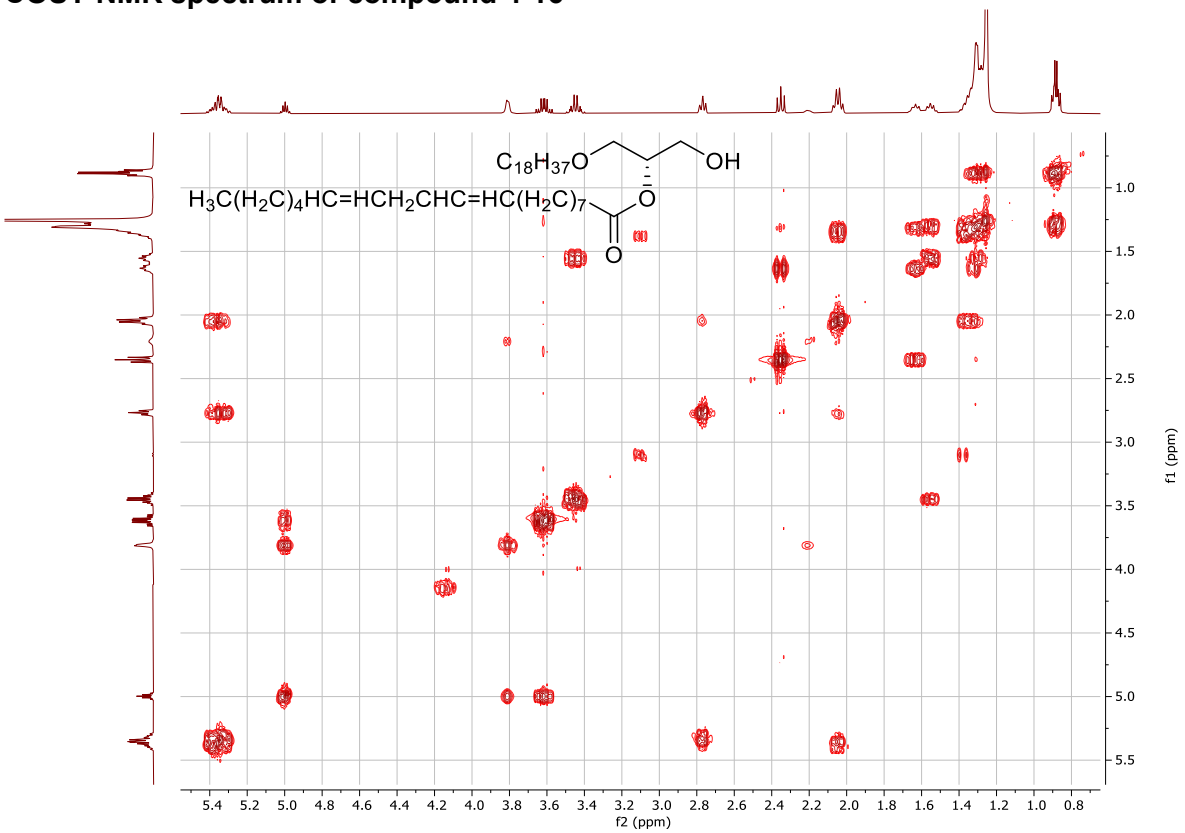

HSQC NMR spectrum of compound 4-16

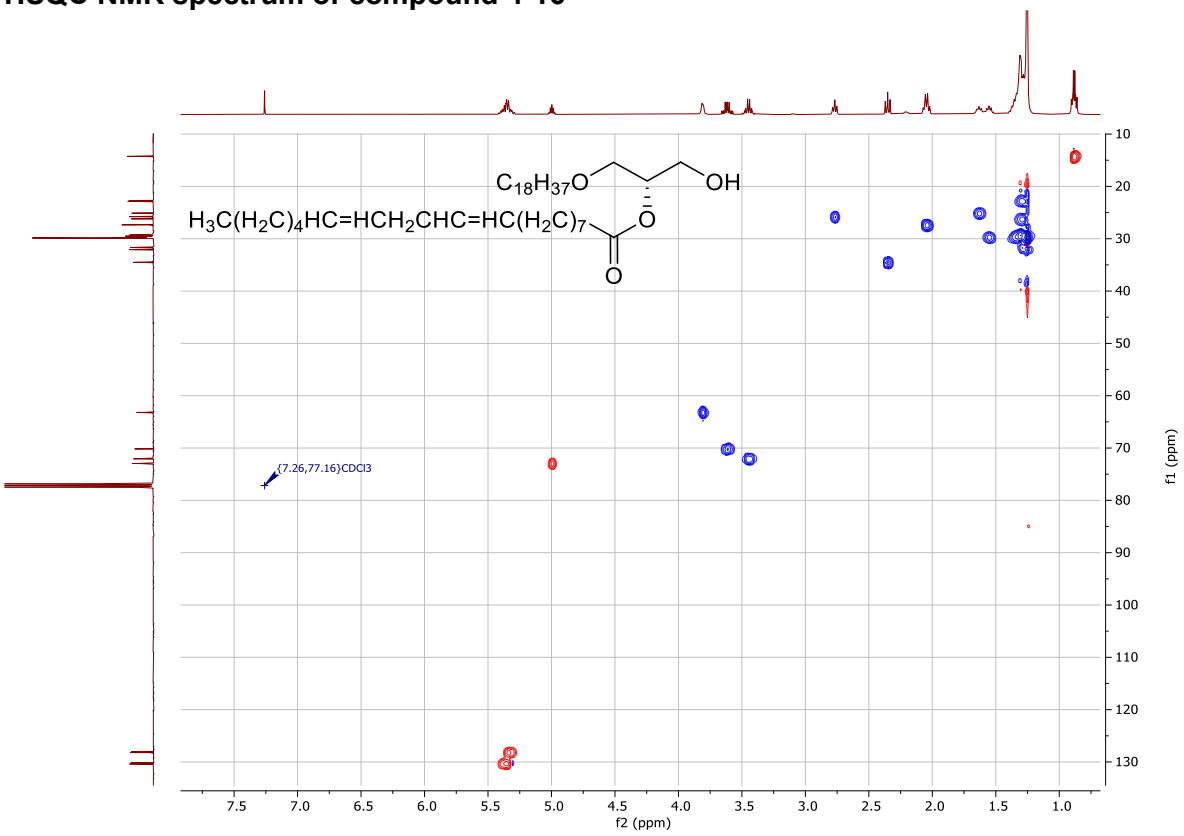

^{1}H NMR spectrum of compound 4-4

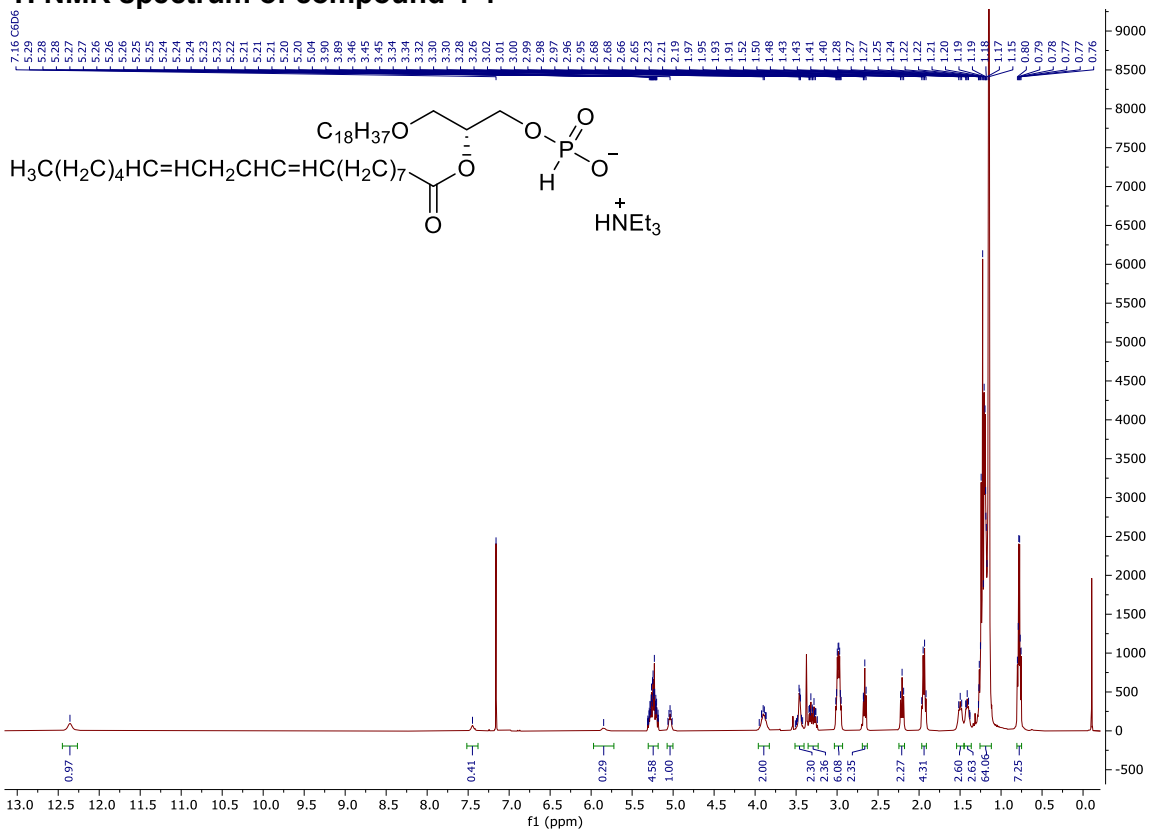

^{13}C NMR spectrum of compound 4-4

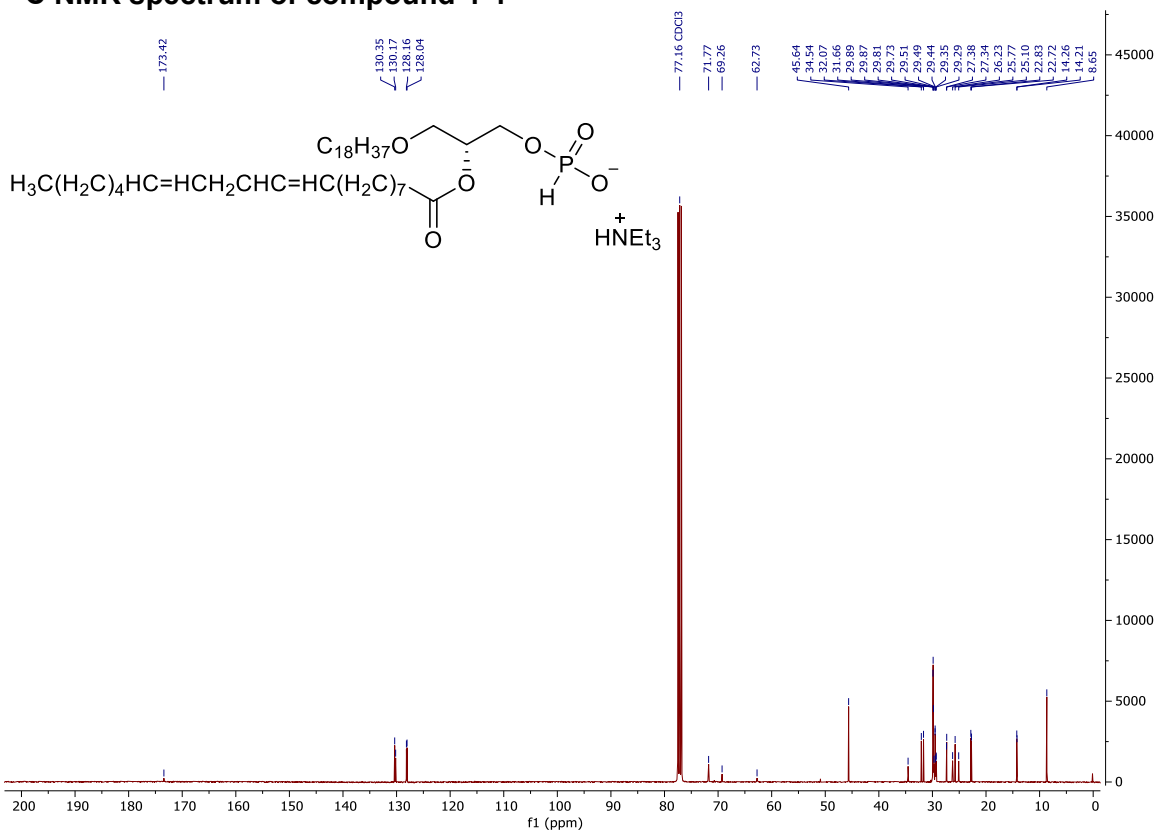

COSY NMR spectrum of compound 4-4

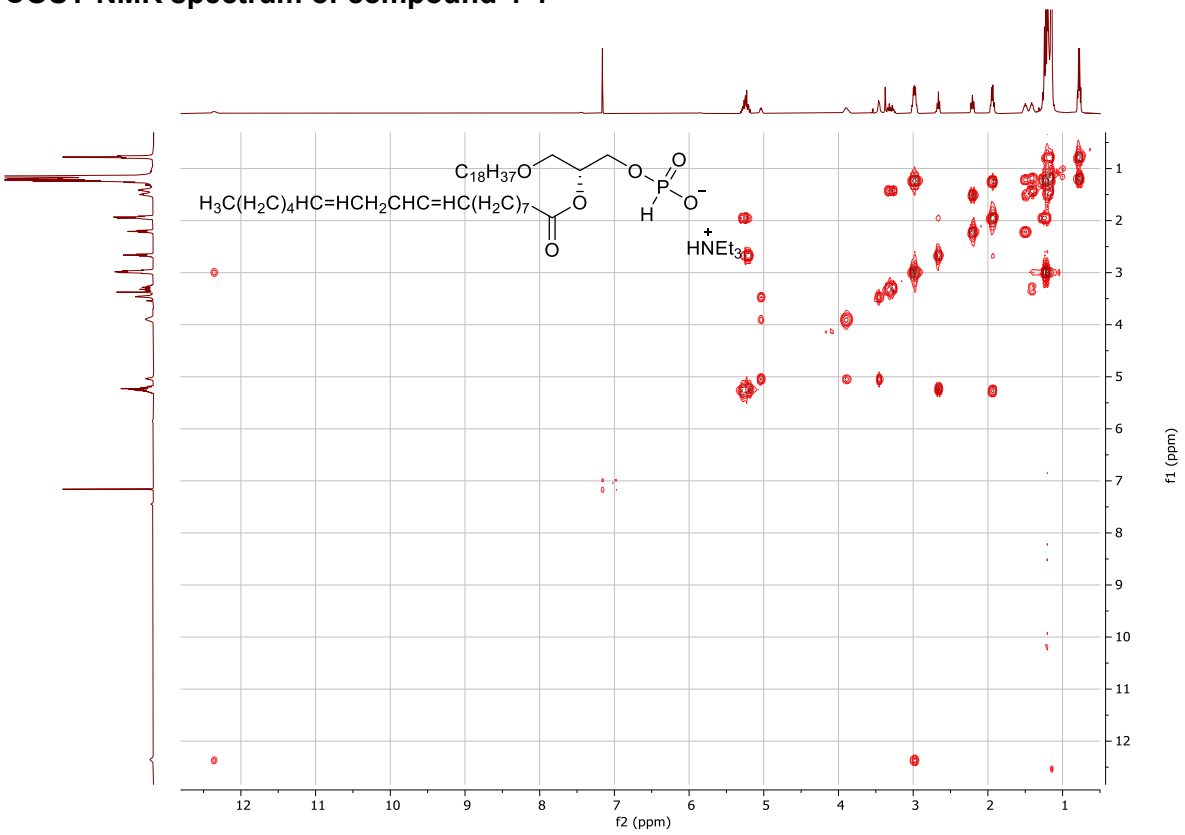

HSQC NMR spectrum of compound 4-4

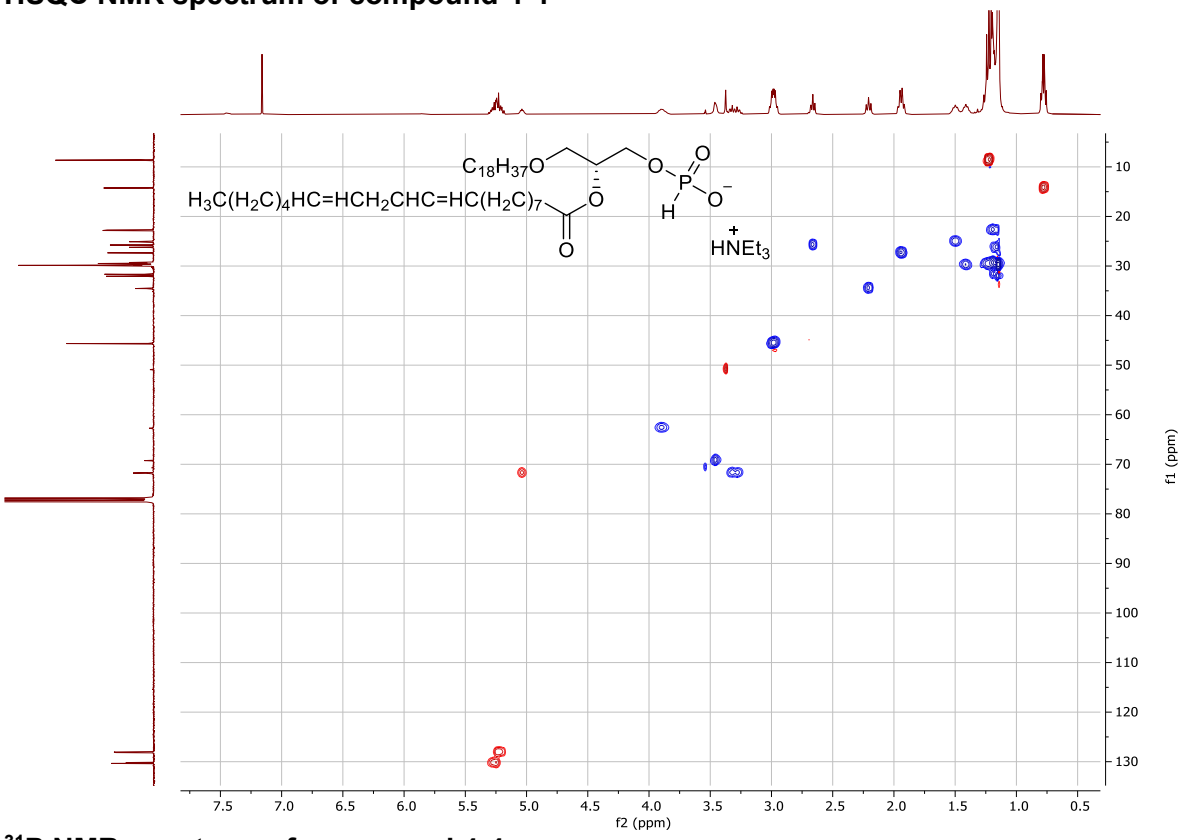

^{31}P NMR spectrum of compound 4-4

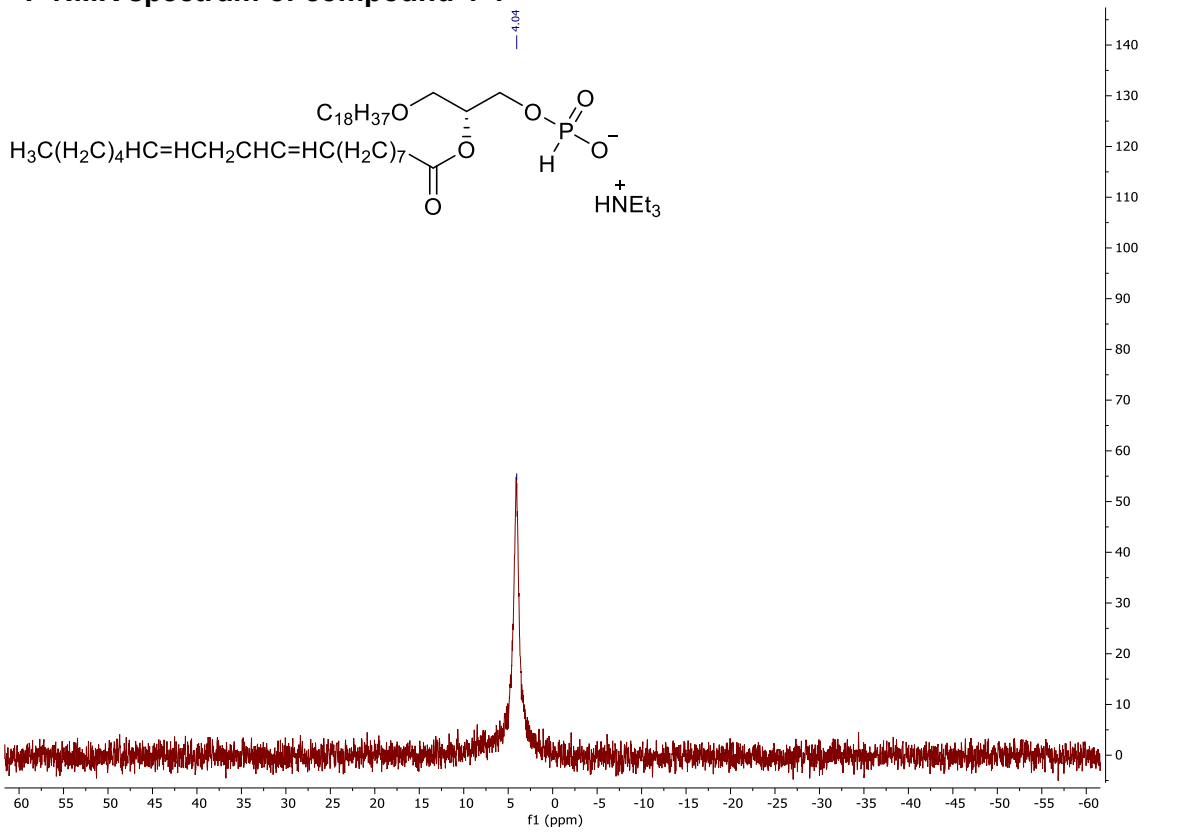

^{1}H NMR spectrum of compound 4-17

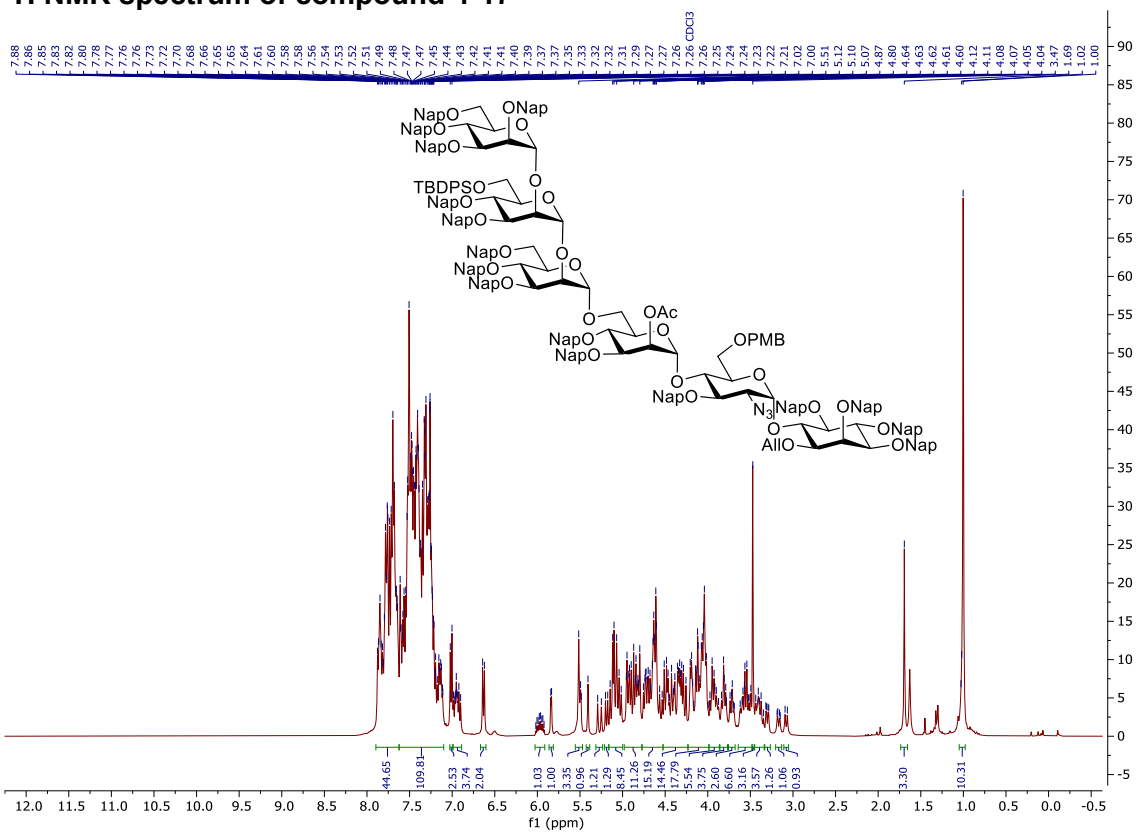

^{13}C NMR spectrum of compound 4-17

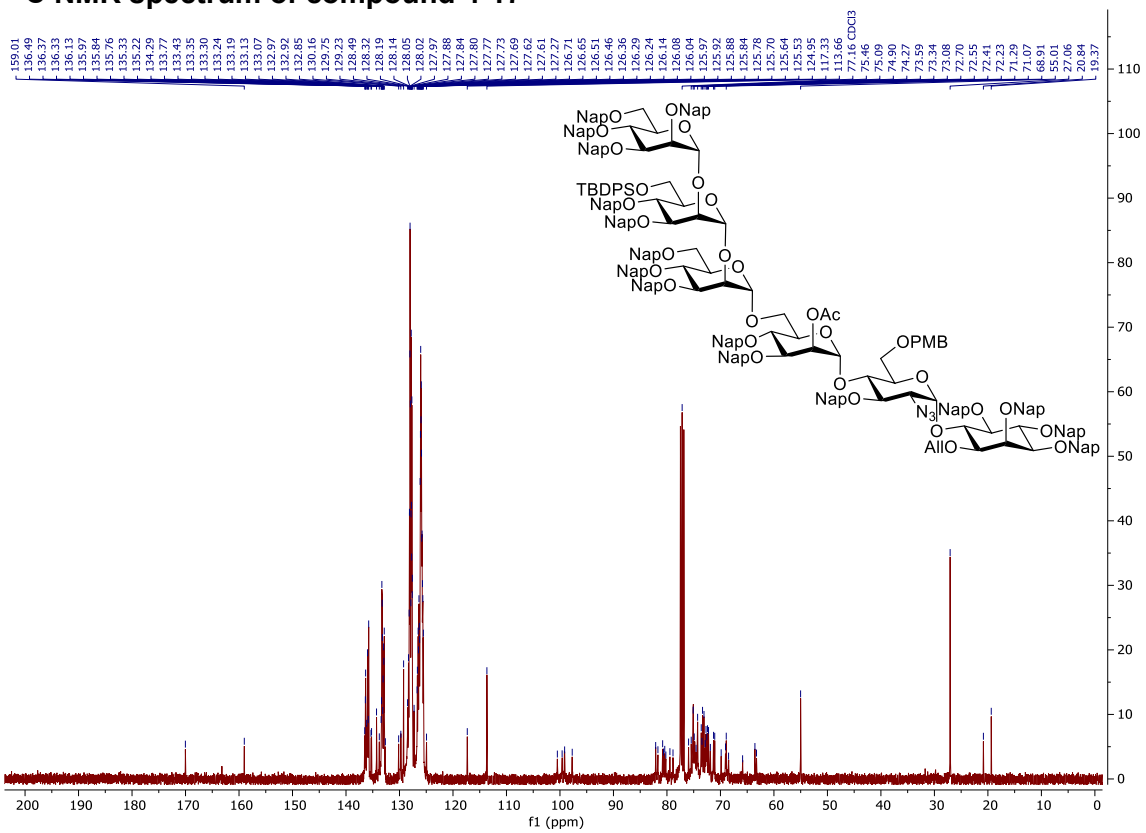

COSY-NMR spectrum of compound 4-17

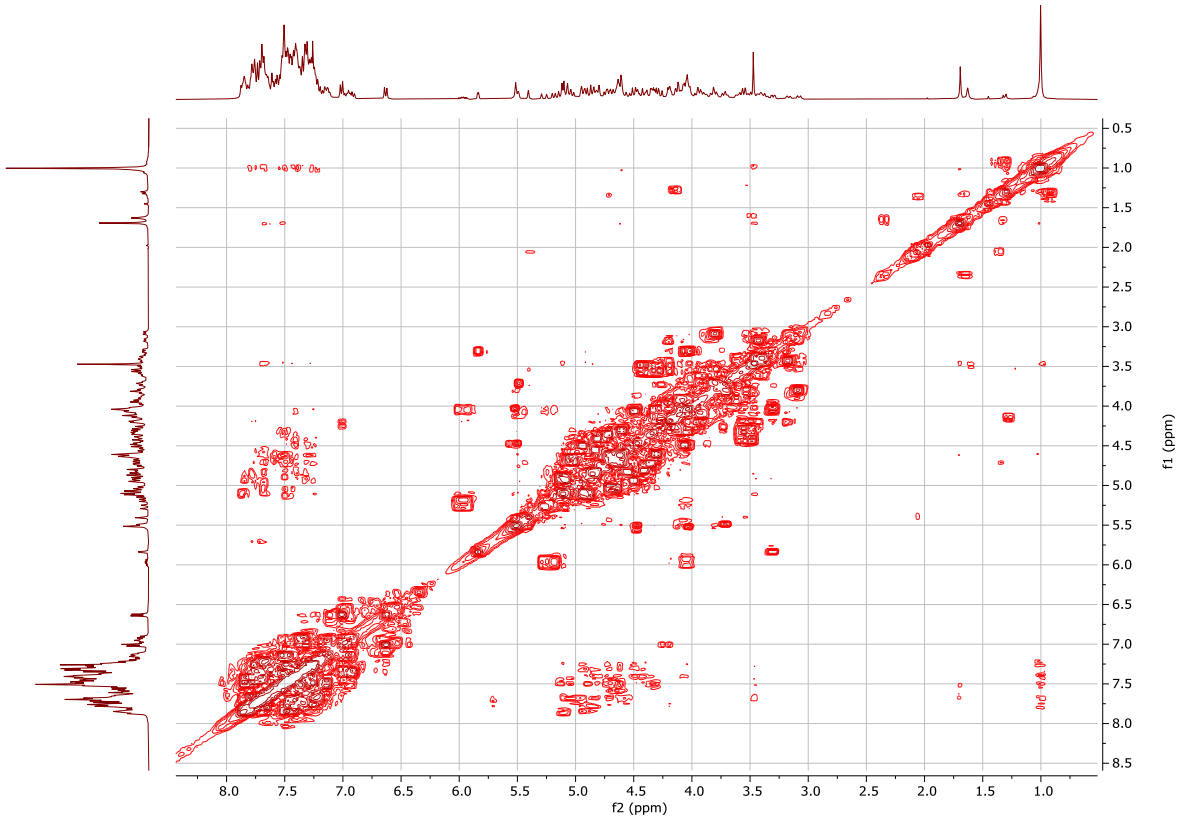

HSQC-NMR spectrum of compound 4-17

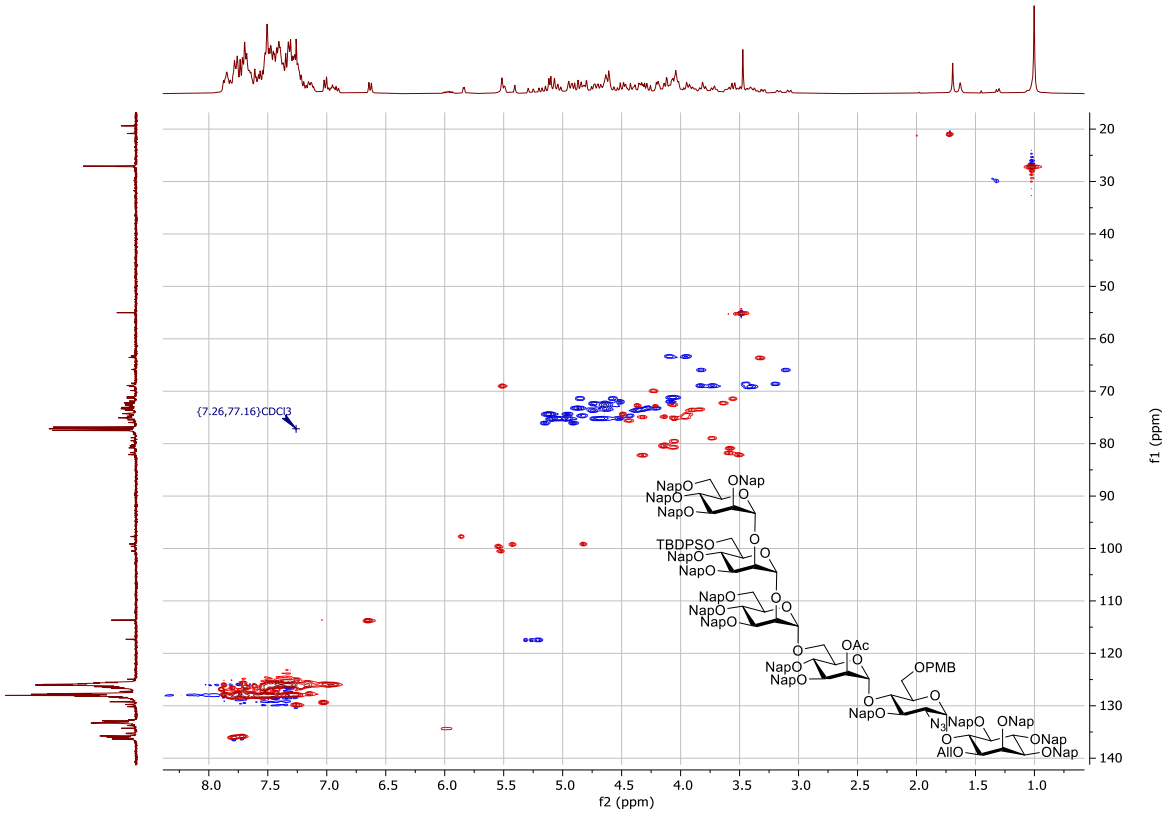

^{1}H NMR spectrum of compound 4-18

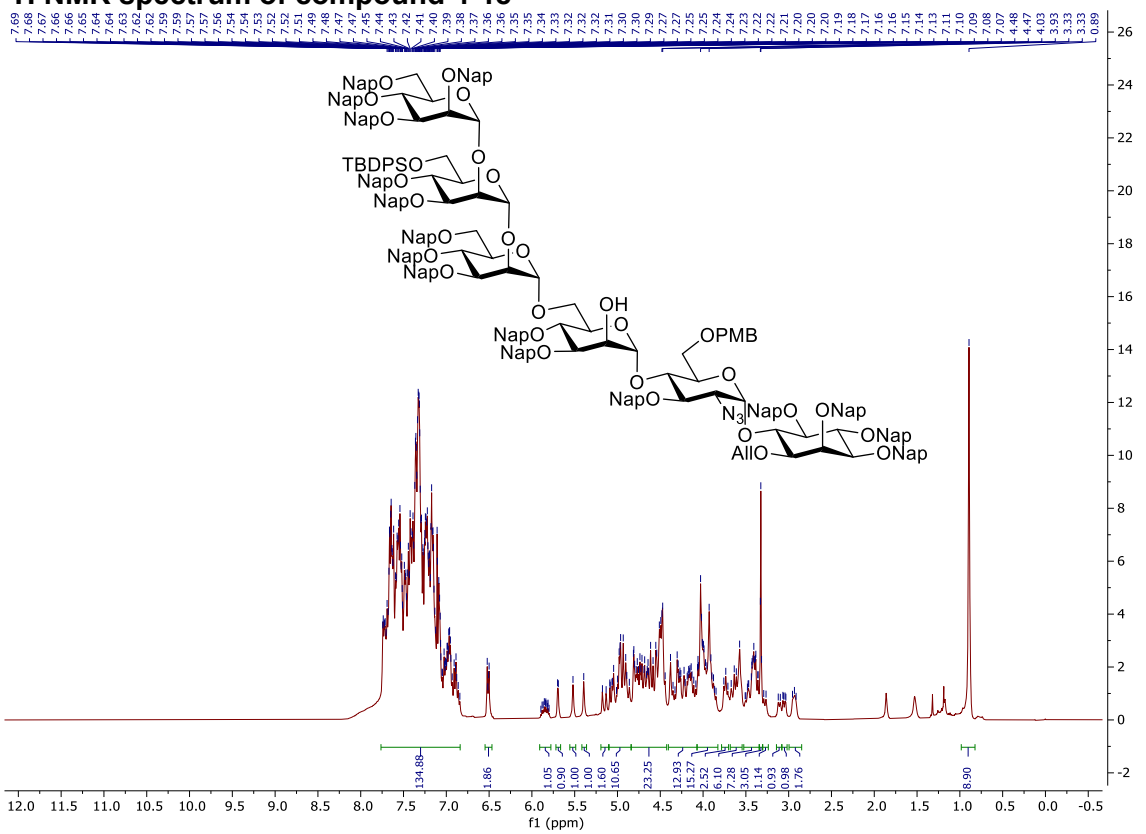

^{13}C NMR spectrum of compound 4-18

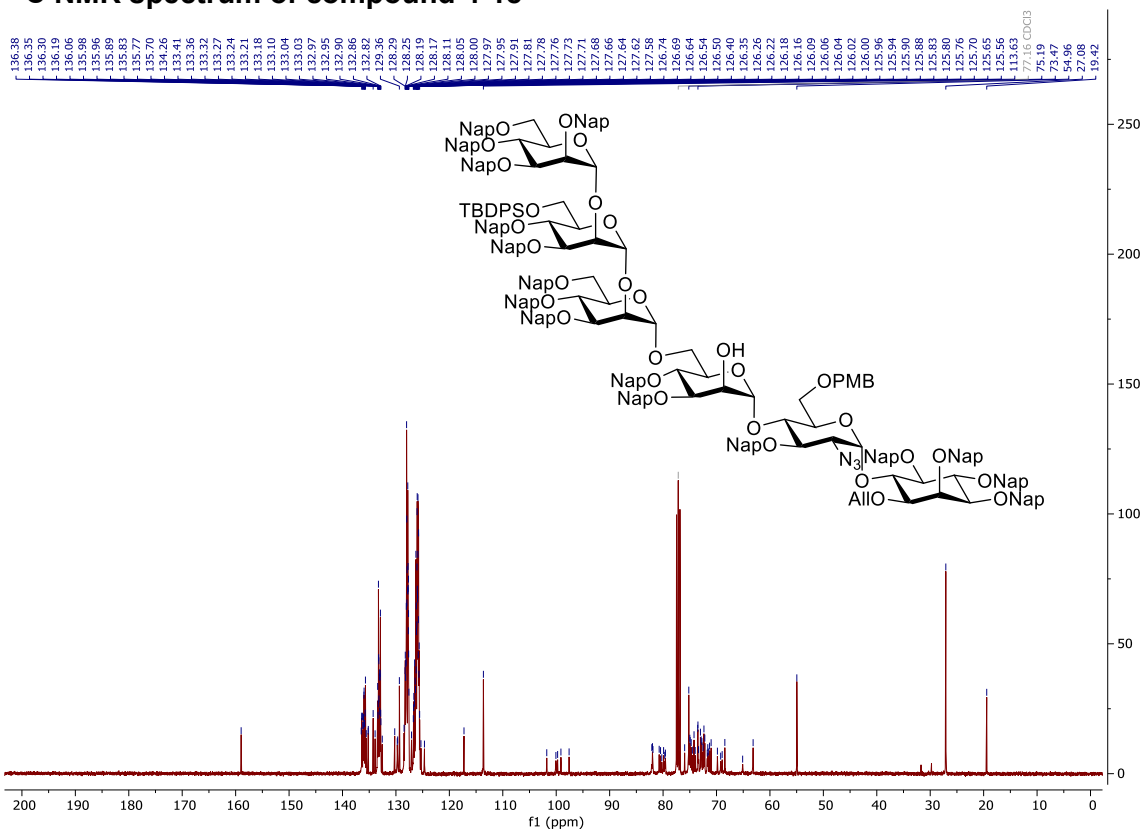

COSY-NMR spectrum of compound 4-18

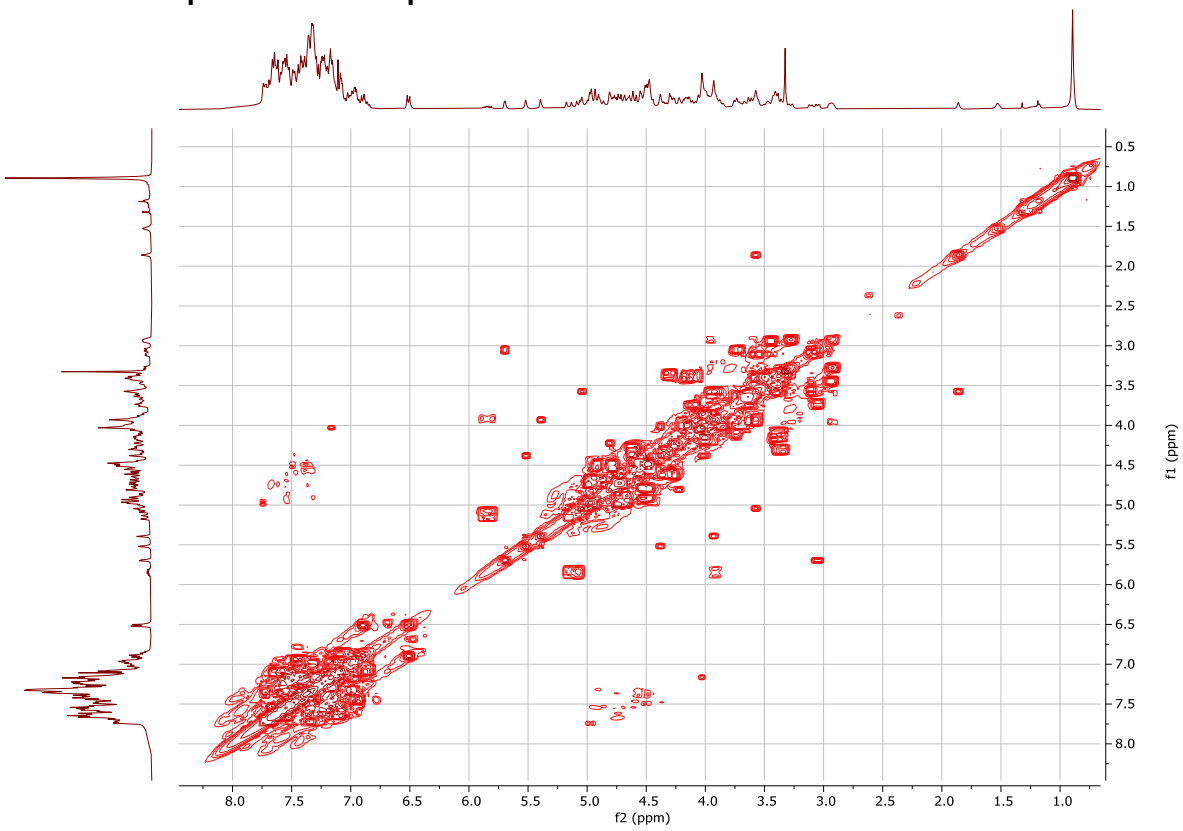

HSQC-NMR spectrum of compound 4-18

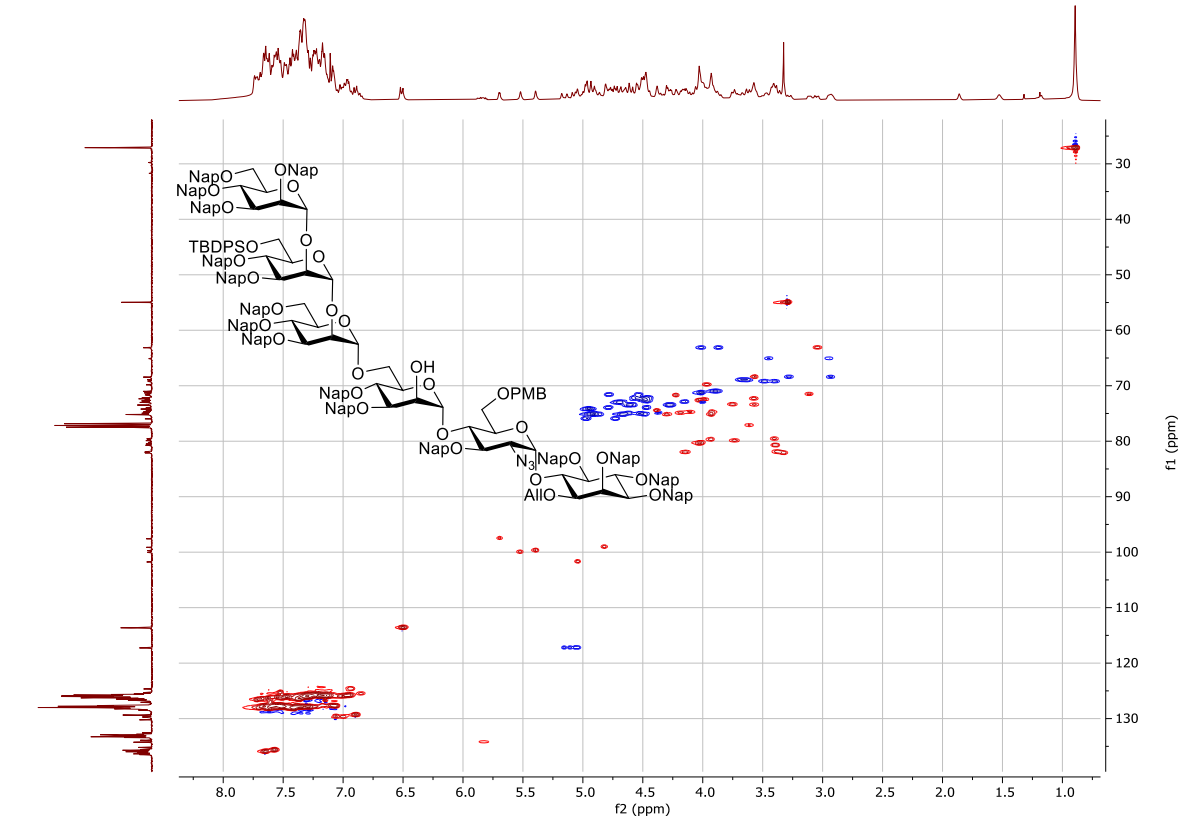

^{1}H NMR spectrum of compound 4-20

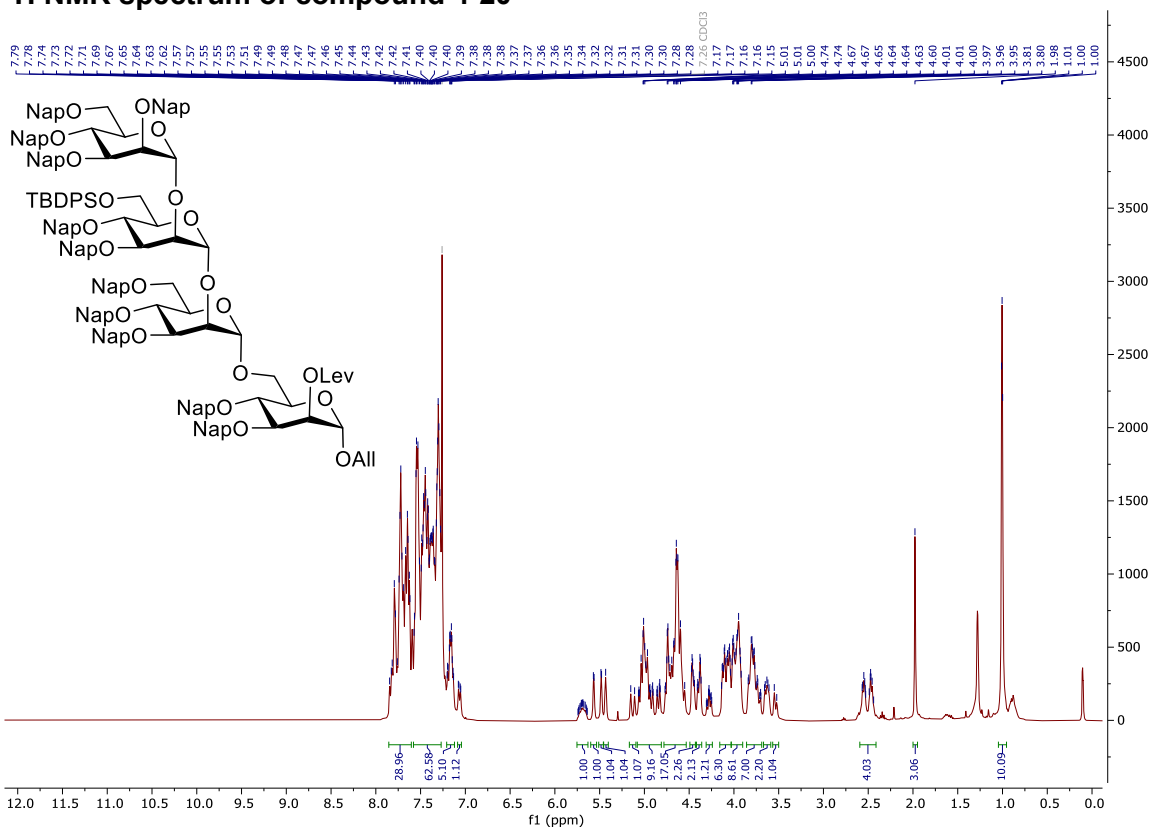

^{13}C NMR spectrum of compound 4-20

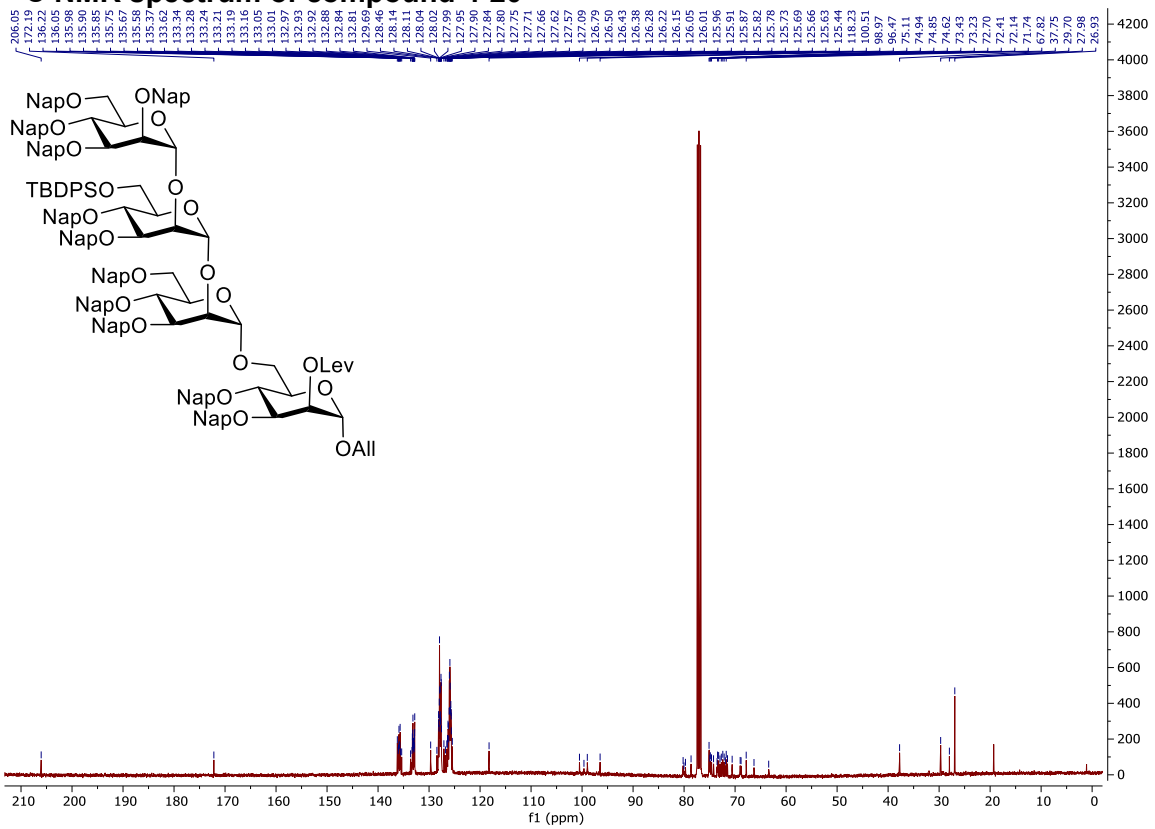

COSY NMR spectrum of compound 4-20

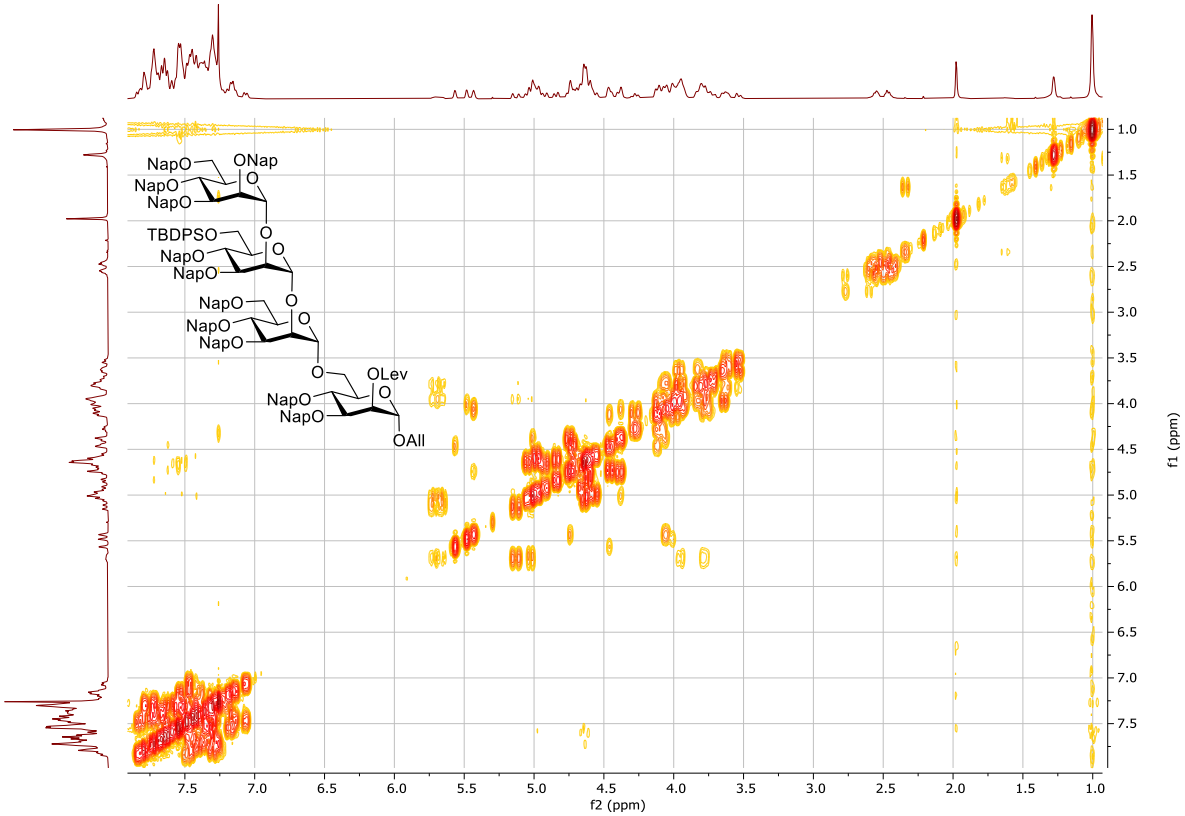

HSQC NMR spectrum of compound 4-20

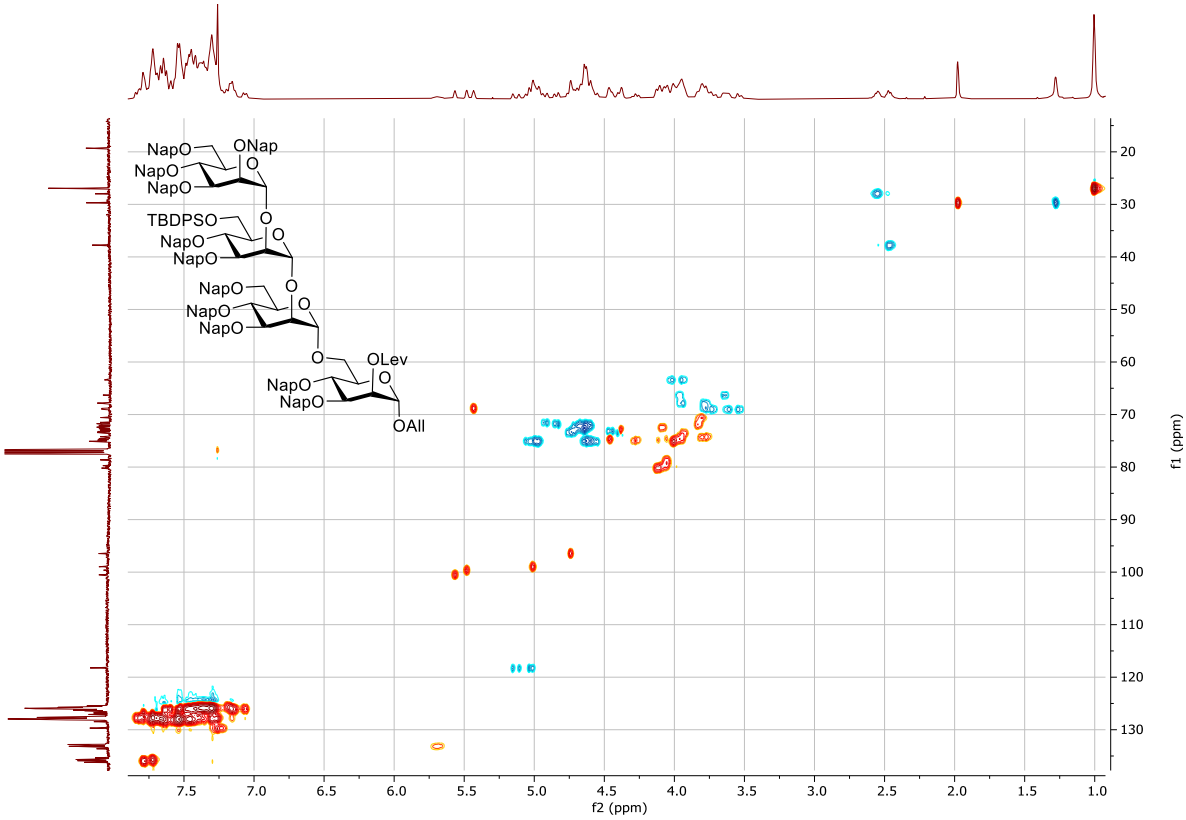

^{1}H NMR spectrum of compound 4-21

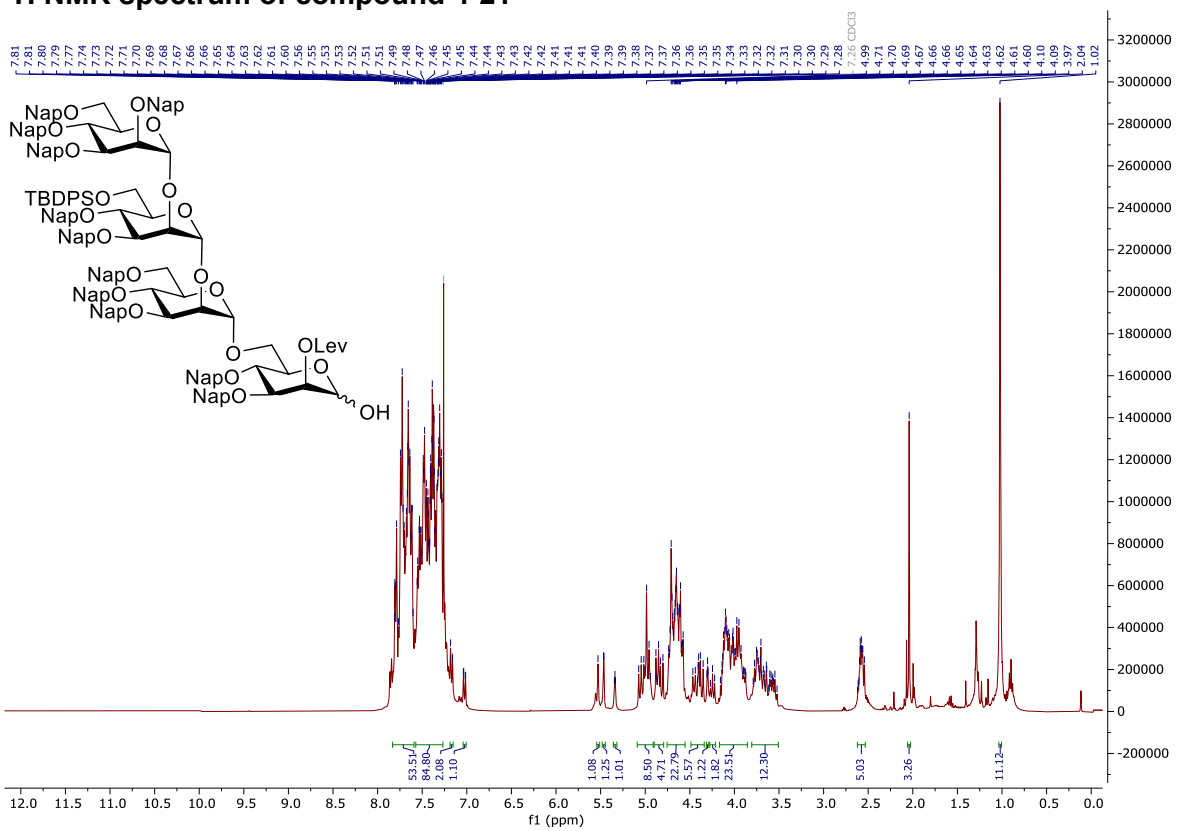

^{13}C NMR spectrum of compound 4-21

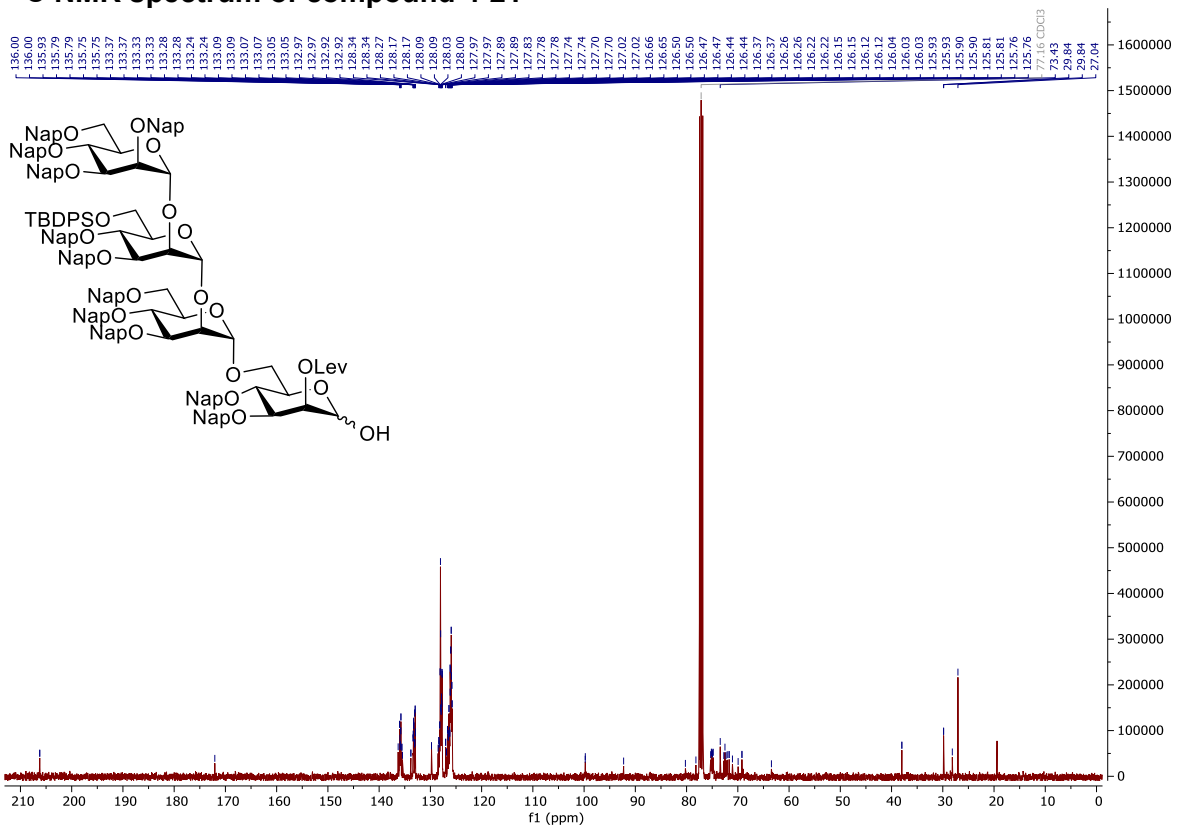

COSY NMR spectrum of compound 4-21

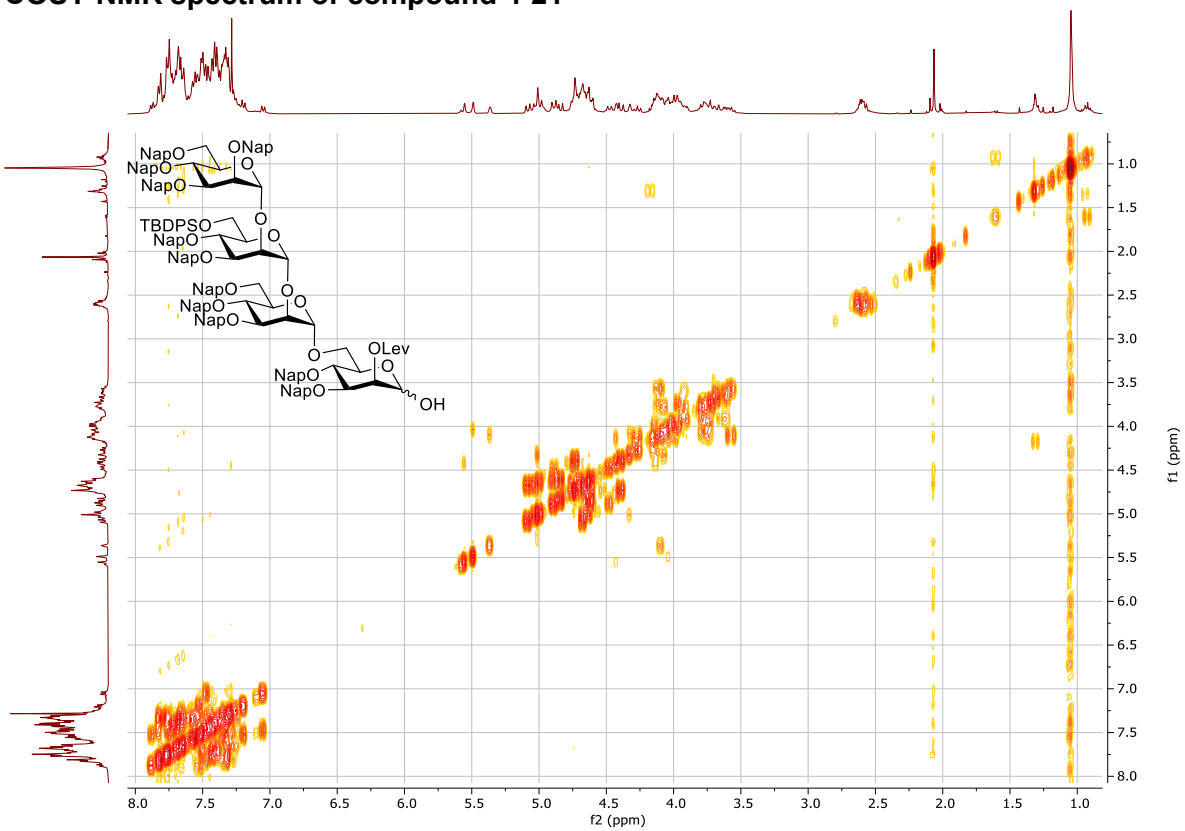

HSQC NMR spectrum of compound 4-21

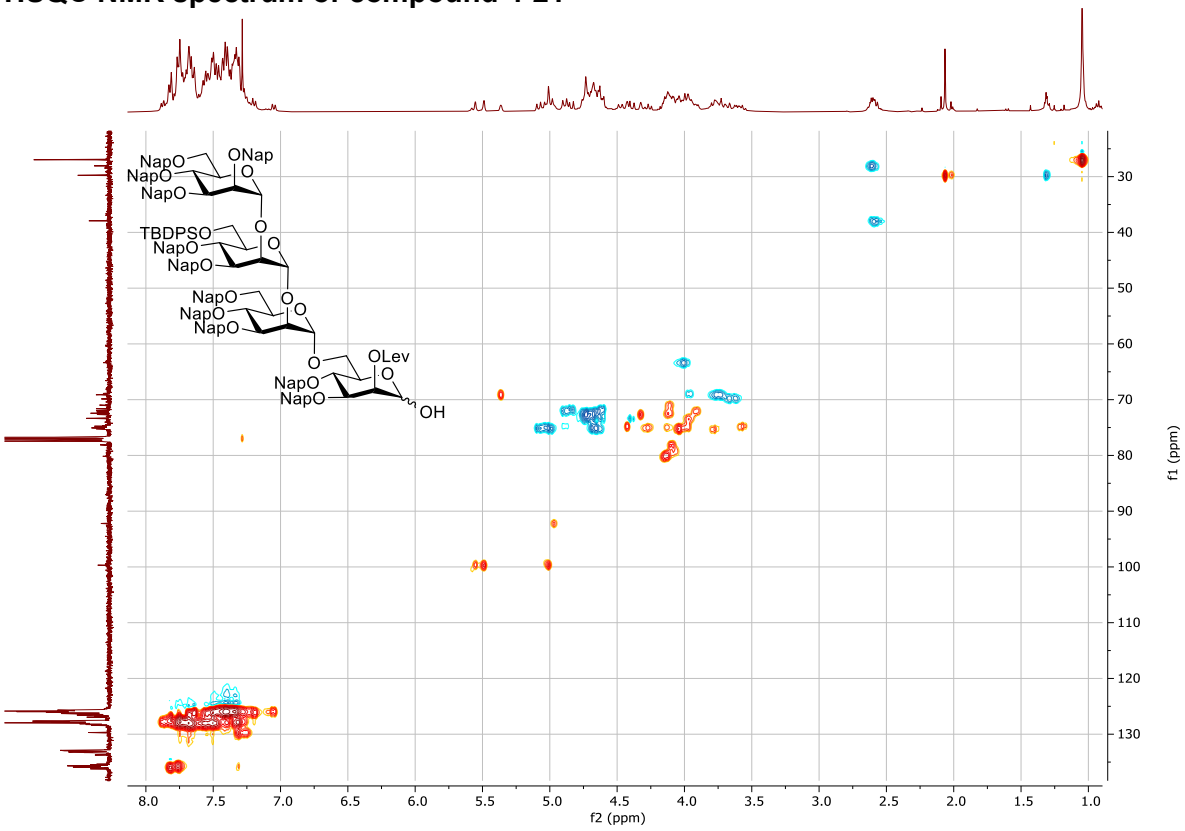

^{1}H NMR spectrum of compound 4-22

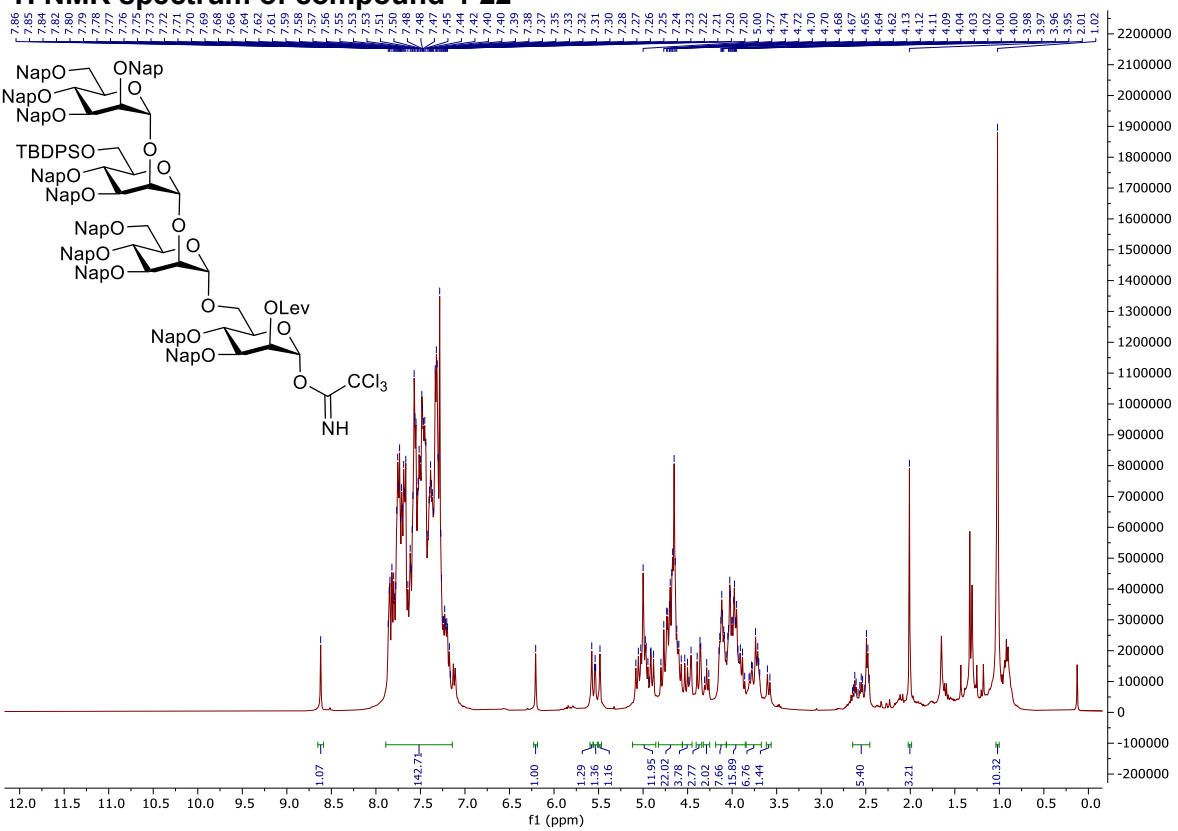

^{13}C NMR spectrum of compound 4-22

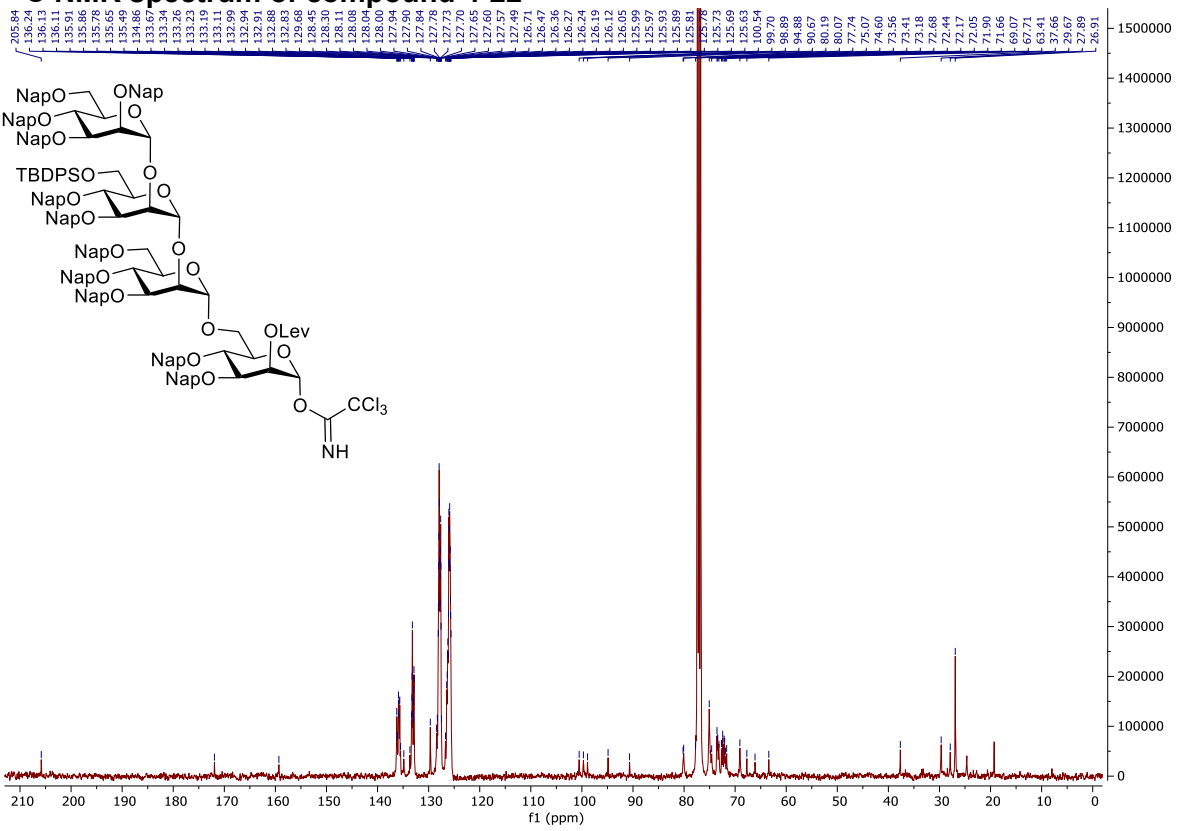

COSY NMR spectrum of compound 4-22

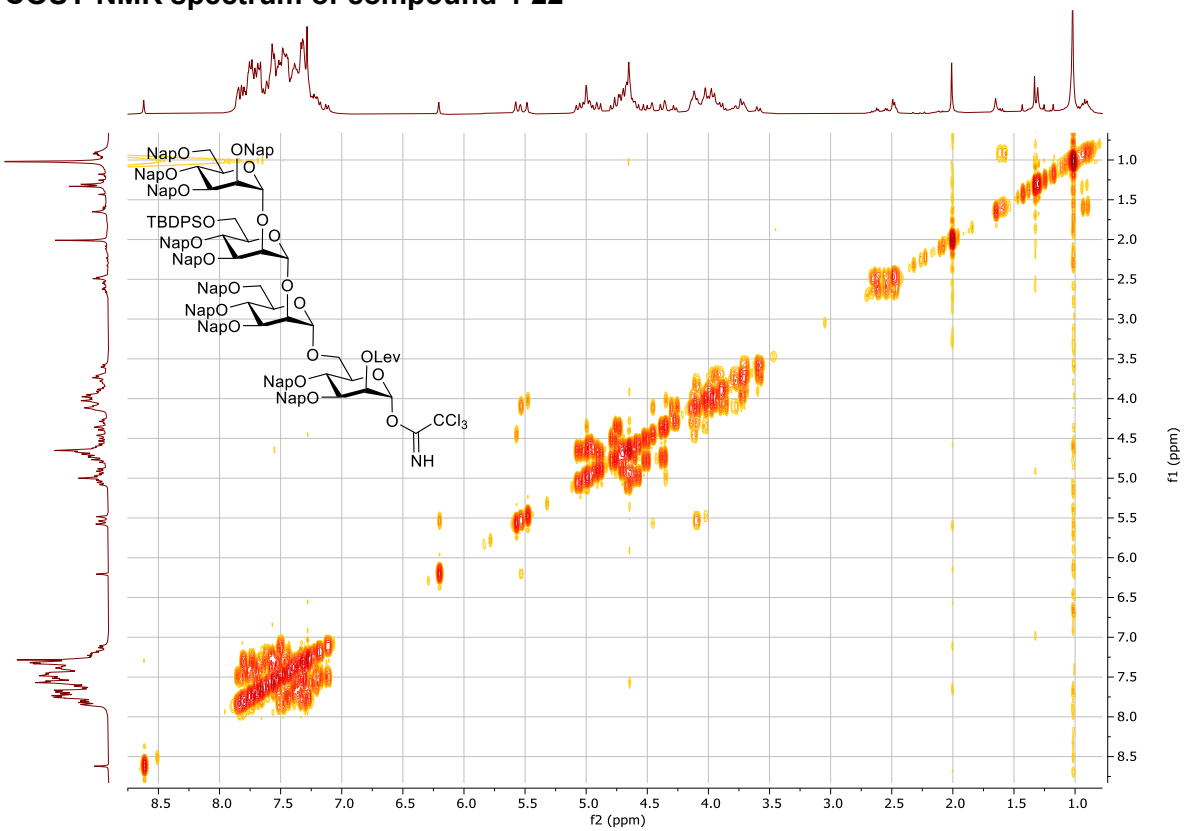

HSQC NMR spectrum of compound 4-22

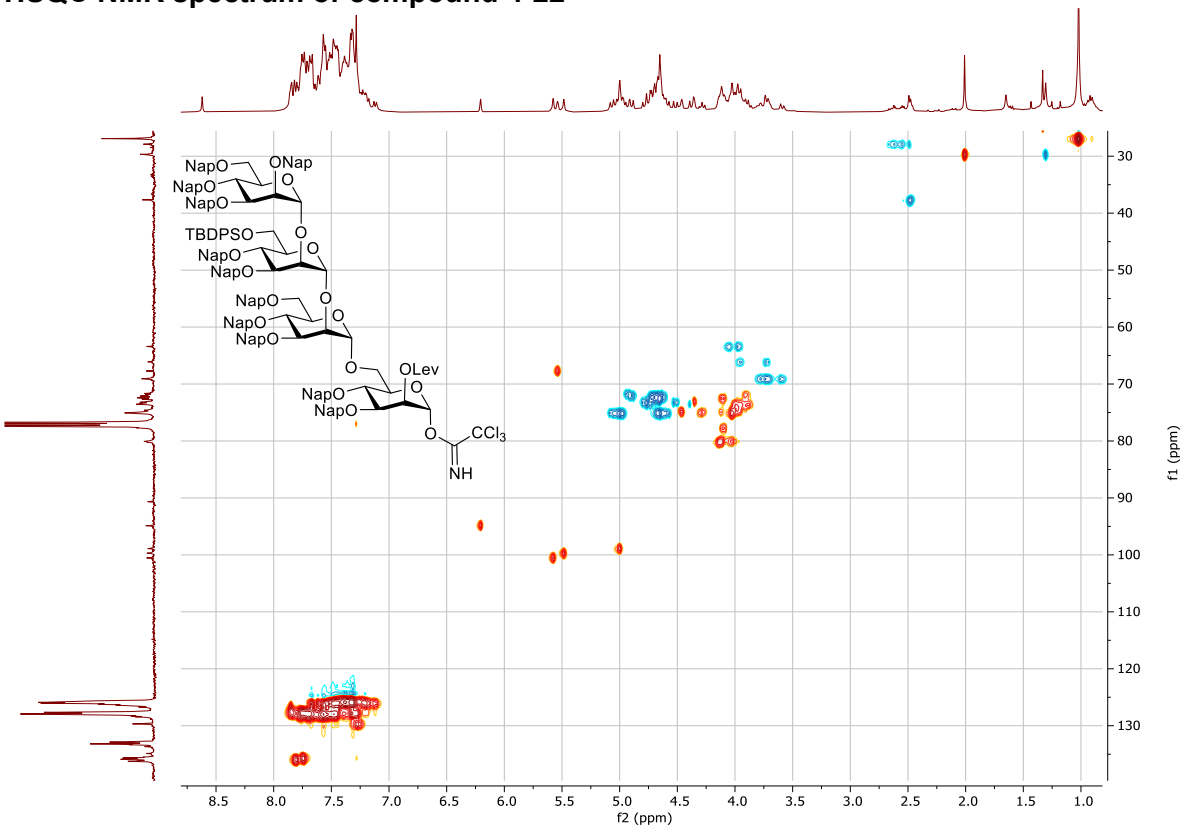

^{1}H NMR spectrum of compound 4-23

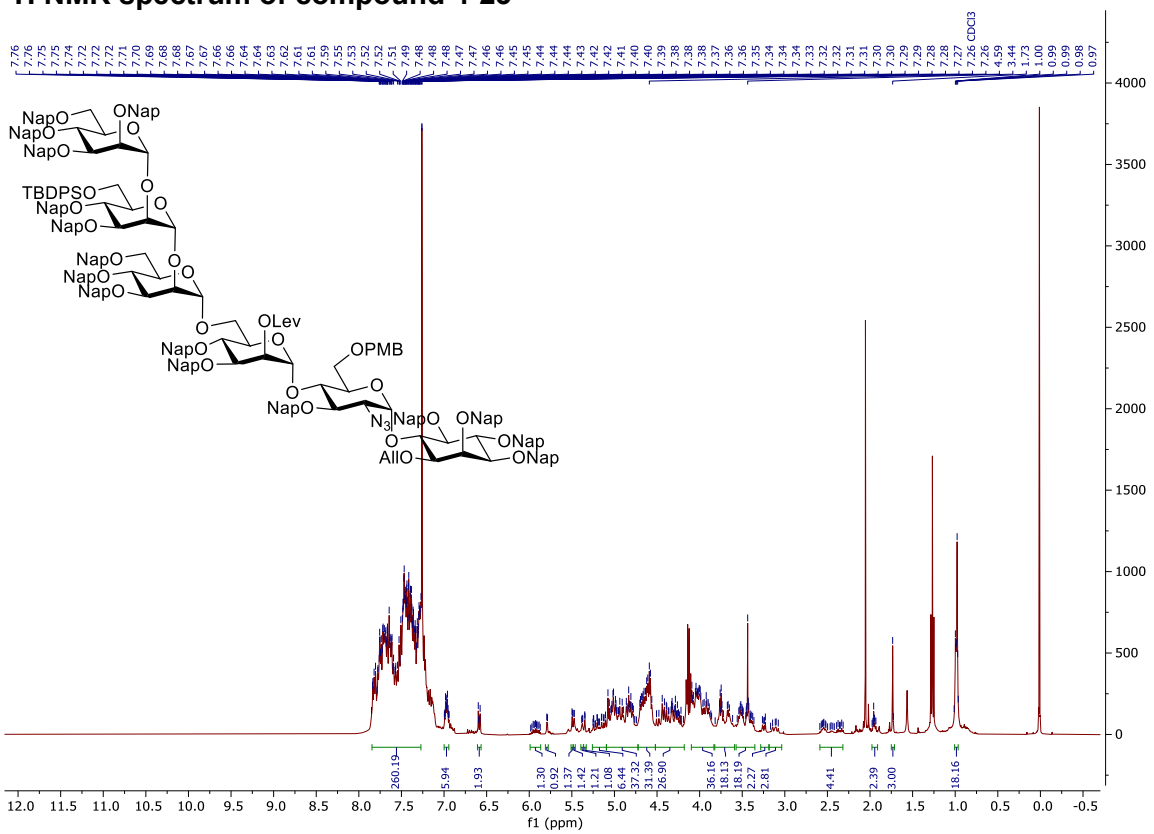

^{13}C NMR spectrum of compound 4-23

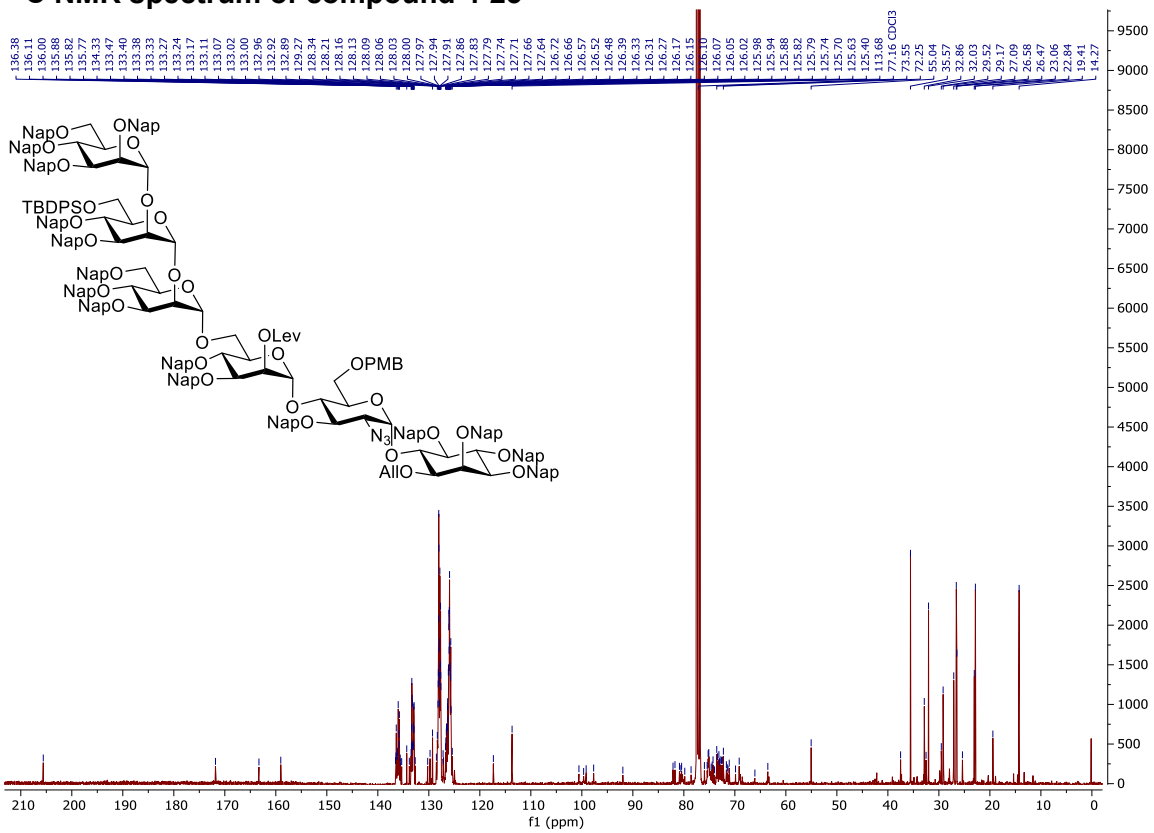

COSY-NMR spectrum of compound 4-23

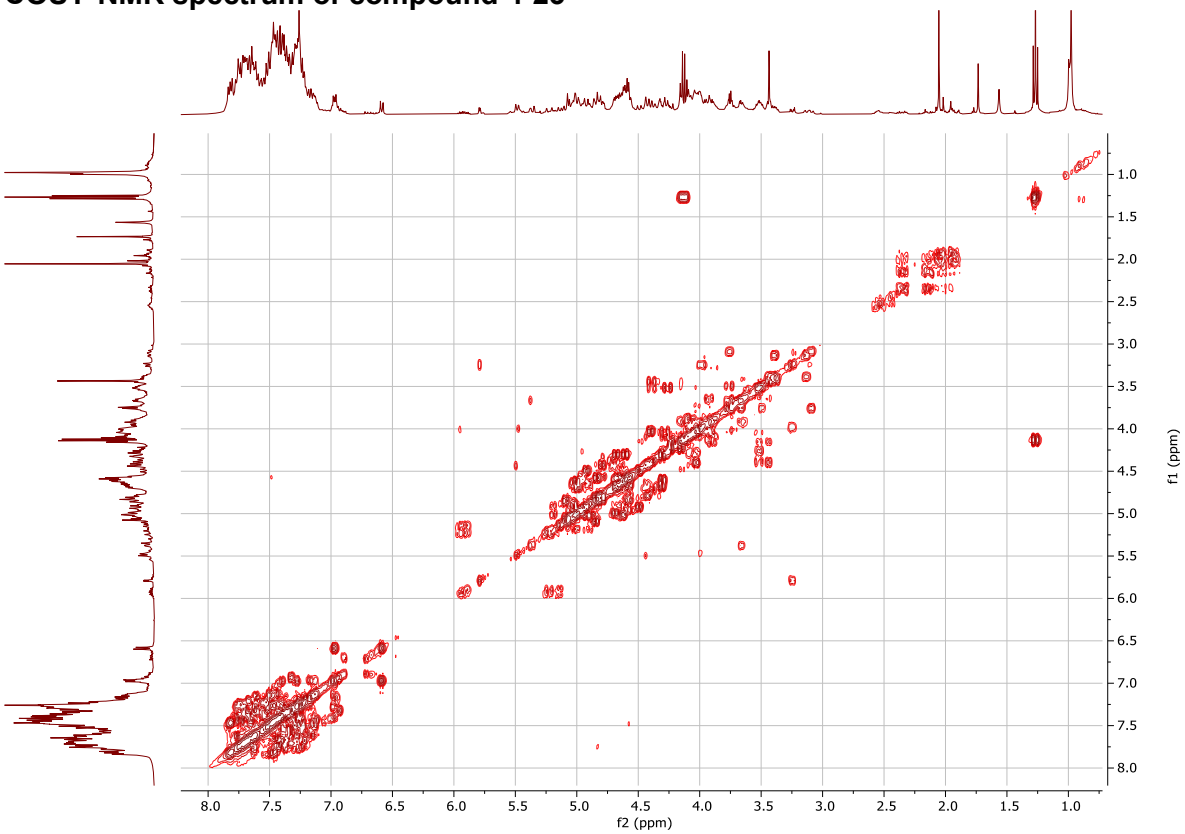

HSQC-NMR spectrum of compound 4-23

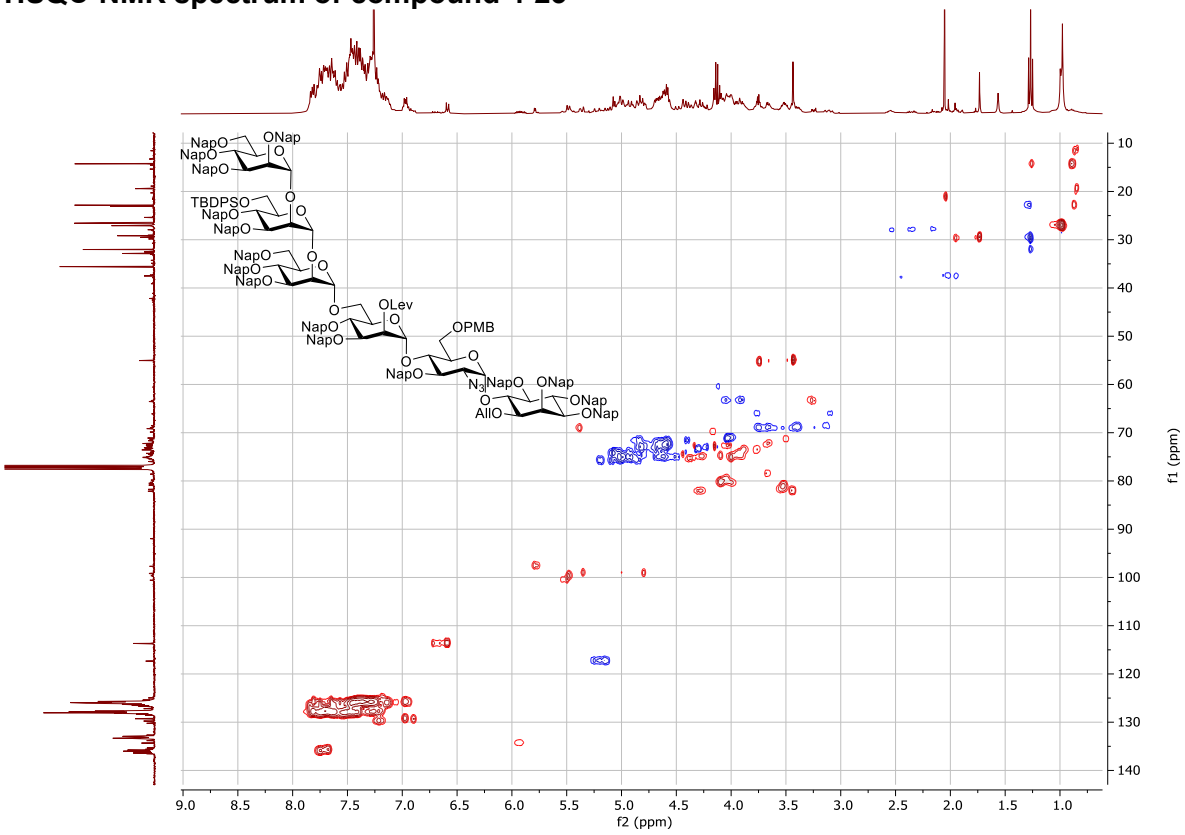

^{1}H NMR spectrum of compound 4-24

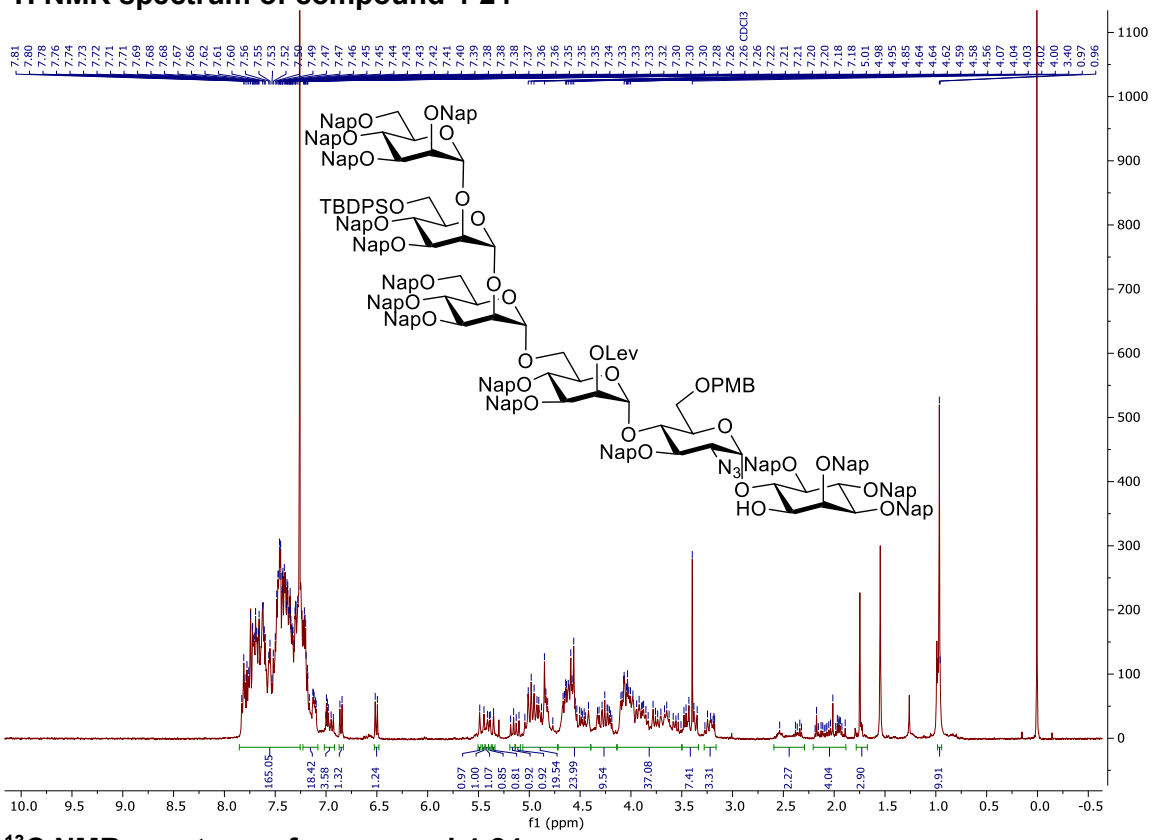

^{13}C NMR spectrum of compound 4-24

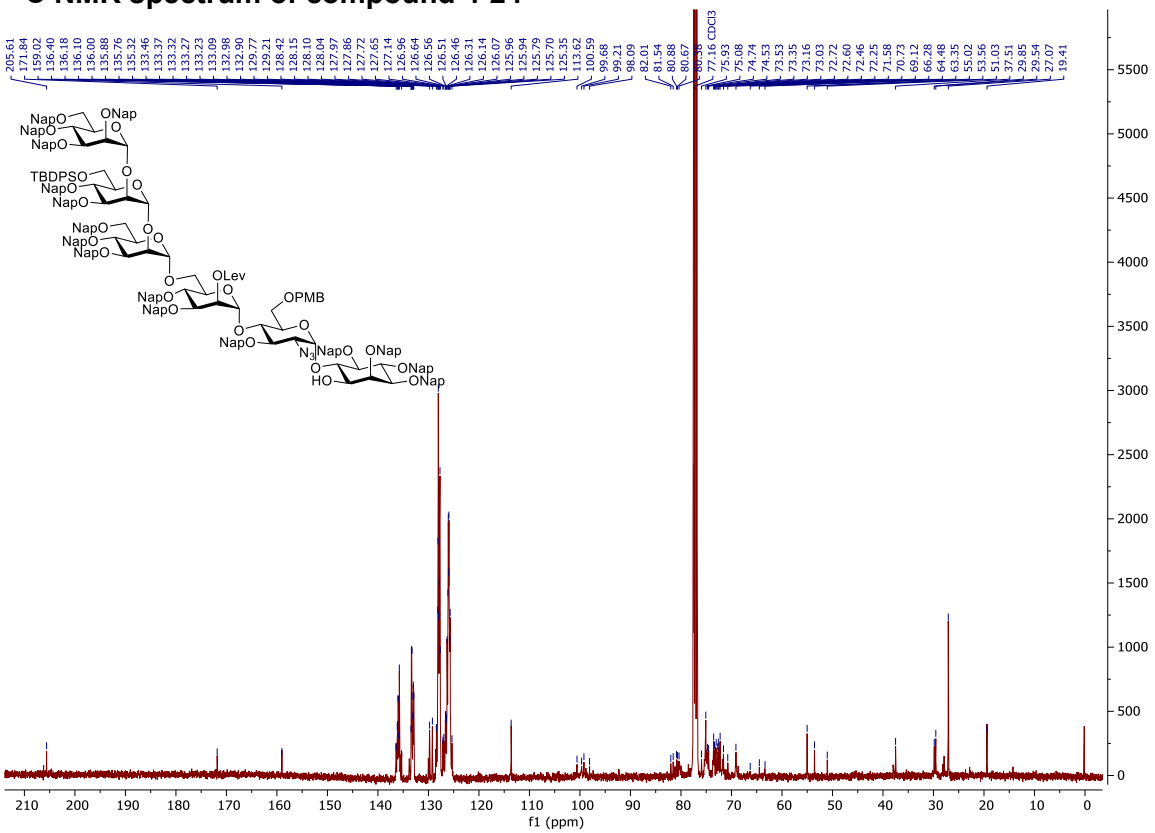

COSY-NMR spectrum of compound 4-24

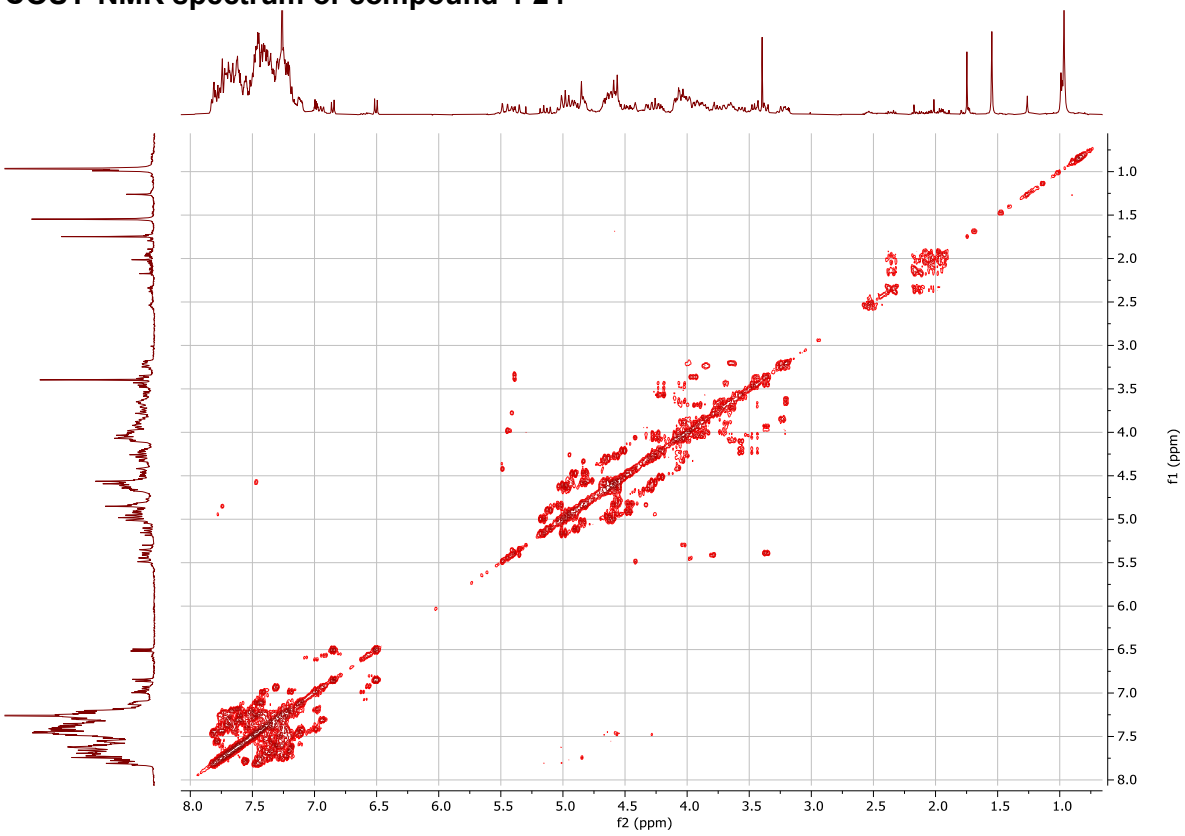

HSQC-NMR spectrum of compound 4-24

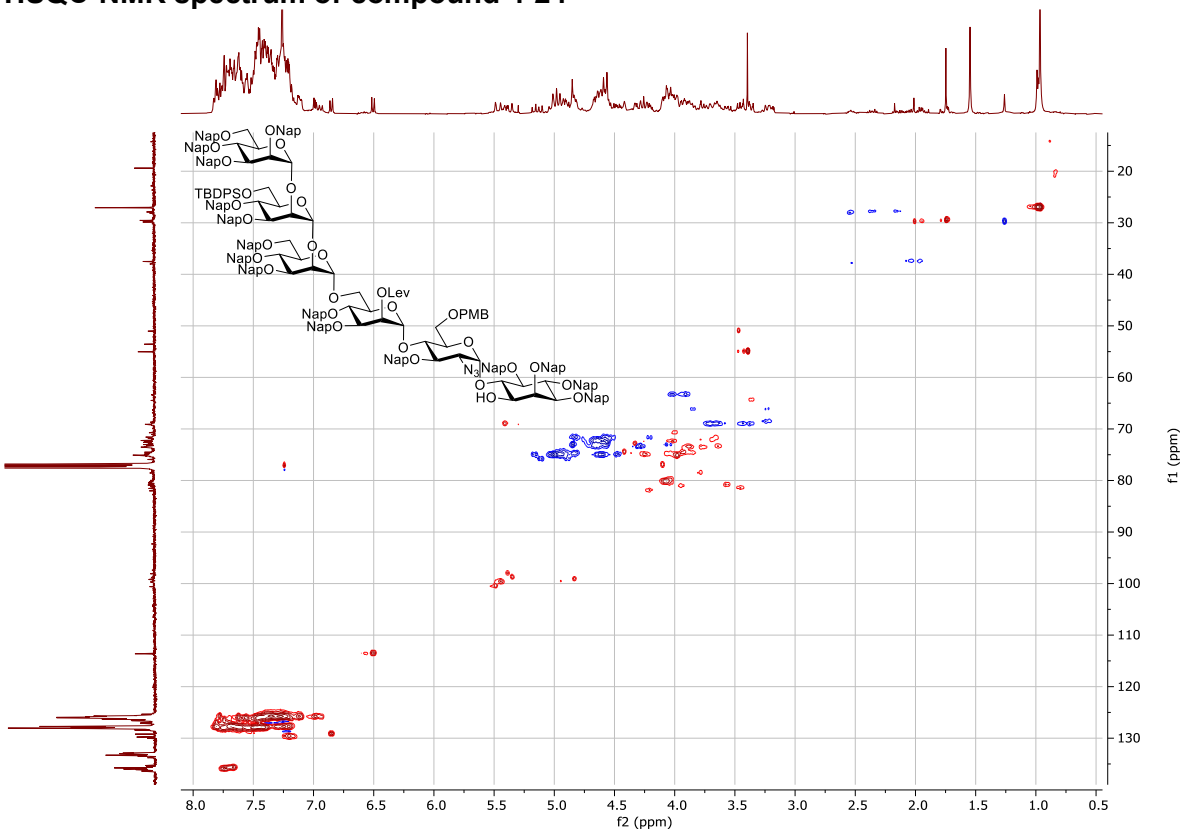

^{1}H NMR spectrum of compound 4-26

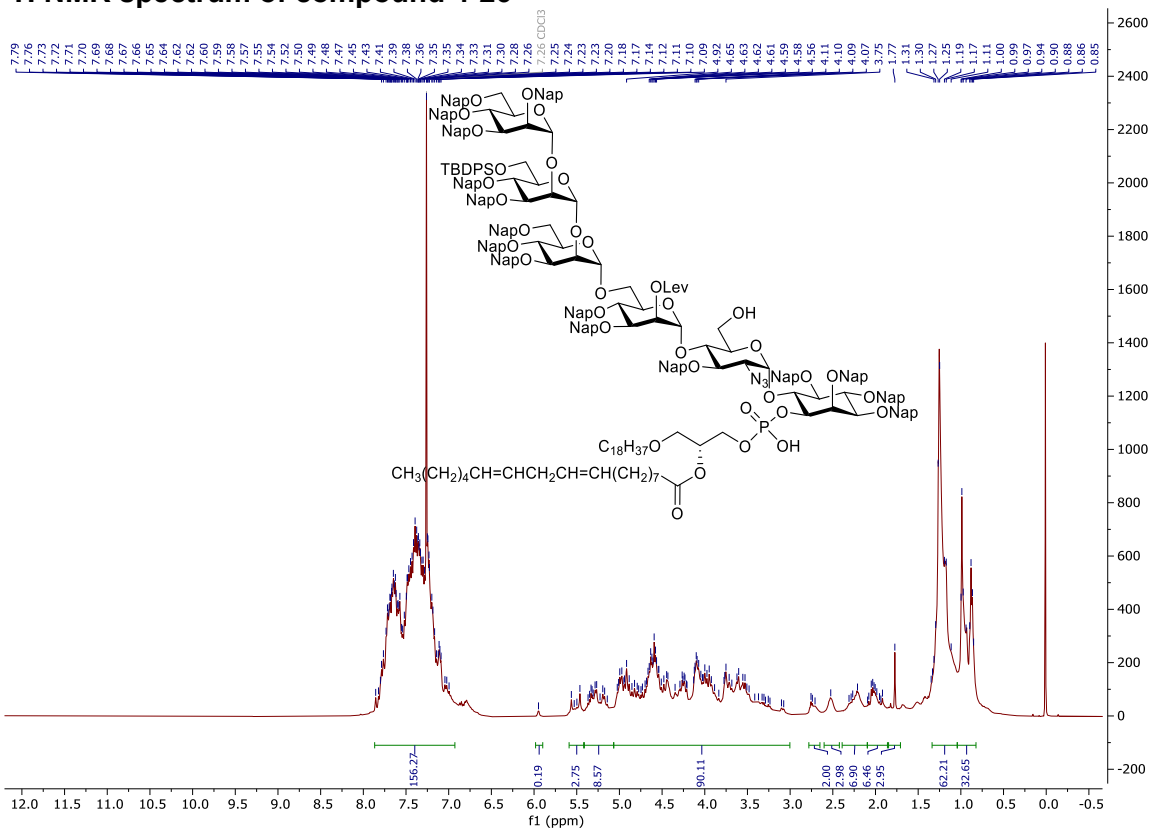

^{13}C NMR spectrum of compound 4-26

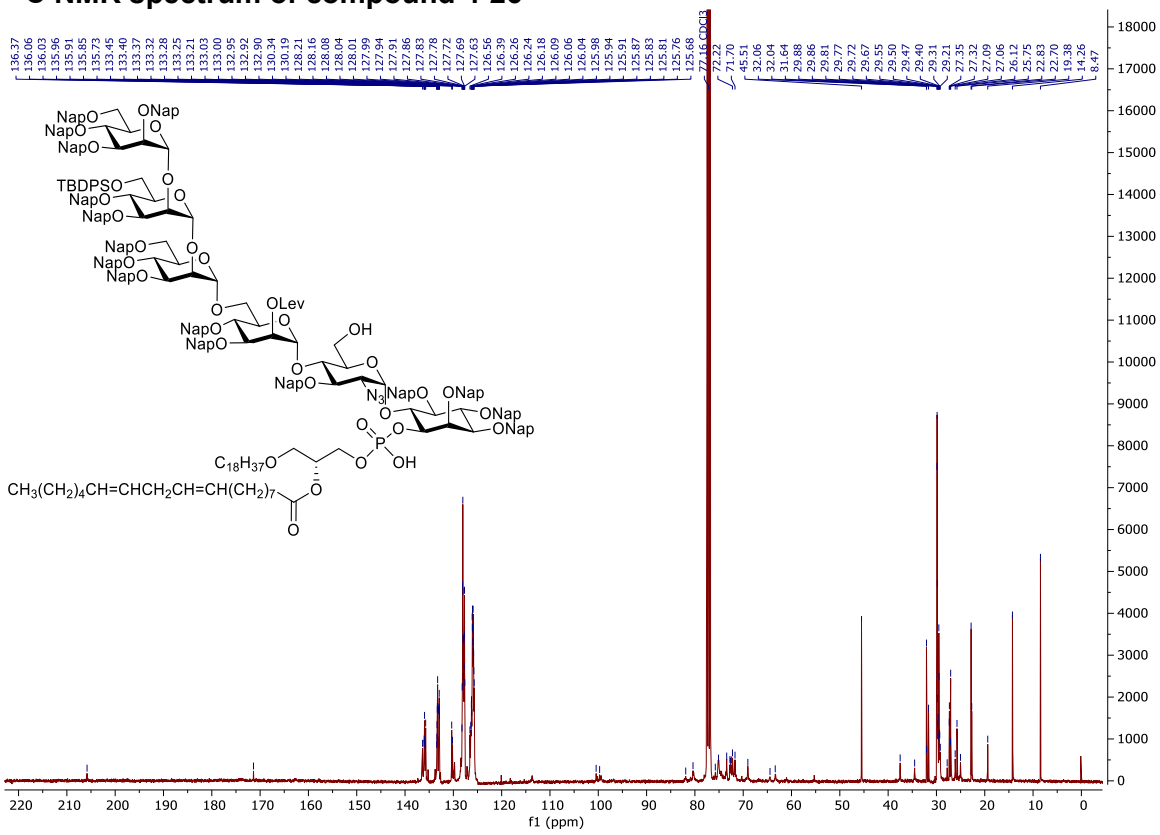

COSY-NMR spectrum of compound 4-26

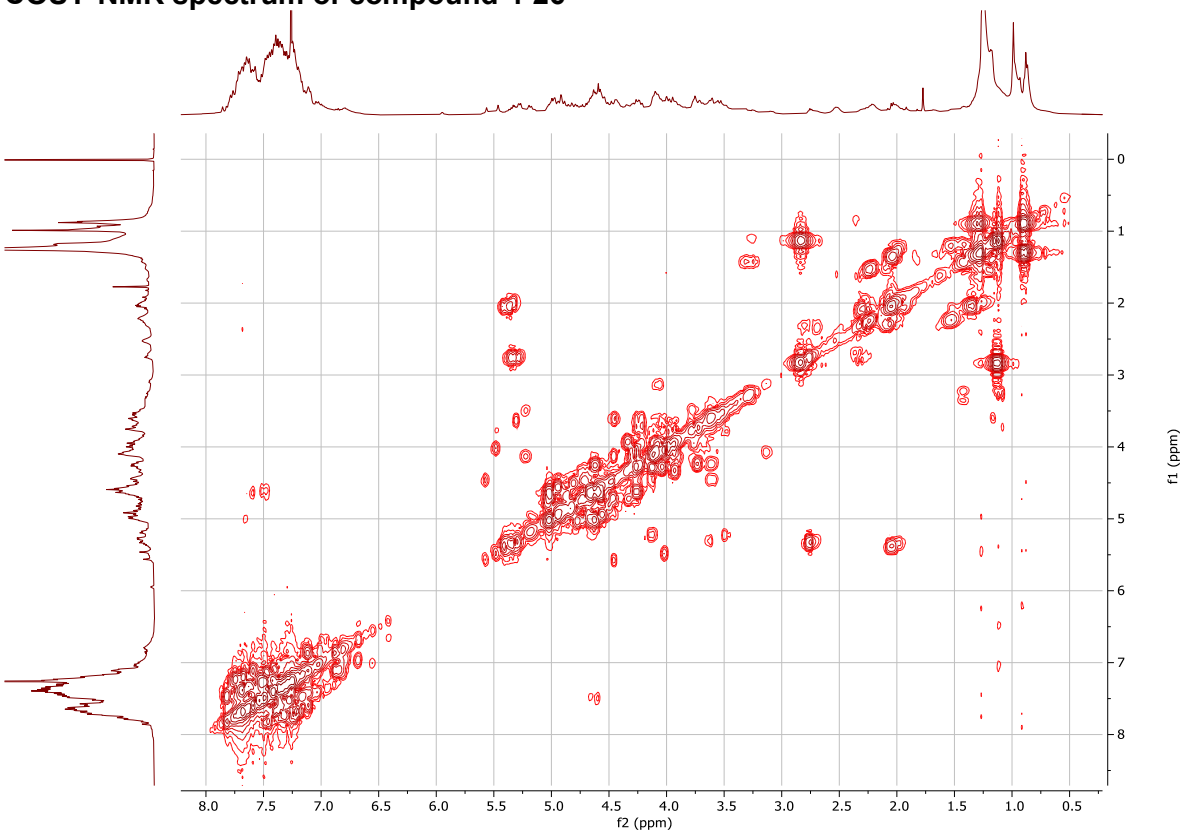

HSQC-NMR spectrum of compound 4-26

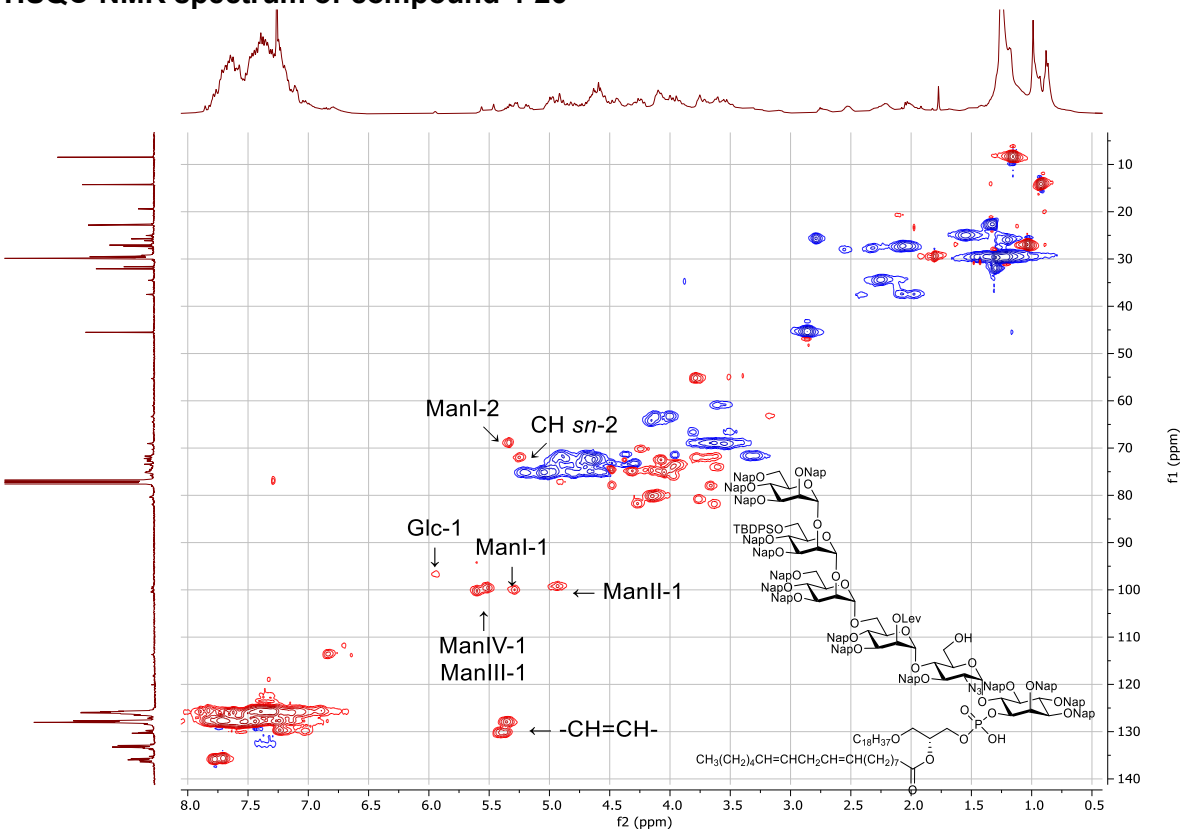

^{31}P NMR spectrum of compound 4-26